Volumes 137–140 (12 Issues), Spring 2007, ISSN: 0273–2289

# Applied Biochemistry and Biotechnology



## Biotechnology for Fuels and Chemicals

*The Twenty-Eighth Symposium*

**Editors**

***Jonathan R. Mielenz***
***K. Thomas Klasson***
***William S. Adney***
***James D. McMillan***

HUMANA PRESS

# Biotechnology for Fuels and Chemicals

*The Twenty-Eighth Symposium*

Presented as Volumes 136–140
of *Applied Biochemistry and Biotechnology*

Proceedings of the Twenty-Eighth Symposium
on Biotechnology for Fuels and Chemicals
Held April 30–May 3, 2006, in Nashville, Tennessee

*Sponsored by*

US Department of Energy Office of the Biomass Program
US Department of Agriculture, Agricultural Research Service
Oak Ridge National Laboratory
National Renewable Energy Laboratory
Idaho National Laboratory
Abengoa Bioenergy Corporation
BRI Energy
Battelle Nanotechnology Innovation Alliance
Cargill
Genencor International
Iogen
Katzen International
Natural Resources Canada
Novozymes
Procter & Gamble
The Samuel Roberts Noble Foundation
Southeastern SunGrant Center
Tate & Lyle

*Editors*
**Jonathan R. Mielenz**
*Oak Ridge National Laboratory*

**K. Thomas Klasson**
*Southern Regional Research Laboratory, USDA-ARS*

**William S. Adney and James D. McMillan**
*National Renewable Energy Laboratory*

HUMANA PRESS TOTOWA, NEW JERSEY

**Applied Biochemistry and Biotechnology**
Volumes 136–140, Complete, Spring 2007


**Applied Biochemistry and Biotechnology** is abstracted or indexed regularly in *Chemical Abstracts, Biological Abstracts, Current Contents, Science Citation Index, Excerpta Medica, Index Medicus,* and appropriate related compendia.

0273-2289/1559-0291 (Online)/07/136–140/iii–viii/$30.00

# Introduction to the Proceedings of the Twenty-Eighth Symposium on Biotechnology for Fuels and Chemicals

**Jonathan R. Mielenz**

*Oak Ridge National Laboratory*
*Oak Ridge. TN 3831*

The Twenty-Eighth Symposium on Biotechnology for Fuels and Chemicals was held April 30-May 3, 2006 in Nashville, Tennessee which provided a new interesting venue as well as a convenient travel destination. The growing interest in alternative fuels and chemicals, driven in part by the rising cost of petroleum, along with the exciting technical program yielded a record attendance at this Symposium with 479 participants, exceeding late year's record attendance in Denver. Notable was a dramatic increase in representation from industry which comprised about 40% of the attendees, signifying the continuing transition of Symposium from biomass research to inclusion of commercial development and deployment. The Symposium continued to receive strong international support with 30% of the attendees coming from 24 counties. As always, the Symposium was a strong supporter of education as shown by the 86 students registered for the meeting at the reduced rate.

The 2006 28$^{th}$ Symposium on Biotechnology for Fuels and Chemicals marked a transition from a meeting organized and managed by the National Renewable Energy Laboratory and the Oak Ridge National Laboratory to transferring these critical duties to a professional not-for-profit scientific society, the Society for Industrial Microbiology (SIM). SIM took on the responsibility for contracting with the host hotel, handling registration, abstract submission and tracking, proceedings publication and overall management of the meeting. The technical aspects continue to be managed by the 21 member organizing committee whose responsibility is to support the meeting Co-Chairs. Session selection, abstract review, manuscript review and editing and proceedings editing is handled by the meeting Co-Chairs and overseen by the committee as it has been in previous years. This transition went very smoothly and the meeting was managed quite well by SIM even in the face of the record attendance.

Selection of the Charles D. Scott awardees marked a small but appropriate departure from tradition with selection of two equally deserving individuals based upon their significant, lengthy support of the Symposium both through their technical contribution for bioenergy research and also by their serving tirelessly as Co-Chairs for the Symposium for ten to twelve years! Brian Davison from Oak Ridge National Laboratory (ORNL) is the Chief Scientist for Systems Biology and Biotechnology. In his twenty years at ORNL he has performed biotechnology research in variety of areas including bioconversion of renewable resources, non-aqueous biocatalysis, systems analysis of microbes, and immobilization of microbes and enzymes among other areas of research. He supported the Symposium many ways before becoming co-chair of the 15th to 26th Symposium on Biotechnology for Fuels and Chemicals and served as editor of Proceedings in *Appl. Biochem. Biotechnol.*, (1994–2005). The Symposium grew from 150 to over 400 attendees during these twelve years (ten with Mark Finkelstein).

Mark Finkelstein joined the National Renewable Energy Laboratory (NREL) in 1992 to introduce industrial approaches to problem solving and helped establish numerous successful business relationships during his tenure at NREL. He helped initiate work on *Zymomonas* within the Biofuels Program that resulted in numerous patents, publications, NREL's first team Staff Award, and an R&D 100 award in 1995. He has served in a variety of capacities in support of the Symposium on Biotechnology for Fuels and Chemicals before becoming co-chair from 1996 to 2004. In 2004 Mark joined Luca Technologies, a small biotechnology company using microbes to create *in-situ* hydrogen/methane as a new source of energy. The Symposium on Biotechnology for Fuels and Chemicals congratulates both Brian and Mark for receiving the CD Scott Award in 2006.

These proceeding cover many of the 62 oral presentations and 255 poster presentations covering topics ranging from Feedstock Supply and Logistics, Microbial Catalysts and Metabolic Engineering, to Bioprocessing and Separations R&D, and Bio/Thermo-chemical Integrated Biorefinery. In addition, the Symposium hosted two special sessions on Life Cycle Analysis/Sustainability, and International Biomass/Biofuels Update.

## Session Chairpersons

***Session 1A: Enzyme Catalysis and Engineering***

Chairs: Michael Himmel, *National Renewable Energy Laboratory, Golden, CO*
Elena Vlasenko, *Novozymes, Inc.,Davis, CA*

***Session 1B: Plant Biotechnology and Genomics***

Chairs: Mariam Sticklen, *Michigan State University, East Lansing, MI*
Gerald Tuskan, *Oak Ridge National Laboratory, Oak Ridge, TN*

***Session 2: Biomass Fractionation and Hydrolysis***
Chairs: Amy Miranda, *USDOE Office of the Biomass Program, Washington, DC*
Charles Wyman, *University of California, Davis, CA*

***Session 3A: New and Developing Industrial Bioproducts***
Chairs: Mohammed Moniruzzaman, *BioEnergy Intl. LLC, Norwell, MA*
Christian Stevens, *Ghent University, Gent, Belgium*

***Session 3B: Feedstock Supply and Logistics***
Chairs: Robert Perlack, *Oak Ridge National Laboratory, Oak Ridge, TN*
Richard Hess, *Idaho National Laboratory, Idaho Falls, ID*

***Session 4: Microbial Catalysis and Metabolic Engineering***
Chairs: Stanley Bower, *Tate & Lyle, Decatur, IL*
Mark Eiteman, *University of Georgia, Athens, GA*

***Session 5: Bioprocessing and Separations R&D***
Chairs: Luca Zullo, *Cargill, Minneapolis, MN*
Seth Synder, *Argonne National Laboratory, Argonne, IL*

***Session 6: Bio/Thermo-chemical Integrated Biorefinery***
Chairs: Art Ragauskas, *Georgia Institute of Technology, Atlanta, GA*
Thomas Foust, *National Renewable Energy Laboratory, Golden, CO*

***Special Topics Session A: Life Cycle Analysis/ Sustainability***
Chairs: Bruce Dale, *Michigan State University, East Lansing, MI*
Michael Wang, *Argonne National Laboratory, Argonne, IL*

***Special Topics Session B: International Biomass/Biofuels Update***
Chairs: Jin-Ho Seo, *Seoul University, Seoul, Korea*
Barbel Hahn-Hagerdal, *Lund University, Lund, Sweden*

## Organizing Committee

Jonathan Mielenz, Conference Chairman, *Oak Ridge National Laboratory, Oak Ridge, TN*
K. Thomas Klasson, Conference Co-Chairman, *USDA Agricultural Research Service, Southern Regional Research Laboratory, New Orleans, LA*
Jim McMillan, Conference Co-Chairman, *National Renewable Energy Laboratory, Golden, CO*
William Adney, *National Renewable Energy Laboratory, Golden, CO*
Doug Cameron, *Khosla Ventures, Menlo Park, CA*
Brian Davison, *Oak Ridge National Laboratory, Oak Ridge, TN*
Jim Duffield, *National Renewable Energy Laboratory, Golden, CO*
Don Erbach, *USDA-Agricultural Research Service, Beltsville, MD*

## Acknowledgments

The 28th Symposium was a success and these Proceedings are available due to the hard work of many people at ORNL, NREL and SIM in addition to the significant contributions of the Co-Chairs. In particular, Ann Luffman and Deneice Daniels at ORNL, Jim Duffield at NREL provided significant help to the Symposium and Proceedings. This author is particularly grateful for the diligent work of Christine Lowe and Demetra Pavidis at SIM for undertaking the difficult task of running the 28th Symposium the first time as it was underway and operating the meeting very successfully and Tracy Catanese at Humana Press for surviving through our delays.

Oak Ridge National Laboratory is operated for the US Department of Energy by the Midwest Research Institute and UT-Battelle under contract DE-AC05-00OR22725.

The National Renewable Energy Laboratory is operated for the US Department of Energy by the Midwest Research Institute and Battelle under contract DE-AC36-99GO10337.

## Other Proceedings in this Series

1. "Proceedings of the First Symposium on Biotechnology in Energy Production and Conservation" (1978), *Biotechnol. Bioeng. Symp.* **8.**
2. "Proceedings of the Second Symposium on Biotechnology in Energy Production and Conservation" (1980), *Biotechnol. Bioeng. Symp.* **10.**
3. "Proceedings of the Third Symposium on Biotechnology in Energy Production and Conservation" (1981), *Biotechnol. Bioeng. Symp.* **11.**
4. "Proceedings of the Fourth Symposium on Biotechnology in Energy Production and Conservation" (1982), *Biotechnol. Bioeng. Symp.* **12.**
5. "Proceedings of the Fifth Symposium on Biotechnology for Fuels and Chemicals" (1983), *Biotechnol. Bioeng. Symp.* **13.**
6. "Proceedings of the Sixth Symposium on Biotechnology for Fuels and Chemicals" (1984), *Biotechnol. Bioeng. Symp.* **14.**
7. "Proceedings of the Seventh Symposium on Biotechnology for Fuels and Chemicals" (1985), *Biotechnol. Bioeng. Symp.* **15.**
8. "Proceedings of the Eigth Symposium on Biotechnology for Fuels and Chemicals" (1986, *Biotechnol. Bioeng. Symp.* **17.**
9. "Proceedings of the Ninth Symposium on Biotechnology for Fuels and Chemicals" (1988), *Appl. Biochem. Biotechnol.* **17,18.**
10. "Proceedings of the Tenth Symposium on Biotechnology for Fuels and Chemicals" (1989), *Appl. Biochem. Biotechnol.* **20,21.**
11. "Proceedings of the Eleventh Symposium on Biotechnology for Fuels and Chemicals" (1990), *Appl. Biochem. Biotechnol.* **24,25.**
12. "Proceedings of the Twelfth Symposium on Biotechnology for Fuels and Chemicals" (1991), *Appl. Biochem. Biotechnol.* **28,29.**
13. "Proceedings of the Thirteenth Symposium on Biotechnology for Fuels and Chemicals" (1992), *Appl. Biochem. Biotechnol.* **34,35.**
14. "Proceedings of the Fourteenth Symposium on Biotechnology for Fuels and Chemicals" (1993), *Appl. Biochem. Biotechnol.* **39,40.**
15. "Proceedings of the Fifteenth Symposium on Biotechnology for Fuels and Chemicals" (1994), *Appl. Biochem. Biotechnol.* **45,46.**
16. "Proceedings of the Sixteenth Symposium on Biotechnology for Fuels and Chemicals" (1995), *Appl. Biochem. Biotechnol.* **51,52.**
17. "Proceedings of the Seventeenth Symposium on Biotechnology for Fuels and Chemicals" (1996), *Appl. Biochem. Biotechnol.* **57,58.**
18. "Proceedings of the Eighteenth Symposium on Biotechnology for Fuels and Chemicals" (1997), *Appl. Biochem. Biotechnol.* **63–65.**
19. "Proceedings of the Nineteenth Symposium on Biotechnology for Fuels and Chemicals" (1998), *Appl. Biochem. Biotechnol.* **70–72.**
20. "Proceedings of the Twentieth Symposium on Biotechnology for Fuels and Chemicals" (1999), *Appl. Biochem. Biotechnol.* **77–79.**
21. "Proceedings of the Twenty-First Symposium on Biotechnology for Fuels and Chemicals" (2000), *Appl. Biochem. Biotechnol.* **84–86.**

22. "Proceedings of the Twenty-Second Symposium on Biotechnology for Fuels and Chemicals" (2001), *Appl. Biochem. Biotechnol.* **91–93.**
23. "Proceedings of the Twenty-Third Symposium on Biotechnology for Fuels and Chemicals" (2002), *Appl. Biochem. Biotechnol.* **98–100.**
24. "Proceedings of the Twenty-Fourth Symposium on Biotechnology for Fuels and Chemicals" (2003), *Appl. Biochem. Biotechnol.* **105–108.**
25. "Proceedings of the Twenty-Fifth Symposium on Biotechnology for Fuels and Chemicals" (2004), *Appl. Biochem. Biotechnol.* **113–116.**
26. "Proceedings of the Twenty-Sixth Symposium on Biotechnology for Fuels and Chemicals" (2005), *Appl. Biochem. Biotechnol.* **121–124.**
27. "Proceedings of the Twenty-Seventh Symposium on Biotechnology for Fuels and Chemicals" (2006), *Appl. Biochem. Biotechnol.* **129–132.**

This symposium has been held annually since 1978. We are pleased to have the proceedings of the Twenty-Seventh Symposium currently published in this special issue to continue the tradition of providing a record of the contributions made.

The Twenty-Eighth Symposium will be April 30–May 3, 2006 in Nashville, Tennessee. More information on the 27th and 28th Symposia is available at the following websites: [http://www.eere.energy.gov/biomass/biotech_symposium/] and [http://www.simhq.org/html/meetings/]. We encourage comments or discussions relevant to the format or content of the meeting.

CONTENTS

Introduction
***Jonathan R. Mielenz*** ..... ***iii***

SESSION 1A: ENZYME CATALYSIS AND ENGINEERING

Introduction to Session 1A
***Michael E. Himmel*** ..... ***1***

Grass Lignocellulose: *Strategies to Overcome Recalcitrance*
***Danny E. Akin*** ..... ***3***

Enzymatic Microreactors for the Determination of Ethanol by an Automatic Sequential Injection Analysis System
***Eliana M. Alhadeff, Andrea M. Salgado, Oriol Cos, Nei Pereira Jr., BelkisValdman, and Francisco Valero*** ..... ***17***

Optimization of Cyclodextrin Glucanotransferase Production From *Bacillus clausii* E16 in Submerged Fermentation Using Response Surface Methodology
***Heloiza Ferreira Alves-Prado, Daniela Alonso Bocchini, Eleni Gomes, Luis Carlos Baida, Jonas Contiero, Inês Conceição Roberto, and Roberto Da Silva*** ..... ***27***

Purification and Characterization of a Cyclomaltodextrin Glucanotransferase From *Paenibacillus campinasensis* Strain H69-3
***Heloiza Ferreira Alves-Prado, Eleni Gomes, and Roberto da Silva*** ..... ***41***

Acetone Powder From Dormant Seeds of Ricinus communis L: *Lipase Activity and Presence of Toxic and Allergenic Compounds*
***Elisa D. C. Cavalcanti, Fábio M. Maciel, Pierre Villeneuve, Regina C. A. Lago, Olga L. T. Machado, and Denise M. G. Freire*** ..... ***57***

Immobilization of *Candida antarctica* Lipase B by Covalent Attachment to Green Coconut Fiber
***Ana I. S. Brígida, Álvaro D. T. Pinheiro, Andrea L. O. Ferreira, Gustavo A. S. Pinto, and Luciana R. B. Gonçalves*** ..... ***67***

Pretreatment of Corn Stover by Soaking in Aqueous Ammonia at Moderate Temperatures
***Tae Hyun Kim and Y.Y. Lee*** ..... ***81***

β-D-Xylosidase From *Selenomonas ruminantium* of Glycoside Hydrolase Family 43
***Douglas B. Jordan, Xin-Liang Li, Christopher A. Dunlap, Terence R. Whitehead, and Michael A. Cotta*** ..... 93

Biodiesel Fuel Production by the Transesterification Reaction of Soybean Oil Using Immobilized Lipase
***Otávio L. Bernardes, Juliana V. Bevilaqua, Márcia C. M. R. Leal, Denise M. G. Freire, and Marta A. P. Langone*** ..... 105

Thermoinactivation Mechanism of Glucose Isomerase
***Leng Hong Lim and Bradley A. Saville*** ..... 115

Measuring Cellulase Activity: *Application of the Filter Paper Assay to Low-Activity Enzyme Preparations*
***Tor Soren Nordmark, Alan Bakalinsky, and Michael H. Penner*** ..... 131

Enzymatic Hydrolysis Optimization to Ethanol Production by Simultaneous Saccharification and Fermentation
***Mariana Peñuela Vásquez, Juliana Nascimento C. Da Silva, Maurício Bezerra de Souza Jr., and Nei Pereira Jr.*** ..... 141

Filter Paper Degrading Ability of a *Trichoderma* Strain With Multinucleate Conidia
***Hideo Toyama, Makiko Yano, Takeshi Hotta, and Nobuo Toyama*** ..... 155

Use of Glucose Oxidase in a Membrane Reactor for Gluconic Acid Production
***Luiz Carlos Martins das Neves and Michele Vitolo*** ..... 161

Enzyme Production by Industrially Relevant Fungi Cultured on Coproduct From Corn Dry Grind Ethanol Plants
***Eduardo A. Ximenes, Bruce S. Dien, Michael R. Ladisch, Nathan Mosier, Michael A. Cotta, and Xin-Liang Li*** ..... 171

Production of Biosurfactant by *Pseudomonas aeruginosa* Grown on Cashew Apple Juice
***Maria V. P. Rocha, Maria C. M. Souza, Sofia C. L. Benedicto, and Márcio S. Bezerra Gorete R. Macedo, Gustavo A. Saavedra Pinto, and Luciana R. B. Gonçalves*** ..... 185

*Thermoascus aurantiacus* CBHI/Cel7A Production in *Trichoderma reesei* on Alternative Carbon Sources
***Zsuzsa Benkő, Eszter Drahos, Zsolt Szengyel, Terhi Puranen, Jari Vehmaanperä, and Kati Réczey*** ..... 195

SESSION 1B: PLANT BIOTECHNOLOGY AND GENOMICS

Introduction to Session 1B
***Mariam B. Sticklen*** ..... ***205***

Heterologous *Acidothermus cellulolyticus* 1, 4-β-Endoglucanase E1 Produced Within the Corn Biomass Converts Corn Stover Into Glucose
***Callista Ransom, Venkatesh Balan, Gadab Biswas, Bruce Dale, Elaine Crockett, and Mariam Sticklen*** ..... ***207***

SESSION 2

The Impact of Enzyme Characteristics on Corn Stover Fiber Degradation and Acid Production During Ensiled Storage
***Haiyu Ren, Tom L. Richard, and Kenneth J. Moore*** ..... ***221***

Fractionation of *Cynara cardunculus* (Cardoon) Biomass by Dilute-Acid Pretreatment
***Mercedes Ballesteros, M. José Negro, Paloma Manzanares, Ignacio Ballesteros, Felicia Sáez, and J. Miguel Oliva*** ..... ***239***

Heat Extraction of Corn Fiber Hemicellulose
***Zsuzsa Benkő, Alexandra Andersson, Zsolt Szengyel, Melinda Gáspár, Kati Réczey, and Henrik Stålbrand*** ..... ***253***

An Evaluation of British Columbian Beetle-Killed Hybrid Spruce for Bioethanol Production
***Alex Berlin, Claudio Muñoz, Neil Gilkes, Sepideh Massoumi Alamouti, Pablo Chung, Kyu-Young Kang, Vera Maximenko, Jaime Baeza, Juanita Freer, Regis Mendonça, and Jack Saddler*** ..... ***267***

Production of Cellulolytic and Hemicellulolytic Enzymes From *Aureobasidium pulluans* on Solid State Fermentation
***Rodrigo Simões Ribeiro Leite, Daniela Alonso Bocchini, Eduardo Da Silva Martins, Dênis Silva, Eleni Gomes, and Roberto Da Silva*** ..... ***281***

The Effect of Particle Size on Hydrolysis Reaction Rates and Rheological Properties in Cellulosic Slurries
***Rajesh K. Dasari and R. Eric Berson*** ..... ***289***

Effect of Dissolved Carbon Dioxide on Accumulation of Organic Acids in Liquid Hot Water Pretreated Biomass Hydrolyzates
***G. Peter Van Walsum, Maurilio Garcia-Gil, Shou-Feng Chen, and Kevin Chambliss*** ..... ***301***

Separation of Glucose and Pentose Sugars by Selective Enzyme Hydrolysis of AFEX-Treated Corn Fiber
*Robert J. Hanchar, Farzaneh Teymouri, Chandra D. Nielson, Darold McCalla, and Mark D. Stowers* ..... 313

The Potential in Bioethanol Production From Waste Fiber Sludges in Pulp Mill-Based Biorefineries
*Anders Sjöde, Björn Alriksson, Leif J. Jönsson, and Nils-Olof Nilvebrant* ..... 327

Dilute Sulfuric Acid Pretreatment of Agricultural and Agro-Industrial Residues for Ethanol Production
*Carlos Martin, Björn Alriksson, Anders Sjöde, Nils-Olof Nilvebrant, and Leif J. Jönsson* ..... 339

Xylanase Contribution to the Efficiency of Cellulose Enzymatic Hydrolysis of Barley Straw
*María P. García-Aparicio, Mercedes Ballesteros, Paloma Manzanares, Ignacio Ballesteros, Alberto González, and M. José Negro* ..... 353

Effect of Organosolv Ethanol Pretreatment Variables on Physical Characteristics of Hybrid Poplar Substrates
*Xuejun Pan, Dan Xie, Kyu-Young Kang, Seung-Lak Yoon, and Jack N. Saddler* ..... 367

Liquid Hot Water Pretreatment of Olive Tree Pruning Residues
*Cristóbal Cara, Inmaculada Romero, Jose Miguel Oliva, Felicia Sáez, and Eulogio Castro* ..... 379

Ammonia Fiber Expansion Pretreatment and Enzymatic Hydrolysis on Two Different Growth Stages of Reed Canarygrass
*Tamika C. Bradshaw, Hasan Alizadeh, Farzaneh Teymouri, Venkatesh Balan, and Bruce E. Dale* ..... 395

Mitigation of Cellulose Recalcitrance to Enzymatic Hydrolysis by Ionic Liquid Pretreatment
*Anantharam P. Dadi, Constance A. Schall, and Sasidhar Varanasi* ..... 407

Evaluation of Different Biomass Materials as Feedstock for Fermentable Sugar Production
*Yi Zheng, Zhongli Pan, Ruihong Zhang, John M. Labavitch, Donghai Wang, Sarah A. Teter, and Bryan M. Jenkins* ..... 423

SESSION 3

Techno-Economic Analysis of Biocatalytic Processes for Production of Alkene Epoxides
***Abhijeet P. Borole and Brian H. Davison*** ..... 437

Evaluation of Liquid–Liquid Extraction Process for Separating Acrylic Acid Produced From Renewable Sugars
***M. E. T. Alvarez, E. B. Moraes, A. B. Machado, R. Maciel Filho, and M. R. Wolf-Maciel*** ..... 451

Enhancement of Rhamnolipid Production in Residual Soybean Oil by an Isolated Strain of *Pseudomonas aeruginosa*
***C. J. B. de Lima, F. P. França, E. F. C. Sérvulo, M. M. Resende, and V. L. Cardoso*** ..... 463

Optimizing Carbon/Nitrogen Ratio for Biosurfactant Production by a *Bacillus subtilis* Strain
***R. R. Fonseca, A. J. R. Silva, F. P. De França, V. L. Cardoso, and E. F. C. Sérvulo*** ..... 471

A New Process for Acrylic Acid Synthesis by Fermentative Process
***B. H. Lunelli, E. R. Duarte, E. C. Vasco de Toledo, M. R. Wolf Maciel, and R. Maciel Filho*** ..... 487

Ethanol/Water Pulps From Sugar Cane Straw and Their Biobleaching With Xylanase From *Bacillus pumilus*
***Regina Y. Moriya, Adilson R. Gonçalves, and Marta C. T. Duarte*** ..... 501

Nisin Production Utilizing Skimmed Milk Aiming to Reduce Process Cost
***Angela Faustino Jozala, Maura Sayuri de Andrade, Luciana Juncioni de Arauz, Adalberto Pessoa Jr., and Thereza Christina Vessoni Penna*** ..... 515

Bacterial Cellulose Production by *Gluconacetobacter* sp. RKY5 in a Rotary Biofilm Contactor
***Yong-Jun Kim, Jin-Nam Kim, Young-Jung Wee, Don-Hee Park, and Hwa-Won Ryu*** ..... 529

Biosurfactant Production by Cultivation of *Bacillus atrophaeus* ATCC 9372 in Semidefined Glucose/Casein-Based Media
***Luiz Carlos Martins das Neves, Kátia Silva de Oliveira, Márcio Junji Kobayashi, Thereza Christina Vessoni Penna, and Attilio Converti*** ..... 539

Evaluation of the pH- and Thermal Stability of the Recombinant Green Fluorescent Protein (GFP) in the Presence of Sodium Chloride
*Marina Ishii, Juliana Sayuri Kunimura, Hélio Tallon Jeng, Thereza Christina Vessoni Penna, and Olivia Cholewa* ..... 555

Carboxymethylcellulose Obtained by Ethanol/Water Organosolv Process Under Acid Conditions
*Denise S. Ruzene, Adilson R. Gonçalves, José A. Teixeira, and Maria T. Pessoa de Amorim* ..... 573

Response Surface Methodological Approach for Optimization of Free Fatty Acid Removal in Feedstock
*Gwi-Taek Jeong, Do-Heyoung Kim, and Don-Hee Park* ..... 583

Optimization of Lipase-Catalyzed Synthesis of Sorbitan Acrylate Using Response Surface Methodology
*Gwi-Taek Jeong and Don-Hee Park* ..... 595

Renewable Energy in the United States: *Is There Enough Land?*
*Alvin O. Converse* ..... 611

Optimizing the Logistics of Anaerobic Digestion of Manure
*Emad Ghafoori and Peter C. Flynn* ..... 625

The Relative Cost of Biomass Energy Transport
*Erin Searcy, Peter Flynn, Emad Ghafoori, and Amit Kumar* ..... 639

SESSION 4

The Effect of Initial Cell Concentration on Xylose Fermentation by *Pichia stipitis*
*Frank K. Agbogbo, Guillermo Coward-Kelly, Mads Torry-Smith, Kevin Wenger, and Thomas W. Jeffries* ..... 653

Construction and Evaluation of a *Clostridium thermocellum* ATCC 27405 Whole-Genome Oligonucleotide Microarray
*Steven D. Brown, Babu Raman, Catherine K. McKeown, Shubha P. Kale, Zhili He, and Jonathan R. Mielenz* ..... 663

Tannase Production by Solid State Fermentation of Cashew Apple Bagasse
*Tigressa H. S. Rodrigues, Maria Alcilene A. Dantas, Gustavo A. S. Pinto, and Luciana R. B. Gonçalves* .....675

Studying Pellet Formation of a Filamentous Fungus *Rhizopus oryzae* to Enhance Organic Acid Production
*Wei Liao, Yan Liu, and Shulin Chen* ..... 689

Comparison of Multiple Gene Assembly Methods for Metabolic Engineering
*Chenfeng Lu, Karen Mansoorabadi, and Thomas Jeffries* ..... 703

Fed-Batch Production of Glucose 6-Phosphate Dehydrogenase Using Recombinant *Saccharomyces cerevisiae*
*Luiz Carlos Martins das Neves, Adalberto Pessoa Jr., and Michele Vitolo* ..... 711

Conversion of Aqueous Ammonia-Treated Corn Stover to Lactic Acid by Simultaneous Saccharification and Cofermentation
*Yongming Zhu, Y. Y. Lee, and Richard T. Elander* ..... 721

SESSION 5: BIOPROCESSING AND SEPARATIONS R&D

Introduction to Session 5
*Luca Zullo and Seth W. Snyder* ..... 739

Economic Evaluation of Isolation of Hemicelluloses From Process Streams From Thermomechanical Pulping of Spruce
*Tobias Persson, Anna-Karin Nordin, Guido Zacchi, and Ann-Sofi Jönsson* ..... 741

Estimation of Temperature Dependent Parameters of a Batch Alcoholic Fermentation Process
*Rafael Ramos de Andrade, Elmer Ccopa Rivera, Aline C. Costa, Daniel I. P. Atala, Francisco Maugeri Filho, and Rubens Maciel Filho* ..... 753

Thermophilic Anaerobic Digester Performance Under Different Feed-Loading Frequency
*John Bombardiere, Teodoro Espinosa-Solares, Max Domaschko, and Mark Chatfield* ..... 765

A Proposed Mechanism for Detergent-Assisted Foam Fractionation of Lysozyme and Cellulase Restored With β-Cyclodextrin
*Vorakan Burapatana, Elizabeth A. Booth, Ian M. Snyder, Ales Prokop, and Robert D. Tanner* ..... 777

Study on the Production of Biodiesel by Magnetic Cell Biocatalyst Based on Lipase-Producing *Bacillus subtilis*
*Ming Ying and Guanyi Chen* ..... 793

Production of ω-3 Polyunsaturated Fatty Acids From Cull Potato Using an Algae Culture Process
*Zhanyou Chi, Bo Hu, Yan Liu, Craig Frear, Zhiyou Wen, and Shulin Chen* ..... 805

Hybrid Neural Network Model of an Industrial Ethanol Fermentation Process Considering the Effect of Temperature
*Ivana C. C. Mantovanelli, Elmer Ccopa Rivera, Aline C. da Costa, and Rubens Maciel Filho* ..... 817

Characterization of Thermostructural Damages Observed in a Seaweed Used for Biosorption of Cadmium: *Effects on the Kinetics and Uptake*
*Antonio Carlos Augusto da Costa, Aderval S. Luna, and Robson Pafumé* ..... 835

Ethanol Fermentation of Various Pretreated and Hydrolyzed Substrates at Low Initial pH
*Zsófia Kádár, San Feng Maltha, Zsolt Szengyel, Kati Réczey, and Wim de Laat* ..... 847

The Effects of Engineering Design on Heterogeneous Biocatalysis in Microchannels
*Frank Jones, Robert Bailey, Stephanie Wilson, and James Hiestand* ..... 859

Utilization of Condensed Distillers Solubles as Nutrient Supplement for Production of Nisin and Lactic Acid from Whey
*Chuanbin Liu, Bo Hu, Shulin Chen, and Richard W. Glass* ..... 875

Optimization of Tocopherol Concentration Process From Soybean Oil Deodorized Distillate Using Response Surface Methodology
*Vanessa Mayumi Ito, César Benedito Batistella, Maria Regina Wolf Maciel, and Rubens Maciel Filho* ..... 885

Semicontinuous Production of Lactic Acid From Cheese Whey Using Integrated Membrane Reactor
*Yebo Li, Abolghasem Shahbazi, Sekou Coulibaly, and Michele M. Mims* ..... 897

Functional Stability of a Mixed Microbial Consortium Producing PHA From Waste Carbon Sources
*Erik R. Coats, Frank J. Loge, William A. Smith, David N. Thompson, and Michael P. Wolcott* ..... 909

Separating a Mixture of Egg Yolk and Egg White Using Foam Fractionation
*Tiffany M. Ward, Ross A. Edwards, and Robert D. Tanner* ..... 927

Synthesis of Poly(Sorbitan Methacrylate) Hydrogel by Free-Radical Polymerization
*Gwi-Taek Jeong, Kyoung-Min Lee, Hee-Seung Yang, Seok-Hwan Park, Jae-Hee Park, Changshin Sunwoo, Hwa-Won Ryu, Doman Kim, Woo-Tae Lee, Hae-Sung Kim, Wol-Seog Cha, and Don-Hee Park* ..... *935*

SESSION 6

Hybrid Thermochemical/Biological Processing: *Putting the Cart Before the Horse?*
*Robert C. Brown* ..... *947*

Physical and Chemical Properties of Bio-Oils From Microwave Pyrolysis of Corn Stover
*Fei Yu, Shaobo Deng, Paul Chen, Yuhuan Liu, Yiqin Wan, Andrew Olson, David Kittelson, and Roger Ruan* ..... *957*

Comparison of Diafiltration and Size-Exclusion Chromatography to Recover Hemicelluloses From Process Water From Thermomechanical Pulping of Spruce
*Alexandra Andersson, Tobias Persson, Guido Zacchi, Henrik Stålbrand, and Ann-Sofi Jönsson* ..... *971*

0273-2289/1559-0291 (Online)/07/136–140/1–2/$30.00

# SESSION 1A
## Enzyme Catalysis and Engineering

# Introduction to Session 1A

**MICHAEL E. HIMMEL***

*National Renewable Energy Laboratory, Golden, CO 80401*
*E-mail: mike_himmel@nrel.gov*

Understanding and overcoming the natural resistance of plant cell walls to enzymatic hydrolysis remains one of the most active research areas in biofuels production (as indicated by the number of abstracts and papers submitted to this session). A number of the oral presentations given during the Enzyme Catalysis and Engineering session highlighted the use of new and innovative tools for advancing our understanding of plant cell wall deconstruction. The oral presentations and posters given for this session included applications of imaging tools and computational models to advance our understanding of biomass recalcitrance relative to enzymatic deconstruction. This session was opened with a presentation by Dr. Danny Akin, who outlined the structural and chemical barriers for the bioconversion of grasses to sugars. Lignocelluloses from grasses, such as switch grass, are resistant to bioconversion by various aromatic constituents, which include both lignins and phenolic acid esters. However, Akin and coworkers demonstrated the use of selected white rot fungal enzymes, which lack cellulases that could be used to produce delignified lignocellulosic materials, resulting in improved bioconversion.

Dr. Shi-You Ding presented an exposé on the use of new imaging tools now available at the National Renewable Energy Laboratory. Dr. Ding presented state-of-the-art applications of imaging and how it can be used to understand how plant cell wall microfibril structure changes during biomass conversion processes. Researchers now have the ability to

*Author to whom all correspondence and reprint requests should be addressed.

examine the microfibril at the nanometer scale using atomic force microscopy, which allows for the imaging of biomaterials at atomic scale without extensive sample preparation or change in the original structure. Dr. Ding described how he has used this technique to visualize cellulases directly under aqueous conditions. His findings have resulted in a new model of the molecular structure of the cellulose microfibril in the plant cell wall.

Other presentations were focused on techniques to reduce biomass recalcitrance by applying thermal tolerant enzymes, supplementation with "accessory enzymes," or by using blocking agents, such as bovine serum albumin to prevent nonspecific absorption of enzymes to lignin. Dr. Deidre Willies from the Thayer School of Engineering at Dartmouth College presented data indicating that corn stover and lignin adsorb large amounts of cellulases and outlined methods that could be used to present adsorption and enhance cellulose digestion.

The presentations and resulting discussion during the session highlighted the need for more research that will advance our understanding of the natural resistance of plant cell walls to microbial deconstruction. It is this property that is largely responsible for the high cost of lignocellulose conversion; and yet to take the steps toward sustainable energy use we must overcome the chemical and structural properties that have evolved in biomass to prevent its deconstruction.

0273-2289/1559-0291 (Online)/07/136–140/3–16/$30.00

# Grass Lignocellulose

## *Strategies to Overcome Recalcitrance*

**DANNY E. AKIN***

*Russell Research Center, PO Box 5677, ARS-USDA, Athens, Georgia 30604, E-mail: danny.abin@ars.usda.gov*

## Abstract

Grass lignocelluloses are limited in bioconversion by aromatic constituents, which include both lignins and phenolic acids esters. Histochemistry, ultraviolet absorption microspectrophotometry, and response to microorganisms and specific enzymes have been used to determine the significance of aromatics toward recalcitrance. Coniferyl lignin appears to be the most effective limitation to biodegradation, existing in xylem cells of vascular tissues; cell walls with syringyl lignin, for example, leaf sclerenchyma, are less recalcitrant. Esterified phenolic acids, i.e., ferulic and *p*-coumaric acids, often constitute a major chemical limitation in nonlignified cell walls to biodegradation in grasses, especially warm-season species. Methods to improve biodegradability through modification of aromatics include: plant breeding, use of lignin-degrading white-rot fungi, and addition of esterases. Plant breeding for new cultivars has been especially effective for nutritionally improved forages, for example, bermudagrasses. In laboratory studies, selective white-rot fungi that lack cellulases delignified the lignocellulosic materials and improved fermentation of residual carbohydrates. Phenolic acid esterases released *p*-coumaric and ferulic acids for potential coproducts, improved the available sugars for fermentation, and improved biodegradation. The separation and removal of the aromatic components for coproducts, while enhancing the availability of sugars for bioconversion, could improve the economics of bioconversion.

**Index Entries:** Lignin; microspectrophotometry; phenolic acid esters; plant breeding; white-rot fungi.

## Introduction

Corn-to-ethanol production and use is rapidly expanding. With the phase-out of methyl tertiary butyl ether, which has been used as an oxygenate for more efficient burning of gasoline, ethanol has been added in ever increasing quantities. Further, the desire to use even higher ratios of ethanol as a fuel related to improved national security, trade imbalance,

*Author to whom all correspondence and reprint requests should be addressed.

and use of agricultural products has driven up the demand, price, and production. With greater emphasis on fuel ethanol, lignocellulose as substrate for fermentation has been given an increased priority (www.ethanolrfa.org) *(1)*. Recently, the Iogen Corporation reported the first commercial batch of ethanol from lignocellulose, using wheatstraw as a substrate (www.iogen.ca).

Cost of lignocellulosic materials is lower than corn grain, but processing for fermentation of this substrate is more costly. The sugars in lignocellulose, i.e., largely polysaccharides such as cellulose and hemicellulose, are not readily available, and pretreatment is necessary to free polysaccharides from lignin and aromatics *(2)*. Dilute sulfuric acid has been proposed for pretreatment by the United States Department of Energy, and this method has been tested in several variations. After pretreatment, enzymatic saccharification of polysaccharides to fermentable sugars is required. Finally, most lignocellulosic materials are rich in xylans and hemicelluloses, and 5-carbon fermentation is needed to take advantage of all the potential substrates *(3)*. Just as distillers dry grains and solubles as a value-added coproduct drives the economics of corn-to-ethanol, high-value coproducts are needed for lignocellulose-to-ethanol processes.

Lignin and other aromatics covalently link with, and at times physically mask, the potential fermentation substrates in lignocelluloses, thus protecting the carbohydrates from degradation *(4–6)*. Pretreatment, therefore, is required for bioconversion of lignocellulosic materials. A considerable body of knowledge is available from the animal nutrition discipline, and indeed many of the same limiting factors are important in bioenergy concerns *(6)*. Whereas woody plants and dicotyledons have rigid, nondegradable lignified cell walls, monocotyledons (e.g., grasses) have lignified cell walls as well as walls rich in low molecular weight phenolic acids, ester-linked to arabinose *(5)*. Another remarkable feature of grasses is that ester-linked *p*-coumaric and ferulic acids occur in nonlignified cell walls *(7)*. Warm-season grasses, which include potential bioenergy crops such as corn stover, sugarcane (bagasse), bermudagrass, and switchgrass, are especially high in the phenolic acid esters *(8)*. Because of the complexities within cell wall types, delineation of the nature, type, and location of aromatics within cell types of specific bioenergy crops can lead to environmentally friendly pretreatments, more efficient bioconversion, and identification of potential coproducts for high-value applications. The objectives of this article are to:

1. Review the structural/chemical barriers to bioconversion in grasses, especially warm-season grasses.
2. Discuss environmentally friendly (nonchemical) strategies to reduce recalcitrance of grass lignocelluloses.
3. Identify potential coproducts.

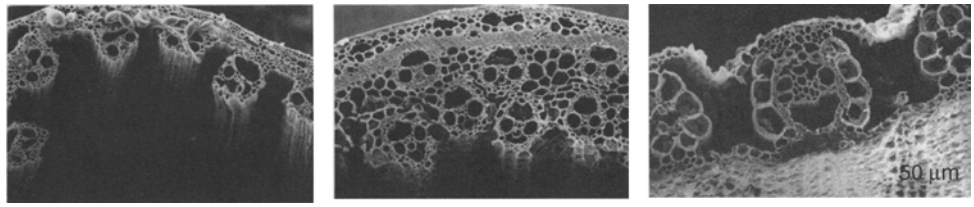


**Fig. 1.** Scanning electron micrographs showing biodegradation of grass fractions. Left—young stem showing resistance of epidermis, sclerenchyma ring, and vascular tissue with other cell types degraded. Center—mature stem showing resistance of epidermis, sclerenchyma ring, vascular tissue, and most of parenchyma cells; parenchyma nearest the stem center is partially degraded. Right—leaf blade showing resistance of vascular bundles, sclerenchyma, and portions of PBS; in addition to partial degradation of parenchyma bundle sheath and epidermis, mesophyll between vascular bundles and phloem cell walls are degraded.

## Structural and Chemical Factors Influencing Recalcitrance in Grass Lignocellulose

### *Biodegradation of Specific Tissue Types*

Response to the actions of fiber-digesting microorganisms within the cattle rumen shows differential cell wall recalcitrance within various lignocellulosic substrates and the influence of specific compounds. Figure 1 indicates the response of cell types in leaf blades and young and old stem internodes of a warm-season grass. The cell walls in the stems of Fig. 1 that resist biodegradation are many of the typically highly lignified cells. Walls are thick and cell contents are lacking, indicating a nonliving support tissue. Such cell types are thought to be the most resistant to degradation owing to the interaction of polymerized phenylpropanoid units with other consistuents. Histochemical stains identify the location of particular lignin types. Vascular cell walls, such as the mestome sheath, show a strong reaction with acid phloroglucinol (AP). Sarkanen and Ludwig *(9)* reported that AP "had universal application to all lignins, although the reaction may be weak or absent in lignins containing high amounts of syringyl propane units." Clifford *(10)* reported that various formulations of AP all detected most aldehydes, with various color responses for different aldehydes and those of cinnamaldehyde compounds giving a purple color. The deep red to purple color is taken to indicate a strong contribution to the cell walls by coniferyl (monomethoxylated) units of lignin. AP positive reactions (AP+) occur in vascular tissues of leaves and stems of grasses and these tissues, as indicated in Fig. 1, have been shown to be the most recalcitrant in grasses *(11)*.

Chlorine water followed by sulfite (CS) is reported to indicate lignin containing large amounts of syringyl (dimethoxylated) units of lignin *(9)*. CS+ reactions occur in leaf blade sclerenchyma (extensions of the vascular bundles) and in the parenchyma cell walls of mature (but not immature)

Table 1
Histochemical Reactions for Lignin and Relative Biodegradation of Cell Walls in Grass Lignocelluloses

| Cell wall type | Histochemical reaction[a] | Area[b] (%) | Biodegradation[c] |
|---|---|---|---|
| *Leaf blade* | | | |
| Xylem/mestome sheath | AP | 4 ± 2 | None |
| Sclerenchyma | CS | 6 ± 3 | Slow to partial |
| Epidermis | – | 35 ± 10[d] | Slow to partial[d] |
| | – | 22 ± 6[e] | Rapid[e] |
| Parenchyma bundle sheath | CS | 15 ± 7[d] | Slow to partial[d] |
| | | 6 ± 2[e] | Rapid[e] |
| Mesophyll | – | 38 ± 9[d] | Rapid |
| | – | 57 ± 5[e] | Rapid |
| *Stem*[f] | | | |
| Epidermis + sclerenchyma | AP | 34 ± 4 | None |
| Ring + vascular (xylem) | – | – | – |
| Parenchyma (mature) | CS | 55 ± 6 | Slow to partial |
| Parenchyma (immature) | – | – | Rapid |

From ref. *11*.
[a]Most dominant staining reaction. No designation means histochemical reaction not prominent.
[b]Calculated from morphometric determinations.
[c]Response to fiber-degrading, rumen microorganisms.
[d]Warm-season.
[e]Cool-season.
[f]Warm-season.

stems *(11,12)*. The mechanism for reaction is unknown, and at times nonlignified cell walls show a positive reaction with chlorine-sulfite, suggesting that compounds other than syringyl lignin react. At times, CS+ tissues are partially degraded and are more susceptible to some chemical treatments, for example, alkali, than AP+ tissues. Table 1 compares many features in cell types of warm- and cool-season grasses related to biodegradation.

Often, and particularly in warm-season grasses, nonlignified cell types that do not show a histochemical reaction for lignin resist biodegradation. An example is shown for bermudagrass leaf blade in which the parenchyma bundle sheath and a portion of the epidermis is not degraded (Fig. 1). It is well established that grasses, and particularly warm-season species, have high levels of ester-linked *p*-coumaric and ferulic within the cell walls *(6,8)*. Use of diazotized sulfanilic acid to show phenolic compounds

Table 2
UV Absorption of Phenolic Esters

| | $\lambda_{max}$ nm | |
|---|---|---|
| Compound | UV spectroscopy | UMSP-80 |
| FAXX | 236 | 238, 242 |
| | 300 | 304 |
| | 324 | 324 |
| PAXX | 230 | 234, 236 |
| | 294 | 286 |
| | 312 | 312, 314 |

Unpublished results by R.D. Hartley.

in cell walls *(13)* has been used to define nonlignified and nonbiodegradable cell walls. The positive histochemical reactions of parenchyma bundle sheath and epidermis in leaf and parenchyma in stem with diazotized sulfanilic acid, suggest a prominent role for these ester-linked phenolic acids as a factor in the recalcitrance of grass lignocellulose *(14)*.

Further evidence for a prominent role for ester-linked phenolic acids is shown by ultraviolet (UV) absorption microspectrophotometry and biodegradation studies of specific cell walls *(15–17)*. These studies were made possible by the use of UV-generated illumination and a scanning monochromator designed into an optical microscope. Further, the preparation of specific compounds, namely coniferyl lignin *(18)* and isolated ferulic acid ester-linked to arabinose linked to xylose units (FAXX) and similar structures but with *p*-coumaric acids (PAXX) *(19)*, allowed for location of these various aromatic compounds within cell wall types. Specific absorbances for the two ester-linked compounds by the microspectrophotometric system are confirmed by UV spectroscopy (Table 2).

UV absorption studies of cell wall types undertaken with the Carl Zeiss, Inc. (Thronwell, NY) UMSP-80 microspectrophotometry system are shown in Fig. 2. The $\lambda_{max}$ near 280 nm is typical for lignin (Fig. 2A). The ester-linked phenolic acids show a bathochromic shift from 280 to a shoulder near 290 nm with $\lambda_{max}$ near 320 nm. FAXX and PAXX can be differentiated by $\lambda_{max}$'s near 326 and 314 nm, respectively (Fig. 2B). With absorbances for these compounds and compositional data on aromatic compounds in grasses, information can be obtained from individual cell types and related to biodegradation and recalcitrance. Mestome sheaths of grasses all show prominent absorbances near 280 nm and near 320 nm (Fig. 2C). This result suggests the presence of lignin and phenolic acid esters within these highly lignified (as shown with AP), nondegradable cell walls. Parenchyma bundle sheaths (PBS), which are a prominent part of the Kranz anatomy of warm-season grasses (Table 1) *(20)*, show a UV spectral pattern identical to phenolic acid esters, suggesting little or no polymeric lignin but a prevalence of

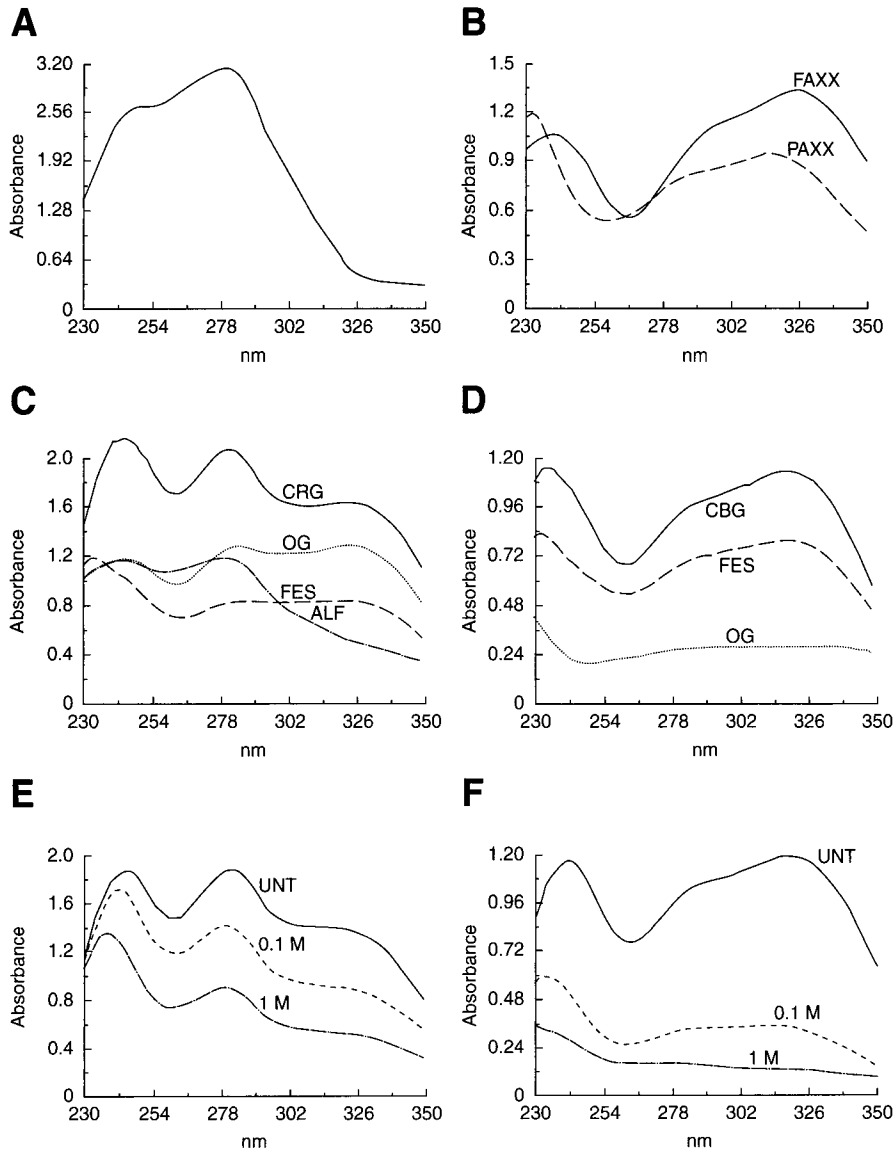


**Fig. 2.** UV absorption microspectrophotometry. **(A)** Synthesized coniferyl lignin showing $\lambda_{max}$ at about 280 nm. **(B)** Phenolic acids esters linked to FAXX and PAXX showing a shoulder near 290 nm and $\lambda_{max}$ at 324 nm for FAXX and 313 for PAXX. **(C)** Highly lignified mestome sheath cell walls of the warm-season Coastal bermudagrass (CBG), cool-season grasses fescue (FES) and orchardgrass (OG), and the legume alfalfa (ALF). Grasses have high-absorbances indicative of lignin and phenolic acids, whereas alfalfa has only the absorbance indicative of lignin. **(D)** PBS of grasses showing strong absorbance indicative of phenolic acid esters in CBG and weaker ones in FES and OG. **(E)** Bermudagrass mestome sheath untreated (UNT) and treated with 0.1 *M* and 1 *M* levels of NaOH. Treatment with NaOH removes absorbance indicative of ester-linked phenolic acids but leaves absorbance indicative of lignin. **(F)** Bermudagrass parenchyma bundle sheath untreated and treated with 0.1 *M* and 1 *M* levels of NaOH showing progressive loss of UV absorbance indicative of ester-linked phenolic acids, with 1 *M* NaOH removing all UV absorbance.

these esters. The slow to partial degradation pattern (Table 1) of warm-season PBS coincides with the presence of phenolic acid esters. In contrast, PBS of cool-season grasses have little to no UV absorbance indicative of lignin or phenolic acids (Fig. 2D), and are rapidly and completely degraded (Table 1). Further evidence for the presence of ester-linked phenolic acids within these tissues is shown in studies using 0.1 *M* and 1 *M* NaOH treatments to compare untreated mestome (Fig. 2E) and PBS (Fig. 2F) cell walls in bermudagrass. The progressive removal of absorbance with increasing NaOH levels suggests alkali-labile, ester linkages. For mestome cell walls, the absorbance near 280 nm is indicative for lignin remains but is reduced. In contrast, the absorbances at 290 and 320 nm for PBS are totally removed.

The use of histochemical stains for lignin, UV absorption microspectrophotometry for lignin and ester-linked phenolic acids, and response of cell types to fiber-degrading, rumen microorganisms provides information on factors influencing recalcitrance of lignocellulose. Certain cell wall types are highly lignified and recalcitrant to biodegradation, even to the potent fiber-degrading, rumen microbial system. However, in warm-season grasses, living, nonlignified tissues are often slow to degrade owing to the presence of ester-linked phenolic acids. The nonlignified cell types in cool-season grasses, in contrast, lack phenolic acid esters and are rapidly degraded (Fig. 2D, Table 1).

Increasing levels of aromatics in cell types, shown by UV absorption, and biodegradability was followed in grass stems *(21)*. In young cell walls, the epidermis, sclerenchyma ring, and vascular tissue gave spectra similar to FAXX and PAXX and were partially degraded, with only the middle lamellae resistant. As the grass internode matured, UV spectral patterns were similar to those for xylem cells with lignin and FAXX/PAXX, with degradation occurring only in cell walls near the cell lumen. In young parenchyma, UV absorbance was low and biodegradability high. As parenchyma cells matured, middle lamellae were the most resistant portions of the cell wall, and UV absorbance spectral patterns resembled those for FAXX/PAXX.

Grassses, especially warm-season species, are high in the phenolic acid–polysaccharide complexes such as FAXX and PAXX and other, related esters *(19)*. The lack of biodegradability is more associated with lignin, but these complexes likely are the predominant factor influencing recalcitrance in living, nonlignified tissues like PBS and epidermis of leaves and mature stem parenchyma. Amounts of these cell wall types are substantial in warm-season grasses.

## Biological Strategies to Overcome Recalcitrance

### *Plant Breeding*

The presence of lignin and aromatics within plants is a protective mechanism against pathogens. Plant breeding to remove these aromatics can result in extremely susceptible plants. An extensive breeding program

Table 3
Comparison of Cell Wall Biodegradability and Chemical Composition of Coastal/Coastcross I

| | Leaf dry weight loss | | | Area of PBS | UV absorbance | | | |
|---|---|---|---|---|---|---|---|---|
| | 24 h | 38 h | 72 h | After 24 h | Parenchyma bundle sheath | | Mestone sheath | |
| | | | | | $\lambda_{max}$ | A | $\lambda_{max}$ | A |
| Coastal | 24%[a] | 36%[a] | 42%[a] | 350 μm²[a] | 291 | 1.2[a] | 285 | 1.8 |
| | | | | | 318 | 1.3[a] | 318 | 1.8 |
| Coastcross I | 34%[a] | 49%[a] | 57%[a] | 196 μm²[a] | 291 | 0.8[a] | 288 | 2.0 |
| | | | | | 322 | 0.9[a] | 321 | 1.9 |

From ref. *15*.
[a]Different between cultivars ($p \leq 0.05$).

that has existed for over 70 yr in the Agricultural Research Service of the United States Department of Agriculture (ARS-USDA) in Tifton, Georgia, has produced several new varieties of sustainable bermudagrasses with improved biodegradability *(22)*. In many of these varieties, the improved biodegradability is related to lowered levels of aromatics. One notable example is Coastcross I bermudagrass (CC I) *(23)*. We studied CC I and one of the parents in the cross, namely Coastal bermudagrass (CBG), which is extensively grown as a forage in the southern United States.

In direct comparison of the biodegradation of leaf blades, CC I was significantly higher in rate and extent of biodegradation compared with CBG (Table 3). Transmission electron micrographs of PBS cell walls colonized and degraded by rumen bacteria further provide evidence that these walls in CC I, although similar in structure, are considerably more biodegradable than those of CBG (Fig. 3). UV absorption data provide an explanation for the greater biodegradability of CC I in showing a significantly lower absorbance of FAXX/PAXX type compounds. The mestome sheath cells, recalcitrant to biodegradation in both cultivars, have similar spectral patterns. In terms of cell wall biodegradability, data support the fact that living, nonlignified cell walls have lower levels of phenolic acid esters in CC I, indicating that these compounds limit biodegradation and such plant breeding can be a strategy to improve fermentation.

A substantial part of ARS-USDA's program for bioenergy crops relies on research by plant breeders. Collaborative work is needed where information such as that on CBG and CC I can provide a comprehensive decision on the most appropriate bioenergy crops. For example, the amount and the susceptibility of phenolic acid esters could be factor chosen for improved fermentation and production of high-levels of aromatic coproducts, such as ferulic acid. Indeed, previous work has shown variation in the germplasm of bermudagrasses that might be exploited in these aspects of bioenergy crops *(24)*.

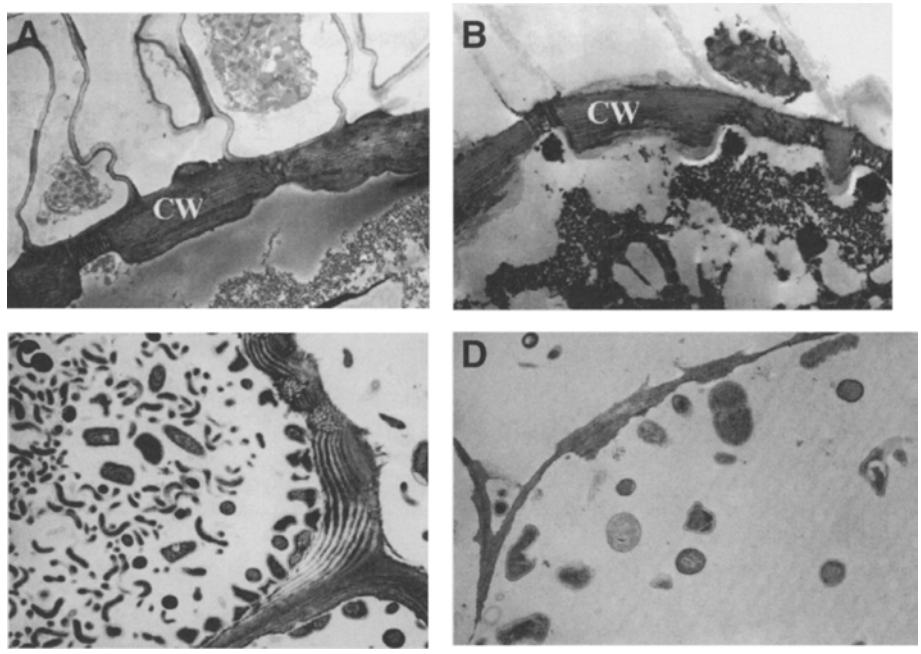


**Fig. 3.** Comparative biodegradation of parenchyma bundle sheath cells walls (CW) of CBG and CC I undigested and 48 h incubation with the potent fiber-digesting action of rumen microorganisms. **(A)** Cell wall of undigested parenchyma bundle sheath of CBG. **(B)** Cell wall of undigested parenchyma bundle sheath of CC I. **(C)** Attack of parenchyma bundle sheath of CBG by rumen bacteria, with slight pitting at this time. **(D)** The PBS of CC I is more susceptible to bacterial attack, with substantial erosion of the cell wall material.

## *Lignin-Degrading Microbes and Enzymes*

White-rot fungi are recognized as the most active lignin-degrading microorganisms *(25)*. Oxidative enzymes produced by the fungi, along with catalysts, attack aromatics and produce free radicals, which results in degradation of aromatic compounds. Well-publicized oxidative enzymes include: laccases, manganese peroxidase, and lignin peroxidase. At least one of these enzymes, laccase with an activator, is commercially available.

A variety of white-rot fungi occur in nature, and their activities differ. The common pattern of attack on lignocellulose by these fungi is a simultaneous decay of polysaccharides and lignin *(25)*. However, patterns of decay and degrees of delignification vary among species and even strains, and some species selectively delignify plant material leaving an unprotected and available carbohydrate for further use *(26)*. Studies have been undertaken using different white-rot fungal species to improve forage utilization with mixed results *(27,28)*. We evaluated several species of white-rot fungi, emphasizing mutants and species reported to lack cellulase and to selectively attack lignin *(29)*.

Data in Table 4 review results obtained with two white-rot fungi having different capablilities. *Phanerochaete chrysosporium* is a well-studied

Table 4
Influence of Pretreatment With Species of White-Rot Fungi on Bioconversion of Plant Lignocellulose

| | Characteristics of pretreated lignocellulose | | | |
|---|---|---|---|---|
| | Residual aromatics | | Bioconversion potential | |
| Fungus | 1 *M* NaOH (mg/g) | 4 *M* NaOH (mg/g) | Dry weight loss (%) | Volatile Fatty Acids (μ moles/mL) |
| Untreated | 13.0 | 22.9 | 34.9 | 47.9 |
| *P. chrysosporium* K-3[a] | 7.1 | 18.9 | 46.9 | 63.8 |
| *C. subvermispora* 90031-sp.[b] | 5.3 | 17.8 | 63.9 | 85.9 |

From ref. *29*.

[a]*P. chrysosporium* is a well-known and studied white-rot fungus that produces cellulases, hemicellulases, and lignin-degrading enzymes.

[b]*C. subvermispora* is a white-rot fungus that does not produce cellulase.

white-rot fungus that nonselectively attacks cell wall components, i.e., lignin and carbohydrates *(25)*. *Ceriporiopsis subvermispora* had been reported to lack cellulase, produce manganese peroxide and laccase, and to selectively delignify several wood species *(30,31)*. Before our work, this fungus had not been evaluated in the improvement of grass lignocellulose. Our data indicated that *C. subvermispora* was better able to attack the aromatics in bermudagrass and improved the utilization of the residue over that by *P. chrysosporium*. *C. subvermispora* removed ester-linked phenolic acids and lignin moieties from bermudagrass and significantly improved the fermentation of the delignified material (Table 4) *(29)*.

## *Release of Phenolic Acids by Esterases*

The ester-linked *p*-coumaric and ferulic acids previously discussed in grass cell walls, especially warm-seasons grasses such as bermudagrass, not only limit lignocellulosic bioconversion but offer a potential value-added coproduct. Earlier work on anaerobic fungi, some of the most potent fiber-digesting microorganisms in ruminants and herbivorous animals, showed highly active phenolic acid esterases (Table 5) *(32)*. It is believed that these enzymes promoted the ability of the fungi to attack and partially degrade aromatic-containing tissues.

More recent work has shown the value of cell-free ferulic acid esterase along with hemicellulases, in releasing ferulic acid from a variety of plant materials *(33–35)*. For example, recent extraction of defatted jojoba meal with ferulic acid esterase from *Clostridium thermocellum* released ferulic acid from

Table 5
Phenolic Acids Released From Plant Cell Walls

| Rumen fungus culture filtrates | *p*-CA[a] (μg/100 mg cell wall) | FA[b] (μg/100 mg cell wall) |
|---|---|---|
| *Neocallimastix* MC-2 | 130 | 376 |
| *Piromyces* MC-1 | 114 | 336 |
| *Anaeromyces* PC-1 | 83 | 254 |
| *Orpinomyces* PC-2 | 93 | 287 |
| *Orpinomyces* PC-3 | 89 | 296 |

From ref. *32*.
[a]*p*-Coumaric acid.
[b]Ferulic acid.

Table 6
Effect of Pretreatment With a Commercial Ferulic Acid Esterase[a]

| Fraction | Treatment[b] | Dry weight loss (%) | Compounds in filtrates after treatment (mg/g) | | | |
|---|---|---|---|---|---|---|
| | | | *p*-CA[c] | FA[d] | Xylose | Glucose |
| Corn leaf | Cellulase | 41 | 0.14 | 0.33 | 8.0 | 53.0 |
| | E + C | 62 | 0.32 | 0.58 | 36.7 | 125.0 |
| Corn stem pith | Cellulase | 17 | 0.26 | 0.22 | 23.0 | 68.6 |
| | E + C | 29 | 0.94 | 0.87 | 34.0 | 83.8 |
| Bermuda leaf | Cellulase | 16 | 0.19 | 0.38 | 8.0 | 17.8 |
| | E + C | 21 | 0.61 | 1.02 | 30.8 | 141.3 |
| Corn fiber | Cellulase | 27 | 0.04 | 0.05 | 2.6 | 36.7 |
| | E + C | 48 | 0.23 | 2.69 | 8.2 | 159.3 |

Adapted in part from ref. *35*.
[a]Depol 740L.
[b]Cellulase incubation for 72 h; E + C incubation with esterase (Depol 740L) for 24 h, removal of filtrate, and subsequent incubation with cellulose 72 h. Values for E + C are summed from the two incubations.
[c]*p*-Coumaric acid.
[d]Ferulic acid.

seven simmondsin ferulates *(34)*. Recently, we evaluated Depol 740 L (Biocatalysts, Ltd., Pontypridd, Wales, UK), a commerical mixture containing ferulic acid esterase, as a pretreatment for grasses before saccharification with cellulases and bioconversion of bermudagrasses *(24)* and corn stover fractions *(35)*. Pretreatment with ferulic acid esterase and saccharification with cellulase is shown for a variety of grass lignocelluloses (Table 6). In all cases, esterase improved release into the filtrate of *p*-coumaric acid, ferulic acid, xylose, and glucose. Particular plants and fractions were more susceptible for release of these particular compounds *(24,35)*. The use of esterases to release ferulic acid

into the filtrate offers the possibility of a value-added coproduct while processing grass lignocellulose for bioconversion to ethanol. *p*-Coumaric and, to a lesser degree ferulic acid can inhibit carbohydrases and biodegradation of plant materials *(36,37)*. The separation and collection of phenolic acids released by esterases may be necessary to optimize subsequent saccharification of pretreated materials. As an inhibitor of microbial growth and enzyme activity, these acids (especially *p*-coumaric acid) may have value for natural compounds for pest control. Other potential uses for ferulic acid are a substrate for vanillin production, UV protection in cosmetics, and food antioxidants *(38)*. Future work should focus on the optimal enzyme cocktail, for example, inclusion of appropriate hemicellulases, optimal substrates, and optimal conditions for the most cost-efficient pretreatment system.

## Acknowledgments

The author of this review is indebted to many colleagues who undertook major parts of this work or had a significant influence on the data and interpretations: (Russell Research Center) Roy D. Hartley for chemistry of cell walls, W. H. Morrison III for chemical analyses, W. S. Borneman for esterase studies, F. E. Barton II and D. S. Himmelsbach for spectroscopy and chemistry of fibers, and L. L. Rigsby for excellent technical support; (University of Georgia) K. -E. L. Eriksson for contributions on white-rot fungi, and L. G. Ljungdahl for contributions on enyzmes, D. Wubah for work on anaerobic fungi; (ARS-USDA, Tifton, GA) W. W. Hanna and W. F. Anderson for work on bermudagrasses. Mention of trade names does not constitute an endorsement of one commercial product over another but is used only for identification purposes.

## References

1. Jung, H. -J. G. and Thompson, D. N. (2005), *Appl. Biochem. Biotechnol.* **121–124,** 3–4.
2. McMillan, J. D. (1994), In: *Enzymatic Conversion of Biomass for Fuels Production.* Himmel, M. E., Baker, J. O., and Overend, R. P. (eds.), American Chemical Society, Washington, DC, pp. 292–324.
3. Li, X. -L., Dien, B. S., Cotta, M. A., Wu, Y. V., and Saha, B. C. (2005), *Appl. Biochem. Biotechnol.* **121–124,** 321–334.
4. Eriksson, K. -L. (1990), In: *Microbial and Plant Opportunities to Improve Lignocellulose Utilization by Ruminants.* Akin, D. E., Ljungdahl, L. G., Wilson, J. R., and Harris, P. J. (eds.), Elsevier Science Publishing Co., New York, pp. 227–233.
5. Hartley, R. D. and Ford, C. W. (1989), In: *Plant Cell Wall Polymers: Biogenesis and Biodegradation.* Lewis, N. G. and Paice, M. G. (eds.), American Chemical Society, Washington, DC, pp. 137–145.
6. Akin, D. E., Ljungdahl, L. G., Wilson, J. R., and Harris, P. J. (eds.), (1990), In: *Microbial and Plant Opportunities to Improve Lignocellulose Utilization by Ruminants,* Elsevier Science Publishing Co., New York, 428p.
7. Carpita, N. C. (1996), *Ann. Rev. Plant Physiol. Plant Mol. Biol.* **47,** 445–476.
8. Akin, D. E. and Chesson, A. (1989), *Proc. Int. Grassl. Congr.* **16,** 1753–1760.
9. Sarkanen, K. V. and Ludwig, C. H. (1971), *Lignins: Occurrence, Formation, Structure, and Reactions.* Wiley-Interscience, New York, pp. 1–18.

10. Clifford, M. N. (1974), *J. Chromatogr.* **94,** 321–324.
11. Akin, D. E. (1989), *Agron. J.* **81,** 17–25.
12. Stafford, H. A. (1962), *Plant Physiol.* **37,** 643–649.
13. Harris, P. J., Hartley, R. D., and Barton, G. E. (1982), *J. Sci. Food Agric.* **33,** 516–520.
14. Akin, D. E., Hartley, R. D., Morrison, W. H. III, and Himmelsbach, D. S. (1990), *Crop Sci.* **30,** 985–989.
15. Akin, D. E., Ames-Gottfred, N., Hartley, R. D., Fulcher, R. G., and Rigsby, L. L. (1990), *Crop Sci.* **30,** 396–401.
16. Ames, N. P., Hartley, R. D., and Akin, D. E. (1992), *Food Struct.* **11,** 25–32.
17. Hartley, R. D., Akin, D. E., Himmelsbach, D. S., and Beach, D. C. (1990), *J. Sci. Food Agric.* **50,** 179–189.
18. Weymouth, N., Dean, J. F. D., Eriksson, K. -E. L., Morrison, W. H. III, Himmelsbach, D. S., and Hartley, R. D. (1993), *Nordic Pulp Pap. Res. J.* No. **4,** 344–349.
19. Borneman, W. S., Ljungdahl, L. G., Hartley, R. D., and Akin, D. E. (1991), *Appl. Environ. Microbiol.* **57,** 2337–2344.
20. Stern, K. R., Jansky, S., and Bidlack, J. E. (2003), *Introductory Plant Biology.* McGraw-Hill, New York, pp. 183–184.
21. Akin, D. E. and Hartley, R. D. (1992), *J. Sci. Food Agric.* **59,** 437–447.
22. Hanna, W. W. and Gates, R. N. (1990), In: *Microbial and Plant Opportunities to Improve Lignocellulose Utilization by Ruminants.* Akin, D. E., Ljungdahl, L. G., Wilson, J. R., and Harris, P. J. (eds.), Elsevier Science Publishing Co., New York, 197–204.
23. Burton, G. W. (1972), *Crop Sci.* **12,** 125.
24. Anderson, W. F., Peterson, J., Akin, D. E., and Morrison, W. H. III. (2005), *Appl. Biochem. Biotechnol.* **121–124,** 303–310.
25. Eriksson, K. -E. L., Blanchette, R. A., and Ander, P. (1990), *Microbial and Enzymatic Degradation of Wood and Wood Components,* Springer-Verlag, New York, 407p.
26. Blanchette, R. A., Burnes, T. A., Leatham, G. F., and Effland, M. J. (1988), *Biomass* **15,** 93–101.
27. Jung, H.-J. G., Valdez, F. R., Abad, A. R., Blanchette, R. A., and Hatfield, R. D. (1992), *J. Anim. Sci.* **70,** 1928–1935.
28. Zadrazil, F. (1985), *Angew. Bot.* **59,** 433–452.
29. Akin, D. E., Sethuraman, A., Morrison, W. H. III, Martin, S. A., and Eriksson, K. -E. L. (1993), *Appl. Environ. Microbiol.* **59,** 4274–4282.
30. Akhtar, M., Attridge, M. C., Myers, G. C., Kirk, T. K., and Blanchette, R. A. (1992), *TAPPI,* February, 105–109.
31. Ruttiman-Johnson, C., Salas, L., Vicuna, R., Kirk, T. K. (1993), *Appl. Environ. Microbiol.* **59,** 1792–1797.
32. Borneman, W. S., Hartley, R. D., Morrison, W. H., Akin, D. E., and Ljungdahl, L. G. (1990), *Appl. Microbiol. Biotechnol.* **33,** 345–351.
33. Faulds, C. B., Zanichelli, D., Crepin, V. F. et al. (2003), *J. Cer. Sci.* **38,** 281–288.
34. Lazlo, J. A., Compton, D. L., and Li, X.-L. (2006), *Ind. Crops Prod.* **23,** 46–53.
35. Akin, D. E., Morrison, W. H. III, Rigsby, L. L., Barton, F. E. II, Himmelsbach, D. S., and Hicks, K. B. (2006), *Appl. Biochem. Biotechnol.* **129–132,** 104–116.
36. Akin, D. E. (1982), *Agron. J.* **74,** 424–428.
37. Martin, S. A. and Akin, D. E. (1988), *Appl. Environ. Microbiol.* **54,** 3019–3022.
38. Graf, E. (1992), *Free Radical Biol. Med.* **13,** 435–448.

0273-2289/1559-0291 (Online)/07/136–140/17–26/$30.00

# Enzymatic Microreactors for the Determination of Ethanol by an Automatic Sequential Injection Analysis System

ELIANA M. ALHADEFF,*[,1] ANDREA M. SALGADO,[1] ORIOL COS,[2] NEI PEREIRA JR.,[1] BELKIS VALDMAN,[1] AND FRANCISCO VALERO[2]

[1]*Escola de Química, Centro de Tecnologia, Universidade Federal do Rio de Janeiro, Ilha do Fundão, Cidade Universitária, CEP: 21.949-900, Rio de Janeiro, Brasil, E-mail: ema@eq.ufrj.br; and* [2]*Department d'Enginyeria Química, Escola Tècnica Superior d'Enginyeria, Universitat Autònoma de Barcelona, 08193 Bellaterra, Barcelona, Spain*

## Abstract

A sequential injection analysis system with two enzymatic microreactors for the determination of ethanol has been designed. Alcohol oxidase and horseradish peroxidase were separately immobilized on glass aminopropyl beads, and packed in 0.91-mL volume microreactors, working in line with the sequential injection analysis system. A stop flow of 120 s was selected for a linear ethanol range of 0.005–0.04 g/L ± 0.6% relative standard deviation with a throughput of seven analyses per hour. The system was applied to measure ethanol concentrations in samples of distilled and nondistilled alcoholic beverages, and of alcoholic fermentation with good performance and no significant difference compared with other analytical procedures (gas chromatography and high-performance liquid chromatography).

**Index Entries:** Alcohol oxidase; ethanol; horseradish peroxidase; immobilized enzymes; sequential injection analysis; biosensors.

## Introduction

Highly sensitive analytical systems for use in the clinical, forensic, pharmaceutical, food, fuels, bioprocess monitoring, and control industries are being developed to obtain fast and reliable results *(1)*. Several analytical techniques that use enzymatic reactions have been applied to quantify low ethanol concentrations. Of these, the use of flow injection analysis (FIA) promises to be reliable, reproducible, reagent saving, and a readily automated technique *(2)*. FIA has been used for ethanol detection in alcoholic beverages and in gasohol mixtures *(3–5)*. The systems use sequential enzymatic

*Author to whom all correspondence and reprint requests should be addressed.

microreactors packed with the alcohol oxidase (AOD) and horseradish peroxidase (HRP) enzymes, immobilized on chitosan or glass beads. Sequential injection analysis (SIA), with a time-based aspiration of defined samples and reagent zones, is an alternative to FIA systems that use smaller sample and indicator volumes, reduce the waste volume, and have more versatile sample handling capabilities *(6,7)*. SIA has been applied with free or immobilized enzymes for bioprocess automation and parameters control *(8–11)*. Amperometric detection of hydrogen peroxide or quinohemoprotein alcohol dehydrogenase complexed with a redox polymer and spectrophotometric detection reaction with $NAD^+$ cofactor dependent enzyme, were reported for ethanol analyses *(9,12,13)*. The aim of this work is to design and develop a sequential injection analysis system with two enzymatic microreactors using AOD and HRP immobilized separately, with a spectrophotometric detection reaction, for the determination of ethanol in distilled and nondistilled beverages and for alcoholic fermentation bioprocess monitoring.

## Materials and Methods

### Chemicals

All reagents were analytical grade and were obtained from Sigma Chemical Co. (St. Louis, MO) unless otherwise noted. AOD and HRP (Toyobo of Brazil) were immobilized separately on aminopropyl glass beads treated with 2.5% (v/v) glutaraldehyde as previously described *(4)*. The composition of the indicator solution was: 4-aminophenazone 0.395 g/L and phenol 0.875 g/L prepared in a 0.1 *M* sodium phosphate buffer solution (pH 7.0). The phosphate buffer was also used as carrier. Reactions were carried out at room temperature (20°C).

### Enzymatic Reactions

$$\text{Ethanol} + O_2 \rightarrow \text{Acetaldehyde} + H_2O_2$$

$$2H_2O_2 + \text{4-aminophenazone} \xrightarrow{\text{AOD}} \text{monoimino-}p\text{-benzoquinone-4-phenazone} + 4H_2O$$

The resulting colored product, monoimino-*p*-benzoquinone-4-phenazone, is detected with a spectrophotometer at 470 nm.

### The Sequential Injection Analysis System

The analyzer (Easi Technologies, Cerdanyola del Vallés, Spain) is consisted of four modules, connected by a RS-485/RS-232 interface and powered by a single 12V/2.5A source. The integrated analyzer system includes a five-way eight-roller peristaltic pump (Model 1201/06-5-0), a colorimeter (Model 1203/470/Z10), a module with two three-port rotary valves (Model 1202/3), and a six-port rotary valve (Cheminert Model 4162510, Valco

Instruments, Houston, TX). The sampling lines of the SIA system were made up of PTFE tubing (0.8 mm i.d.) joined by polyvinylchloride (PVC) fittings. A 1 m length of polytetrafluoroethylene (PTFE) tube was used as a holding coil. Samples and reagent solutions were aspirated and delivered to the six-port rotary valve by two automatic microburettes (Crison MicroBU Model 2031, Alella, Spain) with two syringes of 1-mL and 0.5-mL volume each (Hamilton Model 1002 Teflon Luer Lock, Hamilton Bonaduz AG, Bonaduz, Switzerland). A personal computer with a RS-485/RS-232 interface was used to control and for data acquisition using software developed in $C^{++}$. Figure 1A shows the SIA system schematic. The system has two acrylic microreactors, each with 0.91 mL void volume packed with AOD and HRP immobilized enzymes. The sequence zone structure and the time schedule implemented in the SIA system are shown in Fig. 1B. A 1.2-mL diluted sample was used with 0.14 mL of reagent solution in each run with the proposed time schedule: coil cleaning, 30 s; colorimeter cleaning, 100 s; sequential aspiration of sample and reagent solutions, 89 s; impulsion 1, 9 s; stop-flow at AOD immobilized microreactor, 120 s; impulsion 2, 150 s.

### *Microorganism, Medium, and Culture Conditions*

A batch fermentation with baker's yeast *Saccharomyces cerevisiae* (AB Mauri División, Córdoba, Spain) was monitored in 2-L bioreactor (Braun Biostat ED, Braun Biotech International, Melsungen, Germany), with 1 L of sterilized medium, conducted at 30°C and 500 rpm. The fermentation medium consisted of 100 g/L glucose, 1 g/L $KH_2PO_4$, 1 g/L $MgSO_4{\cdot}7H_2O$, 2 g/L $(NH_4)_2SO_4$, 1 g/L NaCl, and pH 4.5 sterilized at 121°C for 30 min. The samples were centrifuged at 5000*g* and filtered before being diluted for the SIA analyses.

### *Biomass Analysis*

Biomass was measured by withdrawing 3-mL samples from the bioreactor. After filtration and washing (Whatman GF/F, Maidstone, UK) the samples were dried at 105°C to a constant weight. Alternatively, biomass was measured by optical density at 570 nm, using a dry cell weight linear relation (Absorbance = $3.027.C_e + 0.094$) with correlation coefficient 0.9957. Biomass concentration ($C_e$) was expressed as dry cell weight/mL. Both determinations were performed by duplicate and the RSD was about 5%.

### *Off-Line Ethanol Analysis*

A Hewlett Packard (Paolo Alto, CA) 5890 gas chromatograph with a HP-INNOWAX Agilent column (30 m × 0.53 mm × 1 μm) was also used to analyze standard diluted ethanol samples for comparison. Operating conditions were 220°C and 280°C for injection and detector temperatures, respectively; oven temperature profile 40°C for 2 min, followed by 20°C /min up to 180°C , maintained for 2 min. Helium was used as a carrier gas with a flow rate of 8 mL/min. Injection volumes were 1 μL with splitless injection.

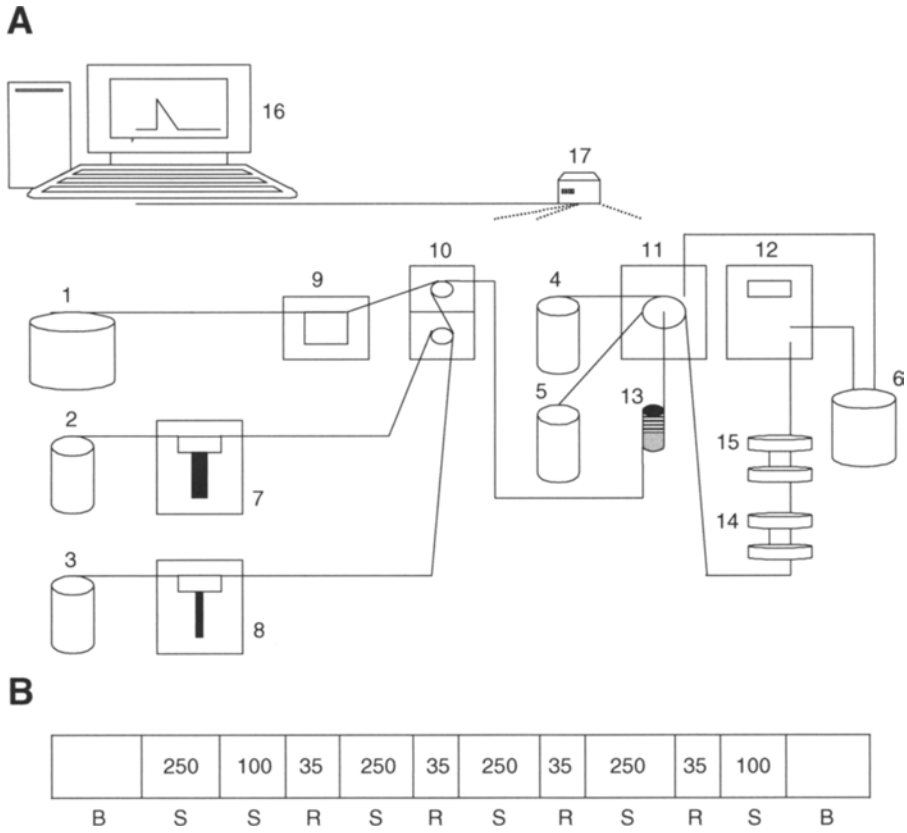


**Fig. 1.** The SIA **(A)** 1–3—pH 7.0 phosphate buffer solutions, 4—diluted ethanol sample, 5—phenol and 4-aminophenazone solution, 6—waste, 7—1000 µL microburette, 8—500 µL microburette, 9—peristaltic pump, 10—two three-way valves, 11—six channels distribution valve, 12—colorimeter at 470 nm, 13—coil, 14—AOD immobilized microreactor, 15—HRP immobilized microreactor, 16—computer and software control, 17—Interface RS-232/RS-485 and **(B)** Schematic diagram of the sequenced zone structure implemented in the SIA system. B, phosphate buffer; S, sample; and R, reagent solution. Quantities are expressed in microliter.

Ethanol was also determined using high-performance liquid chromatography (HPLC) (Hewlett Packard 1050) fpor samples of beverages and for monitoring batch fermentation using an Aminex HPX-87H column, at 25°C, and a refraction index detector. The mobile phase was 15 m*M* sulphuric acid in MilliQ water at 0.6 mL/min, and injection volume was 20 µL.

## *Off-Line Glucose Analysis*

Glucose present in the fermentation medium was measured by the HPLC and confirmed with a YSI (Yellow Springs, OH) 2700 SELECT biochemistry analyzer.

## Results and Discussion

### *Operational Conditions of the SIA System*

The retention efficiencies obtained in the immobilization of AOD and HRP were 95.07 ± 2.33% and 55.60 ± 5.37%, respectively. The retention efficiency was calculated as reported in previous work *(4)*. Preliminary experiments were conducted in the SIA system to select between two different approaches: continuous- and stop-flow strategies, in order to obtain maximum signal response. Three continuous flows of 1.7, 3.3, and 7.4 mL/min were studied in order to analyze the performance of the system in terms of linear range of measurements and sample frequency. Initial results obtained with experiments using a standard solution of 0.05 g/L ethanol rejected the intermediate flow rate. In Table 1 the main parameters obtained for the two flows using a set of ethanol standard solutions are presented.

As can be seen, the selection of the optimum flow is dependent on the detection limit or sample frequency. Trying to amplify the output signal the stop-flow method was used for the same linear range of ethanol solutions. Evaluating different stop-flow times at the first AOD immobilized microreactor with a standard solution sample of 0.05 g/L ethanol, 120 s was selected as an intermediate value between sample frequency and linear range. With this configuration a linear range up to 0.04 g/L ethanol was attained with a coefficient correlation of 0.9922, as shown in Fig. 2. The repeatability of the response signal for different ethanol concentrations is shown in Fig. 3. The sample frequency was seven analyses per hour and the calculated RSD was lower than 0.6% with a detection limit of $2.1 \times 10^{-3}$ g/L, calculated as three times the standard deviation of the background noise. After 60 analyses the enzymatic activity decreased by 50% at which point the immobilized enzymes had to be replaced with new lots.

In Fig. 4, a comparison of results between the proposed SIA and gas chromatography analysis shows with a good correlation ($r^2 = 0.9923$). The performance of the proposed SIA system was also evaluated for the analysis of ethanol concentration of nine diluted samples of distilled and nondistilled beverages. The results obtained are presented in Table 2. A maximum relative error of 7% was observed in samples of white wine, tequila, and vodka. Nevertheless the relative error for the other beverages was lower than 3% compared with HPLC analysis results.

Finally, the proposed SIA system was applied for monitoring a batch of alcoholic fermentation. Culture broth samples were collected every 30 min, filtered to obtain a biomass-free sample, and diluted manually before analysis in the SIA system. Figure 5 shows the production of ethanol measured using the SIA system and fermentation parameters as biomass-glucose, obtained by other measurement techniques. A good agreement between SIA and HPLC results were obtained and no problems of interference with other culture components were detected with a maximum relative error of 4.9%.

Table 1
Continuous Flow Effects on the SIA System

| Flow (mL/min) | Ethanol linear range (g/L) | Correlation factor ($r^2$) | Ethanol detection limit (g/L) | Sample frequency (1/h) | RSD (%) |
|---|---|---|---|---|---|
| 1.7 | 0.005–0.02 | 0.9917 | $2.1 \times 10^{-4}$ | 2 | 0.70 |
| 7.4 | 0.005–0.08 | 0.9717 | $1.5 \times 10^{-3}$ | 9 | 0.74 |

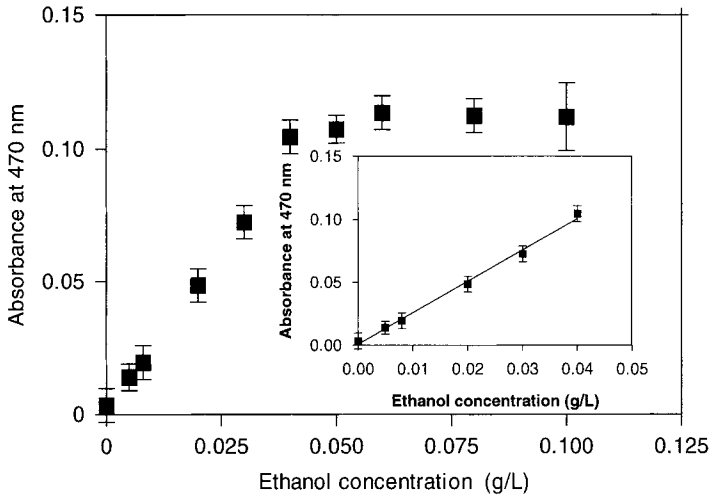


**Fig. 2.** Calibration curve for the 120 s stop-flow at the AOD immobilized microreactor.

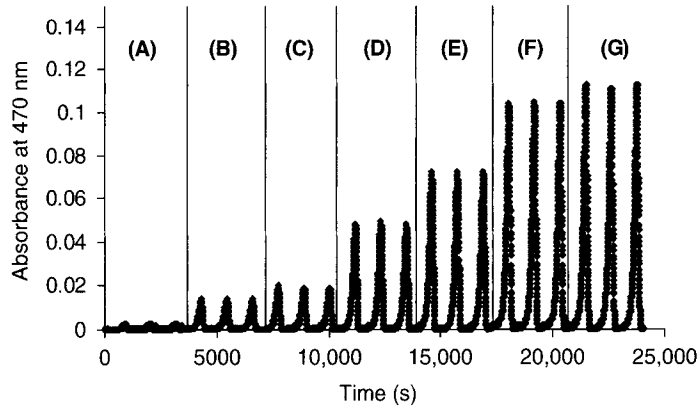


**Fig. 3.** Response signal repeatability obtained in SIA: **(A)** Phosphate buffer pH 7.0, **(B)** 0.005 g/L ethanol, **(C)** 0.008 g/L ethanol, **(D)** 0.020 g/L ethanol, **(E)** 0.030 g/L ethanol, **(F)** 0.040 g/L ethanol, and **(G)** 0.060 g/L ethanol.

Hence, the reliability of the method proposed was corroborated. A relative error of 4.4% was also reported in the literature for ethanol analysis in fermentation samples, working with an amperometric detection device and immobilized AOD in a SIA system (*9*). The advantage of the SIA system

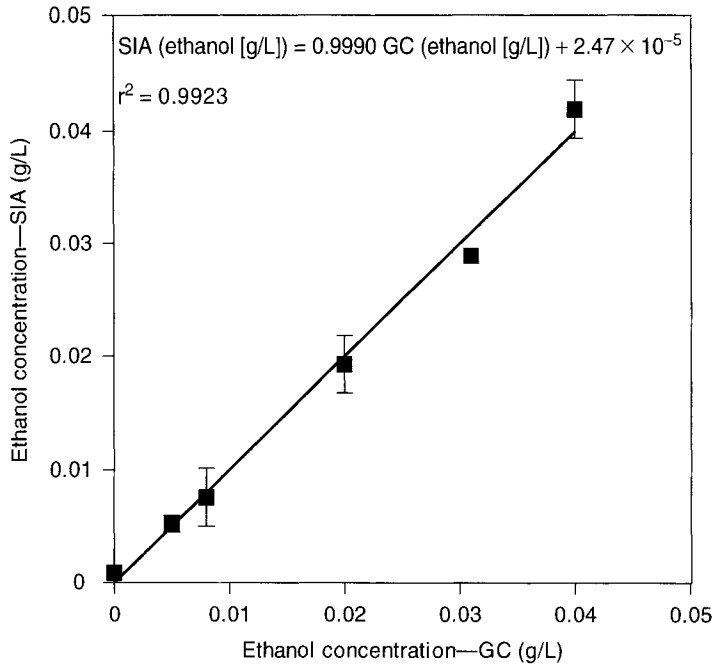


**Fig. 4.** Comparison of SIA and gas chromatography results.

Table 2
SIA and HPLC Analyses of Distilled and Nondistilled Beverage Samples

| Sample | HPLC[a] (g/L ethanol) | SIA[a] (g/L ethanol) | Relative error (%) |
|---|---|---|---|
| Gin | 365.2 ± 0.2 | 378.8 ± 9.0 | −3.7 |
| Tequila | 359.8 ± 1.1 | 336.5 ± 6.6 | 6.5 |
| Vodka | 427.8 ± 1.5 | 455.6 ± 4.5 | −6.5 |
| White wine | 101.9 ± 0.1 | 94.5 ± 3.3 | 7.3 |
| Sugar-cane spirit | 320.6 ± 2.5 | 312.8 ± 5.5 | 2.4 |
| Whisky | 322.8 ± 7.1 | 324.8 ± 5.7 | −0.6 |
| Cognac | 375.6 ± 2.0 | 365.8 ± 9.0 | 2.6 |
| Wine spirit | 254.3 ± 5.1 | 252.9 ± 10.2 | 0.6 |
| Peach liqueur | 181.2 ± 0.3 | 181.4 ± 2.3 | −0.1 |

[a]Mean of two analyses.

proposed in this work is that it works with both AOD and HRP enzymes and a colorimetric detection system for ethanol samples with only a simple dilution for the alcoholic beverages, appropriate for the sensible linear measurement range of 0.005–0.04 g/L ethanol. Other authors *(12,13)* reported similar relative errors working with alcohol dehydrogenase, but needed the cofactor $NAD^+$/NADH, which is not necessary in the present proposed system.

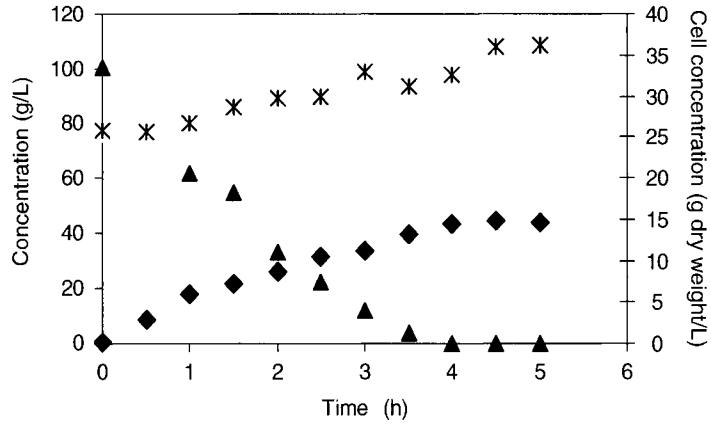


**Fig. 5.** Ethanol monitoring of alcoholic batch fermentation samples by SIA and HPLC. SIA: ethanol (◆), HPLC and biochemistry analyzer: glucose (▲), and dry cell weight (✳).

## Conclusions

A reproducible and reliable SIA analyzer system for ethanol samples was developed. The use of two microreactors with immobilized AOD and HRP permitted an important saving of enzymes reagents in a spectrophotometric detection system. The system was applied to the analysis of distilled and nondistilled beverage samples with similar performances, as reported by other authors working with a more expensive system than the one proposed in this work *(12,13)*. The SIA system performance was also demonstrated to be useful in the monitoring of an alcoholic fermentation showing flexibility and robustness of the analytical equipment. No pretreatment of the samples was needed, simple dilution adequate for the linear range of 0.005–0.04 g/L ethanol was sufficient to analyze the alcoholic beverages and bioprocess medium samples with a detection limit of $2.1 \times 10^{-3}$ g/L ethanol.

## Acknowledgments

We acknowledge the support received from the BI-EURAM Project of the Alpha Program—EU. We also thank Toyobo of Brazil for gently donating the HRP.

## References

1. Patel, P. D. (2002), *Trends Anal. Chem.* **21,** 96–115.
2. Ruzicka, J., Hansen, E. H., and Rietz, B. (1975), *Anal. Chim. Acta* **89,** 241–246.
3. Taniai, T., Sukurragawa, A., and Okitani, T. (2001), *J. AOAC Int.* **84(5),** 1475–1483.
4. Alhadeff, E. M., Salgado, M. A., Pereira, N., Jr., and Valdman, B. (2004), *Appl. Biochem. Biotechnol.* **113,** 125–136.
5. Alhadeff, E. M., Salgado, M. A., Pereira, N., Jr., and Valdman, B. (2005), *Appl. Biochem. Biotechnol.* **121,** 361–372.

6. Keavy, P. J. and Wang, Y. Y. (1997), *TIBTECH* **15,** 76–81.
7. van Staden, J. F. and Stefan, R. I. (2004), *Talanta* **64,** 1109–1113.
8. Surribas, A., Cos, O., Montesinos, J. L., and Valero, F. (2003), *Biotechnol. Lett.* **25,** 1795–1800.
9. Lapa, R. A. S., Lima, J. L. F. C., and Pinto, I. V. O. S. (2003), *Food Chem.* **81,** 141–146.
10. Masini, J. C., Rigobello-Masini, M., Salatino, A., and Aidar, E. (2001), *Latin Am. Appl. Res.* **31,** 463–468.
11. Chung, S. C., Christian, G. D., and Ruzika, J. (1992), *Proc. Contr. Qual.* **3,** 115–125.
12. Niculescu, M., Erichsen, T., Sukharev, V., Kereny, Z., Csregi, E., and Schuhmann, W. (2002), *Anal. Chim. Acta* **463,** 39–51.
13. Segundo, M. A. and Rangel, A. O. S. S. (2002), *Anal. Chim. Acta* **458,** 131–138.

0273-2289/1559-0291 (Online)/07/136–140/27–40/$30.00

# Optimization of Cyclodextrin Glucanotransferase Production From *Bacillus clausii* E16 in Submerged Fermentation Using Response Surface Methodology

HELOIZA FERREIRA ALVES-PRADO,[1,2] DANIELA ALONSO BOCCHINI,[1,3] ELENI GOMES,[1] LUIS CARLOS BAIDA,[4] JONAS CONTIERO,[2] INÊS CONCEIÇÃO ROBERTO,[5] AND ROBERTO DA SILVA*,[1]

[1]*Biochemistry and Applied Microbiology Laboratory—IBILCE/UNESP, São José do Rio Preto, SP, Brazil, E-mail: dasilva@ibilce.unesp.br;* [2]*Biology Institute—UNESP, Rio Claro, SP, Brazil;* [3]*Chemistry Institute—UNESP, Araraquara, SP, Brazil;* [4]*Computation Sciences and Statistic Department—IBILCE/UNESP, São José do Rio Preto, SP, Brazil; and* [5]*Biotechnology Department—School of Engineering of Lorena—EEL/USP—CP: 116, Lorena, SP, Brazil*

## Abstract

Cyclodextrin glucanotransferase production from *Bacillus clausii* E16, a new bacteria isolated from Brazilian soil samples was optimized in shake-flask cultures. A $2^4$ full-factorial central composite design was performed to optimize the culture conditions, using a response surface methodology. The combined effect among the soluble starch concentration, the peptone concentration, the yeast extract concentration, and the initial pH value of the culture medium was investigated. The optimum concentrations of the components, determined by a $2^4$ full-factorial central composite design, were 13.4 g/L soluble starch, 4.9 g/L peptone, 5.9 g/L yeast extract, and initial pH 10.1. Under these optimized conditions, the maximum cyclodextrin glucanotransferase activity was 5.9 U/mL after a 48-h fermentation. This yield was 68% higher than that obtained when the microorganism was cultivated in basal culture medium.

**Index Entries:** Alkalophillus *Bacillus clausii*; CGTase production; cyclodextrin glucanotransferase; experimental design; submerged fermentation; response surface methodology.

## Introduction

Cyclodextrin glucanotransferase (CGTase) (EC 2.4.1.19) is an extracellular bacterial enzyme, used in the production of cyclodextrin from starch. Cyclodextrins (CDs) are cyclic maltoligosaccharides made up of six, seven, or eight D-glucose units, named α-, β-, or γ-cyclodextrin, respectively *(1)*.

*Author to whom all correspondence and reprint requests should be addressed.

The internal cavities of CDs are hydrophobic and the external surface hydrophilic, so they can encapsulate a wide variety of hydrophobic molecules, potentially improving their properties. The modified properties make CDs suitable for numerous applications in the food, cosmetic, and pharmaceutical industries. For example, CDs can be used to capture undesirable tastes or odors, to stabilize volatile compounds, to increase water solubility of hydrophobic substances, or to protect a substance against unwanted modifications *(2–6)*. They are commonly produced from starch through four reactions catalyzed by the CGTase:

1. Intramolecular transglucosylation or cyclization reaction, in which a linear oligosaccharide chain is cleaved and the new reducing-end sugar is transferred to the nonreducing-end sugar of the same chain.
2. Coupling reactions, in which a cyclodextrin ring is cleaved and transferred to an acceptor maltooligosaccharide substrate.
3. Intermolecular transglucosylation or disproportionation, in which a linear maltooligosaccharide is cleaved and the new reducing-end sugar is transferred to an acceptor maltooligosaccharide substrate.
4. A weak hydrolyzing activity on starch *(6,7)*.

CGTase producers are mainly alkalophilic *Bacillus* sp., but they are also reported as *Klebsiella* sp., *Micrococcus* sp., *Brevibacterium* sp., *Paenibacillus* sp., *Themoanaerobacter* sp., *Thermoactinomyces* sp., and others *(2)*. Some studies have shown the improvement of CGTase production through changes in the composition of the culture medium *(8–14)*.

Traditional methods of optimization involve changing one independent variable, whereas fixing the others at a certain level. This single-factor search is laborious, time-consuming, and incapable of reaching the true optimum condition as it fails to reveal interactions among variables. Response surface methodology (RSM), described first by Box and Wilson, is an experimental strategy for seeking the optimum conditions for a multivariable system *(15,16)*. It has been successfully used to optimize the medium ingredients and to operate conditions in enzyme production and many other bioprocesses *(8,9,13,14,17–20)*. In earlier studies we isolated a new CGTase producer, first identified as *Bacillus* sp. subgroup *alcalophilus* E16 *(21)* and we also identified some factors affecting the production of CGTase. In the work reported here, these factors were investigated, using a full-factorial central composite design and RSM, with the aim to improve the CGTase production by optimizing the culture medium.

## Materials and Methods

### *Bacterial Strain Isolation and Identification*

The strain E16 was isolated from a soil crop sample and its microbial properties were investigated by classical taxonomy as described in Bergey's Manual *(22)*. Based on these results, it was identified as a *Bacillus*

sp. strain E16. Molecular techniques based on partial sequence of 16S ribosomal RNA (rRNA) analysis were applied for specie identification. The genomic DNA of strain E16 was isolated and the 16S ribosomal DNA was amplified by polymerase chain reaction using forward primer p27 and reverse primer p1525. These primers are homologous to preserved regions of the 16S rRNA gene of bacteria. The amplified product polymerase chain reaction was purified and sequenced. The 16S ribosomal DNA sequence was aligned with sequences obtained from Ribosomal Database Project (Wisconsin, WI; http://www.cme.msu.edu/RDP/html) and GenBank (http://www.ncbi.nlm.nih.gov/).

The sequences with high similarity and alcalophilic *Bacillus* sp. were compiled into NEXUS files after alignment in CLUSTAL W program *(23)*. The phylogenetic relationships among selected sequences were estimated by using the maximum parsimony method, using a branch-and-bound algorithm as implemented in PAUP v.4.0b10 *(31)*. Branch support was calculated by bootstrap analysis consisting of 500 replicates. The distance matrix used in this work was constructed by "p" method. DNA sequences of *Clostridium butyricum* strain MW (AJ002592), *B. clausii* strain z a w3 (AY066000), *B. clarkii* DSM 8720 (X76444), *B. clausii* strain Y76-A (AB201796), *B. clausii* DSM 8716 (X76440), *Bacillus* sp. strain ikaite 27 (AJ431332), *B. pataginiensis* PAT 05 (AY258614), *Bacillus* sp. DSM 8714 (X76438), *B. alcalophilus* YB380 (AF078812), *B. horti* (D87035), *Bacillus* sp. strain NER (AJ507321), *Bacillus* sp. TS1-1 (AY751538), *Bacillus* sp. G1 (AY754340), *B. oshimae* K-11 (AB188090), *B. pseudalcaliphilus* DSM 8725 (X76449), *B. alcalophilus* DSM 485T (X76436), *B. horikoshii* DSM 8719 (X76443), *B. circulans* ATCC4513 (AY647299), *B. litoralis* IB-B4 (AJ309561), *B. galactosidilyticus* (AJ535638), and *B. thermoamylovorans* (AJ586361) were obtained from the GenBank DNA sequence library.

## Materials

β-Cyclodextrin, maltodextrin, and phenolphthalein were purchased from Sigma (St. Louis, MO). Yeast extract was obtained from Difco (Detroit, MI) and peptone was obtained from Biobrás (Montes Claros, MG, Brazil). Soluble starch was obtained from Mallinckrodt (Paris, France). Other chemicals of analytical grade were obtained from Merck (Darmstadt, Germany).

## Cultivation Medium

Stock culture of the strain E16 was maintained at 5°C on agar slant with the same composition as the following basal liquid culture medium plus 1.5% agar *(24)*. The basal liquid culture medium was made up of soluble starch 10.0 g/L, peptone 5.0 g/L, yeast extract 5.0 g/L, $K_2HPO_4$ 1.0 g/L, $MgSO_4 \cdot 7H_2O$ 0.2 g/L, $Na_2CO_3$ 10.0 g/L (separately sterilized), and pH 10.0 *(25)*. For the optimization experiments the culture medium contained various quantities of soluble starch, peptone, and yeast extract

concentrations; and the initial pH was varied in accordance with the experimental design. Bacteria was transferred by loop to a flask with basal liquid medium and cultured for 24 h to produce the inoculum. The optimization experiments were carried out in 125-mL Erlenmeyer flasks each containing 20 mL of one of the culture media. These flasks were seeded with 0.1 mL from the 24 h-old culture containing $2.6 \times 10^9$ cells/mL, and were incubated for 48 h on a rotary shaker at 37°C and 150 rev/min. After a 48-h fermentation, the contents of each flask was centrifuged at 10,000*g* at 5°C for 15 min, and CGTase activity was measured in the supernatant.

### *CGTase Assay*

CGTase activity was measured as β-CD forming activity based on phenolphthalein method *(26)* with slight modifications as described in Alves-Prado et al. *(27)*. One unit of CGTase activity was defined as the amount of enzyme that produces 1 μmol of β-CD per minute.

### *Experimental Design and Optimization*

The software "Statistica" (version 5.0), from StatSoft Inc., was used for design experiments and for regression and graphical analysis of the data obtained. The dependent variable selected for this study was the CGTase activity, expressed in U/mL, and the independent variables chosen were the concentrations of soluble starch, peptone, and yeast extract, plus the initial pH of the culture medium. These variables and the value ranges were chosen based on previous experiments changing one independent variable and fixing the other variables at a certain level *(28)*. In order to determine the optimal conditions for the production of CGTase by *B. clausii* E16, a $2^4$ full-factorial central composite design with five coded levels was implemented, resulting in twenty-six sets of experiments. Eq. 1 shows the code of independent variables used in the statistical analysis.

$$x_i = \frac{X_i - X_0}{\Delta X_i} \tag{1}$$

where $x_i$ is the independent variable coded value, $X_i$ is the independent variable real value, $X_0$ is the independent variable real value of the center point, and $\Delta X_i$ is the step change.

The ranges and levels of the variables investigated in this study are given in Table 1. In this table, the studied variables are coded as $X_1$ (initial pH), $X_2$ (soluble starch), $X_3$ (peptone), and $X_4$ (yeast extract). The five levels are the results of previous runs based on a path of steepest ascent analysis of which (–1) and (+1) points are the minimum and maximum points, respectively. The (0) point is the central point, which was determined from the arithmetic mean between the minimum and maximum points, for each studied

Table 1
Experimental Ranges and Levels of the Independent Process Variables Used in the $2^4$ Full-Factorial Central Composite Design

| Independent variable | Symbol | Ranges and levels | | | | |
|---|---|---|---|---|---|---|
| | | −1.483 | −1 | 0 | 1 | +1.483 |
| pH | $X_1$ | 9.34 | 9.62 | 10.2 | 10.78 | 11.06 |
| Soluble starch (g/L) | $X_2$ | 11.3 | 12.5 | 15.0 | 17.5 | 18.7 |
| Peptone (g/L) | $X_3$ | 3.8 | 4.4 | 5.6 | 6.8 | 7.4 |
| Yeast extract (g/L) | $X_4$ | 3.7 | 4.2 | 5.3 | 6.4 | 6.9 |

variable. The ($-\alpha = -1.483$) and ($+\alpha = +1.483$) points are levels which result in a star configuration, determined by the mentioned statistic software.

The estimated response surface ($\hat{y}$) was expressed by the second degree Eq. 2:

$$\begin{aligned}\hat{y} = {} & b_0 + b_1X_1 + b_2X_2 + b_3X_3 + b_4X_4 + b_{12}X_1X_2 \\ & + b_3X_1X_3 + b_{14}X_1X_4 + b_{23}X_2X_3 + b_{24}X_2X_4 + b_{34}X_3X_4 \\ & + b_{11}X_1^2 + b_{22}X_2^2 + b_{33}X_3^2 + b_{44}X_4^2 + \varepsilon\end{aligned} \quad (2)$$

where $\hat{y}_i$ represents the response variable, $b_0$ is the intercept, $b_1$, $b_2$, $b_3$, and $b_4$ are the linear terms, $b_{11}$, $b_{22}$, $b_{33}$, and $b_{44}$ are the quadratic terms, $b_{12}$, $b_{13}$, $b_{14}$, $b_{23}$, $b_{24}$, and $b_{34}$ are the cross-product terms, $X_1$, $X_2$, $X_3$, and $X_4$ represent the variables studied, initial pH, soluble starch concentration, peptone concentration, and yeast extract concentration, respectively, and $\varepsilon$ is the random error.

## Results and Discussion

### *Identification of the Isolated Strain*

The cells were grown in nutrient agar in alkaline condition (pH 9.5) at 35°C for 24 h. The cells were rod-shaped with stained positive gram and not motile, the spores were ellipsoidal and subterminal. The colonies were circular with entire margins of light yellow color, and approximate size of up to 2.0 mm. The microorganism was strictly aerobe and positive for catalase and oxidase reaction and negative for nitrate to nitrite reduction. The cellular growth at 30, 35, and 40°C was observed on nutrient medium in pH 6.8. These characteristics comprehend the *Bacillus* sp., a phylogenetic analysis with 16S rRNA sequence was necessary for specie identification. So, the strain E16, was first identified as *Bacillus* sp. subgroup *alcalophillus* in accordance to Nielsen *(29)*.

The aim of the phylogenetic analysis was to determine the relationships among some alcalophilic bacilli sequences. A parsimonious tree was

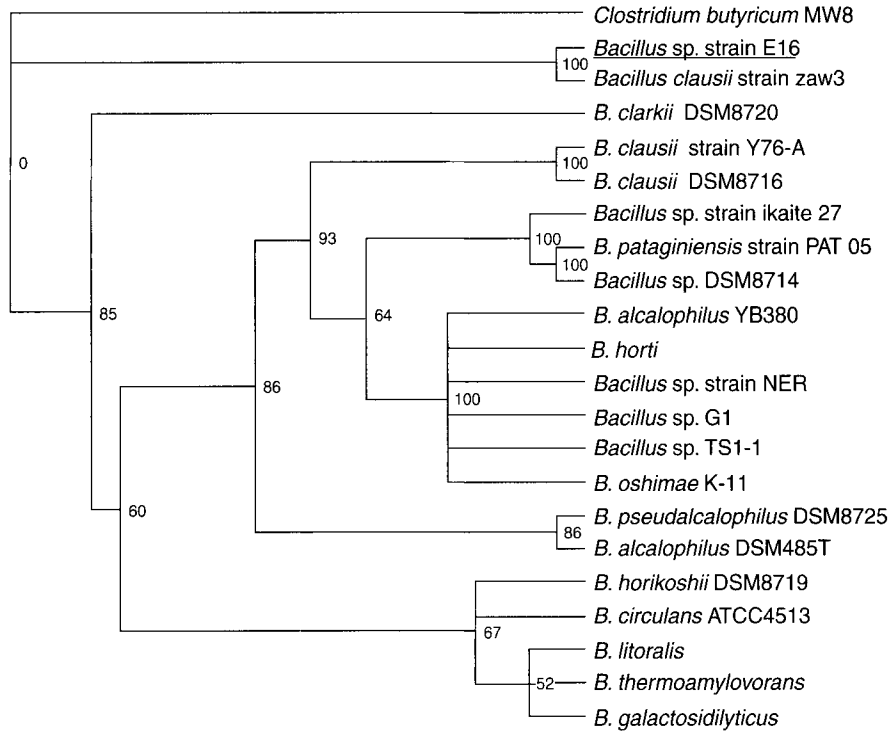


**Fig. 1.** Phylogenetic tree of the alkalophilic isolates based on 16S rRNA gene sequence using the neighbor-joining method. *C. butyricum* strain MW8 (AJ002592) was used as the outgroup. The accession numbers of the additional 16S rRNA sequences used are as follows: *B. clausii* strain z a w3 (AY066000), *B. clarkii* DSM 8720 (X76444), *B. clausii* strain Y76-A (AB201796), *B. clausii* DSM 8716 (X76440), *Bacillus* sp. strain ikaite 27 (AJ431332), *B. pataginiensis* PAT 05 (AY258614), *Bacillus* sp. DSM 8714 (X76438), *B. alcalophilus* YB380 (AF078812), *B. horti* (D87035), *Bacillus* sp. strain NER (AJ507321), *Bacillus* sp. TS1-1 (AY751538), *Bacillus* sp. G1 (AY754340), *B. oshimae* K-11 (AB188090), *B. pseudalcaliphilus* DSM 8725 (X76449), *B. alcalophilus* DSM 485T (X76436), *B. horikoshii* DSM 8719 (X76443), *B. circulans* ATCC4513 (AY647299), *B. litoralis* IB-B4 (AJ309561), *B. galactosidilyticus* (AJ535638), and *B. thermoamylovorans* (AJ586361).

obtained by the analysis of the 22 species (Fig. 1). From a total of 762 characters, 365 were phylogenetically informative. The consistency index was 0.8108 and the retention index was 0.7969. Two clades, one major containing *B. clarkii* DSM 8720, *B. clausii* strain Y76-A, *B. clausii* DSM 8716, *Bacillus* sp. strain ikaite 27, *B. pataginiensis* PAT 05, *Bacillus* sp. DSM 8714, *B. alcalophilus* YB380, *B. horti*, *Bacillus* sp. strain NER, *Bacillus* sp. TS1-1, *Bacillus* sp. G1, *B. oshimae* K-11, *B. pseudalcaliphilus* DSM 8725, *B. alcalophilus* DSM 485T, *B. horikoshii* DSM 8719, *B. circulans* ATCC4513, *B. litoralis* IB-B4, *B. galactosidilyticus*, and *B. thermoamylovorans* (bootstrap value 85) and the other with the *B. clausii* strain zaw3 and *Bacillus* sp. E16 (bootstrap value 100) were highly resolved. These results agree with those observed on the nucleotides sequence. Based on these results, it is suggested that the

*Bacillus* sp. strain E16 be named *B. clausii* strain E16, owing to the low divergence shown on the distance between matrixes (3.8%). This sequence was submitted to GenBank and its access number is DQ924973.

### *Experimental Design and Optimization*

The identification of the major factors affecting the experimental response is the first step in determining the optimum conditions for enzyme production. The culture medium concentrations of the components $K_2HPO_4$, $MgSO_4 \cdot 7H_2O$, soluble starch, peptone and yeast extract, and initial pH of the culture medium were studied previously. Based on these trial runs using a factorial design and a path of steepest ascent, the soluble starch, peptone and yeast extract concentrations, and the initial culture medium pH were identified as important factors in CGTase production *(28)* and were therefore selected for further study of the optimization of CGTase production.

In this study, these variables were statistically optimized with the help of a quadratic model consisting of $2^4$ trials plus a star configuration ($\alpha = \pm 1.483$) and two replicates at the center point. The design of this experiment is given in Table 2, together with the experimental results. The highest CGTase activity (4.82 U/mL) was observed in run number 26 and this run corresponded to the center point. The average CGTase activity obtained on the center points was 4.66 U/mL, where the factors soluble starch, peptone, and yeast concentrations and initial medium pH were 15.0 g/L, 5.6 g/L, 5.3 g/L, and 10.2, respectively. This activity was 30.8% higher than that observed in the control run, where the factors were those used in the basal culture medium.

The regression obtained after analysis of variance gives the production of CGTase from *B. clausii* strain E16 as a function of the different initial pH ($X_1$), soluble starch concentration ($X_2$), peptone concentration ($X_3$), and yeast extract concentration ($X_4$). These terms were included in the following second-order polynomial equation where the mathematical model representing the CGTase activity ($\hat{y}$) in the experimental region studied can be expressed by Eq. 3:

$$\begin{aligned}\hat{y} = {} & 4.472 - 0.296X_1 - 0.363X_2 - 0.384X_3 - 0.181X_4 - 0.362X_1X_2 \\ & + 0.281X_1X_3 + 0.001X_1X_4 - 0.082X_2X_3 - 0.162X_2X_4 \\ & - 0.184X_3X_4 - 0.0674X_1^2 - 0.278X_2^2 - 0.436X_3^2 - 0.362X_4^2\end{aligned} \quad (3)$$

The regression model was generated by Statistica software consisting of 1 offset, 4 linear, 4 quadratic, and 6 interaction terms. Table 3 shows a regression analysis of the estimates and hypothesis tests for the coefficients of regression, which were displayed in Eq. 3. At the 5% probability level, the linear and quadratic coefficients of initial pH ($X_1$) and peptone concentration ($X_3$), the linear coefficient of soluble starch concentration ($X_2$), and the interaction of initial pH and soluble starch concentration ($X_1X_2$)

Table 2
Experimental Design and Results of the $2^4$ Full-factorial Central Composite Design

| Runs | Coded levels $X_1$ $X_2$ $X_3$ $X_4$ | Uncoded levels pH | Soluble starch (g/L) | Peptone (g/L) | Yeast extract (g/L) | Enzymatic activity (U/mL) Observed | Predicted |
|---|---|---|---|---|---|---|---|
| 1 | −1 −1 −1 −1 | 9.62 | 12.5 | 4.4 | 4.2 | 3.85 | 3.58 |
| 2 | −1 −1 −1 +1 | 9.62 | 12.5 | 4.4 | 6.4 | 4.17 | 3.96 |
| 3 | −1 −1 +1 −1 | 9.62 | 12.5 | 6.8 | 4.2 | 2.33 | 2.45 |
| 4 | −1 −1 +1 +1 | 9.62 | 12.5 | 6.8 | 6.4 | 1.85 | 2.09 |
| 5 | −1 +1 −1 −1 | 9.62 | 17.5 | 4.4 | 4.2 | 3.89 | 3.75 |
| 6 | −1 +1 −1 +1 | 9.62 | 17.5 | 4.4 | 6.4 | 3.35 | 3.44 |
| 7 | −1 +1 +1−1 | 9.62 | 17.5 | 6.8 | 4.2 | 2.63 | 2.95 |
| 8 | −1 +1 +1 +1 | 9.62 | 17.5 | 6.8 | 6.4 | 1.83 | 1.92 |
| 9 | +1 −1 −1 −1 | 10.78 | 12.5 | 4.4 | 4.2 | 3.23 | 3.14 |
| 10 | +1 −1 −1 +1 | 10.78 | 12.5 | 4.4 | 6.4 | 3.95 | 3.52 |
| 11 | +1 −1 +1 −1 | 10.78 | 12.5 | 6.8 | 4.2 | 3.37 | 3.14 |
| 12 | +1 −1 +1 +1 | 10.78 | 12.5 | 6.8 | 6.4 | 2.64 | 2.79 |
| 13 | +1 +1 −1 −1 | 10.78 | 17.5 | 4.4 | 4.2 | 2.22 | 1.86 |
| 14 | +1 +1 −1 +1 | 10.78 | 17.5 | 4.4 | 6.4 | 1.70 | 1.58 |
| 15 | +1 +1 +1 −1 | 10.78 | 17.5 | 6.8 | 4.2 | 1.97 | 2.19 |
| 16 | +1 +1 +1 +1 | 10.78 | 17.5 | 6.8 | 6.4 | 1.01 | 1.17 |
| 17 | −1.48 0 0 0 | 9.34 | 15.0 | 5.6 | 5.3 | 3.65 | 3.43 |
| 18 | +1.48 0 0 0 | 11.06 | 15.0 | 5.6 | 5.3 | 2.12 | 2.55 |
| 19 | 0 −1.48 0 0 | 10.20 | 11.3 | 5.6 | 5.3 | 3.97 | 4.40 |
| 20 | 0 +1.48 0 0 | 10.20 | 18.7 | 5.6 | 5.3 | 3.54 | 3.32 |
| 21 | 0 0 −1.48 0 | 10.20 | 15.0 | 3.8 | 5.3 | 3.12 | 4.08 |
| 22 | 0 0 +1.48 0 | 10.20 | 15.0 | 7.4 | 5.3 | 3.70 | 2.94 |
| 23 | 0 0 0 −1.48 | 10.20 | 15.0 | 5.6 | 3.7 | 3.68 | 3.92 |
| 24 | 0 0 0 +1.48 | 10.20 | 15.0 | 5.6 | 6.9 | 3.47 | 3.44 |
| 25 | 0 0 0 0 | 10.20 | 15.0 | 5.6 | 5.3 | 4.49 | 4.42 |
| 26 | 0 0 0 0 | 10.20 | 15.0 | 5.6 | 5.3 | 4.82 | 4.42 |
| Control[a] | – | 10.0 | 10.0 | 5.0 | 5.0 | 3.55 | – |

[a]basal medium composition.

were found to be significant for the enzyme activity. Similar to our results, the quadratic coefficients for sago starch concentration, peptone from casein concentration as well as the interaction sago starch concentration, and initial pH were significant for the CGTase activity from *B. stearothermophilus* HR1 *(14)*.

The statistical significance of this second-order polynomial model equation (Table 4) was evaluated by performing the *F*-test on the analysis of variance (ANOVA) estimates of mean squares, which showed that this regression is statistically significant ($p = 0.004$) at 95% confidence level.

Table 3
Results of Regression Analysis Using the $2^4$ Full-factorial Central Composite Design

| Term | Standard errors | Coefficient | $T_{(11)}$ value | *p*-value |
|---|---|---|---|---|
| Mean | ±0.28 | 4.472 | 15.974[a] | – |
| $X_1$ | ±0.23 | –0.297 | –2.592[a] | 0.0250 |
| $X_1^2$ | ±0.33 | –0.674 | –4.054[a] | 0.0019 |
| $X_2$ | ±0.23 | –0.363 | –3.174[a] | 0.0088 |
| $X_2^2$ | ±0.33 | –0.278 | –1.673 | 0.1225 |
| $X_3$ | ±0.23 | –0.384 | –3.359[a] | 0.0064 |
| $X_3^2$ | ±0.33 | –0.436 | –2.619[a] | 0.0238 |
| $X_4$ | ±0.23 | 0.181 | –1.412 | 0.1856 |
| $X_4^2$ | ±0.33 | –0.362 | –2.175 | 0.0523 |
| $X_1X_2$ | ±0.56 | –0.362 | –2.799[a] | 0.0173 |
| $X_1X_3$ | ±0.56 | 0.281 | –2.178 | 0.0521 |
| $X_1X_4$ | ±0.56 | 0.001 | 0.007 | 0.9943 |
| $X_2X_3$ | ±0.56 | –0.082 | 0.632 | 0.5403 |
| $X_2X_4$ | ±0.56 | –0.162 | –1.292 | 0.2226 |
| $X_3X_4$ | ±0.56 | –0.184 | –1.422 | 0.1827 |

Table 4
Analysis of Variance (ANOVA) for the Regression Model Representing CGTase Activity

| Source | SS | DF | MS | *F*-value | *p*-value |
|---|---|---|---|---|---|
| Model | 20,727 | 14 | 1480 | 554 | 0004 |
| Residue | 2940 | 11 | 0267 | – | – |
| Lack of fit | 2889 | 10 | 0289 | 550 | 0321 |
| Pure error | 0052 | 1 | 0052 | – | – |
| Total | 23,669 | 25 | – | – | – |

R2, 0.88; SS, sum of squares; DF, degrees of freedom; MS, mean square.

The model fitted the data well and gave a good coefficient of determination ($R^2 = 0.88$), explaining 88% of the variability in the response, the rest (12%) being explained by the residues.

The response surface described by model equation ($\hat{y}$) to estimate dependence of CGTase activity on the variables soluble starch concentration ($X_2$) and initial pH of medium ($X_1$) is shown in Fig. 2. This dependence suggests that when the soluble starch concentration is increased, the initial pH value should be decreased to obtain results that tend to maximize CGTase production. For the other studied variables, peptone and yeast extract, there was no significant interaction at the 5% probability level. So, for these variables, the concentrations keep at around the 0 point concentration (central point).

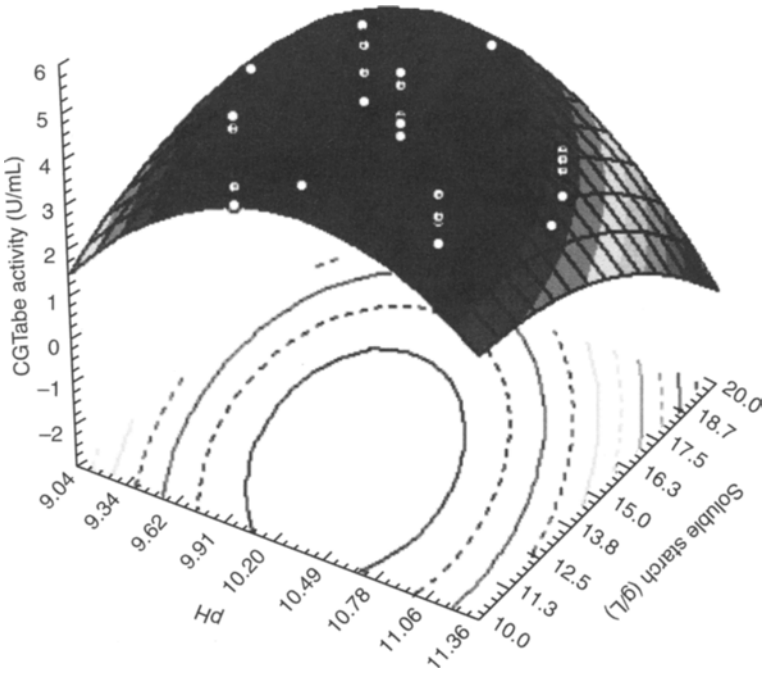


**Fig. 2.** Response surface described by the model $\hat{y}$, which represents CGTase activity (U/mL) produced by *B. clausii* strain E16 after a 48-h fermentation, as a function of soluble starch concentration and initial pH of growth medium.

The second-order polynomial model was significant in the region studied, the optimum coded values (optimum point) of the variables $X_1$, $X_2$, $X_3$, and $X_4$ being determined by Eq. 4, as proposed by Myers *(30)*:

$$x_0 = \mathbf{B}^{-1} \cdot \frac{\mathbf{b}}{2} \tag{4}$$

where $x_0$ is the vector of optimum values; **B** is a matrix of the estimated coefficients of quadratic terms and **b** is a vector of the estimated coefficients of linear terms.

The optimum coded values obtained from the experimental data by Eq. 4 are shown here as components of $x_0$ (Eq. 5):

$$x_0 = \begin{bmatrix} -0.170_{\text{pH}} \\ -0.616_{\text{soluble starch}} \\ -0.548_{\text{peptone}} \\ -0.527_{\text{yeast extract}} \end{bmatrix} \tag{5}$$

The coded values presented above correspond to initial culture medium pH 10.1; soluble starch 13.5 g/L; peptone 4.9 g/L; yeast extract 5.9 g/L. Under these conditions, the model predicts CGTase activity to be at a high

value of 4.64 U/mL, with a possible range from 4.09 to 5.19 U/mL at the 5% probability level. The decrease of CGTase production at higher concentrations of carbon source (soluble starch) was also found in *B. firmus* (Gawande et al., 1998) and *B. stearothermophilus* HR1 *(14)*, similar to our results.

The canonic form was obtained from the second-order polynomial model ($\hat{y}$) as follows:

$$\hat{y} = 4.64 - 0.786w_{\text{pH}}^2 - 0.518w_{\text{soluble starch}}^2 - 0.282w_{\text{peptone}}^2 - 0.165w_{\text{yeast extract}}^2 \quad (6)$$

In this equation, all of the coefficients are negative, indicating that the optimum point found is the maximum for the surface and thus the adjusted response surface model produces the highest results. Equation 6 may also indicate that any change in its values will cause a fall in CGTase activity. The greatest interference is caused by changes in initial pH and soluble starch concentration. The changes in peptone and yeast extract concentrations cause the least interference on CGTase activity.

Figures 3A and 3B are comparisons of growth and activity in the optimized culture medium found in this study with those achieved in the basal medium proposed by Nakamura and Horikoshi *(25)*. Optimized medium produces the highest CGTase activity (5.9 U/mL) after a 48-h fermentation as analyzed in this study. The biomass production peaked between 32 and 40 h (Fig. 3A). However, with basal medium, the highest CGTase activity was 3.5 U/mL after 48-h fermentation, and the maximum biomass production was obtained in a 24-h fermentation (Fig. 3B). These results indicated that it was possible to increase the CGTase activity by 68%, using the optimized medium, in relation to the original basal culture medium. Another important point was that the CGTase activity on base medium after a 48-h fermentation was similar to that obtained on optimized medium after a 24-h fermentation. This shorter time fermentation for the optimized medium can compensate the increase of the medium components and can lead to a decrease in production costs, because the equipments and energy sources are used only half of time when compared with the basal medium for obtaining the same CGTase activity.

Other authors have successfully improved enzyme production, using RSM. Gawande et al *(9)* working with *B. firmus*, obtained the maximum CGTase activity of 7.05 U/mL after a 80-h fermentation. The optimum composition of the culture medium was found at the central point of the $2^3$ full-factorial design, made up of corn starch 21.0 g/L, yeast extract 23.0 g/L, and pharmamedia 22.0 g/L. According to the authors, these results led to an increase of about 20-fold in CGTase activity, compared with the basal medium. Gawande and Patkar *(8)* applied two-level fractional factorial designs to optimize medium composition, in the production of α-CD-specific CGTase from *K. pneumoniae* AS-22. The optimized medium resulted in ninefold higher production of CGTase than in the basal

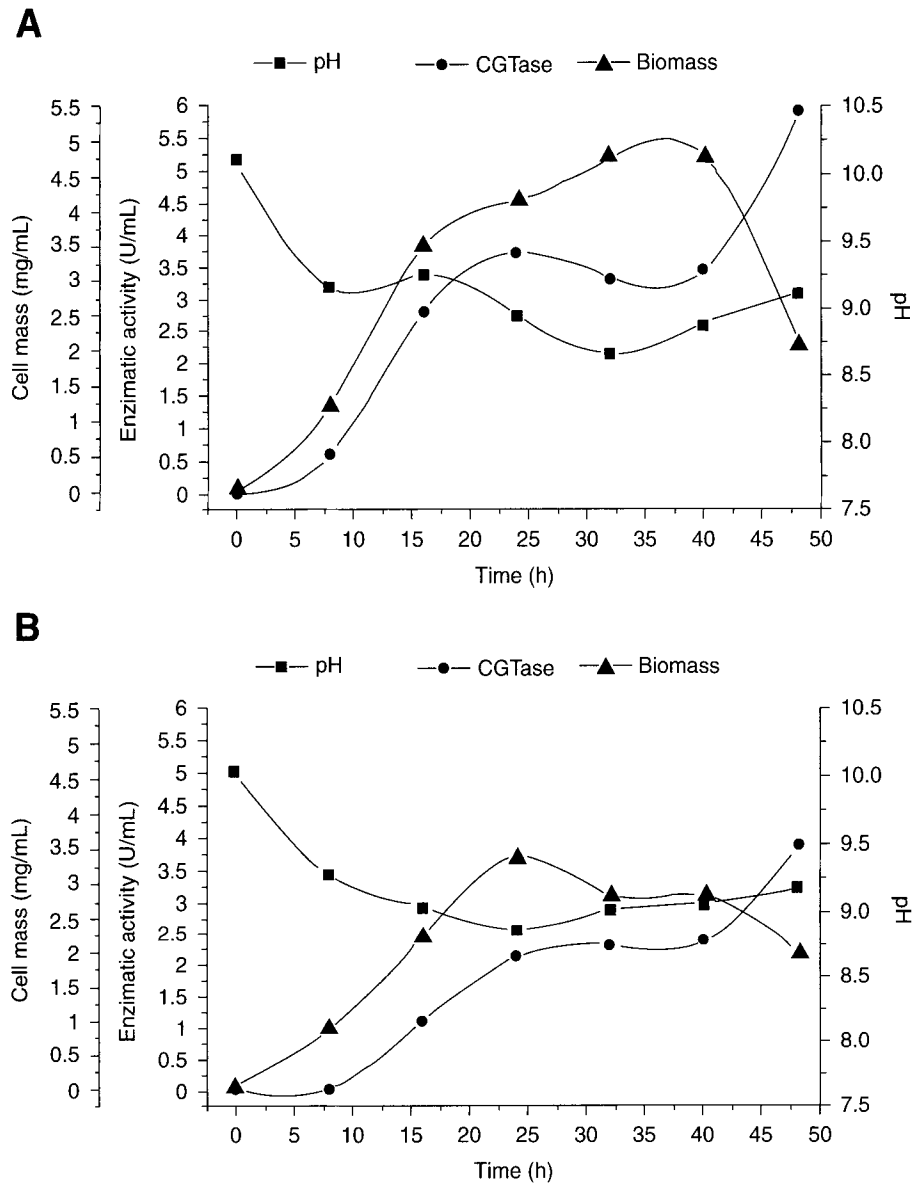


**Fig. 3.** CGTase production in **(A)** optimized medium and **(B)** basal medium by *B. clausii* strain E16 at 37°C. (—■—) pH; (—●—) enzymatic activity; (—▲—) biomass.

medium. The optimum composition of the nutrient medium was dextrin 49.3 g/L, peptone 20.6 g/L, yeast extract 18.3 g/L, ammonium dihydrogen orthophosphate 6.7 g/L, and magnesium sulfate 0.5 g/L. The CGTase production from *B. stearothermophilus* HR1 was analyzed through RSM, an optimized culture medium was performed, which was made up of sago starch 16.02 g/L, peptone from casein 20.0 g/L, $K_2HPO_4$ 1.4 g/L, $CaCl_2$ 0.2 g/L, and initial pH 7.54. The maximum CGTase activity obtained was 14.20 U/mL *(14)*. Ibrahim et al. *(13)* studied the optimal concentration of the culture medium for CGTase production from *Bacillus* sp. G1 using

a $2^5$ central composite design. In this case, the optimized medium increased the CGTase activity by 53% over the basal medium. The optimum composition of the culture medium was tapioca starch 40.0 g/L, peptone 20.0 g/L, $MgSO_4 \cdot 7H_20$ 4.0 g/L, and $Na_2CO_3$ 10 g/L at pH 9.9.

Comparing the literature results, in relation to U/g of substrate, it was observed that better CGTase production was obtained by *Bacillus* sp. G1 (1372.5 U/g of tapioca starch) followed by *B. stearothermophilus* HR1 (886.4 U/g of sago starch), *B. clausii* strain E16 (437.0 U/g of soluble starch), *B. firmus* (434.1 U/g of corn starch), and *K. pneumoniae* AS-22 (335.7 U/g of dextrin). So, better conditions for CGTase production from *B. clausii* strain E16 could be obtained, if other variables such as starch source, inoculum quantities, and time were optimized.

## Conclusion

A new CGTase producer was isolated and identified as *B. clausii* strain E16 and the compounds medium for better CGTase production was studied. The $2^4$ full-factorial central composite design, with independent variables soluble starch, peptone and yeast extract concentrations, and culture medium initial pH were used to optimize the culture medium composition for CGTase production from *B. clausii* strain E16. The optimized medium resulted in a more than 68% higher CGTase production, compared with that in the basal medium. Optimum conditions found in this work were: soluble starch 13.4 g/L, peptone 4.9 g/L, yeast extract 5.9 g/L, $K_2HPO_4$ 1.0 g/L, $MgSO_4 \cdot 7H_2O$ 0.2 g/L, and initial pH 10.1 wherein this pH was obtained using $Na_2CO_3$ 13.0 g/L sterilized separately. The study was carried out in shaker flasks at a 48-h fermentation. These results demonstrated that it is possible to apply statistical design to CGTase production, with a strategy RSM that is relatively simple, and saves both time and material.

## Acknowledgments

The authors thank FAPESP for financial support.

## References

1. Bender, H. (1986), *Adv. Biotechnol. Process.* **6,** 31–71.
2. Alves-Prado, H. F., Gomes, E., and DaSilva, R. (2002), *Bol. SBCTA.* **36,** 43–54.
3. Martin del Valle, E. M. (2004), *Process Biochem.* **39,** 1033–1046.
4. Hedges, A. R. (1998), *Chem. Rev.* **98,** 2035–2044.
5. Szejtli, J. (1997), *J. Mater. Chem.* **7,** 575–587.
6. Tonkova, A. (1998), *Enz. Microbial Technol.* **22,** 678–686.
7. Van der Veen, B. A., Uitdehaag, J. C. M., Dijkstra, B. W. E., and Dijkhuizen, L. (2000), *Biochim. Bioph. Acta* **1543,** 336–360.
8. Gawande, B. N. and Patkar, A. Y. (1999), *Biotechnol. Bioeng.* **64,** 168–173.
9. Gawande, B. N., Singh, R. K., Chauhan, A. K., Goel, A., and Patkar, A. Y. (1998), *Enz. Microbial Technol.* **22,** 288–291.
10. Ramakrishna, S. V., Saswathi, N., Sheela, R., and Jamuna, R. (1994), *Enz. Microbial. Technol.* **16,** 441–444.

11. Turnes, R. E. and Bahar, S. (1996), *Acta Científ. Venez.* **47,** 133–137.
12. Matioli, G., Zanin, G. M., and Moraes, F. F. (2002), *Appl. Biochem. Biotechnol.* **98–100,** 947–961.
13. Ibrahim, H. M., Yusoff, W. M. W., Hamid, A. A., Illias, R. M., Hassan, O., and Omar, O. (2005), *Process Biochem.* **40,** 753–758.
14. Rahman, R. A., Illias, R. M., Nawawi, M. G. M., Ismail, A. F., Hassan, O., and Kamaruddin, K. (2004), *Process Biochem.* **39,** 2053–2060.
15. Box, G. E. P., Hunter, W. G., and Hunter, J. S. (1978), *Statistics for Experimenters. An Introduction to Design, Data Analysis and Model Building.* John Wiley, New York.
16. Barros Neto, B., Scarminio, I. S., and Bruns, R. E. (1996), *Planejamento e Otimização de Experimentos.* 2nd ed., Editora da UNICAMP, Campinas.
17. Dey, G., Mitra, A., Banerjee, R., and Maiti, B. R. (2001), *Biochem. Eng. J.* **7,** 227–231.
18. Haltrich, D., Preiss, M., and Steiner, W. (1993), *Enz. Microbial. Technol.* **15,** 854–860.
19. Bocchini, D. A., Alves-Prado, H. F., Baida, L. C., Roberto, I. C., Gomes, E., and Dasilva, R. (2002), *Process Biochem.* **38,** 727–731.
20. Lee, S. L. and Chen, W. C. (1997), *Enz. Microbial. Technol.* **21,** 436–440.
21. Alves-Prado, H. F., Gomes, E. and DaSilva, R. (2002), *Brazilian J. Food Technol.* **98,** 189–196.
22. Sneath, P. H. A. (1986), In: Bergey's Manual of Systematic Bacteriology. Section 13, Williams &Wilkins, Baltimor, pp. 1105–1139.
23. Thompson, J. D., Higgins, D. G., and Gibson, T. J. (1994), *Nucleic Acid Res.* **22,** 4673–4680.
24. Nakamura, N. and Horikoshi, K. (1976), *Agric. Biol. Chem.* **40,** 1785–1791.
25. Nakamura, N. and Horikoshi, K. (1976), *Agric. Biol. Chem.* **40,** 753–757.
26. Mäkelä, M. J., Korpela, T. K., Puisto, J., and Laakso, S. V. (1988), *Agric. Food Chem.* **36,** 83–88.
27. Alves-Prado, H. F., Gomes, E., and DaSilva, R. (2006), *Appl. Biochem. Biotechnol.* **129–132,** 234–246.
28. Alves-Prado, H. F. (2000), *M.Sc. Dissertation,* UNESP, Rio Claro, Brazil, pp. 144.
29. Nielsen, P., Fritze, D., and Priest, F. G. (1995), *Microbiology* **141,** 1745–1761.
30. Myers, R. H. (1971), Response surface methodology. Allyn and Bacon, Boston.

0273-2289/1559–0291 (Online)/07/136–140/41–56/$30.00

# Purification and Characterization of a Cyclomaltodextrin Glucanotransferase From *Paenibacillus campinasensis* Strain H69-3

**Heloiza Ferreira Alves-Prado,[1,2] Eleni Gomes,[1] and Roberto da Silva*,[1]**

*[1]UNESP—State University of São Paulo, Biochemistry and Applied Microbiology Laboratory, Rua Cristóvão Colombo n 2265, 15054-000, São José do Rio Preto, SP, Brazil, E-mail: dasilva@ibilce.unesp.br; and [2]UNESP—State University of São Paulo, Biology Institute, Rio Claro, SP*

## Abstract

A cyclomaltodextrin glucanotransferase (E.C. 2.4.1.19) from a newly isolated alkalophilic and moderately thermophilic *Paenibacillus campinasensis* strain H69-3 was purified as a homogeneous protein from culture supernatant. Cyclomaltodextrin glucanotransferase was produced during submerged fermentation at 45°C and purified by gel filtration on Sephadex G50 ion exchange using a Q-Sepharose column and ion exchange using a Mono-Q column. The molecular weight of the purified enzyme was 70 kDa by sodium dodecyl sulfate-polyacrylamide gel electrophoresis and the p*I* was 5.3. The optimum pH for enzyme activity was 6.5, and it was stable in the pH range 6.0–11.5. The optimum temperature was 65°C at pH 6.5, and it was thermally stable up to 60°C without substrate during 1 h in the presence of 10 m*M* $CaCl_2$. The enzyme activity increased in the presence of $Co^{2+}$, $Ba^{2+}$, and $Mn^{2+}$. Using maltodextrin as substrate, the $K_m$ and $K_{cat}$ were 1.65 mg/mL and 347.9 μmol/mg·min, respectively.

**Index Entries:** CGTase characterization; CGTase purification; cyclomaltodextrin glucanotransferase; thermostable CGTase.

## Introduction

Cyclomaltodextrin glucanotransferase (CGTase; EC 2.4.1.19) is a member of the α-amylase family (family 13) of glycosyl hydrolase *(1)*. CGTase can also hydrolyze glucan chains in a manner similar to α-amylases, but differs in its ability to form cyclodextrins (CD) as reaction products. CDs are formed from starch molecules through intramolecular transglycosylation (cyclization) and can be made up of 6–8 glucan residues, α-, β-, and γ-CD, respectively. This enzyme is in fact multifunctional; besides cyclization reaction it

*Author to whom all correspondence and reprint requests should be addressed.

displays intermolecular transglycosylation (coupling and disproportionation) and hydrolytic activity on starch and CDs *(2–4)*. CDs are doughnut-shaped molecules with a hydrophilic outer surface and a relatively hydrophobic cavity. Owing to their ability to form inclusion complexes with many organic molecules, CDs have become increasingly useful in pharmacy, food, cosmetics, agriculture, analytical chemistry, and biotechnology. They can be used to capture flavors and odors, stabilize volatile compounds, improve the solubility of hydrophobic substances, and protect substances against undesirable modifications *(2–7)*.

CGTases are produced extracellularly by a variety of bacteria mainly by the alkalophilic, mesophilic, and thermophilic *Bacillus* genus *(4,8)*. However, other producers have also been reported such as *Klebsiella* sp. *(9,10)*, *Brevibacterium* sp. *(11)*, *Paenibacillus* sp. *(12–15)*, *Thermoanaerobacter* sp. *(16,17)*, *Thermoanaerobacterium* sp. *(18)*, *Thermococcus* sp. *(19)*, and *Thermoactinomyces* sp. *(20)*. Most of these CGTase producers are able to produce a mixture of CGTase types, mainly α-CD and/or β-CD.

As the majority of the CGTases studied are produced by mesophilic microorganisms, they possess low-thermostability. In the CD production process, therefore, it is necessary to add a thermostable α-amylase during the liquefaction step carried out at high-temperature (95–105°C). On completion of liquefaction, the stream is cooled to 50–55°C for the CD production by CGTase *(16)*. Thermostable CGTases would make it less necessary to reduce the temperature for CGTase action, and this would decrease the cost of final CD production. On the other hand, the high production cost of CGTase and CDs is considered the limiting factor in CD applications on an industrial scale. Research aimed at decreasing the cost of CGTase production is, therefore, necessary if commercial use of CDs is to become economically feasible. The search for a thermophilic CGTase producing microorganism with high-thermostability is thus of commercial interest.

We have isolated a new CGTase producer from soil cassava crop samples, which grows at 45°C and is classified as *P. campinasensis* strain H69-3 (henceforth referred to as H69-3). Although many studies have been carried out on detection of CGTase in different microorganisms, few reports have described CGTase from the alkalophilic thermophilic *P. campinasensis*. Therefore, in the present study we report its classification and the purification and characterization of its CGTase for the first time.

## Materials and Methods

### *Materials*

CDs (α-, β-, and γ-CD), maltodextrin, phenolphthalein, orange methyl, and bovine serum albumin were purchased from Sigma (St. Louis, MO). Yeast extract, peptone, and agar were obtained from Difco (Detroit, MI). Soluble starch and all other chemicals of analytical grade were obtained

from Merck (Darmstadt, Germany). Resins for enzyme purification were purchased from Amersham Pharmacia Biotech (Uppsala, Sweden).

## Microorganism Isolation and Identification

The bacterial strain H69-3 was isolated from soil cropped with cassava in São José do Rio Preto, SP—Brazil, as described in our previous work *(15)*. The phylogenetic properties of H69-3 were determined with the help of the *Centro Pluridisciplinar de Pesquisas Químicas, Biológicase Agrícolas* (Unicamp, Campinas, SP, Brazil) using molecular techniques of the sequencing and phylogenetic identification analysis of the 16S rRNA gene fragments. The 16S rDNA sequence was amplified by polymerase chain reaction (PCR), using as template the genomic DNA that was isolated off the H69-3 strain. The primers used in PCR were a p27 forward primer and a p1525 reverse primer that corresponded to a homologous conserved region of the 16S rRNA gene in bacteria.

The amplified PCR product was purified and sequenced directly on a MegaBACE 1000 (Amersham Biosciences) automatic sequenator. The forward primers p10 and 765 and reverse primers 782 and p1100 were used during sequencing. The 16S rDNA sequence was compared with known sequences on databases from Ribosomal Database Project (RDP, WI; http://www.cme.msu.edu/RDP/html) and GenBank (http://www.ncbi.nlm.nih.gov/). The 16S rDNA sequences related to H69-3 sequence were selected for phylogenetic analysis. The evaluative distance matrices were calculated with the Kimura model *(21)* and the phylogenetic tree was built using the *Neighbor-Joining* method *(22)* in accordance with analysis software from RDP.

## Assay of CGTase

CGTase activity was measured as β-CD forming activity based on phenolphthalein method *(23)* with slight modifications as described in Alves-Prado et al. *(20)*. One unit of CGTase activity was defined as the amount of enzyme that produced 1 μmol of β-CD per min.

## Protein Determination

Protein concentration was estimated according to the Hartree-Lowry method, using bovine serum albumin as standard *(24)*.

## Purification of CGTase

The culture medium used for CGTase production was based on the proposal by Nakamura and Horikoshi *(25)* with some modifications: soluble starch 10.0 g/L, peptone 5.0 g/L, yeast extract 5.0 g/L, $K_2HPO_4$ 1.0 g/L, $MgSO_4 \cdot 7H_2O$ 0.2 g/L, $Na_2CO_3$ 5 g/L (separately sterilized), pH 9.6.

The CGTase was produced by cultures of H69-3 in 500-mL Erlenmeyer flasks, containing 80 mL culture medium with soluble starch as substrate. The cultures were incubated on a rotary shaker at 45°C, for 48 h at 200 cycles per min. The cells were removed from the medium by centrifugation at 10000*g* for 15 min at 5°C. Supernatant containing crude CGTase was concentrated by ultrafiltration using the Pellicon® system (Millipore, Beldford, MA). The concentrated CGTase was subjected to gel filtration chromatography on a Sephadex superfine G-50 column (2.6 × 100 $cm^2$) that had been preequilibrated with 20 m*M* Tris-HCl buffer (pH 7.5), containing 20 m*M* NaCl. Elution was carried out by the same buffer at a flow rate of 0.3 mL/min at room temperature, and 5 mL fractions were collected using a fraction collector (Pharmacia Biotech Frac-100, Sweden). The CGTase-containing fractions were spin-concentrated using Centricon® YM10 tubes (amicon bioseparations, Millipore, Beldford, MA) with 10 kDa cutting membrane and purified to homogeneity on an ÄKTA purifier system (Pharmacia Biotech, Sweden). The following chromatographic steps were performed using a Q-Sepharose® Fast Flow column (5.0 × 10.0 $cm^2$) followed by a Mono-Q HR 5/5 column with bed volume of 1.0 mL (Pharmacia Biotech, Sweden) using 20 m*M* Tris-HCl buffer (pH 7.5). The purity of the CGTase was determined by sodium dodecyl sulfate-polyacrylamide gel electrophoresis (SDS-PAGE).

## Determination of Protein Molecular Weight

The molecular weight of the pure protein was estimated by SDS-PAGE according to Laemmli *(26)*. The SDS-PAGE was performed on a 10% homogeneous gel using the Mini-Cell electrophoresis apparatus (BioRad Laboratories, Richmond, CA). The gel was stained by means of the Blum silver-staining method *(27)*. BenchMarker™ Protein Ladder (Invitrogen) was used as standard.

## Activity Gel

The native gel was performed on a 10% homogeneous gel using the Mini-Cell electrophoresis apparatus (BioRad Laboratories) in accordance to Laemmli *(26)*, but without SDS. Part of the gel was stained by means of the Blum silver-staining method *(27)* and other part of this gel was incubated on soluble starch solution 1% overnight, rotating at 5°C and after this, the gel was stained with I-IK solution 1%.

## Isoelectric Focusing

Isoelectric focusing (p*I*) was performed in an Ettan IPGphor II two-dimensional electrophoresis apparatus (Amersham Biociences), using a strip holder with a p*I* scale from 3.0 to 10.0 for focusing and a 12% (w/v) acrylamide gel for the second dimension. During isoelectric focusing, the strip

holder was submitted to rehydration loading together with the enzyme sample for 12 h. It was subjected to different voltage steps, with the first step carrier in 500 Vh, the second step carrier in 1000 Vh, and the third step carrier in 12,500 Vh. After focusing, the strip holder was transferred to a polyacrylamide gel (SDS-PAGE) for the two-dimensional. SDS-PAGE was carried out at a constant voltage of 90 V for the first half hour and 220 V for the next 4 h at 25 mA. The gel was stained by the Blum silver-staining method *(27)*.

## Kinetic Parameters

The kinetic parameters were determined by incubating the pure enzyme in maltodextrin with DE 13.0–17.0 (Aldrich, Milwaukee, WI) (from 0 to 10 mg/mL) in 50 m*M* acetate buffer, pH 6.5, at 60°C, for 10 min under phenolphthalein assay conditions. The values of $K_m$ and $V_{max}$ were estimated by fitting the data to a Michaelis-Menten model using the GraFit program, version 5.0 (Erithacus Software).

## Effect of pH and Temperature on Activity and Stability of the Enzyme

The optimum pH of the pure CGTase was determined by measuring activity at 60°C using McIlvaine buffer (pH 2.5–8.0) and glycine–NaOH buffer, 0.1 *M* (pH 8.0–11.5). The reaction was carried out using the CGTase assay as previously mentioned. Optimal pH was the pH where the enzyme displayed its maximal activity, which was considered 100% activity. The optimum temperature of the pure enzyme was determined by incubating the reaction mixture of the CGTase assay in different temperatures, ranging from 5 to 90°C for 10 min. Optimal temperature was the temperature where the enzyme displayed its maximal activity, which was considered 100% activity.

The pH stability was determined by incubating the CGTase preparation without substrate in the same buffer systems used previously, at 25°C for 24 h. The remaining activity was assayed under standard conditions at 60°C. The temperature stability was checked by subjecting the enzyme, without substrate, at various temperatures at 5°C up to 90°C for 60 min and then cooling in ice before measuring the residual activity under standard conditions at 60°C and pH 6.5.

## Results and Discussion

### *Microorganism Isolation*

The bacterial strain H69-3 showed high CGTase activity and growth at 45°C. The strain H69-3 was identified according to 16S rDNA sequence comparisons and correlation with the physiological characteristics of this isolate. H69-3 has rod-shaped cells and Gram coloration was variable. During early growth phase Gram-positive cells could be observed, but

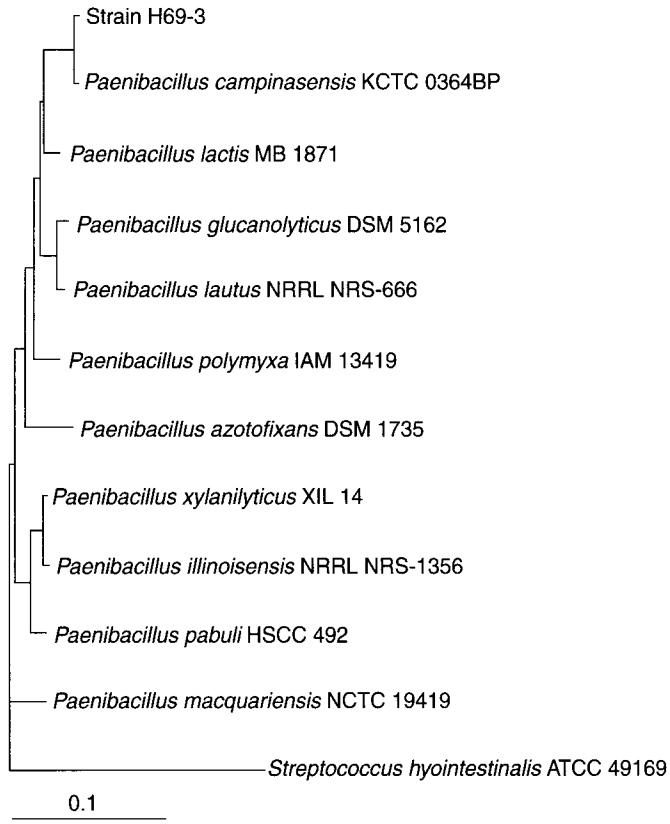


**Fig. 1.** Phylogenetic tree based on the 16S rRNA gene sequence, of the H69-3 strain and other related microorganisms. The *Neighbor-Joining* method was used and *Streptococcus hyointestinalis* was used as the out-group. The GeneBank accession numbers of the additional 16S rRNA sequences used are as follows: *P. campinasensis* KCTC 0364BP (AF021924); *P. lactis* MB 1871 (AY257868); *P. glucanolyticus* DSM 5162 (D78470); *P. lautus* NRRL NRS-666 (D78473); *P. polymyxa* IAM 13419 (D16276); *P. azotofixans* DSM 1735 (X77846); *P. xylanilyticus* XIL14 (AY427832); *P. illinoisensis* NRRL NRS-1356 (D85397); *P. pabuli* HSCC 492 (AB045094); *P. macquariensis* NCTC 10419 (X60625).

after 50 h of growth, only Gram-negative rods were visible. This microorganism was facultative anaerobic, positive for catalase reaction and nitrite to nitrate reduction as well as negative to oxidase reaction. The cellular growth at 30°C, 37°C, 40°C, 50°C, and 55°C was observed for nutrient medium in pH6.8. These physiological properties indicated the gender of the strain H69-3, but only with 16S rRNA was possible to identify correctly this strain. The partial 16S rRNA sequence of H69-3, with 892 pb revealed 99% similarity with sequences of the *P. campinasensis* strain 324 *(28)* and other *Paenibacillus* sp. strains included in RDP and GenBank. Similarity of 94 and 96% was found with other *Paenibacillus* sp., such as *P. lactis* and *P. pabuli*. Phylogenetic analysis and physiological characteristics confirmed the similarity found in databases and clearly grouped the strain H69-3 with *P. campinasensis* (Fig. 1). Based on these results, the studied

microorganism (strain H69-3) was classified as *P. campinasensis* strain H69-3. The partial 16S rDNA sequence has been deposited in the GeneBank and has been assigned the accession number DQ153080.

## CGTase Purification

After 50 h of fermentation, the supernatant from the *P. campinasensis* strain H69-3 culture was used for purification of CGTase in four steps. The supernatant containing crude enzyme was first concentrated by ultrafiltration and subsequently purified by gel filtration and anion exchange (Table 1). These steps resulted in a 115-fold purification with a yield of 13.3%, and specific activity of 8.1 U/mg of protein (Table 1). The purification steps resulted in one homogeneous band on a silver-stained SDS-PAGE (Fig. 2A). A native polyacrylamide gel for activity staining also gave the purified CGTase one single band in the presence of soluble starch (Fig. 2B).

Previously, CGTase purification from *Bacillus* sp. AL-6 was performed using starch adsorption chromatography and two DEAE–Sephadex A-50 chromatographies, with a yield of 14.4% and a 230-fold purification, similar to the yield *(29)*. In another study, CGTase from the *P. campinasensis* (*B. firmus*) strain 324 was purified by ion exchange- and affinity-chromatography resulting in a 26.6% yield and a 90-fold purification *(30)*. Finally, process chromatography was used to purify the CGTase from *P. illinoisensis* ST-12K using a DEAE-cellulose column and a Butyl-Toyopearl column, resulting in a 4.5-fold purification and a 27% yield *(13)*.

## Molecular Weight

The molecular weight of the purified CGTase was estimated by electrophoretic mobility under denaturing conditions to be 70 kDa (Fig. 2A). This molecular weight is in agreement with the majority of purified CGTase reported in literature, which is between 70–88kDa *(4,8–13,25,29–31)*. However, in some cases, CGTase has been reported to have a lower molecular weight, such as those from *B. lentus* (33 kDa) *(32)*, *B. coagulans* (36 kDa) *(33)*, and *Bacillus* sp. 1919 (42 kDa) *(34)*. On the other hand, CGTases with a higher molecular weight have also been reported, such as those from *B. agaradhaerens* (110 kDa) *(35)*, *B. licheniformis* (144 kDa) *(36)*, and *Thermoanaerobacter* sp. (103 kDa) *(16, 17)* (Table 2). The variation of the p*I* values among studied CGTases can be owing to adaptations from environmental properties of the screening place. Different environments can lead to genetic sequence changes of this enzyme during the evolutionary process *(40)*.

### *Isoelectric Focusing*

The p*I* of the purified CGTase was 5.3. The p*I* exhibited by this CGTase is slightly acidic, similar to CGTase from *B. stearothermophilus (37)*, which has a p*I* value of 5.0. Some CGTases have shown high acidic p*I* values, such as CGTase from *Brevibacterium* sp. *(11)* with a p*I* value of 2.8 and from

Table 1
Summary of Purification Results

| Step | Total volume (mL) | Total protein (mg) | Total CGTase activity (U) | Specific activity (U/mg) | Fold purification | Percent yield |
|---|---|---|---|---|---|---|
| Crude enzyme (supernatant) | 350.0 | 1393.0 | 91.0 | 0.07 | – | 100 |
| Concentration by ultrafiltration (Pelicon) | 40.0 | 316.0 | 87.2 | 0.28 | 4.0 | 95.8 |
| Gel filtration Sephadex G-50 | 123 | 32.0 | 49.2 | 1.54 | 22.0 | 54.1 |
| Ion exchange (Q-Sepharose) | 70 | 2.8 | 39.9 | 14.25 | 203.6 | 43.8 |
| Ion exchange (Mono-Q column) | 7.5 | 1.5 | 12.1 | 8.07 | 115.3 | 13.3 |

Enzymatic activity determined by phenolphthalein method.

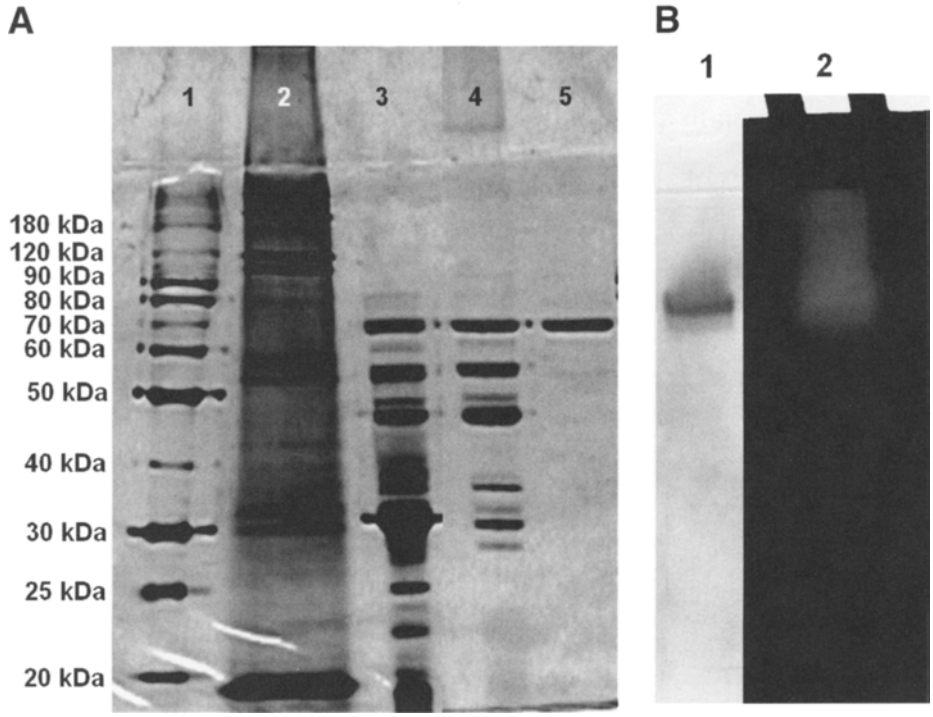


**Fig. 2.** CGTase from *P. campinasensis* strain H69-3 **(A)** determination of molecular weight on SDS-PAGE. Lane 1, molecular weight marker; lane 2, crude enzyme; lane 3, elution from gel filtration; lane 4, Q-Sepharose fast flow elution; and lane 5, purified CGTase (Mono-Q elution). **(B)** Native gel, 1: silver stained and 2: amylolytic activity I-KI stained.

Table 2
Comparison Between the Properties of CGTase From the *P. campinasensis* Strain H69-3 and From Some Other CGTase Producers

| Strain | Molecular weight (kDa) | Optimum temperature (°C) | Stability temperature (°C) | | Optimum pH | Stability pH | $K_m$ (mg/mL) | *p*I | References |
|---|---|---|---|---|---|---|---|---|---|
| | | | +$Ca^{+2}$ | –$Ca^{+2}$ | | | | | |
| Alkalophilic *Bacillus* sp. ATCC 21783 | 85 | 50 | 60 | 70 | 7.0 and 8.0–9.0 | 6.0–9.0 | – | – | *25* |
| *Bacillus* sp. AL-6 | 74 | 55–60 | 40 | – | 8.0 | 5.0–8.0 | – | – | *29* |
| *Bacillus* sp. 1919 | 42 | 55–60 | 50 | – | 4.0 | 5.0–8.0 | – | – | *34* |
| *Bacillus* sp. G1 | 75 | 60 | 60 | 70 | 6.0 | 7.0–9.0 | 0.15[a] | 8.8 | *31* |
| *B. autolyticus* 11149 | 68 | 60 | 40 | – | 5.0–6.0 | 5.0–9.0 | | 3.0–4.0 | *38* |
| *B. agaradhaerens* LS-3C | 110 | 55 | 30 | 40 | 9.0 | 5.0–11.4 | 18.0[b] and 21.2[c] | 6.9 | *35* |
| *B. circulans* E192 | 78 | 60 | – | 45 | 5.5–5.8 | 6.0–9.0 | 0.70[b] and 0.57[d] | 6.9 and 6.7 | *39* |
| *B. coagulans* | 36 | 65 | 65 | – | 6.5 | 5.0–10.0 | – | – | *33* |
| *B. lentus* | 33 | 45–50 | – | 55 | 6.5–7.5 | 6.5–8.5 | – | – | *32* |
| *B. firmus* (NCIM 5119) | 78 | 65 | 30 | – | 5.5–8.5 | 7.0–11.0 | 1.21[c] | – | *41* |
| *B. licheniformis* | 144 | – | 60 | – | 5.0–6.0 | 6.0–8.0 | – | – | *36* |
| *B. stearothermophilus* ET1 | 66.8 | 80 | 60 | 70 | 6.0 | 6.0–8.0 | – | 5.0 | *37* |
| *Brevibacterium* sp. n 9605 | 75 | 45 | 30 | 50 | 10.0 | 6.0–8.0 | – | 2.8 | *11* |
| *K. pneumoniae AS-22* | 72 | 45 | 35 | – | 7.0–7.5 | 5.5–9.0 | 1.35[c] | 7 and 3 | *10* |
| *Paenibacillus* sp. F8 | 72 | 50 | 40 | 50 | 7.5 | 6.0–8.0 | – | – | *12* |
| *Thermoactinomyces* sp. INMIA—A-561 | 64 | – | 70 | – | 6.0–7.0 | 5.5–8.5 | – | – | *20* |
| *Thermoanaerobacter* sp.-ATCC53627 | 103 | 95 | 80 | – | 5.0 | 5.0–6.7 | – | – | *16,17* |
| *P. campinasensis* H69-3 | 70 | 65 | 55 | 60 | 6.5 | 6.0–11.0 | 1.65[b] | 5.3 | This work |

[a]β-cyclodextrin.
[b]maltodextrin.
[c]Soluble starch.
[d]Wheat starch.

*B. autolyticus (38)* with a p*I* s value of 3.0 and 4.0. However, other CGTases have a high basic p*I*, such as that from *Bacillus* sp. G1 *(31)* with a p*I* of 8.8. There are also neutral p*I* CGTases, such as *B. agaradhaerens* LS-3C *(35)* with a p*I* value of 6.9, and *B. circulans* E192 *(39)* with p*I* values of 6.9 and 6.7 (Table 2).

## Kinetic Parameters

The $K_m$ and $V_{max}$ values obtained were 1.69 ± 0.39 mg/mL and 4.97 ± 0.30 μmol/min·mg, respectively. $K_m$ values ranging from 0.15 to 21.2 mg/mL and $V_{max}$ values ranging from 7.4 to 249 U/mg have previously been reported for few CGTases *(10, 30, 31, 35, 39, 41)*. However, only the *B. agaradhaerens* LS-3C *(35) and B. circulans* E192 *(39)* used maltodextrin as substrate. The $K_m$ of CGTase from *P. campinasensis* strain H69-3 was larger than *B. circulans* E192 (0.7 mg/mL) and smaller than CGTase form *B. agaradhaerens* LS-3C (18.0 mg/mL). As $K_m$ might be correlated with the affinity for substrate, by comparison it is possible to infer a good affinity of the CGTase of *P. campinasensis* strain H69-3 for maltodextrin. The $K_{cat}$ and $K_{cat}/K_m$ were calculated and it was 347.9 μ*M*/mg·min and 205.9 min/μmol, respectively. The $K_{cat}$ value exhibited by this CGTase was larger than those obtained by CGTases from *Klebsiella pneumoniae* AS-22 (249 μ*M*/mg·min) *(10)* and *B. firmus* (145.17 μ*M*/mg·min) *(41)*. However, here any conclusion might be obtained, as the used substrates were not the same.

## Effect of pH on Activity and Stability of the Enzyme

The activity CGTase was determined at varying pH values ranging from 2.5 to 11.5 at 60°C. The purified CGTase was highly active between pH values 5.5 and 7.0 with maximum activity at pH 6.5 in MacIlvaine buffer (Fig. 3). The optimum pH value suggests that, in order to effect the cyclization reaction, CGTase from the *P. campinasensis* strain H69-3 needs a pH near to neutral. This optimum pH was also noted for CGTase from *B. lentus (32)* and *B. coagulans (33)*. The pH stability was determined by incubating the crude CGTase on different pH values, ranging from 2.5 to 12.0 for 24 h at 25°C. Then, the residual activity was measured at standard activity conditions. The purified CGTase was found to be stable over a wide range of pH (6.0–11.0) after 24 h of incubation at 25°C (Fig. 3).

## Effect of Temperature On Activity and Stability of The Enzyme

The activity of pure CGTase was measured at temperatures between 30°C and 80°C at pH 6.5. The enzyme exhibited maximum activity at temperatures between 60°C and 65°C (Fig. 4). The effect of temperature on stability of pure CGTase was also investigated. The enzyme was incubated for 1 h at various temperatures (30–70°C) followed by measurement of residual activity under standard assay conditions. Hundred percent CGTase activity was maintained up to 55°C, indicating good thermal stability (Fig. 4). The

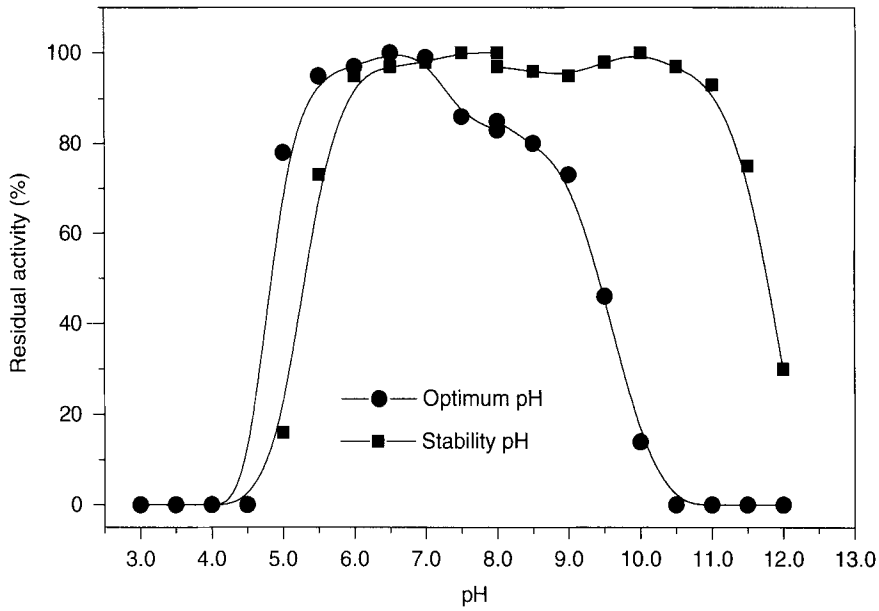


**Fig. 3.** Effect of pH on CGTase activity (—•—) and CGTase stability (—▪—) from the *P. campinasensis* strain H69-3. The buffers used were: MacIlvaine (pH 3.0–8.0) and glycine–NaOH (pH 8.0–11.5).

enzyme was completely inactive at 80°C. The thermal stability increased when the CGTase was incubated in the presence of the $Ca^{2+}$. About 90% of CGTase activity was maintained up to 60°C when it was incubated with 10 m*M* $CaCl_2$ (Fig. 5). Ion $Ca^{2+}$ has been used as enzyme stabilizer and these results were similar to that obtained by Chung *(37)* studying CGTase from *B. stearothermophilus* ET1.

## Effect of Metal Ions and Chemicals on CGTase Activity

The enzyme was incubated with a number of salts and reagents, at 5 m*M* and 1 m*M*, in 100 m*M* acetate buffer, pH 6.5 at 25°C for 60 min. A sample of the mixture was used to determine residual activity under standard assay conditions, while maintaining salt and reagent concentrations. The results are summarized in Table 3. Considering the presence of metallic ions and other reagents, the response of CGTase activity from the *P. campinasensis* strain H69-3 was similar to that reported for other CGTases *(29,35)*. This CGTase was strongly inhibited by $Ag^{1+}$, $Al^{3+}$, $Cr^{2+}$, $Cu^{2+}$, $Fe^{2+}$, $Fe^{3+}$, $Hg^{3+}$, $NH_4^{2+}$, $Sn^{2+}$, and β-CD. It was slightly inhibited by $Cd^{1+}$, $Pb^{2+}$, $Zn^{2+}$, $Zn^{3+}$, $Sr^{2+}$, SDS, and γ-CD with 20–70% of the activity. CGTase activity was not inhibited in the presence of $Mg^{2+}$, $K^{1+}$, $Ca^{2+}$, $Na^{1+}$, $Ni^{2+}$ ethylenediamine tetra acetic acid, phenylmethylsulfonyl fluoride, sodium *m*-arsenite, sodium azide, 2-mercaptoethanol, dithiothreitol, and α-CD and it was enhanced in the presence of $Co^{2+}$, $Ba^{2+}$, and $Mn^{2+}$.

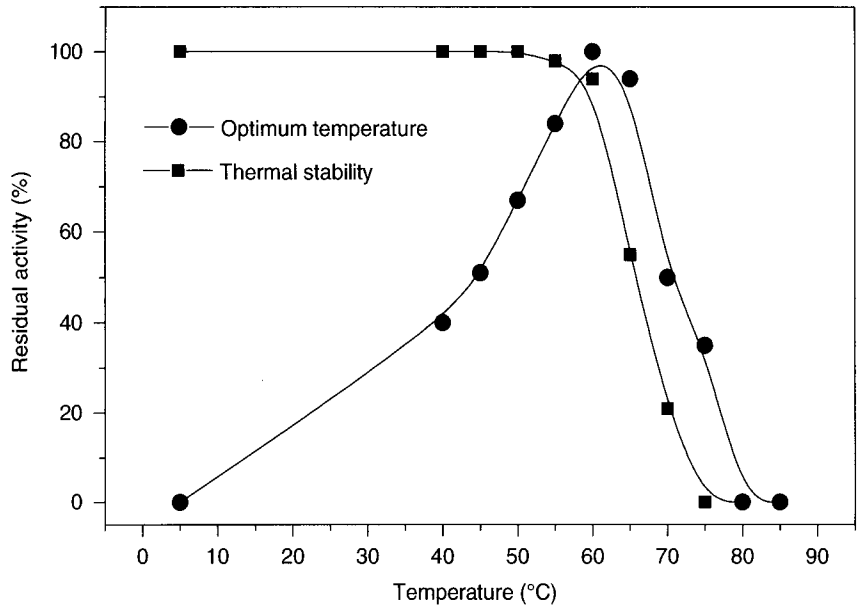


**Fig. 4.** Effect of temperature on CGTase activity (—•—) and CGTase stability (—▪—) from the *P. campinasensis* strain H69-3.

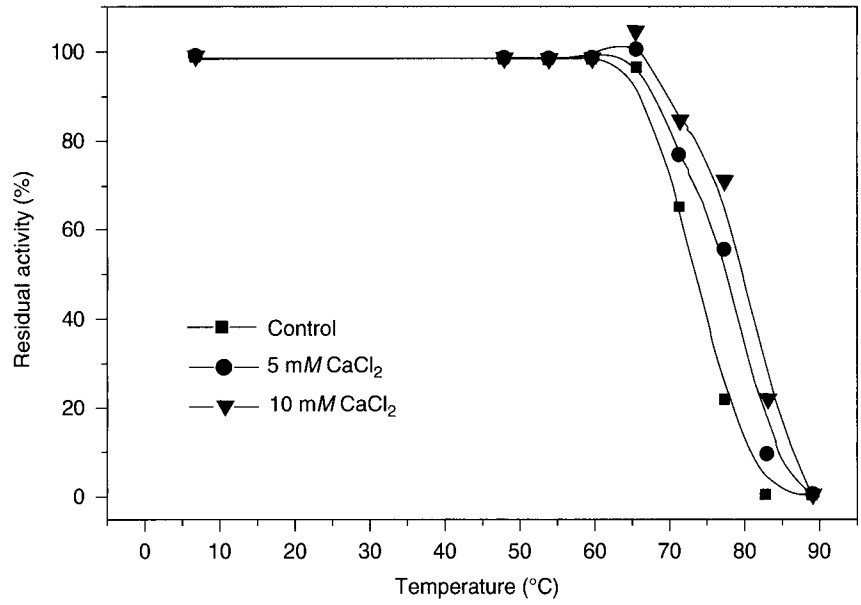


**Fig. 5.** Effect of $CaCl_2$ on temperature stability of CGTase from *P. campinasensis* strain H69-3. (—▪—) control, without $CaCl_2$; (—•—) 5 m*M* $CaCl_2$ and (—▲—) 10 m*M* $CaCl_2$.

Unlike our results, the activity of CGTases from *Bacillus* AL-6 *(29)* was not inhibited by $Fe^{2+}$; the same was reported from *P. campinasensis* strain 324 (*B. firmus*) *(30)*, *B. firmus (42)*, and *B. autolyticus (38)*. The activity was increased using the CGTase from *Brevibacterium* sp. *(22)* and *Bacillus* sp. G1

Table 3
Effects of various reagents on CGTase activity from *P. campinasensis* strain H69-3

| Reagent (1 m*M*) | Residual activity (%) |
|---|---|
| None | 100 |
| SDS[a] | 70.0 |
| EDTA[b] | 84.0 |
| PMSF[c] | 95.0 |
| Sodium azide | 96.5 |
| Sodium *m*-arsenite | 97.0 |
| 2-mercaptoethanol | 98.0 |
| Dithiothreitol | 106.5 |
| α-CD | 90.0 |
| β-CD | 0 |
| γ-CD | 69.0 |

[a] Sodium dodecyl sulfate.
[b]Ethylenediaminetetra acetic acid.
[c]Phenylmethylsulfonyl fluoride.

*(31)*. It has been reported that $Cu^{2+}$ has a significant inhibitory effect on CGTases from *Bacillus* AL-6 *(29)*, *B. firmus (42)*, *Brevibacterium* sp. *(11)*, and B. *agaradhaerens (35)*, whereas CGTases from *B. autolyticus (38)* and *P. campinasensis* strain 324 (*B. firmus*) *(30)* were not inhibited in presence of the $Cu^{2+}$ at 2 m*M*. Also, the CGTase activity from B. *agaradhaerens (35)*, *B. autolyticus (38)*, and *Brevibacterium* sp. *(11)* was maintained in presence of the $Zn^{2+}$, $Pb^{2+}$, and $Sr^{2+}$, unlike the CGTase from *P. campinasensis* strain H69-3. Metal ions such as $Hg^{2+}$, $Ag^{1+}$, $Zn^{2+}$, and $Cu^{2+}$ have been reported as inhibitors of thermostable α-amylases. As one of the mechanism of protein thermostabilization is by formation of disulfite bridges, the presence of cysteine residues are higher in themostable molecules. These metal ions ($Hg^{2+}$, $Ag^{1+}$, and $Cu^{2+}$) have affinity to the sulfhydryl groups. So, these ions inhibit the enzymatic activity of some proteins by oxidation of the functional cysteine residue groups *(43)*. The almost complete inhibition of CGTase activity from the *P. campinasensis* strain H69-3 by $Hg^{2+}$, $Ag^{1+}$, and $Cu^{2+}$ reinforces the hypothesis that the thiol group is essential for the enzymatic activity of the CGTase. About the CD type effect on the CGTase activity, the presence of β-CD and γ-CD has exhibited an inhibitory effect for the CGTase from *B. autolyticus (39)*. In the case of CGTase activity from B. *agaradhaerens (35)*, a slight increase in the presence of β-CD is reported. In common with the studied CGTase, the majority of the CGTase reported present stimulated activity in the presence of $Ca^{2+}$ that also has been reported to be a stabilizer of thermal denaturation *(11,12,21,30,35,38)*.

## Conclusions

The CGTase from new producer *P. campinasensis* strain H69-3 isolated from soil cassava crop was purified and characterized with molecular weight of 70 kDa, optimum pH at 6.5, and optimum temperature at 65°C. So, this bacteria *P. campinasensis* strain H69-3 proved to be a viable alternative microorganism for CGTase production. The moderate optimum temperature and thermostability of the purified CGTase would be advantageous in certain industrial applications.

## Acknowledgments

The authors are grateful to the *Fundação de Amparo à Pesquisa do Estado de São Paulo* (FAPESP) for its financial support. Acknowledgement is due to Dr. Peter James Harris for English-language revision of the text of this article.

## References

1. Henrissat, B. (1991), *Biochem. J.* **280,** 309–316.
2. Bender, H. (1986), *Adv. Biotechnol. Process* **6,** 31–71.
3. Szejtli, J. (1997), *J. Mater. Chem.* **7,** 575–587.
4. Tonkova, A. (1998), *Enzyme Microbial. Technol.* **22,** 678–686.
5. Szejtli, J. (1998), *Chem. Rev.* **98,** 1743–1754.
6. Martin del Valle, E. M. (2004), *Process Biochem.* **39,** 1033–1046.
7. Allegre, M. and Deratani, A. (1994), *J. Agroo Food Ind. Hi Technol.* January/February, 9–17.
8. Alves-Prado, H. F., Gomes, E., and DaSilva, R. (2002), *Bol. SBCTA.* **36,** 43–54.
9. Bender, H. (1985), *Carbohydr. Res.* **135,** 291–302.
10. Gawande, B. N. and Patkar, A. Y. (2001), *Enzyme Microbial. Technol.* **28,** 9–10.
11. Mori, S., Hirose, S., Oya, T., and Kitahata, S. (1994), *Biosci. Biotechnol. Biochem.* **58,** 1968–1972.
12. Larsen, K. L., Duedhal-Olisen, L., Christensen, H. J. S., Mathiesen, F., Pedersen, L. H., and Zimmermann, W. (1998), *Carbohydr. Res.* **310,** 211–219.
13. Doukyu, N., Kuwahara, H., and Aono, R. (2003), *Biosci. Biotechnol. Biochem.* **67,** 334–340.
14. Kaulpiboon, J. and Pongsawasdi, P. (2003), *J. Biochem. Mol. Biol.* **36,** 409–416.
15. Alves-Prado, H. F., Gomes, E., and DaSilva, R. (2006), *Appl. Biochem. Biotechnol.* **132–136.**
16. Starnes, R. L. (1990), *Cereal Foods World* **35,** 1094–1099.
17. Zamost, B. L., Nilsen, H. K., and Starnes, R. L. (1991), *J. Ind. Microbiol.* **8,** 71–82.
18. Wind, R. D., Libl, W., Buitelaar, R. M., et al. (1995), *Appl. Environ. Microbiol.* **61,** 1257–1265.
19. Tachibana, Y., Kuramura, A., Shirasaka, N., et al. (1997), *Appl. Environ. Microbiol.* **65,** 1991–1997.
20. Abelyan, V. A., Afyan, K. B., Avakyan, Z. G., Melkumyan, A. G., and Afrikyan, E. G. (1995), *Biochemistry* **60,** 1223–1229.
21. Kimura, M. (1980), *J. Mol. Evol.* **16,** 111–120.
22. Saitou, N. and Nei, M. (1987), *Mol. Biol. Evol.* **4,** 406–425.
23. Mäkelä, M. J., Korpela, T. K., Puisto, J., and Laakso, S. V. (1988), *Agric. Food Chem.* **36,** 83–88.
24. Hartree, E. F. (1972), *Anal. Biochem.* **48,** 422–427.
25. Nakamura, N. and Horikoshi, K. (1976), *Agric. Biol. Chem.* **40,** 1785–1791.
26. Laemmli, U. K. (1970), *Nature* **27,** 680–685.

27. Blum, H., Bier, H., and Gross, H. J. (1987), *Eletrophoresis* **8,** 93–99.
28. Yoon, J. -H., Yim, D. K., Lee, J. -S., et al. (1998), *Int. J. System. Bacteriol.* **48,** 833–837.
29. Fujita, Y., Tsubouchi, H., Inagi, Y., Tomita, K., Ozaki, A., and Nakanishi, K. (1990), *J. Ferment. Bioeng.* **70,** 150–154.
30. Yim, D. G., Sato, H. H., Park, Y. H. E., and Park, Y. K. (1997), *J. Ind. Microbiol. Biotechnol.* **18,** 402–405.
31. Sian, H. K., Said, M., Hassan, O., et al. (2005), *Process Biochem.* **40,** 1101–1111.
32. Sabioni, J. G. and Park, Y. K. (1992), *Starch/Stärke* **44,** 225–229.
33. Akimura, K., Yagi, T., and Yamamoto, S. (1991), *J. Fermen. Bioeng.* **71,** 322–328.
34. Abelyan, V. A., Avakyan, A. G., Melkumyan, A. G., Balayan, A. M., Uzunyan, L. V., and Gasparyan, A. V. (1992), *Biochem.* **57,** 285–291.
35. Martins, R. F. and Hatti-Kaul, R. (2002), *Enzyme Microbial Technol.* **30,** 116–124.
36. Aoki, H., Yu, E. K. C., and Misawa, M. (1988), Novel Cyclodextrin Glycosyltransferase and its use in Manufacturing Cyclodextrin. US Patent 87-35952, 27p.
37. Chung, H. J., Yoon, S. H., Lee, M. J., et al. (1998), *J. Agric. Food Chem.* **46,** 952–959.
38. Tomita, K., Kaneda, M., Kawamura, K., and Nakanishi, K. (1993), *J. Fermen. Bioeng.* **75,** 89–92.
39. Bovetto, L. J., Backer, D. P., Villette, J. R., Sicard, P. J., and Bouquelet, S. J. -L. (1992), *Biotechnol. Appl. Biochem.* **15,** 48–58.
40. Janecek, S. (2002) *Biologia. Bratislava.* **57,** 29–41.
41. Gawande, B. N., Goel, A., Patkar, A. Y., and Nene, S. N. (1999), *Appl. Microbiol. Biotechnol.* **51,** 504–509.
42. Higuti, I. H., Grande, S. W., Sacco, R., and Nascimento, A. J. (2003), *Brazilian Arch. Biol. Technol.* **46,** 183–186.
43. Vieille, C. and Zeikus, G. J. (2001), *Microbiol. Mol. Biol. Rev.* **65,** 1–43.

0273-2289/1559–0291 (Online)/07/136–140/57–66/$30.00

# Acetone Powder From Dormant Seeds of *Ricinus communis* L

*Lipase Activity and Presence of Toxic and Allergenic Compounds*

ELISA D. C. CAVALCANTI,[1] FÁBIO M. MACIEL,[2] PIERRE VILLENEUVE,[3] REGINA C. A. LAGO,[4] OLGA L. T. MACHADO,[2] AND DENISE M. G. FREIRE*,[1]

[1]*Federal University of Rio de Janeiro, Rio de Janeiro, Brazil, E-mail: freire@iq.ufrj.br;* [2]*UENF, Rio de Janeiro, Brazil;* [3]*CIRAD/AMIS, Montpellier, France; and* [4]*Embrapa Food Technology, Rio de Janeiro, Brazil*

## Abstract

The influence of several factors on the hydrolytic activity of lipase, present in the acetone powder from dormant castor seeds (*Ricinus communis*) was evaluated. The enzyme showed a marked specificity for short-chain substrates. The best reaction conditions were an acid medium, Triton X-100 as the emulsifying agent and a temperature of 30°C. The lipase activity of the acetone powder of different castor oil genotypes showed great variability and storage stability of up to 90%. The toxicology analysis of the acetone powder from genotype Nordestina BRS 149 showed a higher ricin (toxic component) content, a lower 2S albumin (allergenic compound) content, and similar allergenic potential compared with untreated seeds.

**Index Entries:** 2S albumin; castor seeds; lipase; ricin; *Ricinus communis;* acetone powder.

## Introduction

Lipases (glycerol ester hydrolase, enzyme comission [EC] 3.1.1.3) are defined as a group of enzymes that are capable of catalyzing the hydrolysis of long-chain triacylglycerols into glycerol and free fatty acids, although they can also utilize other substrates such as medium or short fatty acid esters. Because of the hydrophobic nature of their substrates, lipases generally act in an aqueous–organic interface. Apart from their hydrolytic activity, lipases may also present reverse activity (esterification and transesterification reactions) in water-restricted environments, such as organic solvents. Their capacity to carry out all these transformations with

*Author to whom all correspondence and reprint requests should be addressed.

a high chimio-, regio-, and enantio-specificity means that lipases have great potential as biocatalysts in technological applications, such as in detergents, foods, pharmaceuticals, oleochemicals, and other industries *(1,2)*.

Lipases are generally found in animals, plants, and microorganisms, but microbial enzymes have been studied the most and applied most to industrial processes. However, in recent years plant lipases have also attracted the attention of researchers. There still exists a huge diversity of plants to be explored and the discovery of lipases with different specificities and stability would extend these enzymes' range of application. Plant lipases generally exhibit a particular specificity, usually a substrate specificity (more pronounced than in microbial enzymes), and are a low-cost raw material. Most of the literature on plant lipases concerns oil seed lipases, of which the most studied seeds are probably from oats, colza, and castor seeds. Lipases from the dormant seed of the castor plant (*Ricinus communis*) could be an option of some interest for industrial applications, given that they are found in large quantities in the ungerminated seed, whereas lipases from oil seeds generally need the seed to start germinating for them to be synthesized, and the quantities produced are very small *(3,4)*. Additionally, the castor bean grows throughout Brazil, it is easy to cultivate and is attracting interest because of its oil, which presents a challenge in finding the best ways to exploit the seeds using the latest scientific and technological approaches.

The lipase activity of dormant castor seeds has been recognized for over a century. Lipases are found in association with the lipid body (small intracellular organelles that store the oil) membranes, and are probably anchored by their hydrophobic region close to the N-terminal end *(4,5)*. The lipase accounts for 5% of the total proteins in the lipid bodies and its molecular weight has been estimated at around 60 kDa *(6)*. Recently, Eastmond *(4)* cloned the lipase of the dormant castor seed with the purpose of clarifying the role this enzyme plays in starting germination; however, its physiological function is still unclear and a new hypothesis is that it might be involved in defending the seed against parasites.

The presence of compounds with a high-toxicity (ricin) and pronounced allergenicity (2S albumin isoforms) *(7,8)* in castor seeds should be taken into account whenever industrial uses are planned for castor seed derivatives, including lipid biotransformation. Ricin is the most lethal of the toxins present in castor cake; it is a member of the family of ribosome-inactivating proteins constituted of two polypeptide chains: the A-chain hydrolyses a conserved region of the 28S rRNA, blocking protein synthesis and bringing about cell death, whereas the B-chain exhibits lectin properties by which the toxin is endocyted *(8,9)*. The castor seed allergen is a non-toxic and unusually stable protein belonging to the 2S albumin class, which exhibits an exceptional capacity to enhance individuals' sensitivity to small concentrations of dust from castor seeds or castor cake *(7)*. The aim of this work was to characterize the lipase activity present in dormant castor seed

acetone powder and to evaluate the acetone treatment for inactivating toxic and allergenic compounds. The castor oil genotypes with the greatest potential as sources of lipases were also selected.

## Materials and Methods

### *Castor Seeds*

The castor bean seeds were supplied by Embrapa Cotton Research Center in Campina Grande, Brazil, and stored at 4°C until use.

### *Extraction of the Acetone Powder*

One hundred and fifty milliliter acetone at 4°C was added to 10.0 g seeds and the mixture was blended (Turmix blender; ARNO) and sieved to obtain particles smaller than 500 μm. These were washed with 300 mL acetone at 4°C and incubated with 150 mL acetone for 16 h. After incubation they were washed with 150 mL acetone. The fat-free powder was left in an open flask for 24 h to complete the removal of the residual acetone and then stored at 4°C until use.

### *Lipase Assay*

Lipase activity was determined by adding 90.0 mg acetone powder to 10 mL emulsion consisting of tributyrin* (5% [w/v]), Triton X-100* (25% [w/v]), and acetate buffer, 0.05 *M*, pH 4.0 (50% [v/v]). This was incubated at 37°C* for 3, 5, and 7 min under agitation (200 rpm). The reactions were stopped by adding 20 mL ethanol and the fatty acids were extracted under agitation (200 rpm) for 10 min and titrated until the end point (pH 11.0) with a NaOH solution (0.04 *N*). The blank assays were performed by adding the acetone powder after the ethanol had been added. The activity (U) was calculated from the α of the graph (μmol free fatty acids vs reaction time), which resulted in the specific activity (U/g acetone powder). One lipase activity unit (U) was defined as the amount of enzyme that produced 1 μmol fatty acid per min under the assay conditions. The reactions were performed in triplicate.

### *Effect of Different Factors on Lipase Activity*

The assays were carried out as previously described except when evaluating the influence of pH.

- *Temperature:* 25, 30, 35, 40, 45, and 50°C.
- *Type of emulsifier:* Triton X-100 (25% [w/v]) and gum arabic (5% [w/v]); the reaction times were 10, 20, 30, and 40 min.
- *Type of substrate:* olive oil, sunflower oil, castor oil (the oils were from local stores), trycaprylin and tributyrin (purchased from Sigma); reaction emulsions contained 10% (w/v) substrate.

*These conditions were changed in some assays.

- *Comparison among different genotypes:* acetone powder from castor genotypes Nordestina BRS 149, Brejeira CNPAM 93-168, CSRN 393, Pernambucana SM-5, and CSRD-2.
- Storage stability: acetone powder was stored for 7 mo at 4∞C before use.

Two experiments were performed to evaluate the influence of pH.

- Hydrolysis catalyzed by the acetone powder: ten milliliter sunflower oil was incubated with 50.0 mg acetone powder in 10-mL buffer (acetate pH 4.0 or phosphate pH 7.2) at 50∞C for 68 h. The blank assays were performed by incubating the oil and buffer solution only.
- *Autohydrolysis:* the action of the endogenous lipase on the seed oil was verified by incubating 1 g ground seed with 10-mL buffer (acetate pH 4.0 or phosphate pH 7.2) at 50°C for 1 h under agitation. The control or blank assay was performed with ground seeds and no addition of a buffer. The thin-layer chromatography (TLC) of the sunflower oil reactions (eluted with 70/30/1 hexane/diethyl ether/acetic acid) and castor seed oil reactions (eluted with 40/60/1 hexane/diethyl ether/acetic acid) were visualized by spraying the TLC plate with a (1 : 1) saturated solution of cupric sulphate : phosphoric acid 85%, followed by 5 min at 180°C.

## *Determination of Toxic and Allergenic Compounds*

In these experiments untreated Nordestina BRS 149 seed and acetone powder were compared.

### Determination of 2S Albumin Content

3.2 mL water at 80°C was added to 16.0 mg acetone powder or ground castor seed and was incubated at 60°C for 6 h under agitation. After decantation, 500 µL from the upper layer was removed and submitted to gel-filtration chromatography using a 50 × 1.5 $cm^2$ Sephadex G-50 column, eluted with trifluoroacetic acid (TFA) 0.1%, at 0.7 mL/min. 200 µL was taken from the fraction containing 2S albumin and injected into the C18 reverse phase chromatography column. The sample was eluted using a solvent gradient consisting of solvent A (TFA 0.1%) and solvent B (acetonitrile 80% and TFA 0.1%): 0–10 min 0% of B; 10–40 min 0 to 80% of B; 40–45 min 80% of B; 50–55 min 80 to 0% of B.

### Immune-Detection of 2S Albumin

The fractions containing 2S albumin that originated from the reverse phase chromatography were concentrated 15-fold and 10 µL of this concentrate was spotted on a nitrocellulose membrane using 2% milk powder as a blocker. After exhaustive washing, an anti-2S albumin rabbit antibody (dilution 1 : 500) and a secondary antibody were added. The primary antibody was not added to the negative control so that any unspecific reactions could be observed.

### Evaluation of Allergenic Properties

The mast cells used came from Wistar rats, which were put down by $CO_2$ asphyxia. The peritoneum cavity was washed with 20 mL Dulbecco's Modified Eagle Medium containing heparin, and 15 mL was incubated in a Petri dish at 37°C for 30 min, after which time 2/3 of the upper phase was discarded. The mast cells (100 µL) resulting from sedimentation in the Petri dish were treated with:

1. Only the preimmune rat serum.
2. Only the anti-2S albumin serum.
3. Anti-2S albumin serum and 2S albumins (10 µg/mL).
4. Negative control (without any treatment).

The pool of IgE obtained from immunized RA/thor rats was diluted at 1 : 100 in the mast cell suspension and subsequently incubated at 37°C for 1 h. In order to observe degranulation, 10 µL cell suspension was incubated for 15 min with 10 µL of a solution containing 0.1% toluidine blue, 10% formaldehyde, and 1% acetic acid at pH 2.8. The count of whole and damaged cells was performed with a microscope using a Neubauer (BOECO, Germany) chamber.

### Determination of Ricin Content

Sixteen milligrams acetone powder or ground castor seed was dissolved in 3.2 mL deionizer and distilled water and incubated at 80°C for 4 h under stirring and a further 16 h at room temperature. The proteins were analyzed in 12% (w/v) SDS-polyacrylamide gel (SDS-PAGE) according to the methodology described by Laemmli *(10)*. Sample preparation: 40 µL sample buffer containing SDS (10%) and β-mercaptoethanol (5%) was added to 80 µL protein extract, and 35 µL of this mixture was used to run the SDS-PAGE.

## Results and Discussion

### *Effect of Different Factors on Lipase Activity*

Acetone powder of genotype Nordestina BRS 149 was used to study the influence of pH, emulsifier type, substrate type, and temperature on the lipase activity of dormant castor seeds.

### Influence of pH

Figure 1A shows the TLC of hydrolysis conducted in acid and neutral reaction media by the acetone powder on sunflower oil. The results for the reaction at pH 4.0 (lane b) show the hydrolysis products: fatty acids (retention factor [Rf] = 0.76) and partial triacylglycerols (Rf 0.60, Rf 0.50, and Rf 0.14). At pH 7.2 (lane c), no reaction took place so the pattern was much the same as for the starting oil (lane a). This result is in agreement with Eastmond *(4)* who only found significant activity from cloned dormant castor seed lipase at pH 3.5–5.0. The same pH influence was observed for autohydrolysis (Fig. 1B). The reaction at pH 4.0 (lane c) shows fatty acids

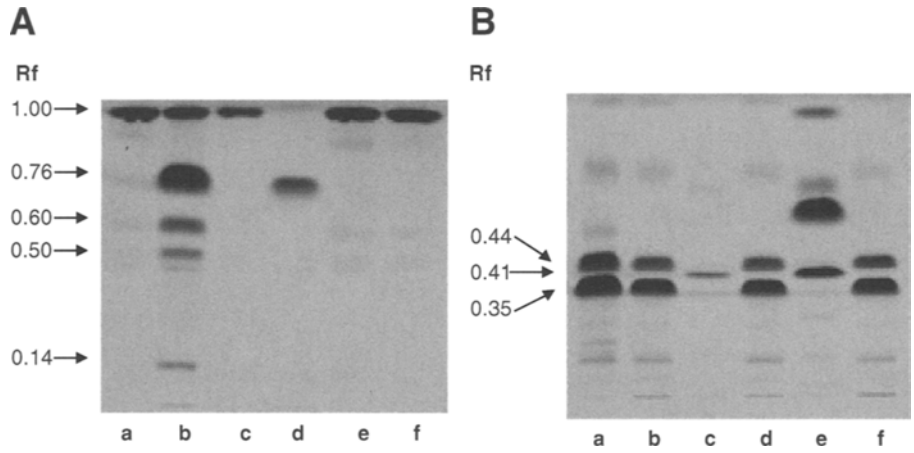


**Fig. 1. (A)** TLC of sunflower oil hydrolysis by acetone powder in neutral and acid media: (a) sunflower oil, (b) hydrolysis at pH 4.0, (c) hydrolysis at pH 7.2, (d) standard fatty acid, (e) negative control at pH 4.0, and (f) negative control at pH 7.2. **(B)** TCL of autohydrolysis in neutral and acid media: (a) commercial castor oil, (b) extracted castor seed oil, (c) hydrolysis at pH 4.0, (d) hydrolysis at pH 7.2, (e) reference sample of ricinoleic acid (Rf 0.41), and (f) negative control of ground seed hydrolysis.

(Rf 0.41), but the reaction at pH 7.2 (lane d) only shows the seed oil triacylglycerols (Rf 0.44 and Rf 0.35), as does the starting oil (lane b).

### Influence of Emulsifier Type

Considerable lipase activity was observed of the acetone powder on tributyrin (5% [w/v]) emulsified with gum arabic (5% [w/v]) or Triton X-100 (25% [w/v]): 139 ± 6 U/g and 220 ± 7 U/g, respectively. The almost twice as high-activity obtained with Triton X-100 may have been caused by alterations to the substrate aggregation state and/or changes to the enzyme's structure *(11)*. One hypothesis is that the lipase's capacity to anchor to the interface may be greater because of the lower interfacial tension of emulsions prepared with Triton X-100 *(12)*, or this lower tension may cause a larger interfacial area that makes a greater amount of lipid available for lipase activity. Some enzymes, not just lipases, have been reported to be activated by triton-X 100 *(13–15)*, possibly by molecular structural changes to a more compact protein *(14)*. The result could also be associated to the composition of the emulsifiers. For example, higher lipase activity has been reported in the presence of nonionic emulsifiers (like Triton X-100) than with ionic emulsifiers (like gum arabic) *(15)*, and castor seed lipase seems to be partially inhibited by some ions *(16)* present in gum arabic (the gum is a plant exudate and has no fixed composition) *(17)*.

### Influence of Substrate Type

The lipase activity of acetone powder with different substrates (10% [w/v] substrate emulsified with 25% [w/v] Triton X-100) was: olive oil

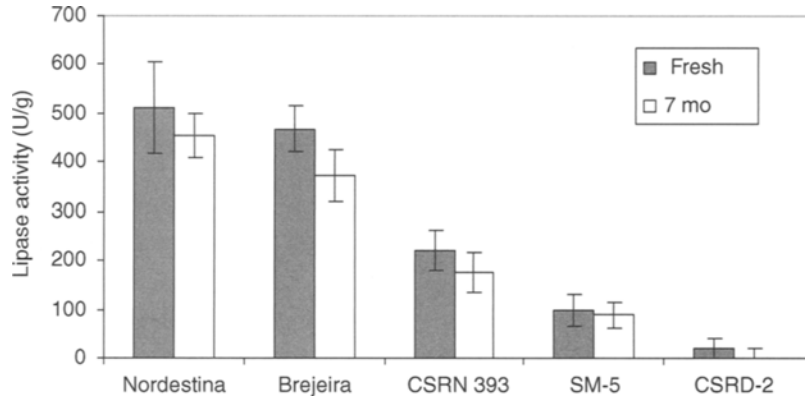


**Fig. 2.** Lipase activity of the fresh acetone powder from different castor genotypes and after storage for 7 mo at 4°C. Reactions were conducted using tributyrin (5% [w/v]) emulsified with Triton X-100 (25% [w/v]) in a buffer, pH 4.0, at 37°C, catalyzed by acetone powder from the different castor genotypes.

28 ± 3 U/g, sunflower oil 24 ± 2 U/g, castor oil 28 ± 2 U/g, tricaprylin 56 ± 7 U/g, and tributyrin 811 ± 54 U/g. The lipase exhibited a marked specificity for triacylglycerols formed by shorter chain fatty acids such as tributyrin (C4). As reported for *Geotrichum candidum* lipase, the chimio-specificity could be attributed to a few aminoacid residues both at the entrance and at the bottom of the active site cavity *(18)*. However, some authors believe that greater lipase activity on a smaller substrate may be caused by the increased water solubility of these short chain compounds, which would create a larger interfacial area and a less pronounced inhibition by products because the free fatty acids would have a stronger tendency to go to the aqueous phase than those of medium and long chains *(19)*.

### Influence of Temperature

The lipase activity of the acetone powder (5% [w/v] tributyrin with 25% [w/v] Triton X-100) was higher in the 25 (429 ± 9 U/g) to 35°C (368 ± 6 U/g) range, and the optimal temperature was 30°C (429 ± 9 U/g). The higher temperatures resulted in lower activities: 216 ± 5 U/g at 40°C; 57 ± 4 U/g at 45°C; and not detectable activity at 50°C.

## *Lipase Activity of Different Castor Genotypes and Storage Stability*

The lipase activity presented by the acetone powders from the different castor genotypes (Fig. 2) shows a great variation (96%) among them. This pronounced variation in lipase activity among different genotypes has also been observed for other plants, such as *Carica papaya* latex (92%) *(20)* and palm fruit (70%) *(21)*. The most promising castor genotypes as sources of dormant seed lipases were Nordestina BRS 149 (511 ± 63 U/g) and Brejeira CNPAM 93-168 (468 ± 47 U/g) (Fig. 2). After the acetone powders had been stored for 7 mo at 4°C, their remaining lipase activity (Fig. 2) was

Table 1
Ricin Content, 2S Albumin Content, and Allergenic Properties of Acetone Powder and Untreated Castor Seed of Genotype Nordestina BRS 149

| Material | Ricin (%)[a] | Albumins 2S (%)[a] | Mast cells degranulation (%)[b] |
|---|---|---|---|
| Castor seed | 0.85 | 2.1 | 43 |
| Acetone powder | 2.15 | 0.7 | 45 |

[a]gram per 10.0 g of material.
[b]number of mast cells degranulated per 100 mast cells.

80–90% of the fresh powders, except for genotype CSRD-2, which lost all its activity (*22*).

### *Toxic and Allergenic Compounds in Acetone Powder*

The ricin protein was isolated by water extraction and gel-filtration chromatography then detected by SDS-PAGE (Table 1); 0.85% (gram per 10.0 g of material) content was found in whole seeds and 2.15% in acetone powder. The higher toxin concentration found in acetone powder may be owing to the elimination of the oil from the seed (about 50% of the seed mass). However, investigations into acetone powder toxicity are recommended because the ricin molecule could be inactive yet present. The 2S albumin was isolated by gel-filtration and reverse phase chromatography (Table 1) and its content dropped by 2.1 to 0.7%. This reduction was confirmed by immune-blot analysis (data not shown). Castor bean allergens demonstrate extreme stability and there are few methodologies for removing the allergen from the cake. Recently, Kim (*23*) proposed a drastic heat- and NaOH- or NaOCl-based treatment to reduce antigenic activity, so the acetone treatment proposed here could be another option. The biological assays to evaluate the allergenic properties of acetone powder based on mast cell degranulation presented very similar degranulation percents to untreated castor seeds (approx 43%) (Table 1).

## Conclusions

The acetone powder from dormant seeds of *R. communis* contains a lipase that is only active in an acid pH. This enzyme activity is stimulated by the Triton X-100 emulsifier, and has a marked specificity for short-chain substrates and a pronounced variability among castor genotypes. The acetone powder also has good storage stability. The ricin content was higher in acetone powder. However, a toxicity investigation is needed to evaluate whether the protein is still in its active form. Given that 2S albumins are stable proteins, and that inactivation treatments have not yet been described, a reduction of their level by acetone treatment could be a promising technique for eliminating these allergenic proteins.

## Acknowledgments

The financial support from CNPq, FAPERJ and Capes, and the castor seeds donated by Rosa M. M. Freire from Embrapa Algodão are gratefully acknowledged.

## References

1. Jaeger, K. -E. and Eggert, T. (2002), *Curr. Opin. Biotechnol.* **13(4),** 390–397.
2. Freire, D. M. G. and Castilho, L. R. (2000), *Rev. Bras. Farm.* **81(1–2),** 48–56.
3. Villeneuve, P. (2003), *Eur. J. Lipid Sci. Technol.* **105(6),** 308–317.
4. Eastmond, P. J. (2004), *J. Biol. Chem.* **279(44),** 45,540–45,545.
5. Ory, R. L., Yatsu, L. Y., and Kircher, H. W. (1968), *Arch. Biochem. Biophys.* **123(2),** 255–264.
6. Altaf, A., Ankers, T. V., Kaderbhai, N., Mercer, E. I., and Kaderbhai, M. A. (1997), *J. Plant Biochem. Biotechnol.* **6(1),** 13–18.
7. Machado, O. L. T., Marcondes, J. A., Souza-Silva, F., et al. (2003), *Allergologie* **26(2),** 45–51.
8. Olsnes, S. and Kozlov, J. V. (2001), *Toxicon* **39,** 1723–1728.
9. Mantis, N. J. (2005), *Adv. Drug Delivery Rev.* **57,** 1424–1439.
10. Laemmli, U. K. (1970), *Nature* **227(5259),** 680–684.
11. Peters, G. H. (2002), *Colloids Surf. B: Biointerfaces* **26(1–2),** 84–101.
12. Tiss, A., Carrière, F., Douchet, I., Patkar, S., Svendsen, A., and Verger, R. (2002), *Colloids Surf. B: Biointerfaces* **26(1–2),** 135–145.
13. Helistö, P. and Korpela, T. (1998), *Enzyme Microb. Technol.* **23(1–2),** 113–117.
14. Yoon, S. H. and Robyt, J. F. (2005), *Enzyme Microb. Technol.* **37,** 556–562.
15. Thakar, A. and Madamwar, D. (2005), *Process Biochem.* **40(10),** 3263–3266.
16. Moulé, Y. (1953), *Oléagineux* **8,** 561–563.
17. Verbeken, D., Dierckx, S., and Dewettinck, K. (2003), *Appl. Microbiol. Biotechnol.* **63,** 10–21.
18. Hellyer, S. A., Chandler, I. C., and Bosley, J. A. (1999), *Biochim. Biophys. Acta.* **1440(2–3),** 215–224.
19. Enujiugha, V. N., Thani, F. A., Sanni, T. M., and Abigor, R. D. (2004), *Food Chem.* **88(3),** 405–410.
20. Caro, Y., Villeneuve, P., Pina, M., Reynes, M., and Graille, J. (2000), *J. Am. Oil Chem. Soc.* **77(8),** 891–901.
21. Sambanthamurthi, R., Oo, K. -C., and Parman, S. -H. (1995), *Plant Physiol. Biochem.* **33(3),** 353–359.
22. Kim B. K. (2006), *Food Sci. Biotech.* **15 (3),** 441–446.

0273-2289/1559-0291 (Online)/07/136–140/67–80/$30.00

# Immobilization of *Candida antarctica* Lipase B by Covalent Attachment to Green Coconut Fiber

ANA I. S. BRÍGIDA,[1] ÁLVARO D. T. PINHEIRO,[1] ANDREA L. O. FERREIRA,[1] GUSTAVO A. S. PINTO,[2] AND LUCIANA R. B. GONÇALVES*,[1]

[1]*Universidade Federal Do Ceará, Departamento De Engenharia Química, Campus Do Pici, Bloco 709, 60455-760, Fortaleza, CE—Brazil, E-mail: lrg@ufc.br; and* [2]*Embrapa Agroindústria Tropical, Caixa Postal: 3761, 60511-110, Fortaleza, CE—Brazil*

## Abstract

The objective of this study was to covalently immobilize *Candida antarctica* type B lipase (CALB) onto silanized green coconut fibers. Variables known to control the number of bonds between enzyme and support were evaluated including contact time, pH, and final reduction with sodium borohydride. Optimal conditions for lipase immobilization were found to be 2 h incubation at both pH 7.0 and 10.0. Thermal stability studies at 60°C showed that the immobilized lipase prepared at pH 10.0 (CALB-10) was 363-fold more stable than the soluble enzyme and 5.4-fold more stable than the biocatalyst prepared at pH 7.0 (CALB-7). CALB-7 was found to have higher specific activity and better stability when stored at 5°C. When sodium borohydride was used as reducing agent on CALB-10 there were no improvement in storage stability and at 60°C stability was reduced for both CALB-7 and CALB-10.

**Index Entries:** Coconut fiber; covalent attachment; enzyme immobilization; lipase; hydrolysis; esterification.

## Introduction

Lipases (triacylglycerol ester hydrolases, E.C. 3.1.1.3) catalyze both the hydrolysis and synthesis of esters from glycerol and long-chain fatty acids *(1)*. They catalyze interesterification, aminolysis, and thiotransesterification reactions *(2)*. Industrial applications of lipases include food processing, detergent formulations, and the synthesis of fine chemicals *(3)*. The use of immobilized enzymes provides for several advantages such as enzyme recycle or reuse and reduced cost. Therefore, many methods have been used to immobilize lipases, such as adsorption *(4)*, covalent attachment *(5)*, and chelation *(4)*. The multipoint attachment of proteins involves

*Author to whom all correspondence and reprint requests should be addressed.

several covalent attachments between one molecule of enzyme and the activated support. Attachment on a solid support should increase the rigidity of the immobilized enzyme molecules, making them more resistant to small conformational changes induced by heat, organic solvents, denaturing agents, and so on. To be successful the support surface should be complementary to that of the enzyme molecule. Not all supports or methods of activation offer the same possibilities to force an intense covalent multipoint attachment and in some conditions the immobilized enzyme can be less stable than the soluble one *(6)*.

Covalent immobilization is based on the retention of enzymes to support surfaces by covalent bonds between functional groups of the enzymes and reactive groups on the support *(7)*. The majority of supports must be activated before immobilization making the technique more expensive than simple adsorption *(4,7)*. Biocatalysts that can be covalently attached are usually more stable and resistant to extreme conditions (pH range and temperature). This stability and resistance are very important characteristics for industrial biocatalysts *(8)*. Lipase immobilization on supports activated with 3-glycidoxypropyltrimethoxysilane ([GPTMS] Sigma-Aldrich Chemical Co, St. Louis) (a silane coupling agent) occurs through a reaction between glyoxyl (aldehyde) groups, present on the support, and amines groups from the enzyme. As a consequence of the amine–aldehyde reaction, Schiff's bases between the enzyme and support are formed. At neutral pH, the reactivity of enzyme lysine residues is very low because of their $pK_a$ (around 10.5). Thus, the covalent attachment under these conditions is said to be one-point. However, at pH 10.0, the multipoint covalent attachment is possible because of the increase in the lysine residues reactivity, and consequently, a larger number of Schiff's bases are formed *(9,10)*.

Considering the high cost of some available commercial support matrixes, studies have been intensified in order to obtain cheaper supports. Some articles have reported the use of agroindustrial wastes as an immobilization matrix for α-amylase *(11)*, invertase *(12)*, and lipase *(13)*. These studies showed that agroindustrial wastes are a suitable raw material source for an immobilization matrix. In Brazil, an increase in the green coconut water market had a direct impact on the increase of coconut husk production, an agroindustrial waste. This waste takes up to seven years to decompose, contributes to spreading tropical diseases, and is responsible for the overfilling of sanitary landfills when not disposed properly *(14)*.

In this study, we examine the immobilization of *Candida antarctica* lipase B by covalent attachment to green coconut fiber. Green coconut fiber was first silanized using GPTMS followed by immobilization of the enzyme. Two covalent immobilization strategies were compared: one-point covalent attachment (pH 7.0) and multipoint covalent attachment (pH 10.0). The derivatives formed by a one-point covalent bound have almost the same properties as the free enzyme and can be used as a standard to test activity/stability of the original enzyme. In this immobilization strategy,

only one (or two) amine residue of the enzyme molecule is involved in the CALB-support covalent bound *(15)*. In general, enzyme stability can be improved if the immobilization occurs through multipoint attachment at multiple lysine residues. Because attachment to the support stabilizes the enzyme structure they should become much more stable than their soluble counterparts or their randomly immobilized derivatives *(9,16)*. High concentrations of aldehyde groups on the support surface may also result in several multipoint bounds between the enzyme and the matrix, which can distort its three-dimensional structure and its active site. Different factors may influence the immobilization process, such as: activating agent, nature of the support, and interaction with enzyme *(17)*. The objective of this work was to study the immobilization of CALB on green coconut fiber by one-point (pH) and multipoint covalent binding (pH 10.0), and investigating the effects of immobilization on the activity and stability of the enzyme.

## Materials and Methods

### *Materials*

Commercial *C. antarctica* lipase type B (1780 U/mL) was kindly donated by Novozymes Latin America Ltd. and was used as received. Methyl butyrate and GPTMS was obtained from Sigma-Aldrich Chemical Co. Butyric acid and butanol were purchased from Merck S. A. (Rio de Janeiro, Brazil). Molecular sieve 4A ($Na_2O[Al_2O_3(5.0SiO_2)]12H_2O$) was from W. R. Grace & Co (Massachusetts, MA). Polyethyleneglycol 6000 was from Vetec (Rio de Janeiro, Brazil). All chemicals were of analytical grade.

### *Support Activation*

Green coconut fiber was obtained from green coconut husks through a process developed by Embrapa Agroindustria Tropical, Ceará State, Brazil *(14)*. It was cut and sieved to obtain particles between 32 and 35 mesh, washed with distilled water, and dried at 60°C before being used as an immobilization matrix. The support was activated using a four-step process. The support was first protonated with nitric acid (10%, [v/v]) under low stirring for 30 min at 30°C. It was then rinsed with nitric acid (10%, [v/v]) and acetone–water solutions (20, 50, and 100%, [v/v]) and dried at 60°C for 1 h. The support was then silanized using GPTMS (1%, [v/v]) at pH 8.5 under low stirring for 5 h at 60°C. The fiber was rinsed with water, acetone–water solutions, and dried. In the third step, the hydrolysis of epoxy groups was done with 0.1 *M* sulphuric acid at 85°C under low stirring for 2 h. Again, the fiber was rinsed with water and acetone–water and dried. For each gram of dry support used in the previous stages, 30 mL of each solution was used. Finally, oxidation was achieved by reaction with 0.04 *M* sodium periodate solution (5 mL/g fiber) under low stirring at room temperature for 1 h. After oxidation, the activated fiber was thoroughly

rinsed with water then with 5 m*M* sodium phosphate buffer pH 7.0. Before immobilization, activated fiber was dried under vacuum *(18)*.

### *Preparation of Immobilized Enzyme*

Lipase was immobilized by covalent attachment by contact at room temperature. The enzyme and support were mixed by repeated inversion using the apparatus shown in Fig. 1. For each gram of dry support, 10 mL of lipase solution (80 U/mL) in 25 m*M* sodium phosphate buffer pH 7.0 or in 200 m*M* sodium bicarbonate buffer pH 10.0, were used. After immobilization, the biocatalyst was separated by filtration, rinsed with phosphate buffer (10 mL) and dried at vacuum for 10 min.

### *Assay of Hydrolytic Activity: Methyl Butyrate Hydrolysis*

Methyl butyrate hydrolysis was used to determine the hydrolytic activity of the immobilized or soluble enzyme *(19)*. Experiments were performed using an automatic titrator (pHstat Netrohm Titrino 751, Switzerland) and 50 m*M* NaOH as titrating agent. The pH was set at 7.0 and the reaction initiated by the addition of 0.1 mL of free enzyme solution or 0.4 g of immobilized enzyme to 30 mL methyl butyrate solution dissolved in 25 m*M* phosphate buffer pH 7.0. One unit (U) of enzymatic activity is defined as the amount of enzyme that releases 1 μmol of methyl butyrate per min at pH 7.0 and 28°C.

### *Esterification Yield: Butyl Butyrate Synthesis*

Stock solutions of butyric acid (150 m*M*) and butanol (150 m*M*) were prepared in *n*-heptane. Experiments were set up in 250-mL flasks containing 20 mL of stock solution, 1.0 g of molecular sieve 4A, and 0.3 g of the biocatalyst *(20)*. The flasks were kept at 30°C under vigorous agitation for 24 h. The consumption of butyric acid was measured by titration with 20 m*M* NaOH using phenolphthalein as an indicator. The total acid content before the reaction was determined by titration of a blank sample, without enzyme. The esterification yield was calculated from the decrease in butyric acid concentration after 24 h of reaction.

### *Operational Stability: Methyl Butyrate Hydrolysis*

Immobilized enzyme stability was assayed by using 0.4 g of the biocatalyst in successive batches of methyl butyrate hydrolysis. Assay conditions were the same as described for the assay of hydrolytic activity. At the end of each batch, the immobilized lipase was removed from the reaction medium, washed with phosphate buffer to remove any remaining substrate or product, dried under vacuum (10 min), and assayed again. The residual activity of the biocatalyst was calculated in terms of percentage of activity (U) of the immobilized enzyme measured after each cycle compared with the activity of the immobilized enzyme before the first cycle.

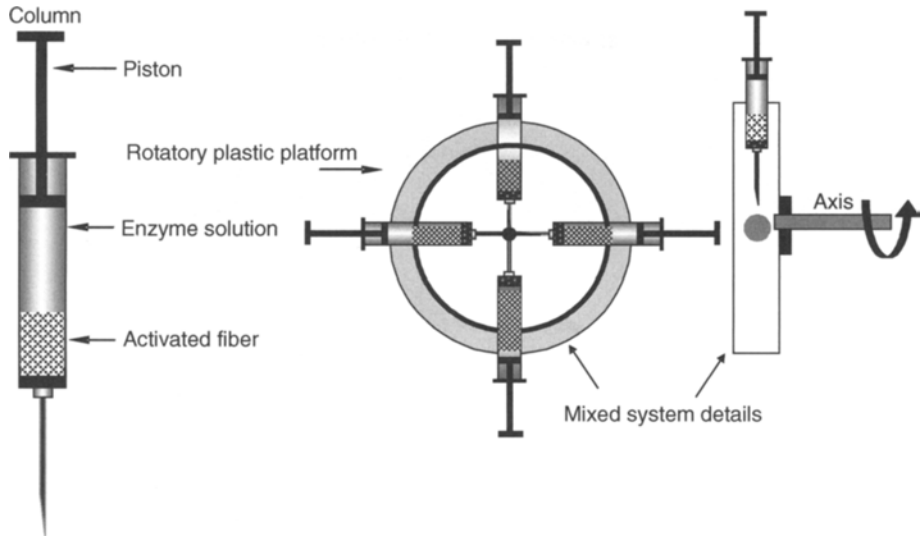


**Fig.1**. Details of the apparatus used for enzyme immobilization *(15)*.

## *Operational Stability: Synthesis of Butyl Butyrate*

Operational stability of the immobilized enzyme was also assayed by using 0.3 g of the biocatalyst in successive batches of butyl butyrate synthesis. The operational conditions were the same as described for the determination of esterification yield. At the end of each batch, the immobilized lipase was removed from the reaction medium and rinsed with hexane (20 mL), in order to extract any substrate or product retained in the matrix. After 1 h at room temperature, the immobilized enzyme was introduced to fresh medium. The residual activity of the biocatalyst was calculated in terms of percentage of activity (U) of the immobilized enzyme measured after each cycle compared with the activity of the immobilized enzyme before the first cycle.

## *Thermal Stability*

The thermal stability of soluble or immobilized enzyme was determined by incubating them in 100 m*M* sodium phosphate buffer at 60°C and pH 7.0. Periodically, samples were withdrawn and their residual activities were assayed by the hydrolysis of methyl butyrate. Residual activity is given as percentage of activity taken as 100% of the hydrolytic activity of the enzyme immobilized before incubation. Thermal deactivation curves follow the first-order deactivation model *(21)*, *see* Eq. 1. First-order deactivation rate coefficients ($K_d$) were estimated from experimental data.

$$\ln(A) = \ln(A_0) - K_d t \quad (1)$$

where $A_0$ is the initial residual activity, $A$ is the residual activity in time $t$, and $K_d$ are first-order deactivation rate coefficients. The biocatalyst half-life

($t_{1/2}$) was estimated by Eq. 2 using the estimated parameter $k_d$. In this article, stabilization factor (F) was considered as the ratio between soluble and immobilized enzymes half-lives.

$$t_{1/2} = \frac{\ln(0.5)}{-k_d} \tag{2}$$

### *Storage Stability*

To evaluate the storage stability of the immobilized enzyme, derivatives produced by covalent attachment were stored dry packed in aluminum paper at 5°C and their residual hydrolytic activities were determined every 24 h.

### *Effect of Sodium Borohydride Reduction*

The effect of sodium borohydride ($NaBH_4$), used as reducing agent, was studied. $NaBH_4$ concentration ranged from 0.5 to 6.0 mg/mL. After immobilization, solid $NaBH_4$ was added directly to the system and the reaction occurred for 30 min at room temperature. At the end of the reaction, the immobilized enzyme was separated by filtration, thoroughly rinsed with phosphate buffer and dried at vacuum for 10 min. The concentration of sodium borohydride that promoted minor loss on hydrolytic activity was selected based on results of thermal and operational stabilities.

### *Scanning Electron Microscopy*

In order to evaluate changes in the surface provoked by the activation process, natural fibers and activated fibers were analyzed by scanning electron microscopy (SEM) using a Zeiss DSM 940A SEM (Zeiss, Germany) operating at 10 kV. All samples were glued onto special stubs and gold-coated with a Sputter Emitech K550 (Emitech Ltd., Kent, UK) to avoid electrostatic charge and to improve image resolution.

## Results and Discussion

### *Green Coconut Fiber Activation With GPTMS*

Lignocellulosic materials, such as coconut fiber, can be activated by inserting functional groups owing to the presence of hydroxyl and carbonyl groups *(22)* on its surface. In the specific case of GPTMS, functional groups are added by reaction with hydroxyl groups *(18)* present in the support. Some techniques allow observing the axial deformation of hydroxyl groups promoted by the addition of functional groups *(23)*. Scanning electron micrographs shown in Fig. 2 demonstrates the presence of this activating agent on the surface of the support. The enzyme was successfully coupled to the activated support, as hydrolytic activity could be measured after immobilization. Other authors have also studied enzyme

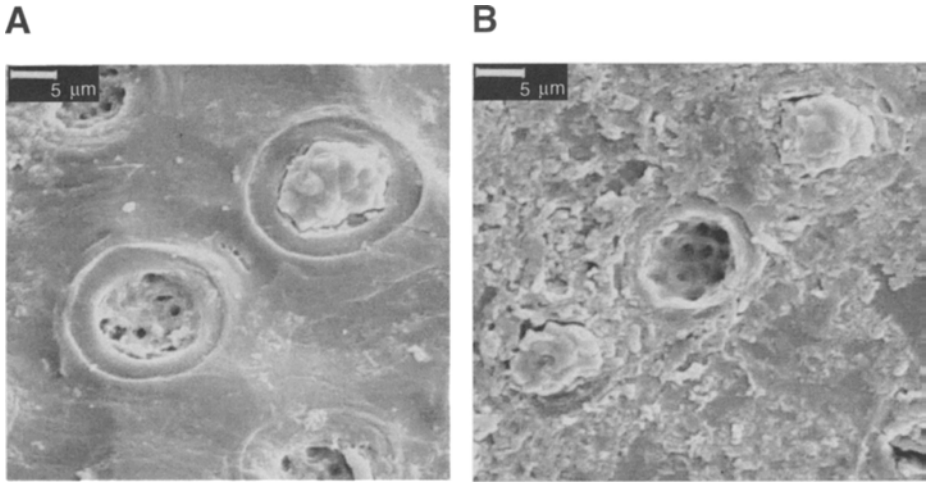


**Fig. 2.** Scanning electron micrographs of **(A)** natural green coconut fiber and **(B)** activated fiber with GPTMS (×2000).

immobilization on nonporous supports *(11,23)*, mainly by covalent attachment *(23)*, obtaining good results.

## *Enzyme Immobilization and Effect of Contact Time on Biocatalyst Hydrolytic Activity*

The influence of lipase contact on fiber activated with GPTMS was investigated for different time intervals. As shown in Fig. 3, when the immobilization was performed at pH 7.0, after 1 h of contact between enzyme and support, no improvement or decrease on immobilized enzyme hydrolytic activity was observed. Nevertheless, when immobilization was performed at pH 10.0, a decrease on immobilized enzyme hydrolytic activity was observed after 2 h of contact. According to the literature *(24)*, this behavior suggests that more than one Schiff's base was formed between enzyme and support, promoting a larger rigidity on the enzyme molecule, and consequently, losses on enzyme activity. Based on these results, the contact time of 2 h was selected for further immobilization studies.

## *Effect of pH of Lipase Solution on Biocatalyst Thermal and Operational Stabilities*

The effect of pH of lipase solution during the binding step of *C. antarctica* lipase B on coconut fiber activated with GPTMS was investigated. The objective of this study was to obtain one-point and multipoint covalent immobilized enzymes. Derivatives prepared at pH 7.0 are expected to be one-point attached. On the other hand, owing to the $pK_a$ of lysine residues on the enzyme surface ($pK_a$ = 10.5), the immobilization at

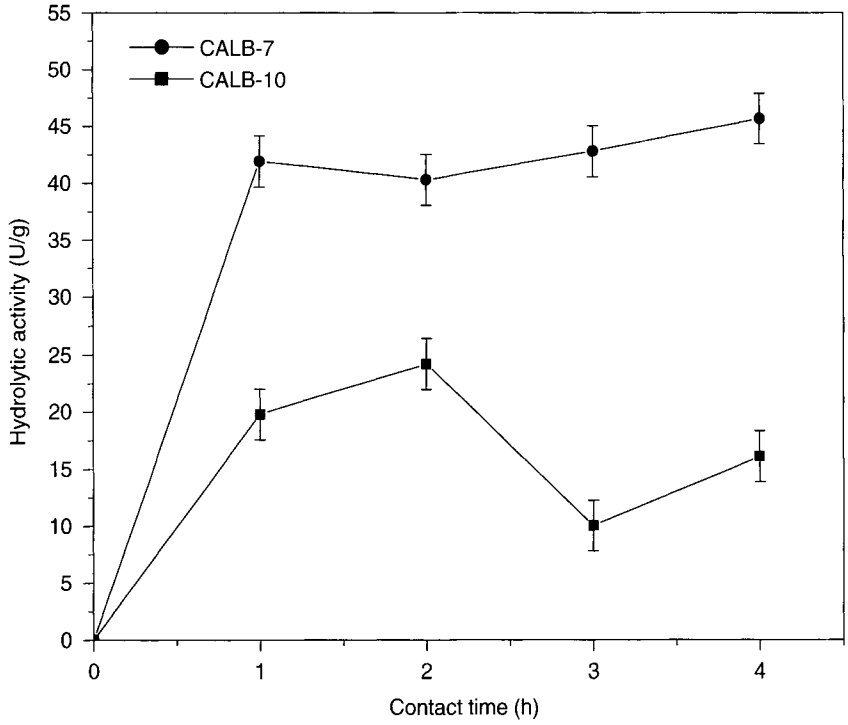


**Fig. 3.** Effect of contact time on the hydrolytic activity of the derivative obtained through lipase immobilization in coconut fiber by covalent attachment at pH 7.0 (CALB-7) or pH 10.0 (CALB-10).

pH 10.0 should be multipoint *(17)*. It can be observed (Fig. 3) that CALB-7 exhibited higher hydrolytic activity than CALB-10, around 42 U/g and 20 U/g, respectively. This result may be an indication of a multiinteraction between enzyme support at pH 10.0. Because a low density of active groups was present on the activated fiber, enzyme immobilization by multipoint attachment would allow a small number of enzyme molecules to bind on the support. However, activity is not the only important parameter when industrial biocatalysts are designed. Therefore, thermal and operational stabilities of the immobilized enzyme were determined.

A direct correlation between the number of attachment points and enzyme thermal stability has been previously reported *(25,26)*. Moreover, multipoint binding between the enzyme and the support, which is responsible for enhancing thermal stability, would provide better stability against deleterious effects of organic solvents *(25)*, which are usually used as reactional media when lipases are used to catalyze the synthesis of esters. Therefore, inactivation profiles at 60°C of free and immobilized lipases (Fig. 4) were studied in this work.

It can be seen in Fig. 4 that the immobilized enzyme is more stable than free enzyme suggesting that immobilization protects the enzyme from

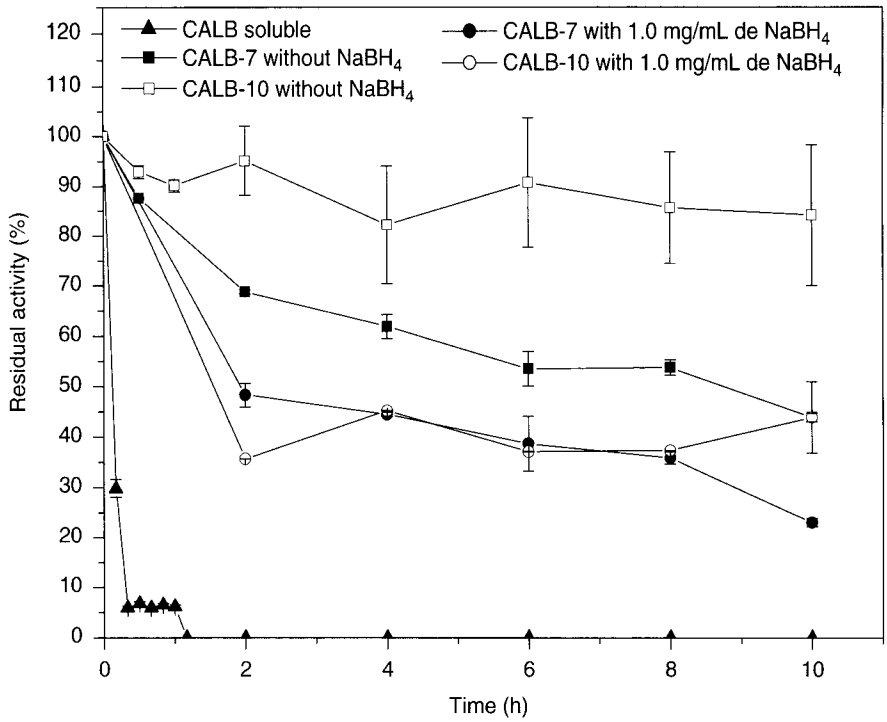


**Fig. 4.** Thermal stability of derivatives from lipase B from *C. antarctica* obtained by covalent attachment at pH 7.0 (CALB-7) or pH 10.0 (CALB-10) with or without reduction with sodium borohydride ($NaBH_4$), incubated in 0.1 *M* sodium phosphate buffer, pH 7.0, at 60°C. Initial hydrolytic activity of the immobilized enzyme (before thermal treatment): (a) Soluble CALB 160 U/mL; (b) CALB-7 without reduction with $NaBH_4$ 42.0 U/g; (c) CALB-7 treated with $NaBH_4$ 32.3 U/g, (d) CALB-10 without reduction with $NaBH_4$ 20.0 U/g; and (e) CALB-10 treated with $NaBH_4$ 12.0 U/g.

thermal inactivity. The plots of residual activity vs incubation time (at pH 7.0 and 60°C) adjust quite well with the proposed model (*see* Eq. 1) and allow calculating the half-lives of inactivation (*see* Table 1). The most stable derivative was prepared at pH 10.0, with stabilization factor (F) equal to 363.71, which is 5.4-fold more stable than the derivative prepared at pH 7.0. Hence, thermal stability is very sensitive to the process of enzyme-support multiinteractions *(25)*, indicating that a multipoint interaction might have occurred when immobilization was conducted at pH 10.0.

The ability to reuse the biocatalyst is of practical importance; the operational stability of lipase preparations was determined. In this work, two model reactions were selected: methyl butyrate hydrolysis (aqueous media) and butyl butyrate synthesis (organic media). The results are summarized in Fig. 5. It can be observed that the biocatalyst prepared at pH 7.0 (CALB-7) retained an activity of about 55% in aqueous media (hydrolysis) and 75% in organic media (synthesis), respectively, after five reuses. The biocatalyst prepared at pH 10.0 (CALB-10) had a similar

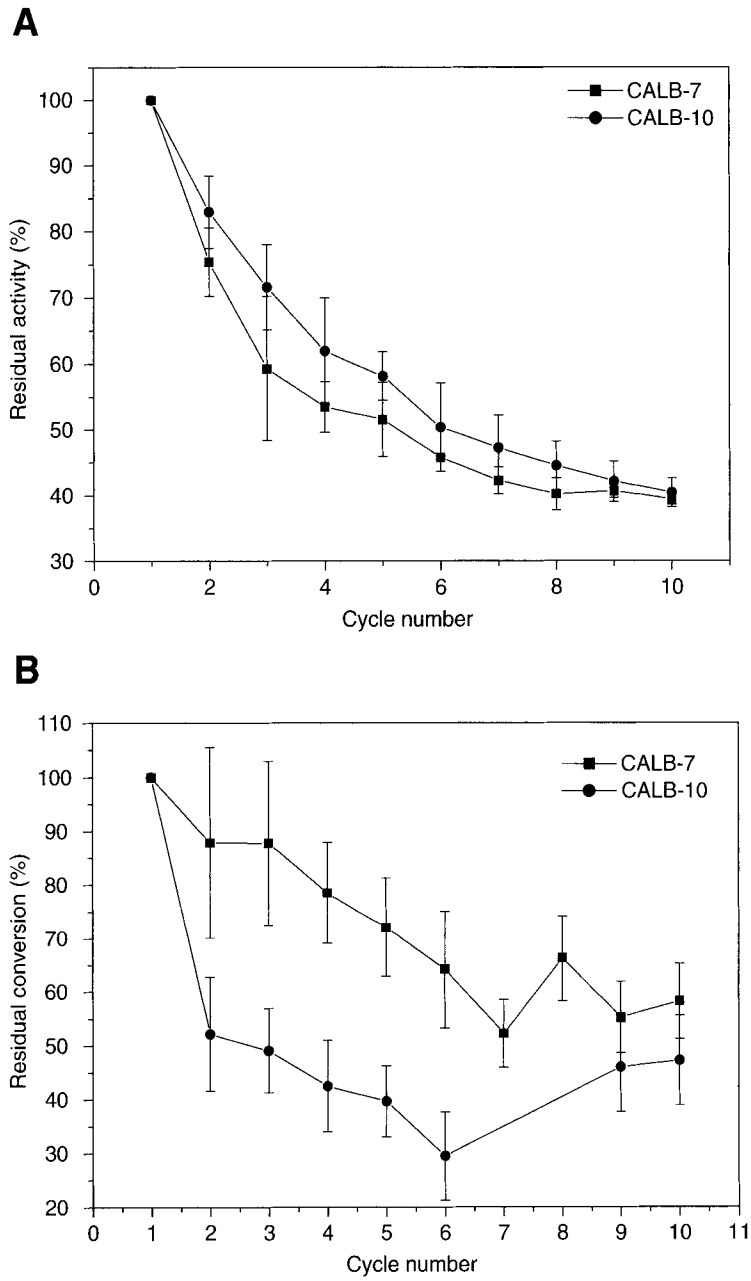


**Fig. 5.** Batch operational stability of covalent immobilized lipase B of *C. antarctica* on coconut green fiber activated with GPTMS: **(A)** methyl butyrate hydrolysis and **(B)** butyl butyrate synthesis. Initial hydrolytic activity of the immobilized enzyme (before operational stability tests): (a) CALB-7 42.0 U/g and (b) CALB-10 20.0 U/g.

behavior in aqueous media, around 55% of residual hydrolytic activity, but presented a poor result of synthetic activity, around 45% of residual activity. After 10 reuses, the residual activities of CALB-7 and CALB-10 were, respectively, around 40% and 45% in aqueous media and 55% and 45% in

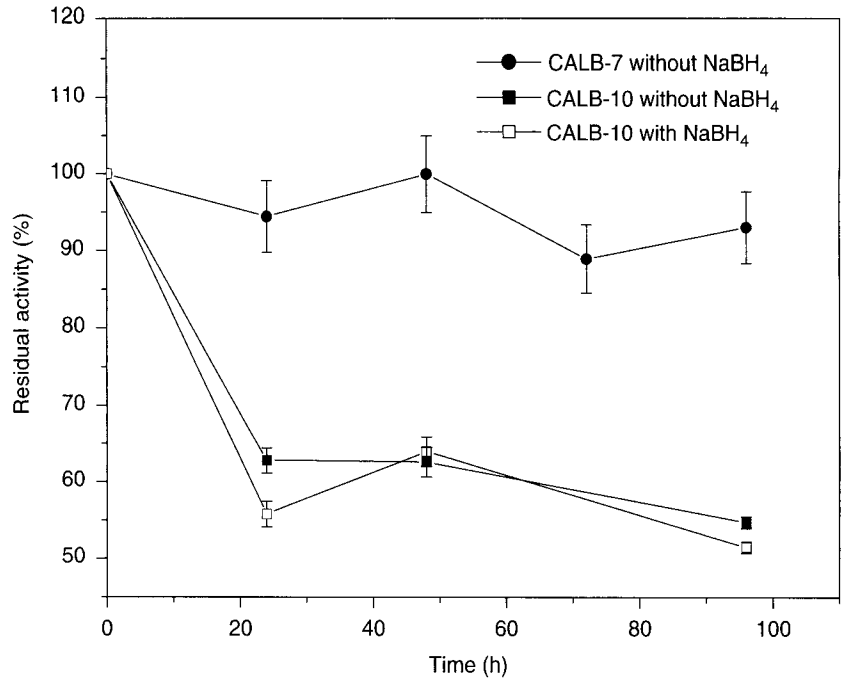


**Fig. 6.** Storage stability at 5°C of derivatives from lipase B from *C. antarctica* obtained by covalent attachment at pH 7.0 (CALB-7) and pH 10.0 (CALB-10), with or without reduction with sodium borohydride. Initial hydrolytic activity of the immobilized enzyme (before storage): (a) CALB-7 without reduction with $NaBH_4$ 42.0 U/g; (b) CALB-10 without reduction with $NaBH_4$ 20.0 U/g; and (c) CALB-10 treated with $NaBH_4$ 12.0 U/g.

Table 1
Kinetics Parameters of Thermal Desativation, at 60°C, of Soluble and Immobilized Lipase B From *C. antarctica* Obtained by Covalent Attachment at pH 7.0 (CALB-7) or pH 10.0 (CALB-10)

| Enzymes | kd ($h^{-1}$) | $t_{1/2}$(h) | R |
|---|---|---|---|
| Soluble enzyme | 7.14 | 0.097 | 1.00 |
| Immobilized enzyme at pH 7.0 | 0.106 | 6.51 | 67.11 |
| Immobilized enzyme at pH 10.0 | 0.020 | 35.28 | 363.71 |

organic media. One possible explanation for the poor operational stability of CALB-10 in organic media is the lower enzyme loading in the support (20 U/g), because one protein molecule is coupled to more than one functional group on the support.

The effect of storage of the immobilized lipases at 5°C was determined and results are illustrated in Fig. 6. It can be observed that CALB-7 is very stable and maintained 100% of activity after 96 h of storage. On the other hand, CALB-10 lost more than 30% of its activity

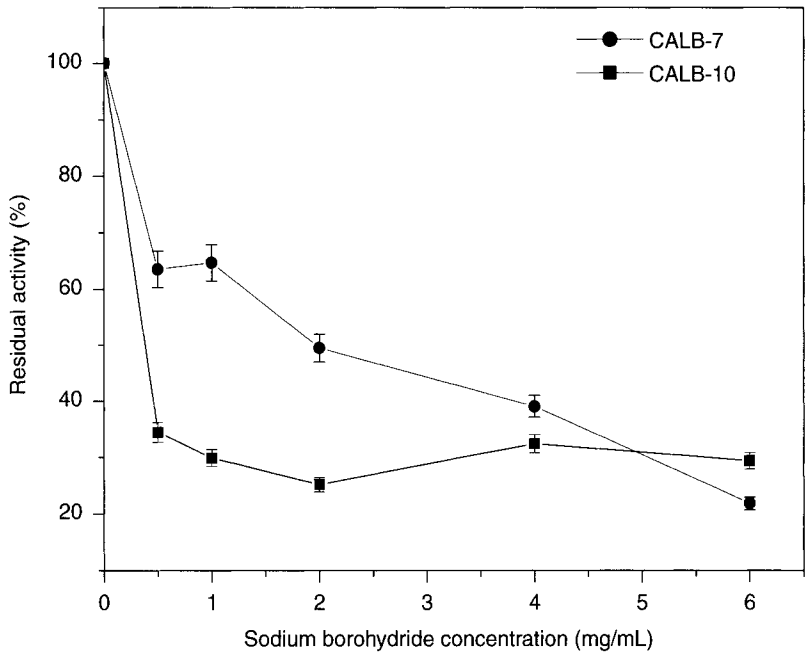


**Fig. 7.** Effect of sodium borohydride on the hydrolytic activity of derivatives obtained by covalent attachment of lipase B from *C. antarctica* in coconut fiber. Initial hydrolytic activity of the immobilized enzyme (before to $NaBH_4$ reduction): (a) CALB-7 42.0 U/g and (b) CALB-10 20.0 U/g.

after 24 h of storage and almost 50% after 96 h. This deactivation profile observed in CALB-10 may be caused by the reaction of amine groups from the bound enzyme with aldehyde groups from the support, because no reduction steps to transform the Schiff's bases into stable secondary amino bonds and the remnant aldehydes into inert hydroxyl groups *(6)* were performed after immobilization. Other possible explanation would be enzyme leakage from the support. Although covalent bound formation is favored, the condensation reaction between amino groups and aldehydes is reversible, which can lead to loss of bound enzyme *(27)*.

## *Effect of the Sodium Borohydride Reduction on the Biocatalyst Activity and Stability*

Sodium borohydride is a double-functional agent, which seems to be a very suitable reducing agent, and also, able to inactivate the remaining aldehydes groups present in the support after immobilization *(10)*. The final reduction of the immobilized enzyme with sodium borohydride transforms weak Shiff's bases into stable secondary amino bounds and remaining aldehyde on the solid support into inert hydroxyl groups. Undesired enzyme-support interactions may be caused by noninert support surfaces, promoting the decrease on enzyme activity and stability *(28,29)*. Therefore, the influence of

sodium borohydride ($NaBH_4$) reduction after the immobilization was evaluated (Fig. 7). All $NaBH_4$ concentrations studied promoted a decrease on the immobilized enzyme hydrolytic activity. For CALB-10, the significant loss in activity might be caused by the low enzyme loading, which is also the probable reason for the false absence of influence of $NaBH_4$ concentration on the biocatalyst activity. For CALB-7, 0.5 mg/mL and 1.0 mg/mL of $NaBH_4$ promoted the smallest reduction in activity values. In spite of the inactivation of bound enzyme, owing to the deleterious effect of $NaBH_4$, the derivatives treated with 1.0 mg/mL of $NaBH_4$ were selected for thermal and storage at 5°C stability studies, as this treatment would prevent further uncontrolled reaction between support and the enzyme that could decrease its stability *(28)*.

Figure 4 shows the thermal stability at 60°C of the immobilized derivatives obtained with and without sodium borohydride reduction. The thermal stability was reduced after the reduction step with sodium borohydride for both CALB-7 and CALB-10. It has been reported that sodium borohydride can have deleterious effects on protein structures: for example, disulfide bond splitting or reductive cleavage of peptide bonds *(30)*, which could justify this thermal stability results. Moreover, the reduction step was not able to improve the storage stability at 5°C (Fig. 6), and therefore, the use of $NaBH_4$ was unsatisfactory for this system. Other authors *(6,17)* have also observed that $NaBH_4$ was not an appropriate reducing agent and found different solutions to solve this problem, such as the use of competitive inhibitor to protect the active center of the enzyme during the reduction step with $NaBH_4$ *(6)* or use another reducing agent, for instance, and amino acids *(27)*.

## Conclusions

The results obtained in this work show that green coconut fiber is a suitable support for lipase immobilization, enabling the preparation of highly stabilized immobilized enzymes, for example, around 363.71-fold (CALB-10) or 67.11-fold (CALB-7) more stable than the soluble enzyme. The higher thermal stabilization observed when immobilized enzyme was prepared at pH 10.0 might be owing to the generation of a multipoint covalent attachment between the aldehyde groups of the support and the lysine residues of the enzyme. Best results of operational stability of synthesis and storage at 5°C were obtained when lipase was covalently immobilized at pH 7.0. The reduction step using sodium borohydride had no influence on CALB-10 storage stability at 5°C. Moreover, it promoted a decrease in thermal stability of both CALB-7 and CALB-10, which shows that it's not an appropriated reducing agent for this system. Other strategies to improve CALB-10 storage and operational stabilities are currently being investigated that include enhancing superficial area of the support. However, we have demonstrated that coconut fiber, a cheap support, is compatible with *C. antarctica* lipase, rendering a biocatalyst with interesting properties that can be used in aqueous or organic media.

## Acknowledgments

The authors would like to thank the Brazilian research-funding agencies FUNCAP (State of Ceará), FINEP, and CNPq (Federal). We are also grateful to Embrapa Agroindustria Tropical for the SEM analysis.

## References

1. Jaeger, K. and Reetz, M. T. (1998), *Trends Biotechnol.* **16,** 396–403.
2. Dalla-Vecchia, R., Nascimento, M. G., and Soldi, V. (2004), *Quím. Nova.* **27,** 623–630.
3. Sharma, R., Chisti, Y., and Banerjee, U. C. (2001), *Biotechnol. Adv.* **19,** 627–662.
4. Villeneuve, P., Muderhwa, J. M., Graille, J., and Haas, M. J. (2000), *J. Mol. Catal. B: Enzyme* **9,** 113–148.
5. Stark, M. -B. and Holmberg, K. (1989), *Biotechnol. Bioeng.* **34,** 942–950.
6. Tardioli, P. W., Fernandez-Lafuente, R., Guisan, J. M., and Giordano, R. L. (2003), *Biotechnol. Prog.* **19,** 564–574.
7. Kennedy, J. F., White, C. A., and Melo, E. H. M. (1988), *Chimicaoggi.* **5,** 21–29.
8. Fernández-Lafuente, R., Rodríguez, V., Mateo, C., et al. (1999), *J. Mol. Catal. B: Enzyme* **7,** 181–189.
9. Mateo, C., Abian, O., Fernández-Lafuente, R., and Guisán, J. M. (2000), *Enzyme Microb. Tech.* **26,** 509–515.
10. Blanco, R. M., Calvete, J. J., and Guisán, J. M. (1989), *Enzyme Microb. Technol.* **11,** 353–359.
11. Dey, G., Nagpal, V., and Banerjee, R. (2002), *Appl. Biochem. Biotechnol.* **102–103,** 303–313.
12. D'Souza, S. F. and Godbole, S. S. (2002), *J. Biochem. Biophys. Methods* **52,** 59–62.
13. Castro, H. F., Lima, R., and Roberto, I. C. (2001), *Biotechnol. Prog.* **17,** 1061–1064.
14. Rosa, M. F., Bezerra, F. C., Brígida, A. I. S., and Brígido, A. K. L. (2002), Aproveitamento de resíduos da indústria da água de coco verde como substrato agrícola: 1—Processo de obtenção. Proceedings of the VI Seminário Nacional de Residuos, Gramado, Brazil (in Portugese).
15. Cardias, H. C. T., Grininger, C. C., Trevisan, H. C., Guisan, J. M., and Giordano, R. L. C. (1999), *Braz. J. Chem. Eng.* **16,** 141–148.
16. Guisan, J. M., Bastida, A., Cuesta, C., Fernandez-Lafuente, R., and Rossel, C. M. (1991), *Biotechnol. Bioeng.* **38,** 1144–1152.
17. Adriano, W. S., Costa-Filho, E. H., Silva, J. A., Giordano, R. L. C., and Goncalves, L. R. B. (2005), *Braz. J. Chem. Eng.* **22,** 529–538.
18. Pereira, G. H. A., Guisán, J. M., and Giordano, R. L. C. (1997), *Braz. J. Chem. Eng.* **14,** 327–332.
19. Rodrigues, D. S. (2005), *Master Thesis,* Estudo da imobilização de lipase B de *Candida antarctica* em carvão i quitorana (in Portugese). Universidade Federal do Ceará, Fortaleza, Brazil.
20. Castro, H. F., Silva, M. L. C. P., and Silva, G. L. J. P. (2000), *Braz. J. Chem. Eng.* **17,** 849–857.
21. Soares, C. M. F., Castro, H. F., Santana, M. H. A., and Zanin, G. M. (2002), *Appl. Biochem. Biotechnol.* **98–100,** 863–874.
22. Pino, G. A. H. (2005), *Master Thesis,* Pontificia Universidade Católica do Rio de Janeiro, Rio de Janeiro, Brazil.
23. Gomes, F. M., Silva, G. S., Pinatti, D. G., Conte, R. A., and Castro, H. F. (2005), *Appl. Biochem. Biotechnol.* **121,** 255–268.
24. Palomo, J. M., Muñoz, G., Fernándes-Lorente, G., et al. (2003), *J. Mol. Catal. B: Enzyme* **21,** 201–210.
25. Otero, C., Ballesteros, A., and Guisan, J. M. (1988), *Appl. Biochem. Biotechnol.* **19,** 163–175.
26. Pedroche, J., Yust, M. M., Mateo, C., et al. (2007), *Enzyme Microb. Technol* in press.
27. Isgrove, F. H., Williams, R. J. H., Niven, G. W., and Andrews, A. T. (2001), *Enzyme Microb. Technol.* **28,** 225–232.
28. Mateo, C., Torres, R., Fernandez-Lorente, G., et al. (2003), *Biomacromolecules* **4,** 772–777.
29. Mateo, C., Palomo, J. M., Fuentes, M., et al. (2006), *Enzyme Microb. Technol.* **39,** 274–280.
30. Blanco, R. M. and Guisán, J. M. (1989), *Enzyme Microb. Technol.* **11,** 360–366.

0273-2289/1559-0291 (Online)/07/136–140/81–92/$30.00

# Pretreatment of Corn Stover by Soaking in Aqueous Ammonia at Moderate Temperatures

TAE HYUN KIM[1] AND Y.Y. LEE*,[2]

*[1]ERRC, ARS, US Department of Agriculture 600 East Mermaid Lane, Wyndmoor, PA 19038-859; and [2]Department of Chemical Engineering, Auburn University, AL 36849, E-mail: leeyoon@auburn.edu*

## Abstract

Soaking in aqueous ammonia at moderate temperatures was investigated as a method of pretreatment for enzymatic hydrolysis as well as simultaneous saccharification and cofermentation (SSCF) of corn stover. The method involves batch treatment of the feedstock with aqueous ammonia (15–30 wt%) at 40–90°C for 6–24 h. The optimum treatment conditions were found to be 15 wt% of $NH_3$, 60°C, 1 : 6 of solid-to-liquid ratio, and 12 h of treatment time. The treated corn stover retained 100% glucan and 85% of xylan, but removed 62% of lignin. The enzymatic digestibility of the glucan content increased from 17 to 85% with 15 FPU/g-glucan enzyme loading, whereas the digestibility of the xylan content increased to 78%. The treated corn stover was also subjected to SSCF test using Spezyme-CP and recombinant *Escherichia coli* (KO11). The SSCF of the soaking in aqueous ammonia treated corn stover resulted in an ethanol concentration of 19.2 g/L from 3% (w/v) glucan loading, which corresponds to 77% of the maximum theoretical yield based on glucan and xylan.

**Index Entries:** Biofuel; bioethanol; biomass conversion; simultaneous saccharification and cofermentation; hemicellulose; lignin.

## Introduction

Hemicellulose is the second largest carbohydrate source in the lignocellulosic biomass. Effective utilization of it is a necessary element in biomass conversion process. In most known process schemes of biomass conversion, the hemicellulose fraction is recovered in liquid during the pretreatment stage. It is so because most pretreatment methods apply temperatures high enough to solubilize the hemicellulose. These conventional pretreatment methods generate hydrolyzates containing a mixture of sugars, lignin, and various decomposed products, which are inhibitor to enzymatic hydrolysis and toxic to bioconversion processes *(1–6)*. A previous study indicates that hemicellulose removal becomes significant at temperatures above 130°C *(7)*. In order to utilize the soluble hemicellulose in the pretreatment hydrolyzate, it must be detoxified before

*Author to whom all correspondence and reprint requests should be addressed.

it is subjected to bioprocessing. Detoxification is not an established process at this time, but it is a significant cost factor in the overall bioconversion scheme.

In our previous work on pretreatment, corn stover was treated in aqueous ammonia at room temperature (soaking in aqueous ammonia [SAA]). We found that with proper operation of this process, one can remove 74% of the lignin, but retain nearly 100% of glucan and more than 85% of xylan *(8)*. It is one of the few pretreatment methods wherein both glucan and xylan are retained. The treated corn stover was found to be highly digestible by cellulase. As the hemicellulose fraction mostly remains intact along with cellulose fraction, they can be hydrolyzed by cellulase enzyme to give glucose and xylose. It is to be noted that most commercial "cellulose" enzymes do exhibit xylanase activity as well as glucanase activity. Such enzyme hydrolyzate is nontoxic, therefore, can be put through a subsequent microbial conversion without detoxification. Elimination of detoxification is a significant cost-saving measure. Retention of hemicellulose in solid during pretreatment is a desirable feature because the overall bioconversion can be carried out without separate recovery and processing of xylose from the pretreatment liquid *(8)*.

In previous SAA at room temperature, a problem arose that the reaction time in the range of 10 d is required to treat the feedstock properly by this method. In this study, SAA with elevated temperatures was investigated to see if the reaction time can be reduced and still retain the hemicellulose fraction. The focus of this work is to evaluate the overall effectiveness of the SAA at moderate temperature as a pretreatment process. The effects of reaction parameters on the composition and the digestibility of the remaining glucan and xylan were investigated. The reaction parameters of interest were solid-to-liquid ratio, reaction time, and ammonia concentration. A recombinant *Escherichia coli*, strain KO11 (American Type Culture Collection (ATCC®) 55124, Manassas, VA) is reported to utilize hexose as well as pentose and convert them into ethanol efficiently *(9,10)*. A simultaneous saccharification and cofermentation (SSCF) using this strain and a cellulase enzyme was used in this work, to evaluate the SAA and the overall conversion scheme as the bioprocess to produce ethanol from lignocellulosic biomass.

## Materials and Methods

### *Materials*

Air-dried ground corn stover was supplied by the National Renewable Energy Laboratory (NREL, Golden, CO). The corn stover was screened to a nominal size of 9–35 mesh. The initial composition of the corn stover, as determined by NREL, was: 36.1 wt% glucan, 21.4 wt% xylan, 3.5 wt% arabinan, 1.8 wt% mannan, 2.5 wt% galactan, 17.2 wt% Klason lignin, 7.1 wt% ash, 3.2 wt% acetyl group, 4.0 wt% protein, and 3.6 wt% uronic acid. α-Cellulose was purchased from Sigma (Cat. No. C-8200, St. Louis, MO Lot No. 11K0246). Cellulase enzyme, Spezyme CP (Genencor, Palo Alto, CH, Lot No. 301-00348-257) was obtained from NREL. The average activity and

the protein content of the enzyme, as determined by NREL were: 31.2 filter paper unit (FPU)/mL and 106.6 mg/mL, respectively. Activity of β-glucosidase (Novozyme 188 from Novo Inc., Sigma Cat. No. C-6150, Lot No. 11K1088) was 750 CBU/mL. Recombinant *E. coli* ATCC 55124 (KO11) was used for the SSCF tests. LB medium (Sigma Cat. No. L-3152) was used for the growth of KO11, which contained 1% tryptone, 0.5% yeast extract, 1% NaCl, and 40 mg/L chloroamphenicol.

### *Experimental Setup and Operation*

Corn stover was treated with 15–30 wt% of aqueous ammonia in screw-capped laboratory bottles at 40–90°C for 6–24 h. Solid-to-liquid ratios ranging 1 : 2–1 : 10 were applied. After soaking, the solids were separated by filtering, washed with DI water until pH reached 7.0, and subjected to the enzymatic digestibility tests. Klason lignin, carbohydrate content, and digestibility were determined by NREL Chemical Analysis and Testing Standard Procedure *(11)*.

### *Digestibility Test*

The enzymatic digestibility of corn stover was determined in duplicates following the procedure of the NREL Chemical Analysis and Testing Standard Procedure *(11)*. The conditions of the enzymatic digestibility tests are 50°C and pH 4.8 (0.05 *M* sodium citrate buffer). Enzyme loadings were: 15 and 60 FPU of Spezyme CP/g-glucan, supplemented with 30 CBU of β-glucosidase (Novozyme 188)/g-glucan. The initial glucan concentration was 1% (w/v). One hundred mL of total liquid was used in the digestibility test. Screw-capped Erlenmeyer flasks (250 mL) containing the enzyme hydrolysis preparations were placed in an incubator shaker (New Brunswick Scientific, Innova-4080). Samples were taken periodically and analyzed for glucose, xylose, and cellobiose content using high-performance liquid chromatography (HPLC). Total released glucose after 72 h of hydrolysis was used to calculate the enzymatic digestibility. α-Cellulose and untreated corn stover were put through the same procedure as a reference and control.

### *Simultaneous Saccharification and Cofermentation*

A 250-mL Erlenmeyer flask was used as the bioreactor. It was shaken in the incubator (New Brunswick Scientific, Innova-4080) at 38°C and 150 rpm (0.64*g*). Into a 100 mL working volume of liquid, treated corn stover sample was introduced to reach 3% (w/v) glucan content in the reactor. α-Cellulose was put through the same procedure as the control. The SSCF runs were performed with buffer without external pH control, starting at pH 7.0 at the beginning of the fermentation and gradually decreasing to pH 6.0 at the end. The loading of cellulase enzyme (Spezyme CP) was 15 FPU/g-glucan, and that of β-glucosidase (Novozyme 188) was 30 CBU/g-glucan. The ethanol yield in SSCF test was calculated as follows:

$$\text{Theoretical maximum ethanol yield (\%)} = \frac{\text{Ethanol produced (g) in reactor}}{\text{Initial sugar (g) in reactor} \times 0.511} \times 100$$

*Note:* Sugar is interpreted as glucose plus xylose in the SSCF work.

### *Analytical Methods*

The solid samples, such as treated/untreated corn stover, α-cellulose, and so on, were analyzed for sugar and Klason lignin following NREL Chemical Analysis and Testing Standard Procedures *(11)*. Each sample was analyzed in duplicates. Sugars were determined by HPLC using a Bio-Rad Aminex HPX-87P column (BioRad Laboratories, Hercules, CA). For the SSCF tests, HPX-87P and 87H columns were used to measure the sugar content and ethanol, respectively. An YSI 2300 Glucose/Lactate analyzer (YSI Incorporated, Yellow Springs, OH) was used for rapid analysis of glucose during inoculums preparation. A refractive index detector was used for HPLC analysis.

### *Scanning Electron Microscope*

Untreated and treated corn stover samples were freeze-dried before observation through a scanning electron microscope (ZEISS, Thornwood, NY Model-DSM940).

## Results and Discussion

### *Effect of Reaction Temperature and Ammonia Concentration*

The effects of reaction temperature and ammonia concentration in SAA were investigated. The results are summarized in Table 1. Two different ammonia concentrations and three different temperatures were applied at each concentration. As seen in Table 1, the major compositional changes are in the lignin. Delignification increased from 50 to 77% as temperature was increased from 40°C to 90°C (Table 1). Increase of ammonia concentration from 15 to 30% showed little effect on delignification. Treatment at 60°C with 15–30 wt% of ammonia achieves 67–71% of delignification. The glucan contents were well preserved over the entire range of treatment condition. About 80% of the xylan is preserved in the SAA. Xylan loss of 20% is much lower than those observed from other treatment methods using aqueous ammonia *(8,12,13)*. Increasing of the ammonia concentration from 15 wt% to 30 wt% resulted in slightly improved enzymatic digestibility of the treated samples. The condition of 15 wt% of ammonia at 60°C carries a special meaning because the system pressure under this condition equals the atmospheric pressure. The SAA can thus be carried out without the use of pressure vessel, a significant cost benefit.

Table 1
Effect of Reaction Temperatures and Ammonia Concentrations on the Compositions and the Enzymatic Digestibility in SAA-Treated Corn Stover[a]

| NH3 concentration (wt%) | Temperature (°C) | S.R. (%)[b] | Lignin (%)[c] | Delignification | Solid (%) | | Enzymatic digestibility (%)[d] | |
|---|---|---|---|---|---|---|---|---|
| | | | | | Glucan | Xylan | Glucan | Xylan |
| Untreated | – | – | 17.2 | – | 36.1 | 21.4 | 17.2 | 12.5 |
| | – | – | ± 0.4 | – | ± 0.3 | ± 0.2 | ± 1.5 | ± 1.2 |
| 30 | 40 | 77.4 | 8.4 | 51.2 | 36.1 | 17.7 | 86.5 | 75.4 |
| | – | ± 2.5 | ± 0.2 | ± 1.2 | ± 0.5 | ± 0.3 | ± 2.5 | ± 1.8 |
| | 60 | 69.6 | 5.1 | 70.4 | 35.9 | 17.5 | 90.3 | 82.2 |
| | – | ± 1.1 | ± 0.4 | ± 2.5 | ± 0.2 | ± 0.4 | ± 1.6 | ± 1.7 |
| | 90 | 68.1 | 3.9 | 77.3 | 35.6 | 16.0 | 98.0 | 85.2 |
| | – | ± 2.0 | ± 0.3 | ± 1.6 | ± 0.4 | ± 0.1 | ± 2.1 | ± 2.2 |
| 15 | 40 | 76.0 | 8.6 | 50.0 | 36.9 | 17.9 | 80.0 | 72.5 |
| | – | ± 1.6 | ± 0.6 | ± 3.7 | ± 0.3 | ± 0.6 | ± 1.5 | ± 1.3 |
| | 60 | 71.4 | 5.6 | 67.4 | 36.1 | 17.2 | 90.1 | 79.8 |
| | – | ± 2.1 | ± 0.5 | ± 2.9 | ± 0.7 | ± 0.4 | ± 2.7 | ± 1.9 |
| | 90 | 67.3 | 3.9 | 77.3 | 35.8 | 16.5 | 93.4 | 81.5 |
| | – | ± 1.0 | ± 0.2 | ± 0.9 | ± 0.6 | ± 0.5 | ± 1.5 | ± 1.1 |

[a]Data in the table are based on the oven-dry untreated biomass. Values are expressed as mean and standard deviation ($n$ = 2 for the composition analysis, $n$ = 4 for the enzymatic digestibility). Pretreatment conditions: 15–30 wt% of ammonia concentration, 40–90°C of reaction temperature, 24 h of reaction time, and 1 : 10 (based on wt) of solid : liquid ratio.

[b]S.R. stands for solid remaining after reaction.

[c]Klason lignin.

[d]Digestibility at 72 h, enzymatic hydrolysis conditions: 15 FPU/g-glucan, pH 4.8, digestibility at 50°C and 150 rpm. Digestibility (%) = ([grams of glucan or xylan digested by enzyme]/[grams of glucan or xylan added]) × 100.

Most of the subsequent experiments were therefore carried out under this condition.

### *Effect of Reaction Time and Solid-to-Liquid Ratio*

In order to study the effect of reaction time, three different reaction times (6, 12, and 24 h) were applied keeping the reaction temperature at 60°C and the ammonia concentration at 15 wt%, and the solid : liquid ratio at 1 : 6. The composition data and enzymatic digestibility after these treatments are summarized in Table 2. The data indicate that the xylan and lignin remaining in the solids generally decrease as reaction time increase. Solubilization of xylan is 17–19%, and lignin removal was in the range of 47–69% with 6–24 h of retention time. However, increase beyond 12 h of treatment was insignificant.

The effect of solid-to-liquid ratio was tested at 60°C. The results are summarized in Table 3. Lignin removal and enzymatic digestibility increased

Table 2
Effect of Reaction Time On The Compositions and Enzymatic Digestibility in SAA-Treated Corn Stover[a]

| Time (h) | S.R. (%)[b] | Lignin (%)[c] | Delignification (%) | Solid (%) | | Enzymatic digestibility (%)[d] | |
|---|---|---|---|---|---|---|---|
| | | | | Glucan | Xylan | Glucan | Xylan |
| Untreated | – | 17.2 | – | 36.1 | 21.4 | 17.2 | 12.5 |
| | – | ± 0.4 | – | ± 0.3 | ± 0.2 | ± 1.5 | ± 1.2 |
| 6 | 75.2 | 9.1 | 47.1 | 36.1 | 18.8 | 79.7 | 71.9 |
| | ± 2.4 | ± 0.6 | ± 3.5 | ± 0.2 | ± 0.3 | ± 1.5 | ± 0.5 |
| 12 | 71.3 | 6.4 | 62.6 | 36.1 | 17.8 | 85.0 | 77.9 |
| | ± 1.5 | ± 0.3 | ± 1.8 | ± 0.0 | ± 0.5 | ± 1.2 | ± 2.2 |
| 24 | 71.1 | 5.3 | 69.3 | 35.9 | 17.4 | 86.4 | 78.4 |
| | ± 1.8 | ± 0.2 | ± 1.0 | ± 0.4 | ± 0.2 | ± 1.1 | ± 17 |

[a]Data in the table are based on the oven-dry untreated biomass. Values are expressed as mean and standard deviation ($n = 2$ for the composition analysis, $n = 4$ for the enzymatic digestibility). Pretreatment conditions: 15 wt% of ammonia concentration, 60°C of reaction temperature, and 1 : 6 of solid : liquid ratio (based on wt).

[b]S.R. stands for solid remaining after reaction.

[c]Klason lignin.

[d]Digestibility at 72 h, enzymatic hydrolysis conditions: 15 FPU/g-glucan, pH 4.8, digestibility at 50°C and 150 rpm. Digestibility (%) = ([grams of glucan or xylan digested by enzyme]/[grams of glucan or xylan added]) × 100.

when the solid-to-liquid ratio was increased from 1 : 2 to 1 : 10. Delignification increased from 38 to 67%. The digestibility (with 15 FPU/g-glucan) also increased steadily from 74 to 91%. However, Xylan removal stayed relatively constant at 17–18%. The overall view is that a 1 : 6 ratio of solid/liquid is near the optimum level as it represents the minimum S : L ratio that can give a satisfactory pretreatment effect (85% glucan digestibility at 72-h). On the basis of the collective experimental data of delignification, xylan remaining, and digestibility we determined the optimum operating condition of the SAA to be: 60°C, 12 h of reaction time, and 1 : 6 of S : L ratio.

The enzymatic digestibility profile of a representative SAA-treated corn stover is shown in Fig. 1. The digestibilities at 72 h with 15 FPU/g-glucan are 85% and 78% for glucan and xylan, respectively. In the initial phase of profile, hydrolysis rate of SAA-treated corn stover is much higher than that of α-cellulose, perhaps owing to the presence of less crystalline cellulose in the treated corn stover. As indicated by the 78% of xylan digestibility, Spezyme CP obviously has a substantial amount of xylanase activity as well as glucanase activity. Judging from the digestibility values, the xylanase activity of Spezyme CP measured against the SAA-treated corn stover is somewhat lower than glucanase activity.

Table 3
Effect of Solid-to-Liquid Ratio on the Compositions and Enzymatic Digestibility in SAA-Treated Corn Stover[a]

| Solid-to-liquid | S.R. (%)[b] | Lignin (%)[c] | Delignification (%) | Solid (%) | | Enzymatic digestibility (%)[d] | |
|---|---|---|---|---|---|---|---|
| | | | | Glucan | Xylan | Glucan | Xylan |
| Untreated | – | 17.2 | – | 36.1 | 21.4 | 17.2 | 12.5 |
| | – | ± 0.4 | – | ± 0.3 | ± 0.2 | ± 1.5 | ± 1.2 |
| 1 : 2 | 79.0 | 10.7 | 37.7 | 36.1 | 18.1 | 74.0 | 66.2 |
| | ± 0.9 | ± 0.7 | ± 4.1 | ± 0.1 | ± 0.2 | ± 1.1 | ± 1.2 |
| 1 : 4 | 74.4 | 8.2 | 52.6 | 36.1 | 17.4 | 81.3 | 73.6 |
| | ± 10.4 | ± 0.4 | ± 2.2 | ± 0.3 | ± 0.4 | ± 0.5 | ± 2.2 |
| 1 : 6 | 71.3 | 6.4 | 62.6 | 36.1 | 17.8 | 85.0 | 77.9 |
| | ± 1.5 | ± 0.3 | ± 1.8 | ± 0.0 | ± 0.5 | ± 1.2 | ± 2.2 |
| 1 : 8 | 71.6 | 6.1 | 64.8 | 35.3 | 18.4 | 87.1 | 77.8 |
| | ± 0.8 | ± 0.1 | ± 0.8 | ± 0.2 | ± 0.1 | ± 0.2 | ± 1.7 |
| 1 : 10 | 71.4 | 5.6 | 67.2 | 36.1 | 17.2 | 90.1 | 79.8 |
| | ± 2.1 | ± 0.5 | ± 2.9 | ± 0.7 | ± 0.4 | ± 2.7 | ± 1.9 |

[a]Data in the table are based on the oven-dry untreated biomass. Values are expressed as mean and standard deviation ($n = 2$ for the composition analysis, $n = 4$ for the enzymatic digestibility). Pretreatment conditions: 15 wt% of ammonia concentration, 60°C of reaction temperature, 1 : 2–1 : 10 of solid : liquid ratio (based on wt), and 12 h of reaction time.

[b]S.R. stands for solid remaining after reaction.

[c]Klason lignin.

[d]Digestibility at 72 h, enzymatic hydrolysis conditions: 15 FPU/g-glucan, pH 4.8, digestibility at 50°C and 150 rpm. Digestibility (%) = ([grams of glucan or xylan digested by enzyme]/[grams of glucan or xylan added]) × 100.

## *Selectivity of Lignin Removal Over Xylan Removal*

Soluble lignin and its derivatives are toxic to microorganism and they also inhibit the enzymatic hydrolysis. The lignin content is, therefore, one of the major factors hindering the SSCF process *(1–6,14)*. Our previous study has also shown that removal of lignin form biomass substrates, which improves the microbial activity and the enzyme efficiency *(8,12,13,15,16)*. Lignin removal and xylan retention are two major factors in the SAA. The main purpose of the SAA is to maximize these factors with a constraint that we attain acceptable level of digestibility. We paid close attention to these reactions, especially the ratio of the lignin removal reaction over xylan removal reaction. We now introduce a selectivity defined as follows:

$$\text{Selectivity} = \frac{m_{\text{Lignin}}}{m_{\text{Xylan}}}$$

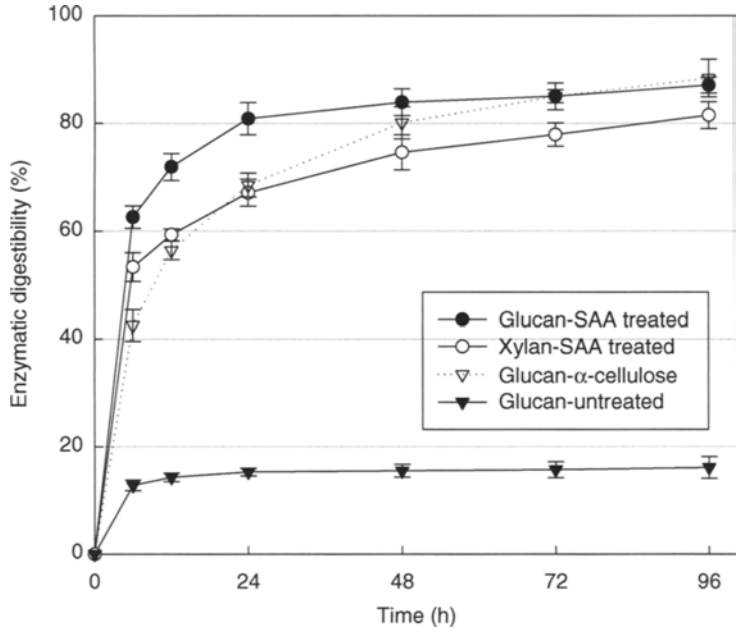


**Fig. 1.** Comparison of enzymatic hydrolysis between untreated and SAA-treated samples (*Note:* 15 FPU of cellulase/g-glucan, 30 CBU of β-glucosidase/g-glucan 50°C, 150 rpm, pretreatment conditions: 15 wt% of ammonia concentration, 60°C of reaction temperature, 12 h of reaction time, and 1 : 6 (based on wt) of solid : liquid ratio. Digestibility (%) = ([grams of glucan or xylan digested by enzyme/grams of glucan or xylan added]) × 100. The data in the figure show the mean value [$n = 4$]).

Where, $m_{\text{Lignin}}$ and $m_{\text{Xylan}}$ are the mass loss rate of lignin and xylan from the solid. The temperature effects on experimentally determined selectivity are presented in Fig. 2. The data clearly show that the selectivity attains maximum at 60°C for the two levels of ammonia concentrations (15 and 30 wt%). The aforementioned optimum temperature of 60°C for SAA is therefore reaffirmed from the standpoint of selectivity as well.

## *Scanning Electron Microscope*

Physical changes because of SAA were observed in the scanning electron microscope pictures of treated and untreated samples. Figure 3 shows that SAA treatment altered the biomass structure significantly. The untreated sample shows rigid, ordered fibrils, and connected structure (Fig. 3A). In the treated samples, the fibers are somewhat separated and exposed. A large amount of mass appears to have been removed from the initial connected structure (Fig. 3B). Pinholes and gaps are also visible in the treated corn stover, leading to a speculation that the surface area and the porosity have also increased.

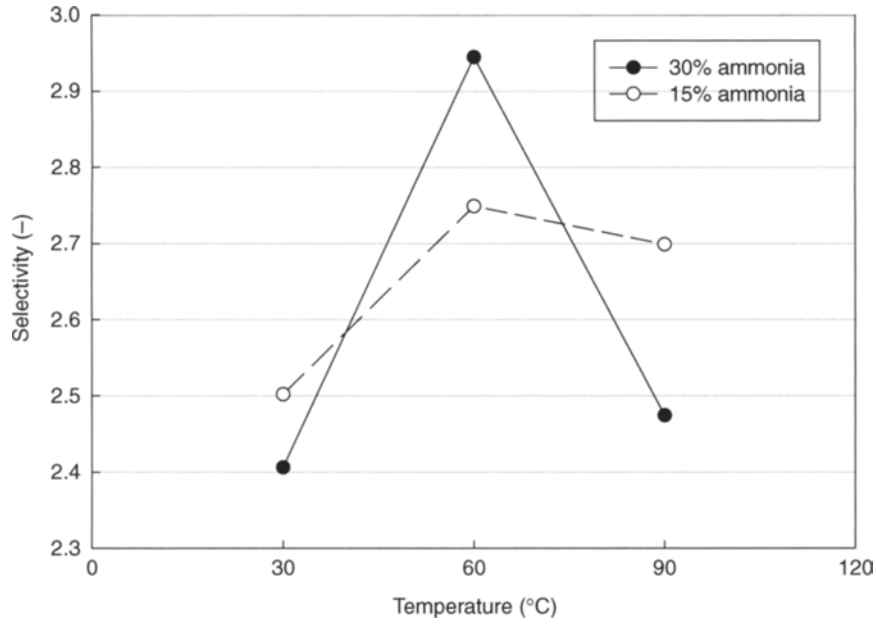


**Fig. 2.** Selectivity plot of the SAA-treated corn stover on various temperature and ammonia concentrations (*Note:* 1. Data in the figure are based on the oven-dry untreated biomass; Pretreatment conditions: 24 h of reaction time, 1 : 10 [based on wt] of solid : liquid ratio, 15 or 30 wt% of ammonia concentration, 40–90°C of reaction temperature. 2. Selectivity = $m_{Lignin}/m_{Xylan}$ [where, $m_{Lignin}$ and $m_{Xylan}$ are the mass loss rate of lignin and xylan in the solid, respectively]. The data in the figure show the mean value [$n = 2$; standard deviation < 0.35]).

## *Simultaneous Saccharification and Cofermentation*

SSCF of SAA-treated corn stover and α-cellulose was performed using recombinant *E. coli* ATCC 55124 (KO11) and Spezyme CP. The SAA conditions for the corn stover were: 15 wt% ammonia, 60°C, 12 h of treatment time, and 1 : 6 of solid-to-liquid ratio. Figures 4 and 5 present ethanol and sugar concentrations in the SSCF performed over an extended period. With initial feed of corn stover equivalent to 3 g of glucan/100 mL, the maximum ethanol concentration reached 19.2 g/L. It was attained after 96 h. This represents 77% of the maximum theoretical yield based on glucan and xylan. The same ethanol yield from SSCF is interpreted as 113% on the basis of glucan alone, a clear indication that both the xylan and glucan were converted to ethanol by the SSCF. The ethanol yield from the treated corn stover is substantially higher than that of α-cellulose performed with same glucan loading. The sugar profiles of Fig. 4 further indicate that glucan and xylan are consumed concurrently by *E. coli* (KO11), an important feature from a process viewpoint. The separate yield of ethanol from glucan and that from xylan were not identifiable in this work. The main purpose of the

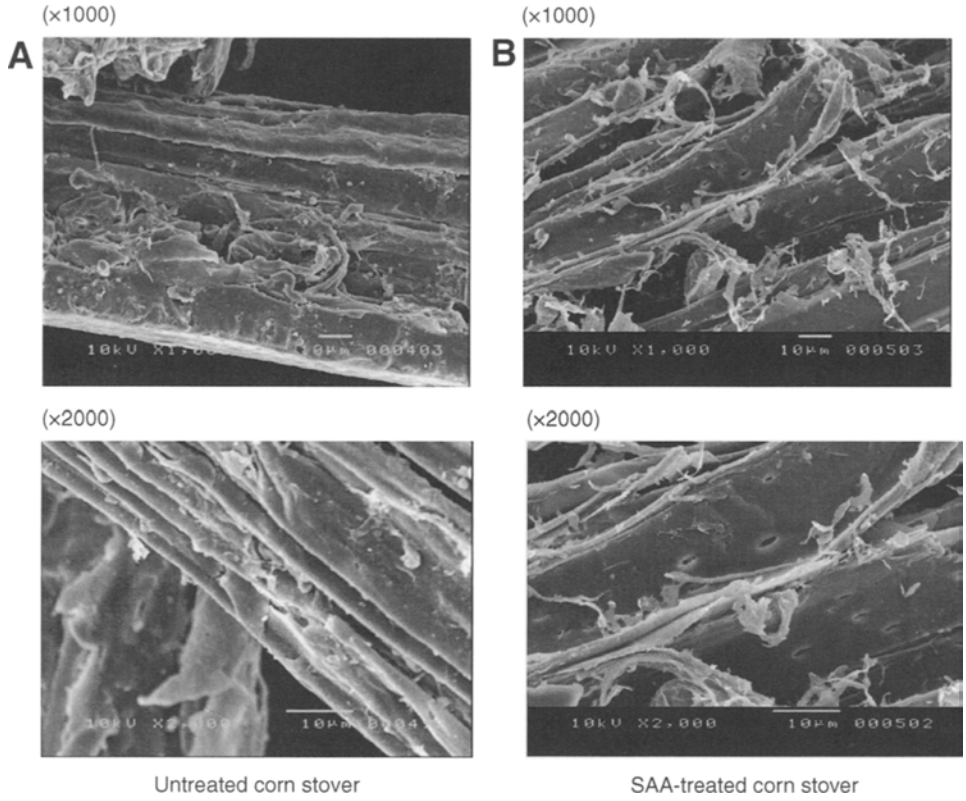


**Fig. 3.** Scanning electron micrographs of treated **(A)** and untreated corn stover **(B)** (*Note:* Pretreatment conditions: 15 wt% of ammonia concentration, 60°C of reaction temperature, 12 h of reaction time, and 1 : 6 [based on wt] of solid : liquid ratio).

SSCF is to convert both hexose and pentose in a single reactor. The SSCF described in this work serves that purpose well.

## Conclusion

SAA at moderate temperatures is a pretreatment method suitable for corn stover. This process is simple and requires low process energy. In this method, most of the xylan and all of glucan are retained after the treatment. SAA operated at 60°C reduces the reaction time from 10 d of room temperature operation to 12 h. The optimum operating conditions for the SAA at moderate temperature are 15 wt% ammonia, 60°C, 12 h, and 1 : 6 of solid : liquid ratio.

The treated corn stover exhibited enzymatic digestibilities of 85% and 78% for glucan and xylan, respectively, with enzyme loading of 15 FPU/g-glucan. The SAA-treated corn stover was subjected to a SSCF test using Spezyme CP (Genencor cellulase) and recombinant *E. coli* (strain KO11). The ethanol yield in the SSCF was 77% of maximum theoretical yield based on glucan and xylan of the treated sample. The same yield is

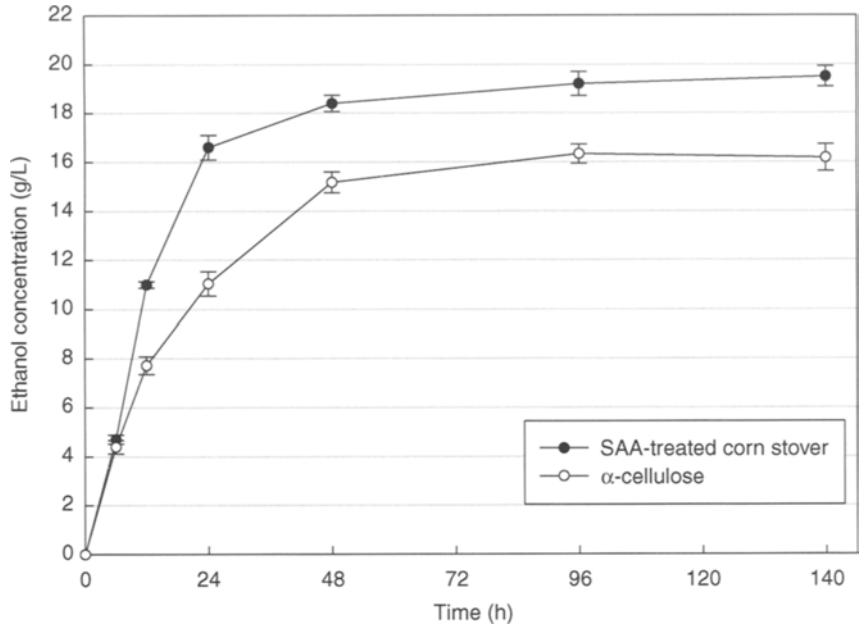


**Fig. 4.** SSCF of SAA-treated corn stover by recombinant *E. coli* (KO11) (*Note:* Microorganism: *E. coli* ATCC 55124; substrate: 3% [w/v] glucan loading/100 mL working volume; SAA-treated corn stover [15 wt% of ammonia concentration, 60°C of reaction temperature, 12 h of reaction time, and 1 : 6 of solid : liquid ratio]; SSCF: 15 FPU of Spezyme CP/g-glucan; 30 CBU of Novozyme 188/g-glucan; LB medium [0.5% of yeast extract and 1% of tryptone]; anaerobic condition; 38°C, 150 rpm. The data in the figure show the mean value and standard deviation [$n = 4$]).

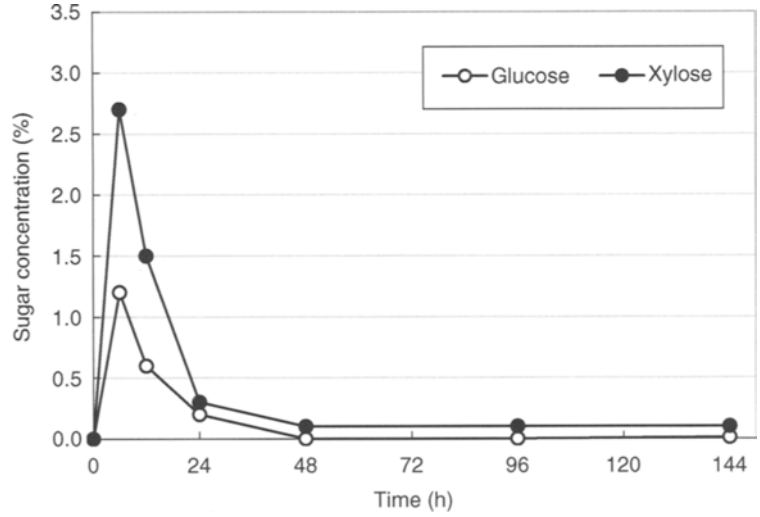


**Fig. 5.** Sugar concentration profiles in SSCF (*Note:* Microorganism: *E. coli* ATCC 55124; substrate: 3% [w/v] glucan loading/100 mL reactor; SAA-treated corn stover [15 wt% of ammonia concentration, 60°C of reaction temperature, 12 h of reaction time, and 1 : 6 of solid : liquid ratio]; SSCF: 15 FPU of Spezyme CP/g-glucan; 30 CBU of Novozyme 188/g-glucan; LB medium [0.5% of yeast extract and 1% of tryptone]; anaerobic condition; 38°C, 150 rpm. The data in the figure show the mean value [$n = 4$; standard deviation <0.7]).

calculated to be 113% on the basis of glucan alone, a clear indication that the SSCF converts both glucan and xylan into ethanol. The SSCF of SAA-treated corn stove proves to be an efficient one-step bioprocess scheme that can convert both the glucan and xylan in biomass into ethanol.

## Acknowledgments

The financial support for this research was provided by EERE/DOE (Contract DE-PS36-00GO10482/Subcontract through Dartmouth College).

## References

1. Chang, V. S. and Holtzapple, M. T. (2000), *Appl. Biochem. Biotechnol.* **84–86,** 5–37.
2. Cowling, E. B. and Kirk, Ti. K. (1976), *Biotechnol. Bioeng. Symp.* **6,** 95–123.
3. Dulap, C. E., Thomson, J., and Chiang, L. C. (1976), *AIChE. Symp. Ser.* **158,** 7258.
4. Lee, D., Yu, A. H. C., and Saddler, J. N. (1995), *Biotechnol. Bioeng.* **45,** 328–336.
5. Mooney, C. A., Mansfield, S. D., Touhy, M. G., and Saddler, J. N. (1998), *Bioresour. Technol.* **64,** 113–119.
6. Schwald, W., Brownell, H. H., and Saddler, J. N. (1988), *J. Wood Chem. Tech.* **8(4),** 543–560.
7. Kim, S. B. (1986), *PhD. Dissertation,* Auburn University.
8. Kim, T. H. and Lee, Y. Y. (2005), *Appl. Biochem. Biotechnol.* **121–124,** 1119–1132.
9. Hahn-Hägerdal, B., Jeppsson, H., Olsson, L., and Mohagheghi, A. (1994), *Appl. Microbiol. Biotechnol.* **41,** 62–72.
10. Ohta, K., Beall, D. S., Mejia, J. P., Shanmugam, K. T., and Ingram, L. O. (2004), *Appl. Environ. Microbiol.* **57,** 893–900.
11. NREL (1996), *Chemical Analysis and Testing Laboratory Analytical Procedures (CAT),* National Renewable Energy Laboratory, Golden, CO.
12. Iyer, P. V., Wu, Z. W., Kim, S. B., and Lee, Y. Y. (1996), *Appl. Biochem. Biotechnol.* **57–58,** 121–132.
13. Kim, T. H., Kim, J. S., Sunwoo, C., and Lee, Y. Y. (2003), *Bioresour. Technol.* **90,** 39–47.
14. Converse, A. O. (1993), *Substrate Factors Limiting Enzymatic Hydrolysis. Biotechnology in Agriculture No. 9,* in CAB Int'l, Oxford, UK, 93–106.
15. Kim, S. B. and Lee, Y. Y. (1996), *Appl. Biochem. Biotechnol.* **57–58,** 147–156.
16. Kim, T. H. and Lee, Y. Y. (2006), *Bioresour. Technol.* **97,** 224–232.

0273-2289/1559–0291 (Online)/07/136–140/93–104/$30.00

# β-D-Xylosidase From *Selenomonas ruminantium* of Glycoside Hydrolase Family 43

DOUGLAS B. JORDAN,*,[1] XIN-LIANG LI,[1] CHRISTOPHER A. DUNLAP,[2] TERENCE R. WHITEHEAD,[1] AND MICHAEL A. COTTA[1]

[1]*Fermentation Biotechnology Research Unit, National Center For Agricultural Utilization Research, US Department of Agriculture, Agricultural Research Service, †1815 N. University Street, Peoria, IL 61604, E-mail: jordand@ncaur.usda.gov; and* [2]*Crop Bioprotection Research Unit, National Center For Agricultural Utilization Research, US Department of Agriculture, Agricultural Research Service, 1815 N. University Street, Peoria, IL 61604*

## Abstract

β-D-Xylosidase from the ruminal anaerobic bacterium, *Selenomonas ruminantium* (SXA), catalyzes hydrolysis of β-1,4-xylooligosacharides and has potential utility in saccharification processes. The enzyme, heterologously produced in *Escherichia coli* and purified to homogeneity, has an isoelectric point of approx 4.4, an intact N terminus, and a Stokes radius that defines a homotetramer. SXA denatures between pH 4.0 and 4.3 at 25°C and between 50 and 60°C at pH 5.3. Following heat or acid treatment, partially inactivated SXA exhibits lower $k_{cat}$ values, but similar $K_m$ values as untreated SXA. D-Glucose and D-xylose protect SXA from inactivation at high temperature and low pH.

**Index Entries:** Fuel ethanol; glycohydrolase; hemicellulose; protein stability; saccharification; arabinofuranosidase; inhibitors; catalysis.

## Introduction

β-D-Xylosidase (EC 3.2.1.37) catalyzes hydrolysis of β-1,4 glycosidic bonds linking D-xylose residues that form xylooligosaccharides *(1–7)*. In conjunction with β-xylanases, which cleave larger polymers of D-xylose (xylans) to xylooligosaccharides, β-xylosidase serves to depolymerize xylan, a major component of plant cell walls and one of the most abundant biopolymers in nature. Auxiliary enzymes catalyze hydrolysis of sugar

*Author to whom all correspondence and reprint requests should be addressed.

†The mention of firm names or trade products does not imply that they are endorsed or recommended by the US Department of Agriculture over other firms or similar products not mentioned.

and acid side chains from the xylose residues. A goal of this laboratory and others is to identify catalytically efficient and robust enzymes that promote complete saccharification of xylans to monosaccharides for fermentation to fuel ethanol and other bioproducts.

Previous studies have shown that strains of the ruminal anaerobic bacterium, *Selenomonas ruminantium*, can enhance utilization of xylooligosaccharides under fermentation conditions *(8–10)*. A crude preparation of β-xylosidase from *S. ruminantium* GA192 (SXA), cloned and expressed in *Escherichia coli*, was shown to catalyze hydrolysis of 4-nitrophenyl-β-D-xylopyranoside (4NPX) and 4-nitrophenyl-α-L-arabinofuranoside with 10-fold preference for the former substrate over the latter *(11)*. Appositely, the preparation of SXA can catalyze hydrolysis of oligosaccharides, produced from partial hydrolysis of oatspelt xylan and wheat arabinoxylan, to smaller oligosaccharides, D-xylose and L-arabinose *(11)*.

The amino acid sequence of SXA places it within glycoside hydrolase family 43. Recently, X-ray structures of glycoside hydrolase family 43 β-xylosidases have been deposited in the Protein Data Bank (http://www.pdb.org/) for the enzyme from *Clostridium acetobutylicum*, *Bacillus subtilis*, and *B. halodurans*. The X-ray structures describe homotetrameric proteins with monomers consisting of two domains, one of which is similar to the five-bladed β propeller domain found in a GH family 43 arabinanase from *Cellvibrio cellulosa (12)*, which is a homodimer of monomers of the single domain. Protein sequence identity of SXA against the family 43 β-xylosidases with reported X-ray structures is 53–72%, making the X-ray structures useful in generating three-dimensional models of SXA. In this work, we explore practical properties of SXA with respect to saccharification of hemicellulose. Destabilization of SXA by extremes of pH and temperature, counteracting stabilization of SXA by monosaccharides, and the pH dependence of monosaccharide binding (inhibition of SXA catalysis) are reported.

## Materials and Methods

### *Materials and General Methods*

The gene encoding β-xylosidase from *S. ruminantium* GA192 was cloned and expressed in *E. coli* as described *(11)*. SXA, produced in *E. coli*, was purified to homogeneity, as judged from SDS-PAGE analysis, by using reverse phase and anionic exchange chromatography steps. Concentrations of homogeneous SXA monomers (active sites) were determined by using an extinction coefficient at 280 nm of 129,600/*M*/cm, calculated from amino acid composition *(13)*. N-terminal Edman sequencing was conducted by the Wistar Proteomics Facility (Philadelphia, PA). Buffers and 4NPX were obtained from Sigma-Aldrich (St. Louis, MO). All other reagents were reagent grade and high purity. A Cary 50 Bio UV-Visible spectrophotometer (Varian; Palo Alto, CA), equipped with a thermostatted holder for cuvettes, was used for spectral and kinetic determinations. Delta extinction coefficients

(product–substrate) at 400 nm were determined for each buffer condition by subtracting the molar absorbance of 4NPX from that of 4-nitrophenol (4NP). The concentration of 4NP was determined by using the published extinction coefficient of 18.3/m*M*/cm at 400 nm for 4NP in NaOH *(14)*. The concentration of 4NPX was determined by incubating the substrate with excess enzyme until an end point was reached, adding an aliquot (0.01–0.1 mL) to 0.1 *M* NaOH, recording the absorbance at 400 nm and using the extinction coefficient of 18.3/m*M*/cm for 4NP. Data were fitted to linear and nonlinear equations by using the computer program Grafit (Erithacus Software; Surrey, UK). Manipulations of X-ray structure coordinates (overlays, distance measurements, and so on.) were through Swiss-PDB Viewer 3.7 (http://www.expasy.org/spdbv/) *(15)*. The Stokes radius was calculated from X-ray coordinates of the homologous β-xylosidase from *C. acetobutylicum* (PDB ID: 1YI7) by using the computer program HYDROPRO, Version 7.C *(16)*. HYDROPRO (Freeware available at http://leonardo.rev.vm.es/macromol/programs/hydropro/hydropro.html) computes hydrodynamic properties of rigid macromolecules from their atomic-level structure.

### *Molecular Mass, Quaternary Structure, and Isoelectric Point SXA*

SDS-PAGE analysis was conducted by using a Criterion gel system, Criterion Tris-HCl 8–16% polyacrylamide gels, Bio-Safe stain, and protein molecular weight standards (all from Bio-Rad Laboratories; Hercules, CA). The Stokes radius of SXA was determined by using a gel filtration method: the column (2.6 × 62 $cm^2$) was packed with Toyapearl 55F resin (Tosoh Bioscience; Montgomeryville, PA) and equilibrated with 100 m*M* sodium phosphate, pH 7.0 at 24–26°C (room temperature) with a flow rate of 2.0 mL/min. Postcolumn eluate was monitored continuously for absorbance at 260, 280, and 405 nm. Elution volumes ($V_e$) were recorded and transformed to $K_{av}$ values by using Eq. 1, where $V_e$ is the recorded elution volume, $V_0$ is the void volume of the column, and $V_t$ is the total volume of the column plus tubing to the absorbance monitor. The value for $V_0$ was determined as 112 mL by using blue dextran 2000. The value of $V_t$ was determined as 330 mL. Protein standards of known Stokes radius ($R_S$) and molecular weight (MW) were obtained from GE Healthcare Life Sciences (Piscataway, NJ): ferritin ($R_S$ = 61.0 Å and MW = 440 kDa), catalase ($R_S$ = 52.2 Å and MW = 232 kDa), and aldolase ($R_S$ = 48.1 Å and MW = 158 kDa). The Stokes radius of SXA was determined from the linear regression of protein standards fitted to eq. 2 where $K_{av}$ is the transformed value of $V_e$, $R_S$ is the Stokes radius, $m$ is the slope and $C$ is the constant of the standard line.

$$K_{av} = \frac{V_e - V_0}{V_t - V_0} \tag{1}$$

$$(\mathrm{Log}K_{av})^{1/2} = m \times R_S + C \tag{2}$$

Isoelectric focusing (IEF) was conducted by using a Criterion electrophoresis system, Criterion pH 3.0–10.0 gels, IEF standards, and Coomasie R-250/Crocein Scarlet IEF gel stain (all from Bio-Rad; Hercules, CA).

### *pH Stability of SXA at 25°C*

Buffers of constant ionic strength ($I$ = 0.3 *M*), adjusted with NaCl, were used as indicated: 100 m*M* succinate–NaOH (pH 3.5–6.0), 100 m*M* sodium phosphate (pH 6.0–8.0), 30 m*M* sodium pyrophosphate (pH 8.0–9.0), and 100 m*M* glycine–NaOH (pH 9.0–10.0). For preincubation, an aliquot (7 µL) of SXA (168 µ*M* with respect to monomer concentration in 50 m*M* Tris-HCl, pH 7.5) was added to 100 µL of buffered solutions at varied pH and 25°C. For ligand protection studies, varied concentrations of D-xylose or D-glucose were included in or omitted from the 100-µL preincubation mixtures containing 100 m*M* succinate–NaOH, pH 4.0, adjusted with NaCl to $I$ = 0.3 *M*. At varied times after enzyme addition, 7 µL of preincubation mixtures were added to 1-mL reaction mixtures containing 100 m*M* sodium phosphate, pH 7.0, adjusted with NaCl to $I$ = 0.3 *M* (buffer A), and 1.95 m*M* 4NPX at 25°C. Initial rates were determined by monitoring reactions continuously at 400 n*M* for 0.3 min. For determination of the expression, "relative activity remaining", initial rates were divided by the rate of enzyme preincubated in buffer A at 0°C and assayed in 1-mL reaction mixtures containing the concentration of monosaccharide (corresponding to the carryover from enzyme preincubated in monosaccharide), the concentration of preincubation buffer (corresponding to the carryover from preincubated enzyme), and 1.95 m*M* 4NPX in buffer A at 25°C. Relative activity remaining data were fitted to Eq. 3, which describes a first-order decay: $A$ is the relative activity remaining at varied times of preincubation, $A_0$ is the relative activity remaining at time zero of the preincubation, $k_{obs}$ is the first-order rate constant, and $t$ is the time of preincubation. Apparent affinities for D-xylose and D-glucose were determined by fitting $k_{obs}$ values from the monosaccharide protection studies to Eq. 4 where $k_{obs}$ is the observed first-order rate constant for the decay, $k_0$ is the first-order rate constant in the absence of ligand (e.g., D-xylose), $I$ is the ligand concentration in the preincubation mixture, and $K_i$ is the dissociation constant of ligand from the enzyme-ligand complex.

$$A = A_0 \times e^{-k_{obs} \times t} \tag{3}$$

$$k_{obs} = \frac{k_0}{1 + I/K_i} \tag{4}$$

To determine the effect on steady-state kinetic parameters caused by low pH treatment, SXA was preincubated in 100 m*M* succinate–NaOH, pH 4.0 (adjusted with NaCl to $I$ = 0.3 *M*) at 25°C until approx 50% of

its catalytic activity was degraded (assessed from reactions containing 1.95 m*M* 4NPX in buffer A at 25°C), the pH of the preincubation mixture was raised to pH 4.9 (where SXA is stable) by adding an equal volume of buffer A at 0°C and mixing 7 µL of the pH-adjusted mixture were added to 1-mL reactions containing varied concentrations of 4NPX (0.2–5.0 m*M*) in buffer A at 25°C, and the reactions were monitored continuously at 400 nm for 0.3 min to determine initial rates. Initial rates of catalysis were fitted to Eq. 5 where $v$ is the initial rate at a specified concentration of 4NPX, $k_{cat}$ is the rate of catalysis when enzyme is saturated with substrate, $S$ is the substrate concentration, and $K_m$ is the Michaelis constant. The parameter, $k_{cat}$, is expressed in moles of substrate hydrolyzed per second per mole of enzyme active sites (monomers), calculated using the delta extinction coefficient for 4NP–4NPX at 400 nm and the extinction coefficient for SXA at 280 nm.

$$v = \frac{k_{cat} \times S}{K_m + S} \tag{5}$$

### *Thermal Stability of SXA at pH 5.3*

For preincubation, 7 µL of SXA (168 µ*M* with respect to monomer concentration in 50 m*M* Tris-HCl, pH 7.5) were added to 100 µL of 100 m*M* succinate–NaOH, pH 5.3 (adjusted with NaCl to $I = 0.3$ *M*) at varied temperatures. Ligand protection studies contained varied concentrations of D-xylose or D-glucose in the pH 5.3 preincubation buffer at 55°C. At varied times after enzyme addition, 15 µL of the preincubation mixtures were added to 15 µL of buffer A at 0°C to cool and bring the pH to 6.3, 7 µL of the enzyme mixture at 0°C were added to 1-mL reaction mixtures containing 1.95 m*M* 4NPX in buffer A at 25°C, and initial rates were determined by monitoring reactions continuously at 400 n*M* for 0.3 min. The expression, "relative activity remaining" $k_{obs}$, and $K_i$ were determined from the initial rate data as described in the Section pH Stability of SXA at 25°C.

To determine the effect on steady-state kinetic parameters caused by heat treatment, SXA was preincubated in 100 m*M* succinate–NaOH, pH 5.3 ($I = 0.3$ *M*) at 55°C until approx 50% of its catalytic activity was degraded (assessed from reactions containing 1.95 m*M* 4NPX in buffer A at 25°C), the temperature of the preincubation mixture was lowered by adding an equal volume of buffer A at 0°C, 7 µL of the cooled enzyme mixture were added to 1-mL reactions containing varied concentrations of 4NPX (0.2–5.0 m*M*) in buffer A at 25°C, and the reactions were monitored continuously at 400 nm for 0.3 min to determine initial rates of catalysis. Steady-state kinetic parameters were determined by fitting initial-rate data to Eq. 5 as described in the Section pH Stability of SXA at 25°C.

### *Inhibition of SXA-Catalyzed Hydrolysis of 4NPX by D-Glucose and D-Xylose*

The 1-mL reaction mixtures at 25°C contained varied concentrations of 4NPX and varied concentrations of D-glucose or D-xylose in buffers of constant ionic strength ($I$ = 0.3 $M$, adjusted with NaCl) as indicated in the Section pH Stability of SXA at 25°C. Reactions were initiated by addition of 7 µL of SXA, preincubated in 10 m$M$ sodium phosphate, pH 7.0 at 0°C. Reactions were monitored continuously for 0.3 min at 400 nm to determine initial rates. Initial-rate data were fitted to Eq. 6, where $v$ is the initial rate, $k_{cat}$ is the rate of the reaction when saturated with substrate, $S$ is the substrate concentration, $K_m$ is the Michaelis constant, $I$ is the inhibitor concentration (e.g., D-glucose), and $K_i$ is the dissociation constant of inhibitor from the enzyme-inhibitor complex.

$$v = \frac{k_{cat} \times S}{K_m(1 + I/K_i) + S} \tag{6}$$

## Results and Discussion

The gene encoding for SXA predicts a protein of 538 amino acids and a molecular mass of 61,140 Da. Edman sequencing of the first ten residues starting at the N terminus of SXA indicated the sequence, MNIQNPVLKG, which agrees with the sequence predicted from the gene and indicates that SXA is produced by *E. coli* with an intact N terminus. SDS-PAGE analysis shows that the purified SXA is homogeneous with a molecular mass of approx 60 kDa (Fig. 1A).

We chose the structure of β-xylosidase from *C. acetobutylicum* (PDB ID: 1YI7) for modeling of SXA because of its 72% protein sequence identity to SXA; as well, within a 9 Å sphere of the active site of 1YI7, all 21 residues are identical in the sequence of SXA. The X-ray coordinates of β-xylosidase from *C. acetobutylicum* contain 534 amino acid residues per subunit of the homotetramer, four fewer residues per subunit than the sequence of SXA. The longest axis of the homotetramer of β-xylosidase from *C. acetobutylicum* is calculated as 123 Å by using the computer program HYDROPRO, and the longest distance, perpendicular to this axis, is approx 90 Å as measured from the coordinates of the tetramer. We determined the Stokes radius of SXA by using a gel filtration method (Fig. 1B). The determined value of 55.4 ± 0.5 Å for the Stokes radius of SXA is similar to the value of 52 Å, calculated by using HYDROPRO and the X-ray structure coordinates of homotetrameric β-xylosidase from *C. acetobutylicum*; consistent with SXA occurring as a homotetramer in solution.

The isoelectric point of native SXA (estimated as approx 4.4) is slightly lower than the lowest isoelectric point (4.5) of the protein standards, but clearly well above the lowest pH (pH = 3.0) of the gel (Fig. 2A).

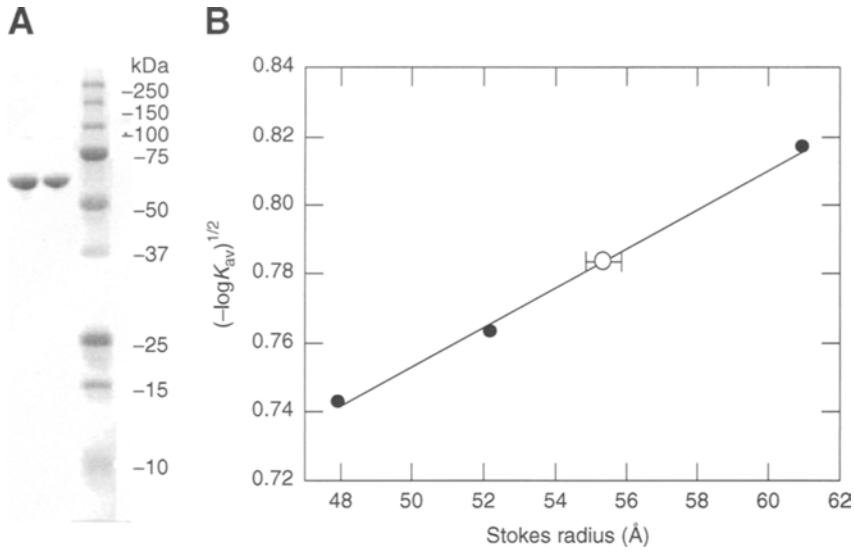


**Fig. 1.** Molecular mass and size of heterologously-produced SXA. **(A)** SDS-PAGE analysis of SXA. From left to right are lanes containing 1 μg SXA, 0.5 μg SXA, protein standards, and molecular masses (in kDa) of the protein standards. **(B)** Stokes radius of SXA. $K_{av}$ values were determined for protein standards (●) of known Stokes radius and the line was drawn by fitting the values to Eq. 2. SXA (○) is positioned by using the value determined for $K_{av}$ and the value determined for its Stokes radius (RS) ± the standard error of the estimate of the standard line (RS = 55.4 ± 0.5 Å).

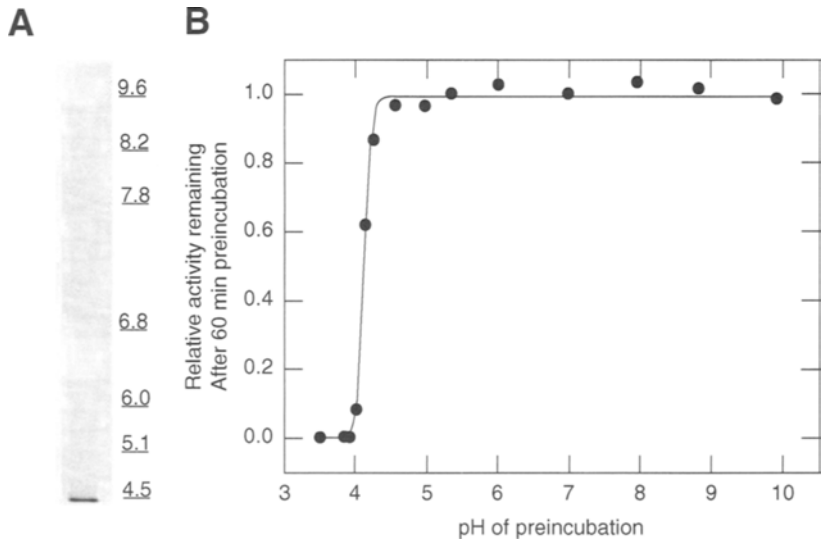


**Fig. 2.** Influence of pH on SXA. **(A)** IEF of native SXA. The left lane contains 0.5 μg SXA. The right lane indicates the positions of protein standards of known isoelectric point. **(B)** pH stability of SXA catalytic activity. SXA was preincubated at the indicated pH values and 25°C for 60 min before analyzing for relative activity remaining (catalytic activity relative to SXA preincubated at 0°C and pH 7.0). Standards deviations (±) of at least three determinations are indicated. The curve is drawn as a visual aid.

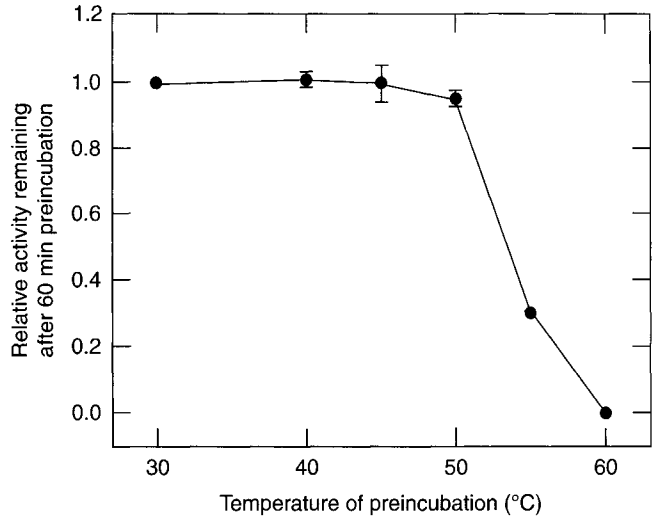


**Fig. 3.** Influence of temperature on SXA stability. SXA was preincubated at the indicated temperatures and pH 5.3 for 60 min before analyzing for relative activity remaining (catalytic activity relative to SXA preincubated at 0°C and pH 7.0). Standards deviations (±) of at least three determinations are indicated. The curve is drawn as a visual aid.

SXA is inactivated by conditions of low pH and high temperature, with a sharp drop in activity between pH 4.0 and 4.3 at 25°C (Fig. 2B) and a broad drop between 50 and 60°C at pH 5.3 (Fig. 3). Loss of catalytic activity at low pH and high temperature was associated with cloudiness in the preincubation mixtures, suggesting that SXA denatures and precipitates. To determine the effect of partially inactivated SXA on steady-state kinetic parameters, the enzyme was preincubated at pH 4.0 and 25°C or at pH 5.3 and 55°C until approx 50% of its catalytic activity remained in each sample. The preincubated samples of SXA were pH adjusted and cooled before the determination of kinetic parameters by fitting initial-rate data (obtained at pH 7.0 and 25°C) to Eq. 5 for comparison with an untreated SXA control sample: partially pH-inactivated SXA ($k_{cat}$ = 6.36 ± 0.041 $s^{-1}$ and $K_m$ = 0.366 ± 0.014 m*M*); partially temperature-inactivated SXA ($k_{cat}$ = 5.39 ± 0.062 $s^{-1}$ and $K_m$ = 0.386 ± 0.084 m*M*); and untreated control SXA ($k_{cat}$ = 12.2 ± 0.05 $s^{-1}$ and $K_m$ = 0.380 ± 0.005 m*M*). Thus, inactivation by low pH or high temperature is attributed to degradation of the $k_{cat}$ parameter without changing $K_m$, consistent with the view that, on limited exposure to the extreme conditions, a portion of the protein denatures and does not contribute to the catalyzed hydrolysis of 4NPX. Complementary experiments have shown that inactivation of SXA by low pH or high temperature is not reversible by simply adjusting the pH or cooling.

At pH 5.3 and 55°C, SXA is inactivated in a first-order process with a rate constant of 0.0252 ± 0.0020 $min^{-1}$ (Fig. 4A). SXA was protected from

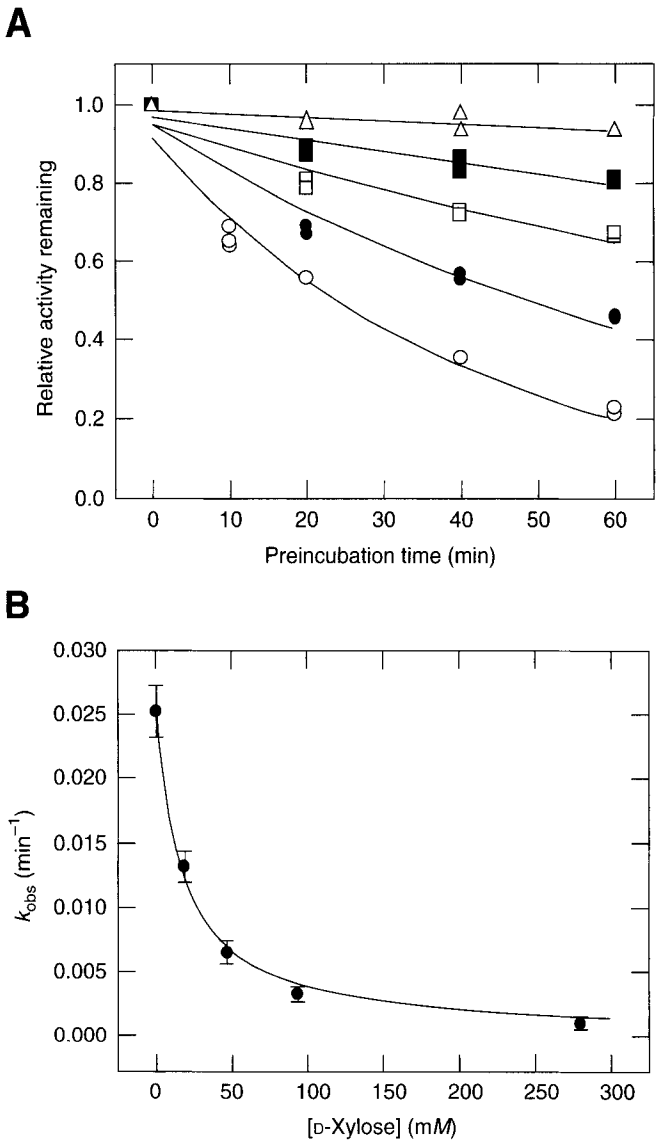


**Fig. 4.** Protection of SXA from thermal inactivation at 55°C by D-xylose. **(A)** Decay curves. Before analyzing for relative activity remaining, SXA was preincubated for the indicated times at pH 5.3 and 55°C in the absence (○) or presence of D-xylose at 18.7 m*M* (●), 46.7 m*M* (□), 93.5 m*M* (■), and 280 m*M* (△). Progress curves were generated by fitting the data for each D-xylose concentration to Eq. 3: 0 m*M* ($k_{obs}$ = 0.0252 ± 0.0020 min$^{-1}$), 18.7 m*M* ($k_{obs}$ = 0.0132 ± 0.0010 min$^{-1}$), 46.7 m*M* ($k_{obs}$ = 0.00649 ± 0.00087 min$^{-1}$), 93.5 m*M* ($k_{obs}$ = 0.00326 ± 0.00056 min$^{-1}$), and 280 m*M* ($k_{obs}$ = 0.000917 ± 0.00033 min$^{-1}$). **(B)** Dependence of first-order decay rates on the concentration of D-xylose. The $k_{obs}$ values determined from the decay rates of panel A (± standard errors) are plotted vs the D-xylose concentration of each preincubation condition. The curve was generated by fitting the $k_{obs}$ values to Eq. 4: $K_{i(D\text{-xylose})}$ = 17.6 ± 1.8 m*M*.

thermal denaturation by including in the preincubation mixture varied concentrations of D-xylose. Protection from temperature denaturation was dependent on the concentration of D-xylose (Fig. 4A), and as the concentration of D-xylose approached saturation the decay rate approaches zero (Fig. 4B), in accordance with Eq. 4, which estimates a dissociation constant ($K_i$ = 17.6 ± 1.8 m*M*) for D-xylose from the $k_{obs}$ values (Fig. 4B). This 55°C value compares with a 25°C value ($K_i$ = 7.62 ± 0.26 m*M*) for inhibition of SXA-catalyzed hydrolysis of 4NPX at pH 5.3 and 25°C by D-xylose. Similarly, SXA was protected from thermal denaturation (55°C at pH 5.3) by including in the preincubation mixture varied concentrations of D-glucose; denaturation rates, determined by fitting the decay data for each D-glucose concentration to Eq. 3, were 0 m*M* ($k_{obs}$ = 0.0256 ± 0.0015 $min^{-1}$), 93.5 m*M* ($k_{obs}$ = 0.00949 ± 0.00069 $min^{-1}$), 187 m*M* ($k_{obs}$ = 0.00588 ± 0.00077 $min^{-1}$), 280 m*M* ($k_{obs}$ = 0.00445 ± 0.00081 $min^{-1}$), and 374 m*M* ($k_{obs}$ = 0.00336 ± 0.00095 $min^{-1}$). A dissociation constant ($K_i$ = 56.1 ± 0.8 m*M*) was estimated for D-glucose from fitting the $k_{obs}$ values to Eq. 4. This 55°C value compares with a 25°C value ($K_i$ = 79.0 ± 2.3 m*M*) for inhibition of SXA-catalyzed hydrolysis of 4NPX at pH 5.3 and 25°C by D-glucose.

At pH 4.0 and 25°C, SXA is inactivated in a first-order process with a rate constant of 0.0784 ± 0.0023 $min^{-1}$, and protection from denaturation at low pH is dependent on the concentration of D-xylose (Fig. 5A). Protection from pH denaturation by D-xylose is saturable with a first-order decay rate of zero at saturating D-xylose in accordance with Eq. 4, which estimates a dissociation constant ($K_i$ = 31.7 ± 2.8 m*M*) for D-xylose (Fig. 5B). This pH 4.0 value compares with a pH 4.3 value ($K_i$ = 43.5 ± 1.1 m*M*) for inhibition of SXA-catalyzed hydrolysis of 4NPX at pH 4.3 and 25°C by D-xylose. Similarly, inactivation rates of SXA at pH 4.0 and 25°C are slowed by D-glucose; denaturation rates, determined by fitting the decay data for each D-glucose concentration to Eq. 3, were 0 m*M* ($k_{obs}$ = 0.0518 ± 0.0037 $min^{-1}$), 234 m*M* ($k_{obs}$ = 0.0210 ± 0.0016 $min^{-1}$), 467 m*M* ($k_{obs}$ = 0.0124 ± 0.0007 $min^{-1}$), and 701 m*M* ($k_{obs}$ = 0.00748 ± 0.00083 $min^{-1}$). A dissociation constant ($K_i$ = 147 ± 12 m*M*) was estimated for D-glucose from fitting the $k_{obs}$ values to Eq. 4. This pH 4.0 value compares with a pH 4.3 value ($K_i$ = 330 ± 8 m*M*) for inhibition of SXA-catalyzed hydrolysis of 4NPX at pH 4.3 and 25°C by D-glucose.

The influence of pH on inhibition of SXA-catalyzed hydrolysis of 4NPX by D-glucose and D-xylose was determined at 25°C by using buffers of constant ionic strength (*I* = 0.3 *M*). D-Glucose and D-xylose inhibited the catalyzed reaction competitively with respect to substrate 4NPX at all pH values examined in accordance with Eq. 6. $K_i$ values for glucose decrease with increasing pH as follows: pH 4.3 (330 ± 8 m*M*), pH 5.3 (79.0 ± 2.3 m*M*), pH 7.0 (34.5 ± 0.7 m*M*), and pH 9.0 (18.7 ± 0.6 m*M*). Similarly, affinities of SXA for D-xylose increase with increasing pH as seen in the progression of $K_i$ values: pH 4.3 (43.5 ± 1.1 m*M*), pH 5.3 (7.62 ± 0.26 m*M*), pH 7.0 (3.82 ± 0.06 m*M*), and pH 9.0 (3.21 ± 0.14 m*M*).

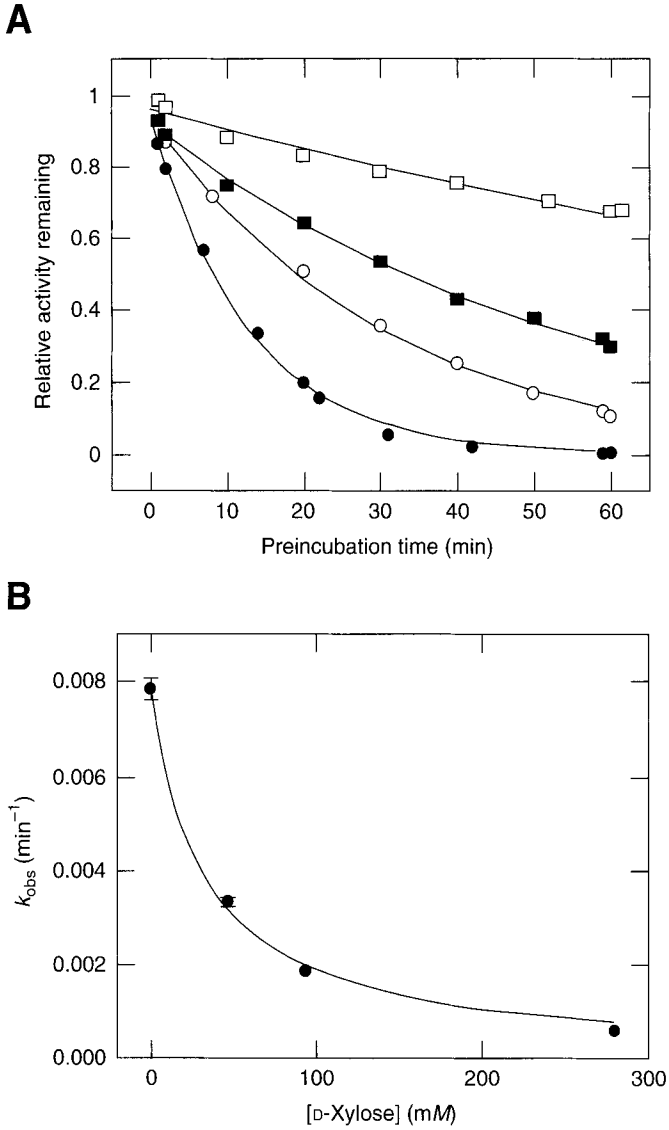


**Fig. 5.** Protection of SXA from low pH inactivation at pH 4.0 by D-xylose. **(A)** Decay curves. Before analyzing for relative activity remaining, SXA was preincubated for the indicated times at pH 4.0 and 25°C in the absence (●) or presence of D-xylose at 46.7 m*M* (○), 93.5 m*M* (■), and 280 m*M* (□). Progress curves were generated by fitting the data for each D-xylose concentration to Eq. 3: 0 m*M* ($k_{obs}$ = 0.0784 ± 0.0023 min$^{-1}$), 46.7 m*M* ($k_{obs}$ = 0.0335 ± 0.0008 min$^{-1}$), 93.5 m*M* ($k_{obs}$ = 0.0186 ± 0.0004 min$^{-1}$), and 280 m*M* ($k_{obs}$ = 0.00614 ± 0.00036 min$^{-1}$). **(B)** Dependence of first-order decay rates on the concentration of D-xylose. The $k_{obs}$ values determined from the decay rates of panel A (± standard errors) are plotted vs the D-xylose concentration of each preincubation condition. The curve was generated by fitting the $k_{obs}$ values to Eq. 4: $K_{i(D\text{-xylose})}$ = 31.7 ± 2.8 m*M*.

Temperature and pH profiles of SXA stability place certain constraints on its application to processes for saccharification of the hemicellulose component of herbaceous biomass, as do $K_i$ values for D-glucose and

D-xylose inhibition of SXA catalysis. Potentially, if saccharification processes require higher temperatures or lower pH than the native SXA withstands, SXA could be modified to better accommodate such assaults on its stability. Similarly, inhibition of catalysis by D-glucose and D-xylose, which constitute two major constituents of herbaceous biomass, potentially could be alleviated by protein engineering approaches. Three-dimensional models of SXA could aid in the design of such modifications. Native SXA is an efficient catalyst for the hydrolysis of xylooligosaccharides, details of which will be reported soon. Owing to the nature of SXA, negative influences of temperature and pH on protein stability and negative influences of inhibition of catalysis by D-glucose and D-xylose are not additive. That is, under conditions of low pH and/or high temperature, the presence of D-glucose and D-xylose could serve to stabilize SXA to an extent similar to their inhibition of catalysis. It is likely that oligosaccharide substrates of SXA afford similar protection from inactivation by low pH and high temperature.

## Acknowledgments

We thank Jay D. Braker and Patrick Kane for excellent technical assistance in contributing to this work.

## References

1. Zechel, D. L. and Withers, S. G. (2001), *Curr. Opin. Chem. Biol.* **5,** 643–649.
2. Vocadlo, D. J., Wicki, J., Rupitz, K., and Withers, S. G. (2002), *Biochemistry* **41,** 9727–9735.
3. Sinnott, M. L. (1990), *Chem. Rev.* **90,** 1171–1202.
4. Shallom, D., Leon, M., Bravman, T., et al. (2005), *Biochemistry* **44,** 387–397.
5. Saha, B. C. (2003), *J. Ind. Microbiol. Biotechnol.* **30,** 279–291.
6. Marshall, P. J. and Sinnott, M. L. (1983), *Biochem. J.* **215,** 67–74.
7. Herrmann, M. C., Vrsanska, M., Jurickova, M., Hirsch, J., Biely, P., and Kubicek, C. P. (1997), *Biochem. J.* **321,** 375–381.
8. Cotta, M. A. (1993), *Appl. Environ. Microbiol.* **59,** 3557–3563.
9. Williams, A. G., Withers, S. E., and Joblin, K. N. (1991), *Lett. Appl. Microbiol.* **12,** 232–235.
10. Cotta, M. A. and Whitehead, T. R. (1998), *Curr. Microbiol.* **36,** 183–189.
11. Whitehead, T. R. and Cotta, M. A. (2001), *Curr. Microbiol.* **43,** 293–298.
12. Nurizzo, D., Turkenburg, J. P., Charnock, S. J., et al. (2002), *Nat. Struct. Biol.* **9,** 665–668.
13. Gill, S. C. and von Hippel, P. H. (1989), *Anal. Biochem.* **182,** 319–326.
14. Kezdy, F. J. and Bender, M. L. (1962), *Biochemistry* **1,** 1097–1106.
15. Guex, N. and Peitsch, M. C. (1997), *Electrophoresis* **18,** 2714–2723.
16. García de la Torre, J., Huertas, M. L., and Carrasco, B. (2000), *Biophys. J.* **78,** 719–730.

0273-2289/1559–0291 (Online)/07/136–140/105–114/$30.00

# Biodiesel Fuel Production by the Transesterification Reaction of Soybean Oil Using Immobilized Lipase

OTÁVIO L. BERNARDES,[1] JULIANA V. BEVILAQUA,[2] MÁRCIA C. M. R. LEAL,[3] DENISE M. G. FREIRE,[3] AND MARTA A. P. LANGONE*,[1]

*[1]Instituto de Química, Universidade do Estado do Rio de Janeiro, Rua São Francisco Xavier, 524, PHLC, sl. 427, CEP: 20559-900, RJ, RJ, Brazil, E-mail: langone@uerj.br; [2]Centro de Pesquisa e Desenvolvimento da Petrobras—Cenpes, Brazil; and [3]Instituto de Química, Universidade Federal do Rio de Janeiro, RJ, CEP: 21949-900, Brazil*

## Abstract

The enzymatic alcoholysis of soybean oil with methanol and ethanol was investigated using a commercial, immobilized lipase (Lipozyme RM IM). The effect of alcohol (methanol or ethanol), enzyme concentration, molar ratio of alcohol to soybean oil, solvent, and temperature on biodiesel production was determined. The best conditions were obtained in a solvent-free system with ethanol/oil molar ratio of 3.0, temperature of 50°C, and enzyme concentration of 7.0% (w/w). Three-step batch ethanolysis was most effective for the production of biodiesel. Ethyl esters yield was about 60% after 4 h of reaction.

**Index Entries:** Enzyme; ethanol; immobilized lipase; methanol; solvent; soybean oil.

## Introduction

The use of an alternative fuel becomes necessary owing to the reduction of oil reserves and, consequently, of the diesel oil supplies and to the increasingly higher amount of gases produced in the combustion reaction of its derivatives. The indirect use of vegetable oils or mixtures of them is usually regarded as impracticable and insufficient for direct/indirect injection in diesel engines because of their high viscosity, the presence of free fatty acids, and the presence of gum from the oxidation and polymerization of diesel oil during their storage and combustion *(1)*. Recently, biodiesel, defined as a mixture of monoalkyl esters derived from fatty acids, has become a more interesting option because of its environmental benefits, as it comes from a renewable source, is biodegradable, and nontoxic.

*Author to whom all correspondence and reprint requests should be addressed.

Biodiesel fuel can be obtained through different reaction pathways. The transesterification of an oil or fat in the presence of an acid or alkaline catalyst is commercially used. The lipase-catalyzed enzymatic production of biodiesel under milder conditions unfolds as a promising option. Under optimum conditions, the cost of production can be reduced and the conversion yield improved (2). Moreover, that reaction uses fewer complex steps for product isolation as well as avoids the elimination of the catalyst and salt produced in the first process (3). This work investigated the effect of reaction parameters such as: temperature, oil/alcohol molar ratio, alcohol, enzyme concentration, solvent, as well as lipase reuse on the transesterification reaction of soybean oil by short-chain alcohols, using an immobilized lipase (Lipozyme RM IM, Novozymes A/S, Denmark).

## Materials and Methods

### Materials

The commercial enzyme used, Lipozyme RM IM, was provided by Novozymes. Other reagents used were commercial soybean oil (Sadia), analytical grade ethanol, methanol, and hexane (Merck, Darmstadt, Germany). Methyl heptadecanoate (a chromatographic standard) was acquired from Sigma (St. Louis, MO).

### Measurement of Lipase Activity

The esterification activity of Lipozyme RM-IM was measured by the consumption of oleic acid at 45°C in the esterification reaction with butanol (oleic acid/butanol molar ratio of 1) with the enzyme concentration of 3% (w/w). One esterification unit of Lipozyme was defined as 1 μmol of oleic acid consumed/min (U) under the experimental conditions described herein. The enzyme used in this work has esterification activity of 3000 U/g.

### Reaction System

The transesterification reactions between soybean oil and alcohol were conducted in closed 15-mL batch reactors, with constant mechanical stirring, coupled to condensers in order to avoid alcohol loss by volatilization. The water circulating in the condenser was cooled by a thermostatic bath. The reaction temperature was kept constant by circulating ethylene glycol from a thermostatic bath (Haake DC 10-B3) into the reactor's jacket. Reaction progress was monitored by taking duplicate samples, which were diluted in hexane and analyzed by gas chromatography.

### Chromatography Analysis

The samples were injected into a Varian gas chromatograph (CP–3380 model), equipped with a flame ionization detector and a CP WAX 52 CB capillary column 30 m × 0.25 mm × 0.25 μm, and split injection system

with a 1 : 20 ratio. Injector and detector temperatures were kept at 250°C. The heating rate was 20°C/min. The oven was initially maintained at 200°C for 4.5 min, then was heated up to 210°C, and was kept constant at this temperature for 0.5 min. After that, it was heated to 220°C for 0.5 min. The oven was heated again to 250°C at a 30°C/min rate and maintained at this temperature for 1.5 min. Hydrogen was used as the carrier gas at a 1.8 mL/min flow rate; column pressure was set at 12 psi. A computer loaded with the Star Workstation 6.2 software was connected to the GC by a Star 800 Module Interface to automatically integrate the peaks obtained. Methyl heptadecanoate was the internal standard used.

### *Transesterification Reaction*

The reaction medium consisted of a mixture of the commercial soybean oil, alcohol, and enzyme. The biodiesel production was also evaluated in the presence of a solvent. In this work, the transesterification reactions took place in the presence of hexane (50% [v/v]). The alkyl esters (biodiesel) synthesis was evaluated as a function of temperature (40, 50, and 60°C), enzyme concentration (3, 5, 7, 9, 11, and 20% [w/w]), alcohol/soybean oil molar ration (3, 6, and 10), type of alcohol used (methanol or ethanol), and in respect to stepwise addition of alcohol (single addition or two or three consecutive alcohol additions, at different times). One molar equivalent of ethanol was 0.72 g for 12.70 g soybean oil.

## Results and Discussion

### *Enzymatic Transesterification in the Presence of a Solvent*

#### Effect of Reactants Molar Ratio

The effect of the ethanol/soybean oil molar ratio over the transesterification reaction was evaluated initially using a 7% (w/w) commercial, immobilized lipase (Lipozyme RM IM) in the presence of hexane (50% [v/v]). An increase in the concentration of any reactant results in a higher yield of ester, because the ethanolysis is a reversible reaction. At least three mols of ethanol are required in the ethanolysis reaction to accomplish a complete conversion of the soybean oil into its ethyl esters. An alcohol/oil molar ratio of six is commonly used in industrial processes to obtain higher yields of esters *(4–6)*. In such case, ethanol/soybean oil molar ratios of 6 and 10 were tested in reactions conducted at 40°C in a closed batch reactor. The results obtained are shown in Table 1 and indicate that the excess of alcohol reduced the ethyl esters production, even in the presence of a nonpolar solvent, hexane. It is well known that, usually, proteins are unstable in a reaction medium containing short-chain alcohols, such as ethanol and methanol. An excess of alcohol can promote the inhibition and/or deactivation of the lipases *(3,7–9)* as observed in Table 1 where the reduced ethyl esters yield is related to the increase in the alcohol molar ratio.

Table 1
Effects of Enzyme Concentration, Alcohol/Soybean Oil Molar Ratio, Type of Alcohol and Solvent Addition on Reaction Yield

| Enzyme concentration (% [w/w]) | Alcohol/ soybean oil molar ratio | Alcohol | Solvent addition (% [v/v]) | Ester yield (%) |
|---|---|---|---|---|
| 7 | 6 | Ethanol | Hexane 50 | 25.0 |
| 7 | 10 | Ethanol | Hexane 50 | 12.0 |
| 20 | 10 | Ethanol | Hexane 50 | 24.7 |
| 7 | 6 | Methanol | Hexane 50 | 5.1 |
| 7 | 6 | Ethanol | No addition | 3.5 |
| 7 | 10 | Ethanol | No addition | 3.3 |
| 7 | 3 | Ethanol | No addition | 16.9 |

The results were obtained after 8 h of reaction at 40°C.

### Effect of Enzyme Concentration

The effect of the enzyme concentration in the ethyl esters production in the reaction was investigated using an ethanol/soybean oil molar ratio of 10 in the presence of hexane (50% [v/v]), at 40°C, in a closed batch reactor. According to the results shown in Table 1, there was an increase in the yield and in the rate of the reaction when 20% (w/w) Lipozyme was used. After 8 h of reaction, the yield obtained was approx 25%, whereas for an enzyme concentration of 7% (w/w), the yield was only 12%. However, taking into account the cost of process and the operational difficulty of working with such a high enzyme concentration (20% [w/w]), the concentration chosen to conduct the experiment was 7% (w/w).

### Effect of Type of Alcohol

The transesterification of triglycerides with methanol is the preferred enzyme-catalyzed reaction for biodiesel production. Nevertheless, the enzymatic alcoholysis of triglycerides using other alcohols, including ethanol, *n*-propanol, isopropyl alcohol, butanol, and pentanol has also been investigated *(4)*. Usually, methanol is the alcohol of choice because of its lower cost in various countries. However, the importance of ethyl alcohol for the Brazilian energy market is well known. The effect of the kind of alcohol used (methanol or ethanol) over the reaction, at 40°C, was investigated using an alcohol/oil molar ratio of 6 and 7% (w/w) Lipozyme RM IM. The reactions were conducted in the presence of 50% (v/v) solution of hexane.

According to the results presented in Table1, the reaction yield when ethanol was used was five times higher than that when methanol was used. This can be explained by the greater enzyme deactivation by an alcohol with fewer carbon atoms. Methanol is a highly hydrophilic solvent, thus able to solubilize and remove the essential water layer that cover the enzymes, which can result in loss of lipase's catalytic activity *(10,11)*.

### Effect of Solvent Addition

The use of organic solvents is not indicated for biodiesel production because of the high risk of explosion and the need for an additional step for solvent removal *(7)*. On the other hand, immobilized lipases show high conversion rates in nonpolar organic solvents, therefore there are several studies of triglyceride enzymatic alcoholysis in organic solvents *(9)*. The biocatalysis of synthetic reactions, such as the biodiesel production reaction, are usually considered possible in solvents immiscible in water and with logP (logP is one of the parameters used to determine the hydrophobicity of a solvent, and is defined as the partition coefficient of a solute in a standard biphasic system formed by water and 1-octanol) more than 4 *(10,11)*. Hexane is one of the most commonly used solvents in synthetic reactions using lipases (logP for hexane = 3.5).

The effect of the addition of 50% v/v hexane was evaluated on the transesterification reaction of soybean oil with ethanol, at 40°C, with 7% (w/w) Lipozyme RM IM. According to the results presented in Table 1, the use of hexane helped the biodiesel production. However, because of the cost and operational difficulties of the process conducted in the presence of a solvent, the effects of certain reaction parameters on the solvent-free transesterification reaction were also investigated.

## *Enzymatic Transesterification in a Solvent-Free Medium*

### Effect of the Reactants Molar Ratio

The effect of the ethanol/soybean oil molar ratio was evaluated in the transesterification reaction conducted at 40°C with 7% (w/w) Lipozyme. The results obtained (Table 1) show that the stoichiometric molar ratio of the reactants (ethanol/oil molar ratio = 3) allowed a higher yield of ethyl esters, which confirms the prejudicial effect of a high concentration of ethanol on the lipase activity. Similar results *(3,12)* were observed for the methanolysis of vegetable oils using Novozym 435 (commercial, immobilized *Candida antarctica* lipase). According to Köse et al. *(12)*, the alcohol can remove the essential water layer which stabilizes the immobilized enzyme, and can form inhibiting binary alcohol-lipase complexes.

### Effect of the Stepwise Addition of Ethanol

At least the stoichiometric amount of ethanol has to be used in order to achieve total conversion of triglycerides into their ethyl esters. Even under these conditions, the yield was low (16.9% in 8 h), as seen in Table 1. The stepwise addition of ethanol (three consecutive steps) was studied in order to avoid the lipase deactivation by a high initial alcohol concentration. The reactions were conducted with 7% (w/w) Lipozyme at 40°C and with the reactants stoichiometric ratio. The results are shown in Fig. 1. When ethanol was added in a stepwise manner (i.e., 1/3 added at time 0, 1/3 after 4 h, and 1/3 after 6 h), the yield (60%) was much higher than that

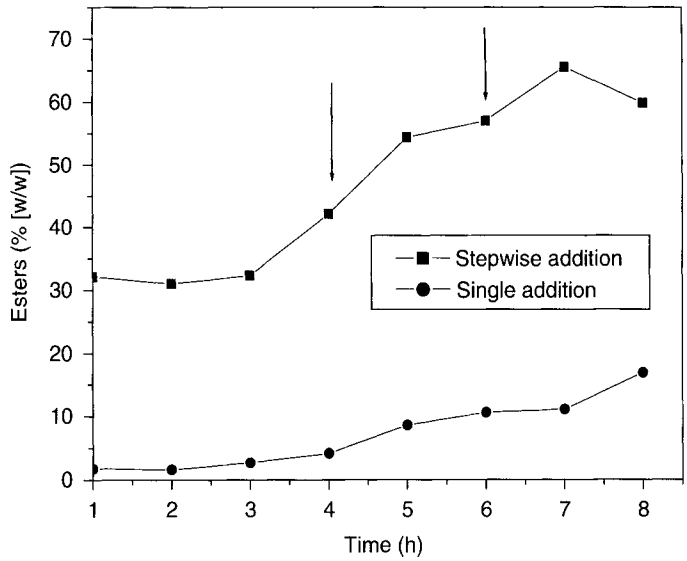


**Fig. 1.** Effect of stepwise ethanol addition on the transesterification of soybean oil using an ethanol/soybean oil molar ratio of 3, 7% (w/w) Lipozyme RM IM at 40°C.

observed when ethanol was added in a single step at the beginning of the reaction.

Shimada et al. (*7*) also verified a higher conversion in the methanolysis reaction of vegetable oil with immobilized *C. antartica* lipase, and three consecutive methanol additions (0, 10, and 24 h).

The stepwise addition also allowed a higher ethyl esters yield, even when an excess of alcohol was used (ethanol/soybean oil molar ratio = 6), as seen in Fig. 2. In this case, ethanol was added in six steps (time: 0, 30, 60, 90, 120, and 150 min). According to the results presented in Figs. 1 and 2, the best molar ratio is the stoichiometric ratio, even when ethanol is added in a stepwise manner.

Because the stepwise addition of ethanol, using the reactants stoichiometric ratio afforded the highest yield of ethyl esters, different ethanol addition times were also investigated. The results show that the ethanol addition at shorter times (0, 30, and 60 min) allowed the highest reaction yield (58.2%) to be reached more rapidly—after about 3 h.

## Effect of Enzyme Concentration

The effect of the enzyme concentration on the reaction yield was investigated under the best reaction conditions established by the previously reported results, (i.e., molar ratio of reactants equal to 3, no solvent, stepwise ethanol addition after 0, 30, and 60 minutes of reaction). According to the results presented in Fig. 3, the highest ethyl esters yield was obtained with 7% (w/w) Lipozyme. The ethanolysis reaction mixture requires constant stirring because of the low solubility of the vegetable oil in ethanol. Initially, the reactants formed a two-phase system, which becomes a three-phase system

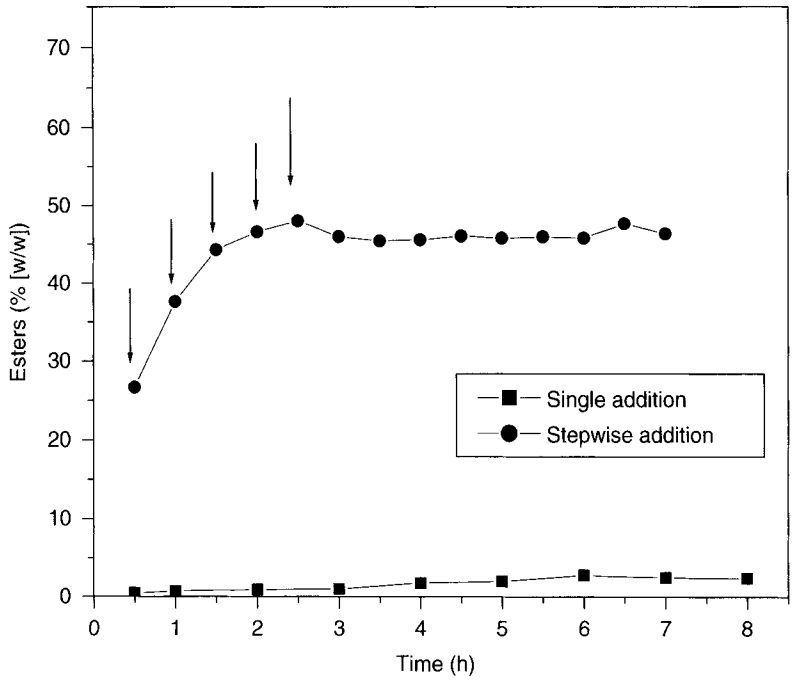


**Fig. 2.** Effect of stepwise ethanol addition on the transesterificaction reaction of soybean oil using an ethanol/soybean oil molar ratio of 6, 7% (w/w) Lipozyme RM IM at 40°C.

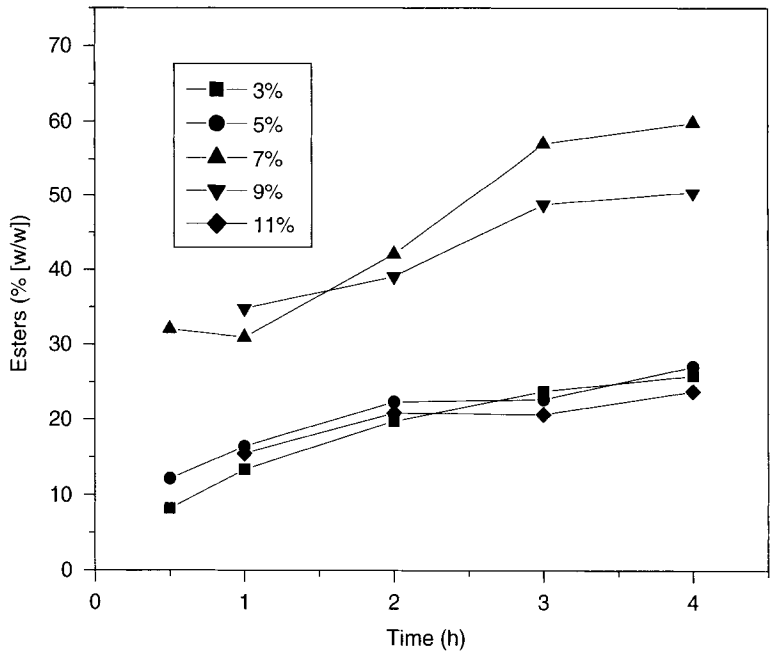


**Fig. 3.** Effect of Lipozyme RM IM concentration on the transesterification of soybean oil using an ethanol/soybean oil molar ratio of 3, with stepwise ethanol addition (1/3 at 0 h, 1/3 after 0.5 h, and 1/3 after 1 h) at 40°C.

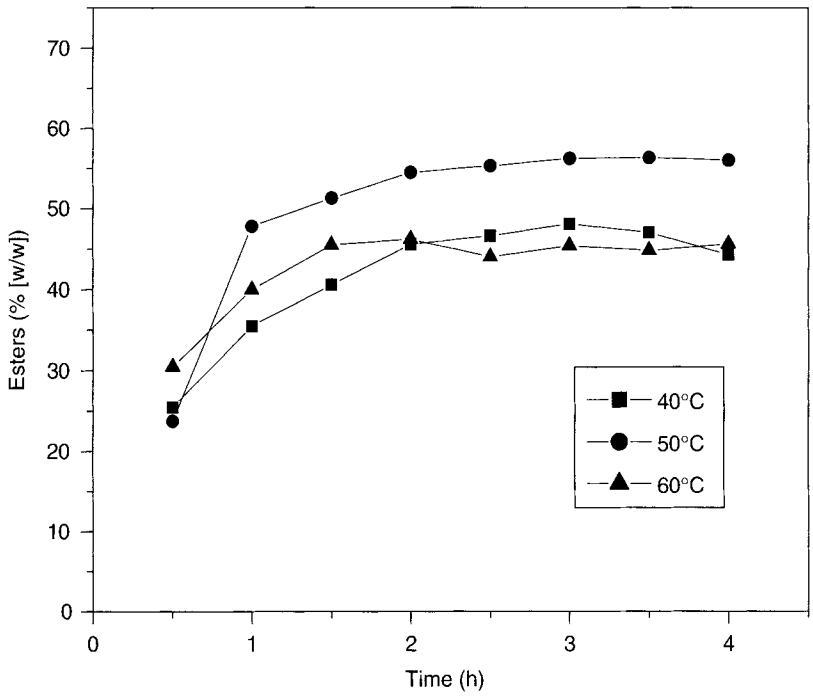


**Fig. 4.** Effect of temperature on the transesterification of soybean oil using an ethanol/soybean oil molar ratio of 3, with stepwise ethanol addition (1/3 at 0 h, 1/3 after 0.5 h, and 1/3 after 1 h), and 7% (w/w) Lipozyme RM IM.

once the immobilized enzyme is added. Higher Lipozyme concentrations (9 and 11% [w/w]) did not allow an appropriate system homogenization with the stirring system used, which can explain the lower ethyl esters yield shown in Fig. 3. After 8 h of reaction, the final yield was basically the same for the reactions conducted with Lipozyme at 7, 9, or 11% (w/w) (these results are not shown in the figures).

## Effect of Temperature

Temperature is another factor that can possibly interfere in the immobilized lipase-catalyzed alcoholysis of vegetable oils. The biodiesel production was investigated at temperatures of 40, 50, and 60°C for reactions using a stoichiometric ratio of reactants and 7% (w/w) Lipozyme. The results obtained show maximum yield at 50°C (Fig. 4). An increase in temperature increases the equilibrium conversion, as verified in the reactions conducted at 40 and 50°C. However, temperatures higher than 50°C deactivate the enzyme as confirmed by the lower yield obtained at 60°C. According to Illanes *(10)*, the thermal stability of enzymes decreases as higher amounts of water are present in the organic solvents, i.e., hydrophilic solvents, such as ethanol, tend to deactivate enzymes by reducing their thermal stability. Köse et al. *(12)* also observed a higher methyl ester yield at 50°C for the immobilized *C. antartica* lipase-catalyzed methanolysis reaction of cottonseed oil.

Table 2
Lipozyme Reuse in the Transesterification of Soybean Oil With Ethanol Using a Reactant Stoichiometric Molar Ratio, Stepwise Ethanol Addition (1/3 at 0 h, 1/3 after 0.5 h, and 1/3 after 1 h), at 50°C

| Batch number | Ester yield after 4 h of reaction (%) |
|---|---|
| First | 56.0 |
| Second (before the enzyme was reused, it was dried in oven at 50°C for 12 h) | 4.1 |
| Second (before the enzyme was reused, it was stored in a desiccator at room temperature for 12 h) | 6.5 |

### Effect of the Stepwise Addition of Enzyme

In order to avoid enzyme deactivation by the ethanol present in the reaction medium, the stepwise addition of Lipozyme (in two steps: 0 and 2 h) to the reaction conducted at 50°C, using the reactants stoichiometric ratio (with stepwise addition of ethanol) and 7% (w/w) Lipozyme was studied. The results show that the final yield after 4 h of reaction was similar for both cases tested. The initial rate of reaction was, evidently, much higher for the reaction in which the whole enzyme was added at time 0 h. In this case, the equilibrium seems to have been reached after about two hours of reaction.

### Enzyme Reuse

One of the major advantages of using immobilized enzymes is the possible reuse of the enzyme preparation, a means of reducing the total costs of reaction. The ethanolysis reaction of soybean oil under the optimum conditions previously reported ($T = 50°C$, $R = 3$ with stepwise ethanol addition, no solvent, 7% [w/w] Lipozyme) was used to investigate the possibility of reusing the enzyme. The enzyme was recovered from the reaction medium, washed with hexane, and placed in a desiccator for 12 h or dried in an oven at 50°C (for 12 h) to remove all the water accumulated on the immobilization support. After this treatment, the enzyme was reused. The results presented in Table 2 indicate that:

- The enzyme drastically loses its activity after the reaction described previously.
- Yields lower than 10% are obtained after the second reuse and after the two types of treatment tested.

According to Lima et al. *(13)*, the loss of lipase's catalytic activity, after being successively reused in the transesterification reactions, is owing to the deposit of water on the enzyme support. The authors have confirmed this effect when the enzyme recovered its catalytic activity after being dried back to its initial water content. However, the results shown in Table 2 indicate that the enzyme deactivation was not only caused by the water

accumulated on the immobilization support during the reaction, because in one of the experiments, the recovered enzyme was stored in an oven at 50°C for 12 h, reaching constant weight. Glycerol, one of the reaction products, could also be adsorbed on the immobilization support, which would promote a change on the enzyme microenvironment, and consequently a decrease in its activity *(14,15)*. According to Soumanou and Bornscheuer *(9)*, glycerol can also inhibit the reaction by limiting the product and substrate diffusion because it is not soluble in oil.

## Conclusions

It is possible to conduct a transesterification reaction of soybean oil with ethanol using a commercial, immobilized lipase in a solvent-free reaction medium as demonstrated by the work presented herein. Under mild reaction conditions (temperature of 50°C, atmospheric pressure), yields higher than 50% were achieved after less than 4 h for a reaction using 7% (w/w) of the biocatalyst with the stepwise addition of ethanol in three steps and using the reactants stoichiometric ratio.

## Acknowledgments

The authors would like to acknowledge Cenpes/Petrobras for financial support and Novozymes for kindly providing the enzyme for this research. Dr. Marta A. P. Langone would also like to thank the Programa Prociência/UERJ.

## References

1. Srivastava, A. and Prasad, R. (2000), *Renew. Sustain Energy Rev.* **4,** 111–133.
2. Shieh, C. J., Liao, H. F., and Lee, C. C. (2003), *Bioresour. Technol.* **88,** 103–106.
3. Du, W., Xu, Y., Liu, D., and Zeng, J. (2004), *J. Mol. Catal. B: Enzym.* **30,** 125–129.
4. Gerpen, J. V. (2005), *Fuel Process. Technol.* **86,** 1097–1107.
5. Meher, L. C., Sagar, D. V., and Naik, S. N. (2004), *Renew. Sustain. Energy Rev.* **20,** 1–21.
6. Barnwal, B. K. and Sharma, M. P. (2005) *Renew. Sustain. Energy Rev.* **9,** 363–378.
7. Shimada, Y., Watanabe, Y., Sugihara, A., and Toninaga, Y. (2002), *J. Mol. Catal. B: Enzym.* **17,** 133–142.
8. Iso, M., Chen, B., Eguchi, M., Kudo, T., and Shrestha, S. (2001), *J. Mol. Catal. B: Enzym.* **16,** 53–58.
9. Soumanou, M. M. and Bornscheuer, U. T. (2003), *Enzyme Microb. Technol.* **33,** 97–103.
10. Illanes, A. (1994), *Biotecnologia de Enzimas*, Ediciones Universitarias de Valparaíso de la Universidad Católica de Valparaíso, Chile: pp. 235–243.
11. Koskinen, A. M. D. and Klibanov, A. M. (1996), *Enzymatic Reactions in Organic Media*, 1st ed., Blackie Academic & Professional, Bishopbriggs, UK: pp. 10–14, 54–57.
12. Köse, Ö., Tüter, M., and Aksoy, H. A. (2002), *Bioresour. Technol.* **83,** 125–129.
13. Lima, F. V., Pyle, D. L., and Ansejo, J. A. (1995), *Biotechnol. Bioeng.* **46,** 69–79.
14. Xu, Y., Du, W., and Liu, D. (2005), *J. Mol. Catal. B: Enzyme* **32,** 241–245.
15. Dossat, V., Combes, D., and Marty, A. (2002), *J. Biotechnol.* **97,** 117–124.

0273-2289/1559-0291 (Online)/07/136–140/115–130/$30.00

# Thermoinactivation Mechanism of Glucose Isomerase

LENG HONG LIM AND BRADLEY A. SAVILLE*

*Department of Chemical Engineering and Applied Chemistry, University of Toronto, 200 College Street, Toronto, Ontario, M5S 3E5, E-mail: saville@chem-eng.utoronto.ca*

## Abstract

In this article, the mechanisms of thermoinactivation of glucose isomerase (GI) from *Streptomyces rubiginosus* (in soluble and immobilized forms) were investigated, particularly the contributions of thiol oxidation of the enzyme's cysteine residue and a "Maillard-like" reaction between the enzyme and sugars in high fructose corn syrup (HFCS). Soluble GI (SGI) was successfully immobilized on silica gel (13.5 μm particle size), with an activity yield between 20 and 40%. The immobilized GI (IGI) has high enzyme retention on the support during the glucose isomerization process. In batch reactors, SGI (half-life = 145 h) was more stable than IGI (half-life = 27 h) at 60°C in HFCS, whereas at 80°C, IGI (half-life = 12 h) was more stable than SGI (half-life = 5.2 h). IGI was subject to thiol oxidation at 60°C, which contributed to the enzyme's deactivation. IGI was subject to thiol oxidation at 80°C, but this did not contribute to the deactivation of the enzyme. SGI did not undergo thiol oxidation at 60°C, but at 80°C SGI underwent severe precipitation and thiol oxidation, which caused the enzyme to deactivate. Experimental results show that immobilization suppresses the destabilizing effect of thiol oxidation on GI. A "Maillard-like" reaction between SGI and the sugars also caused SGI thermoinactivation at 60, 70, and 80°C, but had minimal effect on IGI. At 60 and 80°C, IGI had higher thermostability in continuous reactors than in batch reactors, possibly because of reduced contact with deleterious compounds in HFCS.

**Index Entries:** Deactivation; immobilized enzyme; kinetics; silica gel; thermostability; glucose isomerase.

## Introduction and Background

High fructose corn syrup (HFCS), produced enzymatically using immobilized glucose isomerase (GI), dominates 70% of today's nutritive sweetener market. Because of poor enzyme thermostability and byproduct formation, the current commercial glucose isomerization reaction can only be carried out at 60°C, producing ≤ 50% fructose (55% fructose is more desirable). Identifying the mechanisms that cause GI to deactivate can facilitate

*Author to whom all correspondence and reprint requests should be addressed.

efforts to increase GI thermostability, allowing increased reaction temperatures that could substantially improve the economics of HFCS production.

Volkin and Klibanov *(1)* reported that HFCS and a competitive inhibitor to the enzyme, xylitol, greatly stabilized the immobilized form of GI (IGI) from *Streptomyces olivochromogenes* at high temperatures. The authors also found that at 60°C, IGI deactivation was related to

1. Oxidation of the enzyme's cysteine residues.
2. Heat induced reactions with HFCS.
3. Impurities present in the reaction medium.

In a review published by Quax *(2)*, the author cited that substituting an arginine residue for a lysine residue at the subunit interface of *Actinoplanes missouriensis* GI increased the enzyme's thermostability by two- to threefold. Visuri et al. *(3)*, in turn, reported that the crystalline form of GI from *S. rubiginosus* was more stable in the presence of substrate, whereas in buffer solution, the native enzyme (SGI) was more stable. The loss of activity for SGI was directly proportional to protein precipitation. The enzyme first underwent some precipitation. Once precipitation ceased, the inactivation of the enzyme also stopped. They also claimed that SGI deactivation in HFCS was related to Maillard (browning) reactions that took place between the enzyme and the sugar, which resulted in the formation of a sugar–protein complex. The crosslinked form of GI was not susceptible to the Maillard reaction, possibly because the glutaraldehyde crosslinker had reacted mainly with the GI lysine residues, which were the very residues prone to the deleterious Maillard reaction.

Although previous investigations have identified possible mechanisms for GI inactivation, a thorough investigation of the mechanisms for inactivation of GI from *S. rubiginosus* has not been previously conducted. The objective of this study, therefore, is to further establish the contributions of thiol oxidation of the cysteine residue and the Maillard-like reaction to the thermoinactivation of both SGI and IGI from *S. rubiginosus*, one of the most prevalent commercial forms of GI.

A thorough understanding of the underlying mechanisms of thermoinactivation could facilitate efforts to increase the enzyme's thermostability, ultimately improving economics by reducing the need to purchase new enzymes and hence reduce the cost of HFCS production as a whole. One of the most effective ways to achieve stabilization is by the use of immobilized enzyme *(4)*. Multipoint covalent attachment to solid matrices has been used to stabilize several industrial enzymes *(5)*. The formation of the rigid enzyme-support linkage provides substantial kinetic and thermodynamic stabilization of the 3D structure of the active catalytic site. The immobilized enzyme molecules may also be stabilized against denaturing agents that induce enzyme unfolding that can destroy the active site *(6)*.

In this study, GI has been immobilized on silica gel. The contributions of the Maillard-like reaction and thiol oxidation of the cysteine residue

of both SGI and IGI to the thermoinactivation of the enzyme were then determined.

## Materials and Methods

### *Chemicals*

SGI (E.C. 5.3.1.5. D-xylose ketol isomerase) from a genetically modified strain of *S. rubiginosus*, was supplied by Genencor (Rochester, NY) as Gensweet SGI. Maleic acid, cobalt chloride, magnesium sulfate, D-glucose, D-fructose, sucrose, D-galactose, bovine serum albumin, calcium nitrate, 2-mercaptoethanol, hydrochloric acid, acetone, sodium phosphate dibasic, sodium phosphate monobasic, and activated carbon, were purchased from Fisher Scientific (Unionville, ON, Canada). D-xylose, D-Mannose, guanidine hydrochloride, 5,5′-dithiobis, Tris (Trizma base), Coomassie Blue G250, 3-aminopropyl-triethoxysilane (APES), citric acid, and sodium citrate tribasic dihydrate were supplied by Sigma (Oakville, ON, Canada). Phosphoric acid (85%) and ethanol (95%) were supplied by VWR Scientific. EDTA was purchased from BioShop (Burlington, ON, Canada). Glutaraldehyde (50% [w/v] in water) was purchased from ACROS (Morris Plains, NJ).

The silica gel, supplied by W. R. Grace & Co (Columbia, MD) was of Type 654: 100 × 200 mesh (75–150 μm), 260–340 $m^2/g$ surface area, and average pore diameter of 183–287 Å. GI activity assays were performed at pH 6.85 in 0.2 maleic acid buffer that contained 0.02 *M* magnesium sulphate and 0.001 *M* cobalt chloride. Both batch and continuous GI thermoinactivation studies were carried out at pH 8.0 in 0.05 *M* Tris-HCl buffer that contained 0.02 *M* magnesium sulphate.

### *Immobilization of Enzyme*

The method of enzyme immobilization was adapted from that suggested by Weetall and Filbert *(7)* and Wiseman *(8)*. For the silanization process, 10% APES in acetone was used. In the support activation step, the APES-treated silica gel was incubated in glutaraldehyde, prepared by purification with activated carbon, then diluted to 4% (w/v) using 0.5 *M* citric acid buffer (pH 4.8). In the enzyme-coupling step, the modified silica gel was incubated in dialyzed SGI (0.1 *M* phosphate buffer [pH 7.2]) for about 24 h at room temperature. The moisture content of the resulting IGI was in the range of 60–70%.

### *Standard GI Assay*

The standard GI activity, defined as the change in fructose concentration over 20 min of reaction at 60°C, was used to quantify the catalytic activity of the enzyme, and to quantify the efficiency of immobilization. In the assay, 4 mL of total of 1 *M* glucose substrate in buffer was incubated in a 7-mL glass vial immersed in the jacketed batch reactor at 60°C. For SGI

assays, the enzyme was diluted by a factor of 191. For IGI assays, about 0.4 g of wet IGI was used. One milliliter of the reaction medium was sampled at time zero and 20 min, respectively, and the reaction was stopped by adding 0.25 mL of 20% HCl to 1 mL of sample. The sample was analyzed for fructose and glucose content using an HPX-87C carbohydrate column (BioRad, Mississauga, ON, Canada) in a Perkin Elmer high-performance liquid chromatograph (HPLC) with a refractive index detector. The activity of the immobilized enzyme was based on its dry weight, which was determined gravimetrically.

### *GI Activity Assay for Batch Thermoinactivation Study*

In this assay, 4 mL of 1 *M* glucose in buffer was incubated in a 7-mL glass vial immersed in the jacketed batch reactor at 60°C. When the reaction medium reached 60°C, 0.5 mL of SGI (already diluted about 1 : 17) from the thermoinactivation experiment was added. For the IGI assay, one milliliter of IGI suspension from the thermoinactivation experiment was pipeted into 4 mL of reaction medium that had been preincubated at 60°C. One mL of the reaction medium was sampled at time zero and 20 min, respectively, and the reaction was stopped by adding 0.25 mL of 20% HCl to 1 mL of sample, which was subsequently analyzed using HPLC. The activity of IGI was normalized with respect to its dry weight, which was determined gravimetrically.

### *Protein Assay*

Total protein concentrations of the enzyme solutions were determined by the Bradford method *(9)*.

### *Thiol Assay*

Ellman's reagent was used to test for thiol content in IGI and SGI. The Ellman's reagent stock contained 97.8% (v/v) 6 *M* guanidine HCl and 1 m*M* EDTA, 1.1% m*M* Ellman's reagent, and 1.1% 1 *M* NaOH. For the IGI thiol assay, a 1 mL suspension of IGI in reaction medium (or 1 mL of supernatant of centrifuged reaction medium, which was used as the blank) was incubated in 2.7 mL of Ellman's reagent stock. For the SGI thiol assay, 100 µL of SGI in reaction medium was added to 0.9 mL of Ellman's reagent stock. The mixture was incubated at room temperature for about 15 min and the absorbance at 412 nm was measured. β-Mercaptoethanol was used as the standard.

### *Thermoinactivation Study in Batch Reactors*

GI thermostability experiments in batch reactors were carried out at 60, 70, and 80°C. The contributions of thiol oxidation and Maillard reaction on the thermoinactivation of GI were studied. All thermoinactivation experiments were carried out in stirred jacketed batch reactors. The contents were mixed using a magnetic stirrer. These experiments lasted from about 20 h (for the 80°C runs) to about 60 h (for the 60°C runs).

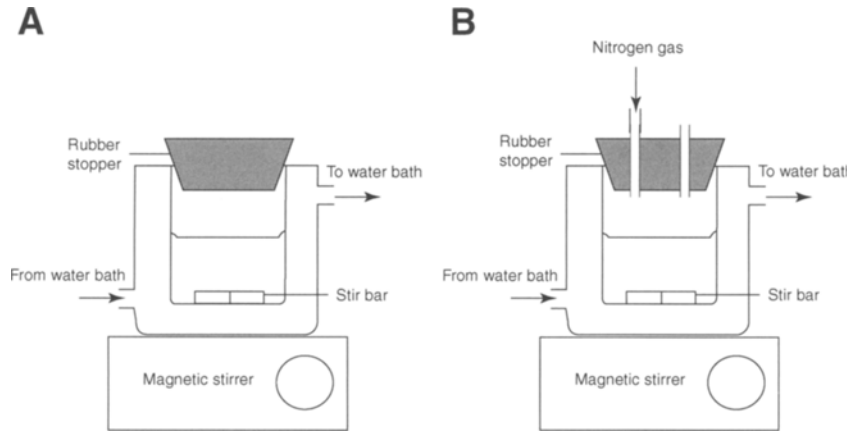


**Fig. 1.** Schematic of jacketed batch reactors for **(A)** GI thermoinactivation study under air-saturated condition and **(B)** GI thermoinactivation study under reduced oxygen conditions (nitrogen sparged).

## *Thiol Oxidation Effect*

The thiol content of IGI and SGI was determined using the procedures previously described under "Thiol assay." For experiments that required reduced dissolved oxygen content, the reaction medium was sparged with nitrogen for at least 30 min before the experiment was started. Initially, the reaction medium (without enzyme) was sparged by submersing the nitrogen supply below the liquid surface. Once the reaction was initiated (by adding enzyme), the nitrogen supply line was withdrawn and placed in the headspace above the reaction medium to maintain oxygen-depleted conditions. Oxygen levels were measured using a Biological Oxygen Monitor from Yellow Springs Instruments (YSI, Yellow Springs, OH) with a high sensitivity membrane (YSI model 5794). Prereaction sparging with nitrogen was able to reduce the dissolved oxygen content by about 95% compared with air saturation, and this was maintained during reaction by the supply of nitrogen into the headspace. Even though nitrogen sparging could not completely eliminate oxygen from the reaction medium, there was nonetheless a significant reduction in oxygen content, so that the impact of oxidation could be studied. A schematic of the experimental setup is shown in Fig. 1. Evaporation of reaction medium at high temperatures was accounted for by replenishing the medium with nitrogen-sparged deionized water, which was heated to the same reaction temperature as the reaction medium. Samples were collected periodically and tested for thiol content and GI activity.

## *Maillard-Like Reaction Effect*

Different sugars, namely, glucose, sucrose, galactose, and xylose were added to the reaction medium to examine the effect of the Maillard-like

reaction on the thermoinactivation of IGI and SGI. Samples were taken and tested for their GI activity.

### *Thermoinactivation Study in Continuous Reactors*

Continuous glucose isomerization using IGI was carried out in a 1 × 30 $cm^2$ jacketed PTFE liquid chromatography column (Sigma) with a bed volume of 24 mL. The reaction medium contained 1 *M* of glucose in 0.05 *M* Tris-HCl buffer (pH 8.0) containing 0.02 *M* $MgSO_4$. The reaction medium was pumped through the reactor at a flow rate of approx 0.4 mL/min using a peristaltic pump. Samples were taken periodically from the outlet of the reactor and analyzed for fructose and glucose using HPLC. To determine the cumulative fructose produced over the entire length of each experiment, the product was collected and tested for the "pooled" glucose and fructose concentrations at the end of the experiment, using HPLC. These experiments lasted between 5 and 15 d, depending on the enzyme loading and temperature. The activity of IGI was determined from the outlet fructose concentration. Once the outlet fructose concentration begins to drop below its equilibrium level, the amount of active enzyme in the reactor is directly proportional to the amount of fructose produced. Beyond this point, the relative activity of the enzyme at time ($t$) can be determined from a ratio of the instantaneous fructose concentration to the fructose concentration at equilibrium. The first-order deactivation kinetics model (Eq. 2) was used to model IGI deactivation under continuous isomerization conditions, following linear regression of the semilog enzyme activity profiles.

The turnover number (TON) of the enzyme is defined as the ratio of the amount of fructose produced by the enzyme from time zero to time ($t$), to the amount of enzyme consumed or inactivated over the same interval. To calculate the TON, the cumulative total mass of fructose produced and determined experimentally, was divided by the total mass of the enzyme consumed (i.e., deactivated) during the reaction.

## Enzyme Deactivation Model

A first-order enzyme deactivation model was used to represent GI deactivation kinetics. First-order deactivation model is consistent with the disruption of a single bond or "sensitive structure," or the occurrence of a single lethal event or a "single hit" *(10)*. Gibbs et al. *(11)* applied the extended Lumry–Eyring model to describe GI deactivation, where the native enzyme (N) first unfolds reversibly to the unfolded species (U), which is catalytically inactive, and then deactivates irreversibly through first-order kinetics to a deactivated species (D). First-order enzyme deactivation kinetics has also been successfully used to describe the deactivation of GI *(12)*. Treating the native and the unfolded forms, i.e., N and U, as one single catalytically active species, (E), and assuming that the subsequent irreversible enzyme

deactivation is a first-order event, the enzyme deactivation kinetics can be described by:

$$\frac{d[E]}{dt} = -k_d[E] \tag{1}$$

Integrating Eq. 1 from $t = 0$ to $t$ gives:

$$\frac{[E]}{[E_0]} = \exp(-k_d t) \tag{2}$$

## Statistical Analysis of Data

Replicates of the kinetics and thermoinactivation studies were produced for most conditions. The HPLC assay was subject to a mean of ±2% and a maximum deviation of ±10%. To account for experimental variability and for statistically justifiable comparisons between experimental runs, 95% confidence intervals (CI) were computed for experiments for the thermoinactivation and kinetics studies. The equation used *(13)* to compute the 95% CI was:

$$95\%\,\text{CI} = t_{\alpha/2} \times s_e / (S_{xx})^{0.5} \tag{3}$$

where $t_{\alpha/2}$, studentized test statistic; $\alpha$, significance level (5%); $s_e$, standard error; and $S_{xx} = \Sigma x^2 - (\Sigma x)^2/(\text{number of data points})$.

Initial comparisons between experimental runs were based on 95% CI, to establish if the results were statistically different. If a difference was confirmed, the degree of difference was then determined using the extreme values of the CIs, i.e., the "worst-case scenario" for each run, based on a 95% confidence level. For example, with A (10 ± 1) and B (5 ± 2), it is apparent that A is statistically different from B, based on a 95% confidence level. In the worst-case scenario, A is at least approx 1.3 times greater than B, calculated using the CIs as follows: $(10-1)/(5+2) = 9/7$ approx 1.3. This approach may not quantify the actual magnitude of the difference between two means, but it serves as a more stringent test of the degree of difference between trial conditions. In comparisons where such an approach has been used, the magnitude of the difference will be stated, preceded by the clause "at least," for example, "at least" 1.3 times greater than B, as written earlier.

## Results and Discussion

### *GI Immobilization*

GI from *S. rubiginosus* was successfully immobilized on silica gel through covalent immobilization with support silanization. The activity yield of the immobilization process was between 20 and 40%, and the IGI

Table 1
Effect of Nitrogen Sparging and Temperature on Thiol Content of IGI and SGI Under Various Conditions in HFCS

| | | Rate of decrease, m, $h^{-1}$ (no. of data points) | |
|---|---|---|---|
| | | 60°C | 80°C |
| IGI | $N_2$ sparging | 0.007 ± 0.003 (18) | 0.037 ± 0.010 (19) |
| | No $N_2$ sparging | 0.014 ± 0.002 (20) | 0.057 ± 0.014 (19) |
| SGI | $N_2$ sparging | 0.008 ± 0.008 (2) | 0.010 ± 0.009 (19) |
| | No $N_2$ sparging | 0.005 ± 0.007 (20) | 0.054 ± 0.015 (19) |

Values of *m* shown as mean ± 95% CI, based on three replicates.

Table 2
First-Order Deactivation Constants and Their Corresponding Half-Lives for IGI and SGI at Various Temperatures in HFCS

| | | First-order $k_d/h^{-1}$ (half-life [h]) | |
|---|---|---|---|
| | | 60°C | 80°C |
| IGI | $N_2$ sparging | 0.008 ± 0.003 (89) | 0.042 ± 0.024 (16) |
| | No $N_2$ sparging | 0.025 ± 0.005 (27) | 0.060 ± 0.018 (12) |
| SGI | $N_2$ sparging | 0.002 ± 0.002 (286) | 0.038 ± 0.012 (18) |
| | No $N_2$ sparging | 0.005 ± 0.002 (145) | 0.133 ± 0.030 (5) |

Values of $k_d$ shown as mean ± 95% CIs, based on three replicates.

was retained on the support during production of HFCS. The IGI produced had an activity of 3.1 ± 0.5 unit GI/g (mean ± standard deviation).

### *Contribution of Thiol Oxidation to GI Thermoinactivation*

The contribution of thiol oxidation of the cysteine residue to the thermoinactivation of SGI and IGI at 60 and 80°C in HFCS, which initially contained only 1 *M* glucose, was investigated. The terms "nitrogen-sparged" or "nitrogen-sparging" are used to denote conditions where the oxygen content of the reaction medium was reduced by approx 95% compared with air-saturated conditions.

Table 1 shows the rate of thiol oxidation (m, in $h^{-1}$), for SGI and IGI under various conditions. The first-order deactivation kinetics model (Eq. 2) was used to describe the enzyme deactivation because of thiol oxidation, and linear regression was performed on the enzyme activity profiles obtained for IGI and SGI at different temperatures in HFCS, which initially contained only 1 *M* glucose. The best-fit first-order deactivation constants, $k_d$, and their corresponding half-lives are listed in Table 2. Figures 2 and 3 show the stabilities of SGI and IGI under air-saturated and nitrogen-sparged conditions at 60 and 80°C, respectively.

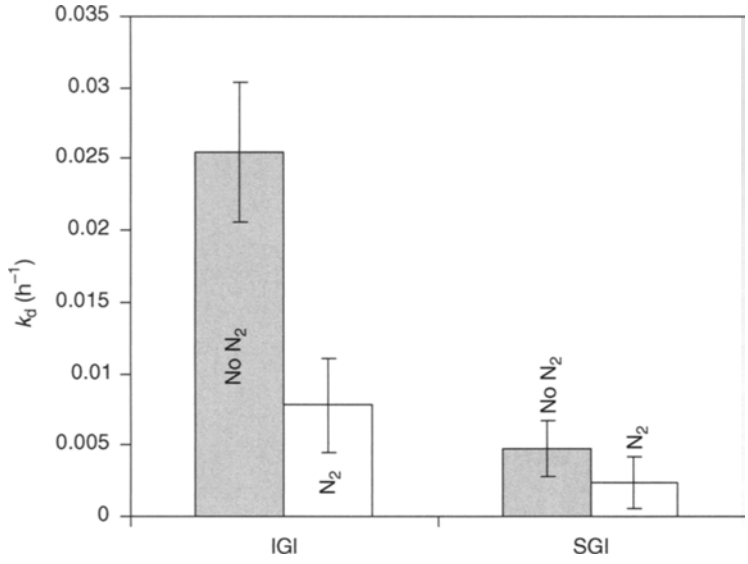


**Fig. 2.** Deactivation constant ($k_d$), for IGI and SGI at 60°C in batch reactors. Data shown as mean ± 95% CI. Enzymes were incubated in Tris-HCl buffer (pH 8.0) that initially contained 1 *M* of glucose.

In general, the rate of thiol oxidation was higher when the enzyme was incubated under air saturation. For SGI at 60°C, experimental data showed a negligible rate of thiol oxidation, based on a 95% CI. There was also no significant difference in the extent of oxidation of the thiol group between the nitrogen-sparged and air-saturated batches, which suggests that the cysteine residue in SGI is not susceptible to oxidation at 60°C. For IGI at 80°C, there was no significant difference between the slopes representing the rates of decrease of thiol content under air and nitrogen saturation. It can also be noted that at 80°C, under air saturation, there was no difference between the rate of thiol oxidation for IGI and SGI. On the other hand, with nitrogen sparging, the rate of thiol oxidation for IGI was *at least* 1.4 times higher than that of SGI at 80°C (0.027/0.019). It was also visually observed that for SGI, protein precipitation became more and more severe at higher temperatures. At 80°C, SGI precipitation occurred within the first 30 min of reaction. Reaction medium browning, measured spectrophotometrically at 330 nm, also became more noticeable for SGI as the temperature increased from 60 to 80°C.

At 60°C without nitrogen sparging, SGI was more stable than IGI. Using nitrogen sparging to reduce the dissolved oxygen content enhanced IGI stability by *at least* 1.8 times (0.020/0.011). Conversely, at a 95% confidence level, no difference was observed between the nitrogen-sparged and air saturation runs for SGI. The thiol concentration profile of IGI at 60°C shows that thiol oxidation occurred in parallel with IGI deactivation. This suggests that thiol oxidation contributed to the thermoinactivation of IGI.

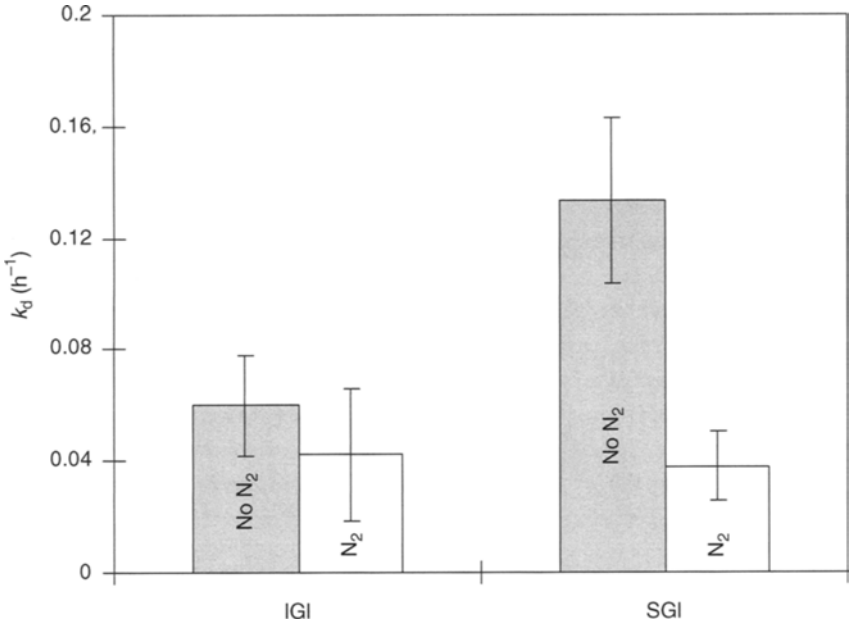


**Fig. 3.** Deactivation constant ($k_d$), for IGI and SGI at 80°C in batch reactors. Data shown as mean ± 95% CIs. Enzymes were incubated in Tris-HCl buffer (pH 8.0) that initially contained 1 *M* of glucose.

No conclusion can be drawn regarding the relation between thiol oxidation and deactivation for SGI because there was little (if any) change in the thiol content of SGI at 60°C, irrespective of the oxygen content in the system.

Nitrogen sparging of SGI at 80°C reduced the extent of thiol oxidation in SGI, and at least doubled the stability of the enzyme compared with that under oxygen saturation. However, for IGI there was no statistically significant difference in half-life between the nitrogen-sparged vs air-saturation conditions. Nitrogen sparging did not reduce the rate of thiol oxidation of the cysteine residue of IGI (Table 1). Therefore, there was not enough evidence to suggest that thiol oxidation was a cause of IGI deactivation, unlike at 60°C. The key conclusion that can be drawn from these observations is that thiol oxidation is a likely reason for the loss of activity of SGI at 80°C.

At 80°C, under air-saturation conditions, IGI was *at least* 1.3 times (0.103/0.078) more stable than SGI, even though there was no statistically significant difference in the rate of thiol oxidation for both enzyme forms. When nitrogen sparging was used, there was no statistically significant difference between the stability of IGI and SGI, in spite of the observation that the rate of thiol oxidation for IGI was *at least* 1.4 times higher than that of SGI. There was also no statistically significant difference between the half-lives of IGI (under air saturation) and SGI (under nitrogen-sparged conditions). These observations indicate that, compared with SGI, the stability of IGI was less sensitive to thiol oxidation. This is also an indication

Table 3
Relative Change in Thiol Oxidation Rate and Half-life for IGI and SGI When Reaction Temperature was Increased From 60 to 80°C

| | | Temperature increased from 60 to 80°C | |
|---|---|---|---|
| | | Relative increase in thiol oxidation rate | Relative decrease in half-life |
| IGI | $N_2$ sparging | 2.7 | 1.6 |
| | No $N_2$ sparging | 2.7 | 1.4 |
| SGI | $N_2$ sparging | 1.0 | 6.5 |
| | No $N_2$ sparging | 3.3 | 15 |

that immobilization protected the enzyme against inactivation owing to thiol oxidation.

The relative increases in the rate of thiol oxidation and the half-life of IGI and SGI when the reaction temperature was increased from 60 to 80°C are shown in Table 3. Based on Table 3, it can be concluded that nitrogen sparging did not reduce the extent of thiol oxidation of IGI. Immobilization of GI probably affected the structure of the enzyme so that the increase in temperature resulted in equal increase in the thiol oxidation rate of the enzyme, regardless of the oxygen content in the reaction medium. Nitrogen sparging did not affect the rate of thiol oxidation in SGI when the temperature was increased from 60 to 80°C; however, the stability of the enzyme still decreased by *at least* a factor of 6.5. On the other hand, under air saturation, the same increase in temperature resulted in *at least* a 15-fold decrease in stability. This suggests that the change in stability was not owing to thiol oxidation alone, even though thiol oxidation was important. Clearly, other processes also contributed to the loss of SGI activity.

Volkin and Klibanov *(1)* reported that the four monomeric subunits of *S. olivochromogenes* GI molecule each contain one cysteine residue imbedded in the interior of the hydrophobic core of the enzyme. At 60°C, it was possible that SGI did not undergo significant conformational change, and the cysteine residue remained protected in the hydrophobic core of the enzyme molecule. Conversely, at 80°C, SGI experienced significant conformational changes, as implied by the severe enzyme precipitation that occurred within the first 30 min of the reaction; these conformational changes exposed the enzyme's cysteine residues to oxygen in the reaction medium. Conversely, when the temperature increased from 60 to 80°C, IGI did not undergo enzyme precipitation, suggesting that IGI did not undergo severe conformational changes, unlike SGI. These observations suggest a relationship between the enzyme's conformational change and the adverse effects of thiol oxidation.

Immobilization made the enzyme more susceptible to thiol oxidation at 60°C, perhaps by a structural change in the enzyme during the immobilization

process that caused the enzyme's cysteine residue to be more readily accessible for oxidation. Such a structural change in the enzyme after immobilization may have also suppressed the destabilizing effect of thiol oxidation on the enzyme at 80°C.

### *Contribution of the Maillard-Like Reaction to GI Thermoinactivation*

Independent reaction kinetics studies by Lim *(14)* on both soluble and immobilized GI from *S. rubiginosus* have shown a reduction in total sugar (glucose and fructose) in the reaction medium that paralleled the loss of the enzyme activity. This is a strong indication of the occurrence of the Maillard-like reaction between the enzyme and the sugars. The effect of different sugars on the deactivation of GI was investigated at 60, 70, and 80°C by incubating the enzyme in 1 mol/L of either sucrose, xylose, or galactose, followed by a subsequent activity assay. Sucrose, a nonreducing disaccharide is the least reactive with proteins, whereas xylose has the greatest reactivity *(3)*.

The first-order deactivation kinetics model (Eq. 2) was used to model GI deactivation. Linear regression was performed on the semilog enzyme activity profiles. The best-fit first-order deactivation constants and their corresponding half-lives are listed in Table 4. These results are based on a single trial with each sugar; each trial contained six data points. The use of data from only a single run for each condition might not reflect the overall variability that would otherwise be observed from experimental replicates under the same condition. However, all the experiments in this study were performed simultaneously, to reduce variability owing to enzyme activity and other biological artifacts. Therefore, it is still reasonable to compare the experimental data within the study.

Experimental trials with xylose showed greater variability/fluctuation, for both IGI and SGI. The fluctuations were also manifested in relatively larger standard deviations of GI stability in xylose (Table 4). This could be because of the fact that xylose, a compound with greater affinity for GI than glucose (the substrate in the activity assay) was bound to the enzyme's active site during incubation. This also accounts for the observation that GI preincubated in xylose had initial activities (i.e., at time zero of incubation) that were 80–87% lower than those for GI preincubated in sucrose and galactose. These relatively low activities ultimately introduced greater variation in the data arising from experiments with xylose.

The stabilities of SGI and IGI depend both on the presence of the sugars and reaction temperature. At 60°C, SGI was *at least* 1.2 times (0.019/0.016) more stable in galactose than in xylose, whereas at 70 and 80°C, there was no statistically significant difference between the stability of SGI in either galactose or xylose. However, at both 60 and 80°C, the stability of SGI incubated in sucrose was dramatically more than that observed when the enzyme was incubated in galactose or xylose. At 80°C, SGI was about three to five times more stable in sucrose than in galactose or xylose, respectively. At 60°C, there was no statistically significant difference in

Table 4
Effect of Exogenous Sugars on the Deactivation of GI

| Sugar used for incubation | Enzyme form | First-order $k_d$, $h^{-1}$ (half-life, h) | | |
|---|---|---|---|---|
| | | 60°C | 70°C | 80°C |
| 1 *M* sucrose (least reactive with proteins) | IGI | 0.020 ± 0.002 (35.0) | No data available | 0.121 ± 0.061 (5.7) |
| | SGI | Very stable $k_d$ approx 0 | No data available | 0.025 ± 0.004 (28.0) |
| 1 *M* galactose | IGI | 0.023 ± 0.012 (30.1) | 0.051 ± 0.026 (13.5) | 0.118 ± 0.054 (5.9) |
| | SGI | 0.014 ± 0.002 (49.5) | 0.088 ± 0.003 (7.8) | 0.172 ± 0.063 (4.0) |
| 1 *M* xylose (most reactive with proteins) | IGI | 0.028 ± 0.021 (24.4) | 0.138 ± 0.056 (5.0) | 0.243 ± 0.040 (2.8) |
| | SGI | 0.073 ± 0.054 (9.5) | 0.104 ± 0.059 (6.7) | 0.308 ± 0.114 (2.2) |

$k_d$ values are shown as mean ± 95% CIs.

stability of IGI incubated in the three different sugars. However, at 70°C, IGI was *at least* 1.1 times more stable in galactose than in xylose, whereas at 80°C, IGI was *at least* 1.1 times more stable in sucrose than in xylose, and *at least* 1.2 times more stable in galactose than xylose. Browning of the reaction medium was also visually observed and was more prevalent at higher temperatures. Browning was most prominent in sucrose, and least prominent in xylose.

Based on changes in enzyme half-life on incubation in different sugars at any particular temperature, it is apparent that immobilization suppressed the effects of the Maillard-like reaction on the thermoinactivation of GI, especially at lower temperatures (<80°C). Such suppression could be because of the glutaraldehyde crosslinker used to activate the silanized support before the enzyme-coupling step. It is expected that glutaraldehyde reacted mainly with the lysine residues on the GI, the very residues most susceptible to the destructive Maillard reaction *(3)*. The Maillard-like reaction between the enzyme's lysine residue and the sugars was less prominent in IGI, possibly because the lysine residues had been used to link the enzyme to the support, and hence, was not available for reaction with the sugars. Even though definitive detection of the Maillard reaction between the enzyme and the sugars was not established in this study, experimental observations of the stability of SGI and IGI under sugars of different reactivities, and the definitive loss of total sugar in the reaction medium that occurred concurrently with the loss of enzyme activity *(14)* are consistent with a Maillard-like reaction between the enzyme and the

Table 5
Comparison of TONs (Gram Fructose Produced/Gram Enzyme Consumed) and Deactivation Rate Constants (Mean Value ± 95% CI) for IGI Under Continuous Isomerization Conditions

| | | 60°C | 80°C |
|---|---|---|---|
| IGI | TON, per g wet mass | 72 | 78 |
| | TON, per g dry mass | $2.4 \times 10^2$ | $2.6 \times 10^2$ |
| | $k_d$, $h^{-1}$ (half-life [h]) | 0.0085 ± 0.0022 (82) | 0.019 ± 0.005 (36) |

sugars. Furthermore, the results from these trials are consistent with those of Quax *(2)*, who previously suggested that the Maillard reaction between a lysine residue and HFCS was responsible for the thermoinactivation of SGI from *A. missouriensis*.

## GI Thermoinactivation in Continuous Reactors

Thermoinactivation studies of the IGIs in continuous reactors provided thermostability information under conditions that more closely reflect actual industrial operation. Batch operation allows inhibitors to accumulate, whereas continuous operation carries out these inhibitors with the effluent, reducing their impact on the enzyme. Therefore, continuous reactors provided another platform to investigate the effect of the Maillard reaction on the thermoinactivation of IGI.

A sample calculation of TON is given as follows: at 60°C, an average of 12.8 g of fructose was produced after 265 h of continuous reaction catalyzed by 2.0 g of IGI, based on two experimental replicates. The fraction of active IGI left at the 265th h was 0.11, calculated using the enzyme deactivation model with the best-fit $k_d$ value. Thus, the total mass of wet IGI consumed was 1.8 g. Therefore, the TON was 7.2 g fructose/g wet IGI consumed, and the TON per gram dry mass was 239. The best-fit first-order deactivation constants and the TONs for all experimental conditions are shown in Table 5.

During continuous isomerization at 60°C, IGI was *at least* 1.9 times more stable than IGI under batch isomerization conditions, based on the computed $k_d$ values. At 80°C, IGI during continuous isomerization was *at least* 1.8 times more stable than it was during batch processing, a similar improvement to that observed at 60°C.

The difference in the relative stability of IGI in batch and in continuous reaction systems might be because of differences in the extent of the Maillard-like reaction in the two systems. During batch processing, equilibrium was reached within 10–20 min, and the enzymes were then continuously exposed to high concentrations of sugars for an extended period of time. During this period, samples were removed and subjected to a kinetics assay for enzyme

Table 6
Factors Contributing to Thermoinactivation of IGI and SGI

| | Factors causing deactivation | | Relative stability (in HFCS, under air-saturation conditions) |
|---|---|---|---|
| | SGI | IGI | |
| 60°C | Maillard-like reaction | Thiol oxidation and Maillard-like reaction (relatively mild) | SGI > IGI |
| 80°C | Thiol oxidation and Maillard-like reaction | Maillard-like reaction (relatively mild) | IGI > SGI |

activity. By comparison, in the continuous systems, certain regions of the bed were exposed to lower concentrations of fructose, and the loss of activity was directly determined from the change in outlet fructose concentrations over time. Consequently, the exposure of the enzymes to sugars responsible for the Maillard-like reaction was different, with higher levels of exposure in the batch system. Furthermore, in the batch system, these sugars had a longer residence time in the reactor and hence, more time for the Maillard-like reaction to proceed. The resulting accumulation of byproducts in the batch system may have enhanced the inactivation of the enzyme under batch conditions. In the continuous reactors, the sugars were constantly removed from the system, which therefore limited the amount of byproduct formation as a result of the Maillard-like reaction. The overall effects of thiol oxidation and the Maillard-like reaction on the stability of SGI and IGI are summarized in Table 6.

## Conclusions

*S. rubiginosus* GI was successfully immobilized onto silica gel using a covalent-binding method following derivitization with APES. The immobilized enzyme had high enzyme retention on the support during glucose isomerization reaction. For SGI, the Maillard-like reaction was the main contributor to inactivation at 60°C, whereas at 80°C, both the Maillard-like reaction and thiol oxidation were significant. For IGI, a mild effect of the Maillard-like reaction was observed at 60°C and 80°C. Thiol oxidation was significant at 60°C, but not at 80°C. Furthermore, SGI was more stable than IGI at 60°C, but the converse was true at 80°C. Therefore, immobilization shifted the thermoinactivation mechanism of GI. At 80°C, there was evidence that thiol oxidation of IGI still occurred, but its impact on IGI deactivation was reduced. Thermoinactivation of IGI at temperatures higher than 60°C could be also caused by deamidation of the asparagine and/or glutamine residues of the enzyme *(1)*.

## Nomenclature

| | |
|---|---|
| $[E]$ | active enzyme concentration ($M$) |
| $[E_0]$ | initial enzyme concentration ($M$) |
| $k_d$ | degradation rate constant in Eq. 2 ($h^{-1}$) |
| IGI | immobilized GI produced at the lab |
| SGI | soluble GI supplied by Genencor |
| $t$ | time (h) |

## References


1. Volkin, D. B. and Klibanov, A. M. (1989), *Biotechnol. Bioeng.* **33,** 1104–1111.
2. Quax, W. J. (1993), *Trends Food Sci. Technol.* **4,** 31–34.
3. Visuri, K., Pastinen, O., Wu, X., Makinen, K., and Leisola, M. (1999), *Biotechnol. Bioeng.* **64(3),** 377–380.
4. Bailey, J. E. and Ollis, D. F. (1986), *Biochemical Engineering Fundamentals.* 2nd ed. McGraw-Hill, New York.
5. Guisan, J. M., Fernandez-Lafuente, R., Rodriguez, V., Bastida, A., Blanco, R. M., and Alvaro, G. (1992), In: *Proceedings of the International Symposium on Enzyme Stability.* Maastricht, The Netherlands, November 22–25.
6. Mozhaev, V. V. (1992), In: *Proceedings of the International Symposium on Enzyme Stability,* Maastricht, The Netherlands, November 22–25.
7. Weetall, H. H. and Filbert, A. M. (1974), In: *Methods in Enzymology.* Jakoby, W. B. and Wilchek, M. (eds.), Academic Press, New York, 59–72.
8. Wiseman, A. (1995), *Handbook of Enzyme Biotechnology.* 3rd ed. Ellis Horwood, London.
9. Ninfa, A. J. and Ballou, B. P. (1998), *Fundamental Laboratory Approaches for Biochemistry and Biotechnology.* Fitzgerald Science Press, Bethesda, MD.
10. Sadana, A. (1992), In: *Thermostability of Enzymes.* Gupta, M. N. (ed.), Springer-Verlag, Berlin, pp. 84–93.
11. Gibbs, P. R., Uehara, C. S., Neunert, U., and Bommarius, A. S. (2005), *Biotechnol. Prog.* **21,** 762–774.
12. Palazzi, E. and Converti, A. (2001), *Enzyme Microb. Technol.* **28,** 246–252.
13. Weiss, N. A. (1999), Elementary Statistics. 4th ed. Addison Wesley Longman, Inc., USA.
14. Lim, L. H. (2006), *PhD Thesis,* Department of Chemical Engineering and Applied Chemistry, University of Toronto.

0273-2289/1559–0291 (Online)/07/136–140/131–140/$30.00

# Measuring Cellulase Activity

## *Application of the Filter Paper Assay to Low-Activity Enzyme Preparations*

**TOR SOREN NORDMARK, ALAN BAKALINSKY, AND MICHAEL H. PENNER***

*Department of Food Science and Technology, Oregon State University Corvallis, Oregon 97331-6602, E-mail: mike.penner@oregonstate.edu*

## Abstract

An approach is presented for obtaining relative filter paper activities for enzyme preparations having activities below that required for application of the traditional International Union of Pure and Applied Chemistry filter paper assay. The approach involves the utilization of protein stabilizers to retard the time-dependent enzyme inactivation that may occur under traditional filter paper assay conditions. Enzyme stabilization allows extended reaction times and the calculation of relative activities based on the time required for saccharification of 3.6% of the traditional substrate, making results proportional to those obtained in the traditional International Union of Pure and Applied Chemistry assay. The assay is demonstrated using a commercial cellulase preparation along with KCl and bovine serum albumin as protein stabilizers.

**Index Entries:** Assay; cellulase; filter paper.

## Introduction

Considerable research is aimed at obtaining novel cellulase enzyme systems for application in the forest products, textile, food, and biomass conversion industries. Microbial enzyme systems capable of catalyzing the degradation of native celluloses include multiple cellulolytic enzymes, either complexed or noncomplexed *(1,2)* that act in concert to solubilize/saccharify crystalline cellulose *(3)*. Assays using cellulose substrates that are somewhat recalcitrant to cellulase-catalyzed hydrolysis are useful for assessing the potential of these enzyme systems because their rates of saccharification are, presumably, dependent on the well-documented synergism that is associated with many cellulase preparations *(4)*. Substrates such as filter paper, microcrystalline cellulose, bacterial cellulose, and cotton are particularly informative because they contain an appreciable amount of crystalline cellulose. The International Union of Pure and

*Author to whom all correspondence and reprint requests should be addressed.

Applied Chemistry (IUPAC) Commission on Biotechnology has endorsed an assay based on the degradation of filter paper *(5)*. The IUPAC filter paper assay is widely accepted as the "standard" method for measuring the activity of noncomplexed cellulolytic enzyme systems.

The IUPAC assay is based on the identification of the amount of enzyme that will solubilize 2.0 mg of reducing sugar equivalents (RSE) from 50.0 mg of filter paper in a 1-h reaction period. Because of the heterogeneous (amorphous/crystalline) nature of filter paper, the assay is based on the conversion of a specified amount of substrate, i.e., 3.6% (2.0 mg soluble glucose is equivalent to approx 3.6% of the glucose in 50.0 mg dry filter paper) *(6)*. The assay itself requires that a minimum of two enzyme concentrations be tested: one mixture producing slightly more and another mixture producing slightly less than 2.0 mg RSE in the assay. The amount of enzyme preparation containing 0.37 filter paper units (FPU) (i.e., that amount that generates 2.0 mg RSE in 1 h) is then calculated based on the empirical observation that, at enzyme concentrations approaching 0.37 FPU per reaction mixture, the amount of RSE in a given reaction mixture is proportional to the log of the enzyme concentration (Eq. 1).

$$\Delta[P_1] = K_1[\Delta \log(E)] \tag{1}$$

where $[P_1]$ is the product (mg RSE) generated in 1-h filter paper assay, $[E]$ is the enzyme concentration, and $K_1$ is the constant of proportionality. The value of the proportionality constant is dependent on the reaction conditions, including the source and history of the enzyme. Thus, if one plots the data from a series of reaction mixtures (as total RSE generated vs log enzyme concentration) it will yield a straight line from which the amount of enzyme preparation corresponding to 0.37 FPU can be obtained. The obvious requirement for this assay is that the enzyme preparation must be sufficiently active to generate ≥2.0 mg of RSE in 1 h. This requirement presents a limitation in using the IUPAC assay for the routine analysis of cellulase preparations whose activity is inherently low. In particular, enzyme samples resulting from native microbial environments, novel microbial culture systems, and plant or microbial extracts will often be of relatively low activity. To measure the filter paper activity (FPA) of these "low-activity" samples require that the enzyme sample be concentrated, such that the concentrated preparation will generate sufficient product. In general, enzyme concentration is achieved by ultrafiltration and/or lyophilization techniques, both operations running the risk of enzyme inactivation *(7)*.

The objective of this note is to explain an approach that may be used in conjunction with the 3.6% conversion rationale, as developed for the standard filter paper-based assay, to obtain relative FPAs for "low-activity" cellulase preparations. The approach is based on the use of enzyme stabilizers; enzyme stabilization allows relative FPAs to be determined based on the time taken to generate a specified amount of

RSE (i.e., 2.0 mg as specified in the IUPAC assay). The presented approach, in which time is varied, is in contrast to the traditional assay in which enzyme concentration is varied, whereas time is fixed. Enzyme stabilization allows activity values to be obtained through Eq. 2, which has the same form as Eq. 1.

$$\Delta[P_t] = K_2(\Delta \log t) \tag{2}$$

where $P_t$ is the product (RSE [mg]) generated at time ($t$), $t$ is the time of reaction, and $K_2$ is the constant of proportionality.

## Materials and Methods

### *Materials*

All chemicals were reagent grade unless specified otherwise. General reagents were obtained from commercial suppliers. Bovine serum albumin (BSA), fraction V, was obtained from Sigma Chemical Co. (St. Louis, MO). The substrate used for all assays was Whatman No. 1 filter paper (Whatman LabSales, Inc., Hillsboro, OR). Fifty milligram substrate strips were weighed to 1.0 mg accuracy. The cellulase preparation (Cellulysin) was purchased from Calbiochem Corp. (San Diego, CA) and used without modification. Enzyme stock solutions were prepared by dissolving enzyme preparations in distilled-deionized water immediately before use.

### *Activity Assay*

Traditional filter paper assays were done according to IUPAC specifications *(5)*. Modified assays for the measurement of "low-activity" enzyme preparations were done according to IUPAC specifications with the following exceptions:

1. Reaction mixtures were supplemented with stabilizers at the concentrations given in Table 1.
2. Where indicated in the text, reaction times were extended beyond the 1 h assay period until a time at which $\geq$2.0 mg RSE could be detected in the reaction mixture.
3. Stabilized reaction mixtures were made 0.02 *M* in sodium azide to prevent microbial growth over the prolonged reaction period. Soluble RSE were determined using the dinitrosalicylic acid assay *(8)*.

## Results and Discussion

Classical enzyme theory dictates that for a specified set of reaction conditions the amount of product generated in any of a series of reaction mixtures differing only with respect to enzyme concentration will be entirely dependent on the product of the enzyme concentration of the

Table 1
Solutes and Combinations of Solutes Tested for Ability to Alleviate Time-Dependent Inactivation of Commercial Cellulase Preparations Under Standard Filter Paper Assay Conditions

| Component | Concentration |
|---|---|
| Glycerol | 1.1 *M* |
| Sorbitol | 1.1 *M* |
| Mannitol | 1.1 *M* |
| Inositol | 1.1 *M* |
| Ascorbic acid | 1.9 m*M* |
| Potassium chloride | 1.0 *M* |
| Potassium chloride | 3.0 *M* |
| Magnesium sulfate | 1.0 *M* |
| BSA | 1.0 mg/mL |
| BSA | 3.0 mg/mL |
| *Combinations* | |
| Mineral oil and degassed buffer | 200 μm layer |
| BSA and calcium chloride | 1.0 mg/mL, 1.0 *M* |
| BSA and glycerol | 1.0 mg/mL, 1.1 *M* |
| BSA, glycerol, and ascorbic acid | 1.0 mg/mL, 1.1 *M*, and 1.9 m*M* |
| BSA, mannitol, and ascorbic acid | 1.0 mg/mL, 1.1 *M*, and 1.9 m*M* |
| BSA, glycerol, and potassium chloride | 1.0 mg/mL, 1.1 *M*, and 2.0 *M* |
| BSA and potassium chloride | 1.0 mg/mL, 2.0 *M* |
| BSA and potassium chloride | 1.0 mg/mL, 1.0 *M* |
| BSA and potassium chloride | 1.0 mg/mL, 0.4 *M* |

reaction mixture and the time of the reaction *(9)*. This general statement may be expressed as in Eq. 3.

$$[E] \times t = f[(P_t)] \tag{3}$$

where $[E]$ is the enzyme concentration, $t$ is the time of reaction, and $[P_t]$ is the product concentration generated at time $t$. In terms of the IUPAC filter paper assay, Eq. 3 indicates that the point on a progress curve corresponding to 2.0 mg of RSE will be directly related to the product of enzyme concentration and time ($[E] \times t$). The equation also suggests that FPA can be determined by using a single enzyme concentration and noting the time required to obtain 2.0 mg of RSE. The activity of a cellulase preparation would then be calculated as in Eq. 4.

$$FPA = \frac{1(h)}{t_2}(0.37) \tag{4}$$

where FPA is the filter paper activity and $t_2$ is the time in hours, required for generation of 2.0 mg RSE. As Eq. 3 must be valid for Eq. 4 to be applied, its validity must be determined. The validity of Eq. 3 is easily tested by

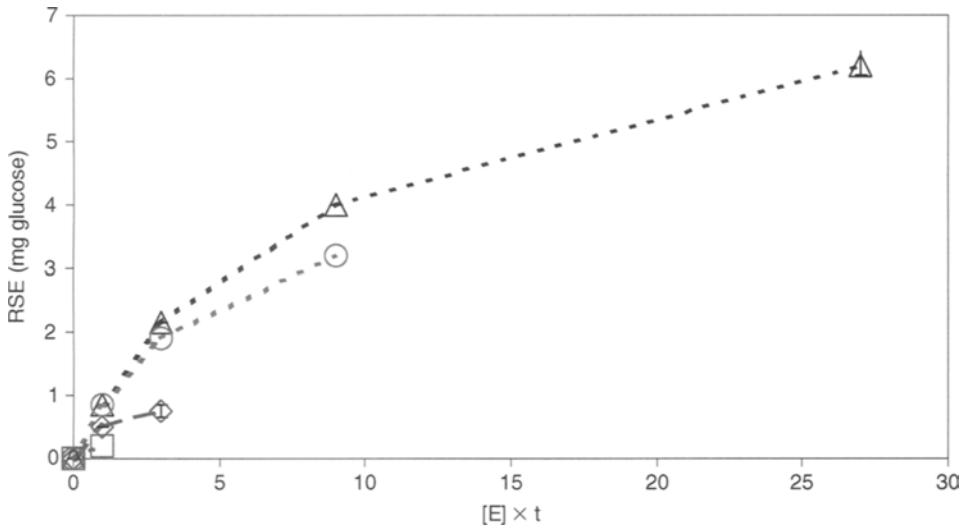


**Fig. 1.** Progress curves of cellulase reaction plotted in terms of soluble RSE vs reaction time (h) multiplied by the amount of enzyme added to the reaction mixture (expressed as the fold dilution of a stock solution). Reaction conditions were as described for the IUPAC filter paper assay. The stock cellulase preparation for this experiment contained 0.14 FPU/mL. Dilutions: 27-fold (□), ninefold (◊), threefold (○), and undiluted (△).

comparing progress curves (as $[P_t]$ vs [E] × $t$) for reaction mixtures containing different enzyme concentrations *(9)*. The progress curves are expected to overlay each other if Eq. 3 is obeyed. And Eq. 3 will be obeyed if the activity of the enzyme is stable over the assay period, or if changes in enzyme activity are a consequence of the percent of substrate converted (such as is expected with a heterogeneous amorphous/crystalline substrate like cellulose) or classical product inhibition. If such theoretical behavior is observed (Eq. 3 is valid), then Eq. 4 may be applied directly. However, if the progress curves are not well behaved, as is the case for the commercial enzyme preparation depicted in Fig. 1, then Eq. 4 is not directly applicable. The nature of the time-courses in Fig. 1 indicate that there is a time-dependent enzyme inactivation that occurs over the course of the assay, and this change in activity is not a simple function of the extent of substrate conversion. Thus, under standard IUPAC conditions (as was used in the experiment generating the data in Fig. 1), one cannot interchange reaction time and enzyme concentration.

Equation 4 may be correctly applied to the enzyme preparation of Fig. 1 only if the time-dependent inactivation is effectively alleviated. Previous studies suggest that the observed inactivation is owing to proteolytic degradation *(10)* and/or thermal inactivation *(11–13)*. Hence, approaches to stabilize the enzyme preparation should likely focus on these mechanisms of inactivation. A number of potential stabilizers, alone or in

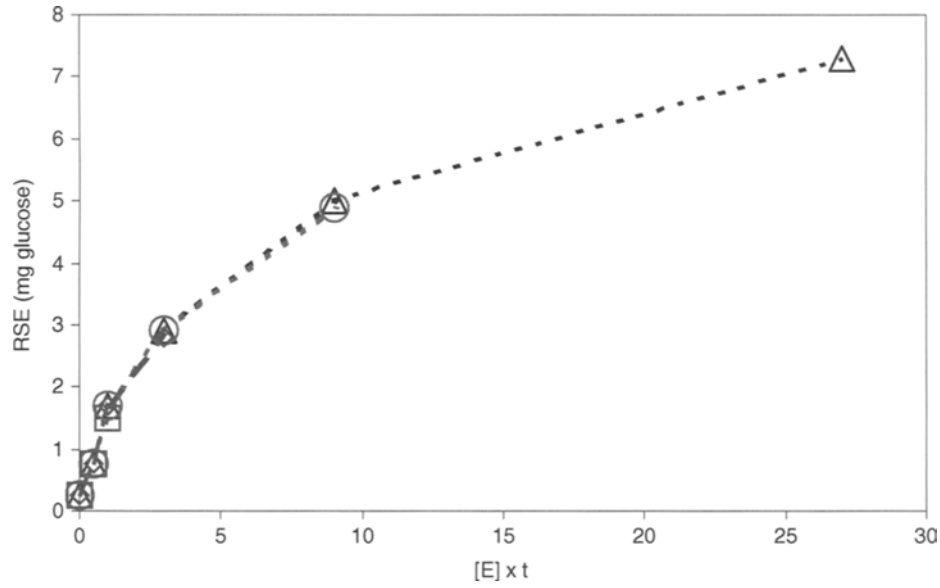


**Fig. 2.** Progress curves of cellulase reaction plotted in terms of soluble RSE vs reaction time (h) multiplied by the amount of enzyme added to the reaction mixture (expressed as the fold dilution of a stock solution). Reaction conditions were as described for the IUPAC filter paper assay with the exception that reaction mixtures were supplemented with enzyme stabilizers (reaction mixtures contained 1.0 mg BSA/mL and were 1.0 *M* in KCl). The stock cellulase preparation for this experiment contained 0.35 FPU/mL. Dilutions: 27-fold (□), ninefold (◊), threefold (○), and undiluted (△).

combination, were tested in this study (Table 1), including glycerol, sugar alcohols, salts, BSA, ascorbic acid, and the exclusion of dissolved gases (particularly oxygen; achieved by degassing the buffer and covering the reaction mixture with mineral oil). In the present case, optimal stability was obtained when reaction mixtures were made 1.0 *M* in KCl and 1.0 mg/mL in BSA. The salt is expected to stabilize the protein through its preferential hydration *(14)*. The BSA may stabilize the system by its hydration properties as well as its ability to act as a competitive substrate for proteolysis. The addition of the stabilizers resulted in an enzyme preparation whose activity was stable for up to 20 h, as evidenced by the overlaying progress curves of Fig. 2 (compare with the analogous curves of Fig. 1). Thus, Eqs. 2–4 appear to be applicable, and a relative FPA can be calculated based on Eqs. 2 and 4 when the stabilizers are used.

An unfortunate consequence of the added stabilizers is that they tend to decrease the measured FPA relative to equivalent enzyme preparations acting in the absence of stabilizers. The "stabilized" enzyme system described earlier, when tested in the standard IUPAC assay with sufficient enzyme to generate 2.0 mg RSE in 1h, had approx 60% of the activity observed for the same enzyme preparation in the absence of stabilizers.

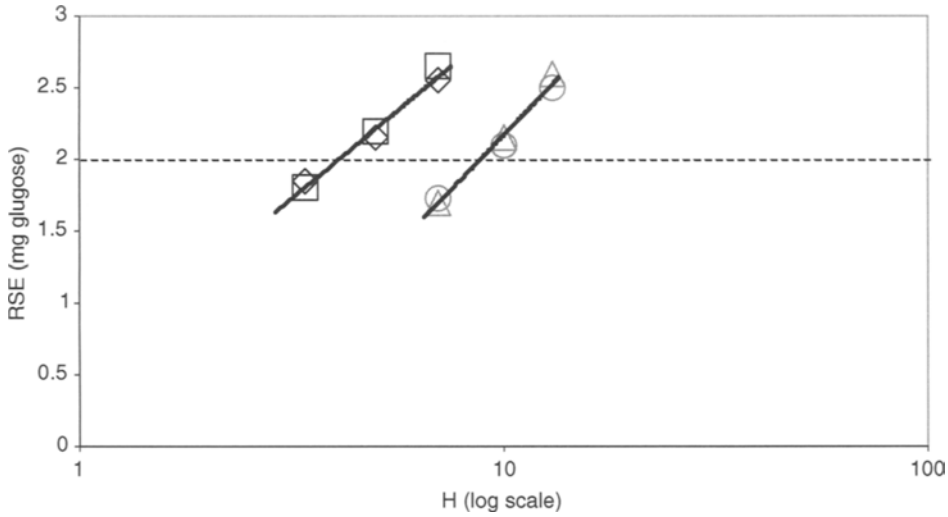


**Fig. 3.** Semilog plot of filter paper-derived soluble RSE vs time for two "low-activity" enzyme preparations. Reaction conditions were as described for the IUPAC filter paper assay with the exception that enzyme stabilizers were added to reaction mixtures (as described in Fig. 2). The enzyme preparations were prepared by diluting approx 0.9 FPU/mL stock enzyme solution sevenfold (□,◊) and 14-fold (○,△).

Hence, the activity measured under stabilizing conditions cannot be directly interpreted in terms of absolute IUPAC FPU. However, this does not limit the use of the presented approach for obtaining relative FPAs. If absolute FPUs are to be calculated for enzyme preparations assayed in the presence of stabilizers, then a correction factor, based on separate kinetic experiments, must be determined. Such correction factors are not necessary for the determination of relative FPAs.

The application of stabilizers in the filter paper assay is illustrated in Fig. 3 and Table 2. In this case, two low-activity enzyme solutions were prepared by diluting (7-fold and 14-fold) an enzyme solution known to contain 0.95 FPU/mL, based on the traditional IUPAC assay. Hence, the diluted enzyme solutions contained approx 2.5- and 5-fold less activity than the minimum required for the traditional assay (0.37 FPU/mL). The test solutions were then assayed in the presence of stabilizers. Total RSE was determined at selected time-points over extended assay periods until at least 2.0 mg RSE could be detected. Times corresponding to the targeted 2.0 mg RSE end point were determined based on Eq. 2 (data presented in Fig. 3), and subsequently, FPAs were calculated based on Eq. 4. The measured activities were found to be directly proportional to the fold dilution used to prepare the test samples (Table 2). Hence, the assay with the incorporated stabilizers correctly measured the relative FPA of the enzyme preparations; these values could not have been obtained using the traditional IUPAC assay because of their relatively low activities.

Table 2
Measured Vs Theoretical Activities for a Series of Diluted Enzyme Preparations[a]

| Enzyme preparations[b] | Measured activity[c] | Theoretical activity[d] | Measured activity/ theoretical activity |
|---|---|---|---|
| Standard solution | 0.56 (0.010) | – | – |
| Sevenfold diluted | 0.078 (0.009) | 0.080 | 0.98 |
| 14-fold diluted | 0.039 (0.001) | 0.040 | 0.98 |

[a]Activity determined as a function of time required to produce 2.0 mg soluble RSE in modified filter paper assay.

[b]The standard solution was prepared from a commercial cellulase preparation and assayed "as prepared," other enzyme preparations were prepared by the indicated dilution of the standard solution. All reaction mixtures contained 1.0 mg BSA/mL and were 1.0 *M* KCl, as described in Fig. 2.

[c]Mean (standard error of mean).

[d]Obtained by dividing the activity of the standard solution by the fold dilution.

It is informative to consider the assay approach described in this note to previously suggested permutations of the filter paper assay. The assay, as adopted by IUPAC, was discussed in some detail in 1976 *(6)*. The emphasis at that time was to fix the extent of conversion of the substrate and the time of the reaction. The chosen extent of conversion was deemed appropriate because 3.6% was considered well past the extent of conversion that would be expected for an incomplete cellulase. In choosing this value, and the corresponding 1-h reaction time, it set a limit as to the minimum activity to which this assay could be applied. This limitation has been addressed in different ways over the years. The "low-activity" assay of Chan et al. *(15)* is based on the conversion of approx 1.5% of the filter paper substrate, the activity then being calculated in Forintek units. Assays based on either Forintek or FPUs are expected to show similar trends with respect to enzyme activity; but Forintek and FPUs are not expected to be directly proportional owing to the two assays being based on different extents of substrate conversion. Another permutation that under certain circumstances may allow the analysis of lower activity samples is the inclusion of supplemental β-glucosidase in the reaction mixture *(16)*. The cited paper was actually addressing the need for a better measure of the extent of saccharification (as have others, *[17]*); but inclusion of β-glucosidase may serve to enhance the rate of filter paper saccharification by those enzyme preparations inherently low in this enzyme and thus, inadvertently make the assay more amenable to lower activity enzyme preparations. However, it is clear that a β-glucosidase-supplemented activity will not be particularly relevant for some applications. A similar argument may be made about the present work that a "stabilized" FPA will not be particularly relevant for some applications. All of the suggested assay permutations that directly or indirectly accommodate low-activity samples have some limitations. We think the method presented here is a

noteworthy addition to the field in that it addresses the mechanistic basis underlying the limitation of the filter paper assay for low-activity samples and it allows one to obtain relative FPA values that were previously unattainable. The merit of any such values, as is the case with activity values obtained with the standard IUPAC assay, is dependent on the particular application of the enzyme system *(18)*.

## References


1. Zhang, Y. -H. P. and Lynd, L. R. (2004), *Biotechnol. Bioeng.* **88,** 797–824.
2. Lynd, L. R., Weimer, P. J., van Zyl, W. H., and Pretorius, I. S. (2002), *Microbiol. Mol. Biol. Rev.* **66,** 506–577.
3. Bayer, E. A., Chanzy, H., Lamed, R., and Shoham, Y. (1998), *Curr. Opin. Struct. Biol.* **8,** 548–557.
4. Jeoh, T., Wilson, D. B., and Walker, L. P. (2006), *Biotechnol. Prog.* **22,** 270–277.
5. Ghose, T. K. (1987), *Pure Appl. Chem.* **59,** 257–268.
6. Mandels, M., Andreotti, R., and Roche, C. (1976), *Biotechnol. Bioeng. Symp.* **6,** 21–33.
7. Roseiro, J. C., Conceicao, A. C., and Amaral-Collaco, M. T. (1993), *Bioresour. Technol.* **43,** 155–160.
8. Breuil, C. and Saddler, J. N. (1985), *Enzyme Microb. Technol.* **7,** 327–332.
9. Selwyn, M. J. (1965), *Biochem. Biophys. Acta* **105,** 193–195.
10. Haab, D., Hagspiel, K., and Szakmary, K. (1990), *J. Biotechnol.* **16,** 187–198.
11. Baker, J. O., Tatsumoto, K., Grohmann, K., et al. (1992), *Appl. Biochem. Biotechnol.* **34–35,** 217–232.
12. Dominguez, J. M., Acebal, C., Jimenez, H., Delamata, I., Macarron, R., and Castillon, M. P. (1992), *Biochem. J.* **287,** 583–588.
13. Lencki, R., Arul, J., and Neufeld, R. (1992), *Biotechnol. Bioeng.* **40,** 1421–1426.
14. Timasheff, S. and Arakawa, T. (1989), In: *Protein Structure: A Practical Approach.* Creighton, T. E. (ed.), pp. 331–345.
15. Chan, M., Breuil, C., Schwald, W., and Saddler, J. N. (1989), *Appl. Microbiol. Biotechnol.* **31,** 413–418.
16. Coward-Kelly, G., Aiello-Mazzari, C., Kim, S., Granda, C., and Holtzapple, M. (2003), *Biotechnol. Bioeng.* **82,** 745–749.
17. Schwald, W., Chan, M., Breuil, C., and Saddler, J. N. (1988), *Appl. Microbiol. Biotechnol.* **28,** 398–403.
18. Kabel, M. A., van der Maarel, M. J. E. C., Klip, G., Voragen, A. G. J., and Schols, H. A. (2006), *Biotechnol. Bioeng.* **93,** 56–63.

0273-2289/1559-0291 (Online)/07/136-140/141-154/$30.00

# Enzymatic Hydrolysis Optimization to Ethanol Production by Simultaneous Saccharification and Fermentation

MARIANA PEÑUELA VÁSQUEZ,[1,2] JULIANA NASCIMENTO C. DA SILVA,[1] MAURÍCIO BEZERRA DE SOUZA JR.,[1] AND NEI PEREIRA JR.*,[1]

[1]*Escola de Química—Universidade Federal do Rio de Janeiro, Centro de Tecnologia—Bloco E—Rio de Janeiro—RJ—Brasil—CEP 21.949-900, E-mail: nei@eq.ufrj.br; and* [2]*Departamento de Ingeniería Química—Universidad de Antioquia—Colombia*

## Abstract

There is tremendous interest in using agro-industrial wastes, such as *cellulignin*, as starting materials for the production of fuels and chemicals. *Cellulignin* are the solids, which result from the acid hydrolysis of the sugarcane bagasse. The objective of this work was to optimize the enzymatic hydrolysis of the cellulose fraction of *cellulignin*, and to study its fermentation to ethanol using *Saccharomyces cerevisiae*. Cellulose conversion was optimized using response surface methods with pH, enzyme loading, solid percentage, and temperature as factor variables. The optimum conditions that maximized the conversion of cellulose to glucose, calculated from the initial dried weight of pretreated *cellulignin*, (43°C, 2%, and 24.4 FPU/g of pretreated *cellulignin*) such as the glucose concentration (47°C, 10%, and 25.6 FPU/g of pretreated *cellulignin*) were found. The *desirability* function was used to find conditions that optimize both, conversion to glucose and glucose concentration (47°C, 10%, and 25.9 FPU/g of pretreated *cellulignin*). The resulting enzymatic hydrolyzate was fermented yielding a final ethanol concentration of 30.0 g/L, in only 10 h, and reaching a volumetric productivity of 3.0 g/L·h, which is close to the values obtained in the conventional ethanol fermentation of sugar cane juice (5.0–8.0 g/L·h) in Brazil.

**Index Entries:** Cellulignin; enzymatic hydrolysis; ethanol production; sugarcane bagasse; cellulases; simultaneous saccharification; *saccharomyces cerevisiae*.

## Introduction

Sugarcane bagasse represents the main lignocellulosic material to be considered in many tropical countries, because it is readily available in the distilleries without additional cost and has high carbohydrate and low

*Author to whom all correspondence and reprint requests should be addressed.

lignin content (1). In Brazil, sugarcane (*Saccharum* sp.) is one of the most important agro-industrial product. According to data of São Paulo State Research Foundation (2), about 60–90% of the generated bagasse from milled sugar cane in the country is used as fuel for steam and energy production and, between 10 and 40% is not used, representing about 5–12 million t annually. In 2003, 340 million t of sugarcane were produced and, consequently, 91.8 millions t of bagasse were generated. Because of the high carbohydrate content, sugar cane bagasse can be potentially used for bioethanol production and/or others products, within the context of biorefinery (3).

Lignocellulosic materials typically contain 55–75% of dry weight of carbohydrates, which are polymers containing sugar units of five and six carbon atoms. Sugarcane bagasse is made up of 38.1 wt% cellulose, 28.4 wt% hemicellulose, 18.4 wt% lignin, and 15.1 wt% proteins and ashes (4). Cellulose is a biopolymer of β-1,4-linked glucose dimers (cellobiose). This abundant biopolymer is made up of crystalline and amorphous regions. The amorphous component is digested more easily by enzymes than the crystalline component (5,6). Crystalline cellulose exists in the form of microfibrils, which are paracrystalline assemblies of several dozen of 1,4-β-D-glucan chains that are tightly linked by numerous hydrogen bonds, both side-to-side and top-to-bottom in a lattice like manner (6).

Hemicellulose are largely made up of aldopentoses (arabinose, xylose, galactose, and manose) and present crosslinking glycans, which are a sort of polysaccharides that can be linked to cellulose microfibrils by hydrogen bonds (6,7). They may coat microfibrils but are also long enough to span the distance between microfibrils and link them together to form a network. Lignin is a complex macromolecule of phenolic polymer, made up of phenylpropanoid units (hydroxycinnamyl, *p*-coumaryl, coniferyl, and sinapyl alcohols that constitute most of the lignin network) (8). Lignin is the most abundant noncarbohydrate constituent of lignocellulosic material. Its presence represents a major problem for the biomass conversion process because the physical structure of native lignocellulose is intrinsically resistant to enzyme attack, especially cellulose, which is further protected by the surrounding matrix of lignin, hemicellulose, and pectin (9,10).

The lignocellulosic biomass must be pretreated to make the cellulose fraction more accessible to enzymatic attack. Diverse pretreatment processes have been evaluated technically and economically aiming at improving enzymatic hydrolysis, these include acid or alkali treatment, steam-explosion, and organic solvents (11,12). Pretreatments are also necessary in order to use sugarcane bagasse in bioconversions, for producing several compounds such as organic acids, xylitol, and mainly ethanol, which represents a promising alternative fuel to reduce environmental problems (13).

In the bioconversion of solid cellulose to a readily fermentable stream of glucose monomers, an enzymatic complex should be used. The enzymatic complex that is able to hydrolyze cellulose to glucose molecules is

called cellulases. This enzymatic complex is usually made up of three types of enzymes that act synergistically. The first is called endoglucanases (EC 3.2.1.4), which cut randomly at amorphous sites in the cellulose yielding smaller chains of cellulose called cello-dextrins *(14)*. The second enzyme group, called exoglucanases (glucohidrolase enzyme commission [EC] 3.2.1.74 and celobiohidrolase EC 3.2.1.91), degrades cello-dextrins and crystalline cellulose, thus liberating glucose and cellobiose as major product *(14,15)*. Finally, the cellobiose is hydrolyzed into glucose by β-glucosidases (EC 3.2.1.21). Currently, the costs of pretreatment and enzymes for cellulose hydrolysis are still the main economic obstacle to the commercialization of biomass bioconversion technologies *(14,15)*.

The aim of this work was to study the different factors that play an important role in the enzymatic hydrolysis of cellulose; those variables were pH, solid content, temperature, and enzymatic loading. In this context, it was required to establish the conditions to obtain optimal values for the response variables (final concentration of glucose and conversion of pretreated *cellulignin* to glucose). Finally, the evaluation of the resulting hydrolyzate fermentability was also the subject of investigation. The fermentation experiments were carried out under the optimal conditions found in the enzymatic hydrolysis stage.

## Materials and Methods

### *Raw Material and Pretreatment of Cellulignin*

The sugarcane bagasse, *Saccharum* sp., was provided by "Usina Costa Pinto," Piracicaba in São Paulo, Brazil. The *cellulignin* was obtained by acid hydrolysis of sugarcane bagasse, from which the hemicellulosic fraction was removed *(16)*. This resulting solid residue was pretreated for increasing the accessability of enzymes to cellulose, by removing partially the lignin. The conditions for this pretreatment were as follows: the *cellulignin* was mixed with a solution of NaOH 4% (w/v), which was further submitted to thermal treatment at 121°C for 30 min *(17)*. The pretreated *cellulignin* was then washed until pH 5.5 and finally, it was dried at 50°C for 24 h, this solid was called *cellulignin*G.

### *Enzyme Activities*

Filter paper activity was determined as recommended by Ghose (1987) *(18)* and it is expressed as *Filter Paper Units* (FPU) per milliliter of mixture. The activity of enzyme used, GC 220 of *Genencor International Inc.* (Leiden, The Netherlands), was 104.27 FPU/mL of mixture.

### *Enzymatic Hydrolysis*

Pretreated *cellulignin* was hydrolyzed by using GC 220 (*Genencor International, Inc.*). The enzymatic hydrolysis was carried out in 125-mL

Table 1
Full Factorial Design ($3^4$)

| Factor | Low label (–1) | Center label (0) | High label (+1) |
|---|---|---|---|
| 1. Temperature (°C) | 30 | 40 | 50 |
| 2. Enzyme loading (FPU/g *CelluligninG*) | 5.0 | 17.5 | 30.0 |
| 3. pH | 5.0 | 5.5 | 6.0 |
| 4. Solid (%) | 2 | 6 | 10 |

flasks on a shaker at 150 rpm. Temperature, pH (citrate buffer), solid percent, and enzyme loading were selected as the most important variables for the optimization of the process.

### *Experimental Design for the Optimization of the Enzymatic Hydrolysis*

Full factorial design of four factors at three levels was developed *(19)*. High, intermediate, and low levels of the factors were considered. The experimental design matrix is shown in Table 1. The analysis of the results of this design includes the computation of the linear (L), quadratic (Q), and interaction effects, and the analyses of the variances ascribed to them. The statistical significance of these effects was evaluated by using *t*-tests and *F*-tests *(19)*.

Final glucose concentration and conversion of *celluligninG* to glucose were considered as response variables for the process analysis. A quadratic model was obtained relating each response variable to the significant effects. These models were used to define the conditions that separately and simultaneously maximize the response variables. The method developed by Derringer and Suich *(20)* was adopted in the case of multiple response optimization. Their procedure makes use of the so-called *desirability* functions *(19–21)*. The STATISTICA 6.0 (Statsoft, Inc., Tulsa, OK) software was used here in order to implement all these statistical analysis.

### *Yeast Cultivation*

A pure culture of *Saccharomyces cerevisiae* was isolated from commercial yeast *Fleischmann* in the Laboratory of Bioprocess Development at the Federal University of Rio de Janeiro, Brazil, and it was used in the fermentation assays. Inoculum was obtained in 500-mL shaker flask with a working volume of 250 mL, and a medium consisting of (g/L): glucose, 30; urea, 1.25; $KH_2PO_4$, 1.1; yeast extract, 1.5; salts, and citric acid solution 40 mL/L *(22)*. Glucose was sterilized separately from the others components to prevent damage to the nutritional qualities of the medium. The sterilization condition, in both cases, was 111°C for 15 min. The pH and temperature were maintained at 5.5 and 37°C, respectively, during 10 h. After cell quantification, the volume required to achieve the initial cell concentration in the bioreactor, was centrifuged at 5000 rpm for 15 min.

### *Fermentation Assay*

Experiments were carried out in a batch bioreactor (BIOFLO III, New Brunswick Scientific, New Brunswick, NJ; 1.5 L) with 1.0 L working volume, at 37°C, 300 rpm, pH 5.0, and an initial cell concentration of 4.0 g (dry weight)/L. The hydrolyzed products obtained after the enzymatic hydrolysis were used as fermentation medium without any nutritional supplements. Three fermentations were run, each one with the hydrolyzate obtained under the conditions established by the separate and simultaneous maximization of the response variables (conversion to glucose and glucose concentration).

### *Analytical Methods*

The cells were measured for absorbance at 570 nm and a calibration curve obtained by the dry weight method was used *(23)*. Glucose, cellobiose, and ethanol concentration were determined by high-performance liquid chromatography-Waters by using a Shodex SC1011 ion exchange column for sugars ($300 \times 8$ mm$^2$; Shoko Co., Ltd., Tokyo) at 80°C as stationary phase and degassed Milli-Q (Molsheim, France) water as the mobile phase at a flow rate of 0.6 mL/min *(24)*.

## Results and Discussion

Several delignification processes were evaluated in a previous study in order to improve or facilitate the accessibility of the enzymes to the cellulose matrix *(25)*. Of the evaluated pretreatments, the one coded as *G*, as described previously, resulted in the best performance of the enzyme preparation. This pretreatment improves 2.4 times the performance of the enzymatic hydrolysis when compared with the analog process with non-pretreated cellulignin (Fig. 1).

The results of 87 experiments, obtained by utilizing a three-level full factorial design with four factors ($3^4$) plus six replicates in the center value, were analyzed by considering glucose concentration and conversion to glucose as output (response) variables. The results of this analysis are shown by using the Pareto charts as they present, very clearly, the most significant effects *(21)*. In these charts, the effects represented by rectangles, which lay to the right side of the 0.05 *p*-value vertical line, are statistically significant and must be considered in the mathematical model. This *p*-value implies in a 95% level of significance, which is the usual level assumed in statistical analysis *(19,21)*.

In the Pareto chart for conversion to glucose (Fig. 2), the largest effect is owing to the enzyme loading followed by temperature, and the quadratic factors (*Q*) for these two factors, all of them affecting positively the glucose formation. In general, the interaction factors exert less significant effects over the conversion to glucose. The negative influence of the solid percentage on the conversion to glucose can be explained by the enzymatic inhibition caused by the increase on the final hydrolysis product concentration (glucose) *(14)*.

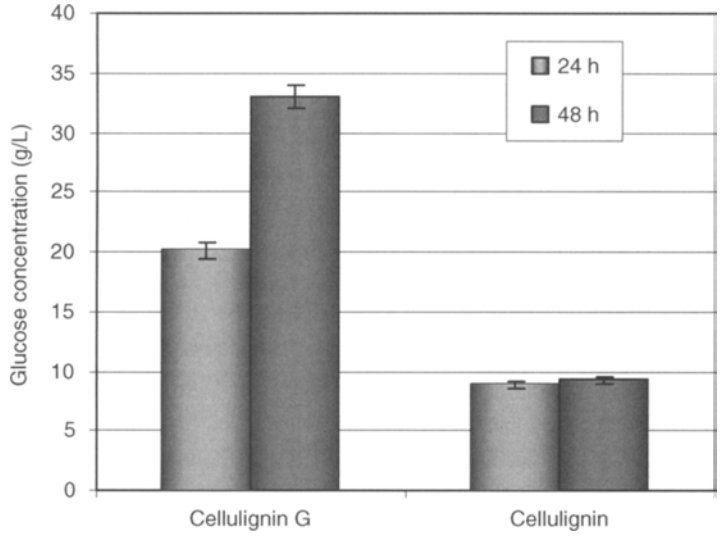


**Fig. 1.** Effect of pretreatment on enzymatic hydrolysis of cellulignin (*T*, 50°C; solid [%], 7; and enzyme concentration, 20 FPU/g cellulignin).

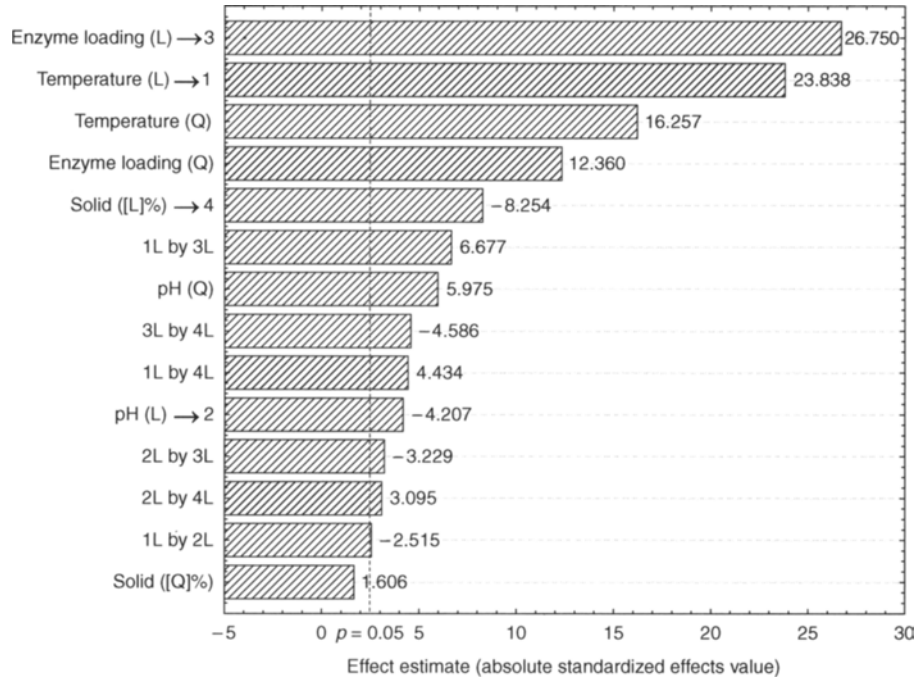


**Fig. 2.** Pareto chart of standardized effects; on conversion to glucose (g glucose/g *cellulignin*G).

When the Pareto chart is analyzed, concerning the glucose concentration variable (Fig. 3), the degree of importance among the factors changes. In this case, the factor that presented the largest effect was the solid percentage (Solid [%]). Similarly to the other analyzed response variable

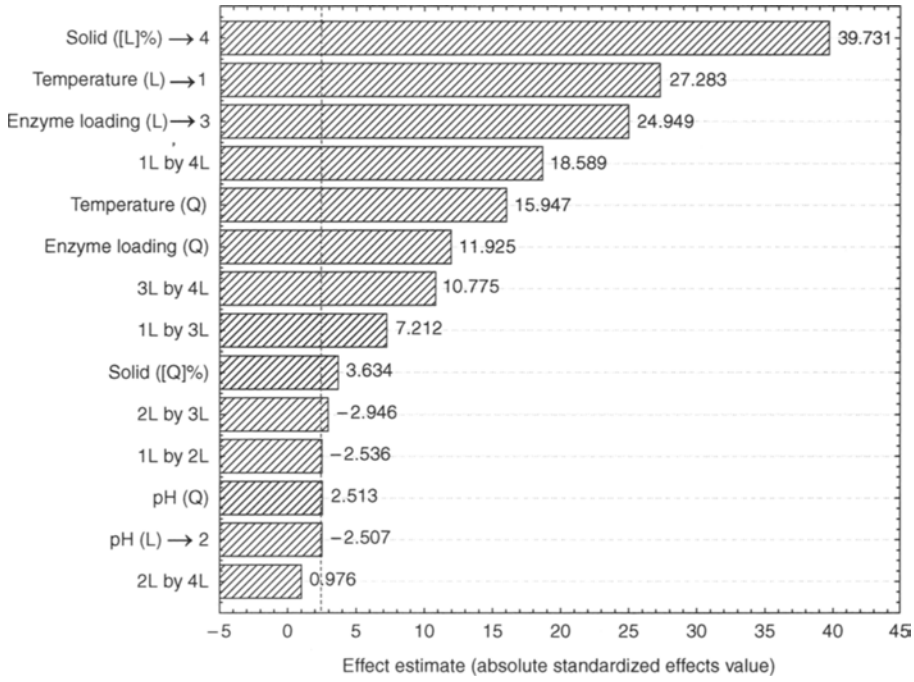


**Fig. 3.** Pareto chart of standardized effects; on glucose concentration (g glucose/L).

(conversion to glucose), the factors temperature and enzyme loading presented highly significant positive effects. However, unlike what was observed in the analysis of conversion to glucose, in which the interaction factors did not show much significance, the positive influence on glucose concentration of the interaction between solid percentage and temperature was evidenced here. For both output variables, it can be depicted from the Pareto chart that the pH presented a linear effect with magnitude lower than the other factors discussed previously. However, it is important to consider that pH variations, outside the range evaluated experimentally, can generate changes in the behavior of the enzyme, leading to a halt of the process.

The pH was eliminated from the model used for the optimization of the enzymatic hydrolysis, because of the fact that it affects the response variables less than the other factors in the range considered. Therefore, a value of pH = 5.0 was selected for further experiments. The use of this value is in accordance with the following facts: the majority of the work presented in literature with cellulosic enzyme preparations uses pH = 5.0 for cellulose hydrolysis; it is a pH value in which the contamination of the fermentation by bacteria is uncommon *(26)*; the yeast (*S. cerevisiae*) displays a good performance in a slightly acid pH range; and finally pH = 5.0 is within the stability range of commercial cellulases *(1,7,11,14,17,27)*.

Analyses of the variances was also performed. The analysis of significance (using *F*-tests) provided exactly the same significant factors already shown in the Pareto charts. Additionally, the percentage of variance

Table 2
Models Coefficients

| Coefficients | Variables | |
|---|---|---|
| | Conversion to glucose | Glucose concentration |
| $\beta_0$ | 0.30 | 18.47 |
| $\beta_1$ | 0.11 | 7.61 |
| $\beta_2$ | 0.12 | 6.95 |
| $\beta_3$ | −0.04 | 11.08 |
| $\beta_4$ | 0.06 | 3.64 |
| $\beta_5$ | 0.05 | 3.75 |
| $\beta_6$ | 0.01 | 0.84 |
| $\beta_7$ | 0.04 | 2.46 |
| $\beta_8$ | 0.02 | 6.35 |
| $\beta_9$ | −0.02 | 3.68 |

explained by the model was 88% for the conversion to glucose (mean squares of pure error: 0,001) and 91.4% for glucose concentration (mean squares of pure error: 4,2).

It should be stressed that for both response variables, the quadratic model fits the experimental data very appropriately as confirmed by the values of the correlation coefficient (0.91 for glucose concentration and 0.88 for conversion to glucose). The models generated in statistic analysis are represented by a quadratic function (Eq. 1) and the coefficient values are shown in the Table 2.

$$\begin{aligned} Y = {} & \beta_0 + \beta_1 \cdot (\text{Temperature}) + \beta_2 \cdot (\text{Enzyme concentration}) \\ & + \beta_3 \cdot [\text{Solid}(\%)] + \beta_4 \cdot (\text{Temperature})^2 \\ & + \beta_5 \cdot (\text{Enzyme concentration})^2 \\ & + \beta_6 \cdot [\text{Solid}(\%)]^2 + \beta_7 \cdot (\text{Temperature} \times \text{Enzyme concentration}) \\ & + \beta_8 \cdot [\text{Temperature} \times \text{Solid}(\%)] \\ & + \beta_9 \cdot [\text{Solid}(\%) \times \text{Enzyme concentration}] \end{aligned} \quad (1)$$

Three optimizations were performed. First, the conditions for maximizing conversion of *celluligninG* to glucose were determined. Second, the conditions for maximizing glucose concentration in the enzymatic hydrolysis were established. The third optimization allowed the definition of values that maximize both variables simultaneously by means of Derringer and Suich function or global *desirability* function *(20,21)*.

Figure 4 shows the response surfaces generated in the simultaneous optimization of both response variables, conversion of *celluligninG* to glucose and glucose concentration. The best results are restricted to temperature ranges between 40 and 50°C, enzyme loading between 18 and 30 FPU/g *celluligninG*, and solid percentage between 8 and 10%, being the last factor, which presents the narrowest range of values that generated the zone of high values of the *desirability* function.

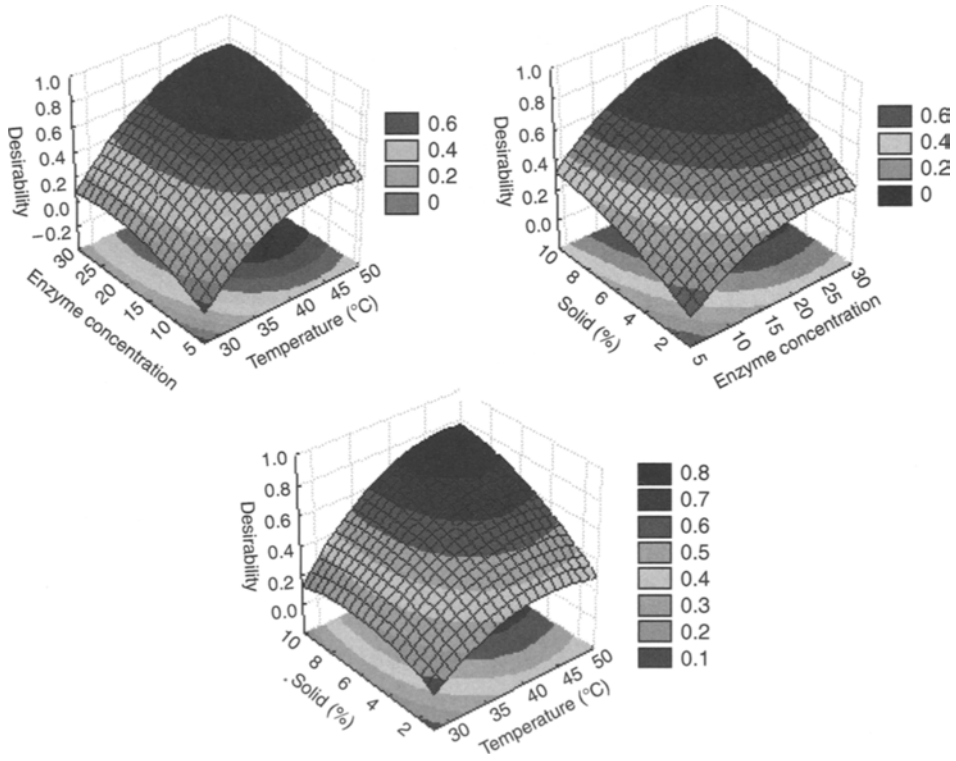


**Fig. 4.** Response surface for *desirability* function.

The optimal values for the response variables, glucose concentration, and conversion to glucose, and the optimal values of the *desirability* function are presented in Table 3. The conditions that lead to maximum values of conversion from *celluligninG* to glucose and glucose concentration are similar for temperature and enzyme load. However, for the solid percentage variable the behavior differs, i.e., it is indicated the upper level (10%) for maximum glucose concentration and the use of its lower level (2%) for conversion to glucose. This makes the solid percentage variable as a decisive factor to reach significant values of both response variables. With the aim of evaluating the fermentability of the hydrolyzate obtained from *celluligninG* arising from sugarcane bagasse, and in order to validate the optimal value predicted by the statistical analysis, the enzymatic hydrolysis was experimentally carried out, and the hydrolyzate was further fermented.

The validation results for the enzymatic hydrolysis were better than those predicted by the model (Table 3). This can be ascribed, probably, to the fact that these validation experiments were performed by using a bioreactor that allowed a better control of the process variables. Conversions of *celluligninG* to glucose of 67% and glucose concentrations around 60.0 g/L were reached experimentally. According to the results obtained, high concentrations of glucose in the medium cannot be expected

Table 3
Predict Values to Statistical Model and Experimental Validations

| Optimal Points | Temperature (°C) | Solid (%) | Enzyme loading (FPU/g) | Predict values: Conversion to glucose (g glucose/g *celluligninG*) | Predict values: Glucose concentration (g glucose/L) | Validation: Conversion to glucose (g glucose/g *celluligninG*) | Validation: Glucose concentration (g glucose/L) |
|---|---|---|---|---|---|---|---|
| For conversion to glucose | 43 | 2 | 24.4 | 0.58 ± 0.06 | – | 0.67 ± 0.09 | 13.05 ± 3.2 |
| For glucose concentration | 47 | 10 | 25.6 | – | 50.98 ± 2.9 | 0.52 ± 0.09 | 58.40 ± 3.2 |
| For *desirability* function | 47 | 10 | 25.9 | 0.47 ± 0.06 | 50.98 ± 2.9 | 0.54 ± 0.09 | 60.08 ± 3.2 |

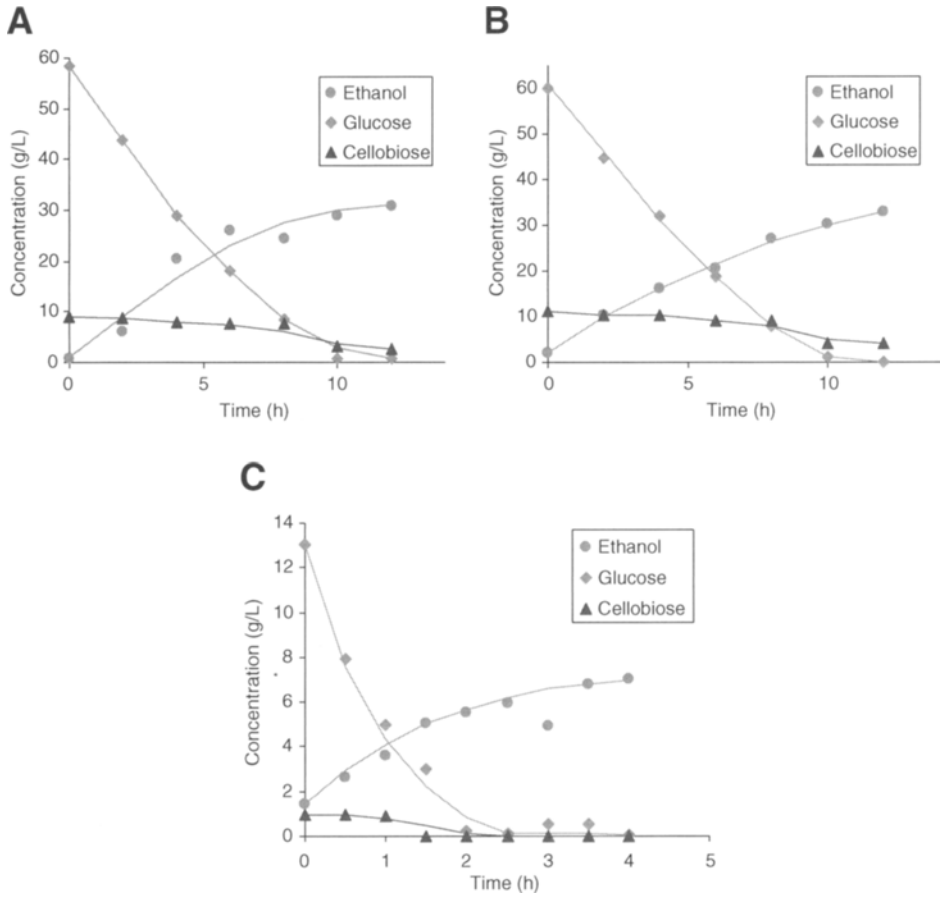


**Fig. 5.** Fermentation kinetics of hydrolyzates obtained by predicted conditions for high-glucose concentration **(A)** for *Desirability* function **(B)**, and for high conversion to glucose **(C)**.

because the conditions for high conversion to glucose are achieved in low solid percentage. The fermentations were carried out by using the hydrolyzate medium containing the hydrolysis residual solid, obtained under the conditions predicted by the statistical model. The fermentation kinetic profiles were obtained and presented in Fig. 5, evidencing the high fermentability of the hydrolyzate medium. Their behaviors are similar to those obtained using glucose synthetic medium (data not shown), evidencing the high fermentability of the hydrolyzate medium.

The similarity of the kinetic profiles of the Fig. 5A, b is owing to the analogous conditions used in the optimization process. For all cases the final ethanol concentration exceeded the theoretical conversion to ethanol considering the initial glucose concentration. This can be explained by the reactivation of the cellulolytic complex enzymes, particularly β-glucosidase, after the consumption of the glucose by the yeast. Thus, diminishing the inhibitory effect of this sugar on the enzymatic action, typical characteristic

of the *simultaneous saccharification and fermentation process*. A reduction of cellobiose concentration is detected after 10 h of fermentation, confirming the enzymatic reactivation.

## Conclusions

The quadratic model generated in the statistical analysis fits adequately the behavior of the response variables (glucose concentration and conversion of *celluligninG* to glucose), in the enzymatic hydrolysis process when the factors (temperature, enzyme loading, and solid percentage) are varied within specified ranges. The conditions of hydrolysis that yielded the highest glucose concentration, 58.40 g/L, were: temperature 47°C, enzyme loading 25.6 FPU/g *celluligninG*, and solid percentage 10%. As far as the conversion of *celluligninG* to glucose, the highest value, 67%, was obtained in the following conditions: temperature 43°C, enzyme loading 24.4 FPU/g *celluligninG*, and solid percentage 2%. The *Desirability* function provided conditions in which both response variables were simultaneously optimized. These conditions were: temperature 47°C, enzyme loading 25.9 FPU/g *celluligninG*, and solid percentage 10%. The pH variable, in the range 5–6, does not present an important influence on the behavior of the enzymatic hydrolysis for any response variables (glucose concentration and conversion of *celluligninG* to glucose).

It is possible to conclude that the hydrolyzate produced in the enzymatic hydrolysis of *celluligninG* is easily fermented by *S. cerevisiae* yeast for the production of ethanol, resulting in a final ethanol concentration of 30.0 g/L, in only 10 h of fermentation. This provides a volumetric productivity value of 3.0 g/L.h, which is not so far from the values obtained in the conventional ethanol fermentation of sucrose in Brazil (5.0–8.0 g/L·h). The fermentation of the hydrolyzate of *celluligninG*, coming from the acid pretreatment of sugar-cane bagasse, stands as an excellent alternative for the production of fuel ethanol from lignocellulosic residues.

## Acknowledgments

The authors acknowledge The Brazilian Oil Company (PETROBRAS) and the Brazilian Council for Research and Postgraduate Studies (CNPq) for financial support. They are also in debt with the Consulting Enterprise of Brazilian Distilleries-FERMENTEC, which dealt with the transportation of sugarcane bagasse from São Paulo State to the Laboratory of Bioprocess Development at the Federal University of Rio de Janeiro.

## References

1. Mais, U., Esteghlalian, A. R., Saddler, J. N., and Mansfield, S. D. (2002), *Appl. Microbiol. Biotechnol.* **98–100**, 815–832.
2. São Paulo State Research Foundation (2004), www.fapesp.gov.br/energia1.htm, access: October, 2004.

3. Garrote, G., Dominguez, H., and Parajó, J. C. (2001), *Bioresour. Technol.* **79,** 155–164.
4. Pandey, A., Soccol, C. R., Nigam, P. E., and Soccol, V. T. (2000), *Bioresource Technology* **74(1),** 69–80.
5. D'Almeida, M. L. O. (1988), *Celulose e Papel.* Ed. Escola SENAI. Capítulo III. São Paulo, Brasil.
6. Buchanan, B., Gruissem, W., and Jones, R. L. (2001), Biochemistry and Molecular Biology of Plants, 3rd ed., Courier Companies, Inc, Rockville, MD.
7. Laureano-Perez, L., Farzaneh, T., Alizadeh, H., and Dale, B. E. (2005), *Appl. Biochem. Biotech.* **121–124,** 1081–1099.
8. Van Soest, P. J. (1994), Nutritional Ecology of the Ruminant. Cornell University Press, Ithaca, NY.
9. Pinto, J. H and Kramden, D. P. (1996), *Appl. Biochem. Biotech.* **60,** 289–297.
10. Berlin, A., Gilkes, N., Arwa, K., et al. (2005), *Appl. Biochem. Biotech.* **121–124,** 163–170.
11. Sewat, V. J. H., Beauchemin, K. A., Rode, L. M., Acharya, S., and Baron, V. S. (1997), *Bioresour. Technol.* **61,** 199–206.
12. Leite, J. L., Pires, A. T. N., Ulson de Souza, S. M. A. G., and Ulson de Souza, A. A. (2004), *Braz. J. Chem. Eng.* **21(2),** 253–260.
13. Sen, R. and Swaminathan, T. (1997), *Appl. Microbiol. Biotechnol.* **47,** 358–363.
14. Lynd, L. R., Weimer, P. J., Van Zyl, W. H., and Pretorius, I. S. (2002), *Microbiol. Mol. Biol. Rev.* **66(3),** 506–577.
15. Bhat, M. K. and Bhat, S. (1997), *Biotecnol. Adv.* **15(3/4),** 583–620.
16. Fogel, R., Garcia, R., Oliveira, R., Palacio, D., Madeira, L., and Pereira N., Jr. (2005), *Appl. Biochem. Biotechnol.* **121–124,** 741–752.
17. Aguiar, C. L. and Menezes, T. J. B. (2002), *Biotecnologia Ciência e Desenvolvimento* **26,** 52–55.
18. Ghose, T. K. (1987), *Pure Appl. Chem.* **59(2),** 257–268.
19. Montgomery, D. C. (2001), Design and Analysis of Experiments, 5th ed., John Wiley & Sons, West Sussex, UK.
20. Derringer, G. and Suich, R. (1980), *J. Qual. Technol.* **12(4),** 214–219.
21. Calado, V. and Montgomery, D. (2003), Planejamento de Experimentos Usando o Statistica. Editorial E-papers Serviços Editoriales, Rio de Janeiro, Brazil.
22. Du Preez, J. C. and Van Der Walt, J. P. (1983), *Biotechnol. Lett.* **6,** 395–400.
23. Borzani, W., Schmidell, W., Lima, U. G., and Aquarone, E. (2001), *Biotecnología Industrial. Vol. 1.* Editora Edgard Blücher LTDA, São Paolo, Brazil.
24. Faria, L. F. F., Couto, M. A. P. G., Nobrega, R., and Pereira, N., Jr. (2002), *Appl. Biochem. Biotechnol.* **98–100,** 449–458.
25. Vásquez, M. P, Silva, J. N., Souza, M. B., and Pereira, N. (2005), VIII Symposium on Enzymatic hydrolysis of Biomass, Maringá, Brazil.
26. Franco, B. D. F. M. and Landgraf, M. (1996), *Microbiologia dos alimentos.* Ed. Atheneu, 182, São Paolo, Brazil.
27. Martin, C., Galbe, M., Nilvebrant, N., and Jönsson, L. J. (2003), *Appl. Microbiol. Biotechnol.* **98–100,** 699–716.

0273-2289/1559-0291 (Online)/07/136-140/155-160/$30.00

# Filter Paper Degrading Ability of a *Trichoderma* Strain With Multinucleate Conidia

HIDEO TOYAMA,* MAKIKO YANO, TAKESHI HOTTA, AND NOBUO TOYAMA

*Minamikyushu University, Kirishima 5-1-2, Miyazaki 880-0032, Japan, E-mail: wonder@iris.dti.ne.jp*

## Abstract

The multinucleate conidia were produced from the green mature conidia of *Trichoderma reesei* Rut C-30 strain by colchicine treatment. The strain with higher Filter paper degrading ability was selected among those conidia using a double layer selection medium. The selected strain, JS-2 was able to collapse the filter paper within 15 min but the original strain took 25 min to collapse it completely. Moreover, the amount of reducing sugar in the L-type glass tube of the strain, JS-2, was greater than that of the original strain. The Avicel, CMC-Na, and Salicin hydrolyzing activity of the strain, JS-2, increased 2.1 times, 1.2 times, and 3.6 times higher than that of the original strain.

**Index Entries:** Cellulase; cellulose; conidia; nuclei; *Trichoderma*; filter paper.

## Introduction

*Trichoderma reesei* is a cellulolytic fungus commonly used for the production of commercial cellulases *(1)*. Colchicine has been shown to induce polyploidy in plants by inhibiting mitosis *(2,3)*. Colchicine has also been shown to induce polyploidy in fungi and Basidiomycetes *(4,5)*. When fungal conidia are incubated in a liquid medium containing colchicine, the diameter of nuclei in conidia gradually increase and generate polyploid nuclei. Multinucleation occurs when multiple smaller nuclei are generated from a polyploid nucleus in a conidium after long-term colchicine treatment *(6)*. Mycelia derived from such a multinucleated conidia contain a larger number of nuclei compared with that of the original strain. The nuclear diameter of the mycelia of multinucleated conidium does not increase, although the DNA content of the mycelia increases. In this report, we selected a strain with a higher filter paper degrading ability from the multinucleated conidia of *T. reesei*.

*Author to whom all correspondence and reprint requests should be addressed.

*T. reesei* Rut C-30 American Type Culture Collection (ATCC56765) was used as a model strain *(7)*. The strain was incubated on potato dextrose agar (PDA) medium (BBL, Cockeysville, USA) at 28°C and preserved at 4°C. A mycelial block ($2 \times 2$ mm$^2$) was placed on the center of a PDA plate and incubated at 28°C to generate green mature conidia. The conidia were suspended in distilled water and filtered with a glass filter (3G-2 type, Iwaki Glass, Funakoshi, Japan) to remove hyphae. The conidia were collected by centrifugation at 5510*g* and desiccated to prepare dried mature green conidia. Conidia that were stained with Giemsa solution (Merck, Darmstadt, Germany) after treatment with 5 *N* HCl (Wako, Osaka, Japan) for 30 min at 50°C were found to be mononucleate *(8)*. Similar results were obtained when the conidia were stained with 4,6′-diamidino-2-phenylindole (Sigma, St. Louis, MO) solution after HCl treatment.

As the basic medium, Mandels' medium $(NH_4)_2SO_4$ (Wako); 1.4 g, $KH_2PO_4$ (Wako); 2.0 g, urea (Wako); 0.3 g, $CaCl_2$ (Wako); 0.3 g, $MgSO_4 \cdot 7H_2O$ (Wako); 0.3 g, $FeSO_4 \cdot 7H_2O$ (Wako); 0.005 g, $MnSO_4 \cdot H_2O$ (Wako); 0.0016 g, $ZnSO_4 \cdot H_2O$ (Wako); 0.0014 g, $CoCl_2$; (Wako) 0.0020 g, and distilled water: 1000 mL was used (pH 6.0) *(9)*. When dried green mature conidia were added to 25 mL of Mandels' medium containing 0.025 g colchicine, 0.25 g glucose, and 0.125 g peptone (Difco, Detroit, USA) in a 50 mL-Erlenmeyer flask and incubated statically for 3 wk at 28°C, multiple smaller nuclei were produced.

These multinucleated conidia were incubated using a double layer selection medium in order to select the strain that has higher degrading ability of a filter paper. The bottom layer medium contained 100 mL of Mandels' medium containing 1.0 g glucose, 0.5 g peptone, 0.3 mL polyoxyethylene (10), octylphenylther (Triton X-100) (Wako), and 3.0 g agar (Difco) in a deep glass plate (150 mm in diameter and 60 mm in depth) (pH 6.0). The upper layer medium contained 100 mL of Mandels' medium containing 1.0 g Avicel (Funakoshi, Tokyo, Japan), 0.5 g peptone, 0.1 mL Triton X-100, and 3.0 g agar (pH 6.0). The multinucleated conidia were added to the bottom layer and left for 30 min at 4°C to harden the agar. After the agar hardened, the upper layer selection medium was overlaid and left for 30 min at 4°C to allow the agar to harden. The conidia were then incubated at 28°C. After 3 d of incubation, colonies began to appear and the largest colony on the surface was selected as strain JS-2 after 6 d of incubation. When the same experiments were carried out using conidia untreated with colchicine, colonies began to appear on the surface after four days of incubation. The colony of strain JS-2 was incubated on a PDA medium and preserved at 4°C.

Cellulase production was carried out using the original strain and strain JS-2. A mycelial mat ($2 \times 2$ mm$^2$) of each strain was added to 50 mL of Mandels' medium containing 0.5 g Avicel and 0.25 g peptone in a 100-mL Erlenmeyer flask followed by incubation using a rotary shaker (TAITEC BR-12FH, Koshigaya, Japan) for 6 d at 28°C. The agitation speed

Table 1
Collapse Time of a Filter Paper and the Amount of Reducing Sugar in an L-type Glass Tube After Enzymatic Reaction

| Strain | Collapse time (min) | Amount of reducing sugar (mg/mL) |
|---|---|---|
| C30 | 25 | 0.74 |
| JS-2 | 15 | 1.86 |

Filter paper (10 × 10 $mm^2$) was added to the enzyme solution in an L-type glass tube followed by incubation for 30 min at 50°C using a Monod shaker. Collapse time of filter paper was measured using a digital stop-watch. After the reaction, the amount of reducing sugar in an L-type glass tube was measured using 3,5-dinitrosalicylic acid.

was 160 rpm at 0.59*g*. After incubation, the medium was filtered with a glass filter (3G-2 type) to remove hyphae. The filtrate was used as the enzyme solution. The pH of the enzyme solution was adjusted to 5.0 using 1 *N* HCl. Five milliliters of the enzyme solution and a filter paper (10 × 10 $mm^2$) (Whatman, No. 2, Maidstone, UK) were added to an L-type glass tube (120 × 68 mm) and incubated for 30 min at 50°C using a Monod shaker (TAITEC MONOD SHAKER PERSONAL-11, Koshigaya, Japan) at an agitation speed of 75 strokes/min. The time of collapse of the filter paper was then measured using a digital stop-watch (CITIZEN, Tokyo, Japan). The term "collapse," was defined as the condition when the reaction mixture contained only fibers without fragments of a filter paper. After collapse, the reaction mixture was filtered with a filter paper (No. 2, Whatman) and the amount of reducing sugar in the filtrate was measured using 3,5-dinitrosalicylic acid (Wako) *(10)*. After examination, it appeared that strain JS-2 was able to collapse the filter paper within 15 min but the original strain, *T. reesei* Rut C-30, took 25 min to collapse it completely as shown in Table 1. After measurement, the amount of reducing sugar in the L-type glass tube of strain JS-2 was more than that of the original strain.

Next, cellulose hydrolyzing activity of the enzyme solution was measured. As the substrates of enzyme reaction, 1.0 g of Avicel, carboxymethylcellulose CMC-Na (D.S. 0.7–0.8) (Wako), or Salicin (Wako) was added to 100 mL of 0.1 *M* acetate buffer (pH 5.0). Two milliliters of the enzyme solution was added to 4 mL of substrate in a glass tube (185 × 18.5 mm) and incubated by a reciprocal shaker (THOMASTAT T-22S, Tokyo, Japan) for 1 h at 50°C at an agitation speed of 125 strokes/min. The glass tubes containing the Avicel substrate were tilted on the shaker and shaken by hand every 30 min in order to avoid the precipitation of Avicel. The reaction mixture was filtered with filter paper ( Whatman, No. 2) and the amount of reducing sugar measured using 3,5-dinitrosalicylic acid. Activity was defined as the amount of enzyme producing reducing sugar equivalent to 1 μmol of glucose/min. The cellulase production was carried out twice using two flasks per strain.

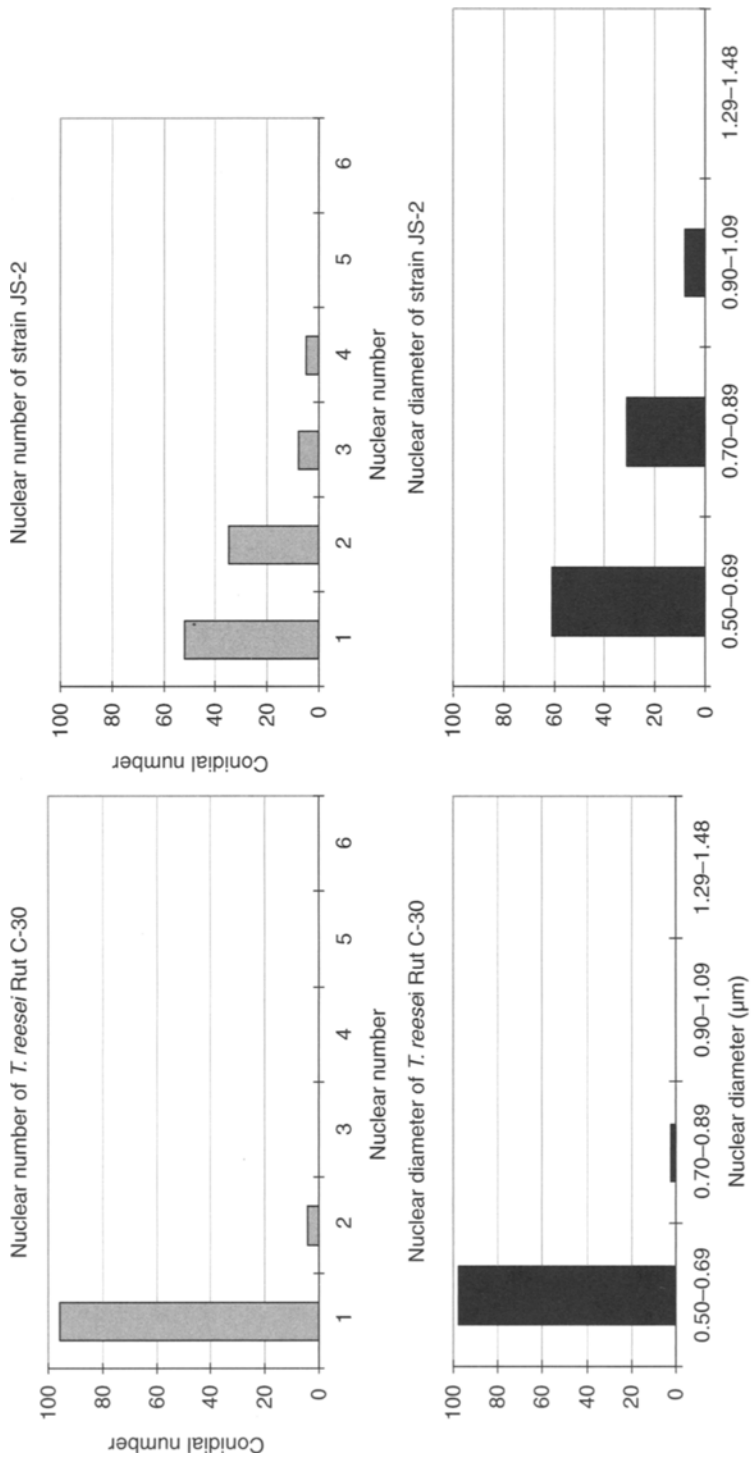


**Fig. 1.** Genetic conditions of the conidia derived from *T. reesei* Rut C-30 and the strain, JS-2.

Table 2
Cellulose Hydrolyzing Activity of the Strain, JS-2 and the Original Strain, *T. reesei* Rut C-30

| | Hydrolyzing activity (IU/mL) | | |
|---|---|---|---|
| Strain | Avicel | CMC-Na | Salicin |
| C30 | 62 | 141 | 10 |
| JS-2 | 130 | 172 | 36 |

Enzyme production was carried out twice using two flasks per strain. Two milliliters of the enzyme solution were added to 4 mL of the substrate in a glass tube incubated by a reciprocal shaker for 1 h at 50°C. The amount of reducing sugar in the reaction mixture was measured using 3,5-dinitrosalicylic acid. The enzyme activity shows average values from two measurements.

Consequently, it was found that the Avicel, CMC-Na, and salicin hydrolyzing activity of strain JS-2 increased by a factor of 2.1, 1.2, and 3.6 over the original strain, respectively, as shown in Table 2.

The diameter and number of the conidia of strain JS-2 were compared with those of *T. reesei* Rut C30 using Giemsa staining after HCl treatment. The nuclear diameter of 100 conidia was measured using a digital caliper (Mitsutoyo, Koshigaya, Japan) on enlarged photomicrographs. The diameter of the original nuclei in an oval conidium ranged from 0.50 to 0.89 μm, whereas the diameter of the nuclei of strain JS-2 ranged from 0.50 to 1.09 μm as shown in Fig. 1.

The nuclear number of the same 100 conidia was counted on the photograph. From the results, the nuclear number of the conidia of strain JS-2 ranged from 1 to 4 and almost half of the conidia were multinucleate. When the mycelia of strain JS-2 were stained with Giemsa solution, it appeared that a larger number of nuclei existed in the mycelia compared with that of the original strain. Therefore, we propose that the higher degrading ability of a filter paper of strain JS-2 may be related to the multinucleated conidia. However, further investigation is necessary to clear the mechanism, which enhances a filter paper degrading ability in strain JS-2.

## Acknowledgments

We wish to thank Tsukishima Kikai Co., Ltd. and Yakult Pharmaceutical Ind. Co., Ltd. for their useful suggestions.

## References

1. Sun, Y. and Cheng, J. (2002), *Bioresour. Technol.* **83,** 1–11.
2. Griesbach, R. J. (1990), *Hortscience* **25,** 802–803.
3. Sackett, D. L. and Varma, J. K. (1993), *Biochemistry* **32,** 13,560–13,565.
4. Toyama, H. and Toyama, N. (1990), *J. Ferment. Bioeng.* **69,** 51–53.

5. Toyama, H. and Toyama, N. (1995), *Microbios* **84,** 221–230.
6. Toyama, H. and Toyama, N. (1995), *J. Ind. Microbiol.* **15,** 121–124.
7. Montenecoute, B. S. and Eveleigh, D. E. (1979), *Adv. Chem. Ser.* **181,** 289–301.
8. Rosen, D., Edelman, M., Galun, E., and Danon, D. (1974), *J. Gen. Microbiol.* **83,** 31–49.
9. Mandels, M. and Sternberg, D. (1976), *J. Ferment. Technol.* **54,** 267–286.
10. Miller, G. L. (1959), *Anal. Chem.* **31,** 426–428.

0273-2289/1559-0291 (Online)/07/136–140/161–170/$30.00

# Use of Glucose Oxidase in a Membrane Reactor for Gluconic Acid Production

**Luiz Carlos Martins das Neves and Michele Vitolo***

*University of São Paulo, School of Pharmaceutical Sciences, Department of Biochemical and Pharmaceutical Technology, Av. Prof. Lineu Prestes, 580, B.16, 05508-900, São Paulo, SP, Brasil, E-mail: michenzi@usp.br.*

## Abstract

This article aims at the evaluation of the catalytic performance of glucose oxidase (GO) (EC.1.1.3.4) for the glucose/gluconic acid conversion in the ultrafiltration cell type membrane reactor (MB-CSTR). The reactor was coupled with a Millipore ultrafiltration-membrane (cutoff of 100 kDa) and operated for 24 h under agitation of 100 rpm, pH 5.5, and 30°C. The experimental conditions varied were the glucose concentration (2.5, 5.0, 10.0, 20.0, and 40.0 m*M*), the feeding rate (0.5, 1.0, 3.0, and 6.0/h), dissolved oxygen (8.0 and 16.0 mg/L), GO concentration (2.5, 5.0, 10.0, and 20.0 $U_{GO}$/mL), and the glucose oxidase/catalase activity ratio ($U_{GO}/U_{CAT}$) (1 : 0, 1 : 10, 1 : 20, and 1 : 30). A conversion yield of 80% and specific reaction rate of $40 \times 10^{-4}$ mmol/h · $U_{GO}$ were attained when the process was carried out under the following conditions: $D$ = 3.0/h, dissolved oxygen = 16.0 mg/L, [*G*] = 40 m*M*, and ($U_{GO}/U_{CAT}$) = 1 : 20. A simplified model for explaining the inhibition of GO activity by hydrogen peroxide, formed during the glucose/gluconic acid conversion, was presented.

**Index Entries:** Catalase; gluconic acid; glucose oxidase; membrane reactor; glucose; continuous process.

## Introduction

The oxidation of glucose into gluconic acid (GA) is one of great interest, not only owing to the high availability of glucose (attained from sucrose and starch, the main and abundant natural sources) but also to the high market demand for GA—over 10,000 t/yr worldwide *(1)*,—a product largely used in the food (as acidulant and surface bleaching), chemical (as surface cleansing agent), and pharmaceutical (gluconate salts) industries *(2)*. GA is obtained from the oxidation of glucose either through the chemical catalysis (bismuth, palladium, platinum, or gold immobilized into active charcoal used as catalyst) or by microbial conversion *(3,4)*. Fermentation is the main process for GA production in which strains of *Aspergillus niger*, *Gluconobacter suboxydans*, or *Acetobacter methanolicus* are used *(4)*. The preference for the

*Author to whom all correspondence and reprint requests should be addressed.

biotechnological process is mainly owing to the good GA yield attained (>80%), the small amount of byproducts formed, the utilization of commercial-grade glucose, and the generation of environmentally inoffensive residues. Despite these advantages on the microbial process, intrinsic problems to be addressed include subsequent cell separation, as well as the discharge and destination of huge volumes of liquid after GA separation. However, the use of glucose oxidase (GO) as catalyst is another valuable way to perform the G/GA conversion. The enzyme catalysis, which presents all the advantages cited for the fermentation plus the mild operational conditions, the low energy requirement, the high specificity for glucose, the generation of nonpollutant residues, and the possibility of carrying out the conversion in a continuous reactor.

Glucose oxidase (EC.1.1.3.4) is a well-characterized enzyme (molecular mass: 150–190 kDa; has two glycoprotein chains linked by disulfide bonds, with each chain having one ferrous ion and one FAD prosthetic group) and largely used in analytical techniques and industrial processes *(5–7)*. Because of the presence of the $Fe^{2+}$/FAD system in the GO structure, the enzyme is sensitive to the presence of any redox agent, mainly hydrogen peroxide, which is one of the reaction products and a strong redox substance. According to Tomotani et al. *(8)*, $H_2O_2$ is a reversible noncompetitive inhibitor of GO, whose inhibition constant is equal to 1.22 m*M*.

Throughout the article several continuous processes—using packed-bed, fluidized-bed, or membrane reactorfor the G/GA conversion catalyzed by GO are described *(7,8)*. Over the last 10 yr the membrane reactor has received high attention for the production of a variety of products *(8)* mainly because of the possibility of using the catalyst in soluble or insoluble form. Such an option is not easily available for the other types of continuous reactors.

A membrane reactor can be assembled through two distinct designs, i.e., as continuous stirred tank reactor (CSTR) coupled with a semipermeable membrane (MB-CSTR) or as a hollow-fiber reactor (a tank without stirring filled with a sheaf of straight-lined hollow-fibers tubes of semipermeable membrane). The MB-CSTR is shaped by connecting in series the CSTR and the 100 kDa UF-membrane module (MB-$CSTR_{Se}$) or by adapting the UF-membrane to the bottom of the CSTR as in a stirring ultrafiltration cell (MB-$CSTR_{UFC}$). The membrane/catalyst arrangement can or cannot involve an interaction between them. If they are linked, the membrane acts as catalysis and separation surface simultaneously; otherwise, it functions only as a separation surface. When the enzyme is in the soluble form, the MB-$CSTR_{Se}$ requires recycling of the catalyst, whereas the MB-$CSTR_{UFC}$ does not. Moreover, the enzyme used may be immobilized in nonmembranous materials (for instance, ion exchange resin beads) *(9)*, in case which the MB-$CSTR_{UFC}$ is preferred over MB-$CSTR_{Se}$ because no recycling of the reaction medium is required. An additional advantage of the MB-$CSTR_{UFC}$ over MB-$CSTR_{Se}$ is the elimination of the pumping step,

surely leading to the reduction of the overall costs, mainly those related to the energy consumption and maintenance of the pumping system.

According to the literature, the enzymatic oxidation of glucose is preferentially conducted in MB-$CSTR_{Se}$ in which the GO is united to the membrane. Nonetheless, there is little information on MB-$CSTR_{UFC}$ using soluble GO, in spite of presenting operational characteristics of homogeneous catalysis, high activity per unit of volume, and absence of conformational and diffusional effects. If needed, the membrane reactor also allows operation under aseptic conditions as well as with multienzymatic systems *(8)*.

In previous work *(8)*, it was reported that the MB-$CSTR_{UFC}$ was suitable for the G/GA conversion provided that the $H_2O_2$ inhibition was minimized. Moreover, a conversion yield of about 75% was achieved under the following conditions: pH 5.5, 30°C, *D* (feeding rate) = 0.15/ min, agitation of 100 rpm, 2.5 m*M* glucose, 1.0 mg/mL of GO, and dissolved oxygen (DO) of 7.0 mg/L. However, the low substrate concentration and the short residence time used in the process, though adequate for controlling the hydrogen peroxide formation, are inadequate for a future scaling-up.

This work aims at the evaluation of the catalytic performance of GO for the G/GA conversion in the MB-$CSTR_{UFC}$. The experimental conditions that varied were the glucose concentration (2.5, 5.0, 10.0, 20.0, and 40 m*M*), the feeding rate (0.5, 1.0, 3.0, and 6.0/h), DO (8.0 and 16.0 mg/L), and the GO/catalase activity ratio ($U_{GO}/U_{CAT}$) (1 : 0, 1 : 10, 1 : 20, and 1 : 30).

## Materials and Methods

### *Chemicals*

GO from *A. niger* and bovine catalase were purchased from Sigma (St. Louis, MO). One gram of GO corresponds to 5100 units. One unit ($U_{GO}$) will oxidize 1 μmol of β-D-glucose to GA and $H_2O_2$ per min at 35°C and pH 5.1. One milligram of catalase corresponds to 2350 units. One unit ($U_{CAT}$) will decompose 1 μmol of $H_2O_2$ per min at 25°C and pH 7.0, while the $H_2O_2$ concentration falls from 10.3 to 9.2 m*M*. The 100-kDa UF-membrane (PLHK07610, made of regenerated cellulose) was purchased from Millipore (Bedford, MA). All other chemicals were of analytical grade.

### *Membrane Reactor*

A 10-mL MB-$CSTR_{UFC}$ (Bioengineering AG, Wald, Germany) was used in all tests. The reactor is a 316-L stainless steel cylinder, whose bottom has an inlet and an outlet for the external water bath for temperature control. The diameter of the UF-membrane used was 63 mm. The reactor can be sterilized (autoclave up to 134°C for 30 min) and resists high temperatures (up to 150°C) and corrosion by most substances (except strong acids, pH < 1.0; and alkalis, pH > 12.0). Moreover, it has a safety valve (set to nominal six bar pressure limit) and can be coupled to a dosing pump, pressure probe, sterile filter, and bubble trap.

### Membrane Reactor Tests

Ten milliliters of buffered GO solution (2.5, 5.0, 10.0, or 20.0 $U_{GO}$/mL in 0.01*M* acetic acid/acetate buffer, pH 5.5) was poured inside the MB-$CSTR_{UFC}$, which had a UF-membrane (PLHK07610) with a molecular mass cutoff of 100 kDa. The reactor was fed continuously with 2.5, 5.0, 10.0, 20.0, or 40.0 m*M* glucose buffered solution (0.01 *M* acetic acid/acetate buffer, pH 5.5) at a feeding rate of 0.5, 1.0, 2.0, 3.0, or 6.0/h. The reaction was carried out for 24 h at 30°C and an agitation of 100 rpm. Pure oxygen was bubbled into the glucose solution, so that the DO concentration in the inlet solution remained around 8.0 mg/L or 16.0 mg/L. Aliquots taken from the outlet solution were measured for the concentration of glucose and $H_2O_2$. The yield (*Y*) and the specific reaction rate (*r*) were calculated through the Eqs. 1 and 2, respectively. The conditions used in all tests realized were presented in Table 1. Each test was carried out in duplicate. When a difference over 5% on *Y* and *r* was observed, then the test was repeated two or more times.

$$Y\ (\%) = \frac{G_{cons}}{G_0} \times 100 \tag{1}$$

$$r\ (\text{mmol/h} \times U_{GO}) = \frac{Q \times G_{cons}}{1000 \times U_{GO}} \tag{2}$$

where $[G]_0$ is the inlet glucose concentration, $[G]_{cons}$ is the $[G]_0 - [G]_{inlet}$, Q is the volumetric rate (mL/h), and $U_{GO}$ is the GO units used. As the stoichiometry of G/GA conversion catalyzed by GO is 1 mol of glucose generating 1 mol of GA and 1 mol of $H_2O_2$ *(7)*, then the $[G]_{cons}$ is equal to the concentration of hydrogen peroxide formed.

### Analytical Techniques

#### Determination of Glucose

The concentration of glucose was measured by using an enzymatic peroxidase/GO kit (Laborlab, São Paulo, SP, Brazil). The procedure was accomplished by mixing 10 μL of the sample with 1.0 mL of peroxidase/GO solution, and incubated at 37°C for 10 min. After that, the absorbance was read in a spectrometer (Beckman DU 640; Beckman Coulter, Fullerton, CA) at λ = 500 nm. The standard curve was attained using glucose solutions whose concentration range was between 0.04 and 0.20 mg/mL. The regression curve established was

$$ABS_{500nm} = 0.168 \times [G] + 0.152\ (r = 0.9990) \tag{3}$$

where [*G*] is the glucose concentration (mg/mL).

The standard deviation and coefficient of variation related to this method were 0.010 mg/mL and 4.5%, respectively.

Table 1
Conditions Under Which all Continuous Experiments Were Conducted and Respective Average Conversion ($Y$) and Specific Reaction Rate ($r$) Attained[a,b]

| Test ($n$) | [G] (m$M$) | [$GO$] ($U_{GO}$/mL) | [$CAT$] ($U_{CAT}$/mL) | $D$ ($h^{-1}$) | DO (mg/L) | $R$ (mmol/ $h \cdot U_{GO}$) $\times 10^4$ | $Y$ (%) |
|---|---|---|---|---|---|---|---|
| 1 | 2.5 | 10 | – | 1.0 | 8.0 | 1.9 | 48 |
| 2 | 2.5 | 10 | – | 3.0 | 8.0 | 2.7 | 29 |
| 3 | 2.5 | 10 | – | 6.0 | 8.0 | 1.9 | 43 |
| 4 | 2.5 | 10 | – | 1.0 | 16.0 | 2.3 | 94 |
| 5 | 2.5 | 10 | – | 3.0 | 16.0 | 3.7 | 50 |
| 6 | 2.5 | 10 | – | 6.0 | 16.0 | 3.1 | 19 |
| 7 | 5.0 | 2.5 | – | 3.0 | 16.0 | 24 | 41 |
| 8 | 5.0 | 5 | – | 3.0 | 16.0 | 11 | 37 |
| 9 | 5.0 | 10 | – | 3.0 | 16.0 | 7.1 | 48 |
| 10 | 5.0 | 20 | – | 3.0 | 16.0 | 5.1 | 70 |
| 11 | 5.0 | 2.5 | – | 1.0 | 16.0 | 9.1 | 45 |
| 12 | 5.0 | 5 | – | 1.0 | 16.0 | 4.7 | 48 |
| 13 | 5.0 | 5 | – | 2.0 | 16.0 | 9.5 | 48 |
| 14 | 5.0 | 10 | – | 0.5 | 16.0 | 3.4 | 83 |
| 15 | 5.0 | 10 | – | 1.0 | 16.0 | 1.9 | 39 |
| 16 | 5.0 | 20 | – | 1.0 | 16.0 | 2.9 | 88 |
| 17 | 5.0 | 10 | 100 | 3.0 | 16.0 | 13 | 88 |
| 18 | 5.0 | 10 | 200 | 3.0 | 16.0 | 13 | 88 |
| 19 | 5.0 | 10 | 300 | 3.0 | 16.0 | 13 | 88 |
| 20 | 10 | 10 | 200 | 3.0 | 16.0 | 25 | 85 |
| 21 | 20 | 10 | 200 | 3.0 | 16.0 | 40 | 80 |
| 22 | 40 | 10 | 200 | 3.0 | 16.0 | 41 | 35 |

[a]In all tests the pH, temperature, and agitation were maintained at 5.5, 30°C, and 100 rpm, respectively.
[b]The yield ($Y$) and the specific reaction rate ($r$) values presented are an average of all the time points.

## Determination of Hydrogen Peroxide

$H_2O_2$ concentration was determined through the ultraviolet absorption method ($\lambda = 240$ nm) as described by Bergmeyer *(10)*. A standard curve was established by measuring the absorbance of $H_2O_2$ solution, whose concentration ranged from 0.18 to 18 m$M$. A pharmaceutical grade $H_2O_2$ was used. The regression curve established was

$$ABS_{240nm} = 4.12 \times 10^{-2} [H_2O_2] - 6.97 \times 10^{-4} \quad (r = 0.9995) \qquad (4)$$

where $[H_2O_2]$ is the $H_2O_2$ concentration (m$M$).The standard deviation and coefficient of variation related to this method were 0.86 m$M$ and 0.33%, respectively.

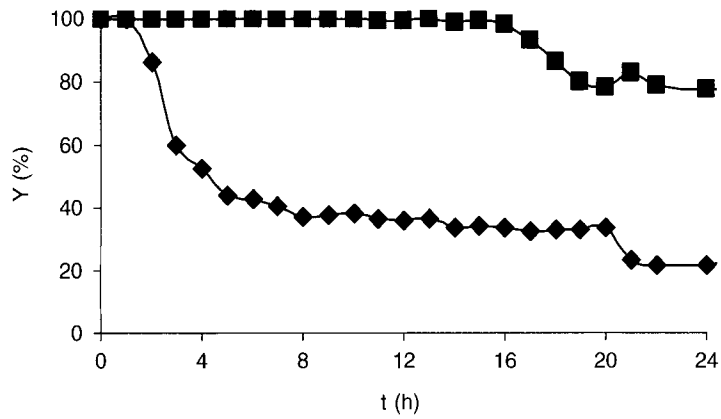


**Fig. 1.** Variation in conversion during continuous glucose oxidation catalyzed by GO for test 1 (◆) and test 4 (■).

### Determination of DO

DO was measured using an oximeter (Digimed, model DM40, São Paulo, Brazil). In all experiments the aqueous glucose solution was bubbled with pure oxygen for attaining the desired concentration 8.0 or 16.0 mg/L.

## Results and Discussion

Taking into account tests 1–6 in which only DO and $D$ were varied, we observed that tests 1 ($D$ = 1.0/h and DO = 8.0 mg/L) and 4 ($D$ = 1.0/h and DO = 16.0 mg/L) presented the highest G/GA conversion yields, respectively, 48% and 94% (Table 1). The G/GA conversion yield of 94% achieved in test 4 was far better than that found by Tomotani et al. *(8)* pointing the importance of the amount of DO in the reaction medium for the GO catalysis. According to Bright *(11)* the G/GA conversion by GO is a two steps process (First: GO-$FAD_{ox}$ + G → GO-$FAD_{red}$ + glucone-δ-lactone; Second: GO-$FAD_{red}$ + $O_2$ → $H_2O_2$ + GO-$FAD_{ox}$) in which the first one is the limiting step. Thereby, under unsaturated $O_2$ concentration the glucose might inhibit the GO.

Figure 1 shows that a steady state of 16 h occurred in tests 4 (average $Y$ near 100% from $t$ = 0 h to $t$ = 16 h) and 1 (average $Y$ near 40% from $t$ = 4 h to $t$ = 20 h). Moreover, the G/GA conversion yield diminished in tests 4 ($Y$ varied from 100 to 80%) and 1 ($Y$ varied from 40 to 25%), respectively, at intervals of 16–24 h and 20–24 h of continuous processing. The perturbation of the stationary phase after several residence times might be owing to the accumulation in the reaction medium of GO molecules containing the iron atom in the $Fe^{+3}$ form instead of $Fe^{+2}$ (the most adequate form for full GO catalysis). In some extension, the redox state of the iron atom contributes to the loss in enzyme stability. According to Tomotani et al. *(8)*, a fraction of GO-$Fe^{+3}$ molecules could arise owing to the accumulation of hydrogen

peroxide in the reaction medium, because the potential of reduction of the pair $H_2O_2/H_2O$ (+1.77V) is higher than the pair $Fe^{+3}/Fe^{+2}$ (+0.771V).

The G/GA conversion yield and the specific reaction rate varied according to the feeding rate or the residence time (inversely correlated with *D*) used. The highest *Y* (94%) and *r* ($3.7 \times 10^{-4}$ mmol/h $\cdot U_{GO}$) occurred at $D = 1.0$/h (test 4) and $D = 3.0$/h (test 5), respectively (Table 1). Thereby, the period under which all reacting species (GO, G, $O_2$, and $H_2O_2$) are left in contact inside the reactor might be adequately set, in order to balance the two steps reaction for the G/GA conversion, as referred earlier.

Undoubtedly, the G/GA conversion yield attained here was significantly improved as compared with that described by Tomotani et al. *(8)*. However, when a scale-up of this process is envisaged, other aspects such as GO and glucose concentration and decomposition of the hydrogen peroxide accumulated in the reaction medium must be evaluated.

The concentration of glucose solution fed in tests 7–10 was set at 5 m*M* and the GO concentration varied from 2.5 to 20 $U_{GO}$/mL (Table 1). As the GO concentration was increased, the specific reaction rate (*r*) decreased from $24 \times 10^{-4}$ mmol/h $\cdot U_{GO}$ (test 7) to $5.1 \times 10^{-4}$ mmol/h $\cdot U_{GO}$ (test 10), whereas the conversion yield increased from 41% (test 7) to 70% (test 10). By varying the feeding rate at fixed amounts of glucose and GO, as in the tests 11–16 (Table 1), we conclude that *D* is not an important parameter for achieving high *Y* and *r* simultaneously. Probably, the presence of hydrogen peroxide in the reaction medium has a role on the final values achieved for *Y* and *r* because it interferes with the overall GO redox state, as mentioned previously. Such influence is easily understood if the $H_2O_2$ strong redox capability is considered. To circumvent the undesirable effect of hydrogen peroxide on the G/GA conversion, the addition of catalase (EC.1.11.1.6) in the reaction medium was evaluated (tests 17–19).

The use of catalase clearly affected the conversion yield and the specific reaction rate as can be seen through the comparison of tests 9 and 17–19 (Table 1). The specific reaction rate (*r*) and the yield (*Y*) increased simultaneously about 46% regarding the test carried out without catalase (test 9). At glucose concentration of 5 m*M* the ratio GO/catalase ($U_{GO}/U_{CAT}$) (test 17: [1 : 10]; test 18: [1 : 20]; and test 19: [1 : 30]) did not affect the reaction rate and the yield (Table 1). In presence of catalase the hydrogen peroxide concentration in the medium diminishes markedly (Fig. 2) leading to the more predictable situation in which *Y* and *r* increase or decrease at the same time. Moreover, the steady-state condition is maintained along the whole process (Fig. 2), differently from what occurred in test 4, whose steady-state condition remained till $t = 16$ h of continuous process (Fig. 1). This result corroborates, albeit indirectly, the kinetic model for the action of GO in presence of $H_2O_2$ proposed by Bao et al. *(12)*, which assumes a competitive inhibition pattern by $H_2O_2$ with respect to the $O_2$ for the GO reduced form ($GO\text{-}FAD_{red}$). Another possibility would be the action of the hydrogen peroxide on the redox state of the iron atom instead

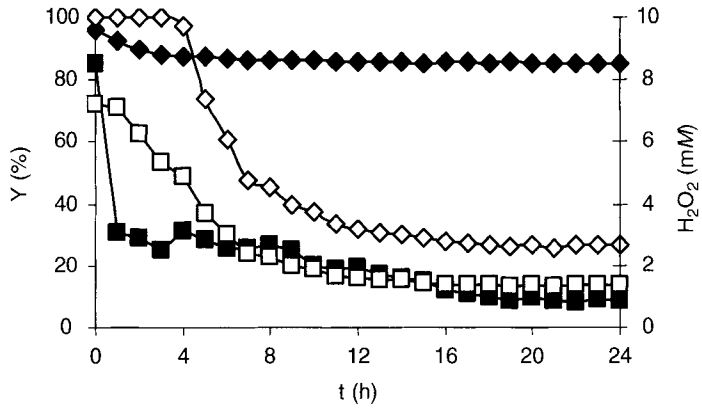


**Fig. 2.** Variation in conversion during continuous glucose oxidation catalyzed by GO for test 9 (◇) and test 17 (◆). Variation of the concentration of hydrogen peroxide in the effluent during the process for test 9 (□) and test 17 (■).

of on the FAD redox state *(8)*. Introducing these assumptions in the Bright's model *(10)*, it becomes a four steps process, i.e.,

First: $\text{GO-FAD}_{ox} + G \rightarrow \text{GO-FAD}_{red} + \text{glucone-}\delta\text{-lactone}$

Second: $\text{GO-FAD}_{red} + O_2 \rightarrow H_2O_2 + \text{GO-FAD}_{ox}$

Third: $\text{GO-FAD}_{red} + H_2O_2 \rightarrow \text{GO-FAD}_{red} + H_2O_2$

Fourth: $\text{GO-Fe}^{+2} + H_2O_2 \rightarrow H_2O + \frac{1}{2} O_2 + \text{GO-Fe}^{+3}$

Therefore, the addition of catalase promotes the $H_2O_2$ decomposition—as consequence, the third and fourth steps are eliminated—leaving the $\text{GO-FAD}_{red}$ available to be oxidized by the oxygen, and the GO turnover is completed.

As the role of catalase in circumventing the inhibition caused by $H_2O_2$ on the GO activity was remarkable, and knowing that the $H_2O_2$ generation is stoichiometrically related to glucose oxidation, the study of G/GA conversion using more concentrated glucose solutions was explored. Tests 20–22 were carried out with glucose solutions of 10, 20, and 40 m*M*, and the results presented in Fig. 3 and Table 1.

Test 21, carried out with 20 m*M* glucose solution, presented the highest $r$ ($40 \times 10^{-4}$ mmol/h · $U_{GO}$) and $Y$ (80%), whereas test 22, carried out with 40 m*M* glucose solution, presented a high $r$ ($41 \times 10^{-4}$ mmol/h · $U_{GO}$) but low $Y$ (35%) (Table 1). On one hand, the similar specific reaction rates observed indicate that catalase at concentration of 200 $U_{CAT}$/mL was enough for maintaining the hydrogen peroxide concentration at noninhibitory level (Fig. 3). On the other hand, the GO at concentration of 10 $U_{GO}$/mL was insufficient to cope with 40 m*M* glucose solution, as shown by the sharp reduction of the G/GA conversion yield (test 22). Therefore, for each glucose concentration over 20 m*M* an adequate $U_{GO}/U_{CAT}$ ratio might be adjusted.

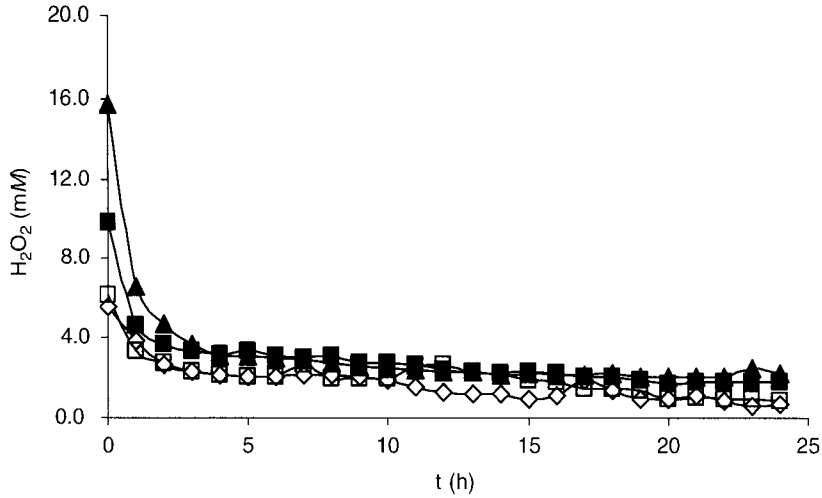


**Fig. 3.** Variation of the concentration of hydrogen peroxide in the effluent during the continuous process for tests (◇) 18, (□) 20, (▲) 21, and (■) 22.

In the present work, tests with still more concentrated glucose solutions were not made because the high bubbling caused by the oxygen generated from $H_2O_2$ decomposition augmented the 10 mL-MB-$CSTR_{UFC}$ internal pressure nearing the up limit of six bar. Going over that pressure would be quite dangerous. Certainly, this handicap might not occur or might be minimized at least, if a large UF-membrane reactor was used. Moreover, such "*in situ*" oxygen generation would allow the elimination of the previous saturation of the substrate solution, which should simplify the overall process.

Finally, comparing the results obtained here with those found by Tomotani et al. *(8)* the boundary for the glucose concentration, which could be used in the G/GA conversion, was enlarged eightfold, i.e., up to 20 m*M*.

## Conclusions

The data presented led us to conclude that the reaction medium must be saturated with oxygen (16.0 mg/L), in order to avoid the GO inhibition by glucose (its natural substrate). However, the hydrogen peroxide—a byproduct resulting from the G/GA conversion—can hinder the GO catalysis either through binding to the $GO\text{-}FAD_{red}$ (an intermediate form of the enzyme) or by oxidizing the $Fe^{+2}$ to $Fe^{+3}$ (another cofactor present in the GO molecule). Such effects are circumvented by maintaining the hydrogen peroxide concentration below 2 m*M* along the whole process, which is achieved by adding catalase into the reactor. The ratio GO/catalase must be adjusted for each glucose concentration over 2.5 m*M*. Finally, the advance of this research might be based on the best conditions for the G/GA conversion established here, i.e., [*G*] = 20 m*M*, [*GO*]/[*CAT*] = 1 : 20, *D* = 3.0/h, 30°C, DO = 16.0 mg/L, and pH 5.5.

## Acknowledgment

This work was supported by research grants from Fundação de Amparo à Pesquisa do Estado de São Paulo (FAPESP).

## References

1. Silveira, M. M. and Jonas, R. (2002), *Appl. Microbiol. Biotechnol.* **59,** 400–408.
2. Jonas, R. and Silveira, M. M. (2004), *Appl. Biochem. Biotechnol.* **118,** 321–336.
3. Bao, J., Furumoto, K., Fukunaga, K., and Nakao, K. (2001), *Biochem. Eng.* **8,** 91–102.
4. Biella, S., Prati, L., and Rossi, M. (2002), *J. Catal.* **206,** 242–247.
5. Beltrame, P., Comotti, M., Della Pina, C., and Rossi, M. (2004), *J. Catal.* **228,** 282–287.
6. Raba, J. and Mottola, H. A. (1995), *Critical Rev. Anal. Chem.* **25(1),** 1–42.
7. Godfrey, T. and West, S. (1996), *Industrial Enzymology.* 2nd ed., MacMillan, London, UK: pp. 64–65.
8. Tomotani, E. J., Das Neves, L. C. M., and Vitolo, M. (2005), *Appl. Biochem. Biotechnol.* **121,** 149–162.
9. Tomotani, E. J. and Vitolo, M. (2006), *Process Biochem.* **41,** 1325–1331.
10. Bergmeyer, H. U. (1984), *Methods of Enzymatic Analysis.* 3rd ed., Verlag Chemie, Weinheim, Germany: pp. 154–160.
11. Bright, H. (1967), *J. Biol. Chem.* **242(5),** 994–1003.
12. Bao, J., Furumoto, K., Yoshimoto, M., Fukunaga, K., and Nakao, K. (2003), *Biochem. Eng. J.* **13,** 69–72.

0273-2289/1559-0291 (Online)/07/136–140/171–184/$30.00

# Enzyme Production by Industrially Relevant Fungi Cultured on Coproduct From Corn Dry Grind Ethanol Plants

EDUARDO A. XIMENES,*,[1] BRUCE S. DIEN,[2] MICHAEL R. LADISCH,[3] NATHAN MOSIER,[3] MICHAEL A. COTTA,[2] AND XIN-LIANG LI[2]

*[1]University of Georgia, Microbiology Department, 204 Biological Sciences, Athens, GA, USA, 30602-2605, E-mail: eximenes@uga.edu; [2]Fermentation Biotechnology Research Unit, National Center for Agricultural Utilization Research, USDA, †ARS, 1815 N. University Street, Peoria, IL 61604; and [3]Purdue University, LORRE, 500 Central Drive, West Lafayette, IN 47907-2022*

## Abstract

Distillers dried grain with solubles (DDGS) is the major coproduct produced at a dry grind ethanol facility. Currently, it is sold primarily as a ruminant animal feed. DDGS is low cost and relatively high in protein and fiber contents. In this study, DDGS was investigated as carbon source for extracellular hydrolytic enzyme production. Two filamentous fungi, noted for their high cellulolytic and hemicellulolytic enzyme titers, were grown on DDGS: *Trichoderma reesei* Rut C-30 and *Aspergillus niger* NRRL 2001. DDGS was either used as delivered from the plant (untreated) or after being pretreated with hot water. Both microorganisms secreted a broad range of enzymes when grown on DDGS. Higher xylanase titers were obtained when cultured on hot water DDGS compared with growth on untreated DDGS. Maximum xylanase titers were produced in 4 d for *A. niger* and 8 d for *T. reesei* in shake flask cultures. Larger amounts of enzymes were produced in bioreactors (5 L) either equipped with Rushton (for *T. reesei*) or updraft marine impellers (*A. niger*). Initial production titers were lower for bioreactor than for flask cultures, especially for *T. reesei* cultures. Improvement of enzyme titers were obtained using fed-batch feeding schemes.

**Index Entries:** *Aspergillus niger*; biomass; DDGS; cellulases; hemicellulases; *Trichoderma reesei*.

*Author to whom all correspondence and reprint requests should be addressed.

†Mention of trade names or commercial products in this article is solely for the purpose of providing specific information and does not imply recommendation or endorsement by the US Department of Agriculture.

## Introduction

The United States corn ethanol market is rapidly growing; production is 4.26 billion gal/yr (National Renewable Fuel Association, 2005) and is mandated to reach 7.5 billion gal/yr by 2012. The soluble and solid residuals from the ethanol fermentation are combined and marketed as an animal feed ingredient under the name of distillers dried grain with solubles (DDGS). Approximately 17 pounds of DDGS is produced per bushel of corn. Expanding ethanol production has raised concerns about finding a sufficiently sized market for DDGS. DDGS is currently priced at only $65/t and the selling price has been declining for the last several years. Therefore, there is a need to develop further markets for DDGS to preserve its future value.

One possible use for DDGS is for the production of industrial enzymes. DDGS is rich in protein (31%), fat (11%), and fiber/carbohydrates (44%) *(1)*. DDGS's low-cost and relatively high protein and carbohydrate contents make it a promising feedstock for industrial fermentations. In particular, the complex carbohydrate profile of DDGS—it includes starch, cellulose, and a complex xylan—should be particularly well suited for production of carbohydrolytic enzymes, such as hemicellulases and cellulases. Cellulases and hemicellulases have multiple industrial uses including biodegradation of lignocellulosic material in biomass conversion, animal feed, foods, textiles, and biopulping in the paper and pulp industry *(2,3)*. The major obstacles for further industrial application of these enzymes are their cost of production and low fermentation yields. In an attempt to overcome these problems, the production of such enzymes by microbial strains in the presence of inexpensive substrates has been investigated *(4)*.

The most commonly used microorganisms for production of acidic hydrolytic enzymes are filamentous fungi. *Trichoderma reesei* is the most widely studied cellulolytic microorganism and is commonly used for production of both cellulases and xylanases. The most important species of the *Aspergillus* genus for the production and utilization of enzymes are *A. oryzae* and members of the group of black aspergilli. Black aspergilli are favored for production of industrial enzymes because they secrete high levels of proteins, are easily cultured in submerged fermentations, and several species are generally regarded as safe for food and feed applications *(5)*, including *A. niger (6)*. In this article, DDGS was used as a substrate for producing hemicellulases by both *T. reesei* and *A. niger*. DDGS has complex carbohydrate structures. To make the DDGS more digestible to the fungi, the DDGS was pretreated with liquid hot water (LHW) (160°C, 20 min) before being added to the culture. LHW is a promising pretreatment that has been shown to be very effective in preparing corn stover *(7)* and corn fiber *(8)* for subsequent cellulose digestion and ethanol fermentation. The method is currently the subject of an industrial scale-up effort at a 100 million gal ethanol/yr corn wet mill facility (Aventine Renewable Energy, Pekin, IL). However, treating with LHW does not saccharify the

xylan sugars, thereby, readying them for fermentation. Instead, this method relies on using hemicellulases for saccharification. So, as a first application for the hemicellulases described in this article, they were applied to LHW–xylan for production of sugars.

## Materials and Methods

### *Materials, Microbial Strains, and Medium*

Microbial strains were obtained from the Agricultural Research Service (ARS) Culture Collection (NCAUR, Peoria, IL). DDGS was generously gifted by Big River Resources (West Burlington, IA). *T. reesei* Rut C-30 and *A. niger* NRRL 2001 were routinely propagated in potato dextrose broth (PD) (0.4% potato and 2.0% dextrose) supplemented with 2% agar for solid medium. All chemicals and medium ingredients were of research quality and were purchased from either Fisher Scientific (Pittsburgh, PA) or Sigma Chemicals (St. Louis, MO).

### *LHW Pretreatment of DDGS*

For flask experiments, 2.0 g of DDGS (10% moisture) was combined with 8 mL water in a stainless steel tube reactor and treated at 160°C for 20 min using a fluidized heating bath. The tube reactors and heating bath arrangement have been previously described *(7)*. The pretreated DDGS, along with 20 mL of distilled wash water used to remove residual solids, was transferred to a presterilized 250-mL baffled Erlenmeyer flask. For destarched DDGS, following the heat treatment, the solids were recovered on glass fiber filter (GF/A, Whatman, England) and washed with distilled water to further remove solids. The solids were transferred to a tared 250-mL Erlenmeyer flask and distilled water was added until the solids and liquid had a weight of 30.0 g. The material was next autoclaved for 15 min. Pretreated DDGS for use in fed-batch experiments was prepared in multiple batches as follows: 45.0 g of DDGS was added to 105 mL of water and treated in the same conditions as described previously. The resulting material was transferred to flasks after three washes with 50 mL water (final volume = 300 mL).

### T. reesei *and* A. niger *Flask Cultures*

Two inoculation loops of *T. reesei* or *A. niger* were transferred to shake flasks (250 mL) containing 50 mL PD medium. Flasks were shaken at 250 rpm at 28°C for 48 h. For both microorganisms, a 5% (v/v) inoculum was transferred to 50 mL of production medium in a 250-mL Erlenmeyer flask. The production media for *T. reesei* and *A. niger* contained per liter 15.0 g $KH_2PO_4$, 20.0 g corn steep liquor (Sigma Chemicals), 0.5 g $NH_4SO_4$, 0.5 g $Mg(SO_4)_2{\cdot}7H_2O$, 1.0 mL Tween 80, and 30 mL solution of untreated or HW-treated DDGS containing a total of 2.0 g DDGS. The basal medium was

adjusted to pH 4.8 and autoclaved separately from the HW treated DDGS. Both microorganisms were grown at 28°C with agitation (250 rpm) for 8 d. Flasks were sampled daily (2 mL). Alternatively, HW-treated DDGS was washed to remove starch before being used for fermentation.

### T. reesei *and* A. niger *Bioreactor Cultures*

Two inoculation loops of *T. reesei* or *A. niger* were transferred to Erlenmeyer flasks (250 mL) containing 50 mL PD medium. Flasks were shaken at 250 rpm at 28°C for 48 h. For both microorganisms, a 5% (v/v) inoculum was transferred to 450 mL of PD medium in a 2800-mL flask and grown under identical conditions as previously described. These cultures were then used to inoculate the bioreactor at 5% (v/v).

Bioreactor runs were conducted in electronically controlled 5-L laboratory bioreactors (BIOSTAT B, B. Braun Biotech International, Melsungen, Germany). The production medium was supplemented with HW-DDGS (at the same concentration used for flask fermentations) and 1 mL of antifoam (PPG2000 from Bayer, Pittsburgh, PA). The oxygen level was set at 20% of saturation and controlled by varying stirring (300–900 rpm). The pH was set at 4.8 and controlled by automatic additions of either 3 *M* $H_3PO_4$ or 4 *M* $NH_4OH$. Samples (approx 10 mL) were taken daily, centrifuged, and the recovered liquid stored at –20°C. At the end of the fermentation, the broth was harvested, centrifuged to remove cell mass, and the recovered liquid (containing the excreted enzymes) was stored at –20°C. Fed-batch fermentations were run in a similar manner to batch fermentations, except they were manually fed at days 3, 6, and 9 by adding 300 mL of a 15% (w/v) DDGS solution.

### *LHW-Treated DDGS Digestion Assays*

A stock supply of LHW pretreated DDGS was prepared as follows for the digestion assay. Pipe reactors were each filled with 1.5 g DDGS (90% wt dry) and 8.5 mL $H_2O$. Using a fluidized heating bath, the reactors were heated to 160°C and kept at that temperature for 20 min. The pipes were quickly cooled by quenching in water. The contents of eight reactors were transferred to a single flask along with 10 mL of 1 *M* sodium citrate buffer (pH 4.5, final concentration of 50 m*M*) and 1 mL of thymol stock solution (50.0 g/L in 70% [v/v] ethanol). Enough water was added for a final volume of 200 mL and a stir bar added to the flask. For individual enzyme assays, DDGS solution was mixed on a stirring plate and 4-mL aliquots transferred to scintillation vials. Following that, appropriate enzyme mixtures were added to the vials. The vials were mixed using a mini tube roller (Belco Glass, Inc., Vineland, NJ) placed in a constant temperature incubator (Innova 4230, News Brunswick, NJ) set to 50°C. The reactions were allowed to proceed for 72 h. Digestion reactions were clarified by centrifugation and the supernatant analyzed for total soluble and monomeric carbohydrates as described in the following sections.

### *Enzyme Assays*

Enzyme activities in the presence of 1% oat-spelt xylan and carboxymethylcellulose (CMC, low viscosity, Sigma Chemicals), and 2.5 m*M* *p*-nitrophenyl (*p*-NP) conjugated substrates were determined at 50°C in the presence of 50 m*M* sodium acetate buffer, pH 4.8 using published methods. Filter paper activity was assayed as described by Mandels et al. *(9)*. The release of reducing sugars was determined in according to Miller *(10)*. One unit of cellulase (for CMC as substrate) and xylanase activities was defined as the release of one µmol of either glucose or xylose per min. For *p*-NP conjugated substrates, one unit of activity was defined as one µmol of *p*-NP released per min.

Feruloyl esterase activity was assayed measuring the conversion of methyl-ferulate (prepared as 100 m*M* in 50% DMSO [v/v] and added to a final concentration of 2 m*M*) to ferulate. Ferulic acid and methyl ferulate were measured by reverse phase SpectraSYSTEM liquid chromatography system (Thermo Finnigan, San Jose, CA) using an Inertsil C18 xolumn (5 µm, ODS3, PN 0396-250X046, Varian, Torrance, CA) combined with a UV2000 ultraviolet detector (310 nm; Thermo Finnigan). Samples were run at room temperature and eluted at 0.8 mL/min with a linear gradient from 5 to 50% acidified methanol (containing 0.25% acetic acid) run over 15 min. One unit of feruloyl esterase activity was defined as the release of one µmol of ferulic acid per min.

### *Analysis of Soluble Carbohydrates*

Total soluble carbohydrates were analyzed by HPLC after being hydrolyzed by treating with 2 *N* trifluoroacetic acid (TFA) for an hour at 100°C, as previously described *(2)*. Samples were analyzed for sugars and acids using a SpectraSYSTEM liquid chromatography system with an organic acids column (Aminex HPX-87H Column, 300 × 7.8 $mm^2$, Bio-Rad Laboratories, Inc, Hercules, CA) and a refractive index detector (RI-150, Thermo Finnigan).

## Results and Discussion

### *Fermentation Results Using Untreated and LHW-Treated DDGS*

*T. reesei* and *A. niger* were grown on either untreated or hot water treated (20 min, 160°C) DDGS and the cultures sampled for production of enzymes. The goal of this experiment was to determine if LHW-treated or -untreated DDGS would be a more suitable carbon source for producing enzymes. The plotted data demonstrate that hot water treated DDGS gave higher final xylanase titers for both *A. niger* and *T. reesei* cultures (Fig. 1A,B). The xylanase enzyme profile for *T. reesei* also showed a long lag phase (5 d) for xylanase production. One possible explanation for the delay in xylanase production is that residual starch present in the DDGS is repressing its production. To test this hypothesis, hot water treated DDGS was

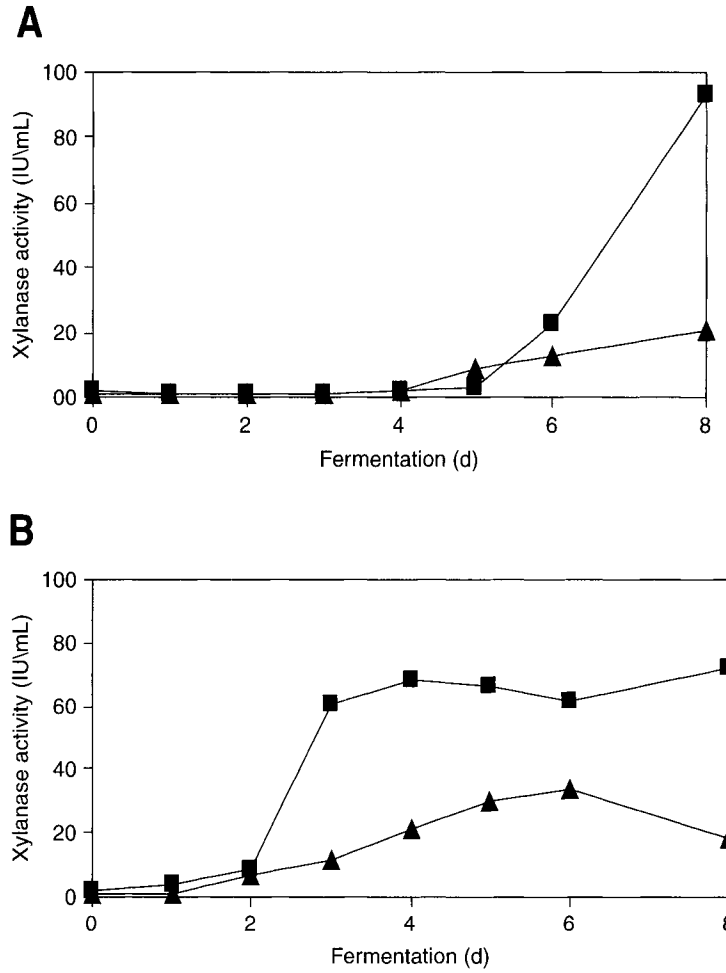


**Fig. 1.** Xylanase production under flask culturing conditions of *T. reesei* Rut C-30 **(A)** and *A. niger* NRRL 2001 **(B)** grown on either DDGS (▲) or hot water pretreated DDGS (■).

washed to remove starch before being used for fermentation. Earlier results have shown that LHW pretreatment solubilizes starch. Therefore, by only adding the washed solids following LHW pretreatment, starch was effectively removed from the medium. Disappointedly, removing the starch failed to shorten the lag phase and only served to lower the final xylanase titer (Fig. 2).

An alternative explanation for the long lag phase of xylanase production might be the adsorption of the xylanases to insoluble DDGS during the early stage of *T. reesei* cultures. A major xylanase produced by *T. reesei* has been found to bind strongly to insoluble xylan (unpublished). This statement is in agreement with the observation that the HW–DDGS resulted in earlier production of xylanase activities than untreated DDGS did (Figs. 1 and 2). Other enzyme activities were also measured. The results are summarized in Table 1. As expected, based on the complex composition of the

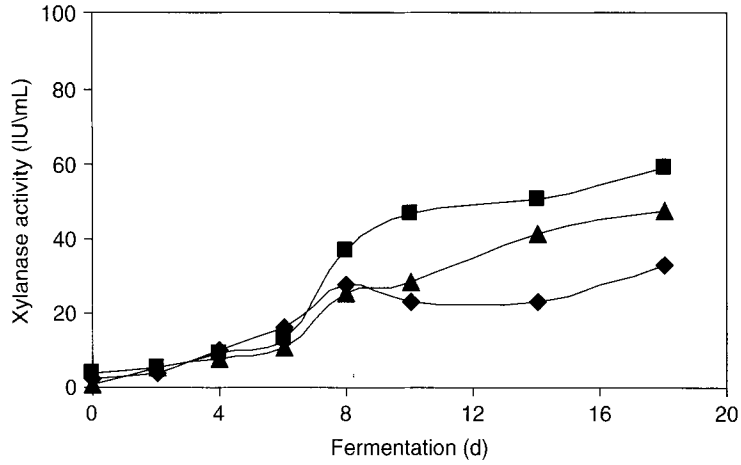


**Fig. 2.** Xylanase production under flask culturing conditions of *T. reesei* Rut C-30 grown on DDGS (◆), hot water pretreated DDGS (■), or washed DDGS for starch removal (▲).

DDGS substrate, a broad range of different enzyme activities were detected. The final enzyme titers using hot water treated DDGS as the substrate were similar or higher than those using DDGS for both microorganisms. A broad range of different enzyme activities was also produced by *T. reesei* QM 9414 and *T. reesei* Rut C-30 grown on corn fiber fractions *(11)*.

As this is the first time DDGS has been reported as a feedstock for production of xylanase, no direct comparison can be made of our results with those from literature. However, there are previous studies that report xylanase yields for fungi grown on other agricultural residues (summarized in Table 2). The xylanase enzyme titers obtained for both microorganisms in shake flask conditions were higher than *Penicillium janthinellum (12)* cultivated in corn cob, and oat husk hydrolysates and *Thermomyces lanuginosus* CAU 44 *(13)* cultivated in wheat straw and rice straw (Table 2). Also, the results for *T. reesei* and *A. niger* were comparable with *T. reesei* QM 9414 and Rut C-30 cultivated in crude corn fiber. On the other hand, much higher enzyme titers were obtained for these two *Trichoderma* strains when grown in corn fiber arabinoxylan (Table 2) *(11)*. Also, Jiang et al. *(13)* reported a xylanase activity of 3260 U/mL when cultivating *T. lanuginosus* CAU 44 in corncob xylan (Table 2).

## Batch and Fed-Batch Bioreactor Cultures for Production of Enzymes

The fungi were next grown in bioreactors to produce larger volumes of enzymes. The first attempt to grow *A. niger* in a bioreactor was unsuccessful (data not shown) because the culture was too viscous to obtain good mixing. It was found that replacing two Rushton impellers with the marine type impellers achieved more homogenous mixing in the reactor. However, the xylanase titer was still lower for *A. niger* (48.8 IU/mL) in the bioreactor compared with flask cultures. In an attempt to increase enzyme titers, the fungi were next grown under fed-batch conditions using the marine impellers.

Table 1
Other Measured Enzyme Activities From Untreated and LHW Treated DDGS Flask Fermentations

| Organism | Substrate | Filter paper (50.0 mg) (FPU) | CMC (1%) (CMCase IU/mL) | *p*-NPG (2.5 m*M*) (β-glucosidase IU/mL) | *p*-NP-gal (2.5 m*M*) (α-galactosidase IU/mL) | *p*-NPX (2.5 m*M*) (β-xylosidase IU/mL) | *p*-NPA (2.5 m*M*) (α-arabinofuranosidase IU/mL) | Ferulic acid (100 mM) (feruloyl esterase IU/mL) |
|---|---|---|---|---|---|---|---|---|
| *A. niger* | Untreated | 0.96[a]/0.00[b] | 3.68[a]/8.21[b] | 1.73[a]/5.71[b] | 2.99[a]/5.6[b] | 0.37[a]/1.20[b] | 1.46[a]/1.86[b] | 0.12[a]/0.01[b] |
| *A. niger* | LHW DDGS | 1.11[a]/0.39[b] | 4.20[a]/22.0[b] | 2.13[a]/3.60[b] | 2.13[a]/4.13[b] | 0.78[a]/1.33[b] | 1.60[a]/1.60[b] | 0.22[a]/0.37[b] |
| *T. reesei* | Untreated | 0.50[a]/0.70[b] | 2.10[a]/21.8[b] | 0.25[a]/1.53[b] | 0.28[a]/1.86[b] | 0.22[a]/1.06[b] | 0.40[a]/0.99[b] | nd[c] |
| *T. reesei* | LHW DDGS | 0.39[a]/1.16[b] | 1.29[a]/44.6[b] | 0.61[a]/4.50[b] | 0.00[a]/0.68[b] | 0.80[a]/2.93[b] | 0.98[a]/1.86[b] | nd[c] |

[a]Activity measured after 4 d.
[b]Activity measured after 8 d.
[c]Not determined (*T. reesei* does not produce feruloyl esterase).

Table 2
The Effect of Various Carbon Sources on the Production of Xylan-degrading Enzymes by Different Microorganisms in Submerged Cultivations

| Organism | Substrate | Cultivation conditions | Substrate for determination of enzyme activity | Xylanase (IU/mL) | Reference |
|---|---|---|---|---|---|
| *T. reesei* Rut C-30 | LHW–DDGS | Shake flask 28°C, 132h | 1% oat spelt xylan | 93.4 | This work |
| *A. niger* NRRL 2001 | LHW–DDGS | Shake flask 28°C, 132h | 1% oat spelt xylan | 72.2 | This work |
| *P. janthinellum* CRC 87M-115 | Corncob | Shake flask 30°C, 132h | 1% birchwood xylan suspension | 55.3 | *12* |
| *P. janthinellum* | Oat husk | Shake flask 30°C, 132h | 1% birchwood xylan suspension | 58.8 | *12* |
| *T. lanuginosus* | Wheat straw | Shake flask 50°C, 96h | 1% birchwood xylan suspension | 53 | *13* |
| *T. lanuginosus* | Rice straw | Shake flask 50°C, 96h | 1% birchwood xylan suspension | 25 | *13* |
| *T. lanuginosus* | Corncob xylan | Shake flask 50°C, 96h | 1% birchwood xylan suspension | 3260 | *13* |
| *T. reesei* QM 9414 | Corn fiber | Shake flask 28°C, 192h | 1% oat spelt xylan | 98.5 | *11* |
| *T. reesei* Rut C-30 | Corn fiber | Shake flask 28°C, 192h | 1% oat spelt xylan | 86.1 | *11* |
| *T. reesei* QM 9414 | Corn fiber xylan | Shake flask 28°C, 192h | 1% oat spelt xylan | 221 | *11* |
| *T. reesei* Rut C-30 | Corn fiber xylan | Shake flask 28°C, 192h | 1% oat spelt xylan | 621 | *11* |
| *T. reesei* Rut C-30 | LHW–DDGS | 4 L fermentation (fed batch) 28°C, 264h | 1% oat spelt xylan | 148 | This work |
| *A. niger* NRRL 2001 | LHW–DDGS | 4 L fermentation (fed batch), 28°C, 264h | 1% oat spelt xylan | 64.3 | This work |
| *P. pinophilum* NTG III/6 | Avicel + barley straw | 12 L fermentation, 35°C, 240h | 1% birchwood xylan suspension | 114 | *14* |
| *A. awamori* mutant AANTG 43 | Ball-milled oat straw | 4 L fermentation 30°C, 48h | 2% oat spelt xylan | 820 | *15* |

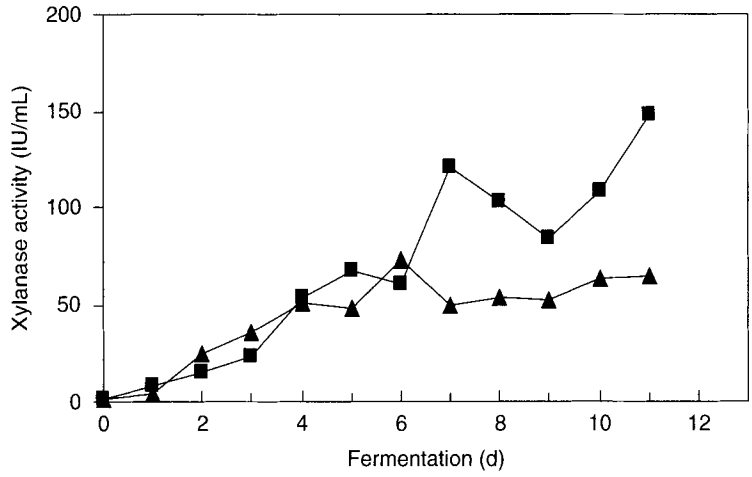


**Fig. 3.** Xylanase production of *T. reesei* Rut C-30 (■) and *A. niger* NRRL 2001 (▲) in repeated fed-batch culture conditions. Three cycles of medium feeding were used (after 3, 6, and 9 d of growth).

Table 3
Other Measured Enzyme Activities From Hot Water Treated DDGS Fermentations Under Fed-Batch Conditions After 11 d of Culturing

| Organism | Filter paper (50.0 mg) (FPAase IU/mL) | CMC (1% [w/v]) (CMCase IU/mL) | *p*-NPG (2.5 m*M*) (β-glucosidase IU/mL) | *p*-NP-gal (2.5 m*M*) (α-galactosidase IU/mL) | *p*-NPX (2.5 m*M*) (β-xylosidase IU/mL) | *p*-NPA (2.5 m*M*) (α-arabinofuranosidase IU/mL) | Ferulic acid (100 m*M*) (feruloyl esterase IU/mL) |
|---|---|---|---|---|---|---|---|
| *T. reesei* | 1.90 | 59.8 | 4.52 | 5.59 | 5.98 | 8.51 | ND[a] |
| *A. niger* | 0.31 | 5.50 | 4.12 | 8.65 | 1.99 | 6.38 | 0.38 |

[a]Not determined (*T. reesei* does not produce feruloyl esterase).

Growing the fungi under fed-batch conditions achieved higher xylanase titers: 3X improved for *T. reesei* (148 IU/mL) and about 1.5X for *A. niger* (64 IU/mL) (Fig. 3).

In comparison with other microorganisms grown in bioreactors (Table 3), the xylanase titers obtained for *T. reesei* and *A. niger* were higher than those reported for *P. pinophilum* NTG III/6 *(14)*, but considerable lower than those for a *A. awamori* mutant (AANTG 43) *(15)*. Other enzyme activity titers are given in Table 3. The data obtained demonstrate that under fed-batch culturing conditions a broad range of different enzyme activities were produced by both fungi. The final enzyme titers were either similar or higher in comparison with the results obtained for flask culturing cultures, except for cellulase production by *A. niger*.

### *Enzymatic Digestion of Pretreated DDGS*

As a first application, the enzymes were evaluated for production of sugars from LHW–DDGS. It was hypothesized that the enzymes would be particularly well suited for this application because the fungi were cultured on LHW–DDGS. LHW is a favorable pretreatment method that has been investigated for preparing biomass for conversion to ethanol. However, although this pretreatment method is effective at increasing the digestibility of cellulose, it does not completely saccharify the xylan fraction. As a result, the method relies on hemicellulases for completing the conversion of xylan to monosaccharides for ethanol fermentation. Converting xylan from DDGS is particularly challenging because it is largely made up of corn pericarp xylan, which is noted in the literature as being particularly recalcitrant to enzymes.

We examined the effects of adding enzymes produced by *T. reesei* and/or *A. niger*, produced in separate fed-batch cultures that used pretreated DDGS, for digesting pretreated DDGS. When added separately, *A. niger* enzymes released more xylose (64%) than *T. reesei* (48%) (Fig. 4A,B), which was expected as a result of superior auxiliary activities (xylanase, feruloyl esterase) found in the *A. niger* preparation. On the other hand, *T. reesei* enzymes released more glucose (84%) compared with *A. niger* (77%) (Fig. 4A,B). This result was expected because *T. reesei* is known as a good cellulase producer with superior activities compared with *A. niger*. The maximum yields for glucose and xylose (99 and 71%, respectively) were obtained using the combined enzymes, albeit there was not improvement in the yield of arabinose (Fig. 4C). The lack of complete conversion of xylan demonstrates the recalcitrant nature of the substrate and the need to identify limiting factors during future research.

## Conclusion

Untreated and LHW–DDGS were evaluated as substrate for producing hydrolytic enzymes using *A. niger* and *T. reesei*. The cultures had xylanase titers higher or comparable with those reported for fungi cultured on other agricultural residues, except for when purified xylan was used as the carbon source. Not surprisingly, these latter gave much higher xylanase titers, but the isolated xylan fractions can also be expected to be a much more expensive fermentation substrate than LHW–DDGS. In addition to having high xylanase titers, the LHW–DDGS grown cultures also contained cellulase and multiple other activities. The mixture of *A. niger* and *T. reesei* enzymes was found to be a highly effective hemicellulase preparation as evidenced by its ability to convert 71% of the xylan from LHW–DDGS to xylose.

## Acknowledgments

The authors wish to thank Patricia J. O'Bryan, Joy Daniel, Jessica Gilles, Loren Iten, and Linda Ericsson for their excellent technical assistance.

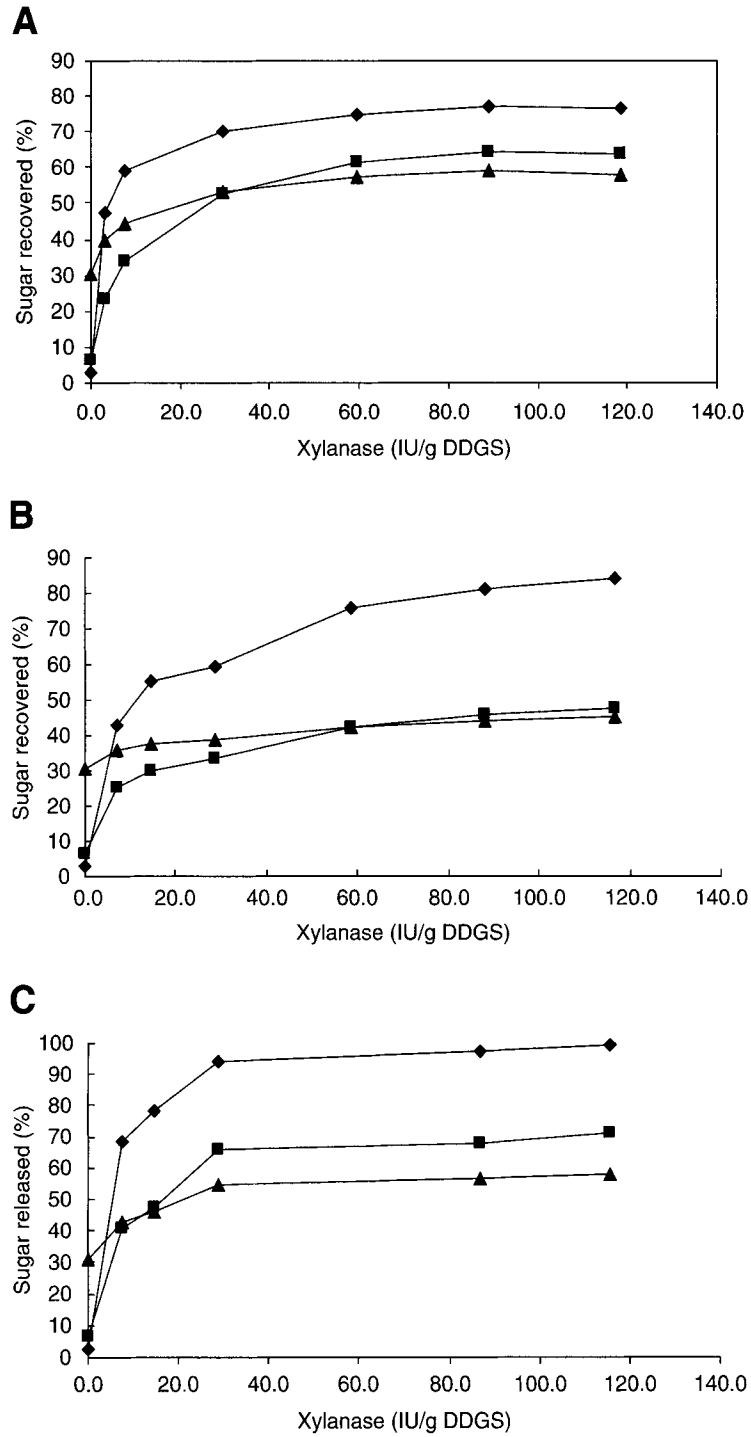


**Fig. 4.** Sugar yields from saccharifying hot water pretreated DDGS hydrolysates using varying loading of *A. niger* NRRL 2001 **(A)**, *T. reesei* Rut C-30 **(B)**, and an equal mixture of *T. reesei* Rut C-30 and *A. niger* NRRL 2001 enzyme preparation **(C)**. Glucose (◆), xylose (■), and arabionose (▲).

## References


1. Belyea, R. L., Rausch, K. D., and Tumbleson, M. E. (2004), *Biores. Technol.* **94,** 293–298.
2. Dien, B. S., Iten, L. B., and Bothast, R. J. (1999), *J. Ind. Microbiol. Biotechnol.* **22,** 575–581.
3. Wong, K. K. Y, Tan, L. U. L, and Saddler, J. N. (1988), *Microbiol. Rev.* **52,** 305–317.
4. Kang, S. W., Park, Y. S., Lee, J. S., Hong, S. I., and Kim, S. W. (2004), *Biores. Technol.* **91,** 153–156.
5. de Vries, R. (2003), *Appl. Microbiol. Biotechnol.* **61,** 10–20.
6. Schuster, E., Dunn-Coleman, N., Frisvad, J. C., and van Dijck, P. W. M. (2002), *Appl. Microbiol. Biotechnol.* **59,** 426–435.
7. Mosier, N. S., Hendrickson, R., Brewer, M., Ho, N., Sedlak, M., and Ladisch, M. R. (2005), *Biores. Technol.* **96(18),** 1986–1993.
8. Mosier, N. S., Hendrickson, R., Brewer, M., et al. (2005), *Appl. Biochem. Biotechnol.* **125,** 1–21.
9. Mandels, M., Andreotti, R., and Roche, C. (1976), *Biotechnol. Bioeng.* **6,** 17–34.
10. Miller, G. L. (1959), *Anal. Chem.* **31,** 426–428.
11. Li, X. -L, Dien, B. S., Cotta, M. A., Wu, Y. V., and Saha B. C. (2005), *Appl. Biochem. Biotechnol.* **121–124,** 321–334.
12. Oliveira, L. A, Porto, A. L. F., and Tambourgi, E. B. (2006), *Biores. Technol.* **97,** 862–867.
13. Jiang, Z. Q., Yang, S. Q., Yan, Q. J, Li, L. T., and Tan, S. S. (2005), *World J. Microbiol. Biotechnol.* **21,** 863–867.
14. Brown, J. A., Cossllin, S. A., and Wood, T. M. (1987), *Enzyme Microb. Technol.* **9,** 355–360.
15. Smith, D. C. and Wood, T. M. (1991), *Biotechnol. Bioeng.* **38,** 883–890.

0273-2289/1559-0291 (Online)/07/136–140/185–194/$30.00

# Production of Biosurfactant by *Pseudomonas aeruginosa* Grown on Cashew Apple Juice

MARIA V. P. ROCHA,[1] MARIA C. M. SOUZA,[1] SOFIA C. L. BENEDICTO,[1] MÁRCIO S. BEZERRA,[2] GORETE R. MACEDO,[2] GUSTAVO A. SAAVEDRA PINTO,[3] AND LUCIANA R. B. GONÇALVES*,[1]

*[1]Universidade Federal do Ceará, Departamento de Engenharia Química, Campus do Pici, Bloco 709, 60455-760, Fortaleza, CE—Brazil, E-mail: lrg@ufc.br; [2]Laboratório de Engenharia Bioquímica (LEB), Departamento de Engenharia Química, Universidade Federal do Rio Grande do Norte, Natal, RN, Brazil; and [3]Laboratório de Bioprocessos, Embrapa Agroindústria Tropical, Rua Dra. Sara Mesquita 2270, Fortaleza, CE, Brazil*

## Abstract

In this work, the ability of biosurfactant production by *Pseudomonas aeruginosa* in batch cultivation using cashew apple juice (CAJ) and mineral media was evaluated. *P. aeruginosa* was cultivated in CAJ, which was supplemented with peptone (5.0 g/L) and nutritive broth. All fermentation assays were performed in Erlenmeyer flasks containing 300 mL, incubated at 30°C and 150 rpm. Cell growth (biomass and cell density), pH, and superficial tension were monitored vs time. Surface tension was reduced by 10.58 and 41% when *P. aeruginosa* was cultivated in nutrient broth and CAJ supplemented with peptone, respectively. These results indicated that CAJ is an adequate medium for growth and biosurfactant production. Best results of biosurfactant production were obtained when CAJ was supplemented with peptone.

**Index Entries:** Biosurfactant; cashew apple juice; *Pseudomonas aeruginosa*; raw materials; rhamnolipid; fermentation.

## Introduction

Biosurfactants are surfactants produced extracellularly or as part of the cell membrane by bacteria, yeasts, and fungi from various substrates including sugars, oils, alkanes, and organic sludges per solids *(1)*. Most microbial surfactants are complex molecules, consisting of different structures that include lipopeptides, glycolipids, polysaccharideprotein complex, fatty acids, and phospholipids *(2)*. They are amphipathic molecules with both hydrophobic and hydrophilic moieties *(3)* and are capable of

*Author to whom all correspondence and reprint requests should be addressed.

reducing surface and interfacial tension *(4)*. Moreover, biosurfactants create micelles, enhancing the solubility of hydrocarbons (such as oil) in water or water in hydrocarbons *(4)*. Because of their surface-active properties and being environmentally friendly, biosurfactants are of great industrial and commercial interest. Potential industrial applications include enhanced oil recovery, crude oil drilling lubricants, surfactant-aided bioremediation of water-insoluble pollutants, and uses in the health care and food processing industries *(3,5)*. Furthermore, biosurfactants may be useful in agriculture, especially in formulation of herbicides and pesticides. In this application, the emulsifier is used to disperse the active compounds and very hydrophobic molecules in the aqueous solution *(6)*. Biosurfactant applications in the environmental industries have received more attention recently owing to their biodegradability, low toxicity, and effectiveness in enhancing biodegradation and solubility of hydrophobic compounds *(1)*. These biological compounds also have potential applications in agriculture, cosmetic, pharmaceuticals, detergents, food processing, laundry supplies, paint industries, and others *(7)*.

Bacteria of the genus *Pseudomonas* are known to produce a glycolipid surfactant containing rhamnose and 3-hydroxy fatty acids. The properties showed by rhamnolipids depend on their homologous composition and distribution that are determined by the bacterial strain, culture conditions, and medium composition *(8)*. Rhamnolipids are isolated from culture broth and can be produced using hydrophobic and hydrophilic substrates *(9)*. Although biosurfactants exhibit such important advantages, they have not been yet used extensively in industry because of relatively high production costs. One possible strategy for reducing costs is the utilization of alternative substrates such as agroindustrial wastes *(10)*. The main problem related to use of alternative substrates as culture medium is to find a waste with the right balance of nutrients that allows cell growth and product accumulation *(11)*. Natural cashew apple juice (CAJ) is an example of an inexpensive substrate in Brazil, as it is a byproduct of the cashew nut industry. In the north coast of Brazil, especially in the state of Ceará, the cashew agroindustry has an outstanding role in the local economy. The cashew apple, a pseudo fruit or peduncle, is the part of the tree that connects it to the cashew nut, the real fruit and a well-known product around the world. The cashew apple is a hard, pear-shaped, small, and nonclimacteric fruit, and is found in three colors: yellow, orange, and red. The most commonly commercialized ones are the yellow and red fruits. The edible portion, representing 90% of the fruit, is a pseudo fruit rich in vitamin C, flavor, and aroma. Internal and external market consumption of cashew nut, in the year of 2004, was about 232,000 t. However, only 12% of the total peduncle is processed *(12–14)* and it does not play an important role to the economy of the state. Furthermore, the majority of the cashew apple production spoils in the soil. These facts together with its rich composition (*see* Table 1), turns CAJ into an interesting and inexpensive (R$1.00/Kg) culture medium.

Table 1
CAJ Composition

| Parameter | CAJ | References |
|---|---|---|
| Vitamin C (mg/100.0 g) | 135.0–372.0 | *12,13* |
| Brix | 7.4 | *13* |
| pH | 3.8–4.2 | *12,13* |
| Malic acid (g/100.0 g) | 0.4 | *13* |
| Total tannins (mg/100.0 g) | 0.6 | *13* |
| Condensed tannins (mg/100.0 g) | 0.2 | *13* |
| Calcium (mg/100.0 g) | 0.9–5.4 | *12* |
| Phosphorous (mg/100.0 g) | 6.1–21.4 | *12* |
| Iron (mg/100.0 g) | 0.2–0.7 | *12* |
| Carotene (mg/100.0 g) | 0.03–0.74 | *12* |
| Carbohydrates (g/100.0 g) | 9.0–9.7 | *12* |
| Reducing sugars (%) | 10.7 | *15* |
| Nonreducing sugars (%) | 0.4 | *15* |
| Starch (%) | 8.5–2.7 | *15* |
| Alanine (μmol/100 mL) | 336.0 | *16* |
| Serine (μmol/100 mL) | 273.0 | *16* |
| Phenylalanine (μmol/100 mL) | 175.6 | *16* |
| Leucine (μmol/100 mL) | 178.0 | *16* |
| Glutamic acid (μmol/100 mL) | 148.4 | *16* |
| Aspartic acid (μmol/100 mL) | 87.6 | *16* |
| Proline (μmol/100 mL) | 158.7 | *16* |
| Tirosine (μmol/100 mL) | 115.5 | *16* |

Therefore, the aim of this work was to investigate the potential use of this alternative substrate (CAJ) as carbon source to rhamnolipid production by *P. aeruginosa* ATCC 10145. Surface-active properties and preliminary characterization of the biosurfactants obtained were also presented.

## Materials and Methods

### *Microorganism*

*P. aeruginosa* ATCC 10145, kindly donated by Dr. Fátima Borges from Empresa Brasileira de Pesquisa Agropecuaria (Embrapa)—Ceará, Brazil, was maintained on nutrient agar (Biolife) slants at 4°C.

### *Substrate Preparation*

CAJ was withdrawn by compressing the cashew apple (*Anarcardium occidentale* L.). After compressing, the substrate was centrifuged at 3500 rpm for 20 min (BIO ENG, BE—6000, São Paolo, Brazil), filtered using a 25 μm filter paper, and diluted with water (1% [v/v]). CAJ supplemented with peptone, here named CAJP, was prepared by adding 5.0 g/L of peptone to diluted CAJ. Afterwards, pH was adjusted to 7.0 and it was sterilized by

filtering through a 0.45 μm Millipore membrane. Nutritive broth (NB) (5.0 g/L of peptone and 3.0 g/L of yeast extract) was distributed in flasks and sterilized in autoclave (Tecnal-AV-75, São Paolo, Brazil) at 1 atm, 121°C for 15 min.

## Media and Growth Conditions

The bacterial strains were streaked in a nutrient agar slant and incubated for 24 h at 30°C. Three loops of culture were inoculated in 50 mL of NB (Biolife) in a 250-mL Erlenmeyer flask and incubated in a rotary shaker (Tecnal—TE240, BR) at 30°C and 150 rpm for 18–24 h. Afterwards, optical density (600 nm) of bacterial suspension was adjusted to 0.1 and an aliquot of 6 mL of inoculum (2%) was transferred to a 500-mL Erlenmeyer flask, containing 300 mL of medium, and incubated at 30°C, 150 rpm in a rotary shaker (Tecnal—TE240, BR). Samples were collected at time-defined intervals and submitted to analysis.

## Biomass Content

Cell growth was determined by measuring the optical density of samples, using a UV-visible spectrophotometer (20 Genesis, BR) at 540 nm. Cell concentration was determined by dry weight by filtering through a 0.45 μm previously weighted Millipore membrane *(17)*.

## Analytical Methods

### Carbohydrates Concentration

Substrate concentration (glucose and fructose), present on CAJ, were measured by high-performance liquid chromatography using a Waters high-performance liquid chromatography equipped with a refractive index detector and a Shodex Sugar SC1011 (Karagawa, Japan) column (8.0 × 300 $mm^2$). Ultrapure water (MiliQ, Millipore, São Paolo, Brazil) was used as mobile phase under the following conditions: flow rate of 0.6 mL/min at 80°C.

### Emulsification Activity

Emulsifying activity was determined according to Cooper and Goldenberg *(18)* with slight modifications: 2 mL of cell free supernatant was added to 2 mL of hydrocarbons (*n*-hexane, *n*-heptane, gasoline, kerosene, or soy oil), containing 0.2 mL of pink dye and the mixture was vortexed for 2 min. After 24 h, the height of emulsion layer was measured. The emulsifying activity ($E_{24}$) was calculated using Eq. 1 *(19)*.

$$E_{24}(\%) = \frac{H_{EL}}{H_S} \times 100 \quad (1)$$

where $H_{EL}$ is the height of the emulsion layer and $H_S$ is the height of total solution.

### Surface Tension Determination

Surface tension was determined with a tensiometer (Torsion Balance of White Electrical Instrument, UK) at 30°C, according to the De Nöuy ring method. The surface tension measurements were performed using cell free supernatants obtained after centrifugation.

### *Rhamnolipid Extraction*

Rhamnolipids mixtures were extracted from culture media after cell removal by filtering through a 0.45 μm Millipore membrane. The pH of supernatant was adjusted to 2.0 with $H_2SO_4$ (6 *N*) and an equal volume of $CHCl_3/CH_3OH$ (2 : 1) was added. The mixture was vigorously shaken for 5 min and allowed to set until phase separation. The organic phase was removed and the operation was repeated again. The rhamnolipid product was concentrated from the pooled organic phase using a rotary evaporator. For further purification the viscous yellowish product obtained was dissolved in methanol and concentrated again by evaporation of the solvent at 45°C *(8)*.

### Carbohydrate and Protein Analysis of Extracted Biosurfactant

The carbohydrate content of extracted biosurfactant was determined by Dubois method *(20)*. Protein concentration was assayed by the Bradford method *(21)*.

### *Statistical Analysis*

All surface tensions and emulsification activities determinations were performed at least three times. Means and standard errors were calculated using the Microsoft Office Excel 2003 (Version 7).

## Results and Discussion

Two complex media (CAJ and CAJP) and a defined media (NB) were used to grow *P. aeruginosa*. The effect of these media on cell growth and rhamnolipid production was investigated and results are pictured on Figs. 1–3. It can be observed that the variation in biomass concentration (optical density), in all media studied, is a typical curve of microbial growth. The same behavior was observed by several authors with different microorganisms *(22–24)*.

Table 2 presents results of growth and production of biosurfactant by *P. aeruginosa* in the different studied media. Maximum biomass concentrations were reached when NB and CAJP were used, 1.08 and 1.00 g/L, respectively. All media tested have favored extracellular production of active surface agent by *P. aeruginosa*. The maximum reduction in the surface tension (41%) was obtained for CAJP after 24 h of culture (Table 2).

A comparison between cell growth, surface tension, and substrate uptake allows observing that the biosurfactant production coincides with the consumption of substrate and the formation of a stationary phase. Several biosurfactants were recognized as secondary metabolites, whereas

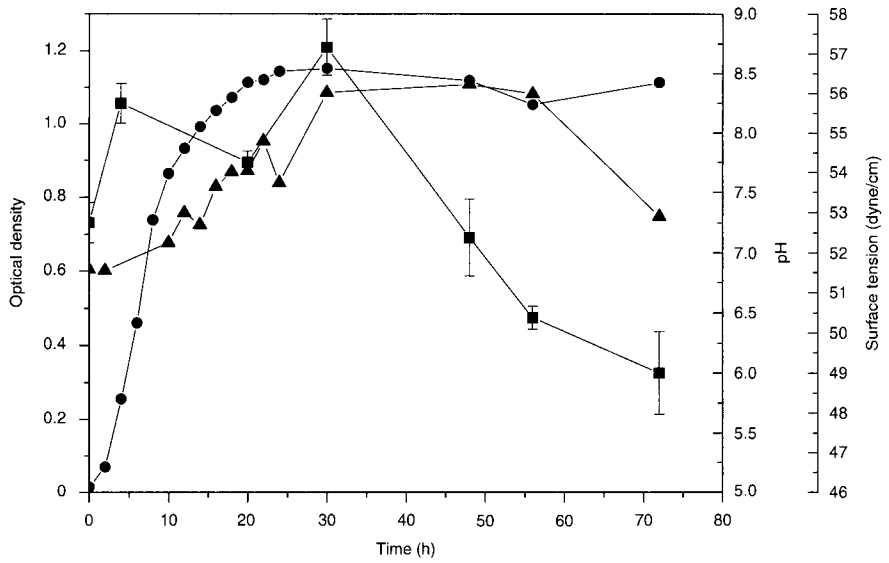


**Fig. 1.** Kinetics of growth and production of biosurfactants at 30°C and 150 rpm in NB by *P. aeruginosa*: (●) optical density ($A_{600}$ nm), (■) surface tension, and (▲) pH.

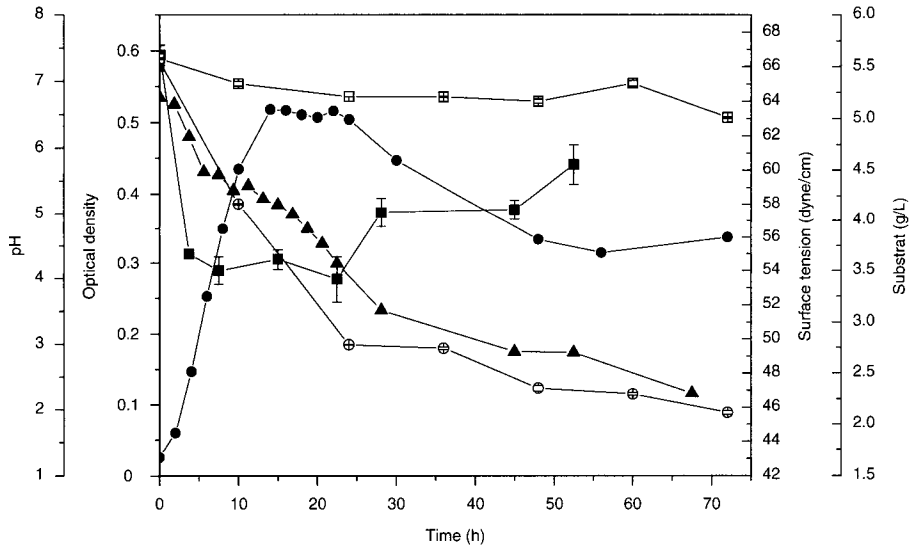


**Fig. 2.** Kinetics of growth and production of biosurfactants at 30°C and 150 rpm in CAJ 1 : 10 by *P. aeruginosa*: (●) optical density ($A_{600}$ nm), (■) surface tension, (▲) pH, (○) glucose concentration (g/L), and (□) fructose concentration (g/L).

others were considered growth associated *(4)*. In this study, the observed behavior is typical of a secondary metabolite.

Other studies evidenced that *P. aeruginosa* was able to reduce the surface tension of soapstock media from 57.5 to 32.9 dyne/cm *(9)*. Brazilian native oils: buriti (*Mauritia flexuosa*), cupuaçu (*Theobroma grandiflora*), passion fruit

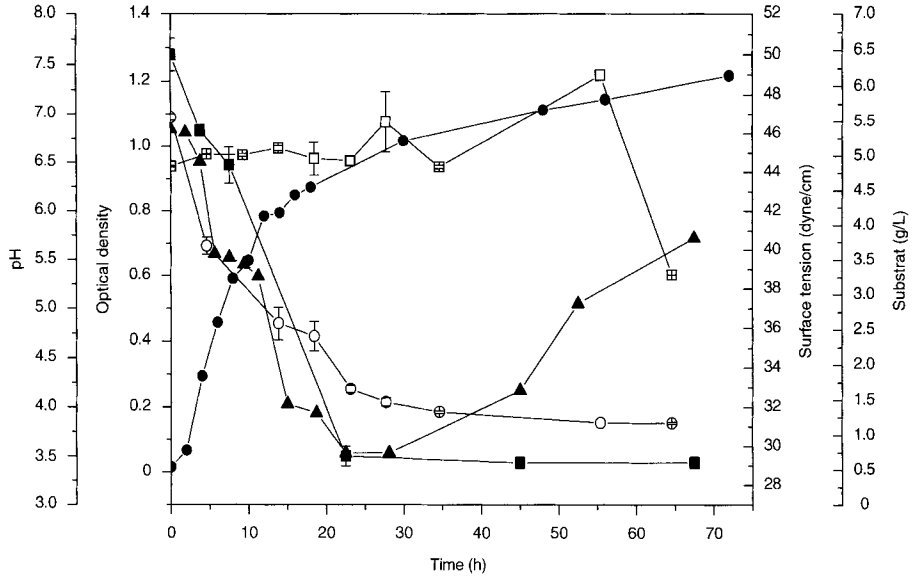


**Fig. 3.** Kinetics of growth and production of biosurfactants at 30°C and 150 rpm in CAJ supplemented with peptone by *P. aeruginosa*: (●) optical density ($A_{600}$ nm), (■) surface tension, (▲) pH, (○) glucose concentration (g/L), and (□) fructose concentration (g/L).

Table 2
Effect of Different Media on Growth and Production of Biosurfactants by *P. aeruginosa*: CAJ 1 : 10, CAJ 1 : 10 Supplemented With Peptone (CAJP), and NB

| Culture media | Biomass (g/L) | Final pH | Surface tension of media (dyne/cm) | Surface tension after cultivation (dyne/cm) | Reduction of surface tension (%) |
|---|---|---|---|---|---|
| CAJ | 0.98 | 2.25 | 66.00 ± 0 | 44.37 ± 0.48[a] | 32.77 |
| CAJP | 1.00 | 5.72 | 50.00 ± 0.81 | 29.50 ± 0.50[b] | 41.00 |
| NB | 1.08 | 8.60 | 52.75 ± 0.5 | 47.17 ± 0.29[c] | 10.58 |

[a]After 72 h of cultive.
[b]After 24 h of cultive.
[c]After 12 h of cultive.

(*Passiflora alata*), andiroba (*Carapa guianensis*), brazilian nut (*Bertholletia excelsa*), and babassu (*Orbignya* sp.) had also been evaluated as carbon sources to produce rhamnolipids for *P. aeruginosa* LB1 *(8)*. The highest rhamnolipids concentrations were obtained from brazilian nut and passion fruit, and surface tension varied from 29.8 and 31.5 dyne/cm, respectively *(8)*. In this article, when CAJP was used, the surface tension of the culture broth fell from 50 to 29.5 dyne/cm, and remained constant up to 70 h. Some authors *(23,25)* report the same behavior and explain that even in the

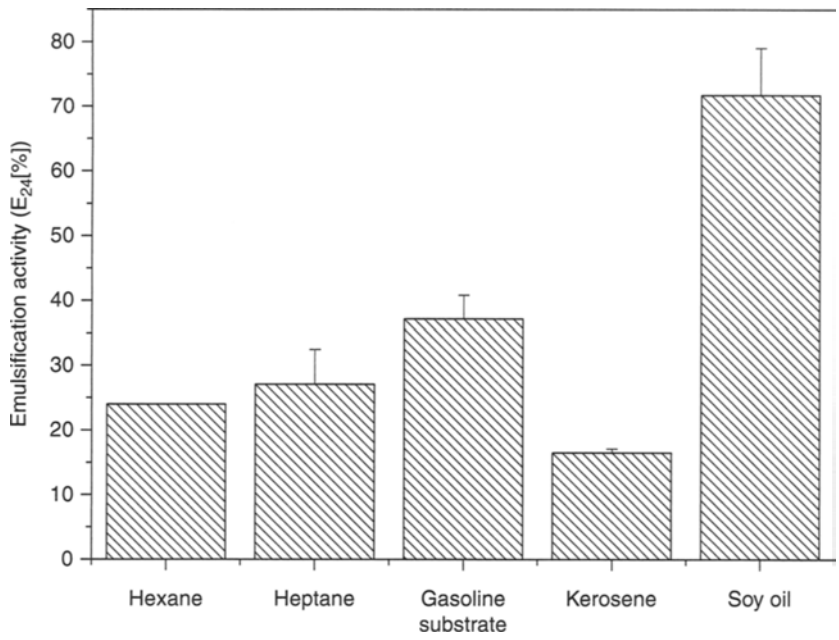


**Fig. 4.** Emulsifying activity ($E_{24}$%) of biosurfactant (produced from medium CAJ supplemented with peptone [CAJP]) obtained for different hydrocarbons. Error bars represent standard deviations.

presence of a small concentration of biosurfactant, the critical micellar concentration may be achieved from which no variation on the surface tension can be observed.

In Figs. 2 and 3, it can be observed that the microorganism consumed only glucose, as fructose concentration remained constant during the fermentation. The pH of the medium increased when using NB and reached values over 8.0, whereas CAJ and CAJP showed acidic conditions. Based on the obtained results, CAJP is a suitable substrate for growth and production of biosurfactant, because it has reduced the surface tension of the media to values below 30 dyne/cm *(24,26)*. Moreover, the exploitation of cashew apple will not only reduce the costs associated with biosurfactant production but will also utilize a surplus raw material that usually spoils in soil and contributes to ambient pollution.

The highest biosurfactant production occurred after 48 h of cultivation using CAJP (3.86 g by biosurfactant for 1000 mL de medium) and the poorest, when NB was used. An emulsion is formed when one liquid phase is dispersed as microscopic droplets in another liquid continuous phase *(4)*. As shown in Fig. 4, all the hydrocarbons and soil oil tested served as substrate for emulsification by the biosurfactant. Soy oil (71.79% emulsified) was the best substrate, whereas kerosene (16.50% emulsified) was the poorest. Most microbial surfactants are substrate specific, solubilizing or emulsifying different hydrocarbons at different rate *(27)*.

No protein was detected in the extracted biosurfactant; however, it did contain carbohydrate (data not shown). The biosurfactant produced by the *P. aeruginosa* may be classified as a rhamnolipid. Rhamnolipids, trelalolipids, and sophorolipids are among the best known glycolipids produced by *P. aeruginosa (28).*

## Conclusion

In this article, three media were studied for the production of biosurfactant by *P. aeruginosa* ATCC 10145. Results indicate that the microorganism was able to grow and produce rhamnolipids when cultivated in all the media studied. However, best results of surface tension reduction were obtained when CAJP was used. Furthermore, *P. aeruginosa* grown on CAJP reduced the surface tension of the media to values below 30 dyne/cm, showing that CAJ, supplemented with peptone, is a suitable substrate for production of biosurfactant. The emulsifying activity of the produced biosurfactant was determined and it was able to emulsify hexane, heptane, gasoline, kerosene, and soy oil. Soy oil (71.79%) was the best substrate, whereas kerosene (16.50%) was the poorest. This initial study indicates that traditional carbon sources for biosurfactant production may be replaced by CAJ. Moreover, the use of CAJ as a culture medium would provide an alternative of waste management for the productive chain of cashew nut, an important industrial segment on the Northeast of Brazil.

## References

1. Muligan, C. N. (2005), *Environ. Pollut.* **133,** 183–198.
2. Nitschke, M. and Pastore, G. M. (2006), *Bioresour. Technol.* **97,** 336–341.
3. Banat, I. M., Makkar, R. S., and Cameotra, S. S. (2000), *Microbiol. Biotechnol.* **53,** 495–508.
4. Desai, J. D. and Banat, I. M. (1997), *Microbiol. Mol. Biol. Rev.* **61,** 47–64.
5. Wei, Y. -H. and Chu, I. -M. (1998), *Enzyme Microbial Technol.* **22(8),** 724–728.
6. Rosenberg, E. and Ron, E. Z. (1999), *Appl. Microbiol. Biotechnol.* **52,** 154–162.
7. Makkar, R. S. and Cameotra, S. S. (2004), *Curr. Opin. Microbiol.* **7,** 262–266.
8. Costa, S. G. V. A. O., Nitschke, M., Haddad, R., Eberlin, M. N., and Contiero, J. (2006), *Process Biochem.* **41,** 483–488.
9. Benincasa, M., Contiero, J., Manresa, A., and Moraes I. O. (2002), *J Food Eng.* **54,** 283–288
10. Mercades, M. E. E., Manresa, M. A., Robert, M., Espuny, M. J., Andres, C., and Guinea, J. (1993), *Bioresour. Technol.* **43,** 1–6.
11. Makkar, R. S. and Cameotra, S. S. (1999), *J. Surf. Det.* **2,** 237–241.
12. Morton, J. F. (1997), In: *Fruits of Warm Climates,* Flair Books, Miami, FL: pp. 239–240.
13. Campos, D. C., Santos, A. S., Wolkoff, D. B., Matta, V. M., Cabral, L. M. C., and Couri, S. (2002), *Desalination* **148,** 61–65.
14. Assunção, R. B. and mercadante, A. Z. (2003), *J. Food Composition Anal.* **16,** 647–657.
15. Souza, A., Simões, A. N., Menezes, J. B., Andrade, J. C., Freitas, D. F., and Mendonça, F. V. S. (2002), in *Proceedings of the XVII Congresso Brasileiro de Fruticultura,* (in portuguese).
16. Oliveira, M. E. B., Oliveira, G. S. F., Maia, G. A., Moreira, R. A., and Monteiro, A. C. O. (2002), *Rev. Bras. Frutic.* **24,** 133–137 (in portuguese).
17. Reis, F. A. S. L., Sérvulo, E. F. C., and De França, P. (2004), *Appl. Biochem. Biotechnol.* 113–116, 899–912.

18. Cooper, D. G. and Goldenberg, B. G. (1987), *Appl. Environ. Microbiol.* **53,** 224–229.
19. Wei, Y. -H., Chou, C. -L., and Chang, J. -S. (2005), *Biochem. Eng. J.* **27(2),** 146–154.
20. Dubois, M., Gilles, K. A., Hamilton, A., Rebers, A., and Smith, F. (1956), *Anal. Chem.* **28,** 350–356.
21. Bradford, M. M. (1976), *Anal. Biochem.* **72,** 248–254.
22. Nitschke, M. and Pastore, G. M. (2002), *Química Nova* **25,** 772–776.
23. Lima Lobato, A. K. C., Macedo, G. R., Magalhães, M. M. A., Bezerra, M. S., Almeida, A. F., and Costa, A. S. S. (2002), Brasiliero de Engenharia Química, Natal, Brazil (in Portugese).
24. Santa Anna, L. M., Sebastian, G. V., Pereira, N., Jr., Alves, T. L. M., Menezes, E., and Freire, D. M. G. (2001), *Appl. Biochem. Biotechnol.* **91–93,** 459–467.
25. Ferraz, C., Nitschke, M., Pastore, G. M. (2002), Proceedings of the XIV Congresso Brasileiro de Engenharia Química, Natal, Brazil (in Portugese).
26. Nitschke, M., Costa, S. G. V. A., and Contiero, J. (2005), *Biotechnol. Prog.* **21,** 1593–1600.
27. Ilori M. O., Amobi, A. C., and Odocha A. C. (2005), *Chemosphere* **61,** 985–992.
28. Robert M., Mercade, M. E., Bosch, M., et al. (1989), *Biotechnol. Lett.* **11,** 871–874.

0273-2289/1559-0291 (Online)/07/136–140/195–204/$30.00

# *Thermoascus aurantiacus* CBHI/Cel7A Production in *Trichoderma reesei* on Alternative Carbon Sources

ZSUZSA BENKŐ,[1] ESZTER DRAHOS,[1] ZSOLT SZENGYEL,[1] TERHI PURANEN,[2] JARI VEHMAANPERÄ,[2] AND KATI RÉCZEY*,[1]

[1]*Department of Agricultural Chemical Technology, Budapest University of Technology and Economics, Szent Gellért tér 4, H-1521 Budapest, Hungary, E-mail: kati_reczey@mkt.bme.hu; and* [2]*ROAL Oy, P.O. Box 57 (Tykkimäentie 15), FI-05200 Rajamäki, Finland*

## Abstract

To develop functional enzymes in cellulose hydrolysis at or above 70°C the cellobiohydrolase (CBHI/Cel7A) of *Thermoascus aurantiacus* was cloned and expressed in *Trichoderma reesei* Rut-C30 under the strong *cbh1* promoter. Cellulase production of the parental strain and the novel strain (RF6026) was examined in submerged fermentation experiments using various carbon sources, which were lactose, Solka Floc 200 cellulose powder, and steam pretreated corn stover. An industrially feasible production medium was used containing only distiller's spent grain, $KH_2PO_4$, and $(NH_4)_2SO_4$. Enzyme production was followed by measurements of protein concentration, total cellulase enzyme activity (filter paper activity), β-glucosidase activity, CBHI activity, and endogenase I (EGI) activity. The *Thermoascus* CBHI/Cel7A activity was taken as an indication of the heterologous gene expression under the *cbh1* promoter.

**Index Entries:** Cellulose; fermentor; lactose; shake flask; Solka Floc 200; steam pretreated corn stover.

## Introduction

Currently, the world's fuel ethanol production is dominated by the United States, Canada, and Brazil. Their contribution to the global production is estimated to be around 90%, whereas the European fuel ethanol production accounts for 7% *(1)*. About 14 billion L of ethanol are produced in Brazil annually from sugar cane. Because of the controlled sugar prices in the United States, sugar cane is too expensive raw material for fuel ethanol production. Therefore, corn and other starch-crops are being used in commercial ethanol production in this country. In Europe, significant amount of ethanol is being produced from sugar beet and

*Author to whom all correspondence and reprint requests should be addressed.

wheat-starch *(1)*. Utilization of lignocellulosic biomass for the production of fuel ethanol could be an interesting option all over the world as lignocellulosic byproducts are generated in huge amounts for example by forestry (wood chip, saw dust, and logging waste), agriculture (various straws), and pulp and paper industry *(2–5)*. In 2005, 280 million t of corn was harvested in the United States and 50 million t in the EU of which 9 million t in Hungary *(6)*. In whole corn plant, corn-stover weighs about 1.5-times as much as corn kernels, thus about 420 million t of corn-stover in the United States and 75 million t in the EU are generated annually. Although, fuel ethanol derived from lignocellulosic biomass can be produced cost competitively with corn-starch based ethanol, the competitiveness with gasoline still remains an issue, which calls for further improvement of such a technology.

Essentially, lignocellulose-to-ethanol processes include three main technological steps. First the polysaccharide content of the feedstock is hydrolyzed to fermentable sugars, which are then converted to ethanol by yeast. In the third step ethanol is refined from the fermentation broth. There are basically three technological concepts available for the hydrolysis of lignocellulosics. These are the one-step concentrated acid hydrolysis, the two-step dilute acid hydrolysis, and the enzymatic hydrolysis, of which the latest seems to have advantages over the former two concepts. The fermentability of hydrolysates obtained in the enzymatic process is significantly better owing to milder processing conditions, resulting in better ethanol yields. On the other hand, for efficient cellulose hydrolysis, high enzyme loading is required making the process economically less favorable because of the high market price of cellulase. Furthermore, the technological margin for economic ethanol distillation has been reported to be 5% ethanol in the fermentation broth, which requires high-density cellulose hydrolysis.

One approach to make the enzymatic process more attractive is to use thermostable cellulases active at high temperatures, thus making the cellulose hydrolysis go faster. Furthermore, the processibility of high-density cellulose slurry could be possible at elevated temperatures. To reach this goal, genetic engineering of different strains has already been carried out *(7,8)*. *Thermoascus aurantiacus* was found to produce thermostable endoglucanase and β-glucosidase in both submerged and solid state cultivation *(9)*.

For economical, large-scale bioethanol production from lignocellulosic material, integrated production plants having the enzyme production on site may be the option. It would be advantageous if the same material could be used for the enzyme production. In the present study, the heterologous production of *T. aurantiacus* cellobiohydrolase (CBHI/Cel7A) in *Trichoderma reesei* RF6026 and the general cellulase enzyme production of the Rut-C30 were investigated and compared on different carbon sources, i.e., on water-soluble (lactose) and water-insoluble carbon sources (cellulose and steam pretreated corn-stover).

## Materials and Methods

### *Carbon Sources for Cellulase Production*

Solka Floc 200 (SF200) cellulose powder (International Fiber, New York, NY), lactose-L-hydrate (SPECTRUM-3D, Hungary) and steam pretreated Italian corn-stover (SPCSI, obtained from ENEA, Italy) were used as carbon sources for cellulase production. Different batches of corn-stover were steam pretreated at 190°C and 210°C for 5 min in continuous reactor, and analyzed for carbohydrate content using the Hägglund method *(10)*. The composition of SPCSI batches obtained after pretreatment at different temperatures were different. The batch pretreated at 190°C contained 36.7% glucan, 15.8% xylan, and 1.0% arabinan on dry matter (DM) basis. The DM content after the treatment was 38.7%. The other batch pretreated at 210°C, contained 32.5% DM glucan, and 2.9% DM xylan. The DM content after the treatment was 59.5%.

### *Microorganisms*

Two different *T. reesei* strains were used in cellulase production experiments, *T. reesei* RF6026 carrying the *T. aurantiacus cbh1/cel7A* under the strong *T. reesei cbh1/cel7A* promoter and the parental strain Rut-C30. In the RF6026 strain the native *T. reesei cbh1/cel7A* gene has been deleted. Freeze-dried conidia of *T. reesei* Rut-C30 (ATCC56765) were obtained from the American Type Culture Collection. Culture of *T. reesei* RF6026 was prepared and kindly supplied from ROAL Oy, Finland.

### *Inoculum Preparation*

The stock culture of the fungus *T. reesei* Rut-C30 was maintained on agar slants containing 50.0 g/L of malt extract, 5.0 g/L of glucose, 1.0 g/L proteose peptone, and 20.0 g/L of bacto agar. *T. reesei* RF6026 was maintained on Potato-dextrose agar slants containing 15.0 g/L starch, 20.0 g/L glucose, and 18.0 g/L bacto agar. After 14 d of incubation at 30°C, the greenish conidia were suspended in 5 mL of sterile water and 1.5 mL of this suspension was transferred to 750-mL Erlenmeyer flask containing 150 mL of sterile and pH adjusted (5.6–5.8) modified Mandels' medium *(11)* in which the concentration of nutrients was added as follows: 0.4 g/L urea, 1.87 g/L of $(NH_4)_2SO_4$, 2.67 g/L of $KH_2PO_4$, 0.53 g/L of $CaCl_2{\cdot}2H_2O$, 0.81 g/L of $MgSO_4{\cdot}7H_2O$, 0.33 g/L of yeast extract, 1.0 g/L of proteose peptone, and 10.0 g/L of lactose. Furthermore, the medium was supplemented with the following trace elements: 6.6 mg/L of $FeSO_4{\cdot}7H_2O$, 2.1 mg/L of $MnSO_4{\cdot}H_2O$, 1.9 mg/L of $ZnSO_4{\cdot}7H_2O$, and 26.7 mg/L of $CoCl_2$. The shake flasks were incubated at 30°C for 3 d on an orbital shaker (350 rpm).

### Enzyme Production in Shake-Flasks

An aliquot of 15 mL 3 d old mycelium suspension obtained from inoculum cultures was used to initiate growth in a 750-mL Erlenmeyer flask containing 150 mL of the Technical Research Centre of Finland (VTT) medium *(8)* in which the concentration of nutrients were 10.0 g/L carbon source (lactose, SF200, and SPCSI), 5.0 g/L distiller's spent grain, 0.83 g/L $KH_2PO_4$, and 0.83 g/L $(NH_4)_2SO_4$. After inoculation, the flasks were incubated for 7 d at 28°C and 200 rpm. Samples were withdrawn daily at the same time and when necessary, the pH in the flasks was adjusted to 5.6 using sterile 10 wt% solutions of NaOH or $H_2SO_4$. Aseptically taken samples were centrifuged at 9000 rpm for 5 min. The collected supernatants were assayed for enzyme activities such as filter paper, β-glucosidase, CBH I, and enduglucanase I, respectively.

### Enzyme Production in Laboratory-Scale Fermentor

Cellulase production was also performed in a 31-L (20 L working volume) double-walled stainless steel laboratory fermentor (Biostat CDCU-3, B Braun Biotech, Germany). The production medium was made up of 60.0 g/L carbon source (lactose, SF200, and SPCSI), 30.0 g/L distiller's spent grain, 5.0 g/L $KH_2PO_4$, and 5.0 g/L $(NH_4)_2SO_4$ *(8)*. The medium components required for 20 L production medium were dissolved in 18 L tap water and sterilized at 121°C for 20 min. After sterilization, 2 L of inoculum culture was aseptically added to initiate growth and enzyme production. During 92 h of fermentation, the temperature was maintained at 28°C and the pH was automatically kept at 5.5 by addition of 10 wt% solutions of either phosphoric acid or ammonium hydroxide. The dissolved oxygen level in the fermentor was controlled to 30% of saturation by cascade controlling first the airflow rate (between 1 and 12 L/min) and agitation speed (300–650 rpm). To avoid foam formation, silicon oil-based Sigma Aldrich Antifoam A (Munich, Germany) in 30% ionic emulsion was added manually. Samples were withdrawn three times a day and centrifuged at 9000 rpm for 5 min. The collected supernatants were assayed for enzyme activities (filter paper activity [FPA], β-glucosidase, CBHI, and EGI).

### Analysis

Reducing sugar (RS) concentration, enzyme activities, and soluble protein content were assayed in sample collected during fermentation. All samples were analyzed in triplicates and the main value was calculated. Relative standard deviation of all measurements was less than 5%. The RS content was measured using 3,5-dinitrosalicylic-acid reagent *(12)*. For fermentation runs carried out using lactose carbon source, the calibration of 3,5-dinitrosalicylic-acid reagent was made using lactose standard, whereas glucose calibration was used for the other two carbon sources. The overall

cellulase activity was measured by FPA *(13)*. In FPA measurements the background RS content was taken into account by subtracting the absorbance of the blank from the absorbance of the activity assay. β-Glucosidase activity was determined against 4-nithrophenyl-β-(D)-glucopyranoside substrate *(14)*. CBHI and EGI activities were assayed using 4-methylumbelliferyl-β-D-lactoside substrate *(15)* in the presence of 100 m*M* glucose to inhibit β-glucosidase. As the reaction is not strictly for CBHI (EGI can also hydrolyze the substrate), for EGI activity measurement 5 m*M* cellobiose is added to inhibit CBHI/Cel7A in the mixture. CBHI activity can be calculated by substracting EGI from the total enzyme activity. Enzyme activities were expressed in international units (IU) except for FPA, wherein filter paper unit (FPU) was used. Enzyme activity measurements from samples collected during the fermentation were carried out at 50°C, if otherwise not indicated. Incubation times and pHs were as following: 60 min and 4.5 for FPA, 10 min and 4.5 for β-glucosidase, and 10 min pH 5.0 for CBHI and EGI activities. Protein content of the samples was also assayed *(16)*.

## Results and Discussion

### *Cellulase Production of* T. reesei *Rut-C30 in Shake-Flask*

In shake flask experiments, cellulase production of *T. reesei* Rut-C30 was examined using the VTT medium in which the carbon source concentration was set to 10.0 g/L. The reason for reducing carbon source concentration from the original 60.0 g/L was owing to the fact that SPCSI at this DM content could not be mixed efficiently in shake-flask cultures. The enzyme production profile obtained on SPCSI carbon source, a potential substrate for ethanol making, was compared with the enzyme profiles obtained on lactose, an industrial standard carbon source, and on purified cellulose powder (SF200), which is regarded as the most effective cellulase inducing carbon source.

The overall cellulase activities were in the range of 1.3–1.9 FPU/mL after 7 d of cultivation. There was no significant difference between the level of cellulase activities on media containing either lactose or SF200, and about 1.3 FPU/mL cellulase titers were reached in both cases. However, when SPCSI carbon source was added to the production medium the overall cellulase activity was 1.9 FPU/mL, which was 45% higher than those obtained for the other two carbon sources. On lactose-containing medium about 1.2 IU/mL β-glucosidase titer was reached in the fermentation; however, the level of this enzyme was considerably lower, around 0.9 IU/mL on solid carbon sources, i.e., SF200 and SPCSI. Levels of CBHI and EGI in the fermentation broth did not show significant variation with different carbon sources. For all three carbon sources the CBHI and EGI activities were around 0.7 and 0.2 IU/mL, respectively (Table 1).

Table 1
Summary of *T. reesei* Rut-C30 Cellulase Production Using Different Carbon Sources

| | Carbon source | | |
|---|---|---|---|
| Enzyme activity | Lactose | SF200 | SPCSI |
| FPA (FPU/mL) | 1.35 | 1.25 | 1.9 |
| β-Glucosidase (IU/mL) | 1.24 | 0.86 | 0.86 |
| CBHI (IU/mL) | 0.66 | 0.72 | 0.75 |
| EGI (IU/mL) | 0.22 | 0.28 | 0.22 |

Enzyme activities obtained in shake flask experiments after 7 d of cultivation.

It has been proven in shake-flask experiments, that SPCSI, a potential substrate for fuel ethanol production, can be efficiently used for cellulase production as well. In spite of the lower carbohydrate content of SPCSI, the overall cellulase activity was increased by 40% compared with lactose. On the other hand the enzyme mixture produced on SPCSI was less balanced in term of the FPA to β-glucosidase ratio. Whereas on lactose carbon source, this proportion was almost 1/1, which is close to the optimal ratio for cellulose hydrolysis, the enzyme cocktail produced on SPCSI was deficient in β-glucosidase enzyme. It is noteworthy to mention that, although significantly higher FPA was measured in case of SPCSI carbon source, individual cellulase (CBHI and EGI) activity assays did not reflect this observation. Unfortunately, with the present set of data and methodology used in this research plausible explanation cannot be provided.

### *Cellulase Production of* T. reesei *Rut-C30 in Fermentor*

Scaled-up cellulase production of *T. reesei* Rut-C30 using the VTT medium supplemented with the previously mentioned carbon sources at 60.0 g/L was performed in a 31 L total volume lab-scale fermentor. Furthermore, with the cultivation of *T. reesei* RF6026 on the same carbon sources the heterologous expression of *T. aurantiacus cbh1/cel7A* was also investigated. Enzyme activities and RS concentration in samples withdrawn during the course of cultivation are summarized in Fig. 1.

Cultivation of *T. reesei* Rut-C30 on medium containing 60.0 g/L lactose resulted in an overall cellulase activity of 3.4 FPU/mL. Significant cellulase production was observed after 20 h of fermentation (Fig. 1A). The activity of β-glucosidase, CBHI, and EGI were quite low at this time, and detectable amounts were only observed in the fermentation broth after 30 h. At end of the fermentation the β-glucosidase, CBHI, and EGI activities were 1.0, 1.5, and 0.4 IU/mL, respectively. About 35% higher, 4.6 FPU/mL FPA was reached at the end of *T. reesei* Rut-C30 cultivation when the cellulase production was induced by SF200 cellulose powder (Fig. 1B).

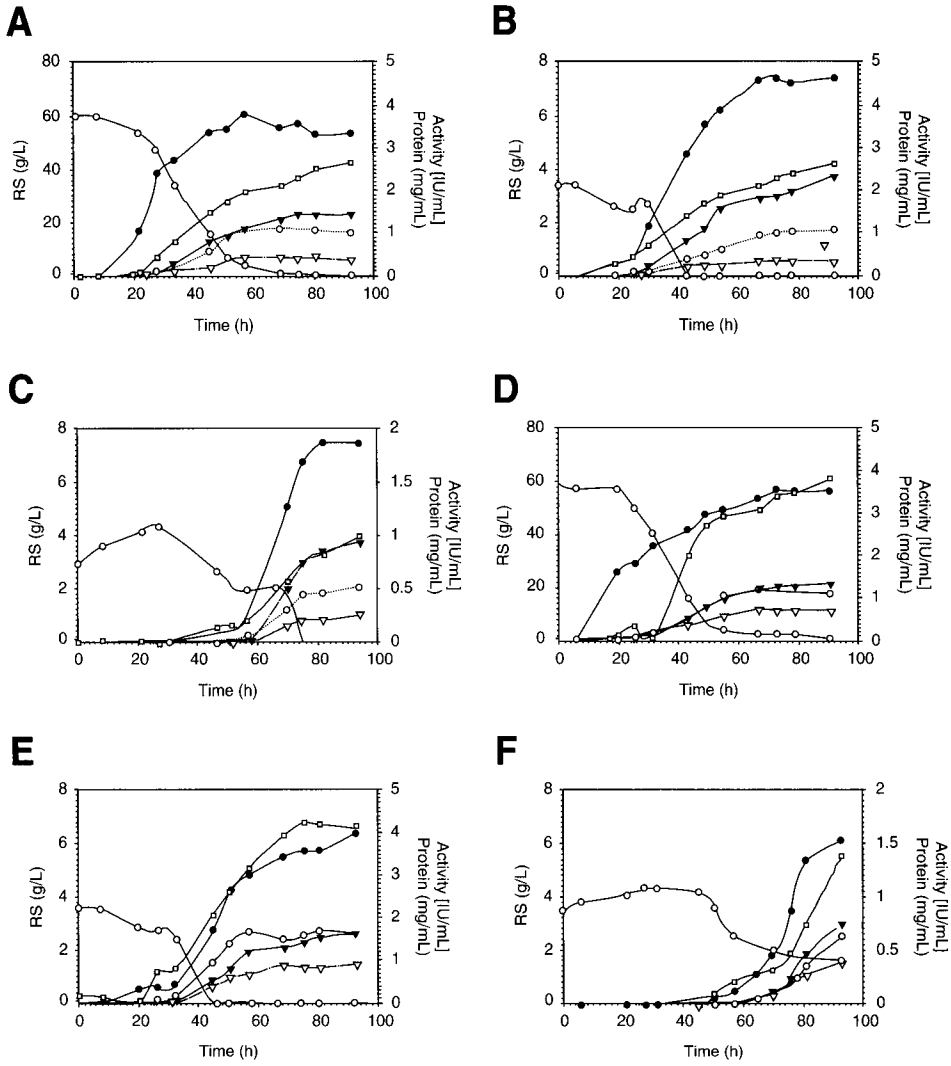


**Fig. 1.** Enzyme production of *T. reesei* strains in lab-scale fermentor using different carbon sources. **(A)** Lactose Rut-C30, **(B)** SF 200 Rut-C30, **(C)** SPCSI Rut-C30, **(D)** Lactose RF6026, **(E)** SF 200 RF6026, and **(F)** SPCSI RF6026; (●) RS, (●) FPA, (○) (β-glucosidase, (▼) CBHI, (▽) EGI, and (□) protein content.

However, the level of β-glucosidase enzyme stayed as low as 1.1 IU/mL. As expected, the expression of CBHI enzyme was clearly higher on SF200 than on lactose carbon source, resulting in a CBHI activity of 2.3 IU/mL at the end of the experiment. On the other hand, the expression of the other cellulase component, EGI, was not influenced by the carbon source at all, and the same level of activity was reached on the strong cellulase inducer as with lactose (Fig. 1 panel A,B). When SPCSI carbon source was used to produce cellulases in the concentration of 60.0 g/L, there was no enzyme

production observed at all. The RS content in the medium (data not shown) increased continuously indicating that cellulase added with the inoculum started to hydrolyze the cellulose fraction of the carbon source, but glucose liberated was not taken up by the fungus. Same phenomenon has been observed elsewhere *(17)*, where the lack of microbial growth and enzyme production was explained by the presence and inhibitory effects of compounds, such as furfural and acetic acid, generated during steam pretreatment of lignocellulosics. The experiment with this carbon source was therefore repeated; however, with reduced amount of SPCSI at 30.0 g/L. As shown in Fig. 1C, even at this lowered SPCSI concentration, a long lag phase could be seen during which the RS concentration was first increasing and then slowly declining as microbial activity picked up. Cellulase production started rather late, at the fortieth hour of the cultivation, compared with the enzyme production carried out with the other two carbon sources. Final enzyme titers were also significantly lower in this case, 1.9 FPU/mL, 0.5 IU/mL, 1.0 IU/mL, and 0.3 IU/mL for FPA, β-glucosidase, CBHI, and EGI activities, respectively. Though it has to be kept in mind that these results were obtained at considerably lower carbon source concentration.

### *CBHI/Cel7A Production of* T. reesei *RF6026 in Fermentor*

Heterologous production of *T. aurantiacus* CBHI in *T. reesei* RF6026 strain was examined by measuring the CBHI activity during the growth of the fungus on lactose, SF200, and SPCSI. Lactose and SF200 were applied in 60.0 g/L concentrations, whereas the concentration of SPCSI in the production medium was 30.0 g/L. Besides FPA, CBHI, EGI, and β-glucosidase activities were also measured. However, when judging the FPA results it should be kept in mind that the CBHI enzyme of *T. aurantiacus* does not have a cellulose binding domain. The enzyme activity and RS curves were very similar to what has been seen during the cultivation of the parental strain on the same carbon sources, except the level of CBHI activities, which were always lower to the same degree as activity measurement was carried out at suboptimal condition of the thermoactive *T. auranticus* CBHI enzyme, for example, 50°C. The enzyme production on lignocellulosics, for example, SF200 and SPCSI, did not seem to be influenced by the facts that:

1. The produced *T. auranticus* CBHI lacks the cellulose binding domain, which would facilitate better hydrolysis of the carbon source thereby supporting growth of the fungus in greater extent.
2. The cultivation of the mesophilic *T. reesei* was performed at 28°C, a definitely suboptimal temperature for the thermo-active CBHI enzyme.

In order to obtain an accurate number on the amount of thermoactive CBHI activity measurement of samples taken at the end of every fermentation have been done at 70°C as well as shown in Fig. 2, where

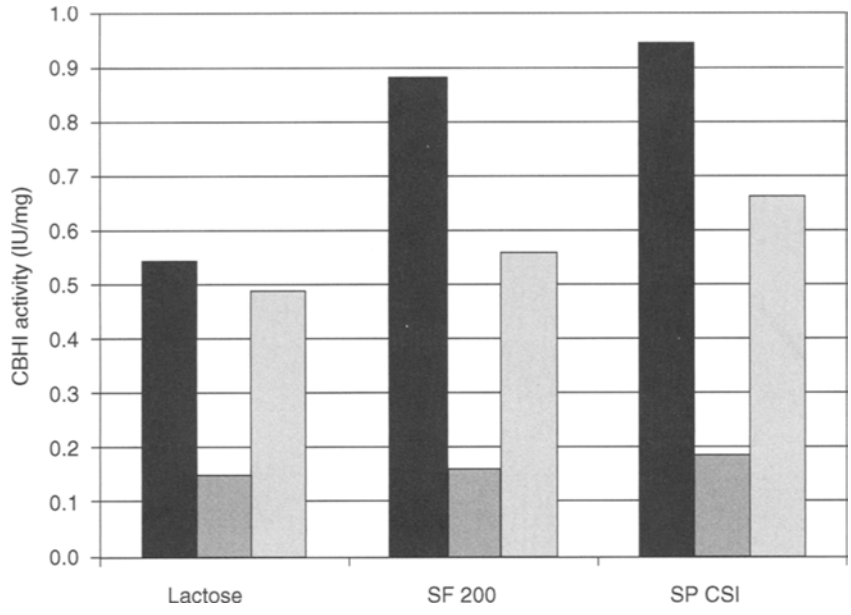


**Fig. 2.** CBHI activities of *T. reesei* Rut-C30 measured at 50°C (■), Rut-C30 measured at 70°C (■) and RF6026 measured at 70°C (▒), produced on different carbon sources.

CBHI specific activities of both endogeneous and cloned CBHI activities measured at optimal temperatures are compared for different carbon sources (CBHI activity of Rut-C30 on elevated temperature is also included for comparison). As expected the protein production pattern under *T. reesei* cbh1 promoter was similar for both strains on cellulosic carbon sources. However, the parental strain loses its CBHI activity at 70°C, whereas CBHI of RF6026 strain still performs well, providing the possibility to work at elevated temperatures.

## Conclusions

The main objective of the present study was primarily to examine the heterologous protein production in a model strain, *T. reesei* RF6026, under the *T. reesei cbh1* promoter. It has been established by CBHI activity measurements at optimal temperatures for both CBHI enzymes that the implementation of the thermo-active enzyme was successful and the target protein was produced. The second objective of this work was to examine the feasibility of utilizing the same material, for example, steam pretreated corn-stover for cellulase enzyme production that could be used as a substrate for fuel ethanol production. It was concluded that the application of SPCSI for enzyme production is limited probably because of the presence of microbial growth inhibiting compound that are liberated during pretreatment of corn-stover.

## Acknowledgments

This work was supported by EC "TIME" project (ENK6-CT-2002-00604). The Hungarian Ministry of Education is acknowledged for its financial contribution (NKFP-OM 00231/2005). Steam pretreated corn-stover was kindly provided by ENEA, Italy. The authors wish to thank the contribution of Éva Sáhó.

## References

1. Licht (2001) www.fo-licht.com. Accessed January 2006.
2. Rudolf, A., Alkasrawi, M., Zacchi, G., and Lindén, G. (2005), *Enzyme Microbiol. Technol.* **37,** 195–204.
3. O'Brien, D. J., Senske, G. E., Kurantz, M. J., and Craig, J. C., Jr. (2004), *Bioresour. Technol.* **92,** 15–19.
4. Kádár, Z. S., Szengyel, Zs., and Réczey, K. (2004), *Ind. Crops Prod.* **20,** 103–110.
5. Réczey, K., Szengyel, Zs., Eklund, R., and Zacchi, G. (1996), *Bioresour. Technol.* **57,** 25–30.
6. www.fao.org/ Last updated in February 2005.
7. Gusakov, A. V., Sinitsyn, A. P., Salanovich, T. N., et al. (2005), *Enzyme Microb. Technol.* **36,** 57–69.
8. Harkki, A., Mäntylä, A., Penttilä, M., et al. (1991), *Enzyme Microb. Technol.* **13,** 227–233.
9. Kalogeris, E., Christakopoulos, P., Katapodis, P., et al. (2003), *Proc. Biochem.* **38,** 1099–1104.
10. Hägglund, E. (1951), *Chemistry of Wood.* Academic Press, New York: pp. 324–332.
11. Mandels, M. and Weber, J. (1969), *Adv. Chem. Ser.* **95,** 391–414.
12. Miller, G. L. (1959), *Sugar Anal. Chem.* **31,** 426–428.
13. Ghose, T. K. (1987), *Pure Appl. Chem.* **59,** 257–268.
14. Berghem, L. E. R. and Petterson, L. G. (1974), *Eur. J. Biochem.* **46,** 295–305.
15. Bailey, M. J. and Tähtiharju, J. (2003), *Appl. Microbiol. Biotechnol.* **62,** 156–162.
16. Bradford, M. M. (1976), *Anal. Biochem.* **72,** 248–254.
17. Szengyel, Zs., and Zacchi, G. (2000), *Appl. Biochem. Biotechnol.* **89,** 31–42.

0273-2289/1559-0291 (Online)/07/136–140/205–206/$30.00

# SESSION 1B
## Plant Biotechnology and Genomics

# Introduction to Session 1B

**MARIAM B. STICKLEN***

*Department of Crop and Soil Sciences, Michigan State University, MI 48824, E-mail: stickle1@msu.edu*

Topics presented in the "Plant Biotechnology and Genomics" session focused on technologies that highlight the important role of plant biotechnology and genomics in the development of future energy crops. Several excellent presentations demonstrated the latest advances in energy crop development through the use of plant cell wall regulation and by engineering new energy crops such as brown midrib sweet sorghum. Approaches included the control of cellulose production by increased expression of cellulase synthase genes and the selection of high-yield varieties of shrub willows. The potential of producing hydrolytic enzymes using transgenic plants as a cost-effective means for the large-scale production of these enzymes was also explored in the session, as was the role of posttranslational modifications on the activities of heterologous expressed cellulases in hosts such as *Pichia pastoris*.

*Author to whom all correspondence and reprint requests should be addressed.

0273-2289/1559-0291 (Online)/07/136–140/207–220/$30.00

# Heterologous *Acidothermus cellulolyticus* 1,4-β-Endoglucanase E1 Produced Within the Corn Biomass Converts Corn Stover Into Glucose

CALLISTA RANSOM,[1] VENKATESH BALAN,[2] GADAB BISWAS,[1] BRUCE DALE,[2] ELAINE CROCKETT,[3] AND MARIAM STICKLEN*,[1]

*[1]Department of Crop and Soil Sciences; [2]Department of Chemical Engineering and Material Science; and [3]Department of Physiology; Michigan State University, MI 48824, E-mail: stickle1@msu.edu*

## Abstract

Commercial conversion of lignocellulosic biomass to fermentable sugars requires inexpensive bulk production of biologically active cellulase enzymes, which might be achieved through direct production of these enzymes within the biomass crops. Transgenic corn plants containing the catalytic domain of *Acidothermus cellulolyticus* E1 endo-1,4-β glucanase and the *bar* bialaphos resistance coding sequences were generated after Biolistic® (BioRad Hercules, CA) bombardment of immature embryo-derived cells. *E1* sequences were regulated under the control of the cauliflower mosaic virus 35S promoter and tobacco mosaic virus translational enhancer, and E1 protein was targeted to the apoplast using the signal peptide of tobacco pathogenesis-related protein to achieve accumulation of this enzyme. The integration, expression, and segregation of *E1* and *bar* transgenes were demonstrated, respectively, through Southern and Western blotting, and progeny analyses. Accumulation of up to 1.13% of transgenic plant total soluble proteins was detected as biologically active E1 by enzymatic activity assay. The corn-produced heterologous E1 could successfully convert ammonia fiber explosion-pretreated corn stover polysaccharides into glucose as a fermentable sugar for ethanol production, confirming that the E1 enzyme is produced in its active form.

**Index Entries:** Ammonia fiber explosion; biomass conversion; cellulose; ethanol; transgenic maize; endoglucanase.

## Introduction

According to a recent report from the Natural Resources Defense Council and the Institute for the Analysis of Global Security, the dependence of the United States on foreign petroleum both undermines its economic strength and threatens its national security *(1)*. Ethanol, obtained either

*Author to whom all correspondence and reprint requests should be addressed.

from grain or from cellulosic materials, has the ability to decrease the need for petroleum fuel *(1)*. Accordingly, the ethanol fuel industry has been growing significantly in many countries throughout the world, and the United States ethanol production capacity reached nearly 13.4 billion L in 2004, up nearly by 1.15 billion L since 2003 *(2)*.

In the United States, ethanol is mostly produced from starch of corn kernels with a net energy balance *(2)*. However, it is believed that with proper management, roughly 1.18 billion mt of crop and forest residues and energy crops can become available in the United States *(3)* and over 1.5 billion mt/yr worldwide *(4)*, which mostly could be used for conversion into alcohol fuels. Some estimate the global availability at 9–45 billion mt of crop biomass annually *(5)*. In the United States, this translates into approx 411 billion L of petroleum in 1 yr *(4)*.

In addition to being cheap and widely available, lignocellulosic biomass has the added benefit of being renewable and thus sustainable *(4,5)*. A current goal for enhancing US economic security is to meet 10% of chemical feedstock demand by 2020 with plant-derived materials, or a fivefold increase over current usage levels *(6)*. Crops that have a high amount of lignocellulosic biomass, such as corn, rice, sugarcane, and fast growing perennial grasses have been recommended for conversion into alcohol fuels *(7,8)*.

Although production of fermentable sugars for alcohol fuels from plant biomass is an exciting and attractive idea, and substantial efforts have been put forth toward improving ethanol yield through this technology and reducing its production costs *(9,10)*, major roadblocks still stand in the way of widespread commercial implementation of this technology. These include prohibitive costs of pretreatment processing of the lignocellulosic matter and production of microbial cellulase enzymes used in the conversion of cellulosic matter into fermentable sugars *(11)*.

Enzymatic hydrolysis of cellulosic matter requires at least three groups of enzymes: 1,4-β-endoglucanase (E1; E.C. 3.2.1.4), cellobiohydrolase (E.C. 3.2.1.91), and β-D-glucosidase (E.C. 3.2.1.21) *(12,13)*. Currently these enzymes are expensively produced in microbial fermentation tanks *(7,14)*. Decades of research have been devoted to reducing microbial production costs of cellulases, resulting in significant decreases since 1980 *(7,15)*. Despite all efforts, enzyme production expenses are still high *(7)*. The latest model designed by the National Renewable Energy Laboratory (Golden, CO) and Genencor (Palo Alto, CA) is producing cellulases at around $0.03–0.05/L of ethanol (http://www.genencor.com/wt/gcor/ethanol).

An alternative strategy might be to use biomass crops as biofactories to produce these enzymes on a large scale, and store them in safe cell compartments until used. Plants are already being used successfully for molecular farming *(16)* of enzymes *(17,18)* and other proteins *(19)*, carbohydrates *(20,21)*, and lipids *(22)*. Plant-based production of enzymes has several critical advantages compared with microbial fermentation or bioreactors.

For example, plants can directly use the energy of the sun. Furthermore, proteins produced in plants mostly display correct folding, glycosylation activity, reduced degradation, and increased stability *(16)*. In addition, the infrastructure and know-how are mostly in place for plant genetic transformation, growing, harvesting, transporting, and processing the corn plant matter *(16)*.

To this end, the thermostable *E1* transgene from *Acidothermus cellulolyticus (23,24)* has successfully been expressed in several plants including *Arabidopsis (12)*, potato *(25)*, and tobacco *(13,26)*. However, none are considered a significant biomass crop for producing adequate amounts of enzymes needed for lower costs of commercial ethanol production. Corn, on the other hand, is an ideal crop for enzyme production, because it produces a large amount of biomass, is an annual crop, and is already grown extensively in the United States.

In this study, we present the successful production and accumulation of E1 in biomass of transgenic corn plants at a relatively high level. This is the first report on the conversion of biomass to fermentable sugars through the use of *A. cellulolyticus* E1 enzyme constitutively produced within the most acknowledged biomass crop, corn.

## Materials and Methods

### *Transformation Vectors*

A combination of pMZ766-$E1_{CAT}$ *(12)* and pBY520 *(27)*, or pMZ766-$E1_{CAT}$ and pDM302 *(28)* was used in transformation research. Vector pMZ766-$E1_{CAT}$ encodes the catalytic domain of E1 from *A. cellulolyticus*, targeted to the apoplast with the signal peptide from tobacco pathogenesis-related protein 1a (Pr1a), under regulation of the cauliflower mosaic virus (CaMV) 35S promoter, the tobacco mosaic virus translational enhancer (Ω), and the polyadenylation signal from nopaline synthase gene (3′ *nos*) (Fig. 1A). Vector pDM302 contains the *bar* coding sequences under the control of the rice actin 1 (Act1) promoter and nos terminator (Fig. 1B). Vector pBY520 contains the barley *HVA1* coding sequences regulated by the Act1 promoter and potato proteinase inhibitor II terminator, as well as the *bar* coding sequences regulated by the CaMV 35S promoter and nos terminator (Fig. 1C).

### *Corn Transformation, Acclimation, and Transfer to Greenhouses*

Highly proliferating, immature embryo-derived type II embryogenic callus *(29)* was used in transformation experiments. Two to four hours before bombardment, callus was transferred in 2 cm circles in the center of a Petri dish containing an osmotic *(30)* or conditioning medium. Conditioned callus was bombarded with ethanol washed tungsten particles combined with a total of 10 μg of 1 : 1 mixture of pMZ766-$E1_{CAT}$ and either pDM302 or pBY520, according to the manufacturer's protocol

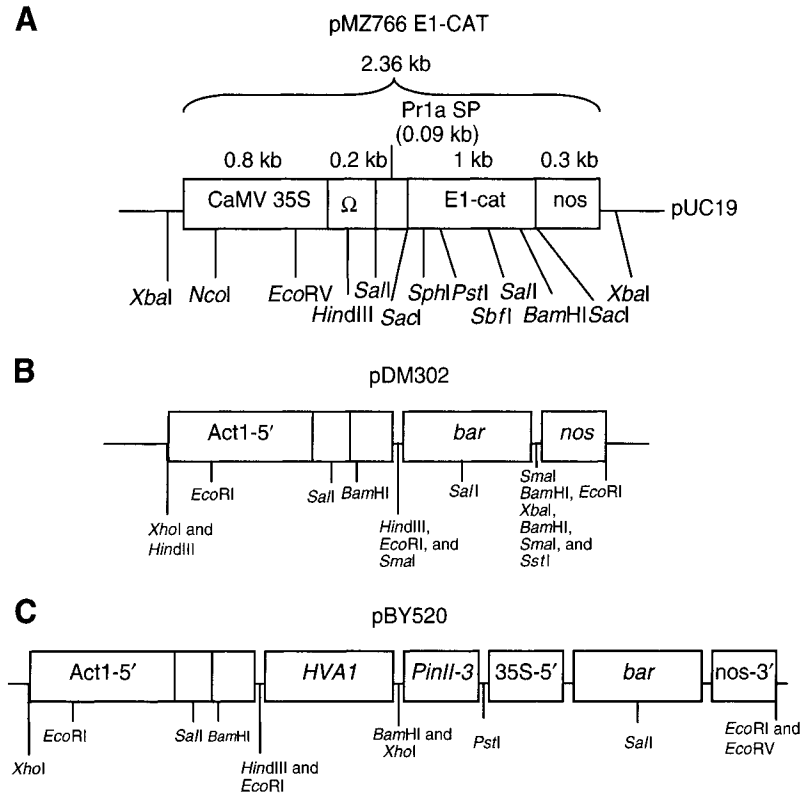


**Fig. 1.** **(A)** Transformation vector pMZ766E1-$_{CAT}$. CaMV 35S, cauliflower mosaic virus 35S promoter; Ω, tobacco mosaic virus Ω translational enhancer; Pr1a SP, the sequence encoding the Pr1a signal peptide; E1-cat, catalytic domain of 1,4-β-glucanase E1 (E1-$_{cat}$, EC 3.2.1.4) from the eubacterium *A. cellulolyticus*; nos, polyadenylation signal of nopaline synthase. **(B)** Transformation vector pDM302. Act1-5′, rice actin 1 promoter; *bar*, bialaphos (herbicide)-resistance gene; nos. **(C)** Transformation vector pBY520. Act1-5′, rice actin 1 promoter; *HVA1*, a barley late embryogenesis abundant protein gene; PinII-3′, potato proteinase inhibitor II terminator; 35S, CaMV 35S promoter; *bar*; and nos.

(PDS 1000/He Biolistic® gun, BioRad, Hercules, CA) at a pressure of 7579 kPa. The pDM302 or pBY520 containing the *bar* selectable marker gene was used to provide the herbicide resistance.

The bombarded callus was kept on the same conditioning medium for 24 h, transferred to callus proliferation medium *(31,32)* for 5 d, and then placed on selection medium containing 2.0 mg/L bialaphos wherein they were maintained for 6–8 wk with 2-wk subcultures into fresh medium. All cultures were maintained in the dark up to this point. The detected bialaphos-resistant surviving callus clones were placed in regeneration medium *(33)* and exposed to light (60 μmol quanta/$m^2$/s from cool-white 40 W Econ-o-watt fluorescent lamps; Philips Westinghouse, Somerset, NJ) for 4–6 wk. Plantlets were transferred further to rooting medium containing

2.0 mg/L bialaphos selectable herbicide *(33)*, and maintained for 2–4 wk under the aforementioned light conditions.

Rooted plantlets of eight to ten centimeters in height were transferred to pots containing soil, and pots were covered with plastic bags and kept under light to mimic the tissue culture conditions. Small holes were made daily in each bag, for 10–14 d acclimating the plants to greenhouse conditions before plants were transplanted into 7.6 L pots and transferred to a long day (16 h/d light) greenhouse.

### *DNA Analyses*

Genomic DNA was extracted from leaf tissue with C-TAB as described *(34)*. For polymerase chain reaction (PCR), the oligonucleotide primers 5′-GCG GGC GGC GGC TAT TG-3′ and 5′-GCC GAC AGG ATC GAA AAT CG-3′ were designed, synthesized, and used to amplify a 1.0 kb fragment spanning the catalytic domain of the *E1* gene. The PCR products were analyzed by electrophoresis in 0.8% agarose gels containing ethidium bromide, and visualized under ultraviolet light.

For Southern blot analyses, 5 µg of genomic DNA and 10.0 pg plasmid DNA (pMZ766-E1$_{CAT}$) were digested with *Hin*dIII or *Sac*I and fractionated on a 1% agarose gel. *Hin*dIII was chosen because it appeared to be a unique site in the construct, and *Sac*I because it cuts out the coding sequence of the catalytic domain (Fig. 1). The DNA was depurinated, denatured, and neutralized, and the gel was blotted onto a Hybond-N+ nylon membrane (Amersham-Pharmacia Biotech, Buckinghamshire, UK) according to the manufacturer's instructions. The PCR DIG Probe Synthesis Kit (Roche Applied Science, Penzberg, Germany, Cat no. 11 636 090 910) was used according to the kit's instructions to generate a probe labeled with digoxigenin–dUTP, representing the E1-$_{CAT}$ coding region. Probe hybridization and immunological detection were carried out using the DIG High Prime DNA Labeling and Detection Starter Kit II (Roche Applied Science, Cat no. 1 585 614) with the instructions therein. Blots were exposed to X-ray film and developed in a Kodak RP X-OMAT Processor (Kodak).

### *Total Soluble Proteins Extraction*

Total soluble proteins (TSP) were extracted from leaf tissues as described *(13)*. Briefly, 100.0 mg fresh leaf tissue was ground in the sodium acetate-grinding buffer and precipitated with saturated ammonium sulfate. Extracts were quantified using the Bradford method *(35)* using a standard curve generated from bovine serum albumin. For the large-scale TSP extraction (to check the activity on biomass), an automatic solvent extractor (Dionex, Sunnyvale, CA) was used. To a total of 9.0 g pulverized transgenic corn residue, 60 mL grinding buffer was added and used by the machine to extract TSP. The extracted TSP were precipitated by adding an equal volume of saturated ammonium sulfate and allowing to stand overnight at 4°C. The precipitated TSP

were collected by centrifugation and concentrated by resuspending in 5 mL grinding buffer. This TSP concentrate was measured for activity (described under "MUCase Activity Assay") and used without any further dilution.

### *MUCase Activity Assay*

E1 activity was assessed as described *(13)*. Briefly, a series of soluble protein dilutions ranging from $10^{-1}$ to $10^{-3}$ were developed, representing concentrations of 0.1–10.0 ng/μL. In a 96-well plate, 10 μL samples (representing 1–100.0 ng TSP) were mixed with 100 μL reaction buffer containing 4-methylumbelliferone β-D-cellobioside (MUC). The fluorophore 4-methyl umbelliferone, as the product of E1 hydrolization of the substrate β-D-cello bioside, was measured as follows. Plates were covered with adhesive lids and incubated at 65°C for 30 min. The reaction was stopped with the addition of the stop buffer, and the fluorescence was read at 465 nm using SPECTRAmax M2 device (Molecular Devices Inc., Sunnyvale, CA) at an excitation wavelength of 360 nm. After subtracting background fluorescence contributed by the control, activity of each sample was calculated using a standard curve representing 4–160 pmol methylumbelliferone and compared with the activity of pure E1 reported in Ziegelhoffer et al. *(13)*.

### *Western Analysis*

For Western blotting, the Invitrogen NuPAGE® Bis-Tris Discontinuous Buffer System with a 10% NuPAGE Novex Bis-Tris Pre-Cast Gel was used (Invitrogen, Carlsbad, CA). One microgram TSP was run on the gel and blotted onto a nitrocellulose membrane (Amersham Hybond™ ECL™; Amersham-Pharmacia Biotech) according to the manufacturer's instructions. The membrane was blocked with 1x PBS, 5% nonfat dry milk, 0.1% Tween-20 and incubated with primary antibody (mouse anti-E1, 1 μg/mL) and secondary enzyme conjugate antimouse IgG : HRPO (BD Transduction Laboratories™, BD Biosciences, San Jose, CA; 1 : 2000). The Pierce SuperSignal® West Pico Chemiluminescent Substrate was used for detection following the manufacturer's protocol (Pierce Biotechnology, Rockford, IL). The blot was exposed to X-ray film for 1 min and developed in a Kodak RP X-OMAT Processor.

### *Progeny Analyses*

Fertile $T_0$ plants expressing the highest percentages of E1 were self-pollinated or cross-pollinated. In some cases, transgenic ears were pollinated with wild-type pollen because of lack of sufficient transgenic pollen. Plants were allowed to mature and seeds were harvested after dry-down when the abscission layer had formed 35–45 d after pollination. $T_1$ seeds were germinated in vitro on 2.0 mg/L bialaphos selection medium *(33)* to determine segregation ratios of the offspring. Then, PCR analysis using the aforementioned primers was used to examine the presence of the *E1* gene in the progeny.

Table 1
Maize Transgenic Lines, Enzymatic Activity, and Percentage E1 Produced in Transgenic Plant TSP

| Plant | 1 | 2 | 3 | 4 | 5 | 6 | 7 | 8 | –C |
|---|---|---|---|---|---|---|---|---|---|
| E1 (%) | 1.16 | 0.35 | 0.27 | 0.26 | 0.18 | 0.05 | 0.03 | 0.02 | 0 |
| Activity (nmol/ μg/min) | 0.464 | 0.1408 | 0.109 | 0.104 | 0.072 | 0.02 | 0.012 | 0.008 | 0 |

### *Pretreatment of Biomass*

Milled corn stover (about 1 cm in length) was pretreated using the ammonia fiber explosion (AFEX) technology *(36)*. In more detail, the crop biomass was transferred to a high-pressure reactor (PARR Instrument Col, IL) with 60% moisture (kg water/kg dry biomass) and liquid ammonia ratio 1.0 (kg of ammonia/kg of dry biomass) was added. The temperature was slowly raised and the pressure in the vessel increased. The temperature was maintained at 90°C for 5 min before explosively releasing the pressure. The instantaneous drop of pressure in the vessel caused the ammonia to vaporize, causing an explosive decompression and considerable fiber disruption. The pretreated material was kept under a hood to remove residual ammonia and was stored in a freezer until further use.

### *Conversion Analyses*

E1 biomass conversion ability was assessed by measuring the reaction of TSP extracted from line 2 ( Fig. 3, Table 1) E1-expressing corn leaves, with soluble cellulose (carboxymethyl cellulose [CMC]), crystalline cellulose (Avicel®, FMC Biopolymer, Philadelphia, PA), and material containing both amorphous and crystalline cellulose, i.e., AFEX-pretreated corn stover *(36)*.

The enzyme hydrolysis was performed in a sealed scintillation vial. A reaction medium, made up of 7.5 mL of 0.1 *M*, pH 4.8 sodium citrate buffer, was added to each vial. In addition, 60 μL (600.0 μg) tetracycline and 45 μL (450.0 μg) cycloheximide were added to prevent the growth of microorganisms during the hydrolysis reaction. The corn stover substrate was hydrolyzed at a glucan loading of 1% (w : v) biomass. The TSP from the plant producing the E1 was concentrated to 1.8%. Two hundred and fifty milliliter of TSP containing 1.8% of E1 protein was used in the enzymatic hydrolysis experiment containing 1% substrate in a 15 mL reaction volume. The reaction was supplemented with 64 pNPGU/g glucan (Novo 188 from Sigma) to convert the cellobiose to glucose. Distilled water was then added to bring the total volume in each vial to 15 mL. All reactions were performed in duplicate to test reproducibility. The hydrolysis reaction was carried out at 50°C with a shaker speed of 90 rpm. About 1 mL of sample was collected at 72 h of hydrolysis, filtered using a 0.2 mm syringe

filter and kept frozen. The amount of glucose produced in the enzyme blank and substrate blank were subtracted from the respective hydrolyzed glucose levels. Hydrolyzate was quantified using Waters high-performance liquid chromatography by running the sample in Aminex HPX-87P (Biorad) column, against sugar standards.

## Results and Discussion

### *E1 Expression in Transgenic Corn*

Recently, the United States Government urged the agricultural and petrochemical industries to find and implement alternatives to fossil fuels to reduce dependence on the foreign oil. One of the specific recommendations has been the development of polysaccharide degrading enzymes within the crop plants *(37,38)*. To date, *A. cellulolyticus* the catalytic domain of E1 has been successfully produced in *Arabidopsis (12)* and tobacco *(13,26)* and the full-length E1 peptide in potato *(25)*. Also, the *Thermomonospora fusca* E2 was produced in alfalfa *(39)*. The apoplast is an ideal compartment for expressing foreign proteins because it is spacious compared with other cellular compartments, thus it has the ability to accumulate large quantities of foreign proteins *(12)*, and for expressing $E1\text{-}_{CAT}$ in particular because its pH matches that of *A. celloulolyticus*, i.e., pH 5.5–5.6. The catalytic domain of E1 has been shown to have more activity than the full-length peptide *(13)*. In the present study, corn Hi-II callus was genetically transformed with the catalytic domain of the *E1* gene, and over 100 herbicide-resistant transgenic plantlets were produced. Of these, 73 regenerated plants survived to the greenhouse stage. Integration of the *E1* coding sequence confirmed through PCR showed that 31 of these (data not shown) plants carried the *E1* transgene. Southern blotting further verified the integration of the *E1* transgene in these plants (Fig. 2).

Among 31 PCR positive transgenic plants, 16 showed biological activity as compared with control untransformed plants, as shown in percent in biologically active E1 in plant leaf extract TSP (Table 1). Percentages of E1 in TSP ranged from 0.01 to 1.16%. The assay was able to detect enzyme activity levels as low as 0.01% E1, which was accurately confirmed in the sample through Western blotting.

Nine plants were chosen for further study owing to having the highest levels of enzymatic activity. Western blotting confirmed the translation of E1, also showing differences in the production levels (Fig. 3).

pDM302 containing the *bar* selectable marker was used in plant numbers 1, 2, 3, and 6. pBY520 was used in plants number 4, 5, 7, 8, and 9 (Fig. 3). In general, the signal strength observed in the Western blot corresponded with the percentage E1 observed in activity assays (Fig. 2).

To obtain second-generation ($T_1$) transgenic seeds, the plants were self- or cross-pollinated in the greenhouse. The most successful crosses

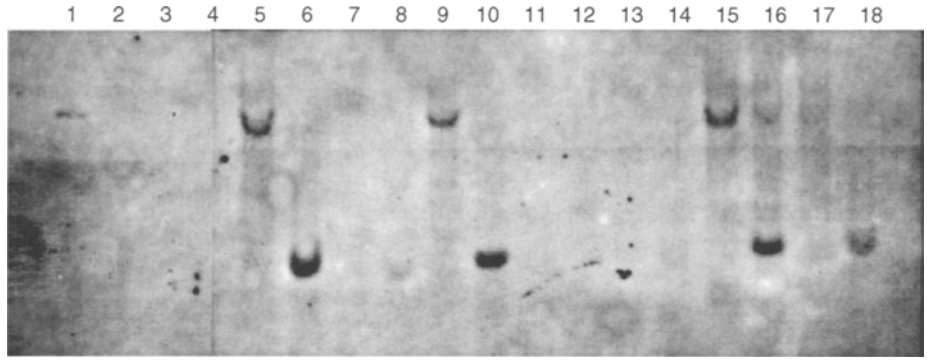


**Fig. 2.** Southern blot of transgenic maize plants. Genomic DNA from maize plants probed with the E1-$_{CAT}$. Lane 1, 10.0 pg of *Hin*dIII digested pMZ766-E1$_{CAT}$; lane 2, 10.0 pg of *Sac*I digested pMZ766-E1$_{CAT}$; lanes 3 and 4, untransformed maize control; lanes 5–18, seven pMZ766-E1$_{CAT}$ transformants; (5, 7, 9, 11, 13, 15, and 17) DNA digested with *Hin*dIII; (6, 8, 10, 12, 14, 16, and 18) DNA digested with *Sac*I.

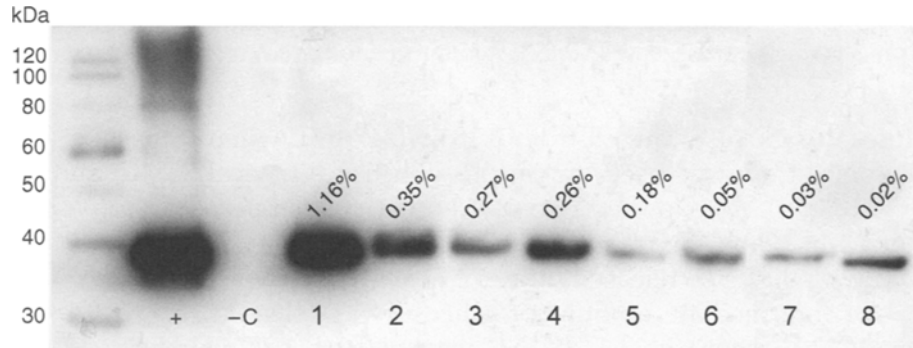


**Fig. 3.** Western blot of transgenic maize plants expressing E1. Western blot of 1.0 μg TSP from transgenic maize plants expressing E1. Lanes: +, positive tobacco control *(39)*; –C: negative maize control (untransformed); 1–9: transgenic maize plants. Invitrogen Magic Mark™ Western Standard used for size markings. Percentages of E1 as determined by enzyme activity assay are displayed above bands for reference, and also in Table 1.

included plant 2 crossed with plant 8; plant 3 crossed with nontransgenic control; plant 7 crossed with plant 8; and plant 8 crossed with plant 9.

When $T_1$ seeds were germinated on bialaphos selective medium, a 3 : 1 ratio was observed suggesting that the gene was transmitted as a single copy in a normal Mendelian fashion (data not shown). PCR analysis confirmed the transmission of the *E1* gene to the progeny (data not shown).

## *Conversion Analyses*

The hydrolytic conversion of corn stover using the plant-produced E1 was confirmed by adding transgenic corn stover TSP to three types of substrates: CMC, Avicel, and AFEX-pretreated corn stover. The conversion of

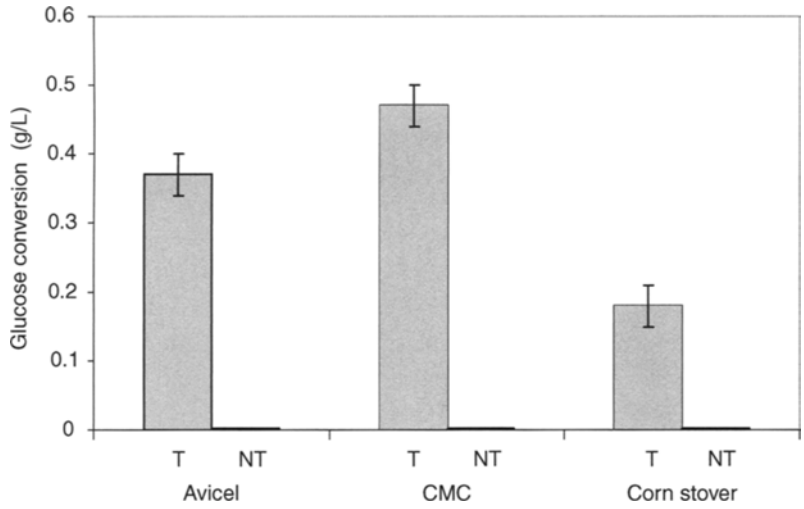


**Fig. 4.** Conversion of cellulose-to-glucose (g/L) using E1 produced from transgenic maize. The substrates used in the experiment were Avicel, CMC, and AFEX treated corn stover. The enzymatic hydrolysis was done for a period of 72 h, at 50°C with 90 rpm shaking. T, transgenic TSP; NT, nontransgenic TSP.

cellulose to glucose ranged from 0.18 to 0.47 g/L when transgenic plant TSP concentrate was used on various substrates (Avicel, CMC, and corn stover; Fig. 4). As expected, we saw higher sugar release up to 0.47 g/L (after 72 h) when the transgenic plant TSP was reacted with CMC compared with 0.37 g/L released (after 72 h) with Avicel (Fig. 4).

An intermediate amount of glucose was released, up to 0.18 g/L (after 72 h), when the E1 of TSP reacted with pretreated corn stover. Overall, the conversion results (Fig. 4) clearly show that there is a significant amount of E1 enzymatic activity in the TSP extracted from corn stover, because we could obtain a higher sugar yield as we increased the amount of TSP (results not shown).

It has been well documented that different cellulases work together synergistically to decrystallize and hydrolyze cellulose. For example, exoglucanases act on cellulose chain ends of crystalline cellulose, endo-1,4-β-glucanase E1 acts on the interior portions of the cellulose chain of amorphous cellulose, and β-glucosidase converts cellobiose released by cellulases to glucose *(40)*. All of the aforementioned enzymes, when derived from thermophilic microorganisms, have interesting characteristics such as stability at high temperature and extreme pH *(41)*. In recent years, use of thermostable enzymes in industry has been increasing wherein high temperatures are favored to reduce microbial contamination. The heterologous E1 produced in this study is from the thermophilic *A. cellulolyticus*. One advantage of using the *E1* gene from a thermophyllic microbe is that the plant in vivo temperature is low, and therefore the E1 enzyme accumulated in the plant apoplast would not harm the plant cell wall integrity.

Although *A. cellulolyticus* E1 enzyme is thermostable, the reaction in this study was performed at 50°C, because β-glucosidase, which has higher cellobiase activity at this temperature, was included in the reaction.

Based on a previous study, AFEX pretreatment destroys as much as two-thirds of the activity of plant-produced heterologous E1 *(36)*. As most of the pretreatment methods including AFEX follow stringent conditions, we extracted the transgenic TSP concentrate containing the biologically active E1 enzyme, and then added to the corn stover after pretreatment, followed by enzymatic hydrolysis. Production of polysaccharide degrading enzymes within the crop biomass may reduce the costs of production of these enzymes for biomass conversion into fermentable sugars. The enzymes could be extracted at the site of hydrolysis and fermentation to gain substantial reduction in the costs. The production of transgenic plant TSP is quick and very easy, and the E1 remains biologically active under freezer conditions for several months.

Although in this study we added the transgenic plant TSP to the AFEX-pretreated corn stover for conversion of cellulosic matter into glucose, it could be added to any other pretreated (acid and/or heat) lignocellulosic matter of any other crops (rice straw, switchgrass, wheat straw, and so on.). However, at the commercial level, it might be best to extract and lyophilize the enzymes for low-cost storage and easy transportation. The E1 and/or other polysaccharide degrading enzymes could be simultaneously produced and targeted to different cellular compartments of the same plants for a maximum enzyme production level *(38)*. This strategy was recently tested by single targeting of a xylanase heterologous enzyme to *Arabidopsis* chloroplasts and peroxysome as compared with its dual targeting to chloroplast and peroxysome *(42)*.

## Acknowledgments

The authors would like to thank National Renewable Energy Laboratory (NERL) for the availability of the E1 antibodies, Dr. K. Danna for the pZM766-$E1_{CAT}$ and Prof. Ray Wu for the pDM302 and pBY520. This study was financially supported by the STTR grant to Edenspace Systems Corp, Consortium for Plant Biotechnology Research (CPBR), Michigan State University Research Excellent Funds (REF), the Corn Marketing Program of Michigan, and the National Corn Growers' Association.

## References

1. Bordetsky, A., Hwang, R., Korin, A., Lovaas, D., and Tonachel, L. (2005), Issue Paper, Natural Resources Defense Council, Institute for the Analysis of Global Security.
2. Renewable Fuels Association (2005), Ethanol Industry Outlook Report, Washington, DC.
3. Perlack, R. D., Wright, L. L., Turhollow, A. F., Graham, R. L., Stokes, B. J., and Erbach, D. C. (2005), Technical Report, US Department of Energy and US Department of Agriculture, Oak Ridge, TN.
4. Kim, S. and Dale, B. E. (2004), *Biomass Bioenergy* **26,** 361–375.

5. Greene, N., Celik, F. E., Dale, B., et al. (2004), Issue Paper, Natural Resources Defense Council.
6. Singh, S. P., Ekanem, E., Wakefield, T., and Comer, S. (2003), *Int. Food Agribusiness Manage. Rev.* **5,** 1–15.
7. Knauf, M. and Moniruzzaman, M. (2004), *Int. Sugar. J.* **106,** 147–150.
8. Sticklen, M. B. (2004), 2nd International Ukrainian Conference on Biomass for Energy, Kyiv, Ukraine, 20–22 September 2004, pp. 133.
9. Ingledew, W. M. (1995), In: *The Alcohol Textbook.* Lyons, T. P., Kelsall, D., and Murtagh, J., (eds.), Nottingham University Press, Nottingham, UK, pp. 55–79.
10. Lynd, L. R., van Zyl, W. H., McBride, J. E., and Laser, M. (2005), *Curr. Opin. Biotechnol.* **16,** 577–583.
11. Kabel, M. A., van der Maarel, M. J. E. C., Klip, G., Voragen, A. G. J., and Schols, H. A. (2006), *Biotechnol. Bioeng.* **93,** 56–63.
12. Ziegler, M. T., Thomas, S. R., and Danna, K. J. (2000), *Mol. Breeding* **6,** 37–46.
13. Ziegelhoffer, T., Raasch, J. A., and Austin-Phillips, S. (2001), *Mol. Breeding* **8,** 147–158.
14. Howard, R. L., Abotsi, E., Jansen van Rensburg, E. L., and Howard, S. (2003), *Afr. J. Biotechnol.* **2,** 602–619.
15. Wyman, C. E. (1999), *Annu. Rev. Energy Environ.* **24,** 189–226.
16. Horn, M. E., Woodard, S. L., and Howard, J. A. (2004), *Plant Cell Rep.* **22,** 711–720.
17. Hong, C. -Y., Cheng, K. -J., Tseng, T. -H., Wang, C. -S., Liu, L. -F., and Yu, S. -M. (2004), *Transgenic Res.* **13,** 29–39.
18. Chiang, C. -M., Yeh, F. -S., Huang, L. -F., et al. (2005), *Mol. Breeding* **15,** 125–143.
19. Liu, H. L., Li, W. S., Lei, T., et al. (2005), *Acta Biochim. Biophys. Sin.* **37,** 153–158.
20. Schulman, A. H. (2002), In: *Plant Biotechnology and Transgenic Plants,* Oksman-Caldenetey, K. -M. and Barz, W. H. (eds.), Basel, New York, pp. 255–282.
21. Sahrawy, M., Avila, C., Chueca, A., Canovas, F. M., and Lopez-Gorge, J. (2004), *J. Exp. Bot.* **55,** 2495–2503.
22. Qi, B., Fraser, T., Mugford, S., Dobson, G., et al. (2004), *Nat. Biotech.* **22,** 739–745.
23. Baker, J. O., Adney, W. S., Nieves, R. A., Thomas, S. R., Wilson, D. B., and Himmel, M. E. (1994), *Appl. Biochem. Biotehnol.* **45–46,** 245–256.
24. Tucker, M. P., Mohegheghi, A., Grohmann, K., and Himmel, M. E. (1989), *Bio/Technol.* **7,** 817–820.
25. Dai, Z., Hooker, B. S., Anderson, D. B., and Thomas, S. R. (2000), *Mol. Breeding* **6,** 277–285.
26. Dai, Z., Hooker, B. S., Anderson, D. B., and Thomas, S. R. (2000), *Transgenic Res.* **9,** 43–54.
27. Xu, D., Duan, X., Wang, B., Hong, B., Ho, T., and Wu, R. (1996), *Plant Physiol.* **110,** 249–257.
28. Cao, J., Duan, X., McElroy, D., and Wu, R. (1992), *Plant Cell Rep.* **11,** 586–591.
29. Armstrong, C. L., Green, C. E., and Phillips, R. L. (1991), *Maize Genet. Coop. Newslett.* **65,** 92–93.
30. Vain, P., McMullen, M. D., and Finer, J. J. (1993), *Plant Cell Rep.* **12,** 84–88.
31. Chu, C. C., Wang, C. C., Sun, C. S., Hus, C., Yin, K. C., and Chu, C. Y. (1975), *Sci. Sinica* **18,** 659–668.
32. Armstrong, C. L. and Green, C. E. (1985), *Planta* **164,** 207–214.
33. Zhang, S., Warkentin, D., Sun, B., Zhong, H., and Sticklen, M. (1996), *Theor. Appl. Genet.* **92,** 752–761.
34. Saghai-Maroof, M. A., Soliman, K. M., Jorgensen, R. A., and Allard, R. W. (1984), *Proc. Natl. Acad. Sci. USA* **81,** 8014–8018.
35. Bradford, M. (1976), *Anal. Biochem.* **72,** 248–254.
36. Teymouri, F., Alizadeh, H., Laureano-Perez, L., Dale, B. E., and Sticklen, M. B. (2004), *Appl. Biochem. Biotehnol.* **116,** 1183–1192.
37. Ragauskas, A. J., Williams, C. K., Davison, B. H., et al. (2006), *Science* **311,** 484–489.
38. Sticklen, M. B. (2006), *Curr. Opin. Biotechnol.* **17(3),** 315–319.

39. Ziegelhoffer, T., Will, J., and Austin-Phillips, S. (1999), *Mol. Breeding* **5,** 309–318.
40. Bayer, E. A., Chanzy, H., Lamed, R., and Shoham, Y. (1998), *Curr. Opin. Struct. Biol.* **8,** 548–557.
41. Bruins, M. E., Janssen, A. E. M., and Boom, R. M. (2001), *Appl. Biochem. Biotehnol.* **90,** 155–186.
42. Hyunjong, B., Lee, D. -S., and Hwang, I. (2006), *J. Exp. Bot.* **57,** 161–169.

0273-2289/1559-0291 (Online)/07/136-140/221-238/$30.00

# The Impact of Enzyme Characteristics on Corn Stover Fiber Degradation and Acid Production During Ensiled Storage

HAIYU REN,[1] TOM L. RICHARD,*[,1] AND KENNETH J. MOORE[2]

*[1]Department of Agricultural and Biological Engineering, 249 Agricultural Engineering Building, University Park, Pennsylvania 16802, E-mail: trichard@psu.edu; and [2]Department of Agronomy, 2101 Agronomy Hall, Iowa State University, Ames, Iowa 50011*

## Abstract

Ensilage can be used to store lignocellulosic biomass before industrial bioprocessing. This study investigated the impacts of seven commercial enzyme mixtures derived from *Aspergillus niger*, *Trichoderma reesei*, and *T. longibrachiatum*. Treatments included three size grades of corn stover, two enzyme levels (1.67 and 5 IU/g dry matter based on hemicellulase), and various ratios of cellulase to hemicellulase (C : H). The highest C : H ratio tested, 2.38, derived from *T. reesei*, resulted in the most effective fermentation, with lactic acid as the dominant product. Enzymatic activity during storage may complement industrial pretreatment; creating synergies that could reduce total bioconversion costs.

**Index Entries:** Biomass; cellulase; hemicellulase; silage; wet storage; pretreatment.

## Introduction

In recent years, corn stover, the above-ground residue of maize plants grown for grain, has attracted intensive interest as lignocellulosic feedstock for bioethanol production because of its considerable availability and biorenewability *(1)*. Around 69 million dry Mg/yr can be sustainably harvested in the United States *(2)*. More than 85% of the available corn stover is concentrated in midwestern states *(3)*, which would reduce industrial-scale harvesting and transportation costs as biomass-based industries develop and mature. The rich content of polysaccharides in corn stover can be hydrolyzed to five- and six-carbon sugars for fermentation and chemical modification to produce value-added products *(4–6)*. Corn stover can also serve as fiber feedstock for particle board manufacturing

*Author to whom all correspondence and reprint requests should be addressed.

*(7,8)*. Considerable efforts have been carried out to develop bioconversion processes and utilization strategies for corn stover *(9–11)*.

Bioconversion of corn stover from its raw form as a plant in the field to final commercial products requires four vital processing phases: harvesting, storage, pretreatment, and bioconversion. Additional steps provide links between these phases, such as transportation of the stover, neutralization of pretreatment chemicals, and removal of toxic byproducts before sugar fermentation. Although technical issues involved in the processes of pretreatment and bioconversion have been extensively investigated, the storage phase has received little attention to date. Because corn stover in the United States can only be harvested once a year, storage is needed to preserve large quantities of stover to provide a continuous supply to future biorefineries. Minimum criteria for storage include: minimizing dry matter (DM) loss, and reducing risk of fire. In addition, it would be preferable if beneficial pretreatment for downstream bioconversion could occur during the preservation period.

Ensilage, a traditional crop preservation method for ruminant feed, has been examined as a preservation method for corn stover and wheat straw *(12–14)*. The high moisture content of silage (up to 60% wet basis) eliminates the risk of accidental fire. A robust lactic acid fermentation initially results in rapidly declining pH, and this low pH then inhibits most microbial activity and DM loss as long as anaerobic conditions are maintained. Ensiled storage can provide stable storage with minimal DM deterioration for as long as 1 yr *(15)*. Acid hydrolysis of the cell wall by lactic and other produced acids can occur during the entire storage period, which may be beneficial for downstream cell wall degradation. However, the low sugar content of corn stover makes it difficult to obtain a robust lactic acid fermentation, resulting in more moderate pH that permits undesirable microbial growth, such as clostridia, whose secondary fermentations reduce stability and degrade the biomass. Amending the corn stover ensilage process with cell wall degrading enzymes has been shown to generate lower pH values, increase fiber hydrolysis to sugars, and conserve water-soluble carbohydrates (WSC), thus providing partial pretreatment for downstream bioconversion into sugar platform chemicals and fuels *(16)*. Enzyme treatment has also been shown to improve downstream manufacturing of stover-based biocomposite materials. Particle board made from ensiled stover had enhanced physical strength and dimensional stability *(12)*.

Enzymes prepared from different aerobic fungi have been observed to have various impacts on improving silage quality, although mechanistic investigations in an ensilage context are lacking. When *Trichoderma reesei* and *Aspergillus niger* were compared as amendments for ryegrass–clover silage, the most active degradation of cellulose and lower pH were found with *T. reesei (17)*. However, the activity of individual enzyme components was not discussed or quantified in their study. Different microorganisms

produce different types and proportions of individual enzymes, and their overall activity is a function of the characteristics and composition of these enzyme components. *T. reesei* excretes a complete set of cellulases with appreciable levels of endoglucanase and cellobiohydrolase *(18)*. However, the level of β-glucosidase is not sufficient to thoroughly hydrolyze cellobiose, thus limiting the complete saccharification of cellulose to glucose *(19)*. *A. niger* is another widely studied and commercially-used enzyme producer. The β-glucosidase productivity was found to be 4.8 times higher that of *T. reesei (20)*. But the activities of endoglucanase and cellobiohydrolase are weaker compared with *T. reesei*, even with genetically improved mutants *(21,22)*. A recent study of enzyme effects on maize silage used enzymes derived from *Flavobacterium xylanivorum*, *T. reesei*, and *Thermoascus acrantiacus*, which are psychrophilic, mesophilic, or thermophilic organisms, respectively *(23)*. Colombatto et al.'s study found that the enzymes derived from *T. reesei* and *T. acrantiacus* reduced pH values and cellulose content significantly more than those of *F. xylanivorum*. These differences may also be caused by the various ratios and activities of individual enzyme components, including xylanase, endoglucanase, exoglucanase, and β-glucosidase, acting in synergistic mixtures.

Similarly, there have been few detailed investigations of the effect of combinations of cellulase and hemicellulase enzymes on silage. The crosslinked spatial orientation of cellulose and hemicellulose in the cell wall is such that complete enzymatic hydrolysis of biomass requires synergistic interactions of cellulases and hemicellulases *(24)*. As most commercial enzyme additives are already mixtures of cellulase and hemicellulase, the effect of these additives on silage chemical composition is actually an integrated effect of these synergistic interactions. As one example of such synergy, hydrolysis of hemicellulose has been reported to increase the effective surface area of cellulose fibrils and, therefore, enhance cellulose hydrolysis *(25)*. But we are not aware of any previous studies that have attempted to optimize the ratios of these enzymes to maximize the synergistic effects.

Effective and economical application of commercial enzymes for corn stover preservation requires a full characterization of the enzyme additives, including the microbial organisms they are derived from and the ratios of individual enzymes in each mixture. The present study

1. Investigated and characterized cell wall degrading enzymes from three microbial sources: *T. reesei*, *A. niger*, and *T. longibrachiatum*.
2. Examined the effect of various ratios of cellulase to hemicellulase from these sources on the biochemical transformations of corn stover during ensilage.

Because stover particle size might influence the contact efficiency and hydrolysis efficacy of the enzymes *(26,27)*, particle size was considered as an additional treatment variable in this study.

## Methods

### Corn Stover and Silage Preparation

Corn stover was harvested by chopping, windrowing, and baling in the fall of 2002. Stover was then milled by using an Art's-Way hammer mill (Art's-Way, Armstrong, IA) 0, 1, and 2 times to obtain three size grades of samples. The original coarse corn stover, once milled (0.5–1.0 cm) and twice milled (0.1–0.5 cm) stover sizes are called course, medium, and fine, respectively. The samples contained 16–20% moisture (wet basis [w.b.]) and were adjusted to 60% (w.b.) by adding water. A moisture level of 60% (w.b.) was previously determined to be the optimum moisture to minimize clostridia and secondary fermentations in a previous study *(28)*.

Six replicates of each treatment (a complete factorial of three size fraction × seven enzyme treatment × enzyme rate) were prepared, with three replicates of each treatment destructively sampled on day 0 and the other three destructively sampled on day 21. For each replicate, 500 g of treated sample was packed tightly into a 20 × 35 $cm^2$ polyethylene bag (200 g dry mass mixed with 300 g water), which was immediately placed under 25 in. mercury vacuum and heat sealed. Samples were incubated at 37 ± 1°C for 21 d. At the end of this preservation period samples were taken for DM and pH measurement. The remainder of each sample was stored frozen for later analysis of lactic acid, volatile fatty acids, WSC, and fiber fractions.

### Industrial Enzyme Additives

Seven enzymes derived from three different filamentous fungi were added to the three size grades of corn stover at two different levels. These seven enzymes were chosen from an initial pool of 15 commercial enzymes to represent a diversity of microbial sources and a wide ratio of cellulase to hemicellulase. A description of the seven enzyme characteristics is summarized in Table 1.

Endo-1,4-β-glucanase, cellobiohydrolase, and cellobiase were measured according to the methods described by Wood and Bhat *(29)* by using carboxymethylcellulose, avicel, and cellobiose as substrate, respectively. Hemicellulase measurement used 1% birchwood 4-*O*-methyl glucoronoxylan (Roth 7500) as substrates *(30)*. The enzymes were applied in liquid solution with water to adjust moisture content and were mixed evenly with the stover. The amount of enzymes applied was based on two constant hemicellulase activities: 1.67 IU/g dry mass and 5.0 IU/g dry mass. The data in each column is the measured activity for each enzyme, with the ratio of the enzyme to hemicellulase in parenthesis. Every enzyme has the same units as presented for hemicellulase. The last column is the code representing each enzyme, with a letter for microbial source and number for the ratio of endo-1,4-β-glucanase to hemicellulase (C : H). Endo-1,4-β-glucanase was chosen to quantify cellulase based on the facts that:

Table 1
Characteristics of Industrial Enzymes Used to Ensile Corn Stover

| Microbial source | Units | Hemi-cellulase | Endo-1, 4-β-glucanase | Cellobio-hydrolase | Cellobioase | ID: source and C : H[a] |
|---|---|---|---|---|---|---|
| *A. niger* | IU/g | 24,805 | 1904 (0.08)[b] | 42.9 (0.002) | 87.4 (0.003) | AN0.08 |
| | IU/g | 1075 | 384 (0.36) | 34.6 (0.03) | 84.3 (0.080) | AN0.36 |
| *T. reesei* | IU/mL | 5712 | 109 (0.02) | 5.31 (0.001) | 3.1 (0.0005) | TR0.02 |
| | IU/g | 1219 | 2607 (2.14) | 247.1 (0.20) | 36.6 (0.03) | TR2.14 |
| | IU/mL | 116 | 278 (2.38) | 45.8 (0.39) | 5.4 (0.047) | TR2.38 |
| *T. longibra-chiatum* | IU/g | 18,624 | 5144 (0.28) | 50.9 (0.003) | 79.5 (0.004) | TL0.28 |
| | IU/mL | 390 | 543 (1.39) | 18.2 (0.05) | 7 (0.018) | TL1.39 |

[a]The ratio of combined cellulase activity to hemicellulase activity.
[b]The ratio of individual cellulase activity to hemicellulase activity.

1. The order of the ratios of filter paper unit to hemicellulase of these seven enzymes is the same as that of the ratio of Endo-1,4-glucanase : H.
2. Endo-1,4-β-glucanase initiates the degradation of cellulose by randomly and rapidly shortening the cellulose chain.

## *Chemical Analysis of Silages*

DM was determined by drying 100 g of fresh samples at 60°C in a forced air oven for 48 h, whereas pH was determined using a pH electrode on samples at a 10 : 1 ($H_2O$ : sample) mass dilution. Lactic acid and volatile fatty acids were determined using gas-liquid chromatography with SP-1000/1200-$H_3PO_4$ columns (Supelco, Inc., Bellefonte, PA) and a flame-ionization detector. The operating temperatures for the oven, injector, and flame detector were 120, 170, and 180°C, respectively. Neutral detergent fiber (NDF), acid detergent fiber (ADF), and acid detergent lignin (ADL) were determined by the method of Vogel et al. *(31)*. Hemicellulose content was calculated as the difference between NDF and ADF, and cellulose as the difference between ADF and ADL. WSCs were determined by the modified phenol-sulfuric acid method described by Guiragossian et al. *(32)*.

## *Statistical Analysis*

Data were analyzed using generalized linear model procedure of Statistical Analysis System edition 9.1 *(33)*. Differences between treatments

Table 2
Initial pH, Fiber Fraction, and WSC of Each Stover Size Fraction

| | Coarse | Medium | Fine |
|---|---|---|---|
| pH | 7.32 ± 0.067[a] | 7.77 ± 0.078 | 7.49 ± 0.017 |
| WSC[b] (% d.b.) | 1.32 ± 0.05 | 1.84 ± 0.09 | 1.88 ± 0.17 |
| NDF[c] (% d.b.) | 80.72 ± 0.08 | 75.61 ± 0.32 | 72.72 ± 0.75 |
| ADF[d] (% d.b.) | 48.32 ± 0.48 | 43.07 ± 0.45 | 43.12 ± 1.16 |
| ADL[e] (% d.b.) | 5.08 ± 0.13 | 5.03 ± 0.21 | 7.56 ± 0.70 |
| Ash (% d.b.) | 1.01 ± 0.10 | 1.62 ± 0.10 | 4.10 ± 0.94 |
| Cellulose (% d.b.) | 43.24 ± 0.57 | 38.04 ± 0.23 | 35.56 ± 1.85 |
| Hemicellulose (% d.b.) | 32.40 ± 0.41 | 32.54 ± 0.19 | 29.59 ± 0.49 |

[a]Average ± standard error.
[b]WSC, water-soluble carbohydrates.
[c]NDF, neutral detergent fiber.
[d]ADF, acid detergent fiber.
[e]ADL, acid detergent lignin.

were determined by Tukey's test. Significance of all analyses was declared at a 5% probability level.

## Results

### *Characterization of Initial Feedstocks*

The initial characteristics of each stover size are shown in Table 2. There were some variations in fiber composition among the three sizes, with concentrations of cellulose decreasing and WSC increasing in the ground fractions relative to the coarse, unground size. These losses may result from natural degradation by plant enzymes or microorganisms acting on surfaces exposed by grinding, which could have occurred during dry storage before the stover was used for experiments. This hypothesis is supported by a lower hemicellulose concentration and increases in ADL and ash concentrations in the fine fraction, suggesting that considerable loss of biodegradable constituents may have occurred in these ground fractions.

### *pH Value of Stover Silage*

The pH value of stover silage dropped from 7.32–7.77 to 3.79–4.76 after a 21-d ensilage process. Increasing C : H ratio resulted in lower final pH values within all three microbial sources of enzymes on medium-sized stover (Fig. 1). However, the enzyme treatments with a low C : H ratio, especially at low enzyme concentrations, did not reduce pH significantly compared with the control sample ($p$ = 0.814 for TR0.02; $p$ = 0.114 for AN0.08) (pH value around 4.73–4.8). The *T. reesei* (TR) treatment with the highest C : H ratio of 2.38 had the lowest pH value, 3.79, which should effectively guarantee low levels of microbial activity and high preservation

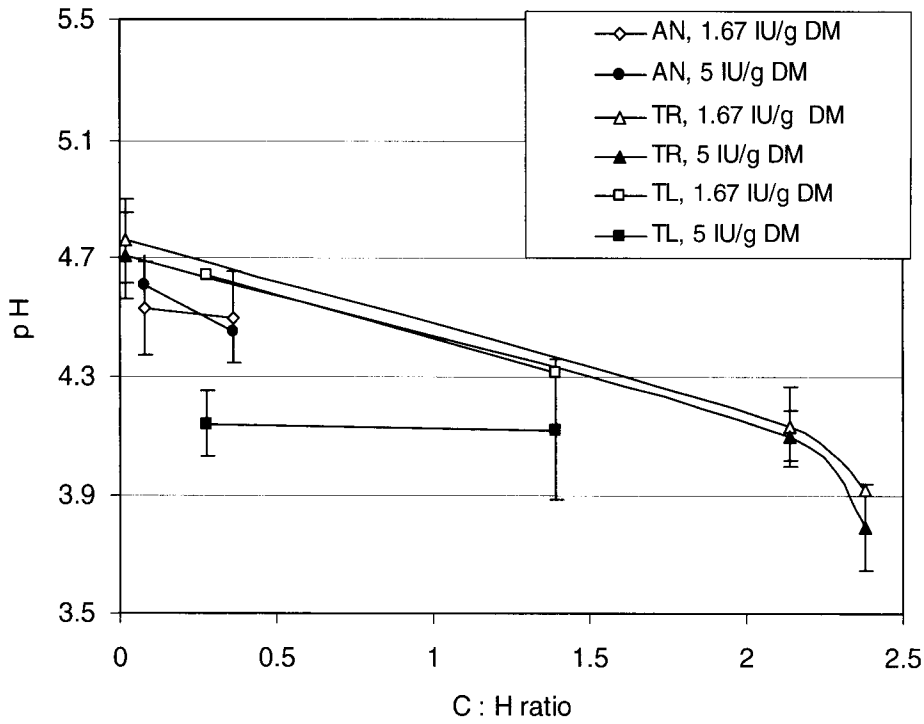


**Fig. 1.** The pH change of ensiled corn stover vs the C : H ratio of enzyme additives for the medium size stover. (AN represents enzymes from the *A. niger* microbial source; TR represents enzymes from *T. reesei*; and TL represents enzymes from *T. longibrachiatum*. Each enzyme product with a specific C : H ratio is represented by data points, with the white color for low-enzyme concentrations and black for the high concentration).

quality. For ensiled storage of biomass, low pH is desired not only for preservation purposes, but also to create an acidic condition to enhance hydrolysis. These acids partially break down the glycosidic linkages of microfibrils of cell walls, especially hemicellulose, during long-term storage. Dewar et al. *(34)* investigated hemicellulose degradation at various pH levels for 90 d and suggested that considerable hydrolysis of hemicelluloses can be obtained at pH 4.0. This can be presumed to be a beneficial pretreatment for downstream degradation.

Differences among microbial sources are reflected in the observation that higher C : H ratios did not guarantee a lower pH value. For example, at 1.67 IU/g DM, TL0.28 did not resulted in a significantly lower pH value than that of AN0.08 ($p = 0.407$). The enzyme complexes produced by different microbial sources generated different responses in terms of pH. Increasing the level of the TR enzymes did not significantly reduce pH ($p = 0.713$), suggesting that this enzyme system's hemicellulase component was already sufficient at the lower 1.67 IU/g DM rate. Increasing C : H ratio did increase the response for the TR enzymes, demonstrating the importance of synergistic effects. For *T. longibrachiatum* (TL) enzymes, the increase of

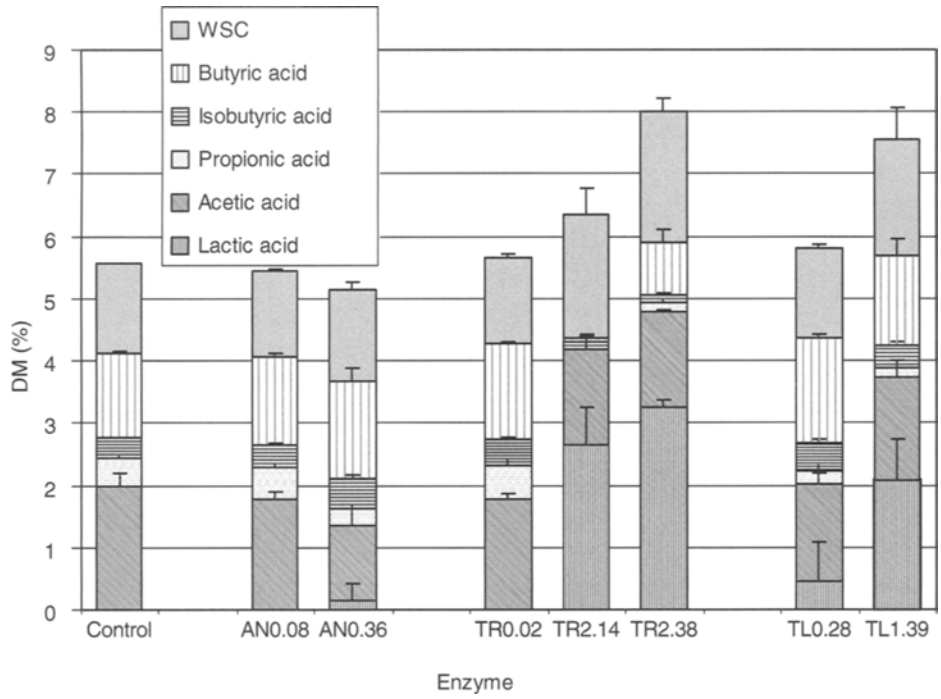


**Fig. 2.** Concentration of water soluble carbohydrate and organic acids with different enzyme treatments at the level of 1.67 IU/g DM for the fine size stover (AN, TR, and TL represent the microbial sources of various enzyme products, standing for *A. niger*, *T. reesei*, and *T. longibrachiatum* respectively. The numbers following AN, TR, and TL are the ratios of endo-1,4-β-glucanase to hemicellulase [C : H] of the enzyme products).

enzyme levels had a more significant effect in reduced pH value at the C : H ratio of 0.28 than at a C : H ratio of 1.39, suggesting that hemicellulase sufficiency for this enzyme complex occurred between these two rates, and that cellulase was sufficient for both C : H ratios at the higher 1.67 IU/g DM hemicellulase rate. Only two relatively low C : H ratios were tested for the *A. niger* (AN) enzymes. For this enzyme source there was not a significant effect of hemicellulase level, suggesting that enzyme concentration was sufficient at the lower rate. Although not significant, there was a slight trend with increasing C : H, which might have been significant if enzyme mixtures had been available over a larger C : H range.

## *Chemical Composition of Corn Stover Silage*

The nature of the mixed fermentation process and the quality of ensiled stover are reflected in the final chemical composition. Combinations of high concentrations of lactic acid and low concentrations of butyric acid in silage indicate a more active lactic acid fermentation and more dormant secondary fermentations *(12,35)*. The chemical composition of stover samples treated

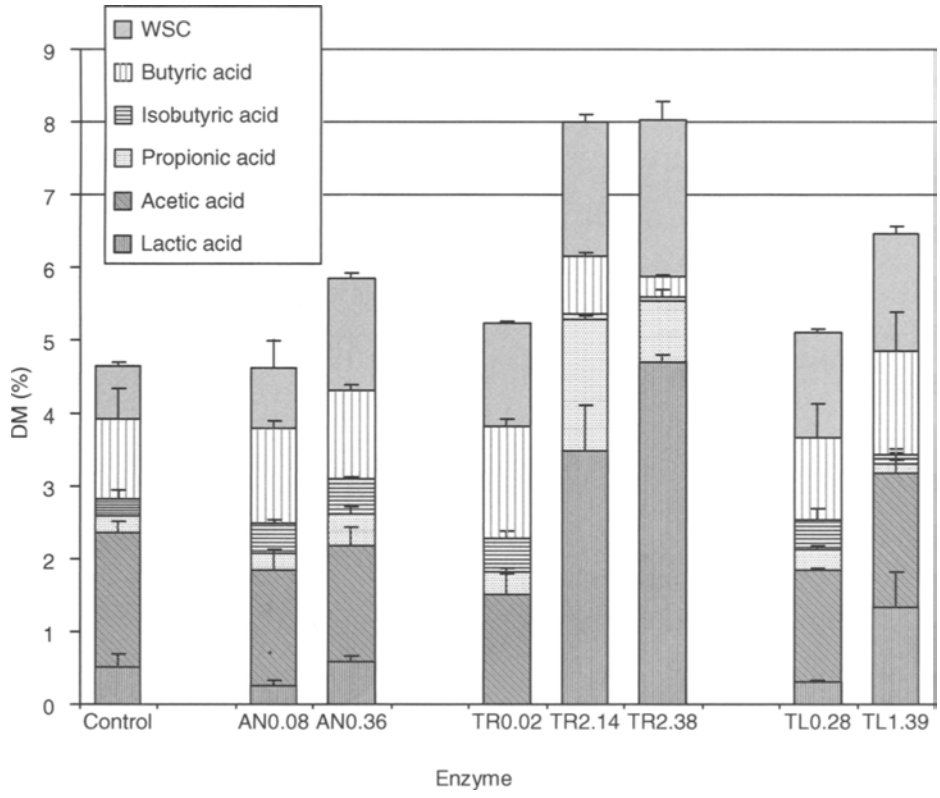


**Fig. 3.** Concentration of water soluble carbohydrate and organic acids with different enzyme treatments at the level of 1.67 IU/g DM for the medium size stover (AN, TR, and TL represent the microbial sources of various enzyme products, standing for *A. niger*, *T. reesei*, and *T. longibrachiatum*, respectively. The numbers following AN, TR, and TL are the ratios of endo-1,4-β-glucanase to hemicellulase [C : H] of the enzyme products).

and stored for 21 d are presented in Figs. 2–4. Each figure is for one stover size, and includes results for all seven enzyme types at 1.67 IU/g DM hemicellulase as well as the control. For each microbial source, increases of C : H ratio generally resulted in higher concentrations of lactic acid and lower concentrations of butyric acid. This trend was most significant for all three sizes of stover treated with enzymes from the TR microbial source ($p < 0.001$ for lactic acid and $p = 0.013$ for butyric acid). The fraction of lactic acid in the total acid products was highest for the TR 2.38 treatment in the medium size, where it was 80%. This represented the most efficient treatment for silage preservation, as fermented WSCs were primarily metabolized into lactic acid to lower the pH. For the enzymes derived from AN and TL microbial sources, increasing the C : H ratio only increased the lactic acid concentration, without consistently decreasing the amount of acetic acid and butyric acid. The fraction of lactic acid was not improved by the increased C : H ratio because of similar or greater increases in total acid products.

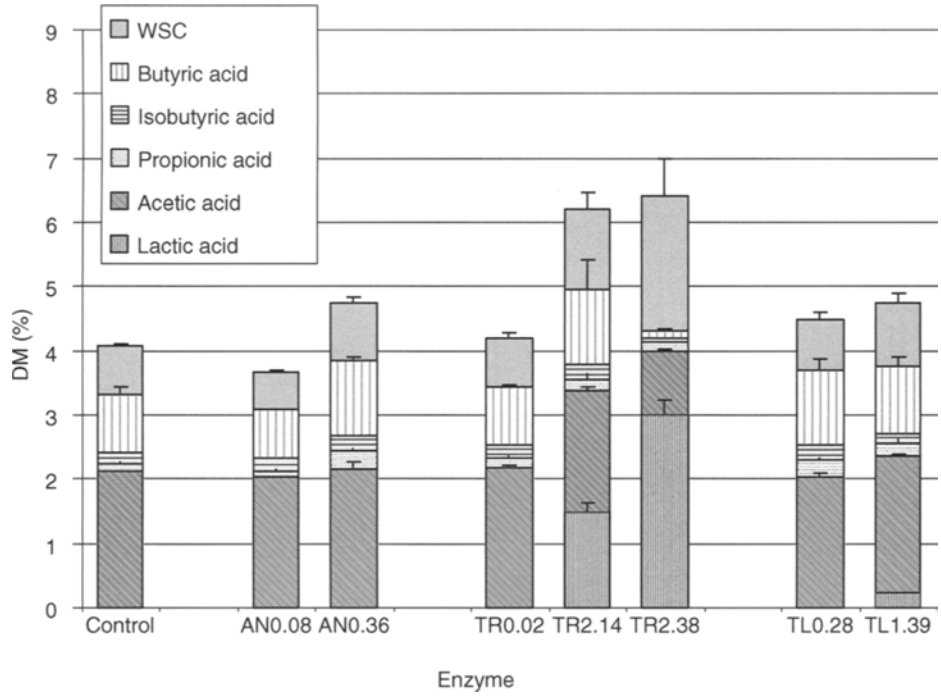


**Fig. 4.** Concentration of water soluble carbohydrate and organic acids with different enzyme treatments at the level of 1.67 IU/g DM for the coarse size stover (AN, TR, and TL represent the microbial sources of various enzyme products, standing for *A. niger*, *T. reesei*, and *T. longibrachiatum*, respectively. The numbers following AN, TR, and TL are the ratios of endo-1,4-β-glucanase to hemicellulase [C : H] of the enzyme products).

Ideally, for silage preservation purposes, the enzyme treatments would exclusively encourage lactic acid fermentation with little or no contribution to secondary fermentation. If the enzyme treatment is not sufficient to encourage lactic acid production and reduce the pH low enough to inhibit clostridia, enzymatically hydrolyzed sugars will be mostly converted to an undesirable acid mixture *(36)*. For example, Mandebvu et al. *(37)* found that the treatment of bermudagrass silage with enzymes increased the butyric acid concentration without improving lactic acid or WSC production. In contrast, Jakhmola et al. *(38)* reported that the addition of cellulase had no significant effect on the forage quality of perennial ryegrass, nor on a mixture of perennial ryegrass and white clover mixed with shredded barley straw. Inadequate enzyme levels may also encourage yeast growth and ethanol production *(36)*. Enzyme treatments will not be beneficial for preservation if degraded sugars are not sufficient to initiate a dominate lactic acid fermentation. If hydrolyzed sugars are instead allowed to assimilate by undesirable microorganisms, these treatments could lead to substantial DM loss. Environmental and chemical conditions in the first hours and days of a silage process are crucial for establishing and maintaining a lactic-acid-dominated system and an appropriate microbial ecosystem.

For all three stover sizes, some enzyme treatments with a low ratio of C : H (AN0.08, AN0.36, TR0.02, and TL0.28) did not produce much lactic acid. It is interesting that for the medium size stover, the lactic acid produced by AN0.08, TR0.02, and TL0.28 treatments was even lower than that of the control samples, although some of these differences were not statistically significant ($p = 0.074$ for AN0.08; $p = 0.007$ for TR0.02; and $p = 0.21$ for TL0.28). Only TR2.14, TR2.38, and TL1.39, which had higher C : H ratios, enhanced lactic acid concentration significantly ($p < 0.001$ for TR2.14; $p < 0.001$ for TR2.38; and $p = 0.033$ for TL1.39). Cellulases play a much more important role in silage preservation than hemicellulase, because most of the hydrolyzed sugars come from the cellulose fraction *(15)*. Ren et al. *(12)* observed that cellulose degradation is more sensitive to enzyme addition than hemicellulose. This difference was attributed to the heterogeneous structure of the hemicellulose and hemicellulase specificity. Thus, for the purpose of encouraging lactic acid fermentation, a certain amount of cellulase is required in the enzyme mixture. A higher ratio of C : H can result in an elevated lactic acid content in the final silage composition.

It is difficult to examine the effects of microbial enzyme sources on stover silage using the present enzyme selection. These enzymes were produced and separated by different processes, and therefore cannot be assumed to have the same composition for individual enzyme components even when produced by the same microbial source. However, the results seem to provide useful insights. When choosing enzymes available in the market for enzyme screening work, it was noticed that enzymes from AN always had a lower ratio of C : H compared with those of TR. Our results indicated that cellulases produced by AN always have lower activity of endo-1,4-β-glucanase per gram enzyme than those of TR when the comparison is based on the same hemicellulase activity , which is consistent with the work of Kang et al. *(21)* and Kim et al. *(22)*.

An expected effect of enzyme addition is increased hydrolysis of the cell wall, releasing sugars that increase WSC content *(39,40)*. However, in this study AN and TL enzymes did not enhance WSC content significantly in fine and coarse size material when compared with control samples ($p = 0.66$ for AN in fine size; $p = 0.93$ for AN in coarse size; $p = 0.227$ for TL in fine size; $p = 0.402$ for TL in coarse size). Only in the medium size, AN0.36, TL0.28, and TL1.39 treatments resulted in significant increase of WSC compared with control samples ($p < 0.001$). TR enzymes did significantly increase WSC content in each of the three sizes with the increase of C : H ratio ($p = 0.006$ for fine size; $p = 0.002$ for medium size; and $p = 0.03$ for coarse size). The different effects of enzyme addition on WSC content depend on the fate of degraded WSC during the ensilage process *(15)*. The WSC content is the difference between the amount of initial WSC and hydrolyzed WSC, and the amount of the WSC metabolized by microorganisms *(17,41)*. The amount of both hydrolyzed WSC and metabolized WSC is influenced by the activity of microbial communities, especially

lactic acid bacteria, throughout the ensilage process. This microbial consumption of hydrolyzed glucose can reduce or eliminate the glucose inhibition effects on cellobioase, resulting in an accelerated and more complete hydrolysis of the cell wall *(42)*.

The net result of these inputs and outputs to the WSC pool is determined by the initial biomass characteristics including its WSC content, the amounts of cellulose and hemicellulose hydrolyzed to WSC by native and introduced enzymes, the population dynamics of vegetative microorganisms, and the metabolic pathways used by the microorganisms. For enzymes with a low ratio of C : H, such as AN0.08, TR0.02, and TR0.28, the relatively constant WSC can be attributed to a low level of cellulase activity that is not sufficient to generate large amounts of WSCs. Low levels of WSCs early in the ensilage process limited lactic acid production and the resulting pH decline, allowing secondary fermentations by clostridia to dominate in these treatments. For TR2.14 and TR2.38, a significant amount of lactic acid was fermented from the available WSCs in silage, and although this lactic acid consumed WSCs, low pH and reduced secondary fermentation resulted in a final WSC that was still significantly higher than the control samples ($p < 0.001$). Previous long-term trials have demonstrated that cell wall hydrolysis continues throughout the ensilage process *(12)*. The conversion of some of the initial sugars to lactic acid encourages more sugar production, resulting in higher final WSC concentrations in these treatments.

### *Fiber Degradation of Corn Stover Silage*

Degradation of cellulose and hemicellulose at the two levels of enzyme addition are presented in Figs. 5 and 6. Degradation is reported as the difference between initial and final concentrations divided by the initial concentration (all on a dry matter basis [d.b.]), and thus assumes negligible DM loss. The average DM loss in previous experiments was 2.7% d.b. with the highest DM loss of 6.1% d.b. Note that these DM losses are considerably less than the fiber degradation indicated in Figs. 5 and 6, as much of the fiber is converted to organic acids and WSC (Figs. 2–4) that are largely conserved at the drying temperature of 60°C. Fine and coarse size material gave similar results of cellulose degradation with medium size, whereas resulting in no significant increase of hemicellulose degradation. In the control sample, only hemicellulose degradation was observed. This is consistent with ensilage results for orchardgrass and lucerne *(43)*, Italian ryegrass *(44)*, and perennial ryegrass *(45)*.

All these studies reported an overwhelming preferential degradation of hemicellulose, relative to cellulose. The degradation of hemicellulose during the ensilage process is catalyzed by indigenous plant hemicellulases, bacterial enzymes produced during ensilage, and resulted from acid hydrolysis by produced acids *(46)*. Although plant enzymes have been credited as contributors to sugar production *(47–49)*, experimental results have been inconsistent. Bousset et al. *(50)* did not observe hemicellulase

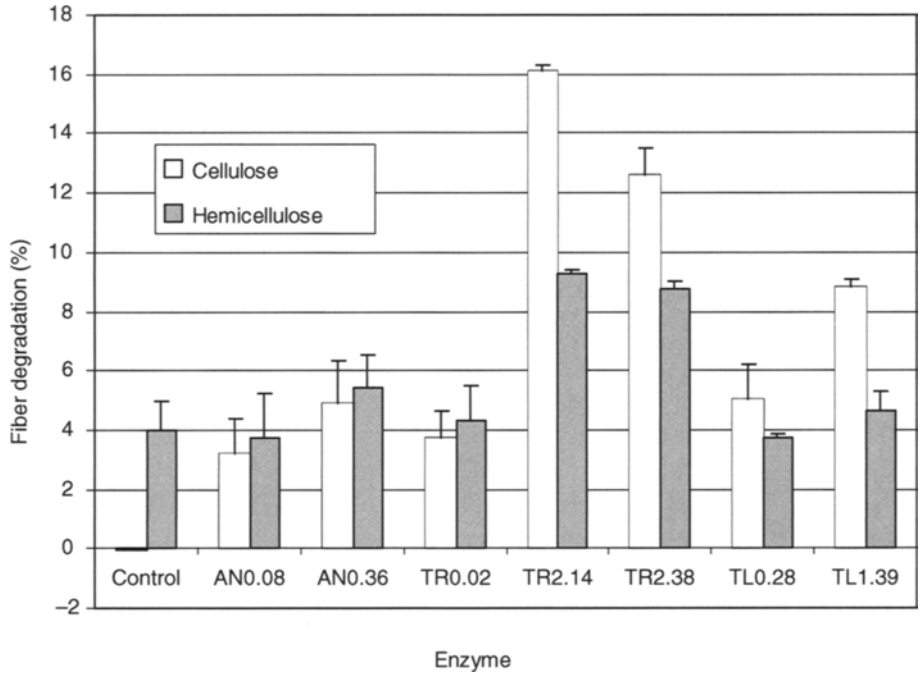


**Fig. 5.** Degradation of cellulose and hemicellulose with different enzyme treatments at the level of 1.67 IU/g DM for the medium size stover (AN, TR, and TL represent the microbial sources of various enzyme products, standing for *A. niger*, *T. reesei*, and *T. longibrachiatum*, respectively. The numbers following AN, TR, and TL are the ratios of endo-1,4-β-glucanase to hemicellulase [C : H] of the enzyme products).

activity in sterilized silage, and argued that if such activity did exist, the activity should be low because of compartmentalization, plasmolysis, and the short life of these enzymes. Dewar et al. *(34)* found that plant enzymes lost most of their activities after 3 d of ensiling. Direct acid hydrolysis has been suggested by Dewar et al. *(34)* and Morrison *(45)* to be mainly responsible for the degradation of hemicellulose. High levels of hemicellulose degradation have been reported to occur at a pH level of 4 *(34)*. Cellulose degradation at this pH is much lower, as cellulose has more resistant microfibrils with extensive crystalline regions, and relatively moderate acid hydrolysis cannot break down the β 1–4 glycosidic links buried in this three-dimensional structure.

It is not surprising that enzyme additions increased cellulose degradation significantly. For treatments with enzymes from the same microbial source, cellulose degradation increased with the increase of C : H ratio, except for TR2.38. This anomalous result may be an artifact of higher DM loss in the TR 2.38 treatment. Increased cell wall degradation would have reduced the DM basis for the measured concentrations, resulting in a higher percentage of cellulose in the silage, and a corresponding smaller

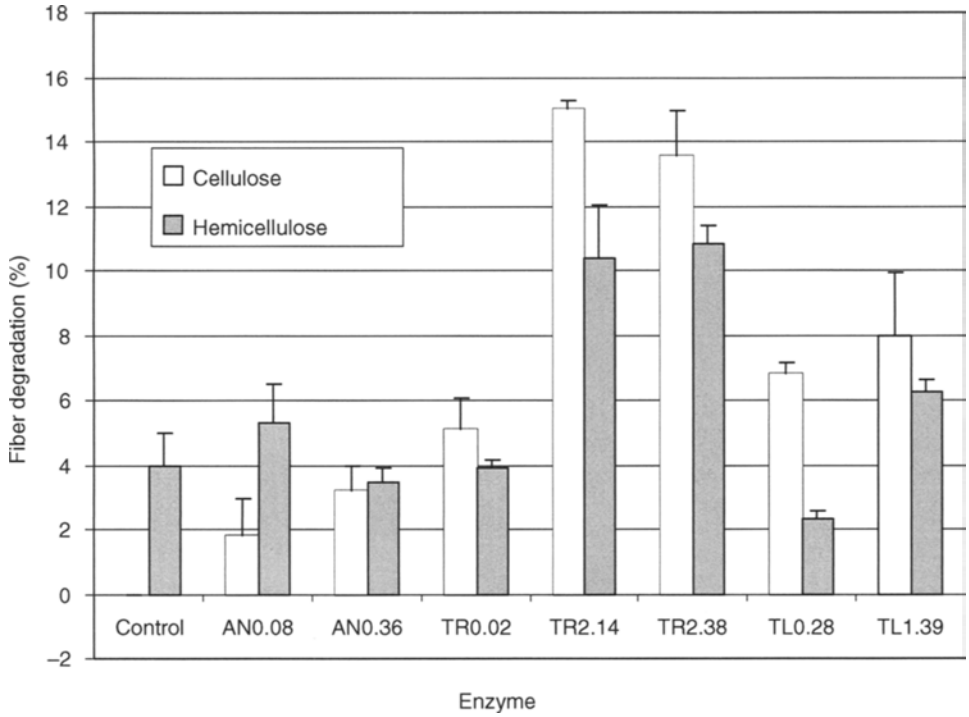


**Fig. 6.** Degradation of cellulose and hemicellulose with different enzyme treatments at the level of 5 IU/g DM for the medium size stover (AN, TR, and TL represent the microbial sources of various enzyme products, standing for *A. niger*, *T. reesei*, and *T. longibrachiatum*, respectively. The numbers following AN, TR, and TL are the ratios of endo-1,4-β-glucanase to hemicellulase [C : H] of the enzyme products).

apparent cellulose loss. Comparing across microbial sources, the cellulose degradation in the TL0.28 treatment was higher than that with AN0.36 at the 5 IU/g DM hemicellulase level, even though the latter had a higher C : H ratio. A similar but smaller difference between these treatments was observed at the 1.67 IU/g DM level. This was also the case when comparing TR0.02 and AN0.08 treatments, with the lower C : H ratio from the *T. reesei* source resulting in higher cellulose degradation. However, we need to be cautious before definitively concluding that enzymes from *T. longibrachiatum* and *T. reesei* are more effective at cellulose degradation than those of *A. niger* at the same C : H ratio. Cellulose degradation is a complicated synergistic process that includes contributions by at least six individual enzyme components *(42)*. Complete elucidation of the effects of the microbial source of enzymes on cell wall degradation requires enzyme characterization on the molecular level.

Significant increases in the degradation of hemicellulose were observed only for the treatments with TR2.14 and TR2.38 in medium size. Other enzyme treatments did not significantly enhance hemicellulose

degradation. Similar results have been reported by Ren et al. *(12)* and Van Vurren et al. *(51)*. The increased hemicellulose degradation observed with TR2.14 and TR2.38 in medium size is probably because the higher lactic acid concentration and lower pH value (<4.0), enhance acid hydrolysis as previously discussed. The higher degradation of cellulose observed with these treatments may also have contributed, by partially removing the structural hindrance around hemicellulose and increasing access of hemicellulase to the substrate *(25)*.

Increasing the hemicellulase enzyme level did not change fiber degradation significantly. The chemical composition of stover silage for enzyme treatments at the higher hemicellulase level were also similar to previously reported data at the lower (1.67 IU/g) level *(12)*. To decrease the cost of enzyme additives in full-scale industrial applications, the lower level of enzyme amendment is preferable.

## Discussion

Mixtures of different ratios of cellulase and hemicellulase enzymes from different microbial sources had varying effects on fiber hydrolysis during ensiled storage of corn stover biomass feedstock. To facilitate comparisons among treatments, mixtures were normalized on the basis of hemicellulase activity. For each enzyme mixture and C : H ratio, two hemicellulase levels were tested, 1.67 and 5 IU/g, and results indicated the lower level of hemicellulase was sufficient to achieve the most beneficial effects. At each of these hemicellulase levels, the ratio of cellulase to hemicellulase was important for improving the quality of stover silage. Increasing ratios of C : H reduced pH, increased lactic acid concentration, and decreased butyric acid concentration.

Successful development of ensilage as a biomass storage strategy will require minimizing DM loss. This loss often results from secondary fermentations, which can be suppressed by high concentrations of lactic acid and the resulting reduced pH. In order to increase the concentration of lactic acid and suppress these secondary fermentations, a critical C : H ratio is required. Mixtures at or more than this critical C : H ratio will have sufficient cellulase to hydrolyze glucose for fermentation into lactic acid. Although this study examined seven different ratios, they were derived from three fungal sources and were not evenly distributed over the entire range. To determine the critical C : H ratio for a particular fungal organism's enzyme suite, additonal C : H ratios derived from that single source should be investigated.

One of the potential benefits of an ensiled storage process would be *in situ* pretreatment and hydrolysis of polymers during storage to produce WSC for downstream bioconversion. This benefit was observed in many of our ensilage treatments. The WSC content of stover silage depended on the ratio of C : H in the applied enzymes as well as the size of stover

material. For each of the stover sizes tested, enzymes from *T. reesei* increased WSC content at increasing rates with increasing C : H ratios. Results for other stover sizes and microbial sources were less consistent, but similar trends were observed. The effect of the microbial source of enzyme mixtures cannot be completely elucidated based on our current results. But enzyme mixtures derived from *T. reesei* and *T. longibrachiatum* appear to hydrolyze more cellulose than those derived from *A. niger*, even when the ratio of C : H in the former mixtures is less than that of the latter. These differences suggest that optimized enzyme mixtures can provide significant pretreatment benefits during ensiled biomass storage.

Hemicellulose is more easily hydrolyzed than cellulose by the acid conditions that prevail during the normal ensilage process. Therefore, it was not surprising that the addition of enzymes improved cellulose degradation more significantly than that of hemicellulose. However, this improved cellulose degradation also contributed to lower pH and presumably increased access of hemicellulase to substrate, resulting in considerably improved hydrolysis of hemicellulose for the high C : H treatments. Development of microbial strains that can convert both five- and six-carbon sugars to ethanol and other value-added chemicals makes increased hemicellulose hydrolysis important for maximizing product yields.

Because the hemicellulase enzyme concentration did not have a significant influence on pH, chemical composition, or fiber degradation of the final stover silage, minimizing the enzyme treatment level should maximize economic returns. For the high C : H ratios of 2.14 and 2.38 in mixtures derived from *T. reesei*, the low 1.67 IU/g hemicellulase level appears more than sufficient to achieve positive results. Further research to optimize these levels and the increase in synergies among enzyme mixture components appears likely to result in attractive ensilage strategies for industrial storage of large volumes of biomass feedstocks.

## Acknowledgments

The authors acknowledge the assistance of Patricia Patrick with laboratory analysis. This research was supported by the Iowa Energy Center, Iowa State University, Penn State University, and the United States Department of Agriculture.

## References

1. Kadam, K. L. and McMillan, J. D. (2003), *Bioresour. Technol.* **88,** 17–25.
2. Perlack, R. D., Wright, L. L., Turhollow, A. F., Graham, R. L., Stokes, B. J., and Erbach, D. C. (2005), *Biomass as Feedstock for Bioenergy and Bioproducts Industry: The Technical Feasibility of a Billion Ton Annual Supply.* Oak Ridge National Laboratory, Oak Ridge, TN.
3. Walsh, M. E., Perlack,R. L., Turhoolow, A., et al. (1999), *Biomass Feedstock Availability in the United States: 1999 State Level Analysis.* Oak Ridge National Laboratory, Oak Ridge, TN.
4. Sudha Rani, K., Swamy, M. V., and Seenayya, G. (1998), *Process Biochem.* **33,** 435–440.
5. Riera, F. A., Alvarez, R., and Coca, J. (1991), *J. Chem. Technol. Biotechnol.* **50,** 149–155.
6. Buhner, J. and Agblevor, F. A. (2004) *Appl. Biochem. Biotechnol.* **119,** 13–30.

7. Wang, D. and Sun, X. S. (2002), *Ind. Crops Prods.* **15,** 43–50.
8. Chow, P., Bowers, T. C., Bajwa, D. S., et al. (1999), *Proceeding of 5th International Conference on Woodfiber-plastic Composites*, Madison, WS, 26–27 May 1999, pp. 312–313.
9. Green, A. E. S. and Feng, J. (2005), *J. Anal. Appl. Pyrolysis* **76,** 60–69.
10. Hu, Z. and Yu, H. (2005), *Process Biochem.* **40,** 2371–2377.
11. Teymouri, F., Laureano-Perez, L., Alizadeh, H., and Dale, B. E. (2005), *Bioresour. Technol.* **98,** 2014–2018.
12. Ren, H., Richard, T. L., Chen, Z., et al. (2006), *Biotechnol. Prog.* **22,** 78–85.
13. Richard, T. L., Moore, K. J., Tobía, C., and Patrick, P. (2002), *Proceedings Institute of Biological Engineering*, Baton Rouge, LA, 18–21 January, vol. 3, pp. 45–53.
14. Thompson, D. N., Barnes, J. M., and Houghton, T. P. (2005), *Appl. Biochem. Biotechnol.* **121–124,** 21–46.
15. McDonald, P., Henderson, A. R., and Heron, S. J. E. (1991), *The Biochemistry of Silage*, 2nd ed. Chalcobe Publications, Marlow, Bucks, UK.
16. Ren, H., Richard, T. L., Moore, K. J., and Patrick, P. (2004), ASAE paper No. 047066. ASAE, Ottawa, Canada.
17. Henderson, A. R. and McDonald, P. (1977), *J. Sci. Food Agric.* **28,** 486–490.
18. Allen, A. L. and Roche, C. D. (1989), *Biotechnol. Bioeng.* **33,** 650–656.
19. Sternberg, D., Vijayakumar, P., and Reese, E. T. (1977), *Can. J. Microbiol* **23,** 139.
20. Flachner, B., Brumbauer, A., and Reczey, K. (1999), *Enzyme Microb. Technol.* **24,** 362–367.
21. Kang, S. W., Park,Y. S., Lee, J. S., Hong, S. I., and Kim, S. W. (2004), *Bioresour. Technol.* **91,** 153–156.
22. Kim, S. W., Kang, S. W., and Lee, J. S. (1997), *Bioresour. Technol.* **59,** 63–67.
23. Colombatto, D., Mould, F. L., Bhat, M. K., Phipps, R. H., and Owen, E. (2004), *Anim. Feed Sci. Technol.* **111,** 145–159.
24. Mielenz, J. R. (2001), *Curr. Opin. Microb.* **4,** 324–329.
25. White, B. A., Mackie, R. I., and Doerner, K. C. (1993), In: *Forage Cell Wall Structure and Digestibility*, American society of Agronomy, Madison, Inc., pp. 715–767
26. Mooney, C. A., Mansfield, S. D., Beatson, R. P., and Saddler, J. N. (1999), *Enzyme Microb. Technol.* **25,** 644–650.
27. Allan, G. G., Ko, Y. C., and Ritzenthaler, P. (1991), *Tappi J.* **74,** 205–212.
28. Richard, T. L., Proulx, S., Moore, K. J., and Shouse, S. (2001). ASAE paper No. 016019. ASAE, St. Joseph, Mich.
29. Wood, T. M. and Bhat, K. M. (1988), *Methods Enzymol.* **160,** 97–112.
30. Bailey, M. J., Biely, P., and Poutanen, K. (1992), *J. Biotechnol.* **23,** 257–270.
31. Vogel, K. P., Pedersen, J. F., Masterson, S. D., and Toy, J. J. (1999), *Crop Sci.* **39,** 276–279.
32. Guiragossian, V. Y., Scoyoc, S. W. V., and Axtell, J. D. (1977), In: *Chemical and Biological Methods for Grain and Forage Sorghum*, Purdue University, W. Lafayette, IN: pp. 174–178.
33. SAS, SAS/STAT User's Guide, Version 9.1. (2004), Statistical Analysis System Institute Inc., Cary, NC. Available at http://support.sas.com/91doc/docMainpage.jsp.
34. Dewar, W. A., McDonald, P., and Whittenbury, R. (1963), *J. Sci. Food Agric.* **14,** 411–417.
35. Leibensperger, R. Y. and Pitt, R. E. (1987), *Grass Forage Sci.* **42,** 297–313.
36. Rauramaa, A., Setala, J., Moisio, T., and Sivela, S. (1987), *J. Agric. Sci. Finland* **59,** 371–377.
37. Mandebvu, P., West, J. W., Froetschel, M. A., Hatfield, R. D., Gates, R. N., and Hill, G. M. (1999), *Anim. Feed Sci. Technol.* **77,** 317–329.
38. Jakhmola, R. C., Weddell, J. R., and Greenhalgh, J. F. D. (1990), *Anim. Feed Sci. Technol.* **28,** 39–50.
39. Nadeau, E. M. G., Buxton, D. R., Russell, J. R., Allison, M. J., and Young, J. W. (2000), *J. Dairy Sci.* **83,** 1487–1502.
40. Adogla-Bessa, T., Owen, E., and Adesogan, A. T. (1999), *Anim. Food Sci. Technol.* **82,** 51–61.
41. Morrison, I. M. (1988), *J. Agric. Sci.* **111,** 35–39.
42. Lynd, L. R., Weimer, P. J., van Zyl, W. H., and Pretorius, I. S. (2002), *Microbiol. Mol. Biol. Rev.* **66,** 506–577.
43. Yahaya, M. S., Kimura, A., Harai, J., et al. (2001), *Anim. Feed Sci. Technol.* **92,** 141–148.

44. Kawamura, O., Fukuyama, K., and Niimi, M. (2001), *Anim. Sci. J.* **72,** 134–138.
45. Morrison, I. M. (1979), *J. Agric. Sci.* **93,** 581–586.
46. McDonald, P., Stirling, A. C., Henderson, A. R., et al. (1960), *Edinburgh School of Agriculture Technical Bulletin* **24,** 70–77.
47. Heron, S. J. E., Edwards, R. A., and McDonald, P. (1986), *J. Sci. Food Agric.* **37,** 979–985.
48. Ohyama, Y. and Masaki, S. (1977), *J. Sci. Food Agric.* **28,** 78–84.
49. Pitt, R. E., Muck, R. E., and Leibensperger, R. Y. (1985), *Grass Forage Sci.* **40,** 279–303.
50. Bousset, J., Bousset-Fatianoff, N., Gouet, Ph., et al. (1972), *Ann. Biol. Anim. Biochim. Biophys.* **12,** 453–477.
51. Van Vuuren, A. M., Bergsma, K., Krol-Kramer, F., and Van Beers, J. A. C. (1989), *Grass Forage Sci.* **44,** 223–230.

0273–2289/1559–0291 (Online)/07/136–140/239–252/$30.00

# Fractionation of *Cynara cardunculus* (Cardoon) Biomass by Dilute-Acid Pretreatment

MERCEDES BALLESTEROS,* M. JOSÉ NEGRO, PALOMA MANZANARES, IGNACIO BALLESTEROS, FELICIA SÁEZ, AND J. MIGUEL OLIVA

*Renewable Energies Department-CIEMAT, Avda. Complutense, 22 28040-Madrid Spain, E-mail: m.ballesteros@ciemat.es*

## Abstract

*Cynara cardunculus* L. (cardoon) is a Mediterranean perennial herb offering good potential as substrate for sustainable production of bioethanol. In this work the first approach to the study of dilute-acid pretreatment of cardoon biomass for biological conversion was made. The influence of temperature (160–200°C), acid concentration (0–0.2% [w/w]), and solid concentration (5–10% [w/v]) in the formation of free sugars and sugar decomposition products in the prehydrolyzate was studied using a response surface methodology. Results show a negative interaction effect between acid concentration and temperature in xylose recovery yield in prehydrolyzate, whereas dry matter concentration does not exert a significant effect. Xylose recovery yield reaches a maximum of about 80% of the content in dry untreated raw material at 180°C and 0.1 or 0.2% acid addition. At these conditions the ratio of monomers found in prehydrolyzate in relation to total sugar yield for xylose is close to 100%. Furfural concentration, the major furan determined in the prehydrolyzate, increases as pretreatment severity rises. Maximum furfural yield of 4.2 g/100 g dry untreated raw material was found at 200°C and 0.2% acid concentration. The yield of furfural at the conditions in which maximum xylose recovery is attained is substantially lower, less than 2 g/100 g dry untreated raw material. This fact supports the idea of using moderate temperatures in dilute-acid processes, which at the same time provides reasonably high sugar recovery yield and avoids high inhibitory products formation.

**Index Entries:** Acid prehydrolyzate; furfural; pretreatment optimization; surface-response methodology; xylose recovery; herbaceous crop.

## Introduction

Cardoon (*Cynara cardunculus* L.) is a dicotyledonous herb originally from the Mediterranean area that can be considered as a potential lignocellulosic feedstock for biofuels production in Spain owing to its good adaptability to the environmental conditions of the country—hot and dry

*Author to whom all correspondence and reprint requests should be addressed.

climates—and high biomass productivities (1). This crop is traditionally cultivated in Spain for food purposes in a shorter artificial cultivation cycle to produce edible blanched leaf petioles using intensive crop management practices. However, it can be cultivated for biomass production in accordance with its natural autumn–spring cycle and whole aboveground biomass can be harvested annually for several years.

Cardoon biomass presents a wide range of applications as raw material for the production of fuels and high-value products. The whole plant has been tested as solid biofuel for power and heat generation (2), seeds for oil production, (3) and stalks as substrate for paper pulping (4). Another alternative use for the aerial part of the plant (stalks and branches) would be as substrate for sustainable production of transportation fuels and chemicals that are now primarily made from petroleum. Some preliminary studies performed by Martinez et al. (5) on cardoon biomass showed good prospects as substrate for biological conversion into ethanol or other products, but more information is needed to establish its real potential.

Regarding biological processing of cellulosic biomass, it is well-known that each type of feedstock, whether wood or agricultural residue, requires a particular pretreatment to minimize the degradation of the substrate and maximize the overall sugar yield. When enzymatic hydrolysis is involved in the process, a pretreatment step is vital to effectively prepare cellulose for enzymes action and provide high sugar yields. So, pretreatment has been frequently highlighted as one of the most costly process steps having a major influence on both previous (e.g., size reduction) and subsequent operations (e.g., enzymatic hydrolysis and fermentation) (6).

There are numerous pretreatment methods or combinations of pretreatment methods available to fractionate lignocellulosic biomass. Among the chemical pretreatment processes used for cellulosic feedstock (dilute acid, alkaline, organic solvent, ammonia, sulfur dioxide, or carbon dioxide), considerable research effort has been carried out on acid catalyzed hydrolysis to depolymerize the hemicellulose fraction contained in biomass (7,8). Xylose, glucose, and other sugars are released in the liquid stream while providing a cellulose-enriched solid more susceptible to further enzymatic hydrolysis. Dilute acid at moderate temperatures has been demonstrated to effectively remove and recover most of the hemicelluloses as dissolved sugars in lignocellulosic substrates. Dilute-acid pretreatment has the advantage of not only solubilizing hemicellulose, but also converting solubilized hemicellulose to fermentable sugars (9). However, with sustained hydrolysis the sugars may be degraded to decomposition products such as furfural and hydroxymethylfurfural (HMF) that lower the sugar yield and affect the subsequent fermentation step. So, to produce fermentable prehydrolyzates and to prevent high losses in yields, it is necessary to choose process conditions that keep at a low level the amount of degradation products produced.

This work represents a first approach to the assessment of dilute-acid pretreatment for biological conversion of *C. cardunculus* biomass into ethanol. In this article, the influence of pretreatment parameters (temperature, acid concentration, and solid concentration) in the formation of free sugars and sugar decomposition products in the prehydrolyzate was investigated by using a statistical experimental design. This statistical model involves fitting an empirical model to the experimental data and identifying the optimal temperature, acid concentration, and solid concentration in the pretreatment stage by using response surface technique.

## Materials and Methods

### *Raw Material*

Cardoon biomass (stalks and branches) (6% moisture content) was obtained from Agroenergy Group of the High School of Agricultural Engineering of Madrid (Spain). Biomass was milled to a particle size smaller than 5 mm using a laboratory hammer mill (Retsch GmbH & Co. KG, Germany), homogenized and stored until used. As the presence of high amounts of alkaline ash in herbaceous feedstock has been reported that can partially neutralize the sulfuric acid and lower the acidity of the reaction mixture in acid pretreatments, the buffering capacity of cardoon biomass in the aqueous phase was determined. The pH of 1% (w/w) sulfuric acid solution was measured before and after mixing with the biomass in the same ratio of substrate, acid, and water as in pretreatment runs. Neutralizing capacity was calculated based on the change of pH of acid solution according to Esteghalian et al. *(10)*.

### *Pretreatment*

Cardoon biomass samples were pretreated in a 2-L stainless steel Hastelloy-C stirred reactor (Model EZE-Seal, Autoclave Engineers, Erie, PA). Process parameters tested were temperature (160–200°C), solid concentration in the reactor (5–10% [w/v]), and acid concentration in the reaction mixture (0–0.2% [w/w]). Biomass samples were loaded into the reactor at the different solid/liquid ratios and heated at selected temperatures by an external heating jacket. The heating rate was between 2 and 4°C/min. When desired temperature was reached, the corresponding amount of sulfuric acid was added to provide final acid content in the reactor, taking into account the buffering capacity of biomass previously determined. After 10 min pretreatment time, the reactor was removed from the heating jacket, and cooled to about 40°C in less than 10 min. The wet material was vacuum-filtered and separated into a water insoluble fraction (WIS) and a filtrate or prehydrolyzate fraction, which contains sugars, furfural, HMF, and other degradation products. Both fractions were analyzed to determine their chemical composition as described under "Analytical Procedures".

Solid recovery yield was then calculated as dry weight of WIS remaining after pretreatment referred to 100 g of dry untreated raw material.

## Analytical Procedures

### Raw Material and Pretreated Substrates Composition

The chemical composition of raw material and WIS fraction from pretreatment was determined using the standard laboratory analytical procedures for biomass analysis described by the National Renewable Energy Laboratory (Colorado) *(11)*.

### Prehydrolyzate Composition

The sugar content of prehydrolyzate after pretreatment was determined "as is" and later by performing a mild acid hydrolysis (3%[v/v] $H_2SO_4$, 120°C, 30 min), measuring glucose, xylose, arabinose, galactose, and mannose concentration by high-performance liquid chromatography (HPLC) in a Waters 2695 liquid chromatograph (Waters, Milford, MA) with refractive index detector. A CARBOSep CHO-682 LEAD column (Transgenomic, Omaha, NE) operating at 80°C with Milli-Q water (Millipore, Billerica, MA) as mobile-phase (0.5 mL/min) was used.

Furfural and HMF, vanillin, syringaldehyde, catechol, cumaric acid, and ferulic acid analyses were performed by HPLC (Hewlett Packard, Palo Alto, CA), using an Aminex ion exclusion HPX-87H cation exchange column (Bio-Rad, Hercules, CA) at 65°C. Mobile phase was 89% $H_2SO_4$ 5 m*M* and 11% acetonitrile at a flow rate of 0.7 mL/min. Column eluent was detected with a 1040A photodiode-array detector (Agilent, Waldbronn, Germany). Acetic, formic, and levulinic acid were quantified by HPLC with a 2414 Waters refractive index detector. A Bio-Rad Aminex HPX-87H (Bio-Rad, Hercules, CA) column maintained at 65°C with a flow rate of 0.6 mL/min was used. Mobile phase was $H_2SO_4$ (5 m*M*).

### Statistical Experiment Design

A response surface methodology was used to study the effects of temperature, acid concentration, and solid concentration in the formation of free sugars and degradation products in the prehydrolyzate. A Box-Behnken design with four center points was created and evaluated with commercial software Statgraphics 5.0 (Manugistics Inc., Rockville, MD). This design allows estimation of the main effects and two factor interactions using analysis of variance. The response surface is calculated using a quadratic polynomic model. The parameters were tested at two levels: temperature (160 and 200°C), acid concentration (0 and 0.2% [w/w]), and solid concentration (5 and 10% [w/v]). Reaction time was fixed at 10 min. The experimental error was estimated in the center point (180°C, 0.1% acid and 7.5% solid content), which was carried out four times. The conditions for each experiment, which were performed in fully randomized order, are shown in Table 1.

Table 1
Conditions for Dilute-Acid Pretreatment of Cardoon Biomass According to Experimental Design

| Experiment | Code | Temperature (°C) | Solid/liquid ratio (w/v [%]) | Acid concentration (w/w [%]) |
|---|---|---|---|---|
| 1 | (–1 –1 0) | 160 | 5 | 0.1 |
| 2 | (1 –1 0) | 200 | 5 | 0.1 |
| 3 | (–1 1 0) | 160 | 10 | 0.1 |
| 4 | (1 1 0) | 200 | 10 | 0.1 |
| 5 | (–1 0 –1) | 160 | 7.5 | 0 |
| 6 | (1 0 –1) | 200 | 7.5 | 0 |
| 7 | (–1 0 1) | 160 | 7.5 | 0.2 |
| 8 | (1 0 1) | 200 | 7.5 | 0.2 |
| 9 | (0 –1 –1) | 180 | 5 | 0 |
| 10 | (0 1 –1) | 180 | 10 | 0 |
| 11 | (0 –1 1) | 180 | 5 | 0.2 |
| 12 | (0 1 1) | 180 | 10 | 0.2 |
| 13 | (0 0 0) | 180 | 7.5 | 0.1 |
| 14 | (0 0 0) | 180 | 7.5 | 0.1 |
| 15 | (0 0 0) | 180 | 7.5 | 0.1 |
| 16 | (0 0 0) | 180 | 7.5 | 0.1 |

## Results and Discussion

### *Raw Material Composition*

The chemical analysis of raw material showed the following composition (dry weight [%]): cellulose, 33.8; hemicellulose, 18.5 (xylans 14.7, arabinans 1.2, galactans 2.0, and mannans, 0.6); acid insoluble lignin, 14.0; acid soluble lignin, 2.4; acetyl groups, 3.8; ash, 6.6; and extractives, 14.3 (total 93.4%). The high ash content of 6.6% suggested a buffering capacity of cardoon biomass in the aqueous phase of dilute-acid pretreatment. The neutralizing ability of cardoon biomass in aqueous phase was determined as 36.0 mg $H_2SO_4$/g dry substrate and it was used to correct the amount of sulfuric acid added in pretreatment experiments. This value is consistent with the high values found in other herbaceous species such as those reported by Esteghalian et al. *(9)* for switch grass and corn stover biomass: 43.7 and 25.8 mg $H_2SO_4$/g dry substrate, respectively. Lower buffering capacities less than 10 mg $H_2SO_4$/g dry substrate have been reported for hardwoods *(12)*, in agreement with the lower ash content of this type of biomass.

### *Sugar Yield in Prehydrolyzate*

The monosaccharide yields in prehydrolyzate from dilute-acid pretreatment experiments of cardoon biomass are shown in Table 2. Values correspond to sugar yield (gram/100 g dry untreated raw material) after mild acid posthydrolysis of prehydrolyzate, so include both oligomers and

Table 2
Sugar Yield in Prehydrolyzate, Solid Fraction (WIS) Composition, and pH and Solid Recovery Values From Dilute-Acid Pretreatment of Cardoon Biomass

| Acid concentration (w/w [%]) | 0 | | | | 0.1 | | | | | 0.2 | | | |
|---|---|---|---|---|---|---|---|---|---|---|---|---|---|
| Temperature (°C) | 160 | 180 | | 200 | 160 | | 180[a] | 200 | | 160 | 180 | | 200 |
| Solid concentration (w/v [%]) | 7.5 | 5 | 10 | 7.5 | 5 | 10 | 7.5[a] | 5 | 10 | 7.5 | 5 | 10 | 7.5 |
| Prehydrolyzate sugar yield (gram/100 g raw material) | | | | | | | | | | | | | |
| Glucose | 0.4 | 0.4 | 0.4 | 0.4 | 0.5 | 0.6 | 1.4 | 5.1 | 3.8 | 1.0 | 2.8 | 2.8 | 7.0 |
| Monomeric form (%) | 34 | 47 | 76 | 27 | 96 | 85 | 98 | 84 | 90 | 100 | 94 | 100 | 98 |
| Xylose | 0.9 | 8.0 | 8.9 | 3.7 | 4.7 | 5.9 | 13.5 | 10.4 | 5.7 | 11.1 | 13.5 | 12.4 | 6.3 |
| Monomeric form (%) | 0 | 2 | 2 | 37 | 83 | 88 | 97 | 84 | 94 | 92 | 96 | 100 | 100 |
| Galactose | 0.9 | 1.3 | 1.3 | 0.5 | 1.2 | 1.4 | 2.1 | 1.7 | 0.8 | 1.9 | 2.3 | 2.1 | 1.3 |
| Arabinose | 0.6 | 0.6 | 0.4 | 0.04 | 1.3 | 1.2 | 1.4 | 0.8 | 0.2 | 1.6 | 1.1 | 1.0 | 0.8 |
| Mannose | 0.05 | 0.04 | 0.08 | 0.25 | 0.2 | 0.1 | 0.5 | 0.7 | 0.3 | 0.3 | 0.6 | 0.5 | 0.5 |
| Total sugars | 2.8 | 12.3 | 13.1 | 4.9 | 7.9 | 9.2 | 18.9 | 18.7 | 10.8 | 15.9 | 20.3 | 18.8 | 15.9 |
| pH | 4.36 | 4.19 | 4.08 | 3.79 | 1.86 | 1.81 | 1.80 | 1.81 | 1.92 | 1.56 | 1.36 | 1.52 | 1.66 |
| WIS composition (w/w [%]) | | | | | | | | | | | | | |
| Glucan | 42.7 | 53.0 | 56.1 | 58.5 | 55.8 | 56.1 | 64.1 | 62.5 | 60.7 | 60.2 | 65.3 | 63.4 | 62.8 |
| Xylan | 16.2 | 9.4 | 7.5 | 5.8 | 14.6 | 13.3 | 3.3 | 0 | 0 | 5.6 | 1.4 | 1.1 | 0 |
| Lignin | 19.4 | 19.8 | 21.1 | 27.9 | 21.4 | 23.0 | 26.0 | 27.5 | 29.7 | 23.5 | 25.4 | 27.4 | 31.2 |
| Solid recovery (g/100 g dry untreated raw material) | 82.7 | 64.7 | 64.2 | 58.6 | 61.9 | 63.5 | 54.6 | 47.4 | 50.2 | 57.8 | 49.8 | 51.1 | 44.1 |

[a]Average values of four center points.

monomers. Soluble sugar monomers ratio, calculated from sugar measurement before such hydrolysis, is shown for glucose and xylose, which are the major sugars present in prehydrolyzate.

Results show that, although significant amounts of xylose can be recovered in prehydrolyzate following dilute-acid pretreatment, xylose recovery is highly dependent on pretreatment conditions. Xylose is the major sugar found in prehydrolyzate, accounting for up to 65–70% of total sugars. Arabinose, glucose, galactose, and mannose are present at lower concentration in most experiments, especially at low temperature and acid concentration. Xylose recovery yield in relation to the content in dry untreated raw material (16.6 g/100g) reached a maximum of about 80% at 180°C and 0.1 or 0.2% acid addition, regardless of solid concentration tested. Higher and lower temperatures led to decreased recovery yields values, depending on acid concentration. Glucose was found in significant amounts at the highest temperature of 200°C in experiments performed with acid, reaching recovery yields from 10% to 20% of initial content (37.2 g/100 g dry untreated raw material). This fact suggests slight cellulose hydrolysis at increased severities.

On the other hand, the ratio of monomers found in prehydrolyzate in relation to total sugar yield for xylose is quite high in all experiments performed with acid (83–100%). The lower pH found in these experiments (Table 2) facilitates the complete depolymerization of oligomeric hemicelluloses. Glucose oligomers were highly hydrolyzed in the presence of diluted acid (95–100% in monomeric form), although considerable amounts of monomers (30–75%) were also found even in nonacid experiments at 180°C. Although for mass balance purposes it is assumed that all glucose is derived from cellulose depolymerization, this easily hydrolyzed glucose could come from depolymerization of xyloglucans, which have been described to make up dicotyledons hemicelluloses *(13)*.

The significance of the effect of temperature, acid concentration, and solid concentration on xylose recovery was determined by analysis of variance and the results can be visualized in standardized Pareto chart shown in Fig. 1A. A negative interaction effect between acid concentration and temperature occurs, which causes different responses at increasing acid concentration depending on temperature tested. Dry matter concentration does not exert a significant effect in xylose recovery, within the limits of the experimental design. Figure 1B shows response surface for xylose recovery in prehydrolyzate at a fixed solid concentration of 7.5% (w/v), calculated using a quadratic polynomic equation. From this graph it can be deduced that conditions resulting in maximum xylose recovery are 180°C and acid concentration close to 0.2%. It also illustrates the aforementioned interaction between acid concentration and temperature, so that the positive effects of increasing acid at lower temperature of 160°C (from 4.7% at 0.1% acid to 11.1% at 0.2% acid) cannot be observed at 200°C, wherein yields even decrease (from 10.4% at 0.1% acid to 6.3% at 0.2% acid).

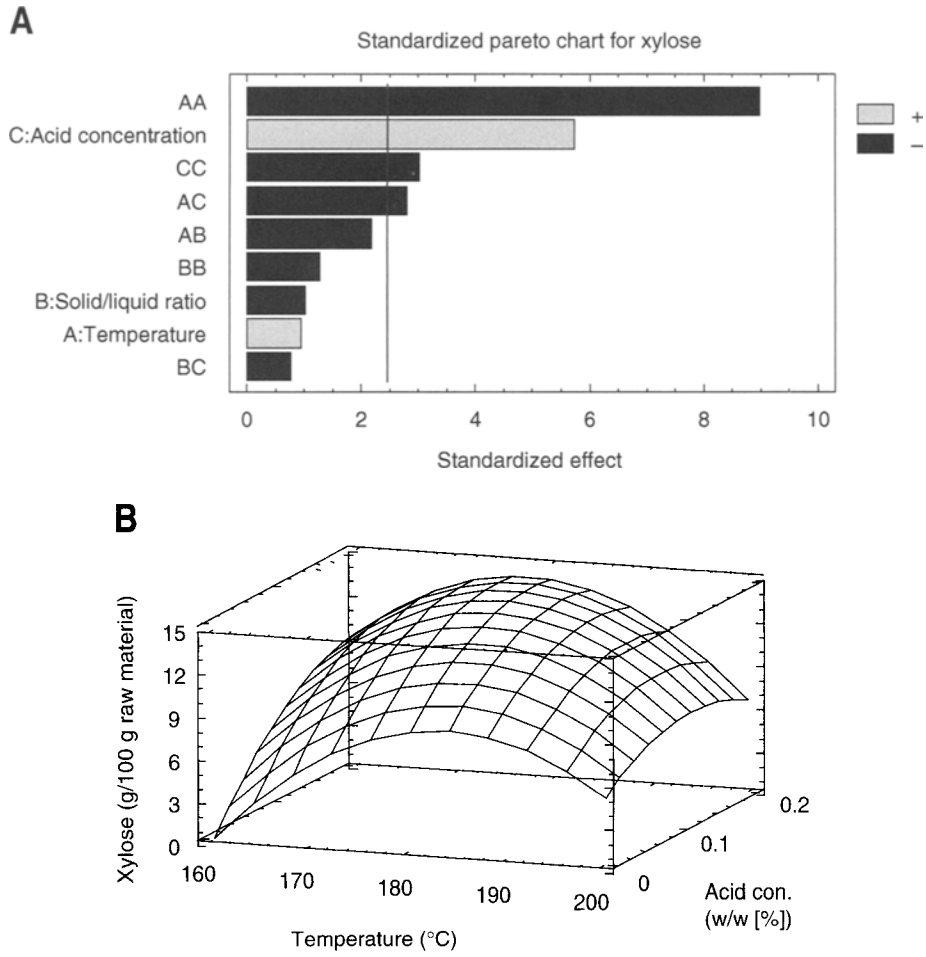


**Fig. 1.** Standardized Pareto chart **(A)** and estimated response surface **(B)** for xylose recovery yield. Solid concentration is fixed at central value (7.5%, [w/v]).

The effectiveness of dilute-acid hydrolysis in xylan depolymerization has been reported in other lignocellulosic herbaceous substrates. Although it is difficult to compare results among different raw materials, xylose yields obtained in this study are similar to those reported in dilute-acid hydrolysis of rice straw (2–15 g/100 g raw material) *(14)* or sugarcane bagasse (9–14 g/100 g raw material) *(15)* in experiments performed in batch hydrolysis reactors. Esteghalian et al. *(9)* reported 80% xylose recovery at temperatures between 170–190°C and 1% (w/w) acid concentration when pretreating corn stover in a Parr reactor similar to that used in this study. Our data of high monomer ratio found in prehydrolyzates obtained in acidic conditions support the idea that satisfactory hydrolysis of cardoon hemicelluloses to monosaccharides can be achieved in a single step reaction within the limits of the selected experimental design, although it is essential to consider degradation products formation.

### *Degradation Products in Prehydrolyzate*

Furfural and HMF are well-known byproducts formed in acid-hydrolysis of lignocellulosic materials originating from pentoses and hexoses degradation in acidic conditions. These compounds can be further degraded to formic and levulinic acid or they can polymerize *(15)*. Moreover, during pretreatment acetic acid is released from hydrolysis of acetyl groups present in hemicelluloses, as a consequence of deacetylation of acetylated pentosans. The amount of these compounds found in prehydrolyzates varies greatly depending on the nature of lignocellulosic substrate and the process conditions. Figure 2 shows the yield of sugar degradation compounds and aliphatic acids in prehydrolyzates from dilute-acid hydrolysis of cardoon biomass at different process conditions. Furfural is the most important furan found in prehydrolyzate (Fig. 2A), which is consistent with the major presence of xylan in hemicelluloses of cardoon biomass (approx 90%). Results show that the yields of both furan compounds increase as the severity of pretreatment rises, attaining maximum values of 4.2 and 0.7 g/100 g dry untreated raw material for furfural and HMF, respectively, at 200°C and 0.2% acid concentration. The yield of furfural at conditions where maximum xylose recovery is attained (180°C and acid concentration close to 0.2%) is substantially lower, less than 2 g/100 g dry untreated raw material.

From statistical analysis of the effect of process parameters on furfural yield, it can be deduced that there is a significant positive interaction between temperature and acid concentration (Fig. 3A). The effect of increasing acid concentration results in considerably higher furfural yield at 200°C; conversely furfural is hardly detectable at 160°C. This fact supports the idea of using moderate temperatures in dilute-acid processes, which, at the same time as providing reasonably high sugar recovery yield, also avoids excessive inhibitory products formation. A complete prevention of sugar degradation products can be achieved by lowering pretreatment temperature below 150°C, but longer reaction times are needed and enzymatic saccharification of pretreated substrate suffers from poor results. Saha et al. *(8)* reported good hemicelluloses solubilization yields without further degradation in dilute-acid pretreatment of rice hulls at 1% (v/v) $H_2SO_4$ and 121°C for 1 h, although the enzymatic saccharification yield of the pretreated slurry remained at 60% based on total carbohydrate content.

The formation of aliphatic acids (acetic, formic, and levulinic) in prehydrolyzate after dilute-acid pretreatment of cardoon biomass is shown in Fig. 2B. The yield of acetic acid fluctuates from low values less than 1 g to a maximum close to 5 g/100 g dry untreated raw material, depending on the severity of pretreatment. As shown in the analysis of raw material, an elevated proportion of acetyl groups are present in hemicelluloses of cardoon biomass and consequently, acetic acid is the prevailing acid present in prehydrolyzate. The maximum amount of acetic acid corresponded to 90%

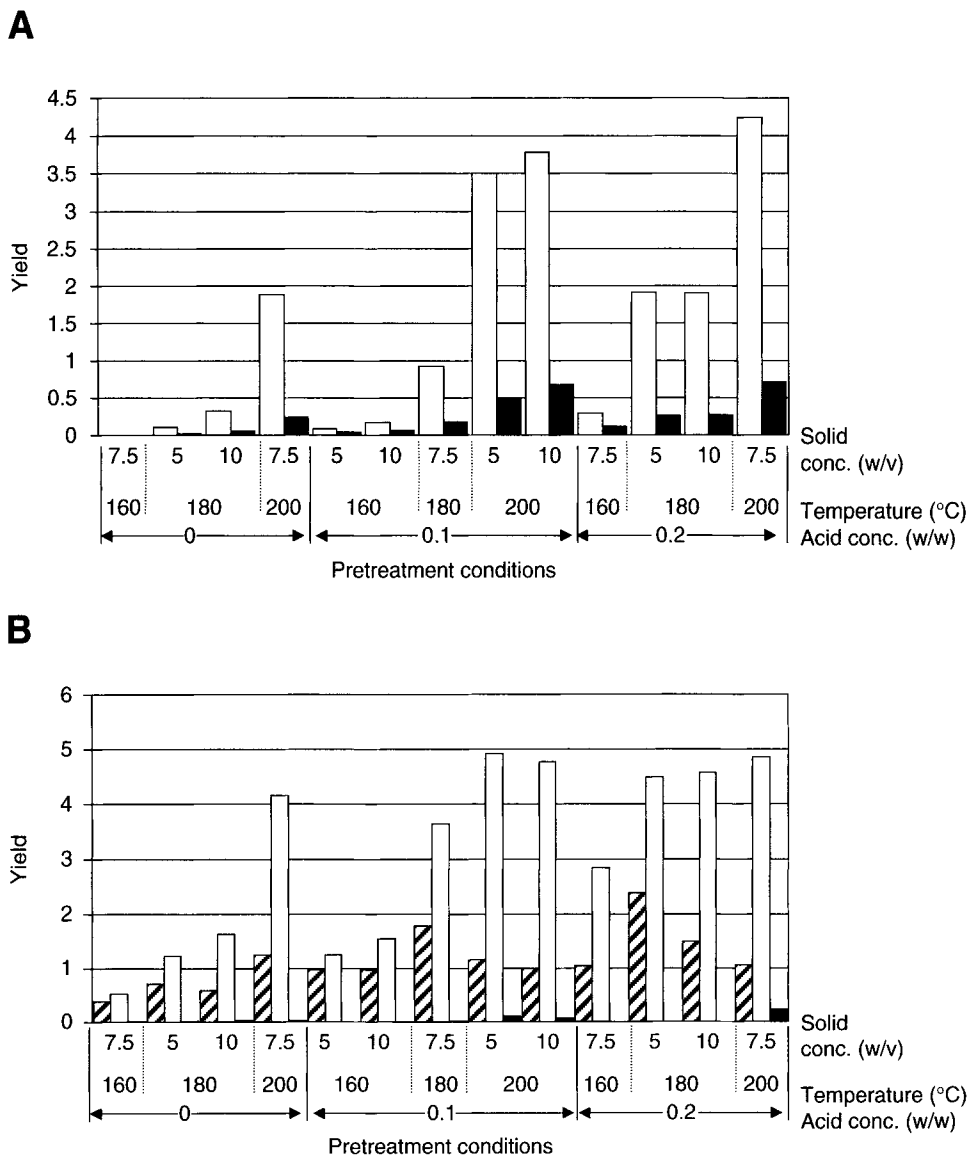


**Fig. 2.** Yields of furfural (□) and HMF (■) **(A)** and formic (▨), acetic (□), and levulinic acid (■) **(B)** in prehydrolyzates from dilute-acid pretreatment of cardoon at different conditions. Results are reported as gram/100 g dry untreated raw material.

of the acetyl groups determined in raw material, which indicates almost complete hydrolysis under the conditions tested. Regarding the effect of process conditions in acetic acid recovery, Fig. 3B illustrates the response surface graph showing a positive effect of the temperature and acid concentration on the formation of acetic acid. The effect of temperature is stronger as even in nonacid conditions increasing acetic acid is formed as temperature rises from 160 to 200°C.

Formic acid, yielding up to 2.5 g/100 g dry untreated raw material, is detected in all experiments, whereas levulinic acid is almost negligible

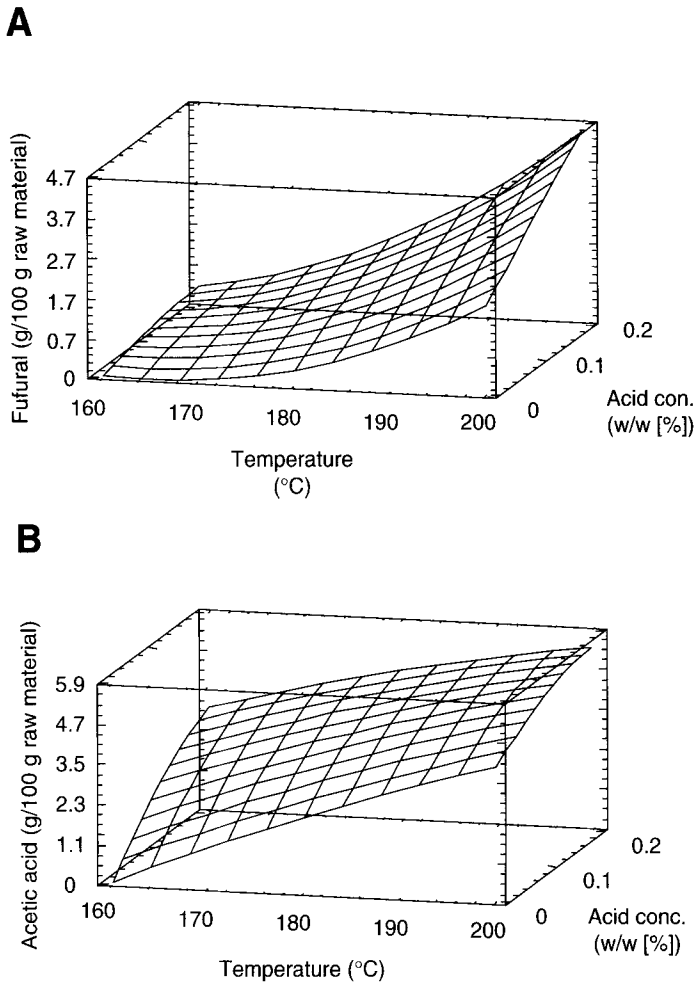


**Fig. 3.** Estimated response surface for furfural **(A)** and acetic acid **(B)** yields. Solid concentration is fixed at central value (7.5%, [w/v]).

(Fig. 2B). As HMF is broken down to equimolar amounts of levulinic and formic acids and HMF yield is rather low (Fig. 2A), most of the formic acid formed probably comes from furfural degradation. The content of some aromatic monomers coming from lignin degradation was also determined. Results of catechol, vanillin, and syringaldehyde in the different experiments are shown in Table 3. The most severe conditions of temperature and acid led to increased yields of catechol, the major phenolic monomer measured in all conditions tested. A higher ratio of syringil derivative (syringaldehyde) was found in relation to guayacil (vanillin). At low severity conditions of 160–180°C without acid, these compounds were not found. Aromatic acids were not detected in any prehydrolyzate.

The maximum yield of soluble lignin-derived compounds, 196 mg/100 g dry untreated raw material, was obtained at 200°C, 5% solid concentration and 0.1% acid concentration. Total concentration in acid prehydrolyzates

Table 3
Yield of Phenolic Compounds (mg/100 g Dry Untreated Raw Material) in Prehydrolyzate From Dilute-Acid Pretreatment of Cardoon Biomass

| Acid concentration (% w/w) | 0 | | | 0.1 | | | 0.2 | | | | | | |
|---|---|---|---|---|---|---|---|---|---|---|---|---|---|
| Temperature (°C) | 160 | 180 | | 200 | 160 | 180 | 200 | 160 | 180 | 200 | | | |
| Solid concentration (% w/v) | 7.5 | 5 | 10 | 7.5 | 5 | 10 | 7.5 | 5 | 10 | 7.5 | 5 | 10 | 7.5 |
| Catechol | 2.6 | 8 | 10 | 39 | 12 | 20 | 61 | 96 | 80 | 39.9 | 86 | 83 | 85.3 |
| Vanillin | nd | 4 | nd | 13 | 8 | 6 | 15 | 20 | 10 | 4 | nd | 20 | 26.6 |
| Syringaldehyde | nd | nd | nd | 13.3 | 17.2 | 14 | 36 | 80 | 70 | nd | nd | 60 | 60.6 |

nd, detected.

ranged from low values about 40 mg/L at 160°C to 196 mg/L at 200°C. Concentrations found in prehydrolyzates produced at 180°C (about 80 mg/L) are lower than those reported by Fenske et al. *(16)* on the aromatic composition of dilute-acid prehydrolyzates prepared from switch grass, corn stover, and poplar biomass at 180°C, 10 min residence time and 1% w/w acid concentration (112.4, 140.8, and 247.3 mg/L). Our results support the idea of the lower toxicity of prehydrolyzates from herbaceous feedstocks in comparison with wood-derived ones, which implies a clear advantage from the point of view of its fermentation.

## *Mass Balance on Xylan*

To complete the assessment of the effectiveness of dilute-acid pretreatment to fractionate cardoon biomass, an overall mass balance for xylose, the major hemicellulose-derived sugar present in cardoon biomass, was carried out (Fig. 4). For this purpose, xylose measured in different fractions from pretreatment (WIS and prehydrolyzate) and furfural content were considered. Xylose recovery yields in WIS and prehydrolyzate (gram xylose/gram xylose in dry untreated raw material) were calculated based on data presented in Table 2. For purposes of mass balance, all furfural found in prehydrolyzate (Fig. 2) was considered to come from xylose degradation. Xylose recovery yield as furfural (gram furfural × 1.56/g xylose in dry untreated raw material) was calculated and summed up to WIS and prehydrolyzate xylose recovery values, as illustrated in Fig. 4.

Results show that at 180°C and 0.1 or 0.2% acid addition, regardless of the solid concentration, a 100% mass closure is attained. At these conditions, the percent of solubilized xylose amounts to 82%. At lower temperatures of 160 and 180°C in experiments without acid addition and at 160°C with 0.1% acid, the mass closure reaches values close to 90%, although a high proportion of xylan remains in the WIS fraction. Contrarily, the highest temperature of 200°C leads to overall recovery decreasing from 78% to 60%

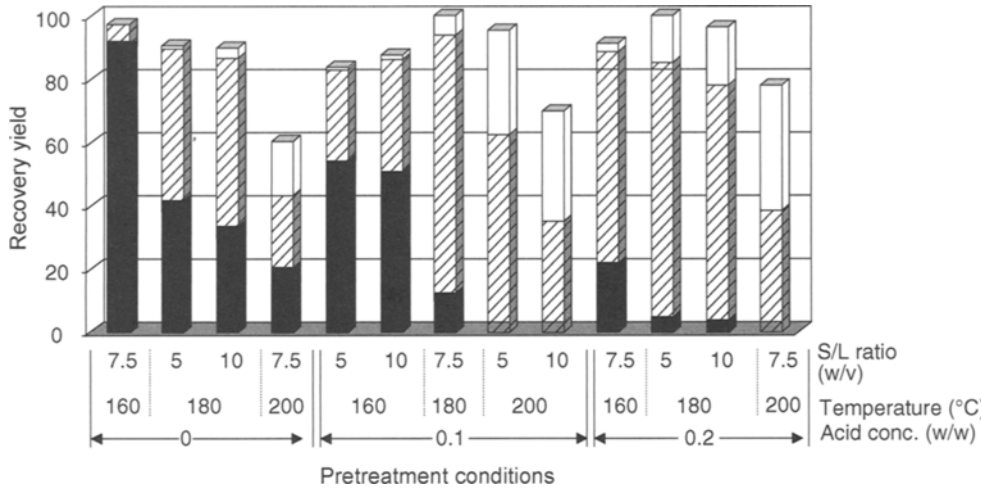


**Fig. 4.** Xylose recovery yields in WIS fraction (■), prehydrolyzate (▨), and xylose recovery as furfural (□), in prehydrolyzates from dilute-acid pretreatment of cardoon at different conditions. Results are reported as gram xylose/100 g xylose in dry untreated raw material.

with increased furfural formation and xylose losses, even in experiments without acid. Summing up, from results obtained in this work it can be concluded that mild temperature of 180°C with the addition of 0.1% (w/w) would be the condition chosen to effectively remove and recover most of the hemicelluloses as dissolved sugars in cardoon biomass. Nevertheless, the presence of inhibitory compounds makes necessary further studies on the fermentability of prehydrolyzate to determine the possibilities of using this fraction, or the whole slurry, for fermentation.

## References

1. Fernandez, J. (1998), In: *Energy Plant Species*. El Bassam N. (ed.), James & James Science, London, pp. 113–117.
2. Fernandez, J. (1990), Commission of the European Communities, Luxemburg, Report EUR 12631 EN-C, 54p.
3. Curt, M. D., Sanchez, G., Fernandez, J. (2002), *Biomass Bioener.* **23,** 33–46.
4. Oliet, M., Gilarranz, M. A., Dominguez, J. C., Alonso, M. V., and Rodriguez, F. (2005), *J. Chem. Technol. Biotechnol.* **80,** 746–753.
5. Martínez, J., Negro, M. J., Sáez, F., Manero, J., Sáez, R., and Martín, C. (1990), *Appl. Biochem. Biotechnol.* **24–25,** 127–134.
6. Wyman, C. E., Dale, B. E., Elander, R. T., Holtzapple, M., Ladisch, M. R., and Lee, Y.Y. (2005), *Bioresour. Technol.* **96(18),** 1959–1966.
7. Sun, Y. and Cheng, J. (2002), *Bioresour. Technol.* **83(1),** 1–11.
8. Saha, B. C., Iten, L. B., Cotta, M. A., and Wu, Y. V. (2005), *Biotechnol. Progr.* **21,** 816–822.
9. Toyd, T. A. and Wyman, C. E. (2205), *Bioresour. Technol.* **96(18),** 1967–1977.
10. Esteghlalian, A., Hashimoto, A. G., Fenske, J. J., and Penner, M. H. (1997), *Bioresour. Technol.* **59,** 129–136.
11. National Renewable Energy Laboratory (NREL). Chemical Analysis and Testing Laboratory Analytical Procedures: LAP-001 to 005, LAP-010 and LAP-017. NREL,

Golden, CO. http://www1.eere.energy.gov/biomass/for_researchers.html. Accessed August 30, 2006.
12. Maloney, M. T., Chapman, T. W., and Baker, A. J. (1986), *Biotechnol. Prog.* **20(4),** 192–202.
13. Fry, S. C. (1989), *J. Exp. Bot.* **40,** 1–11.
14. Karimi, K., Kheradmandinia, S., and Taherzadeh, M. J. (2006), *Biomass Bioener.* **30,** 247–253.
15. Neuriter, M., Danner, H., Thomasser, C., Saidi, B., and Braun, R. (2002), *Appl. Biochem. Biotechnol.* **98–100,** 49–58.
16. Fenske, J. J., Griffin, D. A., and Penner, M. H. (1998), *J. Ind. Microbiol. Biotechnol.* **20,** 364–368.

0273-2289/1559–0291 (Online)/07/136–140/253–266/$30.00

# Heat Extraction of Corn Fiber Hemicellulose

ZSUZSA BENKŐ,[1] ALEXANDRA ANDERSSON,[2] ZSOLT SZENGYEL,[1] MELINDA GÁSPÁR,[1] KATI RÉCZEY,*,[1] AND HENRIK STÅLBRAND[2]

*[1]Department of Agricultural Chemical Technology, Budapest University of Technology and Economics, Szent Gellérttér 4, H-1521 Budapest, Hungary, E-mail: kati_reczey@mkt.bme.hu; and [2]Department of Biochemistry, Center of Chemistry and Chemical Engineering, Lund University, P.O. Box 124, SE-22100 Lund, Sweden*

## Abstract

Water-soluble hemicellulose was extracted from corn fiber with microwave-assisted heat treatment. The effects of treatment temperature and initial pH of the aqueous extraction media were investigated regarding hemicellulose recovery and molecular mass of the isolated polysaccharides. In treatments carried out at neutral pH (simple water extraction), it has been demonstrated that hemicellulose recovery could be increased by applying higher treatment temperatures. However, the molecular weight of isolated hemicellulose gets significantly lower. For example, 10% of the raw materials' xylan was extracted at 160°C and about 30% recovery was reached at 210°C. However, the molecular mass of the isolated polysaccharide at 210°C ($5.82 \times 10^4$) was about half of that measured at 160°C ($1.37 \times 10^5$). Reducing the pH with sulfuric acid resulted in shorter polymer chains ($1.7 \times 10^4$) and lower hemicellulose yields (2.2%). Application of sodium hydroxide in the treatment showed that, compared with acid, considerably higher yields (11%) with longer polysaccharide chains ($1.3 \times 10^5$) could be obtained.

**Index Entries:** Alkaline extraction; carbohydrate analysis; microwave-assisted fractionation; size exclusion chromatography; weight-average molecular weight; maize.

## Introduction

Xylose-rich, water-soluble hemicelluloses have potential applications in numerous industries. They are used as ingredients in functional foods produced in Japan *(1)*, and it is suggested that agriculture might be another target area of utilization as "growth factor-like" properties have been shown *(2)*. Furthermore, using these renewable materials in the polymer industry for the production of biodegradable plastics provides a new

*Author to whom all correspondence and reprint requests should be addressed.

possibility to develop environmentally sound technologies and products (3). Xylan-based dietary fibers (4) can lower blood cholesterol level (5), reduce stomach ulcer lesions (6), stimulate the growth of intestinal Bifidobacteria (7), and xylans might act as human immunodeficiency virus inhibitor as well (8). Hemicelluloses have acceptable odor, low-caloric values, and are noncarcinogenic; thus, as filler substances they could be part of novel, fortified, and specialty foods as well, which are tools of antiobesity diets and enteral nutrition. Finally, these polymers could be constituents of synbiotics consisting of both a prebiotic and a live microbial food ingredient called probiotics (9).

There are two main factors determining the practical use of hemicellulose-originated polysaccharide isolates. On one hand, the chemical (sugar) composition, which primarily is a plant specific feature, needs to be considered. Corn fiber hemicellulose mainly consists of xylose (48%) and arabinose (35%), and also small amounts of galactose (7%) and glucuronic acid (10%) (10). The structure of corn fiber hemicellulose has been studied extensively. It is a branched arabinoglucuronoxylan in which 4-O-methylglucuronic acid groups, arabinose, and trisaccharide groups made up of arabinose, xylose, and galactose are linked directly to the main xylan backbone (11).

On the other hand, the way of lignocellulosics fractionation influences the polymer structure, thus the possible field of application. There are four generally accepted main fractionation categories: physical, chemical, biological, and physico-chemical methods (12). Heat treatments such as steam explosion, microwave irradiation (13,14), and hot water extraction (15,16) are regarded as physico-chemical treatments. Chemical treatment is carried out with the aid of bases (17–19), acids, or organic solvents. Lignin removal can be carried out with biological methods such as the use of lignin degrading microbes.

Lately, biofuels have gained great interest because of environmental considerations as well as global increase in cost of fossil fuels. In the production of ethanol from corn the first step is wet-milling, which yields different byproducts, including corn fiber. Generally, this corn fiber is utilized as animal feed. An anticipated increase in ethanol production is expected to saturate the animal feed market. Therefore, it is of great importance to look for alternative applications of corn fiber and to examine the possibilities to upgrade it to value-added products. One possibility would be to separate the different components in the fiber, thereby obtaining refined products for further processing.

In this study, corn fiber hemicellulose was fractionated using microwave irradiation according to the flow sheet shown in Fig. 1. This treatment involves both physical and chemical methods and has previously been applied for the extraction of galactoglucomannan hemicellulose from spruce (20,21). The effect of treatment temperature and pH were investigated at fixed residence time. Hemicellulose recovery, the molecular weight

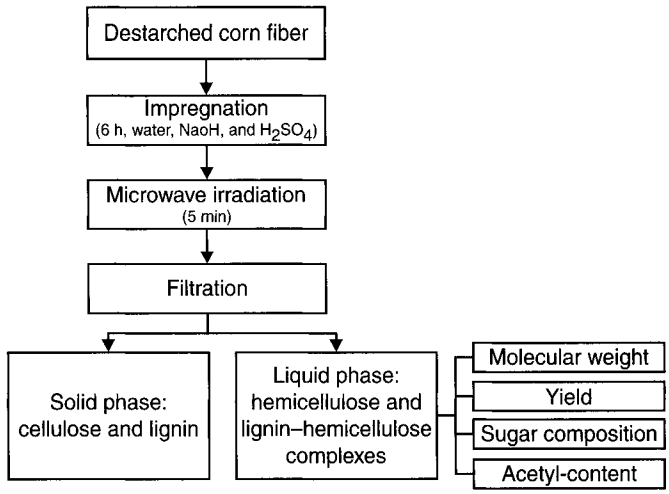


**Fig. 1.** Schematic flowchart of hemicellulose isolation and characterization from corn fiber.

of solubilized hemicellulose, the sugar composition, and the acetyl group content of isolates obtained under different treatment conditions were determined.

## Materials and Methods

### *Preparation and Analysis of Starch Free Corn Fiber*

Corn fiber, which is a byproduct of corn wet-milling starch manufacturing, was kindly provided by Hungrana Co. (Hungary). The average particle size of corn fiber was less than 8 mm and it was not ground before use. Starch was removed in a two-step enzymatic hydrolysis process using thermostable α-amylase (Thermamyl Supra, Novozymes, Denmark) in a 31-L B.Braun DCU-3 laboratory bioreactor (B. Braun Biotech AG, Germany), at 8.7% dry matter content in 0.05 *M* sodium acetate buffer solution (pH 4.8) with continuous stirring at 250 rpm. In the first step 19.4 mL of Thermamyl Supra was added. The mixture was heated up to 120°C and after 20 min the slurry was cooled down to 90°C at this temperature another 19.4 mL of Thermamyl Supra was added and hydrolysis was allowed to continue for another hour. On completion of starch hydrolysis, the slurry was filtered through a 150-mm mesh nylon filter. The liquid fraction was discharged and the filter cake was washed with hot distilled water. The starch free corn fiber (SFCF) was air-dried and stored at room temperature. The dry matter content of air-dried SFCF was 90.9%.

The chemical composition of SFCF was determined with the Hägglund procedure *(22)* followed by high-performance liquid chromatography (HPLC) analysis of the sugars. SFCF contained, given as weight percentages of dried material, 22.1% cellulose, 36.5% hemicellulose, 19.2% lignin, and

22.3% other compounds such as extractives, protein, and ash. On the basis of dry SFCF the hemicellulose fraction contained (expressed in polysaccharide form): 13.7% arabinose, 5.6% galactose, and 17.2% xylose.

### *Microwave-Assisted Heat Treatment of SFCF*

Before heat treatment, 10.0 g air-dried SFCF was soaked with 199.0 g impregnation medium: either distilled water or aqueous solutions of sulfuric acid (0.025% and 0.5%) or sodium hydroxide (0.025% and 0.5%) for 6 h. The whole slurry was transferred into a 350-mL well-sealed Teflon treatment vessel, which was then placed into a microwave oven (Milestone MLS-1200 Mega Microwave Workstation, Sorisole, Italy). The microwave oven was programmed to heat up the reaction mixture in a 2-min cycle to the desired treatment temperature. On reaching the set point, the temperature was controlled at a constant value for another 5 min. The temperature inside the vessel was regulated through a thermocouple immersed into the slurry. Temperatures of 100, 130, 160, 180, 200, and 210°C, respectively were screened. On completion of the heat treatment cycle, the reaction vessel was removed from the oven and cooled down to room temperature with cold water stream. Fibrous residue of the treated SFCF was separated by vacuum filtration of the water-soluble hemicellulose fraction, which was then analyzed for both monomeric sugar and hemicellulose content.

### *Extraction of Hemicellulose-B*

Hemicellulose-B isolation from SFCF was performed according to the procedure described earlier *(23)*. In the first step hemicellulose was extracted from the material by treatment with 2% sodium hydroxide solution at 120°C for 60 min. The dry matter content of the mixture was 10%. After heat treatment, the suspension was rapidly cooled to room temperature and the solid fraction was separated by filtration on a 150-μm mesh nylon filter. The filtrate was collected and the pH of the liquid was adjusted to 4.5 with 35% hydrochloric acid. Double volume of 95% ethanol was added to the filtrate. After 1 d at room temperature the precipitated hemicellulose-B was collected by filtration, rinsed with ethanol, and dried at 105°C. Sugar composition, acetyl group content, and average molecular weight of the isolate were determined as described under "Analysis" for samples obtained in microwave heat treatment.

### *Analysis*

#### Determination of Hemicellulose Content

Supernatants obtained after heat treatment were directly analyzed for monomeric sugars using high-performance liquid chromatography (HPLC) pulsed amperometric detection (PAD) (described under "Carbohydrate Analysis"). For the determination of hemicellulose polymers a milliliter of

each liquid obtained in the heat treatment was hydrolyzed with an equivalent amount of 0.4 *M* sulfuric acid solution in an autoclave at 121°C for 60 min. Samples were subjected to HPLC analysis and the differences between sugar concentrations measured after and before acid hydrolysis were used to calculate the amount of polysaccharides (correction factor of 1.13 for water on hydrolysis was applied).

### Fractionation of Polysaccharides by Size Exclusion Chromatography

Weight-averaged molecular weight ($M_w$) of hemicellulose extracted from SFCF was determined by size exclusion chromatography (SEC). A 500-µL aliquot was loaded on a two-column configuration containing a Superdex 75 and a Superdex 200 column (GE Healthcare, formerly Amersham Biosciences, Uppsala, Sweden) connected in series to an fast protein liquid chromatography (FPLC) system (GE Healthcare). Elution of samples with ultrapure water at a flow rate of 0.5 mL/min was followed by refractive index (RI) detection (RID, Erma-inc, Tokyo, Japan) and ultraviolet detection at 280 nm (GE Healthcare), enabling the detection of both polysaccharides and ultraviolet absorbing compound such as solubilized lignin degradation products. The molecular weight distribution of polysaccharides was determined using dextran (Fluka Chemie AG, Buchs, Switzerland) calibration standards with $M_w$ of 1270, 5220, 11,600, 23,800, and 48,600, respectively. The total dead volume of the two-column configuration (47 mL) was assessed with acetone and the void volume, using Blue Dextran (Fluka Chemie AG) was determined to be 16 mL. During elution, fractions of 2 mL were collected. Fractions showing RI signal in the chromatograms were subjected to further polysaccharide analysis as described in the hemicellulose Analysis section.

### Carbohydrate Analysis

Samples for sugar analysis, obtained during heat treatment or SEC elution, were first filtered through a 0.2-µm syringe filter (Acrodisc, PALL Gelman Laboratory, MI). Sugars were analyzed using high-performance anion-exchange with PAD (Dionex, Sunnyvale CA). The high-performance anion-exchange with pulsed amperometric detection instrument consisted of an ED40 electrochemical detector, a GP40 gradient pump, an AS50 autosampler, and a Carbopac PA-10 guard and analytical column (all from Dionex). Glucose, xylose, arabinose, galactose, and mannose were separated on the analytical column using ultrapure water as mobile phase, at a flow rate of 1.0 mL/min. In order to enable detection of the sugars using PAD, 600 m*M* NaOH was added by a postcolumn pump.

### Determination of Acetyl Groups

The analysis of acetyl groups was based on the release of acetyl groups by alkaline treatment *(24)*. Fractions collected during SEC were first freeze-dried and then dissolved in 1 mL NaOH (1%) solution to remove acetyl

groups from the polysaccharide by 12-h incubation at room temperature. The concentration of liberated acetyl groups was determined by HPLC as acetic acid. Bound acetyl content was calculated by subtracting the free acetate amount in the sample from the amount quantified after treatment with 1% NaOH.

Acetic acid was determined using a GE Healthcare HPLC system equipped with an RI detector. An Aminex HPX-87H organic acid column (BIO-RAD, Hercules, CA) thermostated at 65°C was used to separate acetic acid from other compounds. The mobile phase was 5 mM $H_2SO_4$ at a flow rate of 0.6 mL/min. The system was equipped with a Cation-H Refill Cartridge (BIO-RAD) to protect the analytical column.

## Calculations

### Yield of Xylan in Heat-Treated Samples

Polymer form of extracted hemicellulose was expressed on the basis of polymeric xylose, i.e., xylan. The xylan recovery, i.e., yield of hemicellulose extracted from SFCF, was calculated according to Eq. 1.

$$Y_{xylan} = \frac{X_H - X_F}{f \times X_T} \times 100 \quad (1)$$

where, $X_H$ is the xylose content, calculated in grams, determined after acid hydrolysis of the filtrate obtained in microwave treatment, $X_F$ is the xylose content in the filtrate calculated in grams based on direct sugar analysis of the filtrate obtained in treatment, $f$ is the conversion factor of polymer to monomer hydrolysis (for xylose-based polymers $f = 1.136$ g/g), and $X_T$ is the amount of xylan in grams in SFCF used in the experiments.

### Weight-Average Molecular Weight

A generally accepted formula for the calculation of weight-average molecular weight of polymers *(25)*, based on data obtained from SEC chromatograms is shown in Eq. 2.

$$M_W = \frac{\sum_{i=1}^{N}(c_i \cdot M_i)}{\sum_{i=1}^{N} c_i} \quad (2)$$

where $M_i$ is the molecular weight at elution volume $v_i$ and $c_i$ is the concentration at elution volume $v_i$. The concentration $c_i$, was calculated from the acid hydrolysis of fractions collected during SEC, whereas $M_i$ was calculated from the SEC dextran calibration according to Eq. 3 *(16)*.

$$\log M_i = 0.0968 \times v_i + 6.7103 \quad (3)$$

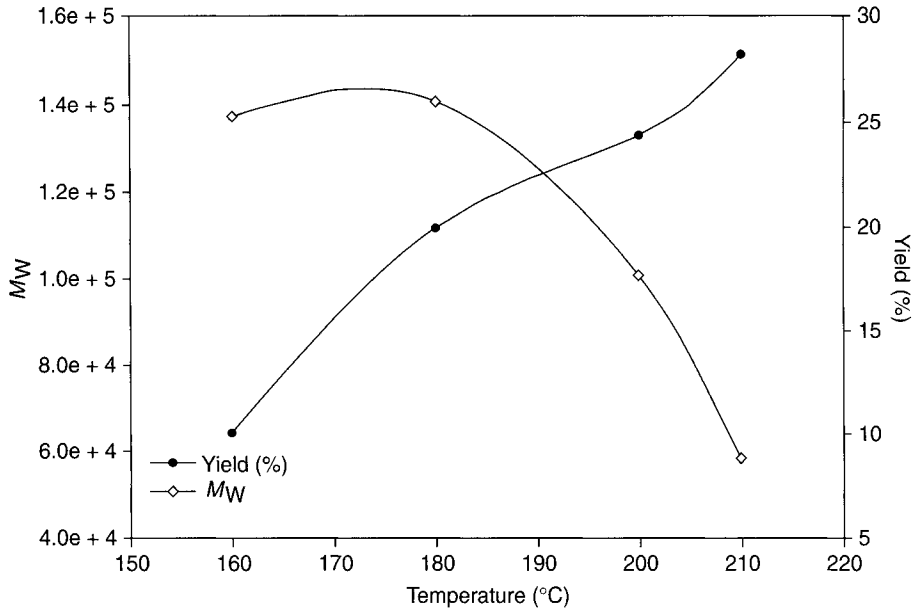


**Fig. 2.** Effect of temperature on the molecular weight and yield of hemicellulose extracted by microwave assisted heat treatment using pure water.

## Results and Discussion

### *Effect of Temperature*

The effect of temperature on the isolation of hemicelluloses from SFCF was examined applying water as the extraction agent without any addition of acidic or alkaline catalysts. Treatment temperature was varied between 100°C and 210°C, which was the highest working temperature of the microwave oven. Water-soluble hemicellulose fractions obtained at different temperature set points were analyzed for molecular weight with SEC. Polymeric hemicellulose recovery was calculated on the basis of xylan recovered (Fig. 2). Treatments carried out at 100°C and 130°C did not produce measurable amounts of solubilized hemicellulose. About 10% hemicellulose extraction, with a polymer $M_w$ of $1.4 \times 10^5$, was reached at 160°C. Increasing treatment temperature significantly influenced the hemicellulose recovery. A maximum of 22.8% hemicellulose yield was obtained at the highest (210°C) temperature value. However, severe degradation of the isolated hemicellulose was observed at higher treatment temperatures, resulting in the lowest $M_w$ of about $6 \times 10^4$ at 210°C. The white–offwhite color of hemicellulose isolates obtained at 160°C and 180°C turned to brown at elevated treatment temperatures.

Optimization of the microwave-assisted heat treatment has to be a compromise between hemicellulose recovery and the molecular weight of the isolated fraction. As shown in Fig. 2, applying higher temperatures than 180°C will significantly lower the molecular weight of isolated

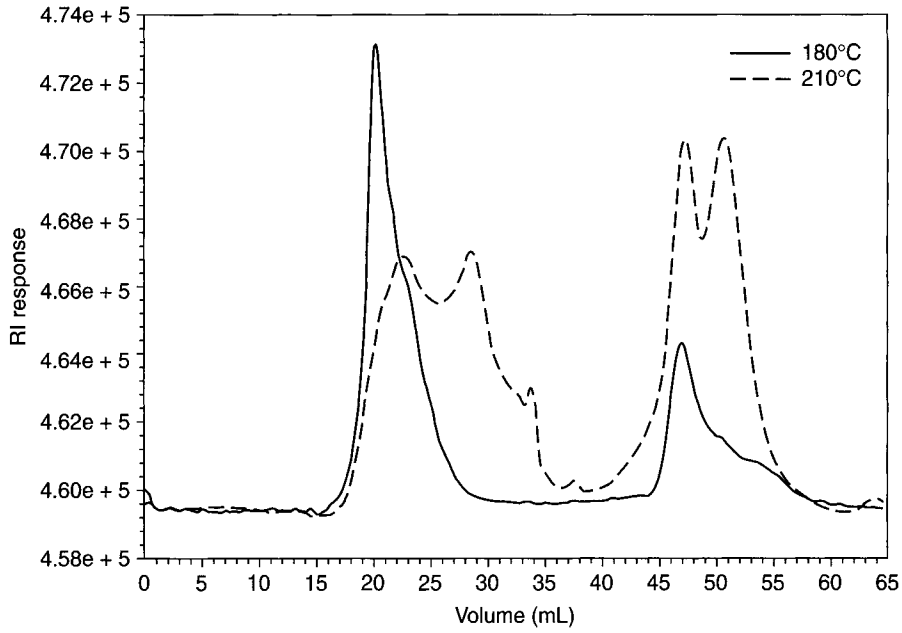


**Fig. 3.** SEC RI chromatograms of hemicellulose samples extracted by microwave assisted heat treatment at 180°C and 210°C using pure water.

hemicellulose. Furthermore, whereas the hemicellulose yield was doubled by a temperature increase from 160°C to 180°C, with no apparent degradation of polymer chains, only 20% higher yield was obtained by another 20°C temperature increase. The pH of the suspension after heat treatment was measured. Compared with the initial pH of 6.2, significantly lower pH values were observed. Increasing treatment temperature resulted in lower pH, for example, at 160°C pH of 5.6, at 180°C pH of 4.3, and at 210°C pH of 3.7 was measured.

The presence of acetyl groups on many types of hemicelluloses present a specific problem. During heat-treatment at certain conditions the acetyl groups can be released yielding acetic acid, thereby causing a decrease in pH. The lower pH, in turn, may cause acid hydrolysis of the glycosidic bonds in the polysaccharide backbone and/or substitutions. In the current case, the pH of the mixture measured after treatment indicated that liberation of acetic acid occurred to a greater extent at high treatment temperatures. These data suggest that acid hydrolysis became the dominant mechanism of hemicellulose recovery over physical extraction of hemicellulose.

Two SEC chromatograms of polysaccharides isolated at 180°C and 210°C are shown in Fig. 3. It can be seen that at 180°C, two dominant fractions were found in the extracts. The peak area of the first peak resulting from the elution of high-molecular weight polymers is significantly greater than the area of the second peak, indicating that the extract contained higher amounts of high-molecular weight polysaccharides. On

Table 1
Molecular Weight and Yield of Microwave Isolated Hemicellulose (at 180°C, Impregnated With Water, Acid, or Alkali) and Alkaline Extracted, Ethanol Precipitated Hemicellulose-B

| Treatment Type | Concentration of impregnation media (%) | Molecular weight ($M_w$) | Yield (%) |
|---|---|---|---|
| Water | – | 127,000 | 20 |
| $H_2SO_4$ | 0.025 | 13,800 | 3.9 |
| $H_2SO_4$ | 0.5 | 17,600 | 2.2 |
| NaOH | 0.025 | 172,000 | 4.6 |
| NaOH | 0.5 | 136,000 | 11 |
| Alkaline extracted ethanol precipitated hemicellulose-B | – | 192,000 | 56 |

the other hand, the extract obtained at 210°C showed more diversity and at least four fractions could be identified. Lower molecular weight polysaccharides were more prominent in this extract.

### *Effect of pH*

Heat treatment of SFCF applying acid or alkaline catalyst was performed at 180°C. Before heat treatment the material was impregnated as written in Materials and Methods section. Both hemicellulose recovery and molecular weight of the isolated hemicellulose were determined (Table 1). The addition of acid did not improve hemicellulose recovery, and considerably lower hemicellulose yields were obtained relative to impregnation with pure water. Not surprisingly, the molecular weight of the recovered hemicellulose fraction was also lower in the presence of the acid catalyst. Furthermore, increasing the acid concentration did not affect hemicellulose molecular weight or recovery. Sodium hydroxide seemed to be a more suitable impregnation agent than sulfuric acid. The molecular weight of the hemicellulose isolates was greater than in case of water extraction; however, hemicellulose yields were far less than those achieved with pure water (Table 1).

### *Comparison of Microwave and Alkaline-Extracted Hemicellulose*

Hemicellulose polymers fractionated by microwave-assisted heat treatment of SFCF were compared with alkaline-extracted and ethanol-precipitated hemicellulose-B. Heat treatment was carried out at 180°C with 5 min of holding time using pure water, whereas hemicellulose-B was isolated as described in the Materials and Methods section of this paper. Molecular weight, acetyl group content, and recoveries based on the

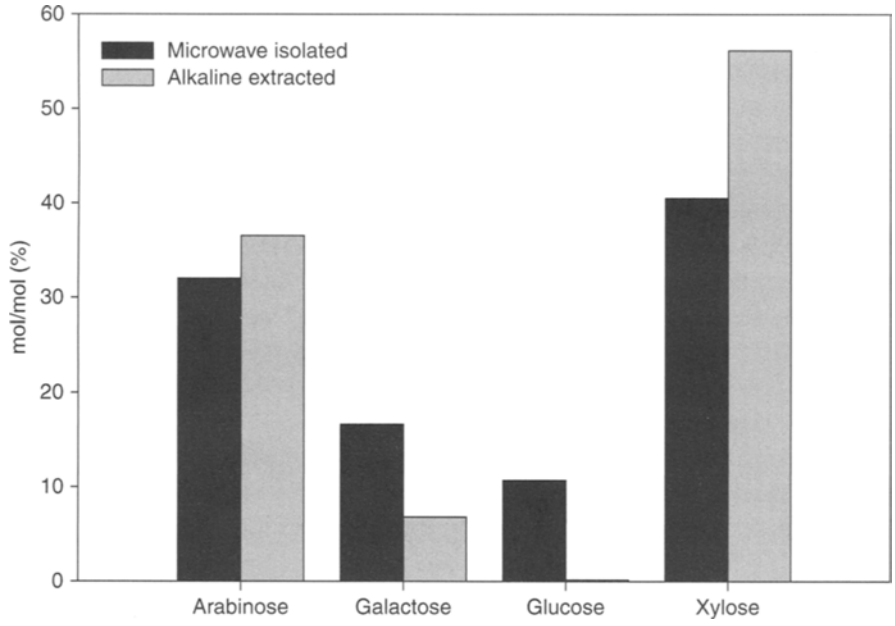


**Fig. 4.** Sugar composition of hemicellulose isolated in microwave assisted heat treatment at 180°C with pure water and alkaline extracted and precipitated hemicellulose-B. (The amounts of different sugars are expressed in the percent of the total sugar content of the sample in moles.)

original raw material xylan content were examined. The molecular weight of hemicellulose-B was higher than that achieved on microwave heat treatment (Table 1). This could be explained with the lower applied temperature of the alkaline treatment; second, liberated acetic acid was neutralized by the sodium hydroxide.

The analysis of fractions during SEC revealed some differences in the composition of polysaccharides obtained in the two preparations. The two dominating sugar residues were xylose and arabinose in both cases (Fig. 4) indicating that, as expected, arabinoxylan is the major polysaccharide. The molecular ratios of xylose : arabinose were also similar: 1.5 for the alkaline extract, and 1.3 for the microwave extract. These values are close to the reported ratio of approx 1.4 for corn hemicellulose *(12)*. The galactose content in the alkaline preparation is also very close to that previously reported for corn fiber hemicellulose (approx galactose : xylose ratio of 0.1). However, the microwave extracted preparation contained a significantly higher amount of galactose (galactose : xylose ratio 0.4). Furthermore, the microwave preparations contained glucose (Fig. 4), possibly indicating minor contamination of starch.

The SEC chromatograms of the two hemicellulose isolates are shown in Fig. 5. Two distinctly separated peaks were observed for both hemicellulose isolates. The analysis of fractions collected during the elution of the first peak, representing high-molecular weight polysaccharides,

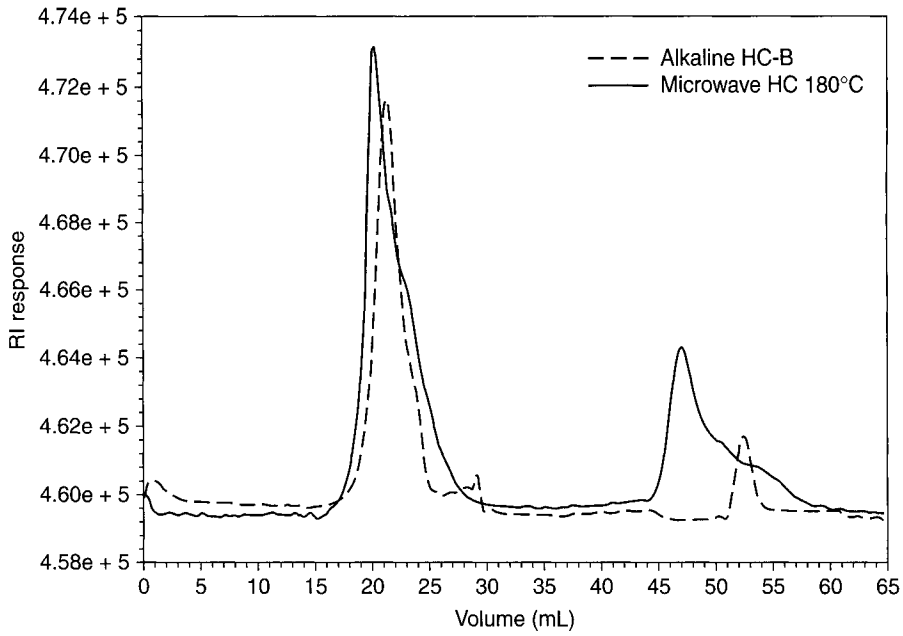


**Fig. 5.** SEC RI chromatograms of hemicellulose extracted by microwave assisted heat treatment at 180°C with pure water and hemicellulose-B.

showed that these polysaccharides were mainly made up of xylose and arabinose, their ratio was 2.2 for the microwave extracted preparation and 2.0 for alkaline treatment. On the other hand, fractions collected later, i.e., the smaller molecular weight polysaccharides, were rich in arabinose. The xylose content of these fractions was about half of the arabinose measured.

Alkaline-extracted hemicellulose-B did not contain a measurable amount of acetyl groups. However, the acetyl group content of hemicellulose isolated on heat treatment at 180°C using around 3 wt% water for the extraction. It is noteworthy to mention that acetyl groups were only detected in those fractions eluted during SEC, which corresponded to the peak containing higher molecular weight polymers. Further experiments will be performed to analyze the assumed position of acetylation.

## Conclusion

The aim of this study was to investigate the possibility of hemicellulose-based polysaccharide isolation from SFCF in microwave-assisted heat treatment and to compare the isolated polysaccharide with hemicellulose-B, a polymer obtained with the well-known alkaline extraction-ethanol precipitation method. The results of aqueous hemicellulose extraction performed at different temperatures showed that hemicellulose recovery could be improved by increasing the temperature of the treatment, but at the same time the molecular weight of the isolated polymers, along with the pH of

the reaction mixture decrease, supporting the assumed mechanism of degradation of polymer chains caused by autohydrolysis.

Application of acid catalyst (sulfuric acid) did not increase hemicellulose recovery and very low molecular weights were obtained. Sodium hydroxide proved to be a more sufficient catalyst. Although, hemicellulose yields were less than those obtained with water, higher molecular weight polysaccharides were isolated. In terms of comparison with alkaline extraction, it could be concluded that microwave treatment provided lower molecular weight and lower polymer recovery, but on the other hand it performed well without application of any chemicals. Thus, it could be a novel environmentally sound way of hemicellulose isolation.

## Acknowledgments

This research was supported by the *European Cooperation in the field of Scientific and Technical Research* (COST Action E-23). *Hungarian Scientific Research Fund* (OTKA TS 049849) is greatly acknowledged for its financial contribution. The authors wish to express their gratitude to the staff of the *Department of Chemical Engineering, Lund University* for helping us to carry out measurement using their research facility. *Carl Tryggers Research Foundation* and *Vinnova* are gratefully acknowledged for grants to H. S. *The Sven and Lilly Lawski* foundation is acknowledged by A. A. for providing a predoctoral scholarship.

## References

1. Crittenden, R. G. and Playne, M. J. (1996), *Trends Food Sci. Technol.* **7,** 353–361.
2. Vázquez, M. J., Alonso, J. L., Domínguez, H., and Parajó, J. C. (2000), *Trends Food Sci. Technol.* **11,** 387–393.
3. Buchanan, C. M., Buchanan, N. L., Debenham, J. S., et al. (2003), *Carbohydr. Polym.* **52,** 345–357.
4. Sugawara, M., Suzuki, T., Totsuka, A., Takeuchi, M., and Ueki, K. (1994), *Starch* **46,** 335–337.
5. Chinen, I. and Sadoyama, K. (1989), Japanese patent JP 89 40,502.
6. Parajó, J. C., Garrote, G., Cruz, J. M., and Dominguez, H. (2004), *Trends Food Sci. Technol.* **15,** 115–120.
7. Dohnalek, M. I. H., Ostrom, K. M., and Hilty, M. D. (1998), US patent 5,827,526.
8. Magerstaedt, M., Meichsner, C., Schlingmann, M., et al. (1991), German patent DE 3,921,761 A1.
9. Vázquez, M. J., Alonso, J. L., Domínguez, H., and Parajó, J. C. (2000), *Trends Food Sci. Technol.* **11,** 387–393.
10. Wolf, M. J., MacMasters, M. M., Cannon, J. A., Rosewall, E. C., and Rist, C. E. (1953), *Cereal Chem.* **30,** 451–470.
11. Montgomery, R., Smith, F., and Srivastava, H. C. (1956), *J. Am. Chem. Soc.* **78,** 2837–2839.
12. Sun, Y. and Cheng, J. (2002), *Bioresour. Technol.* **83,** 1–11.
13. Zhu, S., Wu, Y., Yu, Z., et al. (2005), *Biosyst. Eng.* **92,** 229–235.
14. Zhu, S., Wu, Y., Yu, Z., et al. (2006), *Process Biochem.* **41,** 869–873.
15. Mosier, N. S., Hendrickson, R., Brewer, M., et al. (2005), *Appl. Biochem. Biotechnol.* **125,** 77–97.
16. Allen, S. G., Schulman, D., Lichwa, J., and Antal, M. J., Jr. (2001), *Ind. Eng. Chem. Res.* **40,** 2934–2941.

17. Doner, L. W. and Hicks, K. B. (1997), *Cereal Chem.* **74,** 176–181.
18. Doner, L. W., Chau, H. K., Fishman, M. L., and Hicks, K. B. (1998), *Cereal Chem.* **75,** 408–411.
19. Hespell, R. B. (1998), *J. Agric. Food Chem.* **46,** 2615–2619.
20. Lundqvist, J., Teleman, A., Junel, L., et al. (2002), *Carbohydr. Polym.* **48,** 29–39.
21. Lundqvist, J., Jacobs, A., Palm, M., Zacchi, G., Dahlman, O., and Stålbrand, H. (2003), *Carbohydr. Polym.* **51,** 203–211.
22. Hägglund, E. (1951), Chemistry of Wood. Academic Press, New York. pp. 324–332.
23. Gáspár, M., Juhász, T., Szengyel, Zs., and Réczey, K. (2005), *Process Biochem.* **40,** 1183–1188.
24. Kaar, W. E., Cool, L. G., Merriman, M. M., and Brink, D. L. (1991), *J. Wood Chem. Technol.* **11,** 447–463.
25. Mourey, T. H. and Coll, H. (1995), In: *Chromatographic Characterization of Polymers: Hyphenated and Multidimensional Techniques.* Provder, T., Barth, H. G., and Urban, M. W. (eds.), American Chemical Society, Washington, DC: pp. 123–140.

0273-2289/1559-0291 (Online)/07/136–140/267–280/$30.00

# An Evaluation of British Columbian Beetle-Killed Hybrid Spruce for Bioethanol Production

ALEX BERLIN,*[,1] CLAUDIO MUÑOZ,[2] NEIL GILKES,[1] SEPIDEH MASSOUMI ALAMOUTI,[1] PABLO CHUNG,[1] KYU-YOUNG KANG,[1] VERA MAXIMENKO,[1] JAIME BAEZA,[2] JUANITA FREER,[2] REGIS MENDONÇA,[2] AND JACK SADDLER[1]

*[1]Forest Products Biotechnology, Faculty of Forestry, The University of British Columbia, Vancouver, BC V6T 1Z4, Canada, E-mail: aberlin@interchange.ubc.ca; and [2]Laboratory Renewable Resources, Biotechnology Center, University of Concepción, Concepción, Chile*

## Abstract

The development of bioconversion technologies for production of fuels, chemicals, and power from renewable resources is currently a high priority for developed nations such as the United States, Canada, and the European Union as a way to improve national energy security and reduce greenhouse gas emissions. The widespread implementation of such technologies will require a sustainable supply of biomass from forestry and agriculture. Forests are a major source of feedstocks for biofuels production in Canada. Woody biomass includes residues from logging and forest thinning, and from wood processing and pulp production.

More recently, damaged wood caused by beetle infestations has become available on a large scale in Western Canada. This study evaluates beetle-killed British Columbian hybrid spruce (HS) (*Picea glauca* × *P. engelmannii*) as a feedstock for the production of bioethanol. In the past 30 yr, attack by the beetle *Dendroctonus rufipennis* and associated fungi has resulted in estimated losses of more than three billion board feet in British Columbia alone. Here we describe the chemical and some physical characteristics of both healthy (HHS) and beetle-killed (BKHS) British Columbian HS and evaluate the technical feasibility of using these feedstocks as a source of biomass for bioethanol production. Untreated HHS and BKHS did not differ significantly in chemical composition except for the moisture content, which was significantly lower in BKHS (approx 10%) compared with HHS (approx 18%). However, the yields of carbohydrates in hydrolyzable and fermentable forms were higher at mild pretreatment conditions (H-Factor <1000) for BKHS compared with HHS. At medium (H-Factor 1000–2000) and severe (H-Factor >2000) pretreatment conditions HHS and BKHS behaved similarly.

*Author to whom all correspondence and reprint requests should be addressed.

Organosolv pretreated HHS and BKHS demonstrated good ethanol theoretical yields, approx 70 and 80%, respectively.

**Index Entries:** Cellulase; enzyme; ethanol; hydrolysis; lignocellulose; fermentation.

## Introduction

The expansion of the use of biomass as an energy source is seen by developed nations and many developing countries as a way to reduce the need for fossil oil and gas to secure national energy supply. Furthermore, this principle is considered a feasible approach to support sustainable development of rural economies based on agriculture and forestry. It is also recognized that in order to provide a continuous supply of renewable sources of biomass for bioenergy production, bioethanol in particular, biomass feedstocks from both forest and agricultural sources will be required *(1)*. Forest residues, mainly softwood, are particularly abundant in Northern countries such as Canada. This includes residues from logging and forest thinning, and from wood processing and pulp production.

More recently, damaged wood resulting from insects' attacks, such as beetles, and associated fungi have become available as potential substrates for biomass conversion. These outbreaks of infestation are interpreted as a consequence of global warming trends, which make forests more vulnerable to pest infestations. Moreover, proliferation of global trading is likely to introduce further insect pests; for example, the establishment of brown spruce longhorn beetle *Tetropium fuscum* (Fabricius) in Nova Scotia, Canada. Therefore, it is expected that these types of woody residues will continue to be available for several decades. A representative example of an extensively affected softwood species is the British Columbian hybrid spruce (HS) (*Picea glauca* × *P. engelmannii*).

Spruce is an important component of boreal forests and occupies more than 75% of Canada's forested land *(2)*. Microbial pathogens and outbreak species of insects are the major biotic disturbance agents of spruce forests *(3,4)*. In Canada, the annual volume loss because of growth reduction and mortality caused by insects and pathogens averaged 102.8 million cubic metres between 1982 and 1987, which is equivalent to 70% of the volume harvested nationwide *(5)*. Bark beetles (*Coleoptera*: *Curculionidae*: *Scolytinae*) and their associated fungi currently cause the greatest amount of mortality in Canada and the rest of the world's coniferous forests. Total forest losses as a result of bark beetle–fungal interactions are difficult to estimate but are considered to be greater than those caused by all other insects, pathogens, and fire combined, amounting to millions of dollars every year in British Columbia *(6)*. *Dendroctonus rufipennis* (Kirby) and *Ips typographus* (Linnaeus) are examples of highly aggressive spruce-colonizing bark beetles that have destroyed millions of hectares of spruce forests in North America and Eurasia, respectively *(7–10)*. The capacity of aggressive bark

beetles to overcome the resistance of healthy trees is usually mediated by associated fungi.

Most fungi associated with bark beetles are blue stainers: the filamentous ascomycetes generally referred as Ophiostomatoid fungi *(11)*. These fungi are responsible for significant economic losses to wood and forest industries worldwide. Some of them, for example, *Ophiostoma ulmi* (Buisman), are among the most virulent pathogens and many others are the causal agent of wood discoloration *(11–13)*. The main goal of this study was to perform a preliminary evaluation of the feasibility of utilizing beetle-killed British Columbian HS for bioethanol production.

## Materials and Methods

### *Sampling and Sample Preparation*

Representative samples of approx 125-yr old HHS and BKHS, respectively, were collected from a single stand located in the University of British Columbia (UBC)/Alex Fraser Research Forest (Williams Lake, BC, Canada) at the biogeoclimatic subzone ICHmk3. After harvesting, logs were debarked, split, chipped, and milled to a chip size of approx $\leq 10 \times 10 \times 3$ mm$^3$.

### *Substrate Pretreatment*

Healthy HS and BKHS chips were organosolv-pretreated in aqueous ethanol (50%, w/w), with sulfuric acid as catalyst (1.2%, w/w oven-dried wood) at 7 : 1 liquor : wood ratio in a custom-built, four-vessel, rotating digester (Aurora Products, Ltd., Savona, BC, Canada). Two hundred-gram (oven-dry weight) batches of HHS and BKHS chips were cooked in each 2-L vessel under 12 different conditions, chosen (Table 1) depending on cooking extents described by H-factors *(14)* varying from approx 440 to 5800, corresponding to approx 168°C for about 34 min to approx 195°C for about 50 min, respectively.

The experimental design was performed with the help of SAS v. 9.00 software package (SAS Institute, Inc., Cary, NC). The range of conditions was defined based on our previous experience in organosolv pretreatment of softwoods *(15,16)*. After cooking, vessels were cooled to room temperature in a water bath. Solids and liquor were then separated using a nylon mesh. Solids (pulp and rejects) were homogenized and separated from rejects (recalcitrant, poor-pretreated substrate fraction) by using a standard vibrating screen (Voith, Inc., Appleton, WI) fed with tap water. The resultant fibers, so-called "accepts" or "pulps," were subjected to enzymatic hydrolysis and subsequent fermentation. Carbohydrates dissolved in the spent liquor (liquid fraction) or present in form of rejects were considered as losses for the purpose of this study.

The liquid fractions after ethanol organosolv (OS) pretreatment were diluted with four volumes of tap water to precipitate the dissolved lignin.

Table 1
Ethanol Organosolv Pretreatment Conditions of HHS and BKHS Wood Samples

| | Set variables | | | Observed variables | | | |
|---|---|---|---|---|---|---|---|
| Pulp sample | *T* (°C) | *t* (min) | H-Factor[a] | *T* (°C) | *t* (min) | H-Factor | P (psi) |
| HHS1 | 168 | 34 | 516 | 168 ± 2 | 34 | 510 | 190 |
| HHS2 | 192 | 46 | 4293 | 192 ± 2 | 46 | 3985 | 310 |
| HHS3 | 172 | 40 | 836 | 172 ± 2 | 40 | 911 | 210 |
| HHS4 | 188 | 40 | 2945 | 188 ± 2 | 40 | 3456 | 300 |
| HHS5 | 180 | 36 | 1447 | 180 ± 2 | 36 | 1238 | 235 |
| HHS6 | 180 | 44 | 1724 | 180 ± 2 | 44 | 1505 | 240 |
| HHS7 | 180 | 40 | 1585 | 180 ± 2 | 40 | 1880 | 270 |
| HHS8 | 180 | 40 | 1585 | 180 ± 2 | 40 | 1687 | 255 |
| HHS9 | 180 | 40 | 1585 | 180 ± 2 | 40 | 1390 | 260 |
| HHS10 | 195 | 50 | 5978 | 195 ± 2 | 50 | 5816 | 340 |
| HHS11 | 175 | 45 | 1185 | 175 ± 2 | 45 | 1139 | 230 |
| HHS12 | 185 | 36 | 2125 | 185 ± 2 | 36 | 2090 | 260 |
| BKHS1 | 168 | 34 | 516 | 168 ± 2 | 34 | 437 | 180 |
| BKHS2 | 192 | 46 | 4293 | 192 ± 2 | 46 | 3960 | 330 |
| BKHS3 | 172 | 40 | 836 | 172 ± 2 | 40 | 738 | 210 |
| BKHS4 | 188 | 40 | 2945 | 188 ± 2 | 40 | 2645 | 310 |
| BKHS5 | 180 | 36 | 1447 | 180 ± 2 | 36 | 1265 | 250 |
| BKHS6 | 180 | 44 | 1724 | 180 ± 2 | 44 | 1510 | 230 |
| BKHS7 | 180 | 40 | 1585 | 180 ± 2 | 40 | 1406 | 240 |
| BKHS8 | 180 | 40 | 1585 | 180 ± 2 | 40 | 1515 | 250 |
| BKHS9 | 180 | 40 | 1585 | 180 ± 2 | 40 | 1390 | 230 |
| BKHS10 | 195 | 50 | 5978 | 195 ± 2 | 50 | 5190 | 325 |
| BKHS11 | 175 | 45 | 1185 | 175 ± 2 | 45 | 1043 | 220 |
| BKHS12 | 185 | 36 | 2125 | 185 ± 2 | 36 | 1909 | 275 |

[a]H-Factor values calculated based on Vroom's single variable model *(14)* using the online tool at www.knowpulp.com.

The lignin precipitate, so-called "ethanol organosolv lignin," was collected on a Whatman No. 1 filter and air-dried for 3 d at room temperature.

### *Characterization of Untreated and Pretreated Substrates*

The carbohydrate composition and lignin content of untreated and OS HHS and BKHS were determined using a modified Klason lignin method derived from the Technical Association of the Pulp and Paper Industry (TAPPI) standard method T222 om-88 *(17)*. Acetone extractives were analyzed by Soxhlet extraction according to the standard TAPPI procedure T 280 pm-99 *(17)*. Ash content was determined according to the standard TAPPI method T211 om-02 *(17)*. In addition, high-resolution fiber quality (FQ) analysis (determination of fiber length, width, and percent content of short fibers or so-called "fines") of OS HHS and BKHS was performed as previously described *(18)*.

### *Batch Separate Enzymatic Hydrolysis and Fermentation*

Twenty four OS HHS and BKHS samples (HHS1-12, BKHS1-12) (Table 2) were hydrolyzed using a *Trichoderma reesei* cellulase preparation Celluclast 1.5 L (60.4 filter paper units [FPU]/mL; Novozymes, NC) supplemented with a β-glucosidase preparation (1 : 2 FPU : cellobiase units [CBU] ratio) Novozym 188 (269 CBU/mL; Novozymes, NC) at 2% (w/w) washed substrate consistency, 40 FPU/g glucan, 72 h, pH 5.0, 50°C, 150 rpm. Reactions were run in foam-plugged 125-mL Erlenmeyer flasks in total reaction volume 60 mL. Samples were taken at 3, 6, 12, 24, 48, and 72 h and analyzed by high-pressure liquid chromatography for glucose content as it is described elsewhere *(15)*. The sugar hydrolyzates resulting from the enzymatic hydrolysis were used for the subsequent fermentation.

Fermentation of enzymatic hydrolyzates was performed with the *Saccharomyces cerevisiae* strain Y-1528 (Agricultural Research Service, US Department of Agriculture, Peoria, IL). Fermentations were performed in foam-plugged 125-mL Erlenmeyer flasks containing approx 45 g of sugar hydrolyzates adjusted with 10% NaOH (w/v) to a starting pH of 5.50 in an orbital shaker for 48 h at 36°C and 150 rpm. The hydrolyzates were inoculated to achieve an initial yeast cell concentration of 6.0 g per DCWL-1 (dry cells weight per liter). Samples were taken at 0, 0.25, 2, 4, 6, 8, 12, 18, 24, 30, 36, and 48 h for ethanol analysis.

## Results and Discussion

### *Characteristics of Untreated and Treated HHS and BKHS*

Untreated HHS and BKHS showed no significant differences in carbohydrate composition content (Table 2). However, BKHS moisture content was significantly lower (approx 10%) compared with HHS (approx 18%) leading to formation of a larger amount of small chips during chipping in the case of BKHS. Pretreated HHS and BKHS samples showed higher glucan content, relative to untreated samples (approx 53–84% and approx 62–90%, respectively) and lower xylan content (approx 0.2–4.5% and approx 0.1–3.4%, respectively). Almost all arabinan and galactan was solubilized or degraded. Mannan in pretreated samples was also significantly lower compared with untreated HHS and BKHS (0.1–4.8%). Lignin content in HHS and BKHS was 22–34% and 23–30%, respectively. Ash content in pulped samples was lower or similar to the untreated wood (0–0.3%).

Detailed results of OS BKHS and HHS chemical composition are contained in Table 2. FQ analysis showed that OS BKHS fibers had significantly lower FQ than OS HHS (lower average fiber length and width, and a larger amount of fines). This indicates that BKHS would be a poor source of high quality fiber for papermaking (Fig. 1).

Table 2
Chemical Composition of Untreated and Treated (Pulp) HHS and BKHS (dry weight [%])[a]

| Sample | Arabinan (%) | Galactan (%) | Glucan (%) | Xylan (%) | Mannan (%) | AIL (%) | ASL (%) | Ash (%) | Extractives (%) |
|---|---|---|---|---|---|---|---|---|---|
| HHS | 1.11 | 1.77 | 48.22 | 5.53 | 12.64 | 28.21 | 0.20 | 0.36 | 2.59 |
| HHS1 | 0.16 | 0.23 | 52.79 | 4.51 | 4.78 | 34.29 | 0.22 | 0.32 | n/a |
| HHS2 | 0.06 | 0.05 | 83.95 | 0.25 | 0.22 | 22.60 | 0.46 | 0.15 | n/a |
| HHS3 | 0.15 | 0.06 | 72.15 | 2.20 | 1.41 | 25.55 | 0.41 | 0.20 | n/a |
| HHS4 | 0.06 | 0.03 | 82.38 | 0.31 | 0.23 | 23.90 | 0.61 | 0.33 | n/a |
| HHS5 | 0.01 | 0.00 | 82.23 | 1.36 | 0.87 | 22.23 | 0.48 | 0.14 | n/a |
| HHS6 | 0.06 | 0.05 | 83.64 | 1.19 | 0.91 | 21.85 | 0.52 | 0.11 | n/a |
| HHS7 | 0.08 | 0.03 | 78.77 | 0.96 | 0.69 | 25.46 | 0.52 | 0.21 | n/a |
| HHS8 | 0.00 | 0.00 | 81.56 | 1.18 | 0.77 | 21.99 | 0.44 | 0.19 | n/a |
| HHS9 | 0.00 | 0.00 | 81.73 | 0.78 | 0.62 | 24.47 | 0.62 | 0.00 | n/a |
| HHS10 | 0.00 | 0.00 | 77.42 | 0.20 | 0.10 | 31.85 | 0.31 | 0.22 | n/a |
| HHS11 | 0.00 | 0.00 | 78.18 | 1.22 | 0.84 | 28.20 | 0.38 | 0.13 | n/a |
| HHS12 | 0.14 | 0.04 | 76.57 | 1.15 | 1.21 | 24.08 | 0.19 | 0.07 | n/a |
| BKHS | 1.23 | 2.50 | 48.81 | 7.03 | 11.89 | 28.50 | 0.20 | 0.36 | 2.72 |
| BKHS1 | 0.10 | 0.04 | 62.16 | 3.38 | 2.19 | 26.18 | 0.22 | 0.13 | n/a |
| BKHS2 | 0.06 | 0.05 | 78.08 | 0.14 | 0.16 | 26.83 | 0.65 | 0.06 | n/a |
| BKHS3 | 0.10 | 0.04 | 69.10 | 2.85 | 1.57 | 27.01 | 0.25 | 0.11 | n/a |
| BKHS4 | 0.07 | 0.04 | 82.84 | 0.32 | 0.29 | 26.64 | 0.55 | 0.12 | n/a |
| BKHS5 | 0.06 | 0.06 | 90.08 | 1.14 | 0.82 | 24.09 | 0.32 | 0.08 | n/a |
| BKHS6 | 0.00 | 0 00 | 78.86 | 0.96 | 0.89 | 23.25 | 0.33 | 0.06 | n/a |
| BKHS7 | 0.07 | 0.06 | 81.66 | 1.07 | 0.78 | 23.40 | 0.31 | 0.13 | n/a |
| BKHS8 | 0.06 | 0.06 | 77.36 | 0.48 | 0.41 | 28.28 | 0.41 | 0.14 | n/a |
| BKHS9 | 0.07 | 0.06 | 80.98 | 0.79 | 0.63 | 25.51 | 0.33 | 0.11 | n/a |
| BKHS10 | 0.06 | 0.04 | 76.29 | 0.12 | 0.13 | 29.49 | 0.67 | 0.10 | n/a |
| BKHS11 | 0.06 | 0.06 | 78.57 | 1.59 | 1.17 | 25.74 | 0.28 | 0.11 | n/a |
| BKHS12 | 0.10 | 0.04 | 68.15 | 2.14 | 0.93 | 26.00 | 0.43 | 0.06 | n/a |

AIL, acid-insoluble lignin; ASL, acid-soluble lignin; n/a, not analyzed.
[a]Carbohydrate, lignin, and ash contents untreated HHS and BKHS are based on extractives-free samples.

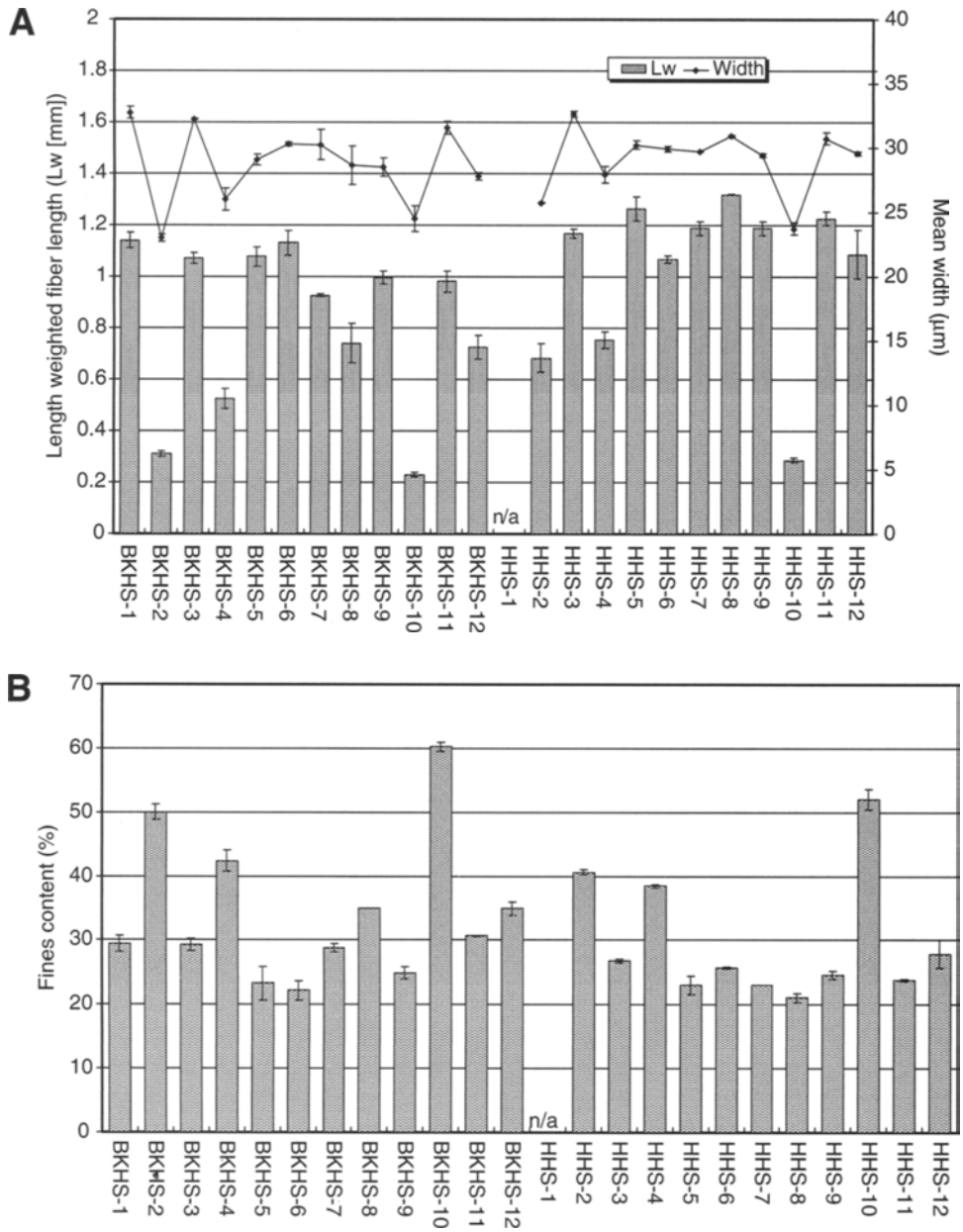


**Fig. 1.** Fiber quality analysis of OS HHS and OS BKHS fibers. **(A)** fiber length and width **(B)** % fines content.

The mass balance of OS HHS1-12 and BKHS1-12 expressed as yields of each component (g) per 100 g (oven-dried weight) untreated HHS and BKHS chips is shown in Table 3. The yields of pretreated carbohydrates (carbohydrates in pulps and liquid fractions) for OS HHS was significantly lower than those for OS BKHS when wood samples were prepared under mild pretreatment conditions (H-Factor <1000) (Table 3). HHS1

Table 3
Mass Balances for Organosolv Pretreatment of HHS and BKHS at a Range of Severities (H-factors)[a]

| Sample | H-factor | Solids (pulp) | | | | | | | | Water-soluble fraction | | | | | Rejects | OS lignin |
|---|---|---|---|---|---|---|---|---|---|---|---|---|---|---|---|---|
| | | Ara | Gal | Glu | Xyl | Man | AIL | ASL | Ash | Ara | Gal | Glu | Xyl | Man | | |
| HHS1 | 510 | 0.01 | 0.01 | 1.71 | 0.15 | 0.15 | 1.01 | 0.01 | 0.01 | 0.32 | 0.39 | 0.54 | 0.58 | 2.28 | 68.99 | 3.41 |
| HHS2 | 3985 | 0.03 | 0.02 | 41.05 | 0.12 | 0.11 | 10.05 | 0.20 | 0.07 | 0.25 | 0.38 | 2.78 | 1.01 | 2.69 | 0.09 | 10.92 |
| HHS3 | 911 | 0.06 | 0.02 | 29.04 | 0.90 | 0.57 | 9.36 | 0.15 | 0.07 | 0.24 | 0.36 | 1.03 | 1.06 | 2.67 | 16.87 | 5.94 |
| HHS4 | 3456 | 0.03 | 0.01 | 40.66 | 0.16 | 0.11 | 10.73 | 0.27 | 0.15 | 0.01 | 0.02 | 0.54 | 0.06 | 0.21 | 0.00 | 10.24 |
| HHS5 | 1238 | 0.01 | 0.00 | 44.51 | 0.75 | 0.47 | 10.95 | 0.24 | 0.07 | 0.57 | 0.86 | 2.89 | 2.46 | 6.11 | 4.48 | 8.20 |
| HHS6 | 1505 | 0.04 | 0.03 | 48.10 | 0.70 | 0.52 | 11.43 | 0.27 | 0.06 | 0.56 | 0.90 | 2.92 | 2.71 | 6.71 | 0.88 | 8.90 |
| HHS7 | 1880 | 0.04 | 0.02 | 42.83 | 0.53 | 0.38 | 12.59 | 0.26 | 0.10 | 0.05 | 0.09 | 1.62 | 0.43 | 0.82 | 1.13 | 8.20 |
| HHS8 | 1687 | 0.00 | 0.00 | 43.64 | 0.64 | 0.41 | 10.71 | 0.21 | 0.09 | 0.06 | 0.13 | 1.96 | 0.50 | 1.01 | 2.53 | 9.00 |
| HHS9 | 1390 | 0.00 | 0.00 | 46.47 | 0.45 | 0.35 | 12.66 | 0.32 | 0.00 | 0.53 | 0.90 | 3.50 | 2.85 | 6.98 | 0.63 | 9.71 |
| HHS10 | 5816 | 0.00 | 0.00 | 35.14 | 0.09 | 0.05 | 13.15 | 0.13 | 0.09 | 0.01 | 0.02 | 2.29 | 0.03 | 0.25 | 0.00 | 10.79 |
| HHS11 | 1139 | 0.00 | 0.00 | 40.17 | 0.64 | 0.43 | 13.18 | 0.18 | 0.06 | 0.26 | 0.57 | 3.27 | 1.36 | 3.60 | 6.39 | 8.36 |
| HHS12 | 2090 | 0.07 | 0.02 | 40.15 | 0.61 | 0.63 | 11.49 | 0.09 | 0.03 | 0.12 | 0.34 | 3.44 | 0.73 | 1.91 | 0.15 | 10.07 |
| BKHS1 | 437 | 0.03 | 0.01 | 17.23 | 0.95 | 0.61 | 6.60 | 0.06 | 0.03 | 0.65 | 1.40 | 1.75 | 2.96 | 6.05 | 47.03 | 8.10 |
| BKHS2 | 3960 | 0.03 | 0.02 | 35.14 | 0.06 | 0.07 | 10.99 | 0.27 | 0.02 | 0.19 | 0.64 | 5.64 | 0.90 | 2.39 | 0.00 | 11.11 |
| BKHS3 | 738 | 0.06 | 0.02 | 37.95 | 1.60 | 0.86 | 13.50 | 0.12 | 0.05 | 0.58 | 1.26 | 2.00 | 3.09 | 5.93 | 8.02 | 9.27 |
| BKHS4 | 2645 | 0.04 | 0.02 | 42.27 | 0.17 | 0.15 | 12.37 | 0.26 | 0.06 | 0.39 | 0.90 | 4.41 | 2.05 | 4.18 | 0.03 | 10.44 |
| BKHS5 | 1265 | 0.03 | 0.03 | 47.82 | 0.62 | 0.44 | 11.64 | 0.15 | 0.04 | 0.54 | 1.12 | 2.82 | 2.97 | 5.41 | 1.46 | 10.26 |
| BKHS6 | 1510 | 0.00 | 0.00 | 43.65 | 0.54 | 0.49 | 11.71 | 0.17 | 0.03 | 0.54 | 1.15 | 2.94 | 2.95 | 5.18 | 1.19 | 8.92 |
| BKHS7 | 1406 | 0.04 | 0.03 | 45.38 | 0.61 | 0.43 | 11.83 | 0.16 | 0.07 | 0.55 | 1.21 | 2.94 | 3.17 | 5.74 | 0.54 | 10.06 |
| BKHS8 | 1515 | 0.03 | 0.03 | 38.78 | 0.25 | 0.21 | 12.90 | 0.19 | 0.06 | 0.39 | 0.96 | 3.25 | 2.02 | 3.86 | 0.20 | 9.01 |
| BKHS9 | 1390 | 0.04 | 0.03 | 40.03 | 0.40 | 0.31 | 11.47 | 0.15 | 0.05 | 0.51 | 1.14 | 3.21 | 3.01 | 5.53 | 0.25 | 10.11 |
| BKHS10 | 5190 | 0.03 | 0.02 | 33.05 | 0.05 | 0.06 | 11.63 | 0.26 | 0.04 | 0.13 | 0.45 | 4.48 | 0.62 | 1.62 | 0.00 | 9.65 |
| BKHS11 | 1043 | 0.03 | 0.03 | 41.53 | 0.86 | 0.62 | 12.38 | 0.13 | 0.05 | 0.57 | 1.35 | 2.75 | 3.42 | 6.23 | 4.80 | 8.39 |
| BKHS12 | 1909 | 0.06 | 0.02 | 37.73 | 1.21 | 0.51 | 13.10 | 0.22 | 0.03 | 0.47 | 1.15 | 4.02 | 2.78 | 5.04 | 0.10 | 7.94 |

All data are yields of each component (g) per 100 g (oven-dried weight) untreated HHS and BKHS chips (*see* untreated HHS and BKHS composition in Table 2). The content of carbohydrate degradation products and low-molecular lignin in liquid fractions was not evaluated.

[a]Ara, arabinose; Gal, galactose; Glu, glucose; Xyl, xylose; Man, mannose.

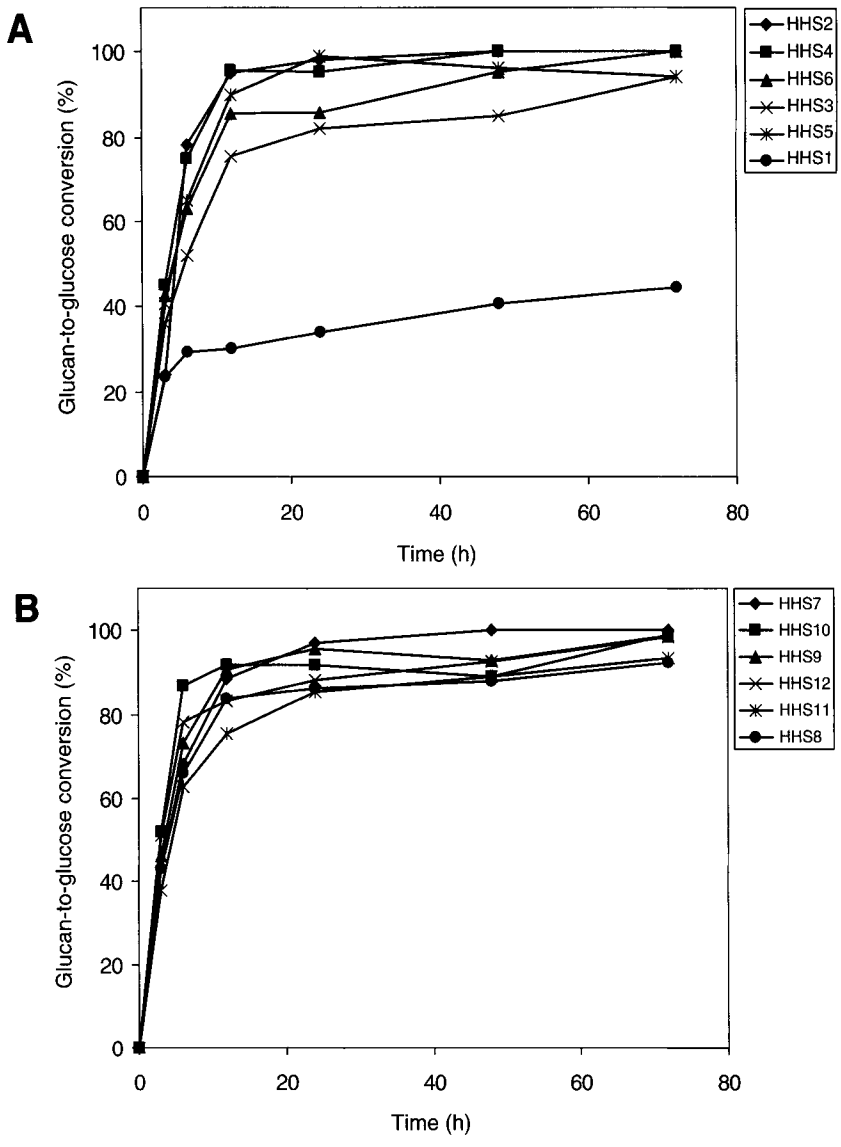


**Fig. 2.** *(Continued)*

(H-Factor –510) and HHS3 (H-Factor –911) yielded approx 6 and 36% carbohydrates, respectively, whereas BKHS1 (H-Factor –437) and BKHS3 (H-Factor –738) yielded approx 32 and 53% carbohydrates, respectively. Furthermore, as it is shown in Table 3 HHS pretreated under mild pretreatment conditions yielded higher rejects content (approx 69 and 17% for HHS1 and HHS3, respectively) compared with BKHS (approx 47 and 8% for BKHS 1 and BKHS3, respectively). These results indicate that BKHS was easier to pretreat than HHS under mild pretreatment conditions. However, under mild or severe pretreatment conditions (H-Factor approx 1000–5000) HHS and BKHS, in general, behaved similarly (Table 3).

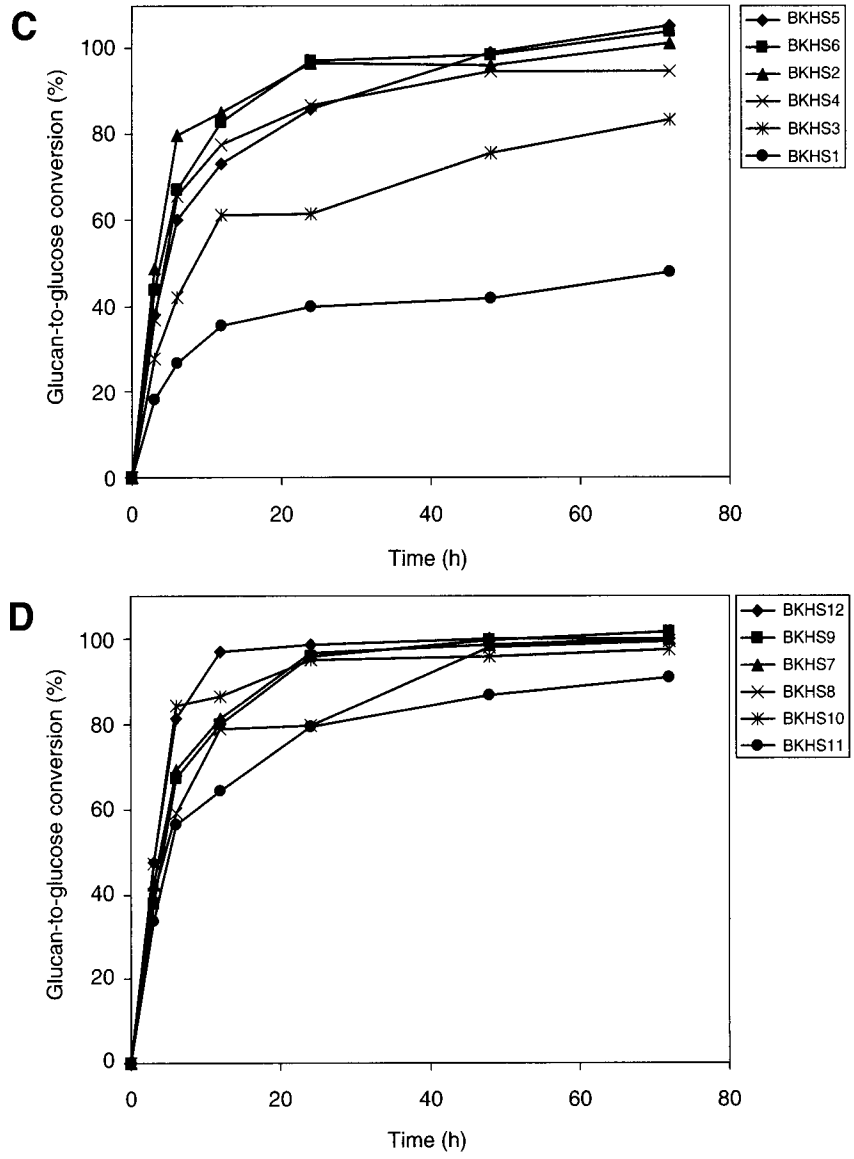


**Fig. 2.** Enzymatic hydrolysis of OS HHS **(A,B)** and OS BKHS **(C,D)**.

## *Enzymatic Hydrolysis and Fermentation*

OS HHS and BKHS showed similar enzymatic hydrolyzability. HHS2, HHS4, HHS5, HHS7, HHS10 and BKHS2, BKHS6-7, BKHS9-10 pulp samples reached more than 90% conversion in 12–24 h; HHS3, HHS6, HHS8-9, HHS11-12 and BKHS3-5, BKHS8, BKHS11–12 yielded more than 90% conversion in 48–72 h. HHS1 and BKHS1 showed significantly lower glucan-to-glucose conversion compared with the other OS-pretreated samples (45 and 48%, respectively). Results of OS HHS and OS BKHS enzymatic hydrolysis are shown in Fig. 2A–D. Fermentation of OS HHS and BKHS

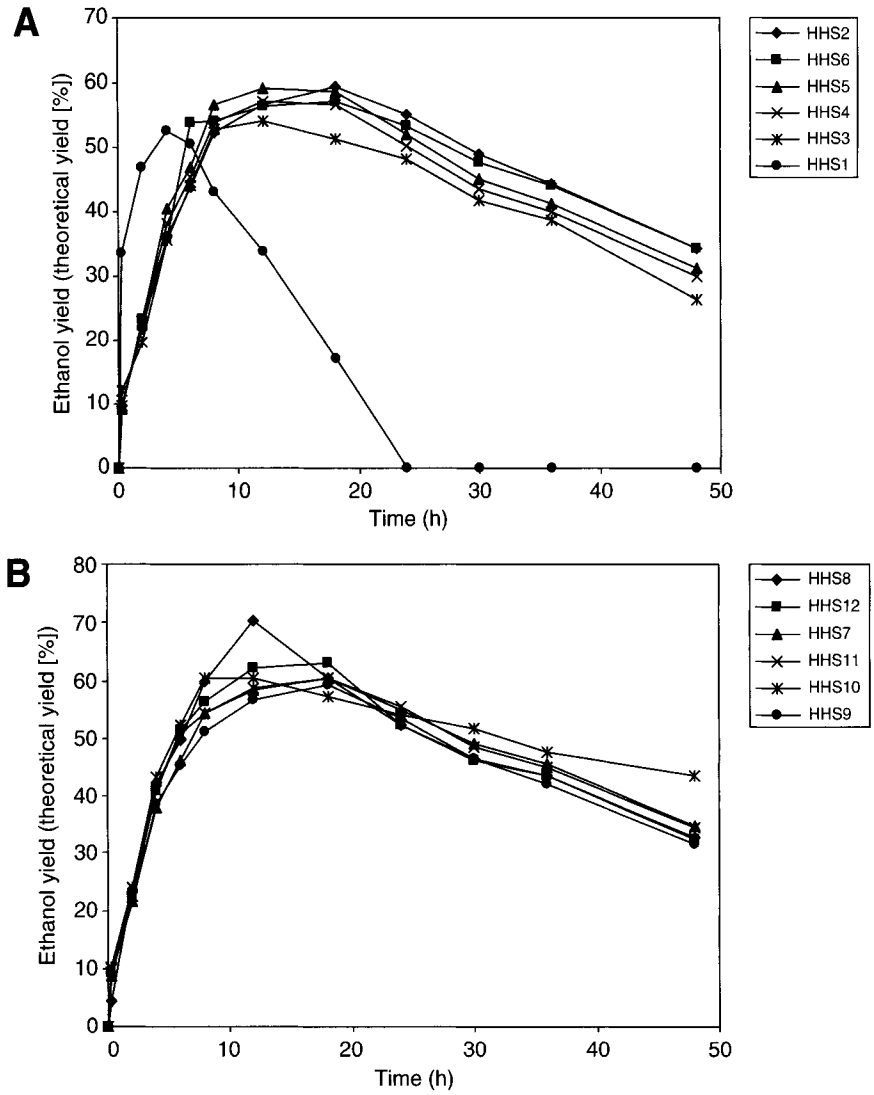


**Fig. 3.** *(Continued)*

hydrolyzates yielded 53–80% theoretical ethanol yield of carbohydrates in pulps in 4–24 h (Fig. 3A–D, Table 4). The best fermentation was observed for hydrolyzates HHS8 (70%, 12 h) and BKHS12 (80%, 24 h). The lowest ethanol yield was shown for HHS1 (53%, 4 h), HHS3 (54%, 12 h), and BKHS5 (53%, 12 h), apparently because of poor substrate hydrolyzability. Relatively low or moderate fermentability was observed for the other substrates (56–64%).

Significant catabolic oxidation of ethanol for all substrates was observed after reaching maximal ethanol yields. After 48 h fermentation, ≥40% reduction in maximum ethanol yield was observed (Fig. 3A–D). This effect can be attributed to the so-called "diauxic shift." characteristic in ethanologenic yeasts fermenting at low sugar concentrations *(19)*.

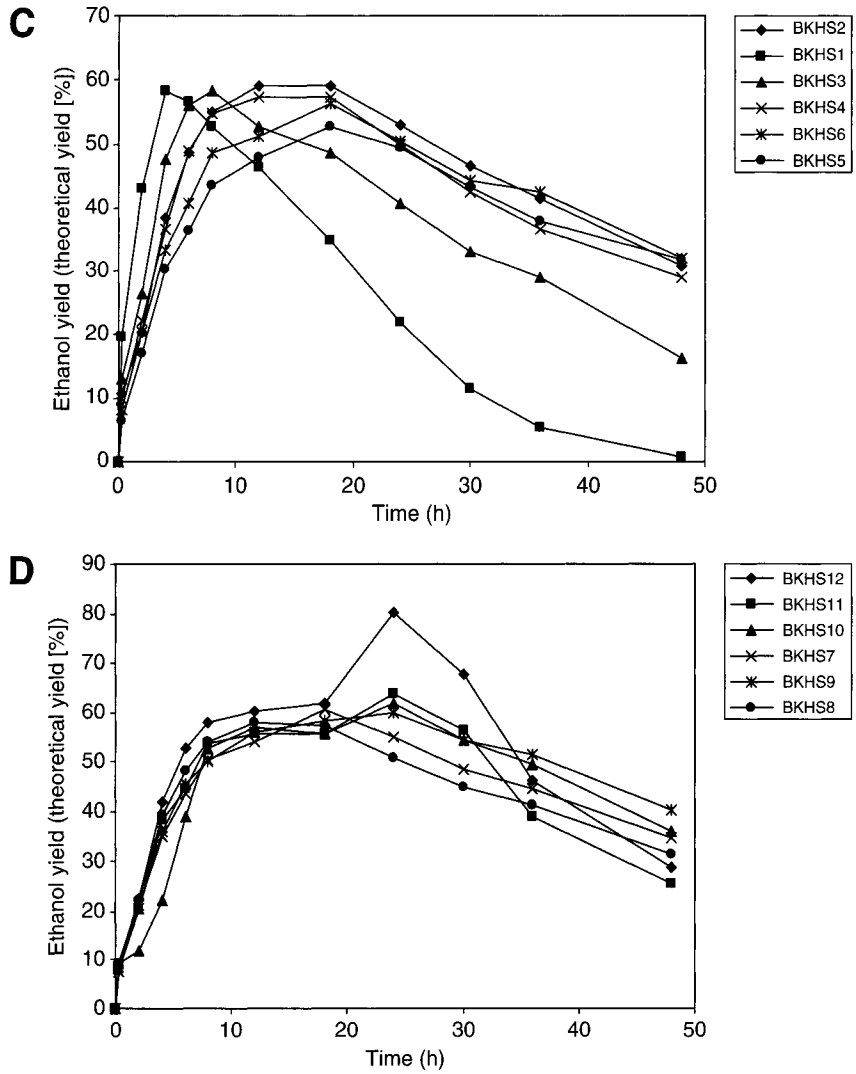


**Fig. 3.** Ethanol fermentation of OS HHS **(A,B)** and OS BKHS **(C,D)** hydrolyzates.

## Conclusion

Beetle-killed HS and HHS pretreated by ethanol organosolv were shown to be good substrates for bioethanol production achieving approx 80 and 70% theoretical ethanol yield, respectively, during relatively brief incubation (Fig. 3, Table 4). Untreated HHS and BKHS did not differ significantly in chemical composition except for the moisture content, which was significantly lower in BKHS (approx 10%) compared with HHS (approx 18%). However, the FQ of OS BKHS pulps was significantly lower than OS HHS pulps (Fig. 1) indicating a poor suitability of BKHS OS pulps for high-quality papermaking. Furthermore, the yields of carbohydrates obtained in hydrolyzable and fermentable forms was higher at mild

Table 4
Maximal Observed BKHS and HHS Ethanol Yields

| Pulp sample | Time (h) | Ethanol yield (%) |
|---|---|---|
| HHS1 | 4 | 52.5 |
| HHS2 | 18 | 59.6 |
| HHS3 | 12 | 54.1 |
| HHS4 | 12 | 57.2 |
| HHS5 | 12 | 59.3 |
| HHS6 | 18 | 57.3 |
| HHS7 | 18 | 60.5 |
| HHS8 | 12 | 70.3 |
| HHS9 | 18 | 59.4 |
| HHS10 | 8 | 60.3 |
| HHS11 | 18 | 60.4 |
| HHS12 | 18 | 62.9 |
| BKHS1 | 4 | 58.2 |
| BKHS2 | 12 | 59.0 |
| BKHS3 | 8 | 58.2 |
| BKHS4 | 12 | 57.3 |
| BKHS5 | 18 | 52.8 |
| BKHS6 | 18 | 56.4 |
| BKHS7 | 18 | 60.7 |
| BKHS8 | 12 | 57.8 |
| BKHS9 | 24 | 60.1 |
| BKHS10 | 24 | 62.0 |
| BKHS11 | 24 | 63.8 |
| BKHS12 | 24 | 80.1 |

Percent of ethanol theoretical yield of carbohydrates in pretreated solids.

pretreatment conditions (H-Factor <1000) for BKHS compared with HHS. At medium (H-Factor 1000–2000) and severe (H-Factor >2000) pretreatment conditions HHS and BKHS behaved similarly (Table 3).

## Acknowledgments

We would like to thank the personnel of the UBC Alex Fraser Research Forest for the help provided in procuring the HHS and BKHS logs for this study. This research was supported by the Natural Sciences and Engineering Council of Canada (NSERC), Natural Resources Canada (NRCAN), and the Chilean National Fund for Scientific and Technologic Development (Fondecyt), Project No. 1040614.

## References

1. Perlack, R. D., Wright, L. L., Turhollow, A. F., Graham, R. L., Stokes, B. J., and Erbach, D. C. (2005), In: Biomass as feedstock for a bioenergy and bioproducts industry: the technical

feasibility of a billion-ton annual supply, *US Department of Energy*, US Department of Agriculture, pp. 1–60. Available electronically at: http://www.osti.gov/bridge. Last accessed date: December 20, 2006.
2. Henry, J. D. (2002), Canada's Boreal Forest, ed. Smithsonian Institution Press, Washington.
3. Armstrong, J. A. and Ives, W. G. H. (1995), Forest insect pestes, In: Natural Resources Canada, Canadian Forest Service, Ottawa, Canada.
4. Malmström, C. M. and Raffa, K. F. (2000), *Global Change Biol.* **6,** 35–48.
5. Hall, J. P. and Moody, B. (1994), Report ST-X-8, Natural Resources Canada, Canadian Forest Service, Ottawa, Canada.
6. Wilson, J., Bell, P., Nettleton, P., Mackey, D., (2001), http://www.governmentcaucus.bc.ca/media/pinebeetle.pdf/2007_update.html. Last date website accessed on January 22, 2007.
7. Schmid, J. M. and Frye, R. H. (1997), Report RM–49, U.S. Department of Agriculture, Colorado.
8. Christiansen, E. and Bakke, A. (1988), In: Dynamics of Forest Insect Populations: Patterns, Causes, Implications. Berryman, A. A. (ed.), Plenum Press, New York: pp. 479–503.
9. Safranyik, L. and Linton, D. A. (1988), *Can. Entomol.* **120,** 85–94.
10. Day, K. R. and Leather, S. R. (1997), In: Forests and Insects. Watt, A. D., Stork, N. E., and Hunter, M. D. (eds.), Chapman and Hall, London, pp. 177–205.
11. Seifert, K. A. (1993), In: *Ceratocystis and ophiostoma:* Taxonomy, Ecology and Pathogenicity. Wingfield, M. J., Seifert, K. A., and Webber, J. F. (eds.), APS Press, St. Paul Minnesota. pp. 141-172.
12. Brasier, C. (1991), *Mycopathologia* **115,** 151–161.
13. Harrington, T. C. (1993), In: *Ceratocystis and Ophiostoma:* Taxonomy, Ecology and Pathogenicity. Wingfield, M. J., Seifert, K. A., and Webber, J. F. (eds.), APS Press, St. Paul Minnesota. pp. 161–172.
14. Vroom, K. E. (1957), *Pulp Pap. Mag. Can.* **58,** 228–231.
15. Kurabi, A., Berlin, A., Gilkes, N, et al. (2005), *Appl. Biochem. Biotechnol.* **121–124,** 219–230.
16. Berlin, A., Gilkes, N., Kilburn, D., et al. (2005), *Enzyme Microb. Technol.* **37,** 175–184.
17. TAPPI (2004), TAPPI test methods in CD–Rom, TAPPI Press, GA.
18. Berlin, A., Maximenko, V., Bura, R., Kang, K., Gilkes, N., and Saddler, J. (2005), *Biotechnol. Bioeng.* **93,** 880–886.
19. Costa, V., Amorim, M. A., Reis, E., Quintanilha, A., and Moradas-Ferreira, P. (1997), *Microbiology* **143,** 1649–1656.

0273-2289/1559-0291 (Online)/07/136–140/281–288/$30.00

# Production of Cellulolytic and Hemicellulolytic Enzymes From *Aureobasidium pulluans* on Solid State Fermentation

**Rodrigo Simões Ribeiro Leite, Daniela Alonso Bocchini, Eduardo Da Silva Martins, Dênis Silva, Eleni Gomes, and Roberto Da Silva***

*Laboratório De Bioquímica E Microbiologia Aplicada, IBILCE—Instituto De Biociências, Letras E Ciências Exatas, UNESP—Universidade Estadual Paulista, Rua Cristóvão, Colombo, 2265, São José Do Rio Preto, São Paulo, CEP 15054-000, Brazil, E-mail: Dasilva@Ibilce.Unesp.Br*

## Abstract

This article investigates a strain of the yeast *Aureobasidium pullulans* for cellulase and hemicellulase production in solid state fermentation. Among the substrates analyzed, the wheat bran culture presented the highest enzymatic production (1.05 U/mL endoglucanase, 1.3 U/mL β-glucosidase, and 5.0 U/mL xylanase). Avicelase activity was not detected. The optimum pH and temperature for xylanase, endoglucanase and β-glucosidase were 5.0 and 50, 4.5 and 60, 4.0 and 75°C, respectively. These enzymes remained stable between a wide range of pH. The β-glucosidase was the most thermostable enzyme, remaining 100% active when incubated at 75°C for 1 h.

**Index Entries:** Cellulases; endoglucanase; hemicellulases; solid state fermentation; β-glucosidase.

## Introduction

The hydrolytic action of cellulases and hemicellulases is of fundamental importance to obtain fermentable sugars from lignocellulosic biomass. These can be used as fermentation substrates to produce liquid fuels, food products, or other chemicals of interest *(1,2)*. The enzymatic hydrolysis of cellulose into glucose involves the synergistic action of at least three different enzymes: endoglucanase or endo-β-1,4-glucanase (EC 3.2.1.4), exoglucanase or exocellobiohydrolase (EC 3.2.1.91), and β-1,4-glucosidase or cellobiase (EC 3.2.1.21). Endoglucanase hydrolyze the polymers internally, resulting in a reduction of the degree of polymerization, whereas the exoglucanases act by removing units of cellobiose from either the reducing or the nonreducing

*Author to whom all correspondence and reprint requests should be addressed.

ends of the molecule. β-glucosidase hydrolyzes cellobiose and other cellodextrins into glucose. β-glucosidase is responsible for the control of the entire speed of the reaction exerting a crucial effect on the enzymatic degradation of the cellulose, preventing the accumulation of cellobiose *(3,4)*. The β-glucosidase can also be used by the food industry to increase the bioavailability of the isoflavones in the human intestine, and by the beverage industry to stabilize the coloration of juices and wines *(5)*.

Because of xylan heterogeneity, the enzymatic hydrolysis of xylan requires different enzymatic activities. Two enzymes, β-1,4-endoxylanase (EC 3.2.1.8) and β-xylosidase (EC 3.2.1.37), are responsible for hydrolysis of the main chain, the former attacking the internal main-chain xylosidic linkages and the latter releasing xylosyl residues by means of endwise attack of xylooligosaccharides *(6)*. However, for complete hydrolysis of hemicellulose, side chain cleaving enzyme activities are also necessary, such as, α-L-arabinofuranosidases (EC 3.2.1.55), endomannanases (EC 3.2.1.78), β-mannosidases (EC 3.2.1.25), and α-galactosidases (EC 3.2.1.22) *(7)*. Solid state fermentation (SSF) is a well-known process for enzyme production and is defined as fermentation involving solids in absence (or near absence) of free water; however, the substrate must possess enough moisture to support growth and metabolism of microorganisms *(8)*. There is a current tendency to apply the SSF process in the development of bioprocesses to attain products with higher added values, such as antibiotics, alkaloids, organic acids, biopesticides, biofuel, aromatic compounds, and enzymes *(8,9)*.

Previous works described the production cellulases and hemicellulases using SSF and agricultural residues *(2,10–12)*. Brazil is an agroindustrial country known for its production of soy, corn, sugar cane, cassava, coffee, and so on, and for its high consumption of wheat, which generate large amounts of residues that have considerable potential for SSF applications *(13)*. On a previous study of screening of cellulolytic microorganisms, a strain of *A. pullulans* with high β-glucosidase activity was isolated. The objective of this work was the study of the production and the characterization of cellulolytic and hemicellulolytic enzymes secreted by *A. pullulans* using agroindustrial residues on SSF.

## Material and Methods

### Microorganism

The yeast *A. pullulans* ER-16 was isolated from orange juice residues in Catanduva, São Paulo State, Brazil. The stock culture was preserved in potato dextrose agar at 4°C.

### Enzyme Production

The microorganism was cultivated using four different types of substrates: wheat bran, soy bran, soy peel, and corn cob. In order to evaluate

enzymatic production, samples were removed every 24 h throughout the period of 144 h.

### *Inoculation*

The yeast was cultivated in 125-mL Erlenmeyer flasks containing 20 mL of potato dextrose agar medium for 48 h at a temperature of 28°C. A suspension was obtained by softly scraping the culture medium surface using 25 mL of mineral solution. Inoculation in the substrate was carried out by transferring 5 mL of the suspension into Erlenmeyer flasks containing the previously prepared production medium.

### *Fermentation*

SSF was carried out in 500-mL Erlenmeyer flasks containing 5 g of moistened substrates (grounded to 2–3 mm size) with 10 mL of mineral solution aiming an initial humidity content of 75%. The mineral solution was made up of 0.1% $(NH_4)_2SO_4$, 0.1% $MgSO_4{\cdot}7H_2O$, and 0.1% $NH_4NO_3$ (w/v). After the inoculation of the microorganism, the fermentation was incubated at 28°C. Enzyme extraction was achieved by adding 50 mL of distilled water to each flask followed by 2 h on a rotary shaker at 80 rpm. Crude extracts were centrifuged (10,000*g*/20 min), and then the supernatant was used for enzyme activities assays.

### *Enzyme Assays*

Xylanase, endoglucanase, and avicelase enzymes activities were measured by determining the release of reducing sugars by the 3,5-dinitrosalicylic acid method *(14)*. The 100 m*M* sodium acetate buffer pH 5.0 was used containing 0.5% of xylan (Birchwood-Sigma), 0.5% of carboxymethylcellulose (C5768 Sigma), and 0.5% of avicel (Co Sigma) as substrates for xylanase, endoglucanase, and avicelase enzymes, respectively. β-glucosidase activity was determined using 50 µL of the extract, 250 µL of 100 m*M* sodium acetate buffer pH 5.0, and 250 µL of 4 m*M* 4-nitrophenyl β-D-glucopyranoside (PNPG, Sigma). After 10 min, the reaction was stopped by the addition of 2 mL of 2 *M* sodium carbonate. The activities were measured at 410 nm and expressed in international units, defined as the amount of enzyme required to produce 1 µmole of nitrophenol (β-glucosidase), xylose (xylanase), and glucose (CMCase and avicelase) per minute, under assay conditions.

### *Enzyme Properties*

The crude enzyme obtained in SSF using wheat bran as substrate was used for enzyme characterization. The activities were determined according to the standard conditions described above, except for the optimum temperature, which was determined in the range of 50–90°C and optimum pH between 3.0–8.0 in 100 m*M* McIlvaine buffer. For pH stability, enzymes were stored for 1 d at room temperature (about 25°C) diluted in 100 m*M*

McIlvaine buffer (pH 3.0–8.0), 100 m*M* Tris/HCI (8.0–9.0), and 100 m*M* glycine-NaOH (9.0–11.0). For temperature stability, enzymes were incubated at different temperatures (30–80°C) for 1 h. Both stabilities were determined by measuring the residual activities under standard conditions at optimum pH and temperature.

## Results and Discussion

### Enzyme Production

*A. pullulans* produced β-glucosidase in all substrates tested, but the production in wheat bran was found to be highest 1.3 U/mL after 120 h (Fig. 1A). The β-glucosidase production obtained in the present work is more than average results found in the literature. Iembo et al. *(10)* related a maximum production of 0.5 U/mL by *Aureobasidium* sp. in 168 h of culture in which wheat bran was used as substrate in SSF. Saha et al. *(15)* used wheat bran and corn bran as carbon source for *A. pullulans* cultivation in submerged fermentation (SMF), and obtained a maximum β-glucosidase production of 0.27 U/mL after 96 h. Wen et al. *(16)* related a β-glucosidase production of 0.0978 U/mL in *Trichoderma reesei* cultivation in SMF by using bovine manure as carbon source.

Wheat bran is a complex substrate rich in proteins (14%), carbohydrates (27%), minerals (5%), fat (6%), and B-vitamin *(17)*, this probably favored the growth and the production of enzymes for the microorganism. Previous works *(3,10–12,18)* report the production of cellulases and hemicelulases, using derived wheat (bran and straw) as substrate. The highest endoglucanase and xylanase production was obtained after 96 h of fermentation in wheat bran—1.05 and 5.0 U/mL, respectively. No endoglucanase production was detected in soy bran and corn-cob cultivation. In addition, no xylanase activity was detected (Figs. 1B,C) in soy bran cultivation. Avicelase activity was not detected from any of the substrates. Avicelase is the activity responsible for crystalline cellulose degradations and it is frequently found in low concentrations or absent on the cellulolytic system of many microorganisms *(19)*. This work confirms that the *A. pullulans* is among these. Previous studies *(1,11,12)*, with other species of fungi, relate endoglucanase and β-glucosidase productions with absence or low avicelase activity.

The xylanase and endoglucanase production for *A. pullulans* was not significant when compared with the production of fungi. Panagiotou et al. *(12)* reported 15.2 U/mL of endoglucanase and 92 U/mL of xylanase, in SSF, from the filamentous fungus *Fusarium oxysporum* using corn bran as substrate. Jecu *(3)* related an endoglucanase production of 14.8 U/mL in *Aspergillus niger* cultivation in a mixture of wheat straw and wheat bran in the ratio of 9 : 1, in SSF. Wen et al. *(16)* reported an endoglucanase production of 12.22 U/mL from *T. reesei*. Jorgensen et al. *(7)* obtained approx 38 U/mL of xylanase from *Penicillium brasilianum*, in SMF. Enzymes

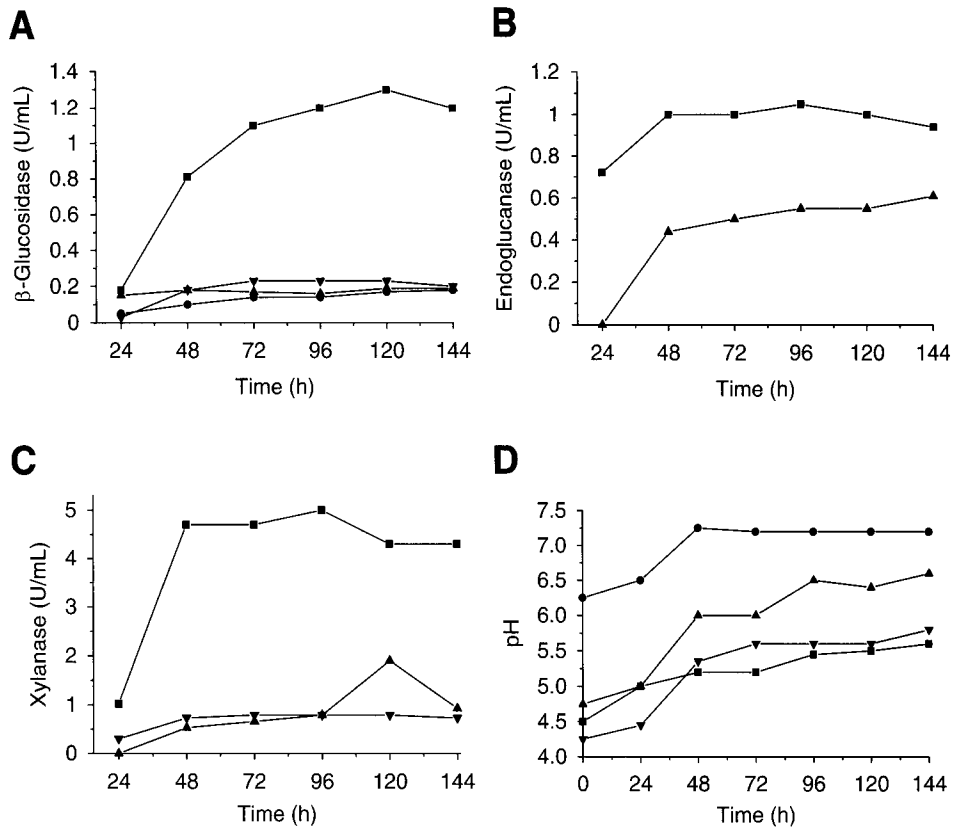


**Fig. 1.** Time-course of enzymatic production by *A. pullulans* in different cellulosic substrates. **(A)** β-glucosidase production, **(B)** endoglucanase production, **(C)** xylanase production, **(D)** pH variation during the fermentative process. (■) wheat bran, (●) soy bran, (▲) soy peel, (▼) corn cob.

production from yeasts is less than the production by filamentous fungi when cultivated on solid substrates. This may be explained because the growth conditions in SSF are very similar with their natural habitat, which favors the spreading of mycelium and consequently, results in a larger production of enzymes and better growth *(8,9)*. Diverse factors can influence enzyme production, such as pH, temperature, type of fermentation, carbon source used, and water availability (SSF). When cultivating *Thermoactinomyces thalophilus* by SSF, Kohli et al. *(20)* found an initial xylanase activities of 6.4 U/mL. After the attainment of the ideal conditions for the microorganism cultivation, the authors related a xylanase production of 42 U/mL in SMF.

A tendency for the pH to increase during the SSF was observed with all substrates tested, and was higher between 24 and 72 h of fermentation. No major alterations were observed after this initial increase, tending to stabilization (Fig. 1D). The pH variation fermentation was caused by the microorganism's metabolic activity, and may increase or decrease according

to what is secreted or consumed in the culture medium. The pH increase may be caused by organic acid consumption, such as citric, acetic, and lactic, or the release of ammonium salts resultant from the hydrolysis of protein and urea *(9,21)*. As proteolytic activity was observed in fermented extracts (data not shown), medium alkalinization was possibly caused by hydrolysis of protein as well as by the microbial metabolic action on the salts added for medium enrichment, such as ammonium sulfate and ammonium nitrate.

### *Enzyme Properties*

The optimum pH and temperature of β-glucosidase produced by *A. pullulans* in this study was determined to be 4.0–4.5 and 75°C, respectively. This enzyme remained stable within a broad range of pH 4.5–10.0 and its original activity was constant after 1 h at 75°C (Fig. 2). When compared with other microbial β-glucosidases found in literature *(4,22–24)*, this enzyme presented a very high level of thermal stability. Previous works *(10,15,25)* described the production of β-glucosidase from *Aureobasidium* sp. and *A. pullulans* as having noticeable stable levels of both pH and temperature. Other research conducted with stable enzymes disclosed very little difference between stable and unstable enzymes regarding amino acid's sequence. Slight alterations in the molecule, such as an increase in hydrophobicity, ionic interaction, and disulfide bridge may lead to major changes in the stability of a molecule *(26)*. Thermostable enzymes are commonly produced by thermophilic microorganisms *(27)*. *A. pullulans* has an optimum growth at around 28°C typical of mesophilic microorganisms. Future studies of β-glucosidase produced by *A. pullulans* may contribute to the understanding of evolutionary interactions between thermophilia and mesophilia, besides presenting characteristics that allow its use in biotechnological processes.

The optimum pH and temperature obtained for endoglucanase were 4.0–4.5 and 60°C, respectively. Xylanase had a maximum activity at pH 5.0 and with temperature at 50°C and remained stable within a wide pH range. Xylanase remained stable after 24 h between pH 3.0–8.0 and maintained 53% of its original activity in pH 11.0. Endoglucanase remained stable within pH 3.5–7.5, maintaining only 54% of its catalytic activity when incubated at pH 8.0. Both enzymes had a considerable reduction in their activity after 1 h of incubation at temperatures more than 50°C (Fig. 2). Thermal inactivation is commonly observed in xylanases and endoglucanases produced by mesophilic microorganisms *(18,28–30)*.

The application of microbial xylanases for biobleaching of pulp by the paper industry is intrinsically related to the absence of cellulases in the fermented medium *(18)*. The hydrolytic action of such enzymes on cellulose fibers may decrease the quality of pulp resulting in inferior paper *(30)*. Hence, the presence of cellulolytic enzymes in the enzymatic extract

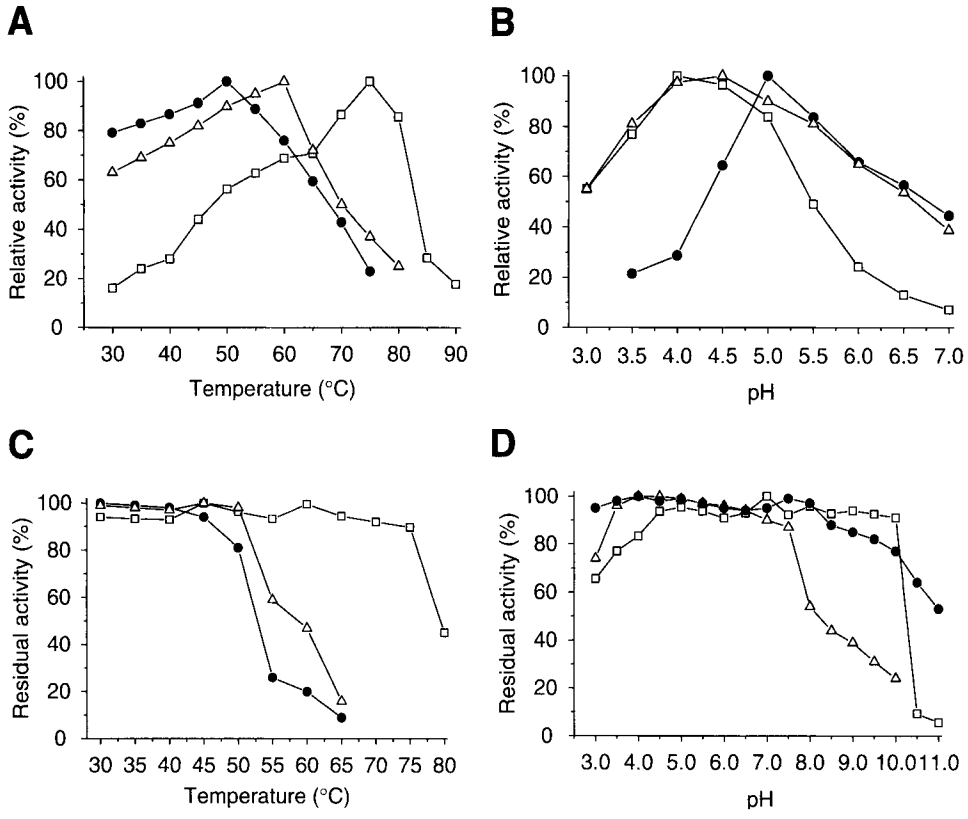


**Fig. 2.** Enzyme activities and stability relative to pH and temperature: **(A)** effect of temperature on the enzyme activities, **(B)** effect of pH on the enzyme activities, **(C)** temperature-stability curve, **(D)** pH-stability curve. (□) β-glucosidase, (●) xylanase, (△) endoglucanase.

produced by *A. pullulans* in SSF along with the low level of activity of xylanase in alkaline pH, impairs its use by the paper industry. On the other hand, the synergistic action of such enzymes benefits the attainment of fermentable sugars from agroindustrial residues that can be used to develop alternative fuels. This fact prompts us to continue with studies of these enzymes in order to contribute to the development of new sources of energy.

## Acknowledgments

This study was supported by the Fundacão de Amparo à Pesquisa do Estado de São Paulo (FAPESP).

## References

1. Romero, M. D., Aguado, J., Gonzales, L., and Ladero, M. (1999), *Enzyme Microb. Technol.* **25,** 244–250.
2. Kang, S. W., Park, Y. S., Lee, J. S., Hong, S. I., and Kim, S. W. (2004), *Bioresour. Technol.* **91,** 153–156.

3. Jecu, L. (2000), *Ind.Crops Product.* **11,** 1–5.
4. Palma-Fernandez, E. R. D., Gomes, E., and da-Silva, R. (2002), *Folia Microbiol.* **47,** 685–690.
5. Bhatia, Y., Mishra, S., and Bisaria, V. S. (2002), *Crit. Rev. Biotechnol.* **22,** 375–407.
6. Bakir, U., Yavascaoglu, S., Guvene, F., and Ersayin, A. (2001), *Enzyme Microb. Technol.* **29,** 328–334.
7. Jorgensen, H., Morkeberg, A., Krogh, K. B. R., and Olsson, L. (2005), *Enzyme Microb. Technol.* **36,** 42–48.
8. Pandey, A. (2003), *Biochem. Eng. J.* **13,** 81–84.
9. Silva, D., Tokuioshi, K., Martins, E. S., Da-Silva, R., and Gomes, E. (2005), *Process Biochem.* **40,** 2885–2889.
10. Iembo, I., Da Silva, R., Pagnocca, F. C., and Gomes, E. (2002), *Appl. Biochem. Microbiol.* **38,** 549–552.
11. Kalogeris, E., Christakopoulos, P., Katapodes, P., et al. (2003), *Process Biochem.* **38,** 1099–1104.
12. Panagiotou, G., Kekos, D., Macris, B. J., and Christakopoulos, P. (2003), *Ind. Crops Product.* **18,** 37–45.
13. Soccol, C. R. and Vandenberghe, L. P. S. (2003), *Biochem. Eng. J.* **13,** 205–218.
14. Miller, G. L. (1959), *Anal. Chem.* **31,** 426–428.
15. Saha, B. C., Freer. S. N., and Bothast, R. J. (1994), *Appl. Environ. Microbiol.* **60,** 3774–3780.
16. Wen, Z., Liao, W., and Chen, S. (2005), *Bioresour. Technol.* **96,** 491–499.
17. Haque, M. A., Shams-Ud-Din, M., and Haque, A. (2002), *Int. J. Food Sci. Technol.* **37,** 453–462.
18. Carmona, E. C., Fialho, M. B., Buchgnani, E. B., Coelho, G. D., Brocheto-Braga, M. R., and Jorge, J. A. (2005), *Process Biochem.* **40,** 359–364.
19. Gomes, I., Gomes, J., Gomes, D.J., and Steiner, W. (2000), *Appl. Microbiol. Biotechnol.* **53,** 461–468.
20. Kohli, U., Nigam, P., Singh, D., and Chaudhary, K. (2001), *Enzyme Microb. Technol.* **28,** 606–610.
21. Raimbault, M. (1998), *Electr. J. Biotechnol.* **1,** 174–188.
22. Mamma, D., Hatzinikolaou, D., and Christakopoulos, P. (2004), *J. Mol. Catal. B: Enzymol.* **27,** 183–190.
23. Villena, M. A., Iranzo, J. F., Gundllapalli, S. B., Otero, R. R. C., and Pérez, A. I. B. (2006), *Enzyme Microb. Technol.* **39,** 229–234.
24. Turan, Y. and Zheng, M. (2005), *Biochemistry (Moscow)* **70,** 1656–1663.
25. Hayashi, S., Sako, S., Yokoi, H., Takasaki, Y., and Imada, K. (1999), *J. Ind. Microbiol. Biotechnol.* **22,** 160–163.
26. Bruins, M. E., Janssen, A. E. M., and Boom, R. M. (2001), *Appl. Biochem. Biotechnol.* **90,** 155–181.
27. Vieille, C. and Zeikus, G. J. (2001), *Microbiol. Mol. Biol. Rev.* **65,** 1–43.
28. Heidorne, F. O., Magalhães, P. O., Ferraz, A. L., and Milagres, A. M. F. (2006), *Enzyme Microb. Technol.* **38,** 436–442.
29. Murashima, K., Nishimura, T., Nakamura, Y., et al. (2002), *Enzyme Microb. Technol.* **30,** 319–326.
30. Christov, L. P., Szakacs, G., and Balakrishnan, H. (1999), *Process Biochem.* **34,** 511–517.

0273-2289/1559-0291 (Online)/07/136-140/289-300/$30.00

# The Effect of Particle Size on Hydrolysis Reaction Rates and Rheological Properties in Cellulosic Slurries

**Rajesh K. Dasari and R. Eric Berson***

*University of Louisville, Department of Chemical Engineering, Louisville, KY 40292, E-mail: Eric.Berson@Louisville.Edu*

## Abstract

The effect of varying initial particle sizes on enzymatic hydrolysis rates and rheological properties of sawdust slurries is investigated. Slurries with four particle size ranges (33 μm < $x \leq$ 75 μm, 150 μm < $x \leq$ 180 μm, 295 μm < $x \leq$ 425 μm, and 590 μm < $x \leq$ 850 μm) were subjected to enzymatic hydrolysis using an enzyme dosage of 15 filter paper units per gram of cellulose at 50°C and 250 rpm in shaker flasks. At lower initial particle sizes, higher enzymatic reaction rates and conversions of cellulose to glucose were observed. After 72 h 50 and 55% more glucose was produced from the smallest size particles than the largest size ones, for initial solids concentration of 10 and 13% (w/w), respectively. The effect of initial particle size on viscosity over a range of shear was also investigated. For equivalent initial solids concentration, smaller particle sizes result in lower viscosities such that at a concentration of 10% (w/w), the viscosity decreased from 3000 cP for 150 μm < $x \leq$ 180 μm particle size slurries to 61.4 cP for 33 μm < $x \leq$ 75 μm particle size slurries. Results indicate particle size reduction may provide a means for reducing the long residence time required for the enzymatic hydrolysis step in the conversion of biomass to ethanol. Furthermore, the corresponding reduction in viscosity may allow for higher solids loading and reduced reactor sizes during large-scale processing.

**Index Entries:** Biomass; enzymatic hydrolysis; non-Newtonian; particle suspension; red oak wood; sawdust slurry; viscosity.

## Introduction

The production of fuel ethanol from renewable lignocellulosic materials continues to receive a great deal of interest as a viable alternative fuel source. Among lignocellulosic materials, the utilization of agricultural residues has the benefit of disposal of problematic solid wastes, which usually does not have any economic alternative *(1)*. The low-cost mill residues from the sawmilling industry can be used as an alternate lignocellulosic substrate as well. Sawdust is used as the substrate because the

*Author to whom all correspondence and reprint requests should be addressed.

material is already mechanically reduced in size as a result of a manufacturing process, and the particles can be easily classified into distinct size ranges. This material offers lower feedstock costs than that of grain and even if further milling is required, may still offset some of the higher processing costs that wood faces *(2)*. A large amount of wood wastes is produced from the lumber industries in the United States. Currently, nearly 63 million mt of this material is generated in the manufacture, use, and disposal of solid wood products each year, which can yield up to 6350 million gallons of ethanol *(3)*.

A significant amount of literature is available regarding the enzymatic hydrolysis of lignocellulosic woods based on the effect of different kinds of pretreatment methods on the enzymatic hydrolysis reaction *(4–7)* and the kinetics of the hydrolysis reactions *(8–12)*. Very few authors have reported the dependence of the course of hydrolysis reaction on the structural features of the cellulosic substrates *(13–18)*. Experiments by Peters et al. *(15)* revealed that the initial particle size over the range between 38 μm and 105 μm had no impact on the rate and the extent of reducing sugar production or on enzyme binding of the microcrystalline cellulose Avicel PH 102 (FMC Corporation, Chalfont, PA). No data appears in the literature regarding the impact of the initial particle size on the viscosity of the lignocellulosic biomass slurries.

This article explores the impact of the initial particle size of red oak sawdust on the rate and extent of enzymatic cellulose conversion to glucose and on the viscosity of the biomass slurry. Experiments were also conducted to study the change of viscosity of the slurry during the course of enzymatic hydrolysis reaction with time. The experiments aim to determine if controlling the initial substrate particle size can maximize the cellulose-to-glucose conversion and reduce the residence time for the enzymatic hydrolysis reaction to achieve maximum glucose yield. Characterization of viscosity aids in reactor design, especially at large scale. And it is necessary for predicting power consumption, which is a significant portion of the operating cost for the process.

## Materials and Methods

### *Cellulose Substrate and Enzyme*

The cellulose substrate used in these experiments is red-oak sawdust obtained from Garrard Wood Products of Lancaster, Kentucky. The carbohydrate components of the sawdust contain 39.7% cellulose and 18.8% hemicellulose. The sawdust was sieved in a set of US standard sieves for 30 min to obtain the following initial particle size ($x$) ranges: 33 μm $< x \leq$ 75 μm, 75 μm $< x \leq$ 104 μm, 104 μm $< x \leq$ 150 μm, 150 μm $< x \leq$ 180 μm, 295 μm $< x \leq$ 425 μm, and 590 μm $< x \leq$ 850 μm. The following sieves were used: 20, 30, 40, 80, 100, 140, and 200 mesh. The sawdust was hydrolyzed without any

pretreatment by the Multifect GC Cellulase enzyme, from Genencor International, Inc. (Rochester, NY) (Lot No. 301-04328-224).

### *Hydrolysis Procedure*

The initial particle size ranges used for the hydrolysis studies were: 33 μm < $x \leq 75$ μm, 150 μm < $x \leq 180$ μm, 295 μm < $x \leq 425$ μm, and 590 μm < $x \leq 850$ μm. The enzyme loading was 15 filter paper units per gram of cellulose. 1 *M* citrate buffer was prepared by adjusting the pH to 4.8 with NaOH, and was used as 5% of the total mass to yield an effective molality of 0.05 mol/kg. All the materials were sterilized in an autoclave at 121°C before use. Enzymatic hydrolysis was performed at 50°C in an Innova 4230 incubator shaker (New Brunswick Scientific Co., Inc., Edison, NJ) at 250 rpm for 72 h. All experiments were performed in 250-mL shake flasks with a working mass of 100 g, and for both 10 and 13% (wt/wt) initial solids concentrations. Samples were collected every 2 h for the first 12 h and every 24 h afterwards for glucose concentration determination. All enzymatic hydrolysis experiments were performed in duplicate and average results were given.

The enzymatic hydrolysis samples were centrifuged at 4000 rpm in a Beckman GPR centrifuge (Beckman Instrument, Inc., Palo Alto, CA) for 15 min, and the glucose concentration was measured by a YSI-Biochemistry analyzer (Yellow Spring Instruments, OH), which was calibrated daily.

### *Viscosity Measurements*

The viscosity of wood particle slurries was measured with a Physica MCR 300 modular compact rheometer from Anton Parr (Ashland, VA) containing a six-bladed vane in a 40-mL cup. The vane dimensions are 1.6 cm long by 0.9 cm wide by 1 mm thick. Sample size used in the cup is 30 mL, which is enough volume to cover the impeller blades. The viscosity of the slurries with the following initial particle size ranges was measured: 33 μm < $x \leq 75$ μm, 75 μm < $x \leq 104$ μm, 104 μm < $x \leq 150$ μm, and 150 μm < $x \leq 180$ μm. Two kinds of viscosity measurements were performed, discrete and continuous. In discrete measurements, the viscosity of the slurries was measured for all four size ranges at an applied shear rate of 10.8/s and at different time intervals of the enzymatic hydrolysis (0, 24, 48, and 72 h). Measurements were made after 10 min of stirring in the viscometer cup, which is the amount of time needed to overcome time dependent changes in viscosity. In continuous measurements, the viscosity of the slurries was measured for the first 12 h of the enzymatic hydrolysis. For these 12 h viscosity tests, the enzymatic hydrolysis reaction was performed directly in the viscometer cup so that the viscosity could be continuously measured. Viscosity data was collected at 10 min intervals. The cup of the viscometer was covered with parafilm to avoid evaporation. The buffer and enzyme concentrations were the same as those in the enzymatic hydrolysis test.

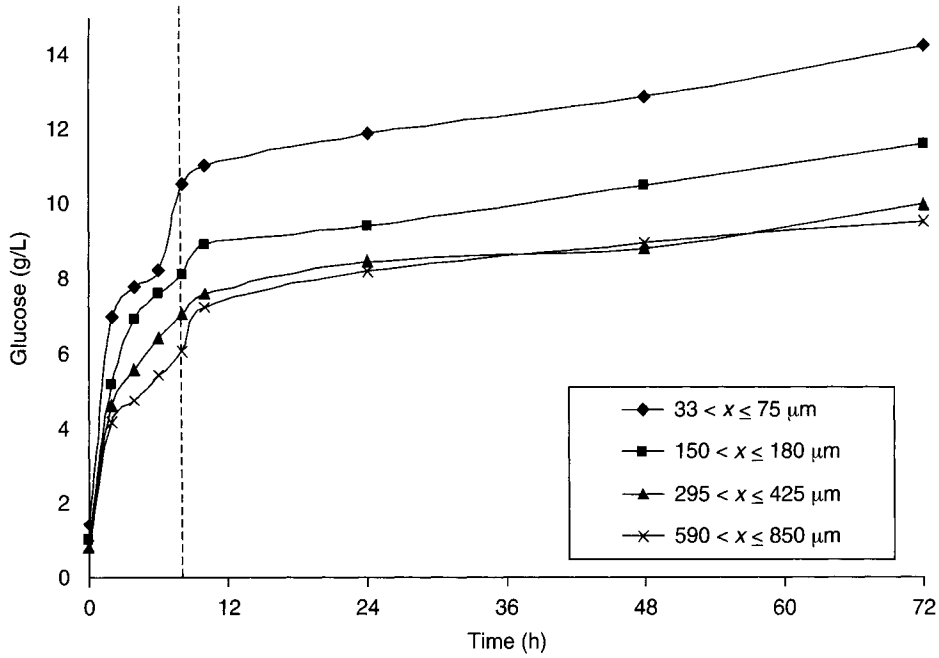


**Fig. 1.** The effect of initial particle size on glucose production with 10% initial solids concentration (glucose ± 0.15 g/L).

## Results and Discussions

The extent of glucose release from cellulose during the course of an enzymatic hydrolysis reaction for four particle size ranges (33 μm < $x$ ≤ 75 μm, 150 μm < $x$ ≤ 180 μm, 295 μm < $x$ ≤ 425 μm, and 590 μm < $x$ ≤ 850 μm) was determined at an enzyme concentration of 15 filter paper units and the results are presented in Figs. 1 and 2. Two phases of the rate are observed during the course of the enzymatic hydrolysis reaction for all particle size ranges. Approximately 70% of the total glucose (obtained in 72 h) is produced within the first 8 h of the hydrolysis reaction. In this first phase the rate is very rapid and the reaction proceeds in a logarithmic fashion and in the second phase the rate declines into zero order kinetics *(19)*.

This observation of two phase kinetics occurs possibly because the easily hydrolysable amorphous form of the cellulose is rapidly converted to glucose (phase 1), followed by the conversion of more recalcitrant crystalline form (phase 2) during the hydrolysis reaction by the enzyme *(8)*. There are a number of other factors that could explain the further slow down in reaction kinetics. One of these is likely because of the nonlinearly varying surface area (Langmuir-type isotherm relationship) for enzyme adsorption with the extent of conversion *(20,21)*. The surface area available on the substrate for the enzyme adsorption is large at the initial stages of the reaction, and it decreases as more cellulose is converted to glucose. The

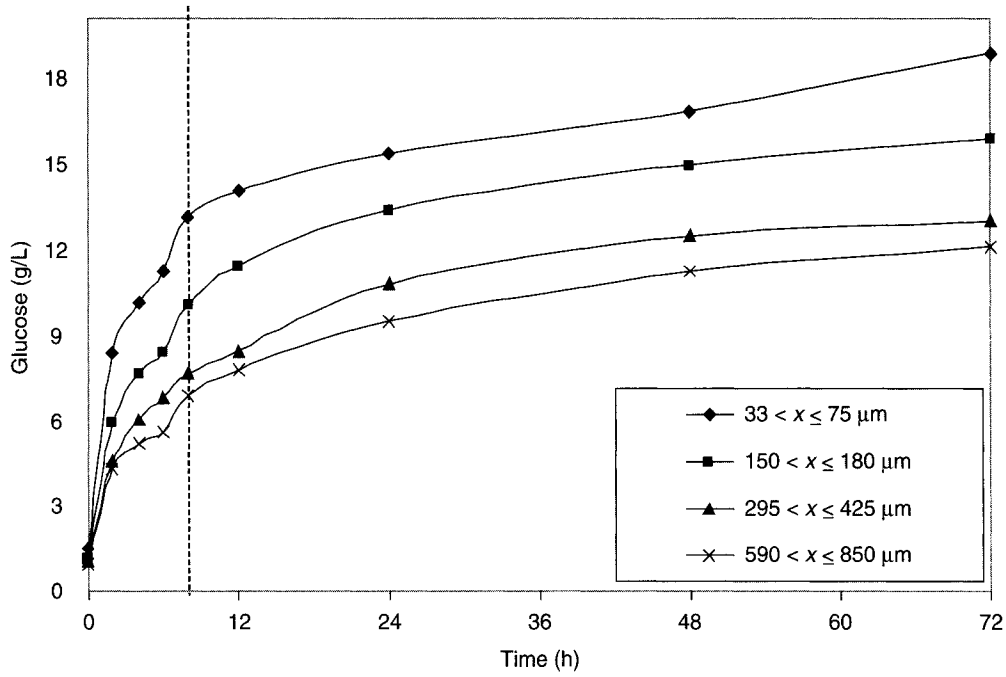


**Fig. 2.** The effect of initial particle size on glucose production with 13% initial solids concentration (glucose ± 0.15 g/L).

drop in the reaction rate of the hydrolysis after the first 8 h may also be because of product inhibition *(11,19)* or the enzyme deactivation by various factors such as thermal deactivation, mechanical deactivation, irreversible binding to lignin, and so on *(22)*. Eriksson et al. *(23)* proposed that this "inactivation" was caused either by the enzyme binding to cellulose at unproductive sites or failure to release from the substrate after catalytically processing a cellulose chain.

It is observed that for smaller particle sizes the rate of release of glucose is higher. An amount of 50 and 55% more glucose is produced for the size range 33 µm $< x \leq$ 75 µm than for the size range 590 µm $< x \leq$ 850 µm for an equivalent initial solids concentration, of 10 and 13%, respectively, in 72 h. Smaller particles have larger surface area per unit volume and, therefore, more cellulose may be accessible for the enzyme to reach and at a faster rate. Another possibility is that smaller particles may have been exposed to more mechanical grinding at the surface, resulting in a reduction of crystallinity and an increase in amorphous nature at the surface *(24,25)*. Peters et al. *(15)* found no significant difference in the extent of sugar produced and the rate of cellulose conversion for the cellulosic substrate Avicel PH 102, as particle size range varies between 38 and 75 µm. Because Avicel is a crystalline structured cellulose and the authors found no significant difference in the rate between different particle sizes, this may

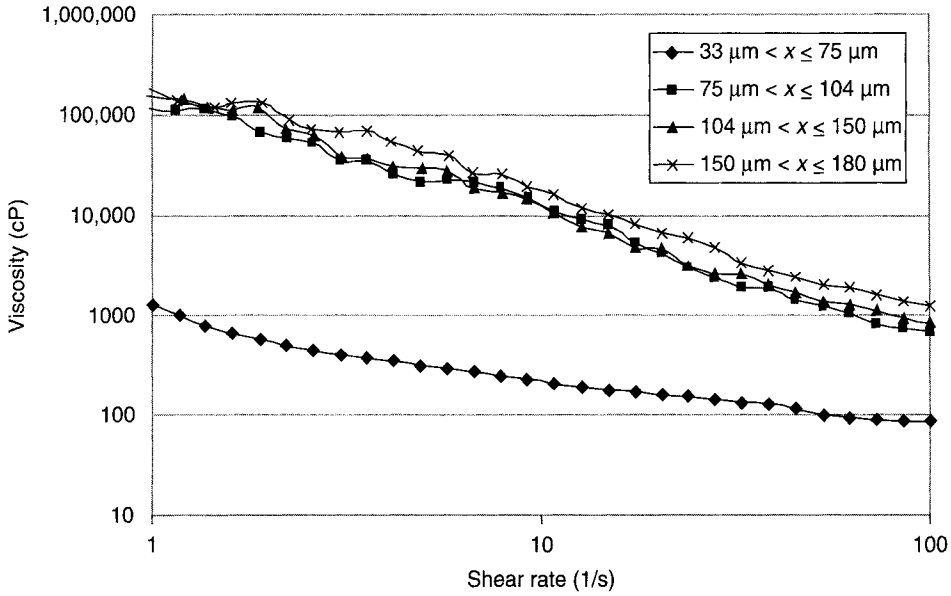


**Fig. 3.** Viscosity and glucose vs time (13% initial solids concentration, 33 μm < $x$ ≤ 75 μm, 10.8/s).

indicate that the latter of the two possible explanations is the more likely reasoning for the increased rate.

Supporting the fact that 70% of the overall cellulose conversion in 72 h is obtained in the first 8 h of the hydrolysis reaction, a significant drop in slurry viscosity is observed within the first 8 h of the hydrolysis reaction. Figure 3 shows as an example the 13% initial solids concentration slurry with the size range 33 μm < $x$ ≤ 75 μm at a shear rate of 10.8/s. The trend is similar for 10% initial solids (not shown). The drop in viscosity is because of a combination of the decrease in solids concentration and the fragmentation of the cellulose particles *(15)*. As the hydrolysis reaction proceeds, the particles break down into smaller particles and eventually the undissolved cellulose particles are converted into dissolved glucose.

Slurry viscosity is generally shear thinning but becomes less associated with shear above a certain applied shear rate. In the cases studied here, this shear rate is near 85/s and is independent of the particle size for slurries before the initiation of the hydrolysis reaction (Fig. 4). The same effect also appears to be independent of the time of the hydrolysis reaction (Fig. 5), with a steadying of the viscosity above a shear near 40/s. The viscosity actually appears to increase slightly with increase in shear above this point, but the apparent effect is likely because of better stirring in the viscometer cup at the higher rotation rate of the impeller. The shear thinning nature of the material is explained by Ebeling et al. *(26)* who reported that the cellulose microcrystal orientation is dependent on the shear rate. At a shear rate more than a certain value, the microcrystals align horizontally along the

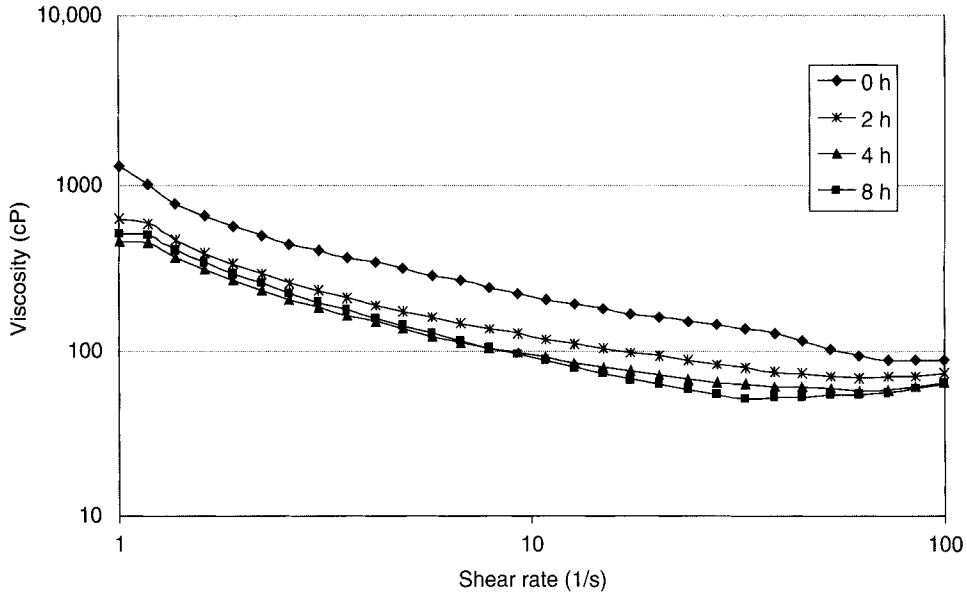


**Fig. 4.** Viscosity vs shear rate ($t$ = 0 h, 13% initial solids concentration).

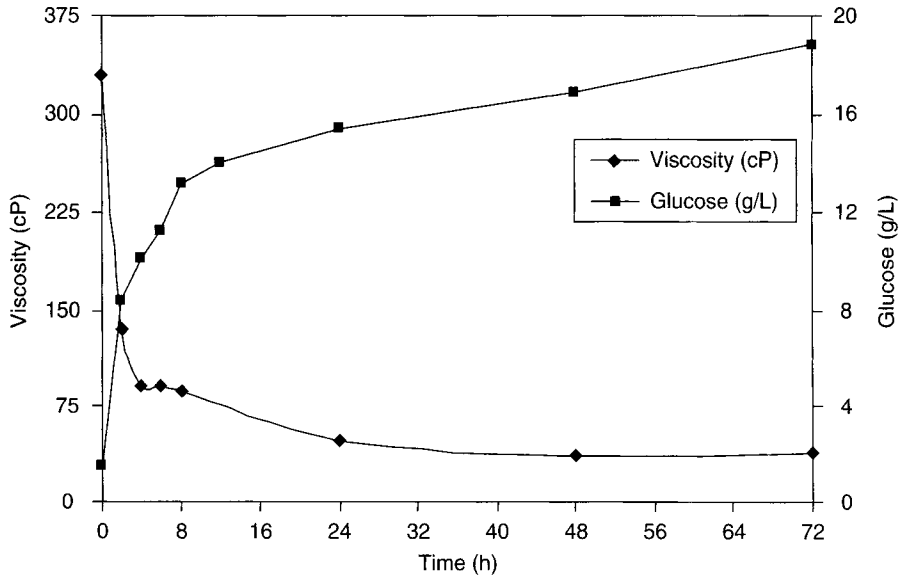


**Fig. 5.** Viscosity vs shear rate at different times during enzymatic hydrolysis (size range: 33 μm < $x$ ≤ 75 μm, 13% initial solids concentration).

shear direction. At a certain degree of alignment, the resistance to the flow becomes approximately constant, and hence, viscosity stops changing. As a side note, the orientation phenomenon is completely reversible *(23)*.

It is well known that as the viscosity of the slurry increases, the power to agitate also increases significantly ($p = \mu_c N^2 D^3$) *(27)*. So, to reduce the power consumption while retaining a high solids loading, it is necessary

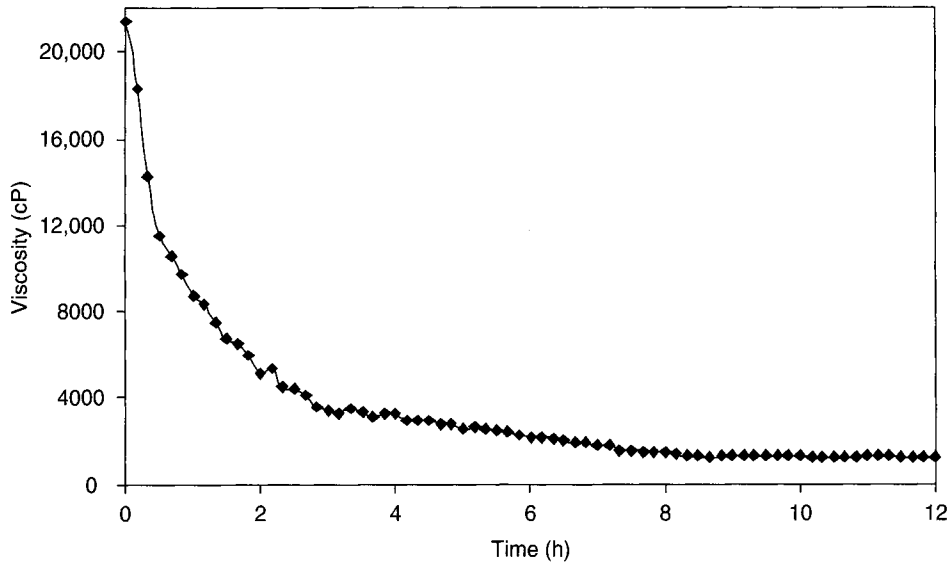


**Fig. 6.** Continuous viscosity vs time measurement (13% initial solids concentration, 150 μm < $x \leq$ 180 μm, 10/s).

to run the reactors at low rpm. For instance, the high solids bioreactor was operated at 7 rpm with 32% of initial insoluble solids by Hodge et al. *(28)*. Therefore, all rheological measurements of the sawdust slurries are measured at a low steady-state shear rate of 10.8/s, which is in the approximate shear rate range of a slow mixing vessel.

In order to better track the viscosity change during the initial stage of the enzymatic hydrolysis reaction, viscosity was measured at 10 min intervals during the first 12 h of the reaction for the size range 150 μm < $x \leq$ 180 μm. The applied shear rate was 10.8/s and the initial solids concentration was 13%. The viscosity data are shown in Fig. 6. From this figure it can be seen that the biggest drop in viscosity occurs in the first 3.5 h of the hydrolysis reaction, indicating the fastest reaction kinetics are actually occurring in this first 3.5-h period.

The effect of the initial particle size of the substrate on the slurry viscosity is studied for the size ranges 33 μm < $x \leq$ 75 μm, 75 μm < $x \leq$ 104 μm, 104 μm < $x \leq$ 150 μm, and 150 μm < $x \leq$ 180 μm for equivalent initial solids concentrations. Results for the case of 10% initial solids are presented in Fig. 7 at a shear rate of 10.8/s. As the particle size range decreases from 150 μm < $x \leq$ 180 μm to 33 μm < $x \leq$ 75 μm, a significant drop in viscosity occurs from 3000 to 61.4 cP. The reason for this significant difference in viscosity with varying particle size is related to the nature of the particle–particle interactions. Amorphous fibers on the surface of particles will affect slurry viscosity as they interact with neighboring particles. Larger fibers will become more entangled than smaller ones, leading to increased resistance to flow and

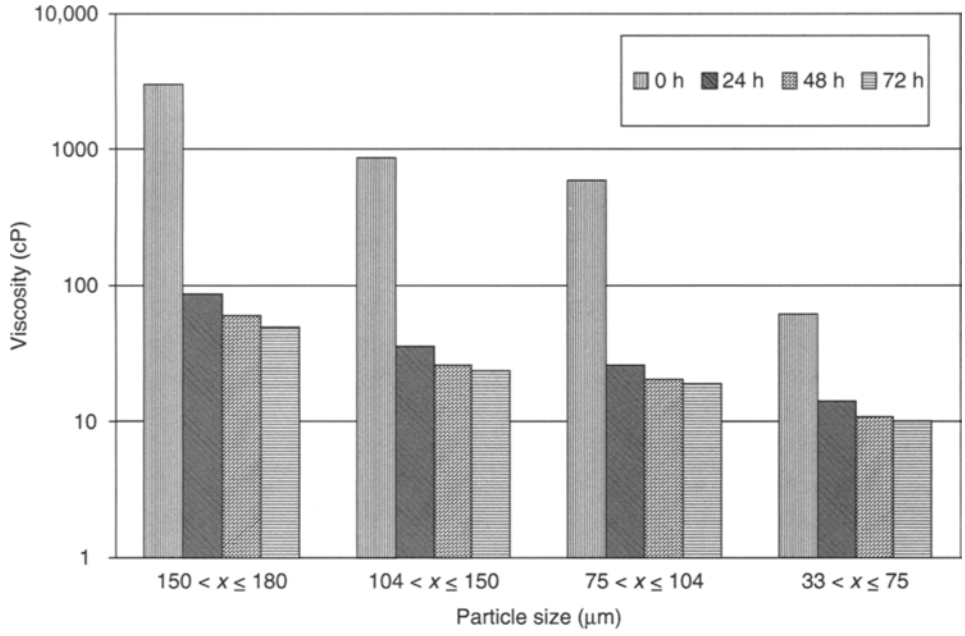


**Fig. 7.** Viscosity vs time of enzymatic hydrolysis for different particle size ranges (10% initial solids concentration, 10.8/s).

hence increased viscosity. Although just speculation, it is reasonable to guess that smaller particles have smaller surface fibers, which would explain the observed lower viscosity for smaller size particle slurries.

The changes of viscosity of the slurries were tracked for initial particle size ranges 33 μm < $x$ ≤ 75 μm, 75 μm < $x$ ≤ 104 μm, 104 μm < $x$ ≤ 150 μm, and 150 μm < $x$ ≤ 180 μm during the course of the hydrolysis reaction and results are presented for the 10% initial solids concentration case. The data at 24-h intervals are presented in Fig. 7 at a shear rate of 10.8/s. For the three larger size ranges (75 μm < $x$ ≤ 104 μm, 104 μm < $x$ ≤ 150 μm, and 150 μm < $x$ ≤ 180 μm) 96% of the initial viscosity is reduced with in the first 24 h of the hydrolysis reaction, whereas only 76% of the initial viscosity is reduced for smaller size particles (33 μm < $x$ ≤ 75 μm). Peters et al. *(15)* reported that the rate of cellulose fragmentation, which results in smaller fragments, is higher for larger size particles. Our results show that the smaller size particles result in lower viscosity. So it is expected that the higher the rate of cellulose fragmentation, the faster the drop in viscosity of the slurry. This explains the bigger viscosity drop in the first 24 h for larger size particles. Hence, the smaller substrate particle size results in lower viscosities of the biomass slurries and therefore lower power consumption and operating costs for the reactor operation at large scale. Also, the lower viscosity may allow for higher solids loading in the reactor.

## Conclusions

These results show that the initial particle size of the biomass substrate has a significant impact on the rates of glucose released and on the viscosity of the biomass slurries. In enzyme hydrolysis, 50–55% more glucose was produced for the size range 33 μm < $x$ ≤ 75 μm than that for the size range 590 μm < $x$ ≤ 850 μm in 72 h of the reaction. Therefore, the minimum particle size range that can be obtained should be used for the maximum cellulose conversion. Further investigation is required to determine the minimum particle size range of substrate at which the reaction rate is no longer affected by the particle size. The viscosity of the sawdust slurry becomes approximately constant above an applied shear rate of 40/s. A correlation was observed between the glucose released and the viscosity reduction during the hydrolysis of cellulose, i.e., 70% of the overall glucose released in 72 h was obtained with in the first 8 h of the hydrolysis reaction and resulted in 70% drop in the viscosity of its initial value. Therefore, reducing particle size can be a way to lower the viscosity of the biomass slurries, to reduce operating costs, or allow for increased solids loading.

## Acknowledgment

This work was funded by the United States Department of Energy award number DE-FC36-046014221. The authors thank Genencor International, Inc., for supplying enzyme used in this study. We wish to thank Garrard Wood Products of Lancaster, KY for supplying saw dust.

## References

1. Cristobal, C., Ruiz, E., Ballesteros, I., Negro, M. J., and Castro, E. (2006), *Process Biochem.* **41,** 423–429.
2. McCloy, B. W. and O'Connor, D. V. (1999), Wood ethanol opportunities and barriers. Report for Forest Sector Table.
3. Robert, H. F. and McKeever, D. B. (2004), Recovering wood for reuse and recycling: a United States perspective. Management of Recovered Wood Recycling, Bioenergy and Other Options, Thessaloniki, European COST E31 Conference.
4. Brownell, H. H. and Saddler, J. N. (1987), *Biotechnology and Bioengineering* **29(2),** 228–235; Mosier, N., et al. (2005), *Bioresource Technology* **96,** 673–686.
5. Hans, E. G. (1991), *Bioresource Techonol.* **36,** 77–82.
6. Ian, F. C., Saddler, J. N., Shawn, D. M. (2004), *Biotechnol. Bioeng.* **85(4),** 413–421.
7. Charles E. W., Lee, Y. Y., Dale, B. E., et al. (2005), 2nd World Congress on Industrial Biotechnology and Bioprocessing.
8. Gusakov, A. V. and Sinitsyn, A. P. (1985), *Enzyme Microb. Technol.* **7,** 346–352.
9. Gonzalez G., Caminal, G., de Mas, C., and Santin, J. L. (1989), *Biotechnol. Bioeng.* **34,** 242–251.
10. Yerkes D. W., Zhang, H., Berson, E. R., Loha, V., Modi, S., and Tanner, R. D. (1995), *Indina Chem. Eng.* **37,** 3,80–89.
11. Kiran, L. K., Rydholm, E. C., and McMillan, J. D. (2004), *Biotechnol. Prog.* **20,** 698–705.
12. Kamyar, M. (2005), *Biochem. Eng. J.* **24,** 217–223.
13. Walker, L. P. and Wilson, D. B. (1991), *Bioresour. Technol.* **36,** 3–14.
14. Abasaeed, A. E. and Lee, Y. Y. (1991), *Bioresour. Technol.* **35,** 15–21.

15. Peters, L. E., Walker, L. P., Wilson, D. B., and Irwin, D. C. (1991), *Bioresource Technol.* **35,** 313–319.
16. Coughlan, M. P. (1992), *Bioresour. Technol.* **39,** 107–115.
17. Perez, L. L., Teymouri, F., Alizadeh, H., and Dale, B. E. (2005), *Appl. Biochem. Biotechnol.* **121–124,** 1081–1099.
18. Kim, S. and Hlotzapple, M. T. (2006), *Bioresour. Technol.* **97,** 583–591.
19. David, J. G. and John, N. S. (1996), *Biotechnol. Bioeng.* **51,** 375–383.
20. Converse, A. O., Ooshima, H., Burns, D. S. (1990), *Appl. Biochem. Biotechnol.* **24–25,** 67–73.
21. Wald, S., Wilke, C. R., and Blanch, H. W. (1984), *Biotechnol. Bioeng.* **26,** 221–230.
22. Palonen, H., Tjerneld, Z. G., Tenkanen, M. (2004), *J. Biotechnol.* **107,** 65–72.
23. Eriksson, T., Karlsson, J., and Tjerneld, F. (2002), *Appl. Biochem. Biotechnol.* **101,** 41–59.
24. Millett, M. A., Baker, A. J., and Scatter, L. D. (1976), *Biotechnol. Bioeng. Symp. No.* **6,** 125–153.
25. Fan, L. T., Lee, Y., and Gharpuray, M. M. (1982), *Adv. Biochem. Eng.* **23,** 157–187.
26. Ebeling, T., Paillet, M., Borsali, R., et al. (1999), *Am. Chem. Soc.* **15(19),** 6123–6126.
27. Oldshue, J. Y. (1983), *Fluid Mixing Technology*, McGraw Hill, New York, NY.
28. Hodge, D., Karim, M. N., Farmer, J., Schell, D. J., and McMillan, J. D. (2005), 27th Symposium on Biotechnology for Fuels and Chemicals, Denver, CO, 1–4 May.

0273-2289/1559-0291 (Online)/07/136–140/301–312/$30.00

# Effect of Dissolved Carbon Dioxide on Accumulation of Organic Acids in Liquid Hot Water Pretreated Biomass Hydrolyzates

G. Peter Van Walsum,*[,1] Maurilio Garcia-Gil,[1] Shou-Feng Chen,[2] and Kevin Chambliss[2]

[1]*Department of Environmental Studies; and* [2]*Department of Chemistry and Biochemistry, One Bear Place No. 97266, Baylor University, Waco, Texas, 76798-7266, E-mail: GPeter_Van_Walsum@Baylor.edu*

## Abstract

Liquid hot water pretreatment has been proposed as a possible means of improving rates of enzymatic hydrolysis of biomass while maintaining low levels of inhibitory compounds. Supplementation of liquid hot water pretreatment with dissolved carbon dioxide, yielding carbonic acid, has been shown to improve hydrolysis of some biomass substrates compared with the use of water alone. Previous studies on the application of carbonic acid to biomass pretreatment have noted a higher pH of hydrolyzates treated with carbonic acid as compared with the samples prepared with water alone. This study has applied recently developed analytical methods to quantify the concentration of organic acids in liquid hot water pretreated hydrolyzates, prepared with and without the addition of carbonic acid. It was observed that the addition of carbon dioxide to liquid hot water pretreatment significantly changed the accumulated concentrations of most measured compounds. However, the measured differences in product concentrations resulting from addition of carbonic acid did not account for the measured differences in hydrolyzate pH.

**Index Entries:** Analysis; aspen wood; carbonic acid; corn stover; pretreatment; organic acids.

## Introduction

Conversion of lignocellulosic material to ethanol requires hydrolysis of carbohydrate polymers to their constituent sugars. Enzymatic hydrolysis is a common approach to hydrolysis and offers the benefits of mild reaction conditions and selective hydrolysis. To achieve useful rates of enzymatic hydrolysis, the lignocellulose must first be pretreated to reduce the recalcitrance of the substance to hydrolysis. Pretreatment accomplishes many alterations of the biomass. Depending on the technology

*Author to whom all correspondence and reprint requests should be addressed.

chosen, these effects typically include, to varying degrees: hydrolysis of the hemicellulose, solubilization of lignin and carbohydrate monomers and oligomers, and increased accessibility of the cellulose to cellulase enzymes *(1)*. Several pretreatment methods have been explored. Among the more commonly reported technologies are water-based methods such as steam explosion or liquid hot water, and dilute-acid pretreatments, in which mineral acids such as sulfur dioxide or sulfuric acid are used at low concentrations (on the order of 1%) and at temperatures usually below 200°C *(2)*.

Water-based and dilute acid pretreatments have undergone research and development for many years. Much of this research has been devoted to fuel production from biomass. Dilute-acid pretreatment offers good performance in terms of recovering hemicellulosic sugars, but the drawback is its use of sulfuric acid. Sulfuric acid is highly corrosive and its neutralization results in copious production of solid wastes, which can be costly to dispose of. The calcium sulfate resulting from neutralization has problematic solubility characteristics in that it becomes less soluble at higher temperatures, such as those encountered in a reboiler *(3)*.

One process that offers some benefits of acid catalysis without the drawbacks of sulfuric acid is the use of carbonic acid. The pH of carbonic acid is determined by the partial pressure of carbon dioxide in contact with water, and thus it can be neutralized by releasing the reactor pressure. Carbonic acid is relatively mild and hence does not offer the same hydrolytic capability of sulfuric acid. However, van Walsum *(3)* has demonstrated that at temperatures on the order of 200°C, carbonic acid does exhibit a catalytic effect on hydrolysis of xylan. Van Walsum observed enhanced release of xylose and low degree of polymerization xylan oligomers compared with pretreatment using hot water alone. On corn stover, Shi and van Walsum *(4)* found enhanced hydrolysis resulting from addition of carbon dioxide.

A curious phenomenon reported in several previous studies *(4–6)* is that the pH of the final hydrolyzate, when measured at ambient temperature and pressure, is higher when carbonic acid is used in the pretreatment, and lower when water alone is used. It has been hypothesized that the two pretreatment methods resulted in differential production and release of organic acids, resulting in the difference in final pH (6.0). This study seeks to test this hypothesis by quantifying the organic acids and other degradation products produced by liquid hot water and carbonic acid-catalyzed pretreatment. These concentration data can then be used to test whether or not the observed pH differences in these hydrolyzates can be explained by the quantity of acid species present. Feedstocks in this study are corn stover and aspen wood. Metrics of pretreatment effects include final pH and chemical concentrations.

## Materials and Methods

### *Feedstock*

Corn stover was kindly supplied by the National Renewable Energy Laboratory in Golden, CO. Aspen wood chips were kindly supplied by the United States Department of Agriculture (USDA) Forest Products Laboratory in Madison, WI. Before pretreatment, the aspen wood was ground in a domestic brand coffee grinder and sifted to a particle size of between 0.5 and 1 mm. Corn stover was used as delivered. Dry weight of the feedstock was determined by oven drying. Carbon dioxide was standard laboratory grade, and $H_2O$ was laboratory deionized quality.

### *Pretreatment*

Two 1 g samples of biomass were weighed out and placed in separate 150-mL, 316 stainless steel reactors, along with 80 mL of deionized water each. One reactor was pressurized with 800 psi of $CO_2$ at room temperature; the other was left with air in the headspace at atmospheric pressure. $CO_2$ was added through a stainless steel tubing connection equipped with a valve and pressure gage *(5)*. Two sand baths equipped with digital temperature controllers were used for temperature control, one heated to the desired reaction temperature, and the second to a temperature 40°C more than the desired reaction temperature. The higher-temperature sand bath was used for preheating the reaction vessels for 3 min to quickly attain the desired reaction temperature. After preheating, the reactors were transferred to the reaction-temperature sand bath for the desired reaction duration. The reaction was quenched in an ice bath immediately after the reaction was complete. Previous research by McWilliams and van Walsum *(6)* had determined that a temperature range of 180–220°C was optimal for xylan solubilization. After pretreatment, suspended particles were removed by filtration using Whatman glass-microfiber membrane filters (90 mm diameter; 0.45-μm pore size; VWR Scientific, Suwanee, GA), and samples were stored at 4°C until processed for high-performance liquid chromatography (HPLC) analysis. Pretreatment conditions investigated in this study are summarized in Table 1. Further description of the pretreatment methods have been published previously *(5,6)*.

### *Analysis*

Quantitative HPLC-ultraviolet (UV) analysis was performed on each sample in triplicate. The HPLC method used has been reported in detail previously *(7)* and is summarized below. For this work, several additional analytes were monitored that were not assessed in our previous work. All analyses were performed using a Dionex® DX-600 BioLC™ system (Dionex

Table 1
Experimental Conditions Applied in This Study

| Experimental conditions | | | | |
|---|---|---|---|---|
| Substrate | Corn stover | | Aspen wood | |
| Cooking temperature (°C) | 180 | | 180 | |
| Cooking time (min) | 16 | | 16 | |
| $CO_2$ presence | 800 psi $CO_2$ | Without $CO_2$ | 800 psi $CO_2$ | Without $CO_2$ |
| Resultant (pH) | 6.90 | 4.81 | 3.68 | 3.05 |
| Predicted reaction pH in $H_2CO_3$ reactor | Approx 3.4 pH | – | Approx 3.4 pH | – |

Resultant pH values were measured on room temperature, degassed hydrolyzate. pH prediction in the carbonic acid pretreatment reactor is after van Walsum *(3,4)*.

Corp., Sunnyvale, CA), equipped with a Model AS50 autosampler, Model DG2410 degassing module, and Model UVD170U ultraviolet detector. After extraction with MTBE, analytes were separated using a 25 cm × 4.6 mm, 5 mm, YMC™ Carotenoid S-3 column (Waters Corporation, Milford, MA) with an RP 18 Opti-Guard® column (Alltech Associates, Deerfield, IL) used to protect the analytical column. Nonlinear gradient separations were carried out using aqueous 0.05% (v/v) phosphoric acid (pH 2.2–2.3) and water–acetonitrile (10 : 90) as the A and B solvents, respectively. Additional parameters used in HPLC analyses were as follows: injection volume, 25 µL; column temperature, 30°C; flow rate, 1 mL/min.

Identification of degradation products in hydrolyzate samples was accomplished by comparing UV absorbance and retention time data with reference standards. Absorbance was monitored at four different wavelengths in each analysis of reference and hydrolyzate samples. Quantitation of target analytes was accomplished using a multipoint internal standard calibration curve, with *p-tert*-butylphenoxyacetic acid as the internal standard. Acceptability criteria for identification of individual components in validation studies using high-purity reference samples required that the retention time for a given analyte be within ± 2% of the average retention time for each respective standard used to construct the calibration curve for that analyte. Since the publication of this analytical method *(7)*, and the conducting of this experimental study, it has been determined that there is a yet unidentified compound coeluting with the peak identified as lactic acid.

## *pH Calculations*

Estimation of the predicted pH of the hydrolyzate was done through iterative calculation of the hydrogen ion concentration at equilibrium conditions, incorporating measured quantities of acid species and their respective p*Ka* values. Compounds for which p*Ka* values were not obtainable were

excluded from the calculation. Prediction of the pH within the carbonic acid pretreatment reactor was determined as per van Walsum and Shi *(3,4)*.

## Results

As noted in Table 1, all reactions were carried out under identical conditions of time and temperature, with only the presence of carbonic acid being varied. Table 1 also presents the measured pH of the hydrolyzates, which shows that the addition of carbonic acid caused the final (room temperature, degassed) hydrolyzate pH to be higher than when reacted with water alone, as has been observed previously *(4–6)*.

### *Corn Stover Pretreatment*

Pretreated samples were analyzed in triplicate and the data shown represent average measurements. Analytical results showed excellent reproducibility, with the average analyte showing a standard deviation of less than 4% of the mean on the corn stover samples. Table 2 presents the mean value data for the samples. It can be seen that most compounds exhibit different concentration levels between the two pretreatment methods. For most measured compounds, the difference in concentrations between hot water and carbonic acid pretreated samples was far more than the standard deviation of the individual analyses. Applying a *t*-test to the data, all but five compounds (itconic, 3,4 dihydroxybenzoic acid, phenol, syringaldehyde, and 4-hydroxybenzaldehyde) showed more than 95% confidence in the difference between mean measurements. Of these five, only 4-hydroxybenzaldehyde showed less than 50% confidence in difference between the means. Thus for corn stover, the addition of carbonic acid appears to significantly change the accumulation of most degradation products. The nine most abundant products present in the two hydrolyzates are highlighted in Fig. 1. It can be seen that carbonic acid results in the increase of some compounds and the decrease in others. These relative differences are plotted in Fig. 2.

### *Aspen Wood Pretreatment*

Parallel results for aspen wood are presented in Figs. 3 and 4 and Table 2. In general, it was found that the aspen wood samples demonstrated weaker analytic reproducibility, with the average standard deviation for the samples rising to about 7% of the mean. A *t*-test on the data shows that fewer compounds have a high level of confidence (95%) in the difference of their means. For aspen wood 13 of the 36 quantified compounds failed to show this level of confidence in the difference of means, compared with 5 of 33 for corn stover. Also for aspen wood, three compounds (fumaric, levulinic, and homovanillic acid) showed less than 50% certainty that the means were different, compared with only one compound for corn stover.

Table 2
Average Analyte Concentrations for Corn Stover and Aspen Wood Pretreated With and Without Dissolved Carbon Dioxide

| | | Aspen wood | | Corn stover | |
|---|---|---|---|---|---|
| Compounds | p*Ka* | With $CO_2$ | Without $CO_2$ | With $CO_2$ | Without $CO_2$ |
| Formic acid | 3.77 | 0.7642 | 0.8634 | 0.9863 | 0.8603 |
| Malonic acid | 2.83 | 0.0116 | 0.0105 | 0.0142 | 0.0244 |
| Lactic acid[a] | 3.86 | 1.3722 | 2.4773 | 1.5815 | 1.4145 |
| Acetic acid | 4.76 | 1.2853 | 1.3881 | 0.7581 | 1.4044 |
| Maleic acid | 1.93 | 0.0035 | 0.0034 | 0.0119 | 0.0073 |
| Succinic acid | 4.19 | 0.0265 | 0.0554 | 0.3093 | 0.5653 |
| Fumaric acid | 3.03 | 0.0034 | 0.0033 | 0.0193 | 0.0111 |
| Propanoic acid | – | 0.0000 | 0.0000 | 1.5315 | 1.2791 |
| t-Aconitic acid | 2.8 | 0.0000 | 0.0065 | 0.0128 | 0.0049 |
| Levulenic acid | – | 0.3879 | 0.3802 | 0.0467 | 0.1979 |
| Glutaric acid | 4.34 | 0.2474 | 0.3094 | 0.0981 | 0.3987 |
| Itaconic acid | – | 0.0008 | 0.0015 | 0.0056 | 0.0069 |
| Gallic acid | 4.41 | 0.0015 | 0.0023 | 0.0005 | 0.0002 |
| 5-Hydroxymethylfurfural | – | 0.0296 | 0.0516 | 0.0599 | 0.0321 |
| 2-Furoic acid | – | 0.0104 | 0.0119 | 0.0168 | 0.0084 |
| Furfural | – | 0.1650 | 0.3304 | 0.7044 | 0.4197 |
| 3,4 Dihydroxybenzoic acid | – | 0.0009 | 0.0015 | 0.0019 | 0.0020 |
| 3,5 Dihydroxybenzoic acid | – | 0.0001 | 0.0001 | 0 | 0 |
| 3,4 Dihydroxybenzaldehyde | – | 0.0015 | 0.0023 | 0.0087 | 0.0038 |
| Phenol | 9.99 | 0.0090 | 0.0152 | 0.0081 | 0.0059 |
| 4-Hydroxybenzoic acid | – | 0.0694 | 0.0837 | 0.0039 | 0.0024 |
| 2,5 Dihydroxybenzoic acid | – | 0.0015 | 0.0022 | 0.0042 | 0.0011 |
| 4-Hydroxybenzaldehyde | – | 0.0242 | 0.0263 | 0.0288 | 0.0324 |
| Vanillic acid | – | 0.0038 | 0.0051 | 0.0057 | 0.0041 |
| Homovanillic acid | – | 0.0007 | 0.0007 | 0.0003 | 0.0007 |
| Caffeic acid | – | 0.0029 | 0.0034 | 0.0035 | 0.0179 |
| Syringic acid | – | 0.0065 | 0.0086 | 0.0087 | 0 |
| 4-Hydroxy-acetophenone | – | 0.0022 | 0.0032 | 0.0065 | 0.0020 |
| Vanillin | – | 0.0241 | 0.0335 | 0.0393 | 0.0368 |
| 4 HO-Coumaric acid | – | 0.0094 | 0.0155 | 0.1921 | 0.2274 |
| Syringaldehyde | – | 0.0329 | 0.0407 | 0.0173 | 0.0176 |
| Benzoic acid | 4.2 | 0.0618 | 0.0665 | 0.0280 | 0.0323 |
| 4-Hydroxy 3-methoxy, ferulic acid | – | 0.0033 | 0.0058 | 0.0342 | 0.0381 |
| Sinapic acid | – | 0.0182 | 0.0148 | 0.0026 | 0.0049 |
| Salicyclic acid | 2.97 | 0.0031 | 0.0034 | 0 | 0 |
| 4-Hydroxycoumarin | – | 0.0094 | 0.0141 | 0.0037 | 0.0039 |
| 2-Toluic acid | – | 0.0138 | 0.0213 | 0.0078 | 0 |
| 4-Toluic acid | 4.36 | 0.0113 | 0.0140 | 0.0074 | 0 |
| Calculated pH | – | 4.69 | 4.61 | 4.61 | 4.63 |

[a]Since the time these analyses were completed, it has been determined that the lactic acid peak detected with the reported method was coeluting with a yet unidentified compound.

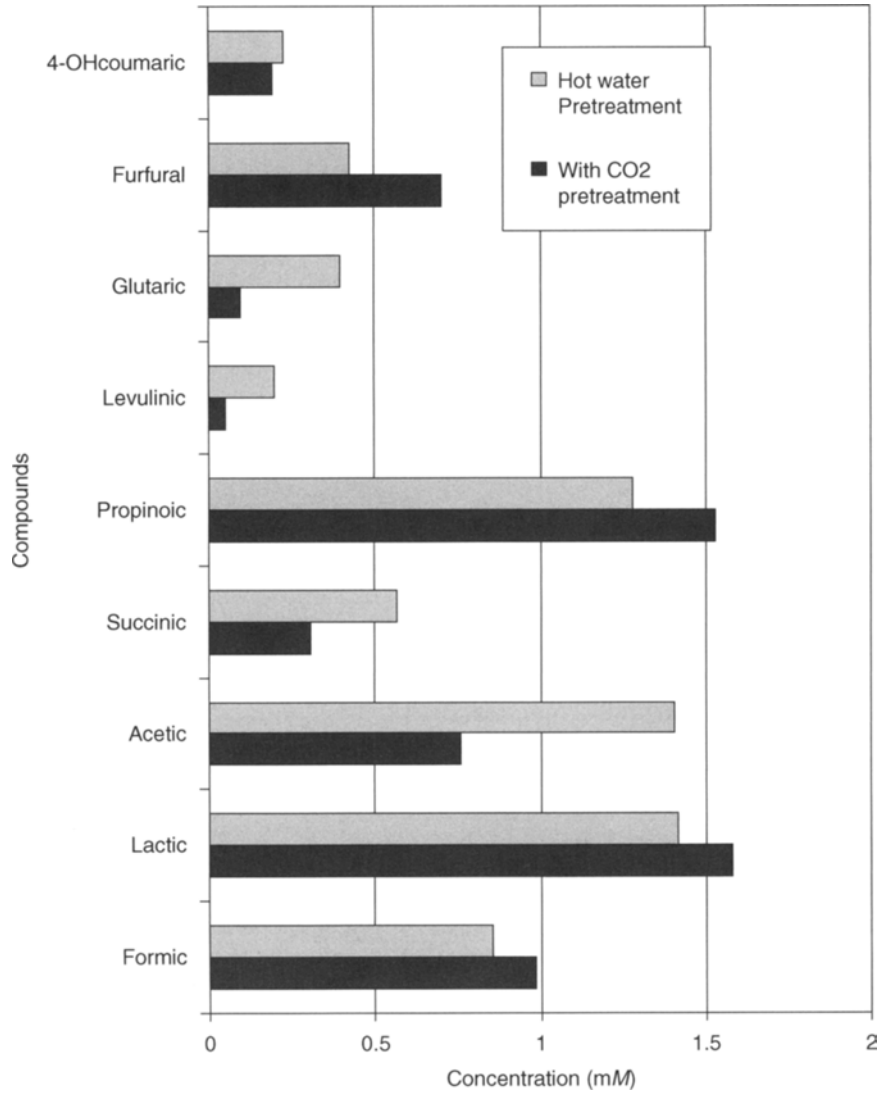


**Fig. 1.** Concentration of selected acid products in corn stover hydrolysate prepared in liquid hot water with and without dissolved carbon dioxide. (*Note*: lactic acid has been determined to coelute with a yet unidentified compound.)

Comparing Figs. 2–4, it can be seen how the variation of the more abundant corn stover products appears to either increase or decrease in response to carbonic acid, whereas on aspen wood, the primary effect of the carbonic acid is to decrease product concentrations.

## *Calculation of pH From Organic Acid Concentrations*

The theoretical pH of the hydrolyzates was calculated based on the concentration and p*Ka* of the various quantified organic acids. p*Ka* values were

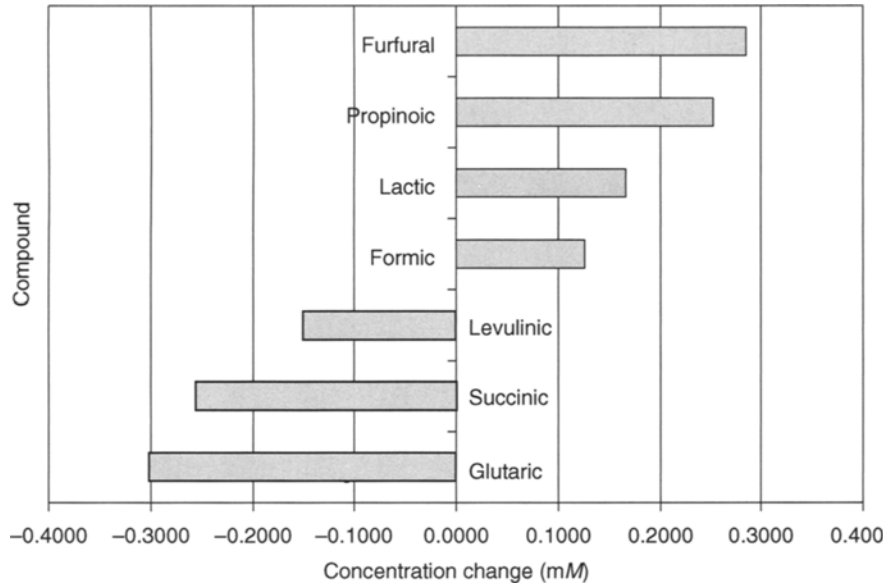


**Fig. 2.** Net difference in concentration of major acid products in corn stover hydrolysate resulting from addition of carbon dioxide. (*Note*: lactic acid has been determined to coelute with a yet unidentified compound.)

not available for some of the compounds present at lower concentration and these were excluded from the calculation. The bottom row of Table 2 lists the outcome of this calculation. It can be seen that the four hydrolyzates represent roughly similar pH ranges for their diverse mixtures of acids, coming in at approx pH 4.64. For aspen wood, the calculated pH values show a slightly higher level for the carbonic acid treated samples, but this difference is far smaller, and manifest at much higher pH, than the values measured experimentally (Table 1). For corn stover, the acid calculations show virtually the same pH in both hydrolyzates. In this case, the calculated pH values fall in the middle of the range measured experimentally.

## Discussion

Corn stover samples were found to demonstrate more response to the presence of carbonic acid than aspen wood. This difference is owing in part to the greater scatter in the analytical results for aspen wood, reducing the confidence levels in the assessment of difference between means. In addition, this result may also reflect reduced influence of carbonic acid on the production of degradation products from aspen wood, in comparison with corn stover. This conclusion is in keeping with previously reported results where it was found that the influence of carbon dioxide on the release of xylose was more pronounced on corn stover than on aspen wood *(4)*.

From Figs. 2 and 4, it appears that the effect of carbon dioxide on aspen wood pretreatment is to reduce the concentration of degradation

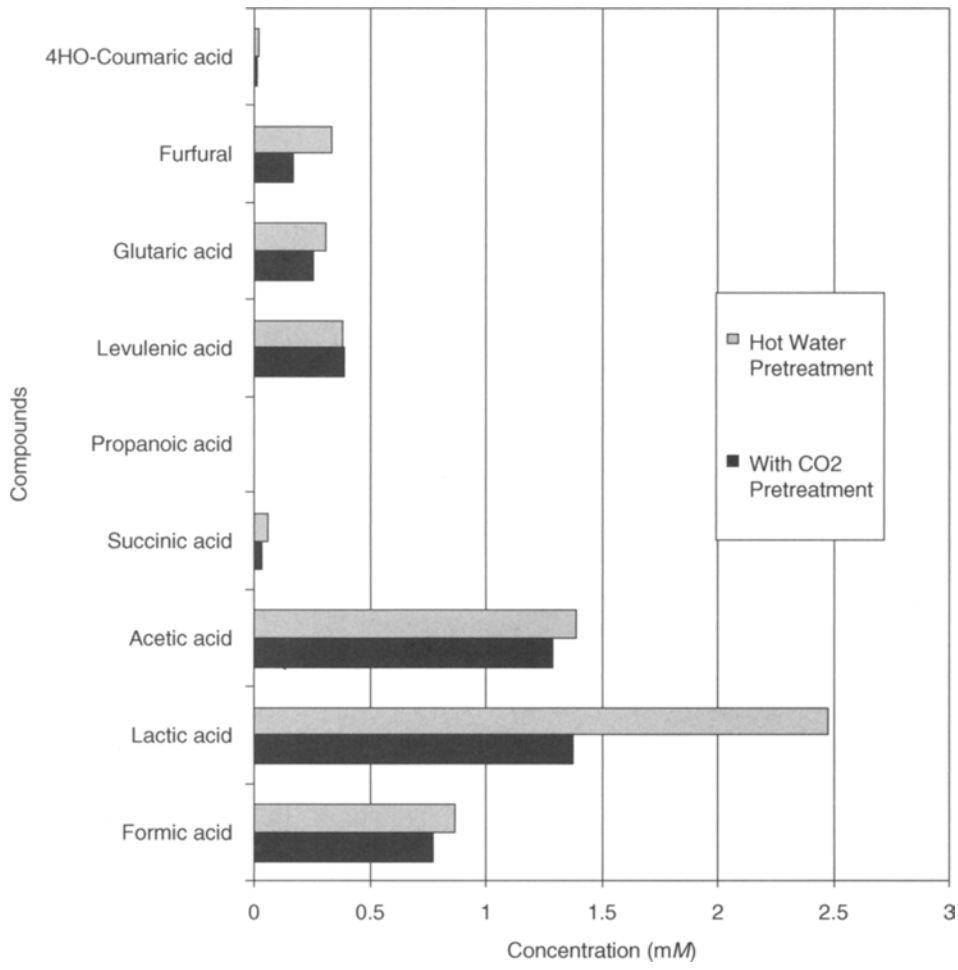


**Fig. 3.** Concentration of selected acid products in aspen wood hydrolysate prepared in liquid hot water with and without dissolved carbon dioxide. (*Note*: lactic acid has been determined to coelute with a yet unidentified compound.)

products, whereas on corn stover it appears to have differing effects for different compounds. The aspen results suggest a lessened degree of hydrolysis action on aspen wood with the addition of carbon dioxide to the reactor, suggesting that with aspen wood, the carbonic acid may possibly be working as a buffer rather than an acid. The predicted pH of the carbonic acid system under reaction conditions is approx 3.4, which is higher than the room temperature p*Ka* of some of the stronger acids present. However, it is not known how the p*Ka* values of the various organic acids present change in response to temperature, making it difficult to further assess this possibility.

The pH values calculated from the concentrations of the organic acids present in the hydrolyzates (Table 2) are in the range to be expected from a mixture containing many diluted organic acids. However, the calculated

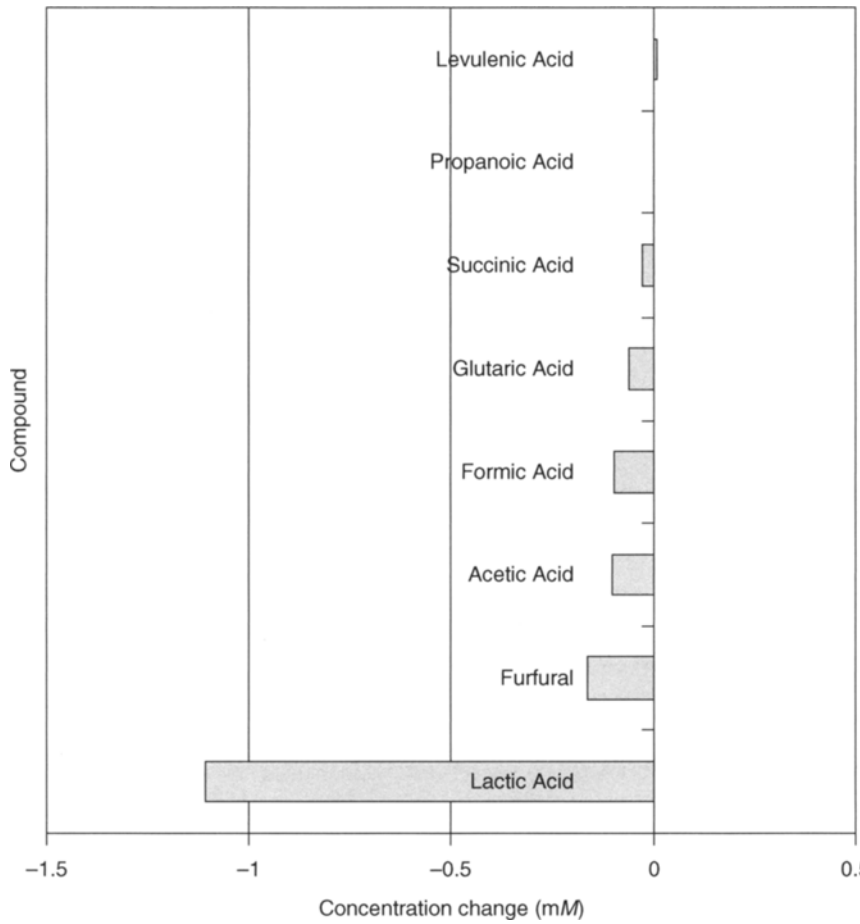


**Fig. 4.** Net difference in concentration of major acid products in aspen wood hydrolysate resulting from addition of carbon dioxide. (*Note*: lactic acid has been determined to coelute with a yet unidentified compound.)

values were not in accord with the measured pH values. For aspen wood, the measured pH values were substantially lower than the calculated values. This indicates that there may remain acid species in the sample that were not quantified in this study. Also, the measured increase in pH resulting from the addition of carbon dioxide, which was observed in this study and has also been consistently reported in previous studies, was not adequately accounted for by the compounds measured in this study. This too suggests an incomplete analysis of the compounds present.

## Conclusions

A newly developed analytical procedure was applied to determine the concentrations of organic acids and other degradation products present in pretreatment hydrolyzates of aspen wood and corn stover. It was observed

that the addition of carbon dioxide to liquid hot water pretreatment significantly changed the accumulated concentrations of most measured compounds. However, these different concentration values failed to explain the consistently observed higher pH levels associated with carbonic acid pretreatment.

## Acknowledgments

Many thanks go to the USDA and the Department of Energy for their partial funding of this research. Also, much gratitude goes to David Roaten and Richard Mowery for their assistance and insight on this work.

## References

1. McMillan, J. D. (1994), *ACS Symp. Ser.* **566,** 292–324.
2. Quang, A. N., Tucker, M. P., Keller, F. A., and Eddy, F. P. (2000), *Appl. Biochem. Biotechnol.* **84–86,** 561–576.
3. van Walsum, G. P. (2001), *Appl. Biochem. Biotechnol.* **91–93,** 317–329.
4. van Walsum, G. P. and Shi, H. (2004), *Biores. Technol.* **93,** 217–216.
5. Yourchisin, D. M. and van Walsum, G. P. (2004), *Appl. Biochem. Biotechnol.* **113–116,** 1073–1086.
6. McWilliams, R. and van Walsum, G. P. (2002), *Appl. Biochem. Biotechnol.* **98–100,** 109–121.
7. Chen, S.-F., Mowery, R., Castleberry, V. A., van Walsum, G. P., and Chambliss, C. N. (2006), *J. Chrom. A.* **1104,** 54–61.

0273–2289/1559–0291 (Online)/07/136–140/313–326/$30.00

# Separation of Glucose and Pentose Sugars by Selective Enzyme Hydrolysis of AFEX-Treated Corn Fiber

ROBERT J. HANCHAR,*[,1] FARZANEH TEYMOURI,[1] CHANDRA D. NIELSON,[1] DAROLD MCCALLA,[1] AND MARK D. STOWERS[2]

*[1]MBI International, 3900 Collins Road, Lansing, MI 48910, USA, E-mail: hanchar@mbi.org; [2]Broin Companies, 2209 E. 57th N., SiouxFalls, SD 57104, USA*

## Abstract

A process was developed to fractionate corn fiber into glucose- and pentose-rich fractions. Corn fiber was ammonia fiber explosion treated at 90°C, using 1 g anhydrous ammonia per gram of dry biomass, 60% moisture, and 30-min residence time. Twenty four hour hydrolysis of ammonia fiber explosion-treated corn fiber with cellulase converted 83% of available glucan-to-glucose. In this hydrolysis the hemicellulose was partially broken down with 81% of the xylan and 68% of the arabinan being contained in the hydrolysate after filtration to remove lignin and other insoluble material. Addition of ethanol was used to precipitate and recover the solubilized hemicellulose from the hydrolysate, followed by hydrolysis with 2% (v/v) sulfuric acid to convert the recovered xylan and arabinan to monomeric sugars. Using this method, 57% of xylose and 54% of arabinose available in corn fiber were recovered in a pentose-rich stream. The carbohydrate composition of the pentose-enriched stream was 5% glucose, 57% xylose, 27% arabinose, and 11% galactose. The carbohydrate composition of the glucose-enriched stream was 87% glucose, 5% xylose, 6% arabinose, and 1% galactose, and contained 83% of glucose available from the corn fiber.

**Index Entries:** Ammonia fiber explosion; arabinose; lignocellulose; sugar separation; xylose; glucose.

## Introduction

According to the Renewable Fuels Association (2006), US ethanol capacity was $4.3 \times 10^9$ US gal in 2005, an increase of $1.4 \times 10^9$ US gall over the production level in 2002. The demand for and production of ethanol is expected to dramatically increase over the next decade to reduce US dependency on foreign oil. The majority of current ethanol processes use glucose derived from corn-starch as the primary feedstock; however, this will not be able to supply all the ethanol needs. An abundant natural and

*Author to whom all correspondence and reprint requests should be addressed.

renewable resource such as lignocellulosic biomass must be utilized to supply our long-term needs for ethanol as a renewable bio-based fuel. In addition to ethanol, forty chemicals and chemical feedstocks have been identified as potential products from renewable plant biomass *(1–4)*.

Lignocellulosic biomass consists of three major components: cellulose, hemicellulose, and lignin. The complex structure of lignocellulosic biomass, the crystalline structure of cellulose, and the physical protection provided by hemicellulose and lignin, prevent efficient hydrolysis and subsequent release of fermentable sugars by hydrolytic enzymes. Therefore, pretreatment is required to alter the structure of cellulosic biomass to make cellulose more accessible to the enzymes that convert the carbohydrate polymers into fermentable sugars.

A number of pretreatment technologies have been proposed and investigated *(5)*. Among these, the ammonia fiber explosion (AFEX) is one of the most effective pretreatments. AFEX disrupts cell wall physical barriers as well as cellulose crystallinity and association with lignin and hemicellulose so that the hydrolytic enzymes can access the biomass macrostructure *(6,7)*. The AFEX process is one of the most environmentally friendly pretreatment processes with several distinguishing features. These features are:

1. Energy requirements are low and reaction temperatures are mild.
2. Ammonia is an abundant and widely available chemical, which can be contained and recycled with residual ammonia serving as a nitrogen source for subsequent fermentation or animal feeding operations.
3. Minimal waste is generated as less than 2% of the ammonia used in the treatment is retained by biomass, therefore, no neutralizing waste or wash streams are created in the process *(6,8,9)*.
4. Dry matter recovery following the AFEX treatment is essentially 100% and is stable for long periods and can be fed at high-solids loadings in fermentation processes *(10)*.
5. Cellulose and hemicellulose are well preserved in the AFEX process, with little or no degradation *(11)*.
6. There is no formation of furfural or furfural derivatives, which are known to have inhibitory effects on the metabolism of the yeast *Saccharomyces cerevisiae* in production of ethanol *(12,13)*.

It has been shown that AFEX treatment of biomass, such as corn stover, corn fiber, and switchgrass followed by enzymatic hydrolysis yields a stream of fermentable sugars containing both C5 sugars (arabinose and xylose) and C6 sugars (glucose), which can be used for production of industrial products such as ethanol and succinic acid *(6,8,14,15)*. However, the individual sugars could be used to produce more highly valued products if the C5 and C6 sugars could be separated from each other and from the lignin. For example, xylose could be

reduced to xylitol, a sweetener that prevents dental caries; arabinose to pharmaceutical intermediates; and glucose could be routed into existing starch-based processes, such as high-fructose corn syrup. An overall process that incorporates the separation of the C5 and C6 streams, would realize increased economic return plus operational and market flexibility.

Corn fiber was selected as the lignocellulosic biomass for this study. The current availability of corn fiber in concentrated amounts at wet mills allows us to model its possibilities as a biomass source without speculating on the gathering and storage costs associated with most other biomass sources. In addition, a limiting factor in the cost effectiveness of current ethanol production processes is the value obtained from the byproducts. The profitability of ethanol production is expected to be enhanced by applying a biorefinery concept and by modifying existing plants to produce value added products *(16)*. A biorefinery, in principle, will process most, if not all, of the incoming feedstocks and byproducts into valuable products while at the same time producing ethanol. Corn fiber is a high cellulose/hemicellulose lignocellulosic biomass with a low market value currently produced in large quantities at corn wet mills and is included in distiller's grains at dry mill ethanol plants. The fractionation of corn fiber into a higher value component would improve the cost effectiveness of current ethanol production processes *(8)*.

Previous studies *(11,15)* have shown the applicability of AFEX to corn fiber. AFEX-treated corn fiber showed significant improvement of glucose production during enzyme hydrolysis relative to untreated material and the generated sugars were readily fermented to ethanol. Unlike cellulose, only a small fraction of the xylan in the AFEX-treated corn fiber (4–6%) was converted to xylose and more than 81% of that was solubilized in the hydrolysate as oligomers during enzyme hydrolysis. Corn fiber xylan is one of the most substituted and complex xylans and is thus highly recalcitrant to enzyme hydrolysis. Available commercial cellulases and xylanases are not able to convert corn fiber xylan into xylose efficiently. In order to have an economically attractive process, all the available polymeric sugars must be utilized. The main objective of this study was to develop a process for maximum hydrolyzation of all the available sugars in corn fiber and to separate C5 and C6 sugars from each other.

## Materials and Methods

*Material:* Corn fiber with 5% moisture content was provided by Bunge Milling (Danville, IL). The composition is listed in Table 1.

*Cellulase:* Spezyme CP (Genencor, Rochester, NY) lot No. 301-01320-216.

β-glucosidase, Novozyme 188 (Sigma, St. Louis, MO) batch No. DCN00206.

*Glucoamylase:* Glucostar L-400 (Dyadic International Inc., Jupiter, FL) lot No. P01311.

Table 1
Corn Fiber Composition (based on dry weight)

| Starch (%) | Cellulose (%) | Xylan (%) | Arabinan (%) | Galactan (%) | Mannan (%) | Lignin (%) |
|---|---|---|---|---|---|---|
| 10.61 | 19.71 | 28.5 | 13.7 | 3.8 | 0.39 | 12.41 |

*Xylanase:* X1-274, X2-275, X3-276, and X4-277 (Dyadic International Inc.), NS50014 and NS50030 (Novozyme, Franklinton, NC).

*Feed enzyme:* Rovabio Excel LC (Adisseo, Alpharetta, GA) lot No. B-04154-01.

*Anhydrous ammonia:* Linde Gas LLC (Lansing, MI). All other chemicals were purchased from Sigma.

## Analytical Methods

Composition (glucan, xylan, galactan, arabinan, lignin, and ash) of the biomass was determined by following the National Renewable Energy Laboratory (NREL) procedure LAP-002: determination of carbohydrates in biomass by high-performance liquid chromatography (HPLC) (NREL LAP-002). NREL procedures are available at http://www.ott.doe.gov/biofuels/analytical_methods.html. The starch analyses were performed by Servi-tech Laboratories (Hastings, NE). Total sugars in the liquid fractions were determined by following the NREL LAP-014: dilute acid hydrolysis procedure for determination of total sugar in the liquid fraction of process samples.

## AFEX Treatment

Corn fiber (500 g) was treated by the AFEX process in a one-gallon pressure reactor (PARR Instrument Co, Moline, IL). The AFEX process parameters were varied, biomass moisture content (20, 40, 60, and 70%), reaction time (10, 15, and 30 min), temperature (80, 90, 100, and 110°C), and ammonia loading (0.7 : 1 and 1 : 1, g ammonia : g dry biomass) to determine conditions that gave the highest glucose yield. Biomass with the desired moisture content level was added to the reactor. To ensure uniform distribution of heat and ammonia, the reactor was equipped with an agitator that mixed the biomass at 100 rpm during the process. The reactor was heated by an electrical heating mantel to approx 10°C lower than the target temperature before addition of the liquid ammonia. While the reactor was heating, the desired amount of ammonia was pumped to the reactor. The reaction timer was started when the reactor was within 5°C of the set-point. Temperature and pressure of the process was recorded every 3 min. When the desired reaction time (30 min) was complete, ammonia was quickly evacuated through a manual ball

valve. The treated biomass was removed from the reactor and left in a fume hood for 1 d to evaporate the residual ammonia. The treated biomass was stored at 4°C until used. All AFEX runs were performed in duplicate and the data for the conditions selected are presented as the average of the duplicates.

### *Small-Scale Enzyme Hydrolysis*

The efficiency of AFEX treatment was evaluated through small-scale enzyme hydrolysis. The hydrolysis was performed in shake flask following NREL's LAP-009: enzymatic saccharification of lignocellulosic biomass procedure with the following modifications. Hydrolyses were performed with 5% solid loading and a mixture of 15 filter paper units of Spezyme CP and 42 cellobiose units of NOVO 188 per gram of cellulose and 0.0032 g of Glucostar L-400/g starch. The hydrolyses were carried out at 50°C and pH 4.8 for 72 h. Samples were taken at 0, 24, 48, and 72 h for sugar analysis.

### *Large-Scale Enzyme Hydrolysis*

The 10 L enzyme hydrolyses were carried out in a New Brunswick Scientific Microferm 14-L fermentor (New Brunswick Scientific, Edison, NJ) equipped with a mechanical stirrer. There were three impellers on the agitation drive shaft, from top to the bottom, two six-blade Rushton impellers 3 in. apart and one lightnin A310 impeller at the bottom. The hydrolyses were mixed at 250 rpm. The hydrolysis used a 10% solids loading of AFEX-treated corn fiber. Fifteen filter paper units of Spezyme CP/g cellulose, 150 U of β-glucosidase/g of cellulose and 0.12 g of Glucostar (glucoamylase)/g of starch were added to the hydrolysis. To minimize potential contamination, all equipment and materials except the biomass were sterilized. Hydrolysis was performed at 50°C and 4.8 pH (active pH control) for 24 h with mixing. Samples were taken for sugar analysis at several time-points. At 24 h, the hydrolysate was removed from the fermentor and centrifuged for 20 min at 5°C at 7500 rpm (9500*g*) to separate the liquid and the solid residuals. Samples were taken from both supernatant and pellet portions for sugar and composition analysis.

### *Ethanol Precipitation*

The supernatant from the enzyme hydrolysis was slowly added to 3X (v : v) cold ethanol (200 proof) to precipitate the solubilized polymeric sugars (mainly hemicellulose). The generated pellet was dried at 45°C in a vacuum oven and was analyzed for carbohydrate composition. The pellet was dissolved in water at 15% solid loading and then concentrated $H_2SO_4$ was added to a final concentration of 2% (v/v). The hydrolysis was carried out at 80°C for 24 h. The hydrolysate was analyzed for sugar content by HPLC. In this procedure, all liquid samples

were analyzed for both monomeric (HPLC) and polymeric (NREL-LAP-014) sugars content. All hydrolyses were performed in duplicate and the data were reported as average. The final hydrolysate was maintained at 4°C until used.

### *Evaluation of Acid Hydrolysis*

Enzyme hydrolysate from corn fiber was prepared as described for the large-scale enzyme hydrolysis above. To a 500-mL flask 100 mL of the enzyme hydrolysate, without filtration, was transferred. Concentrated sulfuric acid was added to achieve the desired acid concentration (2, 1, and 0.5%). With stirring, the reaction was maintained at the appropriate temperature (80 and 100°C). The hydrolysate was periodically sampled and the saccharide concentrations determined following the NREL LAP-014 procedure.

## Results and Discussion

Corn fiber treated under different AFEX conditions was enzyme hydrolyzed (small-scale) to identify the most effective set of AFEX conditions for treatment of corn fiber. The 72 h hydrolysis results showed that corn fiber treated at 90°C, with 60% moisture content for 30 min, with 1 g ammonia per gram of dry biomass gave the highest glucose yield (91 ± 2% based on the available glucose).

The process developed to fractionate AFEX-treated corn fiber to glucose and pentose-rich fractions is shown in Fig. 1. AFEX-treated corn fiber is first hydrolyzed with a cellulase enzyme, converting cellulose to glucose and solubilizing the xylan and arabinan-containing hemicellulose; presumably by partially hydrolyzing it to arabinoxylan oligomers. The insoluble lignins are removed by filtration. The solubilized hemicellulose is precipitated, by addition of ethanol, and collected yielding a glucose-enriched aqueous solution and a filter cake containing the arabinoxylan oligomers. Acid hydrolysis of this filter cake corn fiber gum (CFG) generates the monomeric arabinose and xylose.

### *Effect of Enzyme Hydrolysis Time on Hemicellulose Recovery*

A series of experiments in small-scale (250-mL shake flask) were performed to determine the effect of enzyme hydrolysis time on the recovery of C5 oligomers by ethanol precipitation. Enzyme hydrolysis times of 16, 24, and 48 h were tested with the CFG being precipitated immediately following the hydrolysis. The best yield was obtained from the 24 h hydrolysis where 74% of the xylose and 76% of the arabinose contained in the original AFEX-treated corn fiber was recovered in the CFG. However, statistical analysis showed that the yields from the 16-h and 48-h hydrolyses were not significantly different. The 24-h enzyme hydrolysis was selected for our larger scale (14 L) experiments.

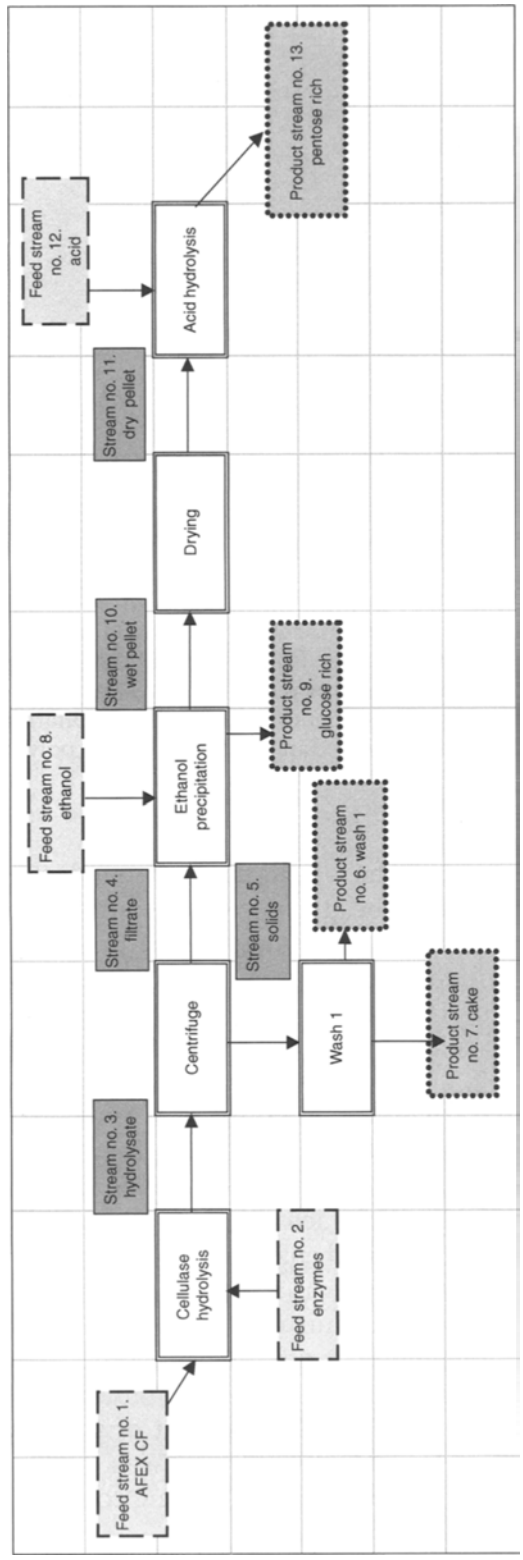


**Fig. 1.** Process flow diagram for separation of arabino/xylan and glucose from AFEX-treated corn fiber.

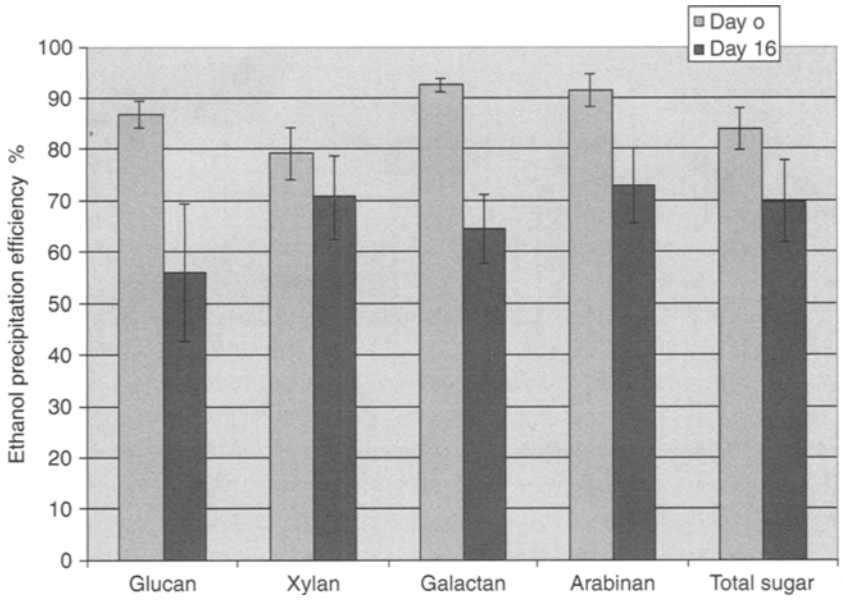


**Fig. 2.** Efficiency of ethanol precipitation of solubilized polysaccharides in enzyme hydrolysate of AFEX-treated corn fiber. Ethanol precipitation was performed immediately after finishing the enzyme hydrolysis (day 0) or after the hydrolysate had been stored at 4°C for 16 d (day 16). (Efficiency of ethanol precipitation was calculated by dividing the amount of sugar recovered in pellet by the total polysaccharides available in the hydrolysate.)

We also investigated the effect that extended storage time of the enzyme hydrolysate had on the efficiency of CFG precipitation. The ethanol precipitation of the arabinoxylan pellet was performed immediately after completing the enzyme hydrolysis (day 0) and after the hydrolysate had been stored at 4°C for 16 d (day 16). After drying, the weight and sugar composition of each pellet was determined. Results of these experiments are presented in Fig. 2. There was a reduction in yield of all the sugars after 16 d and the overall recovery dropped from an average of 83% to an average of 70% (decrease from 4.0 g sugar/10.0 g biomass on day 0, to 3.2 g sugar/10.0 g on day 16). As no attempt was made to denature the enzyme at the end of the hydrolysis, the loss of sugar yield in the precipitation is presumably because of continued enzyme hydrolysis when the hydrolysate is being stored, even though it was maintained at 4°C. This conclusion is also consistent with the mechanism by which the precipitation works; polysaccharides are precipitated, whereas monosaccharides and presumably low molecular weight oligomers are maintained in solution. Extended hydrolysis time should give a higher percent of monosaccharides in the hydrolysate. Based on these observations, it was decided to perform the ethanol precipitation stage within 24 h following completion of the enzyme hydrolysis.

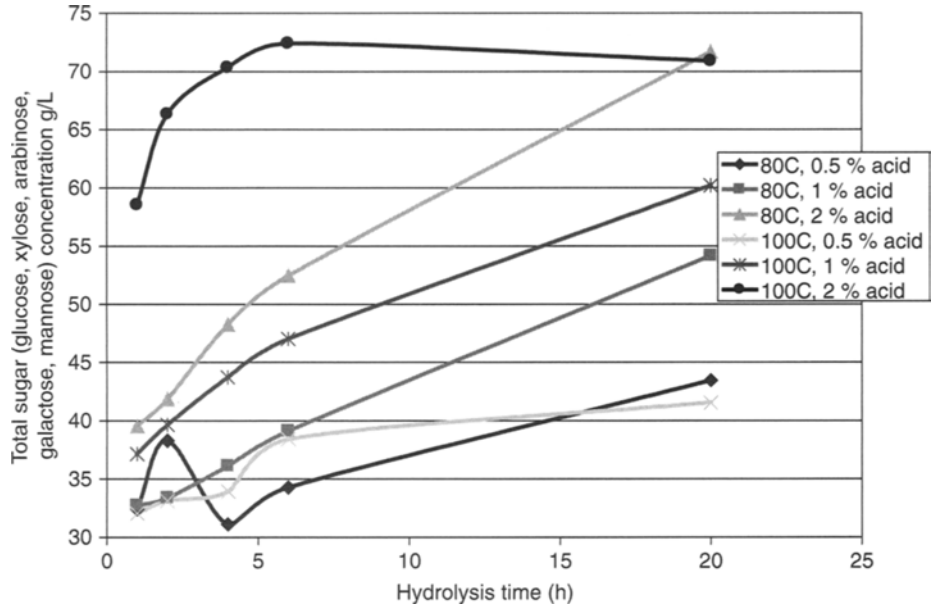


**Fig. 3.** Total sugar (glucose, xylose, arabinose, galactose, and mannose) concentration produced from CFG with different acid hydrolysis conditions.

## *Optimization of Acid Hydrolysis*

To identify the acid hydrolysis conditions that gave the maximum conversion of the enzyme solubilized polysaccharides from corn fiber to monomeric sugars; sulfuric acid concentrations of 0.5, 1, and 2% (v/v) were evaluated at 80 and 100°C. These experiments were performed by adding concentrated sulfuric acid to the unfiltered enzyme hydrolysate. The results from these experiments are summarized in Fig. 3. Data showed that among the tested conditions the maximum sugar conversion was obtained with 2% (v/v) acid, at 100°C for 6 h or 80°C for 20 h.

We also investigated the use of 0.5 and 1% sulfuric acid over a longer period of time to explore the possibility of using lower acid concentration. A temperature of 80°C using 1% acid gave 71% yield after 285 h, and 0.5% acid gave 55% yield after 285 h. Even though the hydrolysis rate was higher at 100°C compared with 80°C, because of equipment limitations (difficult to maintain the 14-L fermentors at 100°C for 6 h) hydrolysis with 2% sulfuric acid at 80°C for 20 h was chosen for acid hydrolysis of CFG.

## *Enzyme Hydrolysis Followed by Ethanol Precipitation of Solubilized Hemicellulose*

Three 10 L hydrolyses of AFEX-treated corn fiber showed that in 24 h 83% of available glucan was converted to glucose. The hemicellulose fraction was partially broken down, with 81% of the xylan and 68% of the arabinan

Table 2
Carbohydrate Composition of Generated CFG (based on dry weight)

| Glucose (%) | Xylose (%) | Galactose (%) | Arabinose (%) | Mannose (%) |
|---|---|---|---|---|
| 3.40 | 43.83 | 7.53 | 20.60 | 0 |

being contained in the hydrolysate after filtration to remove lignin and other insoluble material. An additional 5% of the xylan and 4% of the arabinan were recovered in a water-wash of the filter cake but this material was not added back to the hydrolysate. The xylan and arabinan contained in the hydrolysate was precipitated and collected as CFG by addition of the hydrolysate to three volumes of ethanol. The efficiency of the ethanol precipitation for xylan and for arabinan was 85 and 92.3%, respectively (calculated by dividing the amount of sugar recovered in pellet by the total polysaccharides available in the hydrolysate). This indicates that some of the polysaccharides, probably low-molecular weight oligomers, are not precipitated by the addition of the ethanol. The collected CFG was washed with de-ionized water and dried before acid hydrolysis. The carbohydrate composition of the obtained CFG is presented in Table 2.

Acid hydrolysis (2% $H_2SO_4$ at 80°C for 20 h) of CFG gave the C5-enriched sugar stream. The acid hydrolysis proceeded with 83% yield for the xylose and 86% yield for the arabinose from available oligomers in CFG. The final carbohydrate composition of the C5-enriched sugar stream was 5% glucose, 57.1% xylose, 26.9% arabinose, and 11% galactose, or 84% C5 sugars, and 16% C6 sugars.

### *Yield for Overall Process (Enzyme Hydrolysis, Ethanol Precipitation, and Acid Hydrolysis of CFG)*

For the overall process, we were able to recover 83.2% of available glucose in the C6-rich stream; the C5-rich stream contained 57.1% of the available xylose, 54.1% of the available arabinose, and 58% of the available galactose. The sugar compositions of the product streams are summarized in Table 3 and the overall sugar recovery is provided in Table 4. Analyses of the waste streams from the process were consistent with losses observed in each step, giving a good overall mass balance. The mass balance was 111% for glucose, 94% for xylose, 105% for arabinose, and 90% for galactose (mass balance higher than 100 may be because of analytical error).

### *Enzyme Hydrolysis of CFG*

Enzyme hydrolysis was investigated as an alternative to acid hydrolysis of CFG to produce monomeric sugars. Several different xylanases (X1-274, X2-275, X3-276, X4-277, and Rovabio Excel LC) were tested at the pH and temperature recommended by the manufacturer. Hydrolyses were performed for 72 h at enzyme loadings of 1, 10, 20, and 40% (w/w).

Table 3
Sugar Composition of Product Streams[a] Total sugars recovered (expressed as monomeric)

| Product streams | | | | | | | | |
|---|---|---|---|---|---|---|---|---|
| Stream | No. 6 (wash) | | No. 7 (cake) | | No. 9 (glucose rich) | | No. 13 (pentose rich) | |
| Components | Weight (g) | Percentage | Weight (g) | Percentage | Weight (g) | Percentage | Weight (g) | Percentage |
| Glucan | 0.12 | 0.38 | 2.16 | 7.13 | 3.15 | 10.38 | – | – |
| Xylan | 1.36 | 4.92 | 3.52 | 12.73 | 3.72 | 13.46 | – | – |
| Arabinan | 0.57 | 4.22 | 2.46 | 18.10 | 1.31 | 9.62 | – | – |
| Galactan | 0.21 | 3.98 | 0.72 | 13.58 | 0.40 | 7.53 | – | – |
| Glucose | 1.97 | 5.85 | – | – | 27.90 | 82.84 | 1.55 | 4.60 |
| Xylose | 0.13 | 0.41 | – | – | 1.71 | 5.44 | 17.92 | 57.03 |
| Arabinose | 0.13 | 0.83 | – | – | 1.96 | 12.66 | 8.35 | 54.09 |
| Galactose | 0.03 | 0.49 | – | – | 0.37 | 6.29 | 3.40 | 57.79 |

Expressed as grams per 100 g of starting material (composition is available in Table 1).
[a]Stream numbers are from Fig. 1.

Table 4
Overall Sugar Recovery for Separation of C5 and C6 from AFEX-Treated Corn Fiber[a]

| | Recovered (g) | Recovered (%) |
|---|---|---|
| Glucose | 37.44 | 111.17 |
| Xylose | 29.53 | 93.99 |
| Arabinose | 16.34 | 105.81 |
| Galactose | 5.28 | 89.67 |
| Total | 88.58 | 101.77 |

[a]Expressed as monomeric sugars.

None of the enzymes showed significant activity toward hemicellulose of CFG, presumable because of the complex and highly substituted nature of the xylan contained in corn fiber. Hydrolysis with 40% loading of Rovabio Excel LC resulted in the highest xylose yield (30.2%). Maximum observed xylose yield for the rest of these enzymes was 2.1–4.5%.

## Conclusions

In this study, we demonstrated that 24 h enzyme hydrolysis of AFEX-treated corn fiber hydrolyzed 83% of the cellulose to glucose and solubilized 81 and 68% of the xylan and the arabinan, respectively. It was also demonstrated that 87% of the solubilized hemicellulose (85% of xylan and 92% of arabinan) could be precipitated and collected as CFG by addition of ethanol to the aqueous solution. The collected CFG was hydrolyzed to monomeric sugars with dilute acid, giving a sugar solution made up of 84% C5 sugars and 16% C6 sugars. Attempts were made to identify a xylanase that could hydrolyze the CFG to avoid the acid hydrolysis; however, the best enzyme tested, yielded only 30% xylose at high enzyme loading (40% [w/w]).

The use of AFEX followed by cellulose hydrolysis, ethanol precipitation of CFG, and acid hydrolysis of the precipitated CFG, provides a complete procedure for partially separating the C5 and C6 sugars contained in corn fiber into C5-enriched and C6-enriched sugar streams. Because of the incomplete separation and material losses in the process the recovery of xylose and arabinose in the C5-enriched sugar stream was 57% and 54%, respectively, and recovery of glucose in the C6-enriched stream was 83%. Future work will focus on developing improved methods to fully utilize all available sugars and enhance the purity and yields of glucose and pentose fractions.

## Acknowledgments

The authors would like to thank Nhuan P. Nghiem and Ponnampalam Elankovan for their leadership in the early stage of the project and also we

would like to thank Sirini Rajagopalan and Frank Jere for their technical assistant and advice. This study was funded in part by US Department of Energy Cooperation Agreement No. DE-FC36-02GO12001. Such support does not constitute an endorsement by DOE of the views expressed in the presented work.

## References

1. Ladisch, M. R. and Dyck, K. (1979), *Science* **205(4409),** 898–900.
2. Voloch, M., Janes, N. B., Ladish, M. R., Tsao, G. T., Narayan, R., and Rodwell, V. W. (1985), *Comperihensive Pergamon Press,* Oxford, pp. 934–947.
3. Landucci, R., Goodman, B., Wyman, C. (1996), *Appl. Biochem. Biotechnol.* **57–58,** 741–761.
4. Ladisch, M. R. (2002), *Van Nostrand's Scientific Encyclopedia,* 9th ed. **1,** pp. 434–459.
5. Mosier, N., Wyman, C., Dale, B., et al. (2005), *Bioresour. Technol.* **96,** pp. 673–686.
6. Teymouri, F., Laureano-Perez, L., Alizadeh, H., and Dale, B. (2004), *Appl. Biochem. Biotechnol.* **113–116,** pp. 951–963.
7. Laureano-Perez, L., Teymouri, F., Alizadeh, H., and Dale, B. (2005), *Appl. Biochem. Biotechnol.* **121–124,** pp. 1081–1099.
8. MBI unpublished data.
9. Dale, B. E. and Moreira, M. J. (1982), *Biotechnol. Bioeng. Symp.* No. **12,** 31–43.
10. Teymouri, F., Laureano-Perez, L., Alizadeh, H., and Dale, B. (2005), *Bioresour. Technol.* **96,** 2014–2018.
11. Moniruzzaman, M., Dale, B. E., Hespell, R. B., and Bothast, R. J. (1997), *Appl. Biochem. Biotechnol.* **67,** 113–126.
12. Taherzadeh, M. J., Eklund, R., Gustafsson, L., Niklasson, C., and Liden, G. (1997), *Ind. Eng. Chem. Res.* **36,** 4659–4665.
13. Palmqvist, E. and Hahn-Hagerdal, B. (2000), *Bioresour. Technol.* **74,** 25–33.
14. Alizadeh, H., Teymouri, F., Gilbert, T., and Dale, B. (2005), *Appl. Biochem. Biotechnol.* **121–124,** 1133–1142.
15. Moniruzzaman, M., Dien, B. S., Ferrer, B., et al. (1996), *Biotechnol. Lett.* **18(8),** 985–990.
16. Rajagopalan, S., Elankovan, P., MaCalla, D., and Stowers, M. (2005), *Appl. Biochem. Biotechnol.* **120,** 37–50.

0273-2289/1559-0291 (Online)/07/136–140/327–338/$30.00

# The Potential in Bioethanol Production From Waste Fiber Sludges in Pulp Mill-Based Biorefineries

ANDERS SJÖDE,[1] BJÖRN ALRIKSSON,[1] LEIF J. JÖNSSON,*[,1] AND NILS-OLOF NILVEBRANT[2]

*[1]Biochemistry, Division for Chemistry, Karlstad University, SE-651 88 Karlstad, Sweden, E-mail: Leif.Jonsson@kau.se; and [2]STFI-Packforsk, PO Box 5604, SE-114 86 Stockholm, Sweden*

## Abstract

Industrial production of bioethanol from fibers that are unusable for pulp production in pulp mills offers an approach to product diversification and more efficient exploitation of the raw material. In an attempt to utilize fibers flowing to the biological waste treatment, selected fiber sludges from three different pulp mills were collected, chemically analyzed, enzymatically hydrolyzed, and fermented for bioethanol production. Another aim was to produce solid residues with higher heat values than those of the original fiber sludges to gain a better fuel for combustion. The glucan content ranged between 32 and 66% of the dry matter. The lignin content varied considerably (1–25%), as did the content of wood extractives (0.2–5.8%). Hydrolysates obtained using enzymatic hydrolysis were found to be readily fermentable using *Saccharomyces cerevisiae*. Hydrolysis resulted in improved heat values compared with corresponding untreated fiber sludges. Oligomeric xylan fragments in the solid residue obtained after enzymatic hydrolysis were identified using matrix-assisted laser desorption ionization-time of flight and their potential as a new product of a pulp mill-based biorefinery is discussed.

**Index Entries:** Bioethanol; biorefinery; fiber sludge; lignocellulose; *Saccharomyces cerevisiae;* xylan.

## Introduction

When wood is converted to pulp in kraft mills, the fiber products need to be pure. If the pulp is contaminated with impurities, some of the production instead becomes a fiber waste. Previously, some of the fiber sludge material formed was landfilled. In Sweden, it has been prohibited to landfill organic waste since 2005 and therefore the sediment from the wastewater treatment (Fig. 1) is nowadays burnt. However, waste fiber sludge efficiently binds considerable amounts of water and the heat values (HV) are generally low or even negative.

*Author to whom all correspondence and reprint requests should be addressed.

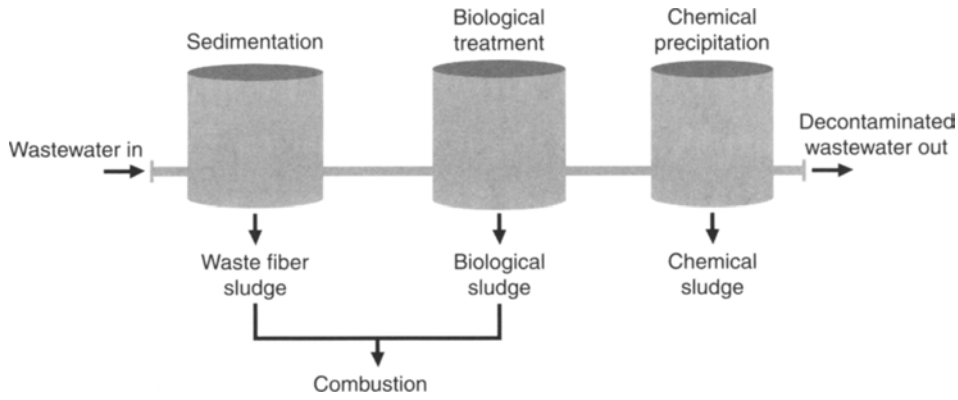


**Fig. 1.** Schematic flow sheet of a pulp and paper mill wastewater treatment system. Fibers from different positions in the mills enter a sedimentation basin with a stream of wastewater. The fiber sludge is collected for combustion. One mill had an addition of bark (sample 1) and one mill added biological sludge (sample 3).

A better way to utilize waste fiber sludges would be to incorporate them in a biorefinery *(1–4)*. Providing that the carbohydrate content of the material is high, it could be converted into bioethanol as a part of a pulp mill-based biorefinery. When bioethanol is made from lignocellulose using enzymatic hydrolysis, a pretreatment step is needed to make the material more accessible to the cellulases. Owing to the processes in the mill, the fiber sludges could be amenable to enzymatic hydrolysis. The chemical composition of the fiber sludge material determines its susceptibility to enzymatic hydrolysis and affects the HV of the solid material left after hydrolysis. To avoid competition for the fiber sludge between ethanol production and heat production, it would be desirable that sugars could be liberated from the fiber sludge for ethanol production without any reduction in HV, leaving the remainder for production of heat.

Samples from three selected Swedish kraft pulp mills were collected and tested to compare the properties of different waste fiber sludges and evaluate their potential as resources in pulp mill-based biorefineries. The aim of this study was to elucidate the potential of the waste fiber fractions for the generation of products with an additional value for the mill. Examples of such products are bioethanol, hemicellulose fractions including xylan, and a solid waste, which contains lignin residues and wood extractives, with improved HV.

## Methods

### *Fiber Sludge Samples*

Fiber sludge samples were collected from three Swedish kraft pulp mills (samples 1–3). The waste fiber sludges were mixtures of fibers diverted from the production through the rejects from the screen room after the pulping process, the outlets from the bleaching plant, the pulp-drying

machine, or the floor drainages. The fiber sludges were collected after the primary sedimentation basins. The samples contained varying amounts of bark residues and wood splinters. The origin of the waste fiber sludges varies from mill to mill because of the specific process solutions of the mills. The samples were selected by the mill operators and would normally have been combusted. All fiber sludge samples were washed with water to stop potential microbial growth. The samples were thereafter air-dried and homogenized by milling (Wiley laboratory mill, 40 mesh; Thomas Scientific, Swedesbaro, NJ) before the ensuing hydrolysis *(5)*.

### *Analysis of Fiber Sludges*

The fiber sludge samples were analyzed for carbohydrates, lignin, extractives, and ash. Carbohydrates and lignin were determined through acid hydrolysis according to TAPPI Method T249 cm-85 (Technical Association of the Pulp and Paper Industry [TAPPI] Norcross, GA). The monosaccharides in the acid hydrolysate were determined using an high-performance anion exchange chromatography (HPAEC) system with an electrochemical detector (Dionex, Sunnyvale, CA) equipped with a CarboPac PA-1 column (Dionex), according to a previously described procedure *(6)*. To determine the amount of extractives, the samples were first extracted with acetone in a Soxtec apparatus (Foss Tecator AB, Höganäs, Sweden). Thereafter, the extracts were evaporated to total dryness and quantified gravimetrically (SCAN-CM 49:03 [Scandinavian Pulp, Paper and Board Testing Committee, Stockholm, Sweden]). The ash content was determined according to International Organization for Standardization (ISO) 2144:1997 (Geneva, Switzerland).

### *Hydrolysis of Fiber Sludges*

The fiber sludge samples were hydrolyzed using the enzyme preparations Celluclast 1.5 (1500 NCU [Novo cellulase units]/g, Novozymes, Bagsvaerd, Denmark) and Novozym 188 (250 cellobiase units/g, Novozymes). The substrate concentration in the reaction mixtures was 15% (w/w) and the concentration of each of the enzyme preparations was 2% (w/w). In addition, 1% (w/w) Tween 20 was added as detergent *(7)*. The initial pH of the hydrolysis reaction mixture was 6.0. The hydrolysis was performed in sealed plastic bags in a water bath at 45°C during 48 h. After the hydrolysis, the remaining solid residue was separated from the liquid fraction (the hydrolysate) by centrifugation and filtration (GF/A, Whatman, Maidstone, UK). All hydrolysis experiments were done as duplicates.

### *Analysis of Fractions Obtained After Hydrolysis*

The monosaccharide contents of the hydrolysates were determined using HPAEC as described under "Analysis of Fiber Sludges." The amounts of solid residue were determined gravimetrically.

### Water Seizing Ability

A small sheet with a grammage of 800 g/m$^2$ was made. The dewatering was done during 60 s and thereafter the sample was weighed and dried at 100°C for 24 h. After the drying, the weight was determined again. The dry content after the dewatering was calculated and is hereafter referred to as the water seizing ability.

### Fermentation Experiments

The fermentations were carried out using *Saccharomyces cerevisiae* (Jästbolaget AB, Rotebro, Sweden). Agar plates with yeast extract peptone dextrose (YEPD) medium (2% yeast extract, 1% peptone, 2% D-glucose, and 2% agar) were used to maintain the strain. Cultures for preparing inocula were grown in 2000-mL cotton-plugged Erlenmeyer flasks containing 1200 mL YEPD medium. The flasks were incubated with agitation at 30°C for approx 12 h. Cells were harvested in the exponential phase by centrifugation at 1500*g* and 4°C for 5 min. Thereafter, the cells were washed with a sodium chloride solution (9.0 g/L) and centrifuged as before.

To determine the dry weight of the inoculum, a 0.45 µm HA filter (Millipore Billerica, MA) was dried in a microwave oven (Husqvarna Micronett, Sweden) set at a power scale of 3 for 15 min, and thereafter placed in a desiccator. After 2 h, the filter was taken from the desiccator and weighed on an analytical scale. The yeast suspension (1.35 mL) was then filtered through the dried filter under the influence of vacuum. The filter was washed with 5 mL of water, dried as previously described, and weighed.

Before fermentation all hydrolysates were adjusted to pH 5.5 using a 5 *M* solution of NaOH. The hydrolysate sample (42.75 mL) (or, alternatively, 42.75 mL of a synthetic sugar solution in water for reference fermentations) was mixed with 0.9 mL of a nutrient solution (consisting of 50.0 g/L yeast extract, 25.0 g/L $(NH_4)_2HPO_4$, 1.25 g/L $MgSO_4 \cdot 7\ H_2O$, and 79.4 g/L $NaH_2PO_4 \cdot H_2O$) and 1.35 mL of the inoculum. The biomass concentration of the inoculum was adjusted to give an initial biomass concentration of 2.0 g/L (dry weight) in the fermentation vessel. The fermentation vessels (55-mL glass flasks) were equipped with magnetic stirrer bars and sealed with rubber stoppers with cannulas for outlet of $CO_2$. The vessels were then placed at 30°C in an incubator with magnetic stirring.

### Analysis of Fermentations

The glucose levels during the fermentation were monitored using a glucometer (Glucometer Elite XL, Bayer, Leverkusen, Germany). Samples (0.2 mL) taken from the vessels were diluted with water (1.8 mL) and centrifuged for 5 min in a microcentrifuge (Minispin Plus, Eppendorf, Hamburg, Germany) at a speed of 14,500 rpm (14,000*g*). The supernatant was collected and stored at –20°C until analysis.

The ethanol concentration was determined using an HP 5890 Series II gas chromatograph with a flame ionization detector (Hewlett Packard, Palo Alto, CA) and a BP-20 column with a film thickness of 1.0 μm (SGE, Austin, TX). The temperature was kept at 30°C for 5 min and then raised to 180°C with a heating rate of 15°C/min. All the hydrolysate samples and the reference were fermented as duplicates.

### *MALDI-TOF Analysis*

Matrix-assisted laser desorption ionization-time of flight (MALDI-TOF) mass spectrometry was used to analyze the residue of sample 2. An HP G2025 A MALDI-TOF system (Hewlett Packard) was operated in positive mode with 0.1–1.3 mJ energy from the laser beam *(8)*. The matrix used for the sample was 2,5-dihydroxybenzoic acid, which was obtained from Fluka (Buchs, Switzerland).

### *HV Analysis*

The HVs of the fiber sludge samples were determined using a bomb calorimeter (Type C110, Janke & Kunkel K.G, Staufen, Germany). A portion (0.400 g) of each sample was combusted in the calorimeter and the change in temperature was noted every 30 s until the maximum temperature was reached. The bomb calorimeter was calibrated using benzoic acid as the standard. The dry weights of the samples were determined using a moisture analyzer (Sartorius MA 50, Sartorius, Goettingen, Germany) set at a temperature of 105°C. The HV was calculated according to the formula $HV = [(\Delta T \cdot C) - E_1 - E_2 - E_3 - E_4]/m_D$, in which $\Delta T$ is the change in temperature in degrees Celsius, C is the heat capacity of the calorimeter (given in J/K), $E_1$ is the correction HV for the cotton thread used as ignition fuse in the calorimeter (given in J), $E_2$ is the correction HV for the chromium-nickel thread used for ignition of the cotton fuse (given in J), $E_3$ is the correction HV for the formation of nitric acid (assumed to be 40 J), $E_4$ is the correction HV for the formation of sulfuric acid (given in J and based on the assumed correction value 9.5 J/mg sulfur), and $m_D$ is the dry weight of the sample (given in gram) *(9)*. The samples were analyzed twice and the HVs are presented in Table 3 as mean values with standard deviations indicated.

## Results

The chemical composition of the fiber sludge samples varied considerably (Table 1). The combined glucan and mannan content varied between 34 and 67%. The xylan content varied between 8.3 and 16.9%. Lignin may have a negative effect on enzymatic hydrolysis, but it is a benefit when the HV is considered. The content of lignin in the samples varied between 1.3 and 25% (Table 1). The fraction of extractives varied between 0.2 and 5.8%. The large variation in the contents of extractives may be explained by differences in the process before the waste sedimentation. Sample 1, which

Table 1
Chemical Analysis of Fiber Sludge Samples (% weight)

| Mill | Arabinan | Galactan | Glucan | Xylan | Mannan | Klason lignin | Acid-soluble lignin | Ash content | Extractives | Total |
|---|---|---|---|---|---|---|---|---|---|---|
| 1 | 0.6 | 1.2 | 32.3 | 12.2 | 2.2 | 22.9 | 1.1 | 3.5 | 5.8 | 81.8 |
| 2 | 0.1 | 0.1 | 65.7 | 16.9 | 1.3 | 1.2 | 0.1 | 1.0 | 0.2 | 86.6 |
| 3 | 0.6 | 0.9 | 42.7 | 9.8 | 3.3 | 22.8 | 1.2 | 2.0 | 1.9 | 85.1 |
| 3 (Washed) | 0.7 | 1.1 | 42.7 | 8.3 | 4.4 | 23.9 | 1.1 | 1.8 | 2.0 | 85.9 |

Table 2
Analysis of Sugars in the Hydrolysates

| Hydrolysate | Sugar concentration (g/L) | | | | | Yield (%) |
|---|---|---|---|---|---|---|
| | Arabinose | Galactose | Glucose | Xylose | Mannose | |
| H1 | 0.0 | 0.2 | 8.2 | 3.1 | 0.8 | 14.0 |
| H2 | 0.0 | 0.3 | 102.6 | 24.3 | 1.0 | 90.4 |
| H3 | 0.2 | 0.3 | 20.6 | 4.9 | 1.6 | 27.7 |

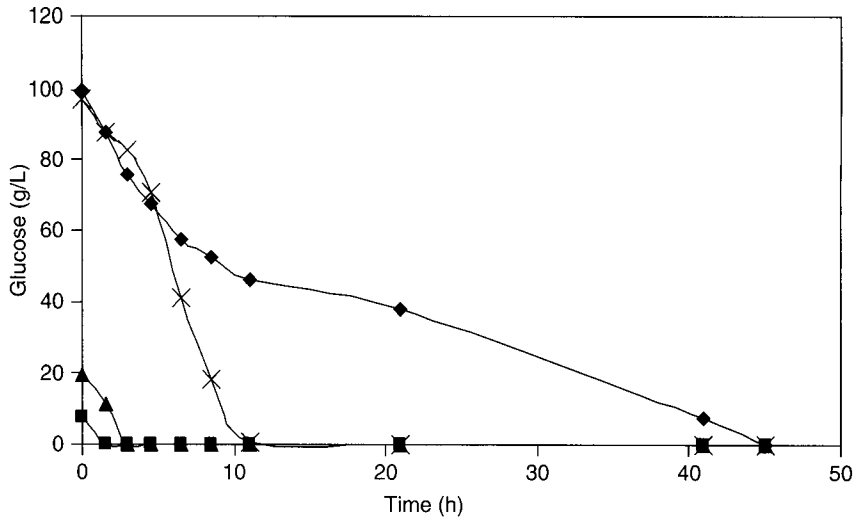


**Fig. 2.** Glucose consumption during fermentation of hydrolysate sample 1 (■), hydrolysate sample 2 (×), hydrolysate sample 3 (▲), and the reference fermentation (◆). The graph shows the mean values of duplicate fermentations. The standard deviation was ≤4.4%.

contained large amounts of extractives, originated from a kraft mill, which had its waste fiber sludge system integrated with a mill producing mechanical pulp fibers rich in extractives and lignin. The other measured components did not vary much and the amounts were very low (Table 1). Washing of sample 3 only resulted in minor changes (Table 1).

Hydrolysates were generated from the fiber sludge samples using enzymatic hydrolysis. The concentrations of monosaccharides in the hydrolysates are presented in Table 2. Hydrolysate 2 contained a high glucose concentration, more than 100.0 g/L. The yields of monosaccharides in the hydrolysates varied between 14 and 90%. The low conversion of carbohydrates in samples 1 and 3 can be correlated to the high lignin content. Sample 1, which showed the lowest yield, had the highest content of extractives. The yield of hexose sugars was generally low except for sample 2. This can probably be related to the high initial content of cellulose and the accessibility of the cellulose to hydrolysis by degrading enzymes. The fibers from mechanical pulping that were present in sample 1 are almost similar to those of native wood and may have had poorer accessibility for cellulose-degrading enzymes *(10)*. The ratio between glucose and xylose was almost one for samples 1 and 3, but for sample 2 the yield of glucose was higher than that of xylose. All three hydrolysate samples were readily fermented by *S. cerevisiae*. The glucose consumption rates of the hydrolysates were equal to or faster than that of the reference fermentation. All glucose in hydrolysate sample 2 was consumed within 11 h, whereas it took 45 h for the corresponding reference fermentation to consume all glucose (Fig. 2).

The offwhite solid residue obtained after enzymatic hydrolysis of sample 2 was analyzed with MALDI-TOF. The mass spectrum showed

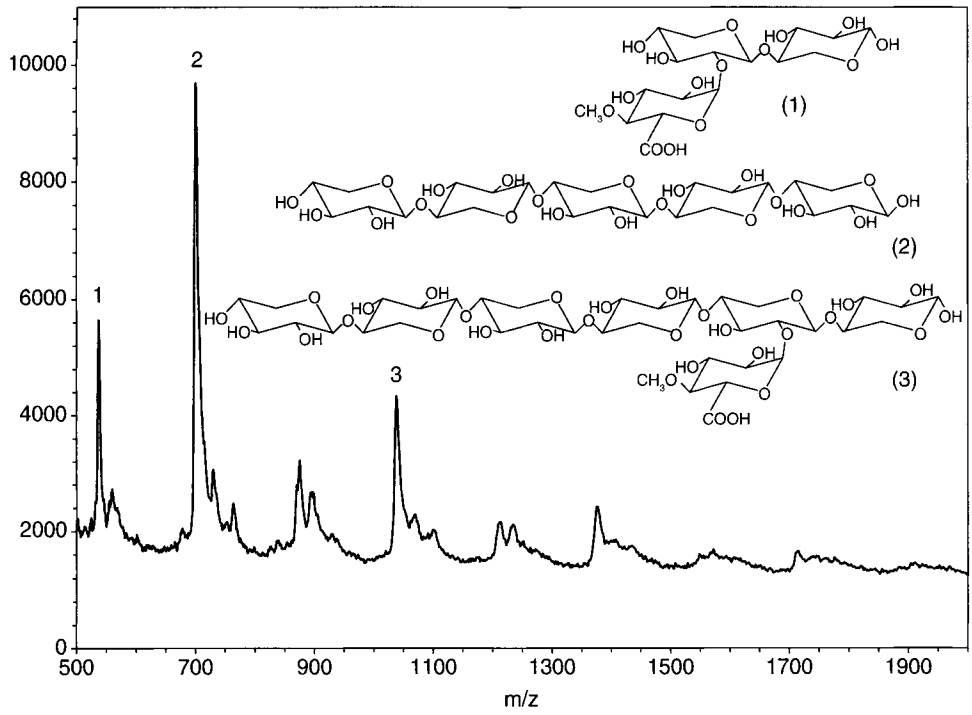


**Fig. 3.** Mass spectrum from the MALDI-TOF analysis. Peak 1 represents 4-*O*-methyl-glucuronic acid with two xylose units, peak 2 corresponds to a xylan fragment with five repeating pentose units, and peak 3 represents six pentose units with a 4-*O*-methyl-glucuronic acid residue (the tentative molecular structures are indicated).

peaks with a mass-to-charge ratio between 500 and 1800 (Fig. 3). The compounds representing the three major peaks were identified. Peaks 1 and 3 represent negatively charged 4-*O*-methyl-glucuronic acid residues, whereas peak 2 represents an uncharged xylan fragment consisting of five linked monomers. Peak 1 had a TOF of 11.6150 μs corresponding to a MW of 537.7, which was interpreted as 4-*O*-methylglucuronic acid-$(xylose)_2$ and a $Na^+$ ion. Peak 3 had a MW of 1038.9, which was interpreted as six pentose units with a 4-*O*-methyl-glucuronic acid residue and a $K^+$ ion. Peak 2, which matched MW 700.4, was interpreted as a xylan fragment with five repeating units and a $Na^+$ ion. The tentative molecular structures are indicated in Fig. 3 and the interpretations have been published previously *(8,11)*. Generally, native as well as pulped xylan fragments are much larger, but because the enzyme cocktail probably contains xylanases the reduced polymer size is not unexpected.

The HVs increased after enzymatic hydrolysis (Table 3). Although the hydrolysis of samples 2 and 3 resulted in improved HVs, they did not reach the level of sample 1. Another important parameter, which is linked to the HV, is the water seizing ability. The water seizing ability is presented in Table 4. The hydrolyzed samples had much higher dry content, which should result in better combustion efficiency.

Table 3
HVs of Fiber Sludge Samples Before and After Enzymatic Hydrolysis

| Sample | HV before hydrolysis (kJ/g dry weight) | HV after hydrolysis (kJ/g dry weight) |
|---|---|---|
| 1 | 20.8 ± 0.11 | 22.2 ± 0.19 |
| 2 | 17.8 ± 0.30 | 18.0 ± 0.36 |
| 3 | 18.3 ± 0.09 | 19.6 ± 0.12 |

Table 4
Dry Content of Fiber Sludge Samples Before and After Enzymatic Hydrolysis

| Sample | Dry content before hydrolysis (% [w/w]) | Dry content after hydrolysis (% [w/w]) |
|---|---|---|
| 1 | 26.2 | 38.7 |
| 2 | 31.9 | 43.4 |
| 3 | 30.0 | 41.8 |

## Discussion

Lignocellulosic fibers, mainly made up of cellulose and hemicelluloses, are produced from wood at large kraft pulp mills. The annual pulp production in a modern kraft mill is often around 700,000 t or even higher. More than 1% of the production may end up as waste fibers of low value for the mill. Deposition of the waste is nowadays often connected with deposition fees or may even be prohibited. The alternative is to burn the waste fibers. However, combustion and recovery of heat is often not effective because of the inherent capacity of the carbohydrates to retain water. Current operational problems with the handling of waste fiber sludges in kraft mills can be turned into benefits in the form of new products in pulp mill-based biorefineries. The dry content and the value of the material as a solid fuel may be increased by removal of water-retaining polysaccharides by hydrolysis. Bioethanol could be produced *(12–14)* and a xylan fraction could be isolated before the residual material is used for combustion.

Waste fiber samples intended for combustion were selected in three Swedish kraft mills and used to investigate production of bioethanol, xylan, and residual material with improved HV. The chemical composition and the HVs of the samples differed considerably. Sample 2 contained only contaminated kraft pulp fibers and was easily degraded to fermentable sugars in high yield. High concentrations of fermentable sugars in the hydrolysates will lower the cost for separation of ethanol by distillation after the fermentation. Sample 1 also contained fibers from production of mechanical pulps. Sample 3 was a mixture that contained considerable amounts of bark and wood pieces. The lower convertibility

of samples 1 and 3 compared with that of sample 2 was probably because of their high lignin content. The kraft process is the most efficient way to remove lignin and wood extractives and to defibrate lignocellulosic materials. Pulp produced through refining, such as thermomechanical pulp and chemithermomechanical pulp, still contains lignin and wood extractives, especially on the fiber surfaces. The presence of such substances on the fibers strongly reduces the activities of polysaccharide-degrading enzymes. However, the negative effect of lipophilic compounds on the fiber surfaces may be reduced by addition of surfactants *(7)*, as in this study. The rapid fermentation rates observed for the hydrolysates suggest that significant amounts of inhibitory compounds were not present. The improved performance of the hydrolysate of sample 2 compared with that of the reference fermentation suggests that this hydrolysate may have contained additional nutrients that affected the yeast in a favorable way.

The HVs of the samples increased after hydrolysis. This can tentatively be explained by the increased content of lignin and extractives, because these substances are not lost during hydrolysis. Sample 2 had the lowest HV and this might be because of its low initial lignin content. The dry content is an important factor when it comes to combustion of fiber sludges. A high dry content will give a higher effective HV. All hydrolyzed samples showed significantly higher dry content compared with untreated material.

The offwhite solid residue after hydrolysis of sample 2 was analyzed using MALDI-TOF. The mass spectrum showed oligomeric xylan fragments, most of which contained 4-*O*-methyl-glucuronic acid groups. The molecular mass was low, less than 1000 Da, compared with the molecular mass of xylan found in kraft pulp fibers, which exceeds 12,000 Da *(15)*. The relatively low molecular mass was expected because the mixture of enzymes used for the hydrolysis would include xylanases. The native glucuronic acid side groups might have hindered a complete enzymatic hydrolysis to monosaccharides. Insoluble charged xylan fragments have a potential as a high-value byproduct. If isolation of a polymeric xylan is the goal, then a mixture of enzymes without xylanase activity should be chosen. As an alternative to isolation of xylan as a byproduct, xylose may be utilized for bioethanol production by pentose-fermenting microorganisms. The results show a potential in the isolation of a solid xylan fraction from a waste fiber stream. Thus, we suggest isolation of charged xylan fragments as a new product.

The xylan residue may be upgraded and used within the kraft mill. The 4-*O*-methyl-glucuronic acid groups in xylan oligomers can be converted to the corresponding unsaturated hexenuronic acid derivatives using alkali. Treatment of a 4-*O*-methyl-glucuronic acid substituted for xylan fragment in 0.5 *M* sodium hydroxide at 150°C for less than 2 h yielded one equivalent of methanol and the corresponding amount of hexenuronic acid *(16,17)*. Such hexenuronic acid substituents in kraft pulp are known as strong metal-ion chelating structures *(18)*. The hexenuronic acid groups are present in unbleached kraft pulp and bind catalytic metal ions like manganese and have

to be removed before a fully bleached pulp can be made *(19)*. The charged xylan fragments have a potential to be used as biodegradable alternatives to complexing agents like ethylenediaminetetraacetic acid and diethylenetriamine pentaacetic acid (DTPA), which are of environmental concern.

## Acknowledgments

Helena Nilsson at STFI-Packforsk AB is acknowledged for help with the MALDI-TOF analysis. We thank the mills that supplied the fiber sludge samples.

## References

1. Wyman, C. E. (2003), *Biotechnol. Prog.* **19,** 254–262.
2. Kamm, B. and Kamm, M. (2004), *Chem. Biochem. Eng. Q.* **18,** 1–6.
3. Ragauskas, A. J., Williams, C. K., Davison, B. H., et al. (2006), *Science* **311,** 484–489.
4. Ragauskas, A. J., Nagy, M., Kim, D. H., Eckert, C. A., Hallett, J. P., and Liotta, C. L. (2006), *Ind. Biotechnol.* **2,** 55–65.
5. Dahlman, O., Jacobs, A., Liljenberg, A., and Olsson, A. I. (2000), *J. Chromatogr.* **891,** 157–174.
6. Sárvári Horváth, I., Sjöde, A., Nilvebrant, N. -O., Zagorodni, A., and Jönsson, L. J. (2004), *Appl. Biochem. Biotechnol.* **114,** 525–538.
7. Eriksson, T., Börjesson, J., and Tjerneld, F. (2002), *Enzyme Microb. Technol.* **31,** 353–364.
8. Jacobs, A. (2001), *PhD Thesis,* Royal Institute of Technology, Stockholm, Sweden.
9. Österholm, L. -H. and Andersson, L. (1987), *Rapport 273: Bestämning av värmevärden för fasta bränslen,* Värmeforsk, Stockholm, Sweden.
10. Helle, S. S., Duff, S. J. B., and Cooper, D. G. (1993), *Biotechnol. Bioeng.* **42,** 611–617.
11. Jacobs, A., Larsson, P. T., and Dahlman, O. (2001), *Biomacromolecules* **2,** 894–905.
12. Jeffries, T. W. and Schartman, R. (1999), *Appl. Biochem. Biotechnol.* **77–79,** 435–444.
13. Fan, Z., South, C., Lyford, K., Munsie, J., van Walsum, P., and Lynd, L. R. (2003), *Bioprocess. Biosyst. Eng.* **26,** 93–101.
14. Kádár, Z., Szengyel, Z., and Réczey, K. (2003), *Ind. Crop. Prod.* **20,** 103–110.
15. Jacobs, A. and Dahlman, O. (2001), *Biomacromolecules* **2,** 894–905.
16. Nilvebrant, N. -O. and Reimann, A. (1996), *Xylan as a source for oxalic acid during ozone bleaching.* 4th European Workshop on Lignocellulosics and Pulp, September 8–11, 1996, Stresa, Italy.
17. Törngren, A. and Ragnar, M. (2002), *Nord. Pulp Pap. Res. J.* **17,** 179–182.
18. Devenyns, J. and Chauveheid, E. (1997), *Uronic acid and metals control.* 9th International symposium on wood and pulping chemistry (ISWPC), Montreal, Quebec, Canada, 9–12 June 1997.
19. Buchert, J., Teleman, A., Harjunpää, V., Tenkanen, M., Viikari, L., and Vuorinen, T. (1995), *Tappi J.* **78,** 125–130.

0273-2289/1559-0291 (Online)/07/136–140/339–352/$30.00

# Dilute Sulfuric Acid Pretreatment of Agricultural and Agro-Industrial Residues for Ethanol Production

CARLOS MARTIN,[1,2] BJÖRN ALRIKSSON,[1] ANDERS SJÖDE,[1] NILS-OLOF NILVEBRANT,[3] AND LEIF J. JÖNSSON,*[,1]

*[1]Biochemistry, Division For Chemistry, Karlstad University, SE-65188 Karlstad, Sweden, E-mail: Leif.Jonsson@kau.se; [2]Bioresource Technology Group, Department of Chemistry and Chemical Engineering, University of Matanzas, Matanzas 44740, Cuba; and [3]STFI-Packforsk, PO Box 5604, SE-11486 Stockholm, Sweden*

## Abstract

The potential of dilute-acid prehydrolysis as a pretreatment method for sugarcane bagasse, rice hulls, peanut shells, and cassava stalks was investigated. The prehydrolysis was performed at 122°C during 20, 40, or 60 min using 2% $H_2SO_4$ at a solid-to-liquid ratio of 1 : 10. Sugar formation increased with increasing reaction time. Xylose, glucose, arabinose, and galactose were detected in all of the prehydrolysates, whereas mannose was found only in the prehydrolysates of peanut shells and cassava stalks. The hemicelluloses of bagasse were hydrolyzed to a high-extent yielding concentrations of xylose and arabinose of 19.1 and 2.2 g/L, respectively, and a xylan conversion of more than 80%. High-glucose concentrations (26–33.5 g/L) were found in the prehydrolysates of rice hulls, probably because of hydrolysis of starch of grain remains in the hulls. Peanut shells and cassava stalks rendered low amounts of sugars on prehydrolysis, indicating that the conditions were not severe enough to hydrolyze the hemicelluloses in these materials quantitatively. All prehydrolysates were readily fermentable by *Saccharomyces cerevisiae*. The dilute-acid prehydrolysis resulted in a 2.7- to 3.7-fold increase of the enzymatic convertibility of bagasse, but was not efficient for improving the enzymatic hydrolysis of peanut shells, cassava stalks, or rice hulls.

**Index Entries:** Bagasse; ethanol; acid hydrolysis; pretreatment; enzymatic hydrolysis; agricultural residues.

## Introduction

Concerns about exhaustion of the world's reserves of fossil fuels and about the greenhouse effect have resulted in an increasing worldwide interest in using fuels from renewable resources, for instance ethanol. However, a reduction of the ethanol production cost is desirable to improve the

*Author to whom all correspondence and reprint requests should be addressed.

competitiveness. As the sugar- and starch-containing feedstocks traditionally used for ethanol production represent the largest share of the total production cost (*1*), the use of cheaper and more abundant raw materials is desirable for increasing the production.

Lignocellulosic materials are the world's most widely available low-cost renewable resources to be considered for ethanol production. A huge diversity of lignocellulosic wastes is available around the world. Sugarcane bagasse, rice hulls, peanut shells, and cassava stalks are agricultural and agro-industrial residues that could be considered for bioconversion in tropical countries (*2*). These lignocellulosic residues are available on a renewable basis as they are generated by the harvest and processing of sugar cane (*Saccharum officinarum*), rice (*Oryza sativa*), peanut (*Arachis hypogaea*), and cassava (*Manihot dulcis*), which are regularly cultivated crops.

Potential applications for these materials include production of activated charcoal (*3*), energy generation (*4*), and pulp production (*5*). However, except bagasse, which is used for energy generation to run sugar mills, pulp and paper production, and cattle feed manufacturing (*6*), the other materials are of low-economic value and cause environmental problems. Therefore, they can be considered for bioethanol production.

Although lignocellulosic residues provide cheap raw material, cost-intensive hydrolysis processes are required to obtain fermentable sugars. The hydrolysis can be catalyzed by acids, either concentrated or diluted, or by enzymes. Hydrolysis of cellulose with diluted acid is performed at high-temperature; whereas hydrolysis with either concentrated acids or enzymes is performed at low-temperature (*7,8*). Dilute acid can also be used for prehydrolysis of hemicelluloses, which is a process performed at relatively low temperatures (*9,10*). After acid-catalyzed hydrolysis of hemicelluloses, a solid residue consisting of cellulose and lignin is obtained and the cellulose can then be hydrolyzed either by using acid under harsher conditions or by using cellulases. Dilute-acid prehydrolysis can be used as a pretreatment method for increasing the reactivity of cellulose toward cellulases (*11*).

A drawback of acid hydrolysis is the formation of byproducts, which can negatively affect the fermentability of the hydrolysates (*12,13*). The fermentation inhibitors include acetic acid, released by deacetylation of hemicelluloses, formic, and levulinic acids, which are sugar degradation products; phenolic compounds that are mainly formed by the partial degradation of lignin, and the furan aldehydes furfural and 5-hydroxymethylfurfural (HMF), which are formed by the degradation of pentoses and hexoses, respectively (*14*). In order to have an efficient fermentation process, it is desirable to reduce the formation of inhibitors during hydrolysis as much as possible.

Considering sugarcane bagasse, rice hulls, peanut shells, and cassava stalks, only dilute-acid prehydrolysis of sugarcane bagasse has been extensively studied previously (*9,10,15,16*). However, much of the previous work concerning dilute-acid hydrolysis of bagasse has been focused on

obtaining high-yields of xylose rather than on the enzymatic convertibility of the pretreated bagasse. In this investigation, the dilute-acid prehydrolysis of these four different agricultural and agro-industrial materials was investigated with respect to the formation of sugars, the fermentability of the prehydrolysates, and the enzymatic convertibility of the pretreated solid materials.

## Materials and Methods

### *Raw Material*

Sugarcane bagasse from the 2004 harvest was generously donated by "Horacio Rodríguez" sugar mill (Matanzas, Cuba). Cassava stalks, peanut shells, and rice hulls were acquired from local producers (Matanzas Provincial Delegation of the Cuban Ministry of Agriculture, Matanzas, Cuba). The rice hulls were obtained from a low-efficiency artisan rice mill. The materials were air-dried to a dry matter (DM) content of 90–92%, milled to pass a 2-mm screen and stored in plastic bags in a dark chamber at room temperature.

### *Dilute-Acid Prehydrolysis*

Thirty-five grams of dried raw material were mixed with a diluted $H_2SO_4$ (Merck, Darmstadt, Germany) solution giving a final concentration of 2 g of acid per 100 g of slurry. The liquid-to-solid ratio was 10 g/g. Treatments were performed at 122°C during 20, 40, or 60 min. Stainless steel cylinders with a total volume of 500 mL were used as reaction vessels. The cylinders were mounted in a rotor and immersed in a polyethylene glycol heating bath, which allowed a relatively rapid heating of the slurries to the work temperatures. A control panel (Jaako Pöyry AB, Karlstad, Sweden) was used for a careful control of the temperature of the bath. The pretreatment was performed in duplicates. When the reaction time had elapsed, the reactors were cooled to room temperature in water-baths and the pretreated slurries were separated by vacuum filtration (Edwards RV8 pump, BOC Ltd., Crawley Sussex, England) into a liquid fraction, hereafter referred to as prehydrolysate, and a solid residue, hereafter referred to as filter cake. The filter cake was washed with two volumes of deionized water. The prehydrolysates were stored in a cold chamber at 4°C until further use. The filter cakes were dried under mild conditions, weighed, and stored in plastic bags in a cold chamber. Samples of the prehydrolysates and the filter cakes were taken for analysis.

### *Analysis of the Solid Fraction*

The DM content was determined using a moisture analyzer (MA40, Sartorius AG, Göttingen, Germany). Extractives were determined gravimetrically after a Soxhlet extraction with 96% (v/v) ethanol during 24 h. For determination of the chemical composition of raw and pretreated

materials, duplicate samples were hydrolyzed first with 72% $H_2SO_4$ during 1 h at 30°C and then for another hour with 4% $H_2SO_4$ at 121°C. The mixture was separated by vacuum filtration through previously weighed filter crucibles and the lignin content was determined gravimetrically (Mettler AE260 Delta Range, Mettler Toledo, Switzerland). The sugar content in the obtained filtrate was analyzed by anion-exchange chromatography using a DX 500 system (Dionex, Sunnyvale, CA) equipped with a CarboPac PA-1 column. The column was eluted with Milli-Q water (Millipore, Billerica, MA) at a flow rate of 1 mL/min. Before the analysis of each sample, the column was activated by a mixture of 200 m*M* NaOH and 70 m*M* NaOAc. A postcolumn addition of 300 m*M* NaOH was applied before the pulse amperometric detection (Dionex ED 40).

### *Analysis of the Liquid Fraction*

Sugars were determined as described under "Analysis of the Solid Fraction." Carboxylic acids were quantified using a Dionex ICS-2000 chromatography system equipped with a conductivity detector. Separation was performed on an IonPac AS 15 (250 × 4 mm) column with an IonPac AG15 (50 × 4 mm) precolumn (Dionex, Sunnyvale, CA), using isocratic elution with 35 m*M* NaOH supplied at a rate of 1.2 mL/min.

The furan aldehydes HMF and furfural were determined by high-performance liquid chromatography using a Shimadzu VP series system (Shimadzu, Kyoto, Japan) with ultraviolet (UV) detection at 282 nm. Separation was performed using an XTerra MS $C_{18}$ column (5 µm, 2.1 × 150 mm) (Waters, Milford, MA) eluted at a flow rate of 0.4 mL/min with a gradient of Milli-Q water and acetonitrile containing 0.016% (v/v) trifluoroacetic acid. The gradient scheme consisted of four steps with a combined time of 26 min:

1. Ten percent acetonitrile was applied for 8 min.
2. The concentration of acetonitrile was increased linearly to 100% during 8 min.
3. Hundred percent acetonitrile was applied for 6 min.
4. The concentration of acetonitrile was decreased linearly to 10% during 4 min.

The total content of phenolic compounds was determined colorimetrically (Unicam UV-visible spectrophotometer, Cambridge, UK) using the Folin-Ciocalteu method *(17)*. Vanillin was used as the calibration standard.

### *Fermentability of the Prehydrolysates*

The pH of the prehydrolysates was adjusted from around 1 to 5.5 with 8 *M* NaOH using a pH meter (WPA Linton, Cambridge, UK). The prehydrolysates were supplemented with 0.5 g/L of $(NH_4)_2HPO_4$, 0.025 g/L of $MgSO_4 \cdot 7H_2O$, 1.38 g/L of $NaH_2PO_4 \cdot H_2O$, and 1 g/L of yeast extract. All prehydrolysates, except the ones from rice hulls, were supplemented with

20 g/L of glucose. The chemicals were supplied by Sigma-Aldrich Chemie GmbH (Steinheim, Germany). A reference solution containing 20 g/L of glucose and supplemented with the same nutrients was also prepared.

The fermentations were carried out in 50-mL flasks, sealed with rubber stoppers and equipped with cannulas for $CO_2$ removal. The flasks were inoculated with baker's yeast (Jästbolaget AB, Rotebro, Sweden) to an initial biomass concentration of 1 g/L (dry weight), and incubated at 30°C in a water-bath with magnetic stirring (IKA-Werke, Staufen, Germany) for 24 h. Samples were withdrawn after 2, 3, 4, 6, 8, 10, and 12 h. Fermentations were performed in duplicates and the mean values were given as results.

Glucose was monitored during the fermentations using a glucometer (Glucometer Elite XL, Bayer AG, Leverkusen, Germany). The final glucose concentration was determined by ion chromatography as described under "Analysis of the Solid Fraction." Ethanol was analyzed with an ethanol kit (Ethanol UV-test, R-Biopharm AG, Darmstadt, Germany). The ethanol yield (g/g), the volumetric productivity of ethanol (g/[L·h]), and the glucose consumption rate (g/[L·h]) were used as criteria of fermentability. For calculation of the yield, the ethanol concentration after 12 h was divided by the initial concentration of glucose. The productivity was based on the ethanol concentration achieved after 3 h of fermentation. The inhibition of the ethanol yield was calculated according to the expression:

$$\text{Yield inhibition (\%)} = [(Y_{ref} - Y_{preh})/Y_{ref}] \times 100$$

where $Y_{ref}$ is the ethanol yield in the reference fermentation and $Y_{preh}$ is the ethanol yield in the fermentation of the prehydrolysate. The inhibition of the volumetric productivity was calculated in an analogous way.

### *Enzymatic Convertibility*

For evaluating the enzymatic convertibility of cellulose, approx 110 mg of the washed pretreated solid fraction was placed in a Falcon tube, and 0.04 *M* acetate buffer (pH 4.8) was added giving a total volume of 5 mL and a DM content of 2%. A commercial preparation of *Trichoderma reesei* cellulases (Celluclast 1.5L) and a β-glycosidase preparation (Novozym 188), both produced by Novozymes A/S (Bagsværd, Denmark), were added at a loading of 25 filter paper units/g DM and 0.46 cellobiose units/mL, respectively. The reaction mixture was incubated in a rotating incubator (New Brunswick Scientific, Edison, NJ) at 50°C and 150 rpm for 24 h. By the end of the hydrolysis, the liquid was separated from the solids by centrifugation, the glucose concentration was determined by ion chromatography, and the results were used for calculating the enzymatic convertibility of cellulose. In a parallel experiment, the enzymatic convertibility of the untreated raw materials was also assayed. The experiments were performed in triplicates.

Table 1
Main Components of the Raw Materials in Percentage

| Material | Glucan | Xylan | Arabinan | Ethanol extractives | Klason lignin | Ash |
|---|---|---|---|---|---|---|
| Bagasse | 36.1 | 20.8 | 2.8 | 6.1 | 17.8 | 2.0 |
| Rice hulls | 49.1 | 8.3 | 1.3 | 6.4 | 12.9 | 15.2 |
| Peanut shells | 22.1 | 10.7 | 1.4 | 8.5 | 35.2 | 7.2 |
| Cassava stalks | 31.0 | 12.3 | 0.9 | 7.6 | 24.8 | 8.0 |

## Results and Discussion

### *Composition of the Materials*

The composition of the raw materials used in this investigation is shown in Table 1. Sugarcane bagasse and rice hulls had the highest carbohydrate content. The high contents of glucan, which were attributed to remaining starch and ash in the rice hulls, are noteworthy. In the other materials, the most notable was the high-lignin content of peanut shells, which is in agreement with previous results *(18)*.

### *Effect of the Prehydrolysis on the Formation of Sugars*

The prehydrolysis conditions studied were selected because they have been successfully used for materials such as sugarcane bagasse *(10)* and sorghum straw *(19)*. As a result of the partial hydrolysis of polysaccharides, sugars were formed during the dilute-acid prehydrolysis. Xylose, derived from hemicelluloses, and glucose, mainly derived from cellulose and starch, were the major sugars found in the prehydrolysates of all the materials (Table 2). The standard deviation of the sugar analyses was 5.7%. Arabinose was the third most abundant sugar, whereas the galactose content was less relevant and mannose was detected only in the prehydrolysates of peanut shells and cassava stalks. The different sugar content of the prehydrolysates indicates that the hemicelluloses of the investigated materials have different composition. However, it is obvious that the different sugar yield is also a consequence of the different susceptibility to dilute-acid prehydrolysis displayed by the different materials.

For all the materials, the glucose and xylose content generally increased with increasing length of the prehydrolysis. Thus, no extensive degradation of monosaccharides was observed, although the furan aldehydes are products of acid-catalyzed degradation. Most of the arabinose and galactose were formed after the shortest prehydrolysis time (Table 2). The high-degree of arabinose release under mild pretreatment conditions has previously been observed for sugarcane bagasse (Martín C. unpublished, *[16]*). The ease of arabinose hydrolysis is supposedly owing to its

Table 2
Sugar Composition of the Prehydrolysates Obtained After Dilute Sulfuric Acid Prehydrolysis of Sugarcane Bagasse, Rice Hulls, Peanut Shells, and Cassava Stalks During 20, 40, and 60 min

| Material | Prehydrolysis time (min) | Glucose (g/L) | Xylose (g/L) | Arabinose (g/L) | Galactose (g/L) | Mannose (g/L) |
|---|---|---|---|---|---|---|
| Bagasse | 20 | 2.1 | 17.2 | 2.0 | 0.7 | ND |
| Bagasse | 40 | 3.7 | 18.9 | 2.1 | 0.8 | ND |
| Bagasse | 60 | 4.0 | 19.1 | 2.2 | 0.8 | ND |
| Rice hulls | 20 | 26 | 4.8 | 1.0 | 0.5 | ND |
| Rice hulls | 40 | 29 | 5.6 | 1.2 | 0.5 | ND |
| Rice hulls | 60 | 33.5 | 6.9 | 1.4 | 0.6 | ND |
| Peanut shells | 20 | 1.3 | 1.7 | 1.5 | 0.7 | 0.1 |
| Peanut shells | 40 | 1.4 | 4.1 | 1.5 | 0.9 | 0.1 |
| Peanut shells | 60 | 1.5 | 5.3 | 1.5 | 1.0 | 0.2 |
| Cassava stalks | 20 | 3.5 | 2.1 | 0.8 | 1.2 | 0.2 |
| Cassava stalks | 40 | 5.1 | 4.9 | 0.8 | 1.5 | 0.5 |
| Cassava stalks | 60 | 5.2 | 6.3 | 0.8 | 1.6 | 0.7 |

ND, not detected.

location in the branches of arabinoxylan, where the cleavage of the glycosidic bonds is easier than in the backbone of the macromolecule *(20,21)*.

### *Sugarcane Bagasse*

Sugarcane bagasse was the most susceptible material to the prehydrolysis conditions used in this work. The hemicellulose fraction of bagasse was hydrolyzed to a high-extent as indicated by the high-concentrations of xylose, arabinose (Table 2), and acetic acid (Table 3) in the prehydrolysates. The conversion of the xylan of the raw bagasse was 73–81% (Fig. 1). The concentrations of hemicellulose degradation products such as xylose, arabinose, and acetic acid increased with less than 30% when the reaction time increased from 40 to 60 min. The relatively low-glucose concentration (Table 2) indicates that cellulose was only marginally hydrolyzed. Even under the harshest conditions, the conversion was no more than 10% (Fig. 2). Evidently, only the noncrystalline part of the cellulose was hydrolyzed, as 72% sulfuric acid was needed to obtain complete hydrolysis. These results on dilute sulfuric acid hydrolysis of Cuban bagasse are comparable with previous reports using bagasse from Australia *(15)*, Brazil *(9)*, and Mexico *(10)*.

### *Rice Hulls*

Although the hydrolysis of the hemicellulose fraction of rice hulls was substantial, the high-degree of glucan hydrolysis was more remarkable. The glucose concentration in the prehydrolysates ranged from 26 to 33.5 g/L (Table 2). The glucose yield ranged between 46.9 and 61.4% (Fig. 2). Because

Table 3
Content of Fermentation Inhibitors in the Prehydrolysates

| Material | Prehydrolysis time (min) | Acetic acid (g/L) | Formic acid (g/L) | Furfural (g/L) | HMF (g/L) | Phenolic compounds (g/L) |
|---|---|---|---|---|---|---|
| Bagasse | 20 | 2.5 | 0.16 | 0.10 | 0.03 | 0.28 |
| Bagasse | 40 | 2.8 | 0.18 | 0.29 | 0.06 | 0.22 |
| Bagasse | 60 | 2.7 | 0.20 | 0.36 | 0.07 | 0.24 |
| Rice hulls | 20 | 0.9 | 0.09 | 0.05 | 0.10 | 0.23 |
| Rice hulls | 40 | 1.0 | 0.12 | 0.11 | 0.17 | 0.23 |
| Rice hulls | 60 | 1.1 | 0.15 | 0.17 | 0.21 | 0.23 |
| Peanut shells | 20 | 1.1 | 0.11 | 0.02 | 0.10 | 0.11 |
| Peanut shells | 40 | 1.7 | 0.19 | 0.05 | 0.15 | 0.12 |
| Peanut shells | 60 | 1.9 | 0.24 | 0.10 | 0.17 | 0.12 |
| Cassava stalks | 20 | 1.5 | 0.10 | 0.01 | 0.01 | 0.04 |
| Cassava stalks | 40 | 1.9 | 0.14 | 0.04 | 0.02 | 0.07 |
| Cassava stalks | 60 | 2.0 | 0.16 | 0.10 | 0.03 | 0.11 |

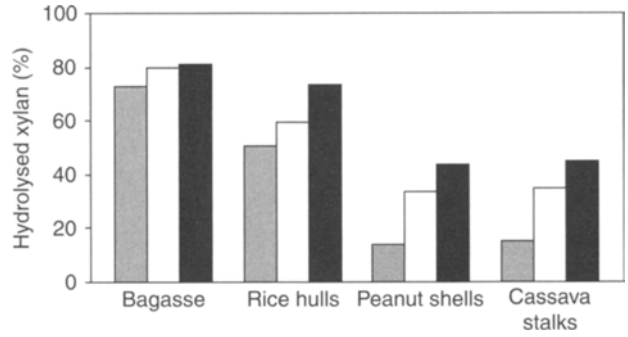


**Fig. 1.** Xylan converted to xylose during dilute acid prehydrolysis of sugarcane bagasse, rice hulls, peanut shells, and cassava stalks. Prehydrolysis time: 20 min (gray bars), 40 min (white bars), and 60 min (black bars).

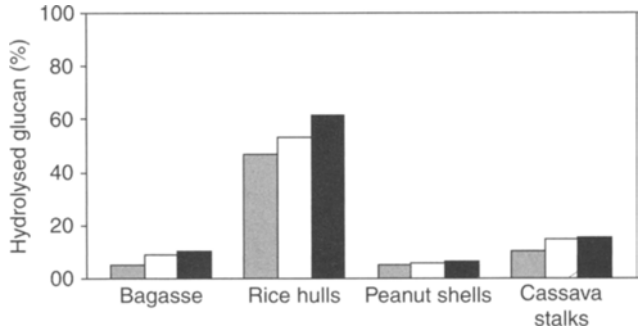


**Fig. 2.** Glucan converted to glucose during dilute acid prehydrolysis of sugarcane bagasse, rice hulls, peanut shells, and cassava stalks. Prehydrolysis time: 20 min (gray bars), 40 min (white bars), and 60 min (black bars).

the conditions used for prehydrolysis should be too weak for cellulose hydrolysis, the glucose should likely be derived from starch in grain remains in the hulls and probably from glucans in the hemicellulose fraction.

### *Peanut Shells and Cassava Stalks*

Peanut shells and cassava stalks rendered low amounts of sugars on prehydrolysis (Table 2) indicating that complete hydrolysis of hemicelluloses would require more severe conditions. Even though xylan conversion increased noticeably with increasing prehydrolysis time, the highest conversion was only 43.6 and 45.1% for peanut shells and cassava stalks, respectively. This is considerably lower than what was achieved for sugarcane bagasse and rice hulls (Fig. 1). The low degree of xylan hydrolysis observed for peanut shells and cassava stalks might be linked to their high-lignin content (Table 1). Although the conditions used for pretreatments were too weak for complete hydrolysis of xylan, they were strong enough for complete hydrolysis of arabinan, even with the shortest prehydrolysis time.

In the prehydrolysates of cassava stalks, including those obtained under mild conditions, glucose was rather abundant. Taking into account that the conditions were far too weak for cellulose hydrolysis, it appears reasonable to assume that glucose is an important component of cassava stalk hemicelluloses. The considerable amounts of galactose and mannose found in the prehydrolysates indicate that those sugars also are important constituents of cassava stalk hemicelluloses. These findings suggest that hemicelluloses of cassava stalks differ considerably from hemicelluloses of other agricultural residues, such as wheat straw *(22)*, rice straw *(23)*, and sugarcane bagasse *(21)*, and are closer to wood hemicelluloses, which contain mannose and galactose heteropolymers *(20)*.

### *Formation of Fermentation Inhibitors*

The data from the pretreatment experiments indicate how the different conditions used influence the formation of inhibitory compounds for each of the different raw materials. As expected, the concentration of most of the inhibitors, except the phenolic compounds, increased with increasing severity of the treatment. However, even under the harshest conditions the inhibitor content of the prehydrolysates was relatively low (Table 3). This is a consequence of the mild prehydrolysis conditions used, which did not lead to any major degradation of the released sugars.

Acetic acid, generated by hydrolysis of hemicelluloses, was the most abundant inhibiting compound found in the prehydrolysates. The highest concentrations were found in bagasse prehydrolysates, wherein hemicelluloses were hydrolyzed to a higher degree. However, in all the prehydrolysates, the concentrations of acetic acid were below the inhibiting limit *(24)*. The low concentration of formic acid and the absence of levulinic

acid in the prehydrolysates indicate that the degradation of furan aldehydes was modest. Higher formation of formic and levulinic acids could be expected if the hydrolysis conditions would be more severe.

The concentrations of furan aldehydes were relatively low, but increased with increasing pretreatment time (Table 3). In the bagasse and cassava stalk prehydrolysates, the concentrations of furfural were higher than the concentrations of HMF, whereas the situation was different in the rice hull and peanut shell prehydrolysates (Table 3). Higher concentrations of furfural could possibly be related to the relatively high-xylan content of bagasse and cassava stalks (Table 1).

The formation of phenolic compounds was most apparent in prehydrolysates of bagasse and rice hulls. Some phenols may originate from low-molecular weight compounds, such as lignans that are soluble in water. Partial degradation of lignin is generally the main source of phenols, but some phenols, such as phenolic acids from gramineous plants, are derived from the hemicellulose fraction *(25,26)*. As the conditions used in this work were too mild to cause extensive lignin degradation, and the highest formation of phenols was observed in the prehydrolysates of residues of sugarcane and rice, two plants belonging to the *Gramineae* family, it might be expected that a considerable part of the phenols found in the prehydrolysates of bagasse and rice hulls result from hydrolysis of lignin-like substituents in hemicelluloses.

### *Fermentability of the Prehydrolysates*

The fermentability of the prehydrolysates was assessed using baker's yeast. The pattern of glucose consumption during fermentation of the prehydrolysates is shown in Fig. 3. Although glucose consumption in the prehydrolysates was slower than in the reference fermentation, all the prehydrolysates fermented relatively rapidly without any detoxification. However, there were some differences between the different raw materials. The highest glucose consumption rates were achieved in prehydrolysates of rice hulls and cassava stalks, where glucose was depleted within 6 h (Fig. 3B,D). The glucose consumption in the 20-min prehydrolysate of cassava stalks was very close to that observed in the reference fermentation. No inhibition of the volumetric ethanol productivity was observed in that prehydrolysate or in the prehydrolysates of rice hulls (Fig. 4). The good fermentability of prehydrolysates of rice hulls, combined with their high-glucose concentration, make them especially attractive for ethanolic fermentation.

In the fermentation of the prehydrolysates of bagasse and peanut shells the consumption of glucose was slower (Fig. 3A,C), and the inhibition of the ethanol productivity was more noticeable (Fig. 4). The slower fermentation rates may be linked to the higher concentrations of inhibitory compounds. However, because the concentrations of all the inhibitors

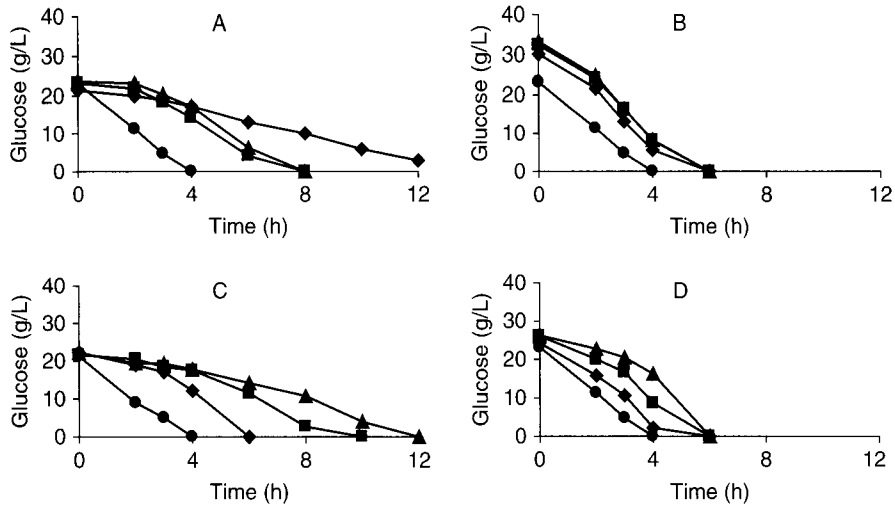


**Fig. 3.** Glucose consumption during fermentation of the prehydrolysates of sugarcane bagasse **(A)**, rice hulls **(B)**, peanut shells **(C)**, and cassava stalks **(D)** obtained by dilute sulfuric acid prehydrolysis at 122°C during 20 (◆), 40 (■), and 60 min (▲). Reference fermentation (●).

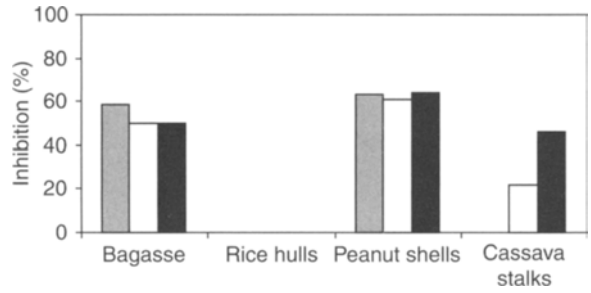


**Fig. 4.** Inhibition of the volumetric productivity of ethanol. Gray bars, 20-min prehydrolysis; white bars, 40-min prehydrolysis; black bars, 60-min prehydrolysis.

were rather low, the inhibitory effect did not last long and all fermentations were completed within 12 h (Fig. 3).

For most materials, the fermentation rate decreased with increasing prehydrolysis time (Fig. 3). This was obviously because of increasing inhibitor content. However, for bagasse, the prehydrolysate obtained with the shortest prehydrolysis time appeared to be most inhibitory (Figs. 3A and 4). One reason could be the higher content of phenolic compounds in that prehydrolysate (Table 3). Another explanation might be related to acetic acid. Assuming that acetic acid exerts a stimulatory effect on the ethanolic fermentations at the concentrations observed in this study, a faster fermentation of the prehydrolysates obtained after 40 and 60 min treatment may be expected.

Table 4
Enzymatic Convertibility (EC) of Sugarcane Bagasse, Rice Hulls, Peanut Shells, and Cassava Stalks Pretreated by Using Dilute Sulfuric Acid

| Material | Prehydrolysis time (min) | Enzymatic convertibility[a] (%) | $EC_{PM}/EC_{UM}$ |
|---|---|---|---|
| Bagasse | 20 | 45.6 | 2.7 |
| Bagasse | 40 | 59.8 | 3.4 |
| Bagasse | 60 | 66.0 | 3.7 |
| Rice hulls | 20 | 14.2 | <1 |
| Rice hulls | 40 | 13.5 | <1 |
| Rice hulls | 60 | 22.2 | <1 |
| Peanut shells | 20 | 15.3 | 1.20 |
| Peanut shells | 40 | 15.4 | 1.20 |
| Peanut shells | 60 | 17.3 | 1.33 |
| Cassava stalks | 20 | 12.6 | <1 |
| Cassava stalks | 40 | 12.9 | <1 |
| Cassava stalks | 60 | 14.8 | <1 |

$EC_{PM}/EC_{UM}$, relative convertibility; PM, pretreated material; UM, unpretreated material.
[a]The enzymatic convertibility is related to the glucan contained in the filter cakes.

### *Enzymatic Convertibility of the Pretreated Materials*

In order to investigate dilute acid prehydrolysis as a pretreatment method for enzymatic hydrolysis of cellulose, the filter cakes obtained after separation of the prehydrolysates were subjected to hydrolysis using cellulolytic enzymes. The best enzymatic convertibilities were achieved for bagasse, whereas the other materials were converted to a lesser extent (Table 4). A *t*-test at 95% confidence level indicated that the differences between the enzymatic convertibility of different materials were statistically significant. The highest degree of conversion was achieved for bagasse pretreated during 60 min, for which 66% of the cellulose of the filter cake was hydrolyzed to glucose. However, taking into account the losses occurring during the pretreatment, the conversion equals only 40% of the cellulose of the raw bagasse. That is relatively low considering the conversion achieved in enzymatic hydrolysis of bagasse pretreated by steam-explosion or wet-oxidation *(27,28)*. Therefore, the optimization of dilute sulfuric acid pretreatment conditions of sugarcane bagasse deserves more attention.

The enzymatic convertibility of the untreated raw materials was also assayed. The relative convertibility indicates how many times higher the enzymatic convertibility of the pretreated materials was compared with that of the unpretreated materials. As can be seen in Table 4, dilute sulfuric acid prehydrolysis improved the enzymatic convertibility of bagasse 2.7–3.7 times. For the rest of the materials, the relative convertibility was low, indicating that the prehydrolysis was not efficient for improving the

enzymatic convertibility. An additional experiment, using a higher enzyme load, did not lead to significant improvements of the enzymatic convertibility of any of the materials investigated (data not shown). More severe conditions have to be considered in future experiments.

The enzymatic convertibility of pretreated rice hulls and cassava stalks was unexpectedly lower than that of the unpretreated materials. This indicates that either the pretreatment used for those materials was inadequate or that easily hydrolysable glucans were present. Rice hulls and cassava stalks contain noncellulose glucans that were not further characterized. Perhaps those glucans can be hydrolyzed by the enzyme preparation used without pretreatment. More severe conditions of dilute sulfuric acid prehydrolysis of rice hulls and cassava stalks appear to be needed for improving the subsequent enzymatic hydrolysis of cellulose.

## Conclusions

Under the conditions tested, prehydrolysis using dilute sulfuric acid was efficient for obtaining sugars from sugarcane bagasse and rice hulls hemicelluloses, and for improving the enzymatic convertibility of bagasse cellulose, but it was not efficient for the other materials. This work demonstrates the potential in using dilute sulfuric acid for pretreatment before enzymatic hydrolysis of bagasse, but further optimization of the conditions is desirable. For rice hulls, peanut shells, and cassava stalks, more severe conditions need to be studied. It is also of interest to investigate rice hulls free of grain remains. An investigation of that issue is underway.

## Acknowledgments

Pia Eriksson and Mikael Andersén are gratefully acknowledged for technical assistance. This work was supported by the Swedish National Energy Administration. CM acknowledges the support of the International Foundation for Science, Stockholm, Sweden, and the Organization for the Prohibition of Chemical Weapons (OPCW), The Hague, The Netherlands, through the grant No. F/3563-1.

## References

1. Claassen, P. A., Sijstma, L., Stams, A. J. M., De Vries, S. S., and Weusthuis, R. A. (1999), *Appl. Microbiol. Biotechnol.* **52,** 741–745.
2. Martín, C., López, Y., Plasencia, Y., and Hernández, E. (2006), *Chem. Biochem. Eng. Q.* **20,** 443–446.
3. Kim, T. Y., Baek, I. H., Jeoung, Y. D., and Park, S. C. (2003), *J. Ind. Eng. Chem.* **9,** 254–260.
4. Ismail, A. F., Yusaf, T. F., Mahdi, F. M. A., and Shamsuddin, A. H. (1997), *Reric Int. Energy J.* **19,** 63–75.
5. Ngamveng, J. N. and Ndikontar, M. (1990), *Cellul. Chem. Technol.* **24,** 523–530.
6. Pandey, A., Soccol, C. R., Nigam, P., and Soccol, V. C. (2000), *Biores. Technol.* **74,** 69–80.
7. Galbe, M. and Zacchi, G. (2002), *Appl. Microbiol. Biotechnol.* **59,** 618–628.
8. Sun, Y. and Cheng, J. (2002), *Biores. Technol.* **83,** 1–11.

9. Pessoa, A., Jr., Mancilha, I. M., and Sato, S. (1997), *Braz. J. Chem. Eng.* **14,** 25–28.
10. Aguilar, R., Ramírez, J. A., Garrote, G., and Vázquez, M. (2002), *J. Food Eng.* **55,** 309–318.
11. Torget, R., Werdene, P., Himmel, M., and Grohmann, K. (1990), *Appl. Biochem. Biotechnol.* **24/25,** 115–126.
12. Parajó, J. C., Domínguez, H., and Domínguez, J. M., (1998), *Biores. Technol.* **66,** 25–40.
13. Palmqvist, E. and Hahn-Hägerdal, B. (2000), *Biores. Technol.* **74,** 25–33.
14. Larsson, S., Palmqvist, E., Hahn-Hägerdal, B., et al. (1999), *Enzyme Microb. Technol.* **24,** 151–159.
15. Lavarack, B. P., Griffin, G. J., and Rodman, D. (2002), *Biomass Bioenergy* **23,** 367–380.
16. Rodríguez-Chong, A., Ramírez, J. A., Garrote, G., and Vázquez, M. (2004), *J. Food Eng.* **61,** 143–152.
17. Singleton, V., Orthofer R., and Lamuela-Raventós, R. (1999), *Methods Enzymol.* **299,** 152–178.
18. Sinner, M., Puls, J., and Dietrichs, H. (1979), *Starch/Stärke* **31,** 267–269.
19. Téllez-Luis, S. J., Ramírez, J. A., and Vázquez, M. (2002), *J. Food Eng.* **52,** 285–291.
20. Sjöström, E. (1993), *Wood Chemistry: Fundamentals and Applications,* 2nd ed. Academic Press, San Diego: pp. 63–70.
21. Sun, J. X., Sun, X. F., Sun, R. C., and Su, Y. Q. (2004), *Carbohydr. Polym.* **56,** 195–204.
22. Sun, R., Mark Lawther, J., and Banks, W. B. (1996), *Carbohydr. Polym.* **29,** 325–331.
23. Sun, R. C. and Sun, X. F. (2002), *Sep. Sci. Technol.* **37,** 2433–2458.
24. Taherzadeh, M. J., Niklasson, C., and Lidén, G. (1997), *Chem. Eng. Sci.* **52,** 2653–2659.
25. Bidlack, J., Malone, M., and Benson, R. (1992), *Proc. Okla. Acad. Sci.* **72,** 51–56.
26. Puls, J. (1997), *Macromol. Symp.* **120,** 183–196.
27. Martín, C., Galbe, M., Nilvebrant, N. -O., and Jönsson, L. J. (2002), *Appl. Biochem. Biotech.* **98/100,** 699–716.
28. Martín, C., González, Y., Fernández, T., and Thomsen, A. B. (2006), *J. Chem. Technol. Biotechnol.* **81,** 1669–1677.

0273-2289/1559-0291 (Online)/07/136-140/353-366/$30.00

# Xylanase Contribution to the Efficiency of Cellulose Enzymatic Hydrolysis of Barley Straw

**María P. García-Aparicio, Mercedes Ballesteros, Paloma Manzanares, Ignacio Ballesteros, Alberto González, and M. José Negro***

*Renewable Energies Department-CIEMAT, Avda. Complutense, 22 28040-Madrid, Spain, E-mail: mariajose.negro@ciemat.es*

## Abstract

In this study, different enzyme preparations available from Novozymes were assessed for their efficiency to hydrolyze lignocellulosic materials. The enzyme mixture was evaluated on a pretreated cellulose-rich material, and steam-exploded barley straw pretreated under different temperatures (190, 200, and 210°C, respectively) in order to produce fermentable sugars. Results show that xylanase supplementation improves initial cellulose hydrolysis effectiveness of water-insoluble solid fraction from all steam-exploded barley straw samples, regardless of the xylan content of substrate. The mixture constituted by cellulase: β-glucosidase: endoxylanase of the new kit for lignocellulose conversion at a ratio 10 : 1 : 5% ([v/w], enzyme [*E*]/substrate [*S*]) provides the highest increment of cellulose conversion in barley straw pretreated at 210°C, for 10 min.

**Index Entries:** Agricultural residues; cellulose conversion; lignocellulose; pretreatment; xylanase supplementation; steam explosion.

## Introduction

Liquid biofuels obtained from biomass feedstock, as ethanol, is regarded as an attractive alternative to fuel oil to reduce dependence on foreign oil and diminish $CO_2$ emissions, main cause of greenhouse effect. The production of ethanol as fuel (i.e., fuel ethanol) from cereal starch in Spain reached about 240,000 t in 2005 *(1)*. Recent legislation *(2)* requires the use of at least 500,000 t/yr of cereal-based ethanol by 2010. Alternative biomass resources as lignocellulosic materials could also be used to supply a large-scale biomass-to-energy industry. This feedstock is interesting because of its abundance and low cost, as a great part of the lignocellulosic materials is generated as remainder in the productive process of agricultural sector. However, the ethanol production and its derivatives

*Author to whom all correspondence and reprint requests should be addressed.

from lignocellulose require advanced conversion technology to make them competitive against fuel oil. Although today there is little commercial production of ethanol from lignocellulosic biomass, R&D is being performed in Canada, the United States, and Europe (3). Among biomass-to-ethanol processes, those based on enzymatic hydrolysis seems to be promising. However, there are physical–chemical, structural, and compositional factors that hinder the enzymatic digestibility of cellulose present in lignocellulose biomass. Barley straw, an important residue from grain industry in Spain, may be a promising substrate for microbial fermentation to ethanol. It contains about 35–40% cellulose, 20–30% hemicellulose, and 8–15% lignin. Currently, the use of cereal straw to produce fuel ethanol faces significant technical and economic challenges. Its success depends largely on the development of an environmentally friendly pretreatment procedure, highly effective enzyme systems for conversion of pretreated barley to fermentable sugars, and an efficient conversion of fermentable sugars to ethanol.

Pretreatment is required to alter the structure of cellulosic biomass making cellulose more accessible to enzymes that convert the carbohydrate polymers into fermentable sugars. The goal is to break the xylan–lignin matrix and disrupt the crystalline structure of cellulose (4). Steam explosion (SE) has been proposed as an efficient pretreatment of lignocellulosic materials owing to its low use of chemicals, low energy consumption, and efficient biomass disruption characteristics for hardwoods and agricultural residues (5). Moreover, it has been developed at commercial scale (6). This pretreatment, based on the combined effect of steam and pressure release, disrupts the lignin barrier and enhances accessibility of cellulose fibers to enzymatic attack.

In addition to the physical barriers that constitute both hemicellulose and lignin, there are difficulties in the enzymatic hydrolysis step. Cellulases have a low specific activity (7). Furthermore, the hydrolysis rate falls off sharply as the hydrolysis proceeds; thus, it is necessary to use great amounts of enzymes in this process. This adds to the higher production cost of the enzymes, making the enzymatic hydrolysis step a critical point in the global cost of ethanol production (8). There are numerous factors that contribute to the reduction in the capacity of cellulose conversion by enzymes: those related to the structure of the substrate, and those related to the mechanisms and interactions of the cellulose enzymes (9). Substrate structure, responsible for the accessibility and susceptibility to the enzymatic attack, is determined by the type and conditions of pretreatment. On the other hand, the nature of the enzymatic complex used and the proportion of each component, and therefore its susceptibility to enzyme product-based inhibition, are going to establish the way of interaction between cellulases and cellulose fiber. The enzymatic conversion of cellulose is a complex process involving the coordinated action of exo/endocellulases and cellobiases, in order to render glucose. On the other hand, enzymatic hydrolysis of the hemicellulose is essential to facilitate complete cellulose

degradation. As xylan is the major hemicellulose in barley straw, xylanase addition would render xylooligomers and xylose. Hence, a complete degradation of xylan-to-xylose would make the production of bioethanol from lignocelulosic materials more profitable, aiming at the possibility to ferment both glucose and xylose to ethanol.

The activities detected in most of the commercial enzymatic preparations are not often sufficient to obtain a complete conversion of the cellulose. The supplementation with greater β-glucosidase doses is essential to reduce cellobiose inhibition in the enzymatic hydrolysis step *(10)*. The use of accessory enzymes as hemicellulases and ligninases could be interesting for the conversion of lignocellulosic materials into monomeric sugars that can be transformed to ethanol by suitable microorganisms *(11)*. In this context, the study of new enzyme mixtures in the enzymatic hydrolysis step is relevant to improve the potentially fermentable sugar yields.

In the present study, different enzyme preparations available from Novozymes A/S (Bagsveard, Denmark) were assessed for their efficiency to hydrolyze lignocellulosic materials. First, these enzyme samples were analyzed for the amount of cellulase, cellobiase, and xylanase activities. Subsequently, the enzyme mixture was evaluated on a pretreated cellulose-rich material, and steam-exploded barley straw pretreated under different temperatures (190, 200, and 210°C, respectively) in order to produce fermentable sugars.

## Materials and Methods

### *Feedstock Material*

Barley straw (*Hordeum vulgare*, 6–8% moisture), supplied by Ecocarburantes de Castilla y León (Spain) was used as raw material. Biomass was coarsely crushed (to a particle size of about 10 mm) using a laboratory hammer mill (Retsch GmbH & Co. KG, Germany), homogenized and stored at room temperature until use. Raw material showed the following composition (dry weight [%]): 37.1 ± 1.3, glucans; 21.3 ± 0.5, xylans; 3.8 ± 0.4, arabinans; 1.2 ± 0.2, galactans; 16.9 acid-insoluble lignin, 2.3 ± 0.8 acid-soluble lignin; 1.8 + 0.01 acetyl groups; 15.4 extractives; and 8.2 ash. The composition of the raw material was determined using the standard laboratory analytical procedures for biomass analysis provided by the National Renewable Energy Laboratory (Colorado) *(12)*.

### *SE Pretreatment*

Barley straw was pretreated in a small SE batch plant based on Mansonite technology, as described in a previous work *(13)*. The reactor was filled with 150.0 g (dry weight) of feedstocks per batch, and then heated to the desired temperature (190, 200, and 210°C, respectively) directly with saturated steam for 10 min. After explosion, the material was recovered in a cyclone. The slurry was cooled to about 40°C and then filtered

for water-insoluble solid (WIS) and liquid-fractions recovery. WIS fraction was thoroughly washed with water and dried at 45°C. The chemical composition of WIS was determined by National Renewable Energy Laboratory standard methods *(12)* and used in enzymatic hydrolysis tests.

### *Enzyme Preparations*

Celluclast 1.5 FG, Novozym 188, Shearzyme, NS50013, NS50010, and NS50030 enzyme preparations were kindly provided by Novozymes. The three last preparations were contained in Novozymes Biomass Kit for conversion of lignocellulosic materials.

### *Measurement of Enzymes Activities*

Enzyme preparations were subjected to standardized tests to determine protein content and main enzymes activities relevant in the conversion of lignocellulose: cellulase, cellobiose, and xylanase activities. Cellulase and β-glucosidase activities were measured according to methods described by Ghose *(14)*. Cellulase activity was defined in terms of filter paper units/milliliter and β-glucosidase as cellobiase unit/milliliter. Xylanase activity was quantified as described by Bailey et al. *(15)* using birchwood xylan (Sigma Aldrich Corp., St. Louis, MO) as substrate. One unit of xylanase activity is the amount of enzyme required to release 1 μmol of reducing sugars (xylose equivalents) per minute (U/mL).

Filter paper activity assay is the most usual measurement of the hydrolytic potential of a cellulase preparation because it allows the determination of the overall cellulase activity. Cellobiase (actually β-glucosidase) activity is responsible for the formation of glucose from cellobiose and its important role in cellulose degradation by relieving cellobiose inhibition is well known. Finally, xylanase (endo-1,4-β-D-xylanase activity) activity catalyzes the random hydrolysis of 1,4-β-D-xylosidic linkages in xylans. The protein content was determined by Bicinohoninic acid [BCA]™ assay (BCA-Compat-Able Protein Assay kit, ref. 23229, Pierce, Rockford, IL) using bovine serum albumin as protein standard.

### *Enzymatic Hydrolysis Experiments*

Different ternary mixtures of enzyme preparations were studied on washed WIS samples after pretreatment: Cellulases (Celluclast 1.5L FG and NS50013): β-glucosidases (Novozym 188 and NS50010) and xylanases (Shearzyme and NS50030). Enzymatic hydrolysis experiments were performed in 250-mL Erlenmeyer flasks at 50°C and 150 rpm and at 5% (w/v) substrate loading in 0.05 *M* citrate buffer (pH 4.8). Enzyme loading of the different enzyme preparations is expressed as volume of enzyme preparation (E)/100.0 g substrate (washed-WIS) (S). Cellulases and xylanases were dosed at 5 and 10% (v/w) E/S, whereas β-glucosidase was dosed always at 1% (v/w) E/S (Table 1).

Table 1
Enzyme Loading in Different Experiments Tested

| Enzyme mixture | Cellulase : β-glucosidase : xylanase | Enzyme loading %(v/w) E/S |
|---|---|---|
| A | Celluclast : Novozym : Shearzyme | 10 : 1 : 0 |
| B | | 10 : 1 : 5 |
| C | | 10 : 1 : 10 |
| D | | 5 : 1 : 5 |
| E | NS50013 : NS50010 : NS50030 | 10 : 1 : 0 |
| F | | 10 : 1 : 5 |
| G | | 10 : 1 : 10 |
| H | | 5 : 1 : 5 |

Samples were withdrawn from the hydrolysis media at 1, 3, 6, 12, 24, and 120 h. The samples were centrifuged at 12,000*g* for 10 min, and sugar concentration (glucose, cellobiose, and xylose) was determined by high-performance liquid chromatography *(16)*. All experiments were performed in duplicate. To compare the time-course of enzymatic hydrolysis of barley straw pretreated at different conditions two indices were calculated: specific conversion (SC) and mean specific rate (MSR). The SC is the percent of total cellulose hydrolyzed to glucose in 12 h/mg, normalized for protein content in 1 mL (%/mg). The MSR is the average of the cellulose hydrolysis rates for 0–1, 1–3, 3–6, and 6–12 h/mg, normalized for protein content in 1 mL (g glucose/L/h/mg). MSR and SC indices were calculated as described by Berlin et al. *(17)*.

The enzymatic hydrolysis yield was calculated as the concentration of the hydrolyzed cellulose (HC) divided by the cellulose content in the pretreated material and expressed as percentage. HC shows glucose and cellobiose content in the media, after applying weight adjustment for analyzed sugars. HC was calculated as follows:

$$HC = [Glu] \cdot 0.9 + [Cell] \cdot 0.95$$

where, [Glu] and [Cell] are the concentrations (g/L) of glucose and cellobiose in the media, respectively. Taking into account that substrate concentration in the enzymatic hydrolysis test was 5% (w/v).

## Results and Discussion

### *SE Pretreatment*

The composition of WIS fraction of pretreated barley straw (dry weight [%]) is shown in Table 2. After SE pretreatment solid recovery (expressed as WIS remaining after pretreatment divided by 100.0 g of raw material) was about 56%. Reduction in WIS was the result of solubilization

Table 2
Composition of WIS Obtained After SE Pretreatment of Barley Straw (Dry Weight [%])

| Pretreatment conditions | Glucans (%) | Xylans (%) | Acid-insoluble lignin (%) | Ash (%) |
|---|---|---|---|---|
| 190°C, 10 min | 58.8 ± 1.1 | 11.8 ± 1.0 | 23.7 ± 1.0 | 7.8 ± 0.4 |
| 200°C, 10 min | 64.5 ± 1.4 | 6.3 ± 0.9 | 24.8 ± 1.2 | 8.4 ± 1.1 |
| 210°C, 10 min | 62.3 ± 1.4 | 3.8 ± 0.9 | 25.4 ± 1.5 | 9.4 ± 0.7 |

Main value + sd.

and/or degradation of hemicellulose and extractives. After SE, the biomass composition changed because of the thermal degradation mainly of the hemicellulose component. Cellulose content in WIS increased in relation to untreated material (37.1%) ranging from 58.8 to 64.5%, depending on the pretreatment conditions. The greatest cellulose content (64.5%) was obtained at 200°C. High temperature pretreatment (210°C) produced lower cellulose content in the pretreated material owing to slight cellulose solubilization. Acid-insoluble lignin was considerably concentrated in comparison with raw material (16.9%), reaching values up to 25.4% at the most severe conditions. At increased pretreatment severity, a decrease in the hemicellulose content was also observed. The chemical composition confirmed that the matter loss primarily occurs at the expense of hemicellulose, the component being more thermally degradable. Glucan and lignin contents in all pretreated substrates were quite similar, and their composition mainly differs on xylan content, which varied from 11.8 to 3.8% depending on pretreatment conditions.

### *Enzyme Activity Assays*

Table 3 presents enzyme activities for the different enzyme preparations used in this work. NS50013, a cellulase complex, and Celluclast 1.5 L FG showed the highest values of filter paper activity (cellulase). In addition, both enzymes presented xylanase activity, being higher in NS50013. This fact is important in enzymatic hydrolysis of lignocellulosic materials because xylans are coating the cellulose fibrils, and therefore, hindering the accessibility of cellulose for cellulases. Xylanase was the highest enzyme activity in Shearzyme, although it also shows some cellulase activity. NS50030 preparation shows the highest xylanase activity (3760.0 IU/mL). In fact, this preparation is a purified endoxylanase and regarding information supplied by Novozymes A/S, it shows high specificity toward the soluble pentosan fraction in wheat.

### *Enzymatic Hydrolysis of Steam-Exploded Barley Straw*

The influence of using different enzyme mixtures has been studied on enzymatic hydrolysis of WIS from pretreated barley straw samples, which

Table 3
Enzyme Activities in Enzymes Preparations

| Enzyme preparations | Protein concentration (mg/mL) | Enzyme activities (U/mL) | | |
|---|---|---|---|---|
| | | FPA | β-Glucosidase | Xylanase |
| Celluclast 1.5 L FG | 151.0 | 65.0 | 12.0 | 660.0 |
| NS50013 | 138.0 | 63.0 | 8.0 | 1117.0 |
| Novozym 188 | 83.0 | n.d. | 664.0 | 69.0 |
| NS50010 | 141.0 | n.d. | 992.0 | 124.0 |
| Shearzyme | 71.0 | 27.0 | 5.0 | 2293.0 |
| NS50030 | 21.0 | n.d. | 1.0 | 3760.0 |

n.d. not detected; FPA, filter paper unit.

mainly differ on their xylan content. Six enzyme mixtures tested in this study (B–D and F–H) consist of cellulases (Celluclast 1.5 L FG or NS50013), β-glucosidases (Novozym 188 or NS50010), and xylanases (Shearzyme or NS50030) preparations. Besides, two binary systems (A and E) consisting only of cellulase and β-glucosidase preparations were studied. β-glucosidase was added in all mixtures studied, because as is well known in literature, β-glucosidase can reduce the inhibiting effect of cellobiose. A reference enzyme mixture (Celluclast 1.5 L FG and Novozym 188) was selected as control. Table 4 shows enzymatic activities for the different enzyme mixtures studied, expressed as unit per milliliter in the hydrolysis test media.

Hydrolysis of steam-exploded barley straw at 5% (w/v) substrate loading by tested enzymes mixtures is shown in Figs. 1–3. Enzymatic hydrolysis followed the same pattern in all experiments. For all pretreated samples, the xylanase addition improved the glucose production in enzymatic hydrolysis. The highest glucose production during the first hour of hydrolysis was found in barley straw pretreated at 210°C. It is worth mentioning that increases in glucose production obtained with the different mixtures compared with control, were always higher in this substrate (up to 7.0 g/L at 12 h of hydrolysis at 210°C with mixtures F and G), in spite of its low xylan content (3.7%). Although the xylan content of the pretreated samples is low, xylanases may significantly increase the accessibility of cellulose to cellulases by removing hemicellulose, including material redeposited on the fibers during pretreatment *(17)*. Increases were less evident as substrate was pretreated at lower temperatures (up to 5.0 g/L at 12 h of hydrolysis at 190°C with mixtures F and G). Similar glucose production was obtained for control and enzyme mixtures D and H (which contained half-cellulase loading with respect to the control and 5% [v/w] of xylanases).

Supplementation with xylanase activity (up to a certain level of 16.0 U/mL) improved glucose production in enzymatic hydrolysis by using enzymes mixtures with similar to both filter paper and β-glucosidase

Table 4
Enzyme Activity and Protein Levels Presents in Hydrolysis Media for Different Enzyme Mixtures Used

| Enzymatic mixture | Cellulase : β-glucosidase : Xylanase | Enzyme loading %(v/w) E/S | Cellulase (filter paper units/mL) | β-glucosidase (U/mL) | Xylanase (U/mL) | Protein (mg/g substrate) |
|---|---|---|---|---|---|---|
| A | Celluclast : Novozym : Shearzyme | 10 : 1 : 0 | 0.35 | 0.42 | 3.6 | 17.0 |
| B | | 10 : 1 : 5 | 0.42 | 0.43 | 9.7 | 20.8 |
| C | | 10 : 1 : 10 | 0.49 | 0.44 | 15.6 | 24.6 |
| D | | 5 : 1 : 5 | 0.25 | 0.40 | 7.9 | 12.8 |
| E | NS50013 : NS50010 : NS50030 | 10 : 1 : 0 | 0.33 | 0.57 | 6.0 | 16.2 |
| F | | 10 : 1 : 5 | 0.33 | 0.57 | 16.0 | 17.2 |
| G | | 10 : 1 : 10 | 0.34 | 0.58 | 26.1 | 18.4 |
| H | | 5 : 1 : 5 | 0.17 | 0.55 | 13.1 | 10.0 |

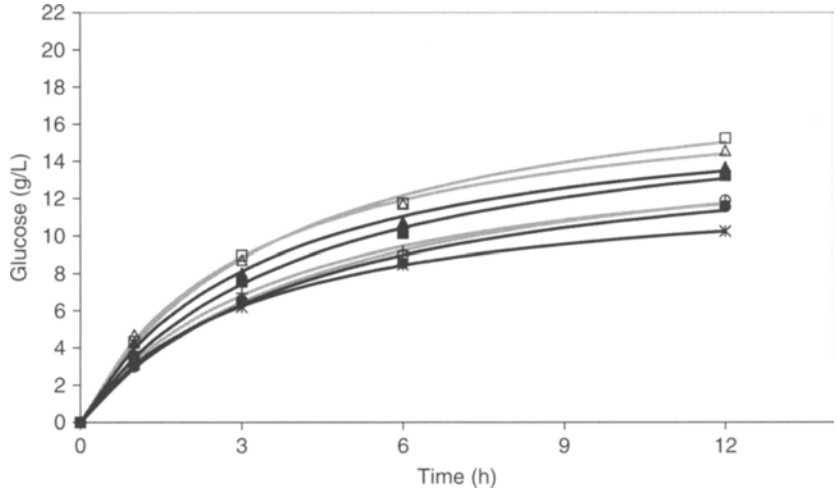


**Fig. 1.** Hydrolysis of WIS fraction of steam-exploded barley straw (190°C 10 min) by different enzymes mixtures. Mixtures A (—*—), B (—■—), C (—▲—), and D (—●—) cellulose : β-glucosidase : xylanase = Celluclast FG 1.5L : Novozym 188 : Shearzyme. Mixtures E (—+—), F (—□—), G (—△—), H (—○—) cellulase : β-glucosidase : xylanase = NS50013 : NS50010 : NS500.

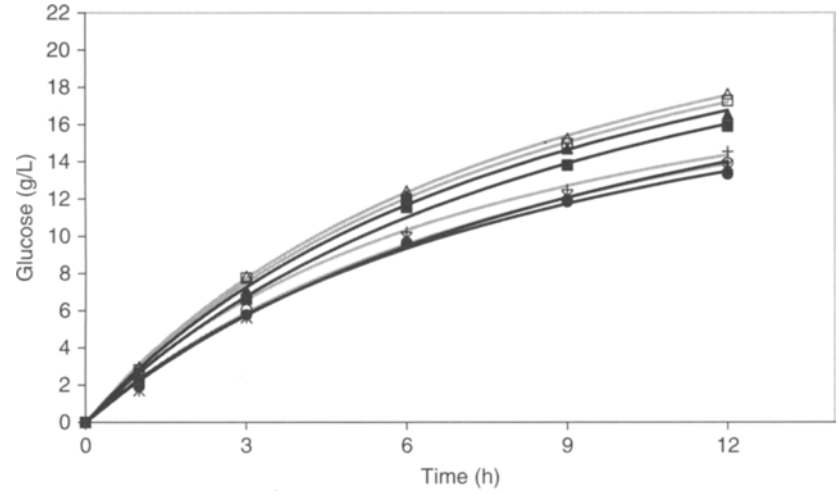


**Fig. 2.** Hydrolysis of WIS fraction of steam-exploded barley straw (200°C 10 min) by different enzymes mixtures. Mixtures A (—*—), B (—■—), C (—▲—), and D (—●—) cellulase : β-glucosidase : xylanase = Celluclast FG 1.5L : Novozym 188 : Shearzyme. Mixtures E (—+—), F (—□—), G (—△—), H (—○—) cellulase : β-glucosidase : xylanase = NS50013 : NS50010 : NS50030.

activities (A and E–G). This fact suggests that filter paper, although commonly used as index of cellulose performance, does not provide a reliable indication of the ability of a preparation to hydrolyze complex lignocellulosic substrates. This fact has been recently indicated by other authors *(18,19)*.

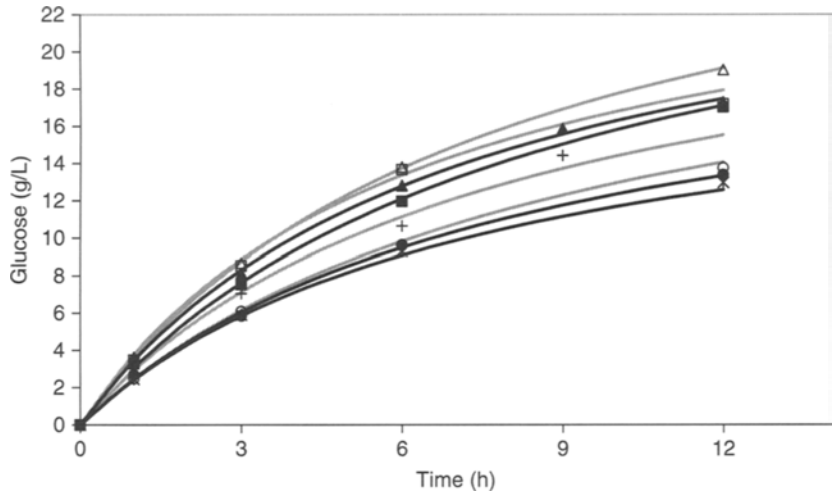


**Fig. 3.** Hydrolysis of WIS fraction of steam-exploded barley straw (210°C 10 min) by different enzymes mixtures. Mixtures A (—*—), B (—■—), C (—▲—), and D (—●—) cellulase : β-glucosidase : xylanase = Celluclast FG 1.5L : Novozym 188 : Shearzyme. Mixtures E (—+—), F (—□—), G (—△—), and H (—○—) cellulase : β-glucosidase : xylanase = NS50013 : NS50010 : NS50030.

The multiple parameters that influence hydrolysis of heterogeneous lignocellulosic substrates (e.g., crystallinity, lignin/hemicellulose content and distribution, and available surface area) result in complex reaction kinetics. In order to compare the performance of different cellulase mixtures on enzymatic hydrolysis of pretreated barley straw substrate, two indices, MSR and SC, were determined as proposed by Berlin et al. *(17)* (Table 5). MSR index provides an estimate of the average reaction rate over the first 12 h of hydrolysis and SC index describes the percentage of the total cellulose in the sample hydrolyzed at 12 h incubation period. Differences in the performance of the various enzyme mixtures tested have been found. MSR indices were similar for all pretreated substrate samples in each enzyme mixture. As aforementioned, higher values for SC index were obtained in the enzymatic hydrolysis of the substrate pretreated at 210°C.

Mixtures D and H provided the highest values of MSR and SC because of their lower protein loadings. Considering enzyme mixtures with similar protein contents (A, E, and F), better results were achieved with mixture F, which includes preparations from the Novozymes Biomass Kit for conversion of lignocellulosic materials. Data obtained using F mixture shows a significant improvement when compared with the control (mixture A), which includes Celluclast and Novozym 188 that are generally used in research studies of enzymatic hydrolysis of lignocellulosic materials.

Table 5
MSR and SCs for Hydrolysis of WIS Steam-Exploded Barley Straw by Different Mixtures Enzymes

| Enzyme mixture | 190°C 10 min | | 200°C 10 min | | 210°C 10 min | |
|---|---|---|---|---|---|---|
| | MSR | SC | MSR | SC | MSR | SC |
| A | 1.8 | 40.8 | 1.8 | 51.2 | 1.7 | 52.0 |
| B | 1.7 | 42.8 | 1.7 | 52.8 | 1.9 | 54.0 |
| C | 1.6 | 37.2 | 1.5 | 46.4 | 1.7 | 63.6 |
| D | 2.4 | 60.4 | 2.3 | 65.6 | 2.4 | 69.2 |
| E | 2.0 | 49.2 | 2.1 | 58.8 | 2.2 | 64.0 |
| F | 2.5 | 59.6 | 2.3 | 65.2 | 2.4 | 67.6 |
| G | 2.3 | 53.2 | 2.2 | 63.6 | 2.4 | 70.4 |
| H | 3.1 | 80.0 | 3.1 | 91.2 | 3.2 | 92.8 |

Table 6
Enzymatic Hydrolysis Yield (%) at 24 h and 120 h of WIS Steam-Exploded Barley Straw by Various Enzyme Mixtures

| Enzyme mixture | 190°C 10 min | | 200°C 10 min | | 210°C 10 min | |
|---|---|---|---|---|---|---|
| | 24 h | 120 h | 24 h | 120 h | 24 h | 120 h |
| A | 47.2 | 54.4 | 60.6 | 74.1 | 58.2 | 85.7 |
| B | 54.8 | 64.5 | 69.8 | 84.4 | 75.6 | 97.0 |
| C | 56.5 | 66.9 | 70.9 | 84.4 | 73.9 | 98.8 |
| D | 50.1 | 60.4 | 59.8 | 78.0 | 62.6 | 97.7 |
| E | 47.5 | 55.2 | 57.5 | 77.2 | 68.7 | 94.1 |
| F | 61.2 | 71.5 | 70.0 | 85.0 | 84.7 | 100 |
| G | 60.2 | 71.3 | 70.3 | 82.7 | 84.5 | 98.1 |
| H | 52.0 | 68.3 | 53.5 | 81.8 | 66.5 | 98.2 |

## *Prolonged Enzymatic Hydrolysis*

Table 6 shows results for cellulose conversion obtained after 24 and 120 h hydrolysis time. Enzymatic hydrolysis yield (expressed as percentage) was calculated as the concentration of the HC divided by the cellulose content in the pretreated substrate. Increased conversions of cellulose to glucose in comparison with the control were obtained in experiments supplemented with xylanases. Comparing mixtures A and D similar cellulose hydrolysis yields at 24 and 120 h were found. This finding is important because in mixture D reduced amounts of cellulase and increased amounts of xylanase are used. Likewise, if mixtures E and H are compared, similar cellulose hydrolysis yields could be attained using reduced cellulase loading and increased xylanase loading. Higher enzymatic hydrolysis yields

were obtained with enzyme mixture F. After 24 h hydrolysis time, the cellulose hydrolysis yield of steam barley straw pretreated at 210°C increased by 45% when using this mixture in comparison with the control (mixture A). In these conditions the increase of xylan hydrolysis yield was by 50%. Complete enzymatic hydrolysis of barley straw pretreated at 210°C was obtained for all enzyme mixtures tested (excluded the control). Regarding results obtained in this work, the ternary mixture of NS50013 : NS50010 : NS50030 at 10 : 1 : 5% ([v/w] E/S) seems to be the most suitable for the cellulose hydrolysis of pretreated barley straw.

## Concluding Remarks

The increase of the accesibility of cellulose to cellulases by the addition of purified endoxylanases has been demonstrated in this work. Although cellulase preparations normally cited in literature include some xylanase activity, xylanase supplementation could maximize enzymatic hydrolysis yield. This fact should be considered when using tailor-made enzyme complex to increase fermentable sugar yield in the hydrolysis step. In this work, xylanase supplementation improved cellulose hydrolysis effectiveness of pretreated barley straw samples, regardless of the xylan content of substrate. The interaction among different enzymatic activities presented in cellulase complex should be further studied.

## Acknowledgments

The authors wish to acknowledge Novozymes for kindly providing enzymes preparations.

## References

1. EurObserver (2005) Biofuels Barometer, May 2006 Paris, Observ'ER.
2. Plan de Fomento de la Energías Renovables en España 2005–2010. IDAE. Ministerio de Industria Comercio y Turismo (2005), 345p.
3. Biofuel in the European Union: a vision for 2030 and beyond. http://europa.eu.int/comm/research/energy/pdf/draft_vision_report_en.pdf. Accessed March 2006.
4. Mosier, N., Wyman, C., Dale, B., et al. (2005), *Bioresour. Technol.* **96,** 673–686.
5. Duff, S. J. B. and Murray, W. D. (1996), *Bioresour. Technol.* **55,** 1–33.
6. www.sunopta.com/(August 2005).
7. Howard, R. L., Abotsi, E., Rensburg, J., and Howard., S. (2003), *Afr. J. Biotechnol.* **2,** 602–619.
8. Sun, Y. and Cheng, J. (2002), *Bioresour. Technol.* **83(1),** 1–11.
9. Mansfield, S. D., Mooney, C., and Saddler, J. N. (1999), *Biotechnol. Prog.* **15,** 804–816.
10. Gruno, M., Väljamaë, P., Pettersson, G., and Johansson, G. (2004), *Biotechnol. Bioeng.* **86,** 503–511.
11. Tuncer, M. and Ball, A. S. (2002), *Appl. Microbiol. Biotechnol.* **58,** 608–611.
12. National Renewable Energy Laboratory (NREL). Chemical Analysis and Testing Laboratory Analytical Procedures: LAP-001 to LAP-005, LAP-010 and LAP-017. NREL, Golden, CO. www.ott.doe.gov/biofuels/analytical_methods.html.

13. Carrasco, J. E., Martínez, J. M., Negro, M. J., et al. (1989), in *5th EC Conference on Biomass for Energy and Industry*, Grassi, G., Gosse, G., and Dos Santos, G. (eds.), vol. 2, Elsevier, Essex, England, UK, pp. 38–44.
14. Ghose, T. K. (1987), *Pure Appl. Chem.* **59,** 257–268.
15. Bailey, M. J., Biely, P., and Poutanen, K. (1992), *J. Biotechnol.* **23,** 257–270.
16. Negro, M. J., Manzanares, P., Ballesteros, I., Oliva, J. M., Cabañas A., and Ballesteros, M. (2003), *Appl. Biochem. Biotechnol.* **105–108,** 87–100.
17. Berlin, A., Gilkes, N., Kilburnn, D., et al. (2005), *Enzyme Microb. Technol.* **37,** 175–184.
18. Kurabi, A., Berlin, A., Gilkes, N., et al. (2005), *Appl. Biochem. Biotechnol.* **121–124,** 119–230.
19. Kabal, M. A., van der, M., Klip, M. J. C., Voagen, G., and Schols, A. G. J. (2006), *Biotechnol. Bioeng.* **93,** 56–63.

0273-2289/1559-0291 (Online)/07/136–140/367–378/$30.00

# Effect of Organosolv Ethanol Pretreatment Variables on Physical Characteristics of Hybrid Poplar Substrates

XUEJUN PAN,*[,1,2] DAN XIE,[2] KYU-YOUNG KANG,[2] SEUNG-LAK YOON,[3] AND JACK N. SADDLER[2]

*[1]Department of Biological Systems Engineering, University of Wisconsin-Madison, 460 Henry Mall, Madison, WI 53706, USA, E-mail: xpan@wisc.edu; [2]Department of Wood Science, University of British Columbia, 2424 Main Mall, Vancouver, BC, Canada, V6T 1Z4; and [3]Department of Interior Materials Engineering, Jinju National University, 150 Chilamdong, Jinju 660-758, Korea*

## Abstract

Hybrid poplar (*Populus nigra* × *P. maximowiczii*) chips were pretreated using an organosolv ethanol process. The effect of pretreatment conditions (temperature, time, catalyst, and ethanol concentration) on the substrate characteristics, including fiber size, crystallinity, and degree of polymerization of cellulose, was investigated using an experimental matrix designed with response surface methodology. The conditions ranged 155–205°C, 26–94 min, 0.83–1.67% catalyst ($H_2SO_4$) on oven-dry wood chip (w/w), and 25–75% ethanol concentration (v/v). The results indicated that the substrate characteristics are controllable and predictable. Desirable substrates can be prepared by fine-tuning the processing parameters. The regression models developed, allowed the quantitative prediction of the substrate characteristics from the pretreatment conditions used.

**Index Entries:** Crystallinity; degree of polymerization; fiber size; hybrid poplar; organosolv ethanol pretreatment; substrate characteristics.

## Introduction

Biorefinery of renewable resources for energy, chemicals, and materials has drawn considerable attention as the concerns for environmental impact and shortage of fossil petroleum are increasing. Fuel ethanol from lignocellulosics is one area receiving particular attention as the feedstocks are generally abundant, inexpensive, and renewable. A typical bioconversion process of lignocellulosics to ethanol consists of pretreatment, saccharification, fermentation, and ethanol distillation steps, whereas in the simultaneous saccharification and fermentation process, saccharification and fermentation are integrated into a single step. A primary techno-economic

*Author to whom all correspondence and reprint requests should be addressed.

challenge in all lignocellulosics-to-ethanol bioconversion processes is the development of cost-effective pretreatment methods to make cellulose more accessible to enzymes *(1,2)*. The most adventitious strategy for an effective pretreatment is to develop a biorefinery platform where not only cellulose is recovered for bioethanol, but also lignin, hemicellulose, and extractive components of the lignocellulosic biomass are converted to valuable coproducts, which offsets the costs of feedstock pretreatment and enzymes for cellulose hydrolysis.

Among the various pretreatment methods, such as steam-explosion *(3)*, dilute acid pretreatment *(4,5)*, organosolv *(6,7)*, and others *(1)*, organosolv ethanol process was initially developed to make clean biofuel for turbine generators. Subsequent modification by the Canadian pulp and paper industry resulted in the Alcell® pulping process for hardwood *(8–10)*. Our initial results *(7)* indicated that the substrates pretreated by organosolv ethanol process from mixed softwoods possessed superior enzymatic digestibility over those pretreated by alternative processes, even at high residual lignin content. Furthermore, the process produces a particularly high-quality lignin fraction with potential in several industrial applications *(11)* and chemicals derived from hemicellulose *(12)*. Another advantage of the organosolv ethanol process is that the solvent (ethanol) used in the pretreatment is one of the final products of the bioconversion. Although the organosolv ethanol process has been largely investigated from the perspective of pulp and paper production from hardwood *(13–16)*, it is not well-studied as a pretreatment/biorefining tool for the bioconversion of lignocellulosic biomass. In particular, the effect of process parameters on the fractionation of major wood components, on the process mass balance, and on the chemical and physical characteristics of the substrate generated has not been investigated.

In previous work *(17)*, we investigated the pretreatment of hybrid poplar using organosolv ethanol process. The process was optimized from the perspective of recovery of cellulose, lignin, and hemicellulose. The enzymatic digestibility of the resulting substrate was also assessed. The organosolv ethanol lignin generated from the poplar was evaluated as an antioxidant *(18)*. In addition, the behaviors of the major wood components (lignin, hemicellulose, and cellulose) during the pretreatment, and chemical composition of resulting substrates and its dependence on process parameters were investigated as well *(17)*. The delignification was greatly dependent on ethanol concentration. Relatively lower ethanol concentration promoted acid-catalyzed cleavage of lignin, whereas higher ethanol concentration enhanced dissolution of depolymerized lignin fragments from the wood matrix. A maximum delignification was achieved at an ethanol concentration of about 70%( (v/v). More hemicellulose was reserved in the substrate and less cellulose was depolymerized at high ethanol concentration, resulting in higher sugar recovery yield. However, retained hemicellulose and less hydrolyzed cellulose might have a negative

impact on enzymatic hydrolysability of the substrate. High-temperature and more catalyst promoted not only delignification but also degradation of cellulose and hemicellulose. Extra high-temperature could result in lignin condensation and further degradation of monosaccharides into furfural, hydroxymethylfurfural, and levulinic acid.

In the present research, physical characteristics influencing enzymatic hydrolysis of the organosolv substrates from hybrid poplar were investigated, including fiber size, crystallinity, and degree of polymerization (DP) of cellulose. The influence of the primary processing variables (temperature, time, catalyst, and ethanol concentration) on the substrate characteristics was discussed. Mathematical equations were regressed to predict quantitatively the effect of the processing variables on the substrate characteristics with the aid of response surface methodology and statistical analysis system (SAS) software (SAS Institute Inc., Cary, NC).

## Materials and Methods

### *Organosolv Ethanol Pretreatment*

Hybrid poplar (*Populus nigra* × *P. maximowiczii*) wood chips, screened to pass one-fourth of an inch (6.4 mm) round screen were generously provided by the National Renewable Energy Laboratory (NREL) (Golden, CO). The chemical composition of the poplar was reported previously *(17)*. Anhydrous ethanol used in pretreatment was purchased from Commercial Alcohol Inc. (Brampton, Ontario, Canada). As described schematically before *(17)*, the poplar chips were pretreated on a customer-designed four-vessel (2 L) digester manufactured by Aurora Products Ltd. (Savona, BC, Canada). Chips of 20.0 g (dry base) were pretreated, each batch in one vessel. After the pretreatment, substrate was separated from the processing liquor containing dissolved lignin and hemicellulose by filtration using nylon cloth. The substrate was first washed three times (300 mL × 3) with warm (60°C) aqueous ethanol of the same concentration as the processing liquor and then washed with warm water thoroughly. After being disintegrated in a standard British disintegrator (Robert Mitchell Co. Ltd., Montreal, Quebec, CA) for 5 min, the washed substrate was screened on a lab flat screen with 0.008 in. (0.203 mm) slits (Voith, Inc., Appleton, WI) to remove undefiberized wood chips (rejects). The screened substrate was stored at 4°C for characterization.

### *Characterization of Organosolv Ethanol Substrates*

Viscosity measurement of the organosolv ethanol substrates from the poplar was conducted according to Technical Association of Pulp and Paper Industry Standard Method T230 om-99. The viscosity of a 0.5% cellulose solution in 0.5 *M* cupriethylenediamine was measured on a capillary viscometer (Cannon Instrument Co., State College, PA). The substrate

was carefully delignified before viscosity measurement, using sodium chlorite according to Useful Method G.10U of Pulp and Paper Technical Association of Canada.

Fiber length of the substrates was measured using a Fiber Quality Analyzer (LDA02, OpTest Equipment Inc., Canada). A dilute suspension of fibers with a fiber frequency of 25–40 EPS (events per second) was transported through a sheath low cell where the fibers are oriented and positioned. The images of fibers were detected by a built-in CCD camera, and the length of the fibers were measured by circular polarized light. The experiment was conducted according to the procedure described by Robertson et al. *(19)*. All samples were run in triplicate.

Crystallinity of the substrates was measured using a Bruker D8 Discover X-ray diffractometer (Madison, WI). X-ray radiation ($\lambda = 1.542$ Å) was generated by a Kristalloflex 780 generator with a Cu anode, powered at 40 kV and 20 mA. An air-dried fiber pad (approx 40 mm diameter and approx 1 mm thickness) was used for crystallinity measurement. The intensity was plotted against the scattering angle $2\theta$ within a range of 5–40°. Two hundred scans were typically recorded for each sample. Crystallinity of the substrates was calculated according to the method described by Vonk *(20)* and Krassig *(21)*.

### *Experimental Design and Data Analysis*

To investigate the influence of four process variables (temperature, reaction time at the temperature, acid catalyst dose, and ethanol concentration) on the characteristics of poplar substrates, an experimental matrix was designed using response surface methodology and a small Hartley composite design *(22)*. The matrix included 21 sets of conditions, including eight factorial points, eight star points, and five center points, as summarized in Table 1. The range of conditions examined was as follows: temperature, 155–205°C; time, 26–94 min; $H_2SO_4$, 0.83–1.67% of wood chips (w/w); and ethanol, 25–75% (v/v). The ratio of liquor to wood was constant (7 : 1, v/w) in all experiments. The condition set of the center point was temperature, 180°C; time, 60 min; $H_2SO_4$, 1.25% of wood chips (w/w); and ethanol, 50% (v/v). Data analysis (regression equations) was conducted and surface plots (figures) were prepared using SAS V9.0 for Windows (SAS Institute Inc.).

## Results and Discussion

### *DP of Cellulose*

The DP of cellulose is one of the substrate features that are known to influence the extent and rate of enzymatic hydrolysis. Some investigations concluded that DP is less important to enzymatic hydrolysis *(23,24)*, whereas other work indicated that substrates with low DP were hydrolyzed more

Table 1
Experimental Matrix of a Small Hartley Composite Design and Results

| No. | Process condition[a] | | | | Viscosity (mPaS) | Crystallinity (%) | Fiber length (mm) |
|---|---|---|---|---|---|---|---|
| | *T* (°C) | *t* (min) | *S* (%) | *C* (%) | | | |
| 1 | 165 | 40 | 1.00 | 65 | 10.9 | 59 | 0.480 |
| 2 | 195 | 40 | 1.00 | 65 | 21.3 | 78 | 0.648 |
| 3 | 165 | 80 | 1.00 | 35 | 20.4 | 63 | 0.702 |
| 4 | 195 | 80 | 1.00 | 35 | 4.5 | 63 | 0.551 |
| 5 | 165 | 40 | 1.50 | 35 | 12.9 | 65 | 0.613 |
| 6 | 195 | 40 | 1.50 | 35 | 2.6 | 76 | 0.392 |
| 7 | 165 | 80 | 1.50 | 65 | 13.6 | 80 | 0.565 |
| 8 | 195 | 80 | 1.50 | 65 | 2.1 | 88 | 0.290 |
| 9 | 155 | 60 | 1.25 | 50 | 14.0 | 69 | 0.521 |
| 10 | 205 | 60 | 1.25 | 50 | 2.8 | 81 | 0.409 |
| 11 | 180 | 26 | 1.25 | 50 | 22.3 | 66 | 0.717 |
| 12 | 180 | 94 | 1.25 | 50 | 9.9 | 70 | 0.560 |
| 13 | 180 | 60 | 0.83 | 50 | 24.8 | 68 | 0.662 |
| 14 | 180 | 60 | 1.67 | 50 | 3.3 | 76 | 0.425 |
| 15 | 180 | 60 | 1.25 | 25 | 6.7 | 73 | 0.525 |
| 16 | 180 | 60 | 1.25 | 75 | 19.9 | 70 | 0.620 |
| 17 | 180 | 60 | 1.25 | 50 | 14.2 | 67 | 0.640 |
| 18 | 180 | 60 | 1.25 | 50 | 13.1 | 66 | 0.624 |
| 19 | 180 | 60 | 1.25 | 50 | 13.5 | 68 | 0.674 |
| 20 | 180 | 60 | 1.25 | 50 | 12.2 | 66 | 0.577 |
| 21 | 180 | 60 | 1.25 | 50 | 12.5 | 65 | 0.633 |

[a]*T*, temperature (°C); *t*, reaction time at the temperature (min); *S*, sulfuric acid dose (percent of dry wood chips [w/w]); *C*, concentration of aqueous ethanol (v/v [%]).

quickly and extensively than those with high DP *(25,26)*. It was believed that longer cellulose chains (high-DP) formed stronger networks by more extensive inter- and intramolecular hydrogen bonding, therefore limiting the accessibility of cellulose to the enzymes and thus diminishing the substrates susceptibility to hydrolysis *(25)*. In addition, the reduction of DP increased the number of cellulose chain ends available to the action of exoglucanase in the cellulase complex, thus generating high-reaction rate and glucose yield *(26–28)*.

The viscosity of the cellulose solution is an indirect measurement of cellulose DP. In the present research, the viscosity of the substrate solution in cupriethylenediamine was used as an indication of cellulose degradation (decrease in molecular weight). The data listed in Table 1 clearly indicate that the viscosity of the substrates greatly depended on process conditions, varying from 2.1 to 24.9 mPaS. The high-viscosity values are within the range of typical wood pulps for paper (15–25 mPaS) but much lower than the viscosity of cotton linters (>40 mPaS) *(29)*, whereas the low-values are too low to meet the strength requirement of pulp for paper. It is apparent that long reaction times reduced the viscosity because of the

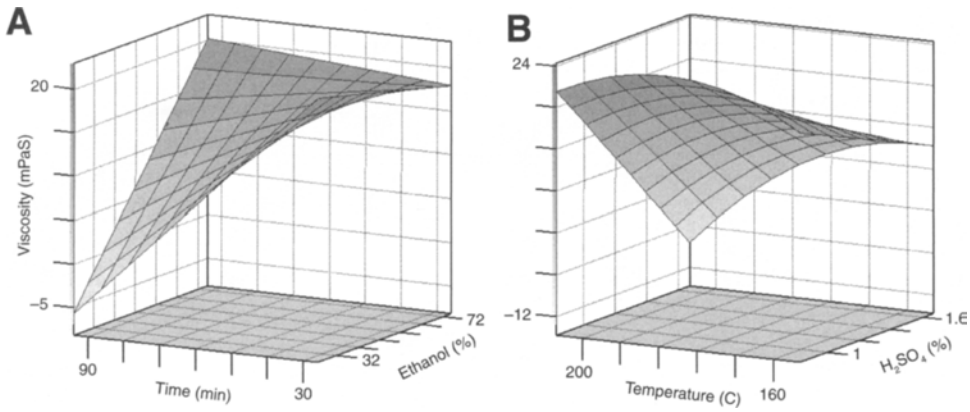


**Fig. 1.** Effect of process parameters on viscosity of the substrates prepared using organosolv ethanol process from hybrid poplar. The fixed variables were set at center point conditions. **A,** 180°C, 1.25% $H_2SO_4$; **B,** 60 min, 50%, ethanol.

acid-catalyzed depolymerization of cellulose when exposed to the acidic processing liquor at high-temperatures and, in particular, at low ethanol concentrations (Fig. 1A). Low ethanol concentration, which generates higher hydrogen ion concentration (lower pH value) at the same dose of $H_2SO_4$ *(30)*, promoted acid-catalyzed hydrolysis of cellulose. As expected, the substrate prepared at high ethanol concentrations had high-viscosity (Fig. 1A), implying that less depolymerization occurred. On the other hand, the substrates prepared at high-temperatures and sulfuric acid concentrations had low-viscosity (Fig. 1B), as the severe conditions enhanced the acidic hydrolysis of glucoside bonds in cellulose.

## *Crystallinity*

The crystallinity of the cellulose is another substrate factor influencing enzymatic hydrolysis. However, contradictory conclusions have been drawn about the effect of crystallinity on enzymatic hydrolysis of cellulose *(24)*. Several studies found a positive correlation between crystallinity and hydrolysis and claimed that the amorphous part of cellulose was hydrolyzed first, leaving the more recalcitrant crystalline part unhydrolyzed *(23,31,32)*. These studies used relatively pure cellulosic substrates; the effect of other substrate features, such as residual hemicellulose and lignin contents, was minor or not considered. Other studies reported no correlation between crystallinity and the rate/extent of enzymatic hydrolysis of substrates. This was particularly true when real lignocellulosic substrates were used because other factors such as residual lignin and hemicellulose played more important roles in inhibiting hydrolysis *(25,33,34)*. In other words, the effect of crystallinity was overlapped in case of real substrate.

The effect of process parameters on the crystallinity of organosolv ethanol substrates is shown in Fig. 2 and Table 1. The crystallinity varied from 59% to 88% (Table 1), depending on processing parameters. Long

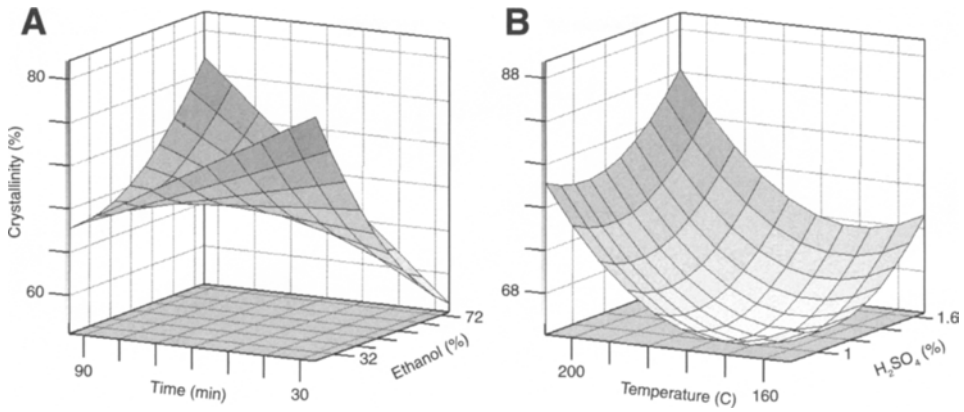


**Fig. 2.** Effect of process parameters on crystallinity of the substrates prepared using organosolv ethanol process from hybrid poplar. The fixed variables were set at center point conditions. **A,** 180°C, 1.25% $H_2SO_4$; **B,** 60 min, 50%, ethanol.

reaction time and relatively low ethanol concentration were expected to generate a substrate with high-crystallinity as these conditions favored the removal of amorphous lignin and hemicellulose. The results indicated that the substrates prepared at high ethanol concentration had lower crystallinity as more hemicellulose was retained in the substrates (right back corner of Fig. 2A). However, it is unclear why low-crystallinity was observed at extended time and low ethanol concentrations (left front corner of Fig. 2A). Figure 2B shows that the substrates generated at high-temperature and sulfuric acid concentration possessed higher crystallinity because of enhanced removal of amorphous lignin and hemicellulose. In addition, selective hydrolysis of amorphous part of cellulose might be another contributor to the high-crystallinity at high-temperature and catalyst dosage.

### *Fiber Size*

It is believed that particle size is an important substrate factor influencing hydrolysis rate. In general, small particle size means large surface area available to enzymes, thus promoting hydrolysis. This is particularly true in case of "real" lignocellulosic substrates *(24)*. The effect of process variables on average length of substrate fibers is shown in Fig. 3 and Table 1. The length of shortest fibers (0.290 mm, no. 8) was only half of that of longer fibers (e.g., no. 17–21), as listed in Table 1. The fiber length of the poplar substrates was linearly related to ethanol concentration and reaction time, as shown in Fig. 3A. Long reaction times produced shorter fibers, whereas high-concentrations of ethanol generated longer fibers. High-temperatures and higher concentrations of sulfuric acid resulted in shorter fibers, as shown in Fig. 3B. The reduction of fiber length was primarily caused by "chemical cutting" occurring during the organosolv ethanol

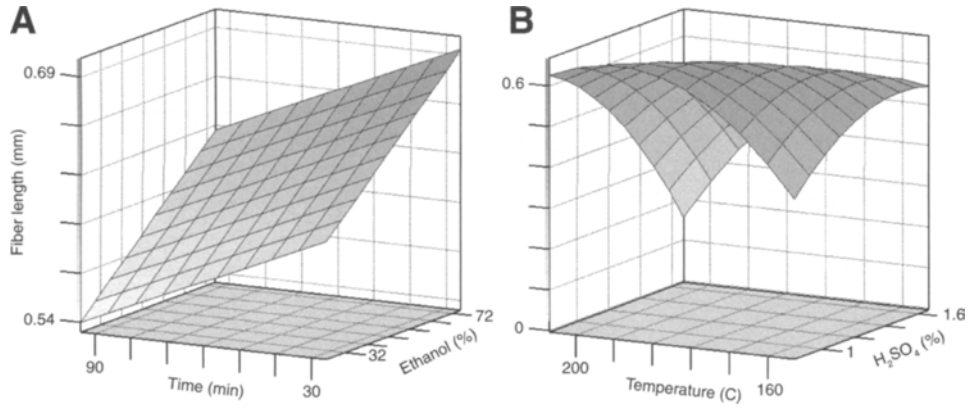


**Fig. 3.** Effect of process parameters on average fiber length of the substrates prepared using organosolv ethanol process from hybrid poplar. The fixed variables were set at center point conditions. **A,** 180°C, 1.25% $H_2SO_4$; **B,** 60 min, 50% ethanol.

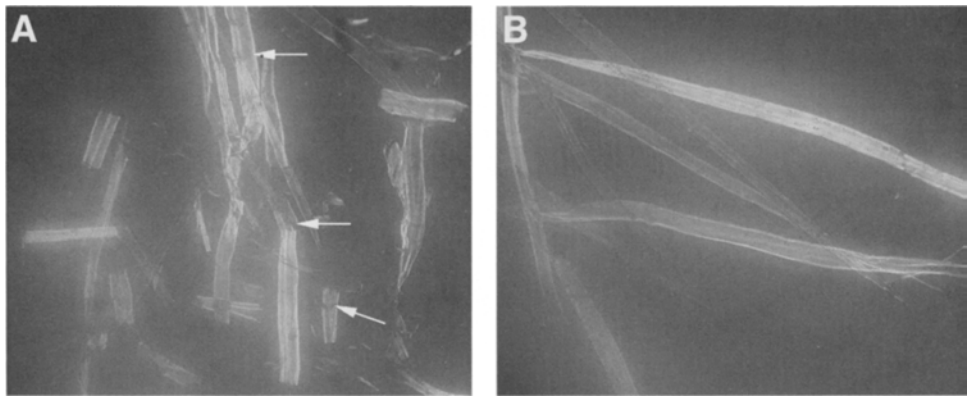


**Fig. 4.** Chemical cutting of fibers occurring during organosolv ethanol pretreatment observed under light microscope.

pretreatment, but the mechanism of the chemical cutting is not clear. The chemical cutting of the fibers was clearly observed under microscope.

Figure 4A shows the short pieces cut off from the fibers. Many cuttings are clearly visible along the fibers, as indicated by the arrows. The images of intact fibers are shown in Fig. 4B for comparison. It was observed that severe pretreatment conditions, for example, long reaction time, low ethanol concentration (high-acidity), high-temperature, and higher concentrations of acid catalyst, promoted the chemical cutting. Similarly, fiber cutting was observed in organosolv acetic acid pulping of wheat straw *(35)*. The chemical cutting is not desirable if the fibers are used for pulp and paper because the cutting weakens the strength of the fibers and papers.

However, from bioconversion point of view, the short fibers might be good substrates to enzymes because of the great surface area.

### *Regression Equations*

The effect of pretreatment conditions on the physical characteristics of the poplar substrates was qualitatively discussed earlier. To quantitatively predict the effect of each process variable on the substrate features, the relationship between substrate features and process variables was fitted to a second-order polynomial equation using SAS software, as shown in Eq. 1.

$$Y = a_0 + \sum_{i=1}^{k} a_i X_i + \sum_{i=1}^{k} a_{ii} X_i^2 + \sum_{i=1}^{k-1} \sum_{j=1}^{k} a_{ij} X_i X_j \quad (1)$$

where $Y$ is the estimated value of the substrate features, $k$ is the total number of independent variables (four in this case), $X_i$s are the independent variables (temperature, time, catalyst dose, and ethanol concentration), the $X_i$, $X_i^2$, and $X_iX_j$ are terms describing linear, quadratic, and two-variable interaction effects, respectively, $a_0$ is a constant and $a_i$, $a_{ii}$, and $a_{ij}$ are linear, quadratic, and interaction coefficients, respectively. The predictive models (Eqs. 2–4) developed for the substrate features are listed in Table 2. These equations can predict the substrate characteristics within the investigated range of process parameters. To validate the regression equations, the calculated values of the substrate characteristics using the equations at center point conditions were compared with the experimental data from five replicate pretreatment experiments. As listed in Table 2, the calculated values are in good agreement with the experimental data, implying the reliability of the equations.

## Conclusion

The results of the present research indicated that the physical characteristics (DP of cellulose, crystallinity, and fiber length) of the organosolv ethanol substrates prepared from hybrid poplar are greatly dependent on the process variables (temperature, reaction time, ethanol concentration, and sulfuric acid dose). In other words, the substrates features are controllable and adjustable by fine-tuning the process variables to generate a desirable substrate for enzymatic hydrolysis. The regression equations developed provide a practical tool to quantitatively predict the substrate characteristics from the pretreatment variables. It is noteworthy that the optimization of the organosolv ethanol pretreatment must consider not only the hydrolysability of resulting substrate but also the recovery of cellulose, hemicellulose, and lignin. Severe processing conditions might generate a readily digestible substrate, but excessive

Table 2
Regression Equations for Prediction of Substrate Characteristics

| Substrate feature | Equation[a] | Equation no. | $R^2$ | Observed value | Calculated value |
|---|---|---|---|---|---|
| Viscosity (mPaS) | Viscosity (mPaS) = $-299.534 + 3.726T + 2.102t + 71.05S - 3.788C - 0.00911T^2 - 0.0115Tt - 0.543TS + 0.0139TC - 0.589tS + 0.0103tC + 0.736SC$ | (2) | 0.9787 | 13.1 | 13.0 |
| Crystallinity (%) | Crystallinity (%) = $512.821 - 3.614T - 0.242t - 116.711S - 2.912C + 0.0111T^2 - 0.00917Tt + 0.00889TC + 1.126tS + 0.0113tC + 23.414S^2 + 0.00574C^2$ | (3) | 0.9764 | 66.4 | 66.2 |
| Fiber length (mm) | Fiber length (mm) = $-12.249 + 0.108T + 0.0425t + 4.672S - 0.0246C - 0.000245T^2 - 0.000155Tt - 0.0171TS + 0.000147TC - 0.0125tS - 0.446S^2$ | (4) | 0.9215 | 0.63 | 0.58 |

[a]$T$, temperature (°C); $t$, reaction time (min) at the temperature; $S$, sulfuric acid dose (percent of dried wood chips [w/w]); $C$, ethanol concentration (v/v [%]).

depolymerization and decomposition of carbohydrate leading to low sugar recovery are undesirable.

## Acknowledgment

The authors are grateful to Jennifer Braun for assistance in measurement of crystallinity. The support of the Natural Sciences and Engineering Research Council of Canada, Natural Resources Canada, and Biological Capital (BIOCAP) Canada Foundation is gratefully acknowledged.

## References

1. Wyman, C. E., Dale, B. E., Elander, R. T., et al. (2005), *Bioresour. Technol.* **96,** 1959–1966.
2. Mosier, N., Wyman, C., Dale, B., et al. (2005), *Bioresour. Technol.* **96,** 673–686.
3. Galbe, M. and Zacchi, G. (2002), *Appl. Microbiol. Biotechnol.* **59,** 618–628.
4. Gorhmann, K., Torget, R., and Himmel, M. (1985), *Biotechnol. Bioeng. Symp.* **15,** 59–80.
5. Allen, S. G., Schulman, D., Lichwa, J., Antal, M. J., Jennings, E., and Elander, R. (2001), *Ind. Eng. Chem. Res.* **40,** 2352–2361.
6. Holtzapple, M. T. and Humphrey, A. E. (1984), *Biotechnol. Bioeng.* **26,** 670–676.

7. Pan, X. J., Arato, C., Gilkes, N., et al. (2005), *Biotechnol. Bioeng.* **90,** 473–481.
8. Stockburger, P. (1993), *Tappi J.* **76,** 71–74.
9. Pye, E. K. and Lora, J. H. (1991), *Tappi J.* **74,** 113–118.
10. Williamson, P. N. (1988), *Sven. Papperstidning-Nord. Cellul.* **91,** 21–23.
11. Lora, J. H. and Glasser, W. G. (2002), *J. Polym. Environ.* **10,** 39–48.
12. Lora, J. H., Creamer, A. W., Wu, L. C. F., and Goyal, G. C. (1991), In: *Proceedings of the 6th International Symposium on Wood and Pulping Chemistry*, May 12–16, Melbourne, Australia Appita, vol. 2, pp. 431–438.
13. Gilarranz, M. A., Oliet, M., Rodriguez, F., and Tijero, J. (1998), *Can. J. Chem. Eng.* **76,** 253–260.
14. Ni, Y. and van Heiningen, A. R. P. (1997), *Pulp Pap. Can.* **98,** 38–41.
15. Diaz, M. J., Alfaro, A., Garcia, M. M., Engenio, M. E., Ariza, J., and Lopez, F. (2004), *Ind. Eng. Chem. Res.* **43,** 1875–1881.
16. Jimenez, L., Perez, I., Garcia, J. C., Lopez, F., and Ariza, J. (2004), *Wood Sci. Technol.* **38,** 127–137.
17. Pan, X. J., Gilkes, N., Kadla, J., et al. (2006), *Biotechnol. Bioeng.* **94,** 851–861.
18. Pan, X. J., Kadla, J. F., Ehara, K., Gilkes, N., and Saddler, J. N. (2006), *J. Agric. Food Chem.* **54,** 5806–5813.
19. Robertson, G., Olson, J., Allen, P., Chan, B., and Seth, R. (1999), *Tappi J.* **82,** 93–98.
20. Vonk, C. G. (1973), *J. Appl. Crystallogr.* **6,** 148–152.
21. Krassig, H. A. (1993), *Cellulose: Structure, Accessibility, and Reactivity*, Gordon and Breach Science Publishers, Yverdon, Switzerland, pp. 88–98.
22. Myers, R. H. and Montgomery, D. C. (2002), *Response Surface Methodology: Process and Product Optimization Using Designed Experiments*, 2nd ed. J. Wiley & Sons, New York, pp. 798.
23. Sinitsyn, A. P., Gusakov, A. V., and Vlasenko, E. Y. (1991), *Appl. Biochem. Biotechnol.* **30,** 43–59.
24. Mansfield, S. D., Mooney, C., and Saddler, J. N. (1999), *Biotechnol. Progr.* **15,** 804–816.
25. Puri, V. P. (1984), *Biotechnol. Bioeng.* **26,** 1219–1222.
26. Martinez, J. M., Reguant, J., Montero, M. A., Montane, D., Salvado, J., and Farriol, X. (1997), *Ind. Eng. Chem. Res.* **36,** 688–696.
27. Valjamae, P., Pettersson, G., and Johansson, G. (2001), *Eur. J. Biochem.* **268,** 4520–4526.
28. Zhang, Y. H. P. and Lynd, L. R. (2004), *Biotechnol. Bioeng.* **88,** 797–824.
29. TAPPI standard (1999), T230 om-99, Viscosity of Pulp (capillary viscometer method), Technical Association of Pulp and Paper Industry (TAPPI).
30. McDonough, T. J. (1993), *Tappi J.* **76,** 186–193.
31. Fan, L. T., Lee, Y. H., and Beardmore, D. R. (1981), *Biotechnol. Bioeng.* **23,** 419–424.
32. Sasaki, T., Tanaka, T., Nanbu, N., Sato, Y., and Kainuma, K. (1979), *Biotechnol. Bioeng.* **21,** 1031–1042.
33. Ramos, L. P., Nazhad, M. M., and Saddler, J. N. (1993), *Enzyme Microb. Technol.* **15,** 821–831.
34. Tanahashi, M., Goto, T., Horii, F., Hirai, A., and Higuchi, T. (1989), *Mokuzai Gakkaishi* **35,** 654–662.
35. Pan, X. J. and Sano, Y. (1999), *J. Wood Sci.* **45,** 319–325.

0273-2289/1559-0291 (Online)/07/136–140/379–394/$30.00

# Liquid Hot Water Pretreatment of Olive Tree Pruning Residues

CRISTÓBAL CARA,[1] INMACULADA ROMERO,[1] JOSE MIGUEL OLIVA,[2] FELICIA SÁEZ,[2] AND EULOGIO CASTRO*,[1]

[1]*Department of Chemical, Environmental and Materials Engineering, University of Jaén, Campus Las Lagunillas, 23071 Jaén, Spain, E-mail: ecastro@ujaen.es; and* [2]*DER-CIEMAT, Avda. Complutense 22, 28040 Madrid, Spain*

## Abstract

Olive tree pruning generates an abundant, renewable lignocellulose residue, which is usually burnt on fields to prevent propagation of vegetal diseases, causing economic costs and environmental concerns. As a first step in an alternative use to produce fuel ethanol, this work is aimed to study the pretreatment of olive tree pruning residues by liquid hot water. Pretreatment was carried out at seven temperature levels in the range 170–230°C for 10 or 60 min. Sugar recoveries in both solid and liquid fractions resulting from pretreatment as well as enzymatic hydrolysis yield of the solid were used to evaluate pretreatment performance. Results show that the enzyme accessibility of cellulose in the pretreated solid fraction increased with pretreatment time and temperature, although sugar degradation in the liquid fraction was concomitantly higher.

**Index Entries:** Biomass; enzymatic hydrolysis; ethanol; liquid hot water pretreatment; olive tree residues; glucose.

## Introduction

Pretreatment is an essential operation in lignocellulosic conversion process because of cellulose resistance to enzymatic hydrolysis *(1)*. Physical pretreatments are usually applied to all biomass feedstock to reduce particle size, thus increasing surface area. Then biomass is pretreated by either water or chemicals at different concentration, temperature, or pressure conditions. Diluted acid pretreatment, especially with $H_2SO_4$, has been extensively applied to lignocellulose raw materials *(2)*. It offers good performance in terms of hemicellulose-derived sugar recoveries but equipment must be acid-resistant, thus increasing costs, and the hydrolyzates must be usually neutralized before using them as a fermentation broth, resulting in a copious solid waste. Water pretreatment, also known as hydrothermal pretreatment, offers several potential advantages compared with diluted acid pretreatment as there is no requirement for purchased acid, for special

*Author to whom all correspondence and reprint requests should be addressed.

equipment materials or for preliminary feedstock size reduction (3), and hydrolyzate neutralization residues are produced in much lower quantities. Steam explosion and liquid hot water (LHW) are common hydrothermal pretreatments applied to lignocellulose materials. Although both pretreatment methods do improve cellulose susceptibility to enzymatic hydrolysis, LHW pretreatment results in higher hemicellulose sugar recovery and lower fermentation inhibiting hydrolyzates than steam explosion pretreatment (4,5). Typical conditions for LHW pretreatment include temperatures around 200°C for a few minutes.

Olive trees are cultivated especially in Mediterranean countries but in the last few years the culture surface is growing worldwide in countries as different as Argentine, Australia, or the United States, reaching more than 8 million ha (6). In olive tree cultivation, old branches must be cut down to regenerate and prepare trees for the next crop. This action, called pruning, is done every 2 yr after olive harvesting and generates a variable amount of lignocellulose residues that has been estimated at 3000.0 kg/ha, as an annual average (7). A typical olive tree pruning lot includes 70% thin branches (by weight, with approx one-third of leaves) and 30% of wood (thick branches, diameter >5 cm approx). Nevertheless, variable amounts and compositions of pruning are possible, depending on culture conditions, production, and local uses. Disposal of pruning residues is necessary to keep fields clean and to prevent propagation of vegetable diseases; usually they are eliminated by either burning or grinding and scattering on fields, causing economic cost and environmental concerns. Olive tree wood is sometimes separated and put to domestic use as firewood but there are no applications on an industrial scale for these residues. As an alternative, olive tree pruning residues may be used as raw material for ethanol production. Pretreatment by steam explosion of olive tree wood has been reported (8) but there is no literature on LHW pretreatment of olive tree pruning residues, to our best knowledge. In this work, LHW pretreatment was applied to olive tree pruning residues at temperatures ranging from 170 to 230°C for 10 or 60 min. The objective of the work is to evaluate the pretreatment performance in terms of sugar yield in the liquid fraction and glucose yield after enzymatic hydrolysis in the solid fraction issued from pretreatment.

## Materials and Methods

### *Raw Material*

Olive tree pruning, discarding thick branches (>5 cm diameter), was collected locally after fruit-harvesting, air-dried at room temperature to equilibrium moisture content of about 10%, milled using a laboratory hammer mill (Retsch GmBH, Haan, Germany) to a particle size smaller than 10 mm, homogenised in a single lot, and stored until used.

### Pretreatment

LHW pretreatment was performed in a laboratory-scale stirred autoclave (model EZE-Seal, Autoclave Engineers, Erie, PA). The reactor has a total volume of 2 L, with an electric heater and magnetic agitation. The temperature/speed controller is a combination of furnace power control and motor speed control with tachometer. Cooling water was circulated through a serpentine coil to cool the reactor content at the end of each run.

Olive tree pruning was pretreated at seven temperature levels in the range of 170–230°C for 10 min and for 60 min at five temperature levels ranging from 170 to 210°C. The amount of dry feedstock loaded was 200.0 g and water was added at 1/5 (w/v) solid/liquid ratio. Both water and raw material were initially at room temperature. Agitation was set at 350 rpm. The average heating rate was 3°C/min. Overpressure in the reactor of 3 MPa was kept to prevent formation of an aqueous vapor phase. Pretreatment time (10 or 60 min) was initiated when the selected pretreatment temperature was reached. After treatment, the reactor was removed from the heating jacket and cooling water was charged through the serpentine coil; furthermore, the reactor vessel was introduced in an ice bath. The content of the reactor cooled down to 80°C in approx 5 min. The reactor was kept sealed, and the slurry agitated until the reactor was cooled to about 40°C. Then the wet material was filtered for solid and liquid recovery. The water-insoluble fraction was washed out with water and analyzed for hemicellulosic sugars, glucose, and acid-insoluble lignin (AIL) content and used as substrate in enzymatic hydrolysis tests. Liquid fraction issued from pretreatment was analyzed for sugars, acetic acid, and sugar-degradation products.

### Enzymatic Hydrolysis Tests

The washed water-insoluble residue of pretreated olive tree pruning was enzymatically hydrolyzed by a cellulolytic complex (Celluclast 1.5 L) kindly provided by Novozymes A/S (Denmark). Cellulase enzyme loading was 15 filter paper units/g substrate. Fungal β-glucosidase (Novozym 188, Novozymes A/S) was used to supplement the β-glucosidase activity with an enzyme loading of 15 international unit/g substrate. Enzymatic hydrolysis was performed in 0.05 *M* sodium citrate buffer (pH 4.8) at 50°C on a rotary shaker (Certomat-R, B-Braun, Germany) at 150 rpm for 72 h and at 5% (w/v) pretreated material concentration. Samples were taken every 24-h for glucose concentration determination. All enzymatic hydrolysis experiments were performed in duplicate and average results were given.

### Analytical Methods

Composition of raw material was determined according to the National Renewable Energy Laboratory (Golden, CO) analytical methods

for biomass (9). Before other determinations, raw material was extracted consecutively with water and with ethanol (two-step extraction procedure). After the first step, the sugar composition of the water-extract was determined by high-performance liquid chromatography (HPLC) in a Waters (Milford, MA) 2695 liquid chromatograph with refractive index detector. An AMINEX HPX-87P carbohydrate analysis column (Bio-Rad, Hercules, CA) operating at 85°C with ultrapure water as a mobile-phase (0.6 mL/min) was used. Free and oligomeric sugar composition were determined before and after a posthydrolysis process consisting in a treatment with sulfuric acid (3% [v/v]) at 121°C and 30 min. The cellulose and hemicellulose content of the extracted solid residue was determined based on monomer content measured after a two-step acid hydrolysis procedure to fractionate the fiber. A first step with 72% (w/w) $H_2SO_4$ at 30°C for 60 min was used. In the second step, the reaction mixture was diluted to 4% (w/w) $H_2SO_4$ and autoclaved at 121°C for 1 h. This hydrolysis liquid was then analyzed for sugar content by HPLC with the Waters liquid chromatograph. The remaining acid-insoluble residue is considered as AIL.

Following LHW-pretreatment, the composition of solid fraction was determined as described for raw material except that no extraction is used. The sugar content (glucose, xylose, arabinose, mannose, and galactose) of the liquid fraction after pretreatment (prehydrolyzate) was determined by HPLC using the same liquid chromatograph. Furfural and hydroxymethylfurfural content was analyzed by HPLC in a 1100 HP (Hewlett Packard, Palo Alto, CA). Liquid chromatograph, equipped with a 1040A Ultraviolet-diode-array detector (Agilent Technologies, Waldbronn, Germany); the separation was performed with a Bio-Rad HPX-87H column, operating at 65°C with 89% $H_2SO_4$ (5 m*M*) and 11% acetonitrile as an eluent at a flow rate of 0.7 mL/min. Acetic, formic, and levulinic acids analysis was carried out with the HPLC system with a refractive index detector mentioned above with a Bio-Rad HPX-87H column at 65°C temperature. The mobile phase was 5 m*M* $H_2SO_4$, at a flow rate of 0.6 mL/min. Glucose concentration from enzymatic hydrolysis samples was measured by an enzymatic determination glucose assay kit (Sigma GAHK-20; Sigma Aldrich Corp., St. Louis, MO). All analytical determinations were performed in duplicate and average results were shown. Relative standard deviations in all cases were less than 5%.

## Results and Discussion

### *Raw Material Composition*

Table 1 summarizes the composition of olive tree pruning residues. Regarding extractives content, water extraction dissolved 27.5% of the raw material. The second extraction step (with ethanol) dissolved 3.9% of the material. Glucose as monomer in the water extract accounted for 3.2% and

Table 1
Raw Material Composition

| Composition | Dry matter (%) |
|---|---|
| Extractives | 31.4 ± 1.6 |
| Glucose | 7.9 ± 0.7 |
| Cellulose as glucose | 25.0 ± 1.2 |
| Hemicellulosic sugars | 15.8 ± 1.2 |
| Xylose | 11.1 ± 0.6 |
| Mannose | 0.8 ± 0.2 |
| Galactose | 1.5 ± 0.2 |
| Arabinose | 2.4 ± 0.2 |
| Acid-insoluble lignin | 16.6 ± 0.5 |
| Acid-soluble lignin | 2.2 ± 0.2 |
| Acetyl groups | 2.5 ± 0.1 |
| Ash | 3.4 ± 0.1 |

Mean values and standard deviations of five determinations.

the subsequent posthydrolysis process led to a total glucose content in extractives of 7.9%.

Cellulose (as glucose) and AIL content (25 and 16.6%, respectively) are smaller than that reported for other agricultural residues *(10)*. Considering acid-soluble lignin content, which refers to the small fraction of lignin that is solubilized during the hydrolysis process used to determine AIL, the total lignin value increases up to 18.8%. Hemicellulosic sugars account for 15.8% of raw material with xylose as the main sugar (70%). Acetyl groups, bound through an ester linkage to branched hemicellulose chains, represented about 2.5% of the initial raw material.

### LHW Pretreatment

Table 2 shows the total gravimetric recovery (solids remaining after pretreatment divided by original oven-dried weight) and the composition of water-insoluble fiber resulting from LHW pretreatment at the different temperatures and times assayed. No influence of pretreatment temperature or time was detected on total material recovery. Around 45% of original material was solubilized as a consequence of pretreatment, except at the softest conditions assayed (170°C, 10 min) wherein the total gravimetric recovery was a little greater. As expected, the content in hemicellulosic sugar of pretreated material decreased as LHW temperature or time increased, vanishing from 220°C in 10 min runs or 200°C in 60 min experiments. Concomitantly, with hemicellulose content decrease, the content in cellulose of pretreated material increased, reaching a maximum of 45.6% at 200°C, and 10 min; beyond this point, a slight solubilization of cellulose was detected increasing in general with time and temperature.

Concerning AIL content, the maximum value of pretreated material should be around 30% (according to initial lignin content and material

Table 2
Composition (Dry Matter [%]) of Water-Insoluble Fiber Resulting From LHW Pretreatment at Different Conditions

| Temperature (°C) | Time (min) | Total gravimetric recovery | Glucose | Xylose | Other sugars[a] | AIL |
|---|---|---|---|---|---|---|
| 170 | 10 | 62.4 | 37.4 | 12.5 | 1.9 | 35.1 |
| | 60 | 55.6 | 42.2 | 4.6 | 0.8 | 45.4 |
| 180 | 10 | 56.8 | 40.5 | 7.2 | 1.5 | 42.7 |
| | 60 | 55.2 | 41.2 | 3.5 | 0.5 | 48.7 |
| 190 | 10 | 54.7 | 43.0 | 4.7 | 1.0 | 43.9 |
| | 60 | 57.4 | 41.9 | 0.9 | 0.3 | 49.7 |
| 200 | 10 | 54.9 | 45.6 | 2.8 | 0.3 | 46.1 |
| | 60 | 57.7 | 41.2 | nd | nd | 52.3 |
| 210 | 10 | 56.0 | 40.7 | 1.0 | nd | 49.4 |
| | 60 | 57.1 | 39.2 | nd | nd | 54.2 |
| 220 | 10 | 56.4 | 40.4 | nd | nd | 52.4 |
| 230 | 10 | 56.6 | 36.3 | nd | nd | 55.9 |

nd: not detected.
[a]Galactose, mannose, and arabinose.

recovery); in contrast, Table 2 shows increasing values of AIL as time or temperature of pretreatment increased. Although this fact is in agreement with hemicellulose solubilization, AIL content values are much greater than they should taking into account just hemicellulose solubilization. A similar result is reported by Ballesteros et al. *(11)* who obtained lignin recovery values that exceeded initial concentration in 20–32% when pretreating olive oil extraction residues, a material with a high extractive content. These results could be explained by the formation of "lignin-like" structures obtained as a result of condensation reactions between lignin and carbohydrate degradation products; interferences in the lignin analysis method from compounds present in the extractive fraction have also been reported in an attempt to explain these unusually high lignin contents *(12)*. In order to clarify this fact, an LHW pretreatment experiment was performed using an olive tree pruning residue lot, which had been previously extracted with ethanol for 24 h. Extraction resulted in the solubilization of about 22% of material (out of 31% present in raw material). When this extractive-free material was submitted to LHW pretreatment at 210°C and 10 min, AIL recovery was significantly lower than that of the unextracted material (22.5% AIL content referred to raw material) (27.6% AIL content referred to raw material), supporting the idea of high extractives content interfering the lignin analysis method. Nonetheless, AIL is still greater than the initial content, probably because of the presence of remaining extractives.

In the water-soluble fraction issued from pretreatment (filtrates), sugars were presented in a considerable proportion as oligomers, so that a posthydrolysis step was performed to determine the total amount of sugars.

Table 3
Composition (Raw Material g/100.0 g) of the Filtrate Resulting From LHW Pretreatment at Different Conditions

| Pretreatment temperature (°C) | 170 | | 180 | | 190 | | 200 | | 210 | | 220 | 230 |
|---|---|---|---|---|---|---|---|---|---|---|---|---|
| Pretreatment time (min) | 10.0 | 60.0 | 10.0 | 60.0 | 10.0 | 60.0 | 10.0 | 60.0 | 10.0 | 60.0 | 10.0 | 10.0 |
| Glucose | 10.1 | 9.2 | 8.9 | 6.2 | 8.2 | 2.6 | 5.9 | 0.5 | 2.8 | 0.1 | 0.8 | 0.2 |
| Xylose | 4.0 | 7.0 | 6.3 | 3.5 | 6.6 | 0.6 | 4.1 | 0.0 | 0.7 | 0.0 | 0.0 | 0.0 |
| Galactose | 1.4 | 1.9 | 1.4 | 0.9 | 1.2 | 0.6 | 1.0 | 0.0 | 0.3 | 0.0 | 0.0 | 0.0 |
| Arabinose | 2.6 | 1.8 | 2.1 | 0.5 | 1.9 | 0.1 | 0.6 | 0.0 | 0.1 | 0.0 | 0.0 | 0.0 |
| Mannose | 0.2 | 0.8 | 0.3 | 0.4 | 0.5 | 0.2 | 0.7 | 0.1 | 0.2 | 0.0 | 0.0 | 0.0 |
| Acetic acid | 0.4 | 1.6 | 0.7 | 2.5 | 1.2 | 3.2 | 2.3 | 3.6 | 2.8 | 4.1 | 3.5 | 3.9 |
| Formic acid | 0.4 | 0.6 | 0.6 | 0.8 | 0.6 | 0.7 | 0.7 | 1.1 | 0.8 | 0.7 | 0.9 | 0.7 |
| Levulinic acid | 0.0 | 0.0 | 0.0 | 0.1 | 0.0 | 0.1 | 0.0 | 0.1 | 0.0 | 0.1 | 0.0 | 0.0 |
| Furfural | 0.1 | 0.4 | 0.2 | 1.4 | 0.5 | 1.7 | 1.2 | 1.3 | 1.6 | 0.7 | 1.7 | 1.2 |
| HMF | 0.2 | 0.5 | 0.3 | 1.1 | 0.6 | 1.8 | 1.0 | 1.9 | 1.4 | 1.1 | 1.7 | 1.5 |
| pH | 3.8 | 3.8 | 3.7 | 3.7 | 3.5 | 3.7 | 3.7 | 3.4 | 3.5 | 3.3 | 3.3 | 3.4 |

The composition of filtrates after LHW pretreatment and posthydrolysis is shown in Table 3. It is worth noting that glucose is the most abundant sugar in the liquid fraction at any conditions; in fact, the highest glucose content (10.1 g/100.0 g raw material, equivalent to a concentration of 20.2 g/L) is found in the filtrate obtained from pretreated material at the softest conditions (170°C, 10 min). Considering that glucose was present at high proportion in the extract fraction of raw material (Table 1), it is likely that the most part of this component was transferred to liquid fraction after pretreatment. This result is in agreement with that reported by Ballesteros et al. *(11)* using olive oil extraction residues. Glucose content of filtrates decreased as a consequence of sugar degradation as either temperature or pretreatment time increased. In contrast, xylose content in the filtrates rose progressively with pretreatment temperature until 190°C (10-min experiments), reaching a maximum value of 13.3 g xylose/L or 6.6 g xylose/100.0 g raw material, and then a decrease was detected; a similar trend was found for the rest of hemicellulosic-derived sugars. Only at the lowest pretreatment temperature (170°C) the content in xylose increased when pretreatment time was changed from 10 to 60 min.

The sugar degradation process observed when the severity of pretreatment was increased is in agreement with the increasing proportion of non-sugar compounds found in the filtrates (Table 3). Acetic acid, furfural, hydroxymethylfurfural (HMF), formic, and levulinic acid are known to act as inhibitors for yeast growth under selected conditions *(13,14)*. For example, the filtrate content in furfural and HMF increased as pretreatment temperature increased, except at 230°C. For a given pretreatment temperature, increasing the process time from 10 to 60 min resulted in an increase of furfural and HMF contents, except at the highest pretreatment (210°C) with 60 min, which showed a decrease, probably owing to further transformation of furfural and HMF into other degradation products, as stated by other authors *(11)*. Regarding other products, organic acids (acetic and formic acid) were observed at all pretreatment conditions; levulinic acid was only detected at 60-min experiments for any pretreatment temperature (except at 170°C). As a whole, the content of filtrates in compounds other than sugars was similar to that reported in the LHW-pretreatment of other lignocellulosic residues as poplar *(15)*, although the proportion of HMF found in olive tree pruning hydrolyzates is somewhat higher, in agreement with a higher glucose composition in filtrates. Moreover, heat-up times (lasting from 40 to 60 min, depending on final process temperature) may also be responsible for the formation of degrading products, especially from extractive soluble glucose.

Table 3 shows also the pH value of hydrolyzates, ranging from 3.3 to 3.8. In general, a slight decrease of pH as a function of pretreatment temperature was detected. Figure 1 illustrates the sugar recovery yield (either referred to glucose or hemicellulosic sugars) in both the water-insoluble fibers and in the filtrates for all experiments performed. This yield is expressed as sugars in the water-insoluble fiber or in the filtrate (referred to

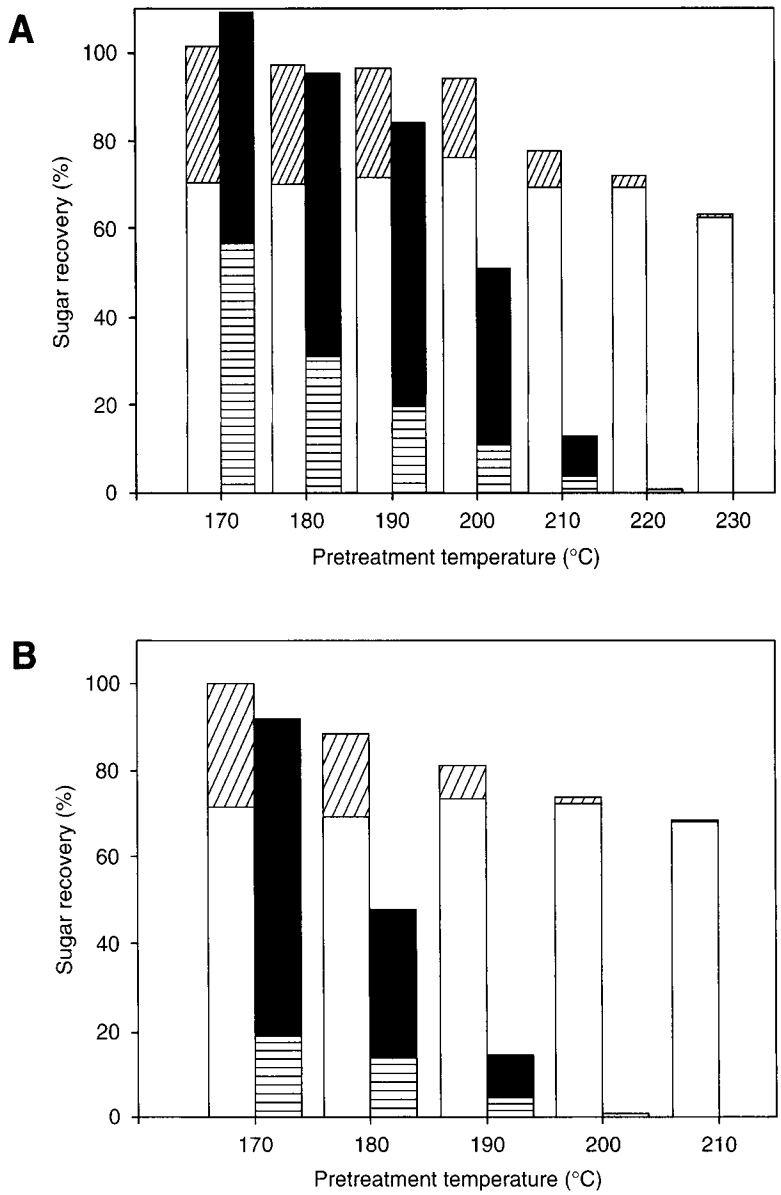


**Fig. 1.** Sugar recovery at different LHW temperatures, expressed as a percentage of the initial content in the raw material. Glucose recovery in solid (▨) and liquid (▨) fractions and hemicellulose-derived sugars recovery in solid (▤) and liquid (■) fractions, **(A)** pretreatment time 10 min and **(B)** pretreatment time 60 min.

original raw material) divided by potential sugars in the raw material. Potential glucose in the raw material (32.9 g/100.0 g, *see* Table 1) has been evaluated taking into account both glucose from cellulose (accounting for 76% of the total glucose) and glucose in the extractive fraction (24%). Glucose recovery yields ranging from 63 to 76% were obtained for pretreated material. However, if just the glucose from cellulose were considered as potential glucose, recovery yields above 90% would be obtained

(regardless of process time) except for the experiment performed at the highest pretreatment temperature (230°C) whereby 82% cellulose recovery yield in solid fraction was determined. This is attributable to cellulose solubilization at these conditions. Regarding the filtrates, glucose recovery yields as high as 30.6% (at the softest conditions) were obtained, owing to glucose from extractives fraction. The higher the pretreatment temperature or time the lower glucose recovery yield. Beyond a pretreatment temperature of 200°C, maintained for 60 min, there is scarcely any glucose left in the filtrates.

Concerning hemicellulose recovery yield in solids, it came down progressively as the pretreatment temperature increased; in the same way, keeping pretreatment temperature for 60 min resulted in a deep decrease of hemicellulose recovery yield, vanishing at a pretreatment temperature of 200°C or above. In the filtrates, a similar drop of hemicellulose recovery yield with pretreatment temperature or time is evidenced for long-time experiments, in agreement with results reported by Laser et al. *(4)*. In the case of 10-min trials, the hemicellulose recovery yield in the liquid fractions rose as a function of pretreatment temperature until 190°C and then it came down; this indicates that sugars released from lignocellulose structure are getting degraded, and hence, poor recoveries in the filtrates are obtained. A different process configuration that better preserves dissolved hemicellulosic sugars, for example, by removing them through continuous percolation, may improve recoveries *(16)*. Although total mass balance (sum of the solubilized and residual solid fractions) moved away from 100% with increasing both pretreatment temperature and time, the susceptibility of the recovered cellulose to enzymatic hydrolysis is also a key aspect in optimizing the overall process and ensuring maximum substrate utilization.

### *Enzymatic Hydrolysis*

To evaluate pretreatment performance the water-insoluble residues were submitted to enzymatic hydrolysis using a cellulose complex (Celluclast 1.5L) supplemented with β-glucosidase (Novozyme 188) and 5% solids concentration. Enzymatic hydrolysis was monitored by sampling every 24 h for a 72-h period. Samples were analyzed for glucose concentration. Results are shown in Table 4. For comparison purposes, enzymatic hydrolysis was also conducted on untreated raw material, with and without enzyme addition. Even when no enzyme was added, 1.6 g glucose/L are solubilized at the hydrolysis conditions (50°C, 72 h), which corresponds to 9.6% of the total potential glucose or 3.2 g/100.0 g raw material, in accordance to the amount detected as free glucose in the first extraction step (*see* Raw Material Composition Section). This amount of glucose will not be available in water-insoluble residues because it is readily solubilized to liquid fractions during pretreatment. When untreated raw material was submitted to enzymatic hydrolysis at the same conditions, the concentration of glucose released after 72 h was greater than that obtained from pretreated material at 170°C for 10 min, because of the

Table 4
Glucose Concentrations (g/L) Obtained by Enzymatic Hydrolysis of Olive Tree Pruning Residues at Varying Pretreatment Conditions

| Pretreatment conditions | | Enzymatic hydrolysis time (h) | | |
|---|---|---|---|---|
| Temperature (°C) | Time (min) | 24 | 48 | 72 |
| 170 | 10 | 2.4 | 2.6 | 2.7 |
| | 60 | 4.3 | 5.5 | 6.6 |
| 180 | 10 | 3 | 3.2 | 3.4 |
| | 60 | 7 | 9.5 | 10.6 |
| 190 | 10 | 4.1 | 4.3 | 4.9 |
| | 60 | 8.4 | 11.6 | 12.7 |
| 200 | 10 | 6.6 | 8.2 | 9.3 |
| | 60 | 11.1 | 13.5 | 15.4 |
| 210 | 10 | 9.8 | 12.8 | 14.3 |
| | 60 | 10.1 | 13.7 | 15.1 |
| 220 | 10 | 11.7 | 14.1 | 15 |
| 230 | 10 | 11.6 | 13.5 | 14 |
| Untreated, no enzyme | | 1.1 | 1.4 | 1.6 |
| Untreated + enzyme | | 2.5 | 2.6 | 2.8 |

aforementioned free glucose present in untreated material. For this reason, comparisons based on enzymatic hydrolysis yields will be done taking into account the difference between glucose concentration obtained from untreated material with and without added enzyme.

Figure 2 shows the enzymatic hydrolysis yields determined from the glucose concentration values at each sampling time (Table 4) and the glucose potential content in the pretreated material (Table 2). As an average, 75% of the enzymatic hydrolysis yield (referred to the yield value at 72 h) was attained within the first 24 h of enzymatic attack. The cellulose digestibility increased as a function of pretreatment temperature and time. This seems to be related to the solubilization of hemicellulosic sugars from the solid (Fig. 1) *(17)*. In fact, the highest enzymatic hydrolysis yields (around 75%) were obtained using solids in which the hemicellulose fraction was completely solubilized, e.g., more than 220°C and 10 min (Fig. 1A) and more than 200°C for 60-min runs (Fig. 1B).

Comparing with untreated material, pretreatment temperatures below 190°C and short times (10 min, Fig. 2A) led to just a slight improvement on enzymatic cellulose accessibility. The pretreatment effect was evidenced from 200°C pretreatment temperature. Enzymatic hydrolysis yields greater than 70% (at 72 h hydrolysis time) were obtained from solids pretreated at 210°C or higher. For a given pretreatment temperature and pretreatment time lasting for 60 min, the enzymatic hydrolysis yields were always higher than those corresponding to short experiments, especially at low pretreatment temperatures. For example, a threefold higher yield was obtained at 180°C for 60 min comparing with 180°C for 10 min.

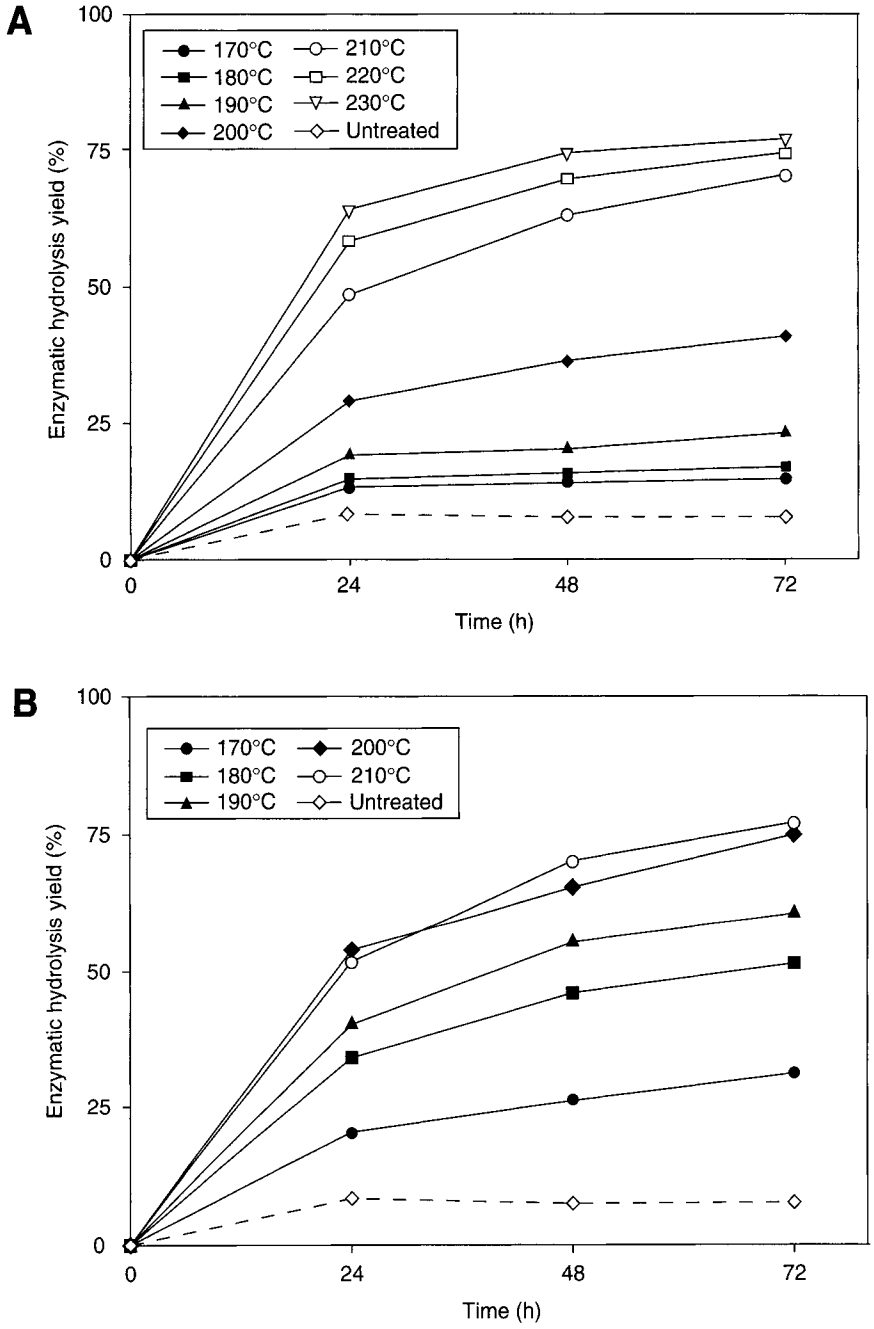


**Fig. 2.** Enzymatic hydrolysis yield expressed as glucose obtained in the enzymatic hydrolysis divided by the potential glucose in pretreated material (%). **(A)** pretreatment time 10 min and **(B)** pretreatment time 60 min.

Although enzymatic hydrolysis yields improved by 10-fold comparing the best results with untreated material, there is still some 20% of cellulose in pretreated materials that is not hydrolyzed after 72 h hydrolysis time. This fraction of unaltered cellulose did not significantly vary even in

7-d hydrolysis experiments. In an attempt to understand whether or not it is possible to attack this cellulose fraction (and to get further improvement on enzymatic yields), a new experimental series was performed by milling previously pretreated solids from 10-min runs until particle sizes decreased to below 1 mm. A slight improvement ranging from 6 to 11% in enzymatic hydrolysis yields was obtained for solids pretreated at low temperatures (170–200°C), whereas no increase on yields was detected when hydrolyzing milled solids pretreated above 210°C. Thus, it seems that there is a recalcitrant cellulose fraction that is not possible to hydrolyze under the assayed operational conditions, probably because of cellulose structural rearrangements that can occur during high-temperature pretreatments *(18)*. Further research on alternative pretreatments or enzymatic hydrolysis configurations should be necessary to improve both glucose yields and raw material utilization.

### *Overall Process Yield*

In order to optimize the overall process, attention must be paid to several partial objectives, e.g., sugars recovery in the filtrate (readily solubilized glucose and hemicellulose-derived sugars), cellulose recovery in the solid residue, and enzymatic hydrolysis performance. Table 5 summarizes the main results achieved when pretreating olive tree pruning residues by LHW. Results are expressed as yields referred to 100.0 g of raw material. Data in liquid-column show yields in sugars (sum of glucose, xylose, mannose, arabinose, and galactose) recovered in filtrates; the highest values are obtained at soft pretreatment conditions (temperatures in the range 170–190°C for 10 min and 170°C for 60 min). It is worth noting that these yields are equivalent to sugars concentrations of around 40.0 g/L in solutions available for fermentation with relatively low concentration of inhibitors (Table 3). Glucose in solid-column in Table 5 includes glucose remaining in solids after pretreatment; significant cellulose losses occurs only at the highest temperature. The subsequent enzymatic hydrolysis performed on pretreated solids led to glucose yields shown in the next column in Table 5. These values take into account both saccharification performance and glucose recovery in pretreated solids (referred to raw material). In contrast to results of liquid-column, the highest glucose yields are obtained at harsh pretreatment conditions. Moreover, enzymatic hydrolysis yields increased as a function of pretreatment temperature and time (Fig. 2), whereas glucose yields in Table 5, which take into account also glucose losses in solids, show a decrease at the experiments performed at the highest pretreatment temperature (230°C, 10 min and 210°C, 60 min). Because of this, no higher values of pretreatment temperatures were assayed. This glucose, released by enzymatic action, is readily fermentable to ethanol, so based on this parameter, best results are obtained in the range of pretreatment temperature of 210–220°C for 10 min or 200–210°C for 60 min.

Table 5
Sugar Yields (Raw Material [g sugar/100.0 g]) From LHW-Pretreatment of Olive Tree Pruning Residues at Varying Pretreatment Conditions

| Temperature (°C) | Time (min) | Liquid[a] | Glucose (in solid)[b] | Glucose from enzyme hydrolysis[c] | Overall glucose yield[d] | Overall sugar yield[e] |
|---|---|---|---|---|---|---|
| 170 | 10 | 18.3 | 23.3 | 3.4 | 13.4 | 21.7 |
| | 60 | 20.7 | 23.5 | 7.3 | 16.5 | 28 |
| 180 | 10 | 19 | 23 | 3.8 | 12.7 | 22.8 |
| | 60 | 11.6 | 22.7 | 11.7 | 17.9 | 23.3 |
| 190 | 10 | 18.3 | 23.5 | 5.4 | 13.6 | 23.8 |
| | 60 | 4.1 | 24.1 | 14.6 | 17.2 | 18.7 |
| 200 | 10 | 12.2 | 25 | 10.2 | 16.1 | 22.4 |
| | 60 | 0.6 | 23.7 | 17.8 | 18.3 | 18.4 |
| 210 | 10 | 4.2 | 22.8 | 16.0 | 18.8 | 20.2 |
| | 60 | 0.1 | 22.4 | 17.2 | 17.3 | 17.3 |
| 220 | 10 | 0.9 | 22.8 | 16.9 | 17.8 | 17.9 |
| 230 | 10 | 0.2 | 20.6 | 15.8 | 16.1 | 16.1 |

[a]Total sugar yield (sum of glucose, xylose, arabinose, mannose, and galactose) in the liquid fraction.

[b]Glucose recovery in solid fractions referred to raw material. Cellulose (as glucose) content in raw material is 25.0 g/100.0 g.

[c]Glucose from 72-h enzymatic hydrolysis at 5% (w/v) pretreated material concentration.

[d]Sum of glucose from enzymatic hydrolysis and glucose in liquid fraction (total glucose content in raw material is 32.9 g/100.0 g).

[e]Sum of glucose from enzymatic hydrolysis and total sugars in liquid fraction (total sugar content in raw material is 48.6 g/100.0 g).

Values in overall glucose yield-column represent the sum of glucose obtained by enzymatic hydrolysis and glucose contained in liquid fractions. Finally, the overall sugar yield-column takes into account all sugars available, e.g., those coming from liquid fractions and glucose from enzymatic hydrolysis. Although relatively good results in terms of overall sugar yields are obtained at soft conditions (170°C for 60 min), the bioconversion of hemicellulose-derived sugars is more difficult as pentose-fermenting microorganisms are required *(19,20)*. Moreover, the pretreated solids would be used in a very limited extension.

To make use of most of the sugars in this raw material under the assayed conditions, some other process configurations might be considered. For example, a two-step process could be an interesting option. In the first one, conducted at low pretreatment temperature, hemicellulosic sugars, and the fraction of glucose easily solubilized would be recovered in the filtrate. The second step, at more severe conditions, would improve cellulose digestibility by enzymatic hydrolysis. Another alternative approach is the use of dilute acids in the pretreatment. Further research on these points is needed.

## Conclusion

A characteristic feature of olive tree pruning residues is the presence of a readily soluble glucose proportion that accounts for up to 7.9% of raw material. When pretreating these residues by LHW this glucose will enter the liquid fraction together with hemicellulose sugars. Up to 57.6% of total sugars (most of them solubilized in the liquid fraction) in raw material may be available at 170°C pretreatment temperature for 60 min. Nevertheless, the resulting solid fraction offers poor digestibility to enzymatic hydrolysis. In contrast, 57.1% of total glucose, easier to convert into ethanol than a sugar mixture, is made available by pretreatment at 210°C for 10 min. The huge amount of olive tree pruning residues yearly generated, the need of disposal, their low cost, and the lack of economic alternatives make these residues deserve a deeper study for ethanol conversion.

## Acknowledgments

This work was partially financed by Ministerio de Educación y Ciencia (Project ENE2005-08822) and FEDER funds. Financial support from Azucareras Reunidas de Jaén, S. A. is also gratefully acknowledged.

## References

1. Mosier, N., Wyman, C., Dale, B., et al. (2005), *Biores. Technol.* **96,** 673–686.
2. Nguyen, Q., Tucker, M. P., Keller, F. A., Beaty, D. A., Connors, K. M., and Eddy, F. P. (1999), *Appl. Biochem. Biotechnol.* **77–79,** 133–142.
3. Van Walsum, G. P., Allen, S. G., Spencer, M. J., Laser, M. S., Antal, M. J., and Lynd, L. R. (1996), *Appl. Biochem. Biotechnol.* **57–58,** 157–169.
4. Laser, M., Schulman, D., Allen, S. G., Lichwa, J., Antal, M. J., and Lynd, L. R. (2002), *Biores. Technol.* **81,** 33–44.
5. Allen, S. G., Kam, L. C., Zemann, A. J., and Antal, M. J., Jr. (1996), *Ind. Eng. Chem. Res.* **35,** 2705–2715.
6. FAO (2006), http://faostat.fao.org/faostat. Accessed May 20, 2004.
7. Sánchez, S., Moya, A. J., Moya, M., et al. (2002), *Ing. Quím.* **34,** 194–202.
8. Cara, C., Ruiz, E., Ballesteros, I., Negro, M. J., and Castro, E. (2006), *Proc. Biochem.* **41,** 423–429.
9. National Renewable Energy Laboratory (NREL). Chemical analysis and testing laboratory analytical procedures. LAP-002 (1996). LAP-003 (1995). LAP-004 (1996). LAP-005 (1994). LAP-010 (1994) and LAP-017 (1998). NREL, Golden, CO, USA. http://www.eere.energy.gov/biomass/analytical_procedures.html. Accessed May 20, 2004.
10. Sun, Y. and Cheng, J. (2002), *Biores. Technol.* **83,** 1–11.
11. Ballesteros, I., Oliva, J. M., Negro, M. J., Manzanares, P., and Ballesteros, M. (2002), *Appl. Biochem. Biotechnol.* **98–100,** 717–732.
12. Zimbardi, F., Ricci, E., Viola, E., Cuna, D., Cardinale, G., and Cardinale, M. (2001), First World Conference on Biomass for Energy and Industry, vol. 2, James & James, London, pp. 1525–1528.
13. Larsson, S., Palmqvist, E., Hahn-Hägerdal, B., et al. (1999), *Enzyme Microb. Technol.* **24,** 151–159.
14. Helle, S., Cameron, D., Lam, J., White, B., and Duff, S. (2003), *Enzyme Microb. Technol.* **33,** 786–792.
15. Negro, M. J., Manzanares, P., Ballesteros, I., Oliva, J. M., Cabañas, A., and Ballesteros, M. (2003), *Appl. Biochem. Biotechnol.* **105–108,** 87–100.

16. Liu, C. and Wyman, C. E. (2005), *Biores. Technol.* **96,** 1978–1985.
17. Yang, B. and Wyman, C. E. (2004), *Biotechnol. Bioeng.* **86(1),** 88–95.
18. Mok, W. S. and Antal, J. (1992), *Ind. Eng. Chem. Res.* **31,** 1157–1161.
19. De Bari, I., Cuna, D., Nanna, F., and Giacobbe, B. (2004), *Appl. Biochem. Biotechnol.* **113–116,** 539–557.
20. Lin, Y. and Tanaka, S. (2006), *Appl. Microbiol. Biotechnol.* **69,** 627–642.

0273-2289/1559-0291 (Online)/07/136–140/395–406/$30.00

# Ammonia Fiber Expansion Pretreatment and Enzymatic Hydrolysis on Two Different Growth Stages of Reed Canarygrass

TAMIKA C. BRADSHAW, HASAN ALIZADEH, FARZANEH TEYMOURI, VENKATESH BALAN, AND BRUCE E. DALE*

*Department of Chemical Engineering and Materials Science, Biomass Conversion Research Laboratory, 2527 Engineering Building, Michigan State University, East Lansing, MI 48824, bdale@egr.msu.edu*

## Abstract

Plant materials from the vegetative growth stage of reed canarygrass and the seed stage of reed canarygrass are pretreated by ammonia fiber expansion (AFEX) and enzymatically hydrolyzed using 15 filter paper units (FPU) cellulase/g glucan to evaluate glucose and xylose yields. Percent conversions of glucose and xylose, effects of temperature and ammonia loading, and hydrolysis profiles are analyzed to determine the most effective AFEX treatment condition for each of the selected materials. The controls used in this study were untreated samples of each biomass material. All pretreatment conditions tested enhanced enzyme digestibility and improved sugar conversions for reed canarygrass compared with their untreated counterparts. Based on 168 h hydrolysis results using 15 FPU Spezyme CP cellulase/g glucan the most effective AFEX treatment conditions were determined as: vegetative growth stage of reed canarygrass—100°C, 60% moisture content, 1.2 : 1 kg ammonia/kg of dry matter (86% glucose and 78% xylose) and seed stage of reed canarygrass—100°C, 60% moisture content, 0.8 : 1 kg ammonia/kg of dry matter (89% glucose and 81% xylose). Supplementation by commercial Multifect 720 xylanase along with cellulase further increased both glucose and xylose yields by 10–12% at the most effective AFEX conditions.

**Index Entries:** Ammonia fiber expansion; biomass; enzymatic hydrolysis; pretreatment; reed canary grass; cellulosic ethanol.

## Introduction

The United States fuel ethanol industry is currently producing over 4 billion gal/yr of ethanol from starch and sugar sources, primarily corn grain *(1–3)*. However, starches and sugars are only a small fraction of total biomass materials. Biomass is the only potentially renewable source of organic chemicals, organic materials, and liquid transportation fuels *(4)*. Biomass is also relatively inexpensive and compares favorably

*Author to whom all correspondence and reprint requests should be addressed.

with petroleum on a cost per pound basis, and frequently, on a cost per unit of energy *(4)*. However, the cellulosic portion of biomass represents an immense potential source of sugars, which await development of the technology necessary for its economical utilization. Cellulose and hemicellulose form the bulk of most biomass, and effective ethanol production from these components can expand the types and availability of feedstock (5). Cellulosic biomass as an alternate feedstock could provide very large quantities of ethanol with considerable environmental benefits. Bioethanol is an alternative fuel currently used as a gasoline additive to reduce carbon monoxide and other toxic air emissions, ground level ozone formation, and to boost octane.

Unfortunately, there is an as-yet unresolved technical problem impeding large-scale bioethanol production. Lignocellulosic biomass is resistant to enzymatic hydrolysis as a result of many physical and chemical factors. The strong bonding between cellulose, hemicellulose, and lignin within the crystalline regions of lignocellulose makes it rather difficult to degrade the sugar polymers in the cell wall. Enzymatic hydrolysis of this material is possible but requires pretreatment of the cellulosic material before the enzymes can access the sugar polymers *(6)*. Pretreatment is an essential process for enhancing the reactivity toward enzymatic hydrolysis. Pretreatment alters the structure of cellulosic biomass to make cellulose more accessible to the enzymes that convert the carbohydrates into fermentable sugars *(7)*. The ammonia fiber expansion (AFEX) process might offer both an effective and economically attractive means of increasing yields of fermentable sugars from lignocellulosic biomass *(8)*. AFEX has been shown to decrease cellulose crystallinity and particle size, whereas increasing the surface area exposed to enzymatic attack *(9,10)*.

This article focuses on the effectiveness of AFEX-pretreated reed canarygrass (RCG) at different plant growth stages. RCG is also a potential biofuel raw material, and is a cool season grass alternative to switch grass (SWG). RCG's rhizomatous growth habit also makes it appealing, particularly on soils wherein SWG, a bunchgrass, does not form thick stands and wherein erosion is a problem *(1)*. The vegetative stage (the period when leaves begin to grow) is the earliest stage of grass maturity. It is followed by the jointing, boot, heading, blooming, and finally, the seed development stages.

The objectives of this study were to evaluate suitable AFEX treatment conditions for different growth stages of RCG, estimate glucose and xylose yields obtainable, and to explore the effects of maturity in plants. The most effective AFEX treatment condition that provides the highest percentage conversions for both glucose and xylose were observed for the selected materials at a fixed enzyme loading. An additional objective was to determine the effects of supplementing the cellulase mixture, which is deficient in xylanase (containing approx 1% xylanase), with additional commercial xylanase.

## Materials and Methods

### Biomass

Materials utilized were the vegetative growth stage of RCG (VRCG) and the seed stage of RCG (SRCG). RCG was dried and ground through a 1-mm screen in a Wiley mill at the Dairy Forage Research Center (Madison, WI). The cell wall carbohydrates (cellulose, xylan, arabinan, galactan, and mannan), soluble carbohydrate (glucose, fructose, sucrose, raffinose, and stachyose), and storage carbohydrate (fructans in RCG) composition for the biomass are summarized in Table 1 for RCG. Ash content and lignin content of these samples were reported elsewhere *(11)*.

### AFEX Pretreatment

AFEX, a physio-chemical pretreatment, is a process in which concentrated ammonia is used to treat biomass at a desired residence time for a given temperature, moisture content, and ammonia loading. The pressure is released rapidly causing the biomass to expand. The pretreated biomass is kept in a fume hood overnight to remove ammonia. After the ammonia has evaporated, the biomass is ready for hydrolysis. More details about the AFEX reactors are available elsewhere *(10,12)*. For this work, AFEX pretreatment conditions varied were temperature (80–120°C) and ammonia loading (0.8, 1.0, and 1.2 kg/1 kg dry biomass) at fixed 60% moisture content (dry weight basis). The moisture condition was fixed at 60% based on our experience in pretreating other grass materials like corn stover and rice straw using AFEX *(13,14)*. Usually, it takes 30–40 min to pretreat 25.0 g of biomass from start to the end. It has to be noted that AFEX is a dry-to-dry process and the glucan content remains the same even after pretreatment unless the sample is washed before hydrolysis. Separate glucan analyses were done using National Renewable Energy Laboratory (NREL, Golden, CO) protocol *(11)* when the samples were washed.

### Enzymatic Hydrolysis

AFEX-treated and untreated materials were washed with water (1.0 g/10 mL water) according to the NREL protocol. Enzymatic hydrolysis was then done using NREL standard procedure (LAP 009) at 15 FPU cellulase/g glucan. Each experiment was done in duplicate *(13,14)*. Hydrolysis was performed simultaneously for each AFEX-treated and untreated sample using Spezyme CP cellulase enzyme (59 FPU/mL and 142 mg/mL; Genencor International, Inc., Rochester, NY) and Novozyme 188 β-glucosidase (64 para-nitro-phenyl glucoside unit [pNPGU]; cellobiase; Sigma, St. Louis, MO). The Spezyme CP cellulase mixture also contains a small amount (about 1% by mass) of hemicellulase activity. The hydrolysis was done using 1% glucan loadings (0.15 g glucan and 15 mL total sample volume) in capped vials, which were placed in an incubator at 50°C, 90 rpm

Table 1
Carbohydrate Composition of Biomass Forage Samples

| | Cell wall structural carbohydrates | | | | | | | | Soluble carbohydrates | | | | | | Total carbohydrates | |
|---|---|---|---|---|---|---|---|---|---|---|---|---|---|---|---|---|
| Biomass | Glc | Xyl | Ara | Gal | Man | Rha | Fuc | UA | Glc | Fru | Suc | Raf | Sta | Storage[a] | NSC | SC |
| *RCG*[b] | | | | | | | | | | | | | | | | |
| VRCG | 209 | 117 | 30 | 16 | 6 | 1 | 1 | 22 | 4 | 5 | 69 | 3 | 0 | 35 | 116 | 402 |
| SRCG | 265 | 163 | 28 | 13 | 6 | 1 | 1 | 21 | 2 | 12 | 30 | 0 | 1 | 54 | 99 | 498 |

NSC, nonstructural carbohydrates; SC, structural carbohydrates; Glc, glucose; Xyl, xylose; Ara, arabinose; Gal, galactose; Man, mannose; Rha, rhamnose; Fuc, fucose; UA, uronic acids; Fru, fructose; Suc, sucrose; Raf, raffinose; Sta, stachyose; RCG, reed canarygrass; VRCG, vegetative stage; SRCG, seed stage.
From ref. *10*.

[a]Storage carbohydrate for SWG was starch. RCG had fructans in the vegetative sample (37.0 g/kg).

[b]Data for RCG are for whole herbage (g/kg DM).

for 168 h as described in the procedure. Samples of 1 mL were taken periodically at 24, 72, and 168 h interval, respectively. Each collected sample was centrifuged and filtered through a 0.2 μm syringe filter containing a nylon membrane into a high-performance liquid chromatography (HPLC) vial and frozen at –20°C, until further analysis.

In some experiments, Multifect 720 xylanase (42.0 mg/mL; Genencor International, Rochester, NY) was added to the cellulase and β-glucosidase mixtures to determine the effect of xylanase on glucose and xylose yields. Each xylanase was loaded at 10–50% (by weight) of the cellulase loading. The samples were hydrolyzed for 168 h and analyzed for glucose and xylose conversions using HPLC. Control experiments were done without adding enzymes to determine the amount of free sugars in both growth stages of RCG. These free sugars were subtracted from the results for enzymatically hydrolyzed samples. Thus, the enhanced sugar yields reported here result from hydrolysis of structural carbohydrates.

### *Analytical Methods*

The HPLC system consisted of Waters (Milford, MA) Pump and Waters 410 refractive index detector, and an Aminex HPX-87P carbohydrate analysis column (Bio-Rad, Hercules, CA) equipped with a deashing guard cartridge (Bio-Rad). Degassed HPLC grade water was used as the mobile phase at 0.6 mL/min at a column temperature of 85°C. The injection volume was 20 μL with a run time of 20 min. Mixed sugar standards were used for quantification of cellobiose and other monosaccharides (glucose, xylose, galactose, arabinose, and mannose) in the samples. More details about the glucose and xylose conversions are given in NREL protocol (LAP009).

## Results and Discussion

### *Vegetative RCG*

Figure 1A shows glucose and xylose yields for VRCG (untreated and treated) after 168 h of hydrolysis. Percent conversions ranged from 48 to 86% for glucan and 33 to 78% for xylan based on cell wall composition. Temperature affects the amount of ammonia vaporized during the explosive flash (for AFEX) *(7)*. It appears that at the lowest temperature (80°C) tested, more ammonia must be used (>1.2 kg ammonia : 1 kg dry matter [DM]) to achieve higher glucose conversion, whereas at a higher temperature (100°C), less ammonia (1 kg ammonia : 1 kg DM) achieved higher glucose conversion. More ammonia vapors flash at higher reactor temperatures, causing greater disruption of the fibrous structure *(7)*. Temperature also likely influences the nature of ammonia's reaction with lignin and the extent of alkaline hydrolysis of hemicellulose. Elevating the temperature beyond 100°C reduced conversion yields for both glucose and xylose. Experimental work to better understand possible deleterious effects of pretreatment done at high temperature is underway. The most effective AFEX condition for

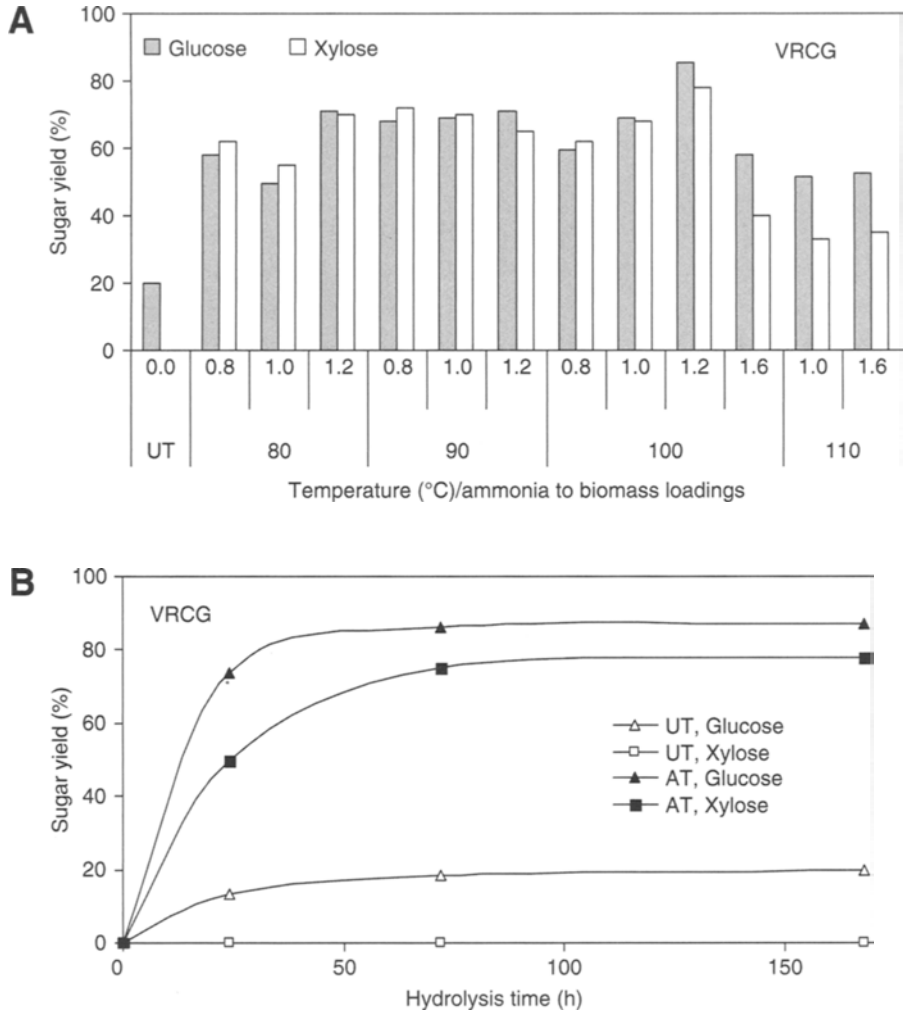


**Fig. 1.** Glucan and xylan conversions for untreated and AFEX-treated VRCG. **(A)** AFEX pretreatment screening was done with 60% moisture in the biomass and by varying the temperature and ammonia-to-biomass loadings. Hydrolysis experiments were done using 15 FPU cellulase/g of glucan and sugar concentration measured at 168 h using HPLC. The sugar conversions are an average of two independent analyses and are consistent with an error range of ±2%. **(B)** Time-course experiments were done to measure glucose and xylose yield for the best AFEX-treated conditions (100°C, 1.2 : 1 ammonia-to-biomass, 60% moisture).

VRCG was found to be 100°C, 60% moisture, 1.2 kg : 1 kg (ammonia : DM), which yielded 86% of theoretical glucose based on cell wall glucan and 78% xylose conversion based on measured cell wall xylan (Table 1).

Although temperature and ammonia loading were increased beyond our usual AFEX pretreatment conditions for SWG *(12)* to explore the possibility of achieving higher yields for both glucose and xylose, VRCG did not behave well under such conditions. Nonetheless, AFEX-treated VRCG

increased glucan conversion by 66 percentage points (pp) and 78 pp for xylan over conversions observed for untreated VRCG.

Figure 1B shows the hydrolysis profile for AFEX-treated and untreated VRCG at an enzyme level of 15 FPU cellulase/g glucan. Results from both the most effective and least effective AFEX treatment conditions for VRCG and untreated VRCG are plotted herein. It is interesting to note that the xylose content of untreated VRCG is completely resistant to enzymatic hydrolysis, whereas about 20% glucose conversion occurs at 168 h hydrolysis. With AFEX pretreatment, more structural carbohydrates are apparently exposed allowing the enzymes to better digest VRCG, increasing both glucose and xylose conversions. For example, after only 24 h of hydrolysis, the most effective AFEX condition observed for VRCG (100°C, 60%, 1.2 kg ammonia : 1 kg DM) generated approx 60 pp more glucose and 50 pp more xylose than did untreated VRCG. By 72 h of hydrolysis, the treated VRCG produced 68 pp more glucose and 75 pp more xylose than did untreated material. The data show that by the end of hydrolysis (for the most effective AFEX condition), glucose and xylose yields increased by 68 and 78 pp, respectively, with AFEX pretreatment. The hydrolysis profile also summarizes the time needed to completely digest the samples. Figure 1B shows that at the most, effective AFEX condition for VRCG reached a peak for glucose and xylose conversion after 72 h hydrolysis.

### *Seed Stage RCG*

Hydrolysis of SRCG (including untreated SRCG) was observed by measuring glucose and xylose conversions under various pretreatment parameters. Figure 2A displays the 168 h conversions for SRCG. The pretreatment effectiveness improved at each temperature with increasing ammonia loading up to 100°C. However, after 100°C, the conversion levels begin to decrease with increasing ammonia loading. Ammonia can react with lignocellulosics by ammonolysis of the ester crosslinks of some uronic acids with the xylan units *(15)*, and by cleaving the bond linkages between hemicellulose and lignin *(16)*. It is possible that extra liquid ammonia plasticizes the cellulose and thereby reduces the disruptive effect of sudden pressure release *(17)*. In Fig. 2A, SRCG treated at different conditions (90°C, 60%, and 1.2), (100°C, 60%, and 0.8), and (100°C, 60%, and 1) provides 89% conversion for glucose and 81% for xylose, respectively.

Figure 2B illustrates the hydrolysis profile for the most and least effective AFEX conditions for SRCG and untreated SRCG at 15 FPU cellulase/g glucan enzyme loadings. It is apparent from Fig. 2B that the structure of SRCG is disrupted by AFEX allowing nearly 4.4 times more glucose and a 50 pp increase in xylose yield with the most effective AFEX condition compared with untreated SRCG at the end of 24 h. At 72 h of hydrolysis, glucose and xylose conversions were consistent with 24 h results for the most effective AFEX condition for SRCG. However, the glucan conversion for the untreated sample increased by 9 pp. By the end of 168 h of

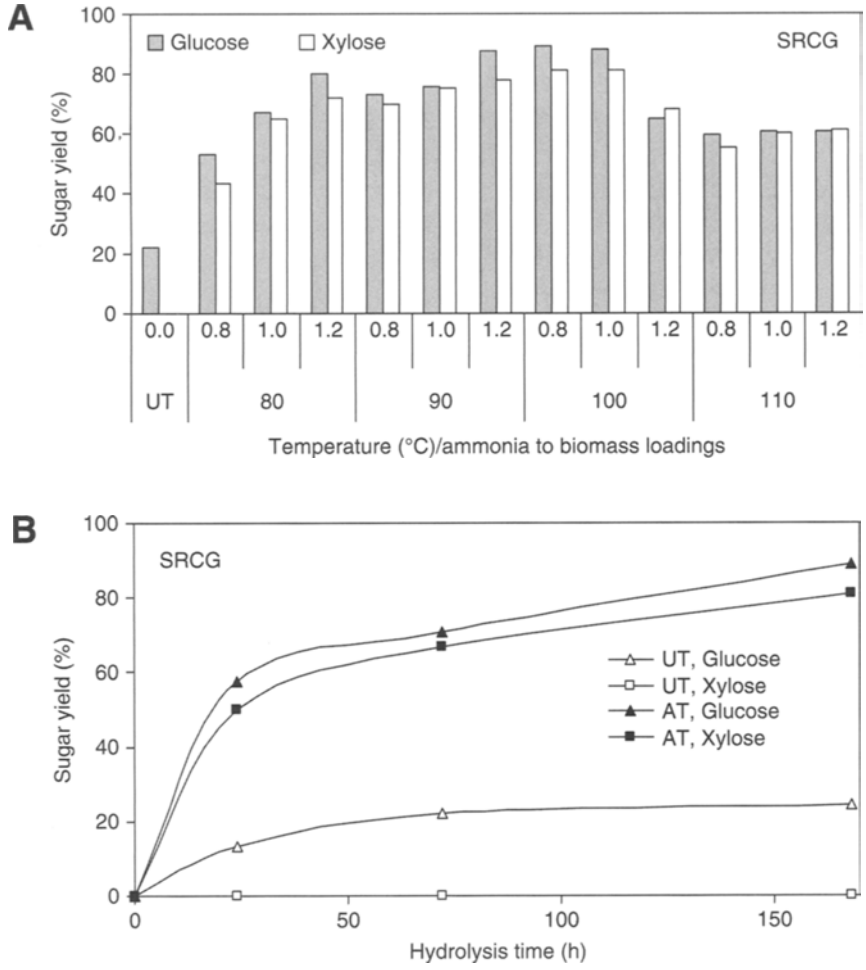


**Fig. 2.** Glucan and xylan conversions for untreated and AFEX-treated SRCG. **(A)** AFEX pretreatment screening was done with 60% moisture in the biomass and by varying the temperature and ammonia-to-biomass loadings. Hydrolysis experiments were done using 15 FPU cellulase/g of glucan and sugar concentration measured at ses. **(B)** Time-course experiments were done to measure glucose and xylose yield for the best AFEX-treated conditions (100°C, 1 : 1 ammonia-to-biomass, 60% moisture).

hydrolysis, conversion of AFEX-treated SRCG increased 18 pp and 14 pp for both glucan and xylan, respectively, compared with the 72 h results. Just 2 pp improvement in glucan conversion was noticed in the untreated sample. Glucose and xylose yields show 65 pp and 81 pp, respectively, enhancement for AFEX-treated SRCG (100°C, 60%, and 0.8) over the untreated sample. Again, as observed for VRCG, the xylan portion of the untreated SRCG is completely resistant to enzymatic hydrolysis. The maximum xylose conversion for the most effective AFEX condition is obtained at 168 h, producing only 80% of theoretical conversion.

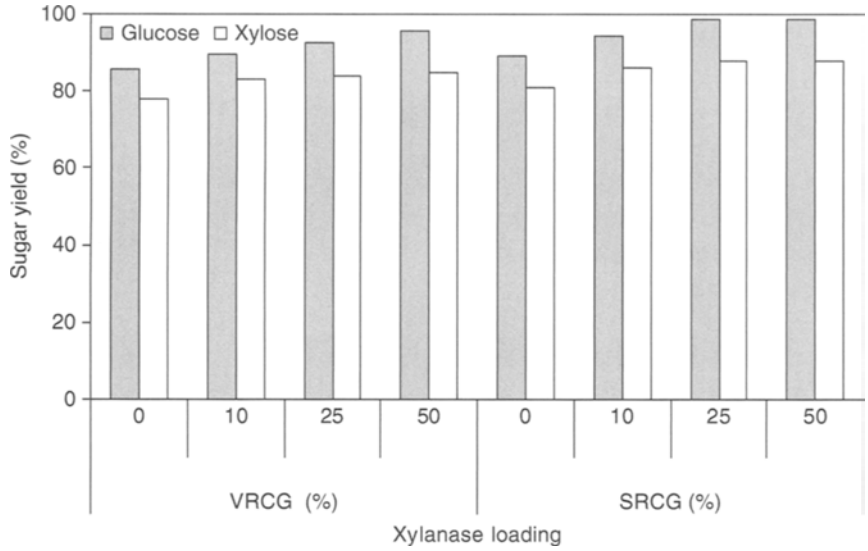


**Fig. 3.** Effect of xylanase supplementation along with cellulase (15FPU/g of glucan), Glucan, and xylan conversions for untreated and AFEX-treated VRCG and SRCG. Hydrolysis experiments were done using 15 FPU cellulase/g of glucan with xylanase (protein concentration 42.0 mg/mL) supplementation (10, 25, or 50%) of the total milligrams of cellulase protein (protein concentration 142 mg/mL). The sugar concentration was measured at 168 h using HPLC.

## *Cellulase and Xylanase Combination*

Samples treated at the most effective AFEX condition found for each of the materials were enzymatically hydrolyzed for 168 h with a combination of Spezyme CP cellulase and Multifect 720 xylanase at 15 FPU cellulase/g glucan. The AFEX-treated samples were tested at various xylanase loadings (10, 25, and 50%, by weight, respectively) of the cellulase loading. Figure 3 shows the increase in glucose and xylose conversions attained for the most effective AFEX conditions for VRCG and SRCG for this specific enzyme combination. Multifect 720 xylanase was shown to enhance both glucose and xylose conversions for all the three samples.

Unlike the glucose conversion shown in Fig. 3, the xylose conversions steadily increased with increasing xylanase loading. At a 10% xylanase loading, both maturity stages for RCG produced about 4 pp higher glucan and xylan conversions. At 25% xylanase loading, the glucan conversion for RCG nearly doubled, whereas the xylan conversion gradually increased by 1 and 2 pp for VRCG and SRCG, respectively. As observed at 50% xylanase loading, VRCG continued to progress, whereas SRCG showed no change with the increase of xylanase compared with 25% xylanase loadings. We conclude that the commercial xylanse is not particularly suited to hydrolyze the hemicellulose in RCG, but that even small increases in xylan conversion promote significant increases in glucan conversion.

*Discussion*

RCG show enhanced glucan and xylan conversions following AFEX pretreatment. The maturity of the materials apparently influenced the conversion of sugars. In a previous study, it was shown that the maturity level for RCG and SWG affected the lignin concentrations, which could explain the rapid digestion observed for vegetative stage compared with seed stage *(11)*. Our results further confirm their hypothesis. Dien et al. *(11)* provided the lignin content as 109 (g/kg DM) for VRCG and 148 (g/kg DM) for SRCG. Consequently, the lignin content is lower for VRCG (which is an earlier stage of RCG) compared with those of SRCG, and might be a major reason why higher percent conversions were achieved with VRCG than with SRCG. Lignin concentrations also increased for the more mature samples *(11,18,19)*. Therefore, more mature stages of RCG gave higher lignin content as well as higher concentrations in structural and nonstructural carbohydrates *(11)*. Because the lignin content is higher for more mature materials, hydrolyzing the sugars from these materials would probably require more enzyme or more extreme pretreatment conditions to achieve higher conversions. A material in its earlier stage growth with lower lignin content would be expected to show higher conversions with less hydrolysis time (or digestion), as observed here *(11,20)*.

The protein content in the vegetative stage is greater compared with the seed stage. Protein could bind degradation products produced during AFEX, and hence, reduce possible enzyme inhibition. Our results also show that xylanase formulations need to be improved in order to get maximal conversion of the hemicellulose to xylose for RCG and likely for other grass materials. However, even small increases in xylan conversion appear to greatly increase glucan conversion. Both the glucan and xylan conversions reported in the paper are understated owing to uncertainties associated with glucan estimation after washing. That is, the actual conversions are somewhat higher than we claim here. More experiments are under way to understand the degradation products formed during pretreatment. Removal of these degradation products may enhance enzyme activity and reduce possible inhibition of microbes in downstream processing.

## Acknowledgments

We sincerely thank our colleagues from the USDA: Drs. Bruce Dien, Hans Jung, Kenneth Vogel, Michael Casler, JoAnn Lamb, Loren Iten, Robert Mitchell, and Gautum Sarath for supplying two different stages of RCG and for the detailed analytical data on these materials that allowed us to perform this work.

## References


1. Dale, B. (2002), *Encyclopedia of Physical Science and Technology*, 3rd ed. vol. 2, pp. 141–157.
2. Gray, K. A., Zhao, L., and Emptage, M. (2006), *Curr. Opin. Chem. Biol.* **10,** 141–146.
3. Dale, B. (1987), *Trends Biotechnol.* **5,** 287–291.
4. Dale, B., Leong, C., Pham, T., Esquivel, V., Rios, I., and Latimer, V. (1996), *Bioresour. Technol.* **56,** 111–116.
5. Williams, K. (1995), http://www.agron.iastate.edu/moore/434/chapter7.htm.
6. Mes-Hartee, M., Dale, B. E., and Craig, W. (1998), *Appl. Microbiol. Biotechnol.* **29,** 462–468.
7. Mosier, N., Wyman, C., Dale, B., et al. (2005), *Bioresour. Technol.* **96,** 673–686.
8. Lemus, R. E., Brummer, C., Moore, K. J., Molstad, N. E., Burras, C. E., and Barker , M. F. (2002), *Biomass Bioenergy* **23,** 433–442.
9. Dale, B., Henk, L., and Shiang, M. (1985), *Dev. Ind. Microbiol.* **26,** 223–233.
10. Chundawat, S. P. S., Venkatesh, B., and Dale, B. E. (2007), *Biotechnol. Bioeng.* **96,** 219–231.
11. Dien, B., Jung, H., Vogel, K., et al. (2006), *Biomass Bioenergy* **30,** 880–891.
12. Alizadeh, H., Teymouri, F., Gilbert, T. I., and Dale, B. E. (2005), *Appl. Biochem. Biotechnol.* **121–124,** 1133–1141.
13. Gollapalli, L. E., Dale, B. E., and Rivers, D. M. (2002), *Appl. Biochem. Biotechnol.* **98–100,** 23–35.
14. Teymouri, F., Laureano-Perez, L., Alizadeh, H., and Dale, B. E. (2004), *Appl. Biochem. Biotechnol.* **113–116,** 951–963.
15. O'Connor, J. J. (1972), *Tappi* **55,** 353.
16. Wang, P., Bolker, H., and Purves, C. (1967), *Tappi* **50,** 123–124.
17. Rowland, S. (1975), *Biotechnol. Bioeng.* **21,** 1031–1042.
18. Holtzapple, M. T., Jun, J. H., Ashok, G., Patibandla, S., and Dale, B. E. (1991), *Appl. Biochem. Biotechnol.* **28–29,** 59–72.
19. McLaughlin, S. B., Bransby, D. I., and Parrish, D. (1994), (http://www.osti.gov/energy citations/servlets/purl/10189529-mvgLAy/webviewable/10189529.pdf) (accessed date Feb. 2007).
20. Fan, L., Lee, Y. Y., and Beardmore, D. (1980), *Biotechnol. Bioeng.* **22,** 177–199.

0273-2289/1559-0291 (Online)/07/136–140/407–422/$30.00

# Mitigation of Cellulose Recalcitrance to Enzymatic Hydrolysis by Ionic Liquid Pretreatment

ANANTHARAM P. DADI, CONSTANCE A. SCHALL, AND SASIDHAR VARANASI*

*Department of Chemical and Environmental Engineering, The University of Toledo, Toledo, OH 43606, USA, E-mail: sasidhar.varanasi@utoledo.edu*

## Abstract

Efficient hydrolysis of cellulose-to-glucose is critically important in producing fuels and chemicals from renewable feedstocks. Cellulose hydrolysis in aqueous media suffers from slow reaction rates because cellulose is a water-insoluble crystalline biopolymer. The high-crystallinity of cellulose fibrils renders the internal surface of cellulose inaccessible to the hydrolyzing enzymes (cellulases) as well as water. Pretreatment methods, which increase the surface area accessible to water and cellulases are vital to improving the hydrolysis kinetics and conversion of cellulose to glucose. In a novel technique, the microcrystalline cellulose was first subjected to an ionic liquid (IL) treatment and then recovered as essentially amorphous or as a mixture of amorphous and partially crystalline cellulose by rapidly quenching the solution with an antisolvent. Because of their extremely low-volatility, ILs are expected to have minimal environmental impact. Two different ILs, 1-*n*-butyl-3-methylimidazolium chloride (BMIMCl) and 1-allyl-3-methylimidazolium chloride (AMIMCl) were investigated. Hydrolysis kinetics of the *IL-treated cellulose* is significantly enhanced. With appropriate selection of IL treatment conditions and enzymes, the initial hydrolysis rates for IL-treated cellulose *were up to 90 times greater* than those of untreated cellulose. We infer that this drastic improvement in the "overall hydrolysis rates" with IL-treated cellulose is mainly because of a significant enhancement in the kinetics of the "primary hydrolysis step" (conversion of solid cellulose to soluble oligomers), which is the rate-limiting step for untreated cellulose. Thus, with IL-treated cellulose, primary hydrolysis rates increase and become comparable with the rates of inherently faster "secondary hydrolysis" (conversion of soluble oligomers to glucose).

**Index Entries:** Cellulose; enzymatic hydrolysis; ionic-liquid; pretreatment crystallinity index; initial rates; reducing sugars.

*Author to whom all correspondence and reprint requests should be addressed.

## Introduction

Cellulose is the most abundant renewable resource in the world. It is a major fraction of plant biomass, which is the feedstock for "future biorefineries" with the potential to replace the conventional petrochemical refineries in an economy based on renewable resources *(1–3)*. In its natural state, cellulose is highly crystalline in structure with individual cellulose polymer chains held together by strong hydrogen bonding and van der Waals forces. The individual cellulose chains are linear condensation polymer molecules made up of anhydroglucose units joined together by β-1,4 glycosidic bonds *(4)*, with degrees of polymerization (DP) ranging, typically, from 1000 to 15,000 units. The high-crystallinity of cellulose, imparts structural integrity and mechanical strength to the material, and also renders it recalcitrant toward hydrolysis aimed at producing glucose—the feedstock for producing fuels and chemicals—from this polysaccharide. In general, neither the water molecules nor the catalysts for hydrolysis (cellulase enzymes) are able to easily penetrate the crystalline matrix *(1)*.

When the DP exceeds six or seven monomer units, even the individual cellulose chains remain insoluble in water *(4)*. Hence the enzymatic hydrolysis of cellulose is inherently a heterogeneous catalytic process in which the component enzymes of the cellulase system adsorb on cellulose surfaces in order to affect hydrolysis. Pretreatments have been investigated as a means of modifying the cellulose structure in such a way that enzyme hydrolysis can occur at high-yields and improved rates, thus making the overall process economically viable *(3,5–7)*.

The goal of our pretreatment approach is to open the structure of cellulose to make it accessible to the component enzymes of cellulases. In this regard, it is helpful to distinguish between "solvent-swollen cellulose" and "regenerated-cellulose" (RC) *(8–10)*. In solvent-swollen cellulose the degree of crystallinity of cellulose is progressively reduced but not eliminated as the extent of swelling increases, whereas with RC the aim is to render cellulose essentially amorphous. The hydrolysis rates of cellulose are expected to depend on the extent of swelling with the maximal improvement expected with amorphous RC. The reproducible physical properties of RC (viz., DP, essential lack of crystallinity, and so on) make it an ideal substrate in fundamental studies aimed at a quantitative understanding of the mode of action and rates of individual components of a cellulase system. The RC would also make an excellent substrate for a "consolidated bioprocess" where cellulase production, cellulose hydrolysis, and fermentation are carried in a single step, which has the potential to convert lignocellulosic biomass to fuels at a much lower cost *(11)*.

Ionic liquids (ILs) show promise as efficient novel solvents for pretreatment of cellulose. Their ability to dissolve large amounts of cellulose at considerably mild conditions and the feasibility of recovering nearly 100% of the used IL to its initial purity makes them attractive *(12)*. Recently,

cellulose solubilities of up to 39, 25, and 10% (w/w) have been reported for the ILs 3-methyl-N-butylpyridinium chloride *(12)*, 1-*n*-butyl-3-methylimidazolium chloride (BMIMCl) *(13)*, and 1-allyl-3-methylimidazolium chloride (AMIMCl) *(14)*, respectively. ILs are salts that are liquids at or near room temperature and are stable up to temperatures of about 300°C. With their low-volatility, fluidity at ambient temperatures, and unique solvent properties, ILs are a class of prospective solvents that are potentially "green" because of their minimal air emissions.

In our approach, ILs were used to dissolve cellulose followed by rapid precipitation with an antisolvent such as water or alcohol. The structure of the RC was examined using X-ray powder diffraction (XRD) and found to lack the crystallinity of untreated cellulose. The hydrolysis kinetics of the RC was studied using a commercial cellulase system, with and without additional β-glucosidase to gain insights into the mechanism of hydrolysis of RC vs untreated cellulose.

An important aspect of our approach is that the IL is able to instantly reject (precipitate) all the dissolved cellulose in presence of antisolvents such as water, methanol, and ethanol through a preferential solute-displacement mechanism. Once the cellulose is precipitated, the antisolvent used for displacement can easily be stripped off the nonvolatile IL through flash distillation and the IL recovered for subsequent reuse. Two different ILs, BMIMCl (melting point 70°C) and AMIMCl (melting point 35°C) *(15)*, displaying appreciable solubility for cellulose were investigated.

## Materials and Methods

Microcrystalline cellulose, Avicel PH-101 (FMC Corp.) was obtained from Sigma Aldrich (Philadelphia, PA). Citric acid monohydrate, sodium citrate, 3,5-dinitrosalicylic acid (DNS), sodium hydroxide, sodium potassium tartarate (Rochelle salt), phenol, sodium metabisulfite, methanol, and ethanol were obtained from Fisher Scientific (Hanover Park, IL). BMIMCl was purchased from Lancaster Synthesis (Alfa Aesar, Pelham, NH) and used without further purification. AMIMCl was prepared according to published procedures *(16)*.

Celluclast 1.5L, a *Trichoderma reesei* cellulase (Novozyme Corp., Bagsvaerd, Denmark), was used in all enzyme hydrolysis experiments. Cellulase activity was determined by the standard filter paper assay and expressed as filter paper units (FPU) per gram of glucan *(17)*. Novozyme 188, a β-glucosidase, was added with Celluclast 1.5L for some hydrolysis experiments. Cellobiase activity was determined by a cellobiose hydrolysis assay *(17)* and expressed as cellobiose units (CBU) per gram of glucan.

### *Cellulose Pretreatment and Regeneration*

Avicel and BMIMCl (or AMIMCl) mixtures containing 5, 10, 15, and 30% (w/w) cellulose were incubated in a 5-mL autoclave vial. The vial and

the contents were heated in a block heater to either 130°C for 10 min or to 120°C for 30 min. The samples were gently stirred by placing the block heater on an orbital shaker. Deionized water was used as an antisolvent for precipitating cellulose from the ILs, BMIMCl, and AMIMCl. About 2 mL of antisolvent was added to the cellulose/IL mixture. Immediately a precipitate was formed. The sample was briefly centrifuged and supernatant was removed. The precipitated sample was washed twice with additional 2-mL aliquots of deionized water followed by the cellulose hydrolysis buffer solution. The resultant cellulose is referred to as RC. It should be noted that, with samples containing initial cellulose weight percent more than its solubility limit in the IL, only partial dissolution of cellulose occurs during incubation. Subsequent antisolvent treatment provides a cellulose mix of RC and partially crystalline cellulose (PCC). In what follows, cellulose samples recovered following antisolvent treatment are referred to as IL-treated cellulose irrespective of whether the resulting cellulose is RC or a mixture of RC and PCC.

### *XRD Measurements*

Smooth films were cast at room temperature on microscopic slides from untreated and IL-treated cellulose samples. XRD data for these films were generated at 25°C with an XPERT' PRO powder diffractometer with Xcelerator' detector (PANalytical, Almelo, The Netherlands) using Nickel filtered CuKα radiation. Samples were scanned over the angular range 6–45°, 2θ, with a step size of 0.05°, and step time of 10 s.

### *Enzymatic Hydrolysis*

Batch enzymatic hydrolysis of IL-treated and untreated cellulose was carried out at 50°C with 50 m*M* citric acid buffer (pH 4.8) in a reciprocating shaker bath. Two different sets of hydrolysis experiments were conducted. In the first set, the effect of augmenting cellulase with additional β-glucosidase (Novozyme 188) on the rates of hydrolysis of untreated cellulose and RC was investigated. A batch volume of 3 mL with a cellulose concentration of 16.7 mg/mL was used with both untreated cellulose and RC (recovered from 5% [w/w] cellulose–IL mixture). The enzyme loadings were varied from 8 to 32 FPU/g glucan of Celluclast 1.5L and 0 to 83 CBU/g glucan Novozyme 188. The second set of experiments was aimed at investigating the effect of crystallinity of cellulose on hydrolysis. In these experiments, batch volumes were adjusted for IL-treated cellulose samples to achieve the same cellulose concentration of 16.7 mg/mL used with untreated cellulose. The resulting volumes were 3, 6, 9, and 18 mL, respectively, for cellulose samples recovered from IL–cellulose mixtures of 5, 10, 15, and 30% (w/w) cellulose. A constant enzyme loading of 16 FPU/g glucan of Celluclast 1.5L and 83 CBU/g glucan Novozyme 188 was used.

The enzyme reaction was monitored by withdrawing 20 μL of samples from the supernatant periodically. Withdrawn samples were diluted

10 times. Untreated and IL-treated cellulose were hydrolyzed using the same cellulase and β-glucosidase (Novozyme 188) stock solutions. The untreated-cellulose controls were run concurrently with all the IL-treated cellulose hydrolysis experiments to eliminate potential differences in temperature history or enzyme loading. The released reducing sugars were measured by the DNS method using D-glucose as a standard *(18)*. Released glucose was determined separately by high-performance liquid chromatography (HPLC) using a HPX-87 P column (Bio-Rad Laboratories Inc., Hercules, CA) at 80°C equipped with a refractive index detector. The mobile phase was deionized water with a flow rate of 0.6 mL/min.

## Results and Discussion

### *Dissolution and Regeneration of Cellulose, and its Crystallinity*

During the incubation of Avicel in ILs at 120°C and 130°C, complete dissolution was observed for 5% (w/w) Avicel solutions in BMIMCl and AMIMCl. Ten percent solutions were completely dissolved in BMIMCl and almost completely dissolved in AMIMCl. For 15 and 30% (w/w) Avicel in ILs, only partial dissolution occurred. The maximum solubility of Avicel observed visually at 120°C was 9% in AMIMCl and 13% in BMIMCl. The dissolution mechanism of cellulose in BMIMCl and AMIMCl can be attributed to the nature of the bulky imidazolium cation and the relatively strong electronegativity and small size of the chloride ion. BMIMCl and AMIMCl have high hydrogen bond basicity and the anion plays a key role in the dissolution of cellulose. The chloride ion attacks the free hydroxyl groups and deprotonates cellulose. The imidazolium cation with its electron rich aromatic π system interacts with cellulose hydroxyl oxygen atoms through nonbonding or π electrons, and in addition prevents cross linking of the cellulose molecules *(16,19)*. Following dissolution in BMIMCl or AMIMCl, Avicel was precipitated from the IL by adding water as antisolvent, which forces the IL to reject dissolved cellulose through a preferential solute-displacement mechanism. During this displacement, the IL is extracted into the antisolvent through hydrogen bonding, dipolar, and columbic interactions between the IL and antisolvent *(20)*.

Samples of cellulose recovered following antisolvent treatment of IL–cellulose mixtures and untreated cellulose were examined by XRD to gain insight into the structural changes resulting from IL-treatment (Figs. 1 and 2). Crystallinity index (CrI) was determined from XRD *(21)* data and calculated using the formula: $\mathrm{CrI} = [(I_{020} - I_{am})/I_{020}] \times 100$, where $I_{020}$ is the intensity above baseline at the 020 peak maximum near 2θ 22.5° and $I_{am}$ is the minimum in peak intensity near 2θ of 18°*(21)*. CrI was reduced for all samples incubated in the ILs (Table 2). For cellulose concentrations less than the solubility limit in the IL (5 and 10% [w/w]), the cellulose recovered

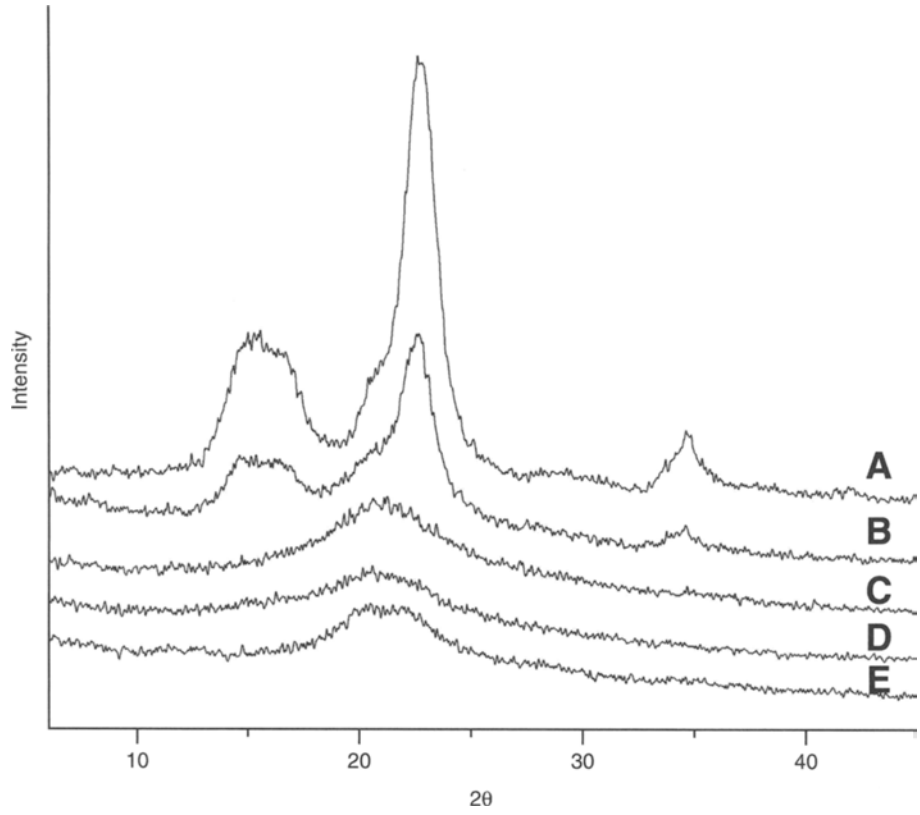


**Fig. 1.** XRD patterns for IL-treated and untreated-Avicel. Untreated Avicel **(A)**, exhibited a significantly greater degree of crystallinity than that of regenerated samples **(B–E)**. Avicel samples were incubated in AMIMCl at 120°C for 30 min and precipitated with deionized water. Samples B–E corresponds to 30, 15, 10, and 5% (w/w) Avicel incubated in AMIMCl. The crystallinity of B is significantly higher than that of C–E (CrI is listed in Table 2).

following antisolvent addition is essentially amorphous. Accordingly, the reduction in the measured CrI was greatest for 5 and 10% (w/w) samples and remains essentially the same for both cases. However, with samples containing initial cellulose weight percent more than its solubility limit in the IL (15 and 30% [w/w]), only partial dissolution of cellulose occurs during incubation. Subsequent antisolvent treatment provides a cellulose mix of RC and PCC. The proportion of PCC is expected to rise as the initial weight percent of cellulose incubated in IL is increased. This gradual increase in PCC will lead to a corresponding increase in CrI as was observed from the CrI obtained from XRD measurement (Table 2).

## *Effect of IL-Treatment on Rate of Hydrolysis of Cellulose*

As noted, cellulose was incubated in BMIMCl or AMIMCl and recovered by quenching with antisolvent water. The IL-treated and untreated

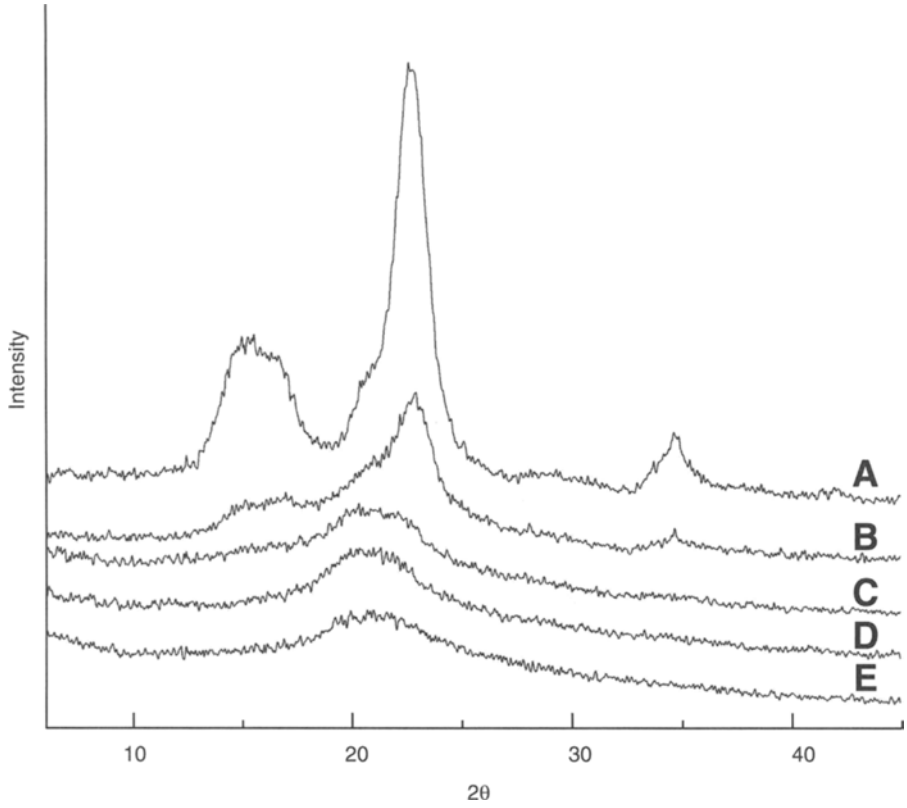


**Fig. 2.** XRD patterns for IL-treated and untreated-Avicel. Untreated Avicel **(A)**, exhibited a significantly greater degree of crystallinity than that of regenerated samples **(B–E)**. Avicel samples were incubated in BMIMCl at 120°C for 30 min and precipitated with deionized water. Samples B–E correspond to 30, 15, 10, and 5% (w/w) Avicel incubated in BMIMCl. The crystallinity of B is significantly higher than that of C–E (CrI is listed in Table 2).

cellulose samples were then enzymatically hydrolyzed using the Celluclast 1.5L cellulase system with and without additional β-glucosidase (Novozyme 188). Total soluble reducing sugars and glucose concentrations were monitored during the course of hydrolysis. The initial rate of formation of total soluble reducing sugars (a measure of hydrolysis) was higher for IL-treated cellulose compared with untreated cellulose for all incubation conditions and enzyme loadings examined (Tables 1 and 2). The concentrations of total soluble sugars and glucose are shown as functions of time in Figs. 3 and 4, respectively.

## *Role of Additional β-Glucosidase on Cellulose Hydrolysis*

The initial rate of soluble reducing sugar formation of untreated cellulose and cellulose regenerated from a 5% cellulose/BMIMCl mixture is shown in Table 1 for various enzyme loadings, with and without

Table 1
Effect of β-Glucosidase on Hydrolysis. Initial Rate of Formation of Total Reducing Sugars, Measured by DNS Assay During the Enzymatic Hydrolysis of Approx 17 mg/mL of Regenerated or Untreated Avicel Samples With Cellulase Loadings Varying From 8 to 32 FPU/g Glucan and 0 to 83 CBU/g Glucan

| Enzyme activity per gram of glucan | | Initial rate (mg/mL/min) | | Rate enhancement[a] |
|---|---|---|---|---|
| Cellulase (FPU) | β-Glucosidase (CBU) | Untreated cellulose | Regenerated cellulose | RC |
| 8 | 0 | 0.0004 | 0.0047 | 12 |
| 8 | 83 | 0.0004 | 0.0320 | 71 |
| 16 | 0 | 0.0043 | 0.0427 | 10 |
| 16 | 83 | 0.0044 | 0.3915 | 89 |
| 32 | 0 | 0.0110 | 0.3953 | 36 |
| 32 | 83 | 0.0140 | 0.5030 | 36 |

Rates are calculated from analysis of supernatant sampled during the first 20 min of hydrolysis. RC was formed by incubating samples of 5% cellulose in ILs (BMIMCl) at 130°C for 10 min followed by precipitation with water.

[a]Rate enhancement is defined as the ratio of initial rate of reducing sugars released for RC divided by that of untreated cellulose.

Table 2
Effect of CrI of IL-Treated Avicel on Hydrolysis. Initial Rate of Formation of Total Soluble Reducing Sugars, Measured by DNS Assay During the Enzymatic Hydrolysis of Approx 17 mg/mL Avicel (With a Cellulase Activity of 16 FPU/g Glucan and β-Glucosidase Activity of 83 CBU/g Glucan)

| Concentration of Avicel in IL | Initial rate (mg/mL/min) | Rate enhancement[a] | Crystallinity index |
|---|---|---|---|
| Untreated | 0.0046 | – | 76.4 |
| 5% in AMIMCl | 0.3274 | 71 | 12.9 |
| 10% in AMIMCl | 0.3397 | 74 | 11.7 |
| 15% in AMIMCl | 0.2304 | 50 | 15 |
| 30% in AMIMCl | 0.1263 | 27 | 47.0 |
| 5% in BMIMCl | 0.3412 | 74 | 11.5 |
| 10% in BMIMCl | 0.3763 | 82 | 11.6 |
| 15% in BMIMCl | 0.289 | 63 | 14.2 |
| 30% in BMIMCl | 0.2140 | 46 | 43.4 |

Rates are calculated from analysis of supernatant sampled during the first 20 min of hydrolysis. RC or a mixture of RC and PCC was formed by incubating cellulose in ILs (AMIMCl/BMIMCl) at 120°C for 30 min followed by contact with water. A mixture of RC and PCC formed at Avicel concentrations in IL more than 10% (w/w).

[a]Rate enhancement is defined as the ratio of initial rate of reducing sugars released for RC divided by that of untreated cellulose.

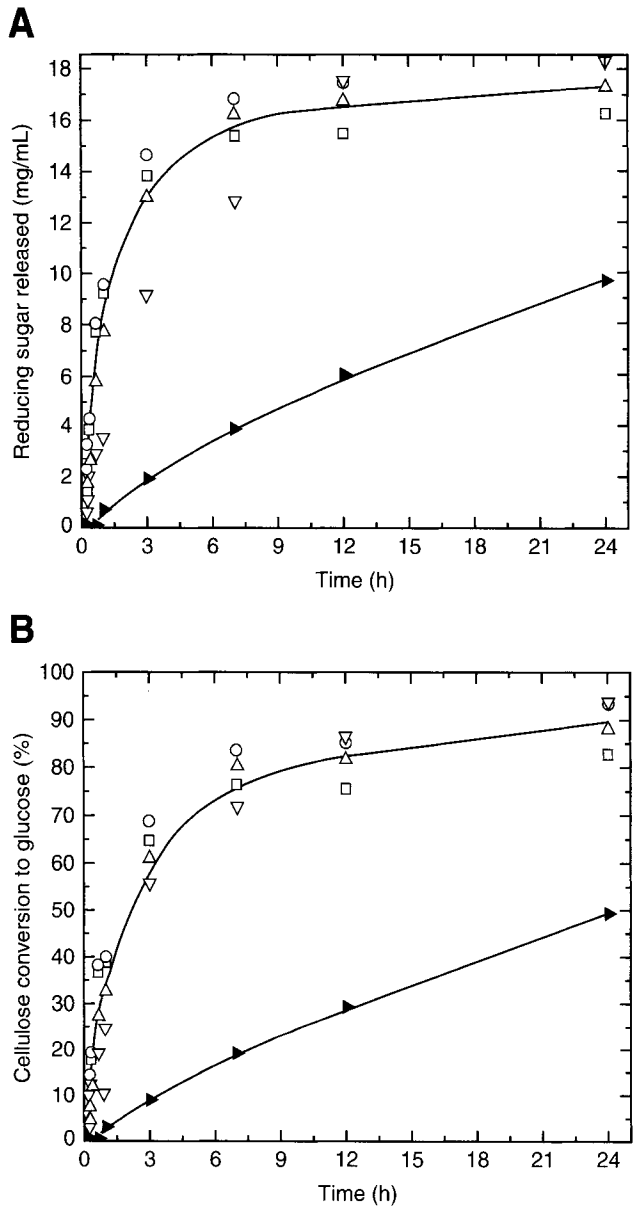


**Fig. 3.** Avicel samples of 5% (□), 10% (○), 15% (△), and 30% (▽) were incubated for 30 min in AMIMCl at 120°C, and precipitated with deionized water. Hydrolysis rates of IL incubated samples are compared with that of untreated Avicel (▶). Conversion of cellulose to sugars for batch samples of approx 17 mg/mL Avicel hydrolyzed with *T. reesei* cellulase activity of 16 FPU/g glucan and 83 CBU/g glucan at 50°C is shown as a function of time for **(A)** total soluble sugars (measured using a DNS assay) and **(B)** as *percent cellulose conversion to* glucose (measured by HPLC).

β-glucosidase addition. In the discussion that follows, the rate of formation of soluble reducing sugars will be referred to as the hydrolysis rate. This hydrolysis rate somewhat underestimates the true hydrolysis rate because hydrolysis of insoluble cellulose into smaller but insoluble fragments is

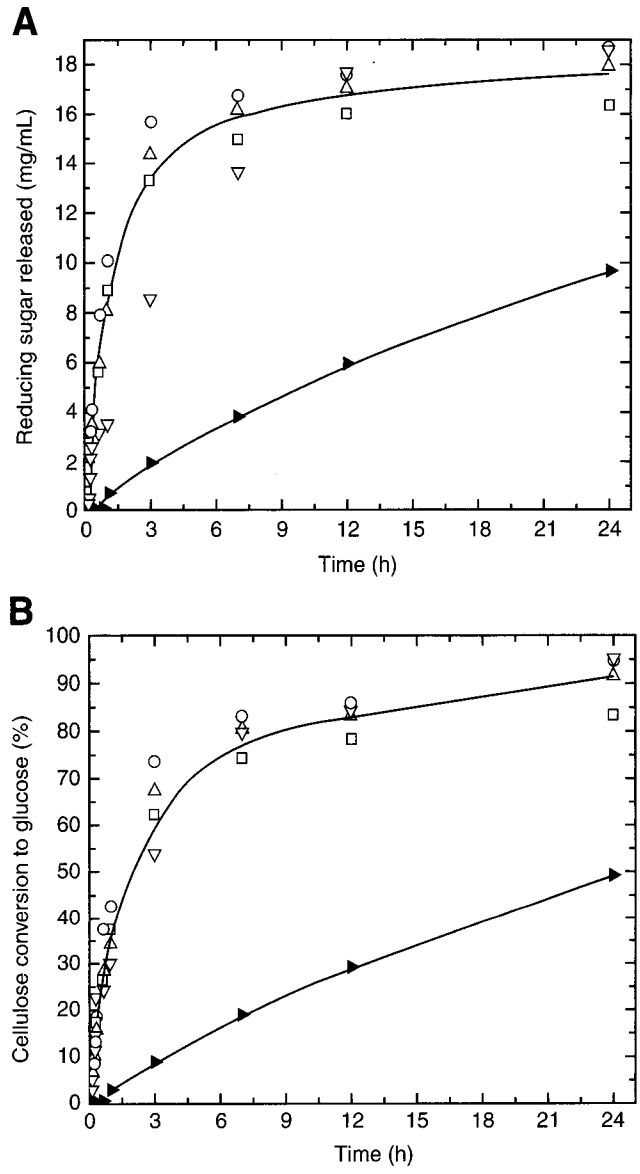


**Fig. 4.** Avicel samples of 5% (□), 10% (○), 15% (△), and 30% (▽) were incubated for 30 min in BMIMCl at 120°C, and precipitated with deionized water. Hydrolysis rates of IL incubated samples are compared with that of untreated Avicel (▶). Conversion of cellulose to sugars for batch samples of 17 mg/mL Avicel hydrolyzed with *T. reesei* cellulase activity of 16 FPU/g glucan and 83 CBU/g glucan at 50°C is shown as a function of time for **(A)** total soluble sugars (measured using a DNS assay) and **(B)** as *percent cellulose conversion to* glucose (measured by HPLC).

not taken into account in the DNS assay of soluble reducing sugars. The rate enhancement, defined as the ratio of initial hydrolysis rate of IL-treated cellulose to that of untreated cellulose, appears highest for an enzyme loading of 16 FPU/g glucan with addition of β-glucosidase at 83 CBU/g glucan. At these enzyme loadings the hydrolysis rate of RC is nearly two

orders of magnitude more than that of untreated cellulose. For modest cellulase activities (8 and 16 FPU/g glucan), the hydrolysis rates of RC increased significantly with addition of β-glucosidase (by six- to ninefold). This increase was not seen in untreated cellulose samples at similar cellulase activities (Table 1).

### *Effect of CrI of Cellulose on Hydrolysis*

A constant enzyme loading of 16 FPU/g glucan with addition of β-glucosidase at 83 CBU/g glucan was used in all experiments conducted with various IL-treated cellulose samples (incubation of 5, 10, 15, and 30% cellulose in the ILs). The initial rates of hydrolysis for untreated and IL-treated cellulose are shown in Table 2. Initial rates of enzymatic hydrolysis of IL-treated cellulose were at least fifty times that of untreated cellulose. Initial rates of enzymatic hydrolysis of completely dissolved and RC samples (5 and 10%) were higher than the IL-treated cellulose samples that were partially dissolved (15 and 30%) as seen in Table 2. Samples containing initial cellulose concentrations less than 10% are within the solubility limit in IL, and more than 10% are above the solubility limit in IL. Addition of antisolvent to IL–cellulose mixtures produced RC when the cellulose concentration is within the solubility limit and produced a mixture of RC and PCC above the solubility limit. Mixture of RC and PCC samples have residual crystallinity (Table 2), which accounted for lower initial rates compared with RC samples.

For both RC (5 and 10%) and a mixture of RC and PCC (15 and 30%) samples, conversion to glucose after 7 h of hydrolysis was about 80–85%, whereas it is only 20% for untreated cellulose (Figs. 3 and 4). Higher conversions were expected for RC samples as the crystallinity of cellulose is almost eliminated in RC samples. Higher conversions obtained for mixtures of RC and PCC (15 and 30%) are somewhat surprising. In spite of the residual crystalliniy of these cases, the conversions were higher and comparable with that of RC samples (5 and 10%) (Figs. 3 and 4). This implies that the crystallinity of 15 and 30% cellulose samples treated in IL was reduced sufficiently to provide enough accessible sites for cellulase enzyme adsorption and activity. This is a promising observation as it suggests that it is not necessary to "totally eliminate" the crystallinity of cellulose to achieve significant enhancement in hydrolysis rates, and even with appreciable residual crystallinity most of the recalcitrance to hydrolysis can be mitigated. This also offers the possibility to process larger amounts of cellulose rapidly (i.e., up to 30 wt% of cellulose can be incubated in the IL-treatment step). All IL-treated cellulose samples reached almost 95% conversions to glucose within 24 h, whereas untreated cellulose only reached 50% conversion in that time period (Figs. 3 and 4).

The hydrolysis rates of IL-treated cellulose samples within the solubility limit (5 and 10%) were comparable for cellulose incubated in either

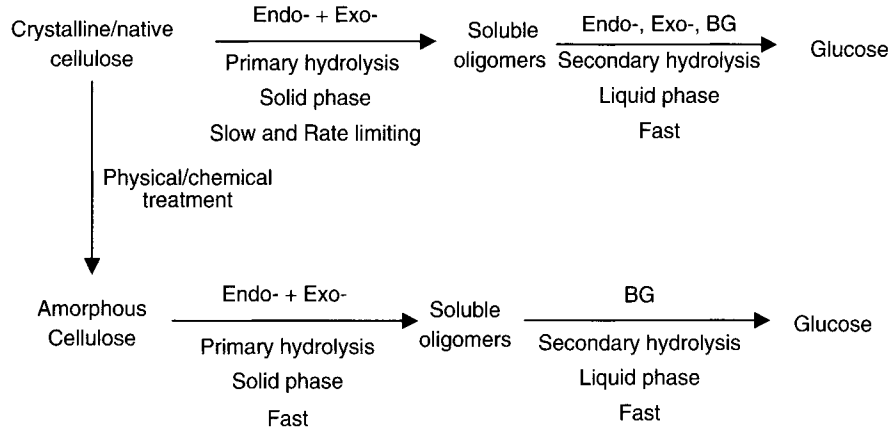


**Fig. 5.** Mechanism of enzymatic hydrolysis of cellulose by *T. reesei* cellulase *(3)*. Endo refers to endoglucanase. Exo, exoglucanase (cellobiohydrolase); BG, β-glucosidase.

AMIMCl or BMIMCl. With IL-treated cellulose samples above the solubility limit (15 and 30%), the hydrolysis rates appear to differ according to the dissolving capabilities of the IL. The hydrolysis rates of IL-treated cellulose prepared from 15% to 30% Avicel incubation in BMIMCl were higher than those prepared with AMIMCl (Table 2).

## *Mechanism of Enzymatic Hydrolysis of RC*

The hydrolysis of insoluble cellulose can be divided into primary and secondary steps *(3)*. Primary hydrolysis (of the solid phase) involves the release of glucose and soluble intermediates such as cellobiose, cellotriose, and soluble cellodextrins from insoluble substrates. Secondary hydrolysis (in the liquid phase) involves the hydrolysis of soluble intermediates to lower molecular weight intermediates and glucose (Fig. 5). Exoglucanases and endoglucanases can hydrolyze solid cellulose substrates by adsorbing on cellulose surface (primary hydrolysis). Exoglucanases act on chain ends and predominantly release cellobiose (a glucose dimer). Endoglucanases hydrolyze cellulose by random chain scission and reduce DP of cellulose more effectively than the exoglucanases. Both exo and endoglucanases are inhibited by cellobiose. β-glucosidase converts cellobiose and soluble oligomers to glucose and only acts on substrates in the liquid phase (secondary hydrolysis). Primary hydrolysis of native crystalline cellulose is much slower than secondary hydrolysis, because of the macro and microstructure and extensive network of inter- and intrahydrogen bonding of cellulose fibrils and crystalline microfibrils, which greatly limits the permeability of enzymes and water to hydrolysis sites *(8,22)*.

For RC, because of the amorphous nature of the cellulose, many β-glucosidic sites are available for endoglucanases, which hydrolyze cellulose rapidly to form short glucose oligomers *(8)*. Within 3–4 h of enzymatic hydrolysis, the RC solutions appeared transparent, whereas

untreated cellulose had a distinct solid phase. This indicates that RC was rapidly hydrolyzed to soluble oligomers of DP <6 (or slightly soluble oligomers of DP <13) *(4,8,23)*. This rapid formation of soluble cellulose oligomers may result in comparable primary and secondary hydrolysis rates for RC.

The hydrolysis rates of RC are increased by about one order of magnitude over those for untreated cellulose for samples hydrolyzed with 8, 16, and 32 FPU/g glucan with no additional β-glucosidase added (Table 1). With the addition of 83 CBU/g glucan, the enzymatic hydrolysis rates increased by almost another order of magnitude for RC samples hydrolyzed with 8 and 16 FPU and to a lesser extent for samples hydrolyzed with 32 FPU/g glucan. The increase in hydrolysis rate with β-glucosidase addition observed for RC can be attributed in part to the relatively fast primary hydrolysis of amorphous cellulose and accumulation of cellobiose which inhibits exo and endoglucanase activity. β-glucosidase addition alleviates this accumulation and also increases the rate of secondary hydrolysis. In contrast, the hydrolysis rates of untreated cellulose were unaffected by β-glucosidase addition at 8 and 16 FPU/g glucan (rates increased modestly at 32 FPU/g glucan similar to the increase seen for RC). For untreated cellulose with modest cellulase loadings, primary hydrolysis appears to be rate limiting in contrast to relatively fast primary hydrolysis for RC. Hence, β-glucosidase addition does not seem to enhance the soluble sugar formation for untreated crystalline cellulose as the endo- and exoglucanase activity is not inhibited during the initial stages of enzymatic hydrolysis, owing to low initial concentrations of cellobiose/soluble oligomers (Table 1).

## Conclusions

In a novel technique, the microcrystalline cellulose was incubated with an IL and then recovered as essentially amorphous or as a mixture of amorphous and PCC, by rapidly quenching the IL–cellulose mixture with an antisolvent. When the incubation samples contained initial cellulose weight percent more than its solubility limit in the IL, subsequent antisolvent treatment provides a cellulose mix of amorphous RC and PCC. The crystallinity index (CrI) obtained from XRD measurement of the IL-treated samples displayed a corresponding increase in CrI when the initial weight percent of cellulose was more than the solubility limit in the IL.

The IL-treated cellulose samples were hydrolyzed to sugars using Celluclast 1.5L and Novozyme 188. IL-treated cellulose exhibited improved hydrolysis kinetics with optically transparent solutions formed after first few hours of reaction, indicating relatively fast hydrolysis kinetics. With optimal IL-treatment conditions and enzyme loadings, initial rates of hydrolysis of IL-treated cellulose were *two orders of magnitude* higher than those observed with untreated cellulose. Among IL-treated cellulose

preparations, the *initial rates* observed with samples containing only RC were higher than the initial rates for the samples that were mixtures of RC and PCC. In spite of the observed differences in the initial rates and CrI, all IL-treated cellulose preparations showed significantly higher glucose conversions compared with untreated cellulose: about 80–85% conversions to glucose were observed for IL-treated cellulose samples in 7 h of hydrolysis where as it was only 20% for untreated cellulose. Thus, it seems that it is not really necessary to completely eliminate the crystallinity of cellulose in order to achieve significant enhancement in hydrolysis rates; even with some residual crystallinity most of the recalcitrance to hydrolysis can be mitigated. This offers the possibility to hydrolyze large amounts of cellulose rapidly using the proposed IL-pretreatment technique.

In the proposed technique, dissolution of cellulose in the IL and its subsequent precipitation with antisolvent, allows separation of the IL/antisolvent solution from cellulose by a simple filtration or centrifugation step. The IL and antisolvent can then be recovered, easily separated, and recycled. Because of the nonvolatility of the IL, antisolvent can be easily stripped from the IL/antisolvent solution for recovery and recycle of both the IL and antisolvent. The synthesis of ILs generally consists of a few steps with relatively high-yields *(16,24)*. The price of ILs is expected to dramatically decrease as commercial uses of ILs are developed and manufacturing scale increases. These considerations point to the promise of the proposed technique in dealing with the recalcitrance of cellulose to hydrolysis.

## Acknowledgments

The authors would like to thank Dr. Jared Anderson of The University of Toledo, Department of Chemistry and Amy Coxe for IL preparation. Funding for this work was provided under a National Science Foundation grant EHR-022789, and a fellowship from Consortium for Plant Biotechnology Research (CPBR) to CS and SV.

## References

1. Lynd, L. R., Weimer, P. J., van Zyl, W. H., and Pretorius, I. S. (2002), *Microbiol. Mol. Biol. Rev.* **66,** 506–577.
2. Lynd, L. R., Wyman, C. E., and Gerngross, T. U. (1999), *Biotechnol. Prog.* **15,** 777–793.
3. Zhang, Y. -H. P. and Lynd, L. R. (2004), *Biotechnol. Bioeng.* **88,** 797–824.
4. Klemm, D., Philipp, B., Heinze, T., Heinze, U., and Wagenknecht, W. (1998), *Fundamentals and analytical methods,* Wiley-VCH, Weinheim.
5. Ladisch, M. R., Ladisch, C. M., and Tsao, G. T. (1978), *Science* **201,** 743–745.
6. Hamilton, T. J., Dale, B. E., Ladisch, M. R., and Tsao, G. T. (1984), *Biotechnol. Bioeng.* **26,** 781–787.
7. Wood, T. M. (1988), *Methods Enzymol.* **160,** 19–25.
8. Zhang, Y. -H. P. and Lynd, L. R. (2005), *Biomacromolecules* **6,** 1510–1515.
9. Dadi, A., Varanasi, S., and Schall, C. A. (2006), *Biotechnol. Bioeng.* **95,** *904–910; Varanasi, S., Schall, C, and Dadi, A;* US Patent filed, December 2006.
10. Zhang, Y. -H. P., Cui, J., Lynd, L. R., and Kuang, R. L. (2006), *Biomacromolecules* **7,** 644–648.

11. Lynd, L. R., van Zyl, W. H., McBride, J. E., and Laser, M. (2005), *Curr. Opin. Biotech.* **16,** 577–583.
12. Heinze, T., Schwikal, K., and Barthel, S. (2005), *Macromol. Biosci.* **5,** 520–525.
13. Swatloski, R. P., Spear, S. K., Holbrey, J. D., and Rogers, R. D. (2002), *J. Am. Chem. Soc.* **124,** 4974–4975.
14. Wu, J., Zhang, J., He, J., Ren, Q., and Guo, M. (2004), *Biomacromolecules* **5,** 266.
15. Moulthrop, J. S., Swatloski, R. P., Moyna, G., and Rogers, R. D. (2005), *Chem. Comm.* **12,** 1557–1559.
16. Zhang, H., Wu, J., Zhang, J., and He, J. (2005), *Macromolecules* **38,** 8272–8277.
17. Ghose, T. K. (1987), *Pure Appl. Chem.* **59,** 257–268.
18. Miller, G. L. (1959), *Anal. Chem.* **31,** 426–428.
19. Anderson, J. L., Ding, J., Welton, T., and Armstrong, D. W. (2002), *J. Am. Chem. Soc.* **124,** 14,247–14,254.
20. Crosthwaite, J. M., Aki, S. N. V. K., Maginn, E. J., and Brennecke, J. F. (2005), *Fluid Phase Eq.* **228–229,** 303–309.
21. Segal, L., Creely, J. J., Martin, A. E., and Conrad, C. M. (1959), *Text. Res. J. 29.*
22. Kleman-Leyer, K. M., Siika-Aho, M., Teeri, T. T., and Kirk, T. K. (1996), *Appl. Envion. Microbiol.* **62,** 2883.
23. Pereira, A. N., Mobedshahni, M., and Ladisch, M. R. (1988), *Methods Enzymol.* **160,** 26–43.
24. Shengdong, Z., Yuanxin, W., Qiming, C., et al. (2006), *Green Chem.* **8,** 325–327.

0273-2289/1559-0291 (Online)/07/136–140/423–436/$30.00

# Evaluation of Different Biomass Materials as Feedstock for Fermentable Sugar Production

YI ZHENG,[1] ZHONGLI PAN,*[,1,2] RUIHONG ZHANG,[1] JOHN M. LABAVITCH,[3] DONGHAI WANG,[4] SARAH A. TETER,[5] AND BRYAN M. JENKINS[1]

*[1]Biological and Agricultural Engineering Department, University of California, Davis, One Shields Avenue, Davis, CA 95616, E-mail: zpan@pw.usda.gov; [2]Processed Foods Research Unit, USDA-ARS Western Regional Research Center, 800 Buchanan, St. Albany, CA 94710; [3]Plant Science Department, University of California, Davis, One Shields Avenue, Davis, CA 95616; [4]Biological and Agricultural Engineering Department, Kansas State University, Manhattan, KS 66506; and [5]Novozymes, Inc., 1445 Drew Ave., Davis, CA 95616*

## Abstract

Saline crops and autoclaved municipal organic solid wastes were evaluated for their potential to be used as feedstock for fermentable sugar production through dilute acid pretreatment and enzymatic hydrolysis. The saline crops included two woods, athel (*Tamarix aphylla* L) and eucalyptus (*Eucalyptus camaldulensis*), and two grasses, Jose tall wheatgrass (*Agropyron elongatum*), and creeping wild rye (*Leymus triticoides*). Each of the biomass materials was first treated with dilute sulfuric acid under selected conditions (acid concentration = 1.4% (w/w), temperature = 165°C, and time = 8 min) and then treated with the enzymes (cellulases and β-glucosidase). The chemical composition (cellulose, hemicellulose, and lignin contents) of each biomass material and the yield of total and different types of sugars after the acid and enzyme treatment were determined. The results showed that among the saline crops evaluated, the two grasses (creeping wild rye and Jose tall wheatgrass) had the highest glucose yield (87% of total cellulose hydrolyzed) and fastest reaction rate during the enzyme treatment. The autoclaved municipal organic solid wastes showed reasonable glucose yield (64%). Of the two wood species evaluated, Athel has higher glucose yield (60% conversion of cellulose) than eucalyptus (38% conversion of cellulose).

**Index Entries:** Dilute acid pretreatment; enzymatic hydrolysis; ethanol potential; municipal solid waste; saline crops; fermentable sugar.

*Author to whom all correspondence and reprint requests should be addressed.

## Introduction

Production of fermentable sugars from biomass materials is an important step for biobased, chemical, and biofuel production. For lignocellulosic materials, sugars are primarily derived from hemicellulose and cellulose components. Naturally, sugar derived from cellulose—glucose—is more easily fermentable, especially for the production of ethanol, than the sugars derived from hemicellulose, which are more complex and mainly include five-carbon sugars, such as xylose. To convert cellulose to glucose, the hydrolysis is a necessary step. Hydrolysis is normally carried out using concentrated acid or enzymes. Compared with concentrated acid hydrolysis, enzymatic hydrolysis is more specific and milder, and it does not cause sugar degradation; however, it requires proper pretreatment of the biomass material to improve cellulose accessibility to enzymes by removing hemicellulose, lignin and/or reducing crystallinity of cellulose *(1)*.

Pretreatment technologies, such as dilute acid, steam-explosion, comminution, ammonia fiber explosion, alkaline, and super critical $CO_2$–$SO_2$ have been extensively investigated *(2–9)*. Herein, dilute sulfuric acid pretreatment has been widely studied because it is considered to be relatively inexpensive and effective for treatment of different biomass species. In addition, dilute sulfuric acid pretreatment can also effectively hydrolyze hemicelluloses into sugars, including monomeric sugars (xylose, arabinose, galactose, glucose, and mannose) and oligomers. With the recent advent of new microorganisms that are capable of fermenting pentoses as well as hexoses to ethanol, dilute acid pretreatment becomes a more viable step in the hydrolysis of lignocellulosic materials *(10)*.

Much previous reported research about the pretreatment of biomass materials with dilute sulfuric acid is mainly related to softwood, hardwood, grass, and agricultural residues. Acid concentration, reaction temperature, and time are the major parameters that influence the treatment effectiveness. For most types of biomass materials, dilute acid pretreatment can release more than 80% of the sugars associated with the hemicellulose fraction and allow for enzymatic conversion of 80% of the cellulose to glucose (Table 1). The amount and type of sugars that can be produced and the conditions required to achieve the optimum production during acid pretreatment and enzymatic treatment are largely dependent on the chemical composition and structure of biomass materials.

This study was focused on the evaluation of saline biomass crops and thermally pretreated municipal organic waste as the feedstock for fermentable sugar production. The saline crops include the two wood species (athel and eucalyptus) and the two grass species (creeping wild rye [CWR], and Jose tall wheatgrass [JTW]). They were planted as experimental crops on the farms located in the San Joaquin valley of California to help mitigate the salt problem in soil and drainage water. The problem caused by using fertilizers and irrigation water exists across agricultural

Table 1
Literature Review of Selected Dilute Sulfuric Acid Pretreatment and Enzymatic Hydrolysis Research

| Feedstock | $T$ (°C) | $t$ (min) | $H_2SO_4$ (w/w, %) | Reactor | Hemicellulose conversion (%) | Enzyme loading (FPU/CBU) | Enzymatic digestibility (%) | References |
|---|---|---|---|---|---|---|---|---|
| Mixed wood (10% birch and 90% maple) | 230 | 0.12 | 1.17 | Flow | – | –/– | 95 | *11* |
| Wheat straw and aspen wood | 140 | 60 | 0.5 (v/v) | Batch | 80 | 26/–33/33 | >80% | *12,13* |
| Three hardwoods (poplar hybrid NE388, poplar hybrid N11, and sweetgum) and three herbaceous crops (switchgrass, weeping lovegrass, and *Sericea lespedeza*) | 160 | 10 | 0.45–0.5 (v/v) | Batch | 94 | 42/4.9 | 90–100 | *14* |
| Corn residues (corn stovers and corn cobs) and three short rotation hardwoods (silver maple, sycamore, and black locust) | 160 | 10 | 0.45–0.5 (v/v) | Batch | 90 | 42/4.9 | 85 | *15* |
| Douglas fir | 200–230 | 1–5 | 0.4 | Batch | 90–95 | 25–60/– | 90 | *16* |
| White fir and ponderosa pine | 200–230 | 1–5 | 0.4 | Two-stage | 95–100 | 60/– | >90 | *17* |
| Corn stover | 121 | 30–120 | 2 | Batch | 90 | 40/8 | 80 | *18* |
| Rye straw and bermudagrass | 121 | 90 | 1.5 | Batch | 55–66 | 25/75 | 52–83 | *1* |

lands in the San Joaquin valley. One of the approaches for solving the salinity problem is to use an integrated on-farm drainage management system, which uses the plantation of different crops and plants sequentially with increasing the salt tolerance levels to utilize drainage water. This has been practiced at Red Rock Ranch (RRR), a farm located near Five Points, California in a 640-acre demonstration project where several salt-tolerant crops, including Athel, eucalyptus, JTW, and CWR, have been planted. The saline biomass production through the integrated on-farm drainage management systems not only helps with transpiration of water and concentration of salt but also serves to capture solar energy through photosynthesis for further use. The produced crops could be used as raw materials for producing bioenergy and biochemicals, such as biogas and sugars, which can be further converted to ethanol and/or other chemicals.

This study was designed to investigate the utilization of the saline crops as feedstock for production of valuable products, such as fermentable sugar, which is important for developing a sustainable agricultural system for their continued production. This study was not focused on addressing the effect of salt contents in saline crops on fermentable sugar production step, although the salt content may influence the fermentation process. The autoclaved municipal organic waste (AMSW) was obtained from the City of San Francisco, CA, and was pretreated with an autoclave process first to partially break down the fibers and reduce the particle size, before it was tested with the hydrolysis experiments. It contained approx 30% food and 25% paper. Currently the municipal solid wastes (MSW) are largely disposed off in landfills. This study also evaluated the feasibility of separating the organic fraction (food and paper) from the MSW and converting it into sugars as valuable products. Although many lignocellulosic biomass materials have been investigated as potential feedstock for sugar and/or ethanol production, little research has been done on the hydrolysis of saline crops and AMSW with high food content. The objectives of this study were to compare different saline crops and AMSW for their potential to be used as feedstock for fermentable sugar production through dilute acid and enzymatic hydrolysis, and determine the amount and types of sugars that can be produced from these biomass materials.

## Materials and Methods

### *Biomass Preparations*

The biomass materials tested in this study include four saline crops and one AMSW. The following is detailed information about the saline crops:

1. Athel pine, *T. aphylla L*, softwood.
2. Eucalyptus, *E. camaldulensis*, hardwood.
3. CWR, *L. triticoides.*
4. JTW, *A. elongatum.*

Athel and eucalyptus from 8-yr old trees were harvested in May 2004 and then cut into approx 40 cm long logs using a chainsaw. The diameter of logs used in this study ranged from 3 to 25.4 cm. The logs were further debarked with chisel and then reduced into 5–10 cm long chips with a Dosko brush chipper (Model 1400-12; Dosko Co., Sacramento, CA). The chips were air-dried to approx 8% moisture content and sealed in plastic bags for storage in the Biomass Laboratory at the University of California, Davis for future use. The JTW and CWR were harvested from the same location as the woods, which was RRR at five points in California. They were cut, field-dried, and baled with an average straw length of 50 cm in September 2004 and in May 2005, respectively. Bales were stored indoors at ambient temperature.

The saline crops were milled into particles using a laboratory hammer mill (Model C269OYB, Franklin Co. Inc., Buffton, IN) equipped with a 0.32-cm rejection screen. After milling, the fiber particles were classified into three groups based on the particle size, more than 0.38, 0.38–0.23, and less than 0.23 mm, using a sieve shaker (RO TAP, The W. S. Tyler Company, Cleveland, OH) with corresponding sieves (Newark Wire Cloth Co., Clifton, NJ). The 0.23–0.38 mm particles were used for this sugar production study. They were stored in sealed 2-gal zip-locked plastic bags at 4°C.

AMSW was prepared from MSW obtained from a waste management company in San Francisco, CA. The MSW was first thermally treated with a process called $CR^3$, which autoclaved the MSW with steam for 2–3 h, at temperature of 127°C and pressure of 172 kPa. AMSW was then screened to separate organic fraction from inorganic fraction. The separated organic fraction was used in this study for the hydrolysis treatment.

### *Dilute Sulfuric Acid Pretreatment*

Biomass was pretreated with dilute sulfuric acid solutions (1.4%, w/w) in a 1-L reactor (Carpenter 20 Cb-3, Parr Co., Moline, IL), equipped with impeller mixers and a pressurized injection device. In this study, a 10% (w/w) solid slurry sample (65 g solids) was chosen to allow for proper mixing. Samples were reacted at 165°C for 8 min, based on results of preliminary tests conducted at different temperatures, durations, and acid concentrations. The duration was clocked from when the mixture of biomass, water, and sulfuric acid in the reactor reached the desired reaction temperature. The warming step before 165°C took approx 30 min.

After dilute sulfuric acid pretreatment was completed, the reaction was terminated by immersing the reactor in ice-water until the reactor pressure became 101 kPa. The reactor was opened slowly and the residues were recovered by washing the reactor with deionized water. The mixture of solid residues and washing water was stored in sealed bottles at 4°C. The pretreated biomass was thoroughly washed with hot deionized water (85°C) and filtered under vacuum to remove water-soluble compounds from solids. During the washing and filtration process, the pH of the filtrate was measured with a pH meter (AR20; Fisher Scientific Inc., Hampton, NH)

and washing was stopped when the pH reached 4.5 or the reducing sugar (RS) concentration reached 0.06 g/L.

A portion of the washed pretreated solid was stored at –20°C for subsequent enzymatic hydrolysis. The remaining solid was dried at 45°C in an oven for subsequent chemical composition analysis. The total volume of wash water was measured and recorded. Then a 20-mL sample was taken from the wash water, neutralized with $CaCO_3$, and filtered with glass filter paper of 0.20-μm pore size. The filtered water was stored at 4°C for analysis of total RS and individual sugars.

### *Enzymatic Hydrolysis*

Enzymatic hydrolysis was carried out in 125-mL screw-capped Erlenmeyer flasks. The enzymes used in the study were cellulase (Novozymes, Celluclast 1.5L, available from Sigma-Aldrich Corp. [St. Louis, MO], Cat. No. C2730) supplemented with extra β-glucosidase (Novozyme188, available from Sigma, Cat. No. C6105). Both enzymes were provided by Novozymes Inc. (Davis, CA). The activities of the two enzyme stocks were determined to be 90 filter paper units (FPU)/mL and 250 cellobiose units (CBU)/mL, respectively. The cellulase and β-glucosidase contained 47.1 and 49.7 mg protein/mL, respectively, as measured by Bio-rad protein assay (Bio-rad Laboratory Hercules, CA). The enzymatic hydrolysis was performed at pH 4.8 with cellulase loading of 15 FPU/g-cellulose (7.9 mg protein/g-cellulose) and β-glucosidase loading of 52.5 CBU/g-cellulose (10.4 mg protein/g-cellulose) in prewarmed (50°C) 50-mL reaction slurry that contained solids equivalent to 2% cellulose, 0.05 *M* sodium citrate buffer (pH 4.8), and 0.3% (w/v) sodium azide. Sodium azide was used to inhibit microbial growth during the enzymatic hydrolysis *(1)*. Before loading of enzymes, the pH of slurry was adjusted with 6 *N* HCl or 6 *N* NaOH to 4.8 as needed. Duplicate 125-mL Erlenmeyer reaction flasks were incubated in a shaking incubator at 50°C with an agitation speed at 140 rpm.

During the enzymatic hydrolysis, 1-mL samples were periodically removed from each flask (0, 2, 8, 18, 24, 72, 120, and 168 h). Each sample was centrifuged for 10 min at 13,500*g*, and 500-μL supernatant was then removed and placed into a 1.5-mL Eppendorf tube, which contained the stop buffer (512 m*M* $Na_2CO_3$ and 288 m*M* $NaHCO_3$; pH 10.0) *(9)*. The buffered samples were stored at 4°C for subsequent glucose measurement.

The glucose yield was calculated as:

$$\text{Glucose yield (\%)} = \frac{\text{Glucose (mg/mL)}}{\text{Cellulose added (mg/mL)} \times 1.11} \quad (1)$$

where the factor 1.11 is used to adjust the weight gained in hydrolyzing cellulose to glucose.

### *Analytical Methods*

The moisture content of biomass was measured according to the American Society of Testing and Materials standard method D4444-92 *(19)*. Total RS was measured with the dinitrosalicylic acid method using glucose as the standard *(20)*. The activities of cellulase and β-glucosidase were measured as FPU and CBU, respectively *(21)*. Glucose content was measured with anthrone colorimetric assay *(22,23)*. Xylose, arabinose, galactose, and mannose were measured by analyzing the alditol acetate derivatives synthesized with gas chromatograph as described by Blakeney et al. *(24)* following hydrolysis with 2 *N* trifluoroacetic acid (TFA) for 1 h at 121°C *(25)*. Ash, acid insoluble lignin (Klason lignin), and acid soluble lignin were determined by standard National Renewable Energy Laboratory's laboratory procedures *(26–28)*.

Solubilized monosaccharides in dilute sulfuric acid hydrolysates, including glucose, xylose, arabinose, galactose, and mannose, were determined using gas chromatography *(24,25)*. The glucose concentrations in the samples obtained from the enzymatic hydrolysis were measured using glucose assay kit purchased from Bioassay Systems (Quantichrom™ Glucose Assay Kit, DIGL-200, CA). All measurements were conducted in duplicate trials and average results were reported.

## Results and Discussion

### *Chemical Composition of Biomass Materials*

The chemical compositions of biomass are shown in Table 2. Glucose was the major component followed by lignin (acid insoluble and soluble lignin) and xylose, and various minor components. Herein, galactose, arabinose, and mannose were minor components. The galactose, arabinose, xylose, and mannose are the major components of hemicellulose matrix *(10)*. In addition, the woody samples (athel and eucalyptus) also contained mannose as part of their xylose. Our results are consistent with the results of Grohmann et al. *(29)*, Torget et al. *(14)*, and Brigham et al. *(30)* who reported that the composition of hemicellulose varied with biomass species and woody xylose contained mannose. Therefore, it can be stated that the hemicellulose of all the biomass used in this study mainly included arabinose, galactose, xylose, and/or mannose with xylose as the dominant carbohydrate. Even though hemicellulose contained some glucose, it was difficult to distinguish the glucose source, because some glucose might come from cellulose during the chemical composition measurement. In addition, AMSW had considerably lower hemicellulose content (5.4%), compared with the saline crops.

### *Dilute Acid Pretreatment*

Weight loss was used to evaluate the effect of dilute acid pretreatment on composition removal for different biomass materials, because the

Table 2
Chemical Composition of Untreated Biomass (dry basis [wt%])

| | Athel | Eucalyptus | CWR | JTW | AMSW |
|---|---|---|---|---|---|
| Glucose | 49.34 | 44.45 | 34.03 | 31.09 | 43.95 |
| Xylose | 11.82 | 10.53 | 16.48 | 16.90 | 2.43 |
| Arabinose | 0.68 | 0.82 | 3.28 | 2.83 | 0.48 |
| Galactose | 0.46 | 2.24 | 0.78 | 0.66 | 0.43 |
| Mannose | 0.27 | 0.28 | ND[a] | ND | 1.98 |
| Acid-insoluble lignin[b] | 25.97 | 32.73 | 20.85 | 17.70 | 22.20 |
| Acid-soluble lignin[b] | 4.45 | 2.45 | 3.51 | 2.70 | 1.66 |
| Ash | 5.43 | 2.14 | 7.37 | 8.61 | 9.89 |
| Other | 1.58 | 4.36 | 13.70 | 19.51 | 16.98 |

[a]ND, not detected.
[b]Lignin contents were measured using unextracted biomass.

Table 3
Removal of Components From Biomass Solids by Dilute Acid Pretreatment (%)[a]

| | Athel | Eucalyptus | CWR | JTW | AMSW |
|---|---|---|---|---|---|
| Glucose | 19 | 16 | 12 | 9 | 12 |
| Xylose | 99 | 98 | 97 | 99 | 99 |
| Arabinose | 100 | 100 | 100 | 100 | 100 |
| Galactose | 100 | 100 | 100 | 100 | 100 |
| Mannose | 100 | 100 | – | – | 100 |
| Acid-insoluble lignin[b] | 22.01 | 29.61 | 13.30 | 27.09 | 18.19 |
| Acid-soluble lignin[b] | 85.08 | 82.07 | 88.69 | 90.31 | 98.63 |

[a]The removal of components (%) = (components in raw solid-components in pretreated solid)/components in raw solid × 100%.
[b]Lignin contents were measured using unextracted biomass.

removal mechanism involves the hydrolysis of the various cell wall components *(14)*. Dry weight losses varied from 59% (JTW) to 35% (AMSW) (Fig. 1). As shown in Table 3, the sugars released from the acid pretreatment included arabinose, galactose, glucose, xylose, and mannose, but no mannose was found from grasses and AMSW. Most of the acid soluble lignin was removed from the solids (82.07–98.63%), but only a relatively small fraction of the acid insoluble lignin was removed (13.30–29.61%). The hydrolysis of cellulose was low (16–19% for athel and eucalyptus and 9–12% for CWR, JTW, and AMSW). Dilute acid pretreatment was equally effective at removing hemicellulose from the woods, grasses, and AMSW.

The sum of the individual sugars and amounts of solubilized RS were also measured (Fig. 2) because the RS contents in the prehydrolyzates can effectively indicate the solubilization of hemicellulose and cellulose during the pretreatment process *(1)*. JTW released the highest amount of RS and individual sugars from hemicellulose. Because of its low content of

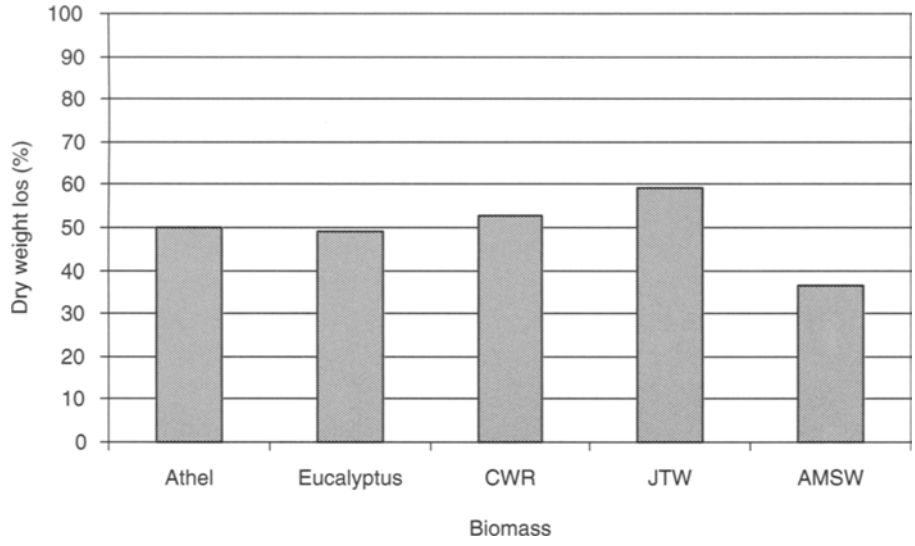


**Fig. 1.** Dry weight losses of different biomass after dilute acid pretreatment.

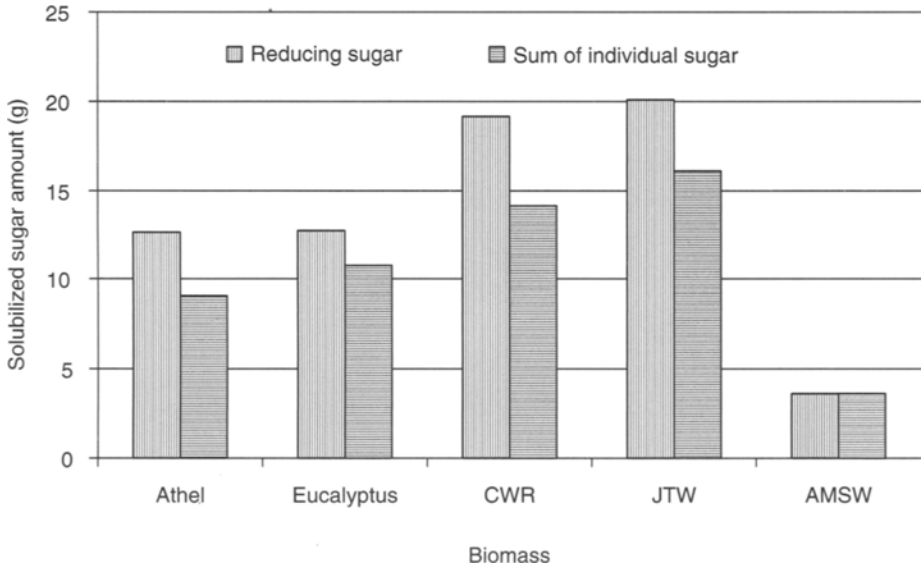


**Fig. 2.** Solubilized RS and sum of individual sugar released from different biomass materials after dilute acid pretreatment.

hemicellulose (5.32%), AMSW had the lowest amount of solubilized RS and individual sugars. In Fig. 2, it can be seen that the amount of RS was higher than the sum of individual sugars. The difference might be because of the presence of other RSs (such as cellobiose) and nonsugar reducing components that were measured as RSs.

The xylose mass balance was done based on the dilute acid pretreatment system. The xylose contents were measured in original solids,

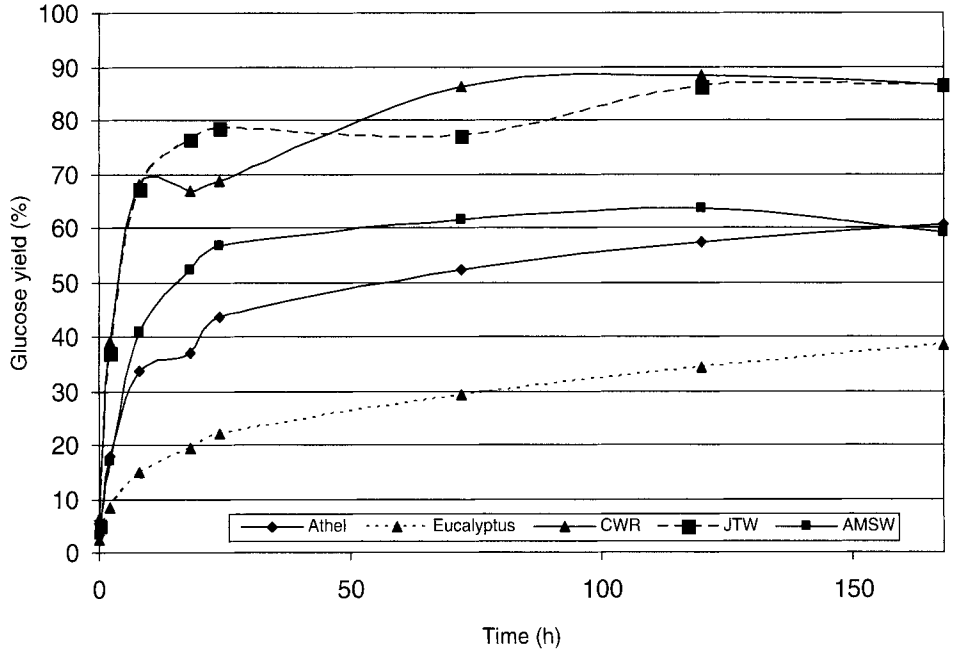


**Fig. 3.** Glucose yield from different acid-treated biomass materials during the enzymatic hydrolysis.

pretreated solids, and prehydrolyzate. It was found that xylose mass balance could not be closed. For example, 33% of the xylose in Athel and 20% in CWR were not recovered as monomeric xylose. These findings were similar to reported results, which indicated that some sugars, such as xylose and glucose, were solubilized in the prehydrolyzate as oligomeric sugar, furfural, hydroxymethylfurfural, and/or other byproducts during the acid pretreatment *(1,7,31)*.

## *Enzymatic Hydrolysis for Glucose Yield*

The glucose yields from different pretreated biomass materials during the enzymatic hydrolysis are shown in Fig. 3. The two grasses, CWR and JTW, had the highest yields (87% cellulose saccharified) after the 168 h treatment. The two woods, athel and eucalyptus, had the lowest glucose yield (60 and 38% cellulose converted, respectively). The glucose yield for AMSW was 63% cellulose converted, which was higher than the glucose yield from the woods. The CWR and JTW also had the fastest rate of sugar release, two to three times faster than Athel and AMSW and five times faster than eucalyptus. In particular, the conversion of cellulose to glucose for JTW was nearly 80% completed after only 24 h of enzymatic hydrolysis. Eucalyptus had the lowest rate of released glucose and even after 168 h the glucose continued to increase in concentration.

The reason for the difference in cellulose hydrolysis rates and final glucose yields among the different biomass materials might be that cellulose

Table 4
Total Sugar Yield From Different Biomass by Dilute Acid Pretreatment and Enzymatic Hydrolysis (gram per gram of Original Dry Matter)

| Biomass | Glucose | Xylose | Arabinose | Galactose | Mannose | Total sugar[a] |
|---|---|---|---|---|---|---|
| Athel | 0.24 | 0.08 | 0.005 | 0.003 | 0.002 | 0.33 |
| Eucalyptus | 0.19 | 0.07 | 0.007 | 0.01 | 0.003 | 0.28 |
| CWR | 0.31 | 0.13 | 0.03 | 0.007 | – | 0.48 |
| JTW | 0.34 | 0.12 | 0.02 | 0.005 | – | 0.49 |
| AMSW | 0.36 | 0.03 | 0.008 | 0.006 | 0.02 | 0.42 |

The sugar is specified as monomeric sugar. For example, total glucose yield = (total monomeric glucose released by dilute acid pretreatment in liquid + total glucose yield from enzymatic hydrolysis)/(total raw dry matter loaded initially in dilute acid pretreatment step). Other sugar yield = (total sugars released by dilute acid pretreatment)/(total raw dry matter loaded initially in dilute acid pretreatment step).

[a]Total sugar is the summation of all the individual sugars released by dilute acid pretreatment and enzymatic hydrolysis.

fibers in pretreated grasses (CWR and JTW) were inherently more digestible than those of pretreated woods (athel and eucalyptus) and AMSW *(14)*. Another possibility could be that lignin condensation during dilute acid pretreatment contributed to the development of higher porosity for grasses than for woods and AMSW, making the cellulose in grasses more accessible by the enzymes *(14)*. More research is needed to identify the mechanism.

### *Total Monomeric Sugars Yield From Dilute Acid Pretreatment and Enzymatic Hydrolysis*

Because of the improvement of genetic engineering, microorganisms now can ferment pentose and hexose sugars to ethanol at the same time *(32–37)*. Therefore, it has become important to measure the total sugar yield from hydrolysis of biomass. In fact, based on either the total or just glucose yield, the grasses and AMSW had higher yields than the woods (Table 4). AMSW had the highest glucose yield (0.36 g/g original dry matter) and eucalyptus had the lowest yield (0.19 g/g original dry matter). For total sugar yields, CWR and JTW had the highest values (0.48 and 0.49 g/g original dry matter, respectively). Eucalyptus had the lowest total sugar yield (0.28 g/g original dry matter). The total sugar yield of AMSW was notable because it was 0.42 g/g original dry matter, which indicated that AMSW could be a good biomass feedstock for ethanol production.

## Conclusions

Athel and eucalyptus had higher cellulose and lignin contents than CWR, JTW, and AMSW. Dilute acid pretreatment was highly effective in hydrolyzing the hemicelluloses in all of the tested biomass materials (over 97%). After dilute acid pretreatment, removal of lignin from the

solids was 13–30%. Overall, the lignins in the grasses were more resistant to dilute acid pretreatment than the woody lignins. Pretreated CWR and JTW had the highest glucose yields (86% of total cellulose converted) and fastest rates of hydrolysis, but the pretreated eucalyptus had the lowest glucose yield (38%) and lowest hydrolysis rate of the samples evaluated in this study. Considering the fact that AMSW is originated from waste streams, its glucose yield of 63% makes it an attractive resource for use as a feedstock for sugar production. CWR and JTW had the highest yield of total monomeric sugars (0.48 and 0.49 g/g original dry matter). AMSW showed promising yield (0.42 g/g original dry matter) of total monomeric sugars. The future research will focus on enzymatic hydrolysis of JTW, CWR, and AMSW with lower enzyme and higher solid loadings.

## Acknowledgment

Authors would like to thank Novozymes, Inc., for providing the enzymes used in this research. The funding support for this research is provided by a research grant from California Department of Water Resources (Grant No. 4600002991).

## References

1. Sun, Y. and Cheng, J. J. (2005), *Bioresour. Technol.* **96,** 1599–1606.
2. Brownell, H. H. and Saddler, J. N. (1984), *Biotechnol. Bioeng. Symp.* **14,** 55–68.
3. Gould, J. M. (1984), *Biotechnol. Bioeng.* **XXVI,** 046–052.
4. Cadoche, L. and Lopez, G. D. (1989), *Biol. Wastes,* **30,** 153–157.
5. Martinez, J., Negro, M. J., Saez, F., Manero, J., Saez, R., and Martin, C. (1990), *Appl. Biochem. Biotechnol.* **24–25,** 127–133.
6. Shah, M. M., Song, S. K., Lee, Y. Y., and Torget, R. (1991), *Appl. Biochem. Biotechnol.* **28–29,** 99–109.
7. Torget, R., Himmel, M. E., and Grohmann, K. (1991), *Bioresour. Technol.* **35,** 239–246.
8. Torget, R., Himmel, M., and Grohmann, K. (1992), *Appl. Biochem. Biotechnol.* **34–35,** 115–123.
9. Vlasenko, E. Y., Ding, H., Labavitch, J. M., and Shoemaker, S. P. (1997), *Bioresour. Technol.* **59,** 109–119.
10. McMillan, J. D. (1996), In: *Handbook on Bioethanol: Production and Utilization.* Wyman, C. E. (ed.), Taylor & Francis, Washington, DC, pp. 287–313.
11. Grethlein, H. E., Allen, D. C., and Converse, A. O. (1984), *Biotechnol. Bioeng.* **XXVI,** 1498–1505.
12. Grohmann, K., Torget, R., and Himmel, M. (1985), *Biotechnol. Bioeng. Symp.* **15,** 59–80.
13. Grohmann, K., Torget, R., and Himmel, M. (1986), *Biotechnol. Bioeng. Symp.* **17,** 135–151.
14. Torget, R., Walter, P., Himmel, M., and Grohmann, K. (1990), *Appl. Biochem. Biotechnol.* **24–25,** 115–126.
15. Torget, R., Walter, P., Himmel, M., and Grohmann, K. (1991), *Appl. Biochem. Biotechnol.* **28–29,** 75–86.
16. Nguyen, Q. A., Tucker, A. P., Boynton, B. L., Keller, F. A., and Schell, D. J. (1998), *Appl. Biochem. Biotechnol.* **70–72,** 77–87.
17. Nguyen, Q. A., Tucker, A. P., Keller, F. A., and Eddy, F. P. (2000), *Appl. Biochem. Biotechnol.* **84–86,** 561–576.
18. Um, B. H., Karim, M. N., and Henk, L. L. (2003), *Appl. Biochem. Biotechnol.* **105–108,** 115–125.

19. American Society of Testing and Materials (1997), Standard test method for direct moisture content measurement of wood and wood-base materials. Designation: ASTM D4444-92, West Conshohocken, PA, pp. 517–521.
20. Miller, G. L. (1959), *Anal. Chem.* **31(3),** 426–428.
21. Ghose, T. K. (1987), *Pure Appl. Chem.* **59(2),** 257–268.
22. Dische, D. (1962), In: *Method in Carbohydrate Chemistry*. Whistler, R. L., and Wolfrom, M. L., (eds.), Academic Press, New York, pp. 480–514.
23. Ahmed, A. E. and Labavitch, J. M. (1980), *Plant Physiol.* **65,** 1009–1013.
24. Blakeney, A. B., Harris, P. J., Henry, R. J., and Stone, B. A. (1983), *Carbohyd. Res.* **113,** 291–299.
25. Albersheim, P., Nevins, D. J., English, P. D., and Karr, A. (1967), *Carbohyd. Res.* **5,** 340–345.
26. Templeton, D. and Ehrman, T. (1995), NREL Analytical Procedure No. LAP-003, National Renewable Energy Laboratory, Golden, CO.
27. Ehrman, T. (1996), NREL Analytical Procedure No. 003, National Renewable Energy Laboratory, Golden, CO.
28. Sluiter, A., Hanes, B., Ruiz, R., Scarlata, C., Sluiter, J., and Templeton, D. (2005), NREL Analytical Procedure No. 004, National Renewable Energy Laboratory, Golden, CO.
29. Grohmann, K., Himmel, M., Rivard, C., et al. (1984), *Biotechnol. Bioeng. Symp.* **14,** 137–157.
30. Brigham, J. S., Adney, W. S., and Himmel, M. E. (1996), In: *Handbook on Bioethanol: Production and Utilization*. Wyman, C. E. (ed.), Taylor & Francis, Washington, DC, pp. 119–141.
31. Prieto, S., Clausen, E. C., and Gaddy, J. L. (1986), *Biotechnol. Bioeng. Symp.* **17,** 123–133.
32. Deanda, K., Zhang, M., Eddy, C., and Picataggio, S. (1996), *Appl. Environ. Microbial.* **62,** 4465–4470.
33. Dien, B. S., Hespell, R. B., Wyckoff, H. A., and Bothast, R. J. (1998), *Enzyme Microbial. Technol.* **23,** 366–371.
34. Aristidou, A. and Penttila, M. (2000), *Curr. Opin. Biotechnol.* **11,** 187–198.
35. Bothast, R. J., Nichols, N. N., Dien, B. S., and Cotta, M. A. (2002), *Society of Industrial Microbiology Annual Meeting*, paper No. 12-1, Philadelphia, PA.
36. Sues, A., Millati, R., Edebo, L., and Taherzadeh, M. J. (2005), *FEMS Yeast Res.* **5,** 669–676.
37. Ruohonen, L., Aristidou, A., Frey, A. D., Penttila, M., and Kallio, P. T. (2006), *Enzyme Microb. Technol.* **39,** 6–14.

0273-2289/1559-0291 (Online)/07/136–140/437–450/$30.00

# Techno-Economic Analysis of Biocatalytic Processes for Production of Alkene Epoxides

ABHIJEET P. BOROLE* AND BRIAN H. DAVISON

*Life Biosciences Division, Oak Ridge National Laboratory, Oak Ridge, TN 37831-6226, E-mail: borolea@ornl.gov*

## Abstract

A techno-economic analysis of two different bioprocesses was conducted, one for the conversion of propylene to propylene oxide (PO) and other for conversion of styrene to styrene epoxide (SO). The first process was a lipase-mediated chemo-enzymatic reaction, whereas the second one was a one-step enzymatic process using chloroperoxidase. The PO produced through the chemo-enzymatic process is a racemic product, whereas the latter process (based on chloroperoxidase) produces an enantio-pure product. The former process thus falls under the category of high-volume commodity chemical (PO); whereas the latter is a low-volume, high-value product (SO).

A simulation of the process was conducted using the bioprocess engineering software SuperPro Designer v6.0 (Intelligen, Inc., Scotch Plains, NJ) to determine the economic feasibility of the process. The purpose of the exercise was to compare biocatalytic processes with existing chemical processes for production of alkene expoxides. The results show that further improvements are needed in improving biocatalyst stability to make these bioprocesses competitive with chemical processes.

**Index Entries:** Bioprocess; chloroperoxidase; economics; enzymatic; epoxides; lipase.

## Introduction

Biocatalytic production of chemicals and intermediates has been studied at the laboratory level for several years; however, few industrial-scale processes have been commercialized. Commercial production of commodity organic chemicals using enzymatic catalysts has been almost nonexistent. However, with the increased use of biocatalytic processes in low-volume high-value chemicals such as pharmaceutical intermediates, newer technologies improving the activity and stability of enzyme biocatalysts *(1,2)* for industrial applications have emerged. Some of these include improved immobilization techniques *(3)*, stabilization through lyophilization with lyoprotectants *(4)*, salts *(5)*, or addition of surfactants *(6,7)*, chemical modification with amphiphilic or hydrophobic polymers *(8,9)*.

*Author to whom all correspondence and reprint requests should be addressed.

Epoxidation of alkenes is of significant industrial interest because of production of a range of products from the epoxides including glycols, polymers such as polyols, plasticizers, and stabilizers for polyurethane manufacturing, pharmaceuticals, agrochemicals, and so on. Biocatalytic epoxidation of alkenes is possible through microbial or enzymatic processes. A microbial process is preferred when cofactor regeneration is necessary, as in monooxygenase-based processes *(10)*. Alternately, an enzymatic process using fatty acids as peroxidation cosubstrates *(11–13)* may be used. Epoxidation of terminal alkenes with carbon atoms ranging from 8 to 16 carbon atoms as well as some cycloalkenes has been demonstrated *(11)*. A second enzymatic route is through the use of haloperoxidases such as chloroperoxidase (CPO) from *Caldariomyces fumago*. This conversion results in epoxides with enantiomeric excess as high as 95%, although yields are generally moderate *(14)*.

Propylene oxide (PO) is one of the largest volume epoxides produced worldwide using chemical routes. A bioprocess route has potential to increase the energy efficiency of producing this commodity chemical. Two biological routes have previously been proposed for production of PO. These include a four-step Cetus process based on corn liquor fermentation and a second route based on methane monooxygenase (MMO) *(15)*. A technical and economic analysis and comparison of various bioreactor types for the latter process was also reported *(16)*. A third route being proposed here is based on a two-step chemo-enzymatic process using lipase as catalyst. A process model based on the two-step reaction was developed for industrial production of PO and an order of magnitude economic analysis was conducted.

Similarly, the epoxidation of styrene through chloroperoxidase was used as a model for developing the process model, followed by the economic feasibility analysis of the process. It should be noted that the chloroperoxidase-based process produces styrene oxide (SO) at high enantiomeric excess, whereas the (PO) is a racemic product. In the latter, whereas the first step is enzymatic, the second step, which produces PO is a chemical step. To develop a process for high-volume commodity chemicals such as PO, enantiopurity is not considered necessary.

## Results and Discussion

### *Propylene Oxide Process Description*

The production of PO is based on a two-step chemo-enzymatic reaction using lipase, a fatty acid, and hydrogen peroxide. The two reaction steps are given below:

$$H_2O_2 + \text{Fatty acid (using lipase as catalyst)} \rightarrow \text{Peroxy acid} + H_2O \quad (1)$$

$$\text{Propylene} + \text{Peroxy acid} \rightarrow \text{PO} + \text{Fatty acid (recycled)} \quad (2)$$

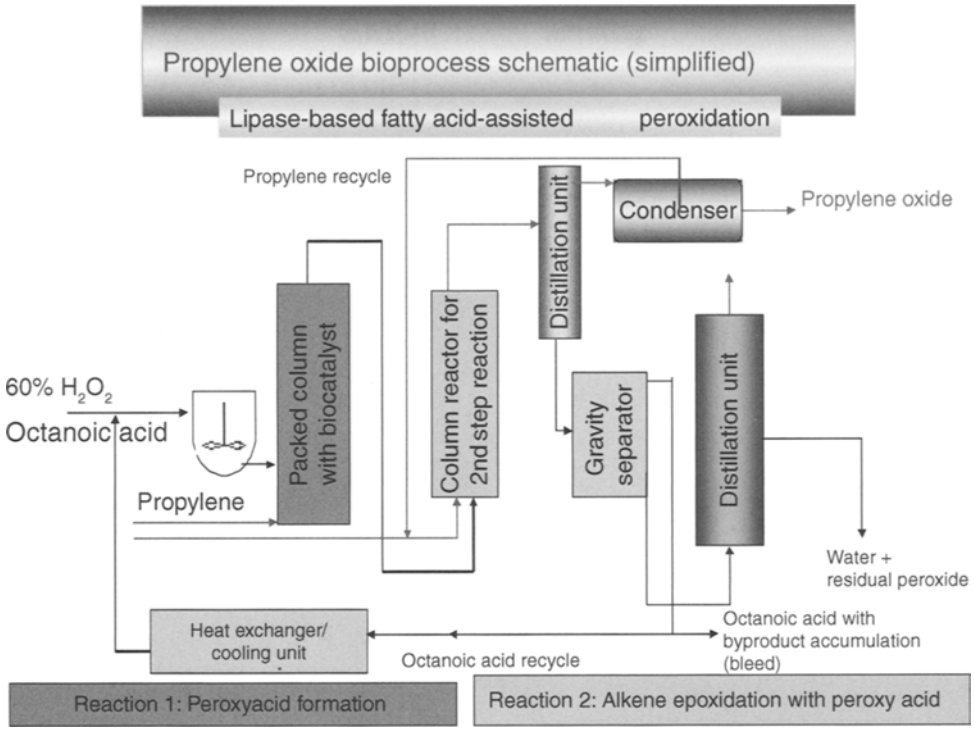


**Fig. 1.** Schematic for conversion of propylene to propylene oxide using a lipase-based chemo-enzymatic peroxidation process.

A chemical route based on peroxy acid as an oxidant has been reported previously. In such a process, acetic acid is suggested as the fatty acid for use. However, use of a low-molecular weight fatty acid interferes with subsequent product separation. Thus, use of higher molecular weight fatty acids is preferable. The enzymatic route allows use of higher fatty acids of up to 20 carbon atoms with very good conversion to peroxy acid *(13)*. Although the reactivity of these higher fatty acids with propylene has not been demonstrated, they have been shown to be effective in epoxidizing terminal alkenes with 8–16 carbon atoms *(11)*. A few assumptions have been made in developing the process model, with the reactivity of specifically, peroxyoctanoic acid with propylene, being one of them. Other assumptions are described later.

The first step in the PO process is conversion of a fatty acid, such as octanoic acid to octane peroxy acid using lipase and $H_2O_2$. The peroxy acid is then used as a chemical oxidant to oxidize propylene-to-propylene oxide in the second step. Such a process is applicable to epoxidation of unsaturated plant oils as well *(17,18)*. A schematic of the process for production of PO is shown in Fig. 1. In this preliminary design developed for the process, octanoic acid and 60% hydrogen peroxide are first mixed in a blending tank. The solubility data on hydrogen peroxide solubility in octanoic acid is not available, so an approximation based on the solubility

data of water in octanoic acid (3.88% at 14.4°C) *(19)* was used. A maximum solubility of 3% was assumed for 60% hydrogen peroxide in octanoic acid at 25°C. The octanoic acid solution containing the dissolved peroxide is then passed through a packed column containing the appropriate biocatalyst. In this study, the biocatalyst used was an immobilized lipase (Novozym-435; Novozymes, Franklinton, NC), for which kinetic data is available for the reaction of epoxidation of unsaturated fatty acids. The kinetic rate constants for alkene epoxidation is not available, although the conversion data is available. However, because rate data is required for determining process conversion, an approximation was used.

Deactivation of the lipase biocatalyst is included as a third reaction (disappearance of the biocatalyst). The rate of deactivation is used from a study by Hilker *(17)*, which gives kinetic constants at various temperatures. The reactor 1 was designed to operate at 40°C and the rate of deactivation of the biocatalyst used was 0.036/min in the organic phase saturated with 60% $H_2O_2$. The propylene gas is flown cocurrent (upward) and recycled to achieve higher conversion. The operating temperature in the reactor is 40°C, allowing the product PO to leave the reactor as a gas along with the unconverted reactant, propylene. This gas mixture is sent to a condenser to remove product PO from propylene. The liquid mixture from the reactor (containing water and residual hydrogen peroxide, dissolved propylene, PO, and octanoic acid) is passed through a gravity separator to remove any aqueous phase carried over with the organic phase. Any aqueous phase collecting in the separator is flash distilled to remove dissolved PO. The organic phase is passed through a distillation tower to remove water (any byproducts formed, such as propylene glycol may also be removed in this manner, although byproduct formation is assumed to be zero in this simulation). The bottoms stream from the distillation tower contains octanoic acid and octane peroxy acid. This stream is recycled to the reactor 1. A recycle loop is also provided for propylene from the condenser outlet as well as the distillation unit.

To enable process design and economic analysis of the process, a simulation of the process was conducted (using SuperPro Designer). A process flow diagram is given in Fig. 2. It should be noted that two reactors in series are used for the two serial steps, wherein the first one is simulation of a packed bed reactor and the second one is a plug flow reactor. Several assumptions were made in designing the process and in its simulation. The major assumptions are listed below:

1. Kinetic data from lauric/stearic acid peroxidation *(17)* is applicable for first step.
2. Kinetic data from oleic acid/alkene epoxidation *(17)* is applicable for second step.
3. Aqueous solubility (water + $H_2O_2$) in octanoic acid of 3% was assumed.

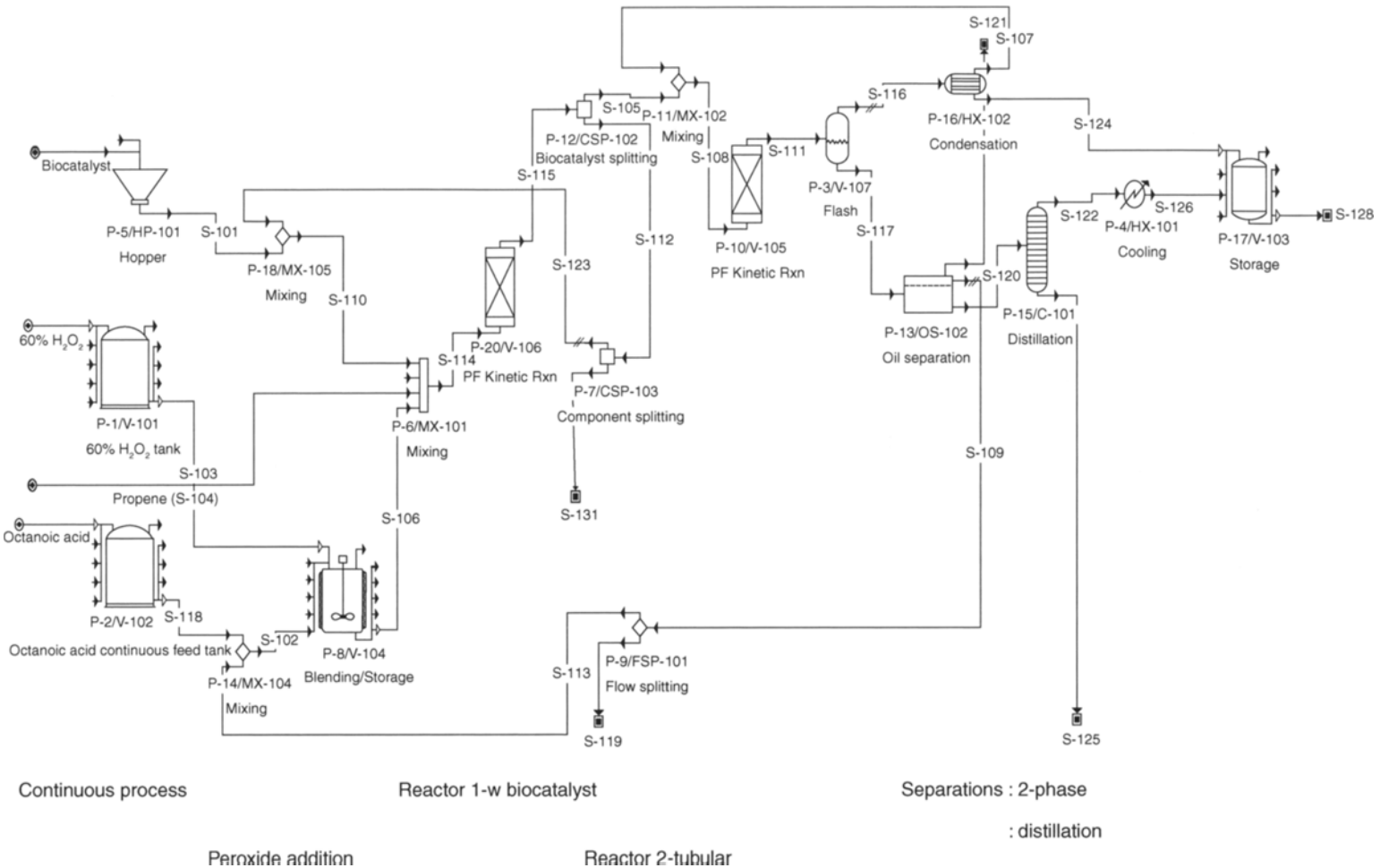


**Fig. 2.** Process flow diagram for propylene oxide production using a lipase-based chemo-enzymatic peroxidation process.

Executive summary (2005 prices)

| | |
|---|---|
| Total capital investment | 169,071,000 $ |
| Capital investment charged to this project | 169,071,000 4 |
| Operating cost | 823,708,000 $/yr |
| Production rate | 199,160,052.85 kg of MP/yr |
| Unit production cost | 4.14 $/kg of MP |
| Total revenues | 290,741,000 $/yr |

Annual operating cost (2005 prices) - Process summary

| Cost item | $ | % |
|---|---|---|
| Raw materials | 752,183,000 | 91.32 |
| Labor-dependent | 6,441,000 | 0.78 |
| Facility-dependent | 17,187,000 | 2.09 |
| Laboratory/QC/QA | 966,000 | 0.12 |
| Consumables | 0 | 0 |
| Waste treatment/disposal | 1,424,000 | 0.17 |
| Utilities | 45,508,000 | 5.52 |
| Transportation | 0 | 0 |
| Miscellaneous | 0 | 0 |
| Advertising/selling | 0 | 0 |
| Running royalties | 0 | 0 |
| Failed product disposal | 0 | 0 |
| Total | 823,708,000 | 100 |

Raw materials cost - Process summary

| Bulk raw material | Unit cost ($/kg) | Annual amount (kg) | Annual cost ($) | % |
|---|---|---|---|---|
| 60% $H_2O_2$ | 0.396 | 196,051,680 | 77,715,000 | 10.33 |
| Octanoic acid | 1,320 | 4,356,000 | 5,750,000 | 0.76 |
| Propene | 0.677 | 145,569,600 | 98,478,000 | 13.09 |
| Biocatalyst | 900 | 633,600 | 570240,000 | 75.81 |
| Total | | 346,610,880 | 752,183,000 | 100 |

**Fig. 3.** Results from preliminary economic analysis of an enzymatic propylene oxide production process.

4. Separation of bulk aqueous phase from octanoic acid phase can be achieved by gravity separation.
5. No royalty cost was assumed in economic analysis.
6. Waste disposal cost was assumed to be negligible.
7. Cost of propylene, hydrogen peroxide, lipase enzyme, and propylene oxide was assumed to be $0.67, 0.66, 900, and 1.58/kg, respectively. This is based on pricing obtained from commercial vendors and Chemical Market Reporter magazine (July 5–12 2004).
8. No byproducts were assumed to be formed in this analysis.
9. No degradation of the peroxy acid occurs in the distillation tower.
10. The biocatalyst deactivation rate (essentially owing to peroxide) obtained for octanoic acid–propylene-Novozym 435 system was presumed to be similar to that reported by Hilker et al. *(17)* for toluene–oleic acid-Novozym 435 system.

The assumptions are presumed suitable for an order-of-magnitude analysis and it should be made clear that many of these assumptions may have to be revised if a more detailed process simulation is to be undertaken. The results of the analysis are shown in Fig. 3. The results indicate

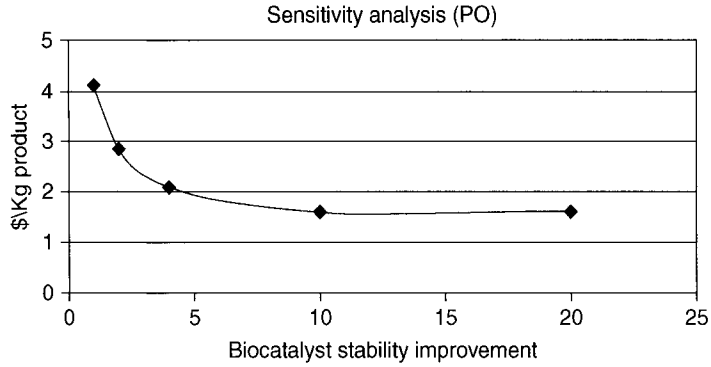


**Fig. 4.** Sensitivity analysis for production of propylene oxide with respect to enzyme stability. An order of magnitude improvement in enzyme stability (reduction in deactivation constant) is needed for the process to produce PO at a cost comparable with current chemical commercial process (PO-Styrene process). The baseline enzyme stability used in the study was for Novozym 435, which is a polyvinyl acetate-immobilized form of the lipase enzyme.

that the process is uneconomical considering the price of biocatalyst used ($900/Kg, Novozym 435). The cost of production of PO was determined to be about $4.14/kg, which is 2.6-fold higher than the current selling price of PO ($1.58/kg). The cost of raw materials (including enzyme) is 91% of the cost of production. Furthermore, the enzyme costs amount to about 75% of the total raw material cost. Thus, improvements are needed either in the biocatalyst activity, stability, or its purchase cost.

A sensitivity analysis was conducted based on the cost and the stability of the enzyme. The cost of the product PO was found to be controlled largely by lipase enzyme and its stability. This cost can potentially be reduced as the demand for the enzyme rises. For the biocatalyst, Novozym 435, used in this analysis, the cost has to drop to $45/kg for the process to produce PO economically, based on this order of magnitude analysis. The sensitivity analysis was done with respect to biocatalyst stability using the price of $900 to find out how stability improvement would affect production cost. The result is given in Fig. 4. The plot shows that a 10- to 20-fold improvement in stability is necessary to bring the production cost near the current product-selling price. It should be noted that the price listed ($900/kg) is for the biocatalyst itself and not the cost for producing a kilogram of product. Second, the price was obtained from enzyme manufacturers that sell the enzymes in bulk. Thus, the prices are realistic prices at this time for the current demand. The prices will certainly decrease as demand increases and technology advances.

A comparison with previously suggested biochemical as well as chemical routes was conducted. Based on the production costs reported previously *(15)*, the three chemical routes, chlorohydrin, *t*-butyl alcohol, and the styrene byproduct routes resulted in PO production cost of $1.548, 1.219, and 0.87/kg of PO, respectively, calculated for 2005 using chemical

plant cost index. The Cetus process gave a production cost of $1.89, whereas the Exxon MMO process gave a cost of $1.14/kg of PO. Although these production costs are relatively low compared with the cost of production using the lipase-based chemo-enzymatic process ($4.14/kg of PO), it should be stressed that in the bioprocess calculations for the Cetus and MMO process, the cost of biocatalyst was not appropriately accounted for. For example, the Cetus process uses three enzymes, glucose isomerase, chloroperoxidase, and epoxide hydrolase as well as a palladium catalyst, and the total catalyst cost (for all four) was assumed to be only 15% of propylene cost. In the MMO process, the cost of the microbial MMO catalyst was about 20% of the propylene cost. A more detailed analysis *(16)* for the MMO process reported a cost of $26.6/kg of PO using a conventional reactor and a cost of $11/kg with an improved reactor (granular-activated carbon-fluidized bed reactor).

### *SO Production Process*

A similar order of magnitude process analysis was also conducted for the production of SO. The design of this process was based on experimental system developed elsewhere *(20,21)*. A batch process was designed for production of 200 *t*/yr of SO. The flow sheet is given in Fig. 5. It consists of a two-phase bioreactor consisting of 1% styrene as the organic phase and 99% aqueous phase containing the enzyme, chloroperoxidase. The organic substrate is emulsified in the aqueous buffer using the surfactant aerosol-OT. Such a system was reported to increase the total turnover number (TTN) by one order of magnitude *(21)*. A process based on the 2-phase system without the surfactant was also evaluated. The process was conducted in batch with a 16 h batch and fed-batch addition of the enzyme, hydrogen peroxide, and the substrate styrene (based on the rate of conversion). The design was based on production of 600 kg of SO per batch, separated through vacuum distillation. The following assumptions were made in the analysis. The first four assumptions are based on experimental work reported elsewhere *(21)*.

1. Assume stoichiometric conversion to obtain 1.3 g/L/h productivity of SO.
2. Assume TTN of 13,000, equivalent to 27.0 mg/L/h of enzyme use.
3. Total volume of aqueous phase approx 28,500 L; 267.0 kg of styrene (added at 1% [w/w]).
4. Provide hydrogen peroxide in stoichiometric amounts, at rate 7.2 mmoles/L/h.
5. Use oil–water separator for phase separation and assume 99% SO recovery from the aqueous–organic mixture.
6. Use batch distillation at 0.01 bar and 75°C *(22)* to achieve 90.3% SO with 9.7% styrene in product, and recover balance styrene approx 224.0 kg for recycle (*Note*: This is shown as revenue stream here, along with SO product, but will be recycled).

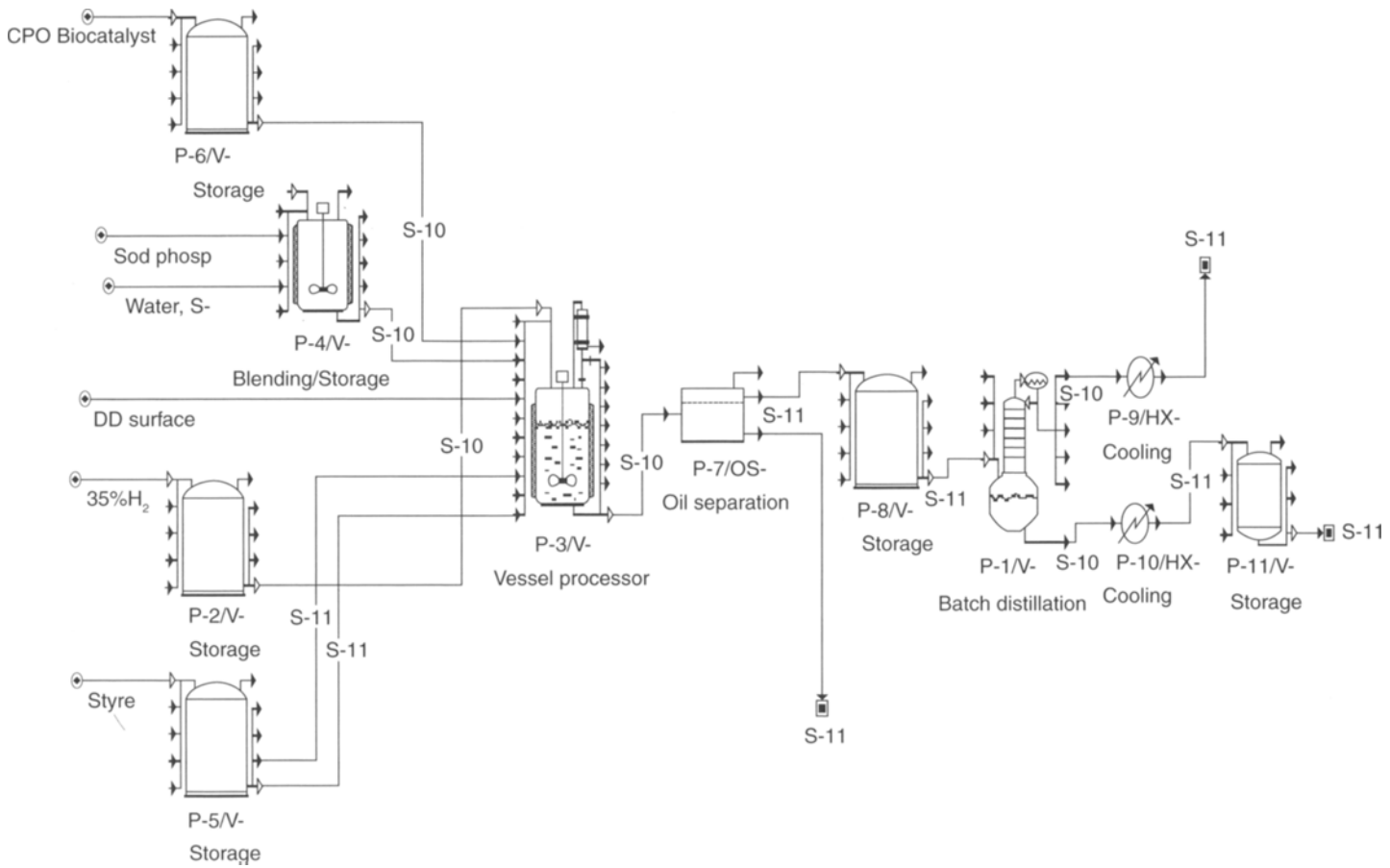


**Fig. 5.** Flow sheet for production of StyOx in a batch process using SuperPro Designer.

Executive summary (2005 prices)

| | |
|---|---|
| Total capital investment | 31,721,000 $ |
| Capital investment charged to this project | 31,721,000 $ |
| Operating cost | 221,672,000 $/yr |
| Production rate | 192,203.78 kg of MP/yr |
| Unit production cost | 1,153.32 $/kg of MP |
| Total revenues | 4,872,000 $/yr |

Annual operating cost (2005 prices) - Process summary

| Cost item | $ | % |
|---|---|---|
| Raw materials | 213,857,000 | 96.47 |
| Labor-dependent | 4,952,000 | 2.23 |
| Facility-dependent | 2,116,000 | 0.95 |
| Laboratory/QC/QA | 743,000 | 0.34 |
| Consumables | 0 | 0 |
| Waste treatment/disposal | 0 | 0 |
| Utilities | 3,000 | 0 |
| Transportation | 0 | 0 |
| Miscellaneous | 0 | 0 |
| Advertising/selling | 0 | 0 |
| Running royalties | 0 | 0 |
| Failed product disposal | 0 | 0 |
| Total | 221,672,000 | 100 |

Raw materials cost - Process summary

| Bulk raw material | Unit cost ($/kg) | Annual amount (kg) | Annual cost ($) | % |
|---|---|---|---|---|
| Sodium phosphate | 0.100 | 117,785 | 12,000 | 0.01 |
| Water | 0.001 | 9,494,579 | 9,000 | 0 |
| Hydroperoxide | 0.660 | 57,749 | 38,000 | 0.02 |
| Styrene | 1.210 | 264,762 | 320,000 | 0.15 |
| Biocatalyst | 50,000 | 4,261 | 213,036,000 | 99.62 |
| Dioctyl sulfosu | 5 | 88,330 | 442,000 | 0.21 |
| Total | | 10,027,465 | 213,857,000 | 100 |

**Fig. 6.** Results from preliminary economic analysis of an enzymatic StyOx production process.

7. A yield of 100% is assumed and no byproducts are assumed to be produced.
8. Biocatalyst (CPO) price was initially assumed to be about $5/mg.

The enzyme price was obtained from vendors who supply the purified enzyme, but have only laboratory-scale operations for production of CPO (price between $5 and $16/mg). In a recent review *(23)*, the price of CPO obtained from Chirazym was $5/mg. Although this is not an appropriate price for evaluating a commercial application, a better estimate for this fungal enzyme is not available. Although research on development of improved methods to produce CPO are under way *(23,24–26)*, a significantly cheaper way to produce this enzyme has not been reported. Assuming a 100-fold decrease in the price of the enzyme compared with current methods of production gives a price of CPO = $0.05/mg. Thus, an approximate estimate of $50,000/kg was used in the analysis.

The results of the economic analysis are shown in Fig. 6. The results show that the biocatalyst cost (using a price of $50,000/kg) contributes to

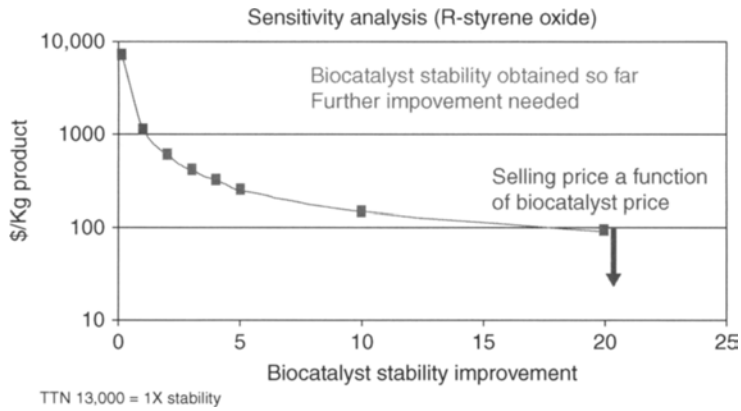


**Fig. 7.** Sensitivity analysis for production of styrene epoxide with respect to enzyme stability. The stabilization procedure developed at University of California, Berkeley accounts for a ninefold decrease in cost compared with existing data.

more than 95% of the production cost. Thus, the biocatalyst cost is the major contributor to the product price. Industrial enzymes are now available at much reduced prices, as genetically engineered strains have been developed to produce the enzymes. Enzymes such as amyloglucosidase and cellulases are available in the range of few hundred dollars per kilogram from Genencor (Palo Alto, CA), Novozymes, and other bulk enzyme manufacturers. However, it should be noted that the source of CPO is the fungus, *C. fumago*, and not all fungal enzymes can be expressed at high levels. Enzymes such as hemicellulases and cellulases from fungal sources have been produced in *Aspergillus niger* and *Trichoderma reesei* at low production costs, so a method for producing CPO may be possible. Recently, expression of CPO was reported in *A. niger*, although the level of production was relatively low *(25)*.

Alternate means to improve the process economics is through activity and stability improvement *(9,25,27,28)*. A sensitivity analysis (Fig. 7) was conducted to determine what other parameters would be important besides the biocatalyst price. Both activity and stability were altered in the process model and it was found that the impact of the biocatalyst stability was much higher. This was because the biocatalyst loses activity rapidly in the presence of the peroxide. Therefore, even if its initial activity is high, the conversion remains low, unless the activity is maintained for a sufficient time. In Fig. 7, the production cost based on a process without the use of a surfactant *(29)* was calculated. This was determined to be more than $9000/kg of SO.

Based on the improvements reported recently in this system, (increase in TTN from 1500 *[29]* to 13,000 with use of a surfactant-based process), the cost of StyOx drops to about $1000/kg. A further 10-fold improvement in biocatalyst stability is needed to enable reduction of production cost to the $100 range. The selling price of enantiopure SO is estimated to be about

$25/kg. Thus, additional reductions in the cost of the enzyme are necessary to make the process economically feasible. An alternate bioprocess to make SO has been reported using a microbial catalyst *(10)*; however, no economic feasibility studies have been reported for the process.

## Conclusions

The preliminary process design for production of PO and SO based on enzymatic processes were conducted. The results indicate that the cost of the enzyme contributes significantly to the production cost and can be as high as 90–95% of the total cost, using current enzyme price. In case of the PO process, which uses an immobilized lipase enzyme available commercially, the cost is still dominated by the biocatalyst cost. This was found to be a result of the instability of the enzyme in presence of hydrogen peroxide, which is a cosubstrate. Thus, improvements are needed in stabilizing the lipase enzyme against hydrogen peroxide deactivation in peroxidation reactions. The feasibility of production of enantiopure SO was similarly found to be controlled by cost of the enzyme, chloroperoxidase. In this case, although the product is of higher value, the economic feasibility was not better because of the higher expected cost of producing the fungal enzyme. Thus, the primary need for demonstrating process feasibility is being able to produce the enzyme CPO at a reduced cost. Furthermore, the stability of the enzyme was important for this enzyme as well and at least an order of magnitude improvement in peroxide stability is needed in each of these enzymes to improve economical feasibility of the process.

## Acknowledgments

The authors would like to acknowledge Douglas S. Clark for providing the data on the SO process and Jonathan S. Dordick for his help in selecting product targets for analysis. The funding from Department of Energy Office of Industrial Technologies is greatly appreciated.

## References

1. Adamczak, M. and Krishna, S. H. (2004), *Food Technol. Biotechnol.* **42,** 251–264.
2. Gupta, M. N. and Roy, I. (2004), *Eur. J. Biochem.* **271,** 2575–2583.
3. D'Souza, S. F. (1999), *Curr. Sci.* **77,** 69–79.
4. Dai, L. Z. and Klibanov, A. M. (1999), *Proc. Natl. Acad. Sci. USA* **96,** 9475–9478.
5. Morgan, J. A. and Clark, D. S. (2004), *Biotechnol. Bioeng.* **85,** 456–459.
6. Sawae, H., Sakoguchi, A., Nakashio, F., and Goto, M. (2002), *J. Chem. Eng. Japan* **35,** 677–680.
7. Song, B. D., Ding, H., Wu, J. C., Hayashi, Y., Talukder, M., and Wang, S. C. (2003), *Chin. J. Chem. Eng.* **11,** 601–603.
8. Mine, Y., Fukunaga, K., Yoshimoto, M., Nakao, K., and Sugimura, Y. (2001), *J. Biosci. Bioeng.* **92,** 539–543.
9. Wang, L. F., Zhu, G. Y., Wang, P., and Newby, B. M. Z. (2005), *Biotechnol. Prog.* **21,** 1321–1328.
10. Panke, S., Wubbolts, M. G., Schmid, A., and Witholt, B. (2000), *Biotechnol. Bioeng.* **69,** 91–100.

11. Bjorkling, F., Frykman, H., Godtfredsen, S. E., and Kirk, O. (1992), *Tetrahedron* **48,** 4587–4592.
12. Bjorkling, F., Godtfredsen, S. E., and Kirk, O. (1990), *J. Chem. Soc. Chem. Commun.* **19,** 1301–1303.
13. Klaas, M. R. G. and Warwel, S. (1997), *J. Mol. Catalysis a-Chem.* **117,** 311–319.
14. Archelas, A. and Furstoss, R. (1997), *Ann. Rev. Microbiol.* **51,** 491–525.
15. Chem Systems, Inc. Report, Assessment of the likely role of biotechnology in commodity chemical production (1988), 20–97, Tarrytown, NY.
16. Soni, B. K., Kelley, R. L., and Srivastava, V. J. (1998), *Appl. Biochem. Biotechnol.* **74,** 115–123.
17. Hilker, I., Bothe, D., Pruss, J., and Warnecke, H. J. (2001), *Chem. Eng. Sci.* **56,** 427–432.
18. Klaas, M. R. and Warwel, S. (1999), *Ind. Crops Prod.* **9,** 125–132.
19. Sober, H. A. and Harte, R. A. (eds.) (1970), *Handbook of Biochemistry*, 2nd ed. The Chemical Rubber Co., Cleveland, OH: pp. E10–E21.
20. Park, J. B. and Clark, D. S. (2006), *Biotechnol. Bioeng.* **93,** 1190–1195.
21. Park, J. B. and Clark, D. S. (2006), *Biotechnol. Bioeng.* **94,** 189–192.
22. Panke, S., Held, M., Wubbolts, M. G., Witholt, B., and Schmid, A. (2002), *Biotechnol. Bioeng.* **80,** 33–41.
23. van de Velde, F., Bakker, M., van Rantwijk, F., Rai, G. P., Hager, L. P., and Sheldon, R. A. (2001), *J. Mol. Catalysis B-Enzymatic* **11,** 765–769.
24. Andersson, M., Andersson, M. M., and Adlercreutz, P. (2000), *Biocatalysis Biotransform.* **18,** 457–469.
25. Conesa, A., van de Velde, F., van Rantwijk, F., Sheldon, R. A., van den Hondel, C., and Punt, P. J. (2001), *J. Biol. Chem.* **276,** 17,635–17,640.
26. Rai, G. P., Zong, Q., and Hager, L. P. (2000), *Isr. J. Chem.* **40,** 63–70.
27. Ayala, M., Horjales, E., Pickard, M. A., and Vazquez-Duhalt, R. (2002), *Biochem. Biophys. Res. Commun.* **295,** 828–831.
28. Borole, A., Dai, S., Cheng, C. L., Rodriguez, M., and Davison, B. H. (2004), *Appl. Biochem. Biotechnol.* **113–116,** 273–285.
29. van Rantwijk, F. and Sheldon, R. A. (2000), *Curr. Opin. Biotechnol.* **11,** 554–564.

0273-2289/1559-0291 (Online)/07/136-140/451-462/$30.00

# Evaluation of Liquid–Liquid Extraction Process for Separating Acrylic Acid Produced From Renewable Sugars

M. E. T. Alvarez, E. B. Moraes, A. B. Machado, R. Maciel Filho, and M. R. Wolf-Maciel*

*Separation Process Development Laboratory (LDPS), Chemical Engineering School, State University of Campinas, (Unicamp), CP 6066, 13081-970, Campinas-SP, Brazil, E-mail: wolf@feq.unicamp.br, mario@feq.unicamp.br*

## Abstract

In this article, the separation and the purification of the acrylic acid produced from renewable sugars were studied using the liquid–liquid extraction process. Nonrandom two-liquids and universal *quasi*-chemical models and the prediction method universal *quasi*-chemical functional activity coefficients were used for generating liquid–liquid equilibrium diagrams for systems made up of acrylic acid, water, and solvents (diisopropyl ether, isopropyl acetate, 2-ethyl hexanol, and methyl isobutyl ketone) and the results were compared with available liquid–liquid equilibrium experimental data. Aspen Plus (Aspen Technology, Inc., version 2004.1) software was used for equilibrium and process calculations. High concentration of acrylic acid was obtained in this article using diisopropyl ether as solvent.

**Index Entries:** Acrylic acid recovery; liquid–liquid extraction; separation; simulation; thermodynamic characterization; renewable sugars.

## Introduction

Renewable sugars, as can be derived from sugar cane, are interesting as alternative carbon sources for the production of chemicals, especially considering the power of modern biotechnological methods. One of the possible routes for obtaining acrylic acid (2-propenoic acid) is through dehydration of lactic acid, which can be obtained through anaerobic fermentation of sugars from biomass. The liquid–liquid extraction process is one option for the separation of acrylic acid from the mixture formed after the dehydration reaction, because it is suitable for dilute systems and is carried out in such a way that avoids thermal degradation of the materials being separated.

*Author to whom all correspondence and reprint requests should be addressed.

Acrylic acid is a commodity chemical that is produced by partial oxidation of propene. This acid could be produced from sugars on bulk industrial scale, as an alternative to its current production from petrochemical feedstocks *(1)*. The major use of acrylic acid and its salts and esters, is in polymeric flocculants, dispersants, coatings, paints, adhesives, and binders for leather, paper, and textiles.

Some authors have been studying possible biotechnology routes to obtain acrylic acid from renewable sugars *(1,2)*. This article will not focus on the conversion of sugars to lactic acid or the dehydration step required to produce acrylic acid; instead, we will focus on the separation of acrylic acid from water, according to data reported by Straathof *(1)*. For this, it is necessary to devise a separation process to obtain acrylic acid with high purity and yield. We thus defined the experiment to consider a dilute stream made up of 3 mol% of acrylic acid and 97 mol% of water, near to the azeotropic point at one atm. The liquid–liquid extraction process being considered in this article was tested under these conditions using several solvents to obtain pure acrylic acid through this process.

Liquid–liquid extraction is an efficient, economical, and environmentally friendly method for separation of organic acids. Extractive recovery of carboxylic acids from dilute aqueous solutions has received attention in recent years because it can be conducted at low temperatures, avoiding material thermal composition. Liquid–liquid extraction is a diffusional separation process, wherein a feed flow is brought into contact with a selected solvent. This solvent will remove a particular chemical compound (the solute) from the feed flow. Two streams leave the column; the solute stream is named extract, and the other stream is named raffinate.

In the open literature, several solvents can be found to extract acrylic acid from aqueous solution through liquid–liquid equilibria (LLE) data. These solvents include diisopropyl ether, 2-ethylhexanol, isopropyl acetate, methyl isobutyl ketone *(3)*, caproic acid, enanthic acid, caprylic acid, pelargonic acid, methyl caproate, methyl enanthate, methyl caprylate, methyl pelargonate *(4)*, and trialkylphosphine oxide *(5)*.

One of the objectives of this article is the characterization of the acrylic acid + water system in order to show the azeotropic point present in this system and, then, include the solvents in the characterization, because of the difficulty associated with separating this mixture through conventional distillation. The solvents must have proper characteristics in terms of solubility with the acid and in terms of facilities of separation from the acid for recycling. The methodology followed here will provide better understanding of the system behavior and will enable evaluation of a liquid–liquid extraction process to obtain pure acrylic acid from dilute aqueous solution. Finally, a liquid–liquid extractor was simulated and optimized to show the robustness of the separation.

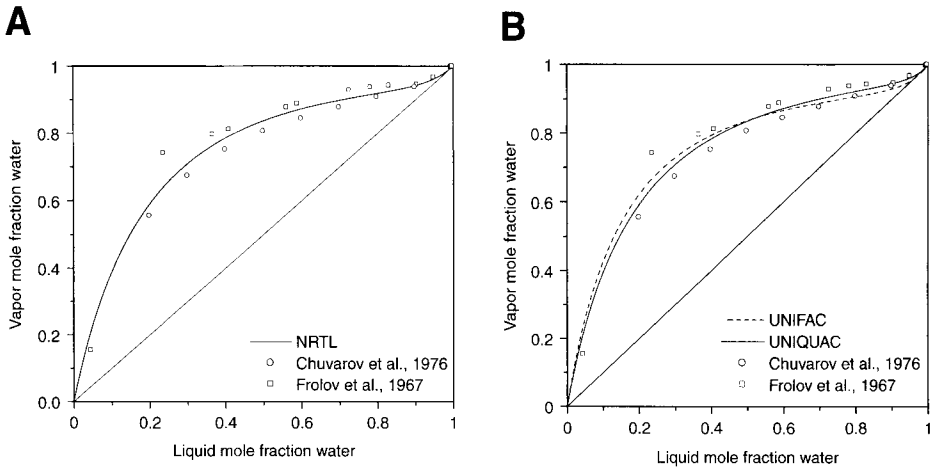


**Fig. 1.** VLE diagram for the system acrylic acid + water **(A)** NRTL and **(B)** UNIQUAC and UNIFAC at 1 atm.

## Characterization of the Systems Acrylic Acid + Water and Acrylic Acid + Water + Solvents

A methodology for characterizing the two systems under consideration, acrylic acid + water and acrylic acid + water + solvents, was developed. The thermodynamic models used were universal *quasi*-chemical (UNIQUAC) and nonrandom two-liquids (NRTL) and the group contribution method UNIQUAC functional activity coefficients (UNIFAC) was used for equilibrium prediction. To evaluate the azeotropic points with the thermodynamic models used for the binary systems involved, the available parameters of vapor-liquid equilibria (VLE) were used. The calculations were made using Aspen Plus simulator; it was possible to find in the Aspen Plus Data Bank both VLE-ideal gas (VLE-IG) and VLE-Hayden-O'Connell data for calculations of activity and fugacity coefficients, respectively. When VLE data were not available for a given system, parameters predicted using UNIFAC activity coefficient method were used. They are called UNIFAC-IG, meaning UNIFAC for predicting activity coefficient and IG model for calculating the vapor phase.

In Fig. 1, the data obtained through simulations were compared with experimental data reported in the literature *(6,7)*. These authors have reported these experimental data in Deutsche Gesellschaft für Chemisches Apparatewesen (DECHEMA), but their data were not ideal for this experiment because both thermodynamic consistency tests are negative. In Fig. 1, the liquid-vapor equilibrium diagram is shown for the acrylic acid + water system. The presence of an azeotrope can be observed at the composition of 2 mol% acrylic acid and 98 mol% water. This behavior indicates that, through a conventional distillation, it is not possible to obtain pure acrylic acid. UNIFAC was also used to predict VLE, as shown in the figure. The

close relationship between UNIFAC and UNIQUAC results indicate that the group contribution method is a powerful method to predict the equilibrium data. Considering this, and as it is a dilute stream, the liquid–liquid extraction process can be used.

According to a search made in the open literature as described, it was found that various solvents are available to extract acrylic acid from dilute aqueous solution. In this article, the following solvents, among the ones listed earlier, will be considered: diisopropyl ether, isopropyl acetate, 2-ethylhexanol, and methyl isobutyl ketone.

## LLE Data, Distribution Coefficient, and Heterogeneous Region

LLE data are essential for the design and development of extraction processes *(8,9)*. First, a literature search was carried out to find LLE experimental data to guide the simulation and/or to validate it. In order to model the LLE, a number of models are available, including NRTL *(10)* and UNIQUAC *(11)*, as well as a prediction method based on group contributions called UNIFAC (and their modifications) *(12–14)*. In this article, the NRTL and UNIQUAC models were used to generate LLE diagrams, and the results were compared with available LLE experimental data. Aspen Plus software was used for these calculations. Group contribution methods as the UNIFAC method for liquid-liquid systems (UNIFAC-LL) can be applied to predict the LLE model parameters if no experimental data are available. The plant size is directly related to the selected solvent used in the liquid–liquid extraction unit, because their characteristics, such as distribution coefficient and selectivity, determine the composition of the raffinate and the extract streams, which will also determine the downstream processing requirements *(8)*.

To evaluate the distribution coefficients and the heterogeneous region, a study was carried out with the unique experimental data reported *(3)*. The outcomes of this study can be seen in Figs. 2 and 3. The distribution coefficient for liquid–liquid extractions involving an aqueous solution is simply equal to the concentration of the solute in the solvent phase divided by its equilibrium concentration in the aqueous phase. This is one of the main parameters used to establish the minimum solvent/feed ratio that must be manipulated in an extraction process. It is necessary that the acrylic acid remains in the organic phase (as indicated in Fig. 2). The heterogeneous region is very wide, avoiding problems in the extremes, wherein partial miscibility could occur, making the posterior recovery of the solvent difficult. The larger that region is, the better the separation through liquid–liquid extraction process will be. In Fig. 3, this region is represented by the binodal curves.

Figure 2 reports that all the solvents studied present higher acrylic acid distribution coefficient between the organic and the aqueous phases, distinguished among them the diisopropyl ether and 2-ethyl hexanol. From the data reported by Linek *(3)* shown in Fig. 3, the solvents present

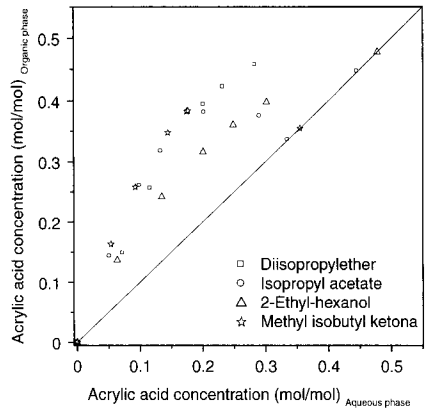


**Fig. 2.** Distribution coefficients of the solvents reported by Linek et al. *(3)*.

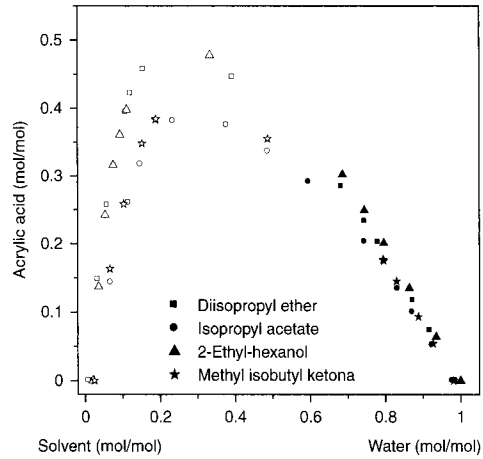


**Fig. 3.** Heterogeneous region of the solvents reported by Linek et al. *(3)*, where closed symbols mean aqueous phase and open symbols mean organic phase.

low water solubility (water mass fraction equal to 0.009 for diisopropyl ether, 0.020 for 2-ethyl hexanol, 0.022 for isopropyl ether, and 0.024 for methyl isobutyl ketone) in the organic phase (heterogeneous region), which can introduce complications when the extract stream is to be treated, or even when the raffinate stream has to be pure water. With this behavior, the azeotropes formed among water + solvents do not affect the separation, because pure water tends to be obtained as rafinatte and only a small amount of water goes to the extract phase.

Among the solvents studied, diisopropyl ether and the 2-ethyl hexanol perform better in terms of distribution coefficients and the range of the heterogeneous region. Thus, these solvents can be chosen for carrying out the extraction process simulations. These solvents were examined using two thermodynamic models for activity coefficients (NRTL and UNIQUAC) as well as the prediction through group contribution method

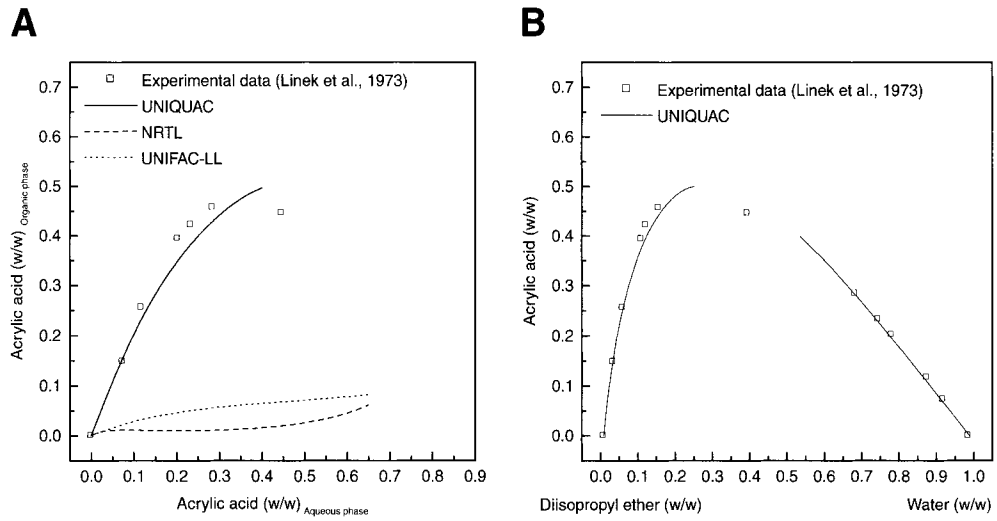


**Fig. 4.** System acrylic acid + water + diisopropyl ether: **(A)** distribution coefficient; **(B)** heterogeneous region.

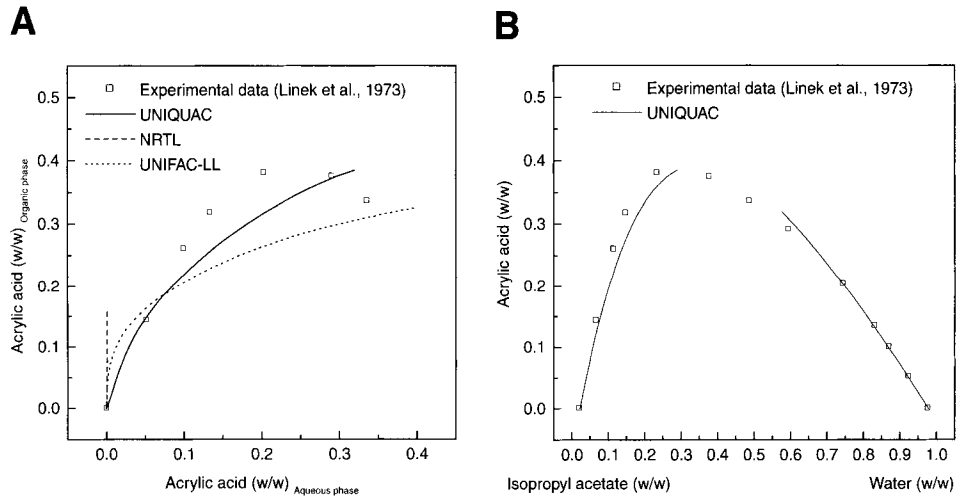


**Fig. 5.** System acrylic acid + water + isopropyl acetate: **(A)** distribution coefficient; **(B)** heterogeneous region.

(UNIFAC-LL), in order to evaluate the representative model of the distribution coefficient and heterogeneous region (Figs. 4–7).

According to the figures, it can be observed that the UNIQUAC model better represents the experimental equilibrium data. The NRTL and UNIFAC-LL models do not approximate the behavior reported in the experimental data. This is likely because of the different inputs that these models use. In the UNIQUAQ model, all LLE binary interaction parameters are reported. In the NRTL model just one pair is reported, whereas the other LLE binary interaction parameters are predicted using UNIFAC-LL method. Using the prediction method (UNIFAC-LL), the simulation does

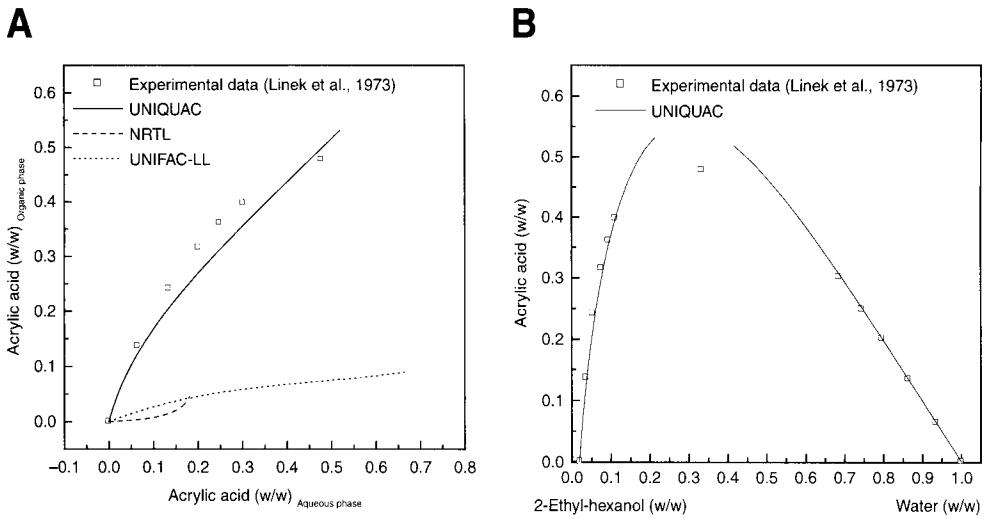


**Fig. 6.** System acrylic acid + water + 2-ethylhexanol: **(A)** distribution coefficient; **(B)** heterogeneous region.

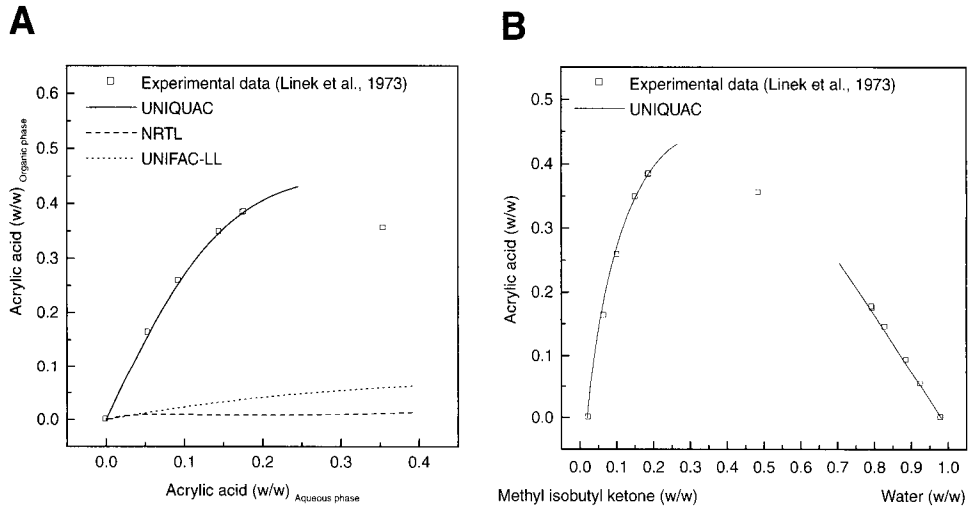


**Fig. 7.** System acrylic acid + water + methyl isobutyl ketone: **(A)** distribution coefficient; **(B)** heterogeneous region.

not represent well the experimental data because it is predictive, and so, more general. It is, indeed, good, when no information on the necessary data are available and evaluations must be made. Based on these results, the most appropriate model to be used is UNIQUAC.

## Simulation of the Liquid–Liquid Extractor—Results and Discussion

Density was used to determine the entrance position of the feed (acrylic acid and water) and of the solvent. In this case, the feed stream enters at the

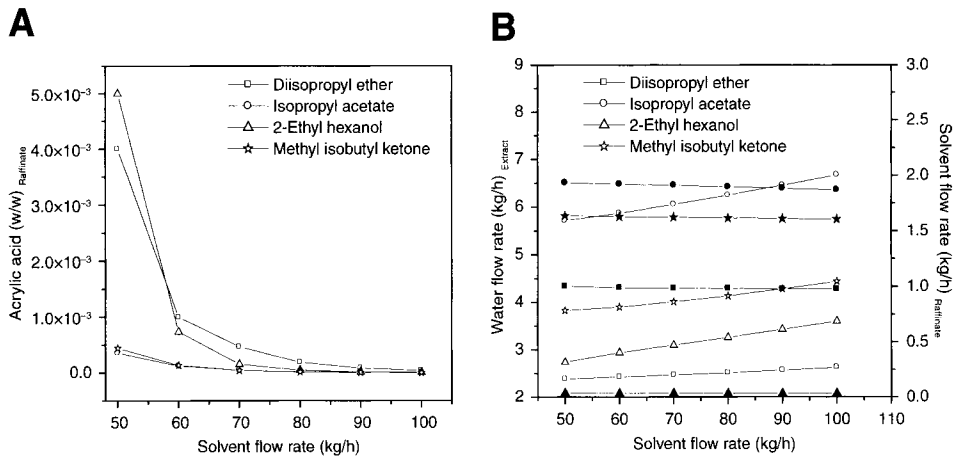


**Fig. 8. (A)** Acrylic acid (w/w) in the raffinate and **(B)** water flow rate (kg/h) in the extract (open symbols) in function of solvent flow rate (kg/h) and solvent flow rate (kg/h) in the raffinate (closed symbols) as a function of solvent flow rate (kg/h).

top and the solvent stream enters at the bottom of the extractor. As stated before, the solute-rich stream is labeled "extract" and the other stream is labeled "raffinate." An Aspen Plus simulator was used for the liquid–liquid extraction process calculations. As stated earlier, the UNIQUAC activity coefficient model was used as it was established as the best in the previous part of the study. The simulation was made in order to analyze the ability of the solvents to extract acrylic acid from a dilute stream.

For all solvents, eight theoretical stages were used; conditions in the extraction column were set at 1 atm and 25°C. The temperature of the feed is 25°C and the mass flow rate is 100 kg/h. The temperature of the solvent is 25°C and its mass flow rate varied from 50 to 100 kg/h. The composition of the feed is 3 mol% of acrylic acid and 97 mol% of water (a composition below the azeotrope). Acrylic acid concentration (w/w) in the raffinate as well as water flow rate (kg/h) and solvent flow rate (kg/h) in the extract stream were determined as a function of the solvent flow rate (kg/h). These results are presented in Fig. 8.

According to Fig. 8A, it can be observed that practically no acrylic acid goes to the raffinate stream when the solvent flow rate is equal to 90 kg/h, for all solvents studied. When Fig. 8B (open symbols) is analyzed, it can be verified that when diisopropyl ether was used, a smaller amount of water goes to the extract stream, which is not desired because water + solvents form azeotropes. This introduces complications when the solvent is to be recovered. In Fig. 8B (closed symbols), the behavior of the solvent flow rate (kg/h) in the raffinate stream is displayed as a function of the variation in the solvent flow rate (kg/h). In this figure, it can be verified that, in terms of the amount in the raffinate stream, the best performance is associated with 2-ethyl hexanol. The extraction column was

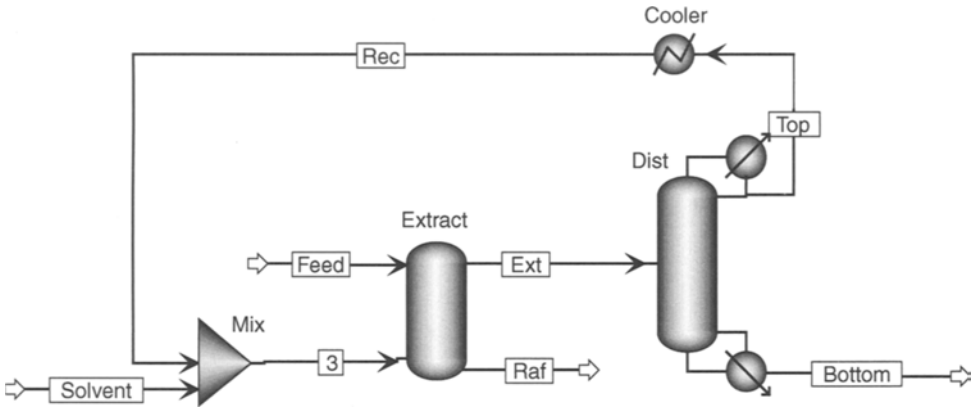


**Fig. 9.** Whole plant for recovering acrylic acid from aqueous stream, including extraction column, distillation column, and solvent recycle.

simulated, with eight theoretical stages for diisopropyl ether, because it is the solvent that present the largest heterogeneous region. The solvent flow rate was set at 90 kg/h (the ratio of solvent to feed, 0.9), based on what was observed in Fig. 8A. With these conditions, it is possible to carry out the complete simulation of the extraction and purification of the acrylic acid.

## Complete Extraction Process—Results and Discussion

The compositions of each stream of the liquid–liquid extraction process (extract or raffinate) determine the next separation units to be used. If high solvent concentrations are found in the raffinate stream, another unit operation (downstream processing) is necessary to remove this component. On the other hand, the presence of water in the extract stream causes further problems for acrylic acid recovery and solvent recycle. These problems have been minimized by the choice of solvent. Calculations for the whole plant, including recycling and distillation column, were made using the NRTL model for representing the activity coefficient with binary interaction parameters from Aspen Databank. For the vapor phase, IG and Hayden-O'Connell models were used. The impact of solvent selection is evident when the complete extraction process is examined. Two separation units are used to recover acrylic acid coming from aqueous stream: extraction- and distillation column (Fig. 9).

The distillation column was used to recover the solvent from the extract stream, to recycle it, and to recover the solute. The simulation conditions were defined for a distillation column with 25 theoretical stages, and extract flow rate was set at 99.232 kg/h (made up of 11.009 kg/h of acrylic acid, 2.551 kg/h of water, and 85.672 kg/h of diisopropyl ether). This column was set to operate at 25°C and 1 atm. The feed stage of this column is 17th and the reflux ratio (mole basis) is equal to three. Table 1 shows the stream

Table 1
Stream Compositions for the System Acrylic Acid + Water + Diisopropyl Ether

| Component | Feed | Solvent | Ext | Raf | Top/rec | Bottom |
|---|---|---|---|---|---|---|
| Component mass fraction in each stream | | | | | | |
| Water | 0.890 | – | 0.026 | 0.989 | 0.029 | 11 ppb |
| Acrylic acid | 0.110 | – | 0.111 | 5 ppm | Trace | 1 |
| Diisopropyl ether | – | 1 | 0.863 | 0.011 | 0.971 | 117 ppm |
| Component mole fraction in each stream | | | | | | |
| Water | 0.970 | – | 0.125 | 0.998 | 0.144 | 42 ppb |
| Acrylic acid | 0.030 | – | 0.135 | 1 ppm | Trace | 1 |
| Diisopropyl ether | – | 1 | 0.740 | 0.002 | 0.856 | 82 ppm |

compositions of the process. It is verified that for the solvent studied, it was possible to produce a raffinate stream of nearly pure water. At the bottom of the distillation column pure acrylic acid can be obtained. The solvent is recovered for recycle at the top of the distillation column.

## Conclusions

The recovery of acrylic acid from water using liquid–liquid extraction process has been presented. A thermodynamic evaluation of the systems involved indicates that UNIQUAC model better represents the LLE experimental data reported in the literature. The complete extraction process was considered (including the extraction column, the distillation column, and recycle). Four solvents for separating acrylic acid from water were examined. Among them, diisopropyl ether was found to be the most suitable in terms of smaller amount of water recovered in the extract stream and in terms of avoiding the problem of azeotrope formation with water and solvent, harming the solvent recovery and recycle.

## Acknowledgments

The authors are grateful to CNPq and FAPESP for the financial support.

## References

1. Straathof, A. J. J., Sie, S., Franco, T. T., and van der Wielen, L. A. M. (2005), *Appl. Microbiol. Biotechnol.* **67,** 727–734.
2. Danner, H., Ürmös, M, Gartner, M., and Braun, R. (1994), *Appl. Biochem. Biotechnol.* **70–72,** 887–894.
3. Linek, J., Hlavatý, K., and Wichterle, I. (1973), *Collect. Czech. Chem. Commun.* **38,** 1840–1845.

4. Chubarov, G. A., Danov, S. M., Logutov, V. I., and Obmelyukhina, T. N. (1984), *J. Appl. Chem. USSR*, **57,** 1671–1673.
5. Li, Y., Wang, Y., Li, Y., and Dai, Y. (2003), *J. Chem. Eng. Data* **48,** 621–624.
6. Chuvarov, G. A., Danov, S. M., and Brovkina, G. V. (1976), *Zr. Prikl. Khim.* **49,** 1413–1415.
7. Frolov, A. F., Loginova, M. A., and Ustavshchikov, B. F. (1967), *Zr. Prikl. Khim.* **41,** 2088–2090.
8. Pinto, R. T. P., Lintomen, L., Luz, L. F. L., Jr., and Wolf-Maciel, M. R. (2005), *Fluid Phase Equilibria*. **228–229,** 447–457.
9. Matsuda, H., Ochi, K., and Surugadai, K. (2003), *J. Chem. Eng. Data* **48,** 184–189.
10. Renon, H. and Prausnitz, J. M. (1968), *AIChE J.* **14,** 135–144.
11. Abrams, D. S. and Prausnitz, J. M. (1975), *AIChE J.* **21,** 116–128.
12. Magnussen, T., Rasmussen, P., and Fredenslund, A. (1981), *Ind. Eng. Chem. Process Des. Dev.* **20,** 331–339.
13. Larsen, B. L., Rasmussen, P., and Fredenslund, A. (1987), *Ind. Eng. Chem. Process Des. Dev.* **26,** 2274–2286.
14. Gmehling, J., Li, J. and Schiller, M. (1993), *Ind. Eng. Chem. Res.* **32,** 178–193.

0273-2289/1559–0291 (Online)/07/136–140/463–470/$30.00

# Enhancement of Rhamnolipid Production in Residual Soybean Oil by an Isolated Strain of *Pseudomonas aeruginosa*

C. J. B. de Lima,[1] F. P. França,[2] E. F. C. Sérvulo,*[,2] M. M. Resende,[1] and V. L. Cardoso[1]

*[1]Universidade Federal de Uberlândia/FEQ, Caixa Postal 593, 38400-902, Uberlândia, MG, Brazil;and [2]Escola de Química, Universidade Federal do Rio de Janeiro, Centro de Tecnologia, Bloco E, Ilha do Fundão, 21.949-900, Rio de Janeiro, RJ, Brazil, E-mail: eliana@eq.ufrj.br*

## Abstract

In the present work, the production of rhamnolipid from residual soybean oil (RSO) from food frying facilities was studied using a strain of *Pseudomonas aeruginosa* of contaminated lagoon, isolated from a hydrocarbon contaminated soil. The optimization of RSO, ammonium nitrate, and brewery residual yeast concentrations was accomplished by a central composite experimental design and surface response analysis. The experiments were performed in 500-mL Erlenmeyer flasks containing 50 mL of mineral medium, at 170 rpm and 30 ± 1°C, for a 48-h fermentation period. Rhamnolipid production has been monitored by measurements of surface tension, rhamnose concentration, and emulsifying activity. The best-planned results, located on the central point, have corresponded to 22 g/L of RSO, 5.625 g/L of $NH_4NO_3$, and 11.5 g/L of brewery yeast. At the maximum point the values for rhamnose and emulsifying index were 2.2 g/L and 100%, respectively.

**Index Entries:** Biosurfactant; experimental design; *Pseudomonas aeruginosa*; rhamnolipids; surface tension; soybean oil.

## Introduction

The surfactants constitute a very important class of chemical compounds widely used in a variety of industrial sectors because they act like dispersants and/or solubilizing agents of organic compounds. Most of the surfactants commercially used are synthesized from petroleum derivatives *(1)*. However, recently, the interest for microbial surfactants has significantly increased, especially because of its biodegradability *(2)*. Microbial compounds that have surfactant properties, i.e., reduce the surface tension (ST) and/or have high emulsifying capacity, are predominantly biosurfactants and consist of bacteria and fungi metabolic

*Author to whom all correspondence and reprint requests should be addressed.

byproducts (3). Microbial-produced surfactants offer several advantages over the equivalent chemical ones: low toxicity, temperature, pH, and ionic force tolerance, besides their possibility of being produced from renewable substrates (4). The biosurfactants can be applied in agriculture for the pesticides and herbicides formulation, in the food industry as additives, and also in the pharmaceutics, textile, cosmetic, and petrochemical industries. In the latter, it is widely used for secondary oil recovery, oil residue removal, and mobilization and for bioremediation (5).

When considering the biosurfactant potential, one must remember that these macromolecules are produced by a variety of microorganisms and that they have different chemical structures and surface properties. The kind and the quantity of the biosurfactant produced depend first on the type of microorganism that is producing it and on the carbon and nitrogen sources, trace elements, aeration, and other factors that can influence the microbial production of these compounds (6). The glycolipids are the best-known microbial surfactants and, among them, the rhamnolipids are the most studied ones. These compounds contain 1 or 2 molecules of rhamnose bonded to 1 or 2 molecules of β-hydroxydecanoic acid (1). Several species of *Pseudomonas* are able to produce large amounts of these compounds (7). Some *Pseudomonas* sp. produce rhamnolipids that, when added to an oil/water system, are able to reduce the interfacial tension from 21 to 0.47 mN/m (7,8). Because of the importance of substitution of chemical surfactants to lower- or nontoxic products, this work had as its main objectives the determination of the best experimental conditions for the rhamnolipid production by an isolated strain of *P. aeruginosa* in relation to the following variables: burnt oil concentration, ammonium nitrate (AN), and residual brewery yeast (RBY) using a central composite experimental design (CCD).

## Materials and Methods

### Microorganisms

The culture was isolated from the soil of a lagoon contaminated with diesel oil and gasoline located at the Rio das Pedras farm, Uberlândia, Minas Gerais, Brazil. The bacterial strain was identified as *P. aeruginosa* called strain PACL. The culture was maintained in bacto nutrient broth (BD, cod. 234000) supplied by BD (Becton Dickinson and Company) at 4°C.

### Culture Isolation

The media proposed by Vecchioli et al. (9), added with 0.5% (v/v) of residual soybean oil (RSO) as the single carbon source, was used for the bacterial cultures isolation, using the pour plate technique. Among the isolated microorganisms, the one that showed the best reduction of the culture medium ST after fermentation was selected and identified. The isolated microorganism was identified at Laboratório de Enterobactérias at Fundação Oswaldo Cruz through classical biochemistry methods.

### *Growth Medium and Conditions*

The bacterial cultures were growth in the medium proposed by Santos et al. *(10)*, containing (g/L): $NH_4NO_3$ 1.7, $Na_2HPO_4$ 7.0, $KH_2PO_4$ 3.0, $MgSO_4 \cdot 7H_2O$ 0.2, yeast extract 5.0, and glucose 10.0. The medium was autoclaved at 121°C for 15 min after adjusting the pH for 7.0. The production medium consisted of the same salts used in the growth medium with added burnt soybean oil (g/L): between 1.4 and 42.6, RBY (g/L): between 0.56 and 22.5, and AN (g/L): between 0.56 and 22.5.

### *Rotary Shaker Experiments*

The experiments were performed in 500-mL Erlenmeyers flasks containing 50 mL of the medium. Typically, three loopfuls from the stock culture were cultivated in 100 mL of the medium proposed by Santos et al. *(10)* at 30 ± 1°C and 170 rpm for 24 h. After inoculating with 5 mL of the inoculum, the flasks were maintained in the rotary shaker at 170 rpm agitation rate for 48 h at 30 ± 1°C.

### *Central Composite Experimental Design*

A central composite experimental design was used in order to optimize the process in relation to the following operational variables: RSO concentration, AN, and RBY. The levels of the studied variables were expressed in the codified form (nondimensional) using the following codifying equation:

$$X_n = \left[\left(X - X_0\right)\right] / \left(X_{+1} - X_{-1}\right) / 2$$

The statistical calculations were done through the Statistic 5.0 Software (Statsof Inc.).Table 1 shows the concentrations used in each of the 16 experiments of the central composite experimental design (CCD).

### *Analytical Methods*

#### Rhamnose Concentration

The rhamnose concentration was determined according to the methodology described by Rahman *(11)*. The ST determination was performed using a Tensiometer (Fisher Scientific, model 21). The analyses were done at 25°C with the tensiometer previously calibrated. The emulsifying activity was determined for aviation kerosene as described by Cooper and Goldenberg *(12)*.

## Results and Discussion

Table 2 shows the results obtained in the central composite design from the studied variables: RSO concentration ($X_1$), AN concentration ($X_2$), and RBY ($X_3$) using the isolated *P. aeruginosa* PATC strain.

Table 1
Concentrations Used for Each Variable in the 16 Experiments of the CCD

| Experiment | Burnt oil (g/L) | AN (g/L) | RBY (g/L) |
|---|---|---|---|
| 1 | 6.0 | 1.25 | 3.0 |
| 2 | 6.0 | 1.25 | 20.0 |
| 3 | 6.0 | 10.0 | 3.0 |
| 4 | 6.0 | 10.0 | 20.0 |
| 5 | 38.0 | 1.25 | 3.0 |
| 6 | 38.0 | 1.25 | 20.0 |
| 7 | 38.0 | 10.0 | 3.0 |
| 8 | 38.0 | 10.0 | 20.0 |
| 9 | 1.4 | 5.625 | 11.5 |
| 10 | 42.6 | 5.625 | 11.5 |
| 11 | 22.0 | 0.0 | 11.5 |
| 12 | 22.0 | 11.25 | 11.5 |
| 13 | 22.0 | 5.625 | 0.56 |
| 14 | 22.0 | 5.625 | 22.5 |
| 15 | 22.0 | 5.625 | 11.5 |
| 16 | 22.0 | 5.625 | 11.5 |

Table 2
Results of Rhamnose Production, EI (E24), and ST Obtained in the Experiments

| Experiment | Rhamnose (g/L) | ST (mN/m) | E24 (%) |
|---|---|---|---|
| 1 | 0.59 | 30.5 | 88 |
| 2 | 0.50 | 31 | 84 |
| 3 | 0.40 | 32 | 64 |
| 4 | 0.43 | 31.5 | 74 |
| 5 | 0.35 | 32.5 | 84 |
| 6 | 0.32 | 32.5 | 79 |
| 7 | 0.31 | 31.875 | 77 |
| 8 | 0.27 | 32.125 | 68 |
| 9 | 0.96 | 27.75 | 86 |
| 10 | 1.63 | 26.375 | 95 |
| 11 | 0.78 | 28.625 | 90 |
| 12 | 1.34 | 27 | 87 |
| 13 | 1.15 | 27.125 | 94 |
| 14 | 1.31 | 26.625 | 96 |
| 15 | 2.20 | 25.75 | 100 |
| 16 | 2.30 | 25.625 | 100 |

The results shown in Table 2 indicate that the maximum rhamnose syntheses were obtained in the fifteenth and sixteenth experiments in which the studied variables' concentrations were at the central point. This indicates that the variable maximum point in the optimization was near the central conditions of the design. The increase in the rhamnose

synthesis (RS) in the experiments promoted an increase in the emulsifying index (EI), demonstrating that both are probably directly related because the higher the biosurfactant concentration in the medium, the higher its capacity of being emulsified. Besides, the increase in the rhamnolipids concentration resulted in a decrease in the medium ST in all experiments performed.

In experiments one to eight, the alterations in the concentrations of RSO, AN, and RBY did not promote significant change in the medium ST. On the other hand, the lowest values of the ST were obtained with concentrations of RSO, AN, and RBY around 22, 5.625, and 11.5 g/L, respectively, which demonstrates that these concentrations are within the optimization region of the process. Besides that, all experiments were able to produce compounds that formed stable emulsions for 24 h. This analysis is a practical measurement of a biosurfactant utility because it gives the compound ability to emulsify nonmiscible liquids with stable emulsions formation. The determination of the significant parameters was performed through a hypothesis test (student's *t*-test) with 10% level of significance. The parameters that show a level of significance higher than this value were dismissed.

The empirically adjusted equations that represent the RS ($R$), ST ($T_S$), and the EI ($I_E$), are respectively, described in Eqs. 1–3.

$$R = 2.218 - 0.55\ X_1X_1 - 0.691\ X_2X_2 - 0.589\ X_3X_3 \quad (1)$$

$$T_S = 24.3769 + 2.209\ X_1X_1 + 2.662\ X_2X_2 + 2.096\ X_3X_3 \quad (2)$$

$$I_E = 102.86 - 4.937X_2 - 8.745X_1X_1 - 9.952\ X_2X_2 - 6.029\ X_3X_3 \quad (3)$$

In Eqs. 1 and 2, the isolated variables did not significantly influence the process, only the quadratic interactions did. But in Eq. 3, besides the quadratic variables, the AN also caused an increase in the EI response because when its concentration is lowered in the system, it promotes an increase in the response. The signs of these variable coefficients indicate a maximum point in the rhamnose production and in the EI, and a minimum point for the ST.

An algorithm done in the Maple V release 4 (Waterloo Maple, Inc., Canada) program was used to calculate the stationary point ($P_0$) for the ST and EI. These values are shown in Table 3. The λ's values that refer to the RS and to the EI indicate that these responses have a maximum point because they have equal and negative signs. However, the λs that refer to the ST indicate that this response has a minimum point as they present equal and positive signs.

The RS, ST, and EI, was 2.218 g/L, 25.372 mN/m, and 100%, respectively, in the optimization point from the codified variable values $x_1$, $x_2$, and $x_3$, as shown in Table 4. As expected, these values are very

Table 3
Stationary Point for the RS (*R*), ST, and EI (E24)

| $P_0$ | *R* | ST | E24 |
|---|---|---|---|
| $\lambda_1$ | −0.619 | 2.095 | −10.812 |
| $\lambda_2$ | −0.587 | 2.141 | −8.385 |
| $\lambda_3$ | −0.548 | 2.733 | −5.530 |

Table 4
Codified Values of the Variables $x_1$, $x_2$, and $x_3$ in the Optimization Point

| Coordinates | *R* | ST | E24 |
|---|---|---|---|
| $x_1$ | 0.015 | 0.015 | 0.003 |
| $x_2$ | 0.023 | 0.015 | −0.249 |
| $x_3$ | 0.007 | 0.008 | −0.071 |

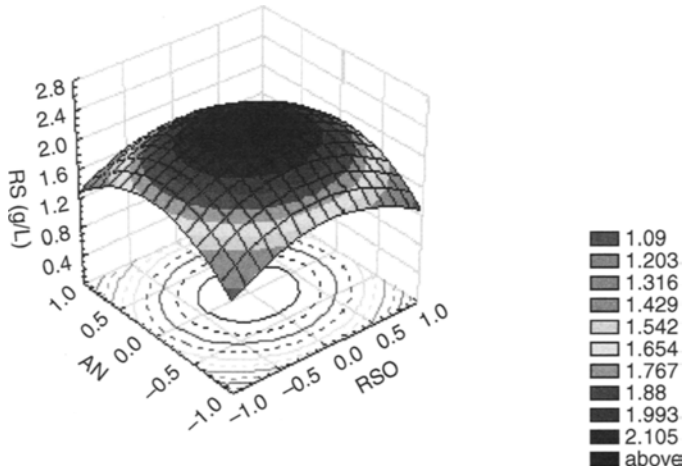


**Fig. 1.** Response surface for the RS in relation to the RSO and AN.

close to the ones obtained in experiments 15 and 16, as the variables of the maximization (rhamnose and EI) and minimization (ST) points are close to the central point.

Response surfaces were generated to facilitate the visualization of the effects of the independent variables: RSO, AN, and RBY on the RS, ST, and EI (Figs. 1–3). The maximum rhamnose production was obtained for values of RSO concentration and AN concentration in the central point region (Fig. 1). Figure 2 shows that the ST decreased for values of RSO a bit under the central point and for the values of residual brewery near the central point. The maximum EI was obtained for values of RBY a bit under the central point.

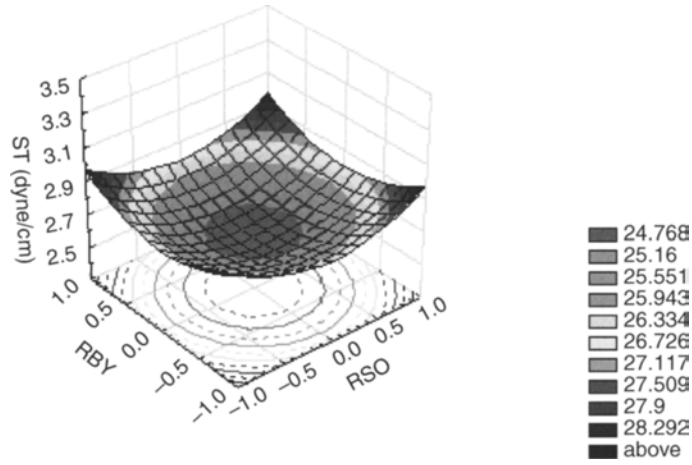


**Fig. 2.** Response surface for the ST in relation to the RSO and the RBY.

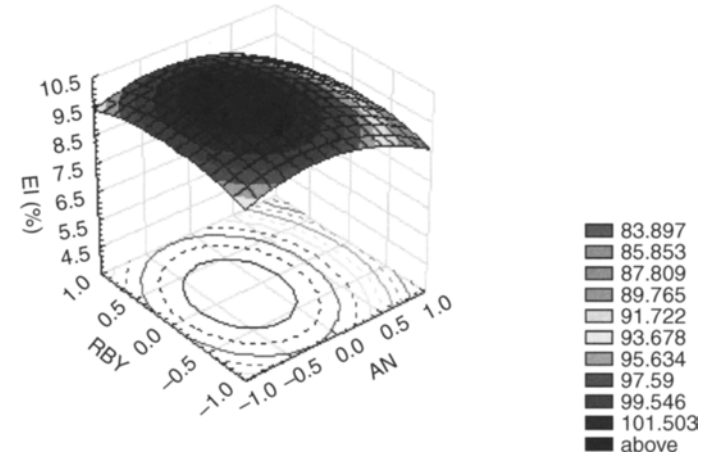


**Fig. 3.** Response surface for the emulsifying index (EI) in relation to the AN and the RBY.

## Conclusions

The experimental design methodology was a very useful tool to determine the independent variables' behavior in rhamnose production, avoiding excessive analyses and showing general information about the influence of the independent parameters in the process. The results obtained in this work show that the isolated *P. aeruginosa* PACL presents good capacity of RSO degradation and great potential for biosurfactant production. Also, all experiments were able to produce compounds that formed stable emulsions for 24 h. The optimization of the analyzed responses showed that the best results found for the rhamnose concentration was 22.0 g/L of RSO, 5.7 g/L

of AN, and 11.0 g/L of residual brewery. All points were localized near the design central point.

## References


1. Desai, A. J. and Banat, I. M. (1997), *Curr. Sci.* **57,** 500–501.
2. Makkar, R. S. and Cameotra, S. S. (2002), *Appl. Microbiol. biotechnol.* **58,** 428–434.
3. Banat, I. M., Samarah, N., Murad, M., Roene, R., and Banerju, S. (1991), *J. Microb. Biotechnol.* **7,** 80–88.
4. Lin, S. C., Sharma, M. M., and Georgiou, G. (1993), *Biotechnol. Program* **9,** 138–145.
5. Ron, E. Z. and Rosenberg, E. (2002), *Curr. Opin. Biotechnol.* **13,** 249–252.
6. Francy, D. S., Thomas, J. M., Raymond, R. L., and Ward, C. H. (1991), *J. Ind. Microb.* **8,** 237–246.
7. Parra, J. L., Guinea, J., and Manresa, M. A. (1989), *JAOCS* **66,** 141–145.
8. Patel, R. M. and Desai, A. J. (1997), *Lett. Appl. Microbiol.* **25,** 91–94.
9. Vecchioli, G. I., Del Panno, M. T., and Painceira, M. T. (1990), *Environ. Pollut.* **67,** 249–258.
10. Santos, A. S., Sampaio, A. P., Vasquez, G. S., Santa Anna, L. M., Pereira, N., Jr., and Freire, D. M. G. (2002), *Appl. Biochem. Biotechnol.* **98–100,** 1025–1035.
11. Rahman, K. S. M., Banat, I. M., Thahira-Rahaman, J., Thayumanavan, T., and Lakshmanaperumalsamy, P. (2002), *Bioresour. Technol.* **81,** 25–32.
12. Cooper, D. G. and Goldenberg, B. G. (1987), *Appl. Environ. Microbiol.* **42,** 224–229.

0273-2289/1559-0291 (Online)/07/136-140/471-486/$30.00

# Optimizing Carbon/Nitrogen Ratio for Biosurfactant Production by a *Bacillus subtilis* Strain

**R. R. Fonseca,[1] A. J. R. Silva,[2] F. P. De França,[1] V. L. Cardoso,[3] and E. F. C. Sérvulo*,[1]**

*[1]Escola de Química, Universidade Federal do Rio de Janeiro, Centro de Tecnologia, Bloco E, Ilha do Fundão, 21.949-900, Rio de Janeiro, RJ, Brazil, E-mail: eliana@eq.ufrj.br; [2]Núcleo de Pesquisa de Produtos Naturais, Universidade Federal do Rio de Janeiro, Centro de Ciências da Saúde, Bloco G, Ilha do Fundão, 21.949-900, Rio de Janeiro, RJ, Brazil; and [3]Universidade Federal de Uberlândia/ FEQ, Caixa Postal 593, 38400-902, Uberlândia, MG, Brazil*

## Abstract

A *Bacillus subtilis* strain isolated from contaminated soil from a refinery has been screened for biosurfactant production in crystal sugar (sucrose) with different nitrogen sources ($NaNO_3$, $(NH_4)_2SO_4$, urea, and residual brewery yeast). The highest reduction in surface tension was achieved with a 48-h fermentation of crystal sugar and ammonium nitrate. Optimization of carbon/nitrogen ratio (3, 9, and 15) and agitation rate (50, 150, and 250 rpm) for biosurfactant production was carried out using complete factorial design and response surface analysis. The condition of C/N 3 and 250 rpm allowed the maximum increase in surface activity of biosurfactant. A suitable model has been developed, having presented great accordance experimental data. Preliminary characterization of the bioproduct suggested it to be a lipopeptide with some isomers differing from those of a commercial surfactin.

**Index Entries:** Biosurfactant/production; crystal sugar; lipopeptide; surface-active substances; surfactin; *Bacillus subtilis*.

## Introduction

Historically, the principal driving force behind the production of surfactants has been the oil industry, which makes use of these compounds, mainly in the secondary recovery of petroleum *(1)*. However, these compounds find applications in an extremely wide variety of industrial fields involving clean-up of oil-storage tanks, transportation of heavy crude oil,

*Author to whom all correspondence and reprint requests should be addressed.

industrial effluent treatment, ecological accident control, heavy metal removal, and bitumen recovery from tar sand, among others (2).

The most commonly used surfactants come from petrochemical sources; though interest in surfactants of microbiological origin has increased considerably in recent years owing mainly to their biodegradability and low toxicity, which offer the advantage of little to no environmental impact and also allow *in situ* production (3). However, the principal focus resides in the high selectivity of these compounds. Being complex organic molecules with specific functional groups gives them greater application efficiency and the capacity to perform even at extreme temperature, pH, and salinity levels (4). In this context, there is a greater possibility for using surface-active microbial compounds, particularly in the areas of agriculture and medicine as well as in the pharmaceutical and textile industries (5). A wide variety of microorganisms including bacteria, yeast, and molds are able to produce biosurfactants with great structural diversity (6,7). However, the quantity and the chemical structure of a biosurfactant do not depend only on the microorganism that is producing it. The culture conditions, such as the carbon and nitrogen sources, trace elements, temperature, oxygen, and pH can also promote changes in the chemical structure of the molecule, and consequently, alter its physicochemical characteristics.

The lipopeptides from *Bacillus subtilis* are particularly interesting because of their strong surface activity (8). Many researchers demonstrated the effectiveness of these biomolecules in reducing the surface tension to around 27 mN/m, even at concentrations as low as 0.05 g/L (9–11). Moreover, these compounds present therapeutic properties, which enable them to be used in a variety of applications (9,11). Some microorganisms only produce surface-active agents when cultivated in hydrocarbons. Nevertheless, biosurfactants can be produced from simple water-soluble substrates such as carbohydrates. This is of significant relevance as fermentation with carbohydrates is simpler than fermentation with hydrocarbons. The choice of the carbon source should be determined not only by its cost, availability, or nutritional characteristics of the microorganism, but also by the kind of application of the biosurfactant that is going to be produced.

Despite the advantages, biosurfactants are still economically uncompetitive because of their high production costs. The promising future of these compounds depends especially on the search for microorganisms able to produce them and on raw materials, which enable high-yields and productivity of biosurfactants with specific ends. The aim of this study was to assess the ability of a *B. subtilis* strain, isolated from a petroleum contaminated soil sample, to produce biosurfactants using low-cost raw materials in order to establish an economically feasible fermentative process. The surface-active compounds produced during fermentation were also preliminary characterized.

## Materials and Methods

### *Microorganism*

The strain *B. subtilis* YRE207 used in this study was isolated from a refinery's petroleum contaminated soil samples. The identification of the strain was done at the Coleção de Culturas do Gênero *Bacillus* e Gêneros Correlatos-CCGB, of Departamento de Bacteriologia of Instituto Oswaldo Cruz (Rio de Janeiro, Brazil), following the classic procedures based on bacteria cytomorphology, biochemistry, and physiology. The culture was maintained on BD/DIFCO nutrient agar (cod. 213000, Becton Dickinson and Company) slants at 4°C and transferred monthly.

### *Inoculum*

The stock culture was reactivated through two successive transfers on BD/DIFCO nutrient agar slants, of 24 h each at 30°C. Then, a loopful of cells culture was inoculated on 100 mL of nutrient broth (cod. 234000), combined with 5.0 g/L glucose (Merck & Co., Brazil), and incubated at 30°C for 16 h on a rotary shaker at 150 rpm.

### *Biosurfactant Production*

Each experiment was performed in triplicate on 500-mL Erlenmeyer flasks containing 100 mL of a mineral medium consisting of 0.1 g/L of KCl, 0.5 g/L of $KH_2PO_4$, 1.0 g/L of $K_2HPO_4$, 0.01 g/L of $CaCl_2$, and 0.5 g/L of $MgSO_4(7H_2O$ *(12,13)*, using 10.0 g/L of crystal sugar (sucrose) as the single carbon source and 4.0 g/L of $NH_4NO_3$, except when specified. The initial pH of the medium was adjusted to 7.0 using 1 *M* NaOH. All reagents were analytical grade (Merck). Inoculation volumes corresponding to about 0.1 g/L of exponential-phase cells were used and the flasks were incubated under the same conditions of the inoculum but this time for 48 h. Periodically, the culture purity was verified through microscopic observations using the Gram stain method.

Initially, five nitrogen sources were tested: 3.0 g/L of urea (Merck), 14.0 mL/L residual brewery yeast (Brewery Co., RJ, Brazil), 6.6 g/L of ammonium sulfate (Merck), 8.5 g/L of sodium nitrate (Merck), and 4.0 g/L of ammonium nitrate (Merck). The concentrations of the different nitrogen sources were calculated in order to obtain an initial nitrogen concentration of 1.4 g/L, a value normally used in culture media for surfactin production *(12,13)*. For the study of carbon/nitrogen ratio, the sucrose concentration was maintained constant at 10.0 g/L and the concentrations of ammonium nitrate varied: 4.0, 1.3, and 0.8 g/L, corresponding to C/N of 3, 9, and 15, respectively. In all experiments, the biosurfactant production was indirectly evaluated through the surface tension determinations in samples of cell-free fermented media.

## Experimental Design

A complete factorial experimental design of two variables and three levels was used, which resulted in nine experiments. In this study, the carbon/nitrogen ratio ($X_1$) and agitation rate ($X_2$) were evaluated as the variables, according to the design matrix shown in Table 2. The variables levels were established through data obtained in the literature *(12–14)* and the percentage of the surface tension reduction adopted as the response variable for this parameter indicates the surface-active agent production.

The data were statistically analyzed using the StatSoft's Statistica 5.0 program (Statsof Inc.) through multiple regression analysis using the quadratic minimums method, taking as factors the isolated terms, the interaction, and the quadratics of the studied variables. The equation below gives the generic representation of the model:

$$Y = \beta_0 + \sum_i \beta_i X_i + \sum_i \sum_j \beta_{ij} X_i X_j + \sum_i \beta_{ii} X_i^2$$

where $Y$ is the predicted response, $\beta_0$ is the interception coefficient, $\beta_i$, $\beta_{ij}$, and $\beta_{ii}$ are, respectively, the measures of the effects of variables $X_i$, $X_iX_j$, and $X_i^2$. The variable $X_iX_j$ represents the first-order interactions between $X_i$ and $X_j$ ($i < j$). The Statistica software was used for regression and graphical analysis of the data obtained. The results of the experiments were analyzed in order to determine the equations, the correlation coefficient $R^2$, the residue curve, the significant variables, the effect and the intensity of the stationary point, i.e., to set up if there was a maximum or minimum point.

## Analytical Methods

### Biomass

The quantifications of viable cells and spores were performed using the pour plate method. For that, samples of the fermented media were serially diluted ($10^{-1}$ to $10^{-10}$) on physiological solution (9.0 g/L NaCl) and plated on BD/DIFCO nutrient agar (cod. 213000). After 48 h of incubation at 30°C, bacteria colonies were counted using a Darkfield Quebec® colony counter (Reichter Inc.), with the results being expressed in colony forming units/mL. For spore counts, samples were heated at 80°C for 12 min before plating in order to inactivate vegetative cells. After the thermal treatment, the samples were diluted and plated as described for quantification of viable cells.

The cell concentration for inoculation of production medium was determined by dry weight according to the methodology described by Reis et al. *(13)*.

### Surface Tension

Surface tensions were used as an indirect measure of surfactant production *(13)*. All measurements were made on cell-free supernatants obtained by centrifugation (13,000*g* for 20 min at 4°C). A KSV SIGMA 70

Surface Tensiometer (KSV Instruments Ltd., Finland) was used, and measurements were performed at 25°C.

### Emulsification Index

The emulsifier activity was determined according to Cooper and Goldenberg *(10)*. Four milliliters of cell-free culture samples were added to six different products (gasoline, diesel oil, aviation kerosene, corn oil, soybean oil, and crude oil). After vortexing at high speed for 2 min, the mixture was allowed to settle for 24 h after which the volume occupied by the emulsion was measured. The emulsification index (E24) is the height of the emulsion layer, divided by the total height of the liquid column.

### Biosurfactant Characterization

The fermented broth, previously centrifuged at 13,000*g* for 20 min at 4°C to remove the cells, was ultrafiltrated in Amicon Systems (Millipore Corporation, Brazil) through 10 kDa membranes, at pressures from $7 \times 10^4$ to $2 \times 10^5$ Pa. Then, the filtrate was analyzed by reverse phase high-performance liquid chromatography (LC10A, Shimadzu, Japan) equipped with an octadecylsilane (C-18) column (250 × 4.9 mm). The mobile phase consisted of 20% trifluoroacetic acid (3.8 m*M*) and 80% acetonitrile. Sample volume was 20.0 µL and the elution rate was 1.0 mL/min. The absorbance of the effluent was monitored at 205 nm. Surfactin from Sigma-Aldrich Co. was served as standard *(15)*.

### Substrate

Sucrose levels were determined by an enzymatic colorimetric glucose-oxidase assay commercially available (Merckotest, Glucose System GOD-PAP, Merck, Germany). The basic principle is the reaction between glucose and water in the presence of oxygen and catalyzed by glucose-oxidase, which leads to gluconate and oxygenated water ($H_2O_2$). Subsequently, a reaction between $H_2O_2$, aminophenazone, and phenol occurs, producing a detectable color change. As the method is specific to glucose, the samples of the fermented broth, previously centrifuged, were hydrolyzed with a solution of 2 *M* HCl in a 1 : 1 proportion and heated at 65–67°C for 10 min. After neutralizing the samples with 1 *M* NaOH, and adequate dilution, a volume of 0.01 mL was mixed with 2.0 mL of the reagent and incubated for 30 min at room temperature (20–25°C). The absorbance of the sample was read at a wavelength of 510 nm on a DR 2500 Spectrophotometer (Hach Company, Colorado).

### pH

The pH was measured using a Digimed DM-20 digital potentiometer, precision ±0.01 (Digimed Analytical, Brazil) and calibrated with pH 4.02 and 6.99 buffer solutions (Merck & Co.) at 25°C.

Table 1
Variation of Surface Tension and pH of *B. subtilis* YRE207 Fermented Media for Different Nitrogen Sources[a]

| Nitrogen source | Surface tension (mN/m)[b] | | Surface tension reduction (%) | Final pH |
|---|---|---|---|---|
| | Initial | Final | | |
| Ammonium nitrate | 66.7 | 31.5 | 52.8 ± 2.1[c] | 7.0 |
| Urea | 62.4 | 37.3 | 40.1 ± 1.3 | 6.0 |
| Brewery residual yeast | 46.5 | 40.3 | 12.9 ± 0.4 | 6.5 |
| Ammonium sulfate | 64.8 | 40.2 | 37.0 ± 4.2 | 6.0 |
| Sodium nitrate | 61.8 | 54.4 | 11.2 ± 1 | 7.0 |

[a]Initial conditions: 10.0 g/L crystal sugar, 1.4 g/L nitrogen, 0.1 g/L cell concentration, 30°C, pH 7.0, 150 rpm, and 48 h.
[b]Mean value from triplicate measurements.
[c]Mean value ± standard deviation.

## Results

### *Influence of the Nitrogen Source*

Table 1 shows the surface tension reduction values and the pH of fermented broth for different nitrogen sources, organic and inorganic ones. A remarkable variation of the surface tension reduction percentage regarding the nitrogen source used was observed, although the final pH has not changed considerably. Among the nitrogen sources tested, ammonium nitrate, ammonium sulfate, and urea were the most favored ones for the biosurfactant production. Nevertheless, ammonium nitrate was the best nitrogen source for surface-active compound synthesis, because the lowest surface tension value and its higher percent reduction were achieved under this nutritional condition. In the final stage of growth, the cells cultivated in the presence of sodium nitrate showed a distinct morphology when compared with that grown in the other tested conditions. Clusters formation could be seen on the fermented medium, which could have favored the cell separation from the medium at the end of the process.

### *Effect of the Carbon/Nitrogen Ratio and the Agitation Rate on the Biosurfactant Production*

The surface tension values determined for the different agitation rates and C/N ratios, using sucrose and ammonium nitrate, and after 48 h, are shown in Figs. 1–3. For C/N 3, the increase in the agitation from 50 to 150 rpm promoted only a slight increase in the total viable cell concentration; however, a remarkable decrease of cellular population at 250 rpm was observed (Fig. 1). Sporulation presented distinct variation, and the highest number of spores were observed under the higher agitation rate condition. Perhaps the increase in the agitation rate caused a greater mass transfer,

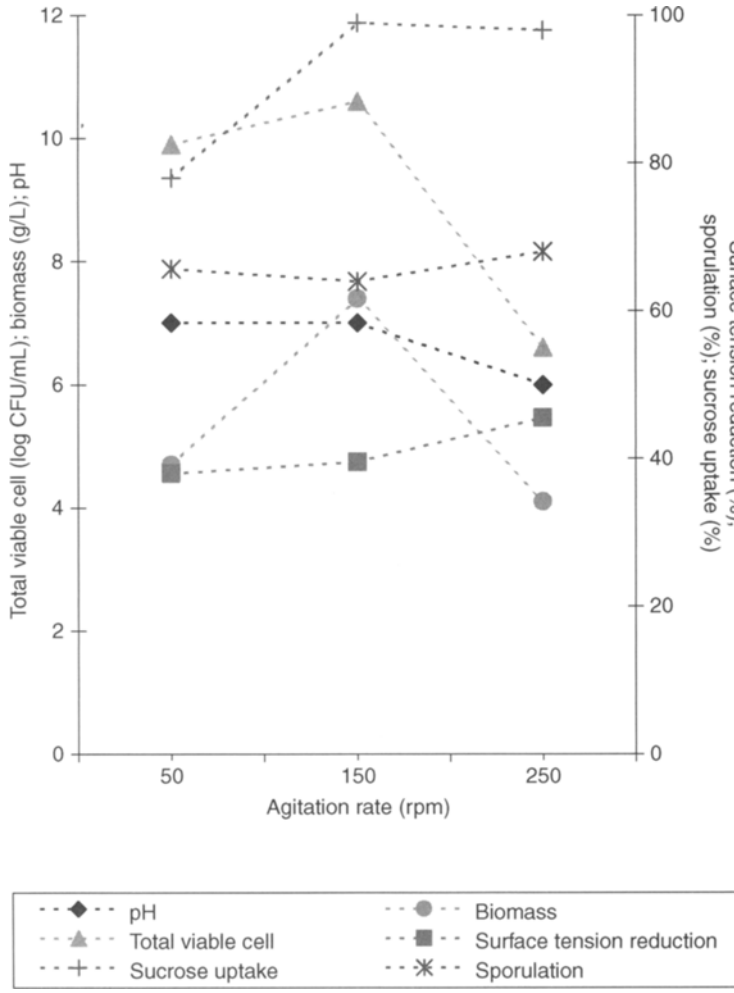


**Fig. 1.** Results for *B. subtilis* YRE207 fermented medium using C/N ratio of 3 at different agitation rates.

which led to faster sugar consumption; sporulation and cell death were a consequence of nutritional depletion.

The reduction of the surface tension was analogous to the percentage of sporulation, suggesting that the synthesis of the surface-active compound was stimulated at the end of the exponential phase of growth with the spore formation. Agitation promotes nutrient and oxygen transfers in the culture media, which in turn favors microbial activity. So, usually, a faster growth of aerobic microorganisms is achieved with high-agitation rates. The oxygen availability favors the biosynthesis reactions, as they are energy-dependent, resulting in a higher quantity of produced biomass, and consequently, in a higher probability of spores formation. However, it is difficult to reach the maximum growth in agitated flasks because in this condition, the oxygen supply is limited. Additionally, in the exponential

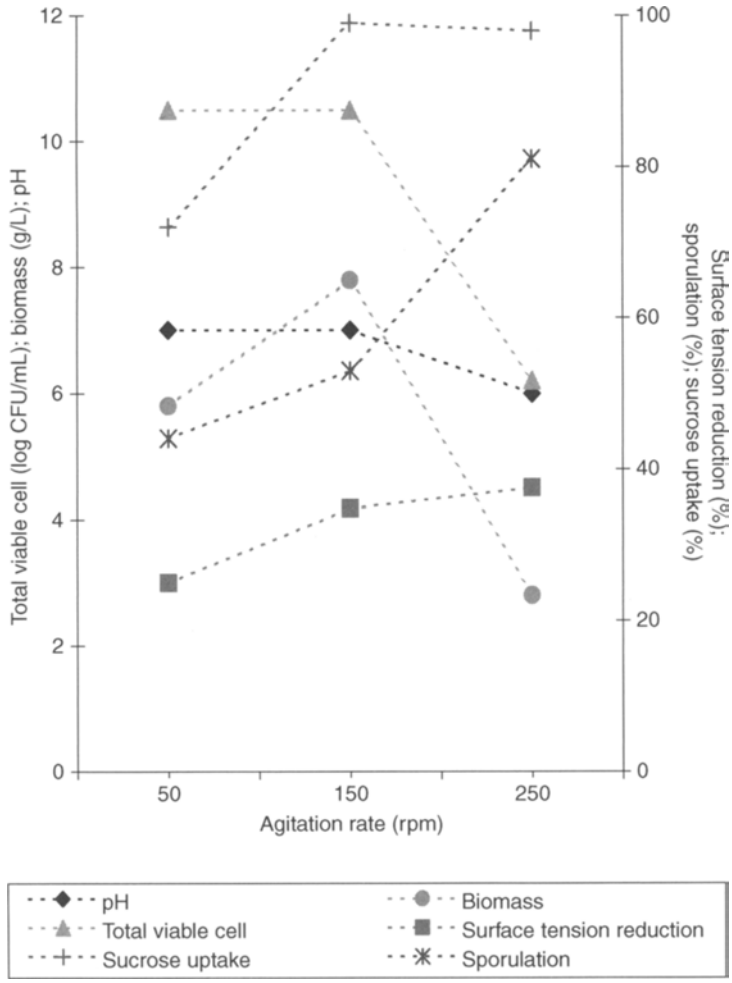


**Fig. 2.** Results for *B. subtilis* YRE207 fermented medium using C/N ratio of 9 at different agitation rates.

phase of growth, the intense propagation of cells causes depletion of oxygen faster than its dissolution on the medium.

A 78% substrate uptake was obtained in the experiment conducted with an agitation rate of 50 rpm. Higher uptakes, of about 99%, were evidenced for the experiments under 150 and 250 rpm. A decrease of the pH was detected when the process was conducted under 250 rpm. A similar behavior was verified for the experiments with C/N ratio of 9 (Fig. 2). Under this condition, a remarkable increase in spore formation directly related to the agitation rate increase was observed. On the other hand, except for the substrate uptake, the bacterial strain showed a different performance when it was cultivated in the media with C/N of 15. In this condition, the increase in the agitation rate promoted an augmentation of the dry weight. However, a reduction in the percentage of sporulation and

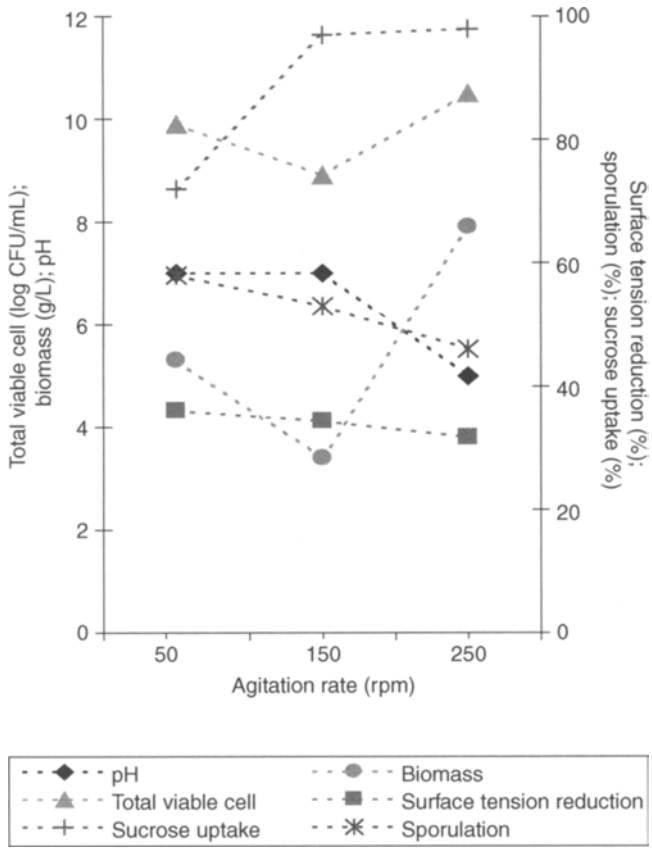


**Fig. 3.** Results for *B. subtilis* YRE207 fermented medium using C/N ratio of 15 at different agitation rates.

surface tension reduction occurred. At the end of the process, samples of the fermented broth were evaluated to its emulsifying activity. All the samples were able to emulsify completely light Arab oil. Nevertheless, no stable emulsions were detected for aviation kerosene, gasoline, diesel oil, and corn and soybean oils. Therefore, the biosurfactant produced may be applied in enhanced oil recovery, bioremediation of oil, and oil tank clean up, but not, as it appears, for use in the food industry.

## *Statistical Analysis*

The optimization of the carbon/nitrogen ratio ($X_1$) and agitation rate ($X_2$) variables was performed considering the percentage of surface tension reduction. From the results obtained, the multiple regressions were done taking as the factors the isolated terms, the interactions, and the quadratics of the variables studied. Table 2 shows the surface tension values for the media before and after fermentation for each experiment.

After the multiple regressions using the Statistica 5.0 program, the parameters with a significance level superior to 10% of the Student's *t*-test

Table 2
Surface Tension Values in Different Experimental Conditions

| Experiment | $X_1$ (C/N) | $X_2$ (agitation rate [rpm]) | Surface tension (mN/m)[a] | | Surface tension reduction (%) |
|---|---|---|---|---|---|
| | | | Initial | Final | |
| 1 | 3 (–) | 50 (–) | 66 | 40.7 | 38.3 ± 0.4[b] |
| 2 | 3 (–) | 150 (0) | 66 | 39.9 | 39.5 ± 1.3 |
| 3 | 3 (–) | 250 (+) | 66 | 35.7 | 45.9 ± 0.6 |
| 4 | 9 (0) | 50 (–) | 57.7 | 40.8 | 29.3 ± 1.2 |
| 5 | 9 (0) | 150 (0) | 57.7 | 37.6 | 34.8 ± 0.7 |
| 6 | 9 (0) | 250 (+) | 57.7 | 36.8 | 36.2 ± 1.1 |
| 7 | 15 (+) | 50 (–) | 60.7 | 38.4 | 36.7 ± 0.1 |
| 8 | 15 (+) | 150 (0) | 60.7 | 39.4 | 35.1 ± 0.9 |
| 9 | 15 (+) | 250 (+) | 60.7 | 41 | 32.5 ± 0.3 |

[a]Mean value from triplicate measurements.
[b]Mean value ± standard deviation.

were eliminated. So, the isolated terms and the agitation quadratic ($X_2$, $X_2^2$) were dismissed. The C/N ratio isolated was the only significant variable on the percentage of surface tension reduction. The correlation coefficient ($R^2$) of 0.803 indicates an adequate adjustment of the experimental data on the percentage of surface tension reduction response, showing that 80.3% of the data variability was explained by the empiric equation that was proposed. The residue distribution around zero and the representation of expected values vs the observed values are shown in Figs. 4 and 5. The residues distribution was at random around zero, presenting no tendency about distribution (Fig. 4). Figure 5 shows that the experimental responses for the percentage of surface tension reduction were near the values given by the empiric equation. Eliminating the insignificant parameters we obtain the following equation:

$$\text{Surface tension reduction (\%)} = 33.4333 - 3.2333\,X_1 + 4.5666\,X_1^2 - 2.95\,X_1X_2$$

This equation represents the adjusted model for the prediction of the surface tension reduction with $X_1$ and $X_2$ in the codified form. The variables were determined through the following codifying equations: carbon/nitrogen ratio ($X_1$) = [C/N – 9]/[(15 – 3)/2] and agitation rate ($X_2$) = [AG (rpm) – 150 (rpm)]/[(250 ( 50)/2] (rpm).

From the complete equation (surface tension reduction (%) = 33.4222 – $3.2333X_1 + 1.7166X_2 + 4.5666X_1^2 + 0.0166X_2^2 - 2.951X_1X_2$), an algorithm of the *Maple V release 4* (Canada) program was used to calculate the stationary point. The calculation of this point gave the following values: $X_1 = 0.590186$ and $X_2 = 0.731199$. The coordinates of the stationary point are between the experimental regions. The λ values that refer to the percentage of the

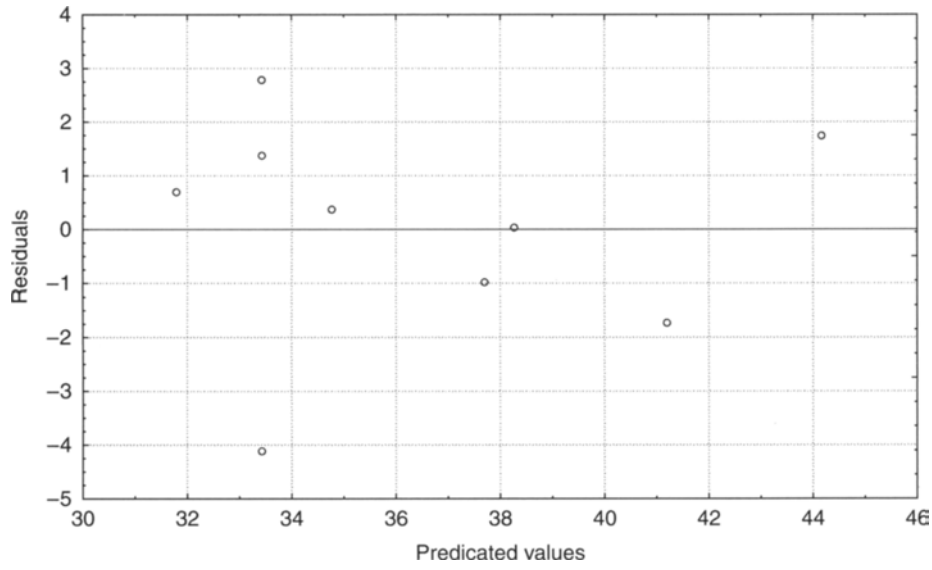


**Fig. 4.** Relative residues distribution in relation to the surface tension reduction.

surface tension reduction indicated that this response has a saddle point because $\lambda_1$ (–0.419649) and $\lambda_2$ (5.002989) have different signs. Using the same algorithm of the *Maple V release 4* program, the codified variable values ($X$'s) were calculated that correspond to the maximization of the response, yielding the following values $X_1 = -1$ and $X_2 = 0.98$. Using the codification equations, the real values may be determined for the variables' concentration in the maximization point of surface tension reduction: $X_1 = 3$ for the C/N ratio and $X_2 = 248$ rpm for the agitation. The determination of the stationary point through canonical analyses using the complete model, in this case, shows that the model really represents the behavior of the surface tension reduction as a function of the studied variables.

Figure 6 illustrates the effect of the studied variables on the surface tension reduction. It is evident that for the lowest values of the C/N ratio, higher rates of agitation cause higher percentage of surface tension reduction. On the other hand, the condition of maximum point of the percentage of surface tension reduction occurs for lower values of the C/N ratio and for higher values of agitation rate. This behavior was also observed in the analyses of the experimental results.

## *Characterization of the Biosurfactant Produced*

Preliminary experiments to determine the presence of surfactin in the fermented broth were performed through chromatographic analyses. Figure 7 shows the chromatograms for the commercial surfactin (Sigma) and for the biosurfactant produced under C/N of 3 and 250 rpm conditions.

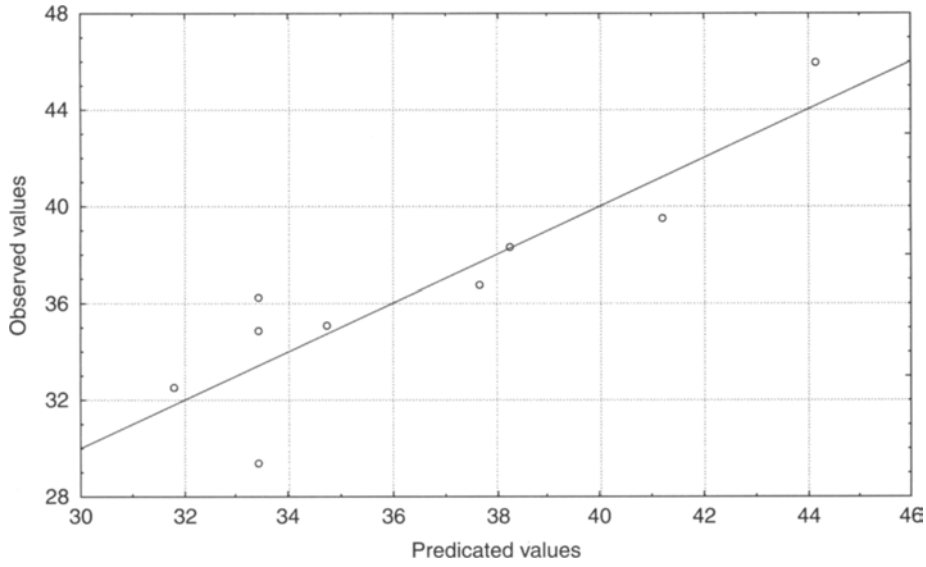


**Fig. 5.** Correlation between experimental values and values predicted by mathematical model.

Surfactin from Sigma presented nine retention peaks. Comparatively, the biosurfactant produced in this study showed similarity with the standard (Sigma) in four retention peaks (number of the peak/retention time: 4/18.593; 5/20.316; 7/25.207; and 8/25.753). Wei and Chu *(15)* observed a chromatographic profile for the surfactin obtained from *B. subtilis* ATCC 21332 similar to the standard (Sigma) also showing nine peaks of which eight were at the same retention time.

## Discussion

Among the nitrogen sources studied, besides the addition of the residual brewery yeast, the addition of sodium nitrate or the ammonium sulfate was not able to significantly reduce the surface tension of the fermented medium (Table 1). According to Davis, Linch, and Varley *(12)*, the type and the concentration of the nitrogen source are important for the optimization of secondary metabolite production, which most of the biosurfactants are. However, the number of publications in the literature about the qualitative and/or quantitative influence of the nitrogen source on the biosurfactant production by *B. subtilis* is still low. Moreover, as stated previously, the production of surfactin by *B. subtilis* in sucrose medium is growth-associated *(13)*.

The production medium containing urea or ammonium nitrate as the nitrogen source was the best in stimulating the biosurfactant production by *B. subtilis* YRE 207, resulting in percentages of surface tension reduction of 40 and 53%, respectively (Table 1). According to Ramnani et al. *(16)*, *Bacillus* spp. are able to reduce the surface tension around 30–60%. Therefore, both

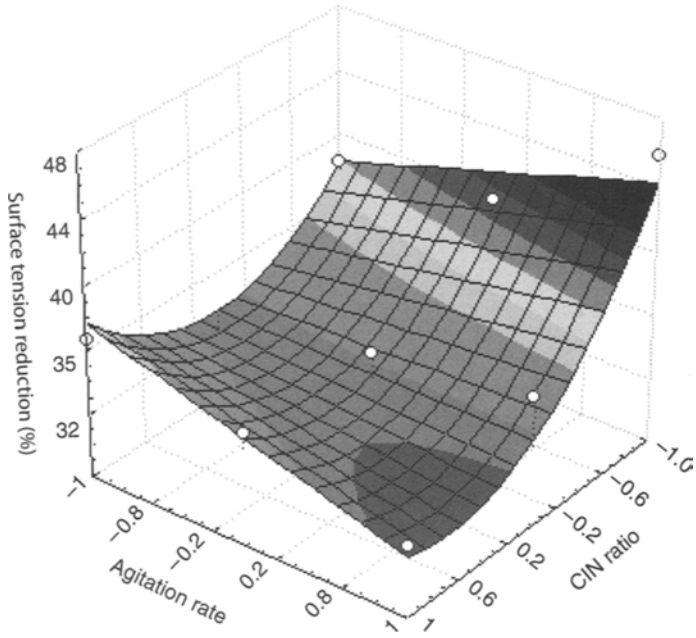


**Fig. 6.** Effect of C/N ratio and agitation rate on surface reduction tension.

nitrogen sources studied were adequate, making the ammonium nitrate the most favorable to the biosurfactant synthesis for the bacterial strain used.

Makkar and Cameotra *(17)* obtained the maximum lipopeptide production by a *B. subtilis* strain after 72 h of cultivation at 45°C with urea and nitrate ion on 3 g/L concentrations. Similarly, the cultivation of *Pseudomonas aeruginosa* strain in different nitrogen sources ($NaNO_3$, $NH_4NO_3$, $(NH_4)_2SO_4$, $NH_4Cl$), with concentrations varying from 2.0 to 5.0 g/L, presented satisfactory surface tension reduction of the medium in the presence of 2.0–3.0 g/L of $NaNO_3$ *(18)*.

Davis, Lynch, and Varley *(12)* concluded that when ammonium ions are used as a nitrogen source, *B. subtilis* ATCC 21332 growth is favored. Meanwhile, the nitrate ion is consumed during *B. subtilis* secondary metabolism, i.e., when the biosurfactant is actually being produced. That is why the evaluation of the nutrients sources is so important. In this work, the effect both of the carbon/nitrogen ratio and the agitation rate were evaluated through an experimental design (Table 2). Variations in the C/N ratio ($X_1$) and in the agitation rate ($X_2$) resulted in alterations of the surface tension reduction (Table 2) varying from 29.3 to 45.9%. Comparing these results, it is possible to establish that in the lower C/N ratio (3 and 9), the increase in the agitation rate promoted an increase in the percentage of surface tension reduction. However, for C/N 15 condition, an increase in the agitation rate caused a small reduction in this percentage. The best results were obtained for the medium containing crystal sugar (10.0 g/L) and $NH_4NO_3$ (4.0 and 1.3 g/L) under 250 rpm agitation rate, corresponding to C/N of 3 and 9.

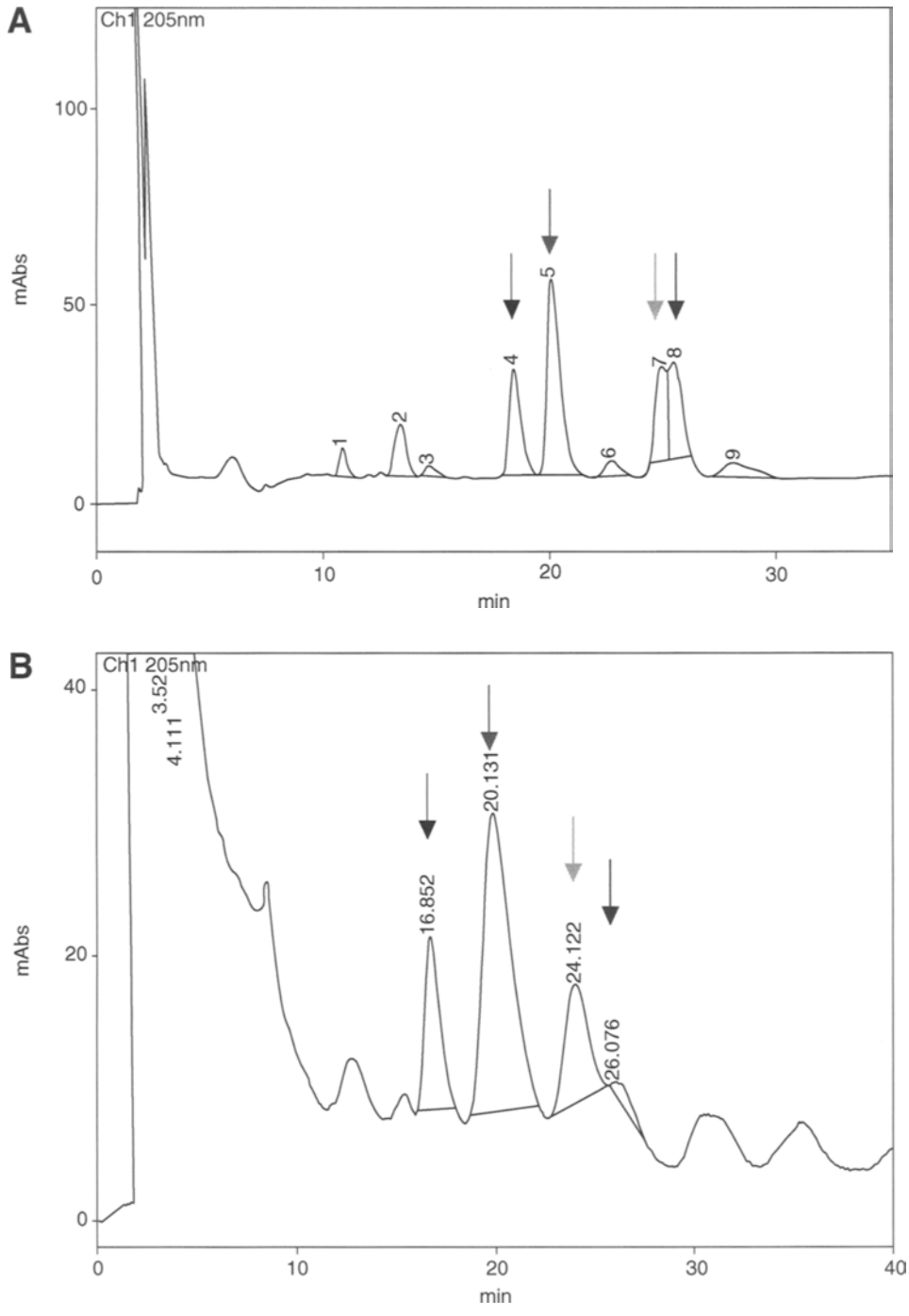


**Fig. 7.** Chromatographic profile of the surfactin **(A)** Sigma and **(B)** fermented broth for C/N ratio of 6 and 250 rpm (peaks and correspondent retention times for Sigma surfactin: 4/18.593; 5/20.316; 7/25.207; and 8/25.753).

The literature usually adopts a carbon/nitrogen ratio around three and agitation of 150 rpm. Davis, Lynch, and Varley *(12)* obtained the highest quantity of surfactin (439.0 mg/L) cultivating *B. subtilis* ATCC 21332 in a medium-containing glucose (10.0 g/L) and ammonium nitrate (4.0 g/L), which corresponds to a C/N ratio of 11. In the experiments performed under 150 and 250 rpm agitation rate, for the different combinations of C/N, an almost total sucrose uptake from the 48 h fermented media was evidenced. Nitschke and Pastore *(11)* showed similar results when using cassava waste water. The pH values obtained at the end of the fermentation were between neutral and acid, 5.5 being the lowest value obtained (Figs. 2 and 3). Wei and Chu *(15)* also observed the existence of an acidogenic metabolic pathway for a high concentration of iron. According to Claus and Berkeley *(19)*, the ideal pH for *B. subtilis* growth is between 5.5 and 8.5. Makkar and Cameotra *(17)* observed remarkable decreases in the growth and mainly in the quantity of biosurfactant produced by a strain of *B. subtilis* when the medium pH was adjusted to 4.5. Additionally, the stability of the surfactin molecule was studied in different pH values *(11)*. The reduction of the pH to values lower than 5.0 favored the microbial surfactant precipitation, which resulted in an elevation of the medium surface tension. So, it may be concluded that there was no influence of the pH on the metabolic activity of the bacterial strain studied.

Analyzing the results obtained, it can be affirmed that there was no correlation between growth and surface tension variation (Figs. 1–3). However, under the conditions in which a higher sporulation was verified (C/N 3—250 rpm; C/N 9—250 rpm, and C/N 15—50 rpm), a decrease in the surface tension was also noted. Branda et al. *(20)* suggest that the surfactin production is related to the sporulation process in *B. subtilis*. The chromatograms of the recovered and partially purified surfactin (C/N 3 and 250 rpm) and of a sample of commercial surfactin (Sigma) showed peaks at different retention times, which prove the existence of different isomers. On the other hand, four peaks were similar to the preponderant peaks of the standard surfactin. Therefore, there is a possibility that the biosurfactant produced in this work has different physicochemical properties that could make it suitable for other types of applications. Obviously, further investigations will be needed.

## Acknowledgments

The authors wish to thank Prof. Leon Rabinovitch (Curator of CCGB, Instituto Oswaldo Cruz, RJ, Brazil) and Assistant Jeane Quintanilha Chaves for carrying out the bacterial strain identification. This work was supported by Coordenação de Aperfeiçoamento de Pessoal de Nível Superior (CAPES), Ministério da Educação, Brazil.

## References


1. Finnerty, W. R. and Singer, M. (1983), *Biotechnology* **1,** 47–54.
2. Morkes, J. (1993), *RD Magazine* **35,** 54–56.
3. Desai, J. D. and Banat, I. M. (1997), *Microbiol. Mol. Biol. Rev.* **61,** 47–64.
4. Kosaric, N. (1996), In: *Biosurfactants*. Rehm, H. -J. and Reed, G., Puhler, A., and Stadler, P., (eds.) *Biotechnology* vol. 6. VCH, Weinheim, Germany: pp. 697–717.
5. Bertrand, J. C., Bonin, P., Goutx, M., Gauthier, M., and Mille, G. (1994), *Res. Microbiol.* **145,** 53–56.
6. Arima, K., Kakinuma, A., and Tamura, G. (1968), *Biochem. Biophys. Res. Commun.* **31,** 488–494.
7. Kakinuma, A.; Sugino, H., Isono, M., Tamura, G., Arima, K. (1969), *Agric. Biol. Chem.* **33,** 973–976.
8. Sandrin, C., Peypoux, F., and Michel, G. (1990), *Biotechnol. Appl. Biochem.* **12,** 370–375.
9. Yeh, M. -S., Wei, Y. -H., and Chang, J. -S. (2005), *Biotechnol. Prog.* **21,** 1329–1334.
10. Cooper, D. G. and Goldenberg, B. G. (1987), *Appl. Environm. Microbiol.* **53,** 224–229.
11. Nitschke, M. and Pastore, G. M. (2005), *Biores. Technol.* **97,** 336–341.
12. Davis, D. A., Lynch, H. C., and Varley, J. (1999), *Enzyme Microb. Technol.* **25,** 322–329.
13. Reis, F. A. S. L., Servulo, E. F. C., and de França, F. P. (2004), *Appl. Biochem. Biotechnol.* **113–116,** 899–912.
14. Davis, D. A., Lynch, H. C., and Varley, J. (2001), *Enzyme Microb. Technol.* **28,** 346–354.
15. Wei, Y. H., and Chu, I. M. (2002), *Biotechnol. Lett.* **24,** 479–482.
16. Ramnani, P., Kumar, S. S., and Gupta, R. (2005), *Proc. Biochem.* **40,** 3352–3359.
17. Makkar, R. S. and Cameotra, S. S. (1997), *J. Ind. Biotechnol.* **18,** 37–42.
18. Robert, M., Mercadé, M. E., Bosch, M. P., et al. (1991), *Biotechnol. Lett.* **11,** 871–874.
19. Claus, D. and Berkeley, R. C. W. (1984), In: *Bergey's Manual of Systematic Bacteriology*. Kieg, N. R. and Holt, J. G., (eds.), Williams & Wilkins, vol. II, London, UK, pp. 1104–1130.
20. Branda, S. S., Gonzalez-Pastor, S. J. E., Ben-Yehuda, S., Losick, R., and Kolter, R. (2001), *Proc. Natl. Acad. Sci. USA* **98,** 11,621–11,626.

0273-2289/1559-0291 (Online)/07/136-140/487-500/$30.00

# A New Process for Acrylic Acid Synthesis by Fermentative Process

**B. H. Lunelli, E. R. Duarte, E. C. Vasco de Toledo, M. R. Wolf Maciel,* and R. Maciel Filho**

*Laboratory of Optimization, Project and Advanced Control—LOPCA, Department of Chemical Process, School of Chemical Engineering, State University of Campinas—UNICAMP, P.O. Box 6066, 13083-970, Campinas, SP, Brazil, E-mail: betania@feq.unicamp.bc*

## Abstract

With the synthesis of chemical products through biotechnological processes, it is possible to discover and to explore innumerable routes that can be used to obtain products of high added value. Each route may have particular advantages in obtaining a desired product, compared with others, especially in terms of yield, productivity, easiness to separate the product, economy, and environmental impact. The purpose of this work is the development of a deterministic model for the biochemical synthesis of acrylic acid in order to explore an alternative process. The model is built-up with the tubular reactor equations together with the kinetic representation based on the structured model. The proposed process makes possible to obtain acrylic acid continuously from the sugar cane fermentation.

**Index Entries:** Acrylic acid; biotechnological processes; bidimensional model; dynamic reduced model; modeling; *Saccharomyces cerevisiae*; tubular bioreactor.

## Introduction

Biological sciences are likely to make the same impact in the formation of new industries in the present and the next centuries, as the physical and chemical sciences have had on industrial development throughout the last century. In fact, the knowledge from biological sciences, when combined with recent and future advances in process engineering, can become the foundation for producing a wide variety of industrial products from renewable plant resources *(1)*.

The present capabilities of genetic engineering for the transfer of specific catalytic functions between organisms can only provide increased opportunities for the future manufacture of chemical commodities from biomass *(2)*. Biotechnological processes, generally, occur under mild conditions.

*Author to whom all correspondence and reprint requests should be addressed.

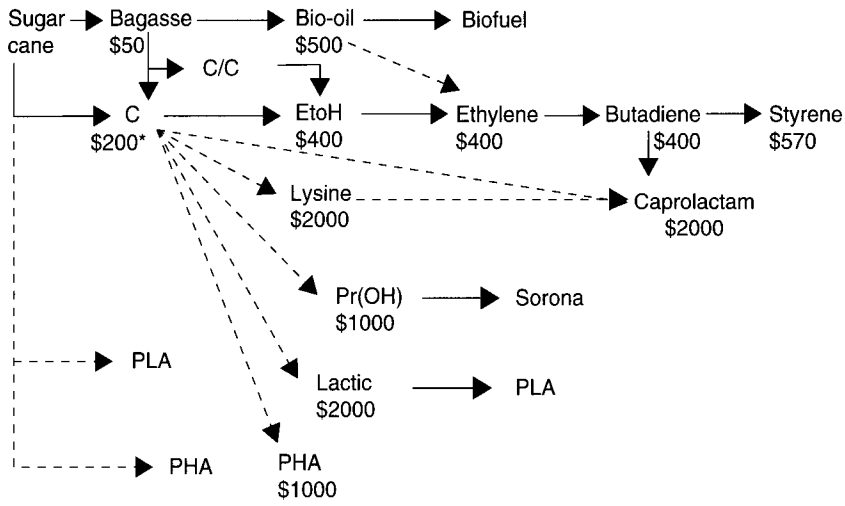


**Fig. 1.** Pathways of several chemical using sugar cane as a feedstock, prices are in USD per ton of compound (*see* ref. *4*).

Biocatalysts, substrates, intermediates, and byproducts, as well as the product itself, are biodegradable. In most cases, water is used as the solvent *(3)*.

With the synthesis of chemical products through biotechnological processes, it is possible to discover and to explore innumerable routes that can be used to obtain products of high added value. Such routes have to be investigated to evaluate their potential in terms of yield, productivity, easiness to recover the product, economy, and environmental impact. A possible feedstock is the sugar cane glucose which is readily available in several countries. Figure 1 depicts possible routes to obtain chemicals from sugar cane, including the use of bagasse *(4)*.

Among these products, acrylic acid is an interesting one. In fact, from the industrial point of view, the acrylic acid production by fermentative process is presented as an innovative process of great importance, because of the possibility of low cost for its production and because of a renewable raw material. This is an important point to be considered, because acrylic acid is used worldwide and its production by fermentation is through environmentally friendly process. In fact, this biochemical route has very low environmental impact, when compared with the conventional petrochemical process. Acrylic acid, known as 2-propenoic acid, is one of the most important industrial chemicals, with an annual production of approx 4.2 mt *(5)*.

Currently, 100% of acrylic acid is produced from fossil fuel. Production from renewable resources is propagated through lactic acid fermentation and subsequent chemical conversion to acrylic acid *(6)*. Bearing this in mind, the purpose of this work is the development of a deterministic model for a biochemical synthesis of acrylic acid, aiming to propose a new methodology for its production. The proposed process makes possible to obtain acrylic acid continuously from the sugar cane fermentation. The reactor is tubular,

continuously operated, and the challenge is to define operating strategy and conditions to achieve the product with the desired specifications.

A deterministic model built-up coupling the reactor and the kinetic equations is developed to study the process. The kinetic model is based on the concepts of structured representation, and adapted from a structured growth model developed by Lei et al. *(7)*, and a structured model for ethanol production developed by Stremel *(10)*, so that the main phenomena taking place in the system is considered. The mathematical models describing the dynamic behavior of the reactor lead to a nonlinear distributed parameter problem requiring excessive computational time. This may be a restriction for control and optimization of online applications. In order to overcome this problem, through the use of reduction techniques, a simplified model is derived. The results show how the model may be used to find out suitable operating conditions and to analyze the effect of kinetic parameters to obtain acrylic acid.

Structured models describing culture kinetics are powerful tools in the control of bioreactors, as they are able to provide a mathematical description of the cellular fermentation mechanism of the process. This is important to help in the optimization and control decisions. The simplest representation of microbial kinetics is the unstructured model, which describes biomass growth, substrate consumption, and extracellular metabolic product formation in a macro balance approach. The unstructured model includes the most fundamental microbial processes: the rate of cell mass production is proportional to biomass concentration; saturation limit growth rate on each substrate is taken into account; and the use of substrate for cell maintenance and the property of the cells to synthesize products even when they do not grow. However, this type of model does not recognize any internal structure of the cell, nor diversity between cell forms, which may be an important feature of certain cell cultures *(8)*.

The application of unstructured models is quite satisfactory in many situations, but there are a large number of applications where such models tend to fail. This is the case when the composition of the system changes drastically, as in any batch process or when the molasses sugar contents change because of the sugar production. In fact, changes in composition affect the initial step of growth as well as in situation where one specific component (protein and RNA in single-cell protein [SCP] production) must be modeled to better use the substrate to a particular pathway. In these cases, a structured model is necessary.

An alternative to simplify the modeling of the bioreactor, even taking into account the cell internal structure is to reduce the dimension of the system of partial differential equations. This can be done taking a mean along a certain position of the reactor, eliminating the dependent variables on radial position, and by formulating an approximation of the variables along that dimension. This dimensionality reduction may be made by application of reduction techniques.

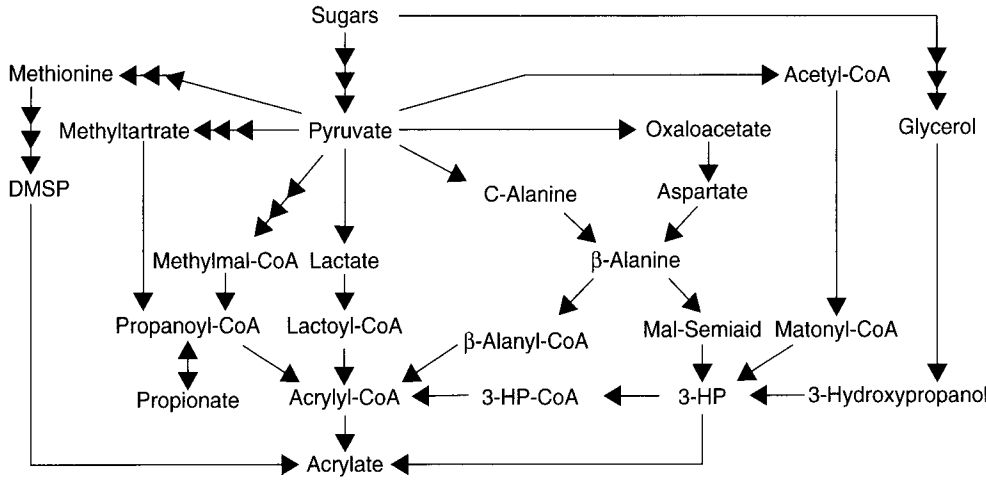


**Fig. 2.** Overview of existing and hypothetical metabolic pathways for biosynthesis of acrylate from sugars (*see* ref. *5*).

## Methods

### *Metabolic Route*

Figure 2 shows the different routes for converting sugars into acrylate. The most direct route is through lactate.

$$\text{Pyruvate} + \text{NADH} + \text{H}^+ \xrightarrow[\text{dehydrogenase}]{\text{Lactate}} \text{Lactate} + \text{NAD}^+$$

Several studies have focused on blocking the enzyme that converts acrylyl-CoA to propanoyl-CoA during the aforementioned lactate fermentation by *Clostridium propionicum*, for example, by using 3-butynoic acid as an inhibitor, to obtain conversion of lactate into acrylate. However, acrylate concentrations never exceed 1% of the initial substrate concentration *(9)*.

There are several problems with production of acrylate through this pathway. First, one-third of the lactate does not lead to acrylate, because it is converted into acetate and $CO_2$. Without this conversion to acetate, no adenosine triphosphate (ATP) for growth and maintenance is generated. The only driving force for the pathway from lactate toward acrylate seems to be the fact that acrylyl-CoA can be used as an electron acceptor for the reducing equivalents produced on formation of acetate and $CO_2$ *(5)*. A method for direct conversion of complex substrate for propionic acid production, with the cultivation of *Lactobacillus* and *Propionibacterium shermanii* and conversion of propionate for acrylate with *C. propionicum* was investigated *(2)*. This route of conversion of propionate to acrylic acid claims to obtain yield more than 18.5%. However, so far it is not clear how to obtain high yields of acrylate from sugars *(5)*. For an economically competitive fermentation process, the molar yield of acrylate on sugar should preferably be almost quantitative. Taking glucose as the sugar, the desired stoichiometry is *(5)*:

$$\text{Glucose} \rightarrow 2\ \text{Acrylate} + 2\ \text{Water}$$

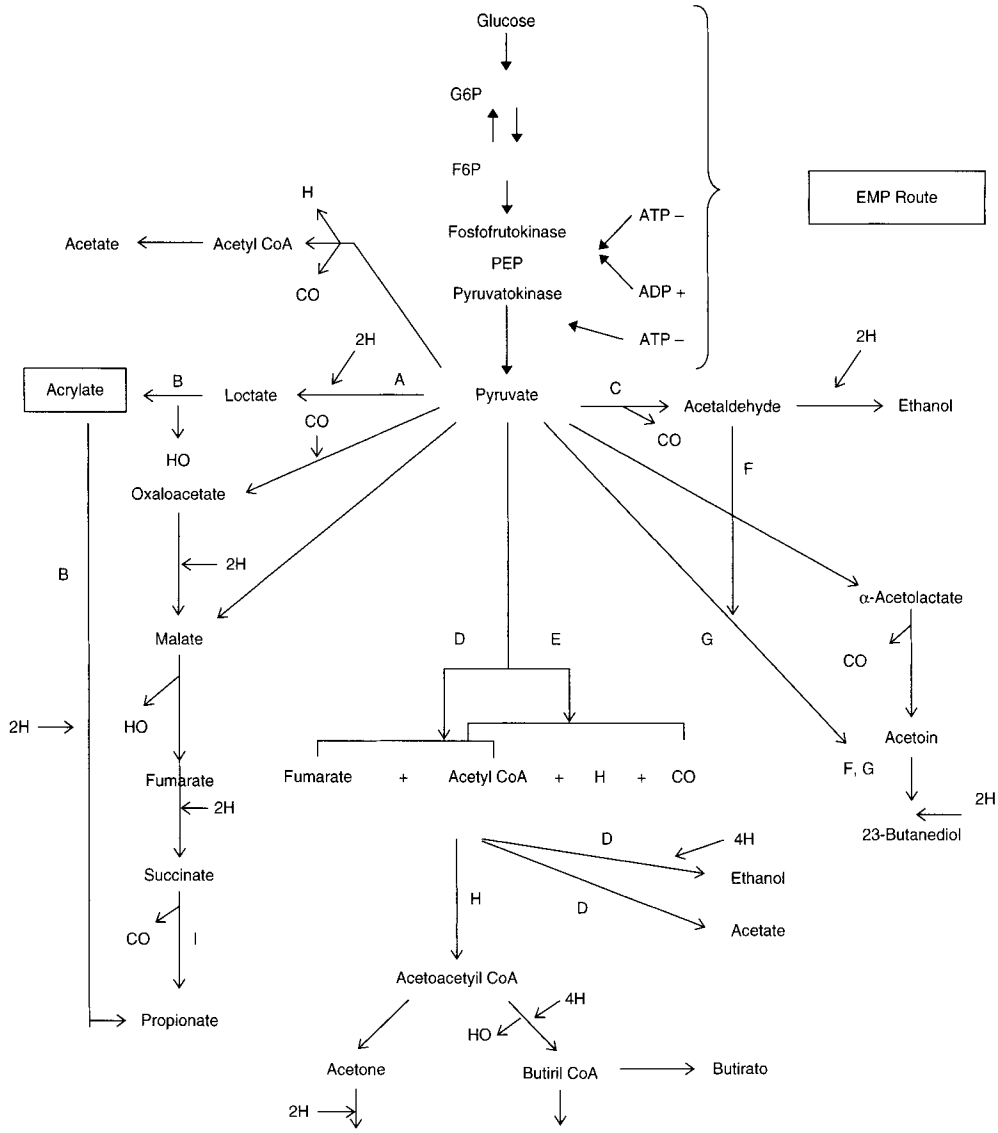


**Fig. 3.** Glycolytic route (*see* ref. *11*).

## Proposed Process

As there is no definitive knowledge on the potential of biotechnological routes for acrylic acid production, and also, because of the few number of structured kinetic models until now developed, in this work, a structured kinetic model for production of acrylic acid by fermentation of sugar cane glucose is developed. The model is based on a structured growth model developed by Lei et al. *(7)*, and on a bioethanol production model developed by Stremel *(10)*. Figure 3 shows the glycolytic route used for the development of the model for acrylic acid and bioethanol production, as they share the same initial route.

The process occurs with the degradation of glucose, which undergoes successive phosphorylations, consuming ATP in the Embden-Meyerhoff-Parnass route, until the pyruvate production. This process is called glycolysis. The pathway of glycolysis can be seen as consisting of two separate phases. In the first phase, two equivalents of ATP are used to convert glucose to fructose-1,6-bisphosphate. In the second phase fructose-1,6-bisphosphate is degraded to pyruvate, with the production of four equivalents of ATP and two equivalents of NADH. Because of action of metabolization through the tricarboxylic acid (TCA) cycle it is converted to lactate the enzyme *lactate dehydrogenase*. The lactate undergoes dehydration, generating acrylate.

### *Bioreactor Mathematical Model*

A mathematical model for the dynamic simulation of a tubular bioreactor that uses *Saccharomyces cerevisiae* immobilized in pellets with 4% of citric pectin for production of bioethanol was developed by Stremel *(10)*, and posteriorly adapted to investigate the acrylate production. As both process share some pathways and the reactor and kinetic structured models are general, the deterministic representation is valid to explore all the possible routes, as the kinetic parameters are available. For the case of bioethanol production, in order to prevent the $CO_2$ accumulation caused for the fermentation process, a type tower fixed-bed bioreactor with gas separator was used. It is important to take this into account as $CO_2$ accumulation may happen in different rates depending on how the process is operated. A scheme of the system is shown in Fig. 4.

The differential balances in the axial direction of the bioreactor take into account the convective terms, assume constant axial dispersion, and the mass interphase transfer and reaction are evaluated in terms of the effectiveness factor. Bearing this in mind the model can be written as:

Substrate in the phase fluid:

$$\frac{\partial S_f}{\partial t} = \frac{D_{ax}}{L^2}\left(\frac{\partial^2 S_f}{\partial z^2}\right) - \frac{u}{L}\left(\frac{\partial S_f}{\partial z}\right) - \frac{1-\varepsilon}{\varepsilon}\eta V_{sup} \tag{1}$$

Ethanol in the phase fluid:

$$\frac{\partial E_f}{\partial t} = \frac{D_{ax}}{L^2}\left(\frac{\partial^2 E_f}{\partial z^2}\right) - \frac{u}{L}\left(\frac{\partial E_f}{\partial z^2}\right) - \frac{1-\varepsilon}{\varepsilon}\eta Y_{ES}\left(V_{sup}\right) \tag{2}$$

## Kinetics for Chemicals Synthesis

A simplification of the glycolytic and respiratory routes (TCA) that was considered in the model, to represent bioethanol synthesis is shown below by stoichiometric expressions.

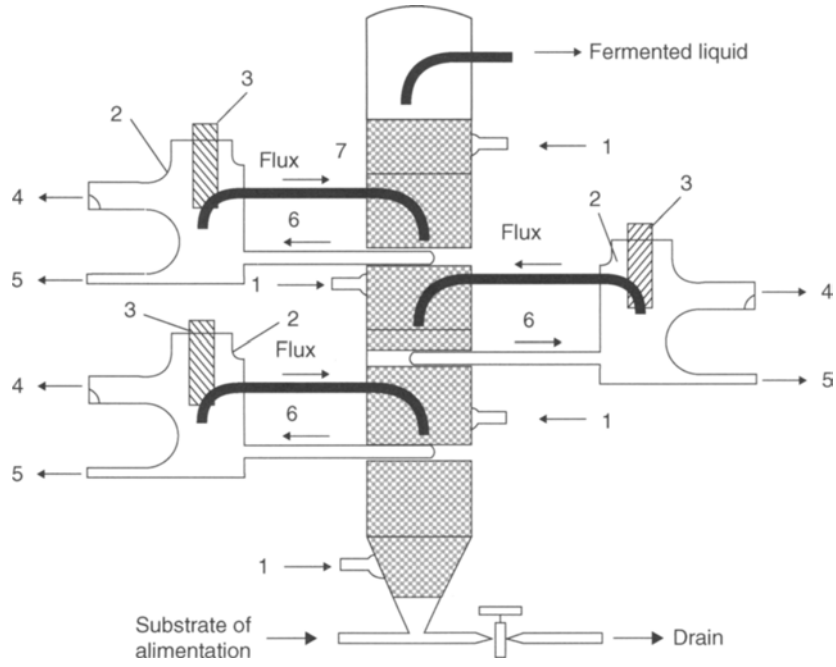


**Fig. 4.** Type tower bioreactor. (1) Pellets of evacuation the alimentation; (2) separator gas-liquid; (3) indutive sensor; (4) exit $CO_2$; (5) evacuation of sample; (6) fermented liquid with flux of $CO_2$; and (7) fermented liquid without flux of $CO_2$.

$$
\begin{aligned}
F_1[\mathrm{S}] &\xrightarrow{R_1} F_1[\mathrm{P}] \\
F_6[\mathrm{S}] &\xrightarrow{R_6} 0.732\,X_{[\mathrm{S}]} \xrightarrow{0.732R_6X_{[\mathrm{S}]}} X_{[\mathrm{T}]} \\
F_4[\mathrm{P}] + \mathrm{O}_2 &\xrightarrow{R_2} \mathrm{TCA} + \mathrm{CO}_2 \\
F_4[\mathrm{P}] &\xrightarrow{R_3} F_3[\mathrm{A}] \\
F_4[\mathrm{A}] + \mathrm{O}_2 + X_{[\mathrm{r}]} &\xrightarrow{R_4} \mathrm{TCA} + X_{[\mathrm{r}]} + \mathrm{CO}_2 \\
F_4[\mathrm{A}] + X_{[\mathrm{fe}]} &\xrightarrow{R_5} F_5[\mathrm{E}] + X_{[\mathrm{fe}]} + \mathrm{CO}_2 \\
F_4[\mathrm{A}] &\xrightarrow{R_7} 0.850\,X_{[\mathrm{S}]} \xrightarrow{0.852R_7X_{[\mathrm{S}]}} X_{[\mathrm{T}]} \\
X_{[\mathrm{S}]} &\xrightarrow{R_8} X_{[\mathrm{P}]} \xrightarrow{(0.732R_6 + 0.850R_7)X_{[\mathrm{P}]}} X_{[\mathrm{T}]} \\
X_{[\mathrm{S}]} &\xrightarrow{R_9} X_{[\mathrm{r}]} \xrightarrow{(0.732R_6 + 0.850R_7)X_{[\mathrm{r}]}} X_{[\mathrm{T}]} \\
X_{[\mathrm{S}]} &\xrightarrow{R_{10}} X_{[\mathrm{fe}]} \xrightarrow{(0.732R_6 + 0.850R_7)X_{[\mathrm{fe}]}} X_{[\mathrm{T}]} \\
X_{[\mathrm{T}]} &\xrightarrow{k_\mathrm{d}} X_{[\mathrm{nv}]}
\end{aligned}
\tag{3}
$$

For the biotechnological production of acrylic acid, three substrates involved in the process are verified. In the first step the glucose is converted into pyruvate, and this into lactate, which is metabolized to produce acrylate. The generic reaction proceeds from the following form:

$$G \xrightarrow{R_p} P \rightarrow La \xrightarrow{R_a} Acryl \tag{4}$$

Balance of mass for glucose in the fluid phase:

$$\frac{d(VG)}{dt} = G_i F_i - GF - \frac{\mu_L X_L}{Y_{XL/G}} V \tag{5}$$

Reaction rate of glucose conversion in pyruvate:

$$R_p = \frac{\mu_L X_L}{Y_{XL/G}} \tag{6}$$

Balance of mass for lactate:

$$\frac{d(VLa)}{dt} = La_i F_i - LaF - \frac{\mu_L X_L}{Y_{XL/G}} V \tag{7}$$

Reaction rate of pyruvate conversion in lactate:

$$R_a = \frac{\mu_L X_L}{Y_{XL/L}} \tag{8}$$

Balance of mass for acrylate:

$$\frac{d(VAcryl)}{dt} = Acryl_i F_i - AcrylF + \frac{\mu_c X_c}{Y_{XC/A}} V \tag{9}$$

## *Reduction Techniques*

The solution for diffusion and reaction multidimensional problems present difficulties associated with a large analytic involvement and also request considerable computational effort. Thus, for practical applications in engineering, online optimization and control is useful to obtain models with lower dimensionality compared with original system of partial differential equations. This may be achieved through the reduction of the number of model independent variables. Therefore, one or more independent variables can be integrated, leading to approximate formulations that retain detailed local information in the remaining variable as well as mean information in the eliminated directions by the integration. The techniques investigated generate models that describe the axial profiles as a function of the time for the convenient explicit elimination of the dependence in the radial variable, in case of the fixed-bed catalytic reactor. The techniques utilized are:

Classic Reduction Technique

This technique is based on the mean value theorem, i.e., each radial mean value is defined for each variable *(12–14)*

$$[\ ]_m = 3\int_0^1 [\ ]\, r^2 dr \tag{10}$$

where $r$ = particle radius and [ ] = radial mean value.

Reduction Technique Based on the Hermite Integrations Formulas

Hermite procedure allows the model order reduction by approaching an integral on the values of the integrating and their derivatives on the limits of the integration, as follow:

$$H_{\alpha,\beta} = \int_{x_{i-1}}^{x_i} y(x)dx = \sum_{v=0}^{\alpha} C_v y^{(v)}(x_{i-1}) + \sum_{v=0}^{\beta} D_v y^{(v)}(x_i) \tag{11}$$

The technique makes use of $H_{0,0}$, $H_{1,1}$ definitions and simultaneously of the spherical coordinates transformation, facilitating the generation of the radial medium variables *(13,15,16)*.

$$H_{0,0} = \int_0^1 y(x)dx \cong \frac{1}{2}[y(0) + y(0)] \tag{12}$$

$$H_{1,1} = \int_0^1 y(x)dx \cong \frac{1}{2}[y(0) + y(1)] + \frac{1}{12}[y'(0) + y'(1)] \tag{13}$$

General Reduction Technique

This technique is a generic mathematical representation, obtained when the Eq. 10 is used with a quadratic equation for the inside particle concentration in function of the mean radial concentration

$$C(r) = C_m b - br^2 \tag{14}$$

## Results

Figure 5 shows the microorganism (*S. cerevisiae*), ethanol ($C_2H_6O$), acetaldehyde ($C_2H_4O$), pyruvate ($C_3H_3O_3$), and substrate ($C_6H_{12}O_6$) concentration at the reactor exit when the steady state is reached. The experimental operation was conducted at pH 4.0 and 30°C using 161.4 g/L initial glucose concentration. The acetaldehyde and pyruvate concentration, intermediary components, appear in low concentration because they are formed and consumed rapidly in the course of respiratory and glycolytic process. At the end of 140 h, 73.0 g/L of ethanol was formed along with 43.0 g/L of cell mass. As can be seen the glucose is used not only to achieve the desired product but also for the maintenance and growth of the microorganism.

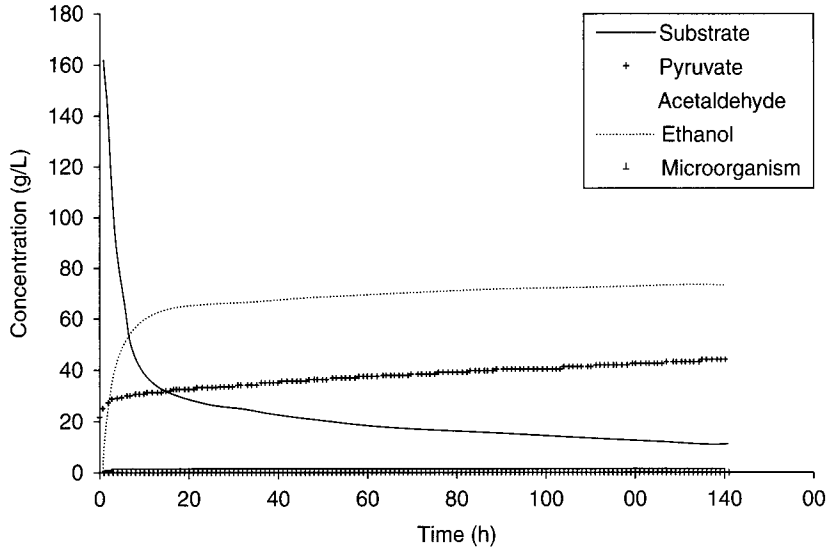


**Fig. 5.** Microorganism, ethanol, acetic acid, pyruvate, and substrate concentration in the reactor exit.

A possible competitive route to obtain the acrylic acid by fermentation through *S. cerevisiae*, is shown in Fig. 6. Acrylate ($C_3H_4O_2$), lactate ($C_3H_5O_3$), pyruvate ($C_3H_3O_3$), and substrate ($C_6H_{12}O_6$) are obtained and their concentrations at the reactor exit when the steady state is established depict the potential to produce acrylic acid. The dynamic behavior follows a system of first order with asymptotic shape for all the species. In fact, an inverse response was not observed because the temperature is constant along the reactor length. This is expected to occur when tubular reactors are used, and it could be a drawback to use this type of design because of difficulties in process control. The steady state operation is achieved in about 140 h.

The Fig. 7 shows the concentration profiles of acrylate and microorganisms concentration at the reactor exit. The product and cell yields obtained from the glucose fermentation were 0.46 g acrylate per gram of glucose and 0.10 g dry cell per gram of glucose, respectively. Changes in the kinetic values alter significantly the specific values of desired product concentration, but what is interesting to realize is that the acrylate production is associated with the microbial growth, i.e., the acrylate production is directly related with energetic metabolic route. This is important information for reactor design and operation because a suitable residence time should be chosen to allow the reactor to operate near the steady state. However, because of the fact that the production is associated with the microbial growth, it is not possible to determine the necessary amount of glucose for the synthesis of the product. This means that it is necessary to find out operating conditions

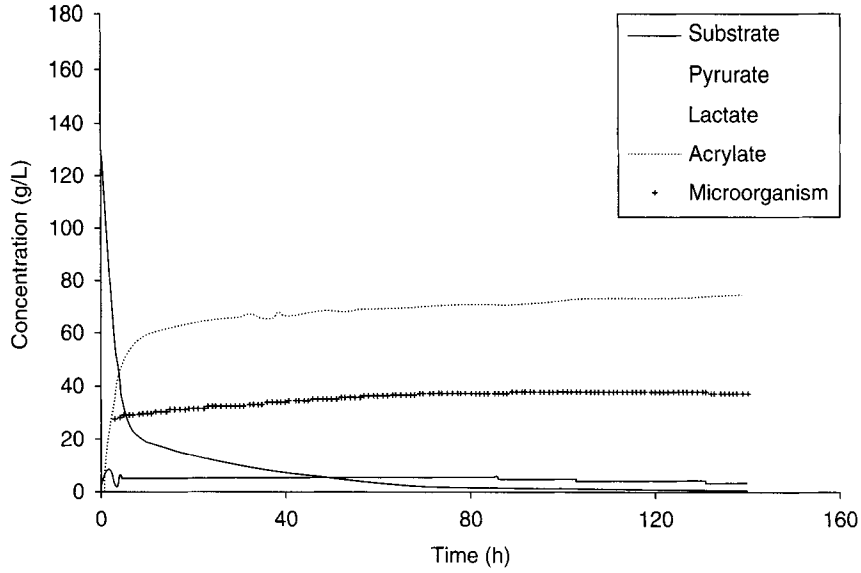


**Fig. 6.** Microorganism, acrylate, lactate, pyruvate, and substrate concentration in the reactor exit.

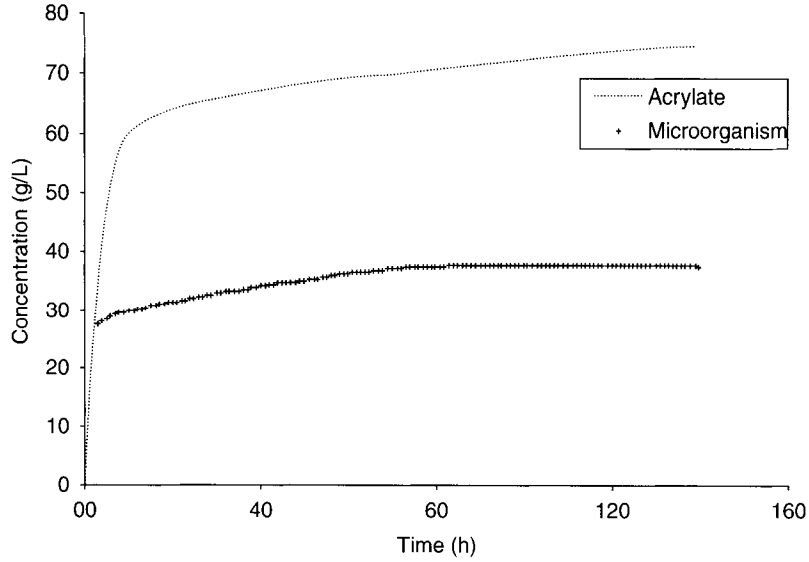


**Fig. 7.** Microorganism, acrylate concentration in the reactor exit.

in such a way that it is possible to achieve desired amount of the product (acrylic acid) with the required amount of substrate for the maintenance and growth of the microorganism.

The kinetic values for a given microorganism, in this case *S. cerevisae*, is dependent on the system operating conditions including substrate

composition. This information may be used to define operating strategies that may drive the system to obtain a desired product. The acrylic acid production by fermentation occurs from glucose degradation and might be expressive depending on the operational conditions, although its conversion as shown in the literature is significantly smaller when compared with the conventional production, i.e., petrochemical via, where the conversion is of approx 90%.

## Conclusions

In this work, a structured deterministic model for the process of production of acrylic acid is proposed. It allowed the understanding of the modeling problem of biochemical processes taking into account the metabolic routes. In this case it is possible to consider the competition among the several product to be formed so that it is possible to foresee operational strategies, which take into account for instance the feed of different substrate compositions as they impact the route that the microorganism will follow. Also it is important to have dynamic information about the time to reach operating conditions around the steady state, so that suitable design can meet required production levels. This is important, as the conversion for biochemical processes is usually low compared with the petrochemical via. For the specific case of acrylic acid production, it is observed that the acid production is strictly related to the microbial growth and this should be considered in the reactor design. Through the application of the reduction techniques it was possible to reduce significantly the number of differential equations to be solved, thus reducing the complexity of the modeling as well as the computer time and burden, whereas still keeping important process information.

## Nomenclature

| | |
|---|---|
| $\eta$ | Effectiveness factor |
| $\mu$ | growth specific velocity ($h^{-1}$) |
| $\varepsilon$ | Porosity of the bed |
| A | Acetaldehyde |
| Acryl | Acrylate |
| $C$ | Concentration (g/L) |
| $C_m$ | Mean radial concentration (g/L) |
| $D_{ax}$ | Axial dispersion of coefficient ($m^2/h$) |
| E | Ethanol |
| $F_1, \ldots, F_6$ | Adjustment of constant |
| G | Glucose |
| $L$ | Length of the bioreactor (m) |
| La | Lactate |
| P | Pyruvate |
| $R$ | Inside radius (m) |

| | |
|---|---|
| $R$ | Particle of the radius (m) |
| $R_{1,\ldots,}R_6$ | Metabolic reaction rate (g/Lh) |
| $R_a$, $R_p$ | Reaction rate (g/h) |
| S | Substrate |
| *Sh* | Sherwood number |
| $t$ | Time (h) |
| $u$ | Fluid interstitial velocity (m/h) |
| $V_{sup}$ | Superficial reaction rate (g/Lh) |
| $X$ | Total mass concentration (g/L) |
| $Y$ | Yield coefficient (g/g [%]) |
| $Z$ | Axial length of the bioreactor (m) |

## Acknowledgments

The authors are thankful to the Fundação de Amparo a Pesquisa do Estado de São Paulo, Brazil, Process number 05/53186-8 for the financial support.

## References

1. Dale, B. E. (2003), *J. Chem. Technol. Biotechnol.* **78,** 1093–1103.
2. O'Brien, D. J., Panzer, C. C., and Eisele, W. P. (1990), *Biotechnol. Prog.* **6,** 237–342.
3. Willke, T. and Vorlop, K. D. (2004), *App. Microbiol. Biotechnol.* **66,** 131–142.
4. Nossin, P., Joosten, J., and Bruggink, A. (2002), Future Feedstocks for Commodity Polymers: EcotheneTM—Sustainability in the 21st century. DSM Research BV, Geleen
5. Straathof, A. J. J, Sie, S., Franco, T. T., and Van der Wielen, L. A. M. (2005), *Appl. Microbiol. Biotechnol.* **67,** 727–734.
6. Danner, H. and Braun, R. (1999), *Chem. Soc. Rev.* **28,** 395–405.
7. Lei, F., Rotboll, M., and Jorgensen, S. B. (2001), *J. Biotechnol.* **88,** 205–221.
8. Birol, G., Kirdar, B., and Onsan, Z. (2002), *J. Ind. Microbiol. Biotechnol.* **29,** 111–116.
9. Akedo, M. Cooney, C. L., and Sinskey, A. J. (1983), *Biotechnol.* **1,** 791–794.
10. Stremel, D. P (2001), In: *Desenvolvimento de Modelos Estruturados Alternativos Para o Processo de Produção de Etanol,* Tese de doutorado, *FEQ/UNICAMP,* Campinas.
11. Bailey, J. E. and Ollis, D. F. (1986), *Biochemical Engineering Fundamentals,* McGraw Hill, New York: pp. 276.
12. Mcgreavy, C. and Naim, H. (1977), *Can. J. Chem. Eng.* **55,** 326–332.
13. Toledo, E. C. V. and Maciel Filho, R. (1997), In: *Modelos reduzidos para controle avançado de reatores de leito fixo.* ELAIQ'94, Chile, pp. 36–41.
14. Stremel, D. P. and Maciel Filho, R. (1998), In: *Aplicação de um modelo estruturado no processo fermentativo em biorreator de alta produtividade para produção de etanol. 12° Congresso Brasileiro de Engenharia Química (COBEQ).* Porto Alegre, RS.
15. Corrêa, E. J. and Cotta, R. M. (1996), Appl. Mathem. Model. **22,** 137–152.
16. Vasco de Toledo, E. C. (1999), In: *Modelagem, simulação e controle de reatores catalíticos de leito fixo.* Tese de doutorado, FEQ/UNICAMP, Campinas.

0273-2289/1559–0291 (Online)/07/136–140/501–514/$30.00

# Ethanol/Water Pulps From Sugar Cane Straw and Their Biobleaching With Xylanase From *Bacillus pumilus*

REGINA Y. MORIYA,[1] ADILSON R. GONÇALVES,*,[1] AND MARTA C. T. DUARTE[2]

[1]*Departamento de Biotecnologia, Escola de Engenharia de Lorena—USP, PO box 116, Lorena 12600-970, SP, Brazil, E-mail: adilson@debiq.faenquil.br, URL: http://debiq.faenquil.br/adilson; and* [2]*CPQBA/UNICAMP, PO box 6171, Campinas 13081-970, SP, Brazil*

## Abstract

The influence of independent variables (temperature and time) on the cooking of sugar cane straw with ethanol/water mixtures was studied to determine operating conditions that obtain pulp with high cellulose contents and a low lignin content. An experimental $2^2$ design was applied for temperatures of 185 and 215°C, and time of 1 and 2.5 h with the ethanol/water mixture concentration and constant straw-to-solvent ratio. The system was scaled-up at 200°C cooking temperature for 2 h with 50% ethanol–water concentration, and 1 : 10 (w/v) straw-to-solvent ratio to obtain a pulp with 3.14 cP viscosity, 58.09 kappa-number, and the chemical composition of the pulps were 3.2% pentosan and 31.5% lignin. Xylanase from *Bacillus pumilus* was then applied at a loading of 5–150 IU/g dry pulp in the sugar cane straw ethanol/water pulp at 50°C for 2 and 20 h. To ethanol/water pulps, the best enzyme dosage was found to be 20 IU/g dry pulp at 20 h, and a high enzyme dosage of 150 IU/g dry pulp did not decrease the kappa-number of the pulp.

**Index Entries:** *Bacillus pumilus*; biobleaching; ethanol/water pulp; organosolv pulping; sugarcane straw; xylanase.

## Introduction

Brazil is the greatest sugar cane producer in the world followed by India and Australia *(1)*. The sugar cane is cultivated in the southeast and northeast portions of the country, and for 2006–2007, the estimated production is more than 410 million t. Sugar cane straw is the material that is removed before the cane is crushed, and 55% of the sugar cane juice is used to produce alcohol and 45% is used for sugar. One ton sugar cane cultivate produces 140 kg sugar cane straw. Sugar cane straw is inclusive of the dried leaves, fresh leaves, and the tip of plant. Thus, Brazil produces about 40 million t/y of sugar cane straw *(2)*. Most of this residue is burned, thereby losing energy and causing significant pollution. From 2005 onward, environmental concerns and legislation

will forbid the burning of sugar cane fields before harvesting in São Paulo State, making a great amount of sugar cane straw available for other uses. This material has not been used as a source of chemicals, but only as solid fuel *(3)*.

Agricultural fibers constitute an alternative to wood as raw material for making pulp because of their high growth rate and adaptability to various soil types. Spain produces more than 16 million t of major agricultural residues each year. With a yield of 40–50%, this mass would provide more than four times the amount of paper currently obtained from wood fibers in this country *(4)*. The annual production of pulp can hardly have current demand, which is growing dramatically in developing countries and, at lesser extent, in developed countries. This is owing to an increasing shortage of wood raw materials and the gradual deforestation of some areas on the planet. For this reason, the use of alternative nonwood materials such as wheat straw *(5,6)*, hemp *(7)*, flax *(8)* were used for pulping and paper making.

Traditionally, the cooking process generates large amounts of concentrated waste-water, especially from sulfite and sulfate processes. One solution for this problem is the use of organic solvents. Although their favorable effects on the pulping process are established, the use of this type of solvent for this purpose is recent and is only on the pilot or small industrial scale *(9)*. Prominent among the pulping processes that use organic solvents are those based on alcohols, particularly the Alcell (ethanol/water) (Alcell Technologies Inc., Montreal Canada), MD Organocell (ethanol soda), (Organocell Thyssen GmbH, Planegg, Germany) and alkali sulfite anthraquinone methanol *(10–13)*. Pulping process that uses organic solvents presents several advantages such as: (a) the required equipment is simple *(14)*, (b) byproducts are suitable for further chemical utilization, (c) this technology can be applied for a variety of raw materials, including hardwoods *(15)*, softwoods *(16)*, nonwood materials *(5–6)*, (d) pulps are susceptible to total chlorine free (TCF) bleaching, and (e) (TCF-bleached pulps present high levels of brightness and intrinsic viscosity *(17)*.

Modifications of the production process at the pulping and bleaching stages have been developed. This includes extending the cooking time and introduction of oxygen delignification as a prebleaching step for additional lignin removal. Biological alternatives to minimize the residual hemicellulose and lignin contents in dissolving pulp are also under investigation. Research has been focused on the use of xylanases *(18)* and white-rot fungi *(19)* in biobleaching of sulfite pulps as means of improving the selectivity and extent of hemicellulose and lignin removal from dissolving pulp. Xylanase prebleaching technology is now in use at several mills, mainly in Scandinavia and Canada; the main motivating factors for this technology are the economic and environmental advantages that xylanase offers to the bleach plant *(20)*. From western countries many reports about using xylanases from different sources for evaluating their interaction with various kinds of pulps are available *(21,22)*. However, it is necessary to assess and study the processes under specific conditions for different countries

with various kinds of pulps, which are locally available. In Maharashtra, (Índia) where sugar cane is an abundantly grown crop, bagasse is one of the major cheap raw materials available for making paper *(23)*. Extremophilic enzymes, which are active under alkaline conditions and high temperatures, have high potential for industrial application, such as the bleaching process, without any need for cooling or change in pH *(24)*. The large variety of potential applications of these enzymes is the main reason for investigating fungal and bacterial xylanase production. The most important application of xylanases is in the prebleaching of kraft pulp *(25)*. A treatment with xylanases can improve the chemical extraction of lignin from pulp *(26,27)*. This leads to significant savings of chemicals required for bleaching and to a reduction of toxic chlorine compounds released into the environment. The use of low-cost substrates for the production of industrial enzymes would be expected to greatly reduce production costs *(28)*.

Only a few microorganisms have been identified to have the capability of producing extremophilic xylanases. One of such strains is *Bacillus pumilus* sp. NCIM 59 *(29)*. The most significant feature of the enzyme from this strain is its cellulase-free nature, which is one of the necessary prerequisites for use in the paper and pulp industry. The objectives of this work are to investigate the conditions for sugar cane straw ethanol/water pulping to obtain dissolved pulps and to evaluate the potential of xylanase obtained from *B. pumilus* on sugar cane straw ethanol/water pulps bleaching. Studies of pulping of sugar cane straw and xylanase biobleaching were done for the first time in this article.

## Materials and Methods

### *Ethanol/Water Pulping in 200-mL Vessel*

Whole sugar cane plant was mechanically cut and fresh sugar cane leaves and the tip of plants were kindly provided by "Usina Ester"(Cosmópolis, SP-Brazil). Sugar cane straw was washed with water, sun-dried to 10% moisture, and scissors chopped to a length of 3–5 cm. Pulping was performed in a 200-mL electrically heated horizontal agitation laboratory stainless steel batch cylindrical reactor (digestor was fabricated in São Paulo University, Brazil). In order to determine optimum ethanol/water pulping conditions of sugar cane straw, a $2^2$ factorial design was used at 150–215°C for 1–4 h. Ethanol concentration of 50% (by volume) and 10 : 1 (v/w) liquor/straw ratio were maintained constant, according to Gonçalves and Ruzene *(30)*. The pulp was filtered and washed with 2500 mL ethanol/water 1 : 1 (v/v).

### *Ethanol/Water Pulping Scale-Up in 40-L Vessel*

The sugar cane leaves, sun-dried to 10% moisture was cut into pieces of approx 3 cm. Scale-up ethanol/water pulping were carried out in a 40-L stainless steel batch cylindrical reactor. An insulated electrical coil arranged

around the reactor provided heating and a manometer was used to read pressure. The reactor rotates around its own axis for agitation. Ethanol/water pulping was performed using ethanol/water mixture 1 : 1 (v/v) at 10 (v/w) liquid/solid ratio. Reaction time was fixed at 2 h and 200°C. After the residence time, the reactor was turned off and cooled for approx 18 h. The pulp was filtered in cotton bag and washed with tap water until wash water was colorless. The moisture content of the washed pulp was 54% (w/w) and it was stored in scaled plastic bags at 4°C until use.

### *Xylanase Assay*

A crude enzyme with high xylanase activity and cellulase-free, produced by bacteria *B. pumilus* was kindly supplied by Duarte *(31)*. Xylanase activity was determined by incubating 0.1 mL suitable diluted enzyme with 0.9 mL of 1% (w/v) xylan (birchwood xylan, Roth, Karlsrule, Germany) in a pH 8.5 glycine–NaOH buffer for 5 min at 50°C as described by Bailey et al. *(32)*. One unit of xylanase activity was defined as the amount of enzyme that catalyses the release of 1 μmol xylose/min of reaction.

### *Xylanase Pretreatment of Pulp*

Before pulping, sugar cane straw pulp was treated with the crude enzyme *B. pumilus*. Optimization of enzyme loading for biobleaching was carried out by treating pulp with varying xylanase charges, ranging from 5 to 50 IU/g of dry pulp for 2 h and 150 IU/g for 20 h pH 8.5 in glycine–NaOH buffer. Samples of ethanol/water pulp with 3% pulp consistency were incubated in transparent plastic bags in a water bath at 50°C with intermittent kneading. Control samples were treated under the same conditions without enzyme. After incubation, the pulp slurry was filtered through a Büchner funnel, and the pulp was washed thoroughly with distilled water. The wet enzyme pretreated straw pulp (3 g dry weight) was placed in Erlenmeyer flask and treated with 1% (w/w) NaOH at 60°C for 1 h. The pulp was filtered and washed with distilled water. A set of samples was treated with NaOH, under the same condition described as used as a control medium.

### *Estimation of Kappa-Number*

A sample of the pulp (0.3–0.35 g dry pulp) was exposed to 0.1 *N* $KMnO_4$ at 25°C for 10 min. The reaction was stopped by adding excess KI solution, and the $KMnO_4$ consumed was determined by back-titrating the liberated iodine with standard sodium thiosulfate. The κ-number so obtained, was the volume in milliliter of 0.1 *N* $KMnO_4$ consumed per gram of pulp and used to measure residual lignin in the pulp *(33)*.

### *Determination of Viscosity*

Viscosity was determined by dissolving sugar cane straw pulp in cupriethylenediamine and measuring the viscosity of 0.5% solution with an Ostwald Fensk viscometer *(34)*.

### *Determination of Pulp Chemical Compounds*

The chemical composition of the sugar cane straw and the pulps treated with xylanase were determined by acid hydrolysis, a method developed at the Laboratory of Biomass Conversion (São Paulo University, São Paulo). Approximately 2.0 g of milled sugar cane straw (Manesco and Ranieri knife mill to pass through a 0.5-mm screen) or 1.0 g of pulp was hydrolyzed with 72% sulfuric acid at 45°C for 7 min. The acid was diluted to a final concentration of 5% (addition of 140 mL of water) and the mixture heated at 125°C/1 atm for 30 min. The residual material was cooled and filtered through fast-filtration paper filter. The solid was dried to constant weight at 105°C and determined gravimetrically as insoluble lignin. The soluble lignin concentration in the filtrate was determined by measurement of the absorbance at 205 nm and using the value of 1101/g/cm as the absorptivity of soluble lignin *(35)*. The concentrations of monomeric sugars in the soluble fraction were analyzed using an Aminex HPX-87H column ($300 \times 7.8$ mm$^2$) (Bio-Rad, Hercules, CA) at 45°C with a Shimadzu chromatograph and refraction-index detector (RI-RID-10A, Shimadzu, Tokyo, Japan). The monosaccharides present in hydrolyzates were converted to percent polysaccharides: D-glucose to glucan, D-xylose to xylan, and D-mannose to mannan. The monosaccharide peak areas were converted using standard equations ascertained with the appropriate internal standards (curves standards of D-glucose, D-xylose, D-mannose, L-arabinose, and acetic acid). The monosaccharide weights were converted to polysaccharide percentage by considering hydrolyzate sample dilution, water of hydrolysis factors, and the original sample dry weight. The factors used to convert sugar monomers to anhydromonomers were 0.90 for glucose and 0.88 for xylose and arabinose. The acetyl content was calculated as the acetic acid content multiplied by 0.7. These factors were calculated based on water addition to polysaccharides during acid hydrolysis *(36)*.

### *Fourier Transform Infrared and Principal Component Analysis of Bleached and Unbleached Pulps*

Fourier transform infrared (FTIR) spectra were obtained directly from the bleached and unbleached refined pulps utilizing attenuated reflexion technique, under the conditions described by Faix *(37)*. Spectra were recorded (32 scans) in an Avatar-320-FT-IR Nicolet spectrometer (Nicolet Instrument Corporation, Madison, WI). After polygonal baseline correction *(37)*, the spectra were normalized by the absorption at 900 cm$^{-1}$, which corresponds to the anomeric carbon atom of O–C–O group in polysaccharides and suffers no interference from other groups *(38)*. Spectra were converted to text files using OMNIC software (Nicolet), and normalized absorbances in the range of 650–4000 cm$^{-1}$ were submitted to principal component analysis (PCA) calculations using the BIOTEC and FAEN programs

compiled in FORTRAN, which were written in our laboratory based on the work of Scarminio and Bruns *(39)*. Graphic presentations were easily made with Microsoft EXCEL 5.0.

## Results and Discussion

### *Optimization of Sugar Cane Straw Ethanol/Water Pulping*

In order to determine the optimum conditions for sugar cane straw ethanol/water pulping to obtain bleached pulps with appropriate dissolving pulp compositions, the temperature and the time of pulping were studied with a $2^2$ factorial design over a temperature range of 150–190°C and a time-span of 1–4 h for an ethanol/water mixture of 50% (by volume), and a sugar cane straw-to-solvent ratio of 1 : 10 (m/v). At 150°C, no pulp was formed more than 1–4 h. Similarly, no pulp was obtained at 170°C and 2.5 h. However, at 190°C, the pulps obtained between 1 and 4 h were very dark. Based on these results, we decided to perform another experimental design $2^2$ over a temperature range of 185–215°C and a time period of 1.5–2.5 h with replicate at the middle point (maximum temperature plus minimum temperature divided by two). Once again, the ethanol/water concentration and biomass-to-solvent ratio were held constant. The second experimental design was carried out in three replicate determinations of the independent variables of the pulping carried out in the 200-mL vessel, as shown in Table 1.

The pulping yield was highest (55.6%) at the highest temperature evaluated. However, pentosan was still degraded (2.3%), and the lignin amount increased to 33%. Pentosan degradation was correlated with the lower viscosity (4.4 cP) for the pulp. At 185°C and 2.5 h, the yield dropped to 47.6%, and the kappa-number, and the glucan and lignin contents were lower than obtained at 200°C, whereas the pentosan content and viscosity were highest. For paper pulp, 185°C and 2.5 h of pulping were optimum conditions for sugar cane straw ethanol/water pulping. Because ethanol/water-dissolving pulps must have a maximum of 10% pentosan *(40)*, we decided the better time and temperature of pulping were 2 h and 200°C, respectively.

The system was scaled-up to a 40-L reactor with sugar cane straw ethanol/water pulping performed for 2 h at 200°C based on the results in Table 1. Now the ethanol/water pulping yield was 50%, and the chemical composition of the pulp obtained was 61.7% glucan, 3.2% pentosan, 31.5% lignin, and 4.1% ash. The viscosity and kappa-number were 3.14 cP and 58.09, respectively. Degradation of the pentosan resulted in a lower viscosity of 3.14 cP compared with the 200-mL vessel at 200°C for 2.5 h. Moriya et al. *(41)* used pulping conditions of an ethanol/water mixture of 1 : 1 (v/v), a bagasse-to-solvent ratio of 1 : 10 (m/v), temperature 185°C, and a 2.5 h cooking time to obtain a pulp viscosity of 8.64 cP and a kappa-number of 50 for sugar cane bagasse. Using these same conditions for pulping of sugar cane straw resulted in a pulp viscosity of 10.6 cP and a kappa-number 54.5.

Table 1
Conditions Used in the Ethanol Pulping of Sugar Cane Straw and Experimental Results for the Yield, Properties Kappa-Number, Viscosity, and the Chemical Composition of the Pulps Obtained

| $X_T$ | $X_t$ | YI (%) | KN | VI (cP) | GL (%) | PE (%) | LI (%) |
|---|---|---|---|---|---|---|---|
| +1 | +1 | 55.6 | 61.4 | 4.4 | 60.3 | 2.3 | 33.0 |
| −1 | −1 | 53.7 | 64.4 | 5.4 | 59.6 | 2.5 | 33.3 |
| −1 | +1 | 47.6 | 54.5 | 10.6 | 58.6 | 11.9 | 26.1 |
| −1 | −1 | 45.2 | 59.1 | 12.2 | 57.5 | 14.2 | 25.6 |
| 0 | 0 | 51.7 | 61.0 | 6.9 | 62.2 | 6.0 | 26.8 |
| 0 | 0 | 52.8 | 64.2 | 7.5 | 63.6 | 6.5 | 25.7 |

$X_T$, temperature (+1 = 215°C, 0 = 200°C, −1 = 185°C); $X_t$, time (+1 = 2.5 h, 0 = 2 h, −1 = 1.5 h); YI, yield; NK, kappa-number; VI, viscosity; GL, Glucan; PE, pentosan; LI, total lignin.

Thus, sugar cane straw pulp gave a higher viscosity than that for sugar cane bagasse pulp, but the kappa-number of sugar cane straw pulp was higher than that for sugar cane bagasse pulp.

### *Effect of Xylanase Concentration on Bleach Boosting and Paper Properties*

The chemical composition of unbleached (control) pulp and different xylanase concentration-treated pulps are shown in Table 2. Xylanase treatment had an influence on content of cellulose and a slight influence on lignin content, which indicated that the treatment alone could not remove lignin and depolymerize cellulose of sugar cane straw pulp effectively. With 10 IU/g of xylanase, the pentosans content decreased, indicating that hemicellulose was degraded by xylanase as expected.

The ethanol/water pulps treated with xylanase were next bleached with NaOH in a single stage. The results of the chemical composition of the pulps treated with xylanase followed by alkaline extraction are shown in Table 3. A long treatment time of 20 h and high enzyme charge were not effective in biobleaching of sugar cane straw pulp. According to Christov and Prior *(17)*, accessibility problems arise for dissolving pulp because chemical bleaching apparently removed more accessible portions of xylan from the cell walls, leaving the remaining part in locations that were less accessible to xylanase. Senior et al. *(42)* reported that prolonged incubation times were not as effective as a series of subsequent short treatments of pulp using xylanase in which about 50% of xylan could be removed.

Sugar cane straw pulps treated with 5 and 10 IU/g of enzyme resulted in a 3.3 cP viscosity, a marginal increase compared with unbleached pulp, and increasing the enzyme charge decreased viscosity. Pulps treated with xylanase followed by alkaline extraction gave higher viscosity than that treated only with enzyme, but only 20 IU/g gave a viscosity increase

Table 2
Chemical Composition of Unbleached and Xylanase Bleached Pulps With Different Enzyme Dosages

| Enzyme dose (U/g) | 0 | 5 | 10 | 20 | 50 | 150 |
|---|---|---|---|---|---|---|
| Glucan (%) | 61.7 ± 2.1 | 66.5 ± 0.7 | 68.9 ± 1.2 | 64.2 ± 2.6 | 64.7 ± 1.5 | 61.8 ± 3 |
| Pentosan (%) | 3.2 ± 0.3 | 3.2 ± 0.1 | 2.4 ± 0.1 | 3.1 ± 0.2 | 3.4 ± 0.2 | 2.8 ± 0.2 |
| Lignin (%) | 31.5 ± 2.4 | 29.0 ± 1.8 | 28.9 ± 2.4 | 28.5 ± 1.9 | 26.9 ± 0.8 | 27.9 ± 0.1 |
| Ash (%) | 4.1 ± 0.3 | 3.5 ± 0.5 | 3.4 ± 0.3 | 3.3 ± 0.1 | 3.2 ± 0.1 | 3.4 ± 0.3 |

Table 3
Chemical Composition of Unbleached, Xylanase Bleached Pulps With Different Enzyme Dosages Followed by Alkaline Extraction

| Enzyme dose (U/g) | 0 | 5 | 10 | 20 | 50 | 150 |
|---|---|---|---|---|---|---|
| Glucan (%) | 70.1 ± 0.6 | 74.5 ± 2.2 | 75.4 ± 1.5 | 73.2 ± 2.2 | 75.6 ± 0.6 | 71 ± 2.7 |
| Pentosan (%) | 2 ± 0.1 | 2.3 ± 0.1 | 2.1 ± 0.1 | 2 ± 0.1 | 2.2 ± 0.1 | 1.8 ± 0.1 |
| Lignin (%) | 13.1 ± 2.3 | 12.3 ± 2.5 | 11.4 ± 0.1 | 11.7 ± 1.3 | 13.5 ± 2.8 | 12.9 ± 0.3 |
| Ash (%) | 2.7 ± 0.1 | 3 ± 0.6 | 2.8 ± 0.2 | 2.8 ± 0.1 | 3 ± 0.1 | 2.8 ± 0.3 |

(Fig. 1A). Enzyme charges of 10 and 20 IU/g of xylanase decreased the kappa-number of sugar cane straw pulps, and pulp treated with 20 IU/g presented the lowest kappa-number *(57)*. The kappa-number of the pulps treated with different enzyme dosages followed by alkaline extraction were virtually the same (Fig. 1B).

Bisson et al. *(43)* evaluated xylanase from *Thermomyces lanuginosus* SSBP on bagasse soda pulp, varying the charge over a range of 5–150 IU and found that increasing the xylanase treatment from 50 to 150 IU/g only changed the kappa-number reductions by 0.5 and 0.6 points, respectively. The kappa-number of the control and xylanase pretreated pulps after DED bleaching were the same. Although kappa-reduction has been attributed to lignin removal, hexeneuronic acid has been shown to account for a significant fraction of the oxidizable components in Kraft pulps *(44)*. Jeffries and Davis *(45)* showed that there is an excellent correlation between xylanase activity and hexeneuronic acid; however, kappa-reduction did not correlate directly with either of these factors. These

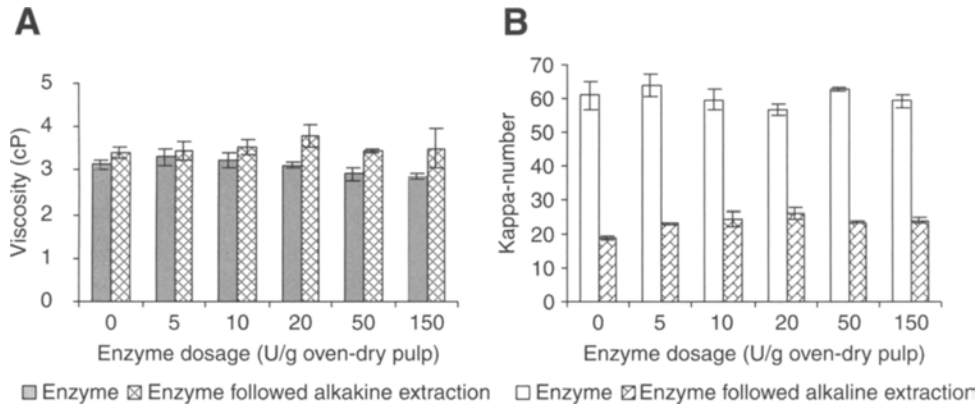


**Fig. 1.** Pulps treated with different enzyme dosages and followed by alkali extraction. **(A)** Viscosity and **(B)** kappa-number.

findings indicate that xylanase pretreatment can result in the release of other compounds, which influence the kappa-number determination *(44)*.

Jiang et al. *(46)* studied the biobleaching boosting effect of recombinant xylanase B from the hyperthermophilic *Thermotoga maritima* on wheat straw soda-anthraquinone pulp and found that an increase in enzyme dosage from 50 to 150 UI/g dry pulp did not decrease the kappa-number in the pulps, but did increase brightness by 4.7%. International Organization for Standardization (ISO) whereas decreased tensile index by 2% and broke length by 2.5%. Ideally, it would be desirable for xylanase treatment to decrease the kappa-number and increase viscosity, resulting in an increase in the viscosity per kappa-number ratio for pulps treated with xylanase. The variation in viscosity with kappa-number (i.e., the selectivity of the process) is shown in Fig. 2. Pulps treated with low enzyme dosage (5 IU/g) presented same seletivity compared with that, control pulp and pulps treated with 20 IU/g presented the higher seletivity (Fig. 2A). The alkali extraction of xylanse-treated pulps provided a similar selectivity in the pulps treated with different enzyme dosage (Fig. 2B). In comparison, Roncero et al. *(4)* treated wheat straw soda pulps by a TCF-bleaching sequence using ozone and xylanase, giving a similar selectivity to the unbleached pulp but low selectivity in the peroxide stage.

## *FT-IR and PCA of the Pulps*

FT-IR spectra of unbleached, xylanase biobleached, and xylanase followed by alkali extraction pulps were recorded and corrected for the 1860 and 780 $cm^{-1}$ fingerprint regions and normalized to the 902 $cm^{-1}$ C–O–C region. PCA is a statistical program and in PCA bidimensional plot, one FT-IR spectra of the pulp represent one point. In the bidimensional plot, the points that are near represent similar pulps. Spectra of the pulps treated with different enzyme charge, unbleached pulp, and xylanase

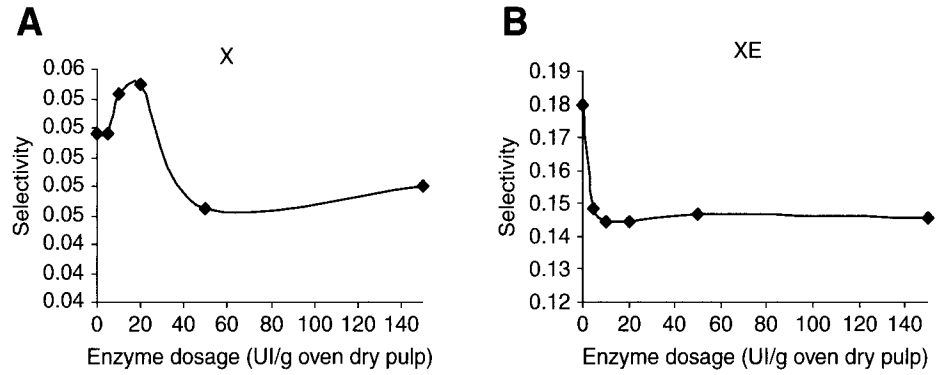


**Fig. 2. (A)** Sugar cane straw ethanol/water pulps treated with different enzyme dosages and **(B)** xylanase followed by alkali extraction pulps.

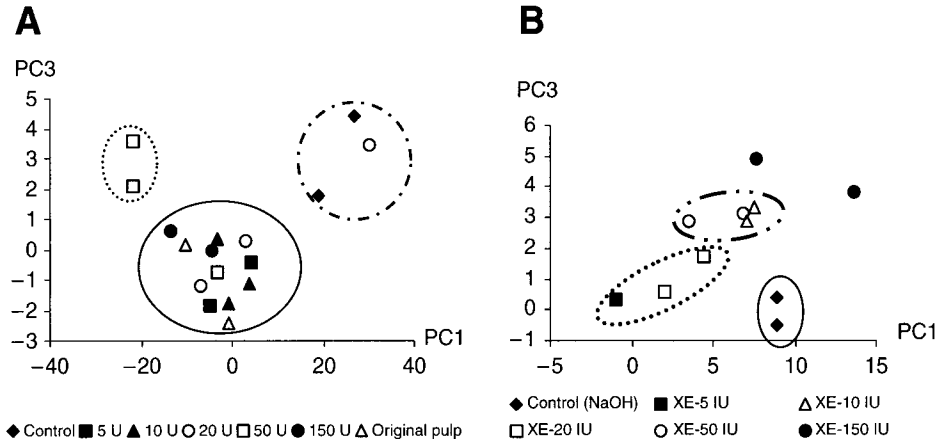


**Fig. 3. (A)** Score values (PC3 × PC1) of the pulps treated with different enzyme dosages and **(B)** score values (PC3 × PC1) from FTIR spectra of unbleached, xylanase bleached, and xylanase followed by alkali extraction sugar cane straw ethanol/water pulps.

followed by alkali extraction-treated pulps were very similar, so FT-IR spectra were better analyzed by PCA, as shown in Fig. 3. Pulps treated with different enzyme charge, three groups of pulps could be identified: unbleached pulps (control pulps) are differentiated (highlighted by non-continuous ellipse), the pulps treated with 20 UI/g enzyme dosage were highlighted by trace ellipse and in the other group were the pulps treated with different enzyme dosages (Fig. 3A). Thus, it was possible to confirm that the pulp treated with 20 IU/g is different from the other pulps and presented reduction in kappa-number. Chemical analysis and the physical properties of pulps treated with different enzyme loading did not provide many differences between the pulps, but in the PCA analysis it was possible to differentiate the pulps treated with xylanase followed by alkali extraction. In Fig. 3B, PC3 × PC1 plot, four groups of pulps were differentiated: control

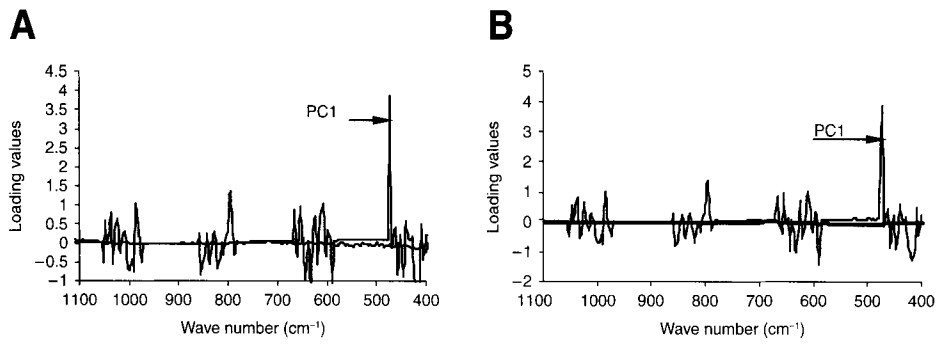


**Fig. 4.** Loading values of PC1 of FTIR spectra of sugarcane straw ethanol/water pulps **(A)** xylanase-treated pulps with different enzyme dosages and **(B)** xylanase followed by alkali-extraction pulps.

pulps were highlighted by continuous ellipse, the pulps treated with 5 and 20 IU/g enzyme dosage were highlighted by trace ellipse, in the middle of PCA plot were pulps treated with 10 and 50 IU/g, and up the plot were pulps treated with higher enzyme dosage (150 IU/g). The first three PCs explain more than 93% of the total variance of the system, PC2 and PC3 being the principal factors for the differentiation between pulp spectra. This is better analyzed by the loading values of each PC (Fig. 4). From Fig. 4, for the sugar cane straw ethanol/water pulps, the influence of infrared bands on PC scores can be evaluated showing that PC1 was influenced by C–O (1000 $cm^{-1}$) bonds present in the esters.

## Conclusions

The temperatures and times required for pulping of sugar cane straw by ethanol/water mixtures were more severe than that needed for the sugar cane bagasse. Furthermore, the pulp obtained had low pentosan (3.2%) and high lignin (31.5%) contents. Thus, the viscosity of the pulp was low (3.14 cP) and the kappa-number was high (58.09). Xylanase enzyme appeared to be effective for loadings less than 20 IU/g. However, it did not produce a direct delignification effect on pulp. A high enzyme dosage (150 IU/g dry pulp) and long time (20 h) of xylanase treatment of the pulp did not decrease the kappa-number of the pulp. There were insignificant differences in the physical properties of the enzyme-treated pulp compared with the reference pulp. Different enzyme dosages resulted in different chemical compositions for the pulps that can be identified through PCA.

## Acknowledgments

This work was supported by Conselho Nacional do Desenvolvimento Científico e Tecnológico, Fundação de Amparo à Pesquisa do Estado de

São Paulo and Coordenação de Aperfeiçoamento de Pessoal de Ensino Superior (all Brazilian Agencies).

## References


1. O Globo. In: www. http://caminhosdocampo.com.br. Access 10 August 2006.
2. CENBIO IN:<http// www.cenbio.br. Access 14 April 2003.
3. Gonçalves, A. R., Benar, P., Costa, S. M., et al. (2005), *Appl. Biochem. Biotechnol.* **121–124,** 821–826.
4. Roncero, M. B., Torres, A. L., Colom, J. F., and Vidal, T. (2003), *Bioresour. Technol.* **87,** 305–314.
5. Jiménez, L., Perez, I., García, J. C., López, F., and Ariza, J. (2000), *Process Biochem.* **35,** 685–691.
6. Jiménez, L., Torre, M. J., Ferrer, J. L., and García, J. C. (1999), *Process Biochem.* **35,** 143–148.
7. Khristova, P., Tomkinson, J., and Jones, G. L. (2003), *Ind. Crops Prod.* **18,** 101–110.
8. Khristova, P., Tomkinson, J., Valchev, L., Dimitrov, I., and Jones, G. L. (2003), *Bioresour. Technol.* **85,** 79–85.
9. Jiménez, L., Bonilla, J. L., Ferrer, J. L., and Pérez, L. (1998), *Afinidad* **55(747),** 133–138.
10. Asiz, S. and Sarkanen K. (1989), *Tappi J.* **72(3),** 169–175.
11. Stockburger, P. (1993), *Tappi J.* **76(6),** 71–74.
12. Dahlmann, G. and Schroeter, M. C. (1990), *Tappi J.* **73(4),** 237–240.
13. Black, N. P. (1991), *Tappi J.* **74(4),** 87–93.
14. Pohjanvesi, S., Saari, K., Poppius-Levlin, K., and Sundquist, J. (1995), in *Proceedings of the 8th International Wood and Pulping Congress*, vol. 2, Helsinki, pp. 231–236.
15. Dapia, S., Santos, V., and Parajo, J. C. (2000), *J. Wood Chem. Technol.* **20(4),** 395–413.
16. Obracea, P. and Cimpoesu, G. (1998), *Cell Chem. Technol.* **32(5–6),** 517–525.
17. Christov, L. P., Akhtar, M., and Prior, B. A. (1996), *Holzforschung* **50,** 579–582.
18. Christov, L. P., Akhtar, M., and Prior, B. A. (1998), *Enzyme Microbiol. Technol.* **23(70–74),** 70–74.
19. Bajpai, P. (1999), *Biotechnol. Prog.* **15(2),** 147–157.
20. Senior, D. J., Mayers, P. R., and Saddler, J. N. (1991), *Biotechnol. Bioeng.* **37,** 274–279.
21. Viikari, L., Kantelinen, A., Buchert, J., and Puls, J. (1994), *Appl. Microbiol. Biotechnol.* **41,** 124–129.
22. Shah, A. K., Sidid, S. S., Ahmed, A., and Rele, M. V. (1999), *Bioresour. Technol.* **68,** 133–140.
23. Sholam, Y., Schwartz, Z., Khasin, A., Gat, O., Zosim, Z., and Rosemberg, E. (1992), *Biodegradation* **3,** 207–218.
24. Bim, M. A. and Franco, T. T. (2000), *J. Chromatogr.* **743,** 349–356.
25. Dhillon, A., Gupta, J. K., Jauhari, B. M., and Khanna, S. (1999), *Bioresour. Technol.* **73,** 273–277.
26. Wizani, N., Esterbauer, H., Steiner, W., and Gomes, J. (1990), AT Patent 1030/90.
27. Duarte, M. C. T., Portugal, E. P., Ponezi, A. N, Bim, M. A., and Tagliari, C. V. (1999), *Bioresour. Technol.* **68,** 49–53.
29. Kulkarni, N. and Rao, M. (1996), *J. Biotechnol.* **51,** 167–173.
30. Gonçalves, A. R. and Ruzene, S. (2003), *Appl. Biochem. Biotechnol.* **105–108,** 769–774.
31. Duarte, M. C. T., Portugal, E. P., Ponezi, A. N., Bim, M. A, and Tagliari, C. V. (1999), *Bioresour. Technol.* **68,** 49–53.
32. Bailey, M. J., Biely, P., and Pourtanen, K. (1992), *J. Biotechnol.* **23,** 257–270.
33. TAPPI (1985), *TAPPI Stand. Methods* T. 236 cm-85.
34. TAPPI (1982), *TAPPI Stand. Methods* T. 230 om-82.
35. Dence, C. W. (1992), In: *Methods in Lignin Chemistry*. Lin, Y. L. and Dence, C. W. (eds.), Springer, Berlin, pp. 33–61.
36. Rocha, G. J. M. (2000), Deslignificação de bagaço de cana-de-açúcar assistida por oxigênio. São Carlos: Universidade de São Paulo/Instituto de Química de São Carlos. *PhD. Thesis*, Brazil, pp. 40,41.

37. Faix, O., Bottcher, J. H., and Berlelt, E. (1992), In: *The International Society for Optical Engineering*. Heise, M., Korte, E. H., and Siesler, H. W. (eds.), San Diego, CA, pp. 428–430.
38. Morohoshi, N. (1991), In: *Wood and Cellulosic Chemistry*. Hon, D. N. S. and Shiraishi, N. (eds.), Marcel Dekker, New York, pp. 331–392.
39. Scarminio, I. S. and Bruns, R. E. (1989). *Trends Anal. Chem.* **8,** 326–327.
40. Biermann, C. J. (1996), *Handbook of Pulping and Papermaking*, 2nd ed. Academic Press, San Diego.
41. Moriya, R. T., Gonçalves, A., and Duarte, M. C. T. (2005). *Appl. Biochem. Biotechnol.* **12,** 171–181.
42. Senior, D. J., Mayers, P. R., Miller, D., Sutcliffe, R., Tan, L., and Saddler, J. N. (1988), *Biotechnol. Lett.* **10,** 907–912.
43. Bisson, S., Christov, L., and Singh, S. (2002), *Process Biochem.* **37,** 567–572.
44. Gellerstedl, G. (1996), *Carbohydr. Res.* **294,** 41–51.
45. Jefries T. W. and Davis, M. (1998), in *Proceedings of the 7th International Conference on Biotechology in the Pulp and Paper Industry*, Vancouver, BC, Canada, June 16–19 C41–43.
46. Jiang, Z. Q., Li, X. T., Yang, S. Q., Li, L. T., Li, Y., and Feng, W. Y. (2006), *Appl. Microbiol. Biotechnol.* **70,** 65–71.

0273-2289/1559-0291 (Online)/07/136–140/515–528/$30.00

# Nisin Production Utilizing Skimmed Milk Aiming to Reduce Process Cost

ANGELA FAUSTINO JOZALA, MAURA SAYURI DE ANDRADE, LUCIANA JUNCIONI DE ARAUZ, ADALBERTO PESSOA JR., AND THEREZA CHRISTINA VESSONI PENNA*

*Department of Biochemical and Pharmaceutical Technology, School of Pharmaceutical Science, University of São Paulo, SP, Brazil, E-mail: tcvpenna@usp.br*

## Abstract

Nisin is a natural additive for conservation of food, pharmaceutical, and dental products and can be used as a therapeutic agent. Nisin inhibits the outgrowth of spores, the growth of a variety of Gram-positive and Gram-negative bacteria. This study was performed to optimize large-scale nisin production in skimmed milk and subproducts aiming at low-costs process and stimulating its utilization. *Lactococcus lactis* American Type Culture Collection (ATCC) 11454 was developed in a rotary shaker (30°C/36 h/100 rpm) in diluted skimmed milk and nisin activity, growth parameters, and media components were also studied. Nisin activity in growth media was expressed in arbitrary units (AU/mL) and converted to standard nisin concentration (Nisaplin®, 25 mg of pure nisin is $1.0 \times 10^6$ AU/mL). Nisin activity in skimmed milk 2.27 $g_{\text{total solids}}$ was up to threefold higher than transfers in skimmed milk 4.54 $g_{\text{total solids}}$ and was up to 85-fold higher than transfers in skimmed milk 1.14 $g_{\text{total solids}}$. *L. lactis* was assayed in a New Brunswick fermentor with 1.5 L of diluted skimmed milk (2.27 $g_{\text{total solids}}$) and airflow of 1.5 mL/min (30°C/36/200 rpm), without pH control. In this condition nisin activity was observed after 4 h (45.07 AU/mL) and in the end of 36 h process (3312.07 AU/mL). This work shows the utilization of a low-cost growth medium (diluted skimmed milk) to nisin production with wide applications. Furthermore, milk subproducts (milk whey) can be exploited in nisin production, because in Brazil 50% of milk whey is disposed with no treatment in rivers and because of high organic matter concentrations it is considered an important pollutant. In this particular case an optimized production of an antimicrobial would be lined up with industrial disposal recycling.

**Index Entries:** Artificial compounds; EDTA; fermentation processes; Gram-negative; Gram-positive; *Lactococcus lactis*; nisin.

*Author to whom all correspondence and reprint requests should be addressed.

## Introduction

Nisin, a naturally occurring antimicrobial polypeptide, discovered in 1928 *(1,2)*, is a monomeric pentacyclic subtype A antibiotic peptide (3.35 kDa with 34 amino acid residues), synthesized by *Lactococcus lactis* subsp. lactis *(3,4)* during exponential phase of bacteria growth *(5,6)*. Nisin is used as a natural preservative in food and dairy industries, approved by Food and Drug Administration and GRAS *(7)*, meeting the requirements of safe food with fewer chemical additives.

Applications of nisin include dental-care products *(8)*, pharmaceutical products such as stomach ulcers and colon infection treatment and potential birth control *(9–11)*. Nisin solubility and stability improves substantially with a decrease in pH values. Nisin is stable at pH 2.0, insoluble at pH 8.5, and can be autoclaved at 121°C without denaturation *(12)*. The complete inactivation of nisin activity is observed after 30 min at 63°C and pH 11.0 *(13)*.

Nisin is not generally active against Gram-negative bacteria, yeasts, and fungi. The outer membrane of Gram-negative bacteria prevents nisin from reaching the site of action. Outer membrane permeability can be altered by treatment with chelators, such as disodium ethylenediamine tetraacetate (EDTA) or high hydrostatic pressure, resulting in increased sensitivity toward nisin *(14–20)*. The mechanism of growth inhibition by EDTA is not fully understood, but generally attributed to its chelating activity. EDTA binds primarily divalent cations *(21)* that are present in the supernatant obtained from the growth media, which salts decrease the amount of EDTA added. Therefore, we can imply that the washing of the cells should be enough to extract the majority of salts from the culture media, in order not to compete with EDTA main activity of destabilizing the membrane of some Gram-negative strains by chelating Ca and Mg salts, which are necessary for lipopolysaccharide to bind to cell wall *(21–23)*.

In a system combining different antimicrobials, treatment with nisin/EDTA or nisin/potassium sorbate at 10°C showed a meaningful inhibition in *Escherichia coli* O157-α5 compared with samples treated with nisin, EDTA, or potassium sorbate alone *(17,25)*. The inhibitory activity of nisin on Gram-negative organisms can be improved by combining nisin with EDTA in culture media *(26)*. Vessoni Penna et al. *(27)* using *L. lactis* ATCC 11454 observed that nisin production was the highest in a growth medium containing 25% skimmed milk added to either 25% M17 or MRS, it was showed that nisin production depend on the nutrients concentration and the transfers renewed the media each at 36 h. The influence of milk compounds on nisin activity was observed in previous work *(28)* and skimmed milk (9.09% dry matter) increased nisin activity and release into the media for all five transfers. Although the formulations of skimmed milk diluted with MRS broth were found to stimulate optimal nisin production.

Lactic acid bacteria are fastidious microorganisms and require a medium containing nutrients, which enhance the growth and production of nisin *(29)*.

In this study, diluted skimmed milk in different concentrations was used to improve nisin production and also examined the utilization of skimmed milk compounds (artificial reproduction) to determine which nutrient is essential to nisin production. With nisin activity related to growth conditions of *L. lactis*, the effects of culturing parameters such as media components were evaluated in this study to optimize the expression of nisin and release into media.

## Material and Methods

The nisin-producing strain of *L. lactis* ATCC 11454 and the nisin-sensitive indicator strain of *L. sake* ATCC 15521 (Gram-positive) were used in this study. The cultures of *L. lactis* and *L. sake* were maintained at –80°C in MRS broth (Man Rugosa Shepeer-Bacto Lactobacilli MRS broth, DIFCO) with 40% (v/v) of glycerol *(26–28)*.

## Growth Medium and Inoculum

The influence of milk components on nisin activity was studied in previous work *(27,28)*. In this present work different medium were elaborated with diluted skimmed milk to improve the growth conditions for *L. lactis*. Before inoculating experimental media, 100 µL of the stock culture of *L. lactis* was grown (preinoculum) in MRS broth (DIFCO) into 50 mL of broth in 250-mL Erlenmeyer flasks and incubated on a rotary shaker (100 rpm) at 30°C for 36 h. From the growth culture, 5-mL aliquots of bacterial suspension were transferred to 50 mL of the experimental medium in 250-mL flasks, which were incubated for another period of 36 h (100 rpm/30°C). The transfer and incubation of a new volume of each medium was repeated five times (first, second, third, fourth, and fifth transfers).

In the first group of assays, utilized skimmed milk (9.09 $g_{total\ solids}$, standard concentration) was developed with following experimental medium: (a) skimmed milk at 50% of standard concentration (4.54 $g_{total\ solids}$); (b) skimmed milk at 25% of standard concentration (2.27 $g_{total\ solids}$); (c) skimmed milk at 12.5% of standard concentration (1.14 $g_{total\ solids}$). All medium was diluted in sterile distillated water (Table 1).

In Second group of assays, utilized skimmed milk compounds (artificial reproduction) was developed with following experimental medium: (a) casein (0.75 g) and lactose (1.25 g); (b) casein (0.75 g), lactose (1.25 g) plus calcium (0.06 g); (c) casein (0.75 g), lactose (1.25 g) plus sodium citrate (0.01 g); and (d) casein (0.75 g), lactose (1.25 g), calcium chloride (0.06 g) plus sodium citrate (0.01 g) (Table 2).

## Fermentation Process

Preinoculum was prepared with 100 µL of the stock culture of *L. lactis* and was grown into 150 mL of MRS broth (36 h/100 rpm/30°C). The entire 150 mL of this culture was poured into 1.5 L of the diluted skimmed milk

Table 1
Nisin Production, Specific Production, Productivity, Proteins, and Sugar Consumption of *L. lactis* Growth for Every Transfer After 36 h to Diluted Skimmed Milk

| | | Nisin production | | | | | Biomass | Productivity | Proteins | Sugars |
|---|---|---|---|---|---|---|---|---|---|---|
| | Transfers | pH | Halo (mm) | $10^{(0.2408x - 0.8745)}$ (AU/mL) | Log (AU/mL) | 0.025 (mg/L) | $y = 2.1042x + 0.124$ ($g_{DCW}$/L) | $mg_{nisin}$.mg $_{DCW}$/h | $y = 0.9023x - 0.0329$ ($g_{casein}$/L) | $y = 0.537x - 0.0127$ ($g_{lactose}$/L) |
| Compounds | Preculture | 4.5 | 17 | 1656.15 | 3.22 | 41.40 | 0.87 | – | – | – |
| | 1 | 4.8 | 11.75 | 90.14 | 1.95 | 2.25 | 0.47 | – | 17.67 | 21.53 |
| | 2 | 4.45 | 12.5 | 136.62 | 2.14 | 3.42 | 0.36 | – | 17.28 | 21.06 |
| 4.54 g and pH 6.8 | 3 | 4.5 | 15.5 | 720.94 | 2.86 | 18.02 | 1.37 | – | 14.04 | 21.52 |
| | 4 | 4.35 | 19 | 5019.96 | 3.70 | 125.50 | 1.43 | 0.0 | 14.86 | 22.74 |
| | 5 | 4.43 | 20 | 8739.77 | 3.94 | 218.49 | 0.94 | 0.01 | 11.98 | 18.45 |
| | Preculture | 4.55 | 17.5 | 2185.24 | 3.34 | 54.63 | 0.85 | <0.01 | – | – |
| | 1 | 5.33 | 16.5 | 1255.16 | 3.10 | 31.38 | 0.49 | <0.01 | 17.67 | 13.45 |
| | 2 | 5.63 | 17.5 | 2185.24 | 3.34 | 54.63 | 0.34 | <0.01 | 17.28 | 13.16 |
| 2.27 g and pH 6.8 | 3 | 4.36 | 18.25 | 3312.07 | 3.52 | 82.80 | 1.58 | <0.01 | 14.04 | 10.76 |
| | 4 | 4.51 | 18.75 | 4370.19 | 3.64 | 109.25 | 1.64 | <0.01 | 14.86 | 11.37 |
| | 5 | 4.34 | 21.5 | 20077.05 | 4.30 | 501.93 | 1.78 | 0.01 | 11.98 | 9.22 |
| | Preculture | 4.55 | 12 | 103.54 | 2.02 | 2.59 | 0.84 | – | – | – |
| | 1 | 4.3 | 13.75 | 273.21 | 2.44 | 6.83 | 0.28 | – | 2.94 | 4.96 |
| | 2 | 5.75 | 11.25 | 68.31 | 1.83 | 1.71 | 0.09 | – | 8.87 | 2.22 |
| 1.14 g and pH 6.8 | 3 | 5.92 | – | – | – | – | 0.55 | – | 2.28 | 4.89 |
| | 4 | 6.47 | 9.5 | 25.89 | 1.41 | 0.65 | 0.41 | – | 3.70 | 4.18 |
| | 5 | 6.73 | – | – | – | – | 1.91 | – | 4.50 | 2.94 |

Table 2
Nisin Production, Specific Production, Productivity, Proteins, and Sugar Consumption of *L. lactis* Growth, for Every Transfer After 36 h to Artificial Compounds

| | | Nisin production | | | | | Biomass | Productivity | Proteins | Sugars |
|---|---|---|---|---|---|---|---|---|---|---|
| | Transfers | pH | Halo (mm) | $10^{(0.2408x - 0.8745)}$ (AU/mL) | Log (AU/mL) | 0.025 (mg/L) | $y = 2.1042$ $x + 0.124$ ($g_{DCW}$/L) | $mg_{nisin}$ .mg $_{DCW}$/h | $y = 0.9023$ $x - 0.0329$ ($g_{casein}$/L) | $y = 0.537$ $x - 0.0127$ ($g_{lactose}$/L) |
| Compounds | 1 | 3.9 | 14.5 | 414.10 | 2.62 | 10.35 | 0.15 | – | 1.08 | 13.41 |
| | 2 | 6.29 | 9.75 | 29.74 | 1.47 | 0.74 | 0.42 | – | 8.32 | 16.19 |
| Media A | 3 | 6.14 | – | – | – | – | 1.56 | – | 10.46 | 19.79 |
| | 4 | 6.52 | 11.25 | 68.31 | 1.83 | 1.71 | 1.31 | – | 13.13 | 19.68 |
| | 5 | 6.35 | – | – | – | – | 1.50 | – | 15.26 | 11.05 |
| | 1 | 4.23 | 14.75 | 475.66 | 2.68 | 11.89 | 0.14 | – | 0.40 | 13.33 |
| | 2 | 6.14 | 10.5 | 45.07 | 1.65 | 1.13 | 0.20 | – | 8.73 | 15.45 |
| Media B | 3 | 6.27 | – | – | – | – | 0.26 | – | 9.91 | 15.05 |
| | 4 | 6.64 | – | – | – | – | 0.23 | – | 13.70 | 18.14 |
| | 5 | 6.43 | – | – | – | – | 0.19 | – | 14.80 | 10.50 |
| | 1 | 4.36 | 11.25 | 68.31 | 1.83 | 1.71 | 0.18 | – | 1.08 | 13.41 |
| | 2 | 6.61 | 10.5 | 45.07 | 1.65 | 1.13 | 0.15 | – | 8.32 | 16.19 |
| Media C | 3 | 6.26 | – | – | – | – | 0.20 | – | 10.46 | 19.79 |
| | 4 | 6.51 | – | – | – | – | 0.25 | – | 13.13 | 19.68 |
| | 5 | 6.73 | – | – | – | – | 0.23 | – | 14.70 | 10.50 |
| | 1 | 4.6 | 12.75 | 156.93 | 2.20 | 3.92 | 0.14 | – | 0.06 | 12.84 |
| | 2 | 6.11 | 11 | 59.47 | 1.77 | 1.49 | 0.15 | – | 17.01 | 18.14 |
| Media D | 3 | 5.9 | – | – | – | – | 0.19 | – | 6.53 | 16.29 |
| | 4 | 6.37 | – | – | – | – | 0.26 | – | 13.48 | 19.84 |
| | 5 | 6.43 | – | – | – | – | 0.24 | – | 14.75 | 10.21 |

(2.27 $g_{total\ solids}$, pH 6.8) in a 2-L bench-scale fermentor (NBS-MF 105, New Brunswick Scientific, New Brunswick, NJ). The initial cell concentration in the fermentor was 0.58 ± 0.10 g/L. The total incubation time was 36 h at 30°C to observe variations of nisin activity associated with growth conditions. Foaming was controlled as needed by adding 0.5 mL of dimethylpolysiloxane (Sigma-Aldrich, Saint Louis, MO). Agitation and aeration were 200 rpm and 1.5 vvm, respectively. The airflow was measured by an online rotameter and set using a needle valve. The pH of the medium during cultivation was measured by an electrode (Ingold, Woburn, MA). Before the addition of inoculum to the fermentor, the propeller speed, aeration rate, and the temperature (30°C) were adjusted.

## Analytical Procedures

Assays in rotator shaker in each transfer cell suspensions were aseptically withdrawn from the flasks and tested for pH, cellular density, colony number, and nisin concentrations. For this study, each fermentor culture was performed in triplicate. Samples were aseptically withdrawn from fermentor with interval of 4 h (10 sample points) and were collected and tested for biomass, nisin activity, and nutrients consumed. For this study, each sample was performed in triplicate.

## Biomass, Total Sugars, and Total Proteins

The cellular biomass concentration, expressed in mg of dried cellular weight per liter of broth (mg · DCW/L), was determined from the optical density at 660 nm ($OD_{660}$) by the calibration curve [biomass (mg · DCW/L) = $2.1042 \times OD_{660} + 0.124$, $R^2 = 0.998$], as described in the previous work *(26–28)*. The lactose concentration, expressed in gram of lactose per liter of broth (g/L) was determined from the samples in the optical density at 540 nm ($OD_{540}$) through colorimetric Somogyi-Nelson methodology *(30)*. The standard curve [lactose g/L = $(0.537 \times OD_{540\ nm})$ (0.0127], was developed for different concentrations (0.25–0.01 g/L) with standard lactose solution (Merk, Darmstadt, Germany).

The protein concentration, expressed in gram of casein per liter of broth (g/L) was determined from the samples in the optical density at 660 nm ($OD_{660}$) through colorimetric Folin-phenol methodology described by Lowry *(31)*. The standard curve [casein g/L = $(0.9023 \times OD_{660\ nm})$ –0.0329] was developed for different concentrations (0.25–0.01 g/L) with the standard casein solution (Sigma, St. Louis, MO).

## Nisin Activity

For nisin activity detection, the cell suspension was centrifuged at 12,000 rpm for 10 min at 25°C and the supernatant collected was filtered through a 0.22-μm membrane filter (Millipore®). The titers of nisin expressed

and released in culture media were quantified and expressed in arbitrary units (AU/mL of medium) by the agar diffusion assay *(6,22)* utilizing *L. sake* as a sensitive indicator microorganism. *L. sake* was grown in MRS broth and incubated (100 rpm/30°C/24 h). A 1.5-mL aliquot of the suspension ($OD_{660}$ = 0.7) was transferred and mixed with 250 mL of soft agar (MRS broth with 0.8% w/v of bacteriological grade agar). Each 20 mL of inoculated medium was transferred to Petri plates (100-mm diameter). After the agar solidified, 3-mm wells were cut out with a sterile metal pipe with 5 mm total diameter. The relation between (AU/mL) and international units (IU/mL) was determined by using Nisaplin® (a commercial purified nisin preparation containing 2.5 mg of nisin per gram of Nisaplin, corresponding to $10^6$ IU/g Nisaplin; Aplin & Barret Ltd, Beaminster, UK, distributed by Sigma Chemical). Standard solution of nisin were prepared by dissolving 1 g of Nisaplin into 10 mL of 0.02 *N* HCl with 0.75% (w/v) NaCl (pH = 1.6–1.8).

The solution was autoclaved at 121°C for 15 min, and stored at 4°C. Further dilutions of the standard nisin solution were made as necessary by diluting in 0.02 *N* HCl and water. With the standard curve (AU/mL = $10^{0.2408\ H-0.8745}$), the concentrations of standard nisin ($10^0$–$10^5$ AU/mL) were related by the diameter of the inhibition halo (H, mm), and the activity of nisin from cells grown in the experimental media was determined and expressed in arbitrary units per mL ($10^0$–$10^5$ AU/mL). Based on the calibration curves between AU per mL and IU per mL, 1.09 ± 0.17 AU corresponded to 1.0 IU (40 IU = 1 μg of pure nisin A).

Using the standard solutions for calibration of nisin activity in all the assays, $10^6$ AU of nisin corresponded to 0.025 $\mu g_{nisin}$/mL. The activity of nisin expressed in AU/mL was converted to nisin in milligrams per milliliters (mg/mL), through the relation: Nisin (mg/L) = ($z \times 0.025$), where z = AU/mL. The concentration of nisin was also expressed in milligrams per liters (mg/L); and in the production of nisin (mg/L/h), the formation of nisin in milligrams per liters related to incubation time (h). The specific production of nisin (mg/mg) is the ratio between nisin concentration (mg/L) and the dry weight cell (mg · DCW/L). Productivity was expressed in milligrams nisin per milligram of DCW per hour as the ratio of the hourly milligrams of nisin (mg/L/h) and biomass (DCW).

## Results and Discussion

*L. lactis* was transferred consecutively five times in the same growth medium and incubated under the same conditions (100 rpm/30°C/36 h) as proceeded in our previous works *(26–28)*. Tables 1 and 2 show the results for nisin activity (AU/mL) and concentration (mg/L) in the analyzed samples.

### *Dilution of Milk*

Vessoni Penna et al. *(27)* observed that milk at standard concentration (9.09% dry matter) increased nisin activity and released it into the media

Table 3
Compounds of Skimmed Milk in Different Dilutions

| Nutrients | 50 mL | 25 mL | 12.5 mL | 6.25 mL |
|---|---|---|---|---|
| Carbohydrates | 5.0 | 2.5 | 1.25 | 0.63 |
| Proteins | 3.0 | 1.5 | 0.75 | 0.38 |
| Iron | 0.0001 | 0.00005 | 0.0 | 0.0 |
| Calcium | 0.2 | 0.1 | 0.05 | 0.03 |
| Cholesterol | 0.0025 | 0.00125 | 0.0 | 0.0 |
| Total fat | 0.33 | 0.165 | 0.08 | 0.04 |
| Saturated fats | 0.05 | 0.025 | 0.01 | 0.01 |
| Sodium | 0.5 | 0.25 | 0.13 | 0.06 |
| Vit A | 0.006 | 0.003 | 0.0 | 0.0 |
| Vit B | 0.00038 | 0.00019 | 0.0 | 0.0 |
| Total solids (g) | 9.09 | 4.54 | 2.27 | 1.14 |

for all five transfers, from 408.02 to 884.74 mg/L, similar to that attained at the first transfer for both 25% MRS plus 25% milk and 25% M17 plus 25% milk. The highest nisin concentration (3563.20 mg/L) before the fifth transfer was observed for MRS 25% plus skimmed milk 25%. A dilution of both media (MRS plus milk and M17 plus milk) provided levels of nisin activity (63.68 mg/L for 17.36% M17 plus 17.36% milk and 161.19 mg/L for 17.36% MRS plus 17.36% milk) five times lower than detected relatively to 25% concentration for the media assayed.

Jozala et al. *(28)* indicated that the preculture growth in MRS allowed nisin release by *L. lactis*; when compared with M17, nisin concentration was 1.7 times higher. Although nisin activity improved when milk was diluted with MRS and M17 broth to 25% of the original compounds. The nutrients and corresponding concentrations for three different media used in this work (Table 3), were shown to be correlated to the nisin activity data presented in Table 4. Nisin activity increased up to 97-fold from the first to the fifth transfer (90.14–8739.77 AU/mL) in milk diluted with water (4.54 $g_{\text{total solids}}$ at pH 6.8). Biomass (cells growth) increased up to threefold from the first to the fourth transfer (0.47–1.43 g/L) and in the fifth transfer decreased 1.5-fold (0.97g/L) (Fig. 1, Table 1).

Biomass ($g_{DCW}$/L) and nisin activity (AU/mL) in diluted skimmed milk (2.27 $g_{\text{total solids}}$ at pH 6.8) increased gradually through the transfers (Table 1). The levels of *L. lactis* biomass (0.49–1.78 $g_{DCW}$/L) and nisin activity (1255.16–20077.05 AU/mL) ranged from first to fifth transfer for each period of 36 h. However, in diluted skimmed milk with half total solids (1.14 $g_{\text{total solids}}$, pH 6.8), nisin activity reduced 11-fold from the first (273.21 AU/mL) to the fourth (25.89 AU/mL) transfers (Fig. 1, Table 1).

Comparing these results, the nisin activity through the transfers in the media with 2.27 $g_{\text{total solids}}$ was up to threefold and 85-fold higher than in those with 4.54 $g_{\text{total solids}}$ and 1.14 $g_{\text{total solids}}$, respectively (Fig. 1). From culture media 2.27 $g_{\text{total solids}}$ the maximum biomass (1.78 $g_{DCW}$/L)

Table 4
Nisin Production, Specific Production, Productivity, Proteins, and Sugar Consumption of *L. lactis* Growth, After 36 h, in Fermentation Processes to Diluted Skimmed Milk 2.27 $g_{total\ solids}$

| | Parameters | | | | | Nisin production | | | | | | |
|---|---|---|---|---|---|---|---|---|---|---|---|---|
| Samples | Time (h) | Temperature (°C) | pH | $O_2$ (%) | rpm | Halo (mm) | AU/mL | Log AU/mL | mg/L | Biomass $g_{DCW}/L$ | Proteins $g_{casein}/L$ | Sugars $g_{lactose}/L$ |
| 0 | 0 | 30 | 5.78 | 119.8 | 200 | 10.5 | 45.07 | 1.65 | 1.13 | 0.6 | 0.26 | 0.11 |
| 1 | 4 | 30 | 4.74 | 111.4 | 200 | 13.75 | 273.21 | 2.44 | 6.83 | 5.8 | 0.39 | 0.07 |
| 2 | 8 | 30 | 4.73 | 107.4 | 200 | 14.75 | 475.66 | 2.68 | 11.89 | 5.7 | 0.40 | 0.09 |
| 3 | 12 | 30 | 4.72 | 107 | 200 | 15.25 | 627.62 | 2.80 | 15.69 | 5.2 | 0.38 | 0.10 |
| 4 | 16 | 30 | 4.72 | 106.2 | 200 | 16.25 | 1092.70 | 3.04 | 27.32 | 6.5 | 0.40 | 0.20 |
| 5 | 20 | 30 | 4.72 | 104.5 | 200 | 16.5 | 1255.16 | 3.10 | 31.38 | 5.7 | 0.44 | 0.21 |
| 6 | 24 | 30 | 4.73 | 103.8 | 200 | 16.5 | 1255.16 | 3.10 | 31.38 | 6.4 | 0.44 | 0.21 |
| 7 | 28 | 30 | 4.73 | 103.3 | 200 | 16.5 | 1255.16 | 3.10 | 31.38 | 6.6 | 0.42 | 0.24 |
| 8 | 32 | 30 | 4.73 | 88.1 | 200 | 16.5 | 1255.16 | 3.10 | 31.38 | 5.9 | 0.28 | 0.23 |
| 9 | 36 | 30 | 4.74 | 88.5 | 200 | 18.25 | 3312.07 | 3.52 | 82.80 | 6.6 | 0.25 | 0.25 |

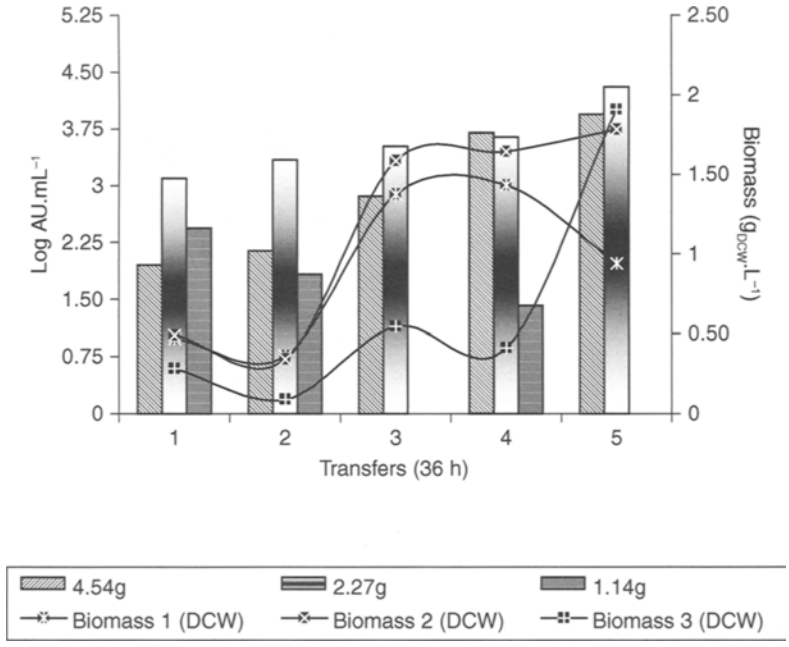


**Fig. 1.** Relation between nisin activity (log AU/mL) and biomass (gDCW/L) through the transfers in rotatory shaker assays into media with diluted skimmed milk at 4.54 $g_{\text{total solids}}$, 2.27 $g_{\text{total solids}}$, 1.14 $g_{\text{total solids}}$. AU/mL (log AU) and inhibition halo (H [mm]) was calculated through the equation: log [AU/mL = $10^{(0.2408 \times H - 0.8745)}$].

corresponded to the maximum nisin activity 20077.39 AU/mL = 501.93 mg/L, in the fifth transfer. However, in the same transfer from media with 4.54 $g_{\text{total solids}}$, the maximum biomass did not correspond to the maximum nisin activity 8799.77 AU/mL = 218.93 mg/L (Fig. 1, Table 1).

## *Milk Components to Formulate Artificial Media*

Four different groups of assays were developed utilizing artificial compounds based on proportions of skimmed milk with 2.27 $g_{\text{total solids}}$, to evaluate which nutrient influenced more nisin activity (Table 5). In the assay made up of casein (0.75 g) and lactose (1.25 g), nisin activity was reduced 14-fold from the first to the second transfer (414.10–29.70 AU/mL) and increased up to twofold from the second to the fourth transfer (29.70–68.31AU/mL).

In the systems: (a) casein (0.75 g), lactose (1.25 g) plus calcium chloride (0.06 g); (b) casein (0.75 g), lactose (1.25 g) plus sodium citrate (0.01 g); and (c) casein (0.75 g), lactose (1.25 g), calcium chloride (0.06 g) plus sodium citrate (0.01 g), nisin activity was observed on the first and second transfers (Fig. 2, Table 2), the respective values were: (a) 475.66 and 45.07 AU/mL, (b) 68.31 and 45.07 AU/mL, and (c) 156.93 and 59.47 AU/mL.

The pH values on the assays with artificial compounds were high (ratio pH 6.5) and inhibited nisin activity. Release of intracellular nisin

Table 5
Artificial Media Compounds Based on Skimmed Milk 2.27 $g_{total\ solids}$

| Nutrients | A | B | C | D |
|---|---|---|---|---|
| Carbohydrates | 1.25 | 1.25 | 1.25 | 1.25 |
| Proteins | 0.75 | 0.75 | 0.75 | 0.75 |
| Sodium | – | – | 0.01 | 0.01 |
| Calcium | – | 0.06 | – | 0.06 |
| Total solids (g) | 2.0 | 2.06 | 2.01 | 2.07 |

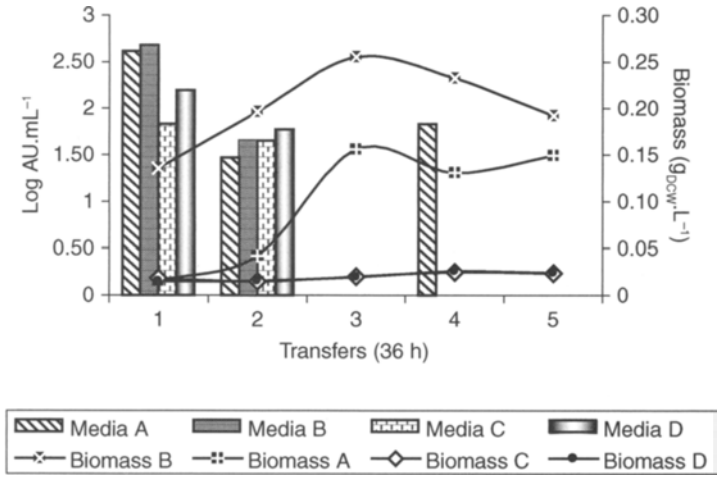


**Fig. 2.** Relation between nisin activity (log AU/mL) and biomass ($g_{DCW}$/L) through the transfers in rotatory shaker assays into media with artificial compounds media A; media B; media C; media D. AU/mL (log AU) and inhibition halo (H [mm]) was calculated through the equation: log [AU/mL = $10^{(0.2408 \times H - 0.8745)}$].

depends on the pH value of the growth media, in pH values lower than 6.0, the 80% expressed nisin is delivered to the media. On the other hand, when *L. lactis* grows in alkaline pH (pH > 6.0), most of the nisin is retained intracellular or within the cell membrane *(32–35)*.

Cheigh et al. *(36)* observed the highest nisin activity early in the stationary phase (20 h, 30°C) of *L. lactis* during batch fermentation in M17 broth (pH = 6.0) with 3% lactose added. In fact, M17 broth with 3% lactose resulted in eightfold greater nisin activity than either M17 supplemented with 0.5% glucose or in MRS broth. The authors confirmed low levels of nisin activity in both MRS and M17 broth, although these media favored cellular growth, with similar results obtained in this study ($10^7$–$10^9$ CFU/mL). Chandrapati and O'Sullivan *(34)* observed a 50% increment in nisin activity using sucrose as the carbon source in M17 broth for *L. lactis* culturing, over two transfers. The authors observed that glucose was the optimal carbon source tested, with glycerol the least suitable. They also

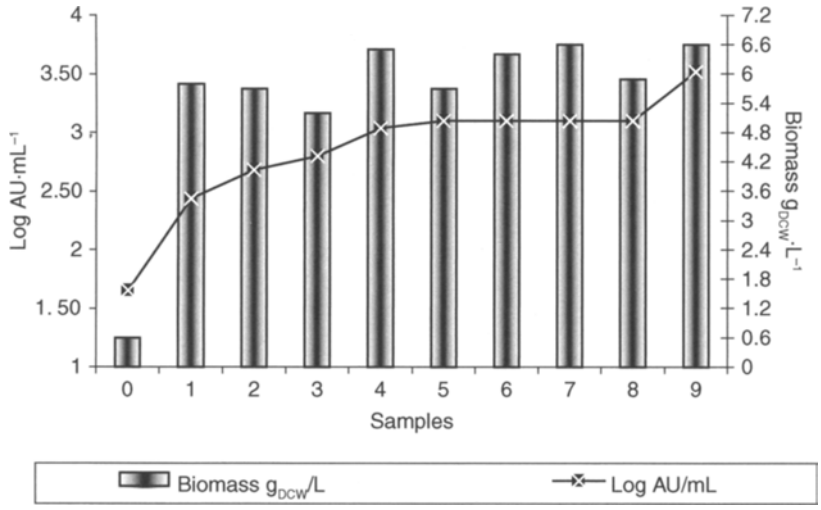


**Fig. 3.** Relation between nisin activity (log AU/mL) and biomass ($g_{DCW}$/L) of the samples in fermentor assay with skimmed milk 2.27 $g_{total\ solids}$ · AU/mL (log AU) and inhibition halo (H [mm]) was calculated through the equation: log [AU/mL = $10^{(0.2408 \times H - 0.8745)}$].

verified that the incorporation of either sodium or potassium phosphate into an artificial medium did not improve nisin production.

## Single Batch Fermentation

In fermentation conditions, nisin activity was observed after 4 h (45.07 AU/mL) and stabilized in between 20 and 32 h process (1255.16 AU/mL). For the last 4 h fermentation (performing 36 h total process) the nisin production speeded up to threefold (3312.07 AU/mL). Oxygen demand was low in entire process and did not influence biomass or nisin production. The pH value was stabilized in 4 h cultivation (pH = 4.74 ± 0.2) and was maintained through the process. (Fig. 3, Table 4).

Flôres and Monte Alegre *(37)* investigated nisin activity during the fermentation batch with *L. lactis* ATCC 7962, nisin bactericidal effect was detected after 4 h fermentation when 40% biomass had been produced. Furthermore, the maximum nisin activity was in 9 h fermentation (pH 4.9); however it decreased in the following 24 h process. Previous work *(26)* utilized in single batch fermentation culture media with skimmed milk plus MRS broth and the maximal nisin activity ranged from 1376.97 AU/mL (8 h fermentation) to 5934.03 AU/mL (16 h fermentation).

In the present work, the composition of the diluted skimmed milk (2.27 $g_{total\ solids}$) with no extra supplementation was verified to be enough for *L. lactis* growth with concomitant nisin production. Nisin activity in diluted skimmed milk (2.27 $g_{total\ solids}$) with no supplementation was similar to the activity of nisin expressed in the mixture of 25% skimmed milk

with 25% MRS broth in the previous work *(27)*. Liu et al. *(38)* observed a specific nisin formation of $5.4 \times 10^6$ AU/g at pH 5.5 in M17 broth added with lactose as a carbon source, for immobilized *L. lactis* in continuous fermentation, where nisin formation was reported to be greatly influenced by medium dilution rate.

## Conclusions

The culture media made up of diluted skimmed milk (2.27 $g_{\text{total solids}}$) was shown to support better conditions for nisin production and activity by *L. lactis*. The mechanism for this improvement is unclear. Quality of a natural product cannot be reproduced in an artificial way, because milk composition is an extremely complex group of the natural nutrients. In this work *L. lactis* cells developed in minimum concentration of diluted skimmed milk; however, artificial compounded media did not favor cell adaptation and, consequently, failed nisin production.

Besides that skimmed milk dilution for fermentation batch and nisin by *L. lactis* cells showed similar behavior when compared with fermentation with skimmed milk plus MRS broth *(26)*. This research shows the utilization of a low-cost growth media (diluted skimmed milk) to antimicrobial production with wide applications. Furthermore, the utilization of milk subproducts can be exploited (milk whey), because milk whey contains considerable levels of casein and lactose and these nutrients are observed to improve nisin production. In Brazil, 50% of milk whey is disposed with no treatment in rivers and because of high-organic matter concentrations milk whey is considered an important pollutant. In this particular case, an optimized production of an antimicrobial would be lined up with industrial disposal recycling.

## Acknowledgment

The authors thank the Brazilian Committees for the Scientific Technology Research (CNPq, FAPESP, and CAPES) for financial support and scholarship.

## References

1. Hurst, M. (1981), *Appl. Microbiol.* **27,** 85–123.
2. Cleveland, J., Montville, T. J., Nes, I. F., and Chikindas, M. L. (2001), *Int. J. Food Microbiol.* **71,** 1–20.
3. Jung, G. (1991), *Angew. Chem. Int. Ed. Engl.* **30,** 1051–1192.
4. de Vuyst, L. and Vandamme, E. J. (1992), *J. Gen. Microbiol.* **138,** 571–578.
5. Buchman, G. W., Banerjee, S., and Hansen, J. N. (1988), *J. Biol. Chem.* **263,** 16,260–16,266.
6. Vessoni Penna, T. C. and Moraes, D. A. (2002), *Appl. Biochem. Biotech.* **98–100,** 775–789.
7. Hansen, J. N. (1994), *Crit. Rev. Food Sci. Nutr.* **34,** 69–93.
8. Turner, S. R., Love, R. M., and Lyons, K. M. (2004), *Int. Endodontic J.* **37,** 664–671.
9. Aranha, C., Gupta, S., and Reddy, K. V. R. (2004), *Contraception* **69,** 333–338.
10. Dubois, A. (1995), *EID Dig. Dis. Div.* **1(3),** 79–88.

11. Sakamoto, I., Igarashi, M., and Kimura, K. (2001), *J. Antimicob. Chemother.* **47,** 709–710.
12. Biswas, S. R., Ray, P., Johnson, M. C., and Ray, B. (1991), *Appl. Environ. Microbiol.* **57,** 1265–1267.
13. Hansen, J. N., Chung, Y., and Liu, W. (1991), *ESCOM Science Publishers,* pp. 287–302.
14. Stevens, K. A., Sheldon, B. W., Klapes, N. A., and Klaenhammer, T. R. (1991), *J. Food Protection.* **55,** 763–776.
15. Ganzle, M. G., Hertel, C., and Hammes, W. P. (1999), *J. Food Microbiol.* **48,** 37–50.
16. Thomas, L. V., Clarkson, M., and Delves-Broughton, J. (2000), In: *Natural Food antimicrobial systems.* Naidu, A. S. (ed.), CRC Press, Washington D.C., pp. 463–524.
17. Fang, T. J. and Hung-Chi Tsai. (2004), *Food Microbiol.* **20,** 243–253.
18. Ukuku, D. O. and Fett, W. (2004), *J. Food Prot.* **67(10),** 2143–2150.
19. Vaara, M. (1992), *Microbiol. Rev.* **56,** 395–411.
20. Hauben, K. J. A., Wuytack, E. Y., Soontjens, C. C. F., and Michiels, C. W. (1996), *J. Food Prot.* **59,** 350–355.
21. Shelef, L. A. and Seiter, J. (1993), In: *Antimicrobial in Foods.* Davidson, P. M. and Branen, A. L. (eds.), Marcel Dekker, New York, pp. 539–569.
22. Gray, G. W. and Wilkson, S. G. (1965), *J. Appl. Microbiol.* **28,** 153.
23. Leive, L. (1965), *Biochem, biophys. Res. Commun.* **21,** 290–296.
24. Vessoni Penna, T. C., Ishii, M., Pessoa Júnior, A., Nascimento, L. O. A., Souza, L. C., and Cholewa, O. (2003), *Appl. Biochem. Biotechnol.* **113–116,** 453–468.
25. Gill, A. O. and Holley, R. A. (2003), *Int. J. Food Microbiol.* **80,** 251–259.
26. Vessoni Penna, T. C., Jozala, A. F., Gentille, T. R., Pessoa Júnior, A., and Cholewa, O. (2006), *Appl. Biochem. Biotechnol.* (in press).
27. Vessoni Penna, T. C., Jozala, A. F., Novaes, L. C. L., Pessoa Júnior, A., and Cholewa, O. (2005), *Appl. Biochem. Biotech.* **121–124,** 1–20.
28. Jozala, A. F., Novaes, L. C. L., Cholewa, O., Moraes, D., and Penna, T. C. V. (2005), *A. J. Biotech.* **4,** 262–265.
29. Kim, W. S., Hall, R. J., and Dunn, N. W. (1997), *Appl. Microbiol. Biotech.* **48,** 449–453.
30. Somogyi, M. (1952), *J. Biol. Chem.* **195,** 19–23.
31. Lowry, O. H., Rosebough, N. J., Farr, A. L., and Randall, R. J. (1951), *J. Biol. Chem.* **193,** 265–375.
32. Hurst, A. and Kruse, H. (1972), *Antimicrob. Agents Chemother.* **1,** 277–279.
33. Parente, E., Ricciardi, A., and Addario, G. (1994), *Appl. Microbiol. Biotechnol.* **41,** 388–394.
34. Parente, E. and Ricciardi, A. (1994), *Lett. Appl. Microbiol.* **19,** 12–15.
35. Chandrapatti, S. and O'Sullivan, D. J. (1998), *J. Biotech.* **63,** 229–233.
36. Cheigh, C. I., Choi, H. J., Park, H., et al. (2002), *J. Biotech.* **95,** 225–235.
37. Flôres, S. A. and Monte Alegre, R. (2001), *Biotech. Appl. Biochem.* **34,** 103–107.
38. Liu, X., Yoon-Kyung Chung, Shang-Tian Yang, and Yousef, A. E. (2005), *Process Biochem.* **40,** 13–24.
39. Cutter, C. N. and Siragusa G. R. (1995), *J. Food Prot.* **58,** 977–983.

0273-2289/1559-0291 (Online)/07/136-140/529-538/$30.00

# Bacterial Cellulose Production by *Gluconacetobacter* sp. RKY5 in a Rotary Biofilm Contactor

YONG-JUN KIM,[1] JIN-NAM KIM,[1] YOUNG-JUNG WEE,[2] DON-HEE PARK,[2] AND HWA-WON RYU*,[2]

[1]*Department of Material Chemical and Biochemical Engineering, Chonnam National University, Gwangju 500-757, Korea; and* [2]*School of Biological Sciences and Technology, Chonnam National University, Gwangju 500-757, Korea, E-mail: hwryu@chonnam.ac.kr*

## Abstract

A rotary biofilm contactor (RBC) inoculated with *Gluconacetobacter* sp. RKY5 was used as a bioreactor for improved bacterial cellulose production. The optimal number of disk for bacterial cellulose production was found to be eight, at which bacterial cellulose and cell concentrations were 5.52 and 4.98 g/L. When the aeration rate was maintained at 1.25 vvm, bacterial cellulose and cell concentrations were maximized (5.67 and 5.25 g/L, respectively). The optimal rotation speed of impeller in RBC was 15 rpm. When the culture pH in RBC was not controlled during fermentation, the maximal amount of bacterial cellulose (5.53 g/L) and cells (4.91 g/L) was obtained. Under the optimized culture conditions, bacterial cellulose and cell concentrations in RBC reached to 6.17 and 5.58 g/L, respectively.

**Index Entries:** Bacterial cellulose; bioreactor; fermentation; *Gluconacetobacter*; optimization; rotary biofilm contactor.

## Introduction

Cellulose is one of the most abundant biological macromolecules in nature, wherein it plays a crucial role in the integrity of plant cell walls *(1)*. Cellulose is a linear insoluble biopolymer, made up of the repeated unit of β-1,4 glycosidic bonds *(2)*. Cellulose molecules are chain or microfibrils, of up to 14,000 units of D-glucose that occurs in twisted rope-like bundles held together by hydrogen bond *(3)*. Bacterial cellulose synthesized by microorganisms differs from plant cellulose in its structure. Bacterial cellulose is extremely pure and exhibits a higher degree of polymerization and crystallization in respect of the fibrous with lignin, hemicellulose, and waxy aromatic substances *(4)*. On account of these physicochemical properties, there

*Author to whom all correspondence and reprint requests should be addressed.

has been recently interest in new fields of application and development of new methods for mass production of bacterial cellulose *(5–7)*.

A rotary biofilm contactor (RBC) has become a popular method for the treatment of domestic and industrial wastewater during the last decades. Tyagi et al. *(8)* previously investigated biodegradation of petroleum refinery wastewater in a polyurethane-attached RBC, and they found that RBC was capable of retaining considerable amounts of attached biomass, which when coupled with a good oxygen transfer capability of the system, could provide successful performance. The RBC generally consists of a series of circular disks mounted on a horizontal shaft *(9)*. The disks within the RBC are rotated, and alternatively exposed to the fermentation medium and air space *(8)*. Bacterial cellulose has been conventionally produced by static culture method, which requires a long culture period and intensive manpower, thus resulting in a low productivity. An agitated culture method converts bacterial cellulose-producing strains into cellulose-negative ($Cel^-$) mutants, which become more enriched than wild-type strain because of their rapid growth, thereby resulting in the lower productivity of bacterial cellulose *(10)*.

A cultivation of bacterial cellulose-producing bacteria in an RBC may not have a strong shear stress and an air bubble at the surface of liquid medium, which seems to be very excellent in terms of oxygen transferability by which the microorganisms can be readily contacted with air in comparison with stirred-tank bioreactor. In this study, the cultivation of *Gluconacetobacter* sp. RKY5 in RBC was attempted to improve the bacterial cellulose production, which might be a first trial for the production of bacterial cellulose using RBC as a bioreactor. This work mainly aimed at maximization of bacterial cellulose production through optimization of fermentation conditions in the RBC.

## Materials and Methods

### Microorganism

Microorganism used in this study was *Gluconacetobacter* sp. RKY5 KCTC 10683BP, which was previously isolated from persimmon vinegar *(11)*. *Gluconacetobacter* sp. RKY5 belongs to the group of Gram-negative aerobic bacterium, and it is rod-shaped without motility. It was maintained on 2% (w/v) agar plates containing Hestrin and Shramm (HS) medium *(12)*.

### Composition of Medium

The standard medium for regeneration of the strain and precultivation was HS medium, which consisted of 20.0 g/L of glucose, 5.0 g/L of peptone, 5.0 g/L of yeast extract, 2.7 g/L of $Na_2HPO_4$, and 1.2 g/L of citric acid monohydrate. A modified HS medium, consisted of 15.0 g/L of glycerol, 8.0 g/L of yeast extract, 3.0 g/L of $K_2HPO_4$, and 3.0 g/L of acetic

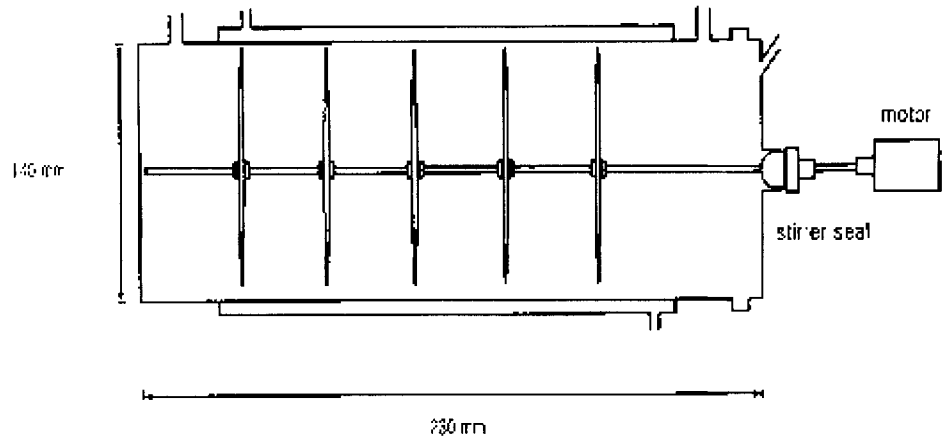


**Fig. 1.** Schematic diagram of a RBC.

acid was used for main fermentation. Before sterilization of each medium at 121°C, the pH value of the medium was adjusted to 6.0.

### Cultivation Conditions

Precultivation was carried out by inoculation of a single colony into 50 mL of HS medium in a 250-mL Erlenmeyer flask, and then incubated at 30°C and 150 rpm for 1 d in a shaking incubator (KMC-8480SF; Vision Scientific, Daejeon, Korea). Fifty milliliters of the preculture broth were homogenized by a homogenizer (X520D; CAT Ingenieurbüro M. Zipperer GmbH, Staufen, Germany) at 10,000 rpm for 1 min, and then 2% (v/v) of the homogenate was used as an inoculum.

### Experimental Setup

A schematic diagram of RBC used in this study is shown in Fig. 1, whereas the specifications of RBC are documented in Table 1. All disks were made of polypropylene and 34% of the disk was immersed in the medium. Disk diameter was 12 cm and disk thickness was 0.3 cm. A surface area of each disk was 226.2 $cm^2$, whereas an effective surface area of each disk was 221.1 $cm^2$. The RBC used in this study was made of pyrex, which was constructed with a double jacket to maintain the temperature through the circulation of constant temperature water. Total volume of the RBC was 3.5 L. Five to nine disks were mounted on a horizontal steel shaft and rotated with a variety of speeds from 15 to 35 rpm using a direct driven digital stirrer with a 50 W electric motor (SS-200; Global Lab, Seoul, Korea). Gas aeration was provided by an air pump through a filter (0.45-μm pore size) and controlled by an airflow meter. The overall experimental setup of RBC for bacterial cellulose production is schematically illustrated in Fig. 2. Bacterial cellulose fermentation was conducted in a 3.5-L RBC containing 1.0 L of working volume at 30°C for 96 h.

Table 1
Summary of the Dimensions of a RBC

| Parameter | Unit | Specification |
|---|---|---|
| Disk diameter | cm | 12 |
| Disk thickness | cm | 0.3 |
| Total surface area | $cm^2$ | 1131–2035.8 |
| Submergence | % | 34 |
| Effective area | $cm^2$ | 1105.6–2021.2 |
| Total volume | $cm^3$ | 3540 |
| Working volume | $cm^3$ | 1000 |
| Rotation speed | rpm | 15–35 |
| Temperature | °C | 30 |

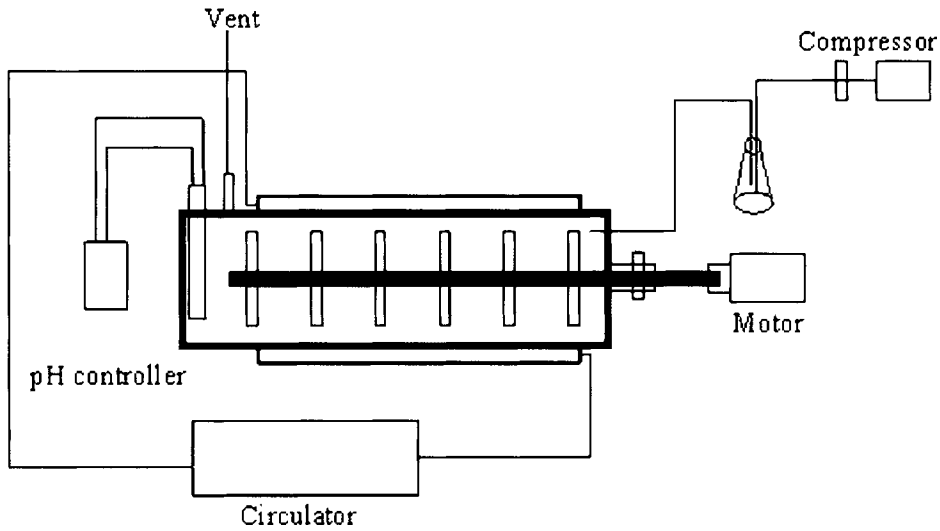


**Fig. 2.** Experimental setup of a RBC for bacterial cellulose production.

## *Analytical Methods*

Cell concentration was determined by measuring the optical density at 660 nm ($OD_{660}$) using a UV-1700 spectrophotometer (Shimadzu, Kyoto, Japan). The $OD_{660}$ was measured after the culture broth containing cellulose pellicle was treated with 0.1% (v/v) cellulase (Celluclast 1.5 L; Novozymes A/S, Bagsvaerd, Denmark) at 50°C with shaking at 150 rpm for 1 h. Dry cell weight was then calculated by using a predetermined calibration curve *(13,14)*. The thick cellulose membrane formed on the surface of the disk was flaked with tweezers, which was washed with distilled water several times to remove the medium components and then treated with 0.1 *N* NaOH at 80°C for 30 min in order to dissolve the microorganisms *(3)*. After these treatments were done, bacterial cellulose was rinsed

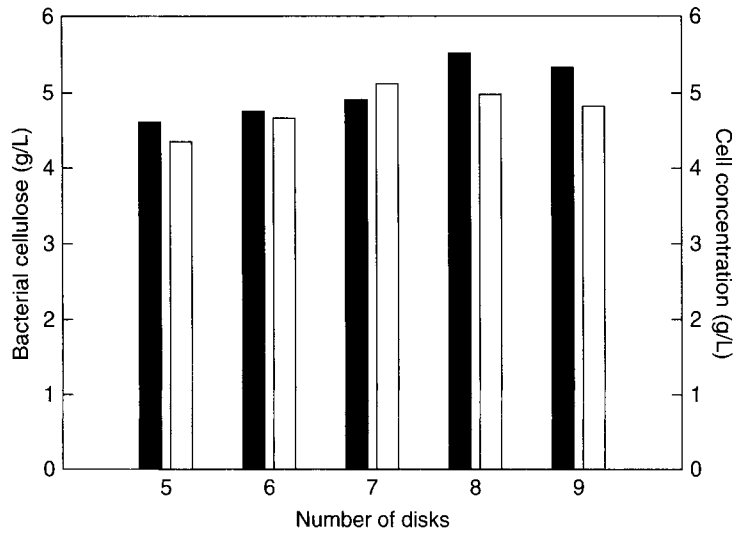


**Fig. 3.** Effect of number of disks on bacterial cellulose production and cell concentration by *Gluconacetobacter* sp. RKY5 cultured in a RBC. (Culture conditions: pH, uncontrolled; temperature, 30°C; rotation speed, 15 rpm; aeration rate, 1 vvm; fermentation time, 96 h.) Symbols: ■, bacterial cellulose and □, cell concentration.

again with distilled water until the pH of water became neutral. Purified bacterial cellulose was dried at 80°C until constant weight was obtained, and then weighed.

## Results and Discussion

### *Influence of the Number of Disks*

In order to determine the optimal number of disk, fermentation was conducted with different number of disks using a modified HS medium. *Gluconacetobacter* sp. RKY5 was cultured in a 3.5-L RBC, containing 1 L working volume, at 30°C, 15 rpm, and 1 vvm for 96 h. Before sterilization at 121°C, the pH value of medium was adjusted to 6.0. During the cultivation, the pH of culture broth was not controlled. Figure 3 shows the amount of bacterial cellulose produced and cell concentration at different number of disks. As shown in Fig. 3, the amount of bacterial cellulose gradually increased with the number of disks up to eight disks, but then somewhat decreased beyond eight disks. Therefore, the optimal number of disks seemed to be eight, at which the amount of bacterial cellulose produced and cell concentration was 5.52 and 4.98 g/L, respectively.

### *Influence of Aeration Rates*

To investigate the effects of aeration rate on bacterial cellulose production, fermentation was conducted with 0–1.5 vvm in a 3.5-L RBC, containing 1 L working volume, at 30°C, 15 rpm, and eight disks for 96 h.

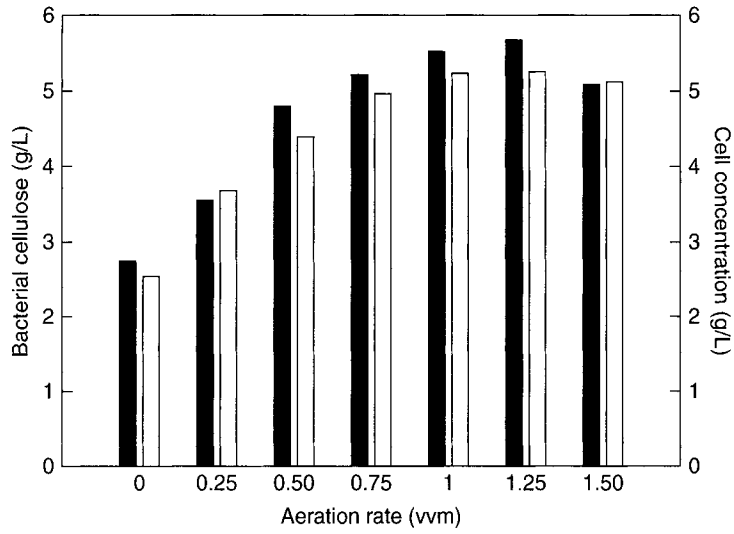


**Fig. 4.** Effect of aeration rates on bacterial cellulose production and cell concentration by *Gluconacetobacter* sp. RKY5 cultured in a RBC. (Culture conditions: pH, uncontrolled; temperature, 30°C; rotation speed, 15 rpm; number of disk, 8; fermentation, 96 h.) Symbols: ■, bacterial cellulose and □, cell concentration.

During the cultivation, culture pH was not controlled. Figure 4 shows the amount of bacterial cellulose produced and cell concentration according to the respective aeration rates. As shown in Fig. 4, the amount of bacterial cellulose produced and cell concentration increased in accordance with increases in aeration rate. When aeration rate was 1.25 vvm, the maximal bacterial cellulose was 5.67 g/L and cell concentration was 5.25 g/L. In contrast, the excessive air supply higher than 1.25 vvm lowered both bacterial cellulose production and cell concentration.

### *Influence of Rotation Speeds*

Fermentations were conducted with 15–35 rpm in a 3.5-L RBC, containing 1 L working volume, at 30°C, 1.25 vvm, and eight disks for 96 h, in order to find the optimal rotation speed for enhancement of bacterial cellulose production. Before sterilization, the pH value of medium was adjusted to 6.0. During the cultivation, the pH of culture broth was uncontrolled. Figure 5 shows the amount of bacterial cellulose produced and cell concentration at various rotation speeds of the impeller. As shown in Fig. 5, both the amount of bacterial cellulose produced and cell concentration showed quite similar trends between 15 and 25 rpm, but then slightly decreased beyond this value. The highest amount of bacterial cellulose (5.41 g/L) and cell concentration (5.15 g/L) were obtained when the rotation speed was 15 rpm.

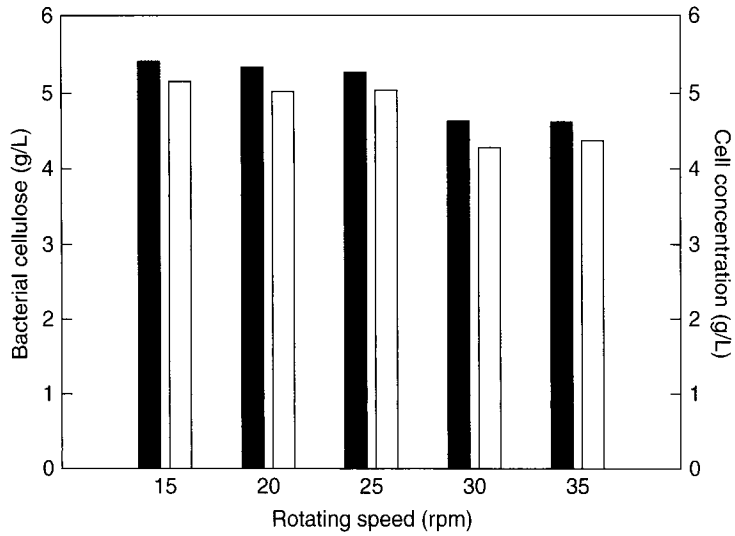


**Fig. 5.** Effect of rotation speeds on bacterial cellulose production and cell concentration by *Gluconacetobacter* sp. RKY5 cultured in a RBC. (Culture conditions: pH, uncontrolled; temperature, 30°C; aeration rate, 1.25 vvm; number of disk, 8; fermentation time, 96 h.) Symbols: ■, bacterial cellulose and □, cell concentration.

## *Influence of Culture pH*

To investigate the effect of culture pH on bacterial cellulose fermentation, fermentation was conducted in a 3.5-L RBC, containing 1 L working volume, at 30°C, 15 rpm, 1.25 vvm, and eight disks for 96 h. The pH of culture broth was maintained at a constant value by automatic addition of 5 *N* NaOH and 5 *N* HCl. Figure 6 shows the amount of bacterial cellulose produced and cell concentration at pH values of 5.0, 6.0, 7.0, 8.0, and uncontrolled. As shown in Fig. 6, when the culture pH was not controlled, both bacterial cellulose production and cell concentration were considerably higher than those of the pH controlled fermentations. This was probably because of the inhibitory effect of nonuniformly mixed alkali and/or acid solution used for pH control, because the culture broth in the RBC was almost static. The maximal amount of bacterial cellulose produced (5.53 g/L) and cell concentration (4.91 g/L) was obtained at uncontrolled pH.

The optimal conditions for bacterial cellulose production in a RBC were established from the aforementioned results, and the amounts of bacterial cellulose produced and cell concentration were 6.17 and 5.58 g/L, respectively, under the aforementioned optimal conditions. Furthermore, bacterial cellulose concentration produced was generally associated with cell growth. From this observation, it can be deduced that bacterial cellulose fermentation should be severely associated with the growth of microorganism. Figure 7 shows a photograph of the thick cellulose membrane formed on the surface of the disk in a RBC.

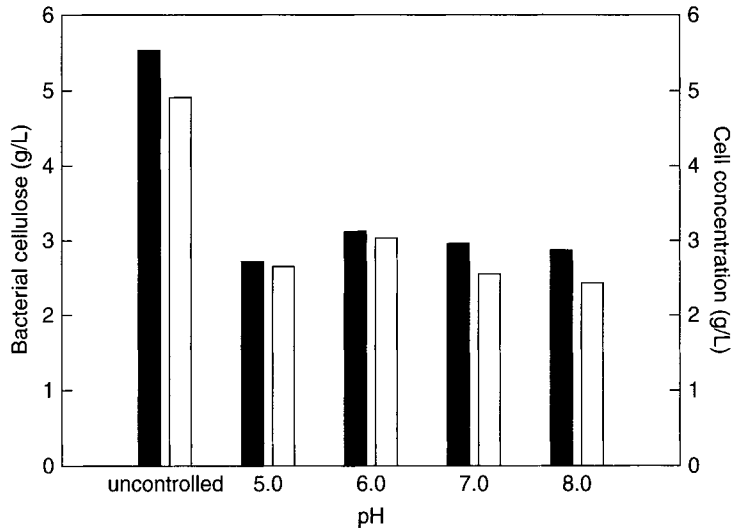


**Fig. 6.** Effect of culture pHs on bacterial cellulose production and cell concentration by *Gluconacetobacter* sp. RKY5 cultured in a RBC. (Culture conditions: temperature, 30°C; aeration rate, 1.25 vvm; rotation speed, 15 rpm; number of disk, 8; fermentation time, 96 h.) Symbols: ■, bacterial cellulose and □, cell concentration.

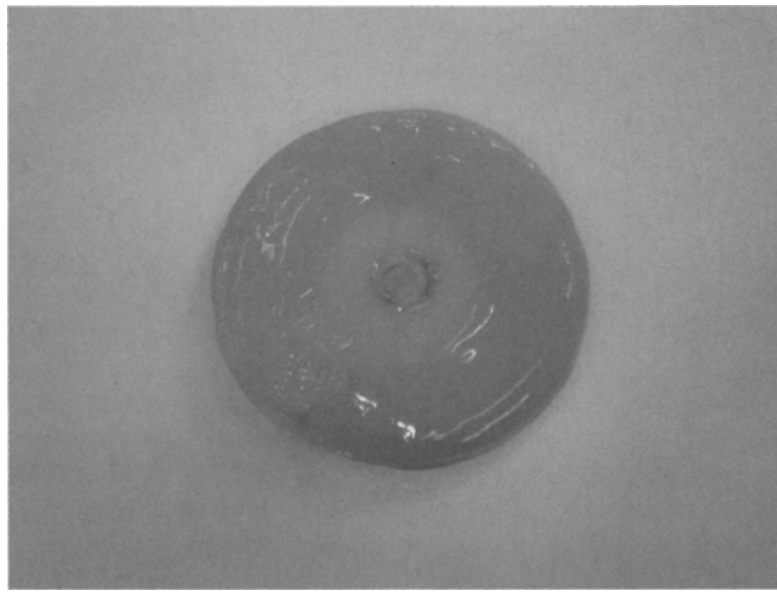

**Fig. 7.** Photograph of bacterial cellulose membrane formed on the surface of the disk during the fermentation using a RBC.

## Conclusions

The optimal fermentation conditions were investigated by using *Gluconacetobacter* sp. RKY5 in a RBC in order to improve bacterial cellulose production. The optimal number of disks was eight, at which the amount of bacterial cellulose produced and cell concentration was 5.52 and 4.98 g/L, respectively, and the aeration rate was 1.25 vvm with the maximal bacterial cellulose and cell concentration of 5.67 and 5.25 g/L, respectively. The highest amount of bacterial cellulose (5.41 g/L) and cell concentration (5.15 g/L) was obtained when the rotation speed was 15 rpm. The maximal amount of bacterial cellulose (5.53 g/L) and cell concentration (4.91 g/L) was obtained when the culture pH was not controlled at fixed value. After optimizing the operational parameters of RBC for bacterial cellulose production, the amounts of bacterial cellulose and cell concentration could be increased to 6.17 and 5.58 g/L, respectively.

## Acknowledgments

This article was supported by the Korea Research Foundation Grant funded by the Korean Ministry of Education and Human Resources Development (KRF-2006-521-D00118), and further supported partly by the Korean Government through the second stage of BK21 program.

## References

1. Delmer, D. P. and Amor, Y. (1995), *Plant Cell* **7,** 987–1000.
2. Desvaux, M. (2005), *FEMS Microbiol. Rev.* **29,** 741–764.
3. Ralph, J. F., Fessenden, J. S., and Marshall, W. L. (1998), *Organic Chemistry*, 6th ed. Brooks/Cole Publishing Company, USA, 952p.
4. Richmond, P. A. (1991), In: *Biosynthesis and Biodegradation of Cellulose*, Haigler, C. H. and Weimer, P. J., (eds.), Marcel Dekker, New York, pp. 5–23.
5. Tsuchida, T. and Yohinaga, F. (1997), *Pure Appl. Chem.* **69,** 2453–2548.
6. Tahara, N., Tabuchi, M., Watanabe, K., Yano, H., Morinaga, Y., and Yoshinaga, F. (1997), *Biosci. Biotechnol. Biochem.* **61,** 1862–1865.
7. Naritomi, T., Kouda, T., Yano, H., and Yoshinaga, F. (1998), *J. Ferment. Bioeng. 85,* 89–95.
8. Jianlong, W. (2000), *Bioresour. Technol.* **75,** 245–247.
9. Zheng, Z. and Obbard, J. P. (2002) *J. Biotechnol.* **96,** 241–249.
10. Valla, S. and Kjosbakken, J. (1981), *J. Gen. Microbiol.* **128,** 1401–1418.
11. Kim, S. Y., Kim, J. N., Wee, Y. J., Park, D. H., and Ryu, H. W. (2006), *Appl. Biochem. Biotechnol.* **129,** 705–715.
12. Schramm, M. and Hestrin, S. (1954), *Biochem. J.* **56,** 163–166.
13. Kouda, T., Yano, H., and Yoshinaga, F. (1997), *J. Ferment. Bioeng.* **83,** 371–376.
14. Naritomi, T., Kouda, T., Yano, H., and Yoshinaga, F. (1998), *J. Ferment. Bioeng.* **85,** 89–95.

0273-2289/1559-0291 (Online)/07/136–140/539–554/$30.00

# Biosurfactant Production by Cultivation of *Bacillus atrophaeus* ATCC 9372 in Semidefined Glucose/Casein-Based Media

LUIZ CARLOS MARTINS DAS NEVES,*,[1] KÁTIA SILVA DE OLIVEIRA,[1] MÁRCIO JUNJI KOBAYASHI,[1] THEREZA CHRISTINA VESSONI PENNA,[1] AND ATTILIO CONVERTI[2]

*[1]University of São Paulo, School of Pharmaceutical Sciences, Biochemical and Pharmaceutical Technology Department, São Paulo, Brazil, E-mail: lucaneves@usp.br; and [2]Dipartimento di Ingegneria Chimica e di Processo, Università degli Studi di Genova, Genova, Italy, E-mail: converti@unige.it*

## Abstract

Biosurfactants are proteins with detergent, emulsifier, and antimicrobial actions that have potential application in environmental applications such as the treatment of organic pollutants and oil recovery. *Bacillus atrophaeus* strains are nonpathogenic and are suitable source of biosurfactants, among which is surfactin. The aim of this work is to establish a culture medium composition able to stimulate biosurfactants production by *B. atrophaeus* ATCC 9372. Batch cultivations were carried out in a rotary shaker at 150 rpm and 35°C for 24 h on glucose- and/or casein-based semidefined culture media also containing sodium chloride, dibasic sodium phosphate, and soy flour. The addition of 14.0 g/L glucose in a culture medium containing 10.0 g/L of casein resulted in 17 times higher biosurfactant production ($B_{max}$ = 635.0 mg/L). Besides, the simultaneous presence of digested casein (10.0 g/L), digested soy flour (3.0 g/L), and glucose (18.0 g/L) in the medium was responsible for a diauxic effect during cell growth. Once the diauxie started, the average biosurfactants concentration was 16.8% less than that observed before this phenomenon. The capability of *B. atrophaeus* strain to adapt its own metabolism to use several nutrients as energy sources and to preserve high levels of biosurfactants in the medium during the stationary phase is a promising feature for its possible application in biological treatments.

**Index Entries:** *Bacillus atrophaeus;* batch cultivation; biosurfactant production; casein; glucose; kinetics.

## Introduction

Biological surfactants or biosurfactants are a diverse group of natural surface-active chemical compounds *(1,2)* produced spontaneously by microorganisms, extracellularly or as part of the cellular membrane.

*Author to whom all correspondence and reprint requests should be addressed.

Biosurfactants are proteins with detergent, emulsifier, and surfactant power to lower the surface tension of water and other solvents, and have potential application in environmental uses such as organic pollutants treatment and oil recovery. The production of biosurfactants is related to the consumption of hydrocarbons, including oily residues, and occurs during exponential cellular growth.

Cyclic lipopeptide biosurfactants with antimicrobial activity (surfactin, iturin, and fengicin), also reduce surface tension, critical micelle concentration, and interfacial tension in both aqueous and hydrocarbon mixtures *(2)*. Surfactin, one of the most effective cyclic lipopeptide biosurfactants produced by *Bacillus subtilis (3–5)* can lower the surface tension of water from 72 to 50 mN/m and has a critical micelle concentration of $2.5 \times 10^{-5}$ *M (6,7)*. When compared with chemically synthesized surfactants, biosurfactants exhibit a higher specific activity, lower toxicity, and environmental impact, higher biodegradability, and lower costs *(3,5,8)*.

*B. subtilis* is considered a suitable source for biosurfactant production owing to the absence of pathogenicity, which permits the use of its products in the food and pharmaceutical industries *(9,10)*. Cell viability is easily assayed and its spores have successfully been used as biological indicators *(11–13)*. Therefore, the development of improved strains and culturing methods of *B. subtilis* can provide a safe source of surfactants for waste treatment.

Biosurfactants can be produced in *B. subtilis* cultures using sugars (sucrose, glucose, and lactose), vegetable oils, or starch as carbon sources *(14–19)*. However, the high cost of the process and recuperation of these proteins and low productivity can limit their application for environmental purposes *(20)*. Alternative sources of culture media as sugar cane molasses, water of maize *(21)*, and industrial effluent wastes *(22,23)* have been considered to reduce the final cost of the process to obtain higher productivity of biosurfactants.

Among several industrial effluents, milk serum, a residue of the milk derivative industries, is distinguished as potential source of biosurfactants based on a rich composition in proteins (6%), fats (3.2%), sugars, and salts. In Brazil, for each 1000 L of milk used in the manufacture of cheese, approx 820 L of milk serum are produced and about 50% is poured directly in rivers, with no previous treatment, causing a serious environmental problem *(24)*. The use of milk serum as a culture medium to produce biosurfactants at low costs is an interesting alternative to reduce this environmental problem.

However, the use of this residue as substrate to obtain biosurfactants for industrial use, or as a nutritional source during the biological treatment of effluents, can be an interesting alternative to reduce environmental impact.

The use of casein in the culture of microorganisms is usually associated to the production of proteases or to the research of its properties *(25–27)*. However, few studies have developed a culture medium with casein associated with other nutrients to improve the production of valuable

biotechnological products. Thus, it is interesting to evaluate the productivity yield of biosurfactants by *B. subtilis* in an alternative culture medium with other sources of carbon, including casein, which is abundant in milk serum. The aim of this work is to develop a growth medium able to stimulate biosurfactants production by *B. atrophaeus* ATCC 9372. Batch cultivations are carried out at 150 rpm and 35°C for 24 h on glucose- and/or casein-based culture media to relate the biosurfactant production with cellular growth and nutrient consumption.

## Materials and Methods

### *Maintenance of the Strains*

A strain of *B. atrophaeus* ATCC 9372 was maintained according to the following procedure. All the materials and 500 mL of culture medium were sterilized at 121°C for 30 min. Spore suspensions stored at 4°C in 0.02 mol/L calcium acetate (pH 9.0) were directly utilized for these experiments. Five 7-mL glass tubes containing slants of plate count agar (Merck, Darmstadt, Germany) were inoculated with spores of *B. atrophaeus* ATCC 9372 and incubated for 24 h at 35°C. Cells were suspended in 2 mL of physiological solution (0.9% NaCl) and transferred to Roux flasks containing 200 mL of tryptone soy agar (Merck). After incubation at 35°C for 24 h, the flasks were washed with 100 mL of 0.02 mol/L calcium acetate solution, and their contents transferred to sterilized capped flasks containing 30.0 g of glass beads with 3-mm diameter. The pH of these suspensions was adjusted to 9.6 with 1 mol/L NaOH solution.

### *Cultivations*

250-mL Erlenmeyers containing 100 mL of culture media, containing glucose and casein at variable concentrations, 5.0 g/L of sodium chloride, 2.5 g/L of dibasic sodium phosphate, and 3.0 g/L of soy flour, were inoculated with cell suspensions to give a starting biomass concentration ($X_o$) of 0.2 $g_X$/L ($OD_{600\ nm} = 0.014$). All batch runs were performed in triplicate at 35°C utilizing a rotary shaker at 150 rpm. Samples were collected every 1–2 h, transferred to Eppendorfs, and then centrifuged at 17,091*g* for 20 min. 10°C. Both liquid and precipitated fractions were stored at 4°C and subsequently analyzed for determinations of extracellular and intracellular concentrations of glucose, total proteins, and biosurfactant, according to circumstances.

### *Cell Disruption*

Cell mass separated by centrifugation at 17,091*g* was resuspended in 1 mL of a buffer solution containing protease inhibitors consisting of (mmol/L) 50 Tris-HCl buffer (pH 7.5), 5 $MgCl_2$, 10 β-mercaptoethanol, 2 aminocaproic acid, and 0.2 ethylenediaminetetraacetic acid. Glass

spheres with 0.5-mm diameter were then added to the suspension as abrasive agent up to 1/300 w/w ratio. After mixing for 12 min in a water bath cooled at 4°C with ice, cell debris and glass spheres were removed by centrifugation at 4°C and 17,091*g*, and the supernatant was utilized for determinations of biosurfactant concentration and total protein content *(28)*.

### *Analytical Determinations*

Biomass concentration ($X$ [$g_X$/L]) was determined in cell suspension before centrifugation using a calibration curve ($OD_{600\ nm} = 0.5820\ X - 0.1022$) obtained relating optical density at 600 nm (Beckman DU-640, Fullerton, CA) to dry mass of *B. atrophaeus* ATCC 9372 cells in the exponential growth phase *(29–30)*. Average deviation of the experimental data from the fitting curve ($\sigma$) and determination coefficient ($r^2$) were 4.5% and 0.996, respectively. Glucose concentration ($G$ [g/L]) in the liquid phase was determined by the glucose oxidase peroxidase (GOD-POD) enzymatic assay no. 11538 (Biosystem, São Paulo, Brazil), using an absorbance calibration curve ($OD_{500\ nm} = 0.3496\ G - 0.0011$; $r^2 = 0.999$; $\sigma = 0.06\%$) obtained from glucose solutions with variable known concentrations *(30)*.

Casein concentration was determined as total proteins (TP [g/L]) on aliquots of the liquid phase from centrifugation after cell disruption. This methodology was based on the direct absorbance of samples at 660 nm after a color-developing reaction *(31)*. The calibration curve, obtained using casein solutions with different concentrations, was described by the linear equation $OD_{660\ nm} = 0.663\ TP + 0.0133$ ($r^2 = 0.993$; $\sigma = 0.2\%$). Aliquots of samples of the supernatant were used to determine biosurfactant concentrations. According to Morikawa et al. *(6)*, the concentration of biosurfactant ($B$) was related to the diameter of the halos ($D$) formed by 10 µL samples on a thin layer of 10 mL oil dispersed in 40 mL water. Comparison of sample diameters with those obtained with standard water/surfactin dispersions allowed expressing the biosurfactant concentration as $mg_B$/L. The calibration curve, obtained using surfactin solutions with different concentrations, was described by the linear equation $D = 0.0133\ B - 0.0007$ ($r^2 = 0.999$; $\sigma = 1.8\%$).

Protease assay was determined according to Ahamed et al. *(32)* in aliquots of the supernatant. Samples (0.5 mL) were incubated with buffered casein (bovine milk, Sigma, St. Louis, MO) solution (2.5 mg/mL in 0.05 *M* sodium phosphate buffer) at pH 6.5 and 37°C in a final assay volume of 2 mL. The reaction was stopped, and residual protein was precipitated by addition of 4 mL trichloroacetic acid (10% [w/w]). After standing 1 h, supernatant was obtained by centrifugation (3000*g*, 6 min). To 1 mL of supernatant, 5 mL of 0.4 *M* sodium carbonate was added followed by 0.5 mL folin-phenol reagent. After 10 min, tyrosine liberated by the action of protease was measured at 660 nm. One unit of protease activity liberates 1.0 mg of tyrosine per minute under assay conditions. The calibration curve, obtained using subtilisin solutions, a characteristic protease

produced by *B. subtilis* with different concentrations, was described by the linear equation $C = 0.0133\ E - 0.0007$ ($r^2 = 0.999$; $\sigma = 2.0\%$) when $C$ is the casein concentration and $E$ is the enzymatic activity of subtilisin.

### *Calculation of Fermentation Parameters*

The specific rates of cell growth ($\mu_X$), biosurfactant formation ($\mu_B$), and substrate consumption ($\mu_S$) were expressed, respectively, as 1/h, $mg_B/g_X \cdot h$, and $g_S/g_X \cdot h$ and defined as:

$$\mu_x = \frac{1}{X}\frac{dX}{dt} \tag{1}$$

$$\mu_B = \frac{1}{X}\frac{dB}{dt} \tag{2}$$

$$\mu_S = \frac{1}{X}\frac{dS}{dt} \tag{3}$$

where $S$ is the substrate concentration and $t$ the time. Maximum specific growth rate ($\mu_{Xmax}$) was determined during the exponential growth phase according to the equation:

$$\mu_{X_{max}} = \frac{1}{t}\ln\frac{X}{X'} \tag{4}$$

where $X'$ and $X$ are cell concentrations at the start of the exponential phase and after a time ($t$), respectively.

Generation time was determined according to the equation:

$$t_g = \frac{\ln 2}{\mu_{max}} \tag{5}$$

Volumetric cell productivity ($P_X$), expressed as $g_X/L \cdot h$, was calculated according to the equation:

$$P_X = \frac{\Delta X}{\Delta t} = \frac{(X_{max} - X_0)}{t} \tag{6}$$

where $X_{max}$ and $X_0$ are the maximum and initial values of biomass concentration, respectively, whereas $t$ is the time needed to reach $X_{max}$. Volumetric biosurfactant productivity ($P_B$), expressed as $mg_B/L \cdot h$, was calculated according to the equation:

$$P_B = \frac{\Delta B}{\Delta t} = \frac{(B_f - B_0)}{t} \tag{7}$$

where $B_0$ and $B_f$ are the initial and final biosurfactant concentrations attained after the time $t$. The yield of biosurfactant on cell mass, expressed as $mg_B/g_X$, was calculated as the ratio of the biosurfactant concentration ($\Delta B$) to the corresponding biomass concentration after the same time ($\Delta X$).

The average value of this yield ($Y_{B/X}$) was calculated as the ratio of the variation in biosurfactant concentration from the start to the maximum cell concentration to the corresponding variation in biomass concentration.

The yield of biosurfactant on total proteins, expressed as $mg_B/g_{TP}$, was calculated as the ratio of the biosurfactant concentration ($\Delta B$) to the corresponding total proteins concentration ($\Delta$TP) after the same time. The average value of this yield ($Y_{B/TP}$) was calculated as the ratio of the variation in biosurfactant concentration from the start to the maximum cell concentration to the corresponding variation in total proteins concentration. The yield of biomass on consumed substrate ($Y_{X/S}$), expressed as $g_X/g_S$, was calculated as the ratio of the difference between maximum and initial cell concentrations ($X_{max} - X_0$) to the corresponding substrate consumption (glucose, $\Delta G$ and casein, $\Delta C$) after the same time interval.

The yield of biosurfactant concentration on consumed substrate ($Y_{B/S}$), expressed as $mg_B/g_S$, was calculated as the ratio of the difference between final and initial biosurfactant concentration ($B_f - B_0$) to the corresponding substrate consumption (glucose, $\Delta G$ and casein, $\Delta C$) after the same interval.

## Results and Discussion

Batch cultivations of *B. atrophaeus* ATCC 9372 were performed on medium containing variable levels of hydrolyzed casein (0.0–10.0 g/L) and glucose (0.0–18.0 g/L) to follow the production of biosurfactants associated with cell growth. The concentration ranges of these ingredients were selected on the basis of the values most widely accepted in the literature for the growth of different microorganisms in synthetic media *(20–21,33–34)*. Table 1 lists the values of the main fermentation parameters obtained under different nutritional conditions, i.e., either in the presence of both nutrients or in the presence of only one of them.

A look at the data of the volumetric cell productivity points out that the lowest values of this parameter in the presence of both glucose and casein were obtained in tests 1 ($P_X = 0.36\ g_X/L \cdot h$) and 2 ($P_X = 0.34\ g_X/L \cdot h$), i.e., cultivations in which the casein level was almost the same or higher than that of glucose. On the other hand, when glucose concentration was 80% higher than that of casein (test 3), this parameter exhibited an average increase by 50%.

The simultaneous presence of these metabolizable nutrients seemed to influence the relation between carbon source uptake and cell growth. Glucose behaved as the preferential carbon source in all cultivations performed in its presence (tests 1–5), being consumed since the beginning. However, when glucose concentration was increased from 2.5 g/L (test 1) to 14.0 g/L (test 2) in the medium containing casein as well, the yield of biomass on consumed substrate (glucose, $\Delta G$) decreased by 67%, hence suggesting that glucose was likely present in excess with respect to the

Table 1
Main Kinetic Results of Batch Cultivations of *B. atrophaeus* ATCC 9372 Performed at Different Initial Glucose and Casein Concentrations

| Test | $G_0$[a] ($g_S$/L) | $C_0$[b] (g/L) | pH[c] | $Y_{B/X}$[d] ($mg_B/g_X$) | $Y_{B/TP}$[e] ($mg_B/g_{TP}$) | $\mu_{Xmax}$[f] ($h^{-1}$) | $t_g$[g] (h) | $\Delta G$[h] ($g_S$/L) | $\Delta C$[i] (g/L) | $B_{max}$[j] ($mg_B$/L) | $P_X$[k] ($g_X$/L·h) | $P_B$[l] ($mg_B$/L·h) | $Y_{X/S}$[m] ($g_X/g_S$) | $Y_{B/S}$[n] ($mg_B/g_S$) |
|---|---|---|---|---|---|---|---|---|---|---|---|---|---|---|
| 1 | 2.5 | 10.0 | 6.7 ± 0.3 | 121 | 25.4 | 0.180 | 3.8 | 1.78 | 1.10 | 346 | 0.36 | 58 | 1.20 | 36.1 |
| 2 | 14.0 | 10.0 | 6.7 ± 0.3 | 162 | 53.6 | 0.084 | 8.2 | 13.8 | 0.80 | 635 | 0.34 | 29 | 0.40 | 43.9 |
| 3 | 18.0 | 10.0 | 5.8 ± 0.5 | 256 | 53.8 | 0.247 | 2.8 | 16.3 | 4.31 | 574 | 0.54 | 191 | 0.73 | 4.70 |
| 4 | 2.5 | 0.0 | 6.3 ± 0.03 | 30.1 | 22.8 | 0.104 | 6.7 | 2.4 | – | 53.9 | 0.15 | 3.4 | 1.38 | 7.90 |
| 5 | 5.0 | 0.0 | 6.6 ± 0.04 | 5.50 | 3.40 | 0.242 | 2.9 | 2.6 | – | 10.0 | 0.14 | 1.4 | 1.15 | 0.00 |
| 6 | 0.0 | 10 | 5.7 ± 0.5 | 70.1 | 15.2 | 0.117 | 5.9 | – | 1.70 | 537 | 0.39 | 23 | 3.71 | 68.0 |

The average kinetic parameters were calculated at the end of the cell growth phase.
[a]Initial glucose concentration.
[b]Initial casein concentration.
[c]pH variation during cultivation.
[d]Average yield of biosurfactant on cell mass.
[e]Average yield of biosurfactant on total proteins.
[f]Maximum specific growth rate.
[g]Generation time.
[h]Glucose consumption during the growth phase.
[i]Casein consumption during the growth phase.
[j]Maximum biosurfactant concentration.
[k]Volumetric biomass productivity.
[l]Volumetric biosurfactant productivity.
[m]Yield of biomass on consumed substrate during growth phase.
[n]Yield of biosurfactant on consumed substrate during growth phase.

uptake ability of the microorganism, and the exponential phase took twice longer (16 h). In both cases the occurrence of stationary growth phase was coincident with total glucose consumption.

Comparison of the results listed in Table 1 shows that casein was simultaneously consumed, although never completely, and that its consumption ($\Delta C$) in test 1 was 27% larger than in test 2, likely because the low glucose concentration in the medium made this substrate limiting for the growth and forced the microorganism to metabolize other carbon sources. These results confirm that glucose was the primary carbon source and that the initial concentration of casein used in this cultivation (10.0 g/L) was higher than the needs of the microorganism.

The results of biosurfactants produced during cultivations performed at glucose levels comparable with that of casein (test 2) or less (test 1) point out that these compounds were metabolized insofar as they were released during cell growth. The maximum concentration of biosurfactants ($B_{max}$ = 346.0 mg/L) detected at the end of the exponential growth phase of test 1 ($t$ = 6 h) does in fact suggest that this production was associated to growth (Fig. 1A). The connection between curves of specific growth rate ($\mu_X$), substrate consumption rate ($\mu_S$), and biosurfactant formation rate ($\mu_B$) suggests a primary metabolism to biosurfactant production in tests 1 (Fig. 1B) and 2 (Fig. 2B). When glucose concentration was increased (test 2), the production of biosurfactants exhibited almost the same behavior as that observed in test 1 (Fig. 2A), in that it increased during the exponential growth phase (8–10 h), achieved a maximum value of 635.0 mg/L, and then decreased ($t$ = 14 h, $B_{max}$ = 278.0 mg/L). Because the occurrence of the stationary phase was related in both cultivations to the depletion of the primary carbon source (glucose), it was likely that, under these nutritional stress conditions, not only the production of biosurfactants was strongly affected but also biosurfactants were utilized as the preferred carbon source. It is noteworthy that the concentration of total proteins, related to the presence of casein, did not show large variations during tests 1 ($\Delta C$ = 1.10.0 g/L) and 2 ($\Delta C$ = 0.80 g/L) (Table 1), which suggests that the microorganism preferred the biosurfactant to casein as a secondary carbon source. A possible cause of this behavior could be the simpler structure of biosurfactants, which are simple lipopeptides containing only 7–10 aminoacids, and then could have been hydrolyzed and metabolized more quickly than casein. The production of biosurfactants can alternatively be evaluated through the yield of biosurfactants on biomass ($Y_{B/X}$), a volume-independent parameter very useful in scale-up operations. Comparing the results of tests 1 and 3 (Table 1) shows that a sevenfold glucose concentration in the medium led to a >200% increase in this parameter.

When initial glucose level was higher (18.0 g/L) than that of casein (10.0 g/L) (test 3), *B. atrophaeus* growth curve exhibited a clear inflection after 10 h of cultivation. Such a sort of diauxic growth (Fig. 3A) could be ascribed to the activation of alternative routes to metabolize the new

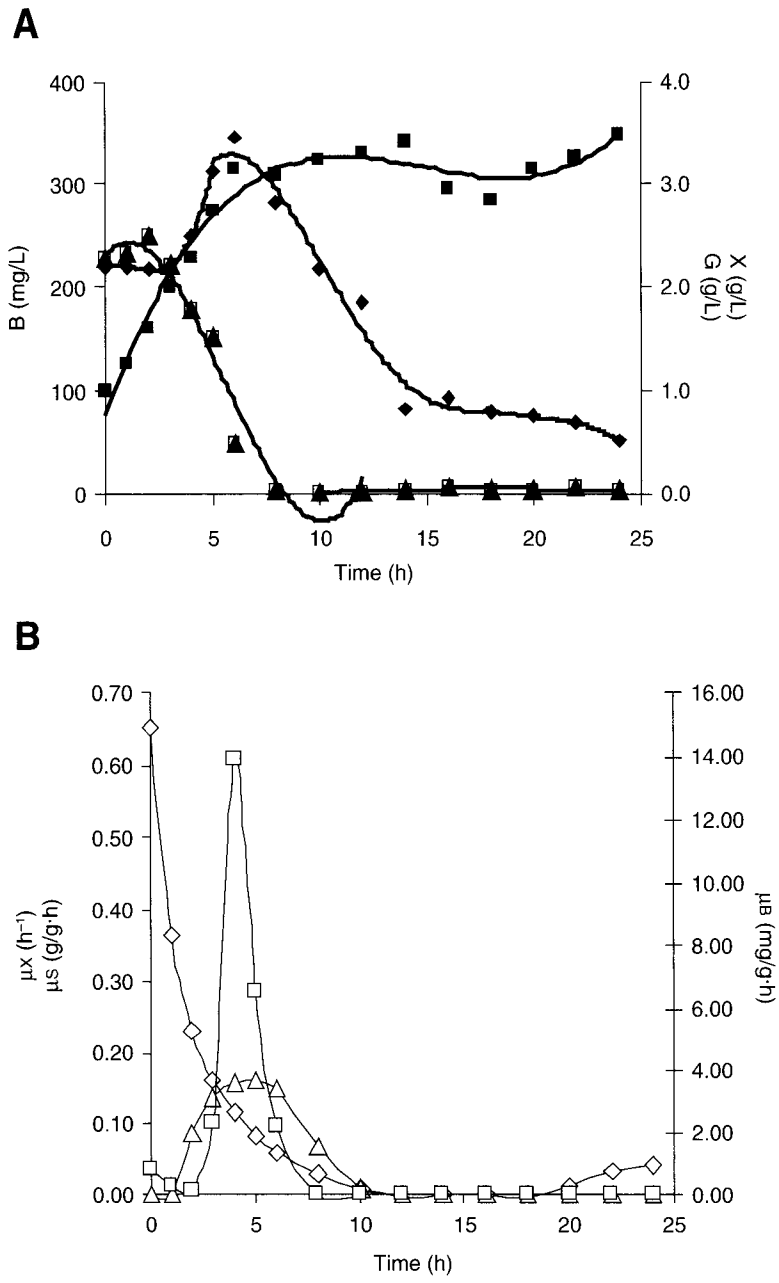


**Fig. 1.** Time behaviors of **(A)** the concentrations of (X-■) biomass, (G-▲) glucose, and (B-◆) biosurfactants and **(B)** the specific rates of growth ($\mu_X$-□), substrate consumption ($\mu_S$-△), and biosurfactant formation ($\mu_B$-◇) during the cultivation of *B. atrophaeus* ATCC 9372 on 2.5 g/L glucose and 10.0 g/L casein.

carbon source, when the concentration of glucose, the less-energy consuming substrate, decreased to less than 10.0 g/L. Casein uptake started at the beginning of the stationary phase preceding the diauxic phenomenon, then went on simultaneously to that of glucose (Fig. 3A, Table 1), and was

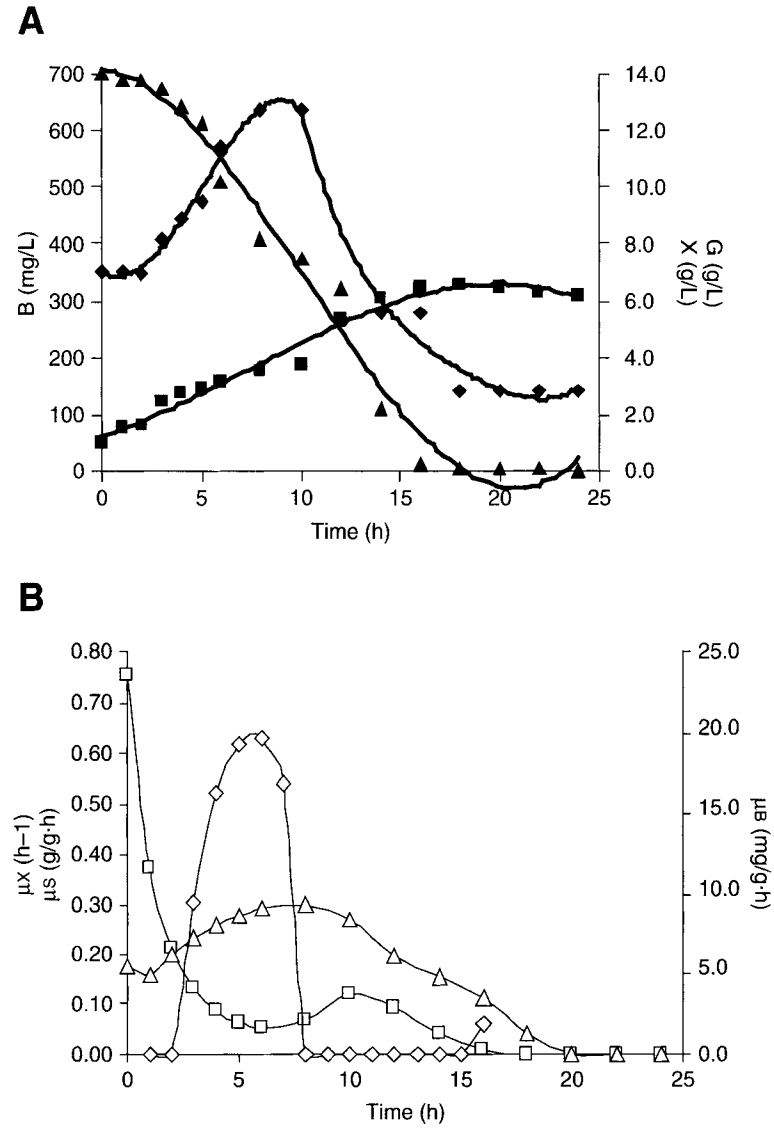


**Fig. 2.** Time behaviors of **(A)** the concentrations of (X-■) biomass, (G-▲) glucose, and (B-◆) biosurfactants and **(B)** the specific rates of growth ($\mu_X$-□), substrate consumption ($\mu_S$-△), and biosurfactant formation ($\mu_B$-◇) during the cultivation of *B. atrophaeus* ATCC 9372 on 14.0 g/L glucose and 10.0 g/L casein.

about fourfold that obtained at lower initial glucose levels (tests 1 and 2). Therefore, we can believe in the existence of a relationship between the metabolic change associated to casein consumption and diauxic growth, which resulted in a new phase of cell growth up to 22 h. This behavior is confirmed by the curves of Fig. 3B showing two different phases of cell growth at $G_0$ = 18.0 g/L and an intermediate interval of quick increase in the specific growth rate ($\mu_X$).

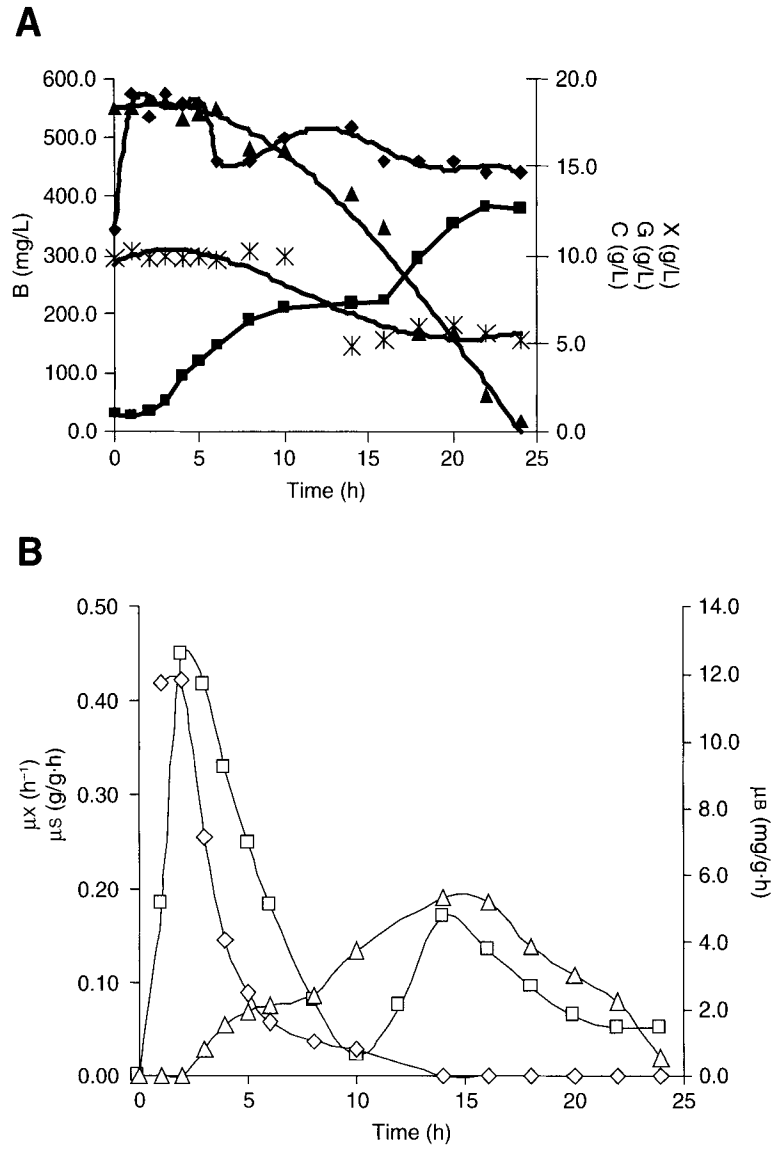


**Fig. 3.** Time behaviors of **(A)** the concentrations of (X-■) biomass, (G-▲) glucose, (B-◆) biosurfactants, and (C-*) casein and **(B)** the specific rates of growth ($\mu_X$-□), substrate consumption ($\mu_S$-△), and biosurfactant formation ($\mu_B$-◇) during the cultivation of *B. atrophaeus* ATCC 9372 on 18.0 g/L glucose and 10.0 g/L casein.

The simultaneous uptake of glucose and casein can explain the scarce consumption of biosurfactants, whose concentration in the extracellular medium decreased only by 135.0 mg/L from the beginning to the end of test 3 (Fig. 3A). This means that biosurfactants released by the cell almost stopped to be utilized as carbon and energy source, contrary to what it was observed at lower glucose levels (tests 1 and 2).

The significance of casein in the production of biosurfactants can be deduced from the results of tests 4 and 5, which were performed using only

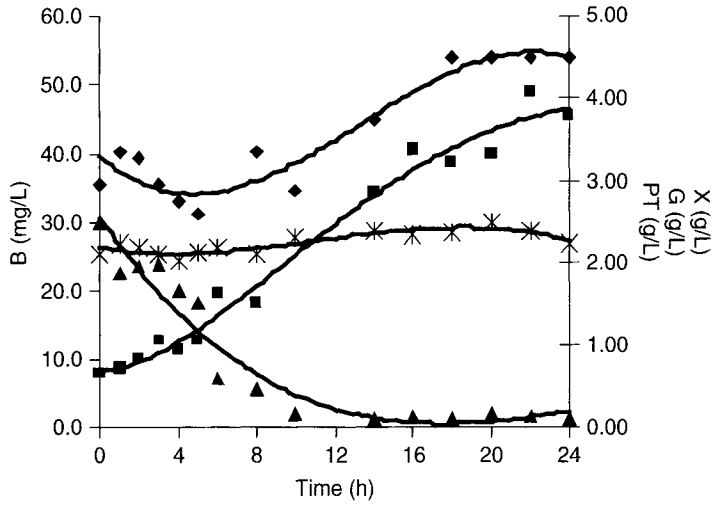


**Fig. 4.** Time behaviors of **(A)** the concentrations of (X-■) biomass, (G-▲) glucose, (B-◆) biosurfactants, and (PT-*) total extracellular proteins during the cultivation of *B. atrophaeus* ATCC 9372 on 2.5 g/L glucose without casein.

glucose as a carbon and energy source. As an example, comparing test 4 with test 1, the yield of biosurfactants on biomass did in fact dramatically decrease (by 75%) when using a medium lacking of casein. Figures 4 and 5, which deal with cultivations in the absence of casein performed at glucose concentrations of 2.5 and 5.0 g/L, respectively, show that the concentration of total extracellular proteins in the medium kept almost unvaried, hence demonstrating that soy flour was not utilized as energy source by the system. Moreover, at the higher glucose level a reduction of biosurfactant concentration was observed throughout the whole experiment. Although biosurfactants are products of primary metabolism, i.e., their formation is associated to cell growth, high-starting level of glucose as the only carbon and energy source did not favor their production. Therefore, the 25% increase in the concentration of total extracellular proteins, illustrated in Fig. 5, was likely the result of the synthesis of some other protein without surfactant activity.

Test 6 demonstrated the ability of the microorganism to adapt its metabolism to uptake casein as energy source. This change led to a lag phase period of 10 h before starting cell growth (Fig. 6A). Casein was consumed throughout the whole cultivation, bringing about a decoupling of the curves of the specific rates of growth ($\mu_x$) and substrate consumption ($\mu_S$) (Fig. 6B). Besides, the occurrence of diauxie is demonstrated by the presence of two separated exponential growth phases, i.e., two peaks of $\mu_x$ in Fig. 6B. Similar to the situation in which glucose and casein were simultaneously present in the medium, growth acceleration after diauxie was less marked with respect to the former peak at the beginning of the cultivation.

Comparison of the volumetric cell productivities ($P_x$) listed in Table 1 shows that, in cultivations performed with both nutrients at starting glucose

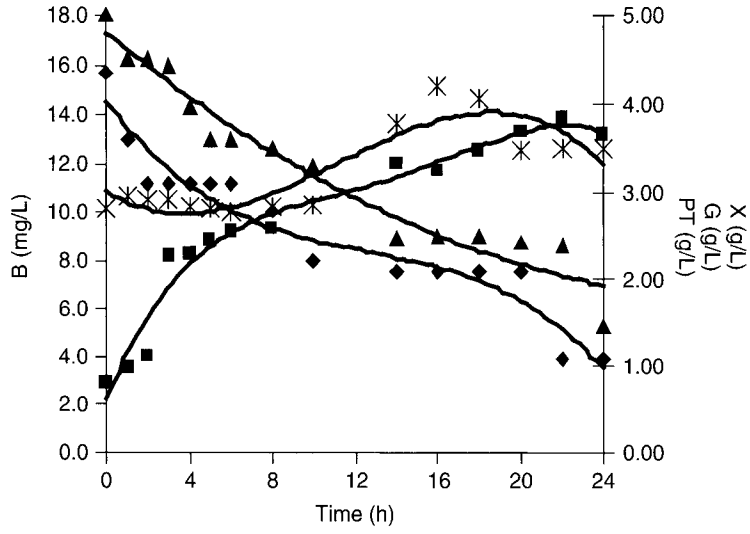


**Fig. 5.** Time behaviors of **(A)** the concentrations of (X-■) biomass, (G-▲) glucose, (B-◆) biosurfactants, and (PT-✳) total extracellular proteins during the cultivation of *B. atrophaeus* ATCC 9372 on 5.0 g/L glucose without casein.

level comparable with that of casein or less (tests 1–2), this parameter was almost the same as that obtained in the presence of casein alone (test 6), whereas a 27–37% increase was observed at the highest glucose level (test 3). Nevertheless, in the presence of casein as the only energy source, the microorganism exhibited higher yield of biomass on substrate ($Y_{X/S} = 3.71\ g_X/g_S$).

The release of biosurfactants started only after the lag phase (10 h), and deceleration of casein consumption ($\mu_s$) simultaneously took place (Fig. 6B). The possibility to metabolize casein can only be associated to the capability of the microorganism to synthesize and release extracellular proteases, mainly subtilisin, which also exhibits biosurfactant properties (*35*). Therefore, the behavior of Fig. 6A suggests coupling of subtilisin release and cell growth after diauxie. After 15 h of cultivation, the decrease in $\mu_S$ (Fig. 6B) did in fact occur together with certain maintenance of TP level (Fig. 6A), after the achievement of stationary growth phase. However, this condition appeared not to affect the synthesis of biosurfactants, as suggested by the continuous increase in their concentration along the whole cultivation. Resuming the addition of casein in a medium containing sugars and salts favored either the production or the stability of biosurfactants. The microorganism did in fact shift its metabolism to utilize the excess protein (casein) as a carbon source. The significance of the use of media containing both sugar and casein is associated to the possibility of maintaining high biosurfactant levels in environmental applications, even after the microorganism has entered the stationary growth phase.

As is well known, the major limitations in the application of biotechnologies to environmental applications are related to their high costs.

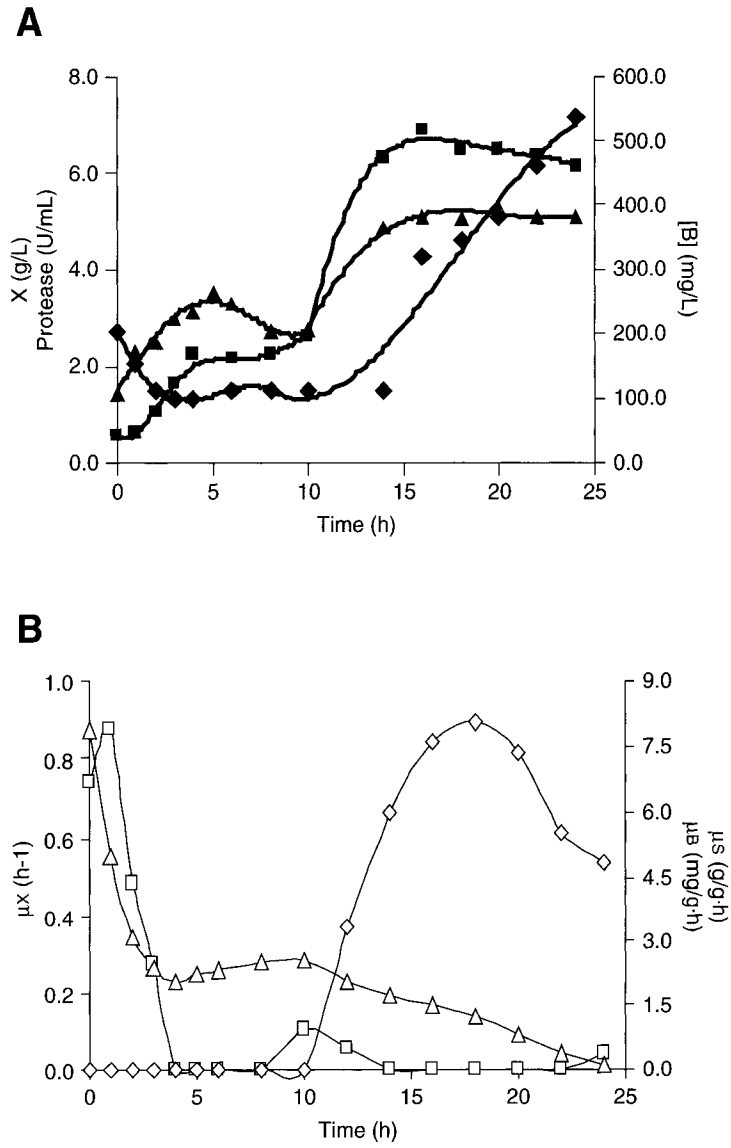


**Fig. 6.** Time behaviors of **(A)** the concentrations of (X-■) biomass, (▲) protease, and (B-◆) biosurfactants, and **(B)** the specific rates of growth ($\mu_X$-□), substrate consumption ($\mu_S$-△), and biosurfactant formation ($\mu_B$-◇) during the cultivation of *B. atrophaeus* ATCC 9372 on 10.0 g/L casein without glucose.

Among the possibilities to reduce them there is the substitution of synthetic media with natural media having almost the same nutritional composition and less purity. To this purpose, industrial residues could be used as alternative media for the production of biosurfactants to be used in environmental applications. Mixtures of sugars, salts, and casein can in fact be obtained from residual sources such as whey, after adjustment of the concentrations of the main ingredients to the best values previously determined in

synthetic medium. The next attempt will deal with (a) the use of whey as alternative medium for biosurfactant production by *B. atrophaeus* ATCC9372 cultivations and (b) the application of such a system to biotreatments in which relatively stable levels of biosurfactants are required.

## Conclusions

The inclusion of casein in a sugar-based medium for *B. atrophaeus* ATCC 9372 cultivation favored the synthesis and release of biosurfactants thanks to the ability of the microorganism to simultaneously metabolize them. The highest concentration of biosurfactants ($B_{max}$= 635.0 mg/L) was obtained in the presence of 14.0 g/L glucose and 10.0 g/L casein. Under these conditions, biosurfactants were released in the medium only during the exponential growth phase, after which they were metabolized. At the highest glucose level tested in this work (18.0 g/L), biosurfactants kept at high levels in the medium even after the microorganism entered its stationary growth phase. These results are promising for possible application of this biosystem to biological, enviromental applications.

## References

1. Banat, I. M. (1993), *Biotechnol. Lett.* **15,** 591–594.
2. Banat, I. M. (1995), *Biores. Technol.* **51(1),** 1–12.
3. Rosengerg, E. (1986), *CRC Crit. Rev. Biotechnol.* **3(2),** 109–132.
4. Peypoux, F., Bonmatin, J. M., and Wallach, J. (1999), *Appl. Microbiol. Biotechnol.* **51,** 553–563.
5. Haferburg, D., Hommel, R., Claus, R., and Kleber, H. P. (1986), *Adv. Biochem. Eng. Biotechnol.* **33,** 53–93.
6. Morikawa, M., Hirata, Y., and Imanaka, T. (2000), *Biochem. Biophys. Acta* **1488,** 211–218.
7. Noah, C. W., Shaw, C. I., and Ikeda, J. S. (2005), *J. Food Prot.* **68(4),** 680–686.
8. Cooper, D. G. (1986), *Microbiol. Sci.* **3(5),** 145–149.
9. Neves, L. C. M., Miyamura, T. T. M. O., Moraes, D. A., Vessoni-Penna, T. C., and Converti, A. (2006), *Appl. Biochem. Biotechnol.* **129(1–3),** 130–152.
10. Singh, P. and Cameotra, S. S. (2004), *Trends Biotechnol.* **22(3),** 142–146.
11. Vessoni-Penna, T. C., Ishii, M., Machoshvili, I. A., and Marques, M. (2002), *Appl. Biochem. Biotechnol.* **98–100,** 539–551.
12. Vessoni-Penna, T. C.., Ishii, M., Machoshvili, I. A., and Marques, M. (2002), *Appl. Biochem. Biotechnol.* **98–100,** 525–538.
13. Vessoni-Penna, T. C., Chiarini, E., Machoshvili, I. A., Ishii, M., and Pessoa, A., Jr. (2002), *Appl. Biochem. Biotechol.* **98–100,** 791–802.
14. Kosaric, N. (1992), In: *Biotechnology.* Rehm, H. J., Reed, G., Puhler, A., and Stadler, P. (eds.), vol. 6, VCH, Weinheim, pp. 659–717.
15. Lang, S. and Wullbrandt, T. (1999), *Appl. Microbiol. Biotechnol.* **51,** 22–32.
16. Makkar, R. S. and Comeotra, S. S. (1998), *J. Ind. Microbiol. Biotechnol.* **20,** 48–52.
17. Adamczak, M. and Bednarski, W. (2000), *Biotechnol. Lett.* **22,** 313–316.
18. Ferraz, C., De Araújo, A. A., and Pastore, G. M. (2002), *Appl. Biochem. Biotechnol.* **98–100,** 841–847.
19. Mukherjee, A. K. and Das, K. (2005), *FEMS Microbiol. Ecol.* **54,** 479–489.
20. Davis, D. A., Lynch, H. C., and Varley, J. (1999), *Enzyme Microb. Technol.* **25,** 322–329.
21. Patel, R. M. and Desai, A. J. (1997), *Lett. Appl. Microbiol.* **26,** 91–94.
22. Lang, S. and Wagner, F. (1987), *In: Biosurfaotants and Biotechnology.* Kosaric, N., Cairns, W. L., Gray, N. C. C. (Eds.), Surfactant Science Series, vol. 25, Marcel Dekker, NY, 247–331.

23. Nitschke, M. and Pastore, G. M. (2003), *Appl. Biochem. Biotech,* **105–108,** 295–301.
24. Petrus, J. C. C. Reutilização do soro de leite, CTC-UFSC, http://inventabrasilnet.t5.com.br/soro.htm (March 20, 2006).
25. Fall, R., Kinsinger, R. F., and Wheeler, K. A. (2004), *Syst. Appl. Microbiol.* **27,** 372–379.
26. Çalik, P., Çelik, E., Telli, I. E., Oktar, C., and Özdemir, E. (2003), *Enzyme Microb. Technol.* **33,** 975–986.
27. Kim, J. M., Lim, W. J., and Suh, H. J. (2001), *Process Biochem.* **37,** 287–291.
28. Neves, L. C. M., Pessoa, A. Jr., and Vitolo, M. (2003), *Braz. J. Pharm. Sci.* **39(3),** 160–163.
29. Neves, L. C. M., Pessoa, A. pJr., and Vitolo, M. (2005), *Biotechnol. Prog.* **21,** 1135–1139.
30. Rossi, F. G., Ribeiro, M. Z., Converti, A., Vitolo, M., and Pessoa, A., Jr. (2003), *Enzyme Microb. Technol.* **32,** 107–113.
31. Lowry, O. H., Rosebrough, N. J., Farr, A. L., and Randall, R. J. (1951), *J. Biol. Chem.* **193(1),** 265–275.
32. Ahamed, A., Singh, A., and Ward, O. P. (2006), *Process Biochem.* **41,** 789–793.
33. Shimogaki, H., Takeuchi, K., Nishino, T., et al. (1991), *Agric. Biol. Chem.* **55(9),** 2251–2258.
34. Prakash, M., Banik, R. M., and Koch-Brandt, C. (2005), *Appl. Biochem. Biotechnol.* **127(3),** 143–155.
35. Bognolo, G. (1999), *Coll. Surf. A: Physicochem. Eng. Aspects* **152,** 41–52.

0273-2289/1559-0291 (Online)/07/136–140/555–572/$30.00

# Evaluation of the pH- and Thermal Stability of the Recombinant Green Fluorescent Protein (GFP) in the Presence of Sodium Chloride

MARINA ISHII,*[,1] JULIANA SAYURI KUNIMURA,[1] HÉLIO TALLON JENG,[1] THEREZA CHRISTINA VESSONI PENNA,[1] AND OLIVIA CHOLEWA[2]

[1]*Department of Biochemical and Pharmaceutical Technology, School of Pharmaceutical Science, University of São Paulo, SP, Brazil, E-mail: marishii@usp.br; and* [2]*Molecular Probes, Inc., Eugene, OR, USA, 97402*

## Abstract

The thermal stability of recombinant green fluorescent protein (GFP) in sodium chloride (NaCl) solutions at different concentrations, pH, and temperatures was evaluated by assaying the loss of fluorescence intensity as a measure of denaturation. GFP, extracted from *Escherichia coli* cells by the three-phase partitioning method and purified through a butyl hydrophobic interaction chromatography (HIC) column, was diluted in water for injection (WFI) (pH 6.0–7.0) and in 10 m*M* buffer solutions (acetate, pH 5.0; phosphate, pH 7.0; and Tris-EDTA, pH 8.0) with 0.9–30% NaCl or without and incubated at 80–95°C. The extent of protein denaturation was expressed as a percentage of the calculated decimal reduction time (*D*-value). In acetate buffer (pH 4.84 ± 0.12), the mean *D*-values for 90% reduction in GFP fluorescence ranged from 2.3 to 3.6 min, independent of NaCl concentration and temperature. GFP thermal stability diluted in WFI (pH 5.94 ± 0.60) was half that observed in phosphate buffer (pH 6.08 ± 0.60); but in both systems, *D*-values decreased linearly with increasing NaCl concentration, with *D*-values (at 80°C) ranging from 3.44, min (WFI) to 6.1 min (phosphate buffer), both with 30% NaCl. However, *D*-values in Tris-EDTA (pH 7.65 ± 0.17) were directly dependent on the NaCl concentration and 5–10 times higher than *D*-values for GFP in WFI at 80°C. GFP pH- and thermal stability can be easily monitored by the convenient measure of fluorescence intensity and potentially be used as an indicator to monitor that processing times and temperatures were attained.

**Index Entries:** Bioindicator; *D*-value; green fluorescent protein; pH-stability; sodium chloride; thermal stability.

*Author to whom all correspondence and reprint requests should be addressed.

## Introduction

The green fluorescent protein (GFP), is an acidic (p*I* 4.9–5.1) thermostable protein that can be expressed in a wide variety of organisms, in vivo, or in cell cultures. It is used extensively to monitor biological events in a variety of experimental applications as well as a biosensor to monitor industrial and medical processes to ensure product quality or process efficacy. Water activity ($a_w$), which is defined as the ratio of the vapor pressure of water in a material to the vapor pressure of pure water at the same temperature *(1)*, has become a useful determinant of food stability to measure potential microbial growth and, together with temperature and pH, is one of the major parameters influencing bacterial growth and survival. Water activity is related to solute species and concentration and their effects on microbial growth and protein stability *(1,2)*. Therefore, $a_w$, which is a measure of the energy status of the water in a system, can be influenced by several factors. Colligative effects of dissolved species (e.g., salt or sugar) interact with water through dipole–dipole, ionic, and hydrogen bonds *(1,2)*. Electrostatic interactions between charged groups on a protein surface are often modified by the presence of salts in the solution. Salt ions are highly mobile and compact units of charge, compared with the amino acid side chains and thus, compete effectively for charged sites on the protein. In this manner, electrostatic interactions among amino acid residues on the protein surface might be shielded by high concentrations of salts and these interactions impact protein stability.

The minimal water activity with glycerol or sodium chloride (NaCl) added to the medium was evaluated for various microorganisms *(3)*. For several microorganisms, glycerol is less inhibitory than NaCl, but in the case of *Staphylococcus aureus*, NaCl is less inhibitory than glycerol. *S. aureus* is known to be the most halo-tolerant nonhalophilic eubacterium that can grow at $a_w$-values as low as 0.86 (around 20% NaCl) *(4)* owing to its highly effective transport systems. With added sucrose or NaCl, microbial growth is affected not only by the reduction of water activity but also to specific molecular and/or ionic interactions.

The antimicrobial effects of brine solutions on the survival characteristics of nonspore forming bacteria at $a_w$ from 0.90 (15% NaCl) to 0.75 (30% NaCl) were analyzed in other studies. Gram-positive bacteria were less sensitive to lowered $a_w$ than Gram-negative bacteria, as observed: (1) there was a decrease of one log reduction of *Salmonella* sp. after 3 d at 0.75 $a_w$; (2) 0.14 $\log_{10}$ colony forming unit/g/d decrease at 20°C and 0.90 $a_w$ in salami, and 4.40 $\log_{10}$ colony forming unit/g/d reduction in starch for *Escherichia coli* O157:H7, and, (3) 5 log-cycles reduction in 7 d at 0.91 $a_w$ for *Listeria monocytogenes* cultivated in trypticase soy broth (TSB) yeast extract (YE) and TSB-YE supplemented with NaCl *(3)*.

In the presence of NaCl the thermal stability of thermolysin, a metalloproteinase produced by *Bacillus thermoproteolyticus*, was enhanced, dependent

on the salt concentration. The enzyme's catalytic activity also improved, which can be related to the electrostatic interaction between thermolysin and ions in the medium *(5)*. The activity was enhanced 13–15 times with 4 *M* NaCl (around 25–30% NaCl) at 25°C, pH 7.0 *(6)*. The thermal unfolding of lysozyme, α-chymotrypsinogen A, and yeast alcohol dehydrogenase in aqueous solution showed that water activity ($a_w$) determined the extent of change in the stability of these proteins and the solvent influenced the direction of the change *(7)*. The effect of unfolding was not evaluated for GFP in this study, but these studies show that solutes and $a_w$ significantly influence protein stability.

The evaluation of GFP thermal stability in brine solutions of up to 30% NaCl allows us to study the behavior of this protein for use as a biosensor in the thermal processing of parenteral solutions (solutions from 0.9 to 20% NaCl or KCl), foods (pasteurization and blanching), and their disposal as effluents into waterways, as well as in the study of halophilic bacteria. GFP thermal stability is dependent on pH and temperature as well as the concentration of ions in the solvent system. The aim of this work was to determine the thermal stability of extracted, purified GFP by heating aqueous solutions with NaCl concentrations ranging from 0.9 (physiological saline) to 30% with $a_w$ ranging from 0.75 to 1.00. This work evaluates the potential utility of GFP as a biosensor for moist-heat treatments, environmental diagnosis, and bioremediation purposes.

## Materials and Methods

### *Green Fluorescent Protein*

The expression of recombinant GFP by *E. coli* DH5-α, the extraction and purification of GFP have been outlined in previous experiments *(8–12)*. GFP fluorescence intensity was measured in a spectrofluorometer ($\lambda_{Excitation}$ = 394 nm, $\lambda_{Emission}$ = 509 nm) (RF 5301 PC; Shimadzu Corporation, Kyoto, Japan). Purified recombinant GFP (95% purity, Clontech Laboratories, Palo Alto, CA) was used to generate a standard curve to determine three-phase partitioning-extracted GFP concentration related to fluorescence intensity in Eq. 1:

$$(I) = 134.64 + 103.61 \times (\text{GFP } \mu\text{g / mL}) \quad R^2 = 0.98 \tag{1}$$

### *Buffer Solutions*

To study GFP pH- and thermal stability, solutions with 0.9 to 30% NaCl (w/v) were prepared in: (1) 10 m*M* sodium acetate/acetic acid buffer (pH 5.0), (2) 10 m*M* potassium phosphate buffer (monobasic/dibasic; pH 7.0), (3) 10 m*M* Tris-EDTA buffer (pH 8.0), and (4) water for injection ("WFI," from the Milli-Q system, Millipore®, Bedford, MA). Buffered solutions and WFI without NaCl were the controls for each system. A defined weight of NaCl (99.5% purity) was diluted in each buffer solution or WFI. After

complete dissolution, the solution was transferred to a 250-mL volumetric flask and the volume was adjusted. The solutions were filter-sterilized (Millipore 0.22 μm membrane), transferred to sterile flasks and stored at 4°C until use. To monitor contamination, 1 mL of each solution, before and after filtration, was plated (plate count agar) and incubated at 35–37°C for 24 h.

### *Sample Preparation for GFP Stability Determination*

To each 4.9 mL of buffered solution or WFI at 25°C, 100 μL three-phase partitioning-extracted GFP (concentration around 400.0 μg/μL) was added to provide a final concentration of 8.0–10.0 μg/mL. GFP fluorescence intensity and pH were measured before heating, immediately after heating, and after storing samples for 24 h at 4°C. Immediately on the addition of GFP into the buffered or WFI solutions, the mixture was gently stirred for 30 s, placed into the cuvet and incubated at a constant temperature of 80, 85, 90, or 95°C. All fluorescence intensities and pH readings of the samples before and after heat treatment were recorded with the solutions at 25°C.

A 2-mL aliquot of sample was transferred to a quartz cuvet (1 cm light path length × 45 mm height) and sealed with a plastic cover. Each cuvet was inserted into an adapter assembly and adjusted in the cell holder. A constant temperature (±0.05°C) was maintained by continuous circulation of water from the water bath to the cell holder and the sample in the cuvet through a circulation pump (Thermo-bath TB-85, P/N 200-65022, Shimadzu Corporation). The moment the sample-filled cuvet was placed in the cell holder and the treatment was initiated, fluorescence readings were recorded at intervals of 5 s with the samples incubated at a constant 80, 85, 90, or 95°C for 1.5 h. With all samples starting at 25°C before heating, the 2 mL sample volume attained the final assay temperatures of 80 or 85°C after 20–30 s, and attained a final 90 or 95°C in 10 s. All samples were tested in triplicate.

### *Analysis of the Kinetic Parameters*

#### Thermal Treatment

The extent of protein denaturation was evaluated by measuring the loss of fluorescence intensity over time for GFP exposed at temperatures ranging from 80 to 95°C and converted to denatured GFP concentrations (μg/mL). The GFP fluorescence data provided curves that were considered first order models represented by $\mathrm{Log}_{10} I_f = \mathrm{Log}_{10} I_o - (1/D) \times t$ where $I_o$ was the initial fluorescence intensity of native GFP and $I_f$ was the final fluorescence intensity of remaining native GFP, after the exposure time (min) at a constant temperature of either 80, 85, 90, or 95°C. The decimal reduction time, ($D$-value = k/2.303), the interval of time required to reduce one decimal logarithm of the initial fluorescence intensity of GFP at reference temperature, was determined from the negative reciprocal of the slopes of the regression lines, using the linear portions of the inactivation curves ($\log_{10}$ fluorescence

intensity GFP/mL vs incubation time at a constant temperature). The *z*-value may be related to the coefficient $Q_{10}$ of the process by Eq. 2:

$$Q_{10} = \left(10^{10/z}\right) \tag{2}$$

Activation energy ($E_a$, kcal/mol), represents the energy present in a system, the energy necessary to destabilize a system and can be defined using the Arrhenius equation 3:

$$\mathrm{Log}_{10}k_1 = \mathrm{Log}_{10}k_2 - \left\{\left(E_a / 2.303 \times R\right)\left[\left(1/T\right) - \left(1/T\right)\right]\right\} \tag{3}$$

where $T_1$ and $T_2$ are the incubation temperatures in degrees Kelvin (K), $R$ is the universal gas constant (1.987 cal × mol/K) and $k$ is the inactivation rate constant.

## Results and Discussion

The extent of protein denaturation was expressed as a percentage of the calculated *D*-value; the interval of time required for a 90% reduction, or one decimal logarithm of the initial fluorescence intensity of GFP. The denaturation of GFP in NaCl solutions, as measured by the loss of fluorescence intensity, was expressed in the decimal logarithm of the decrease in native GFP concentration vs the incubation time at a constant temperature. To estimate *D*-values at constant heating temperatures and pH, the range of native GFP concentrations evaluated was between 10.0 μg/mL for initial concentration ($C_o$) to 2.0 μg/mL for final concentrations ($C_f$), which corresponded to the linear portion of the inactivation curves ($\log_{10}$ fluorescence intensity GFP/mL vs incubation time at a constant temperature). Table 1 shows *D*-values obtained for GFP diluted in WFI, acetate, phosphate, and Tris-EDTA buffered solutions incubated at 80, 85, 90 and 95°C, respectively.

### *Evaluation of pH for GFP in Sodium Chloride Solutions*

The pH of GFP in the NaCl solutions was measured at room temperature (25°C) with mean values: (1) pH 7.65 (±0.17) in Tris-EDTA buffer (pH 8.0); (2) pH 6.08 (±0.60) in phosphate buffer (pH 7.0); and (3) pH 4.84 (±0.12) in acetate buffer (pH 5.0). The mean pH for WFI was 5.94 (±0.60) (Table 1).

### *Loss of Fluorescence Intensity Before Heating GFP in Solution*

The loss of initial GFP fluorescence intensity at 25°C immediately after diluting into the buffered or WFI solutions was dependent on the NaCl concentration and the composition of the solution. The maximum loss of fluorescence was observed for solutions with 30% NaCl in acetate buffer (94.5% loss in fluorescence intensity). Solutions prepared in Tris-EDTA buffer provided optimal conditions for GFP stability, with a maximum loss of 25% fluorescence intensity in solutions with up to 30% NaCl. In WFI or in phosphate buffer with up to 30% NaCl, a 70% drop in fluorescence intensity was

Table 1
*D*-Values for GFP in NaCl Solutions[a]

| | | | pH | | *D*-values (min) | | | |
|---|---|---|---|---|---|---|---|---|
| | NaCl (%) | [b]$a_w$ | Initial | 24 h | 80°C | 85°C | 90°C | 95°C |
| Tris-EDTA | 0 | 0.99 | 7.89 | 8.07 | 24.88 | 8.7 | 5.02 | 3.82 |
| | 0.9 | 0.99 | 7.90 | 7.90 | 37.04 | 9.88 | 6.12 | 4.81 |
| | 5 | 0.98 | 7.73 | 7.79 | 40.00 | 11.61 | 6.54 | 4.83 |
| | 10 | 0.918 | 7.63 | 7.62 | 49.26 | 9.73 | 7.17 | 5.14 |
| | 15 | 0.885 | 7.54 | 7.54 | 65.79 | 14.71 | 6.75 | 5.12 |
| | 20 | 0.845 | 7.50 | 7.48 | 52.63 | 18.12 | 6.78 | 5.26 |
| | 25 | 0.795 | 7.51 | 7.49 | 46.95 | 15.22 | 7.96 | 5.45 |
| | 30 | 0.759 | 7.48 | 7.48 | 33.78 | 13.30 | 7.26 | 5.08 |
| | Mean | – | 7.65 | 7.67 | – | – | 6.94 | 5.10 |
| | [c]SD | – | 0.17 | 0.23 | – | – | 0.59 | 0.23 |
| WFI | 0 | 0.99 | 6.63 | 6.47 | 13.85 | 4.64 | 3.46 | 3.21 |
| | 0.9 | 0.99 | 6.99 | 6.72 | 20.12 | 8.29 | 5.42 | 4.55 |
| | 5 | 0.98 | 6.12 | 6.10 | 8.26 | 5.67 | 3.49 | 3.19 |
| | 10 | 0.918 | 5.86 | 5.75 | 5.74 | 4.34 | 2.46 | 5.48 |
| | 15 | 0.885 | 5.66 | 5.63 | 4.75 | 3.78 | 2.76 | 2.44 |
| | 20 | 0.845 | 5.53 | 5.54 | 4.21 | 3.56 | 2.59 | 2.3 |
| | 25 | 0.795 | 5.42 | 5.46 | 3.58 | 3.21 | 2.43 | 2.14 |
| | 30 | 0.759 | 5.30 | 5.40 | 3.44 | 2.91 | 2.32 | 2.37 |
| | Mean | – | 5.94 | 5.88 | – | – | – | – |
| | SD | – | 0.60 | 0.49 | – | – | – | – |
| Phosphate | 0 | 0.99 | 7.08 | 7.05 | 40.32 | 9.28 | 5.52 | 4.38 |
| | 0.9 | 0.99 | 6.77 | 6.81 | 35.34 | 10.34 | 6.15 | 4.78 |
| | 5 | 0.98 | 6.33 | 6.29 | 21.19 | 10.39 | 5.41 | 4.64 |
| | 10 | 0.918 | 6.01 | 6.01 | 14.25 | 9.46 | 5.55 | 4.82 |
| | 15 | 0.885 | 5.80 | 5.81 | 11.57 | 8.49 | 4.87 | 4.21 |
| | 20 | 0.845 | 5.6 | 5.68 | 8.79 | 7.45 | 5.13 | 4.14 |
| | 25 | 0.795 | 5.49 | 5.45 | 6.99 | 6.84 | 4.5 | 4.02 |
| | 30 | 0.759 | 5.43 | 5.38 | 6.10 | 6.51 | 4.49 | 4.03 |
| | Mean | – | 6.08 | 6.06 | – | – | 5.16 | 4.38 |
| | SD | – | 0.60 | 0.61 | – | – | 0.60 | 0.36 |
| Acetate | 0 | 0.99 | 5.05 | 5.05 | 4.08 | 3.12 | 2.42 | 2.68 |
| | 0.9 | 0.99 | 5.00 | 5.00 | 3.82 | 3.44 | 3.03 | 3.04 |
| | 5 | 0.98 | 4.89 | 4.87 | 3.72 | 2.90 | 2.52 | 2.11 |
| | 10 | 0.918 | 4.82 | 4.80 | 3.47 | 3.38 | 2.12 | 1.83 |
| | 15 | 0.885 | 4.80 | 4.78 | 3.08 | 2.50 | 2.51 | 2.17 |
| | 20 | 0.845 | 4.76 | 4.75 | – | – | 3.32 | 3.30 |
| | 25 | 0.795 | 4.75 | 4.74 | – | – | – | – |
| | 30 | 0.759 | 4.71 | 4.69 | – | – | – | – |
| | Mean | – | 4.84 | 4.83 | – | – | – | – |
| | SD | – | 0.12 | 0.13 | – | – | – | – |

[a]WFI, water for injection; acetate 10 m*M*; phosphate 10 m*M*; Tris-EDTA 10 m*M* buffers, at 80, 85, 90, and 95°C, respectively.
[b]$a_w$, water activity.
[c]SD, standard deviation at $p < 0.05$.

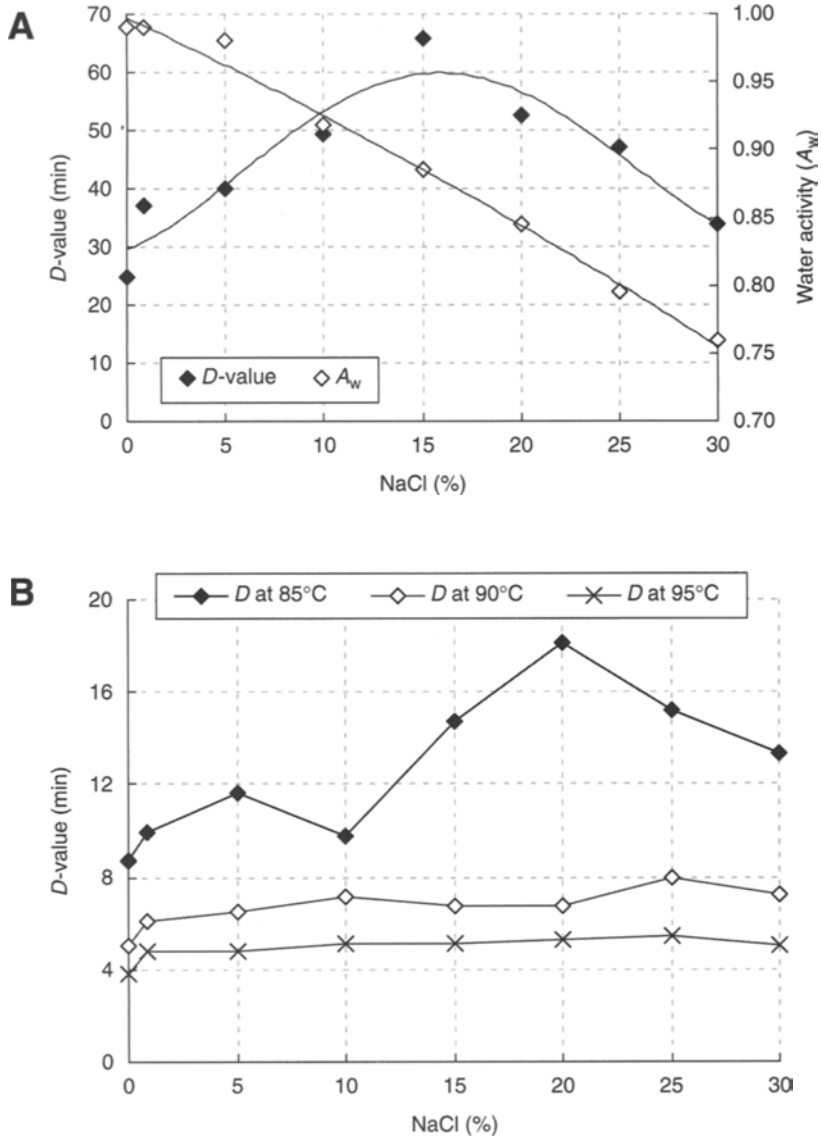


**Fig. 1.** *D*-value behavior for GFP in Tris-EDTA buffer 10 m*M* at: **(A)** 80°C (bell-shaped, -♦-) and **(B)** 85°C (-♦-), 90°C (-◊-), and 95°C (-×-).

observed. These results confirm that the presence of salts can affect GFP stability, altering either its structure or propensity for self-aggregation, which in these samples did not develop to any visible precipitation.

## *Thermal Stability of GFP in Tris-EDTA (pH 7.65 ± 0.17) Buffered Solutions*

The pH of Tris-EDTA buffered solutions were relatively constant (pH 7.65 ± 0.17) and independent of the solute added (with up to 30% NaCl, Table 1). At 80°C, GFP showed increasing stability in NaCl solutions

(Fig. 1A) with the maximum *D*-value of 65.79 min with 15% NaCl, less than 2- to 2.5-fold greater than the control (*D* = 24.88 min), 0.9% NaCl (37.04 min) and 30% NaCl (33.78 min).

The *D*-value for GFP in Tris-EDTA/0.9% NaCl at 80°C (37.04 min) was comparable to phosphate buffer (pH 6.77 ± 0.01), 1.8-fold greater than in WFI (pH 6.99 ± 0.21) and 10-fold greater than in acetate buffer (pH 5.0; *D*-value = 3.82 min) at the same salt concentration (0.9% NaCl). At 85°C, ≥10% NaCl provided an equivalent thermal stability (mean *D*-value = 10.40 min) relative to the control (8.70 min). The highest *D*-value was attained for 20% NaCl (18.12 min). At 90°C and 95°C, GFP thermal stability was independent of the solute concentrations, but related to temperature, providing mean $D_{90°C}$ = 6.94 (±0.59) min and $D_{95°C}$ = 5.10 (±0.23) min, respectively for the same solution.

GFP thermal stability improved with the addition of 15–20% NaCl, wherein the highest *D*-value was observed at 80°C (65.79 min) and dropped 3.6-fold at 85°C (18.12 min). In contrast, the mean *D*-value decreased 9.5-fold at 90°C (mean 6.94 min) and 13-fold at 95°C (mean 5.10 min), highlighting the dependence at higher temperatures (Fig. 1B). At 90°C and 95°C, GFP showed the same thermal stability in phosphate and Tris-EDTA buffered solution, showing that GFP thermal stability was related to solution composition. In this case, buffer composition was not the main factor involved with thermal stability.

In our previous work, the presence of NaCl into solutions improved GFP thermal stability compared with glucose solutions made with the same buffers used in this work *(11)*. The buffered glucose/NaCl solutions at pH 7.0 provided the highest *D*-values ($D_{90°C}$ = 6.52 min and $D_{95°C}$ = 4.93 min), equivalent for glucose/Tris-EDTA buffered solution (pH 8.0; $D_{90°C}$ = 6.64 min and $D_{95°C}$ = 5.20 min), for the same concentration of glucose, proving that the addition of glucose and NaCl in the same solution affected GFP thermal stability favorably.

### *Stability of GFP in Phosphate (pH 6.08 ± 0.60) Buffered Solutions*

In phosphate buffer at 80°C, the *D*-value for GFP in the control (40.32 min) dropped 14% in 0.9% NaCl, and half in 5% NaCl (21.19 min). The *D*-value varied linearly with the pH of the phosphate-buffered solutions, according to the Eq. 4:

$$D\text{-value} = 21.578 \times \text{pH} - 113.05 \quad (R^2 = 0.98) \tag{4}$$

For solutions with 0.9% NaCl in phosphate buffer (pH 6.77) and Tris-EDTA (pH 7.90), the *D*-values at 80°C were similar, 35.34 and 37.04 min, respectively. At 80°C, *D*-values changed exponentially with NaCl concentration, and were related by the Eq. 5:

$$\text{Log}_{10}\ D\text{-values} = -0.0271 \times [\text{NaCl}(\%)] + 1.5172 \ (R^2 = 0.95) \quad (5)$$

This exponential relation between *D*-value and NaCl concentration shows that for every interval of NaCl concentration, the *D*-value will change 10-fold. For example, the addition of 30% NaCl lowered the $a_w$ from 1.00 to 0.759, which shows less available water at the GFP surface, promoting aggregation of the protein and the loss in fluorescence intensity from both aggregation and denaturation. At 85°C and 90°C, *D*-values related directly with NaCl concentration, by the Eqs. 6 and 7:

$$\text{Log}_{10}\ D\text{-values}\ (85°\text{C}) = -0.1617 \times [\text{NaCl}(\%)] + 11.02 \ (R^2 = 0.97) \quad (6)$$

$$\text{Log}_{10}\ D\text{-values}\ (90°\text{C}) = -0.0523 \times [\text{NaCl}(\%)] + 5.95 \ (R^2 = 0.94) \quad (7)$$

For every 5% increase in NaCl, the *D*-value dropped 10% at 85°C and 5% at 90°C. At 90°C and 95°C, the mean *D*-values were respectively 5.16 ± 0.60) min and 4.38 (±0.36) min, both independent of NaCl concentration and pH. The mean *D*-values at 90°C for GFP in phosphate-buffered solutions (pH = 6.08 ± 0.60) were comparable to the mean *D*-value (5.10 ± 0.23 min) in Tris-EDTA (pH 7.65 ± 0.17). In phosphate buffer (pH 6.08 ± 0.60), although pH decreased with increasing NaCl concentration, this buffer system favored GFP thermal stability compared with WFI solutions, whereby the drop in *D*-values were at least double at comparable pH (Fig. 2).

### *Stability of GFP in WFI (pH 5.88 ± 0.49)*

The initial pH of the WFI solutions dropped with up to 30% NaCl, from pH 6.99 to 5.30, for a mean of pH 5.94 (±0.60), but was stable around a pH 5.88 (±0.49) after 24 h storage at 4°C. Similar changes in pH were observed in the phosphate-buffered solutions, reinforcing the observation that buffer composition was not the main factor responsible for the drop in pH with increasing NaCl concentration. The *D*-values for GFP at 80°C can be considered linearly dependent on the pH by the Eq. 8:

$$D\text{-values} = 9.6865 \times \text{pH} - 49.52 \ (R^2 = 0.95) \quad (8)$$

Through the analysis of the angular coefficients (θ), the dependence of WFI solutions on pH was observed to be twice lower than that determined (θ = 21.578, Eq. 2) for GFP in phosphate-buffered solutions with up to 30% NaCl. *D*-values were also shown to decrease exponentially with increasing NaCl of up to 30% in WFI, owing to the drop in pH in these solutions. The remarkable influence of pH on GPF thermal stability at 80°C can be represented by the Eq. 9:

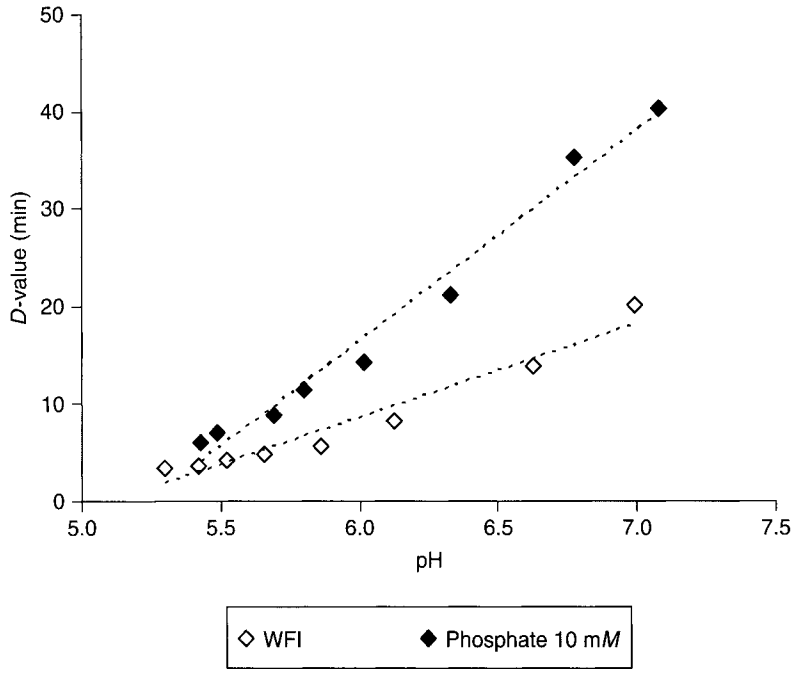


**Fig. 2.** *D*-value for GFP related to the pH solution in WFI (-◊-), (*D*-value is 9.6865 × pH –49.52, $R^2$ is 0.95) and phosphate 10 m*M* (-♦-), (*D*-value is 21.578 × pH –113.05, $R^2$ is 0.98), at 80°C.

$$\mathrm{Log}_{10} D = 0.147 \times \mathrm{pH} - 1.96 \left(R^2 = 0.997\right) \quad (9)$$

The *D*-value for the control (13.85 min) was close to 0.9% NaCl (20.12 min), fell by half with 5% NaCl (8.26 min) and fivefold in the presence of 25–30% NaCl in WFI ($\mathrm{mean}_{25\text{–}30\%}$ = 3.51 min; Table 1). At 85, 90, and 95°C, the presence of 0.9% NaCl in WFI favored GFP thermal stability, with the *D*-values of 8.29, 5.42, and 4.55 min, respectively. The *D*-values for GFP for concentrations ≥10% of NaCl were comparable to the control.

## *Stability of GFP in Acetate-Buffered Solutions (pH 4.84 ± 0.12)*

In acetate-buffered solutions the mean pH of 4.84 ± 0.12 was close to the p*I* for GFP (p*I* = 4.9-5.1) and remarkably, lowered GFP thermal stability independent of either NaCl concentration or temperature. In this case, the addition of solutes did not influence GFP thermal stability compared with the control for every temperature studied, up to 15% NaCl between 80–85°C and up to 20% NaCl between 90–95°C. There was a slight tendency for *D*-values to drop at 80–85°C from the control and up to 15% NaCl (at 80°C, $D_{\mathrm{control}}$ = 4.08 min; $D_{15\%}$ = 3.08 min and at 85°C, $D_{\mathrm{control}}$ = 3.12 min; $D_{15\%}$ = 2.5 min). However, between 90 and 95°C, a drop in *D*-values from 0.9% NaCl (3.03 and 3.04 min, respectively) to 10% NaCl (2.12 and 1.83 min) increased to a mean *D* = 3.3 min in up to 20% NaCl, corresponding to an $a_w$ = 0.845 (Fig. 3).

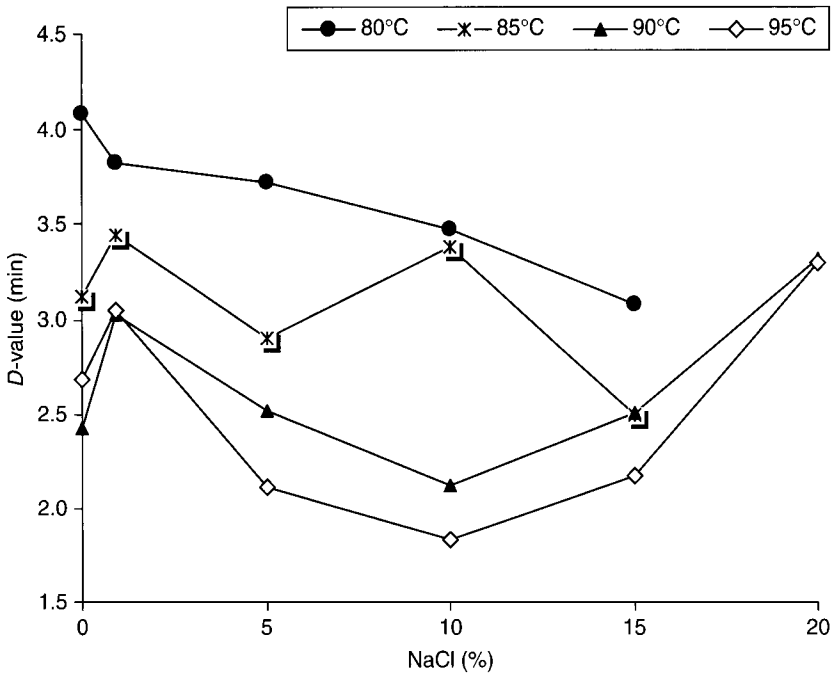


**Fig. 3.** *D*-value behavior for GFP in acetate buffer 10 m*M* at 80°C (-●-), 85°C (-*-), 90°C (-▲-), and 95°C (-◊-).

## *Kinetic Parameters z-Value, $Q_{10}$ Coefficients, and Activation Energy*

The kinetic parameters, *z*-value and the related $Q_{10}$ coefficient ($Q_{10} = 10^{10/z}$), reflect the temperature dependence of GFP denaturation (as measured by fluorescence intensity decrease) subjected to the heating in solutions of different composition (Fig. 4A). The greater the *z*-value, the more stable GFP is in the system.

### z-Value

For the range of temperatures from 80 to 95°C for the controls, solutions without NaCl, the *z*-values varied from: (1) $z$ = 24.63°C in WFI; (2) $z$ = 75.76°C in acetate buffer; (3) $z$ = 16.03°C in phosphate buffer, and (4) $z$ = 18.66°C in Tris-EDTA. For the same range of temperatures and the interval of NaCl concentrations, between 0.9 and 30% NaCl, *z*-values varied from: (1) $z$ = 23.58–85.47°C for solutions in WFI; (2) $z$ = 142.86–109.89°C in acetate buffer; (3) $z$ = 17.67–71.43°C in phosphate buffer, and (4) $z$ = 17.45–18.32°C in Tris-EDTA solutions.

*z*-Values of the systems delineated GFP behavior in the temperature interval from 80 to 95°C. Tris-EDTA influenced the system the least with the addition of NaCl, with *z*-value (mean = 16.16 ± 1.6°C) unchanged with up to 30% NaCl. WFI and phosphate-buffered systems exhibited the positive influence of NaCl on GFP thermal stability. The *z*-values were linearly

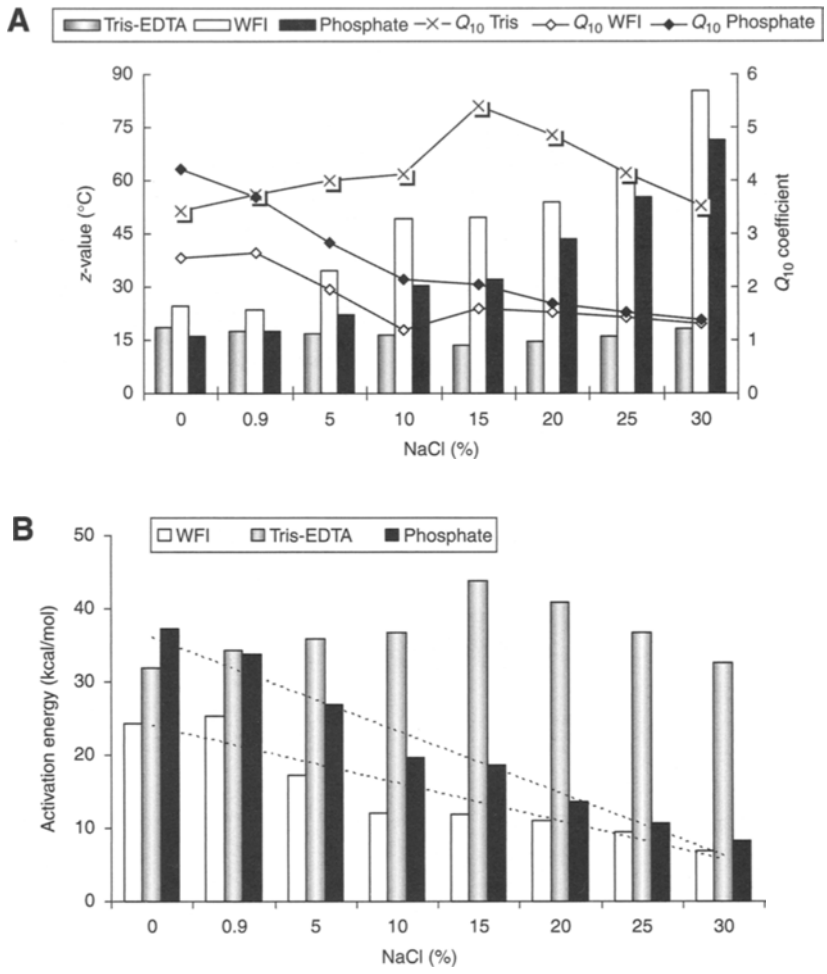


**Fig. 4.** Kinetic parameters for GFP in WFI, phosphate buffer 10 m*M*, and Tris-EDTA buffer 10 m*M* systems at the interval from 80 to 95°C: **(A)** *z*-value (°C) and **(B)** $E_a$ (kcal/mol) and $Q_{10}$ coefficient.

dependent with increasing NaCl concentration in WFI and phosphate-buffered solutions by the relations: (1) *z*-value (°C) = 1.7962 × (NaCl, %) = 24.288, $R^2 = 0.93$ and (2) *z*-value (°C) = 1.7028 × (NaCl, %) + 13.535, $R^2 = 0.95$, respectively.

## $Q_{10}$-Coefficient

For the range of temperatures from 80 to 95°C, the GFP $Q_{10}$ *coefficients* shifted from: $Q_{10}$ = 2.55, $Q_{10}$ = 1.36, $Q_{10}$ = 4.21, and $Q_{10}$ = 3.44 in WFI, acetate, phosphate, and Tris-EDTA buffered control solutions, respectively. With the addition of NaCl and GFP, acetate-buffered solutions exhibited less influence from external conditions, a stable system with $Q_{10}$ varying from 1.36 to 1.23 for the interval up to 15% of NaCl. The Tris-EDTA buffered system provided optimal conditions for GFP stability for the range of

increasing temperatures with $Q_{10}$ coefficients ranging from 3.44 to 5.41, for the control and 15% NaCl. Comparing z-values, acetate buffer provided the most uniform system for GFP ($Q_{10} < 1.5$), as well as WFI systems with more than 10% NaCl, and phosphate-buffered solutions with more than 20% NaCl. WFI and phosphate buffer (pH 7.0) up to 5% and between 5 and 15% NaCl respectively, provided intermediate stability ($1.5 < Q_{10} < 3.5$). Tris-EDTA buffered solutions (pH 8.0; $3.5 < Q_{10} < 6.0$) showed that GFP can be less affected by external influences.

### Activation Energy

The parameter $E_a$ is related to the intrinsic energy of the system and is correlated with the stability of the system during heating (Fig. 4B). Therefore, stable systems have lower energy than unstable ones. Consequently, systems that exhibit small $E_a$ are less influenced by temperature, as shown in Table 2. Differences in the kinetics of heat activation of GFP result from different solution composition. It is well-known that the water content in the media is an important parameter for the activity of enzymes, and enzyme activity is better quantified in terms of water activity. Water is believed to increase the internal flexibility of the enzyme and thereby increase catalytic activity. $a_w$ is important for protein stability because water is involved in many of the mechanisms influencing protein denaturation *(13)*.

Between 80°C and 95°C, GFP thermal stability ($E_a$) was highest in acetate-buffered solutions (pH 5.0) owing to aggregation of the protein, promoted by the low pH close to the p*I*. At pH 4.0–5.0, sodium acetate is totally dissociated, the ions compete for water molecules, which have preferential interaction with the ions in the solution, promoting a tendency for GFP to aggregate, which enhanced GFP thermal stability. The acetate-buffered system with the lowest intrinsic energy for spontaneous transformation was independent of either the temperature or NaCl concentrations. Citric and phosphoric acids are commonly used in processed foods to control pH. Sodium chloride can have a huge effect on the environmental pH because of the changes in the ionized state of the food product *(14)*. The addition of sucrose can change the p$K_a$ of the buffer solution, shifting the buffer equilibrium. Citrate buffer was shown to be more resistant to pH changes from added polyols than phosphate buffer *(15)*.

The thermal inactivation of polyphenoloxidase in pineapple puree when heated from 70°C to 90°C, with *D*-values varying from 91.3 and 11.4 min, corresponded to a z-value of 21.5°C and $E_a$ of 82.8 kJ/mol (1 cal = 4.18 J; 19.81 kcal/mol) *(16)*. GFP showed greater stability than polyphenoloxidase in the systems composed with water (>5% NaCl), or with phosphate (>10% NaCl) and acetate-buffered solutions (up to 30% NaCl). The $E_a$ for thermolysin was observed to increase up to 30–33 kcal/mol by addition of 0.5–1.5 *M* NaCl (5–15% NaCl). Further increases in NaCl concentration were verified to decrease the $E_a$ to 15 kcal/mol in 4 *M* NaCl (around 25%

Table 2
$z$-Values, $Q_{10}$ Coefficient, and $E_a$ of Thermal Stability for GFP in NaCl Systems[a]

| | Tris-EDTA | | | WFI | | | Acetate | | | Phosphate | | |
|---|---|---|---|---|---|---|---|---|---|---|---|---|
| Nacl (%) | $E_a$ (kcal/mol) | $z$-Value (°C) | $Q_{10}$ | $E_a$ (kcal/mol) | $z$-Value (°C) | $Q_{10}$ | $E_a$ (kcal/mol) | $z$-Value (°C) | $Q_{10}$ | $E_a$ (kcal/mol) | $z$-Value (°C) | $Q_{10}$ |
| 0.0 | 31.97 | 18.66 | 3.44 | 24.31 | 24.63 | 2.55 | 7.87 | `75.76 | 1.36 | 37.24 | 16.03 | 4.21 |
| 0.9 | 34.23 | 17.45 | 3.74 | 25.32 | 23.58 | 2.65 | 4.2 | 142.86 | 1.17 | 33.79 | 17.67 | 3.68 |
| 5.0 | 35.84 | 16.64 | 3.99 | 17.28 | 34.48 | 1.95 | 9.52 | 62.5 | 1.45 | 26.97 | 22.12 | 2.83 |
| 10.0 | 36.77 | 16.26 | 4.12 | 12.15 | 49.26 | 1.2 | 12.3 | 48.31 | 1.61 | 19.58 | 30.4 | 2.13 |
| 15.0 | 43.74 | 13.64 | 5.41 | 11.96 | 49.75 | 1.59 | 5.41 | 109.89 | 1.23 | 18.55 | 32.05 | 2.05 |
| 20.0 | 40.86 | 14.58 | 4.85 | 11.01 | 54.05 | 1.53 | – | – | – | 13.58 | 43.67 | 1.69 |
| 25.0 | 36.81 | 16.21 | 4.14 | 9.40 | 63.29 | 1.44 | – | – | – | 10.72 | 55.25 | 1.52 |
| 30.0 | 32.55 | 18.32 | 3.52 | 6.97 | 85.47 | 1.31 | – | – | – | 8.31 | 71.43 | 1.38 |

WFI (pH 6.0–7.0); 10 m*M* acetate buffer; 10 m*M* phosphate buffer; 10 m*M* Tris-EDTA buffer.

NaCl). In this study, it was observed that the $E_a$ value for GFP also decreased in the presence of increasing concentrations of up to 30% NaCl in WFI, acetate, and phosphate-buffered systems. However, for GFP in Tris-EDTA-buffered system with 30% NaCl, the $E_a$ value (32.55 kcal/mol) was almost the same as that measured for GFP in the control solution, without NaCl ($E_a$ = 31.97 kcal/mol), similar to behavior observed for thermolysin in no salt and 4 *M* NaCl, at pH 7.0 *(6)*.

The stability of scallop transglutaminases (TGase) in the presence of neutral salts (around pH 7.0) showed that NaCl was an effective enhancer of TGase activity, which occurs instantly and reversibly, suggesting small conformational changes of the TGase *(17)*. In this and prior results, GFP did not show fluorescence recovery (renaturation) in all conditions studied. The solubility of lysozyme in aqueous NaCl solutions (pH 4.5 and 7.0), in aqueous sodium acetate (pH 8.3), and in aqueous magnesium chloride solutions (pH 4.1), was observed and related with a preferential solvation of protein in a binary aqueous solution and its solubility *(18)*. Considering the systems wherein GFP thermal stability was evaluated, the activation energies ($E_a$) are as follows (Table 2):

1. In WFI, the $E_a$ of 24.31 kcal/mol for GFP in the control increased to 25.32 kcal/mol with 0.9% NaCl, decreasing up to 6.97 kcal/mol with 30% NaCl.
2. In acetate buffer (pH 5.0), the smallest $E_a$ value of 4.20 kcal/mol was observed for GFP in 0.9% NaCl solutions, lower than 7.87 kcal/mol for the control, increasing to 12.30 kcal/mol with 10% NaCl.
3. In phosphate buffer (pH 7.0), the $E_a$ range decreased from 33.79 to 8.31 kcal/mol for NaCl concentrations between 0.9 and 30%, showing that the addition of 30% NaCl into solution reduced $E_a$ up to 4.5-fold compared with the control solution, $E_a$ = 37.24 kcal/mol.
4. In Tris-EDTA buffered solutions, the intrinsic energy and change in GFP stability was higher than in WFI, with $E_a$ of 31.97 kcal/mol (control), increasing to 34.23 kcal/mol and attaining the maximum value ($E_a$ = 43.74 kcal/mol) in 15% NaCl, equivalent to results for GFP in 5% glucose solutions ($E_a$ = 43.81 kcal/mol) obtained in prior work (*11*), dropping to 32.55 kcal/mol (30% NaCl), at the interval ranging from 0.9 to 30% NaCl.

As observed in previous work, GFP thermal stability, in terms of *D*-value, was dependent on the pH of the solutions with: *D*-values in acetate buffer < WFI < phosphate buffer < Tris-EDTA buffer and NaCl concentration. Between 80°C and 95°C, the amount of activation energy to destabilize the molecule was dependent on the buffer pH: $E_a$ in acetate buffer < phosphate buffer < WFI < Tris-EDTA. From pH 7.0 to 8.0, GFP is in its native conformation, unfolding in these systems at 80–95°C requires greater energy than that required in WFI. NaCl added to phosphate-buffered solutions and WFI exhibited equal changes in pH, but these

systems influenced GFP thermal stability differently. In acetate buffer (pH 5.0) GFP has a tendency to aggregate, the pH of the solutions is close to the p*I* for the protein, between 4.9 and 5.1. Aggregation promotes an increase in the thermal stability of the protein in this system. The presence of NaCl associated to the ions of the buffer systems provided a positive influence on the stability of the molecule for the systems and range of temperatures studied.

## Conclusion

The performance of GFP under these conditions confirmed its potential utility as a biological indicator for use in a variety of applications: in the decontamination of parenteral solutions and WFI, and in disinfection and pasteurization processes. GFP was shown to be an efficient marker in a system with up to 30% NaCl when exposed to the typical temperature range used for decontamination processing of solutions with added NaCl. This indicates the high stability of GFP under these conditions, dependent on the processing temperature, as observed in the evaluation of the *z*-value, $Q_{10}$ coefficient, and free energy of these systems.

## Acknowledgments

We thank our personal assistants for providing technical support Irene A. Machoshvili and Ricardo Alves Silva. This study was made possible by financial support provided by the Brazilian Committees for Scientific Technology Research (Conselho Nacional de Pesquisa e Desenvolvimento (CNPq), and Fundação de Amparo à Pesquisa do Estado de São Paulo (FAPESP).

## References

1. Fennema, O. R. (1985), In: *Food Chemistry—Second Edition, Revised and Expanded.* Fennema, O. R. (ed.), Marcell Dekker Inc, New York, pp. 46–50.
2. Kets, E. P. W., de Bont, J. A. M., and Heipieper, H. J. (1996), *FEMS Microbiol. Lett.* **139,** 133–137.
3. Chirife, J. (1994), *J. Food Eng.* **22,** 409–419.
4. Wijnker, J. J., Koop, G., and Lipman, L. J. A. (2006), *Food Microbiol.* **23,** 657–662.
5. Inouye, K., Kuzuya, K., and Tonomura, B. (1998), *Biochim. Biophys. Acta* **1338,** 209–214.
6. Inouye, K. (1992), *J. Biochem.* **112,** 335–340.
7. Matsue, S., Tomoyuki, F., and Miyawaki, O. (2001), *Int. J. Biol. Macromol.* **28,** 343–349.
8. Vessoni Penna, T. C. and Ishii, M. (2002), *BMC Biotechnol.* Available from http://www.biomedcentral.com/1472-6750/2/7/qc, 2, 7 (Accessed February 22, 2007).
9. Vessoni Penna, T. C., Ishii, M., Pessoa, A., Jr., Nascimento, L. O., De Souza, L. C., and Cholewa, O. (2004), *Appl. Biochem. Biotechnol.* **113–116,** 453–468.
10. Vessoni Penna, T. C., Ishii, M., Cholewa, O., and De Souza, L. C. (2004), *Afr. J. Biotechnol.* **3,** 105–111.
11. Vessoni Penna, T. C., Ishii, M., Cholewa, O., and De Souza, L. C. (2004), *Lett. Appl. Microbiol.* **38,** 135–139.
12. Vessoni Penna, T. C., Ishii, M., Kunimura, J. S., and Cholewa, O. (2006), In: *Trends in Biotechnology Research.* Hearns E. C., (ed.), Nova Publishers, New York, pp. 181–197.

13. Persson, M., Costes, D., Wehtje, E., and Adlercreutz, P. (2002),w *Enzyme Microb. Technol.* **30,** 916–923.
14. Chuy, S. and Bell, L. N. (2006), *Food Res. Int.* **39,** 342–348.
15. Bell, L. N. and Labuza, T. P. (1992), *J. Food Sci.* **57,** 732–734.
16. Chutintrasri, B. and Noomhorm, A. (2006), *Lebenson. Wiss. Technol.* **39,** 492–495.
17. Nozawa, H., Mamegoshi, S., and Seki, N. (1999), *Comp. Biochem. Physiol. B* **124,** 181–186.
18. Shulgin, I. L. and Ruckenstein, E. (2005), *Biophys. Chem.* **118,** 128–134.

0273-2289/1559-0291 (Online)/07/136–140/573–582/$30.00

# Carboxymethylcellulose Obtained by Ethanol/Water Organosolv Process Under Acid Conditions

DENISE S. RUZENE,[1] ADILSON R. GONÇALVES,*,[1] JOSÉ A. TEIXEIRA,[2] AND MARIA T. PESSOA DE AMORIM[3]

*[1]Departamento de Biotecnologia, Escola de Engenharia de Lorena–USP, CxPostal 116, CEP 12.600-970 Lorena-SP, Brazil; E-mail:adilson@debiq.faenquil.br; [2]Centre for Biological Engineering, Universidade do Minho, Campus de Gualtar, 4710–057, Braga, Portugal; and [3]Centro de Engenharia Têxtil, Universidade do Minho, Campus de Azurém, Portugal*

## Abstract

Sugar cane bagasse pulps were obtained by ethanol/water organosolv process under acid and alkaline conditions. The best condition of acid pulping for the sugarcane bagasse was 0.02 mol/L sulfuric acid at 160°C, for 1 h, whereas the best condition for alkaline pulping was 5% sodium hydroxide (base pulp) at 160°C, for 3 h. For the residual lignin removal, the acid and alkaline pulps were submitted to a chemical bleaching using sodium chlorite. Pulps under acid and alkaline conditions bleached with sodium chlorite presented viscosities of 3.6 and 7.8 mPa·s, respectively, and μ–kappa numbers of 1.1 and 2.4, respectively. The pulp under acid condition, bleached with sodium chlorite was used to obtain carboxymethylcellulose (CMC). CMC yield was 35% (pulp based), showing mass gain after the carboxymethylation reaction corresponding to 23.6% of substitution or 0.70 groups $-CH_2COONa$ per unit of glucose residue. The infrared spectra showed the CMC characteristic bands and by the infrared technique it was possible to obtain a substitution degree (0.63), similar to the substitution degree calculated by mass gain (0.70).

**Index Entries:** Acid and alkaline catalyzed ethanol pulping; carboxymethylcellulose; chemical bleaching; infrared spectra; sugarcane bagasse; Organosolv pulping.

## Introduction

Currently, there is a great interest in using renewable resources for obtaining of industrial products, specially those obtained from residues. Sugar cane bagasse is an agricultural waste abundant in several countries. Brazil has many sugar cane plantations, mainly for the manufacture of sugar and ethanol, which is used as fuel for automobiles. The production of sugar cane bagasse for the year 2004/2005 was $56 \times 10^6$ t. About 90% of

*Author to whom all correspondence and reprint requests should be addressed.

this biomass was burned to generate energy for the ethanol distillation and the remaining 10% constitutes a surplus corresponding to $5 \times 10^6$ t that could be used for the production of other chemicals and materials, such as cellulose derivatives *(1)*.

Alternative pulping processes utilizing aqueous organic solvents, known as Organosolv, have been extensively studied in the last 30 yr as an alternative to conventional chemical processes of pulping *(2–7)*. These processes can collaborate largely with the decreased environmental impact caused by conventional delignification processes, besides allowing for the integral use of lignocellulosic components in chemical products of commercial interest *(3,8,9)*. Organosolv pulping has been proposed as a promising alternative to chemical pulping. The ethanol/water process combines high efficiency, low cost, and ethanol abundance in countries where sugar cane is economically important *(3,10,11)*. Organosolv pulping methods can be divided into two great groups: (a) acid-catalyzed processes *(3)*, often operated without the addition of an acid catalyst; in such cases, acetic acid released during the pulping process provides the needed acidity *(3,12–14)* and (b) alkaline organosolv processes, commonly using delignification agents such as NaOH or $Na_2SO_3$; the role of the organic solvent is to promote the solubilization of lignin *(3)*.

Cellulose is a linear and high-molecular weight polymer as well as natural, renewable, and biodegradable material *(15)*. However, because of its inter- and intramolecular hydrogen bonds, cellulose is not dissolved by common solvents *(16)*. In order to utilize cellulose industrially, cellulose must be converted to soluble derivatives. Cellulose derivatives have gained acceptance for pharmaceutical, cosmetic, food, adhesives, textiles, and packaging uses. They must be nontoxic, noncarcinogenic, biocompatible, and nonharmful to the biological environment. Cellulose ether is the most widely used cellulose derivative in food and pharmaceutical industries. Conversion of cellulose to sodium carboxymethylcellulose (CMC), an anionic linear cellulose ether, is another example.

CMC is an important industrial polymer with a wide range of applications in detergents, textiles, paper, drag reduction, foods, drugs, and oil. It is prepared by treating cellulose with aqueous sodium hydroxide followed by reaction with chloroacetic acid. Sodium carboxymethyl groups ($-CH_2COONa$) are introduced into the cellulose molecule, which promote water solubility *(17,18)*. The various properties of CMC depend on three factors: molecular weight of the polymer, average carboxyl content per anhydroglucose unit, and the distribution of carboxyl substituents along the polymer chains *(19)*. The CMC structure is based on the $\beta(1\rightarrow4)$-D-glucopyranose polymer of cellulose. Different preparations may have different degrees of substitution, but are generally in the range 0.6–0.95 carboxymethyl groups per monomer units *(20)*. The structure of CMC is shown in Fig. 1. The objective of this work was to produce CMC from an ethanol/water organosolv lignocellulosic process under acid conditions.

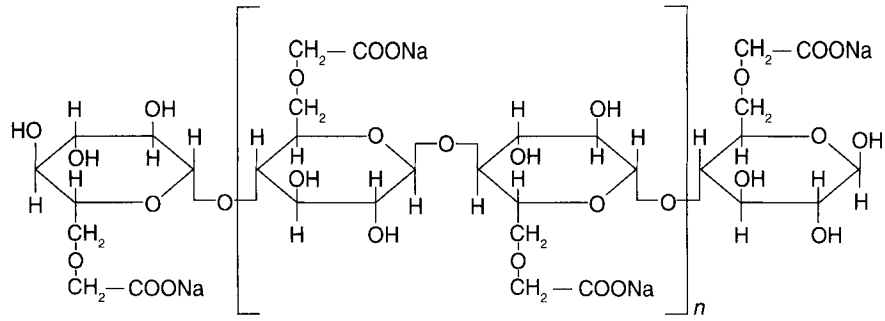


**Fig. 1.** Sodium CMC molecule structure.

## Materials and Methods

### *Pulping and Bleaching*

Pulping of depithed sugar cane bagasse with ethanol/water 1 : 1 (v/v) mixture was carried out in a closed and pressurized vessel (gram bagasse, liquor to bagasse ratio). The pulping was conducted using $H_2SO_4$ in the concentration range of 0.01–0.05 mol/L for 0.5–2 h and NaOH (5–10% dry bagasse) for 3 h. The products were filtered and the pulp was dried for yield determination. Dried and refined pulps (10 g) were suspended in 333 mL of water (3% consistency) and heated to 70 ± 5°C. Sodium chlorite (8.4 g) and glacial acetic acid (3.4 mL) were added. The solution was further heated to 70 ± 5°C for 60 min. Afterward, the samples were cooled in ice bath to 10°C. Bleached pulp was filtered, washed with water (3 L), and dried *(21)*.

### *Analysis and Chemical Composition of the Pulps*

Kappa-number and viscosities of the pulps were determined by standard methods *(22,23)*. One gram of dry pulp was treated with 10 mL of 72% $H_2SO_4$ with stirring at 45°C for 7 min. The reaction was interrupted by adding 50 mL of distilled water, and the mixture was then transferred to a 500-mL Erlenmeyer flask, and the volume brought to 275 mL. The flask was autoclaved for 30 min at 1.05 bar for the complete hydrolysis of oligomers. The mixture was filtered and the hydrolysate brought to 500 mL. A sample (40 mL) of the hydrolysate was diluted to 50 mL and the pH was adjusted to 2.0 with 2 mol/L of NaOH. After filtration through a Sep-Pak $C_{18}$ cartridge (Waters, Milford, MA) to remove aromatic compounds, the hydrolysate was analyzed in an Aminex HPX-87H column (300 × 7.8 $mm^2$) (Bio-Rad Laboratories Ltd., Hercules, CA) at 45°C using a Shimadzu chromatograph LC-10AD (Shimadzu Co., Tokyo, Japan) with refractive-index detector. The mobile phase was 0.005 mol/L $H_2SO_4$ at 0.6 mL/min flow rate. Sugar concentrations, reported as xylan and glucan, were determined from calibration curves of pure compounds. Lignin was determined by gravimetric analysis *(24)*.

### Determination of Brightness

The brightness of pulps was determined in agreement with Technical Association of the Pulp and Paper Industry (TAPPI) *(25)*. Samples were prepared following the TAPPI norm *(26)*: 3 g of pulp (dry base) were disaggregated by 5 min at pH 5.5 and 0.3% consistency. The pulp suspension was filtered in Büchner funnel (110-mm diameter). After filtration, the funnel was inverted and pulp was liberated using airflow. The formed leaf was pressed (10–12 $kgf/cm^2$) for 90 s and dried in the dark. After 1 d, the sheets with thickness between 310 and 315 $g/m^2$ were analyzed using Photovolt 577 equipment (Photovolt Instruments Minneapolis, MN). The reflection percentage was determined at five different points and the results were presented as average values.

### Determination of Holocellulose

Five-gram samples of dry pulp (with known moisture) were transferred to 250-mL Erlenmeyer flasks with 160 mL of distilled water, 0.5 mL of acetic acid, and 1.5 g of sodium chlorite. The samples were heated in water bath at 70–80°C with agitation every 10 min for 60 min. Then, 0.5 mL of acetic acid and 1.5 g of sodium chlorite were added. This addition was repeated at 60 min intervals for 4-h reaction time. After 4 h the Erlenmeyer flask was put in ice bath and cooled to 10°C, then the samples were filtered in crucibles of porosity 2. The residue was washed with 1.6 L of hot distilled water under suction. Subsequently, samples were washed with acetone and dried at room temperature *(21)*.

### Determination of α-Cellulose

One-gram samples of holocellulose (with known humidity) were transferred to 150-mL beakers and put in water bath at 20°C. Then, 11.8 mL of 17.5% NaOH solution were added with stirring, 5 mL being added in the first 1 min, 3.4 mL in the next 45 s, and 3.4 mL in the next 15 s. The samples were left at rest by 3 min and then 13.6 mL of 17.5% NaOH was added over 10 min, 3.4 mL with stirring initially, 3.4 mL were added in the 2.5nd min, 3.4 mL in the 5th min, and 3.4 mL in the 7.5th min. Samples were covered and left in for 30 min at 20°C. Afterwards, 33.4 mL of distilled water was added, and the mixture was left for another 30 min at 20°C. The samples were filtered in crucible of porosity 2, washed with 8 mL of 8.3% NaOH, and washed with 400 mL of distilled water. The volume was completed with acetic acid 2 mol/L and left at rest for 3 min. The samples were filtered to remove acetic acid, washed with 3 L of distilled water to room temperature and dried overnight *(21)*.

### Synthesis of Sodium CMC

A sample of 5 g bleached pulp was transferred to 500-mL two-necked flask with 92.5 g ethanol and 3.7 g water. A solution of sodium hydroxide (5 g

of NaOH and 8 g of water) was added in the mixture, within the addition time of 30 min, under mechanical agitation and put in water bath at 15 ± 5°C. On completion of the addition, the mixture was agitated for 1 h, maintained in the water bath at 15–25°C. After the alkalization, a solution of monochloracetic acid and ethanol to 50% of the mass (6.5 g of monochloracetic acid and 6.5 g of ethanol) was added in the reactional mixture with 30 min addition time, mechanical agitation, and water bath at 20 ± 5°C. At the end of the addition, the sample was heated at 60°C and agitated for 3 h. Afterward, the mixture was drained and the solid phase suspended in 70% methanol and neutralized while in suspension with 90% acetic acid. The suspension was filtered, and the precipitate washed repeatedly with ethanol, methanol, and dried at 60 ± 5°C. The mass gain of CMC was determined by the Eq. 1 *(27)*.

$$\mathrm{MG}(\%) = \frac{\mathrm{CMCM} - \mathrm{Mbp}}{\mathrm{Mbp}} \times 100 \quad (1)$$

where MG (%) is the mass gain of the CMC, CMCM is the CMC mass (gram dry base), and Mbp is the mass of bleached pulp (gram dry base).

### *Fourier Transform Infrared of CMC*

Fourier-transform infrared (FTIR) spectra were obtained directly from sample of CMC utilizing the high attenuated total reflectance technique in Nicolet Avatar 360 FTIR spectrometer (Nicold Instrument Corporation, Madison, WI).

## Results and Discussion

The composition of sugar cane bagasse pulps is given in Table 1. Yield values (using refined pulps) were 19% greater for the pulp under alkaline treatment. Viscosity values were 53% lower for the acid treatment because of higher degradation of fibers, in other words, the degree of polymerization of cellulose decreased. The kappa-number remained around 40, indicating that residual lignin still remained in the pulp. The amount of glucan was 27% higher for the acid treatment in respect to the total amount evaluated. Values for xylan and total lignin were 90.1 and 33.6% higher for the alkaline treatment. The holocellulose values were around 90%. Values for α-cellulose were 70%, whereas the brightness for acid and alkaline conditions was of 30.5 ± 1.2 and 25.0 ± 1.2%, respectively. Faria *(28)* found brightness of 35.4% for NaOH pulps of bagasse, indicating that the results were close to those reported in the literature *(29)*.

Table 2 gives the composition of bleached pulps. The classified yield values of the bleached pulps were higher than 89%. Viscosity was preserved after chemical bleaching and fiber degradation did not occur. In general, the reagents used in the bleaching sequence partially removed the lignin, without reducing the viscosity. The kappa-number was reduced significantly showing

Table 1
Chemical Composition and Analysis of Sugar cane Bagasse Pulps

| | Puping conditions | |
|---|---|---|
| | Acid[a] | Alkaline[b] |
| Classified yield (%) | 33.1 | 40.9 |
| Viscosity (mPa·s) | 3.8 ± 0.2 | 8.1 ± 0.2 |
| Kappa-number | 41.1 ± 0.4 | 46.2 ± 0.6 |
| Glucan (%) | 75.9 ± 3.2 | 55.3 ± 0.6 |
| Xylan (%) | 2.2 ± 0.1 | 23.1 ± 0.5 |
| Klason lignin (%) | 9.7 ± 0.3 | 14.6 ± 0.9 |
| Holocellulose (%) | 91.2 ± 0.1 | 89.1 ± 1.1 |
| α-Cellulose (%) | 70.4 ± 0.9 | 68.4 ± 0.3 |
| Brightness | 30.5 ± 1.2 | 25.1 ± 1.2 |

[a]Acid (0.02 mol/L $H_2SO_4$), 1 h at 160°C.
[b]Alkaline (5% NaOH), 3 h at 160°C.

Table 2
Chemical Composition and Analysis of Bleached Pulps

| | Bleached pulp | |
|---|---|---|
| | Acid condition[a] | Alkaline condition[b] |
| Classified yield (%) | 92.6 | 89.7 |
| Viscosity (mPa·s) | 3.6 | 7.8 |
| Kappa-number | 1.1[c] | 2.4[c] |
| Glucan (%) | 69.5 | 64.6 |
| Xylan (%) | 2.3 | 21.9 |
| Klason lignin (%) | 1.8 | 6.2 |
| Holocellulose (%) | 98.4 | 98.1 |
| α-cellulose (%) | 69.8 | 69.4 |
| Brightness | 82.3 ± 0.8 | 68.3 ± 1.6 |

[a]Acid (0.02 mol/L $H_2SO_4$), 1 h at 160°C.
[b]Alkaline (5% NaOH), 3 h at 160°C.
[c]μ–κ number.

after bleaching a μ–kappa value of 1.1 (acid condition) or 2.4 (alkaline condition), indicating that the residual lignin of the pulp was practically removed. The glucan and xylan were preserved after bleaching. The total lignin was also reduced with the bleaching. Values of α-cellulose were not changed indicating no reduction in the polymerization degree of the cellulose. The brightness was elevated to 63% for the two bleaching conditions showing that with the removal of the residual lignin the value for brightness increased.

In contrast, with the pulps used for papermaking, both xylan and lignin are undesirable and should be removed during the pulping and

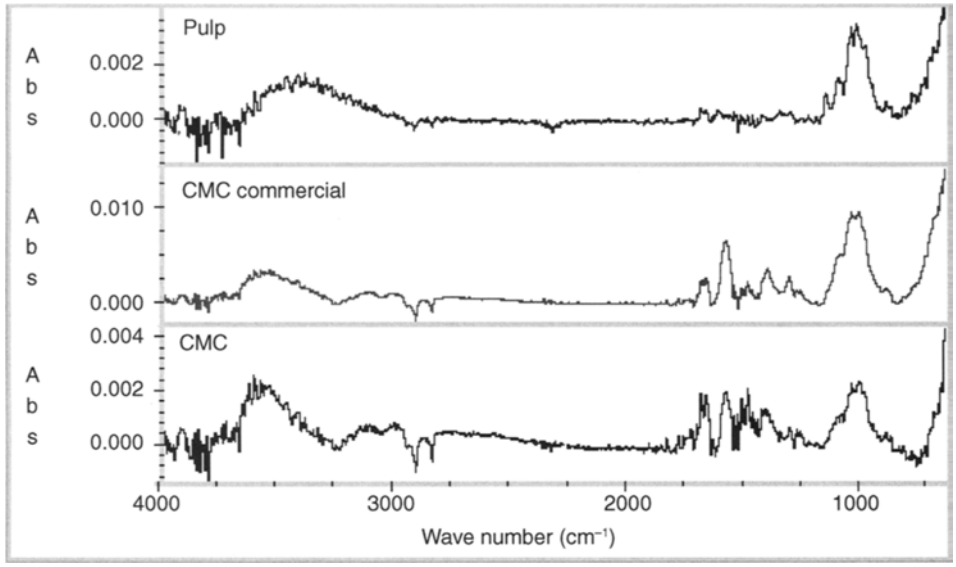


**Fig. 2.** FTIR spectra of the pulp in acid condition bleached with sodium chlorite, CMC commercial, and CMC obtained in this article.

bleaching sequences *(30)*. The pulp used for CMC production was the ethanol/water/$H_2SO_4$ (acid condition) pulp. This pulp presented the best conditions of κ-number, brightness and smaller amount of xylan.

## *Carboxymethylcelulose*

Figure 2 shows the FTIR spectra of the ethanol/water/acid organosolv pulp bleached with sodium chlorite, commercial CMC, and of CMC obtained in this work. The carboxymethylation reaction occurs through the substitution of one hydrogen atom of the group hydroxyl for a carboxymethyl group. A decrease in the absorbance of the band in the region related to the axial stretching of O–H at 3600 $cm^{-1}$ and a displacement of this band in the region around 3650–3700 $cm^{-1}$ were observed.

The decrease of the absorbance is because of the etherification of the cellulose O–H groups for carboxymethylic groups and the displacement to the decrease of the intramolecular hydrogen bonds. Another evidence is observed in the region of 1150–1000 $cm^{-1}$, in which the bands occur as a result of the C–O and C–O–C links, typical of ethers. The introduction of the $CH_2COONa$ group in the cellulose structure (this group possesses the carbonyl bond inserted in the carboxylate group) absorbs in the 1650–1550 $cm^{-1}$ range because of the asymmetrical axial deformation. This band differentiates the spectrum of the cellulose from that of CMC. Acid pulp bleached with sodium chlorite was used to produce CMC and the mass gain was 35%. After 3 h reaction a white powder, denser than water, was obtained. A test of the water body was carried out *(31)* to verify CMC

Table 3
Bands of Characteristic Oscillations in IR Region for the Cellulose[a]

| Functional group | Type of deformation | Band region ($cm^{-1}$) |
|---|---|---|
| –C–H; $–CH_2$ | Axial antisymmetrical, symmetrical | 2926–2853 |
| | Angular symmetrical in the plan and outside plan | 1465–1350 |
| | Angular antisymmetrical in the plan and outside plan | 720–1150 |
| –O–H | Axial | 3550–3200 |
| | Angular in the plan | 1420–1330 |
| | Angular outside plan | 769–650 |
| –C–O; C–O–C | Axial | 1260–1000 |
| Adsorbed $H_2O$ | Angular symmetrical in the plan | Approx 1600 |

[a]*See* refs. *15* and *36*.

affinity with the water. Water was put in a glass and CMC was added (spatula tip) to the water surface. After some minutes, CMC sample had a gelatinous aspect and soon afterward it was dissolved in the water.

CMC is a polar molecule with a great affinity for water. The dissolution of CMC in water confirmed the success in obtaining this material. The original cellulose (bleached pulp) does not dissolve in water. A CMC mass gain of 35% was observed, in other words, after the reaction the material was incorporated to the product. There is introduction of functional groups in the molecule chain of the cellulose. In the case of CMC, the hydrogen of the cellulose hydroxyl is substituted for the $CH_2COONa$ group. The introduction of the functional group in the cellulose results in the obtainment of a product of molar mass higher than that of the original cellulose, causing a mass gain, corresponding to 23.6% of substitution or 0.70 $CH_2COONa$ group per unit of glucose residue. The maximum theoretical value of substitution is 3, but this value reached up to 1.2 according to the literature *(27,31)*.

### *Infrared Spectroscopy*

IR spectroscopy has been largely used for the characterization of lignocellulosic materials and studied in some works involving characterization of the compounds with or without modification *(32–34)*. Samples were analyzed by spectroscopy in IR region and cellulose characteristic bands are presented in Table 3.

Using the IR spectra of the Fig. 2, the evaluation of the substitution degree (DS) was made through the analysis of the absorption band in the 1600 $cm^{-1}$ area in relation to the band in the region of 901 $cm^{-1}$ (Absorbance [Abs] 1600/Abs901). A 901 $cm^{-1}$ band corresponds to the vibration of the O–C–O group involving the carbon-1 (anomeric) of the polysaccharides and does not suffer influence of the other groups *(35)*. Abs1600/Abs901 ratios of 4.89 and 2.63 were obtained for commercial

CMCNa and CMC, respectively. Other methods of determination of the DS were not tested. It was calculated using the ratio values between the absorbances (1600/cm and 901/cm), and a 0.63 DS was obtained (value found using 1.18 DS of commercial CMCNa, according to Machado *[31]*).

Machado *(31)* determined the DS of CMCNa by conductometric titration, obtaining 1.18 DS for commercial CMCNa and 1.0 DS for CMCNa obtained by the author (isopropanol as solvent). In work accomplished by Silva *(27)*, DS of CMCNa, produced using isopropanol and ethanol as solvents, was determined by potentiometric titration. DS of CMCNa (isopropanol) was 0.73, whereas DS using ethanol as solvent was 0.64. This fact shows that the result obtained in the present work (0.63 DS), using the IR technique, was similar to that determined by other methods and it was also similar to the result of DS calculated by the mass gain (0.70).

## Conclusions

The mass gain of CMC was 35%, corresponding to 23.6% of substitution or 0.70 $CH_2COONa$ group per unit of glucose residue (DS = 0.70). The IR spectra showed characteristic bands of CMC in the region of 1150–1000 $cm^{-1}$ typical of ethers and band in the region of 1650–1550 $cm^{-1}$ that differentiates basically the spectrum of the cellulose form of CMC. Using the IR technique it was possible to obtain a DS of 0.63, similar to that determined by other methods (conductometric titration, DS [1.00] and potentiometric titration, DS [0.63] and it was also similar to the result of DS calculated by the gain mass [0.70]).

## Acknowledgments

The authors acknowledge financial support from Fundação de Amparo à Pesquisa do Estado Científico e Tecnológico (FAPESP) and Conselho Nacional de Desenvolvimento Científico e Tecnológico (CNPq).

## References

1. Ruzene, D. S. (2005), *PhD. Thesis*, Faenquil/Debiq, Lorena, Brazil.
2. Kleinert, T. N. (1974), *Tappi J.* **57,** 99–102.
3. Aziz, S. and Sarkanen, K. (1989), *Tappi J.* **72,** 169–175.
4. Young, R. A. and Akhtar, M. (1998), In: *Environmentally Friendly Technologies for the Pulp and Paper Industry*. Wiley, New York, pp. 5–69.
5. Gonçalves, A. R. and Ruzene, D. S. (2001), *Appl. Biochem. Biotechnol.* **91–93,** 63–70.
6. Gonçalves, A. R. and Ruzene, D. S. (2003), *Appl. Biochem. Biotechnol.* **105–108,** 195–204.
7. Shatalov, A. A. and Pereira, H. (2005), *Carbohydr. Polym.* **59,** 435–442.
8. Paszner, L. and Cho, H. J. (1989), *Tappi J.* **72,** 135–142.
9. Bendzala, J. and Kokta, B. V. (1995), *Wood Sci. Technol.* **29,** 467–479.
10. Goyal, G. C., Lora, J. H., and Pye, E. K. (1992), *Tappi J.* **75,** 110–116.
11. Raymond, A. Y. and Akhtar, M. (1998), In: *Environmentally Friendly Technologies for the Pulp and Paper Industry*. Wiley, New York.
12. Sarkanen, K. V. (1990), *Tappi J.* **73,** 215–219.
13. McDonough, T. J. (1993), *Tappi J.* **76,** 186–193.

14. Gilarranz, M. A., Oliet, M., Rodrigues, F., and Tijero, J. (1998), *Can. J. Chem. Eng.* **76(2),** 253–260.
15. Fengel, D. and Wegener, G. (1989), In: *Wood Chemistry, Ultrastruture, Reactions*. Walter de Gruyter, Berlin.
16. Hon, D. N. S. (1996), Chemical modification of lignocellulosic materials. Marcel Dekker.
17. Heinze, T. (1998), *Macromol. Chem. Phys.* **199,** 2341–2364.
18. Sjöström, E. (1993), In: *Wood Chemistry: Fundamentals and Applications*, Academic Press, New York.
19. Juste, K. E. and Majewicz, T. G. (1985), In: *Encyclopedia of Polymer Science and Engineering*. vol. 3, Wiley, New York, pp. 226–269.
20. Biswal, D. R. and Singh, R. P. (2004), *Carbohydr. Polym.* **57,** 379–387.
21. Browing, B. L. (1963), In: *The Chemistry of Wood*. New York, Interscience.
22. TAPPI—Technical Association of the Pulp and Paper Industry (1985), TAPPI Standard Methods. T 236 cm-85 (kappa number).
23. TAPPI—Technical Association of the Pulp and Paper Industry (1982), TAPPI Standard Methods. T 230 om-82 (viscosity).
24. Rocha, G. J. M. (2000), *PhD. Thesis*, São Carlos/Universidade de São Paulo, Brazil.
25. TAPPI—Technical Association of the Pulp and Paper Industry (1999), TAPPI Standard Methods T 230 om-99 (brightness of pulps).
26. TAPPI—Technical Association of the Pulp and Paper Industry (1999), TAPPI Standard Methods. T 236 om-99 (samples prepared).
27. Silva, P. J. (1997), *MS Thesis*, São Carlos/Instituto de Química, Brazil.
28. Faria, L. F. F. (1994), *MS Thesis*, Faenquil/Demar, Brazil.
29. Biermann, C. J. (1996), In: *Handbook of Pulping and Papermaking*. Academic Press, San Diego.
30. Mosai, S., Wolfaardt, J. F., Prior, B. A., and Christov, L. P. (1999), *Bioresour. Technol.* **68,** 89–93.
31. Machado, G. O. (2000), *MS Thesis*, São Carlos/Instituto de Química, Brazil.
32. Collier, W. E., Schultz, T. P., and Kalasinsky, V. F. (1992), *Holzforschung* **46(6),** 523–528.
33. Kimura, F., Kimura, T., and Gray, D. G. (1992), *Holzforschung* **46(6),** 529–532.
34. Ferraz, A., Rodriguez, J., Freer, J., and Baeza, J. (2000), *Bioresour. Tecnhol.* **74,** 201–212.
35. Morohoshi, N. (1991), In: *Wood and Cellulosic Chemistry* (Hon, D. N. S. and Shiraishi, N., eds.). Marcel Dekker, New York, pp. 331–392.
36. Silverstein R. M. and Bassler. (1974) In: *G. C. Spectrometric Identification of Organic Compounds, 5th Ed.* John Wiley, New York.

0273-2289/1559-0291 (Online)/07/136–140/583–594/$30.00

# Response Surface Methodological Approach for Optimization of Free Fatty Acid Removal in Feedstock

GWI-TAEK JEONG,[1,2] DO-HEYOUNG KIM,[3] AND DON-HEE PARK*,[2–6]

*[1]Engineering Research Institute; [2]School of Biological Sciences and Technology, E-mail: dhpark@chonnam.ac.kr; [3]Faculty of Applied Chemical Engineering; [4]Biotechnology Research Institute; [5]Institute of Bioindustrial Technology; and [6]Research Institute for Catalysis, Chonnam National University, Gwangju 500-757, Korea*

## Abstract

Fatty acid methyl esters, also referred to as biodiesel, have been determined to have a great deal of potential as substitutes for petro-diesel. In order to optimize conversion yield in the biodiesel production process, feedstocks were previously recommended to be anhydrous, with a free fatty acid content of less than 0.5%. In this study, we removed free fatty acid from feedstock through the use of solid catalysts and response surface methodology. In order to optimize free fatty acid removal, response surface methodology was applied to delineate the effects of five-level-four-factors and their reciprocal interactions on free fatty acid removal. A total of 30 individual experiments were conducted, each of which was designed to study reaction temperature, reaction time, catalyst amounts, or methanol amounts. A statistical model was used to estimate that the optimal free fatty acid removal yield would be 100%, under the following optimized reaction conditions: a reaction temperature of 66.96°C, a catalyst amount of 12.66% (w/v), and a reaction time of 37.65 min. Using these optimal factor values under experimental conditions in three independent replicates, an average conversion yield was well achieved within the values predicted by the model.

**Index Entries:** Biodiesel; free fatty acid; optimization; response surface methodology.

## Introduction

Fatty acid methyl esters (FAMEs) derived from a variety of vegetable oils, animal fats, and waste oils have been shown to evidence low viscosities, similar to those associated with petro-diesel. Additionally, many of the salient characteristics of FAMEs, most notably volumetric heating value,

*Author to whom all correspondence and reprint requests should be addressed.

cetan number, and flash point have also been shown to be comparable with those of petro-diesel *(1–3)*. Several processes have been previously developed for the production of FAMEs through acid-, alkali-, and enzyme-catalyzed transesterification processes *(3–5)*. Transesterification, also called alcoholysis, involves the displacement of alcohol from an ester by another alcohol, in a process comparable to hydrolysis. Transesterification is generally characterized by a number of consecutive, reversible reactions. The reaction step involves the conversion of triglycerides to diglycerides, followed by the conversion of diglycerides to monoglycerides and of monoglycerides to glycerol at each step *(6,7)*. In the process of transesterification, as it is presently conducted, and is the most used, under alkali-catalyst and short-chain alcohol it tends to produce the highest conversion yields with the shortest reaction times. The primary parameters relevant to transesterification include the molar ratio of vegetable oil to alcohol, the catalysts, reaction temperature and time, free fatty acid contents, and water contents in the oils and fats *(5)*. In alkali-catalyzed transesterification, the oils and alcohol must be substantially anhydrous, as water induces saponification with the oils *(5,8)*. Ma et al. *(9)* suggested that the free fatty acid contents of the refined oil should be as low as possible, less than 0.5%. The recommended amount of alkali-catalyst for the transesterification is between 0.1 and 1% (w/w) of oils and fats *(10)*.

Feedstocks used in the production of FAMEs are generally divided into vegetable oils, animal fats, and waste oils. It has been established that high free fatty acid content in oils induces the destruction and decreases the activity of catalysts, and also results in soap conversion *(11)*. As free fatty acid levels increase, this effect becomes increasingly undesirable, owing to the loss of feedstock, as well as the deleterious effects of soap on glycerin separation. The soaps tend to promote the formation of unstable emulsions, which prevent the separation of FAMEs from glycerin during processing *(12)*. A great deal of research has focused on the evaluation of feedstocks regarding the effects of free fatty acid levels. However, in most cases, alkaline catalysts have been utilized in the process, and the free fatty acids were removed from the process stream as soap, and considered to be waste *(5,12,13)*.

Response surface methodology (RSM) utilizes multiple regression and correlation analyses as tools in order to assess the effects of two or more independent factors on the dependent factors. Central composite rotatable design (CCRD) is a RSM, which is used in the optimization processes of biotechnological procedures *(14–17)*. In this study, we removed the free fatty acids from feedstocks through the application of solid catalysts and RSM. In order to optimize free fatty acid removal, we applied RSM to delineate the effects of five-level-four-factors and their reciprocal interactions on the removal of free fatty acids.

## Materials and Methods

### Chemicals

The crude rapeseed oil was supplied by Onbio Co. Ltd. (Bucheon, Korea), and its characteristics are summarized in Table 1. The oleic acid was supplied by Duksan Pure Chemical Co. Ltd. (Korea). The Lewatit S1467 and Ionac NM60 were obtained from Hankook Baychemical Co. Ltd. (Korea). The characteristics of Ionac NM60 are summarized in Table 2. The Amberlite IR-120 (Duksan Pure Chemical Co. Ltd., Korea), Amberlite IRA-900 (Sigma-Aldrich Co. Ltd.), and Amberlite 200C (Fluka, Switzerland) used in this study were of reagent grade. The anhydrous methanol was obtained from Fisher Scientific. All other chemicals used were of analytical grade, and the solvent used in the study was dried for 1 d before use, with molecular sieves.

### Experimental Procedure

In order to select the appropriate solid catalyst, Ionac NM 60, Lewatit S1467, Amberlite IR-120, Amberlite IRA-900, and Amberlite 200C were applied to the removal reaction with refined rapeseed oil combined with 15% oleic acid, for 30 min at 65°C. During the reactions, some of the samples were withdrawn at set intervals, and the acid values of the samples were determined. The results are expressed as the mean values of at least two independent measurements. In order to optimize the CCRD experimental design, a five-level-four-factor CCRD was adopted in this study, requiring 30 experiments, which included 16 factorial points, eight axial points, and six central points to provide information about the interior of the experiment region, allowing evaluation for curvature *(16,17)*. The variables, selected for the study of free fatty acid removal, and their respective levels, were as follows: reaction temperature (30–70°C), catalyst amount (5–20 wt%), reaction time (5–60 min), and methanol amount (0–20 wt%). Table 3 shows the coded and uncoded independent factors ($X_i$), levels, and experimental design.

All experiments concerning the removal of free fatty acid from oil with a solid catalyst were conducted using a bottle apparatus, with a working volume of 25 mL. The reaction temperature was controlled with a water bath equipped with a PID temperature controller. Mixing was conducted with a magnetic stirrer, spinning at approx 200 rpm. The condenser prevented evaporation of the reactants. During the reactions, some of the samples were withdrawn at set intervals, and the acid values of the samples were determined.

### Statistical Analysis

The experimental data (Table 4) were analyzed by means of RSM to fit the following second-order polynomial equation, using Design-Expert 6

Table 1
Composition of Crude Rapeseed Oil

| Composition | Content (%) |
|---|---|
| Triglyceride | 94.1 |
| Free fatty acid | 4.0 |
| Phospholipid | 0.1 |
| Unsaponicable material | 1.5 |
| Moisture | 0.3 |

Table 2
Typical Physical and Chemical Properties of Catalyst

| | |
|---|---|
| Ionic forms | $H^+/OH^-$ |
| Bead size (mm) | >90; 0.3–1.25 |
| Effective size (mm) | 0.47 ± 0.06 |
| Density (g/mL) | 1.2 |
| Water retention | 55–60 |
| Total capacity (min) | 20,000 Ohm-cm; 0.55 eq/L |
| Stability | Temperature range: 1–49°C; pH range: 0.0–14.0 |

Table 3
Factors and Their Levels for Central Composite Design

| | | Coded factor levels | | | | |
|---|---|---|---|---|---|---|
| Variable | Symbol | –2 | –1 | 0 | 1 | 2 |
| Reaction temperature (°C) | $X_1$ | 30 | 40 | 50 | 60 | 70 |
| Catalyst amount (wt%) | $X_2$ | 5.00 | 8.75 | 12.50 | 16.25 | 20.00 |
| Reaction time (min) | $X_3$ | 5.00 | 18.75 | 32.50 | 46.25 | 60.00 |
| Methanol amount (wt%) | $X_4$ | 0.00 | 5.00 | 10.00 | 15.00 | 20.00 |

software (Stat-Ease Inc.). The second-order coefficients were generated through regression with stepwise elimination. The response was initially fitted to the factors through multiple regression. The quality of fit of the model was evaluated through coefficients of determination ($R^2$) and analysis of variances (ANOVA). The insignificant coefficients were eliminated after the examination of the coefficients, and the model was finally refined. The quadratic response surface model was then fitted to the following equation:

$$Y = \beta_{k0} + \sum_{i=1}^{4} \beta_{ki} x_i + \sum_{i=1}^{4} \beta_{kii} x_i^2 + \sum_{i=1}^{3} \sum_{j=i+1}^{4} \beta_{kij} x_i x_j \quad (1)$$

Table 4
Central Composite Rotatable Second-Order Design, Experimental and Estimated Data for Five-Level-Four-Factor Response Surface Analysis

| Standard | Run | Temperature $X_1$ (°C) | Catalyst amount (wt%), $X_2$ | Reaction time (min), $X_3$ | Methanol amount (wt%), $X_4$ | Conversion yield (%) | |
|---|---|---|---|---|---|---|---|
| | | | | | | Experimental | Estimated |
| 1 | 2 | −1 | −1 | −1 | −1 | 62.1 | 65.0 |
| 2 | 21 | 1 | −1 | −1 | −1 | 85.3 | 81.8 |
| 3 | 22 | −1 | 1 | −1 | −1 | 87.4 | 85.3 |
| 4 | 11 | 1 | 1 | −1 | −1 | 93.7 | 93.3 |
| 5 | 29 | −1 | −1 | 1 | −1 | 90.5 | 90.8 |
| 6 | 10 | 1 | −1 | 1 | −1 | 93.7 | 96.2 |
| 7 | 3 | −1 | 1 | 1 | −1 | 93.7 | 97.6 |
| 8 | 6 | 1 | 1 | 1 | −1 | 95.8 | 94.4 |
| 9 | 27 | −1 | −1 | −1 | 1 | 66.3 | 65.0 |
| 10 | 9 | 1 | −1 | −1 | 1 | 87.4 | 81.8 |
| 11 | 4 | −1 | 1 | −1 | 1 | 87.4 | 85.3 |
| 12 | 16 | 1 | 1 | −1 | 1 | 93.7 | 93.3 |
| 13 | 1 | −1 | −1 | 1 | 1 | 91.6 | 90.8 |
| 14 | 28 | 1 | −1 | 1 | 1 | 95.8 | 96.2 |
| 15 | 17 | −1 | 1 | 1 | 1 | 93.7 | 97.6 |
| 16 | 24 | 1 | 1 | 1 | 1 | 95.8 | 94.4 |
| 17 | 8 | −2 | 0 | 0 | 0 | 89.5 | 87.4 |
| 18 | 30 | 2 | 0 | 0 | 0 | 95.8 | 100.9 |
| 19 | 14 | 0 | −2 | 0 | 0 | 74.7 | 76.7 |
| 20 | 25 | 0 | 2 | 0 | 0 | 95.8 | 95.1 |
| 21 | 20 | 0 | 0 | −2 | 0 | 59.0 | 64.6 |
| 22 | 23 | 0 | 0 | 2 | 0 | 95.8 | 91.4 |
| 23 | 13 | 0 | 0 | 0 | −2 | 93.7 | 94.1 |
| 24 | 7 | 0 | 0 | 0 | 2 | 95.8 | 94.1 |
| 25 | 12 | 0 | 0 | 0 | 0 | 93.7 | 94.1 |
| 26 | 5 | 0 | 0 | 0 | 0 | 93.7 | 94.1 |
| 27 | 15 | 0 | 0 | 0 | 0 | 95.8 | 94.1 |
| 28 | 26 | 0 | 0 | 0 | 0 | 93.7 | 94.1 |
| 29 | 19 | 0 | 0 | 0 | 0 | 93.7 | 94.1 |
| 30 | 18 | 0 | 0 | 0 | 0 | 93.7 | 94.1 |

where $Y$ is the response factor (conversion yield), $x_i$ the $i$th independent factor, $\beta_0$ the intercept, $\beta_i$ the first-order model coefficients, $\beta_{ii}$ the quadratic coefficients for the factor $i$, and $\beta_{ij}$ is the linear model coefficient for the interaction between factors $i$ and $j$.

## *Quantitative Analysis*

The free fatty acid contents were determined through AOCS Cd 3a-63. Two to ten grams of each sample was dissolved in 100 mL of diethyl ether : EtOH (1:1) solution. After the addition of 2–3 drops of 1% phenolphthalein

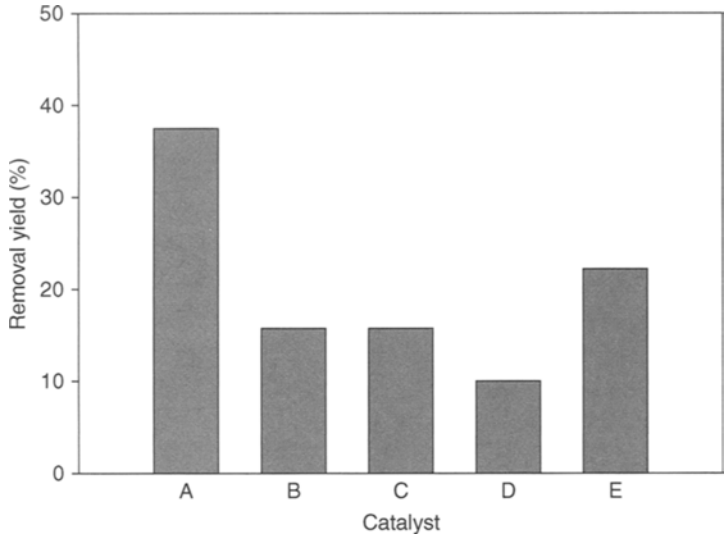


**Fig. 1.** Effect of kind of catalyst on removal of free fatty acid in prepared rapeseed oil with 15% oleic acid. Reaction temperature was 65°C. A: Ionac NM 60, B: Lewatit S1467, C: Amberlite IR-120, D: Amberlite IRA-900, E: Amberlite 200C.

indicator, the mixed solution was subjected to a titration analysis with alcoholic 0.1 *N* KOH. The free fatty acid contents were calculated as below.

$$\text{Free fatty acid (\%)} = (\text{volume of used KOH solution} - \text{blank}) \times \text{factor} \times 0.1\ N \times 56.11 / \text{weight of sample} \times 0.5034.$$

## Results and Discussion

In order to optimize the conversion yield of FAMEs production process, it has been previously recommended that the feedstocks be as anhydrous as possible, with a free fatty acid content of less than 0.5% *(5,6,9)*. The primary objective of this study was to optimize free fatty acid removal in crude rapeseed oil using a solid catalyst, coupled with RSM.

First, in order to select the most appropriate solid catalyst for free fatty acid removal, Ionac NM 60, Lewatit S1467, Amberlite IR-120, Amberlite IRA-900, and Amberlite 200C were applied to the removal reaction, with refined rapeseed oil combined with 15% oleic acid for 30 min at 65°C. As is shown in Fig. 1, the removal yield was approx 37.5% with Ionac NM 60. This yield was higher approx 1.7–3.7 times than that of other solid catalysts. For the next experiment, involving the removal of free fatty acids from crude rapeseed oil, Ionac NM 60 was selected as the solid catalyst. Next, in order to estimate the reaction time, waste vegetable oil with an acid value of 2.65 was reacted with the Ionac NM 60 catalyst at 75°C for 1 h. The acid value was decreased to 0.01 after approx 20 min of reaction time (data not shown). In the alkali-catalyzed transesterification process, the free fatty acid amount should be less than 0.5% on the basis of oil weight, in order to obtain a sufficiently high conversion

Table 5
ANOVA for Response Surface-Reduced Quadratic Model

| Source | Sum of squares | DF | Mean square | *F*-value | Probability > $F^{a,b}$ |
|---|---|---|---|---|---|
| Model | 2784.92 | 8 | 348.11 | 36.99 | <0.0001 |
| $X_1$ | 273.62 | 1 | 273.62 | 29.07 | <0.0001 |
| $X_2$ | 508.81 | 1 | 508.81 | 54.06 | <0.0001 |
| $X_3$ | 1080.33 | 1 | 1080.33 | 114.79 | <0.0001 |
| $X_2^2$ | 121.15 | 1 | 121.15 | 12.87 | 0.0017 |
| $X_3^2$ | 463.58 | 1 | 463.58 | 49.26 | <0.0001 |
| $X_1 X_2$ | 75.39 | 1 | 75.39 | 8.01 | 0.0100 |
| $X_1 X_3$ | 128.00 | 1 | 128.00 | 13.60 | 0.0014 |
| $X_2 X_3$ | 180.06 | 1 | 180.06 | 19.13 | 0.0003 |
| Residual | 197.64 | 21 | 9.41 | – | – |
| Lack of fit | 193.95 | 16 | 12.12 | 16.42 | 0.0029 |
| Pure error | 3.69 | 5 | 0.74 | – | – |
| Correlation total | 2982.56 | 29 | – | – | – |

[a]Probability > *F*, level of significance.
[b]Values of probability > $F < 0.05$ indicate model terms are significant.

yield (*9*). Because of its relatively high acid value, the activity of the catalyst was diminished in the transesterification reaction. As is shown in Table 1, the fatty acid content of the crude rapeseed oil used in this experiment was 4%, a value, which is far higher than the proposed value (<0.5%) (*9*).

In order to construct a proper model for the optimization of free fatty acid removal, the CCRD, which is generally the preferred design for response surface optimization, was selected with five-level-four-factors: reaction temperature, reaction time, catalyst amount, and methanol amount. Table 3 shows the experimental variables settings and the results based on the experimental design. All 30 of the designed experiments were conducted and the results were analyzed through multiregression. The coefficients of the full model were evaluated through regression analysis, and tested for significance. The insignificant coefficients were eliminated in a stepwise manner, on the basis of the *p*-values after the testing of the coefficients. Three linear coefficients ($X_1$, $X_2$, $X_3$), two quadratic coefficients ($X_2^2$, $X_3^2$), and three cross-product coefficients ($X_1X_2$, $X_1X_3$, $X_2X_3$) were ultimately determined to be significant (Tables 5 and 6). The final estimative response model equation, after clearing the insignificant variables for the estimation of the effectiveness of free fatty acid removal by stepwise elimination, was as follows.

$$Y = -95.462 + 1.730\,X_1 + 9.905\,X_2 + 3.718\,X_3 - 0.147\,X_2^2 - 0.021\,X_3^2 - 0.058\,X_1X_2 - 0.021\,X_1X_3 - 0.065\,X_2X_3 \quad (2)$$

Table 6
Regression Coefficients and Significance of Response Surface-Reduced Quadratic Model After a Stepwise Elimination

| Factor | Coefficient estimate[a] | DF | Standard error | 95% CI low | 95% CI high |
|---|---|---|---|---|---|
| Intercept | 94.15 | 1 | 0.886 | 92.304 | 95.988 |
| $X_1$ | 3.38 | 1 | 0.626 | 2.074 | 4.679 |
| $X_2$ | 4.60 | 1 | 0.626 | 3.302 | 5.907 |
| $X_3$ | 6.71 | 1 | 0.626 | 5.407 | 8.012 |
| $X_2^2$ | –2.06 | 1 | 0.575 | –3.260 | –0.868 |
| $X_3^2$ | –4.04 | 1 | 0.575 | –5.233 | –2.841 |
| $X_1X_2$ | –2.17 | 1 | 0.767 | –3.766 | –0.576 |
| $X_1X_3$ | –2.83 | 1 | 0.767 | –4.423 | –1.233 |
| $X_2X_3$ | –3.35 | 1 | 0.767 | –4.950 | –1.760 |

[a]This value of "coefficient estimate" is calculated on the basis of "coded factor level."

where $Y$ is the response factor, conversion yield (%). $X_1$, $X_2$, and $X_3$ are the real values of the independent factors, reaction temperature (°C), catalyst amount (wt%), and reaction time (minutes), respectively. The model coefficients (based on coded factor level) and probability values are fully provided in Table 6. The $p$-values of all of the coefficients were less than 0.05, and the coefficient of determination ($R^2$) was 0.934, thereby indicating that the model was sufficient to adequately represent the actual relationship among the selected factors. The ANOVA for the response surface-reduced quadratic model is given in Table 5. The coefficients of the response surface model, as are shown by Eq. 1 were evaluated. The $p$-value test showed that all the linear coefficients were all more highly significant than their quadratic and cross-product terms. However, in order to minimize error, all of the coefficients were considered in this design.

Figure 2A shows the effects of reaction temperature, catalyst amount, and their reciprocal interactions on free fatty acid removal at reaction times of 18.75, 32.00, and 135 min. Reaction temperature also appeared to exert a significant degree of influence on removal rates. Increases in the reaction temperature resulted in higher removal yields at any catalyst amount. Removal yields increased in a linear fashion with increasing reaction temperature and catalyst amounts under short reaction time conditions (18.72 min). However, under long reaction time conditions, a saddle-type free fatty acid removal pattern was observed in the experiments in which reaction temperature and catalyst amount were varied.

Figure 2B shows the effects of different catalyst amounts and reaction times on removal yields at constant reaction temperature (50°C). At any of the tested catalyst amounts, from 8.8 to 16.3%, the enhancement of linear removal yields resulted in a low reaction temperature (40°C). As is shown in Figs. 2B (b) and (c), removal yield was maximized at a catalyst amount of 15%

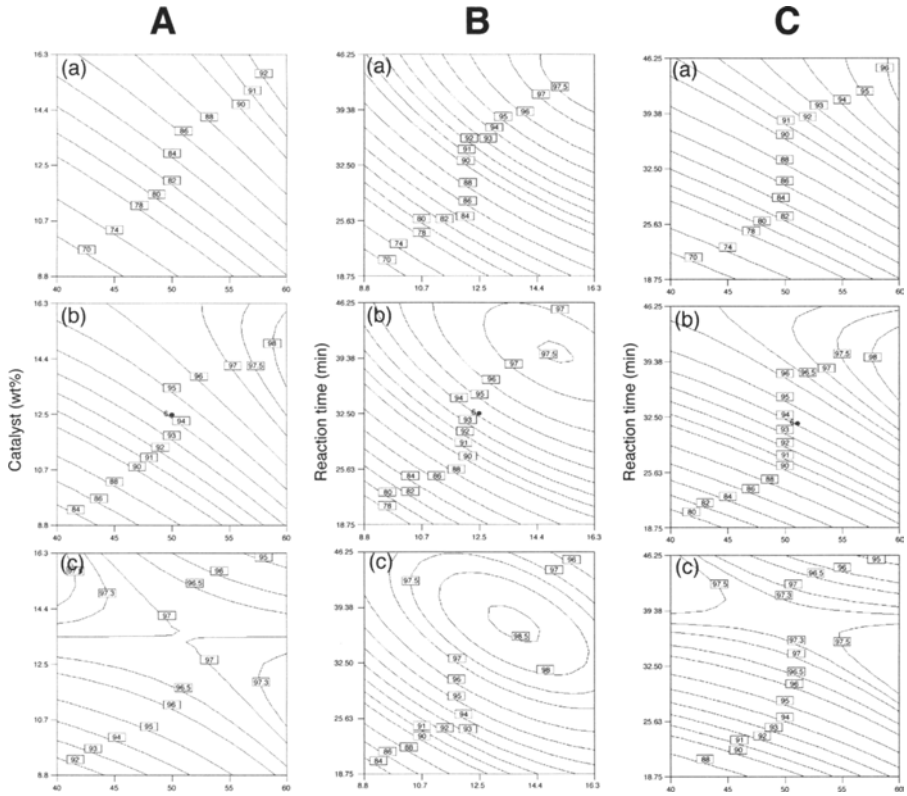


**Fig. 2.** Contour plots representing the effect of reaction temperature, catalyst amount, reaction time, and their reciprocal interaction on removal yield of free fatty acid in crude rapeseed oil. **(A)** (a) reaction time 18.75 min, (b) 32.00 min, and (c) 46.25 min. **(B)** (a) reaction temperature 40°C, (b) 50°C, and (c) 60°C. **(C)** (a) Catalyst amount 8.75% (w/v), (b) 12.50% (w/v), and (c) 16.25% (w/v).

at 40 min of reaction time at 50°C; however, these values peaked at a catalyst amount of 13% and 37 min. Maximal yield was accomplished with a high catalyst amount and a long reaction time, at a high reaction temperature. At any of the designed reaction temperatures, increases in the catalyst amount resulted in a linear enhancement of removal yields to optimum conditions.

Figure 2C shows the effects of reaction temperature, reaction time, and the reciprocal interaction of these factors with free fatty acid removal rates at constant catalyst amounts of 8.75, 12.50, and 16.25% (w/v). As is shown in Figs. 2C (a) and (c), reaction temperature also exerted a significant degree of influence on removal rates. Increases in reaction temperature resulted in high removal yields at any of the tested constant catalyst amounts. Removal yields were shown to increase in a linear fashion with reaction temperature and reaction times at low catalyst amounts (8.75%). However, at high catalyst amounts, a saddle pattern of free fatty acid removal was observed in the experiments in which reaction temperature and time were varied.

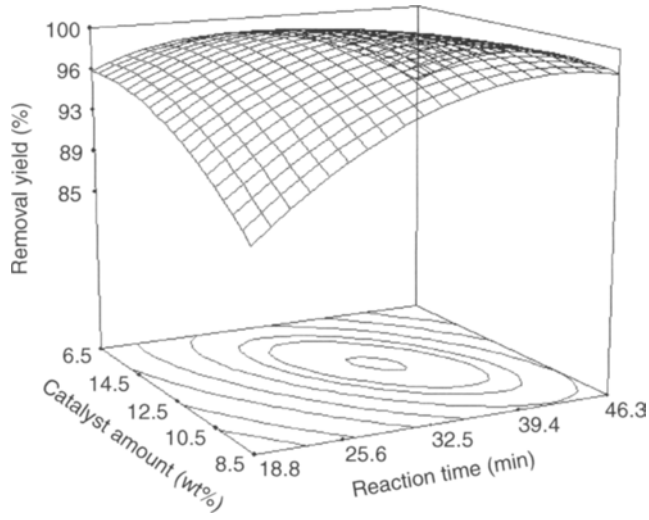


**Fig. 3.** Response surface plot representing the effect of reaction time and catalyst amount of the optimal removal of free fatty acid in crude rapeseed oil at the stationary point (reaction temperature 66.96°C).

Figure 3 contains the response surface plot showing the effects of reaction time and catalyst amount on free fatty acid removal rates in crude rapeseed oil. The optimal conditions for free fatty acid removal estimated by the model equation were as follows: $X_1 = 66.96$°C, $X_2 = 12.66\%$, and $X_3 = 37.65$ min. The theoretical removal yield estimated under the aforementioned conditions was $Y = 100\%$. In order to confirm this model-based estimation, the predicted optimal conditions were applied to three independent replicates for free fatty acid removal. The average removal yield proved to be well within the values estimated through the model equation. This shows that RSM coupled with the appropriate experimental design can be applied effectively to the optimization of factors in a reaction *(17)*. This study focused specifically on the application of RSM for the optimization of conditions for free fatty acid removal using a solid catalyst in feedstock. Our results may provide useful information regarding the development of more economical and efficient solid catalyst system for biodiesel production processes.

## Acknowledgments

The authors would like to thank the Korea Energy Management Corporation for their financial support of this study.

## References

1. Lang, X., Dalai, A. K., Bakhshi, N. N., Reaney, M. J., and Hertz, P. B. (2001), *Bioresour. Technol.* **80,** 53–62.
2. Cvengros, J. and Povazanec, F. (1996), *Bioresour. Technol.* **55,** 145–152.

3. Jeong, G. T., Oh, Y. T., and Park, D. H. (2006), *Appl. Biochem. Biotechnol.* **129–132,** 165–178.
4. Jeong, G. T. and Park, D. H. (2006), *Appl. Biochem. Biotechnol.* **129–132,** 668–679.
5. Freedman, B., Pryde, E. H., and Mounts, T. L. (1984), *JAOCS* **61(10),** 1638–1643.
6. Darnoko, D. and Cheryan, M. (2000), *JAOCS* **77(12),** 1263–1267.
7. Noureddini, H. and Zhu, D. (1997), *JAOCS* **74(11),** 1457–1463.
8. Jeong, G. T., Park, D. H., Kang, C. H., et al. (2004), *Appl. Biochem. Biotechnol.* **114,** 747–758.
9. Ma, F., Clements, L. D., and Hanna, M. A. (1998), *Ind. Eng. Chem. Res.* **37,** 3768–3771.
10. Kim, H. S. and Kang, Y. M. (2001), *J. Korean Oil Chem. Soc.* **18(4),** 298–305.
11. Dorado, M. P., Ballesteros, E., Almeida, J. A., Schellert, C., Lohrlein, H. P., and Krause, R. (2002), *Trans. ASAE* **45(3),** 525–529.
12. Canakci, M. and Gerpen, V. J. (2001), *Trans. ASAE* **44(6),** 1492–1436.
13. Wimmer, T. (1995), US patent 5399731.
14. Fukuda, H., Kondo, A., and Noda, H. (2001), *J. Biosci. Bioeng.* **92(5),** 405–416.
15. Lin, C. Y. and Huang, J. C. (2003), *Ocean Eng.* **30,** 1699–1715.
16. Usta, N. (2005), *Biomass Bioenergy* **28(1),** 77–86.
17. Jeong, G. T. and Park, D. H. (2006), *Enzyme Microbial. Technol.* **39,** 381–386.

0273-2289/1559–0291 (Online)/07/136–140/595–610/$30.00

# Optimization of Lipase-Catalyzed Synthesis of Sorbitan Acrylate Using Response Surface Methodology

GWI-TAEK JEONG[1,2] AND DON-HEE PARK*[,1,3–6]

*[1]School of Biological Sciences and Technology, E-mail: dhpark@chonnam.ac.kr; [2]Engineering Research Institute; [3]Faculty of Applied Chemical Engineering; [4]Biotechnology Research Institute; [5]Institute of Bioindustrial Technology; and [6]Research Institute for Catalysis, Chonnam National University, Gwangju 500-757, Korea*

## Abstract

In this study, we have synthesized sorbitan acrylate through response surface methodology, using sorbitan and vinyl acrylate that catalyze immobilized lipase. In order to optimize the enzymatic synthesis of the sorbitan acrylate, we applied response surface techniques to determine the effects of five-level-four-factors and their reciprocal interactions with the biosynthesis of sorbitan acrylate. Our statistical model predicted that the highest conversion yield of sorbitan acrylate would be approx 100%, under the following optimized reaction conditions: a reaction temperature of 40.1°C, a reaction time of 237.4 min, an enzyme concentration of 8%, and a 4.49 : 1 acyl donor/acceptor molar ratio. Using these optimal conditions in three independent replicates, the conversion yield reached 97.6 ± 1.3%.

**Index Entries:** Bioconversion; central composite rotatable design; esterification; lipase; optimization; response surface methodology; sorbitan ester.

## Introduction

Esterification is the principal process in the synthesis of sugar esters. This process has been extensively studied, and is achievable through both chemical and enzymatic processes. Chemical esterification has been associated with low regioselectivity, which results in poor selectivity, undesirable side reactions, and low yields. However, enzymatic esterification can be applied to the regioselective transformation of several sugars, and does not tend to result in any undue complications *(1–6)*. As compared with conventional chemical processes, enzymatic esterification can be conducted under mild conditions, and exhibits an excellent degree of selectivity, allowing for the generation of pure materials through more efficient and environmentally friendly processes, than are associated with more

*Author to whom all correspondence and reprint requests should be addressed.

conventional chemical methods. Enzymatic esterification carries the advantages of high material stability, low energy costs, a high degree of selectivity, and low purification costs. Therefore, enzymatic esterification appears to constitute a favorable alternative synthesis technique *(1–6)*.

Recently, a host of reports have noted the myriad possible applications of sugar-harboring polymeric materials synthesized from sugar esters. Sugars constitute an attractive group of multifunctional compounds, as they are both biologically relevant, and harbor multiple hydroxyl groups. Sugar esters have become the focus of increased interest of late, and have already been utilized in several fields, and a variety of applications. They have proven useful in diverse industries, and have been used as detergents, emulsifiers, lubricants, flavorings, and cosmetic additives. Sugar esters are also biodegradable, biocompatible, and nontoxic *(4,7,8)*.

Sorbitan esters are prepared either in one- or two-step reactions. In the one-step reaction, sorbitol and acyl donor are converted simultaneously to the sorbitan ester. In two-step reaction, first, sorbitol is dehydrated to sorbitan with acid catalyst (*p*-toluenesulfonic acid, sulfuric acid, and phosphoric acid). Second, formed sorbitan is esterified to sorbitan ester with the acyl donor and catalyst (alkali catalyst and enzyme) *(2,4–6,9)*.

In this study, we have evaluated two distinct esterification schemes: acylation and alcoholysis (transesterification). Acylation is the esterification of a carboxylic acid (e.g., acrylic acid [AA]) with the hydroxyl group on the acyl acceptor (e.g., 1,4-sorbitan), and generates an ester and a water byproduct. However, transesterification involves the esterification of an ester (e.g., methyl acrylate [MA], ethyl acrylate [EA], and vinyl acrylate [VA]) with the hydroxyl group on the acyl acceptor (e.g., 1,4-sorbitan). Alcoholysis generates another ester, but yields alcohol, rather than water, as a byproduct *(4–6)*. In the enzymatic process utilized in the production of sorbitan acrylate from 1,4-sorbitan, several factors can affect both glycosylation yields and rates. These factors include the reaction solvent, reaction temperature, the type and concentration of the acyl donor, the quantity of enzyme in the reaction, the water content, and the initial concentration of substrate *(3–5)*. In particular, the difficulty inherent to the dissolution of both hydrophobic and hydrophilic substrates in a common reaction solvent of low toxicity has been the principal limitation of biological synthesis *(1,4,6)*.

In all of our experiments, *t*-butanol was used as the reaction solvent owing primarily to its high substrate solubility, remarkable affinity for glycoside, its regioselective effect with glycoside, and the ease inherent to the separation/purification of the products, which is attributable to its low boiling point *(3–5,10)*. In our study, we have conducted the enzymatic synthesis of sorbitan acrylate using Novozym 435, a well-known nonspecific lipase. Novozym 435 facilitates reactions between a wide range of alcohols and vinyl esters, and is a remarkably heat-tolerant enzyme *(11)*.

Response surface methodology (RSM) is an effective statistical technique used in the research of complex processes. RSM uses multiple regression and correlation analyses as tools to test the effects of two or more independent factors on the dependent factors. The primary advantage of RSM is the reduced number of experimental runs required to generate sufficient information for a statistically acceptable result. It is both faster and less expensive than the classical research method. RSM has been successfully applied to the study and optimization of the enzyme synthesis of sugar esters. In addition, central composite rotatable design (CCRD) is a RSM that has previously been successfully used in the optimization of several biotechnological processes *(4,8,12–16)*.

In this study, we conducted acylation and alcoholysis using immobilized lipase, in order to synthesize sorbitan acrylate. First, several acyl donors were tested in order to select the optimal acyl donor for esterification. Second, the effects of different initial sorbitan concentrations, water contents, and molecular sieves were tested. Finally, RSM, consisting of a five-level-four-factor CCRD, was applied in order to evaluate the interactive effects, and to optimize the conditions for the enzymatic synthesis of sorbitan acrylate, with VA being used as the acyl donor.

## Materials and Methods

### Chemicals

The Novozym 435 (lipase B from *Candida antarctica*, EC 3.1.1.3, a nonspecific lipase immobilized on a macroporous acrylic resin, 1–2% water content, 10,000 propyl laurate units/g) was purchased from Novo Nordisk A/S (Bagsvaerd, Denmark). The D-sorbitol, VA, and *t*-butanol were purchased from the Sigma-Aldrich Chemical Co. (St. Louis, MO). The AA, MA, and EA were obtained from Daejung Chemicals & Metals Co., Ltd. (Korea), Junsei Chemical Co., Ltd. (Japan), and Yakuri Pure Chem. Co., Ltd. (Japan), respectively. The acetonitrile was obtained from Fisher Scientific. All other chemicals were of analytical grade, and the solvents were dried using molecular sieves (4 Å, Yakuri Pure Chem. Co., Ltd.) 1 d before use.

### 1,4-Sorbitan Preparation

All dehydration reactions (sorbitol cyclization) for the synthesis of 1,4-sorbitan, using *p*-toluenesulfonic acid in a solvent-free process, were conducted according to the previously reported methods *(3)*.

### Enzymatic Esterification and Experimental Design

In this study, two distinct esterification schemes were conducted: acylation (AA) and alcoholysis (MA, EA, and VA). All esterification reactions for the synthesis of 1,4-sorbitan esters were performed using immobilized

lipase (Novozym 435). The reaction temperature was controlled using a water bath equipped with a PID temperature controller. Mixing was performed with a magnetic stirrer, which spun at approx 200 rpm. The condenser prevented the evaporation of the reactants. During all of the reactions, 0.2 mL of the samples were withdrawn at set intervals, and then monitored through high-performance liquid chromatography. In all experiments with no water content, there was no set initial amount of water, with the exception of the water contained in the enzymes themselves. The results of the experiments are expressed as the mean values from at least two independent measurements.

In order to select the optimal acyl donor for enzymatic esterification, we assessed the effects of four acyl donors, as is described below. 30 g/L of prepared 1,4-sorbitan was added to the bottle, and either AA, VA, EA, or MA were subsequently added at a 1 : 3 molar ratio, in order to determine the most favorable acyl donor at 45°C and 5% (w/v) Novozym 435. In order to determine the optimal initial 1,4-sorbitan concentration for enzymatic esterification, 25–100 g/L of prepared 1,4-sorbitan was added to the bottle, at a molar ratio of 1 : 3 with VA, and 5% (w/v) Novozym 435 at 45°C. In order to determine the optimal initial water content and molecular sieve amounts for enzymatic esterification, 0–5% (v/v) water or 0–2% (w/v) molecular sieves were added to the reactant, coupled with 50 g/L of prepared 1,4-sorbitan, at a molar ratio of 1 : 3 with VA, and 5% (w/v) Novozym 435 at 45°C.

In order to apply RSM in the enzymatic synthesis of sorbitan acrylate, a five-level-four-factor CCRD scheme was adopted in this study, requiring 30 experiments, which included 16 factorial points, eight axial points, and six central points in order to provide information regarding the interior of the experiment region, allowing for the evaluation of curvature *(9)*. When applying RSM to our sorbitan acrylate synthesis scheme, we set an initial concentration of 1,4-sorbitan of 50 g/L. The variables, and their levels, selected for the study of sorbitan acrylate synthesis, were as follows: reaction temperature (25–65°C), reaction time (30–240 min), enzyme amount (1–7% [w/v]), and acyl donor/acyl acceptor molar ratio (1 : 1–5 : 1; VA : sorbitan molar ratio). Table 1 provides the coded and uncoded independent factors ($X_i$), the levels, and the experimental design.

### *Statistical Analysis*

Our experimental data (Table 2) were analyzed through RSM, to fit the following second-order polynomial equation generated by Design-Expert 6 software (Stat-Ease, Inc.). Second-order coefficients were generated through regression with stepwise elimination. The response was first fitted to the factors through multiple regression. The quality of the fit of the model was evaluated using the coefficients of determination ($R^2$) and the analysis of variances (ANOVA). The insignificant coefficients were eliminated after examining the coefficients, and the model was finally

Table 1
Factors and Their Levels for Central Composite Design

| | | Coded factor levels | | | | |
|---|---|---|---|---|---|---|
| Variable | Symbol | −2 | −1 | 0 | 1 | 2 |
| Reaction temperature (°C) | $X_1$ | 25 | 35 | 45 | 55 | 65 |
| Reaction time (min) | $X_2$ | 30 | 82.5 | 135 | 187.5 | 240 |
| Enzyme amount (wt%) | $X_3$ | 1 | 3 | 5 | 7 | 9 |
| Substrate molar ratio (acyl donor/acyl acceptor) | $X_4$ | 1 | 2 | 3 | 4 | 5 |

refined. The quadratic response surface model was fitted to the following equation:

$$Y = \beta_{k0} + \sum_{i=1}^{4} \beta_{ki} x_i + \sum_{i=1}^{4} \beta_{kii} x_i^2 + \sum_{i=1}^{3} \sum_{j=i+1}^{4} \beta_{kij} x_i x_j \quad (1)$$

where $Y$ is the response factor (conversion yield), $x_i$ is the $i$th independent factor, $\beta_0$ is the intercept, $\beta_i$ is the first-order model coefficient, $\beta_{ii}$ is the quadratic coefficient for the factor $i$, and $\beta_{ij}$ is the linear model coefficient for the interaction between factors $i$ and $j$.

### *Quantitative Analysis*

The enzymatic reactions were monitored through analysis of the conversion yield of 1,4-sorbitan. The reactant and product measurements were obtained through high-performance liquid chromatography with a ZORBAX carbohydrate column (5 μm, 120 Å, 250 × 4.6 $mm^2$, Agilent), and maintained at a constant 35°C. In order to measure the amount of sorbitan and its ester concentrations, we used a mixture of acetonitrile : water (75 : 25 [v/v]) as a mobile phase, at a flow rate of 1.0 mL/min. A 0.2 mL sample was extracted from each of the reaction mixtures at set time intervals throughout the reaction. The enzymes were removed through the filtration and dilution of the sample with buffer solution (acetonitrile : water, 50 : 50 [v/v]). 20 μL of a prepared sample was then administered. Detection was conducted using an RI detector (Shimazu RID-10A, Japan).

## Results and Discussion

In the enzymatic process used in the synthesis of sorbitan acrylate from 1,4-sorbitan, several factors can affect both the conversion yield and rate, including the reaction solvent, reaction temperature, acyl donor type and concentration, enzyme amount, water content, and initial substrate

Table 2
Central Composite Rotatable Second-Order Design, Experimental, and Estimated Data for 5-Level-4-Factor Response Surface Analysis

| Standard | Run | Temperature (°C), $X_1$ | Time (min), $X_2$ | Enzyme amount (wt%), $X_3$ | Substrate molar ratio (acyl donor/acceptor), $X_4$ | Conversion yield (%) | |
|---|---|---|---|---|---|---|---|
| | | | | | | Experimental | Estimated |
| 1 | 25 | −1 | −1 | −1 | −1 | 23.4 | 19.5 |
| 2 | 19 | 1 | −1 | −1 | −1 | 14.3 | 10.0 |
| 3 | 17 | −1 | 1 | −1 | −1 | 40.5 | 40.4 |
| 4 | 11 | 1 | 1 | −1 | −1 | 15.2 | 14.1 |
| 5 | 7 | −1 | −1 | 1 | −1 | 49.8 | 48.4 |
| 6 | 16 | 1 | −1 | 1 | −1 | 38.7 | 38.9 |
| 7 | 6 | −1 | 1 | 1 | −1 | 73.8 | 77.2 |
| 8 | 26 | 1 | 1 | 1 | −1 | 43.5 | 50.9 |
| 9 | 3 | −1 | −1 | −1 | 1 | 32.6 | 32.7 |
| 10 | 23 | 1 | −1 | −1 | 1 | 24.1 | 23.2 |
| 11 | 20 | −1 | 1 | −1 | 1 | 50.8 | 53.6 |
| 12 | 12 | 1 | 1 | −1 | 1 | 23.4 | 27.3 |
| 13 | 18 | −1 | −1 | 1 | 1 | 60.7 | 61.6 |
| 14 | 21 | 1 | −1 | 1 | 1 | 52.5 | 52.1 |
| 15 | 2 | −1 | 1 | 1 | 1 | 86.3 | 90.4 |
| 16 | 10 | 1 | 1 | 1 | 1 | 65.2 | 64.1 |
| 17 | 9 | −2 | 0 | 0 | 0 | 51.7 | 49.9 |
| 18 | 27 | 2 | 0 | 0 | 0 | 14.6 | 14.0 |
| 19 | 28 | 0 | −2 | 0 | 0 | 26.0 | 32.0 |
| 20 | 13 | 0 | 2 | 0 | 0 | 73.4 | 65.0 |
| 21 | 15 | 0 | 0 | −2 | 0 | 11.2 | 14.1 |
| 22 | 30 | 0 | 0 | 2 | 0 | 85.2 | 79.8 |
| 23 | 5 | 0 | 0 | 0 | −2 | 34.3 | 35.5 |
| 24 | 1 | 0 | 0 | 0 | 2 | 65.5 | 61.9 |
| 25 | 4 | 0 | 0 | 0 | 0 | 62.6 | 58.6 |
| 26 | 8 | 0 | 0 | 0 | 0 | 59.9 | 58.6 |
| 27 | 22 | 0 | 0 | 0 | 0 | 57.2 | 58.6 |
| 28 | 24 | 0 | 0 | 0 | 0 | 56.5 | 58.6 |
| 29 | 29 | 0 | 0 | 0 | 0 | 57.9 | 58.6 |
| 30 | 14 | 0 | 0 | 0 | 0 | 57.2 | 58.6 |

concentration (*3*). The first step of this study was the identification of factors likely to affect the conversion yield. Therefore, we assessed several screening factors for the RSM experiments, including several different acyl donors, initial sorbitan concentrations, water contents, and molecular sieves.

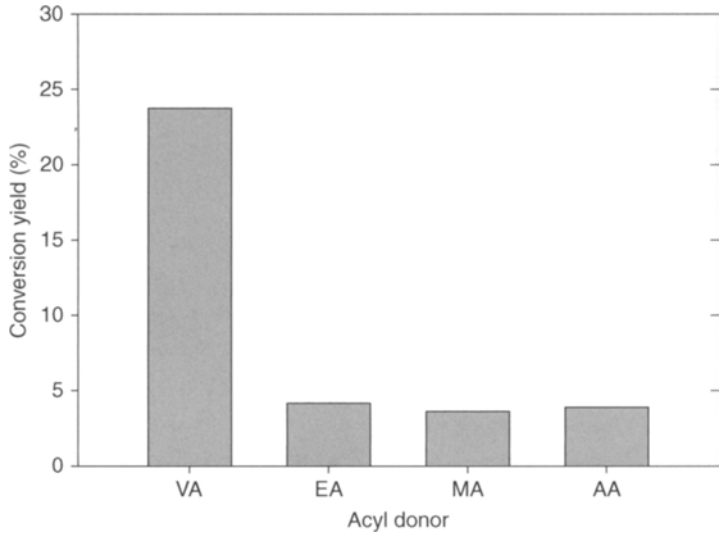


**Fig. 1.** Effect of acyl donor on enzymatic synthesis of sorbitan acrylate. Sorbitan concentration 30 g/L, acyl acceptor : acyl donor molar ratio 1 : 3, enzyme amount 5% (w/v), and reaction temperature 45°C. AA, MA, EA, and VA.

## *Effect of Acyl Donor*

In this study, we carried out two distinct esterification schemes (acylation and alcoholysis). In the acylation, AA was used as an acyl donor. In the alcoholysis, MA, EA, and VA were used as acyl donors. Figure 1 shows the effects of different acyl donors on the enzymatic esterification of sorbitan acrylate. The application of VA to the reaction was shown to result in a higher conversion yield than was observed with AA, MA, or EA. In cases in which VA was used as an acyl donor, vinyl alcohol was produced during periods in which glycosylation occurred. Therefore, we were able to determine that this process facilitates an irreversible glycosylation, which results in higher conversion yields *(3,5,10,17)*.

## *Effects of Initial Sorbitan Concentration*

In a previous experiment, we had identified VA as the optimal acyl donor. The effects of initial sorbitan concentrations on the conversion of 1,4-sorbitan with VA to sorbitan acrylate were investigated using Novozym 435. As has been shown in Fig. 2, the conversion of 1,4-sorbitan to sorbitan acrylate was approx 19.2% at 135 min, with a 25 g/L sorbitan concentration. High initial sorbitan concentrations, in excess of 50 g/L, resulted in low conversion yields. Sorbitan acrylate was synthesized at a conversion yield of approx 31.1% at an initial 1,4-sorbitan concentration of 100 g/L. In contrast to the final conversion yield of 55%, the initial conversion rate was found to be higher at a sorbitan concentration of 50 g/L within 135 min than was seen when 100 g/L of sorbitan was applied.

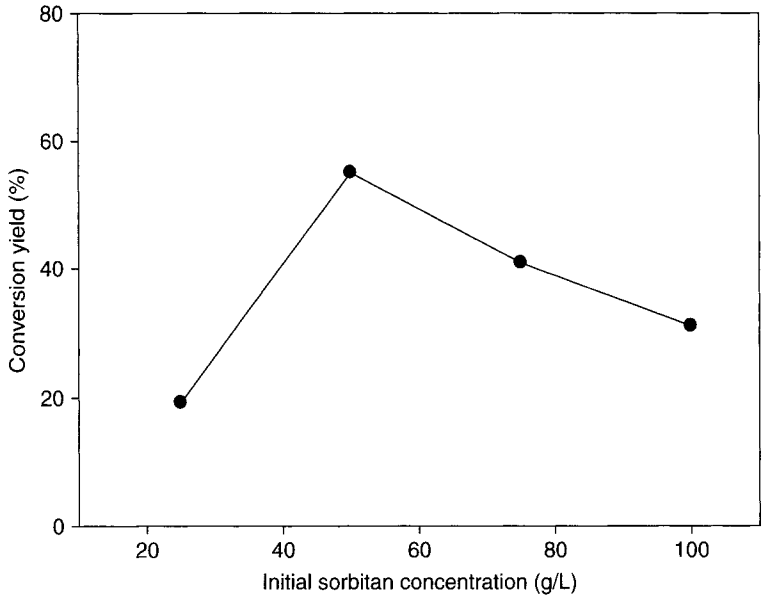


**Fig. 2.** Effect of initial sorbitan concentration on enzymatic synthesis of sorbitan acrylate. Sorbitan : VA molar ratio 1 : 3, enzyme amount 5% (w/v), and reaction temperature 45°C.

## *Effects of Water Content and Molecular Sieve*

In a previous experiment, the optimal initial sorbitan concentration was determined to be 50 g/L, and so this concentration was used in all subsequent experiments. Generally, at least a trace of water is required for enzymatic bioconversion. Enzymes manifest different reaction and selectivity behavior in organic solvents than in water *(3–6,17)*. In this experiment, the effects of water content (0–5% [v/v]) and molecular sieve amount (0–2% [w/v]) on the synthesis of sorbitan acrylate were investigated under the following conditions: 50 g/L of 1,4-sorbitan, a 1 : 3 molar ratio of VA, 0.15% (w/v) Novozym 435, and a reaction time of 135 min at 45°C.

As shown in Fig. 3, the addition of water resulted in an inhibition of the conversion of sorbitan acrylate. High water content induced low-conversion yields in a range of 1–5% (v/v). At 5% (v/v) water content, sorbitan acrylate was synthesized with a yield of approx 29.8%. Compared with the yields achieved under other conditions, the final conversion yield was 57.2% under conditions in which no water had been added, except for the inherent water content of the immobilized enzymes used.

Figure 4 shows the effects of the application of molecular sieves as water absorbents on the enzymatic synthesis of sorbitan acrylate, when using VA as the acyl donor. The addition of molecular sieves was found to generally inhibit sorbitan conversion. As compared with the 57.2% conversion yield achieved when no molecular sieves were added, the application of 2% (w/v) molecular sieves resulted in an approx 48.8% sorbitan

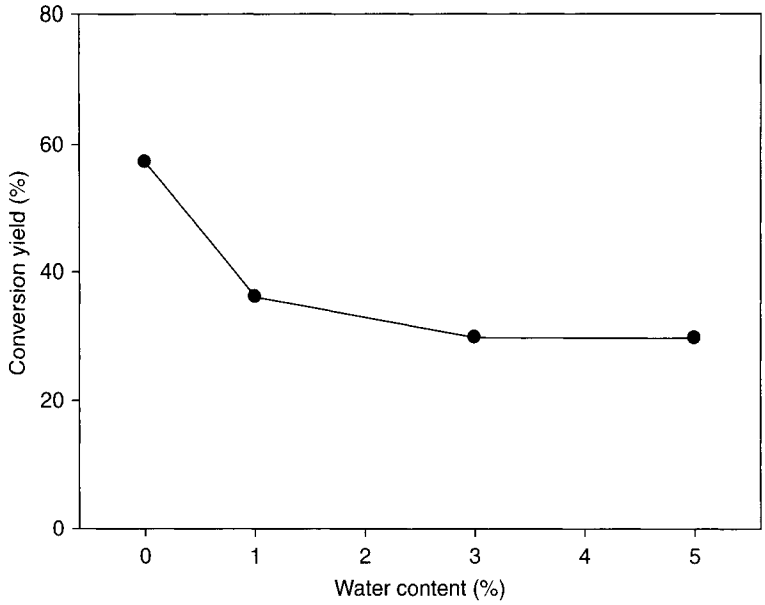


**Fig. 3.** Effect of water content on enzymatic synthesis of sorbitan acrylate. Sorbitan concentration 50 g/L, sorbitan : VA molar ratio 1 : 3, enzyme amount 5% (w/v), and reaction temperature 45°C.

acrylate conversion rate. As is shown in Figs. 3 and 4, neither the addition of water nor the dehydration of water with molecular sieves was required for the enzymatic synthesis of sorbitan acrylate using Novozym 435. In subsequent experiments, then, the reaction mixtures contained no water, except for the inherent water content of the enzymes used.

### *RSM of Esterification*

In order to construct a proper model for the optimization of sorbitan acrylate synthesis, we elected to use a CCRD, generally considered to be the best design for response surface optimization. This design featured the following five-level four-factors: reaction temperature, reaction time, enzyme amount, and acyl donor/acyl acceptor molar ratio. Table 2 shows the experimental parameter settings and results on the basis of the experimental design. A total of 30 designed experiments were then conducted, and the results were analyzed through multiple regression. The coefficients of the full model were then evaluated through regression analysis, and tested for their significance. The insignificant coefficients were eliminated in a stepwise fashion on the basis of p-values after the coefficients had been tested. Finally, the best fitting model was determined through regression and stepwise elimination. Ultimately, four linear coefficients (X1, X2, X3, and X4), three quadratic coefficients ($X_1^2$, $X_2^2$, $X_3^2$, and $X_4^2$, and two cross-product coefficients (X1X2 and X2X3) were determined to be significant (Tables 3 and 4).

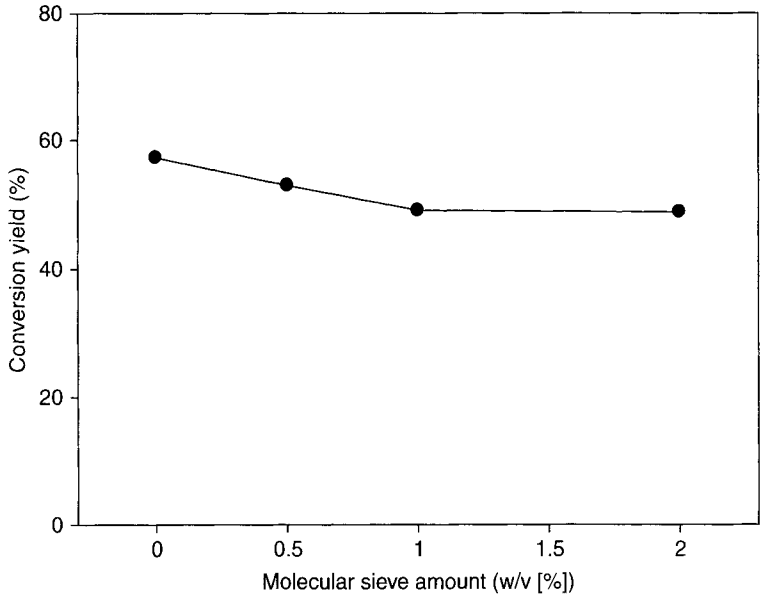


**Fig. 4.** Effect of molecular sieve on enzymatic synthesis of sorbitan acrylate. Sorbitan concentration 50 g/L, sorbitan : VA molar ratio 1 : 3, enzyme amount 5% (w/v), and reaction temperature 45°C.

Table 3
Regression Coefficients and Significance of Response Surface-Reduced Quadratic Model After a Stepwise Elimination

| Factor | Coefficient estimate | DF | Standard error | 95% CI low | 95% CI high |
|---|---|---|---|---|---|
| Intercept | 58.56 | 1 | 1.721 | 54.954 | 62.156 |
| $X_1$ | −8.96 | 1 | 0.860 | −10.760 | −7.159 |
| $X_2$ | 8.23 | 1 | 0.860 | 6.432 | 10.034 |
| $X_3$ | 16.43 | 1 | 0.860 | 14.626 | 18.227 |
| $X_4$ | 6.61 | 1 | 0.860 | 4.810 | 8.411 |
| $X_1^2$ | −6.65 | 1 | 0.805 | −8.337 | −4.968 |
| $X_2^2$ | −2.51 | 1 | 0.805 | −4.199 | −0.831 |
| $X_3^2$ | −2.90 | 1 | 0.805 | −4.582 | −1.213 |
| $X_4^2$ | −2.46 | 1 | 0.805 | −4.147 | −0.778 |
| $X_1X_2$ | −4.21 | 1 | 1.054 | −6.411 | −2.000 |
| $X_2X_3$ | 1.97 | 1 | 1.054 | −0.240 | 4.171 |

CI, confidence interval.

The final estimative response model equation, after the elimination of the insignificant variables in order to estimate the enzymatic synthesis of sorbitan acrylate, was as follows:

$$Y = -210.833 + 6.173\,X_1 + 0.670\,X_2 + 12.929\,X_3 + 21.3859\,X_4 - 0.067\,X_1^2 - 0.001\,X_2^2 - 0.724\,X_3^2 - 2.462\,X_4^2 - 0.008\,X_1X_2 + 0.019\,X_2X_3 \quad (2)$$

Table 4
ANOVA for Response Surface-Reduced Quadratic Model

| Source | Sum of squares | DF | Mean square | *F*-value | Probability > $F^{a,b}$ |
|---|---|---|---|---|---|
| Model | 12828.48 | 10 | 1282.848 | 72.217 | <0.0001 |
| $X_1$ | 1926.58 | 1 | 1926.579 | 108.455 | <0.0001 |
| $X_2$ | 1626.74 | 1 | 1626.742 | 91.576 | <0.0001 |
| $X_3$ | 6475.72 | 1 | 6475.721 | 364.545 | <0.0001 |
| $X_4$ | 1048.74 | 1 | 1048.743 | 59.038 | <0.0001 |
| $X_1^2$ | 1213.83 | 1 | 1213.834 | 68.332 | <0.0001 |
| $X_2^2$ | 173.48 | 1 | 173.478 | 9.766 | 0.0056 |
| $X_3^2$ | 230.26 | 1 | 230.260 | 12.962 | 0.0019 |
| $X_4^2$ | 166.31 | 1 | 166.310 | 9.362 | 0.0064 |
| $X_1X_2$ | 283.00 | 1 | 282.997 | 15.931 | 0.0008 |
| $X_2X_3$ | 61.82 | 1 | 61.819 | 3.480 | 0.0776 |
| Residual | 337.51 | 19 | 17.764 | – | – |
| Lack of fit | 310.83 | 14 | 22.202 | 4.160 | 0.0621 |
| Pure error | 26.69 | 5 | 5.337 | – | – |
| Correlation total | 13165.99 | 29 | – | – | – |

[a]*Probality* > *F*, level of significance.
[b]Values of probality > *F* < 0.0500 indicate model terms are significant. Values more than 0.1000 indicate the model terms are not significant.

where Y is the response factor, and conversion yield (%). X1, X2, X3, and X4 represent the real values of the independent factors—reaction temperature (°C), reaction time (min), enzyme amount (wt%), and acyl donor/acyl acceptor molar ratio (–), respectively. The model coefficients and probability values are shown in Table 4. All p-values of the coefficients were less than 0.05, and the coefficient of determination (R2) was 0.974 (R2 = 0.90 estimated by model Eq. 2), thereby indicating that the model adequately represented the real relationship among the factors selected. The ANOVA for the response surface-reduced quadratic model is given in Table 4. The coefficients of the response surface model, as are provided in Eq. 1, were evaluated. A Probability > F-value indicated that all of the linear coefficients were more highly significant than were their quadratic and cross-product terms. According to the results of our analysis of factors, there was a low lack of fit. This indicates that the model represents the actual relationships of the reaction parameters, well within the selected ranges.

Figure 5 shows the responses of surface plots representing the effects of reaction temperature, acyl donor/acceptor molar ratio, reaction time, and enzyme amount as well as their reciprocal interaction with the synthesis of sorbitan acrylate, by holding two factors constant at zero level. The relationships between the reaction factors and responses can be better understood

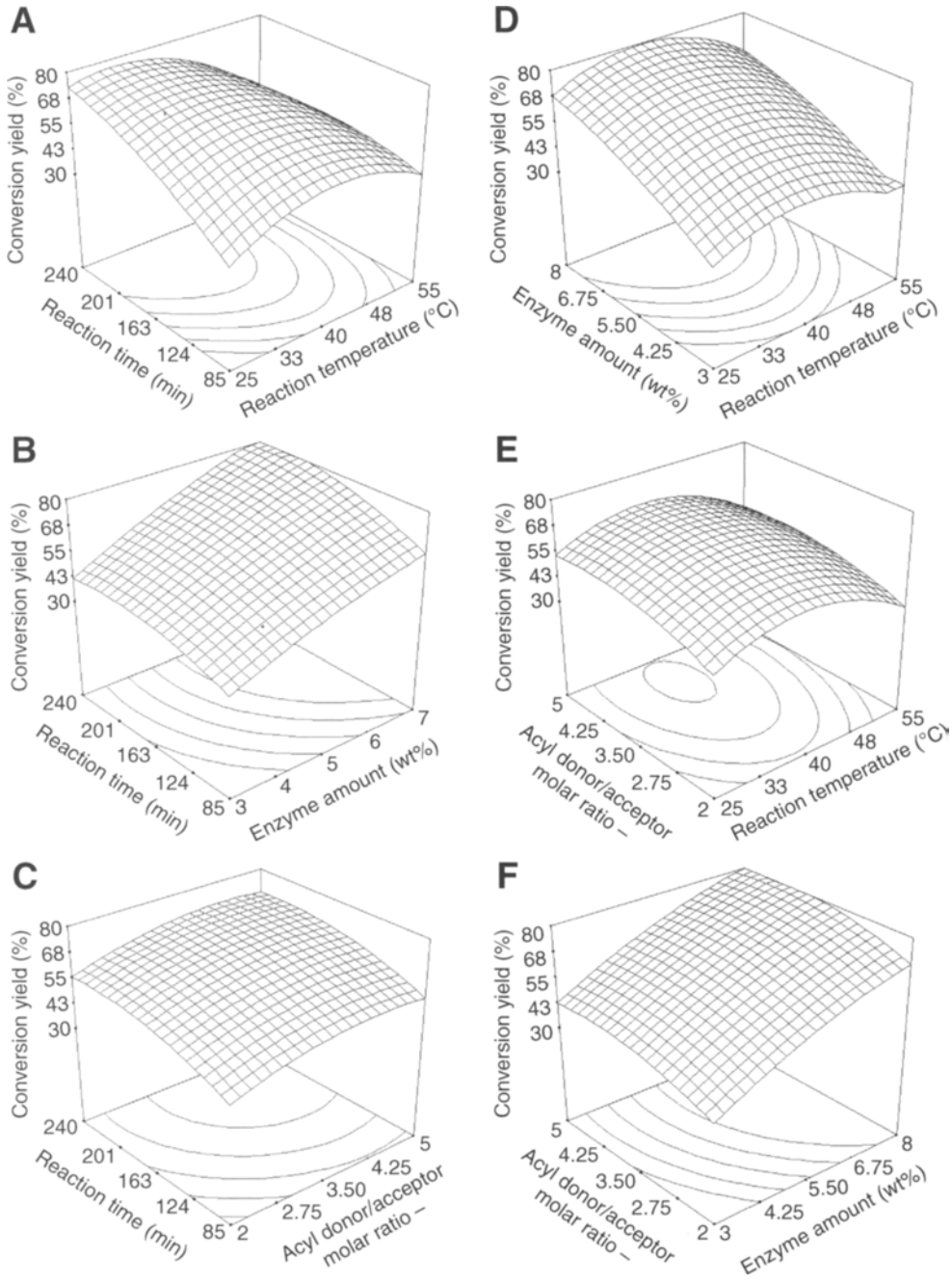


**Fig. 5.** Response surface plots representing the effect of reaction temperature, enzyme amount, substrate molar ratio, reaction time, and their reciprocal interaction with sorbitan acrylate synthesis. Other factors are constant at zero levels.

with an explanation of the planned series of plots generated from the predicted model, in Eq. 2. As shown in Fig. 5A, the low reaction temperature (35–40°C) results in an increased conversion yield, with an increase in reaction time with the other factors at zero level. Conversion was affected slightly by reaction temperature, and the optimal reaction temperature for sorbitan acrylate synthesis was determined to be between 30 and 40°C.

Figure 5B represents the effects of different enzyme amounts and reaction times on sorbitan conversion at constant reaction temperature (45°C) and substrate molar ratio (3 : 1). At any enzyme concentration between 3 and 7%, an enhancement of conversion yield leads to an increase in reaction time. An increase in the amount of introduced enzyme amount results in a linear increase in conversion yield at a constant reaction time. The maximal yield was obtained through the administration of a high enzyme amount and a long reaction time, using a moderate reaction temperature. At any of the reaction temperatures within the limits of the experimental design, an increase in the enzyme concentrations enhances the conversion yield in a linear fashion. Also, with increases in the acyl donor/acceptor molar ratio, conversion yields were enhanced in a linear fashion with reaction time, when other factors were maintained at zero level (Fig. 5C).

The effects of reaction temperature and differing enzyme concentrations on the enzymatic synthesis of sorbitan acrylate, with a acyl donor/acceptor molar ratio of 3 : 1 and a 135 min reaction time, are shown in Fig. 5D. Within the entire range of introduced enzyme amounts, maximal sorbitan conversion was accomplished at a mild reaction temperature, of between 35 and 40°C. At constant reaction temperature, an increase in the amount of introduced enzymes resulted in a linear increase in sorbitan conversion. Reaction temperature also evidenced a high degree of influence on the conversion rate. High reaction temperatures clearly tended to induce enzyme inactivation. Increases in the reaction temperature more than 55°C resulted in low-conversion yields at any enzyme amount because of the inactivation of enzymes at such high temperatures. This showed that the optimal temperature for Novozym 435 was between 40 and 60°C, as previously reported *(4–6)*.

Figure 5E shows the effects of different reaction temperatures and acyl donor/acceptor molar ratios on sorbitan conversion conducted with a constant reaction time (135 min) and enzyme amount (5%). An increase in the introduced acyl donor/acceptor molar ratio resulted in a general increase in conversion yields at constant reaction temperature. The optimal yield was obtained at a 4.25 : 1 acyl donor/acceptor molar ratio and a 40°C reaction temperature.

The effects of different enzyme amounts and acyl donor/acceptor molar ratios on the enzymatic synthesis of sorbitan acrylate at zero level are shown in Fig. 5F. Increases in the amount of introduced enzymes or in the acyl donor/acceptor molar ratio both resulted in a linear increase in conversion yields, when reaction temperature and time were constant. Maximal conversion was achieved using a high enzyme content and a

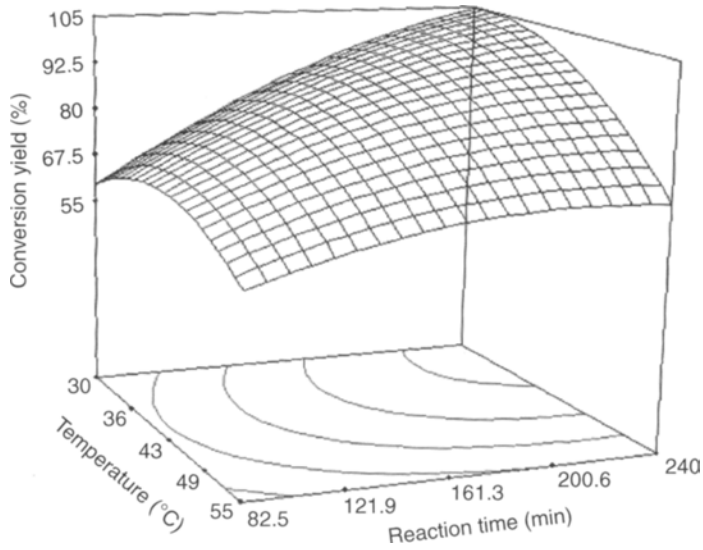


**Fig. 6.** Response surface plot representing the effect of reaction temperature and reaction time of the optimal enzymatic synthesis condition at the stationary point (enzyme amount 8%, and acyl donor/acceptor molar ratio 4.49 : 1).

high acyl donor/acceptor molar ratio. As compared with the results shown in Fig. 5, the optimal conversion yields were achieved using a high enzyme amount and a high acyl donor/acceptor molar ratio, as well as a long reaction time, at a reaction temperature of between 40 and 45°C. This pattern is similar to the previous report *(4)*.

The optimum values of the selected factors were obtained by solving the regression equation (Eq. 2), using Design-Expert 6 software. The optimal conditions for the lipase-catalyzed enzymatic synthesis of sorbitan acrylate, as estimated by the model equation, were as follows: $X_1 = 40.1$°C, $X_2 = 237$ min, $X_3 = 8\%$, and $X_4 = 4.49 : 1$ (Fig. 6). The theoretical conversion yield predicted under the above conditions was $Y = 100.1\%$. In order to conform the prediction value by the model, using these optimal conditions in three independent replicates, the average yield reached 97.6 ± 1.3%. This confirms that RSM coupled with proper experimental design can be effectively used in the optimization of lipase-catalyzed processes.

## Acknowledgments

This work was supported by Korea Research Foundation Grant funded by the Korean Government (MOEHRD) (R05-2004-000-11185-0).

## References

1. Castillo, E., Pezzotti, F., Navarro, A., and López-Munguía, A. (2003), *J. Biotechnol.* **102,** 251–259.
2. Park, D. H., Lim, G. G., Jeong, G. T., et al. (2003), *Korean J. Biotechnol. Bioeng.* **18,** 222–228.

3. Torres, C. and Otero, C. (2001), *Enzyme Microb. Technol.* **29,** 3–12.
4. Jeong, G. T. and Park, D. H. (2006), *Enzyme Microb. Technol.* **39,** 381–386.
5. Jeong, G. T., Lee, H. J., Kim, H. S., and Park, D. H. (2006), *Appl. Biochem. Biotechnol.* **129–132,** 265–277.
6. Jeong, G. T., Byun, K. Y., Lee, W. T., et al. (2006), *Biochem. Eng. J.* **29,** 69–74.
7. Park, O. J., Kim, D. Y., and Dordick, J. S. (2000), *Biotechnol. Bioeng.* **70,** 208–216.
8. Shaw, J. F., Wu, H. Z., and Shieh, C. J. (2003), *Food Chem.* **81,** 91–96.
9. Smidrkal, J., Cervenkova, R., and Filip, V. (2004), *Eur. J. lipid Sci. Technol.* **106,** 851–855.
10. Park, D. H. and Kim, H. S. (2001), *Korean J. Biotechnol. Bioeng.* **16,** 82–86.
11. Virto, C. and Adlercreutz, P. (2000), *Enzyme Microb. Technol.* **26,** 630–635.
13. Tu, Y. Y., Xu, X. Q., Xia, H. L., and Watanabe, N. (2005), *Biotechnol. Lett.* **27,** 269–274.
14. Park, S. H. (2004), *Design of Experiments*, 2nd ed. MinYoungSa, Seoul, Korea.
15. Kiran, K. R., Manohar, B., and Divakar, S. (2001), *Enzyme Microb. Technol.* **29,** 122–128.
16. Gunawan, E. R., Basri, M., Rahman, M. B. A., Salleh, A. B., and Rahman, R. N. Z. A. (2005), *Enzyme Microb. Technol.* **37,** 739–744.
17. Park, D. W., Haam, S., Ahn, I. S., Lee, T. G., Kim, H. S., and Kim, W. S. (2004), *J. Biotechnol.* **107,** 151–160.

0273-2289/1559-0291 (Online)/07/136-140/611-624/$30.00

# Renewable Energy in the United States

*Is There Enough Land?*

**ALVIN O. CONVERSE***

*Thayer School of Engineering, Dartmouth College, Hanover, NH 03755,*
*E-mail: alvin.o.converse@dartmouth.edu*

## Abstract

A review of studies of biomass potential in the United States finds a wide variation in the estimates. A number of specific policy-relevant questions about the potential of biofuels in the United States are answered. A recently published global analysis of the potential conflict between land needed for bioenergy and land needed for food is extended to the situation in the United States. A renewable energy supply scenario, capable of meeting the 2001 US energy demand, indicates that there is enough land to support a renewable energy system but that the utilization of biomass would be limited by its land requirement.

**Index Entries:** Agriculture; forest; postfossil; renewable energy; scenario; land requirements.

## Introduction

Oil production in the United States peaked in 1970 and many expect world oil production to peak by 2020. Odell *(1)* expects that natural gas will fill in for oil, and peak about 2060, followed by unconventional oil and gas, which in his projection will peak about 2080 and 2100. This allows the global oil and gas consumption rate to increase from the current rate of 263 EJ/yr at a rate of 1.6%/yr for the first half of the present century, to a level of 702 EJ/yr, then level off, and finally decrease rapidly at the beginning of the next century. At this point, the use of coal, nuclear breeder energy, and/or some forms of renewable energy must expand rapidly to fill in for the declining production of oil and gas. In a similar vein, Turton *(2)* projects a rapid expansion in the use of biomass for fuels beginning in 2050 and reaching 180 EJ in fuels, requiring 320 EJ in raw biomass by 2100. What role can we expect biomass and other forms of renewable energy to play in this postpetroleum age? Will land availability limit the ability of renewable sources to meet the demand? Will biomass energy become a big new customer for land, reducing the availability of land for food?

*Author to whom all correspondence and reprint requests should be addressed.

## Review of Studies of the Bioenergy Potential in the United States

According to the following five studies, the potential amount of liquid fuel from cellulosic biomass in the United States ranges from less than 10 to 30 EJ. Lynd et al. *(3)* estimate 30 EJ of ethanol from 160 Mha devoted to energy crops. Ethanol productivity is assumed to increase to 168 GJ/ha because of improved biomass productivity (18.0 Mg/ha) and process yield (0.53 J ethanol/J biomass). Hoogwijk et al. *(4)* estimate 20 EJ largely from agricultural land no longer needed for food production because food productivity is assumed to outpace population growth, but the land area is not specified. Green et al. *(5)* estimate 15 EJ from 37 Mha plus the use of corn stover. They assume that by 2050 ethanol productivity will increase to 335 GJ/ha. This study calls for the unusual measure of replacing soybeans with switchgrass, justified on the claim that much more ligno-cellulosic biomass can be produced while producing the same amount of protein. Perlack et al. *(6)* estimate a potential of about 8.5 EJ of liquid biofuels, largely from residues of existing biomass operations and improved agricultural yields. They require only 22 Mha of land exclusively for energy crops. McLaughlin et al. *(7)* base their estimate on the modeled economic response to prices paid for switchgrass; at 44 US$/Mg they find only 1.4 EJ of ethanol is produced. This requires 16.4 Mha, reducing crop production and increasing the price of corn, wheat, and so on, by 10–15%. This study is particularly important because it is the only study that examines the economic effect of energy crop production on food production. In none of these studies is the role of biomass in a total renewable energy system of the country considered. The section entitled "A Renewable Energy Scenario to Produce the Energy Used in the United States in 2001" in this article is an attempt to rectify this situation; it calls for 16 EJ of liquid fuel and 3.1 EJ of solid fuel from biomass.

## Biomass Energy, is There Enough Land in the United States?

The question is a little vague. Is there enough land to do what, with what technology, and on whose land? Let us begin by examining some more specific questions.

### *Is There Sufficient Cropland in the United States to Provide Enough Ethanol From Corn to Make a 10% by Volume Blend, Often Referred to as E-10, of All the Gasoline Used in 2001?*

The gross ethanol yield per acre from corn is taken to be 74.2 GJ/ha (equivalent to 3516 L of ethanol/ha) *(8)*, and it is the *gross* land-energy productivity that should be used in this case because we just want to know whether biomass can supply enough ethanol, regardless of the source of the energy to produce it. (The net energy will come later.) In 2001, 479 GL (126.6 billion gal) of gasoline were used in the United States *(9)*. Hence, for

a 10% volume blend, 13.7 Mha (33.8 million acres) would be required. Inspection of the United States land use *(10)* indicates that this amount could be met from the idled and reserve program land. However, note that this amount of land area is half the total land currently allocated to corn *(11)*. Hence, corn might be able to support the current effort to promote E-10 but not much more, and E10 replaces only 10% of the gasoline.

### *How Much Could the Required Land Area be Reduced by Converting Some of the Corn Stover to Ethanol?*

Kim and Dale *(8)* analyzed the case in which 70% of the stover as well as the corn grain, was converted, and wheat was grown as a winter cover crop to offset the loss of the organic matter as a result of the removal of a portion of the stover. In their study the corn grain yield was 8.12 Mg/ha-yr and the corn stover 5.70 Mg/ha-yr. From the corn they obtained 2.88 Mg/ha-yr of ethanol; and from the stover, 1.68 Mg/ha-yr. Important byproducts included corn gluten meal, 0.46 Mg/ha-yr; corn gluten feed, 1.96 Mg/ha-yr; and corn oil, 0.36 Mg/ha-yr. In addition 1.28 MWH/ha of electricity was obtained.

In this case they found the gross land-ethanol productivity to be 122 GJ/ha (617 gal/a). The energy inputs for the corn grain are summarized as follows, in GJ/ha: agricultural processes, 22.7; wet-milling, 42.5; and energy avoided owing to coproduct production, –49.5. The energy inputs for the corn stover, in GJ/ha, are for corn stover conversion, 5.0; and avoided electricity, –15; for a subtotal of 5.7 for both aspects of the process. Thus, the overall net land-ethanol productivity is 122 – 5.7 = 116.3 GJ/ha, or 588 gal ethanol/acre.

Note the importance of the avoided energy of the byproducts in reducing the energy required to produce the ethanol. The stover adds not only cellulose to increase the ethanol output, but also adds thermal energy to power the process and supply excess electricity. The *net* ethanol land productivity is 116.3 GJ/ha (588 gal/acre), whereas without the stover, the *gross* land ethanol productivity is only 74.2 GJ/ha (375 gal/acre). Hence, the land required to make the ethanol for a 10% blend is reduced from 13.7 to 8.66 Mha. In this case the energy required to grow and process the ethanol is supplied by process residuals (largely lignin) and a portion of the product ethanol.

### *How Much Energy is Saved When Ethanol is Made From Corn?*

Ferrell et al. *(12)* have reviewed a number of conflicting papers and come to the following conclusions.

#### For Corn Ethanol

Per amount of energy in the ethanol, the nonrenewable energy inputs are: 0.05 of petroleum, 0.3 of natural gas, 0.4 of coal, and 0.04 of hydro and nuclear for a total of 0.79. Per unit of energy in gasoline the energy inputs

Table 1
Land Requirements for Food and Energy

| Item | World | | United States |
|---|---|---|---|
| | Poor | Rich | |
| Arable land ($m^2$/person) | 2500 | | 6140 |
| Forests and pastures ($m^2$/person) | 12,400 | | 15,300 |
| Food consumption (Kg wheat equivalent) | 200 | 800 | 800 |
| Food production (Kg wheat eq./$m^2$) | 0.2 | 1.0 | 0.233 |
| Arable land needed for food ($m^2$) | 1000 | 800 | 3400 |
| Energy consumption (GJ/person-yr) | 35 | 200 | 330 |
| Biomass production (Mg/ha) | 1.0 | 15 | 15 |
| Energy production (GJ/ha-yr) | 18 | 270 | 270 |
| Land required for energy ($m^2$/person) | 19,000 | 7400 | 12,200 |
| Land required for food and energy ($m^2$/person) | 20,000 | 8200 | 15,600 |

Sources from ref. *13* and this work.

are: 1.1 of petroleum, 0.03 of natural gas, 0.05 of coal, and 0.011 of hydro and nuclear, for a total of 1.191. So when one unit of gasoline energy is replaced with one unit of corn ethanol energy, 1.1 – 0.05 = 1.05 units of petroleum energy are saved. However, 0.3 – 0.03 = 0.27 units of natural gas energy are expended and 0.4 – 0.05 = 0.35 units of coal are expended. Regarding the total energy when one unit of corn gasoline energy is replaced with one unit of corn ethanol energy, 1.19 – 0.79 = 0.40 units of energy are saved. So, if corn ethanol is used in an effort to reduce petroleum imports, it is quite effective; the reduction in imported petroleum energy is 105% of the energy in the ethanol. However, if corn ethanol is used to reduce fossil fuel use, such as would be the case when greenhouse gases are of concern, it is much less effective; the reduction in fossil fuel use is only 44% of the energy in the ethanol. And the reduction in total nonrenewable energy is only 40%.

### For Ethanol From Cellulosics

The substitution of one unit of energy in cellulosic ethanol for one in gasoline saves 1.09 units of nonrenewable energy. Not only does the use of cellulosics greatly expand the resource base, it is far more energy efficient than corn.

## *Can Biomass Supply the Primary Energy Consumption Without Compromising Food Production?*

The global analysis, summarized in the first three columns of Table 1, taken from Nonhebel *(13)*, is based on the current world population of six billion; the extension to the United States in the fourth column is based on the current United States population of 300 million. The analysis distinguishes between so-called "poor" and "rich" societies. Food

consumption (line 3) in "rich" societies is high owing primarily to the inclusion of meat in the diet. Food productivities (line 4) are based on the world average for the "poor" and Holland's maximum for the "rich". The corresponding land requirements for food (line 5) are nearly the same for "rich" and "poor," the higher productivity of the "rich" being offset by their greater consumption. Note that if the average United States wheat yield, 0.233 kg/m$^2$ *(10)*, had been used for the "rich" food productivity, the land requirement would be much higher, specifically, 3433 m$^2$, as shown in the United States column. This does not exceed the United States arable land per capita but it does exceed the world average of 2500 m$^2$, indicating that the rich diet and the United States wheat productivity cannot be shared by all. Assumptions concerning energy consumption are presented in row 6; as indicated, the US energy consumption exceeds Nonhebel's rich level. Biomass productivity is given on lines 7 and 8. The value of 15 Mg/ha is based on the performance of plantations of short-rotation woody biomass. The value of 1 Mg/ha seems low. The author indicates a value of 2 Mg/ha for unfertilized plots earlier in the article; and values of 3–8 are given in the literature *(14)*. However, the productivity of a typical Swedish forest is 1 Mg/ha-yr *(15)*. Furthermore, many who use biomass for fuel live in areas of poor rainfall. Hence, the biomass productivity has not been changed. Even if it were as high as 3 Mg/ha there still would not be enough arable land. The energy productivity (line 8) is based on the heat content of biomass with no consideration of product yield or processing and harvesting requirements. Thus, it is an upper limit. The corresponding land requirements for primary energy are given in line 9. In all three cases the land required for food and biomass greatly exceeds the arable land indicating that food production would have to be reduced if sufficient arable land were allocated to bioenergy to meet the full primary energy demand.

### *What can be Expected From the United States Forests?*

From forest surveys *(16)*, the total live biomass in the 202 Mha (500 million acres) of US Timberland, including Alaska, is 21.9 Pg (24,120 million dry t). The gross growth rate is 3.55% of live biomass. This is partially offset by the death rate, 0.75%, and the removals rate, 1.9%, leaving a net accumulation rate of 0.9% *(17)*. Thus, the annual increase in live biomass is 0.197 Pg/yr (217 million dry t/yr). In addition Perlack et al. *(6)* estimate that 0.260 Pg/yr. (287 million dry t/yr) could be obtained from residues and fire hazard reduction. (*see* Review of Studies of the Bioenergy Potential in the United States section) Adding this to the net annual increase in live biomass yields 0.457 Pg/yr (503 million dry t/yr) for the total. The energy content of this (using 17.6 MJ/kg) is 8.0 EJ (7.5 quads), which would yield about 3.7 EJ of liquid biofuel. However, at present some residues are in use for direct heating and the generation of electricity.

The aforementioned figures are based on surveys of only 206 Mha (500 million acres) of "productive unreserved forest" whereas the total

forest area is 309 Mha (750 million acres). However, the remaining 103 Mha (250 million acres) consists of low-productivity forest in the west and in the interior of Alaska, and protected acres in wilderness areas and national parks *(18)*. The availability of cheap oil has been a disincentive to producing fuels from cellulosic biomass. Without this restraint and with improved technology for converting cellulosic biomass to liquid fuels, regulation to preserve the sustainability of forest growth may well be even more important than now.

### *How Much Additional Liquid Fuel Could be Made if Animal Production Were Reduced by 50%?*

According to the mass flow diagram of Heller and Keoleian *(19)*, 177 Tg/yr (390e9 lbs/yr) of grains are fed to animals. This is slightly more than the 162 Tg (356e9 lbs) exported, which required 37.2 Mha (92 million acres) (*see* Appendix A). This indicates that approx 41 Mha (100 million acres) are used to produce grain to be fed to animals, not counting the extensive land used for pasture. In addition to the land used for grain production and pasture, 42 Mha (103 million acres) are used to grow hay (Appendix A). Hence, if animal production were reduced by 50% there would be about 41 Mha (100 million more acres) for biomass, which according to the value of 116.3 GJ/ha (588 gal/acre) *(8)*, would yield 4.77 EJ ethanol (58 billion gal ethanol), about 30% of the gasoline (on an energy basis) used in 2001.

### *How Does the Land Productivity for Photovoltaic Hydrogen Compare With That of Biomass?*

Long-term photovoltaic (PV) efficiency based on insolation on the horizontal is assumed to be 10%. Average insolation in the United States is taken to be 59,000 GJ/ha-yr. (*Source:* Inspection of insolation contour plots from de Jong *[20]*). This is supported by the fact that a typical year's insolation in Madison, WI is 51,500 GJ/ha-yr *(21)*. The land-PV electricity productivity = 0.1 × 59,000 GJ/ha-yr = 5900 GJ-electric/ha-yr. Electrolysis efficiency is assumed to be 80%. The land-hydrogen energy productivity = 0.8 × 5900 = 4720 GJ-hydrogen/ha-yr. (23,883 gal/acre ethanol equivalent). Note how much greater this is than the current value of 49 GJ/ha-yr or even the optimistic value of 335 GJ/ha-yr *(5)* presented in Section "Review of studies of the Bioenergy Potential in the United States".

### *What is the Land-Energy Productivity for Biodiesel Compared With Bioethanol?*

For biodiesel made by esterification of oil from soybeans grown in a corn-soybean rotation, soybean production was 2.60 Mg/ha-yr, yielding 0.46 Mg/ha-yr of diesel fuel *(8)*. Based on 37.8 MJ/Mg this corresponds to a land-energy productivity of 17.4 GJ/ha-yr. The aforementioned figure

of 2.60 Mg/ha-yr is supported by the value of 2.51 Mg/ha-yr found in Table A1, which is drawn from total United States production data. The result of 17.4 GJ/ha-yr is in rough agreement with the value of 25 obtained independently *(22)*. Hence, the gross land liquid-fuel productivity is much smaller than that obtained for corn ethanol, 74.2GJ/ha-yr *(8)*. However, a recent study *(23)* found that without byproducts considered, the net energy in biodiesel was 73% of the gross, and 20% in ethanol from corn. Hence, the net land liquid-fuel productivity would be 12.7 GJ/ha for soy diesel and 14.8 GJ/ha for corn ethanol.

### *Is There Enough Cropland in the United States for Ethanol From Biomass to Replace all the Gasoline Used in the United States in 2001?*

On an energy equivalent basis, it would require 727 billion L (192 billion gal) of ethanol to replace the 480 billion L (126.6 billion gal) of gasoline used in 2001 *(9)*. Using the land-ethanol productivity of 116 GJ/ha (588 gal/acre), (developed in the answer to question 2) this would require 132 Mha (326 million acres). This is greater than the currently harvested cropland; however, this land might be found if one looked hard:

1. From reserve programs, cropland used for pasture, and 'other' land, 65 Mha *(10)*.
2. By eliminating export grains, 37 Mha (Appendix).
3. By reducing animal production by 50%, 40 Mha (*see* above discussion).
4. By replacing soybeans with switchgrass, 29 Mha (*see* Review of Studies of the Bioenergy Potential in the United States section and ref. *5*), for a total of 171 Mha.

## A Renewable Energy Scenario to Produce the Energy Used in the United States in 2001

The extent to which biomass energy is used will depend on how much is needed, and this means that the energy demand and other sources of supply need to be spelled out in detail. The following scenario is based on the energy used in the United States in 2001 and the constraint that neither fossil fuel nor nuclear power be used. The underlying rationale is to determine whether an energy system using only renewable energy sources available in the United States is possible, or better expressed, what the land requirements might be. It is based on a set of plausible assumptions, and is meant to give a rough sketch of the role biomass might play.

The land-energy productivities on which the scenario is based, are presented in Table 2. The nonelectrical 2001 demands are presented, along with renewable means of satisfying them, in Table 3. The 2001 electrical demands are presented, along with the renewable means of satisfying

Table 2
Land Renewable Energy Factors

| Technology | Solar efficiency (%) | Factor (GJ/ha-yr) | Sources |
|---|---|---|---|
| Wind electric | n. a. | 416 | *24* |
| Photovoltaic | 10 | 5886 | *29* |
| Solar–thermal–electric (STE) | 11.5 | 6771 | *30* |
| Solar–thermal | 34.5 | 20,371 | Based on three times's the output of STE |
| Liquid biofuel | 0.19 | 113 | Corn and 70% stover *(8)* |
| Switchgrass, advanced | 0.56 | 331 | Dependent on R&D *(5)* |
| Wind hydrogen | n. a. | 354 | Based on wind-electric and 85% electrolysis efficency |
| Biomass solid | 0.30 | 180 | Based on 282 GJ/ha for less 15% loss in harvesting and 25% loss in combustion |

n. a., not applicable.

Table 3
Renewable Energy Scenario to Cover 2001 Nonelectric Energy Use

| | | Renewable energy scenario | | |
|---|---|---|---|---|
| Type of use | In 2001 EJ/yr | EJ/yr | TWh/yr | Energy source |
| Transportation | | | | |
| Aviation fuel *(31)* | 3.0 | 3.0 | – | Hydrogen |
| Gasoline *(10)* | 15.4 | 7.7 | – | Biomass liquid |
| | – | 7.7 | 725[a] | Electricity |
| Diesel fuel *(10)* | 5.0 | 4.0 | – | Biomass liquid |
| | – | 1.0 | 98 | Electricity |
| Other fuel *(10)* | 4.4 | 3.2 | 314 | Electricity |
| | – | 1.2 | | Biomass liquid |
| Total transportation *(32)* | 27.8 | 27.8 | – | – |
| Nonfuel (Chemicals and so on) *(33)* | 6.2 | 3.1 | – | Biomass liquid |
| | – | 3.1 | – | Hydrogen |
| Residential, commercial, and industrial nonfuel *(32)* | 28.3 | 3.1 | – | Biomass solid |
| | – | 14.7 | – | Solar thermal |
| | – | 10.5 | – | Conservation |
| Electric storage loss[b] | – | – | 284 | – |
| Total | 62.3 | 62.3 | 1421 | – |

[a]Based on 10.6 MJ/kWh rather than 3.6 to account for thermal conversion.
[b]It is assumed that 50% of the electricity is stored and that 25% of this is lost because of electrochemical conversions.

Table 4
Renewable Energy Scenario to Cover 2001 Electrical Energy Use

| Source | 2001[a] TWh | Renewable energy scenario TWh | Land (Mha) |
|---|---|---|---|
| Fossil | 2677 | 0 | – |
| Nuclear | 769 | 0 | – |
| Hydro | 217 | 434 | – |
| Biomass | 35.2 | 0 | – |
| Waste (MSW) | 21.8 | 30 | – |
| Geothermal | 13.7 | 137 | – |
| STE | 0.25 | 943 | 0.57 |
| Photovoltaic | 0.25 | 313 | 0.21 |
| Wind | 6.7 | 1883 | 20.8 |
| Other | 4.7 | 5 | – |
| Storage loss[b] | – | 936 | – |
| Total | 3737 | 4460 | 21.6 |

[a]DOE Annual Energy Review, Table 8.2a *(34)*.

[b]It is assumed that 50% of the electricity is stored and that 25% is lost in electrical conversions. Supply divided among STE, 30%; PV, 10%; and Wind, 60%.

Table 5
Summary of Land Requirements

| Item | Energy content EJ | Energy content TWh | Land factor GJ/ha | Land factor MWh/ha | Land Mha |
|---|---|---|---|---|---|
| Biomass liquid | 16.0 | – | 113 | – | 142 |
| Biomass solid | 3.16 | – | 180 | – | 17.5 |
| Hydrogen (wind) | 6.12 | – | 354 | – | 17.2 |
| Solar–thermal | 14.7 | – | 20,371 | – | 0.7 |
| Electricity | – | 5881 | – | – | – |
| Wind (60%) | – | 3529 | 416 | 116 | 30.4 |
| STE (30%) | – | 1764 | 6771 | 1882 | 0.93 |
| PV (10%) | – | 588 | 5886 | 1636 | 0.36 |
| Total | 40.0 | 5881 | – | – | 209.1 |
| | – | 21.1 EJe | – | – | – |

*Note.* This scenario calls for 15.7 EJ (14.9 quads) of biomass liquid. According to Lynd et al. *(3)* this option would also produce 349 TWh of electricity. Using the land wind electrical energy factor of 116 MWh/ha (0.47 e5 kWh/acre), this would reduce the wind land requirement by 3.0 Mha (7.4 million acres).

them, in Table 4. Finally, the amounts of the various forms of renewable energy and their land requirements, are presented in Table 5.

This scenario calls for a great deal of wind energy; it requires 6.0% of the land in the lower 48 states to be used for wind power. There is enough land if some class 3 sites are used. Elliot and Swartz *(24)* conclude that, while avoiding all environmentally sensitive areas, class 3 and above wind sites occupy 18% of the land area and have a potential of 14,300 TWh/yr. Class 4 characteristics were used to compute the average wind energy land productivity in this study. One of the desirable aspects of wind power is that the use of an area of land for wind power does not preclude its use for agriculture. In fact, combining a biomass plantation with a wind farm makes good sense. *(25)*

156 Mha (385 million acres) for biomass is also very large but some of the studies reviewed in previous sections indicate that this might be possible, especially, if exports were reduced, agricultural and dietary practices were changed, forest and agricultural residues were utilized, and/or bioenergy technology improved as expected. Several alternatives (solar–thermal, solar–thermal–electric, wind–electric, and hydrogen from electricity) that are less land intensive, are available if necessary.

Obviously many other menus of energy supply are possible. Wind energy is emphasized over photovoltaic conversion because it is less expensive and does not cover the land. Hydrogen was selected for aviation fuel because of its high energy density, and the fact that there is some experience with hydrogen as an aviation fuel *(26)*. I chose a mixture of biofuels and electricity for vehicles over hydrogen because of the low cost and efficiency *(27)* and the promise of hybrid vehicles.

The storage requirement (50% of electrical generation to be stored and 25% of this lost owing to conversion) is speculative. I have assumed that electro-chemical batteries would be used but hydrogen could be used for electrical storage; however, the energy loss is very large, although the cost of storage is less *(28)*. Hydrogen in this scenario is for uses that do not require it to be converted back into electricity.

The land-energy productivity used in this scenario for biomass liquid fuel, 116 GJ/ha, is based on corn kernels plus 75% of the stover *(8)*. Although it is higher than the current technology of using only corn kernels, it does not represent a particularly optimistic value. A more optimistic value, projected to occur by 2050 in Green et al. *(5)* on the basis of improvements in switch grass productivity, which have been achieved in experimental plots, the use of Fischer–Tropsch synthesis as well as fermentation, and expected fermentation improvements, is 331 GJ/ha. This would reduce the land required for biomass liquid fuels from 142 to 48 Mha, obviously a much more accessible amount.

Hopefully, the scenario puts biomass energy into context and begins to lay open the nature of a sustainable renewable energy system at the 2001 level of demand in the United States. The study indicates that there

Table A1
Agriculture Land Use

| | Units | Area (Mha) *(11)* | Production (M units) *(11)* | Average yield (units/ha) | Density (kg/unit) *(11)* | Producsts (Tg) | Yield (Mg/ha) |
|---|---|---|---|---|---|---|---|
| Corn for grain | bu | 27.62 | 8807.0 | 318.9 | 25.4 | 223.7 | 8.10 |
| Corn sillage | tons | 2.7 | 97.3 | 36.0 | 907 | 88.2 | 32.67 |
| Sorgum for grain | bu | 2.73 | 333.6 | 122.2 | 25.4 | 8.5 | 3.10 |
| Wheat for grain | bu | 18.43 | 1577.8 | 85.6 | 27.2 | 42.9 | 2.33 |
| Oats for grain | bu | 0.81 | 110.0 | 135.8 | 14.8 | 1.6 | 2.01 |
| Barley for grain | bu | 1.62 | 214.4 | 132.3 | 21.8 | 4.7 | 2.89 |
| Rice | cwt | 1.3 | 210.4 | 161.8 | 45.3 | 9.5 | 7.33 |
| Soybeans for beans | bu | 29.3 | 2708.8 | 92.5 | 27.2 | 73.7 | 2.51 |
| Peanuts for nuts | Lbs | 0.49 | 3134.0 | 6395.9 | 0.454 | 1.4 | 2.90 |
| Dry edible beans | Lbs | 0.68 | 32.0 | 47.1 | 27.2 | 0.9 | 1.28 |
| Cotton | bales | 5.04 | 17.3 | 3.4 | 218 | 3.8 | 0.75 |
| Tobacco | Lbs | 0.17 | 870.0 | 5117.6 | 0.45 | 0.4 | 2.30 |
| Potatoes | cwt | 0.51 | 451.0 | 884.3 | 45.35 | 20.5 | 40.10 |
| Sugarbeets | tons | 0.55 | 27.8 | 50.5 | 907 | 25.2 | 45.84 |
| Sugarcane | tons | 0.4 | 35.3 | 88.3 | 907 | 32.0 | 80.04 |
| Forage used for hay | tons | 25.92 | 211.3 | 8.2 | 907 | 191.6 | 7.39 |
| Alfalfa hay, (dry) | tons | 9.16 | 68.8 | 7.5 | 907 | 62.4 | 6.81 |
| Small- grain hay (dry) | tons | 1.76 | 7.8 | 4.4 | 907 | 7.1 | 4.02 |
| Tame hay (dry) | tons | 10.89 | 52.4 | 4.8 | 907 | 47.5 | 4.36 |
| Wild hay (dry) | tons | 2.72 | 8.1 | 3.0 | 907 | 7.3 | 2.70 |
| Haylage from alfalfa (green) | tons | 1.44 | 23.3 | 16.2 | 907 | 21.1 | 14.68 |
| Other haylage (green) | tons | 0.72 | 11.2 | 15.6 | 907 | 10.2 | 14.11 |
| Total | – | 145.0 | – | – | – | 884.2 | – |

Table A2
Agriculture Land Use

| | Export *(1)* 1e6 Mg | Export land Mha | Int. land Mha | Net Int. use 1e6 Mg | Residue yield kg/kg *(3)* | Residue 1e6 Mg |
|---|---|---|---|---|---|---|
| Corn for grain | 47.06 | 5.81 | 21.81 | 176.6 | 1 | 223.7 |
| Corn sillage | – | 0.00 | 2.70 | 88.2 | – | – |
| Sorgum for grain | 3 | 0.97 | 1.76 | 5.5 | – | – |
| Wheat for grain | 25.4 | 10.91 | 7.52 | 17.5 | 1.23 | 52.8 |
| Oats for grain | 1 | 0.50 | 0.31 | 0.6 | 1.16 | 1.9 |
| Barley for grain | 2.56 | 0.89 | 0.73 | 2.1 | 1.45 | 6.8 |
| Rice | 3.54 | 0.48 | 0.82 | 6.0 | 0.78 | 7.4 |
| Soybeans for beans | 36.88 | 14.67 | 14.63 | 36.8 | – | – |
| Peanuts for nuts | – | 0.00 | 0.49 | 1.4 | – | – |
| Dry edible beans | – | 0.00 | 0.68 | 0.9 | – | – |
| Cotton | 2.21 | 2.95 | – | – | – | – |
| Tobacco | 0.16 | 0.07 | 0.10 | 0.2 | – | – |
| Potatoes | – | 0.00 | 0.51 | 20.5 | – | – |
| Sugarbeets | – | 0.00 | 0.55 | 25.2 | 0.95 | 24.0 |
| Sugarcane | – | 0.00 | 0.40 | 32.0 | – | – |
| Forage used for hay | – | 0.00 | 25.92 | 191.6 | – | – |
| Alfalfa hay (dry) | – | 0.00 | 9.16 | 62.4 | – | – |
| Small-grain hay (dry) | – | 0.00 | 1.76 | 7.1 | – | – |
| Tame hay (dry) | – | 0.00 | 10.89 | 47.5 | – | – |
| Wild hay (dry) | – | 0.00 | 2.72 | 7.3 | – | – |
| Haylage from alfalfa (green) | – | 0.00 | 1.44 | 21.1 | – | – |
| Other haylage (green) | – | 0.00 | 0.72 | 10.2 | – | – |
| Total | 121.8 | 37.2 | 105.6 | 760.9 | 6.57 | 316.5 |

is enough land for a sustainable renewable energy system at the level of demand experienced in 2001, and that the utilization of biomass, although quite significant, would be limited by its land requirement.

## Acknowledgment

I would like to acknowledge those who contributed the articles that I have reviewed in this piece, especially my colleagues at Dartmouth, as well as the use of the facilities at the Thayer School.

## Appendix A Agriculture Land Use

The following worksheets, Tables A1 and A2, are based on data from the 2002 Census of Agriculture *(11)* and other references as indicated on the worksheet. It contains information on crop production, crop yields, acreage, exports, acreage used for exports, and residue production. In Table A1, values for the area, production in terms of the units given in the units column, and density are entered directly. This allows the yields and the production in Mg to be computed. In Table A2 the exports and residue yields are entered directly. This allows the land area required for exports to be computed from the known yield given in Table A1. Similarly, the land left for internal use can be computed and along with it the production used internally. Finally the amount of residue can be computed from the residue yield and the total production.

## References

1. Odell, P. R. (2004), *Why Carbon Fuels Will Dominate the 21st Century's Global Energy Economy*. Multi-Science Pub. Co., Essex, UK.
2. Turton H. (2005), *Biomass Bioenergy* **29,** 225–257.
3. Lynd, L. R., Cushman, J. H., Nichols, R. J., and Wyman, C. E. (1991), *Science* **251,** 1318–1323.
4. Hoogwijk, M., Faaij, A., Eickhout, B., de Vries, B., and Turkenburg, W. (2005), *Biomass Bioenergy* **29,** 225–257.
5. Greene, N., et al. (2004), Growing Energy, how biofuels can help end America's oil dependence, Natural Resources Defense Council, NewYork.
6. Perlack, R. D., Wright, L. L., Turhollow, A., Graham, R. L., Stokes, B., and Erbach, D. C. (2005), Biomass as a feedstock for a bioenergy and bioproducts industry: the technical feasibility of a billion-ton annual supply, USDA and DOE, http://www.osti.gov/bridge.
7. McLaughlin, S. B., Ugarte, D. G., Garten, C. T., et al. (2002), *Environ. Sci. Technol.* **29,** 426–439.
8. Kim, S. and Dale, B. E. (2005), *Biomass Bioenergy* **29,** 426–439.
9. Statistical Abstracts (2003), US Department Commerce, ESA, Census Bureau Statistical Abstracts of the United States, Table 1096.
10. USDA—NASS (2005) Agriculture Statistics, Table 12.39.
11. USDA, NASS (2002) Census of Agriculture, and http://www.ers.usda.gov/Briefing/LandUSe/majorlandusechapter.htm.
12. Ferrell, A. E., Plevin R. J., Turner B. T., Jones, A. D., O'Hare, M., and Kammen, D. M. (2006), *Science* **311,** 506–508.
13. Nonhebel, S. (2005), *Renewable Sustainable Energy Rev.* **9,** 191–201.

14. White, L. P. and Plaskett, L. G. (1981), *Biomass as Fuel*, Academic Press, Chapter 3.
15. Schelhaas, M. J. and Nabuurs, G. J. (2001), Spatial distribution of regional whole tree carbon stocksand fluxes of forests in Europe. Alterra-rapport. 300, Wageningen, UR.
16. US Forest Service (2004), Smith, W. B., Miles, P. D., Vissage, J. S., and Pugh, S. A., Forest Resources of the United States, 2002, published 2004, Table 38, available at http://fia.fs.fed.us/
17. US Forest Service (2004), Trend Data, available at http://fia.fs.fed.us/
18. Smith, Brad (2006), Personal communication.
19. Heller, M. C. and Keoleian, G. A. (2000), Life Cycle-Based Sustainability Indicators fo Assessment of the US Food System, Center for Sustainable Systems, U. Michigan, Report No CSS00-04, Dec 6 2000.
20. de Jong, B. (1973), *Net Radiation Received by a Horizonal Surface on the Earth*, Delft University Press, Netherlands.
21. Duffie, J. A. and Beckman, W. A. (1974), *Solar Energy Thermal Processes*, John Wiley and Sons, New York: pp. 34–37.
22. British Assoc. for Biofuels and Oils, http://www.biodiesel.co.uk/levington_tables.htm#Table%201 (accessed 3/12/06).
23. Hill, D., Nelson, E., Tilman, D., Polasky, S., and Tiffany, D. (2006), *PNAS* 11206–11210.
24. Elliot D. L. and Schwartz M. N. (1993), Wind Energy Potential In the United States, Sept. 1993. PNL-SA-23109, Richland WA: Pacific NW Lab. DE4001667. (Available on the internet at http://www.nrel.gov/wind/wind_potential.html).
25. Mazza, P. and Heitz, E. (2005), The New Harvest, biofuels and wind power for rural revitalization and national energy security, The Energy Foundation, available at http://www.eesi.org/programs/Agriculture/reports/EFbioenergy1.06.pdf and http://www.ef.org
26. Dickson, E. M., Ryan, J. W., and Smulyan, M. H. (1977), *The Hydrogen Economy*, Prager, NY, pp. 89–95.
27. Shinnar, R. (2003), *Tech. in Society*, **25,** 455–476.
28. Converse, A. O. (2006), *Energy Policy* **34,** 3374–3376.
29. Kelly, H. (1993), In: Johansson, T.B., Kelley, H., Reddy, A.K.N., and Williams, R.H. (eds.) *Renewable Energy, Sources for Fuels and Electricity.* Island, Washington, D.C.: pp. 297ff.
30. de Laquil III, P., Kearney, D., Séller, M., and Diver, R. (1993), In: Johansson, T.B., Kelley, H., Reddy, A.K.N., and Williams, R.H., (eds.) Renewable Energy, Sources for Fuels and Electricity. Island, Washington, D.C.: pp. 213ff.
31. US Federal Aeronautics Admin. (2003), http://apo.faa.gov/forcas03/start.htm
32. US Department of Energy, EIA (2003), Annual Energy Review, Table2.1a.
33. US Department of Energy, EIA (2003), Annual Energy Review, Table 1.15.
34. US Department of Energy, EIA (2003), Annual Energy Review, Table 8.2a.
35. USDA, ERS (2005), Outlook for Agricultural Trade/AES-48.

0273-2289/1559-0291 (Online)/07/136–140/625–638/$30.00

# Optimizing the Logistics of Anaerobic Digestion of Manure

**EMAD GHAFOORI AND PETER C. FLYNN***

*Mechanical Engineering Department, University of Alberta, Edmonton, AB, Canada, E-mail: peter.flynn@ualberta.ca*

## Abstract

Electrical power production from the combustion of biogas from anaerobic digestion (AD) of manure is a means of recovering energy from animal waste. We evaluate the lowest cost method of moving material to and from centralized AD plants serving multiple confined feeding operations. Two areas are modeled, Lethbridge County, Alberta, Canada, an area of concentrated beef cattle feedlots, and Red Deer County, Alberta, a mixed-farming area with hog, dairy, chicken and beef cattle farms, and feedlots. We evaluate two types of AD plant: ones that return digestate to the source confined feeding operation for land spreading (current technology), and ones that process digestate to produce solid fertilizer and a dischargeable water stream (technology under development). We evaluate manure and digestate trucking, trucking of manure with return of digestate by pipelines, and pipelining of manure plus digestate. We compare the overall cost of power from these scenarios to farm or feedlot-based AD units. For a centralized AD plant with digestate return for land spreading the most economical transport option for manure plus digestate is by truck for the mixed-farming area and by pipelines for the concentrated feedlot area. For a centralized AD plant with digestate processing, the most economical transport option is trucking of manure for both cases.

However, for the concentrated feedlot area, pipeline transport of manure is close in cost to trucking, and the impact of truck congestion would likely lead to selection of pipeline transport. For the mixed-farming area, centralized AD is more economical than for any individual farm or feedlot unit. For the concentrated feedlot area, a centralized AD plant is less economical than a feedlot-based AD unit more than 55,000 head (digestate return) and 300,000 head (digestate processing). The study demonstrates the viability of centralized AD plants vs farm-based units in most farming environments, and that careful analysis of the cost of pipeline vs truck transport of manure and digestate is required on a case-by-case basis.

**Index Entries:** Anaerobic digestion; biogas plant; digestate processing; manure; manure pipeline; optimum size; trucking.

*Author to whom all correspondence and reprint requests should be addressed.

## Introduction

There are three reasons to process manure to biogas (a mixture of methane, carbon dioxide, and trace gases) through anaerobic digestion (AD). The first reason is to recover useable energy that contributes no net carbon to the atmosphere *(1,2)*. Biogas from small AD plants is typically used for heat or combined heat and power, with power being produced from an internal combustion engine-driven generator. Typical generator efficiencies based on lower heating value are 37–43% *(3,4)*. The amount of heat recovered depends on the available heat sink; European AD plants often feed biogas to a combined heat and power plant that utilizes waste heat in a district heating system *(5)*. Larger amounts of biogas can be processed in a combined cycle power plant with thermal efficiencies of 55% or higher *(6)*. As an alternative, biogas can be scrubbed to remove $H_2S$ and $CO_2$ and compressed to produce a pipeline quality natural gas *(7,8)*. If the $CO_2$ is recovered and sequestered a double-carbon credit can be claimed, one for displacing fossil fuel for power generation and one for carbon capture *(9)*.

A second reason to use AD for biogas is to reduce the risk from pathogens, for example, *Escherichia coli*, from land spreading, the most common manure disposal step today. Thermophilic or mesophilic AD with a sanitization step destroys all or virtually all pathogens *(10–12)*. Note that current AD technology does not eliminate the need for land spreading, but rather changes what is spread from raw manure to digestate (the material left after biogas production) or its liquid component.

A third and prospective benefit from AD processing of manure is the potential to recover nutrients from digestate, leaving a disposable water stream. As discussed below in the results of the study this has the potential to significantly reduce transport costs associated with centralized AD plants. In addition, it has the potential to alleviate serious nutrient imbalance problems, reducing the risk to human health from excess phosphate in drinking water *(13–15)*, by producing a concentrated fertilizer that can be economically moved to areas that need the nutrients. Full digestate processing is an area of intense research, but the only commercially available and fully demonstrated treatment of digestate today is solid–liquid separation, which can remove half or more of phosphate into a transportable solid fraction *(16,17)*.

AD has a strong economy of scale. Both analysis of actual capital cost data from Danish plants and theoretical studies show a scale factor of about 0.6 *(18)*, where scale factor is the exponent in the relationship:

$$\text{Cost}_{\text{plant2}} = \text{Cost}_{\text{plant1}} \times (\text{Capacity}_{\text{plant2}}/\text{Capacity}_{\text{plant1}})^{\text{scale factor}}$$

In biomass processing plants that transport biomass from external sources, there is a tradeoff in two cost factors. As plant capacity increases, biomass must be moved to the plant from longer distances, increasing the transportation cost. As plant capacity increases, the economy of scale that

arises from the scale factor reduces the cost of capital recovery and operating costs per unit of output. Competition between these two cost factors leads to an optimum size of processing for biomass processing *(19–24)*. As biomass availability per overall unit area surrounding a plant (which we call gross yield to distinguish from species-specific yields of biomass) increases, optimum plant size increases.

In previous work we used two locations in the province of Alberta, Canada, to model the economics of AD of manure in centralized plants vs plants based at the confined feeding operation (CFO) *(18)*. Lethbridge County is an area of intense processing of beef cattle and is unique in Canada; typical feedlots contain 25,000 to 100,000 head, and the overall county contains an average of 570,000 beef cattle *(25)*. Average gross yield of manure is 280 dry $t/km^2/yr$ (for clarity, gross manure yield is the yield per total area in the county). Manure as recovered has an estimated moisture content of 70% *(26)*. A similar area in North America is the large meat processing industry supported by feedlots in the area of eastern Colorado, western Kansas, western Oklahoma, and North Texas *(27,28)*.

The western half of Red Deer County is a mixed-farming area, typical of many such areas in North America, in which grain and forage farms are mixed with beef cattle (cow calf and small feedlot), dairy, hog, and poultry operations. A detailed analysis of virtually all manure sources in the county was completed in 2005 *(29)*. The manure gross yield is 34 dry $t/km^2/yr$. Forty percent of manure is in the form of liquid and would be shipped in a tanker truck; the remaining 60% would arrive as a solid with estimated moisture content of 70%.

Pipeline transport of manure and digestate is an alternative to truck transport *(30,31)*. Pipelining of biomass has a significant economy of scale, with a scale factor less than 0.5 *(30–32)*, whereas truck transport has no economy of scale: more material simply requires more truck trips, with no or very minor variation in unit cost of transport. Hence at large scale, pipeline transport will become more economical than truck transport. As all pipelined manure initially is moved by truck, either from farm or individual feedlot pens, the fixed cost of loading a truck, about \$4–5/t, is always incurred. (All costs in this study are reported in 2005 US dollars; where required a conversion factor of 1\$ USD = 1.2\$ Cdn was used.)

Transshipment from truck to pipeline incurs some additional costs that are independent of the length of the pipeline (called distance fixed costs [DFC]), for example, for incremental labor to operate the pipeline. Large pipelines will have a lower unit cost of transport, including operating and capital recovery costs, per unit distance (called distance variable cost [DVC]). Therefore a minimum shipping distance is required for transshipment to be economical, in that the reduction in DVC must offset the increased DFC that arises from transshipment. This analysis of pipelining of manure and digestate is based on economic factors, and we note that other site-specific noneconomic factors can enter into decisions to choose pipelining over trucking, for

example, impact on communities from odor concerns and traffic congestion. Such factors played a role in the recently announced AD plant in Maabjerg, Denmark, discussed below in the Discussion section *(33)*.

In this study we use Lethbridge and Red Deer counties to model pipeline vs truck transport of manure and digestate to and from centralized AD plants. We consider only manure as a feedstock. Other organic feed streams such as purpose grown crops, crop residues, and various waste streams give higher yields of biogas per mass than manures, which represent material already once processed by bacteria in the gut of an animal. However, the availability of other organic streams is highly site specific, as are regulations that may prohibit the use of ruminant meat scraps or the blending of municipal solid wastes into processes for which digestate will be land spread.

## Modeling Pipeline Vs Truck Transportation of Manure

We analyzed two technologies, AD biogas production and digestate return to the source CFO for land spreading, and AD biogas production and digestate processing to solid fertilizer and dischargeable water, for two locations, Lethbridge County and the western half of Red Deer County. For centralized plants we evaluated three transportation modes: trucking of manure plus digestate, pipelining of manure and digestate, and trucking manure and pipelining digestate. In each case we used a 12% pretax return on capital and compared the cost of power production from a centralized AD plant to the cost of a farm or feedlot-based unit.

Point-specific CFO locations were not available for Lethbridge County, only county-wide statistics on beef cattle feedlot population. To simplify comparison, the study areas were assumed to be a square, and manure sources were assumed to be evenly distributed within the area. Red Deer County has manure from many types of CFOs; in this study the reported number of head is the equivalent number of feedlot beef cattle that would generate the same amount of dry mass of manure. A simplified model of a spoke and hub pipeline system was developed (Fig. 1), and contrasted to truck transport for both Lethbridge and the western half of Red Deer County. The study area was divided into five subregions of equal area. Manure in the central region 1 (Fig. 1) was transported to the plant by truck, whereas manure in the remaining four regions was transported by truck to the closest pipeline inlet. Digestate return was by a similar mechanism: truck to region 1, and pipeline plus truck to the remaining four regions. Table 1 shows the key parameters for the model.

Details for the calculation of trucking and pipelining costs were developed in previous studies *(30,31)*. Table 2 shows the values of DFC and DVC for trucking, and for pipelining at three different scales of manure and digestate volume. The scale factors for DVC for one- and two-way pipelines were about 0.40; pipeline capital costs were derived from

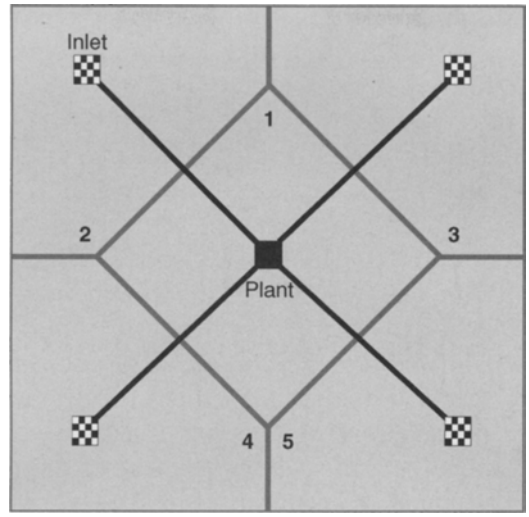


**Fig. 1.** Simplified model of a spoke- and hub-pipeline system used for both counties.

Table 1
Key Parameters Used for the Modeling

| Parameters (unit) | Value | |
|---|---|---|
| | Red Deer | Lethbridge |
| Total manure produced (dt/yr) | 93,000 | 780,000 |
| Total county area ($km^2$) | 2700 | 2800 |
| Gross yield of manure ($dt/km^2/yr$) | 34 | 280 |
| Average trucking distance for entire county (km) | 37 | 37 |
| Average trucking distance for each region (km) | 16 | 17 |
| Length of each pipeline (km) | 30 | 31 |

Table 2
Impact of Scale on the Values of DVC and DFC for Trucking and Pipelining of Solid Beef Cattle Manure

| Head | 25,000 | 50,000 | 1,00,000 |
|---|---|---|---|
| *DVC ($/dt/km)* | | | |
| Manure trucking[a] | 0.25 | 0.25 | 0.25 |
| Digestate trucking[b] | 0.96 | 0.96 | 0.96 |
| One-way pipeline | 0.54 | 0.33 | 0.20 |
| Two-way pipeline | 0.86 | 0.56 | 0.35 |
| *DFC ($/dt)* | | | |
| Manure trucking[a] | 17 | 17 | 17 |
| Digestate trucking[b] | 64 | 64 | 64 |
| One-way pipeline | 13 | 7 | 3 |
| Two-way pipeline | 15 | 8 | 4 |

[a]Solid manure shipped at 70% moisture content.
[b]Digestate returned at 92% moisture content.

(34), and pipeline pump power consumption was developed from detailed pressure drop calculations. Capital and operating costs for the AD plant were also developed in a previous study (18).

For each manure source, the moisture content at time of collection was factored into the volume and mass calculations for manure and digestate. A manure source that has a solids level of 12%, typical of some dairy operations, would be pipelined and processed "as is," and the AD process would destroy 45% of the volatile solids, which represent 85% of the solids in the manure (35,36). Hence for this manure source, digestate volume is about 95% of the original volume of manure. However, beef cattle manure from an Alberta feedlot typically contains 30% solids at time of collection, as noted above in the Introduction section and is diluted to 12% for AD processing (26), so digestate volume is about 2.4 times that of the initial manure. For areas of concentrated beef cattle feedlots such as Lethbridge County, this increase in volume becomes a significant factor in the relative economics of pipelining digestate vs manure. Note that if manure is pipelined it is diluted to 12% solids content at the pipeline inlet rather than the AD plant, as pipeline cost is minimized at this concentration (31). Hence, pipeline inlets would require a significant water supply.

Whether the manure is liquid or solid also affects the cost of digestate return. Solid manure is delivered in an open truck, and the truck is empty on the return route. Digestate from solid manure CFOs is returned in a separate truck. Hence, for solid manures (e.g., all manure sources in Lethbridge County), each truck-load of incoming manure causes 2.4 digestate truck trips in a separate vehicle. Liquid manure makes up 40% of sources in Red Deer County, and digestate is returned by backhaul, which generates an incremental DFC charge for loading and unloading digestate but no incremental DVC.

## Results of the Study

Figure 2 shows the cost of farm or feedlot-based processing plants (solid line and upper axis) and large centralized processing plant (bars) for production of power from biogas with digestate land spreading; several conclusions can be drawn.

1. For centralized processing in the mixed-farming area of Red Deer County the lowest cost for moving manure and digestate is by two-way trucking. Note, however, that the cost difference between two-way pipeline transport of manure and digestate through four pipelines is very small compared with two-way trucking.
2. Centralized processing of manure with digestate return is more economical than on-farm processing for up to a farm or feedlot size equivalent to about 10,000 head of beef cattle. As the largest single source of manure in Red Deer County is a feedlot containing 7500

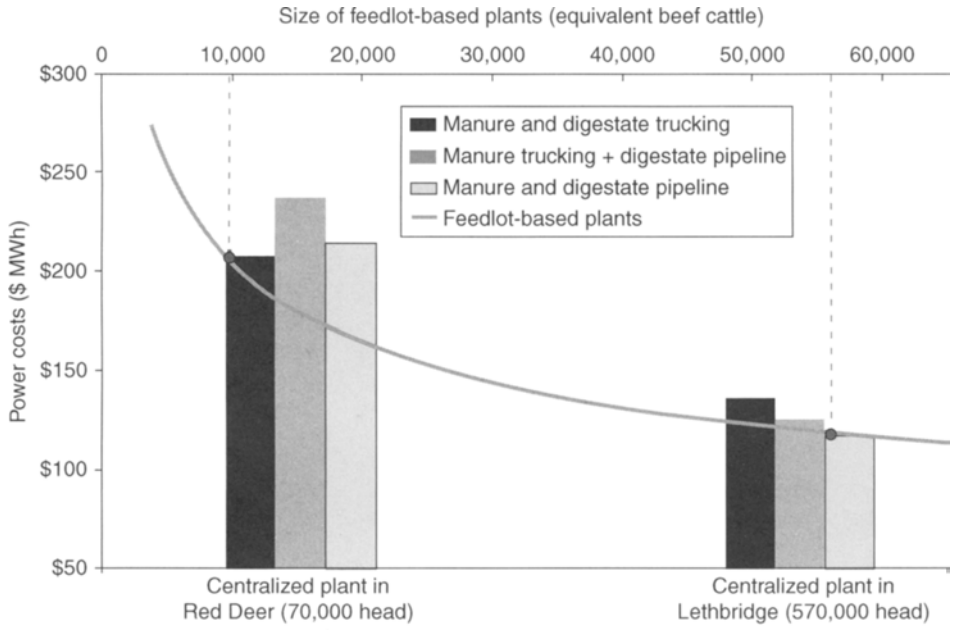


**Fig. 2.** Biogas power cost at farm-based plants vs centralized plants ( the dotted line identifies the size of farm-based plants in which power cost is the same as a centralized plant).

head, centralized processing was the most economical alternative for conventional production of power from biogas *(18)*.

3. Third, for the concentrated beef cattle feedlot operations in Lethbridge County the lowest cost for moving manure and digestate was by two-way pipelines.
4. Centralized processing of manure is a more costly method of producing electrical power than feedlot-based processing for any feedlot more than 55,000 head when the most economical transport mode is chosen. Feedlot sizes of 50,000–1,00,000 head are common in North America, and hence there is not a significant incentive to move manure to and return digestate from a centralized plant.
5. For centralized processing the cost in the area of concentrated feedlots is significantly lower than the mixed-farming area, $120 vs $210/mwh. Two factors contribute to this reduction in power cost: an eightfold increase in both plant size and the gross yield of manure per square km. The larger plant size reduces capital recovery and operating costs, and the higher manure yield reduces transportation cost per unit of power output.

Figure 3 shows the cost of farm or feedlot-based processing (solid line and upper axis) and large centralized processing (bars) for production of power from biogas with digestate processing to recover solid fertilizer and

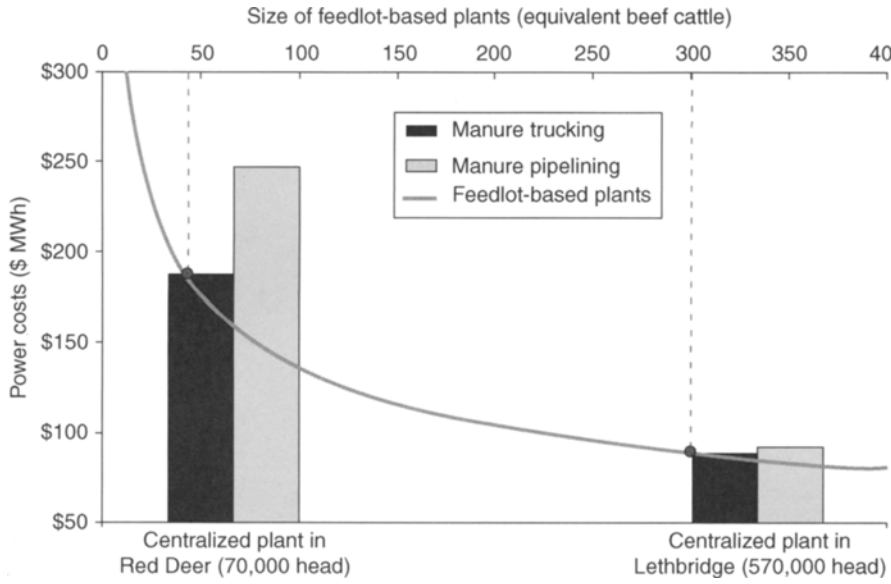


**Fig. 3.** Biogas power cost at farm-based plants vs centralized plants with digestate processing (the dotted line identifies the size of farm-based plants in which power cost is the same as a centralized plant).

a dischargeable water stream. Note that the power cost does not include any credit for the sale of fertilizer, because fertilizer value will be highly site-specific and based on the expected transport distance to a market for phosphate rich fertilizer, and an offsetting payment to the CFO may be required. For centralized processing in the mixed-farming area the lowest cost-way of moving manure was by truck only and the cost difference between trucking and a single pipeline carrying manure was significant.

Digestate processing gives centralized processing of manure an even larger advantage over individual farm or feedlot-based units, because AD plus digestate processing is more capital intensive than AD with digestate return. This increased capital intensity increases the impact of the economy of scale in capital recovery cost relative to transportation costs. For the area of concentrated feedlot operations, manure trucking was slightly more economical than pipelining, although it raises congestion problems that are discussed further below in the Discussion section. Because of the increased capital intensity of AD plus digestate processing, centralized AD was more economical than feedlot-based processing of manure for feedlots up to 300,000 head in size. As no individual feedlot in Lethbridge County is even close to that size, we can conclude that digestate processing tips the balance in favor of centralized processing of manure. It also significantly reduces the cost of power from centralized AD, $90 vs $120/mwh for digestate return. This cost reduction reflects the high volume increase in digestate vs incoming solid manure, the need to use a different truck to

Table 3
The Number of Truck Arrivals per Day and the Interval Between Arrivals

| | Red Deer | | Lethbridge | |
|---|---|---|---|---|
| Centralized plant at: | Truck only | Truck + pipeline | Truck only | Truck + pipeline |
| *Without digestate processing* | | | | |
| Manure delivery (arrival/d) | 69 | 14 | 363 | 73 |
| Digestate return (arrival/d) | 59 | 12 | 867 | 173 |
| Arrival intervals at 16/7 (min) | 8 | 38 | 0.8 | 4 |
| Arrival intervals at 24/7 (min) | 11 | 56 | 1.2 | 6 |
| *With digestate processing* | | | | |
| Manure delivery (arrival/d) | 69 | 14 | 363 | 73 |
| Digestate return (arrival/d) | – | – | – | – |
| Arrival intervals at 16/7 (min) | 14 | 70 | 3 | 13 |
| Arrival intervals at 24/7 (min) | 21 | 105 | 4 | 20 |

return digestate than to move manure, and the cost of pipeline and truck movement of digestate. Note, however, that the scope of digestate processing is poorly defined and the estimated capital and operating cost has a very high degree of uncertainty.

As noted earlier, large-scale centralized AD plants would concentrate truck traffic and raise questions of both road congestion and nuisance odors. Table 3 shows the number of truck arrivals per day, and the interval between truck arrivals. Digestate processing reduces truck traffic by eliminating the need for return of digestate to the source CFO. Liquid manure, for example, from hog barns and some dairy operations, also reduces net truck traffic because, as discussed above (*see* "Modeling"), digestate can be returned by backhaul rather than by a separate truck going out full and returning empty.

## Discussion

Whether pipelining, or truck transport is more economical requires a case-by-case analysis, because pipelining has a strong economy of scale and truck transport does not. Increasing plant size reduces the unit cost of pipelining of manure and digestate relative to trucking. Two-way pipelining of manure and digestate has an economy of scale relative to one-way pipelining of digestate for two reasons: (a) The second pipeline can be laid in the same trench as the first and (b) the cost of building a duplicate facility is estimated to be 95% of the cost of the first *(34)*. The savings on the second duplicate pipeline arises because marshaling costs are saved and efficiencies are realized in construction.

Noneconomic reasons also arise for pipelining manure and digestate, and the recently announced proposed Maabjerg Bioenergy project in

Denmark is an example of this (33). Although this project is half the size of the Red Deer County centralized digester evaluated in this study, it will use a 200-km network of pipelines to move both digestate and manure. The high population density and semirural area of the plant presumably present issues related to community acceptance of a manure-based energy project. Table 3 illustrates the very high traffic density caused by AD plants supplied by truck. Careful siting would be required to manage community resistance to such a project. This study concludes that trucking of manure in Lethbridge County is more economical than pipelining for the case of digestate processing, but the difference in cost is small. We think that traffic congestion and community resistance issues would tip such a project into selecting pipeline delivery of manure.

This study illustrates the significant impact of processing plant size on the overall economics of utilizing manure as an energy source, a result found for other biomass sources (19–24). Centralizing manure processing improves the economics up to a cutoff size of farm or feedlot because the increase in capital and operating cost efficiency is greater than the cost of transporting even a low-energy density material like manure. This conclusion is reflected in the practice widespread in Denmark of forming farmer cooperatives to centrally process manure (37,38), usually with heat recovery into a district heating system.

The impact of economy of scale is further illustrated by the impact of digestate processing on the relative economics of feedlot vs centralized processing of manure. In the absence of digestate processing increasing transportation cost exceeds incremental capital saving in the concentrated feedlot area at about 55,000 head of beef cattle. However, if digestate processing is included then a larger amount of capital is subject to the benefit of economy of scale, and this tips the balance to centralized processing against feedlots up to 300,000 head in size. In North America no individual feedlot is larger than 150,000 animals, perhaps to control the magnitude of loss in the event of an epidemic disease. Hence, a key conclusion of this study is that extensive digestate processing will favor very large centralized AD plants.

Digestate processing to recover phosphate as a transportable solid, some in separated fiber and some as crystallized phosphate salts, gives the potential to sell a phosphate rich fertilizer in areas that need the nutrient, whereas reducing phosphate buildup in areas of excess. However, the challenge of total nutrient recovery from phosphate is daunting and requires additional research to develop a commercially proven process. Given the developmental stage of digestate processing, capital and operating cost estimates in this study are approximate. However, they demonstrate that digestate processing has the potential to significantly reduce the cost of energy production from manure by eliminating the need to return digestate to the source CFO for land spreading.

For the mixed-farming area the calculated cost of power from manure is about $210/mwh, about three times the cost of power from straw in a

study based on the same area *(24)*. The estimated power cost of $120/mwh from the area of intense feedlots is also significantly higher than power from straw. We note, however, that control of pathogens in manure is a potential incentive for using biomass as an energy source; digestate is safer to land spread than raw manure.

The model accuracy will be improved if additional data on capital and operating costs, and biogas yield specific to manure types become available. The model uses an idealized configuration that assumes that manure sources are evenly distributed throughout an agricultural area and a processing plant can be located central to that area. In real cases farms and feedlots will have specific locations, and plus the distribution of population will influence plant siting. The conclusions of this study illustrate the sensitivity of decisions about mode of transport and centralized vs farm or feedlot-based processing to specific factors of cost, yield, size, and distance of transport. Hence, in optimizing transport to centralized AD plants project specific factors will have to be analyzed.

Finally, it should be noted that although this study uses electrical power as the end product of biogas, production of pipeline-grade natural gas is an alternative. Natural gas may have higher value than electrical power, particularly if that power is produced from an internal combustion engine-powered generator with efficiencies less than 43%. Production of pipeline-grade natural gas also produces a byproduct stream rich in $CO_2$, creating the possibility of carbon sequestration and a double carbon credit if a suitable sink can be found *(9)*.

## Conclusions

For Lethbridge County, an area of concentrated beef feedlots, pipeline is the least cost means of moving manure and digestate to a centralized AD plant when digestate is returned to the source CFO for land spreading. This conclusion is dependent on manure quantity because pipeline transport has a significant scale factor whereas the cost of trucking is virtually independent of size. When digestate is processed and hence only manure is transported, truck hauling has a slightly lower cost than pipelining. However, road congestion factors would likely lead to the selection of pipelines for very large AD plants. Centralized processing of manure is favored for AD plants that return digestate to the source CFO compared with processing at farm or feedlot up to a size equivalent to 55,000 head of beef cattle. If digestate is processed, then based on a preliminary estimate of the capital cost of digestate processing, centralized processing of manure is favored up to a size equivalent to 300,000 head of beef cattle. This size is larger than any known feedlot in North America, and hence digestate processing will tip the balance in favor of large centralized AD plants for all CFOs. For Red Deer County, a typical mixed-farming area, truck transport of manure and digestate is the least cost means of moving manure and

digestate to a centralized AD plant for either digestate return or processing. Centralized processing of manure is more cost effective than farm-based processing for all manure sources in the county. This study illustrates the cost effectiveness of centralized processing of manure, and the need for a case specific analysis of alternative transportation modes for AD plants.

## Acknowledgments

The authors gratefully acknowledge financial support from the Alberta Energy Research Institute and Alberta Agricultural Research Institute, which have supported this research by a grant, and from the Poole Family. We appreciated helpful discussions with Xiaomei Li, Alberta Research Council, David Williams, Chief Estimator with the Bantrel Corporation, an affiliate of Bechtel and Graham Harrison of Waterous Power Systems, an affiliate of GE Jenbacher. However, all conclusions in this study are from the authors.

## References

1. Martin, J. H. (2003), Report submitted to US Environmental Protection Agency. EPA Contract No. 68-W7-0068.
2. Schneider, U. A. and McCarl, B. A. (2003), *Environ. Resour. Econo.* **24,** 291–312.
3. Harrison, G. (2005), Manager, GE Jenbacher, Waterous Power Systems. Contacted May 2004, personal communication. Calgary, Alberta, Canada.
4. GE Energy (2006), GE Jenbacher Gas Engines. http://www.gepower.com/prod_serv/products/recip_engines/en/index.htm (accessed March 2006).
5. Mahony, T., O'Flaherty, V., Colleran, E., et al. (1999), Feasibility Study for Centralized Anaerobic Digestion for Treatment of Various Waste and Wastewaters on Sensitive Catchment Areas. Environmental Protection Agency. Ireland.
6. Shilling, N. (2004), Product Line Manager General Electric Corporation. Rochester, NY, USA. Contacted June 2004, personal communication.
7. Quest Air Technologies (2004), Website: http://questairinc.com/applications/biogas.htm (accessed February 2006).
8. Environmental Power Corporation (2005), News Release: http://ir.environmentalpower.com/ReleaseDetail.cfm?ReleaseID=172199, (accessed February 2006).
9. Ghafoori, E., Flynn, P. C., and Checkel, M. D. (2007), *Int. J. Green Energy* (in press).
10. Birkmose, T. (2000), The Danish Agricultural Advisory Centre, The National Department of Crop Production. ISBN 87 7470 829 5.
11. Sahlstrom, L. (2003), *Bioresour. Technol.* **87,** 161–166.
12. Demirer, G. N. and Chen, S. (2005), *Process Biochem.* **40,** 3542–3549.
13. Cooke, G. W. and Williams, R. J. B. (1973), *Water Res.* **7(1–2),** 19–33.
14. Hooda, P. S., Edwards, A. C., Anderson, H. A., and Miller, A. (2000), *Sci. Total Environ.* **250,** 143–167.
15. Savard, M. (2000), *Ecol. Modeling* **125,** 51–66.
16. Møller, H. B., Lund, I., and Sommer, S. G. (2000), *Bioresour. Technol.* **74,** 223–229.
17. Møller, H. B., Sommer, S. G., and Ahring, B. K. (2002), *Bioresour. Technol.* **85,** 189–196.
18. Ghafoori, E. and Flynn, P. C. (2006), Optimizing the size of anaerobic digester. The 2006 CSBE Annual Conference, Edmonton, AB, 16–19 July.
19. Overend, R. P. (1982), *Biomass* **2,** 75–79.
20. Nguyen, M. H. and Prince, R. G. H. (1996), *Biomass Bioenergy* **10(5–6),** 361–365.
21. Jenkins, B. M. (1997), *Biomass Bioenergy* **13(1–2),** 1–9.
22. Larson, E. D. and Marrison, C. I. (1997), *J. Eng. Gas Turbines Power* **119,** 285–290.

23. Dornburg, V. and Faaij, A. P. C. (2001), *Biomass Bioenergy* **21(2),** 91–108.
24. Kumar, A., Cameron, J. B., and Flynn, P. C. (2003), *Biomass Bioenergy* **24(6),** 445–464.
25. CANFAX (2006), website: http://www.canfax.ca/default.htm (accessed January 2006).
26. Li, X. (2005), Environmental Technologies, Alberta Research Council Inc (Contacted January 2006), Edmonton, Alberta, Canada. Personal communication.
27. Dhuyvetter, K. C., Graff, J., and Kuhl, G. L. (1998), Kansas State University Agricultural Experiment Station and Cooperative Extension Service, Report MF-1057.
28. Ward, C. E. and Schroeder, T. C. (2004), Oklahoma Cooperative Extension Fact Sheets. Oklahoma State University, F-553, p. 2.
29. RDC (Red Deer County) Office (2005), Red Deer County Biomass Survey Database prepared for the Red Deer Country Biogas Plant Feasibility Study.
30. Ghafoori, E. and Flynn, P. C. (2006), *Trans. ASABE* **49(6)**, 2069–2075.
31. Ghafoori, E., Flynn, P. C., and Feddes, J. J. (2005), *Biomass Bioenergy* **31(2–3),** 168–175.
32. Kumar, A., Cameron, J. B., and Flynn, P. C. (2004), *Appl. Biochem. Biotechnol.* **113(1–3),** 27–39.
33. Munster, M. and Juul-Kristensen, B. (2005), http://www.maabjerg-bioenergy.dk/Default.aspx?ID=362, (accessed February, 2006).
34. Williams, D. (2004), Chief Estimator at Bantrel Corporation (a subsidiary of Bechtel), Calgary, Alberta, Canada (contacted May 2004), personal communication.
35. ASAE Standards (2003), ASAE. D384.1: Manure production and characteristic. St. Joseph, Michigan.
36. CBC—California Biomass Collaborative (2005), Department of Biological and Agricultural Engineering, University of California, Davis, CA.
37. H-Gregersen, K. (1999), Centralized biogas plants–integrated energy production, waste treatment and nutrient redistribution facilities. Danish Institute of Agricultural and Fisheries Economics.
38. Al Seadi, T. (2000), Danish centralized biogas plants—plant descriptions. Bioenergy Department, University of Southern Denmark.

0273-2289/1559-0291 (Online)/07/136–140/639–652/$30.00

# The Relative Cost of Biomass Energy Transport

ERIN SEARCY, PETER FLYNN,* EMAD GHAFOORI, AND AMIT KUMAR

*Mechanical Engineering Department, University of Alberta, Edmonton, AB, Canada, E-mail: peter.flynn@ualberta.ca*

## Abstract

Logistics cost, the cost of moving feedstock or products, is a key component of the overall cost of recovering energy from biomass. In this study, we calculate for small- and large-project sizes, the relative cost of transportation by truck, rail, ship, and pipeline for three biomass feedstocks, by truck and pipeline for ethanol, and by transmission line for electrical power. Distance fixed costs (loading and unloading) and distance variable costs (transport, including power losses during transmission), are calculated for each biomass type and mode of transportation. Costs are normalized to a common basis of a giga Joules of biomass. The relative cost of moving products vs feedstock is an approximate measure of the incentive for location of biomass processing at the source of biomass, rather than at the point of ultimate consumption of produced energy. In general, the cost of transporting biomass is more than the cost of transporting its energy products. The gap in cost for transporting biomass vs power is significantly higher than the incremental cost of building and operating a power plant remote from a transmission grid. The cost of power transmission and ethanol transport by pipeline is highly dependent on scale of project. Transport of ethanol by truck has a lower cost than by pipeline up to capacities of 1800 t/d. The high cost of transshipment to a ship precludes shipping from being an economical mode of transport for distances less than 800 km (woodchips) and 1500 km (baled agricultural residues).

**Index Entries:** Biomass transportation; ethanol transport; pipeline transport; power transmission; rail transport; ship transport; transportation cost; truck transport.

## Introduction

Biomass can be used as a power source either directly, such as by combustion or gasification to generate electricity, or by creating a fuel such as ethanol, which can be used to power a vehicle. Significant use of biomass as an energy source will require the collection of biomass from the field, for example, agricultural or forestry residues or purpose grown crops. Many field sources of biomass are, by their nature, remote from the

*Author to whom all correspondence and reprint requests should be addressed.

population centers that will use the produced energy. Thus, developers of such biomass projects will have the alternative of moving the biomass to a plant near the energy consumer, or moving the produced energy from a remote biomass processing plant.

Factors affecting location of biomass plants are both noneconomic and economic. Noneconomic factors include community concerns about traffic congestion and possible emissions such as dust or odors. Economic factors include the relative transportation cost of biomass vs produced energy, the cost of constructing and operating a plant in a location remote from rather than near population centers, and the potential benefit from large-scale integrated processing of biomass, for example, a multiproduct biomass refinery. In this article, we focus on the relative transportation cost of biomass and its energy products to provide a database against which other economic and noneconomic factors can be weighed.

Two cost components are critical in analyzing transportation cost: distance variable costs (DVC), the component that is directly dependent on the distance traveled, and distance fixed costs (DFC), which are independent of the distance traveled. DVC depends on the transportation mode and the specific location; an example is the "per ton kilometer" cost of trucking or rail shipment. DFC depends on the type of biomass being transported and the equipment and contractual arrangements involved, which are both case specific; examples include the cost of loading and unloading biomass from a truck, railcar, or ship. Hence, DFC will vary based on the specific form of biomass to a far greater extent than DVC. For example, this study is based on large round bales of stover or straw, which would require different treatment for transshipment from truck to rail than woodchips. The impact of DFC on overall transportation cost diminishes with increasing distance.

Biomass transportation costs are often reported in units that do not relate to the true determinant of cost of transport, for example, cost dry/ton/kilometer for trucking. In reality, a trucker is not concerned with the number of dry metric tons moved, but rather the total number of actual metric tons as road limits, and hence truck-load limits are based on total weight of material moved. Thus, increases in the moisture level of biomass reduce the amount of dry metric tons per load, and as trucking costs are charged per actual metric ton, the calculated transport cost per dry metric ton will vary for every biomass source.

For truck, rail, and ship transport, mass is the primary factor setting the cost of shipment, although for low density loads volume can become the limiting factor. This has been previously noted for straw shipments by truck *(1)* and railcar *(2)*. For pipelines transporting a single phase liquid, for example ethanol, liquid volume is the primary factor, whereas for two-phase slurry pipelines carrying biomass the amount of dry matter is the primary factor, because moisture level reaches equilibrium during transport *(3)*. For electrical power, the primary factor for costing is the power or

Table 1
Biomass Properties

| | Straw | Stover | Woodchips from FHR |
|---|---|---|---|
| Moisture content (%) | 15 *(1)* | 15 *(5)* | 45 *(1)* |
| Hydrogen content (wt%) *(12)* | 5.46 | 5.46 | 6.08 |
| Bulk density (dry kg/m$^3$) | 140 *(1)* | 145 *(5)* | 350 *(1)* |
| HHV (dry basis [MJ/kg]) *(13)* | 18 | 18 | 20 |
| LHV (MJ/kg) *(14)* | 13.9 | 13.9 | 8.8 |
| Gross yield (actual t [GJ/ha])[a] | 0.440 *(1)* | 0.882 *(5)* | 0.449 *(1)* |
| Gross yield (GJ/ha) | 6.12 | 12.25 | 3.95 |
| Transport form | Bale | Bale | Chips |

[a]Gross hectares refers to the total land area, including towns, roads, and other nonagriculturally productive area.

energy carried in the line, i.e., MW or MWh. In this study, we relate all transport cost for biomass and its conversion products to the primary factor governing the cost, and then apply these relations to calculate the cost of moving biomass or the amount of product that can be produced from that biomass.

## Modeling Biomass Transportation Costs

### *Biomass Sources*

We study three biomass residue sources: straw from grain in western Canada, corn stover from the midwestern United States, and woodchips from forest harvest residues (FHR) (the limbs and tops of trees harvested for pulp or lumber) from the boreal forest in Canada. These three sources were selected because they represent large sources of field biomass for which supply is contiguous over large areas. The two agricultural residues are somewhat remote from major centers of population, whereas boreal forest operations are often very remote, for instance across the northern half of Provinces in Canada. Table 1 identifies the properties of the biomass used in this study.

### *Processing Alternatives*

We analyze two conversion alternatives for each biomass source, electrical power and ethanol. Electrical power is produced by direct combustion of biomass; thermal efficiency figures are based on the performance of the largest biomass boiler, the Alholmens 240-MW power plant in Pietarsaari, Finland *(4)*. Values for ethanol production through fermentation are derived from previous studies for both corn stover and woodchips from the US National Renewable Energy Laboratory (NREL) *(5,6)*.

NREL estimates show a significantly lower conversion efficiency for woody biomass as compared with agricultural residues.

Each processing alternative was evaluated at both small and large scale. For all three biomass sources the small-scale plant size is identical in biomass energy input. The small power plant processes enough biomass to produce 50 MW (gross) power. Differing values of lower heating value (LHV) result in a higher biomass requirement from woodchips than from straw to produce an equivalent amount of power. The small-scale ethanol plant processes the same mass of biomass feed as required to produce 50 MW of power. For straw and stover the large-scale plant is a 500 MW (gross) power plant or an ethanol plant processing the same amount of biomass to ethanol. For woodchips from FHR the large-scale plant is a 150 MW (gross) power plant or an ethanol plant processing the same amount of biomass to ethanol. The difference in large-scale size reflects previous studies of optimum size of biomass processing *(1)*: larger processing plants are economic for biomass sources with a lower overall transportation cost. Higher gross yield of energy (the energy content of the biomass available in the total draw area) is a key factor in transportation costs. Compared with woodchips from FHR, straw has a 50% higher energy yield per gross hectare (gross hectare refers to the total draw area for the biomass), and stover has 300% the energy yield of woodchips from FHR. The higher energy yield for agricultural residue justifies the 500 MW plant size vs 150 MW for FHR. Table 2 outlines the processing parameters used in this study.

### *Transportation Modes*

We evaluate a short and a long transport distance, i.e., the assumed distance between the centers of the biomass collection area and the product usage area, arbitrarily chosen as 100 and 500 km. The study is not focused on moving biomass to a centralized processing plant, but rather moving either biomass or its products from source to market. All costs in this study are reported in 2004 US dollars.

Four modes of biomass transportation are evaluated in this study:

- **Truck transport**—straw is transported using a 20 t capacity flatbed truck, and woodchips using a 40 t chip van. Costs for both are derived from previously reported actual costs in western Canada, where bale and chip movement are routine *(1)*. We note, however, that transport of woodchips is subject to long-term high volume contracts, whereas straw movement is seasonal and usually moves a much lower volume of biomass per contract. Hence, straw costs in this study might be higher than if long-term contracts to move straw on a year round basis were used to support a straw processing industry, as such contracts ensure high equipment utilization.
- **Truck plus rail transport**—straw and woodchips are moved to a rail siding where they are loaded on a unit train for transport over the

Table 2

| Processing plant parameters | Small | | Large | |
|---|---|---|---|---|
| | Straw/stover | Woodchip | Straw/stover | Woodchip |
| *Biomass* | | | | |
| Biomass feed (actual Mt/yr) | 0.269 | 0.427 | 2.69 | 1.28 |
| Draw area ($km^2$) | 6125 | 9500 | 61,250 | 28,500 |
| Average driving distance (km) | 55 | 68 | 173 | 118 |
| *Ethanol* | | | | |
| Ethanol yield (t/d) | 174 | 83 | 1743 | 315 |
| Ethanol yield as fraction of dry mass (wt%) *(5)* | 25 | 11.6 | 25 | 11.6 |
| Ethanol pipeline diameter (in.) *(10)* | 4 | 3 | 8 | 4 |
| *Power* | | | | |
| Capacity (mW) | 50 | 50 | 500 | 150 |
| Thermal efficiency (LHV [%]) *(4)* | 38 | 38 | 38 | 38 |
| Availability (%) | 90 | 90 | 90 | 90 |
| Parasitic load (%) | 8.5 | 8.5 | 8.5 | 8.5 |

specified distance. Costs for the truck transport are calculated with the average trucking distance calculated from the biomass gross yield, assuming that the biomass source is contiguously available around the railhead. A rectilinear road system, common in the western United States and Canada, is assumed. Costs for rail are taken from a previous study of rail transport *(2)*. Straw transport by rail is assumed to be on flatbed cars without tarping; however, it would need to be verified whether a unit train of uncovered straw would present an unacceptable risk of fire. Truck plus rail transport would only make sense for the long distance case. At 100 km the collection area of biomass is so large that the cost of transshipping from truck to rail cannot be recovered by the savings in DVC *(2)*.

- **Truck plus pipeline transport**—straw and woodchips are moved to a pipeline inlet where they are slurried with water. Costs for truck transport to the pipeline inlet are identical to those for rail transport. Pipeline costs are derived from a previous study *(7)*. Note that pipeline costs show a significant economy of scale, whereas truck and rail transport do not. The previous study noted that pipeline transport of biomass is not compatible with a combustion-based utilization of the biomass, because uptake of carrier fluid by the biomass reduces the LHV. Hence, this transportation mode would

only be compatible in this study with the production of ethanol. Like rail transport, this option is only evaluated for the long distance case.

- **Truck plus ship transport**—straw and woodchips are moved to a ship where they are loaded for transport. The draw area for biomass is assumed to surround the ship loading area, an ideal case. Costs for truck transport to the ship are identical to those for rail transport, and ship costs are derived from a previous study *(8)*. Like rail transport, this option is only evaluated for the long distance case.

For power generation cases we assume that a power plant using the biomass is located remote from existing transmission lines, and we develop the cost of transmission based on the construction and operation of a dedicated line. Capital and operating costs for transmission lines are developed from detailed data from an integrated power company (Manitoba Hydro, Winnipeg, Canada). A single circuit 230 kV transmission line is used up to 200 MW, and capital cost is virtually independent of capacity. Larger capacity transmission lines use multiple circuits to reduce line loss of power. Thus, at 500 MW a two circuit 230 kV line would be built, at a premium of 50% in capital cost to a single circuit 200 MW line. A 12% pretax return is applied in calculating capital recovery. Operating costs are line losses, which are proportional to the square of the line capacity in megawatt, and maintenance costs. Maintenance cost for transmission lines is primarily vegetation control and is independent of capacity.

Two modes of ethanol transportation are evaluated in this study:

- **Truck**—the study basis is a tandem tanker carrying 40 t of ethanol. Costs are developed from industry charge rates for long-term contracts *(9)* and are based on a truck loading and unloading time of 45 min each and an average transport speed of 100 km/h.
- **Pipeline**—the cost of ethanol pipelining was developed from an analysis of capital and operating costs. Pipeline capital costs are based on discussions with a major contractor *(10)*; a 12% pretax return is used in calculating capital recovery. Pump station number and power requirement are based on detailed calculations of pressure drop; a power cost of $60 MW/h is used in this study. Annual maintenance costs are estimated based on percentages of capital cost drawn from industry norms: 0.5% for the pipeline and 3% for pumping stations.

## Results

### *Transportation Cost Factors*

Table 3 lists the DVC and DFC for all modes of transportation in this study. The units for DVC and DVC reflect the actual basis by which the cost of transportation is primarily affected, for example, actual mass for truck transport, volume for ethanol pipelining, and mass of dry matter for biomass pipelining. The economy of scale is negligible for some modes of

Table 3
Distance Variable and Distance Fixed Transportation Parameters[a]

| Mode | Item transported | DVC | Units | DFC | Units |
|---|---|---|---|---|---|
| Truck | Straw/stover *(2)* | 0.12 | $ Actual t/km | 4.39 | $/Actual t |
| | Woodchips *(2)* | 0.07 | $ Actual t/km | 3.01 | $/Actual t |
| | Ethanol *(9)* | 0.05 | $ Actual t/km | 3.86 | $/Actual t |
| Rail *(2)* | Straw/stover | 0.023 | $ Actual t/km | 14.15 | $/Actual t |
| | Woodchips | 0.017 | $ Actual t/km | 5.48 | $/Actual t |
| Ship *(8)* | Straw/stover | 0.01 | $ Actual t/km | 34.01 | $/Actual t |
| | Woodchips | 0.01 | $ Actual t/km | 11.15 | $/Actual t |
| Pipeline | Biomass[b] *(7)* | $23.4\ C^{-0.4086}$ | $ Dry t/km | $4{,}19{,}000\ C^{-0.8656}$ | $/Dry t |
| | Ethanol[c] *(10)* | $4.13\ E_m^{-0.5885}$ | $ t Ethanol/km | 0 | $/t Ethanol |
| | Ethanol[d] *(10)* | $0.062\ E_v^{-0.5885}$ | $/L/km | 0 | $/L |
| Power *(15)* | 46 MW net | 321 | $/MW/km | 0 | $/MW |
| | 137 MW net | 195 | $/MW/km | 0 | $/MW |
| | 458 MW net | 208 | $/MW/km | 0 | $/MW |
| | 46 MW net | 0.04 | $/MWh/km | 0 | $/MWh |
| | 137 MW net | 0.02 | $/MWh/km | 0 | $/MWh |
| | 458 MW net | 0.03 | $/MWh/km | 0 | $/MWh |

[a]Source data have been adjusted to consistent units and a common currency (2004 US dollars).
[b]$C$, pipeline capacity in dry metric tons biomass per year.
[c]$E_m$, pipeline capacity in metric tons of ethanol produced per day.
[d]$E_v$, pipeline capacity in liters of ethanol produced per day.

transport, such as truck, rail, and ship: more biomass means more loads at a set cost per load that depends on distance traveled. The economy of scale is strong for pipelining, as reflected in the low exponent relating DVC to capacity. Power transmission show a discontinuity in cost between 150 and 500 MW because the line design changes from single circuit to double circuit.

DFC values in Table 3 show a wide range. Ship transport, for example, has the lowest DVC cost, but the cost of getting biomass onto and off a ship is high relative to the cost of loading a truck. Rail cars are intermediate. Note that for both ship and rail the DFC for straw/stover is significantly higher than for woodchips. Woodchips lend themselves to bulk handling by methods such as conveying or pneumatic transfer, whereas straw/stover is moved as a large bale. As noted earlier, pipeline transport of biomass can only be used for aqueous-based processing, and DFC for pipelining is low because the cost of slurrying biomass is not incremental to the overall processing cost. Rather, slurrying of biomass can be thought of as shifting equipment from the processing plant to the pipeline inlet. Hence, DFC for pipeline transport of biomass reflects incremental labor, typically one extra person at the pipeline inlet compared with the staffing required for biomass receipt by truck or rail at a central pipeline facility *(11)*. An ethanol pipeline located within a biomass processing plant would have no DFC: pipelines would typically be connected directly to product storage tanks. Similarly, power transmission has no incremental DFC.

### *Relative Transportation Costs*

The transportation cost factors were then used to calculate the cost of transporting biomass or the equivalent amount of ethanol or power that could be produced from that biomass for eight cases: straw/stover and woodchips from FHR to ethanol and power at large and small scale. Results are normalized to the transport cost per unit of energy in the incoming biomass, and are shown in Figs. 1–4.

Many observations can be drawn from Figs. 1 to 4; we highlight some key observations.

- In all cases a product transportation option is available that is significantly lower than the cost of moving biomass. Two factors contribute to this: biomass has a low energy density, and the energy produced from biomass is lower than the energy in the biomass as a result of conversion losses. The latter is especially true for ethanol from wood, which has a very low conversion efficiency compared with ethanol from straw or power from any biomass source. Note also that at 500 km the cost of transporting biomass by truck is more than \$4/GJ, a significant cost considering that the current wholesale price of natural gas is about \$6–8/GJ in North America.

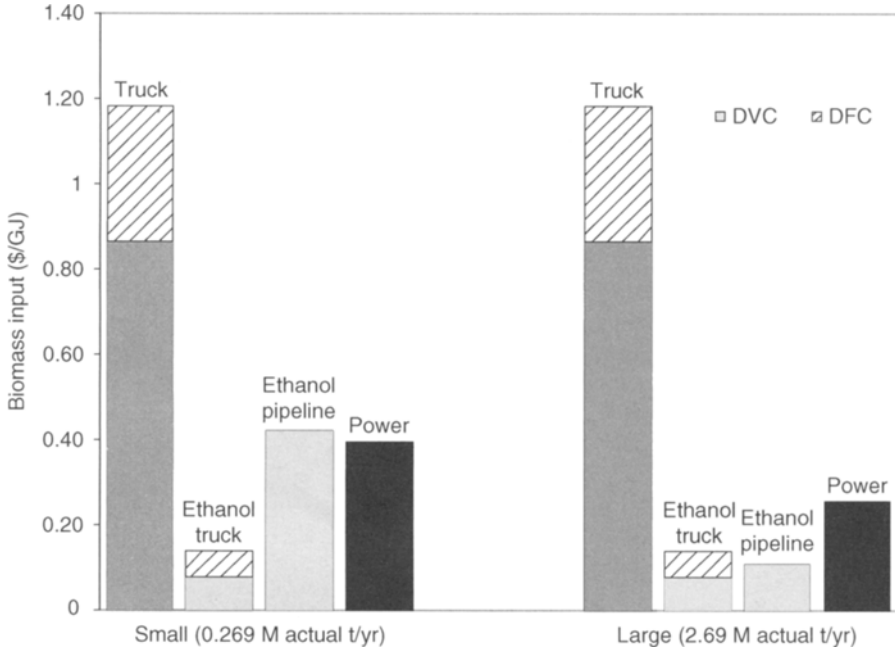


**Fig. 1.** Agricultural residue transportation costs for biomass and products more than 100 km.

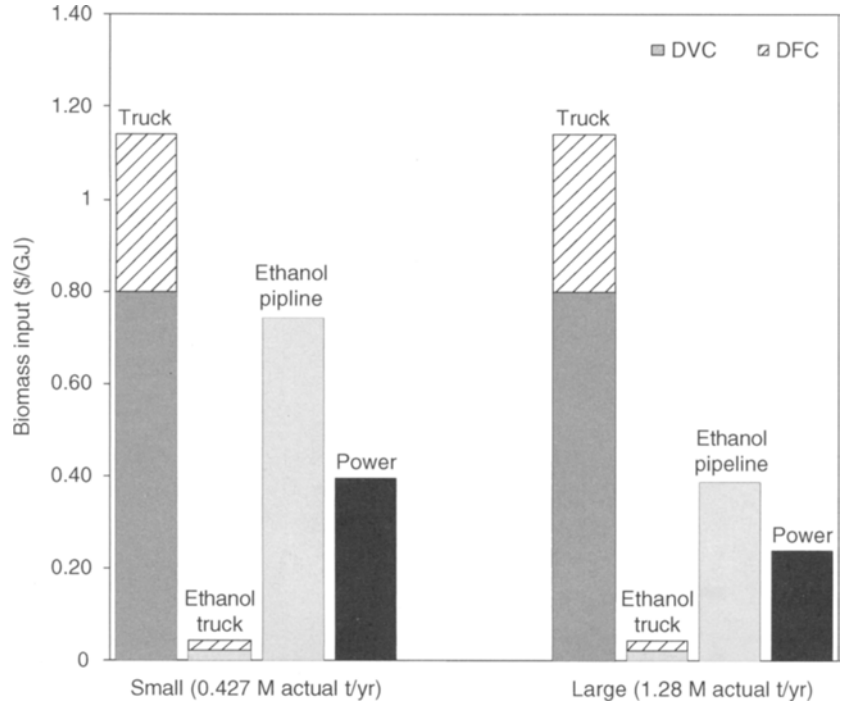


**Fig. 2.** Woodchip transportation costs for biomass and products more than 100 km.

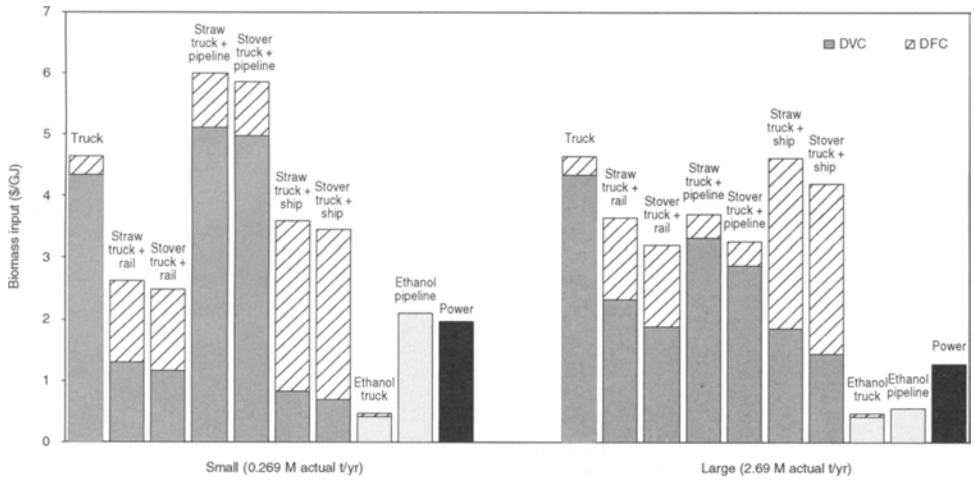


**Fig. 3.** Agricultural residue transportation costs for biomass and products more than 500 km.

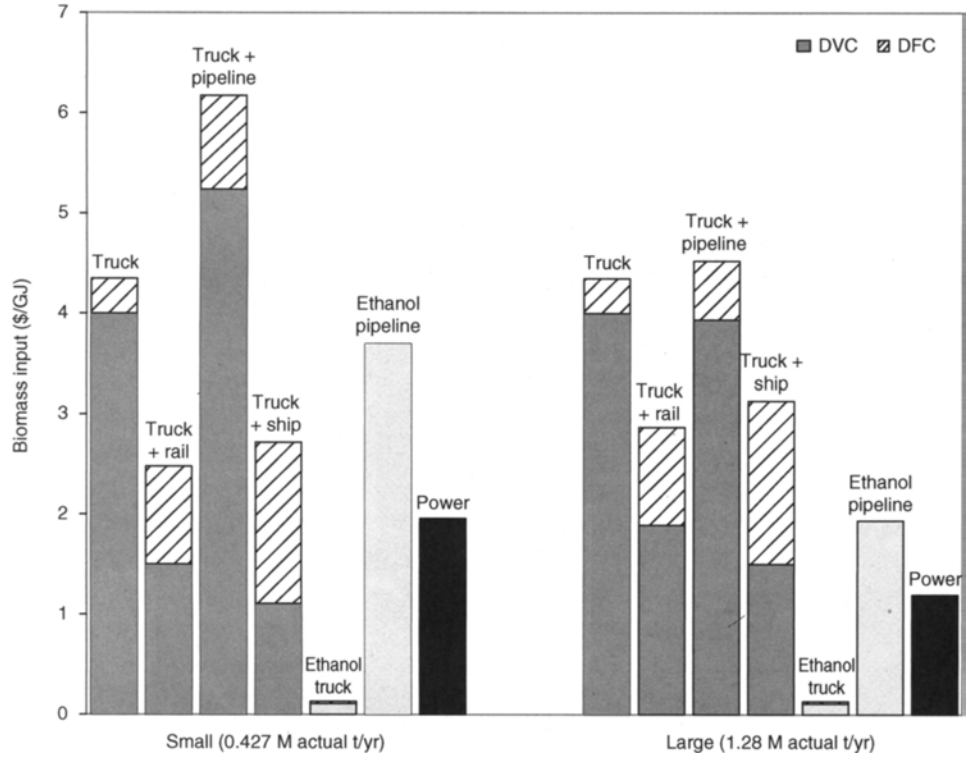


**Fig. 4.** Woodchip transportation costs for biomass and products more than 500 km.

- If rail transport is available it is more economical to transship biomass to rail for transport distances of 500 km.
- Pipelining of biomass is not economical at small scale, nor at the large-scale for wood chips, 1900 dry t/d of biomass. It is competitive with rail transport at large-scale for straw, i.e., about 2.5 Mt/yr).
- Ship transport is not economical relative to rail at a transport distance of 500 km because the high DFC cost offsets the benefit of a low DVC.
- Pipelining of ethanol is uneconomical from small-scale plants, and is about as economical as truck transport for the large-scale straw/stover to ethanol plant in this study, producing 1700 t/d (2.3 ML/d) of ethanol. Ethanol pipelining does not have a DVC, so pipelining is more economical than truck shipment for the large case at 100 km, and slightly less economical at 500 km. From Table 3 one can calculate that the DVC for pipelining ethanol is lower than truck haul more than 1800 t/d ethanol, making pipelining more economical than truck hauling at any distance.
- The transmission lines for the small and large woodchip power plants are identical, and therefore have the same capital and maintenance costs. However, line losses increase with the square of the power transmitted. The large-plant transmission cost is 60% of the small-plant transmission cost.

The high DFC for loading and unloading biomass from ships means that long distances are required for the saving in DVC to offset the DFC. Figure 5 shows the cost of rail vs ship transport of biomass as a function of distance. Shipping of straw incurs a very high DFC, as noted earlier, and a shipping distance of about 1500 km is required before the lower DVC of shipping offsets the incremental DFC. DFC for woodchips is lower, and shipping is more economical than rail transport at a distance of about 800 km.

## Discussion

Transportation is a cost element in any energy project, and this is especially true for biomass because of the lower energy density compared with fossil fuels. Woodchips with a moisture content of 45% have an LHV of less than 10 MJ/kg, whereas the comparable figure for surface-mined coal in western North America is about 20 MJ/kg. However, there are at least two incentives for aggregating large amounts of biomass in an energy project: the economy of scale in processing, and the ability to create a multiproduct integrated biorefinery maximizing the production of higher value products and using all of the energy in the biomass. Assessing these tradeoffs requires a careful analysis of the cost of moving both biomass and its products.

For example, the relative cost of transporting biomass and its products can be used to do some preliminary screening of plant-site location.

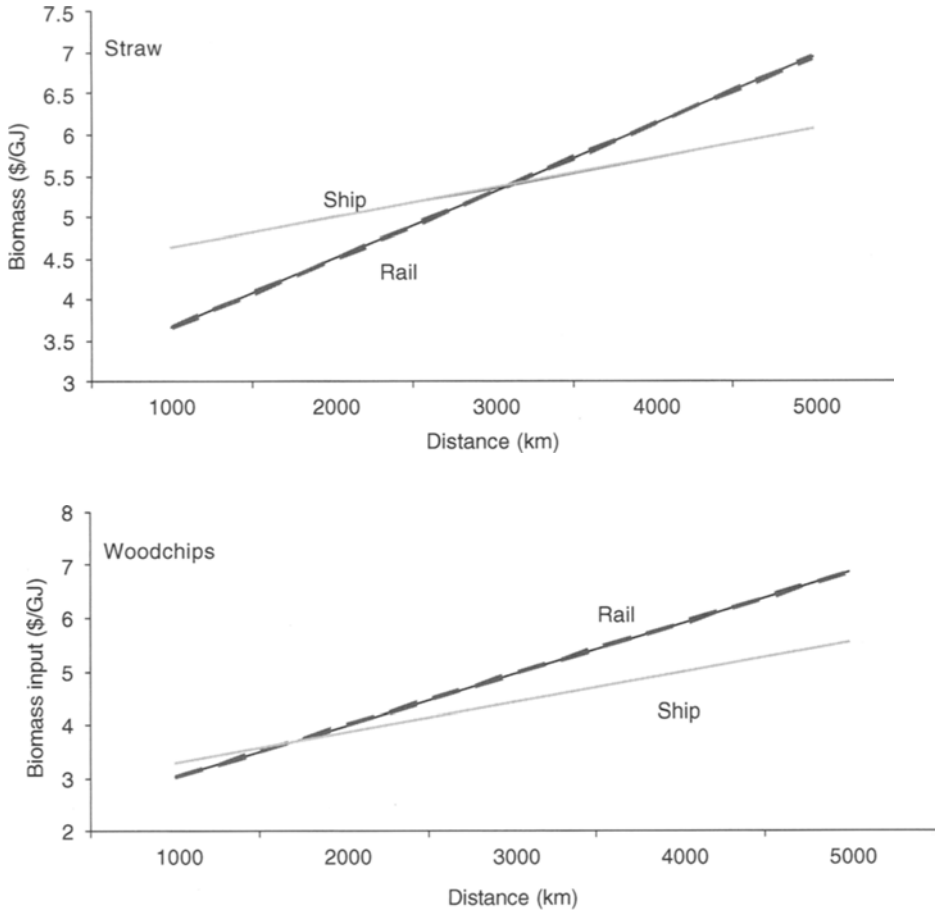


**Fig. 5.** Determination of the minimum distance where the cost per GJ biomass input is lower for ship than for rail transport.

A previous detailed study of producing power at optimum plant size from biomass in western Canada *(1)* showed a total power plant operating cost including administration, operating labor, maintenance, and capital recovery of $25/MWh for straw and $34 for woodchips, adjusted to 2004 USD; the difference arises from the larger optimum plant size for straw relative to FHR. This range of cost is equivalent to $2.40–3.20/GJ in the biomass for a thermal efficiency of the power plant of 34%, the value used in the study. As a general guideline, plants built in remote areas will have capital and operating costs that are 10% higher than those built near a large population center, because of the need to build an access road and a camp to house construction labor, and the need for higher salaries to attract operating and maintenance staff to a remote setting *(10)*. At 10% premium the impact is therefore, about $0.24–0.32 of increased cost per GJ of biomass. The cost savings from transporting power rather than biomass for the two large-scale cases is more than $2/GJ in the biomass at 500 km, and about $1 at 100 km. Hence, the cost of remote construction is not likely to be the

deciding factor for moving biomass from a remote area to a location adjacent to an existing transmission grid: it is cheaper to move the power and pay the location premium.

Ethanol production raises two transportation issues. First, yield of ethanol per metric ton of biomass is low, 25% on a dry basis for straw and 12% on a dry basis for woodchips. Factoring in moisture content, the mass of biomass moved is about five times higher than the ethanol produced from straw, and 15 times higher for woodchips. At large scale, 1800 t/d, ethanol pipelining becomes more economical than truck transport at any distance. This scale is too large to be economically supplied by a low-gross yield biomass such as woodchips from FHR. In addition, ethanol production produces large amounts of unconverted biomass. Transporting biomass to a distant ethanol plant might require that the residue from processing be transported back to the point of origin, creating a further disincentive.

A biorefinery has the potential to increase the value of biomass by producing fuels, chemicals, and power, for example, ethanol form fermentation coupled with combustion or gasification of lignin to produce power. If biomass is being moved an average of 100 km to a biorefinery the integration would have to yield a value of $1/GJ in the biomass to justify the transportation premium.

## Conclusions

Transportation costs for biomass and its products have a distance fixed component that is incurred regardless of the distance traveled, and a distance variable component that is directly related to the distance traveled. Both factors must be included in an analysis of transportation costs. Some modes of transportation, for example, trucking, have a negligible economy of scale and DVC is constant; others such as pipelining have a high economy of scale, and DVC is a function of capacity. Shipping of biomass has a low DVC but a high DFC, and hence is not economic below 800 km (woodchips) and 1500 km (straw/stover). Transshipment from truck to rail is economical at 500 km for both woodchips and straw/stover if rail lines are available. Ethanol transport by pipeline is more economical than trucking at production rates of 1800 t/d of ethanol; this is well above the economic size of producing ethanol from a dispersed low-yield biomass source like FHR. The gap in cost between the cost of transporting power and biomass is far more than the expected higher cost of building and operating a power plant in a location remote from an existing transmission grid.

## Acknowledgments

We gratefully acknowledge EPCOR Utilities Inc. and the Canadian Natural Sciences and Engineering Research Council (NSERC), whose financial support made this research possible. Shane Mailey, manager,

transmission projects department, Manitoba Hydro (an integrated Canadian utility) provided invaluable insight into transmission cost information, and Wally Pyl, transmission network planning engineer at Manitoba Hydro, provided useful guidance online loss costs. Previous conversations with Colin Johnson and Roger Stenvold of Canadian National Railway Company (CN), were helpful. David Williams, Chief Estimator for Bantrel (an affiliate of Bechtel), provided insightful comments concerning capital cost estimation of pipeline. Jeff Taylor, regional manager of Gibson's trucking company, provided helpful information on trucking costs. All conclusions and opinions are solely the authors' and have not been reviewed or endorsed by any other party.

## References

1. Kumar, A., Cameron, J., and Flynn, P. (2003), *J. Biomass Bioenergy* **24,** 445–464.
2. Mahmudi, H. and Flynn, P. (2006), *J. Appl. Biochem. Biotechnol.* **129–132,** 88–103.
3. Kumar, A., Cameron, J., and Flynn, P. (2004), *J. Appl. Biochem. Biotechnol.* **113,** 27–40.
4. Flynn, P. and Kumar, A. (2005), Trip Report, Pietarsaari, Finland. University of Alberta, Canada (May 1, 2006). www.biocap.ca/files/reports.
5. Aden, A., Ruth, M., Ibsen, K. Lignocellulosic biomass to ethanol process design and economics utilizzing co-carrent diulte acid prehydrolsis for corn stoner, TP-5-32438 (2002), National Renewable Energy Laboratory, Golden, Colorado.
6. Wooley, R., Ruth, M., Sheehan, J., and Ibsen, K. (1999), Lignocellulosic biomass to ethanol process design and economics utilizing co-corrent dilute acid prehydrolysis and enzymatic hydrolysis—current and futuristic scenarios, TP-580-26157. National Renewable Energy Laboratory, Golden, Colorado.
7. Kumar, A., Cameron, J., and Flynn, P. (2005), *J. Bioresour. Technol.* **96,** 819–829.
8. Borjesson, P. and Gustavsson, L. (1996), *J. Energy* **21,** 747–764.
9. Taylor, J. (2002), Regional Manager of Gibson's Trucking Company, Alberta, Canada, personal communication.
10. Williams, D. (2002), Chief Estimator for Bantrel Corporation (an affiliate of Bechtel), Edmonton, Calgary, Alberta, Canada, personal communication.
11. Ghafoori, E. and Feddes, J. (2005), Pipeline vs beef transport of beef cattle manure. ASAE Pacific Northwest Section Meeting Presentation, PNW05-1012, Lethbridge, Alberta, Canada.
12. Rao, M., Singh, S., Sodha, M., Dubey, A., and Shyam, M. (2004), *J. Biomass Bioenergy* **27,** 155–171.
13. Cameron, J., Kumar, A., and Flynn, P. (2004), ASAE/CSAE Annual International Meeting, PN 048039, Ottawa, Ontario, Canada.
14. Van den Broek, R., Faaij, A., and Van Wijk, A. (1995), Department of Science, Technology and Society, Utrecht University, Netherlands.
15. Mailey, S. (2006), Transmission information engineer, Manitoba Hydro, Winnipeg, Manitoba, Canada, personal communication.

0273-2289/1559-0291 (Online)/07/136–140/653–662/$30.00

# The Effect of Initial Cell Concentration on Xylose Fermentation by *Pichia stipitis*

**Frank K. Agbogbo,*[,1] Guillermo Coward-Kelly,[1] Mads Torry-Smith,[1] Kevin Wenger,[1] and Thomas W. Jeffries[2]**

*[1]Novozymes North America Inc., 77 Perry Chapel Church Road, Franklinton, NC 27525, E-mail: fkag@novozymes.com; and*
*[2]Institute from Microbial and Biochemical Technology, Forest products Laboratory, One Gifford Pinchot Dr., Madison, WI 53705*

## Abstract

Xylose was fermented using *Pichia stipitis* CBS 6054 at different initial cell concentrations. A high initial cell concentration increased the rate of xylose utilization, ethanol formation, and the ethanol yield. The highest ethanol concentration of 41.0 g/L and a yield of 0.38 g/g was obtained using an initial cell concentration of 6.5 g/L. Even though more xylitol was produced when the initial cell concentrations were high, cell density had no effect on the final ethanol yield. A two-parameter mathematical model was used to predict the cell population dynamics at the different initial cell concentrations. The model parameters, $a$ and $b$ correlate with the initial cell concentrations used with an $R^2$ of 0.99.

**Index Entries:** Cell concentration; fermentation; model; *Pichia stipitis*; xylose.

## Introduction

Cost-effective production of fuel ethanol from lignocellulosic biomass requires fermentation of the hemicellulose fraction, which contains xylose as the major sugar component in agricultural residues *(1)*. Hemicellulose includes 24–35% of the dry biomass of some lignocellulosic materials, such as corn fiber, corn cob, corn stover, and sugar cane bagasse *(1)*. Native strains of *Pichia stipitis* have the ability to ferment xylose, glucose, and cellobiose *(2,3)*.

Low levels of oxygen (1.5–5 mmol/L·h) are necessary for the conversion of xylose to ethanol in order to maintain cell viability and NADH balance *(4–7)*. A high level of oxygen leads to ethanol reassimilation and biomass production, and therefore, low yields *(8–10)*. Under anaerobic conditions, cell growth and ethanol production are severely restricted *(11)*. The cell growth of *P. stipitis* is inhibited at low ethanol concentrations (approx 34.0 g/L) *(12–13)* and the highest ethanol tolerance reported for

*Author to whom all correspondence and reprint requests should be addressed.

growth is 64.0 g/L *(11)*. Previous studies have shown that the fermentation rate can be increased by addition of 10.0 mg/L zinc *(14)* and that it can be decreased by forced cycling of pH *(15)*. The initial cell concentrations used in *P. stipitis* fermentations varies from 0.01 to 6 g/L *(14,16)*. However, how the initial cell concentration affects fermentation rate, final ethanol concentration, and yield has not been documented. The purpose of this work is to look at the effect of the initial cell concentration on the rate of fermentation, final ethanol concentrations, and yield using synthetic media containing xylose.

## Materials and Methods

### *Microorganism and Media*

*P. stipitis* CBS 6054 stock cultures were maintained on 20% glycerol at −15°C. Stock culture (100 µL) of *P. stipitis* CBS 6054 was cultured on yeast extract, peptone, xylose agar plates at 30°C for 3 d. The plates were prepared from 10.0 g/L yeast extract, 20.0 g/L peptone, 20.0 g/L xylose, and 20.0 g/L agar. Colonies from the plates were grown overnight in a filter-sterilized fermentation medium containing 1.7 g/L yeast nitrogen base (without amino acid and ammonium sulfate), 2.27 g/L urea, 6.56 g/L peptone, and 20.0 g/L xylose. The cells were centrifuged at 3000 rpm for 5 min and the supernatant was discarded. The cells were resuspended in distilled water media to have a cell concentration of 55.0 g/L.

### *Synthetic Media Preparation*

Xylose solution (140.0 g/L) was prepared and filter-sterilized. Nutrient solution (50X the concentration used) was prepared by dissolving 1.7 g of yeast nitrogen base, 2.27 g of urea, and 6.56 g of peptone in 20 mL of water.

### *Fermentation*

Fermentations were performed in sterile 125-mL Erlenmeyer flasks (with 0.2 µm vent cap) using an air-shaker incubator at 30°C and 100 rpm. The initial pH was 6.3. Each Erlenmeyer flask contained 50 mL of xylose solution, 1 mL of nutrient solution, and 7 mL of inoculum, which had been diluted to the appropriate cell concentration. Initial cell concentrations of 1.8, 4.3, and 6.5 g/L were investigated in this study. All experiments were performed in triplicate.

### *Analytical Methods*

Fermentation was monitored for 8 d by taking 1 mL of sample for xylose, ethanol, and xylitol analyses. The concentration of xylose, ethanol, and xylitol was determined using an Agilent high-performance liquid

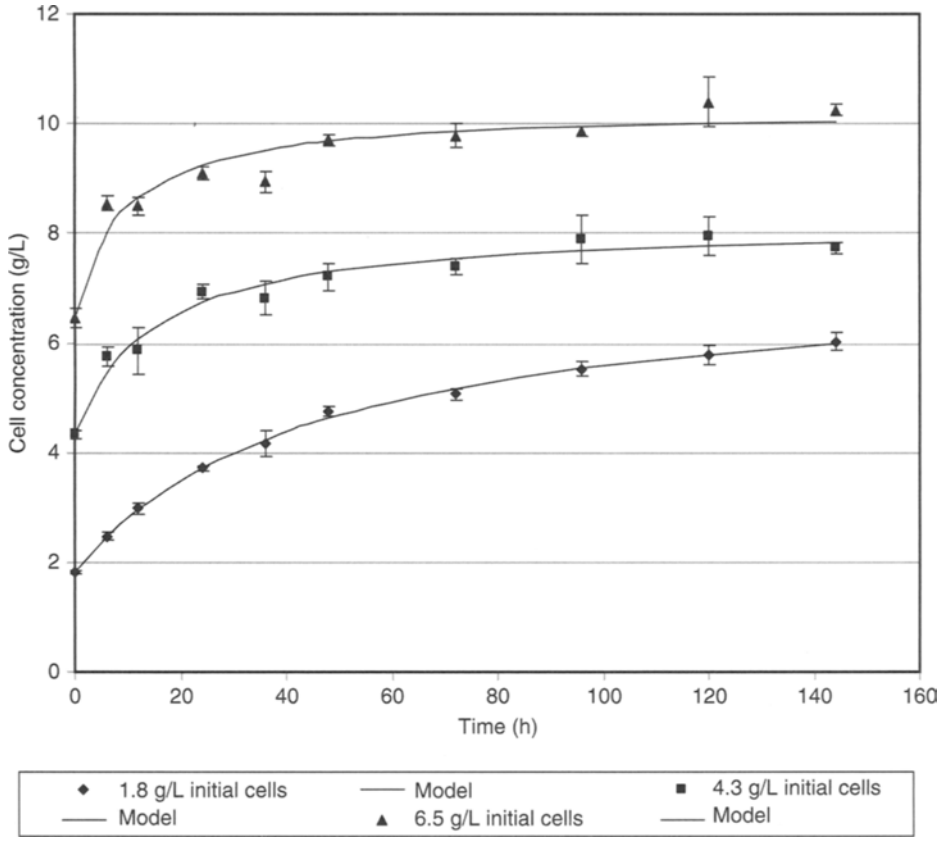


**Fig. 1.** Cell concentrations during fermentation. Error bars are ±1 standard deviation.

chromatography System with an analytical BIO-RAD Aminex HPX-87H column and a BIO-RAD Cation H refill guard column. Cell concentration was determined from optical density measurement of the cells using Cary 3C Ultraviolet-visible spectrophotometer at 600 nm. An optical density of 1 is equivalent to 0.23 g of dry cells/L.

## Results and Discussion

### *Cell Growth and Mathematical Model*

The cell concentrations of *P. stipitis* during fermentation on xylose are shown in Fig. 1. From Fig. 1, an initial cell concentration of 1.8, 4.3, and 6.5 g/L increased to 6.0, 7.7, and 10.3 g/L, respectively, after 144 h of fermentation. The average specific cell growth rates decrease at high initial cell concentrations. Previous attempts to model *P. stipitis* fermentation used the Monod model *(11,17–19)*. The Monod model describes substrate-limited growth in which environmental conditions are only related to the substrate concentration. However, the fermentation performed in this work is not limited solely by the amount of substrate supplied initially.

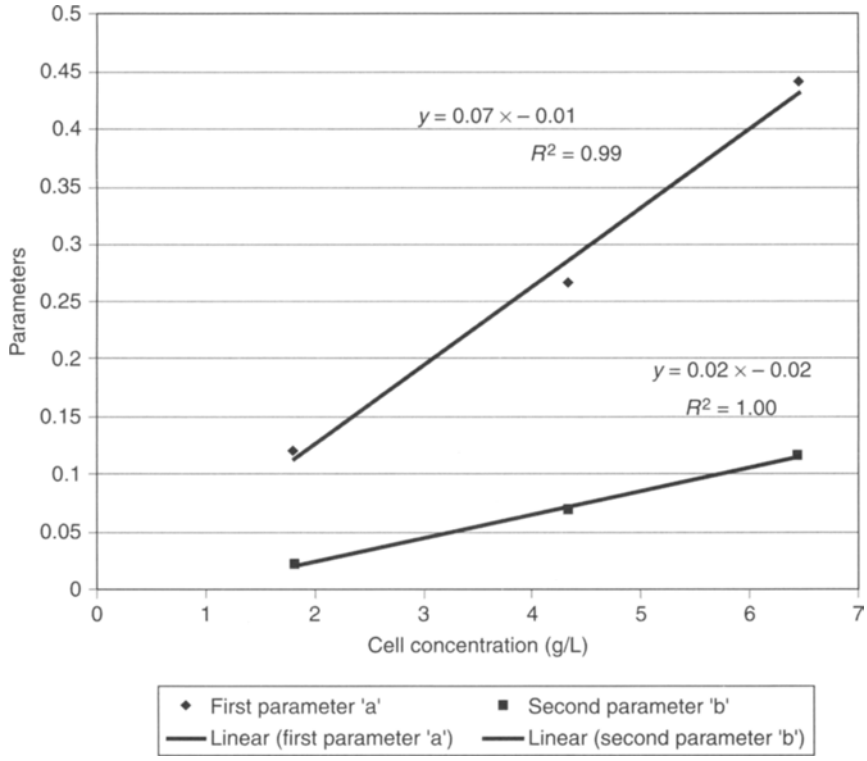


**Fig. 2.** Variation of model parameters during fermentation on xylose.

Therefore, a two-parameter empirical mathematical model was used to fit the cell concentrations during the fermentation. The different initial cell concentrations were fit to Eq. 1, using least-square analysis of the error between experimental and predicted values.

$$X = X_0 + \frac{at}{1+bt} \tag{1}$$

where $X$ is the cell concentration during fermentation (g/L), $X_0$ is the cell concentration initially (g/L), $t$ is the time (h), $a$ is a parameter with units (g/L · h), and $b$ is a parameter with units (1/h).

The parameters $a$ and $b$ were determined at the different initial cell concentrations used in the fermentation. The variation of these parameters with the initial cell concentration is shown in Fig. 2. From Fig. 2, a linear correlation fits the parameters, $a$ and $b$, with a correlation coefficient of 0.99 and 1, respectively. Therefore, Eq. 1 predicts the population dynamics with parameters that correlate very well with the initial cell concentrations used in the fermentation. From the graphs in Fig. 2, it is possible to determine the parameters $a$ and $b$, in the range 1.8–6.5 g/L and then determine the cell concentrations during the fermentation. Although these studies were done in shake flasks at a shaking rate of 100 rpm and sugar concentration of

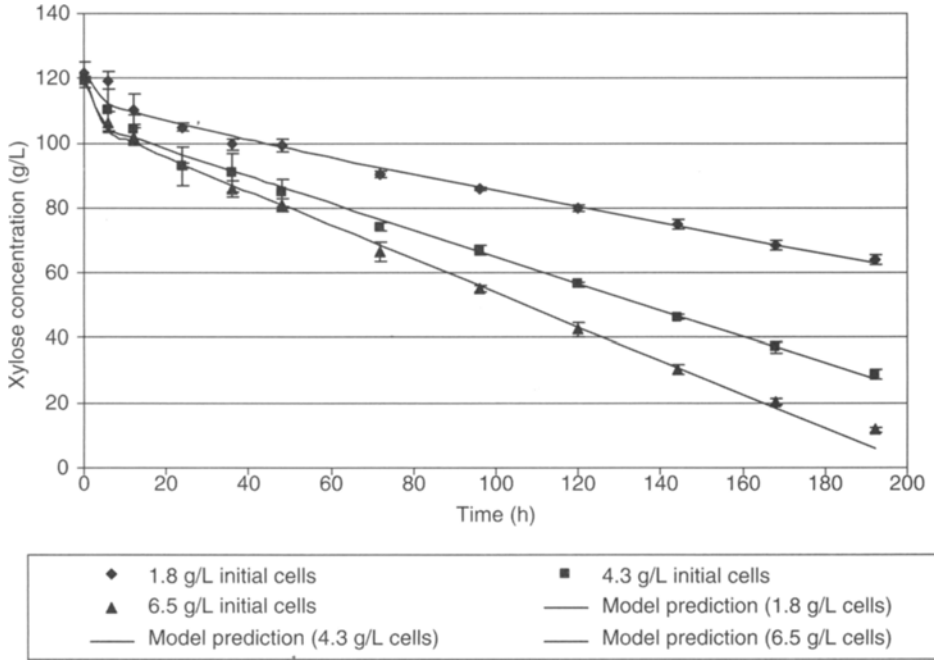


**Fig. 3.** Xylose concentration at different initial cell concentrations. Error bars are ±1 standard deviation.

120 g/L, a working population dynamics model for this system could be applied to other systems.

## *Substrate Consumption*

The xylose concentrations at the different initial cell concentrations are shown in Fig. 3. From the graph, the amounts of xylose consumed after 192 h of fermentation were 58.0, 92.0, and 108.0 g/L at initial cell concentrations of 1.8, 4.3, and 6.5 g/L, respectively. At high initial cell concentrations, the amount of substrate consumed was high. As the amount of substrate consumed depends on the initial cell concentration used, inoculating with the right initial cell concentration is vital for complete substrate consumption with *P. stipitis*. In a recent study *(20)*, using xylose at a concentration of 60.0 g/L and an initial cell concentration of 2.0 g/L, approx 60.0 g/L of the substrate was consumed in 120 h compared with 192 h in this study. The decrease in the ethanol yield and the rate of substrate utilization in this work compared with our previous study *(20)* is similar to observations made by Du Preez et al *(21)*.

The rate of substrate consumption is modeled using the Leudeking-Piret kinetics *(22)* as shown in Eq. 2.

$$\frac{dS}{dt} = -\alpha X - \beta \frac{dX}{dt} \tag{2}$$

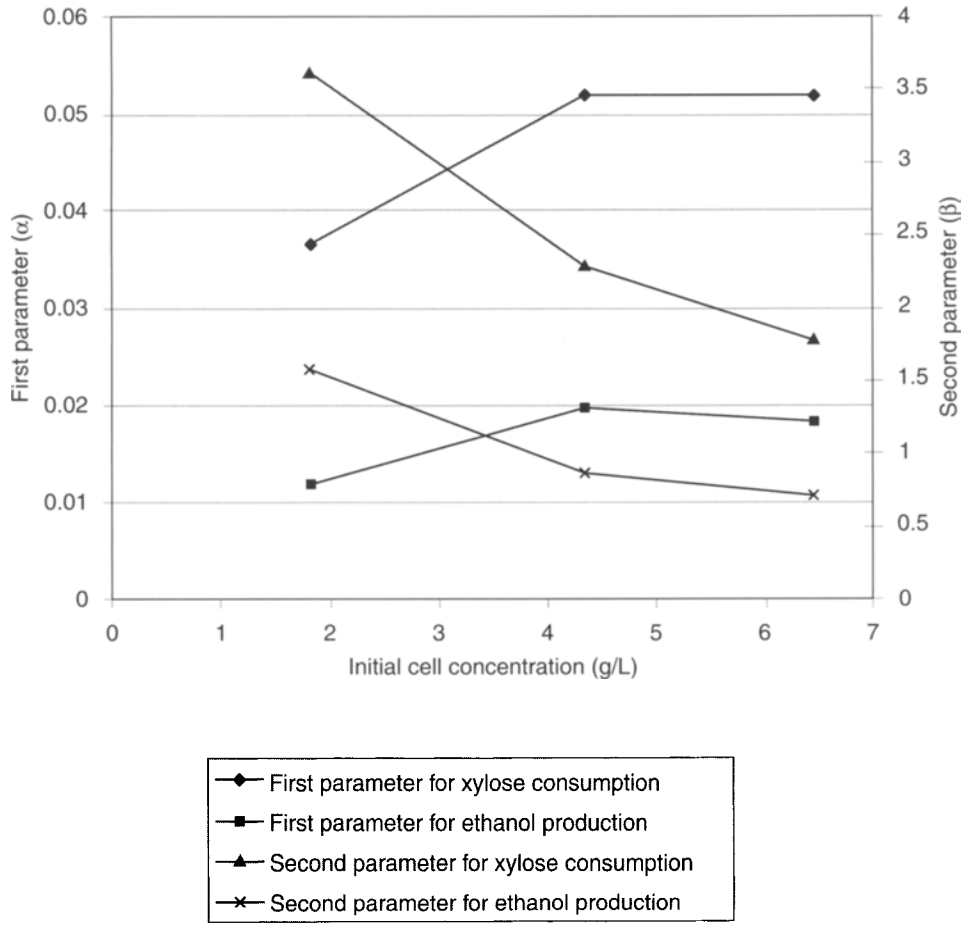


**Fig. 4.** Variation of model parameters with initial cell concentrations.

where α is a parameter associated with cell maintenance (1/h) and β is a parameter associated with growth (g substrate/g cells). Substituting Eq. 1 and its differential in Eq. 2 and integrating, we obtain Eq. 3.

$$S = S_0 - \alpha\left[X_0 t + \frac{at}{b} - \frac{a}{b^2}\ln(1+bt)\right] - \beta\left[X_0 + \frac{at}{1+bt}\right] \quad (3)$$

where $S$ is the substrate concentration at time $t$ (g/L) and $S_0$ is the initial substrate concentration (g/L). Equation 3 was fitted to experimental data using least square minimization of the error between experimental and predicted values. The experimental and predicted substrate concentrations at the different initial cell concentrations are shown in Fig. 3. The model parameters (α and β), at the different initial cell concentrations are shown in Fig. 4. From Fig. 4, the first parameter (α), which is related to the maintenance coefficient, increased when the initial cell concentration increased from 1.8 to 4.3 g/L. However, the parameter remained essentially constant when initial cell concentrations increased from 4.3 to 6.5 g/L. The first

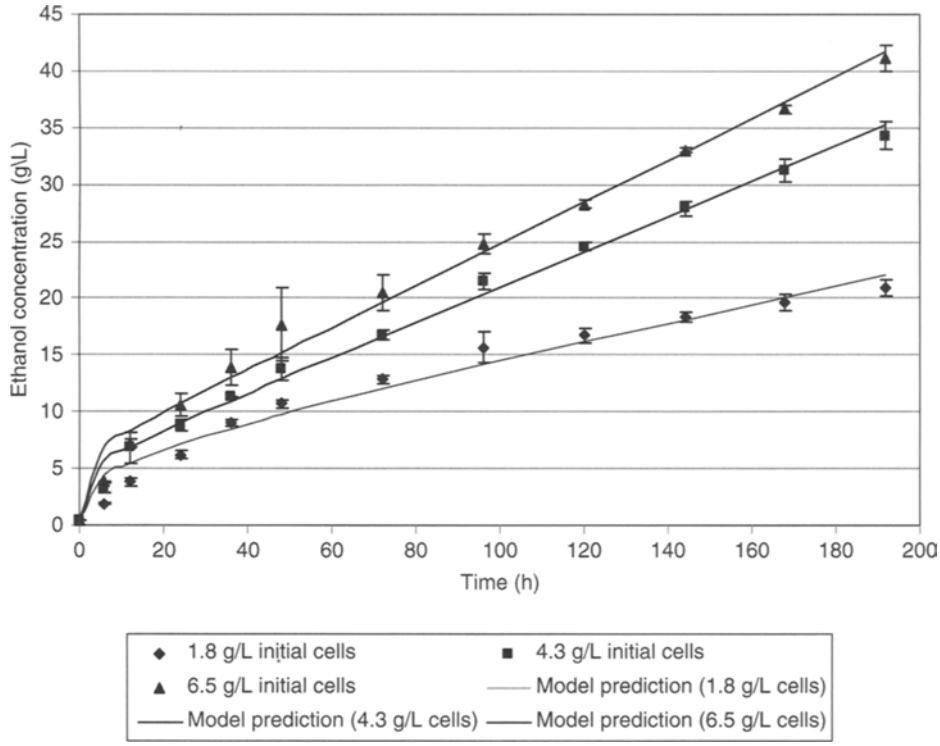


**Fig. 5.** Ethanol concentration at different initial cell concentrations. Error bars are ±1 standard deviation.

parameter is the major contributor to the rate of substrate consumption after the initial growth period ($t > 48$ h). The results indicate that the initial cell concentration needs to be more than some threshold value in order to get substantial substrate consumption. The second parameter β, which is the growth associated parameter, decreased as the initial cell concentrations increased (*see* Fig. 4). As the cells grow more when the initial cell concentration is low, this parameter is high when the initial cell concentrations are low. Although β is high at low initial cell concentrations, it has no significant effect on the initial fermentation rate.

## *Ethanol Production*

Figure 5 shows the ethanol concentration at the different initial cell concentrations. The final ethanol concentrations after 192 h of fermentation were 20.9, 34.3, and 41.1 g/L at the initial cell concentrations of 1.8, 4.3, and 6.5 g/L, respectively. The final ethanol concentration was high when the initial cell concentration was high because there were more cells to convert the xylose into ethanol. The amount of ethanol produced in the fermentation depends on the amount of cells used in the initial inoculum. Xylitol, a byproduct of the fermentation, was at concentrations of 2.2, 6.9, and 10.4 g/L at the initial cell concentrations of 1.8, 4.3, and 6.5 g/L,

Table 1
Summary of Fermentation Results After 192 h of Fermentation

| Substrate | | Xylose | |
|---|---|---|---|
| Substrate concentration (g/L) | | 120.3 ± 1.4 | |
| Initial cell concentration (g/L) | 1.82 ± 0.04 | 4.33 ± 0.08 | 6.45 ± 0.16 |
| Maximum ethanol concentration (g/L) | 20.9 ± 0.72 | 34.3 ± 1.22 | 41.09 ± 1.12 |
| Ethanol yield (g/g) | 0.363 ± 0.019 | 0.381 ± 0.017 | 0.378 ± 0.006 |
| Xylitol yield (g/g) | 0.038 ± 0.003 | 0.077 ± 0.007 | 0.096 ± 0.002 |
| Substrate consumption rate (g/L·h) | 0.301 ± 0.021 | 0.470 ± 0.006 | 0.565 ± 0.007 |
| Ethanol production rate (g/L·h) | 0.109 ± 0.004 | 0.179 ± 0.006 | 0.214 ± 0.006 |
| Ethanol selectivity (g/g) | 0.906 ± 0.002 | 0.832 ± 0.013 | 0.798 ± 0.006 |

Errors are ±1 standard deviation.

respectively, after 192 h of fermentation. The xylitol concentrations and fraction of the total product converted to xylitol, increased with an increase in the initial cell concentration.

A summary of the fermentation results are shown in Table 1. The ethanol yield was 0.36, 0.38, and 0.38 g/g at the initial cell concentrations of 1.8, 4.3, and 6.5 g/L, respectively. The ethanol yield was slightly higher at initial cell concentrations of 4.3 and 6.5 g/L because the substrate was used for ethanol production rather than for cell biomass production. There was no significant difference between the yield at initial cell concentrations of 4.3 and 6.5 g/L, although the fraction of the substrate converted to xylitol was higher at initial cell concentration of 6.5 g/L. This might be owing to the neutralizing effect of the two factors, an increased yield owing to less cell biomass production, and a decreased yield owing to xylitol production. The selectivity for ethanol was high at low initial cell concentrations and decreased as the initial cell concentrations increased.

The rate of ethanol production modeled using the Leudeking–Piret kinetics for product formation as shown in Eq. 4.

$$\frac{dP}{dt} = -\alpha X + \beta \frac{dX}{dt} \tag{4}$$

where $\alpha$ is a parameter associated with cell maintenance (1/h) and $\beta$ is a parameter associated with growth. Substituting Eq. 1 and its differential in Eq. 4 and integrating, we obtain Eq. 5.

$$P = P_0 + \alpha\left[X_0 t + \frac{at}{b} - \frac{a}{b^2}\ln(1+bt)\right] + \beta\left[X_0 + \frac{at}{1+bt}\right] \tag{5}$$

where $P$ is the ethanol concentration at time $t$ (g/L) and $P_0$ is the initial ethanol concentration (g/L). Equation 5 was fit to experimental data using least square minimization of the error between experimental and predicted values. The experimental and predicted substrate concentrations at the different initial cell concentrations are shown in Fig. 5. The model parameters at the different initial cell concentrations are shown in Fig. 4.

From Fig. 5, the observations made for the substrate consumption are similar to that made for ethanol production. The first parameter ($\alpha$), which is related to the maintenance coefficient, is the major contributor to the rate of ethanol production after the initial growth period. The results from this study indicate that the initial cell concentration needs to be more than some threshold in order to get substantial product formation rate. The second parameter ($\beta$), decreased as the initial cell concentrations increased (*see* Fig. 5). The parameter $\beta$, is a growth associated parameter and has a significant effect on the initial ethanol production rate.

## Conclusions

This work shows that the initial cell concentration of *P. stipitis* affects the fermentation rate, ethanol concentrations, and yield. At low initial cell concentrations, cell growth was higher compared with fermentations with high initial cell concentrations. The rate of xylose consumption and ethanol production was high when the initial cell concentrations were high. Ethanol yield was high when the initial cell concentration was high because the cells used the substrate for ethanol production rather than for cell growth. However, the ethanol selectivity was low at higher initial cell concentrations.

The cell growth curve is a function of the initial cell concentration used in the fermentation. The form of the empirical mathematical model used in this work describes the population dynamics with just two parameters, which correlate very well with the initial cell concentration used. This cell concentration model was used with the Leudeking-Piret kinetics to predict substrate consumption and product formation during the fermentation. From the results, the substrate consumption and ethanol production rate are both functions of the initial cell concentration used. In the use of *P. stipitis* for biomass fermentation, an adequate amount of cells is necessary for complete substrate utilization and adequate ethanol yield.

## Acknowledgment

This investigation was supported by the Abengoa-DOE project. We like to thank David Milam for helping with the high-performance liquid chromatography analysis.

## References


1. Saha, B. C. (2003), *J. Ind. Microbiol. Biotechnol.* **30,** 279–291.
2. Toivola, A., Yarrow, D., van den Bosch, E., van Dijken, J. P., and Scheffers, W. A. (1984), *Appl. Environ. Microbiol.* 1221–1223.
3. Du Preez, J. C., Bosch, M., and Prior, B. A. (1986), *Appl. Microbiol. Biotechnol.* **23(3–4),** 228–233.
4. Chandakant, P. and Bisaria, V. S. (1998), *Crit. Rev. Biotechnol.* **18(4),** 295–331.
5. Moniruzzaman, M. (1995), *World J. Microbiol. Biotechnol.* **11,** 646–648.
6. Grootjen, D. R. J., van der Lans, R. G. J. M., and Luyben, K. Ch. A. M. (1990), *Enzyme Microb. Technol.* **12,** 20–23.
7. Grootjen, D. R. J., van der Lans, R. G. J. M., and Luyben, K. Ch. A. M. (1991), *Enzyme Microb. Technol.* **13,** 648–654.
8. Passoth, V., Zimmermann, M., and Klinner, U. (2003), *Appl. Biochem. Biotechnol.* **57/58,** 201_212.
9. du Preez, J. C. (1994), *Enzyme Microb. Technol.* **16,** 944–956.
10. Gorgens, J. F., Passoth, V., van Zyl, W. H., Knoetze, J. H., and Hahn-Hagerdal, B. (2005), *FEMS Yeast Res.* **5,** 677–683.
11. Slininger, P. J., Branstrator, L. E., Bothast, R. J., Okos, M. R., and Ladisch, M. R. (1991), *Biotechnol. Bioeng.* **37,** 973–980.
12. Meyrial, V., Delgenes, J. P., Romieu, C., Moletta, R., and Gounot, A. M. (1995), *Enzyme Microb. Technol.* **17,** 535–540.
13. Delgenes, J. P., Moletta, R., and Navarro, J. M. (1988), *J. Ferment. Technol.* **66(4),** 417–422.
14. Sreenath, H. K. and Jeffries, T. W. (2000), *Bioresour. Technol.* **72,** 253–260.
15. Ryding, P. -O., Niklasson, C., and Liden, G. (1993), *Can. J. Chem. Eng.* **71,** 911–915.
16. Sanchez, S., Bravo, V., Castro, E., Moya, A. J., and Camacho, F. (2002), *J. Chem. Technol. Biotechnol.* **77,** 641–648.
17. Dominguez, H., Nunez, M. J., Chamy, R., and Lema, J. M. (1993), *Biotechnol. Bioeng.* **41,** 1129–1132.
18. Kompala, D. S., Ramkrishna, D., and Tsao, G. T. (1984), *Biotechnol. Bioeng.* **26,** 1272–1281.
19. Dhurjati, P., Ramkrishna, D., Flickinger, M. C., and Tsao, G. T. (1985), *Biotechnol. Bioeng.* **27,** 1–9.
20. Agbogbo, F. K., Coward-Kelly, G., Torry-Smith, M., and Wenger, K. S. (2006), *Process Biochem.* (Accepted).
21. du Preez, J. C., Bosch, M., and Prior, B. A. (1986), *Enzyme Microb. Technol.* **8,** 360–364.
22. Leudeking, R. and Piret, E. L. (1959), *J. Microbiol. Technol. Eng.* **1(4),** 393–412.

0273-2289/1559-0291 (Online)/07/136–140/663–674/$30.00

# Construction and Evaluation of a *Clostridium thermocellum* ATCC 27405 Whole-Genome Oligonucleotide Microarray

STEVEN D. BROWN,[1] BABU RAMAN,[2] CATHERINE K. MCKEOWN,[2] SHUBHA P. KALE,[3] ZHILI HE,[1,4] AND JONATHAN R. MIELENZ*,[2]

*[1]Microbial Ecology and Physiology Group; [2]Bioconversion Science and Technology Group, Biosciences Division, Oak Ridge National Laboratory, Oak Ridge, TN, E-mail: mielenzjr@ornl.gov; [3]Department of Biology, Xavier University of Louisiana, New Orleans, LA; and [4]Current address: Institute of Environmental Genomics, Department of Botany and Microbiology, University of Oklahoma, Norman, OK*

## Abstract

*Clostridium thermocellum* is an anaerobic, thermophilic bacterium that can directly convert cellulosic substrates into ethanol. Microarray technology is a powerful tool to gain insights into cellular processes by examining gene expression under various physiological states. Oligonucleotide microarray probes were designed for 96.7% of the 3163 *C. thermocellum* ATCC 27405 candidate protein-encoding genes and then a partial-genome microarray containing 70 *C. thermocellum* specific probes was constructed and evaluated. We detected a signal-to-noise ratio of three with as little as 1.0 ng of genomic DNA and only low signals from negative control probes (nonclostridial DNA), indicating the probes were sensitive and specific. In order to further test the specificity of the array we amplified and hybridized 10 *C. thermocellum* polymerase chain reaction products that represented different genes and found gene specific hybridization in each case. We also constructed a whole-genome microarray and prepared total cellular RNA from the same point in early-logarithmic growth phase from two technical replicates during cellobiose fermentation. The reliability of the microarray data was assessed by cohybridization of labeled complementary DNA from the cellobiose fermentation samples and the pattern of hybridization revealed a linear correlation. These results taken together suggest that our oligonucleotide probe set can be used for sensitive and specific *C. thermocellum* transcriptomic studies in the future.

**Index Entries:** Biomass; cellulose; ethanol; fermentation; transcriptomics.

*Author to whom all correspondence and reprint requests should be addressed.

## Introduction

In 2004, 3.4 billion gal of ethanol was blended into gasoline, which was approx 2% of gasoline sold in the United States by volume or 1.3% ($2.5 \times 10^{17}$ J) of its energy content *(1)*. Transportation ethanol is derived primarily from corn; however, there is need to develop an emerging industry to produce ethanol from lignocellulosic biomass to meet expected future demand *(2)*. Because of the complexities of biomass, extraction and hydrolysis of the cellulose requires thermochemical pretreatment of the biomass followed by the addition of enzymes needed to hydrolyze these polymers to simple sugars that can be fermented to ethanol by an added fermentative microorganism *(3)*. However, a game-changing technology is being developed for a process to simultaneously convert the cellulosic component of biomass to end products with a *single processing step* that consolidates cellulase enzyme production, cellulose hydrolysis, and fermentation *(4)*. Particularly important is that no added cellulase enzymes are needed, thus avoiding the added cellulose production costs, recently been reported in the range of 10–20 ¢/gal of ethanol produced *(5)*. Central to this consolidated bioprocessing approach is a thermophilic (high-temperature) bacterium called *Clostridium thermocellum*, which has the critical ability to produce its own cellulases that permit it to very rapidly hydrolyze cellulose, using a structure called the cellulosome, for growth and energy. In fact, *C. thermocellum* exhibits the highest rate of cellulose hydrolysis known and as a result the protein chemistry of this process has been extensively studied for 20 yr *(6)*.

There has been significant for cellulosome structural biology, and cellulose fermentation *(6)*, however, little is known regarding key enzyme expression levels that might be either bottlenecks or key catalytic steps that will serve as targets for further metabolic engineering of this organism to maximize ethanol yields from biomass. Therefore, this article outlines initial progress aimed at investigating the intrinsic biology of this unique organism, especially toward gene expression during cellobiose and cellulose fermentation.

The application of microarray technology to study gene expression at the level of whole transcriptome has been widely used for many years *(7,8)* and more recently transcriptomic studies have been conducted in ethanologenic bacteria and yeast *(9–14)*. The availability of the 3.8 Mb *C. thermocellum* genome sequence (http://genome.ornl.gov/microbial/cthe) predicted to encode 3163 candidate protein-encoding genes permitted the development of a whole-genome microarray, thus allowing the application of microarray technology to investigate patterns of gene expression during fermentation of cellulose to ethanol in *C. thermocellum*. As a first step, in this study, we present the design, fabrication, and assessment of a whole-genome microarray for *C. thermocellum* ATCC 27405.

## Materials and Methods

### *Bacterial Strains, Culture Conditions, and Chemicals*

*C. thermocellum* strain ATCC 27405 was a kind gift from Prof. Herb Strobel, University of Kentucky, Lexington, KY. A 1 : 25 dilution of a fresh overnight culture (16 h, optical density [$OD_{600}$] approx 0.9) of *C. thermocellum* was used to inoculate 2 L of MTC medium containing 5.0 g/L cellobiose and 1.0 g/L yeast extract in a Braun BioStat B fermentor (Sartorius BBI Systems Inc., Bethlehem, PA), essentially as described previously *(15)*, except that *C. thermocellum* was cultured at 58°C and pH 7.0 (controlled through addition of 3 *N* NaOH) with an agitation of 250 rpm. Reagent grade chemicals were obtained from Sigma (St. Louis, MO) unless indicated otherwise. Cell free culture supernatants were analyzed by high-performance liquid chromatography (Waters Corp, Milford, MA) to measure cellobiose, acetate, lactate, and ethanol concentrations.

### *Whole-Genome DNA Microarray Construction and Design of Polymerase Chain Reaction Primers*

DNA sequences for the 3163 *C. thermocellum* ATCC 27405 predicted protein-encoding genes were obtained from The Joint Genome Institute (http://genome.ornl.gov/microbial/cthe/17nov03_obsolete/) using sequence assembled in November 2003. Oligonucleotide probes that represented the whole genome of *C. thermocellum* were designed using the CommOligo software *(16,17)* and were commercially synthesized without modification (MWG Biotech, High Point, NC) in 96-well plates. The concentration of the probes was adjusted to 100 pmol/μL, transferred to 384-well printing plates in a final concentration of 50% dimethyl sulfoxide using a BioMek FX liquid handling robot (Beckman-Coulter, Fullerton, CA) and then spotted onto UltraGAPS glass slides (Corning Life Sciences, Corning, NY) using a BioRobotics Microgrid II microarrayer (Genomic Solutions, Ann Arbor, MI) in a dust-free clean room maintained at 21°C and 50% relative humidity. Spotted DNA was stabilized on slides by ultraviolet crosslinking using an Ultraviolet 1800 Stratalinker (Stratagene, La Jolla, CA) according to slide manufacturer's instructions (Corning Life Sciences). A partial genome microarray that contained 16 replicates for 72 *C. thermocellum* and control probes was constructed initially, and subsequently, whole-genome microarrays were fabricated, which contained two replicates per probe on each slide. The Primer3 software (http://frodo.wi.mit.edu/cgi-bin/primer3/ primer3_www.cgi) was used to design primers to amplify gene specific polymerase chain reaction (PCR) products for hybridizations.

### *Nucleic Acid Isolation and Preparation of Labeled complementary DNA Targets*

Early-exponential phase ($OD_{600}$, 0.25) batch cultures were used for RNA isolation. Total cellular RNA was isolated using a lysozyme

coupled with TRIzol reagent (Invitrogen, Carlsbad, CA) treatment as described previously *(18)*. Precipitated RNA was further treated with RNase-free DNase I (Qiagen, Valencia, CA) to digest any residual chromosomal DNA, and subsequently purified with RNeasy Mini kit according to the manufacturer's instructions (Qiagen). *C. thermocellum* genomic DNA was isolated using the DNeasy Tissue kit (Qiagen). The concentration and purity of the extracted nucleic acids was determined at $OD_{260}$ and $OD_{280}$ with a NanoDrop ND-1000 spectrophotometer (NanoDrop Technologies, Wilmington, DE). Purified RNA was used as the template to generate complementary DNA (cDNA) copies labeled with either Cy3-dUTP or Cy5-dUTP (Amersham Biosciences, Piscataway, NJ) and in a duplicate set of reactions the fluorescent Cy dyes were reversed for the different technical replicates to analyze dye-specific variations in hybridization signal intensity. Genomic DNA and PCR products were labeled with Cy-3dUTP and Cy-5dUTP, respectively, using a Bioprime Labeling kit (Invitrogen) with random-primers and then purified using a Qiaquick PCR kit (Qiagen) *(19)*. The labeled and purified cDNA were then dried using the SDP1010 SpeedVac System (ThermoSavant, Holbrook, NY). The sequences for the oligonucleotides used to amplify the probe-specific PCR products are shown in Table 1.

### *Microarray Hybridization, Scanning, Image Quantification, and Data Analysis*

Preliminary microarray quality assessments were made by staining the microarrays with a 1 : 1000 dilution of Syto61 dye (Invitrogen) pure containing 10.0 μg/mL of bovine serum albumin (New England Biolabs, Ipswich, MA) for 20 min at room temperature, followed by two 0.1X SSC (Ambion, Austin, TX) washes. Hybridization and washing conditions for oligonucleotide microarrays have been described elsewhere *(20)*. Microarray images were scanned using a ScanArray Express (PerkinElmer) scanner, and spot signal, quality, and background fluorescent intensities were quantified using ImaGene version 6.0 (Biodiscovery, Marina Del Rey, CA). Signal-to-noise ratio were calculated as described previously *(21)* in Microsoft Excel, and GeneSpring 7.0 (Agilent Technologies, Palo Alto, CA) was used to transform microarray data with the locally weighted scatterplot smoothing method of normalization and to remove poor/empty spots.

## Results and Discussion

### C. thermocellum *Cellobiose Fermentations*

Initially, we investigated the growth of *C. thermocellum* during fermentation of cellobiose. Cells were grown in amended MTC medium and growth was monitored for approx 12 h. Two independent experiments

Table 1
Oligonucleotides Used to Amplify Gene-Specific PCR Products

| Number[a] | Gene | Forward primer (5′–3′) | Reverse primer (5′–3′) | Gene product |
|---|---|---|---|---|
| 1 | *Ct3187* | GCATAGGAACATCCCTGTGTG | CATTGTCCACAGGAAGCAAG | Phosphoglycerate kinase |
| 2 | *Ct0462* | GCTGTCAATTCCACTGCAAA | CGCAATCGGCATATACAAAG | Phosphotransacetylase |
| 3 | *Ct0463* | TCACAAGCTTGCCATACAGG | CGGAGCCAGTTCAACACAAT | Acetate kinase |
| 4 | *Ct3150* | GGACTTTTTCTGTGGCAAGG | ACATTCCCCGTTTGTACAGG | Iron-containing alcohol dehydrogenase |
| 5 | *Ct3185* | TGTACAACAAACTGCCTTGCTC | TGAGTTGCAGTTGTAGCGTGT | Glyceraldehyde-3-phosphate dehydrogenase |
| 6 | *Ct3012* | CGGGAGGAGAAGGTACCAG | TTCAGAAGTTCAATAATATGCTCCA | Nucleotidyl transferase |
| 7 | *Ct1135* | GTGGAGCTGCACACATATCG | GCACCCGCAGTTTTAACATC | L-lactate dehydrogenase |
| 8 | *Ct2924* | ATTATTGGCGAACACGGTGA | AATCTGCTCCTCGCACTGAT | L-lactate dehydrogenase |
| 9 | *Ct3589* | TCGTTCTGCCTGAGAAACCT | CCCCTTCGGCAACTATAACA | 6-Phosphofructokinase |
| 10 | *Ct3735* | ACAGGGAAGAATTTkCGAGA | TGGAATGAGTGGGAAAGCAT | Glucose-6-phosphate isomerase |

[a]Corresponds to labeled PCR targets in Fig. 3 and primer pairs that will be used for Q-PCR for genes involved in cellulose fermentation identified in Fig. 6.

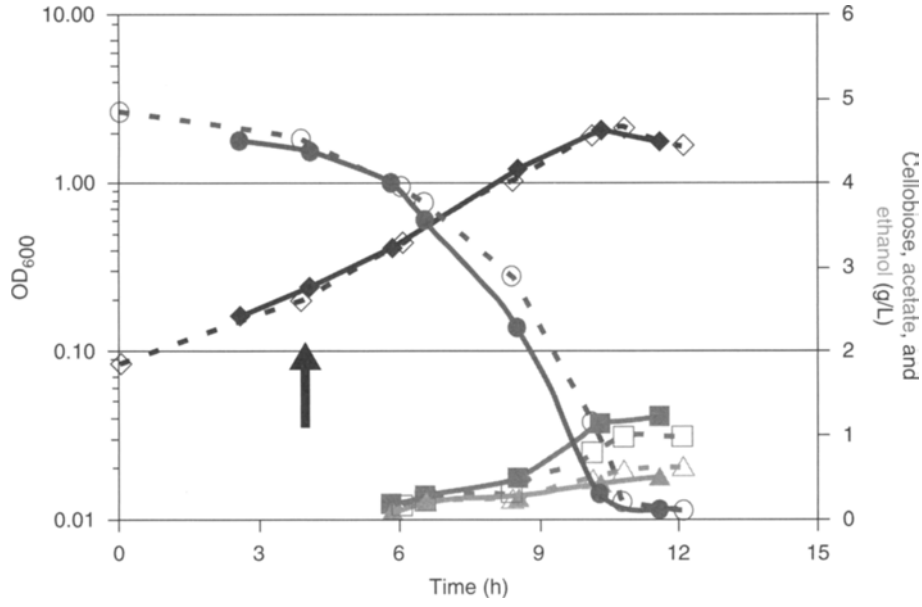


**Fig. 1.** *C. thermocellum* cellobiose fermentations. OD at 600 nm ($OD_{600}$) (blue lines), cellobiose (red lines), acetate (pink lines), and ethanol (green lines) concentration (g/L) is plotted against fermentation time (h). Open and closed symbols correspond to data from two independent fermentations. Arrow indicates sample harvest time for total RNA isolation.

based on culture turbidity measurements and high-performance liquid chromatography analysis of substrate (cellobiose) consumption and byproduct (acetate and ethanol) formation, indicated that batch cultures of *C. thermocellum* had typical bacterial growth cycle kinetics (Fig. 1). Total cellular RNA was extracted from two technical replicates at the same point in early-logarithmic growth phase during single cellobiose fermentation (Fig. 1).

## C. thermocellum *Microarray Probe Design*

Unique 70-mer oligonucleotide probes were designed for 94.2% of the 3163 *C. thermocellum* candidate protein-encoding genes by the CommOligo software *(16)*. A further 10 probes were designed for groups of highly similar genes, so that 96.7% of the putative coding sequences were represented and only 104 coding sequences remained unrepresented on the whole-genome microarray. The *C. thermocellum* genome sequence contains a large number of putative genes whose products are predicted to encode proteins with transposon-related functions *(22)*. Wherein sequences were highly similar, such as for genes encoding proteins with transposon-related functions, individual gene probes could not be designed. Group probes 1–10 represented putative hypothetical, transposase, transposase (IS116/IS110/IS902), phage/plasmid primase P4, hypothetical, transposase (mutator type),

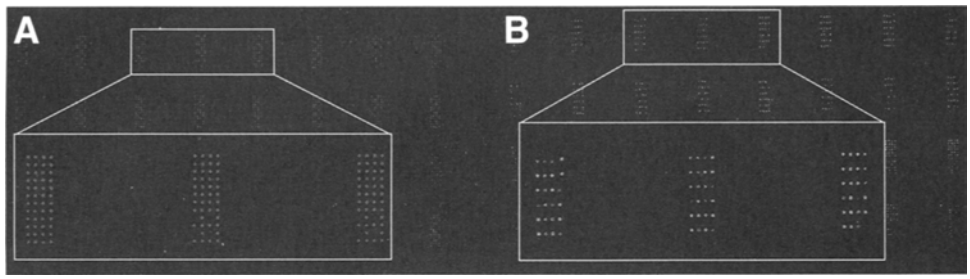


**Fig. 2.** Specificity of *C. thermocellum* microarray probes. *C. thermocellum* partial-genome microarray stained with nonspecific Syto61 dye for DNA **(A)** and hybridized with gDNA labeled with Cy3 dye (green), which hybridizes to all *C. thermocellum* probes and *Ct3187* PCR product labeled with Cy5 dye (red) that hybridizes to replicates of *Ct3187* probe **(B)**.

transposase (IS3/IS911), transposase (mutator type, transposase (IS30 family), and transposase proteins, respectively. The percentage of *C. thermocellum* probes designed for the whole genome is similar to several recently constructed whole-genome microarrays for *Desulfovibrio vulgaris* (Hildenborough) and *Shewanella oneidensis* MR-1, which had 98.6 and 94.3% probe coverage of the genomes, respectively *(20,23)*. The group probe design feature of CommOligo enabled probes to be designed for highly homologous sequences, thus extending the fraction of gene expression comparisons that will be able to be made in the future.

## *Microarray Probe Specificity and Sensitivity*

Initially, a subset of the whole-genome microarray probes was tested for sensitivity and specificity by producing partial-genome microarrays that contained 70 *C. thermocellum* probes representing the range of functional diversity in the predicted gene products. The DNA stain Syto61 was used to assess the quality of the partial-genome microarrays and to confirm signal was observed from negative control probes (Fig. 2A). PCR products designed to hybridize to individual probes that represented specific genes were labeled with Cy-5 and hybridized to the partial array to confirm signal specificity of the designed oligonucleotide probes (Fig. 2B). In each case the 10-labeled PCR products gave signal-to-noise ratios of more than three, or positive for probe-target hybridization interaction *(24)*, whereas only low values and SNRs below three were observed from negative control probes (Fig. 3).

The hybridization of different amounts of *C. thermocellum* genomic DNA labeled with Cy-dye to *C. thermocellum* partial microarrays showed that as little as 1.0 ng of genomic DNA could be labeled and give signal-to-noise ratios more than three (Fig. 4). A signal-to-noise ratio more than three is a general criterion considered as the minimum probe signal necessary that can be quantified accurately *(24)*. Our results were in keeping with other studies *(25,26)* and were indicative of the *C. thermocellum* microarray probes

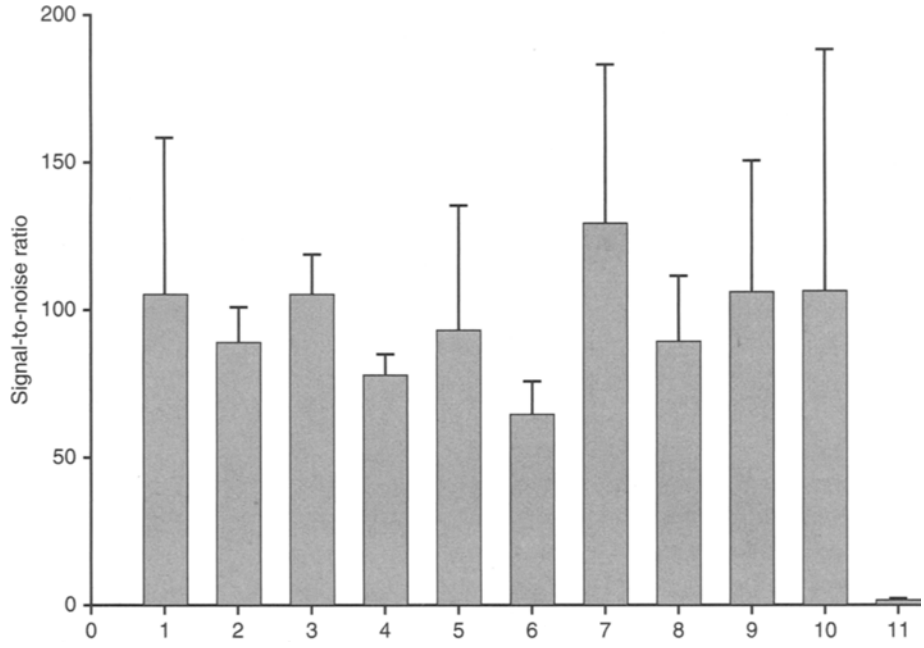


**Fig. 3.** Hybridization of PCR products for specific *C. thermocellum* genes to partial-genome microarray. Signal-to-noise ratios for gene-specific probes: 1, *Ct3187*; 2, *Ct0462*; 3, *Ct0463*; 4, *Ct3150*; 5, *Ct3185*; 6, *Ct3012*; 7, *Ct1135*; 8, *Ct2924*; 9, *Ct3589*; 10, *Ct3735*; and 11, remaining *C. thermocellum* probes. Primer sequences used to amplify PCR products and probe descriptions are given in Table 1.

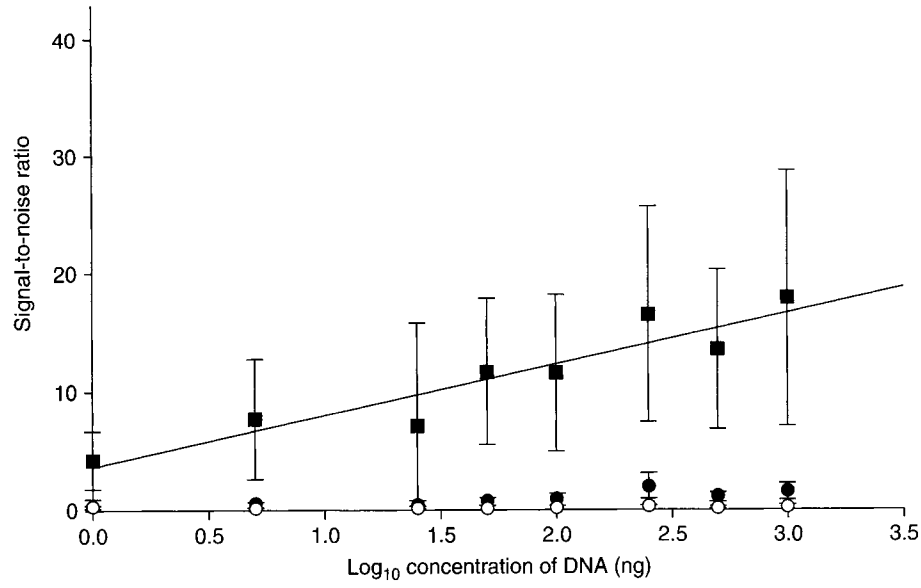


**Fig. 4.** Hybridization of *C. thermocellum* genomic DNA to *C. thermocellum* partial microarray. Average of all *C. thermocellum* probes, ■ and ▬ regression plot; negative control 1, ●; negative control 2, ○.

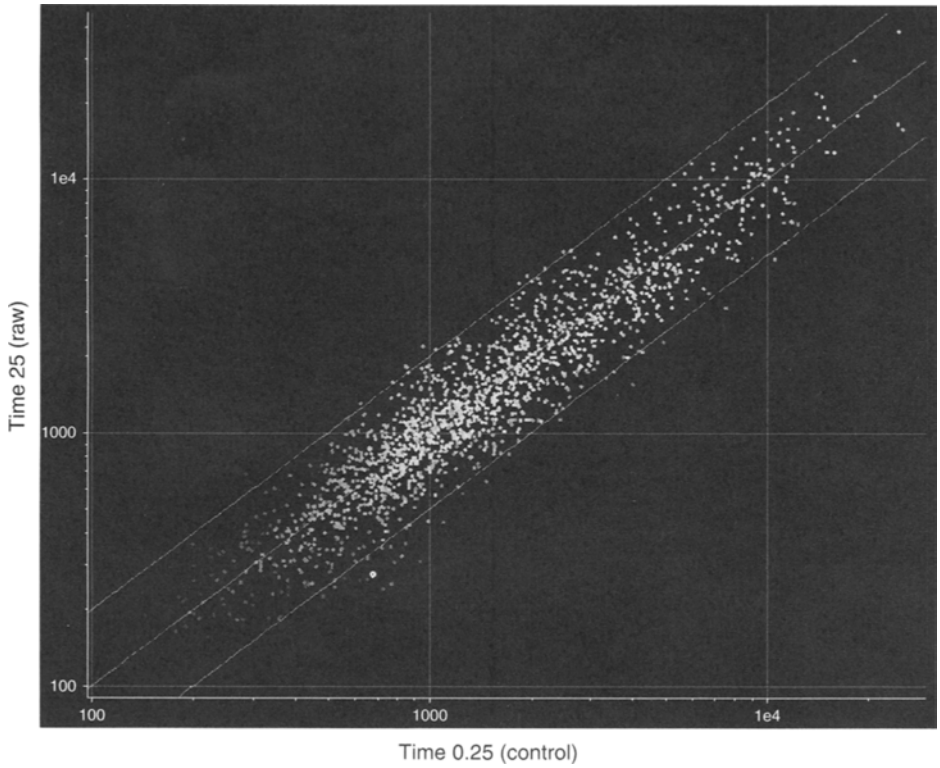


**Fig. 5.** Scatterplot of whole-genome microarray data. The upper and lower green lines represent twofold levels of differential expression and the middle green line represents no change in expression.

being sensitive as well as specific. In order to further assess the reliability of the microarray data we constructed a whole-genome microarray and cohybridized cDNA prepared from total cellular RNA extracted from two technical replicates from the same *C. thermocellum* cellobiose fermentation in early-logarithmic growth phase. The pattern of hybridization revealed a linear relationship between the samples and 97.4% of the genes fell within a twofold threshold after data normalization and poor/empty spot removal by GeneSpring (Fig. 5). This value may be further improved on in future studies, as one potential source of variation was average incorporation of the Cy-dye, which was less than 1 pmol/μL of purified target DNA. In this experiment only three of the 1708 genes were slightly outside the bounds of a threefold change in expression value between samples. Overall, the results described above suggest our oligonucleotide probe set can be used for sensitive and specific *C. thermocellum* transcriptomic studies in the future.

## Conclusion

To our knowledge this is the first whole-genome microarray for a thermophile capable of converting cellulose to ethanol in a consolidated

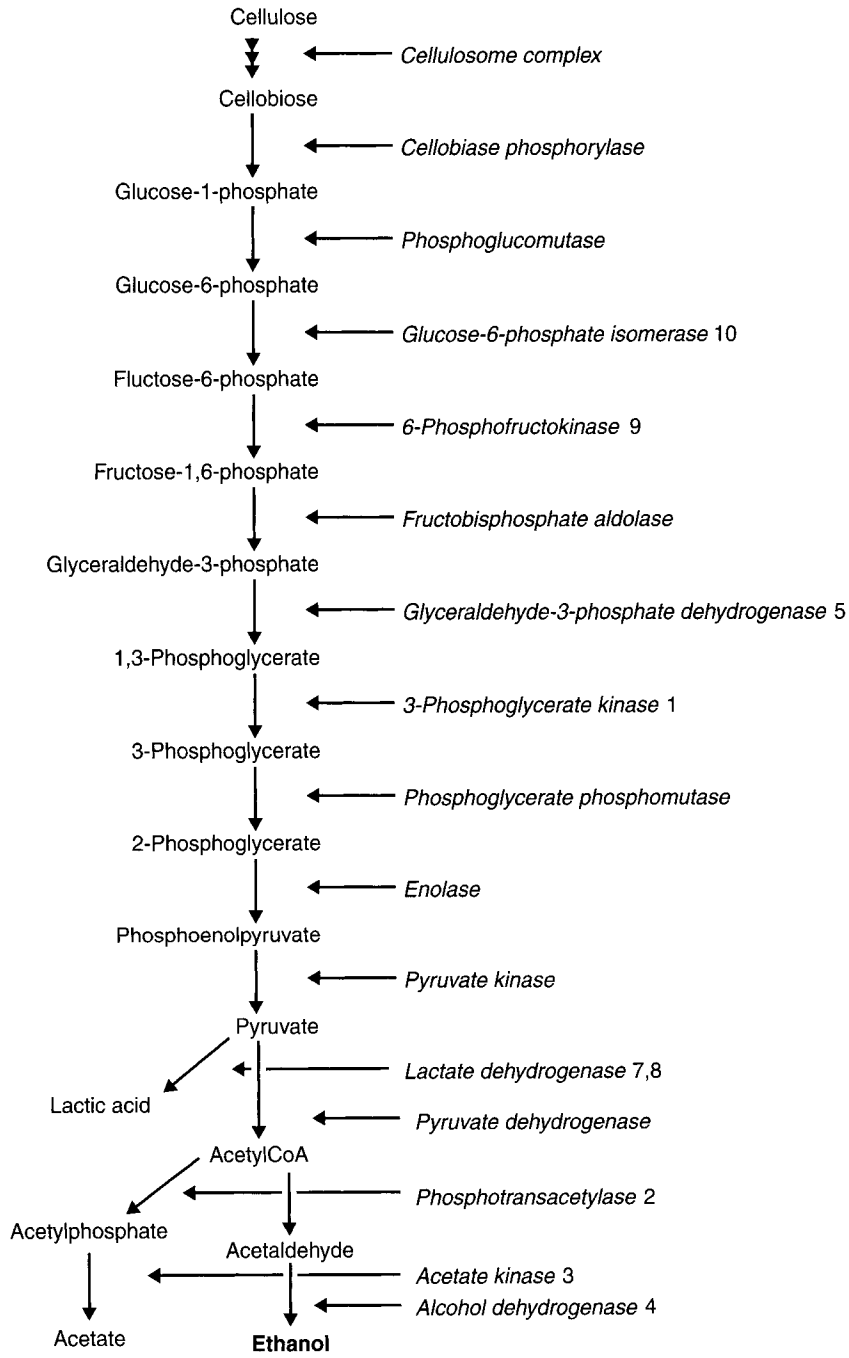


**Fig. 6.** Metabolic pathway for conversion of cellulose to ethanol, lactic acid, and acetic acid. The numbered genes correspond to PCR products in Table 1 and their location in this metabolic pathway.

process. The PCR products shown in Table 1 were chosen not only to verify the quality of the *C. thermocellum* microarray, but also for future quantitative-PCR primer analysis of key genes in the pathway from cellulose to the final metabolic end products of ethanol, lactic acid, and acetic acid (Fig. 6).

Future transcriptomics using the whole-genome microarray will provide insight into the expression genes whose products are thought to be important for cellulose fermentation and also potentially provide insight into the roles of other genes whose importance cannot be inferred by *a priori* assumptions. Interestingly, such experiments will answer questions whether both genomic copies of lactate dehydrogenase are expressed (Table 1, genes 7 and 8) or if transcription occurs from only one locus during fermentation of either cellobiose and/or cellulose. Information on these and other genes contributing to or detracting from the pathway for ethanol production will be invaluable as the complexities of *C. thermocellum* metabolic circuits are unraveled. In conclusion, the application of transcriptomic profiling, along with other molecular biology tools and physiological studies offer the opportunity to better understand fundamental biology of ethanologenic bacteria and the potential for improved production of ethanol.

## Acknowledgments

Research sponsored by the Laboratory Directed Research and Development Program of Oak Ridge National Laboratory (ORNL), managed by UT-Battelle, LLC for the US Department of Energy under Contract No. DE-AC05-00OR22725. S.P.K was supported by the DOE Faculty Sabbatical Program sponsored by the DOE Office of Science. We thank Liyou Wu for assistance with microarray printing.

## Note Added in Proof

As this paper was going to press, the *C. thermocellum* ATCC 27405 genome was closed and finished. The finished genome sequence can be found at http://genome.jgi.psf.org/finished_microbes/cloth/cloth.home.html.

## References

1. Davis, S. C. and Diegel, S. W. (2004), In: *Transportation Energy Data Book: Technical Report No. ORNL-6973*. Oak Ridge National Laboratory, Oak Ridge, TN.
2. http://www.ethanolrfa.org/industry/locations/. Accessed March 19, 2007.
3. Mielenz, J. R. (2001), *Curr. Opin. Microbiol.* **4,** 324–329.
4. Lynd, L. R., van Zyl, W. H., McBride, J. E., and Laser, M. (2005), *Curr. Opin. Biotechnol.* **16,** 577–583.
5. Greer, D. (2005), *Biocycle* **46,** 61–65.
6. Lynd, L. R., Weimer, P. J., van Zyl, W. H., and Pretorius, I. S. (2002), *Microbiol. Mol. Biol. Rev.* **66,** 506–577.
7. DeRisi, J., Penland, L., Brown, P. O., et al. (1996), *Nat. Genet.* **14,** 457–460.
8. Schena, M., Shalon, D., Heller, R., Chai, A., Brown, P. O., and Davis, R. W. (1996), *Proc. Natl. Acad. Sci. USA* **93,** 10,614–10,619.
9. Sonderegger, M., Jeppsson, M., Hahn-Hagerdal, B., and Sauer, U. (2004), *Appl. Environ. Microbiol.* **70,** 2307–2317.
10. Tomas, C. A., Welker, N. E., and Papoutsakis, E. T. (2003), *Appl. Environ. Microbiol.* **69,** 4951–4965.
11. Sedlak, M., Edenberg, H. J., and Ho, N. W. Y. (2003), *Enzyme Microbial Technol.* **33,** 19–28.

12. Jewett, M. C., Oliveira, A. P., Patil, K. R., and Nielsen, J. (2005), *Biotech. Bioprocess Eng.* **10,** 385–399.
13. Wahlbom, C. F., Otero, R. R. C., van Zyl, W. H., Hahn-Hägerdal, B., and Jonsson, L. J. (2003), *Appl. Environ. Microbiol.* **69,** 740–746.
14. Salusjärvi, L., Pitkänen, J. -P., Aristidou, A., Ruohonen, L., and Penttilä, M. (2006), *Appl. Biochem. Biotechnol.* **128,** 237–274.
15. Zhang, Y. -H. P. and Lynd, L. R. (2005), *J. Bacteriol.* **187,** 99–106.
16. Li, X., He, Z., and Zhou, J. (2005), *Nucleic Acids Res.* **33,** 6114–6123.
17. Bozdech, Z., Zhu, J., Joachimiak, M. P., Cohen, F. E., Pulliam, B., and DeRisi, J. L. (2003), *Genome Biol.* **4,** R9.
18. Tomas, C. A., Alsaker, K. V., Bonarius, H. P. J., et al. (2003), *J. Bacteriol.* **185,** 4539–4547.
19. Pollack, J. R., Perou, C. M., Alizadeh, A. A., et al. (1999), *Nat. Genet.* **23,** 41–46.
20. Chhabra, S. R., He, Q., Huang, K. H., et al. (2006), *J. Bacteriol.* **188,** 1817–1828.
21. Tiquia, S. M., Chong, S. C., Fields, M. W., and Zhou, J. (2004), In: *Molecular Microbial Ecology Manual,* Kowalchuk, G. A., de Bruijn, F. J., Head, I. M., Lakkennans, A. D., and van Elsas, J. D. (eds.), Kluwer Academic Publishers, Dordrecht, The Netherlands, pp. 1743–1763.
22. http://genome.ornl.gov/microbial/cthe/.
23. Gao, H. C., Wang, Y., Liu, X. D., et al. (2004), *J. Bacteriol.* **186,** 7796–7803.
24. Verdnik, D., Handran, S., and Pickett, S. (2002), In: *DNA image analysis: Nuts & bolts,* Kamberova, G. (ed.), DNA Press, Salem, MA, pp. 89–98.
25. Tiquia, S. M., Wu, L., C. Chong, S. C., et al. (2004), *BioTechniques* **36,** 664–675.
26. He, Z. L., Wu, L. Y., Li, X. Y., Fields, M. W., and Zhou, J. Z. (2005), *Appl. Environ. Microbiol.* **71,** 3753–3760.

0273-2289/1559-0291 (Online)/07/136–140/675–688/$30.00

# Tannase Production by Solid State Fermentation of Cashew Apple Bagasse

**Tigressa H. S. Rodrigues,[1] Maria Alcilene A. Dantas,[1] Gustavo A. S. Pinto,[2] and Luciana R. B. Gonçalves*,[1]**

*[1]Universidade Federal do Ceará, Departamento de Engenharia Química, Campus do Pici, Bloco 709, 60455-760, Fortaleza, CE—Brazil, E-mail: lrg@ufc.br; and [2]Embrapa Agroindústria Tropical, Rua Dra Sara Mesquita, 2270, Planalto do Pici, CEP 60511-110, Fortaleza—CE, Brazil*

## Abstract

The ability of *Aspergillus oryzae* for the production of tannase by solid state fermentation was investigated using cashew apple bagasse (CAB) as substrate. The effect of initial water content was studied and maximum enzyme production was obtained when 60 mL of water was added to 100.0 g of CAB. The fungal strain was able to grow on CAB without any supplementation but a low enzyme activity was obtained, 0.576 U/g of dry substrate ($g_{ds}$). Optimization of process parameters such as supplementation with tannic acid, phosphorous, and different organic and inorganic nitrogen sources was studied. The addition of tannic acid affected the enzyme production and maximum tannase activity (2.40 $U/g_{ds}$) was obtained with 2.5% (w/w) supplementation. Supplementation with ammonium nitrate, peptone, and yeast extract exerted no influence on tannase production. Ammonium sulphate improved the enzyme production in 3.75-fold compared with control. Based on the experimental results, CAB is a promising substrate for solid state fermentation, enabling *A. oryzae* growth and the production of tannase, with a maximum activity of 3.42 $U/g_{ds}$ and enzyme productivity of $128.5 \times 10^{-3}$ $U \cdot g_{ds}^{-1} \cdot h^{-1}$.

**Index Entries:** Cashew apple bagasse; solid state fermentation; tannase; *Aspergillus oryzae*; tannic acid; ammonium sulfate.

## Introduction

In the north coast of Brazil, especially in the state of Ceará, the cashew agroindustry has an outstanding role in the local economy. The cashew apple, a pseudofruit or peduncle, is the part of the tree that connects it to the cashew nut, the real fruit and a well-known product around the world. The cashew apple is a hard, pear-shaped, small, and nonclimacteric fruit, and is found in three colors: yellow, orange, and red. The most commonly commercialized ones are the yellow and red fruits. The edible portion,

*Author to whom all correspondence and reprint requests should be addressed.

Table 1
Physico-chemical Characterization of Natural Bagasses of Cashew (*Anacardium ocidentale* L)

| Parameters | Natural cashew bagasse (CAB) |
|---|---|
| pH | 4.01 |
| Acidity (gram of citric acid/100.0 g of sample) | 1.34 |
| Soluble solids (Brix) | 12.0 |
| Reducing sugars (mg/100.0 g) | 6.84 |
| Total sugars (mg/100.0 g) | 7.68 |
| Proteins (%) | 1.83 |
| Lipids (%) | 0.38 |
| Fibers (%) | 33.10 |
| Moisture (%) | 78.76 |

From ref. 7.

representing 90% of the fruit, is rich in vitamin C, flavor, and aroma. Internal and external market consumption of cashew nut, in the year of 2004, was about 232,000 t. However, only 12% of the total peduncle is consumed *"in natura"* or processed industrially to produce a wide range of products from concentrated juice to desserts. The industrially processed products are basically consumed by the local market and they do not play an important role in the state or Brazil economy. Furthermore, the majority of the cashew apple spoils in the soil *(1–4)*. When peduncle is industrially processed for the production of juice, 40% (w/w) of bagasse is produced, which is not used for human consumption and is usually discarded by the local industry. These facts, together with its composition (*see* Table 1), turns cashew apple bagasse (CAB) into an interesting and inexpensive (<$0.50/Kg) substrate for several potential applications *(5–7)*, including the production of microbial enzymes by solid state fermentation (SSF).

SSF has been defined as a bioprocess in which microorganisms are grown on solid substances in the absence or near absence of free water *(8)*. Two types of substrates are used in SSF—one in which the solid substrate itself is used by the microorganisms as the carbon and energy source and other in which the substrate acts only as support. SSF mainly deals with the utilization of agroindustrial residues as substrates. Application of such residues as substrates is certainly economical and it also reduces environmental pollution *(9)*. In this work, CAB, a coproduct of cashew apple juice, is investigated for the production of tannase through SSF.

Tannase (tannin-acyl-hydrolase, Enzyme Commission [EC], 3.1.1.20) catalyzes the breakdown of hydrolysable tannis and gallic acid esters *(10)*. Hydrolysable tannins are present in most of the residues obtained from higher plants, which is the case of CAB, and are polyphenolic compounds formed by the association of sugars with ellagic acids through esters linkages *(11)*. Tannase

Table 2
Physico-chemical Characterization of the CAB

| Parameters | Natural cashew bagasse (CAB) |
|---|---|
| Proteins (% [w/w]) | 16.7 |
| Lipids (% [w/w]) | 5.22 |
| Glucose (% [w/w]) | 0.25 |
| *Micronutrients (ppm)* | |
| Zn | 14.92 |
| Fe | 49.72 |
| Mn | 14.82 |
| Cu | 18.31 |
| Mg | 8.13 |

CAB (*A. ocidentale*, L.) used in this work.

can be obtained from plant sources; the enzyme is present in tannin rich vegetables, mainly in their fruits, leaves, branches, and barks of trees *(10,12,13)* as well as in bovine intestine and other ruminant mucous *(10)*. However, the most important source of industrial tannase is microbial production, as these enzymes are more stable than similar ones obtained from other sources *(10)*.

Tannases are widely used in the food and pharmaceutical industry, especially in tea clarification and also for the production of pharmaceutically important compounds, such as gallic acid. Gallic acid, a tannin product, is the substrate for chemical synthesis of propyl gallate and trimethoprim, which are important in food and pharmaceutical industries, respectively. Tannase is also used in the treatment of tannery effluents for the stabilization of malt polyphenols, clarification of beer and fruit juices, for the prevention of phenol-induced madeirization in wine and fruit juices, and for the reduction of antinutritional effects of tannins in animal feed *(14–16)*. Therefore, the objective of this work was to study the potential of CAB for the production of tannase, by SSF using *Aspergillus oryzae*.

## Materials and Methods

### Solid Substrate Preparation

CAB was used as a substrate and was kindly donated by the Kraft Foods unit located in Aracati, State of Ceará, Brazil. Before storage, it was washed three times with water and dried for 24 h at 50°C and characterized, because the CAB composition varies depending on the fruit type and harvest. The average composition of the CAB used in this work is described in Table 2.

### Microorganism and Inoculum Preparation

A fungal strain of *A. oryzae* from the Embrapa Agroindústria Tropical, Ceará, Brazil was used in this study. The microorganism was grown and

maintained on Nutrient Agar slants at 32°C. Spore suspensions were extracted with 10 mL of a sterile water solution containing 0.4% Tween 80. Afterwards, 1 mL of spore suspension was placed in flasks, containing 10.0 g of corn brain, 4 mL of a solution 1.7% (w/v) $NaHPO_4$ and 2.0% (w/v) $(NH_4)_2SO_4$, and incubated at 30°C for 3 d. Viable spores were scraped with 40 mL of sterile 0.4% (w/v) Tween 80 solution and determined by plate count technique.

### *Humidity Determination*

Two gram of sample was analytically weighted and dried at 90°C for 24 h in an air circulation oven.

### *Water Activity Determination*

Water activity ($a_w$) is defined as the relative humidity of the gaseous atmosphere in equilibrium with the substrate. In SSF process, water activity of the substrate quantitatively express water requirements for microbial activity. Pure water has $a_w$ equal to 1.0, which diminishes with increase in amounts of substrate *(17)*. In this work, water activity was determined using an Aqualab CX-2 (Decagon Devices, Pullman, WA) device at 30°C.

### *Preparation of SSF Medium for Inoculation*

SSF was carried out in 500-mL conical flasks containing 40.0 g of medium, CAB enriched or not with tannic acid and moistened with water. Flasks were autoclaved at 121°C for 15 min, cooled to room temperature, and inoculated with fungal spores ($10^7$ spores/g). The contents were mixed thoroughly and incubated at 30°C for 96 h. Every 24 h, samples were withdrawn by removing a single Erlenmeyer flask from the incubator.

### *Enzyme Extraction*

Tannase was extracted from the fermented substrate by adding 100 mL of acetate buffer (pH 5.0). The contents were incubated at 30°C for 60 min and the crude enzyme was separated by filtration through Whatman No. 1 paper. The filtrate, here denominated as enzymatic extract, was colleted in vials and preserved for further analysis.

### *Gallic Acid Assay*

Gallic acid concentration in the enzymatic extract was determined according to alcoholic rhodanine method that is based on the formation of a chromogen. The developed color was read at 520 nm using a Cary 50 spectrophotometer (Varian, Melbourne, Australia) *(18)*.

### *Tannase Assay*

For tannase determination, the enzymatic extract was incubated with buffered solution (acetate 20 m*M*, pH 5.0) of tannic acid 200 mg/L at 30°C

for 5 min *(19)*. The gallic acid released was quantified by alcoholic rhodanine method *(18)*. One unit of tannase activity was defined as the amount of enzyme that catalyses the production of 1 μmol of gallic acid/min under assay conditions.

### *Determination of Total Phenolics*

Tannic acid concentration in the enzymatic extract was determined with the method proposed by Folin and Denis *(20)*.

### *Optimization of Process Parameters*

SSF was carried out to study the effect of several parameters required for the optimal production of tannase by *A. oryzae*. Initial amount of water added to the substrate (40, 60, 80, and 100 mL for 100.0 g of dry CAB), incubation time (0–96 h), supplementation with tannic acid (2.5, 5.0, 7.5, 10.0, and 12.5% [w/w] of tannic acid for 100.0 g of CAB), phosphorous (0.5, 1.0, 1.5, and 2.0 % [w/v]), and different organic (peptone and yeast extract at 1% [w/v]) and inorganic nitrogen sources (ammonium nitrate at 1% [w/v] and ammonium sulfate from 0.5 to 4.0% [w/v]) were the studied parameters.

### *Tannase Productivity*

In this work tannase productivity ($P_{EN}$) is defined as the amount of the desired product formed (tannase activity—$A_{EN}$) per reaction time ($t_{max}$) to achieve the highest enzyme activity *(21)*, *see* Eq. 1.

$$P_{EN} = \frac{A_{EN}}{t_{max}} \tag{1}$$

## Results and Discussion

### *Effect of Initial Water Content*

Several studies have showed that initial water content is a critical factor for growth and enzyme production and it is intimately related to the definition of SSF because it is necessary for new cell synthesis *(9,17,22–24)*. Water is needed for cooling and also for incorporation into new microbial cells. Moreover, some authors *(25)* observed that fungal growth could be hampered by limited water availability. Therefore, in this work, the effect of initial water content on tannase production was investigated and results are pictured in Fig. 1.

It can be observed that maximum enzyme production was obtained when 60 mL of water was added to 100.0 g of dry CAB and 0.576 U/g of dry substrate ($g_{ds}$). In this medium the humidity and water activity were 40.4% and 0.978, respectively (Table 3). The increase in water content beyond 60 mL inhibited enzyme production. With increasing water content, keeping

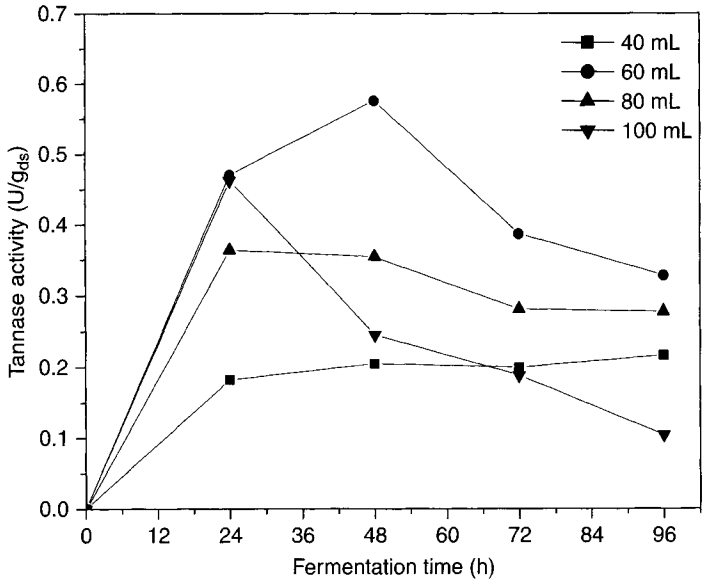


**Fig. 1.** Effect of water content on tannase yield production by *A. oryzae* in SSF of CAB (100.0 g) at 30°C.

Table 3
Humidity and Water Activity of the CAB Used in This Work for Different Amounts of Added Water

| Added volume (mL) | Humidity (%) | $a_w$ |
|---|---|---|
| 40 | 31.6 | 0.965 |
| 60 | 40.4 | 0.978 |
| 80 | 47.2 | 0.983 |
| 100 | 51.8 | 0.993 |

substrate volume constant, the air content of the substrate occupied within the interparticle space, decreases. Moreover, the scarcity or excess of water affects the decomposition rate of the organic matter, which was found to decrease, affecting enzyme production *(9,24)*. Low substrate water content may result in poor microbial growth and product formation owing to the poor access to nutrients arising from reduced mass transfer of gas and solute to the cells *(26)*. Some experiments have showed the influence of water content on the metabolism of microorganisms. The influence of water content on a solid substrate on growth rate and sporogenesis of filamentous fungi was reported *(27)*. Others authors *(28)* studied the influence of water activity on enzyme biosynthesis and enzyme activities produced by fungi. The water content of the medium is a fundamental parameter for mass transfer of water and solutes across the cell membrane. The control of this parameter could be used to modify the metabolic production or excretion of a microorganism *(17)*. Optimal water content allows the entry of nutrients

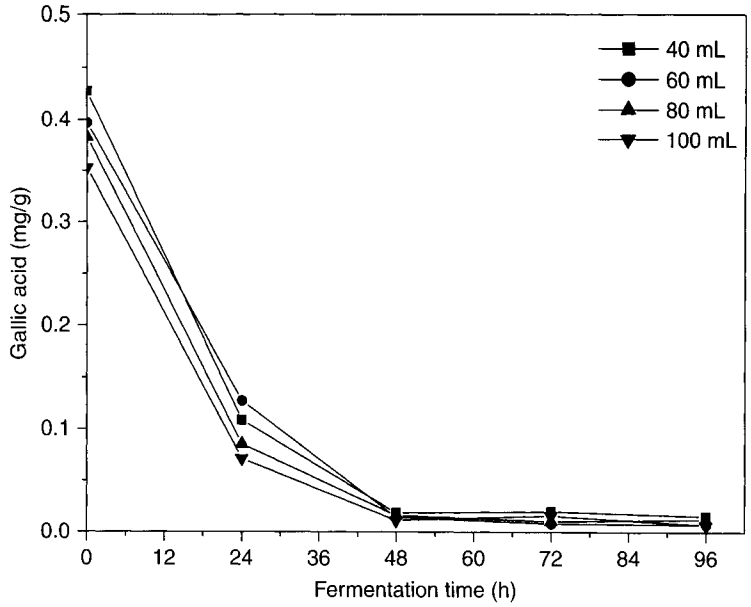


**Fig. 2.** Gallic acid concentration during SSF of CAB supplemented with different amounts of water.

through the cell walls, which enhances enzyme production. Any deviation from optimal may decrease enzyme production owing to osmotic imbalance inside the cells *(29)*.

Tannase production is a response of an induction process *(10)*. However, in this stage no inducer was added to the culture media, but tannase activity was detected. The analysis of fermentation extracts showed that phenolic compounds were presented in all fermentation media, from 0.50 to 0.55 mg/g (data not shown). Specifically, gallic acid, a pointed tannase inducer, was observed as a natural component of culture media from 0.35 to 0.43 mg/g (Fig. 2). In fermentation process, the gallic acid content decreased, probably as a result of microorganism consumption (Fig. 2). Based on the obtained results, all the subsequent fermentations were performed using 60 mL of initial water content.

## *Effect of Addition With Tannic Acid*

The supplementation of CAB with different amounts of tannic acid was investigated and the results are presented in Fig. 3. It can be observed that addition of tannic acid affected the enzyme production and maximum tannase activity (2.40 $U/g_{ds}$) was obtained with 2.5% (w/w) supplementation. Moreover, the addition of 2.5% of tannic acid stimulated tannase production about 4.2-fold, when compared with the results presented in Section *Effect of Initial Water Content*. Other authors observed an improvement in tannase production when tannic acid was added to the culture media *(9,24)*. An increase in tannic acid concentration over 2.5%, did not correspond to more tannase production. These results are similar to those observed by

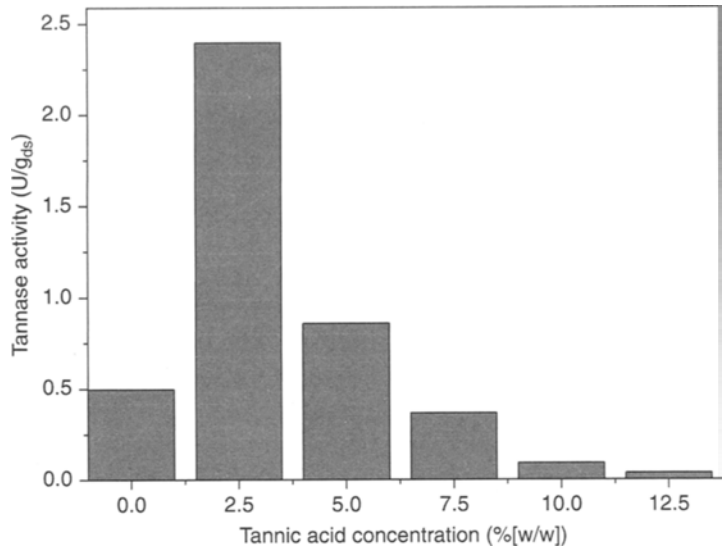


**Fig. 3.** Effect of tannic acid supplementation (% [w/w]) on tannase production by SSF at 30°C, 40.4% humidity, 40.0 g of CAB, and 48 h of incubation period.

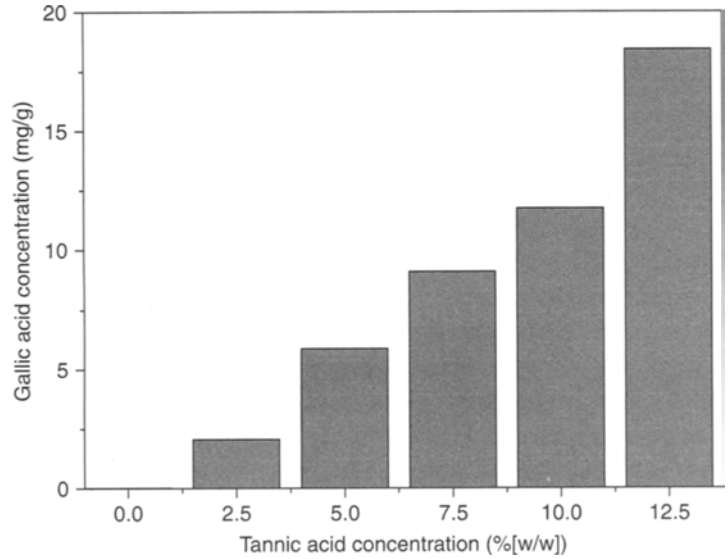


**Fig. 4.** Gallic acid concentration during SSF of 40.0 g of CAB supplemented with 2.5% (w/w) tannic acid at 30°C, 40.4% humidity, and 48 h of incubation period.

Lekha and Lonsane *(10,30)*. For high concentrations of tannic acid, ranging from 4 to 20%, tannase production by *A. niger* PKL104 and *A. oryzae* were negatively affected. The authors suggested that a growth inhibition, and consequently less enzyme synthesis, was related to high tannin concentration.

Figure 4 presents gallic acid profile in culture media. In all media supplemented with tannic acid, a gallic acid accumulation until 48 h was

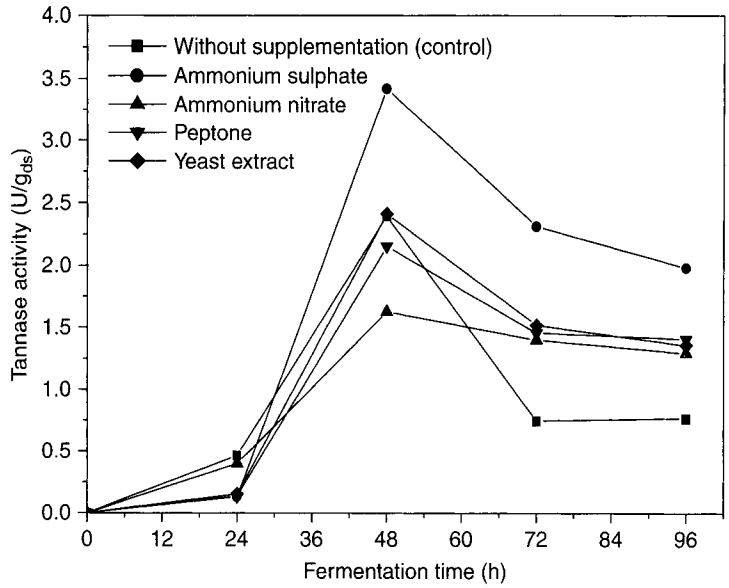


**Fig. 5.** Effect of supplementation of different nitrogen sources (1% [w/v]) on tannase production by *A. oryzae* in SSF of 40.0 g of CAB supplemented with 2.5% (w/w) tannic acid at 30°C and 40.4% humidity.

observed. The relation between the presence of high amounts of this compound and enzyme activity is not clear. Some authors *(10, 31–33)*, showed that gallic acid acts as inductor of synthesis. In opposite way, other authors *(34,35)* point gallic acid out as a great feedback repressor. Based on the obtained results, all the subsequent fermentation media were supplemented with 2.5% (w/w) of tannic acid.

### *Effect of Supplementation of Nitrogen Sources*

The effect of supplementation of different organic (peptone and yeast extract) and inorganic (ammonium nitrate and ammonium sulfate) nitrogen sources on tannase production was evaluated and results are shown in Fig. 5. It can be observed that ammonium nitrate, peptone, and yeast extract exerted no influence on tannase production. These results were similar to those obtained by other authors studying the production of tannase by *A. niger* 3T5B8 in wheat straw *(33)*. These authors point the distinct assimilation of inorganic ions and the possibility of complex formation between tannins and proteic structures of yeast extract and peptone. Ammonium sulphate, at a concentration of 1%, on the other hand, improved the enzyme production in 1.43-fold compared with control (fermentation in the absence of nitrogen sources). Nitrogen can be an important limiting factor in the microbial production of enzymes. The presence of an additional nitrogen source in the substrate may have promoted cell growth and enzyme production *(9)*.

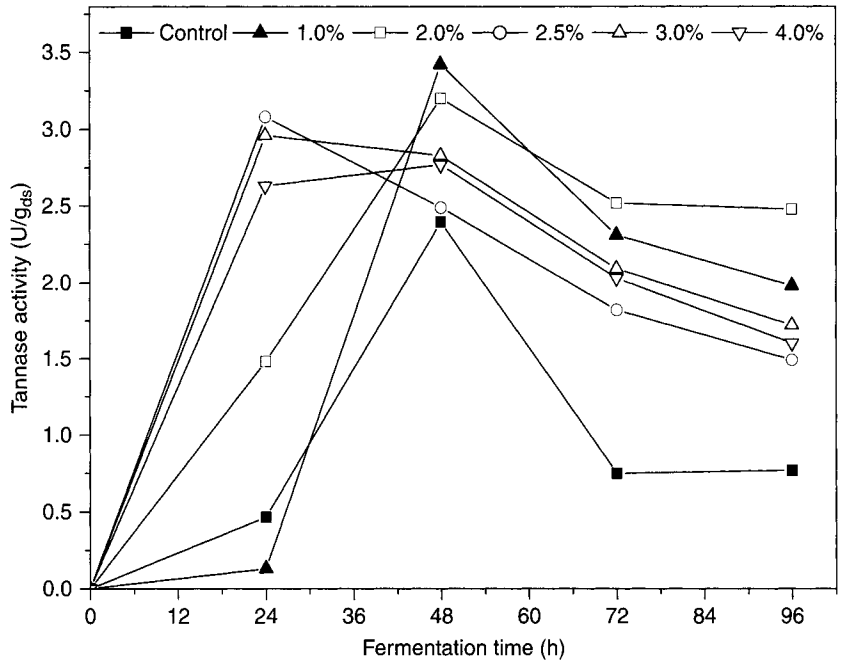


**Fig. 6.** Effect of ammonium sulphate concentration on tannase production by *A. oryzae* in SSF of 40.0 g of CAB supplemented with 2.5% (w/w) tannic acid at 30°C and 40.4% humidity.

Media supplementation with different amounts of ammonium sulfate was investigated and the results are presented in Fig. 6. It can be observed that increasing ammonium sulfate concentration exerted no influence on the amount of tannase produced; however, it has influenced the kinetics of enzyme production. Table 4 shows enzyme activity and productivity of tannase obtained in this work (SSF using *A. oryzae* and CAB supplemented with 2.5% (w/w) of tannic acid and ammonium sulphate) and by other authors *(9,24)* using different substrates and microorganisms.

Results pictured in Fig. 7 show an acceleration of the microbial metabolism when more than 2.0% (w/v) of ammonium sulphate was added to CAB, and consequently, better tannase productivities ($128.5 \times 10^{-3}$ $U \cdot g_{ds}^{-1} \cdot h^{-1}$) were achieved, *see* also Table 4. These productivity results, compared with other authors' results, indicate that CAB is a promising substrate for tannase production.

## *Effect Phosphorous Supplementation*

The effect of supplementation of CAB, enriched with 1% (w/v) of ammonium sulphate, with $NaH_2PO_4 \cdot H_2O$ on tannase production was evaluated and results are shown in Fig. 8. It can be observed that $NaH_2PO_4 \cdot H_2O$ exerted no influence on tannase production. Pinto *(33)* observed that the addition of phosphorus to the fermentation media (wheat

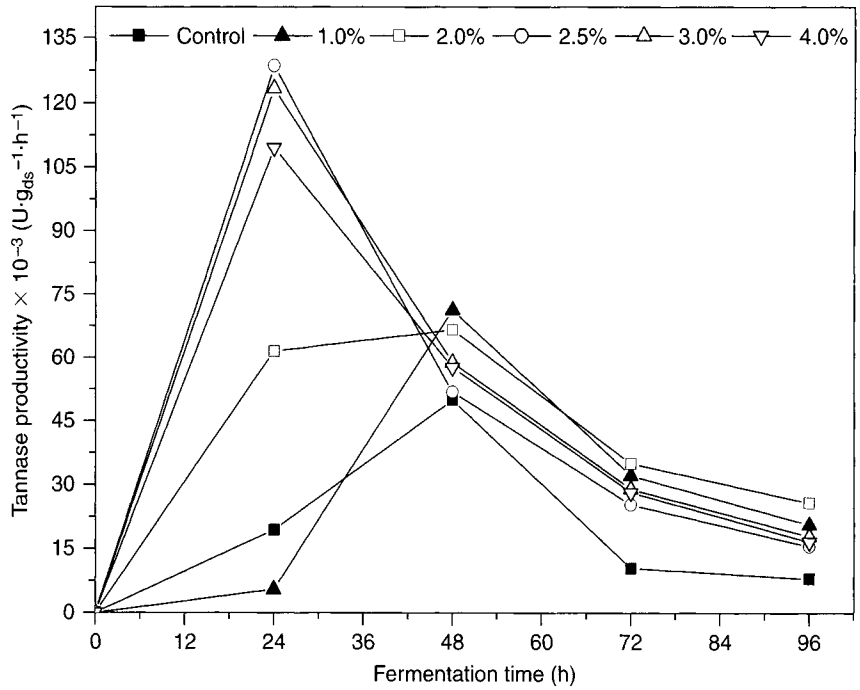


**Fig. 7.** Effect of ammonium sulphate concentration on tannase productivity by *A. oryzae* in SSF of 40.0 g of CAB supplemented with 2.5% (w/w) tannic acid at 30°C and 40.4% humidity.

Table 4
Tannase Activity ($U/g_{ds}$) and Productivity ($U \cdot g_{ds}^{-1} \cdot h^{-1}$) in SSF Using Different Microorganisms and Culture Media

| Substrate | Microorganism | Tannase activity ($U/g_{ds}$) | Tannase productivity $\times 10^3$ ($U \cdot g_{ds}^{-1} \cdot h^{-1}$) |
|---|---|---|---|
| CAB supplemented with 2.5% (w/w) tannic acid and 1% (w/v) ammonium sulphate | *A. oryzae* | 3.42 | 71.3 |
| CAB supplemented with 2.5% (w/w) tannic acid and 2.5% (w/v) ammonium sulphate | *A. oryzae* | 3.08 | 128.5 |
| Coffee husk *(24)* | *Lactobacillus* sp. | 0.70 | 14.5 |
| Tamarind seed power *(24)* | *Lactobacillus* sp. | 0.65 | 13.5 |
| Palm kernel cake *(9)* | *A. niger* ATCC16620 | 13.03 | 135.7 |

In this work, *A. oryzae* was able to grow in 40.0 g of CAB supplemented with 2.5% (w/w) tannic acid and ammonium sulphate at 30°C and 40.4% humidity.

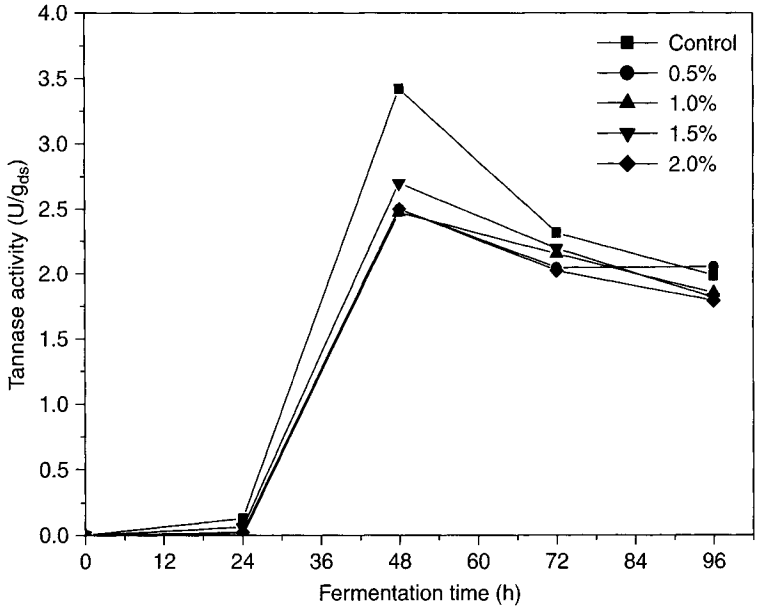


**Fig. 8.** Effect of sodium phosphate supplementation on tannase production by *A. oryzae* in SSF of 40.0 g of CAB supplemented with 2.5% (w/w) tannic acid and 1% (w/v) ammonium sulphate at 30°C and 40.4% humidity.

straw) promoted an increase in enzyme yield and productivity, which was not the observed in this work.

### *Effect of Incubation Period*

Maximum amount of tannase activity was obtained after 48 h or 24 h of fermentation (Figs. 1, 5, 6, and 8) for all conditions studied in this work. A decrease in enzyme yield with further increase of incubation time was also observed. This behavior could be owing to the reduced nutrient level of the media, affecting the enzyme synthesis. Some authors claim that tannase is produced during the primary phase of growth, and therefore, the activity decreases either because of decrease in production or because of enzyme degradation *(9)*. The consumption of gallic acid (Fig. 2) may contribute to a decrease in the level of induction. Nevertheless, the increase of ammonium sulphate concentration in culture media improved enzyme productivity (Figs. 6 and 7), allowing to produce almost the same amount of enzyme in 24 h of fermentation.

## Conclusions

Results obtained in this work showed that CAB was a promising substrate, enabling *A. oryzae* growth and the production of tannase. The physico-chemical parameters that influenced the enzyme production were: water content (60 mL), supplementation with tannic acid (2.5% [w/w]), and supplementation with nitrogen source (2.5% [w/v] ammonium sulphate).

The increase in ammonium sulphate concentration in the media improved enzyme productivity to $128.5 \times 10^{-3}$ U · $g_{ds}^{-1}$ · $h^{-1}$, when 2.5% was added. Supplementation of the medium with phosphorous ($NaH_2PO_4 \cdot H_2O$), ammonium nitrate, peptone and yeast extract exerted no influence on tannase production.

## Acknowledgments

The authors would like to thank the Brazilian research-funding agencies FINEP, CAPES, and CNPq (Federal).

## References

1. Morton, J. F. (1997), *Fruits of Warm Climates*, Florida Flair Books, Miami: pp. 239–240.
2. Campos, D. C. P., Santos, A. S., Wolkoff, D. B., Matta, V. M., Cabral, L. M. C., and Couri, S. (2002), *Desalination* **148,** 61–65.
3. Assunção, R. B. and Mercadante, A. Z. (2003), *J. Food Composition Anal.* **16,** 647–657.
4. Azevedo, D. C. S. and Rodrigues, A. (2000), *J. Sep. Technol.* **35,** 2561–2581.
5. Rocha, M. V. P., Oliveira, A. H. S., Souza, M. C. M., and Gonçalves, L. R. B. (2006), *World J. Microb. Biot.* **22,** 1295–1299.
6. Ferreira, A. C. H., Neiva, J. N. M., Rodríguez, N. M., Lobo, R. N. B., and Vasconcenlos, V. R. (2004), *R. Bras. Zootec.* **33,** 1380–1385.
7. Matias, M. F. O., Oliveira, E. L., Gertrudes, E., and Magalhães, M. M. A. (2005), *Braz. Archives Biol. Technol.* **48,** 143–150.
8. Cannel, E. and Moo-Young, M. (1980), *Proc. Biochem.* **15,** 2–7.
9. Sabu, A., Pandey, A., Jaafar Daud, M., and Szakacs G. (2005), *Bioresour. Technol.* **96,** 1223–1228.
10. Lekha, P. K. and Lonsane, B. K. (1997), *Adv. Appl. Microbiol.* **44,** 215–260.
11. Kurmar, R. and Singh, M. (1984), *J. Agric. Food Chem.* **32,** 447–453.
12. Madhavakrishna, W., Bose. S., and Nayudamma, Y. (1960), *Bull. Cent. Leather Res. Inst.* **7,** 1–11.
13. Pourrat, H., Regerat, F., Pourrat, A., and Jean, D. (1985), *J. Fermentation Technol.* **63,** 401–403.
14. Adachi, O., Watanabe, M., and Yamada, H. (1968), *Agric. Biol. Chem.* **32,** 1079–1085.
15. Aguillar, C. N. and Sanchez, G. (2001), *Food Sci. Tech. Int.* **7,** 373–382.
16. Pinto, G. A. S., Leite, S. G. F., Terzi, S. C., and Couri, S. (2001), *Braz. J. Microb.* **32,** 24–26.
17. Pandey, A. (1992), *Process Biochem.* **27,** 109–117.
18. Inoue, K. H. and Hagerman, A. E. (1988), *Anal. Biochem.* **169,** 363–369.
19. Sharma, S., Bhat, T. K., and Dawra, R. K. (2000), *Anal. Biochem.* **279,** 85–89.
20. Folin, O. and Denis, J. (1912), *J. Biol. Chem.* **12,** 239–243.
21. Gonçalves, L. R. B., Giordano, R. L. C., and Giordano, R. C. (2005), *Process Biochem.* **40,** 247–256.
22. Robinson, T. and Nigam, P. (2003), *Biochem. Eng.* **13,** 197–203.
23. Francis, F., Sabu, A., Nampoothiri, K. M., et al. (2003), *Bioch. Eng. J.* **15,** 107–115.
24. Sabu, A., Augur, C., Swati, C., and Pandey, A. (2006), *Process Biochem.* **41,** 575–580.
25. Oriol, E., Schettino, B., Viniegra-Gonalez, G., and Raimbault, M. (1988), *J. Ferment. Technol.* **66,** 57–62.
26. Bradoo, S., Gupta, R., and Saxena, R. K. (1996), *J. Gen. Appl. Microbiol.* **42,** 325–329.
27. Gervais, P., Grajek, W., Bensoussan, M., and Molin, P. (1988), *Biotechnol. Bioeng.* **31,** 457–463.
28. Grajek, W. and Gervais, P. (1987), *Enzyme Microbial. Technol.* **9,** 658–662.
29. Banerjee, R., Mukherjee, G., and Patra, K. C. (2005), *Bioresource Technology* **96,** 949–953.
30. Lekha, P. K. and Lonsane, B. K. (1994), *Process Biochem.* **29,** 497–503.

31. Knudson, L. J. (1913), *Biol. Chem.* **14,** 159–184.
32. Nishira, H. and Mugibayashi, N. (1953), *Hyogo Noka Diagaku Kenkyu hokoku Nogeikagaku Hen* **4,** 113–116.
33. Pinto, G. A. S. (2003), *PhD Thesis,* Universidade do Rio de Janeiro, Rio de Janeiro, Brasil.
34. Bradoo, S. and Gupta, R. (1997), *J. Gen. Appl. Microbiol.* **42,** 325–329.
35. Aguilar, C. N., Augur, C., Favela-Torres, E., and Viniegra-González, G. (2001), *Process Biochem.* **36,** 565–570.

0273-2289/1559-0291 (Online)/07/136–140/689–702/$30.00

# Studying Pellet Formation of a Filamentous Fungus *Rhizopus oryzae* to Enhance Organic Acid Production

**Wei Liao,* Yan Liu, and Shulin Chen**

*Department of Biological Systems Engineering, and Center for Bioenergy and Bioproducts, Washington State University, Pullman, WA 99163, E-mail: wliao@mail.wsu.edu*

## Abstract

Using pelletized fungal biomass can effectively improve the fermentation performance for most of fugal strains. This article studied the effects of inoculum and medium compositions such as potato dextrose broth (PDB) as carbon source, soybean peptone, calcium carbonate, and metal ions on pellet formation of *Rhizopus oryzae*. It has been found that metal ions had significantly negative effects on pellet formation whereas soybean peptone had positive effects. In addition PDB and calcium carbonate were beneficial to *R. oryzae* for growing small smooth pellets during the culture. The study also demonstrated that an inoculum size of less than $1.5 \times 10^9$ spores/L had no significant influence on pellet formation. Thus, a new approach to form pellets has been developed using only PDB, soybean peptone, and calcium carbonate. Meanwhile, palletized fungal fermentation significantly enhanced organic acid production. Lactic acid concentration reached 65.0 g/L in 30 h using pelletized *R. oryzae* NRRL 395, and fumeric acid concentration reached 31.0 g/L in 96 h using pelletized *R. oryzae* ATCC 20344.

**Index Entries:** Calcium carbonate; fumaric acid; fungal pellet; inoculum size; lactic acid; metal ions; potato dextrose broth; *Rhizopus oryzae*.

## Introduction

Filamentous fungal fermentation is widely used to commercially produce useful products such as organic acids, enzymes, antibiotics and the cholesterol lowering drugs (Statins), and so on *(1–7)*. Fungi can be grown in submerged cultures by several different morphological forms: suspended mycelia, clumps, or pellets *(8)*. Many studies have discussed the advantages and disadvantages of growth morphologies in terms of different product *(9–11)*. It has been concluded that the fungal growth in pellet form is a favorable alternative to benefit the most of fungal fermentations because it not only makes fungal biomass reuse possible but also significantly improve the culture rheology, which results in better mass and oxygen transfer into the biomass, and lower energy consumption for aeration and agitation *(12)*.

The change of fungal morphology is mainly influenced by medium compositions, inoculum, pH, medium shear, additives (polymers, surfactants, and chelators), culture temperature, and medium viscosity *(5,8,13,14)*. For individual strains, each factor has different importance to the growth morphologies; some strains such as *Rhizopus* sp. need strong agitation to form pellets, whereas some strains such as *Penicillium chrysogenum* require high pH to form pellets *(8)*. Thus, the study on fungal pellet formation is limited at the level of the individual strain.

Strains of *R. oryzae* have the capability to produce fumaric acid, lactic acid, pectinase, amylogucosidase, α-amlyase, and so on *(1,4,5,15)*. Zhou et al. *(16)* investigated the effects of different metal ions ($Mg^{2+}$, $Zn^{2+}$, and $Fe^{2+}$) and pH on the pellet formation of *R. oryzae* ATCC 20344 under glucose as a carbon source and urea as a nitrogen source. Byrne studied the effects of glucose concentration, peptone concentration, pH, and some additives on the pellet formation of *R. oryzae* ATCC 10260 *(17,18)*. However, the comprehensive investigation of the effects of medium compositions and inoculum on the pellet formation and the effects of pellets on the improvement of organic acid production has not been fulfilled. This article is focused on studying the factors such as carbon source, nitrogen source, metal ions, neutralizer, and inoculum in order to develop a new approach to form *R. oryzae* pellets, and further enhance organic acid production.

## Materials and Methods

### Microorganism

*R. oryzae* ATCC 20344 and *R. oryzae* NRRL 395 were obtained from the American Type Culture Collection (ATCC) (Manassas, VA). The strains were first cultured on potato dextrose agar (Difco, Franklin Lakes, NJ) slants, and further propagated on potato dextrose agar in 500-mL Erlenmeyer flasks to form spores. The culture temperature was 25°C. The spores were washed from the agar with sterile distilled water, and collected as a spore suspension for the study. The spore concentrations of the suspension were $7.5 \times 10^7$ spores/mL for *R. oryzae* ATCC 20344, $9.0 \times 10^7$ spores/mL for *R. oryzae* NRRL 395, respectively. *R. oryzae* ATCC 20344 was used for studying pellet formation.

### Pellet Formation

The effects of factors such as different carbon source, nitrogen source, mineral ions, and neutralizer on pellet formation were carried out by a $2^4$ full-factorial design with replicates (Table 1). Two different carbon sources Potato dextrose broth (PDB) and glucose under two levels of nitrogen (with and without), mineral ions (with and without), and neutralizer (with and without) were studied. The glucose concentration in the carbon sources was 20.0 g/L. The nitrogen source was soybean peptone (Sigma,

Table 1
$2^4$ Full-factorial Design With Replicates for Pellet Formation[a,b]

| Run | Factors | | | |
|---|---|---|---|---|
| | Carbon source | Nitrogen source | Mineral ions | Neutralizer |
| 1 | PDB ((+1) | Yes (+1) | Yes (+1) | Yes (+1) |
| 2 | PDB (+1) | Yes (+1) | Yes (+1) | No (–1) |
| 3 | PDB (+1) | Yes (+1) | No (–1) | Yes (+1) |
| 4 | PDB (+1) | Yes (+1) | No (–1) | No (–1) |
| 5 | PDB (+1) | No (–1) | Yes (+1) | Yes (+1) |
| 6 | PDB (+1) | No (–1) | Yes (+1) | No (–1) |
| 7 | PDB (+1) | No (–1) | No (–1) | Yes (+1) |
| 8 | PDB (+1) | No (–1) | No (–1) | No (–1) |
| 9 | Glucose (–1) | Yes (+1) | Yes (+1) | Yes (+1) |
| 10 | Glucose (–1) | Yes (+1) | Yes (+1) | No (–1) |
| 11 | Glucose (–1) | Yes (+1) | No (–1) | Yes (+1) |
| 12 | Glucose (–1) | Yes (+1) | No (–1) | No (–1) |
| 13 | Glucose (–1) | No (–1) | Yes (+1) | Yes (+1) |
| 14 | Glucose (–1) | No (–1) | Yes (+1) | No (–1) |
| 15 | Glucose (–1) | No (–1) | No (–1) | Yes (+1) |
| 16 | Glucose (–1) | No (–1) | No (–1) | No (–1) |

[a]Code values are in the parentheses.
[b]The strain is *R. oryzae* ATCC 20344.

St. Louis, MO) with a concentration of 6.0 g/L. The mineral ions included: 0.6 g/L $KH_2PO_4$, 0.25 g/L $MgSO_4 \cdot 7H_2O$, and 0.088 g/L $ZnSO_4 \cdot 7H_2O$. The neutralizer was $CaCO_3$ (6.0 g/L). The cultures were performed at 27°C for 48 h on a rotary shaker at 190 rpm.

### *Effects of Inoculum Size on Pellet Formation and Growth*

Four spore concentrations ($1.5 \times 10^8$, $3.75 \times 10^8$, $7.5 \times 10^8$, and $1.5 \times 10^9$ spores/L) were run on the selected media, which were identified in the previous section as favorable media to form pellets. The cultures were carried out under the same conditions described under "Pellet Formation."

### *Comparison of Pelletized Fungal Fermentation and Clump-Like Fungal Fermentation on Organic Acid Production*

*R. oryzae* NRRL 395 was used to produce lactic acid. The fermentation conditions for lactic acid production were: 120.0 g/L of glucose, 60.0 g/L of $CaCO_3$, and 6.5 g/L (dry basis) of biomass for both pellets and clump. *R. oryzae* ATCC 20344 was the strain used to produce fumaric acid. The fermentation conditions for fumaric acid production were: 100.0 g/L of glucose, 60.0 g/L of $CaCO_3$, and 11.5 g/L (dry basis) of biomass for both pellets and clumps. The cultures were carried out at 27°C in 250-mL flasks

containing 100 mL of culture medium on a rotary shaker at 190 rpm. All media were autoclaved at 121°C for 15 min before inoculation.

### *Statistical Analysis*

The effects of carbon source, nitrogen, mineral ions, and neutralizer on pellet formation were compared using the special property of factorial designs whose effects can be simply estimated by the differences in average response values between the high and low codes of each factor. A ranked list that presented the relative importance among factors was formed by the comparison. The list is given in the Pareto chart *(19)*.

### *Analytical Methods*

The morphology of the cultures was determined by examining submerged cultures dispersed on Petri dishes. An Olympus microphotograph (Tokyo, Japan) was used to observe the pellet morphology and measure the size of the pellets. The pH value was measured with a Fisher portable pH meter (Fisher Scientific, Pittsburgh, PA). Dry biomass was determined by washing the pellet mycelia with 6 *N* HCL to neutralize excess $CaCO_3$ attached in the pellets, and then washing to pH 6.0 with deionized water. The washed biomass was dried at 100°C overnight before weight analysis. The fumaric acid and lactic acid in the broth were analyzed using a Dionex DX-500 system (Sunnyvale, CA) including an AS11-HC (4 mm 10-32) column, a quaternary gradient pump (GP40), a CD20 conductivity detector, and an AS3500 autosampler *(20)*.

## Results

### *Pellet Formation*

The effects of carbon source, nitrogen source, metal ions, and neutralizer on fungal morphology were investigated (Table 2). Fungal morphologies varied from different combination of factors (Fig. 1). There were only four runs (Nos. 3, 4, 11, and 12), which were able to form pellets. In order to run statistical analysis on a qualitative data of morphologies, the qualitative value has to be assigned to describe it. The uniform pellet form of fungal biomass was represented by the value of 1, and other nonpellet forms such as clump, less/nongrowth, and nonuniform pellet/clump were represented by the value of 0. The analysis demonstrated that peptone, metal ions, and their combined interaction together had 100% of total effect, which means that peptone and metal ions were the two main factors on pellet formation (Fig. 2). The data also showed that peptone had a positive effect (33% of total effect) on pellet formation, whereas metal ions and the interaction of metal ions and peptone (33% each of total effect) had negative effects.

Table 2
Experimental Results From $2^4$ Full-Factorial design[a,b]

| Run | Fungal morphology[c] | Pellet size (mm)[d] | Biomass (g dry matter/L) | Initial pH | Final pH |
|---|---|---|---|---|---|
| 1 | Clump (0) | – | 6.344 | 6.06 | 7.10 |
| 2 | Clump (0) | – | 3.62 | 5.76 | 7.13 |
| 3 | Uniform pellet (1) | 1.98 ± 0.41 | 3.992 | 6.84 | 6.81 |
| 4 | Uniform pellet (1) | 1.03 ± 0.15 | 3.158 | 5.99 | 3.77 |
| 5 | Clump (0) | – | 2.818 | 5.58 | 5.59 |
| 6 | Nonuniform pellet and clump (0) | – | 2.318 | 4.65 | 3.11 |
| 7 | Nonuniform pellet and clump (0) | – | 2.366 | 6.58 | 6.21 |
| 8 | Nonuniform pellet and clump (0) | – | 0.912 | 4.93 | 3.31 |
| 9 | Clump (0) | – | 4.574 | 6.44 | 7.18 |
| 10 | Clump (0) | – | 3.03 | 6.20 | 6.11 |
| 11 | Uniform pellet (1) | 2.57 ± 0.22 | 2.408 | 7.42 | 5.88 |
| 12 | Uniform pellet (1) | 1.47 ± 0.35 | 1.842 | 7.13 | 3.43 |
| 13 | Nongrowth (0) | – | 0.008 | 5.43 | 5.84 |
| 14 | Nongrowth (0) | – | 0.008 | 4.64 | 4.52 |
| 15 | Less-growth (0) | – | 0.016 | 6.81 | 6.74 |
| 16 | Less-growth (0) | – | 0.036 | 6.05 | 6.09 |

[a]All data except pellet size are the mean of two replicates, pellet size is the mean of 200 replicates with standard deviation at $\alpha = 0.05$.
[b]The strain is *R. oryzae* ATCC 20344.
[c]Code values are in the parentheses. 1 is the value to represent the pellet, 0 is the value to represent the nonpellet forms such as clump, nongrowth, and so on.
[d]"–" means nonpellet.

Statistical analysis concluded that the other two factors of carbon source and neutralizer were not the main factor on pellet formation. However, both of them had significant influences on fungal pellet growth. Pellets from cultures with calcium carbonate and PDB had an average diameter of 1.98 mm and 3.99 g biomass, whereas pellets from corresponding cultures without calcium carbonate only had 1.03 mm and 3.16 g, respectively (Fig. 3). Pellets cultured on glucose had the same trend as those on PDB (Fig. 3). In addition, pellets cultured on both PDB and glucose with calcium carbonate were much smoother than those

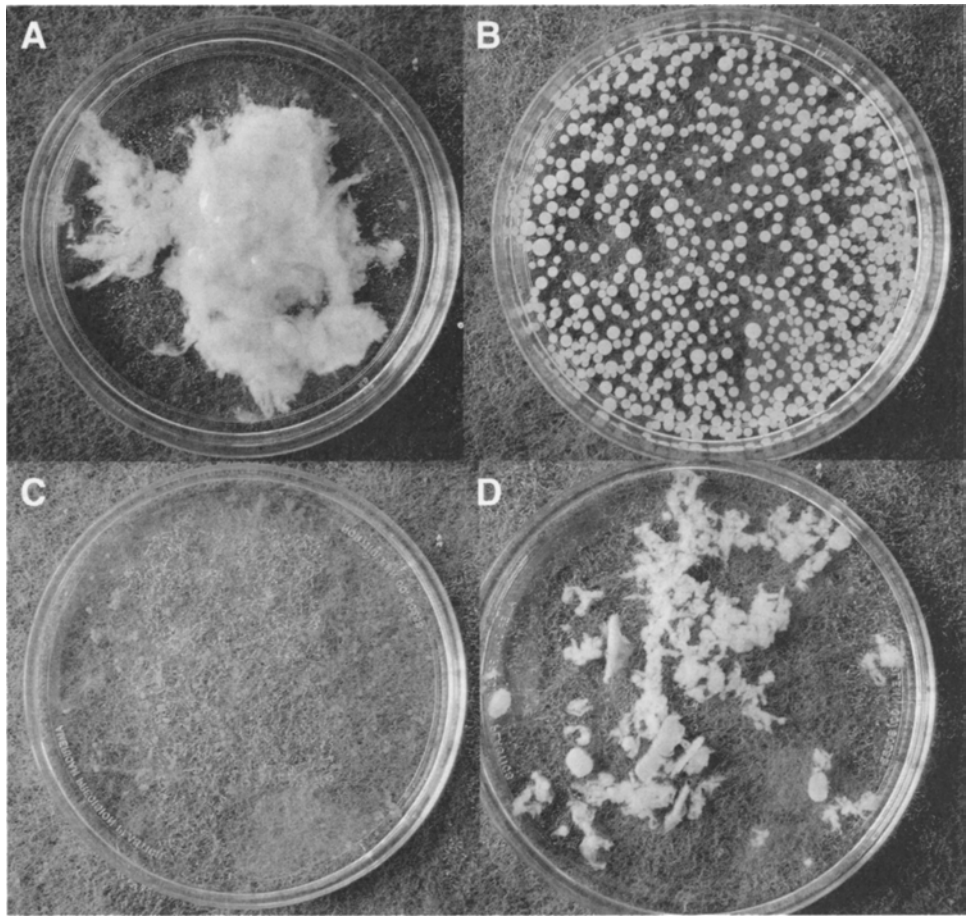


**Fig. 1.** Morphology of fungal biomass (the strain is *R. oryzae* ATCC 20344). **(A)** Clump from run 2, **(B)** pellet from run 3, **(C)** less-growth from run 15, and **(D)** nonuniform pellet and clump.

without calcium carbonate (Fig. 4). As for carbon sources, on the media with calcium carbonate the size of pellets cultured on PDB was 1.98 mm, which was smaller than the 2.57 mm from cultures on glucose, and PDB medium produced 1.58 g/L more biomass than the glucose medium (Fig. 3). The same trend was on the media without calcium carbonate (Fig. 3). In terms of effects of carbon sources on fungal pellets, PDB was a benefit for producing more biomass and pellets with a smaller size compared with glucose. The data also demonstrated that pH differences caused by different components in the culture medium among experimental runs had no significant influence on pellet formation compared with other factors (Table 2). Run Nos. 3 and 4 formed pellets at final pH 6.81 and 3.77, respectively. Run No. 11 and 12 formed pellets at the pH values of 5.88 and 3.43.

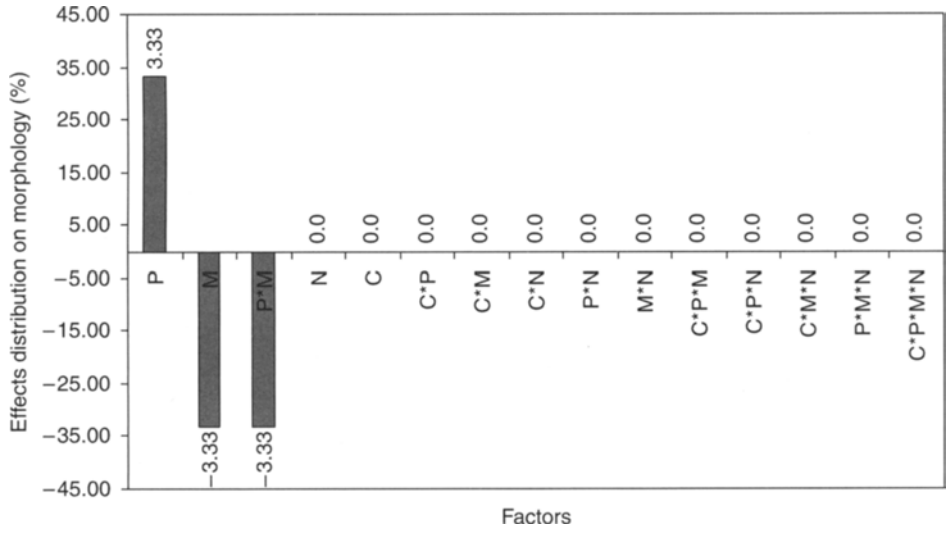


**Fig. 2.** Pareto charts of effects of medium composition on pellet formation. Where P is peptone, M is mineral ions, N is neutralizer, and C is carbon source. The strain is *R. oryzae* ATCC 20344.

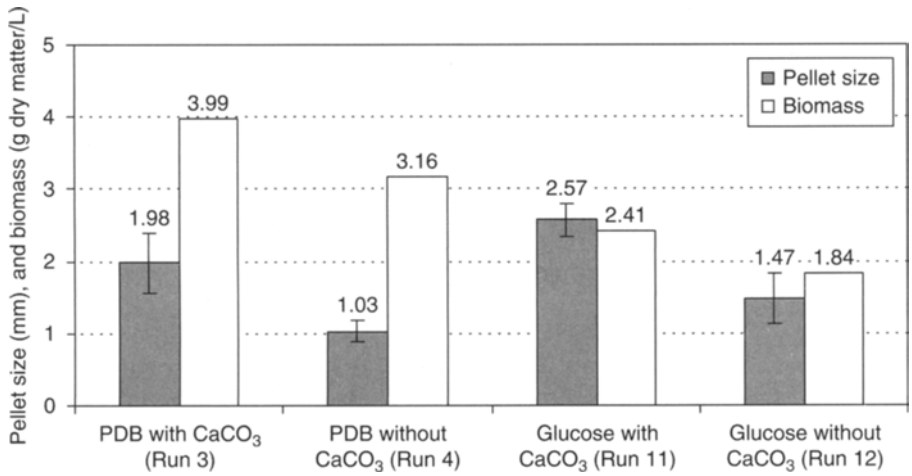


**Fig. 3.** Effects of carbon source and neutralizer on pellet morphology during pellet formation (the strain is *R. oryzae* ATCC 20344).

## *Effects of Inoculum Size on Pellet Formation and Growth*

Spore concentration did not influence the pellet formation. All four different spore concentrations ($1.5 \times 10^8$, $3.75 \times 10^8$, $7.5 \times 10^8$, and $1.5 \times 10^9$ spores/L) formed smooth pellets on both PDB pellet-formed culture medium (24.0 g/L PDB, 6.0 g/L soybean peptone, and 6.0 g/L $CaCO_3$) and glucose pellet-formed culture medium (20.0 g/L glucose, 6.0 g/L soybean peptone, 6.0 g/L $CaCO_3$). Pellet numbers and total amount of biomass

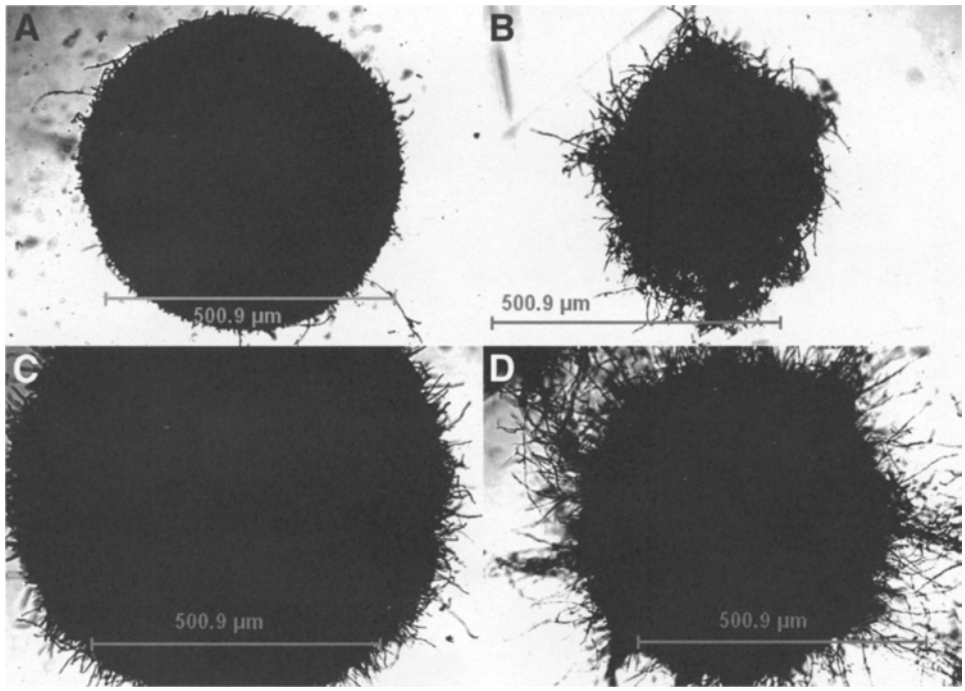


**Fig. 4.** Surface structure of fungal pellets from different cultural conditions (the strain is *R. oryzae* ATCC 20344). **(A)** From run 3 (PDB with $CaCO_3$), **(B)** from run 4 (PDB without $CaCO_3$), **(C)** from run 11 (glucose with $CaCO_3$), and **(D)** from run 12 (glucose without $CaCO_3$).

increased, and pellet size decreased following the increase of spore concentration no matter what type of carbon source the cultures were on (Fig. 5). The changes of total pellet numbers and pellet size with the increase of inoculum concentration was much more significant than the change of biomass because the biomass increase in the certain range of inoculum is mainly controlled by the nutrients rather than spore concentration.

## *Comparison of Pelletized Fungal Fermentation and Clump-Like Fungal Fermentation on Organic Acid Production*

The pelletized fungal biomass for both lactic acid and fumaric acid production were obtained from culturing *R. oryzae* NRRL 395 and *R. oryzae* ATCC 20344 on the medium (24.0 g/L PDB, 6.0 g/L soybean peptone, 6.0 g/L $CaCO_3$) with inoculum size of $1.5 \times 10^9$ spores/L at 27°C and 190 rpm for 48 h. The average pellet diameters of biomass for *R. oryzae* NRRL 395 and *R. oryzae* ATCC 20344 are 1.7 mm and 1.5 mm, respectively. Organic acid fermentations comparing clump and pellet morphologies demonstrated that there were significant ($p < 0.05$) differences on lactic acid and fumaric acid production between clump and pellet morphologies. The lactic acid concentration of clump fermentation reached 32.0 g/L in 60 h of culture duration,

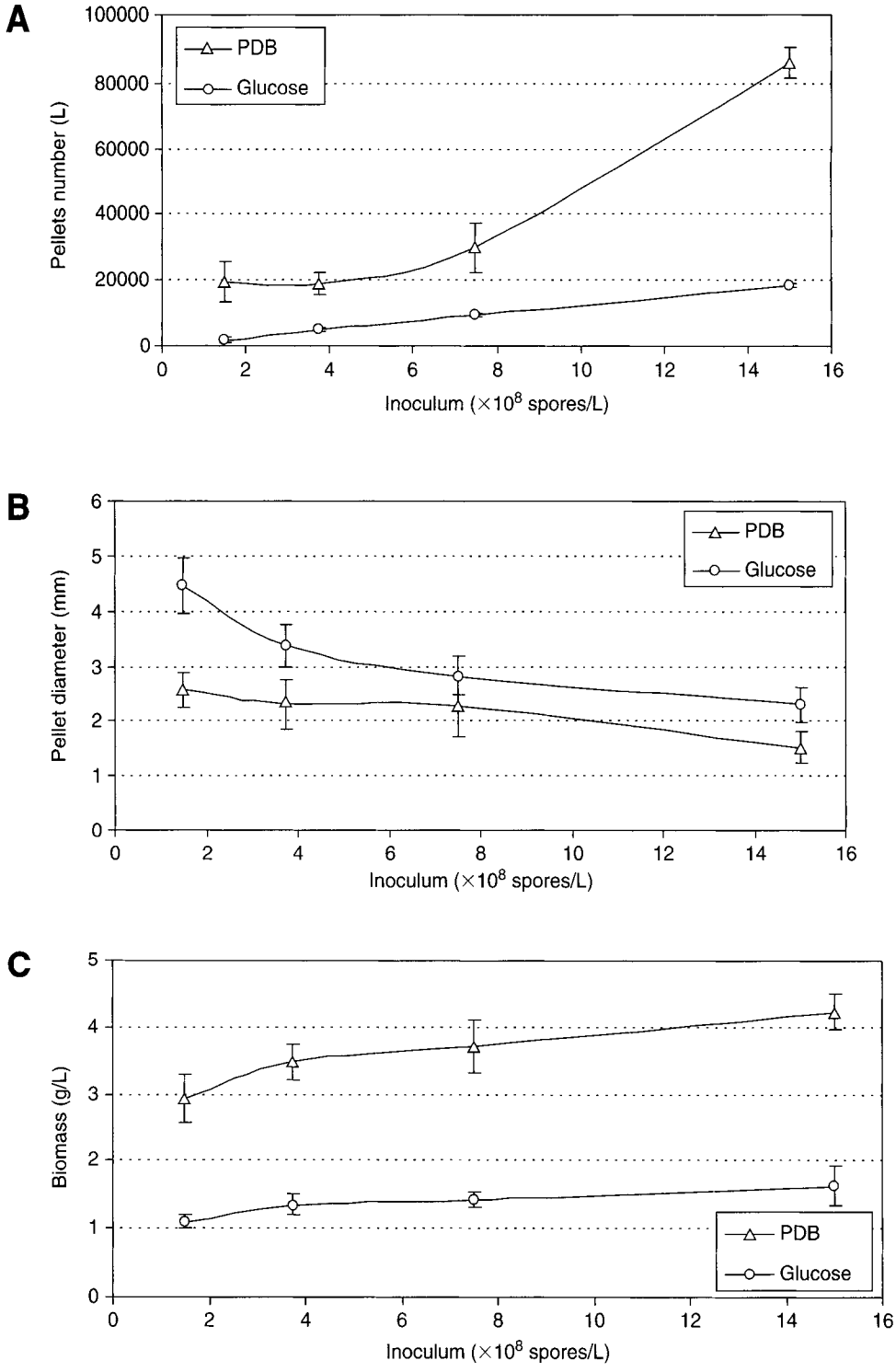


**Fig. 5.** Effects of inoculum on pellet formation (the strain is *R. oryzae* ATCC 20344). **(A)** Pellet number, **(B)** pellet size, and **(C)** biomass.

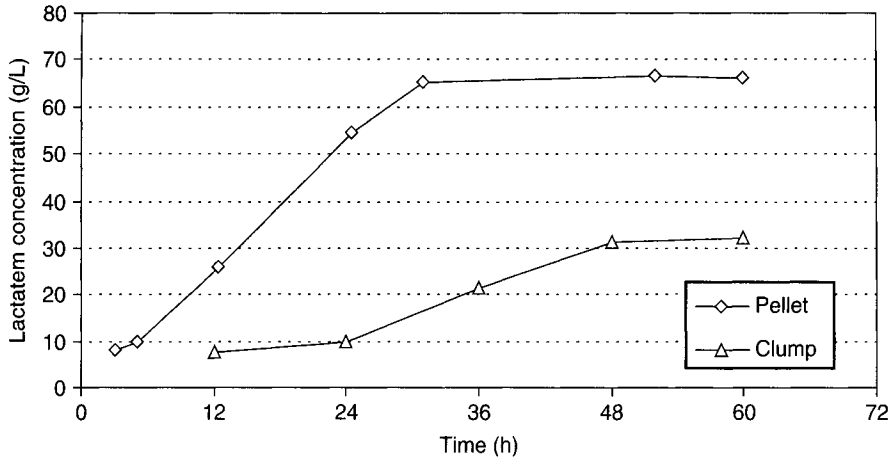


**Fig. 6.** Comparison of lactic acid production using pellet and clump morphology (the strain is *R. oryzae* ATCC NRRL 395). Data are presented as the mean of two replicates.

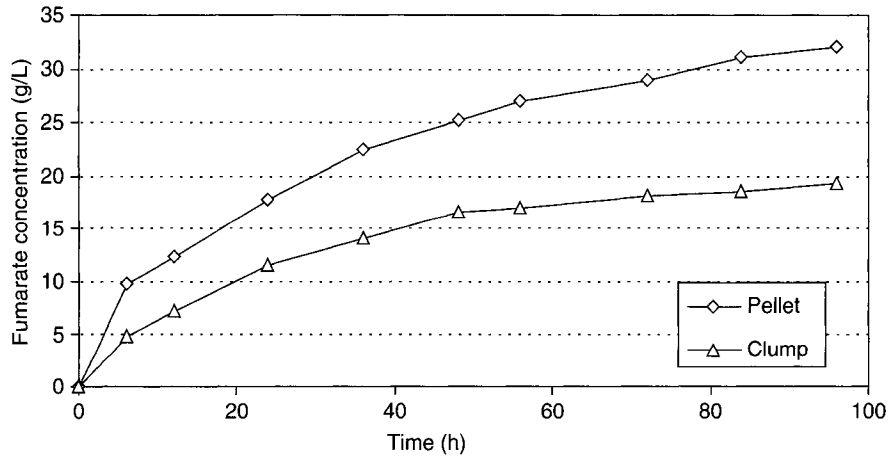


**Fig. 7.** Comparison of fumaric acid production using pellet and clump morphology (the strain is *R. oryzae* ATCC 20344). Data are presented as the mean of two replicates.

whereas the pellet fermentation produced 65.0 g/L in 30 h of culture duration (Fig. 6). Meanwhile, the clump and pellet fermentations of fumaric acid reached 21.5 and 31.0 g/L, respectively, during 96 h of culture duration (Fig. 7). The data indicated that both of lactic acid and fumaric acid production were significantly increased using pelletized fungal fermentation.

## Discussion

Metal ions are very important factor in the metabolism of *R. oryzae*. The organism utilized the energy three times more efficiently when metal ions were added to the medium, which made for a relatively fast and abundant fungal growth *(21)*. It has been proved by the study that the cultures with metal ions produced more biomass than those without metal

ions (Table 2). Meanwhile, in terms of fungal morphology, metal ions in the media made *R. oryzae* difficult to form the pellet as well, because the fungus grew so fast on the media with metal ions, the filaments tangled with each other and leaned to clumpy morphology (Fig. 1A). Thus, in order to form *R. oryzae* pellet, metal ions had to be eliminated in the culture media.

The pH of medium has also been reported as a very important factor for various fungi to form pellets. Generally, pH could change the surface properties of fungi, further influencing the pellet formation, and different strains have different sensibility to pH value *(8)*. However, for this particular strain of *R. oryzae*, the results showed that there were no significant differences on pellet formation with a pH range of 3.0–7.0, which means that this strain is not as sensitive to pH as some other strains such as *Aspergillus niger* and *P. chrysogenum (7,22,23)*.

Inoculum size is generally recognized as of great importance in the process of fungal pellet formation. Generally, the interaction of hyphae is considered as the main force to form clump. In the early stage of growth, the higher the inoculum size, the more interaction with the hyphae, and the more possibility the clump would be formed. Thus, it has been concluded by other researchers that low inoculum concentrations are beneficial for pellet production *(24)*. However, the maximum inoculum size varied from strain to strain *(8)*. Most of studies on pellet formation of strains of *Rhizopus* were conducted at relatively low concentrations ($<10^7$ spores/L) *(14,17,18,25)*. The study on the effects of inoculum on *R. oryzae* pellet formation demonstrated that there were no significant ($p > 0.05$) influences on pellet formation once the inoculum concentration was increased up to $10^9$ spores/L. The result elucidated that the particular strain of *R. oryzae* is able to prevent hyphae growth from forming clumps at relatively higher inoculum concentrations compared with other strain in the genus *Rhizopus*.

Peptone as nitrogen source was one of the two main factors on fungal pellet formation based on the statistical analysis. It had positive effect on pellet formation mainly because nitrogen is the limiting factor on the growth of *R. oryzae (26)*. Meanwhile, the type of nitrogen compound also has a considerable influence on fungal pellet formation *(23)*. A study of different nitrogen sources on *R. oryzae* ATCC 20344 showed that peptone produced much smaller, more unique, and heavier pellets than other nitrogen sources such as urea (W. Liao and S. Chen, unpublished data).

Although the carbon source was not a main factor on pellet formation, the result showed that PDB is a better carbon source on the pellet formation of *R. oryzae* compared with glucose. PDB as a good nutrient source has been widely used for fungal and yeast cultures. It contains mainly glucose, some vitamins, and a little nitrogen. The effects of PDB on fungal morphology have not been reported to date. It has been found by this study that PDB had a large impact on pellet such as pellet size and total biomass. This means that

the vitamins in PDB might be the main substances causing the difference in fungal pellet growth. Furthermore, studies on the effects of PDB components on pellet growth need to be carried out.

Calcium carbonate, as a neutralizer, prevents pH from dropping into the low pH range of 2.0–3.0, which is not favorable for the biomass accumulation *(16)*. Total amount of biomass from a medium with calcium carbonate were significantly higher than those without it (Fig. 3). In addition, during fungal pellet formation, calcium carbonate is not only a neutralizer to keep pH stable, but it also supplies $Ca^{2+}$ ions. It has been reported that calcium ions were usually recognized to induce mycelial aggregation during fungal growth *(27)*, which has been proved by this study that media with calcium carbonate produced smoother and larger pellets than those without calcium carbonate (Fig. 4).

## Conclusion

This study developed a new, simple culture medium to grow pellets for *R. oryzae*. The fungal pellets can be formed from the culture on a medium with only three components of PDB, soybean peptone, and calcium carbonate without any additives such as metal ions, polymers, and so on. Pelletized fungal fermentation significantly enhanced organic acid production. Lactic acid concentration reached 65.0 g/L in 30 h using pelletized *R. oryzae* NRRL 395, and fumeric acid concentration reached 31.0 g/L in 96 h using pelletized *R. oryzae* ATCC 20344.

## Acknowledgment

The authors gratefully acknowledge Mr. Dan Hardesty and Mr. Craig Frear for critically reading the manuscript.

## References

1. Cao, N., Du, J., Gong, C. S., and Tsao, G. T. (1996), *Appl. Environ. Microbiol.* **62,** 2926–2931.
2. Casas Lopez, J. L., Sanchez Perez, J. A., Fernandez sevilla, J. M., Acien Fernandez, F. G., Molina Grima, E., and Chisti, Y. (2004), *J. Chem. Technol. Biotechnol.* **79(10),** 1119–1126.
3. Chahal, D. S. (1985), *Appl. Environ. Microbiol.* **49(1),** 205–210.
4. Hang, Y. D. (1989), *Biotechnol. Lett.* **11(4),** 299–300.
5. Papagianni, M. (2004), *Biotechnol. Adv.* **22,** 189–259.
6. Schuurmans, D. M., Olson, B. H., and San clemente, C. L. (1956), *Appl. Microbiol.* **4(2),** 61–66.
7. Steel, R., Martin, S. M., and Lentz, C. P. (1954), *Can. J. Microbiol.* **1(3),** 150–157.
8. Metz, B. and Kossen, N. W. F. (1977), *Biotechnol. Bioeng.* **19(6),** 781–799.
9. Calam, C. T. (1976), *Process Biochem.* **4,** 7–12.
10. Konig, B., Schugerl, K., and Seewald, C. (1982), *Biotechnol. Bioeng.* **24(2),** 259–280.
11. Martin, S. M. and Waters, W. R. (1952), *J. Ind. Eng. Chem.* **44,** 2229–2233.
12. Van Sjijdam, J. C., Kossen, N. W. F., and Paul, P. G. (1980), *Eur. J. Appl. Microbiol. Biotechnol.* **10(3),** 211–221.
13. Nielsen, J. and Carlsen, M. (1996), In: *Immobilised Living Cell Systems.* Willaert, R. G., Baron, G. V., and De Backer L. (eds.), John Wiley & Sons Ltd., New York: pp. 273–293.

14. Znidarsic, P., Komel, R., and Pavko, A. (1998), *J. Biotechnol.* **60,** 207–216.
15. Soccol, C. R., Iloki, I., Marin, B., and Raimbault, M. (1994), *J. Food Sci. Technol.* **31(4),** 320–323.
16. Zhou, Y., Du, J., and Tsao, G. T. (2000), *Appl. Biochem. Biotechnol.* **84–86,** 779–789.
17. Byrne, G. S. and Ward, O. P. (1989). *Biotechnol Bioeng.* **33,** 912–914.
18. Byrne, G. S. and Ward, O. P. (1989). *J. Ind. Microbiol.* **4,** 155–161.
19. Haaland, P. D. (1989), *Experimental Design in Biotechnology.* Marcel Dekker, Inc. New York: pp. 23–29.
20. Liu, Y., Wen, Z., Liao, W., Liu, C., and Chen, S. (2005), *Eng. Life Sci.* **5(4),** 343–349.
21. Foster, J. W. and Waksman, S. A. (1939), *J. Bacteriol.* **37,** 599–617.
22. Galbraith J. C. and Smith, J. E. (1969), *J. Gen. Microbiol.* **59(1),** 31–45.
23. Pirt, S. J. and Callow, D. S. (1959), *Nature* **184,** 307–310.
24. Foster, J. W. (1949), *Chemical Activities of Fungi.* Academic, New York.
25. Znidarsic, P., Komel, R., and Pavko, A. (2000), *World J. Microbiol. Biotechnol.* **16,** 589–593.
26. Foster, J. W. and Waksman, S. A. (1939), *J. Am. Chem. Soc.* **61,** 127–135.
27. Jackson, S. L. and Heath, I. B. (1993), *Microbiol. Rev.* **57(2),** 367–382.

0273-2289/1559-0291 (Online)/07/136-140/703-710/$30.00

# Comparison of Multiple Gene Assembly Methods for Metabolic Engineering

CHENFENG LU,[1] KAREN MANSOORABADI,[2] AND THOMAS JEFFRIES*,[1-3]

[1]*Department of Food Science;* [2]*Department of Bacteriology, University of Wisconsin, Madison, WI 53706, E-mail: twjeffri@wisc.edu; and* [3]*USDA Forest Service, Forest Products Laboratory, Madison, WI 53726*

## Abstract

A universal, rapid DNA assembly method for efficient multigene plasmid construction is important for biological research and for optimizing gene expression in industrial microbes. Three different approaches to achieve this goal were evaluated. These included creating long complementary extensions using a uracil-DNA glycosylase technique, overlap extension polymerase chain reaction, and a *Sfi*I-based ligation method. *Sfi*I ligation was the only successful approach for assembling large DNA fragments that contained repeated homologous regions. In addition, the *Sfi*I method has been improved over a similar, previous published technique so that it is more flexible and does not require polymerase chain reaction to incorporate adaptors. In the present study, *Saccharomyces cerevisiae* genes *TAL1*, *TKL1*, and *PYK1* under control of the 6-phosphogluconate dehydrogenase promoter were successfully ligated together using multiple unique *Sfi*I restriction sites. The desired construct was obtained 65% of the time during vector construction using four-piece ligations. The *Sfi*I method consists of three steps: first a *Sfi*I linker vector is constructed, whose multiple cloning site is flanked by two three-base linkers matching the neighboring *Sfi*I linkers on *Sfi*I digestion; second, the linkers are attached to the desired genes by cloning them into *Sfi*I linker vectors; third, the genes flanked by the three-base linkers, are released by *Sfi*I digestion. In the final step, genes of interest are joined together in a simple one-step ligation.

**Index Entries:** Gene expression; cloning; ligation; optimization; xylose; yeast.

## Introduction

Most metabolic engineering approaches use genetic tools to alter a target metabolic pathway. This is usually done by sequential gene overexpression, deletion, or promoter replacement to alter gene activity *(1)*. To implement these tools, traditional cloning methods based on restriction sites are often used. This is sufficient in the construction of single insert or knockout vectors. Tweaking the activity of a single gene, however; usually

*Author to whom all correspondence and reprint requests should be addressed.

has little effect on the metabolite flux (2,3), because flux control is usually exerted at multiple steps. Also changing expression level of a single gene is not usually enough to perturb fluxes in a tightly regulated pathway, such as the glycolytic pathway (4). In addition, engineering a *de novo* metabolic pathway for a more complex product, such as polyketide, usually requires multiple steps (5). This makes the identification of target genes for strain improvement difficult. If one wishes to approach the optimal expression or activity of several different genes in a pathway by altering multiple promoters or by using genes for enzymes with various kinetic or regulatory properties, the problem spirals out of control. Simultaneous multiple-gene overexpression could help overcome such problems, so we have developed a multigene vector construction approach as a tool for strain improvement (6).

Construction of multigene vectors, especially those in which multiple variants are incorporated, calls for a more efficient vector assembly method than what can be achieved with single gene inserts. Conventional cloning methods based on restriction sites are too time-consuming and awkward for this purpose. As the number and length of gene inserts increases, the efficiency of vector assembly decreases. If multiple genes and multiple variants of each gene are required in each vector, the problem becomes similar to that encountered in assembling a library, and the efficiency of target vector construction decreases rapidly. Although, direct construction from overlapping oligonucleotides is feasible with smaller genes, the error frequency inherent with oligonucleotide synthesis (7) prohibits direct construction of larger genes.

Several techniques that are potentially suitable for multiple gene assembly, including methods involving exonuclease (8–11), uracil-DNA glycosylase (UDG) (12,13), polymerase chain reaction (PCR) (14), and enzymes with degenerate recognition sequence such as *Sfi*I (15). These methods, although diverse, are based on two mechanisms: either create compatible but different overhangs for each DNA fragment, or piece together unique fragments using overlap extension PCR. The exonuclease, UDG, and *Sfi*I methods belong to the first category. In the exonuclease method, a mild exonuclease, such as T4 DNA polymerase, is used to create a 5′ overhang by removing bases from one DNA strand from 3′ to 5′. The 5′ region of each DNA fragment is homologous to the 3′ end of the neighboring DNA fragment, thus creating sticky ends (10). Multiple DNA fragments can be joined together by exonuclease treatment and ligation. The UDG method also generates sticky ends. Primers containing uracil bases are used to amplify the genes of interest. The three prime (3′) overhangs are created by releasing the uracil bases from the dsDNA fragments with UDG treatment (12). The *Sfi*I method takes advantage of the degenerate *Sfi*I restriction site, and produces 3′ overhangs by *Sfi*I digestion. Most PCR methods are based on the overlap extension mechanism. Although these

methods are able to construct a multigene assembly, they require several PCR amplifications of each DNA fragment and are not versatile enough for assembling large multicistronic vectors. In this study, multigene assembly by joint PCR, UDG, and *Sfi*I was evaluated and a new PCR-free *Sfi*I method was developed, which we have shown to be efficient, flexible, and able to join relatively large DNA fragments (>1 kb).

## Materials and Methods

### *DNA Manipulation*

*Escherichia coli* DH5 (Gibco-BRL, Gaithersburg, MD) was routinely used for transformation of ligation products. The transformants obtained were plated on ampicillin containing Luria Bertani medium. PCR amplifications were performed in 50 μL volumes containing primers (0.5 m*M* each) custom-made by Invitrogen (Carlsbad, CA), deoxynucleotide triphospates in varying concentrations, chromosomal DNA (0.5 mg), and Taq polymerase (1 U) in the buffer recommended by the manufacturer (Promega, Madison, WI). Temperature cycling was performed by a programmable thermocycler (PTC-200 thermal cycler; MJ Research Inc., Watertown, MA) following standard protocols with minor modifications based on specific primers and amplification results.

### *UDG Method*

UDG method was performed with minor modification to the published protocol *(12)*. After UDG treatment, the reaction mix was incubated at 70°C for 10 min to disassociate the uracil-containing single stranded DNA. The DNA fragments were purified with a Qiaquick PCR purification kit (Qiagen, Hilden, Germany) and ligated in equal molar using T4 DNA ligase (New England Lab, Ipswich, MA) overnight.

### *SfiI Method*

The DNA inserts consisting of a 2.3 kb 6-phosphogluconate dehydrogenase (*GND2*) promoter-controlled transaldolase (*TAL1*) gene, 3.4 kb *GND2* promoter-controlled transketolase (*TKL1*) gene, and 2.9 kb *GND2* promoter-controlled pyruvate kinase (*PYK1*) gene, were prepared by PCR from genomic *Saccharomyces cerevisiae* DNA. The ligation strategy is shown in Fig. 1. The vector p*Sfi*-linker was constructed by subcloning the modified multiple cloning site (MCS) into pBluescript (Stratagene, La Jolla, CA) through *Sac*I and *Kpn*I sites. This modified MCS was flanked by three different *Sfi*I sites, each of which contained the desired three base overhang. Each modified MCS was synthesized by phosphorylation of two pairs of o*Sfi*-linker oligos using T4 polynucleotidekinase (New England Lab) and annealing at room temperature. The adaptors for the three *Sfi*I-linkers

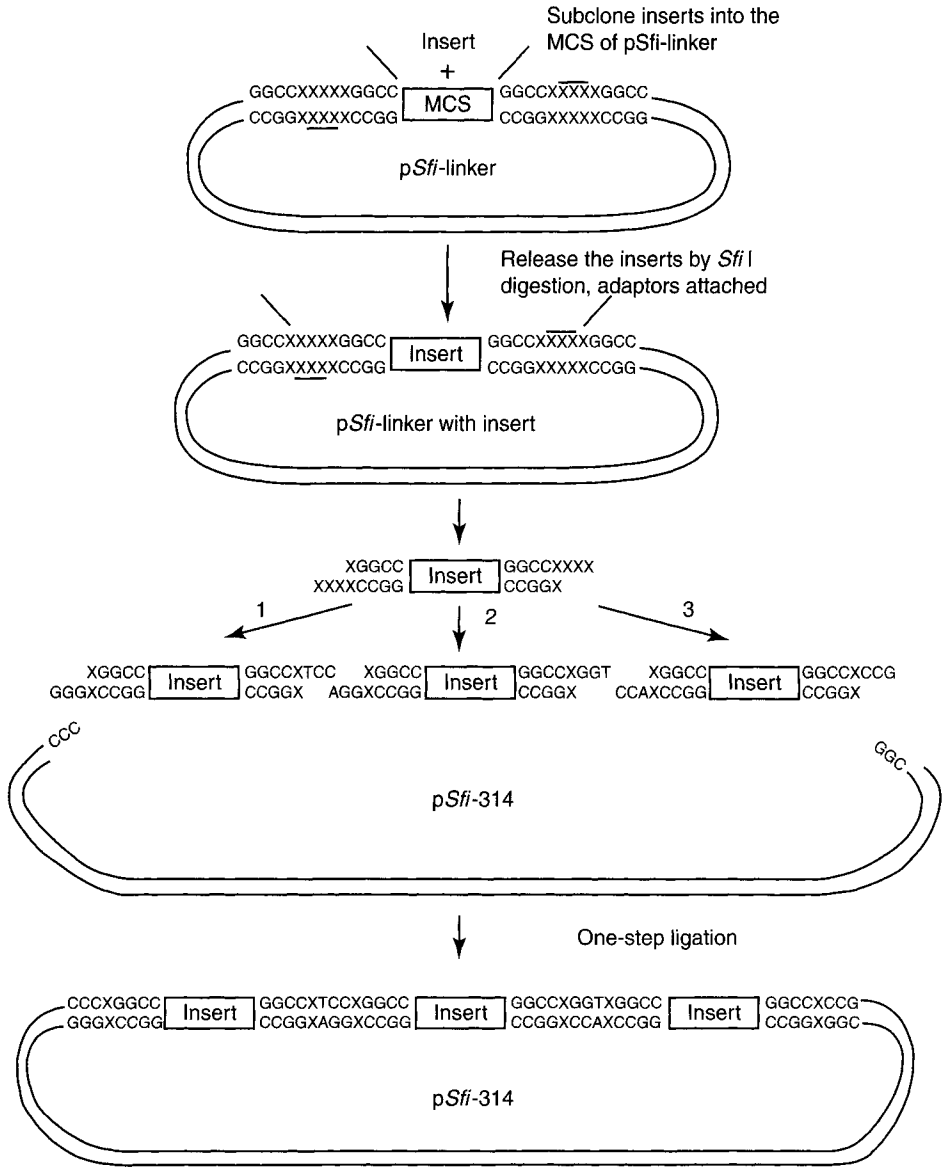


**Fig. 1.** Experimental strategy for PCR free *Sfi*I assembly method. In the first step, desired inserts were subcloned to the p*Sfi*-linker vector through *Apa*I and *Bam*HI. In the second step, inserts were released from the linker vector by *Sfi*I digestion, three base adaptors were attached to 5′ ends of the insertion on digestion. Finally inserts were joined together through these compatible adaptors.

were CCC-TCC, TCC-CCT, and CCT-CCG. For one-step assembly of the three inserts and p*Sfi*-314 *(16)*, which has the adaptor CCC-CCG, each promoter-gene cassette was subcloned to the p*Sfi*-linker through *Apa*I and *Bam*HI sites, digested with *Sfi*I, gel purified using Geneclean kit (Qbiogene, Morgan Irvine, CA), and ligated together with p*Sfi*-314 through *Sfi*I sites in equal molar concentration using T4 DNA ligase (Table 1).

Table 1
Oligos Used in This Study[a]

| Oligo name | Description | Sequence |
|---|---|---|
| ocfl 113 | Amplify *GND2* promoter region for UDG method | AGAACTAGTGGATCCCC CUCCGTCATAAC TTTGA ATCCT GTCAT |
| ocfl 114 | Amplify *RPE1* open reading frame (ORF) downstream with 23-mer linker to *GND2* promoter upstream for UDG method | ATTCAAAGTTATGACGGC GAAAUGGA TATT GATCTAGATGGC |
| ocfl 115 | Amplify *GND2* promoter region and 23-mer linker with cfl114 for UDG method | ATTTCGCCGTCATAA CTTTGAAUCCTGTCAT |
| ocfl 116 | Amplify *TAL1* ORF downstream with 22-mer linker to *GND2* promoter for UDG method | AGTTATGACGGGGGACG TTGAUTTAAGGTGGTTCC |
| oGND2p-for | Forward primer to amplify *GND2* promoter | GGGCCCCCGTCATAACT TTGAATCCTGTCAT |
| oGND2p-rev | Reverse primer to amplify *GND2* promoter | GTCGACTCTGTTCCTCG TGTTTTTTTAATTGTAG |
| oTAL1-for | Forward primer to amplify *TAL1* ORF | CTCGAGATGTCTGAAC CA GCTCAAAAGAAAC |
| oTAL1-rev | Reverse primer to amplify *TAL1* ORF | GGATCCGGGACGTTGA TTTAAGGTGGTTCC |
| oTKL1-for | Forward primer to amplify *TKL1* ORF | CTCGAGATGACTCAATTCA CTGACATTGATAAGC |
| oTKL1-rev | Reverse primer to amplify *TKL1* ORF | GGATCCTTCTTTATTGGCT TTATACTTGAATGGTG |
| oPYK1-for | Forward primer to amplify *PYK1* ORF | CTCGAGATGTCTAGATTA GAAAGATT GACCTCAT TAAACG |
| oPYK1-rev | Reverse primer to amplify *PYK1* ORF | GGATCCGAATTTTTAGC GTATCCTTTCGC C |
| oSfi-linker1 | One of the four oligos to make *Sfi*I-linker vector | TGGCCXXXXXGGCCCAC CGCGGTGGCGGCCGCTC TAGAACTAGTGGATCCC CCGGGCTGCAGGAA[b] |
| oSfi-linker2 | One of the four oligos to make *Sfi*I-linker vector | TTCGATATCAAGCTTATC GATACCGTCGACCTC GAGGGGGGGCCCGGC CXXXXXGGCCTGTAC[b] |
| oSfi-linker3 | One of the four oligos to make *Sfi*I-linker vector | AGGCCXXXXXGGCCGGGC CCCCCCTCGAGGT CGACGGTATCGATAA GCTTGATATCGAA TTCCTG[b] |

*(Continued)*

Table 1 *(Continued)*

| Oligo name | Description | Sequence |
|---|---|---|
| oSfi-linker4 | One of the four oligos to make *Sfi*I-linker vector | CAGCCCGGGGGATCCAC<br>TAGTTCTAGAGCGGC<br>CGCCACCGCGGTGGGC<br>CXXXXXGGCCAAGCT[b] |

[a]*XYL3* orf was amplified from *Pichia stipitis* wild type strain CBS6054, all other promoters and genes are amplified from *S. cerevisiae* strain YSX3. All PCR products were subcloned to TOPO vector (TOPO PCR 2.1 kit, Invitrogen) and sequenced before further cloning.

[b]XXXXX is CCCCC, ATCCA, TGGAT, GGGGG for insert 1 (TAL1 cassette); ATCCA, ACCTA, TAGGT, TGGAT for insert 2 (*TKL1* cassette); and ACCTA, ACCGA, TCGGT, TAGGT for insert 3 (*PYK1* cassette).

## Results and Discussion

We were unsuccessful in using PCR method to assemble DNA fragments with homologous regions. In our preliminary experiments, the joint PCR method worked well for joining DNA fragments without significant homology, but failed to join DNA fragments with significant homology, such as two genes driven by the same promoter (data not shown). This is probably because of the binding of homologous regions. The UDG method is based on the use of primers that contain dUTP at the 5′ end. A 3′ sticky end is formed by treatment of the PCR products with UDG, which releases the uracil bases *(12)*. Pairwise ligation was used to determine the quality of the ligation products formed with different fragments. The pairwise ligation pattern at different time-points is shown in Fig. 2. Some smearing was observed after the 30 min incubation. This became stronger with prolonged incubation, indicating residual exonuclease activity in the enzyme UDG. Hence, there could be some nonspecific activity resulting in degradation of the DNA. This may have contributed to the unsuccessful multiple DNA assembly of longer inserts (2 kb or larger) (data not shown).

### *Experimental Strategy and Results of PCR-Free SfiI Method*

A previous published *Sfi*I method *(15)* was modified by incorporating linker vectors into the assembly process (*see* Fig. 2). The linker vector was constructed by subcloning a 127 bp fragment into the pBluescript. This 127 bp fragment is generated by annealing four oligomers, which contain polylinkers, two *Sfi*I sites, and all the restriction sites in the pBluescript MCS, except *Kpn*I and *Sac*I. It adds versatility to the existing *Sfi*I method *(15)* and does not require PCR to incorporate the *Sfi*I sites. Adaptors were attached to the 5′ and 3′ ends of the DNA fragment by subcloning it into the linker vector and subsequent *Sfi*I digestion. After the fragment was attached to the adaptors onto both ends, each DNA fragment was gel purified and ligated using T4 DNA ligase in a final volume of 50 µL in

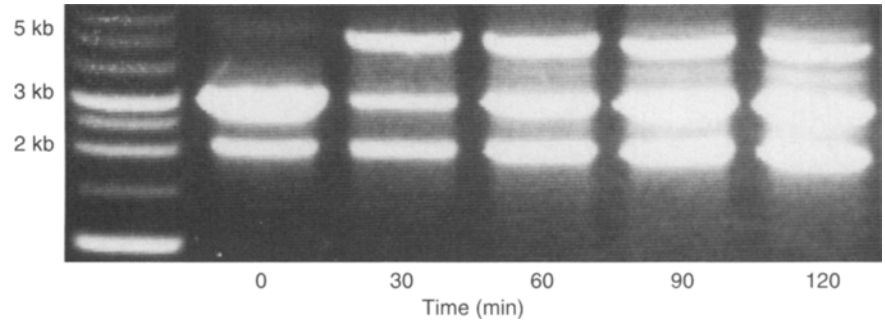


**Fig. 2.** Effect of prolonged UDG incubation on pairwise ligation. *Rpe*1 cassette (2.0 kb) and *TAL1* (2.4 kb) cassette were ligated in vitro at varied incubation time. At each time-point, the reaction was stopped by heating the samples at 70°C for 10 min. Subsequently samples were purified and ligated overnight at room temperature. Ligated products were loaded onto a 0.8% agarose gel.

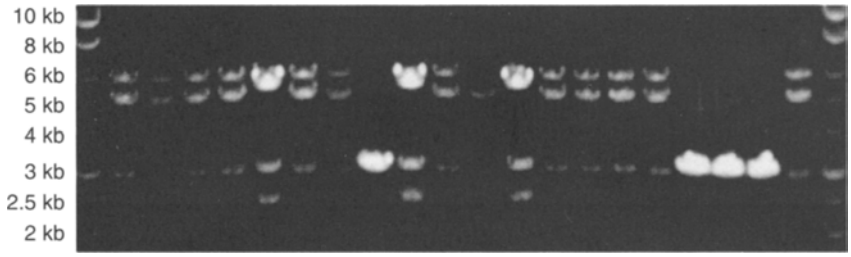


**Fig. 3.** Restriction digestion of the four piece ligation clones. About 0.5 µg of plasmid DNA were digested by 20 U *Sfi*I enzyme for 1 h in a total volume of 20 µL, and 5 µL samples were loaded onto a 0.8% agarose gel. The first and last lane were loaded with 0.2 µg of 1 kb DNA ladder (Promega). The rest of the lanes were loaded with *Sfi*I digested four piece ligation products.

equal molar. The ligation was performed at room temperature overnight. About 1.0–2.0 ng of ligation product was transformed into *E. coli* DH5α and plated on Luria Bertani-ampicillin. Plasmid DNA was isolated from 20 of the 325 ampicillin-resistant colonies. Restriction analysis showed 65% of the recovered plasmids to be correct. Results from the restriction analysis are shown in Fig. 3. Bands are present at 4.9 kb (vector), 2.3 kb (*TAL1*), 3.4 kb (*TKL1*), 2.9 kb (*PYK1*), and 5.7 kb (dimeric product of *TAL1* and *TKL1*) in Fig. 3. This dimeric digestion product likely caused the higher band intensity of *PYK1*, and lower intensities for *TAL1* and *TKL1*. Four of the correct construct were subject to additional PCR verification, and proved to be bonafide constructs (data not shown). Among the 20 plasmids subject to restriction digestion, three were nonspecific ligation products, showing band sizes of 2.3 kb (*TAL1*) and 2.9 kb (*PYK1*), missing the middle DNA *TKL1* cassette. The other three incorrect constructs were beyond our understanding. These results demonstrated that our PCR-free *Sfi*I method successfully ligated four DNA fragments together in a very flexible way: each

insert is interchangeable and can be easily replaced. Among the five nucleotide degenerate nucleotides in the *Sfi*I site, three are capable of forming "sticky" overlaps *(17)* and can be used as an adaptor. This gives $4^3 = 64$ choices of adaptors. In practice, adaptors consisting of three A/T bases do not work well *(15)*, probably because of less hydrogen bonding than G/C rich adaptors. We observed that adaptors containing at least two C/G worked much better. There are P(2 G/C) + P(3 G/C) = 32 possible adaptors, which is plenty for multiple DNA fragment assembly.

## Conclusions

Three multiple DNA assembly methods were tested. The joint PCR method and the UDG method were not successful for assembling DNA fragments. A novel assembly method based on *Sfi*I was developed and found to be efficient for joining multiple DNA fragments. Sixty five percentage of the four-piece ligation clones were correct after restriction digestion and PCR confirmation. In addition, it is versatile and does not require PCR to incorporate adaptors. Adaptors can be attached to any insert by subcloning it into a *Sfi*I-linker vector and releasing by *Sfi*I digestion.

## Acknowledgment

This work was supported by NIH grant GM67933-03 to TWJ.

## References

1. Alper, H., Fischer, C., Nevoigt, E., and Stephanopoulos, G. (2005), *Proc. Natl. Acad. Sci. USA* **102,** 12,678–12,683.
2. Cornish-Bowden, A. and Hofmeyr, J. H. (1994), *Biochem. J.* **298 (Pt 2),** 367–375.
3. van Heeswijk, W. C., Bakker, B. M., Teusink, B., et al. (1999), *Biochem. Soc. Trans.* **27,** 261–264.
4. Schaaff, I., Heinisch, J., and Zimmermann, F. K. (1989), *Yeast* **5,** 285–290.
5. Palaniappan, N., Kim, B. S., Sekiyama, Y., Osada, H., and Reynolds, K. A. (2003), *J. Biol. Chem.* **278,** 35,552–35,557.
6. Bailey, J. E. (1999), *Nat. Biotechnol.* **17,** 616–618.
7. Gao, X., Yo, P., Keith, A., Ragan, T. J., and Harris, T. K. (2003), *Nucleic Acids Res.* **31,** E143.
8. Yang, Y. S., Watson, W. J., Tucker, P. W., and Capra, J. D. (1993), *Nucleic Acids Res.* **21,** 1889–1893.
9. Kuijper, J. L., Wiren, K. M., Mathies, L. D., Gray, C. L., and Hagen, F. S. (1992), *Gene* **112,** 147–155.
10. Hsiao, K. (1993), *Nucleic Acids Res.* **21,** 5528–5529.
11. Lohff, C. J. and Cease, K. B. (1992), *Nucleic Acids Res.* **20,** 144.
12. Rashtchian, A., Buchman, G. W., Schuster, D. M., and Berninger, M. S. (1992), *Anal. Biochem.* **206,** 91–97.
13. Booth, P. M., Buchman, G. W., and Rashtchian, A. (1994), *Gene* **146,** 303–308.
14. Pachuk, C. J., Samuel, M., Zurawski, J. A., Snyder, L., Phillips, P., and Satishchandran, C. (2000), *Gene* **243,** 19–25.
15. Tsuge, K., Matsui, K., and Itaya, M. (2003), *Nucleic Acids Res.* **31,** E133.
16. Ni, H. Y. (2004), *Master Thesis,* University of Wisconsin, Madison, USA.
17. Qiang, B. Q. and Schildkraut, I. (1984), *Nucleic Acids Res.* **12,** 4507–4516.

0273-2289/1559-0291 (Online)/07/136–140/711–720/$30.00

# Fed-Batch Production of Glucose 6-Phosphate Dehydrogenase Using Recombinant *Saccharomyces cerevisiae*

LUIZ CARLOS MARTINS DAS NEVES, ADALBERTO PESSOA JR., AND MICHELE VITOLO*

*Department of Biochemical and Pharmaceutical Technology, School of Pharmaceutical Sciences, University of São Paulo. Av. Prof. Lineu Prestes, 580 B.16, 05508-900, São Paulo, SP, Brazil, E-mail: michenzi@usp.br*

## Abstract

The strain *Saccharomyces cerevisiae* W303-181, having the plasmid YEpPGK-G6P (built by coupling the vector YEPLAC 181 with the promoter phosphoglycerate kinase 1), was cultured by fed-batch process in order to evaluate its capability in the formation of glucose 6-phosphate dehydrogenase (EC.1.1.1.49). Two liters of culture medium (10.0 g/L glucose, 3.7 g/L yeast nitrogen broth (YNB), 0.02 g/L L-tryptophan, 0.02 g/L L-histidine, 0.02 g/L uracil, and 0.02 g/L adenine) were inoculated with 1.5 g dry cell/L and left fermenting in the batch mode at pH 5.7, aeration of 2.2 vvm, 30°C, and agitation of 400 rpm. After glucose concentration in the medium was lower than 1.0 g/L, the cell culture was fed with a solution of glucose (10.0 g/L) or micronutrients (L-tryptophan, L-histidine, uracil, and adenine each one at a concentration of 0.02 g/L) following the constant, linear, or exponential mode. The volume of the culture medium in the fed-batch process was varied from 2 L up to 3 L during 5 h. The highest glucose 6-phosphate dehydrogenase activity (350 U/L; 1 U = 1 μmol of NADP/min) occurred when the glucose solution was fed into the fermenter through the decreasing linear mode.

**Index Entries:** Fed-batch; glucose 6-phosphate dehydrogenase; glucose; recombinant strain; *Saccharomyces cerevisiae;* fermentation.

## Introduction

Glucose 6-phosphate dehydrogenase (G6PD) (EC.1.1.1.49), a constitutive enzyme present in all cells, is largely used as reagent in clinical diagnostic and chemical analysis methods *(1)*. Among all G6PD available sources, the *Saccharomyces cerevisiae* deserves special attention because it is a nonpathogenic microorganism, its biochemistry and genetic mechanisms have been intensely studied throughout the 20th century and it is intensely used in industry (ethanol distilleries, bakery, for instance) *(2)*. To circumvent the metabolic control on the formation of G6PD by the

*Author to whom all correspondence and reprint requests should be addressed.

wild *S. cerevisiae* strain, a quite common event for a constitutive enzyme, genetically modified yeast was used, aiming to overproduce the enzyme. Lojudice et al. *(3)* attained the recombinant strain *S. cerevisiae* W303-181 by introducing the plasmid YEpPGK-G6P in the wild yeast strain. The plasmid, in turn, was constructed from the vector YEPLAC 181—a mutant allele of *LEU2* gene of wild *S. cerevisiae* fully described *(4)*—combined with the promoter phosphoglycerate kinase 1.

Lojudice et al. *(3)* evaluated the growing and G6PD formation capability by the engineered yeast through a batch culture carried out at 35°C, pH 4.0, aeration of 2.3 vvm, and in a medium constituted of glucose (20.0 g/L), peptone (5.0 g/L), yeast extract (3.0 g/L), $Na_2HPO_4 \cdot 12H_2O$ (2.4 g/L), $MgSO_4 \cdot 7H_2O$ (0.075 g/L), and $(NH_4)_2SO_4$ (5.1 g/L). The G6PD specific activity attained under these conditions was equal to 0.300 $U/g_{cell}$. Indeed, the authors directed their efforts preferentially to the retention of the plasmid YEpPGK-G6P and not to the formation of G6PD by the modified yeast. However, it was observed through batch culture that the G6PD formation was stimulated at glucose concentration in the medium higher than 7.0 g/L *(5)*. Such a result prompted to carry out fed-batch tests in order to establish the correlation between G6PD formation and glucose concentration. The fed-batch culture, as well known, allows maintaining the substrate concentration in the medium inside well-defined interval, provided that the substrate addition into the fermenter obeys a defined feeding strategy *(6)*. From the literature consulted *([7,8]*, among others), studies have demonstrated that the optimization of the fed-batch culture can improve the gene expression by the vector. Moreover, an initial study of the *S. cerevisiae* W303-181 grown in fed-batch cultivations was performed by glucose addition according to exponential mode and the results obtained demonstrated that the high-level of G6PD formation was related to cell growth and the plasmid not excreted to the extracellular medium *(9)*. Nevertheless, more studies are necessary to establish the best fed condition including nutrient and feeding strategies. Thereby, the present work aims to evaluate the effect of the feeding strategies on the G6PD formation by *S. cerevisiae* W303-181 cultured through a fed-batch process.

## Materials and Methods

### *Microorganism and Maintenance Culture Medium*

*S. cerevisiae* W303-181 was kindly assigned by the Chemical Institute of University of São Paulo through Dra. Carla Columbano Oliveira. Lojudice et al. *(3)* described all the genetic engineering techniques used in modifying the yeast strain as well as the culture medium (CM) for maintaining its viability. The maintenance culture medium (MCM) consisted of 20.0 g/L glucose, 7.4 g/L YNB, 15.0 g/L agar, 0.02 g/L L-histidine, 0.02 g/L L-tryptophan, 0.02 g/L uracil, and 0.02 g/L adenine.

Subcultivation was done every month at 30°C for 48 h. After that the plates (stock cultures) were stored at 4°C.

### *Preparation of the Inoculum*

A loopful of the stock culture was transferred to tubes containing 5 mL of CM (the MCM without agar) and incubated at 30°C for 24 h. The content of one tube was then transferred to 500-mL Erlenmeyer flask with 95 mL of CM and incubated on a rotary shaker (NBS Gyratory Shaker, New Brunswick Scientific Co., Edison, NJ) at 150 rpm at 30°C for 18 h. A total of sixteen 500-mL Erlenmeyer flasks were used (total volume = 1.6 L).

### *Fed-Batch Culture*

A volume of 0.10 L of inoculum (total cell mass of 3.0 g on dry basis) was introduced into a 5-L bench fermenter (NBS-MF 105, coupled with a DO-81 dissolved oxygen controller) containing 1.9 L of CM. The glucose solution (20.0 g/L), the micronutrients solution (constituted of L-histidine, L-tryptophan, uracil, and adenine each one at a concentration of 0.020 g/L), or the solution containing glucose (20.0 g/L) and micronutrients (each one at 0.020 g/L) was then fed into the reactor (in pulses at intervals of 30 min) from the initial volume ($V_0$) of 2 L up to a final volume ($V_f$) of 3 L through constant, linear, or exponential mode. In all tests the fermenter filling-up-time was set at 5 h. The culture was carried out at 30°C, pH 5.7, impeller speed of 400 rpm, and aeration of 2.2 vvm. Once the feeding was completed, the fermentation was continued until the glucose concentration in the medium was negligible. Fifteen milliliter aliquots of the CM were collected at each hour for analysis. After sampling, 15.0 mL of sterile water was added back to the fermenter. A total of ten tests were realized (Table 1). On the feeding plan, the feed rates were well controlled and reproducible. Air was bubbled for 15 min before adding the inoculum. The pH of the medium was maintained at the chosen value by the controlled addition of 0.5 *M* NaOH or 0.5 *M* $H_2SO_4$. The foam was controlled, whenever needed, by addition of drops of dimethylpolysiloxane.

### *Cell Disruption*

At each hour a sample of 5 mL of the fermenting broth was centrifuged (4100*g*, 20 min) and the pellet was rinsed twofold with 5 mL of distilled water. The pellet was suspended in 50 m*M* TRIS-HCl buffer (pH 7.5), 5.0 m*M* $MgCl_2$, 0.2 m*M* ethylenediamine tetra acetic acid, 10.0 m*M* β-mercaptoethanol, 2.0 m*M* aminocaproic, and 1.0 m*M* phenylmethylsulfonyl fluoride. The cells were disrupted through stirring with 0.5-mm glass beads for 12 min (dry cell matter/mass glass beads ratio of 1 : 300). Cell debris and glass beads were removed by centrifugation (4100*g*, 20 min). The supernatant was used to measure enzyme activity.

Table 1
Identification of the Tests Regarding the Nutrient Fed and the Feeding Strategy Used

| Test (no.) | Nutrient fed | Feeding mode[a] | Equations[b] | $k$ (L/h$^2$) | $F_0$ (L/h) |
|---|---|---|---|---|---|
| 1 | G[c] | $F = F_0$ | $(V - V_0) = 0.2 \cdot t$ | – | 0.2 |
| 2 | M[d] | $F = F_0$ | $(V - V_0) = 0.2 \cdot t$ | – | 0.2 |
| 3 | G | $F = F_0 - k \cdot t$ | $(V - V_0) = 0.4 \cdot t - 0.04 \cdot t^2$ | 0.08 | 0.4 |
| 4 | M | $F = F_0 - k \cdot t$ | $(V - V_0) = 0.4 \cdot t - 0.04 \cdot t^2$ | 0.08 | 0.4 |
| 5 | G | $F = F_0 + k \cdot t$ | $(V - V_0) = 0.04 \cdot t^2$ | 0.08 | 0 |
| 6 | M | $F = F_0 + k \cdot t$ | $(V - V_0) = 0.04 \cdot t^2$ | 0.08 | 0 |
| 7 | G | $F = F_0 \cdot e^{-k \cdot t}$ | $0.92 \cdot (V - V_0) = (V_0 - V_f) \cdot (e^{-0.5 \cdot t} - 1)$ | 0.5 | 0.54 |
| 8 | M | $F = F_0 \cdot e^{-k \cdot t}$ | $0.92 \cdot (V - V_0) = (V_0 - V_f) \cdot (e^{-0.5 \cdot t} - 1)$ | 0.5 | 0.54 |
| 9 | G | $F = F_0 \cdot e^{k \cdot t}$ | $11.2 \cdot (V - V_0) = (V_f - V_0) \cdot (e^{0.5 \cdot t} - 1)$ | 0.5 | 0.045 |
| 10 | M | $F = F_0 \cdot e^{k \cdot t}$ | $11.2 \cdot (V - V_0) = (V_f - V_0) \cdot (e^{0.5 \cdot t} - 1)$ | 0.5 | 0.045 |
| 11 | G/M[e] | $F = F_0 - k \cdot t$ | $(V - V_0) = 0.4 \cdot t - 0.04 \cdot t^2$ | 0.08 | 0.4 |

For all tests the fermentor filling-up time was 5 h.
[a]Feeding mode:F (reactor feeding rate [L/h]), $F_0$ (initial reactor feeding rate [L/h]), $k$ (feeding constant [L/h$^2$]), and $t$ (time [h]).
[b]These equations were obtained by assuming that $V = V_f$ when $t = T$ and integrating as previously reported *(14)*.
[c]G, glucose.
[d]M, micronutrients (solution containing L-tryptophan, L-histidine, uracil, and adenine each one at concentration of 0.02 g/L).
[e]G/M, glucose plus micronutrients (solution containing 20 g/L of glucose and 0.02 g/L of each micronutrient cited).

## *Analytical Procedures*

### Measurement of Cell Concentration

At each hour a sample of 10 mL of the fermenting broth was filtered through a microfiltration membrane (Millipore® HAWP04700), and the cell cake was rinsed twofold with distilled water. The cell concentration, expressed as gram of dry matter/L was determined *(6)*. The variation coefficient of this technique was 4.49%.

### Measurement of Glucose Concentration

The glucose concentration was determined as the total reducing sugars present in the sample of the fermenting broth *(6)*. The variation coefficient related to this method was 3.86%.

### Measurement of G6PD

The determination of G6PD activity was made through the continuous reduction of NADP at 30°C in a spectrophotometer (Beckman DU650, $\lambda = 340$ nm) (Beckman Coulter, Fullerton, CA) as described by Bergmeyer *(10)*. One G6PD unit (U) was defined as the amount of enzyme catalyzing the reduction of 1 μmol of NADP/min under the assay conditions. Each determination was made in triplicate and the variation coefficient was less than 1%. Throughout the work the G6PD activity was expressed as U/L ($A$) and U/g dry cell ($U/g_{cell}$) ($A_{cell}$).

### Detection of Cell Viability

Samples of 1.0 mL were taken each 2 h or 3 h during the culture for detecting the cell viability. The approaches considered as viability criteria were:

- **Methylene blue colorant absorption by the cells**—the blue colored cells were counted through a conventional Neubauer chamber ($1/400 \times 0.100$ mm$^3$). One percent of colored cells was considered as the superior limit for high-viability.
- **Cell cultivation in MCM**—the appearance of a characteristic pink color in the solid medium was taken as indication of viability. The intensity of coloration was visually compared with a standard stock culture of *S. cerevisiae* W303-181, prepared as already described.

In all tests the realized yeast cells remained viable during the cultivation (through the methylen blue adsorption criteria) as well as retained the plasmid (through the criteria of cultivation in MCM).

### Kinetic Parameters

The generation time ($t_g$) was calculated as proposed by Vitolo et al. *(11)*. The cell ($P_x$) and G6PD ($P_{G6PD}$) productivity were calculated, respectively, as the ratio of cell mass ($\Delta$Mx) and enzyme activity ($\Delta A$) to the cultivation time

Table 2
Parameters Related to the Fed-batch Cultures of *S. cerevisiae* W303-181

| Test (no.) | $t_g$ (h) | $t_{max}$ (h) | $A$ (U/L) | $A_{cell}$ (U/$g_{cell}$) | $P_{G6PD}$ (U/L·h) |
|---|---|---|---|---|---|
| 1 | Nd | 6 | 190 | 65 | 32 |
| 2 | 13 | 8 | 240 | 50 | 30 |
| 3 | 4 | 5 | 350 | 65 | 70 |
| 4 | 3 | 10 | 200 | 105 | 20 |
| 5 | 7 | 12 | 270 | 61 | 23 |
| 6 | 5 | 10 | 140 | 31 | 14 |
| 7 | 6 | 12 | 234 | 36 | 20 |
| 8 | 8 | 10 | 300 | 45 | 30 |
| 9 | 5 | 5 | 300 | 48 | 60 |
| 10 | 11 | 5 | 185 | 32 | 37 |
| 11 | 15 | 7 | 96 | 22 | 14 |

Generation time ($t_g$), duration of the fermentation process ($t_{max}$), highest G6PD activity ($A$), and G6PD specific activity ($A_{cell}$). Nd, not determined.

($\Delta t$). The whole duration of the fermentation process ($t_{max}$) was set as the period of time elapsed between the beginning of fermenter feeding and the completion of glucose consumption.

## Results and Discussion

The high G6PD activities attained were 350 U/L and 300 U/L, respectively, in tests 3 (glucose fed; $t_{max}$ = 5 h; linear decreasing feeding mode) and 8 (micronutrients fed; $t_{max}$ = 10 h; exponential decreasing feeding mode) (Table 2). Taking into account the enzyme formed in test 3 was about 18% higher than in test 8, the glucose was better than the micronutrients as the fed substrate for stimulating the G6PD formation by the recombinant yeast. This result is understandable considering that glucose is the source of carbon and energy utilized by the yeast for growing as well as fulfilling the necessities of its overall metabolism, whereas the micronutrients are funneled preferentially to specific metabolic pathways (for instance, biosynthesis of nucleic acids and proteins).

From Figs. 1 and 2 it can be seen that the feeding mode as well as the type of nutrient fed influenced the G6PD specific activity ($A_{cell}$) formed by *S. cerevisiae* W303-181 along the culture. When the substrate fed through the linear decreasing strategy was the glucose (test 3), the highest $A_{cell}$ (about 65 U/$g_{cell}$) was reached at $t$ = 2 h remaining constant till the end of the culture (Fig. 1). However, when the substrate fed through the same strategy was the micronutrient solution (test 4), the highest $A_{cell}$ (about 105 U/$g_{cell}$) was reached between $t$ = 3 h and $t$ = 4 h, followed by a reduction of about 52% till the end of the fermentation (Fig. 2). Probably

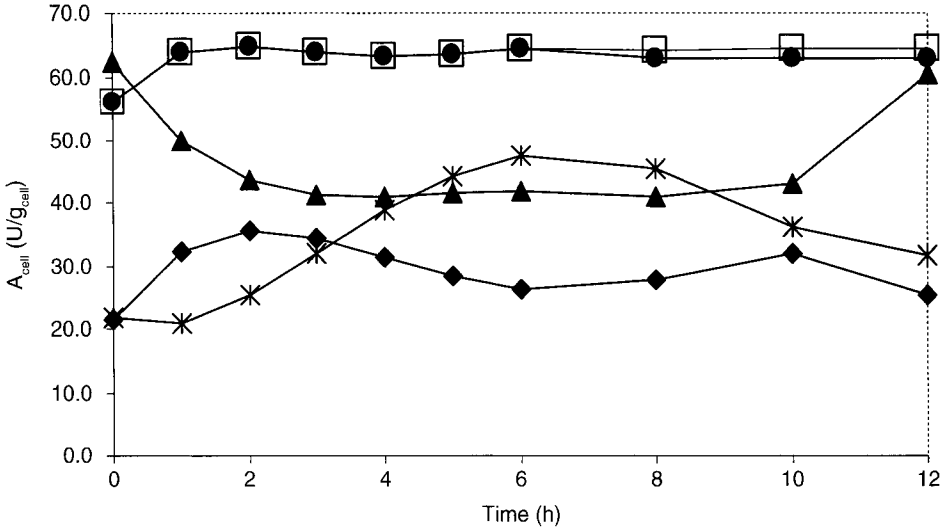


**Fig. 1.** Variation of G6PD specific activity ($A_{cell}$) during the culture time ($t$), when glucose was the fed nutrient. Tests 1 (●), 3 (□), 5 (▲), 7 (◆), and 9 (✳).

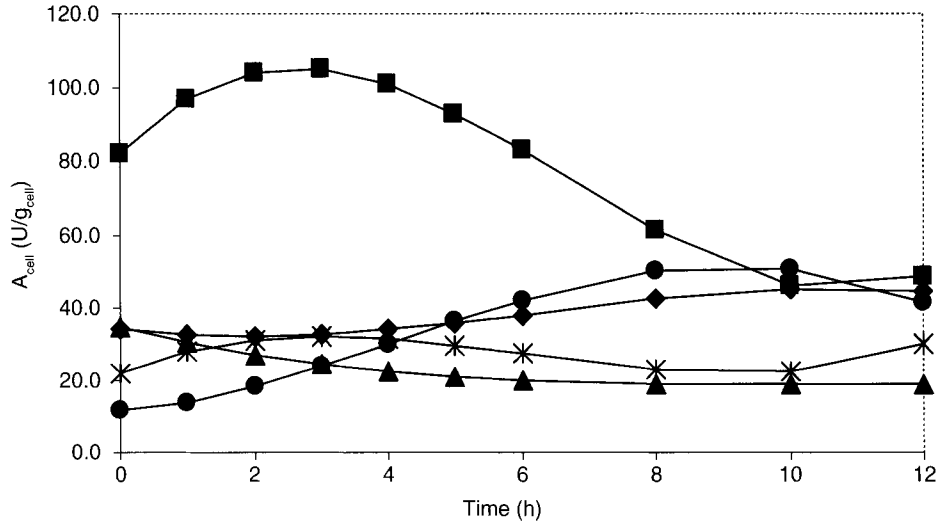


**Fig. 2.** Variation of G6PD activity ($A_{cell}$) during the culture time ($t$), when micronutrients were the fed substrate. Tests 2 (●), 4 (■), 6 (▲), 8 (◆), and 10 (✳).

an amino acid/nucleotide limitation occurred in test 4, insofar as the generation time ($t_g$) of 3 h was 25% lower than that of test 3 ($t_g$ = 4 h) (Table 2). As the *S. cerevisiae* W303-181 has in the nucleus one additional G6PD codifying gene, the dependence on amino acids and nucleotides can be more conspicuous.

The best G6PD activities attained through the decreasing feeding strategy (linear or exponential) might be because of the availability of glucose or micronutrients present in the medium to the cells. In any

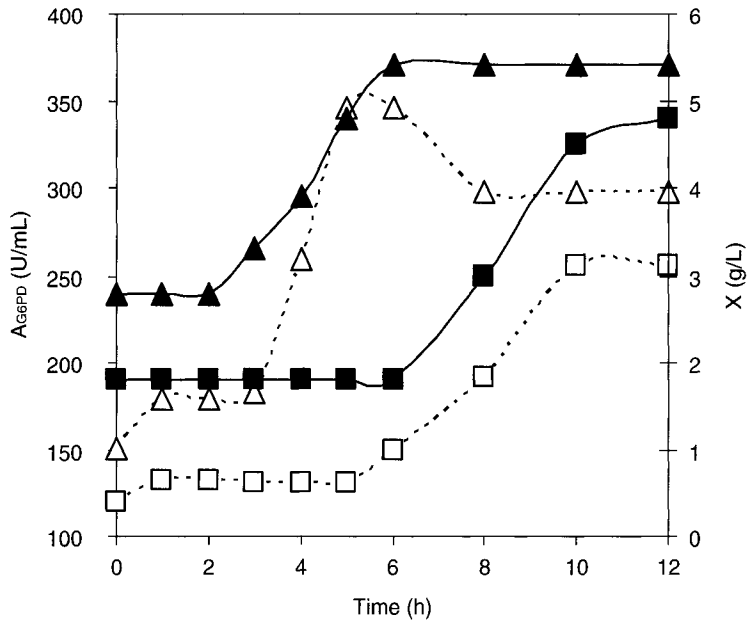


**Fig. 3.** Variation of G6PD activity concentration during the fed-batch culture of *S. cerevisiae* W303-181 in which glucose ([▲] $A_{G6PD}$ and [■] X) and micronutrients ([△] $A_{G6PD}$ and [□] X) were added according to the decreasing linear mode.

decreasing feeding strategy the amount of substrate available to the cells is always high at the beginning of the culture, diminishing afterwards. From the correspondent feeding equations (Table 1) $[(V-V_0) = 0.4 \cdot t - 0.04 \cdot t^2$ and $0.92 \cdot (V - V_0) = (V_0 - V_f) \times (e^{-0.5\,t} - 1)]$ the starting volumes for glucose (linear decreasing strategy) and micronutrients (exponential decreasing strategy) are 190 and 241 mL, respectively. According to Brown et al. *(12)* the cell growth must be stimulated over the enzyme formation in the beginning of culture, so that after a period of time (say about 2 h, in the present work) the *G6PD* gene can be derepressed and the enzyme synthesis proceeds. Such a behavior is attained as the linear or exponential feeding strategy is used.

Figure 3 shows clearly that the formation of a constitutive enzyme is linked to the cell mass formed, a well-known phenomenon *(13)*. However, what is notorious is the different behavior presented by *S. cerevisiae* W303-181 regarding the type of substrate added into the CM. When the fed substrate was glucose the cell and G6PD formation ceased after $t = 5$ h. Moreover, the final enzyme activity diminished about 14%. In the case of feeding with the micronutrients solution, a pronounced lag phase occurred before the formation of cell and G6PD. Because of the amino acid/nucleotide limitation the strain might need an adaptation period for its metabolism to the culture conditions. This might explain the oscillation of $A_{cell}$ along the time observed when comparing tests 3, 4, and 11 (Fig. 4) with the fermenter being fed, respectively, with glucose,

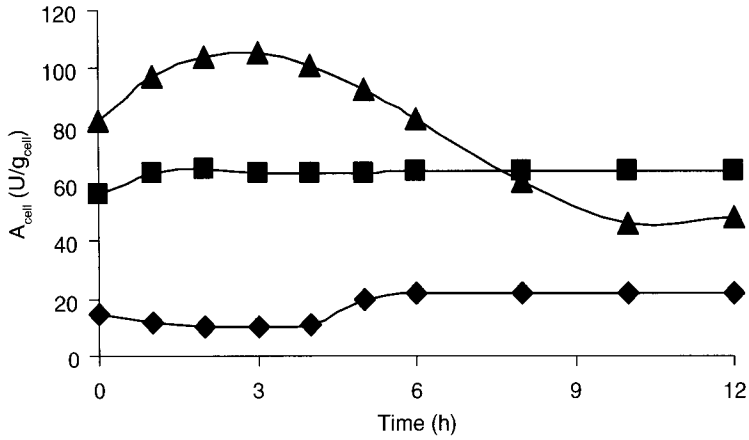


**Fig. 4.** Variation of G6PD specific activity ($A_{cell}$) during the culture time ($t$), when glucose (■), micronutrients (▲), and both (glucose and micronutrients) (◆) were the fed nutrients added according to the decreasing linear mode.

micronutrients, and both nutrients (glucose and micronutrients) according to the decreasing linear mode. The $A_{cell}$ in test 11 was 66% less than obtained in test 3 (fed with glucose) and 79% less than test 4 (fed with micronutrients). Moreover, test 11 presented the lowest G6PD specific activity ($A_{cell}$ = 22 U/$g_{cell}$) when comparing with the nutrients fed isolated in all feeding modes.

In spite of the best fed-batch culture conditions for the G6PD, formation by *S. cerevisiae* W303-181 must be still established. The result attained in test 3 ($P_{G6PD}$ = 70 U/L·h) (Table 2) is sevenfold higher than that found in the best batch fermentation process ($P_{G6PD}$ = 10.5 U/L·h), which was carried out under the same conditions, except the feeding rate *(5)*. However, the $P_{G6PD}$ was 47% lower than that found by Miguel et al. *(9)*, whose conditions differed on glucose concentration (5.0 g/L instead of 10.0 g/L as used in the present work), concentration of micronutrients (8.0 μg/L instead of 20 μg/L), and the feeding rate (0.2/h instead of 0.5/h). Through the fed-batch approach it is possible to couple the end of the substrate addition with the high formation of a desired product, which can reduce costs when the process is operated in an industrial plant *(12)*. In the present work the condition $T = t_{max}$ occurred in tests 3, 9, and 10 (Table 1).

Finally, having alternatives for G6PD production is quite important for an enzyme-importing country (like Brazil), because this particular enzyme has a large use in accurate diagnostic tests (mainly, enzyme-immunoassay technique) for the identification of several diseases, most of them endemic in developing countries. Nevertheless, the cost of the CM utilized in this work for the growth of the recombinant strain is very high, because expensive micronutrients are required. However, significant cost reduction might be attained using a low expensive CM constituted of sugarcane blackstrap molasses and yeast extract *(14)*. Other important aspect refers to the fact that the strain *S. cerevisiae* W303-181 belongs to a

public Institution (University of São Paulo), eliminating the payment of royalties to a foreign supplier by a Brazilian company, if the process is scaled up to an industrial plant.

## Conclusions

The data presented lead to conclude that the fed-batch process was suitable for G6PD production insofar as the linear or exponential decreasing feeding strategy was used. Moreover, *S. cerevisiae* W303-181 had a behavior like any yeast of the genus *Saccharomyces* in which growth and G6PD synthesis are coupled events. The G6PD synthesis depended on the amount of glucose and micronutrients present in the medium culture. The cell free extract achieved had a G6PD activity (350 U/L) comparable with those G6PD preparations already marketed.

## Acknowledgments

This work was supported by Fundação de Amparo à Pesquisa no Estado de São Paulo (FAPESP), São Paulo, SP, Brazil, Conselho Nacional de Pesquisas (CNPq) and Coordenadoria de Aperfeiçoamento de Pessoal de Nível Superior (CAPES), Brasília, DF, Brazil.

## References

1. Godfrey, T. and West, S. (1996), *Industrial Enzymology*, 2nd ed. MacMillan, London, UK: pp. 64–65.
2. Vitolo, M. (2004), In: *Enzymes as Biotechnological agents*, Said, S. and Pietro, R. C. L. R. (eds.), Legis Summa, Ribeirão Preto, SP, Brazil, pp. 207–222.
3. Lojudice, F. H., Silva, D. P., Zanchiw, N. I. T., Oliveira, C. C., and Pessoa, A., Jr. (2001), *Appl. Biochem. Biotechnol.* **91–93,** 161–169.
4. Gietz, R. D. and Sugino, A. (1988), *Gene* **74,** 527–534.
5. Das Neves, L. C. M., Pessoa, A., Jr., and Vitolo, M. (2005), *Biotechnol. Prog.* **21,** 1135–1139.
6. Echegaray, O. F., Carvalho, J. C. M., Fernandes, A. N. R., Sato, S., Aquarone, E., and Vitolo, M. (2000), *Biomass* **19,** 39–50.
7. Song, G. Y. and Chung, B. H. (1999), *Process Biochem.* **35,** 503–508.
8. Kim, C. H., Rao, K. J., Youn, D. J., and Rhee, S. K. (2003), *Biotechnol. Bioprocess Eng.* **8(5),** 303–305.
9. Miguel, A. S. M., Das Neves, L. C. M., Vitolo, M., and Pessoa, A., Jr. (2003), *Biotechnol. Prog.* **19,** 320–324.
10. Bergmeyer, H. U. (1983), In: *Methods of Enzymatic Analysis*, 3rd ed. Weinheim: Verlag Chemie, vol. 2, 539p.
11. Vitolo, M., Duranti, M. A., and Pellegrim, M. B. (1995), *J. Ind. Microbiol.* **15,** 75–79.
12. Brown, J. A., Segal, H. L., Maley, F., and Chu, F. (1987) *J. Biol. Chem.* **254,** 3689–3691.
13. Schmidell, W. and Facciotti, M. C. R. (2001), In: *Industrial Biotechnology*, Schmidell, W., Lima, U. A. L., Aquarone, E., and Borzani, W. (eds.), Edgard Blücher, São Paulo, SP, Brazil, pp. 179–192.
14. Danesi, E. D. G., Miguel, A. S. M., Yagui, C. O. R., Carvalho, J. C. M., and Pessoa, A., Jr. (2006), *J. Food Eng.* **75,** 96–103.
15. Vitolo, M., Carvalho, J. C. M., Duranti, M. A., and Breda, M. (1991), *Biomass Bioenergy* **1(5),** 301–304.

0273-2289/1559-0291 (Online)/07/136–140/721–738/$30.00

# Conversion of Aqueous Ammonia-Treated Corn Stover to Lactic Acid by Simultaneous Saccharification and Cofermentation

YONGMING ZHU,[1] Y. Y. LEE,*[,1] AND RICHARD T. ELANDER[2]

[1]*Department of Chemical Engineering, Auburn University, AL 36849, E-mail: yylee@eng.auburn.edu; and* [2]*National Bioenergy Center, National Renewable Energy Laboratory, Golden, CO 80401*

## Abstract

Treatment of corn stover with aqueous ammonia removes most of the structural lignin, whereas retaining the majority of the carbohydrates in the solids. After treatment, both the cellulose and hemicellulose in corn stover become highly susceptible to enzymatic digestion. In this study, corn stover treated by aqueous ammonia was investigated as the substrate for lactic acid production by simultaneous saccharification and cofermentation (SSCF). A commercial cellulase (Spezyme-CP) and *Lactobacillus pentosus* American Type Culture Collection (ATCC) 8041 (Spanish Type Culture Collection [CECT]-4023) were used for hydrolysis and fermentation, respectively. In batch SSCF operation, the carbohydrates in the treated corn stover were converted to lactic acid with high yields, the maximum lactic acid yield reaching 92% of the stoichiometric maximum based on total fermentable carbohydrates (glucose, xylose, and arabinose). A small amount of acetic acid was also produced from pentoses through the phosphoketolase pathway. Among the major process variables for batch SSCF, enzyme loading and the amount of yeast extract were found to be the key factors affecting lactic acid production. Further tests on nutrients indicated that corn steep liquor could be substituted for yeast extract as a nitrogen source to achieve the same lactic acid yield. Fed-batch operation of the SSCF was beneficial in raising the concentration of lactic acid to a maximum value of 75.0 g/L.

**Index Entries:** Aqueous ammonia pretreatment; biomass; cofermentation; lactic acid; simultaneous saccharification; response surface method.

## Introduction

Lactic acid is a commodity chemical widely used in the food industry, cosmetics, pharmaceuticals, and plastics. Currently, its commercial production is primarily based on microbial fermentation of starch-derived glucose or sucrose *(1)*. With the concern on feedstock cost, the use of lignocellulosic materials (LCM) as an inexpensive carbon source for lactic acid production has been

*Author to whom all correspondence and reprint requests should be addressed.

pursued (2–4). The most important component in LCM is cellulose, complete hydrolysis of which leads to glucose. Conventional fermentation technology can be integrated with cellulose hydrolysis for lactic acid production (5–7).

Next to cellulose, hemicellulose represents the other important carbohydrate fraction in LCM. Hemicellulose is a heteropolymer made up of a variety of sugar units including glucose, xylose, galactose, arabinose, and mannose. For a lignocellulosic conversion process to be economically viable, both the cellulose and hemicellulose fractions must be utilized effectively. One conversion scheme applicable for this purpose is simultaneous saccharification and cofermentation (SSCF). In this process, cellulose and hemicellulose are hydrolyzed by "cellulase" enzyme to soluble sugars (hexose and pentose sugars), which are converted into desired products by microorganism that are present in the same vessel as the enzymes.

Production of ethanol by SSCF has been investigated rather extensively (8–10). However, few studies have been made on lactic acid production from lignocellulosic substrates by this method. The key to the success of the SSCF is finding the right microorganism because very few organisms are known to efficiently utilize both hexoses and pentoses. A number of studies have been made to develop new strains for lactic acid cofermentation (11–14). Among the promising strains for our purpose is *Lactobacillus pentosus* (15–17). As a facultative heterofermentative species, *L. pentosus* ferments hexose (glucose) through the Embden–Meryerhof–Parnas (EMP) pathway under anaerobic conditions giving lactic acid as the sole product (homofermentation), and uses the phosphoketolase (PK) pathway for conversion of pentoses (xylose and arabinose) to equal moles of lactic acid and acetic acid (heterofermentation) (3). Therefore, this species has a theoretical yield of 2 mol of lactic acid/mol of hexose and 1 mol of lactic acid/mol of pentose during anaerobic fermentation.

This investigation was focused on SSCF of the cellulose and hemicellulose in corn stover pretreated by aqueous ammonia for lactic acid production using *L. pentosus* bacteria ATCC 8041. Corn stover is one of the most abundant lignocellulosic feedstocks in the United States. In this work, corn stover was pretreated by the aqueous ammonia pretreatment method developed in our laboratory and designated as soaking in aqueous ammonia (SAA) (10). Our recent study proved that SAA-treated corn stover retains most of glucan and xylan in the biomass, becomes highly susceptible to enzyme attack, and has low lignin content (10,18), making the pretreated corn stover suitable as a SSCF substrate. The microorganism *L. pentosus* ATCC 8041 was originally introduced from the Spanish Collection of Type Cultures (Valencia, Spain; No. CECT-4023). It has been reported to work well for the cofermentation of glucose, xylose, and arabinose in hemicellulose hydrolyzate from trimming wastes of vine shoots (17).

The primary objective of this study was to develop a SSCF process for production of lactic acid from SAA-treated corn stover based on the organism above. Attempts were also made to evaluate and refine the

SSCF bioprocess. For this purpose, statistical experimental design and a response surface methodology were used to analyze the effects of key variables on the SSCF process. Fed-batch operation was then applied to improve the process.

## Materials and Methods

### *Feedstock and Chemicals*

Corn stover was supplied by the National Renewable Energy Laboratory (NREL), Golden, CO, and stored at 5°C. The moisture content was 9–14%. The chemical composition of the feedstock was ([w/w], dry basis): 36.8% glucan, 21.7% xylan, 2.6% arabinan, 0.68% galactan, 0.3% mannan, and 17.2% lignin. Ammonia hydroxide (30% [w/w]) and MRS broth, the medium introduced by DeMan et. al. *(19)*, were purchased from Fisher Scientific Co., whereas yeast extract, corn steep liquor (CSL) (containing approx 50% [w/w] solids), and agar were purchased from Sigma Co (St. Louis, MO). The corn steep liquor was centrifuged at 3823 g for 20 min to separate the solids, and the supernatant—clarified corn steep liquor (cCSL)—was used as a nutritional supplement for SSCF. The recovery of the solids for marketing as animal feed has been proposed to improve wet-milling process economics *(20)*.

### *Aqueous Ammonia Treatment (SAA Pretreatment)*

SAA treatment was conducted in a 600-mL stainless steel autoclave. Heating and temperature control were done in a GC oven (Varian Model 3700, Varian, Palo Alto, CA). The treatment conditions were: liquid-to-solids ratio of 10 ([w/w]; air-dried corn stover containing 40.0 g of solids soaked in 400.0 g of 15% [w/w] ammonia solution), 90°C, and 24 h. The treated materials were washed with deionized water until the pH became near neutral. The washed corn stover was then transferred onto a piece of cheesecloth, wrapped, and squeezed by hand to remove most of the free water. By this means the moisture content of the pretreated corn stover was reduced to 69–71%, and the recovery of the corn stover solids was 65% (w/w) on the basis of the untreated solids. The dewatered solids were then subjected to composition analysis and used as the substrate for SSCF experiments. The composition of the treated solids was ([w/w] dry basis): 54.4% glucan, 24.9% xylan, 3.1% arabinan, 1.0% galactan, 0.6% mannan, and 7.7% lignin.

### *Enzyme*

The enzyme used in the SSCF experiments was Spezyme CP cellulase (Genencor Co, Palo Alto, CA). The cellulolytic activity (filter paper units [FPU]/mL) was determined using the NREL Standard Analytic Protocol 007 and found to be 30 FPU/mL *(20)*. This enzyme has proved capability of hydrolyzing both cellulose and hemicellulose in LCM *(22)*.

### Inocula Preparation

The *L. pentosus* ATCC 8041 (CECT-4023, Valencia, Spain) strain was grown aerobically on plates made up of 5.5% (w/v) MRS broth and 1% (w/v) agar at 37°C for 36 h in the presence of 10% (v/v) carbon dioxide. A fresh colony was transferred to 10 mL of 5.5% (w/v) MRS medium that was placed in a 20-mL glass tube. The headspace of the test tube was filled with 10% (v/v) of carbon dioxide, capped and placed in an incubator, which was set at 37°C without shaking. After 12 h of growth, 1 mL of the medium was transferred to 100 mL of 5.5% (w/v) MRS medium in a 250-mL Erlenmeyer flask. The headspace of the flask was also filled with 10% (v/v) of carbon dioxide and incubated at the same condition for 12 h, and then the medium was used as inocula for SSCF experiments. The dry cell mass of the inocula was determined to be 2.1–2.3 g/L. All the medium and solutions were sterilized at 121°C for 10 min before inoculation.

### SSCF in Batch Mode

SSCF batch experiments were carried out anaerobically in 250-mL Erlenmeyer flasks with a working volume of 100 mL. An Innova 4080 incubator shaker (New Brunswick Scientific Co., NJ) was used to control the temperature (37°C) and provide agitation (150 rpm). The addition of substrate (SAA-pretreated and water-washed corn stover) was based on 3.0 g of glucan input. The pH of the fermentation media was automatically controlled by addition of 6.0 g calcium carbonate. The predetermined, pretreated corn stover, calcium carbonate, yeast extract, and cCSL were added into the flasks and sterilized together at 121°C for 10 min. After the flasks cooled down, inocula and enzyme were added. The flasks were then flushed with sterile nitrogen, capped, and placed in the incubator to start the SSCF. Samples were taken at given times and after sampling, the flasks were flushed with nitrogen again to maintain the anaerobic environment.

### SSCF in Fed-Batch Mode

Assays for fed-batch SSCF were run in duplicates. The start of the fed-batch experiments was generally identical to that of the batch experiments with the only exception that a double amount of calcium carbonate (12.0 *g*) was added for pH control. Feeding of solid was applied every 36 h. At each feeding, SAA-treated and water-washed corn stover containing 3.0 g glucan were added into each of the flasks along with 2 mL of diluted Spezyme CP enzyme having a specific activity of 7.5 FPU/mL. By this procedure, the enzyme loading was maintained at 5 FPU/g-glucan throughout the experiments. The flasks were flushed with nitrogen before being placed back into the incubator shaker.

Table 1
Factors and Levels in Statistical Experimental Design

| Factor | Label | Levels | | | | |
|---|---|---|---|---|---|---|
| | | −2 | −1 | 0 | 1 | 2 |
| X1 | Enzyme loading (FPU/g-glucan) | 2.5 | 5 | 7.5 | 10 | 12.5 |
| X2 | Inoculum (% [v/v]) | 1 | 2 | 3 | 4 | 5 |
| X3 | Yeast extract (% [w/v]) | 0 | 0.2 | 0.4 | 0.6 | 0.8 |
| X4 | cCSL (% [w/v]) | 0 | 0.5 | 1.0 | 1.5 | 2.0 |

### *Statistical Experimental Design and Result Analysis*

A central composite design *(23)* with eight star points and four replicates in the center point was used to identify the significance of the variables to lactic acid yield. The experimental runs were carried out in random order. The four independent variables were enzyme loading (X1), inocula size (X2), yeast extract concentration (X3), and cCSL concentration (X4); and their respective levels (uncoded and coded) are listed in Table 1. The results were assessed by using the SAS 9.1 ADX program (SAS Institute Inc., Cary, NC). A response surface analysis was applied to examine the feasibility of substituting an inexpensive nitrogen source (cCSL) for the more expensive yeast extract in SSCF.

### *Analysis*

Vials containing slurry samples from SSCF flasks were boiled for 5 min to denature the enzyme and kill the cells. The boiled slurry samples were centrifuged at 60,000 g for 5 min, and the supernatant was taken for analyses of sugars and acids by high-performance liquid chromatography (HPLC) operated with Bio-Rad Aminex HPX-87H column (Bio-Rad Laboratories, Inc., Hercules, CA). The HPLC system includes Liquid Pump (LabAlliance, Accuflow Series III, State College, PA), RI detector (Shodex Model-71, NY), Autosampler (Alcott Chromatography, Model-718, Norcross, GA), and PeakSimple Chromatography Data System. The HPLC was operated at 85°C with a flow rate of 0.55 mL/min of DI water for sugar analysis, and at 65°C and 0.05 M $H_2SO_4$ as mobile phase for acid analysis. The carbohydrate, acetyl, and lignin contents in the solids were measured by following the NREL Standard Analytical Procedure *(21)*.

## Results and Discussion

### *Formation of Sugars and Acids in SSCF Process*

Figure 1 shows the time-course of sugars and acids in a replicated SSCF conducted in batch mode with 7.5 FPU/g-glucan, 3% (v/v) inoculum,

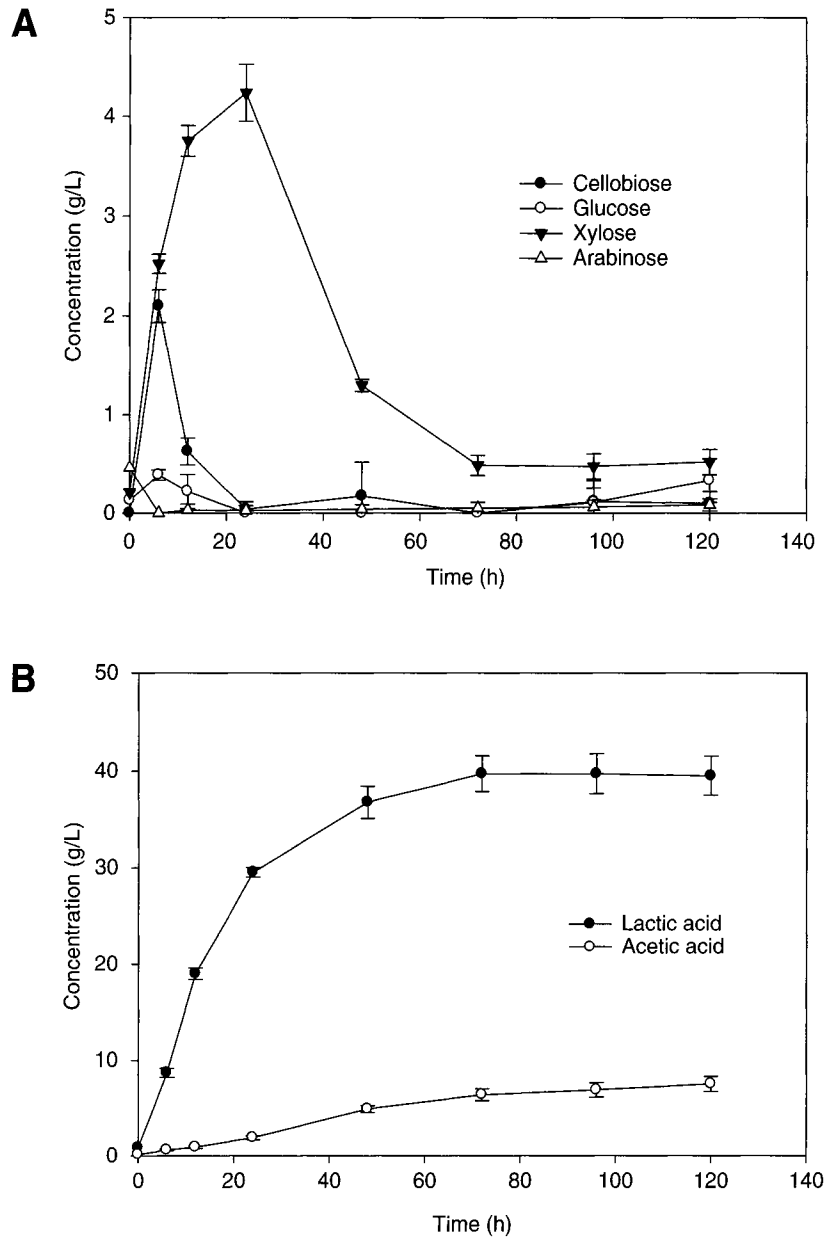


**Fig. 1.** Profiles of sugars **(A)** and acids **(B)** in SSCF of aqueous ammonia-treated corn stover. Average data from four replicates with standard deviations are presented. SSCF conditions: 3% (w/v) glucan loading, 7.5 FPU/g-glucan, 3% (v/v) inocula, 0.4% (w/v) yeast extract, 1% (w/v) cCSL, 37°C, pH 5.7, and 150 rpm.

0.4% (w/v) yeast extract, and 1% (w/v) cCSL. These data were used as the basis of the statistical experimental design (Table 1). The sugars and acids were traced from time zero when the inocula and enzyme were introduced. Glucose and arabinose remained at low levels throughout (<0.5 g/L), indicating that these sugars were efficiently assimilated after release from

biomass by hydrolysis (Fig. 1A). The cellobiose profile showed a similar pattern except that before 6 h, cellobiose accumulated up to 2.0 g/L because of the insufficient cellobiase activity of the cellulase enzyme and the lack of cellobiose-assimilating capability of this microorganism. The profiles of these three sugars (glucose, arabinose, and cellobiose) in Fig. 1 resemble those of most simultaneous saccharification and fermentation (SSF) or SSCF processes, wherein consumption of sugars are much more rapid than hydrolysis, the latter being the controlling step *(8,23,24)*. However, the assimilation of xylose was rather slow compared with that of glucose or arabinose. As the curve indicates, the xylose concentration increased almost linearly before 12 h and further increased up to 4.2 g/L before it started to decrease. Xylose consumption occurred shortly after depletion of glucose. This is a classic example of diauxic consumption of substrates wherein glucose is preferred to xylose. At this stage, glucose (and probably arabinose as well) was depleted, and xylose assimilation became the predominant reaction. Coinciding with the transition in sugar consumption, lactic acid production decelerated, whereas acetic acid accumulation accelerated (Fig. 1B). This is because xylose was converted into acetic acid in addition to lactic acid, whereas glucose assimilation under anaerobic conditions gave only lactic acid *(3)*.

Table 2 shows lactic acid and acetic acid yields as a percent of theoretical maximum under different SSCF conditions, as defined by the central composite design and represented by coded factors. Because galactose and mannose exist in very small quantities relative to glucose, xylose, and arabinose, only the latter three were used as the basis for yield calculations. The yields were calculated after deducting the contributions of acids at time zero, and assuming the assimilations of hexose (glucose) and pentoses (xylose and arabinose), respectively, follow EMP and PK pathways. The data indicate that the final (120 h) lactic acid yield fell between 0.79–0.92. It is also seen that the lactic acid yield can easily reach above 0.85 under most of the reaction conditions applied in this study. In addition, Table 2 shows that the acetic acid yield varies between 0.7 and 1.2, depending on the reaction conditions. Some of the acetic acid yields exceeded 1.0 probably because of difficulty of tightly controlling the anaerobic condition, which allowed seepage of small amount of oxygen into the flasks. This could divert part of the glucose to take PK pathway, leading to the production of acetic acid in addition to lactic acid *(1)*. Another source of the excess acetic acid production might be the conversion of galactose and mannose, which were present in small amount in the substrate and thus not accounted for in the yield calculation.

Figure 2 depicts the average yields of lactic acid and acetic acid from all 28 runs at different time intervals. The average lactic acid yield leveled off after 72 h, whereas the acetic acid yield continuously increased even after 120 h. The reason for the discrepancy is unclear at this point. We speculate that under high lactate/acetate concentrations, the metabolic pathway for

Table 2
Statistical Experimental Design and Acid Yields

| Coded levels | | | | Lactic acid (h) | | | | | | | Acetic acid (h) | | | | | | |
|---|---|---|---|---|---|---|---|---|---|---|---|---|---|---|---|---|---|
| X1 | X2 | X3 | X4 | 6 h | 12 | 24 | 48 | 72 | 96 | 120 | 6 | 12 | 24 | 48 | 72 | 96 | 120 |
| –1 | –1 | –1 | –1 | 0.11 | 0.22 | 0.40 | 0.66 | 0.74 | 0.82 | 0.87 | 0.04 | 0.08 | 0.11 | 0.21 | 0.38 | 0.58 | 0.72 |
| –1 | –1 | –1 | 1 | 0.11 | 0.28 | 0.53 | 0.77 | 0.88 | 0.89 | 0.90 | 0.05 | 0.10 | 0.17 | 0.47 | 0.72 | 0.85 | 0.95 |
| –1 | –1 | 1 | –1 | 0.13 | 0.38 | 0.61 | 0.80 | 0.83 | 0.82 | 0.83 | 0.06 | 0.16 | 0.38 | 0.77 | 0.94 | 1.03 | 1.13 |
| –1 | –1 | 1 | 1 | 0.11 | 0.38 | 0.62 | 0.78 | 0.85 | 0.86 | 0.87 | 0.07 | 0.13 | 0.32 | 0.70 | 0.84 | 0.89 | 0.95 |
| –1 | 1 | –1 | –1 | 0.14 | 0.27 | 0.52 | 0.73 | 0.82 | 0.86 | 0.90 | 0.07 | 0.10 | 0.18 | 0.43 | 0.65 | 0.79 | 0.86 |
| –1 | 1 | –1 | 1 | 0.15 | 0.32 | 0.56 | 0.71 | 0.76 | 0.77 | 0.80 | 0.09 | 0.15 | 0.26 | 0.60 | 0.92 | 1.10 | 1.21 |
| –1 | 1 | 1 | –1 | 0.16 | 0.40 | 0.61 | 0.77 | 0.85 | 0.83 | 0.83 | 0.08 | 0.17 | 0.39 | 0.73 | 0.95 | 1.02 | 1.19 |
| –1 | 1 | 1 | 1 | 0.17 | 0.42 | 0.64 | 0.78 | 0.87 | 0.86 | 0.87 | 0.08 | 0.15 | 0.37 | 0.70 | 0.92 | 0.95 | 1.05 |
| 1 | –1 | –1 | –1 | 0.12 | 0.26 | 0.49 | 0.70 | 0.78 | 0.81 | 0.85 | 0 | 0.03 | 0.06 | 0.24 | 0.47 | 0.66 | 0.80 |
| 1 | –1 | –1 | 1 | 0.13 | 0.33 | 0.60 | 0.76 | 0.89 | 0.91 | 0.91 | –0.01 | 0.04 | 0.10 | 0.37 | 0.69 | 0.89 | 0.97 |
| 1 | –1 | 1 | –1 | 0.13 | 0.45 | 0.70 | 0.86 | 0.89 | 0.90 | 0.91 | 0.03 | 0.11 | 0.30 | 0.71 | 0.82 | 0.83 | 0.89 |
| 1 | –1 | 1 | 1 | 0.13 | 0.48 | 0.74 | 0.89 | 0.92 | 0.88 | 0.90 | 0.03 | 0.11 | 0.35 | 0.76 | 0.93 | 0.96 | 1.18 |
| 1 | 1 | –1 | –1 | 0.15 | 0.30 | 0.52 | 0.73 | 0.8 | 0.86 | 0.91 | 0.03 | 0.05 | 0.05 | 0.25 | 0.48 | 0.66 | 0.77 |

| | | | | | | | | | | | | | | | | | |
|---|---|---|---|---|---|---|---|---|---|---|---|---|---|---|---|---|---|
| 1 | 1 | −1 | 1 | 0.17 | 0.38 | 0.64 | 0.79 | 0.85 | 0.89 | 0.90 | 0.06 | 0.11 | 0.17 | 0.41 | 0.69 | 0.89 | 1.01 |
| 1 | 1 | 1 | −1 | 0.21 | 0.52 | 0.73 | 0.82 | 0.89 | 0.89 | 0.89 | 0.09 | 0.15 | 0.39 | 0.75 | 0.89 | 1.03 | 1.07 |
| 1 | 1 | 1 | 1 | 0.20 | 0.53 | 0.78 | 0.91 | 0.93 | 0.92 | 0.92 | 0.08 | 0.15 | 0.44 | 0.82 | 0.89 | 0.89 | 0.98 |
| −2 | 0 | 0 | 0 | 0.11 | 0.26 | 0.42 | 0.59 | 0.68 | 0.74 | 0.80 | 0.07 | 0.11 | 0.27 | 0.50 | 0.66 | 0.87 | 0.98 |
| 2 | 0 | 0 | 0 | 0.19 | 0.46 | 0.73 | 0.84 | 0.89 | 0.88 | 0.90 | 0.05 | 0.14 | 0.35 | 0.65 | 0.84 | 0.98 | 1.13 |
| 0 | −2 | 0 | 0 | 0.09 | 0.35 | 0.62 | 0.76 | 0.91 | 0.84 | 0.90 | 0.02 | 0.10 | 0.22 | 0.64 | 0.92 | 0.91 | 1.03 |
| 0 | 2 | 0 | 0 | 0.20 | 0.45 | 0.68 | 0.89 | 0.87 | 0.90 | 0.85 | 0.09 | 0.15 | 0.33 | 0.80 | 0.96 | 1.08 | 1.25 |
| 0 | 0 | −2 | 0 | 0.08 | 0.17 | 0.33 | 0.62 | 0.71 | 0.72 | 0.79 | 0.02 | 0.04 | 0.06 | 0.07 | 0.16 | 0.25 | 0.34 |
| 0 | 0 | 2 | 0 | 0.15 | 0.48 | 0.72 | 0.87 | 0.88 | 0.91 | 0.86 | 0.08 | 0.15 | 0.45 | 0.80 | 0.91 | 1.00 | 1.08 |
| 0 | 0 | 0 | −2 | 0.16 | 0.36 | 0.59 | 0.68 | 0.82 | 0.81 | 0.86 | 0.08 | 0.13 | 0.25 | 0.60 | 0.88 | 0.91 | 0.99 |
| 0 | 0 | 0 | 2 | 0.15 | 0.43 | 0.69 | 0.88 | 0.89 | 0.84 | 0.86 | 0.07 | 0.12 | 0.30 | 0.74 | 1.02 | 1.09 | 1.24 |
| 0 | 0 | 0 | 0 | 0.18 | 0.41 | 0.65 | 0.78 | 0.79 | 0.80 | 0.79 | 0.09 | 0.12 | 0.30 | 0.76 | 1.01 | 1.10 | 1.19 |
| 0 | 0 | 0 | 0 | 0.17 | 0.41 | 0.64 | 0.84 | 0.90 | 0.90 | 0.92 | 0.07 | 0.15 | 0.23 | 0.65 | 0.80 | 0.84 | 0.92 |
| 0 | 0 | 0 | 0 | 0.15 | 0.40 | 0.63 | 0.79 | 0.88 | 0.89 | 0.88 | 0.06 | 0.10 | 0.26 | 0.66 | 0.90 | 0.98 | 1.09 |
| 0 | 0 | 0 | 0 | 0.16 | 0.38 | 0.64 | 0.83 | 0.88 | 0.90 | 0.89 | 0.07 | 0.11 | 0.26 | 0.70 | 0.91 | 0.99 | 1.11 |

*Note:* The assimilations of glucose and xylose are assumed to follow the EMP and PK pathways, respectively.

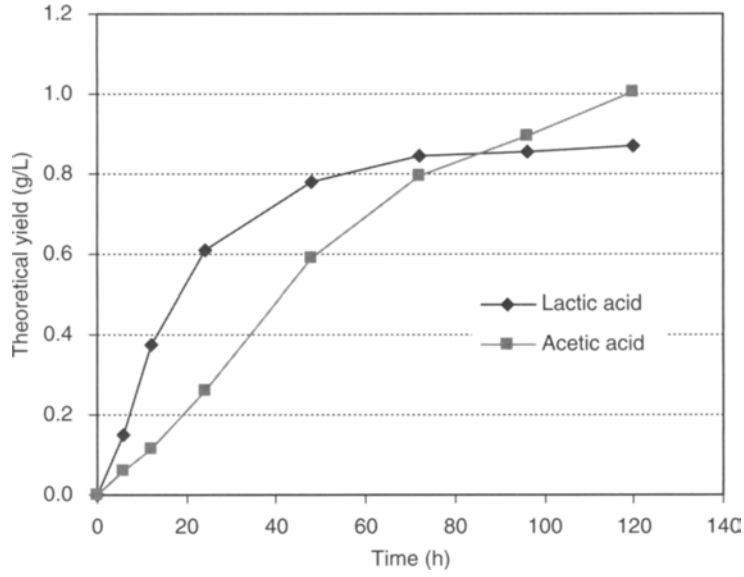


**Fig. 2.** Average acid yields from 28 runs at different time intervals. The assimilations of glucose and xylose are assumed to follow the EMP and PK pathways, respectively.

xylose utilization shifts significantly in such a way that acetic acid becomes the primary, if not the sole, product of the fermentation. As lactic acid is the product of interest in this study, the data obtained at 72 h is taken for response surface study.

### *Statistical Analysis and Response Surface*

The data associated with lactic acid yield were analyzed, and the estimates of the main effects and the interactions of the factors are listed in Table 3, with the significance of each factor represented by probability levels (*p*-values). Among the four factors under investigation, enzyme loading (X1) and yeast extract concentration (X3) were the most important for lactic acid production, followed by cCSL concentration (X4) and inoculum size (X2). Besides the main effects, the quadratic term of enzyme loading (X1) also was found to be important in lactic acid production. It is notable that the inoculum size was insignificant for final lactic acid yield despite the fact that it affected lactic acid productivity during the early stage (<24 h), implying that inocula addition for the SSCF process can be maintained at a rather low level.

In general, lactic acid bacteria are nutritionally fastidious, and costly nitrogen sources such as yeast extract and peptone have been commonly provided for lactic acid bacteria to grow fast and function effectively *(26–28)*. In order to improve the process profitability, a number of efforts have focused on substituting inexpensive nitrogen sources. Corn steep liquor has been proposed as an alternative cost-effective nitrogen source for

Table 3
Coefficient Estimates of Polynomial Models (Using Coded Levels) for Lactic Acid Yield and Significance Examination

| Term | 12 h | | | 24 h | | | 48 h | | | 72 h | | |
|---|---|---|---|---|---|---|---|---|---|---|---|---|
| | Estimate | Standard error | *t* value | Estimate | Standard error | *t* value | Estimate | Standard error | *t* value | Estimate | Standard error | *t* value |
| X1 | 0.040408 | 0.002464 | 16.3964[a] | 0.055415 | 0.006664 | 8.315467[a] | 0.040398 | 0.009114 | 4.432355[a] | 0.031773 | 0.008461 | 3.755105[b] |
| X2 | 0.022379 | 0.002464 | 9.080788[a] | 0.017545 | 0.006664 | 2.63269[c] | 0.011352 | 0.009114 | 1.245449 | −0.003163 | 0.008461 | −0.37387 |
| X3 | 0.07632 | 0.002464 | 30.96807[a] | 0.081493 | 0.006664 | 12.22858[a] | 0.052529 | 0.009114 | 5.763356[a] | 0.035861 | 0.008461 | 4.238344[a] |
| X4 | 0.020053 | 0.002464 | 8.136795[a] | 0.030001 | 0.006664 | 4.501869[a] | 0.029809 | 0.009114 | 3.270491[b] | 0.020496 | 0.008461 | 2.422365[d] |
| X1 × X1 | −0.00944 | 0.002464 | −3.82926[b] | −0.01531 | 0.006664 | −2.29738[c] | −0.020952 | 0.009114 | −2.29878[c] | −0.016618 | 0.008461 | −1.96404[d] |
| X1 × X2 | 0.003612 | 0.003018 | 1.196645 | −0.002035 | 0.008162 | −0.24932 | 0.004215 | 0.011163 | 0.377627 | 1.62E-05 | 0.010363 | 0.001562 |
| X1 × X3 | 0.013821 | 0.003018 | 4.578959[a] | 0.015459 | 0.008162 | 1.894112 | 0.014918 | 0.011163 | 1.336404 | 0.006814 | 0.010363 | 0.657579 |
| X1 × X4 | 0.00314 | 0.003018 | 1.040322 | 0.007216 | 0.008162 | 0.884107 | 0.009693 | 0.011163 | 0.868298 | 0.007069 | 0.010363 | 0.68215 |
| X2 × X2 | 0.000212 | 0.002464 | 0.086155 | 0.003968 | 0.006664 | 0.595405 | 0.006501 | 0.009114 | 0.71331 | 0.009067 | 0.008461 | 1.071636 |
| X2 × X3 | −2.20E-05 | 0.003018 | −0.00727 | −0.008185 | 0.008162 | −1.00283 | −0.007012 | 0.011163 | −0.62817 | 0.008594 | 0.010363 | 0.8293 |
| X2 × X4 | 0.000964 | 0.003018 | 0.319473 | −0.002577 | 0.008162 | −0.3157 | −0.001427 | 0.011163 | −0.12781 | −0.015373 | 0.010363 | −1.48345 |

*(Continued)*

Table 3 (Continued)

| Term | 12 h | | | 24 h | | | 48 h | | | 72 h | | |
|---|---|---|---|---|---|---|---|---|---|---|---|---|
| | Estimate | Standard error | *t* value | Estimate | Standard error | *t* value | Estimate | Standard error | *t* value | Estimate | Standard error | *t* value |
| X3 × X3 | –0.01763 | 0.002464 | –7.15521[a] | –0.026139 | 0.006664 | –3.92241[b] | –0.012758 | 0.009114 | –1.39975 | –0.014194 | 0.008461 | –1.67758 |
| X3 × X4 | –0.0109 | 0.003018 | –3.61063[b] | –0.016209 | 0.008162 | –1.98593 | –0.007115 | 0.011163 | –0.6374 | –0.007789 | 0.010363 | –0.75163 |
| X4 × X4 | –0.00017 | 0.002464 | –0.07025 | 0.002656 | 0.006664 | 0.398492 | –0.005246 | 0.009114 | –0.57559 | 0.00112 | 0.008461 | 0.132371 |
| $R^2$ | – | 0.9913 | – | – | 0.9554 | – | – | 0.8555 | – | – | 0.7992 | – |

[a] $p < 0.001$.
[b] $p < 0.01$.
[c] $p < 0.05$.
[d] $p < 0.1$.

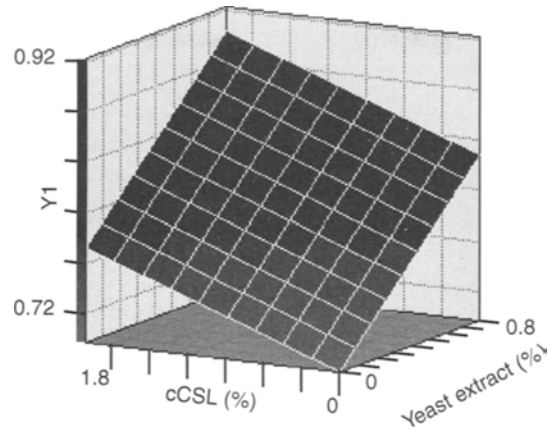


**Fig. 3.** Response surface representing lactic acid yield (Y1) as a function of yeast extract and cCSL additions. Enzyme loading: 5 FPU/g-glucan; inoculum size: 1% (w/w).

a range of microbes *(20,24,29,30)*. For example, Lawford and Rousseau *(20)* reported that in the SSCF biomass-to-ethanol process using recombinant *Zymomonas* yeast extract could be entirely replaced with corn steep liquor without affecting the growth and fermentation performance of the microorganism. Patel et al. *(13)* reported that in the lactic acid fermentation of hemicellulose hydrolyzate obtained from acid hydrolysis of sugar cane bagasse, a theoretical yield of 89% was attainable by using 0.5% corn steep liquor as the only organic nitrogen source for a thermotolerant acidophilic *Bacillus* sp.

In this study, cCSL was tested as a nutritional supplement for *L. pentosus* ATCC 8041. Figure 3 shows the response surface representing the 72-h lactic acid yield as a function of yeast extract and cCSL concentrations. The lactic acid yield increased linearly with both yeast extract and cCSL concentration, consistent with the almost linear effect of yeast extract concentration on lactic acid production by *L. casei* reported by Hujanen and Linko *(27)* using the same statistical analysis method. Further examination of the response surface shows that yeast extract can be replaced by cCSL, with an estimated ratio of 1 : 5 (g yeast extract/g cCSL), to achieve equivalent lactic acid yield.

## *Fed-Batch Experiment*

Lactic acid concentration is a key factor affecting the costs of the downstream recovery process. In this study, the concentration of lactic acid was improved by using fed-batch technique. In accordance with the statistical analysis and taking the costs into consideration, the enzyme loading was set at 5 FPU/g-glucan and inoculum size 1% (v/v). The yeast extract was maintained at a low level of 0.2% (w/v), whereas cCSL was at a comparatively high level (2% [w/v]) to compensate for the low yeast extract concentration. Four batches of SAA-treated and washed corn stover were fed to the vessels at 0, 36, 72, and 108 h, resulting in a cumulative glucan addition of 12.0 g. The time intervals for substrate additions were chosen

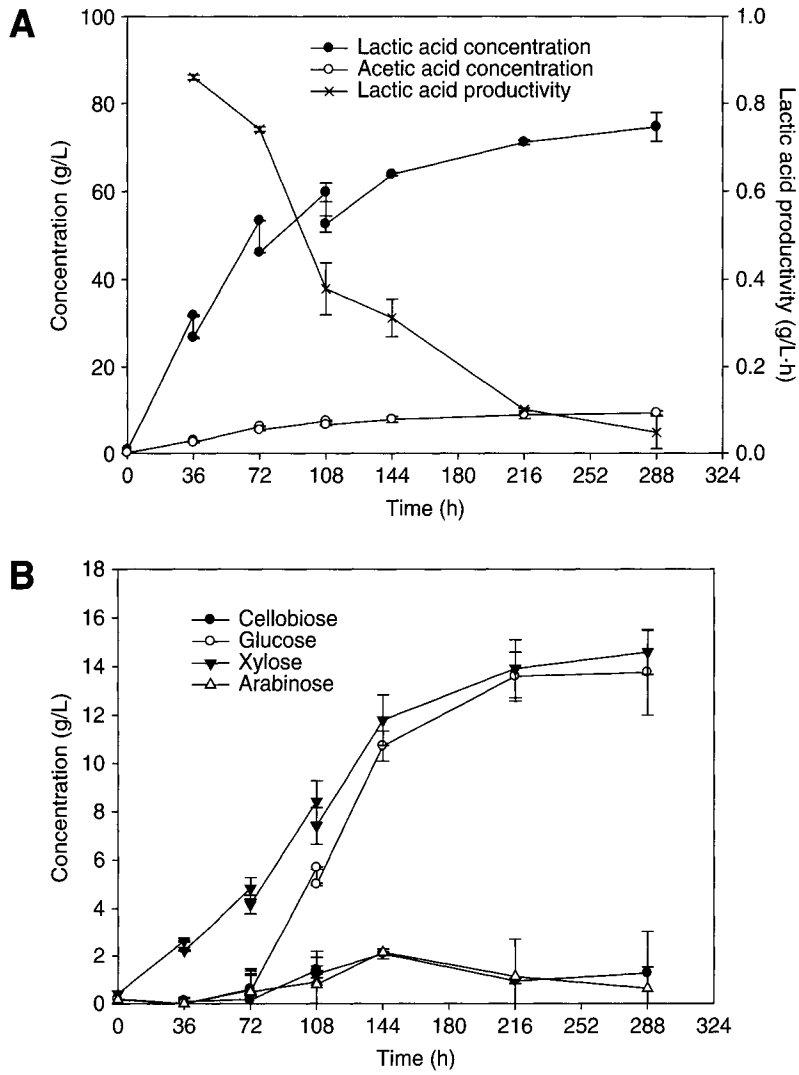


**Fig. 4.** Changes of sugar concentrations **(A)**, acid concentrations and lactic acid productivity **(B)** in fed-batch SSCF experiments. Average data from duplicates with standard deviations are presented.

in such a manner that the previous batch of solids were well liquefied as evidenced by observation. Cellulase enzyme was added in a quantity to maintain its level in the SSCF media at 5 FPU/g-glucan.

Shown in Fig. 4B are the concentrations of lactic acid and acetic acid, as well as the lactic acid productivity in the fed-batch experiment. The abrupt drops at certain points (36, 72, and 108 h) were owing to the feeding operations, which suddenly increased the working volume of the SSCF medium. The maximum lactic acid concentration achieved in these experiments was 74.8 g/L. Lactic acid concentrations increased rapidly before 72 h with an average productivity of more than 0.7 g/L·h, indicating that the microorganisms exerted high activity at the early stage. This value is comparable

with that reported by Bustos et al. *(14)* in the fermentation of hemicellulose hydrolyzate from vine-trimming waste, which was 0.800 g/L·h after 24 h. On the other hand, the productivity of lactic acid in this study rapidly dropped with time. For example, at 108 h, the productivity decreased to 0.38 g/L·h, and further decreased to 0.05 g/L·h at 288 h. The final yield of lactic acid was determined to be 0.65 g/L. It is unlikely that the decrease in productivity resulted from the lack of available carbon sources in the fermentation medium, as evidenced by the accumulations of sugars in the reaction (Fig. 4A). Also, agar plates verified that the cells remained highly viable at the end of the operation (approx $10^6$ colony forming units/mL). Therefore, it is concluded that the drastic decrease in lactic acid productivity was because of the strong inhibition of the elevated concentration of lactate/acetate anions to the lactic acid bacteria, consistent with the inhibitory effect of lactic acid (lactate ions) on *Lactobacillus* strains documented by others. Iyer and Lee *(5)* reported that the *L. delbrueckii* NRRL-B445 strain was strongly inhibited when lactic acid reached 65.0 g/L. Bustos et al. *(31)* observed marked inhibition to *L. pentosus* ATCC 8041 by lactic acid as the lactic acid concentration reached up to 46.0 g/L.

Besides the inferior glucose assimilation, xylose utilization was also inefficient, as can be seen from the comparatively low acetic acid concentration throughout the experiment (Fig. 4B) and the low final acetic acid yield (0.51 at 288 h). Therefore, if the complete utilization of carbohydrates is desirable, the inhibitory effect of the acid products must be taken into consideration before substrate additions. As an illustration, another series of fed-batch experiments was conducted with reduced substrate addition. In this experiment, SAA-treated and water-washed corn stover containing 6.0 g of glucan (in contrast to 12.0 g of glucan in the earlier fed-batch SSCF) was evenly added in two batches, one at time zero and the other at 36 h. The results are summarized in Fig. 5. Unlike in the earlier fed-batch SSCF, the xylose concentration decreased at the late stage of this experiment, although at a fairly low rate as compared with that of batch SSCF (Fig. 1A). At the end of the run (144 h), the lactic acid concentration reached 61.8 g/L, and the acetic acid 8.8 g/L. In comparison with the earlier fed-batch experiments, both lactic and acetic yields obtained in this experiment were remarkably higher (0.81 and 0.80 vs 0.65 and 0.61), indicating that inhibition was much less pronounced.

## Conclusions

This study showed that SAA-pretreated corn stover is a substrate suitable for lactic acid production. The cellulose and hemicellulose fractions in the pretreated corn stover were effectively converted to lactic acid by SSCF. The maximum lactic acid yield was more than 90% of the theoretical maximum on the basis of all available fermentable sugars. The significances of enzyme, inocula, yeast extract, and cCSL for lactic acid production were

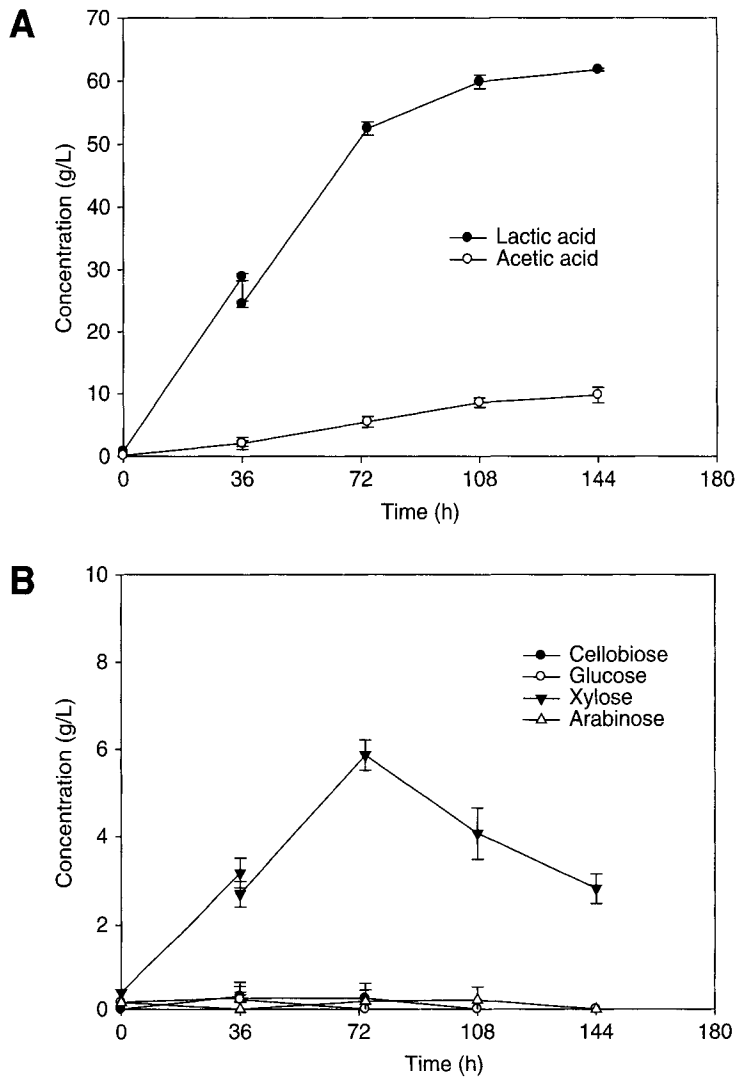


**Fig. 5.** Changes of sugar concentrations **(A)**, and acid concentrations **(B)** in reduced-feeding fed-batch SSCF experiments. Average data from duplicates with standard deviations are presented.

tested by way of statistical experiment design. It was found that the concentrations of enzyme and yeast extract are the two most significant factors affecting lactic acid yield. On the other hand, inocula size had an insignificant effect within the range of 1–5% (w/w). The response surface study indicated that yeast extract can be replaced by cCSL, without adversely affecting lactic acid yield. Acetic acid was also produced as a result of pentose assimilation (xylose and arabinose) through PK pathway. Fed-batch operation increased the lactic acid product concentration to 74.8 g/L, although at a relatively low yield (65%). Further improvement of the product concentration was difficult owing to end-product inhibition of the organism.

## Acknowledgment

The authors acknowledge the financial support provided for this research by the US/EPA through Grant-EPA-RD-83164501 (a Technology for a Sustaining Environment project).

## References

1. Litchfield, J. H. (1996), *Adv. Appl. Microbiol.* **42,** 45–95.
2. Parajo, J. C., Alonso, J. L., and Moldes, A. B. (1997), *Food Biotechnol.* **11(1),** 45–58.
3. Garde, A., Jonsson, G., Schmidt, A. S., and Ahring, B. K. (2002), *Bioresour. Technol.* **81(3),** 217–223.
4. Neureiter, M., Danner, H., Madzingaidzo, L., et al. (2004), *Chem. Biochem. Eng. Q.* **18(1),** 55–63.
5. Iyer, P. V. and Lee, Y. Y. (1999), *Biotechnol. Lett.* **21(5),** 371–373.
6. Lee, S. -M., Koo, Y. -M., and Lin, J. (2004), *Adv. Biochem. Eng./Biotechnol.* **87,** 173–194.
7. Naveena, B. J., Altaf, M.; Bhadriah, K., and Reddy, G. (2005), *Bioresour. Technol.* **96(4),** 485–490.
8. McMillan, J. D., Newman, M. M., Templeton, D. W., and Mohagheghi, A. (1999), *Appl. Biochem. Biotechnol.* **77–79,** 649–665.
9. Sedlak, M. and Ho, N. W. Y. (2004), *Appl. Biochem. Biotechnol.* **113–116,** 403–416.
10. Kim, T. H. and Lee, Y. Y. (2005), *Appl. Biochem. Biotechnol.* **121–124,** 1119–1131.
11. Dien, B. S., Nichols, N. N., and Bothast, R. J. (2001), *J. Ind. Microbiol. Biotechnol.* **27(4),** 259–264.
12. Dien, B. S., Nichols, N. N., and Bothast, R. J. (2002), *J. Ind. Microbiol. Biotechnol.* **29(5),** 221–227.
13. Patel, M., Ou, M., Ingram, L. O., and Shanmugam, K. T. (2004), *Biotechnol. Lett.* **26(11),** 865–868.
14. Patel, M., Ou, M., Ingram, M., and Shanmugam, K. T. (2005) *Biotechnol. Progress* **21(5),** 1453–1460.
15. McCaskey, T. A., Zhou, S. D., Britt, S. N., and Strickland, R. (1994), *Appl. Biochem. Biotechnol.* **45–46,** 555–563.
16. Perttunen, J., Myllykoski, L., and Keiski, R. L. (2001), Lactic acid fermentation of hemicellulose liquors and their activated carbon pretreatments. Focus on Biotechnology, 4 (Engineering and Manufacturing for Biotechnology), 29–38.
17. Bustos, G., Moldes, A. B., Cruz, J. M., and Dominguez, J. M. (2004), *J. Sci. Food Agric.* **84(15),** 2105–2112.
18. Zhu, Y., Kim, T. H., Lee, Y. Y., Chen, R., and Elander, R. T. (2005), *Appl. Biochem. Biotechnol.* **129–132,** 586–598.
19. DeMan, J. D., Rogosa, M., and Sharp, M. E. (1960) *J. Appl. Bact.* **23,** 130–135.
20. Lawford, H. G. and Rousseau, J. D. (1997), *Appl. Biochem. Biotechnol.* **63–65,** 287–304.
21. NREL (1996), Laboratory analytical procedures, National Renewable Energy Laboratory, Golden, CO.
22. Zhu, Y., Lee, Y.Y., and Elander, R .T. (2004), *Appl. Biochem. Biotechnol.* **117,** 103–114.
23. Box, G. E. P. and Draper, N. R. (1987), *Empirical Model-building and Response Surfaces,* John Wiley & Sons, Inc.
24. Rivas, B., Moldes, A. B., Dominguez, J. M., and Parajo, J. C. (2004), *Int. J. Food Microbiol.* **97(1),** 93–98.
25. Spindler, D. D., Wyman, C. E., and Grohmann, K. (1989), *Biotechnol. Bioeng.* **34(2),** 189–195.
26. Mercier, P., Yerushalmi, L., Rouleau, D., and Dochain, D. (1992), *J. Chem. Technol. Biotechnol.* **55(2),** 111–121.
27. Hujanen, M. and Linko, Y. -Y. (1996), *Appl. Microbiol. Biotechnol.* **45(3),** 307–313.
28. Nancib, N., Nancib, A., Boudjelal, A., Benslimane, C., Blanchard, F., and Boudrant, J. (2001), *Bioresour. Technol.* **78(2),** 149–153.

29. Amartey, S. and Jeffries, T. W. (1994), *Biotechnol Lett.* **16(2),** 211–214.
30. Tellez-Luis, S. J., Moldes, A. B., Vazquez, M., and Alonso, J. L. (2003), *Food Bioprod. Proc.* **81(C3),** 250–256.
31. Bustos, G., Moldes, A. B., Cruz, J. M., and Dominguez, J. M. (2005), *Biotechnol. Prog.* **21(3),** 793–798.

0273-2289/1559-0291 (Online)/07/136–140/739–740/$30.00

SESSION 5
Bioprocessing and Separations R&D

# Introduction to Session 5

LUCA ZULLO*,[1] AND SETH W. SNYDER†,[2]

[1]*Cargill, Inc., Minneapolis, MN 55440, E-mail: luca_zullo@cargill;*
*and* [2]*Chemical and Biological Technology, Argonne National Laboratory, Argonne IL 60439, E-mail: seth@anl.gov*

Production of bio-based products that are cost competitive in the market place requires well-developed operations that include innovative processes and separation solutions. Separations costs can make the difference between an interesting laboratory project and a successful commercial process. Bioprocessing and separations research and development addresses some of the most significant cost barriers in production of biofuels and bio-based chemicals. Models of integrated biorefineries indicate that success will require production of higher volume fuels in conjunction with high margin chemical products. Addressing the bioprocessing and separations cost barriers will be critical to the overall success of the integrated biorefinery.

Production of fuels and chemicals offers distinct technical challenges in comparison with related fields. In pharmaceuticals, high-valued products can support complex and expensive separation processes. In petrochemicals, product concentrations are typically significantly higher than possible with aqueous fermentations. The field has focused on technologies such as designing bioreactors to facilitate product recovery, or development of novel membrane materials and technologies that reduce the energy burden in separating dilute aqueous products. Modeling and simulations have played

*Author to whom all correspondence and reprint requests should be addressed.
†Also for correspondence.

strong roles is designing new processes and evaluating their potential performance. Session 5 included oral presentations on scaling up fed-batch processes, innovative membrane bioreactors and product recovery systems, evaluation of processes to extract products from wood pulping, and mathematical models and CFD simulations of reactors and fermentations.

The poster session described a wide variety of projects including production of ethanol and organic acids, sugar separations, pretreatment, esterification of organic acids, anaerobic digestion, biodegradation, fatty acid and biodiesel production, utilization of coproducts, new materials, strains, catalysts, processes, and simulations to improve fermentations, and so on. In addition, bioprocessing and separations of different biomass sources was presented in several posters. What is apparent is that the field is open and has drawn the attention of international distribution of researchers from microbiologists through chemical engineers. There is no single bullet, but a suite of technology solutions that are developing. Some will be valuable for large volume products such as ethanol whereas others will have specific product or feedstock niches. The work directly addresses some of the most significant cost barriers to production of fuels and chemicals from biomass.

0273-2289/1559-0291 (Online)/07/136–140/741–752/$30.00

# Economic Evaluation of Isolation of Hemicelluloses From Process Streams From Thermomechanical Pulping of Spruce

TOBIAS PERSSON, ANNA-KARIN NORDIN, GUIDO ZACCHI, AND ANN-SOFI JÖNSSON*

*Department of Chemical Engineering Lund University, P.O. Box 124, SE-221 00 Lund, Sweden, E-mail: ann-sofi.jonsson@chemeng.lth.se*

## Abstract

Hemicelluloses, which are abundant in nature and have potential use in a wide variety of applications, may make an important contribution in helping relieve society of its dependence on petrochemicals. However, cost-efficient methods for the isolation of hemicelluloses are required. This article presents an economic evaluation of a full-scale process to isolate hemicelluloses from process water from a thermomechanical pulp mill. Experimental data obtained in laboratory scale were used for the scale up of the process by computer simulation. The isolation method consisted of two process steps. The suspended matter in the process water was removed by microfiltration and thereafter the hemicelluloses were concentrated by ultrafiltration, and at the same time, separated from smaller molecules and ions in the process water. The isolated hemicelluloses were intended for the production of oxygen barriers for food packaging, an application for which they have been shown to have suitable properties. The solution produced contained 30 g hemicelluloses/L with a purity (defined as the ratio between the hemicelluloses and the total solids) of approx 80%. The evaluation was performed for a plant with a daily production of 4 metric tonnes (t) of hemicelluloses, which is the estimated future need of barrier films at Tetra Pak (Lund, Sweden). The production cost was calculated to be € 670/t of hemicelluloses. This is approx 9 times lower than the price of ethylene vinyl alcohol, which is produced by petrochemicals and is currently used as an oxygen barrier in fiber-based packaging materials. This indicates that it is possible to produce oxygen barriers made of hemicelluloses at a price that is competitive with the materials used today.

**Index Entries:** Barrier film; economic evaluation; galactoglucomannan; hemicelluloses; ultrafiltration; thermomechanical pulp.

*Author to whom all correspondence and reprint requests should be addressed.

## Introduction

Lignocelluloses, i.e., celluloses, hemicelluloses, and lignin constitute approx 80% of the biomass on earth and could be utilized much more widely in the future. Hemicelluloses (i.e., heteropolysaccharides found in plant cell walls) may make an important contribution in helping relieve society of its dependence on petrochemicals, but cost-efficient methods for the isolation of hemicelluloses are required. Examples of potential applications of hemicelluloses are the production of barrier films *(1,2)* and hydrogels *(3)*, hydrolysis and fermentation to produce ethanol *(4)*, and as a feedstock for xylitol production *(5)*. The extraction of hemicelluloses from different raw materials has long been studied *(6–11)*. A promising hemicellulose source is the process streams in thermomechanical pulp mills. A method using membrane filtration to isolate hemicelluloses from process water from thermomechanical pulping of spruce has been developed in a previous study *(12)*. A screening of several different membranes was performed in this work to find the most suitable membrane material for this process.

The aim of the present study was to perform an economic evaluation of the isolation of hemicelluloses from process water from thermomechanical pulping of spruce. The purified and concentrated hemicelluloses were intended for the production of barrier films in fiber-based packaging materials. The dominating hemicellulose in spruce is *O*-acetyl galactoglucomannan, which has been shown to have suitable properties for the production of oxygen barriers intended for food packaging *(1)*. To enable an economic evaluation, experimental results are needed. Experiments were therefore performed in laboratory scale. The choice of membranes and operating conditions in the experiments was based on results from a previous investigation *(12)*.

## Materials and Methods

### *Raw Material*

The raw material was process water from thermomechanical pulping of spruce from Stora Enso Kvarnsveden Mill AB, Sweden. The process water was collected from the final dewatering step of the pulp. The pH of the process water was approx 4.6 and the amount of dissolved hemicelluloses, defined as oligo- and polysaccharides including acetyl groups, was around 0.5 g/L. The average molecular mass of the hemicelluloses in the process water was approx 10 kDa and the monosaccharide composition of the oligo- and polysaccharides was similar to that found in the hemicellulose galactoglucomannan.

### *Experimental Procedure*

The method used to isolate hemicelluloses from the process water involves two steps: (a) pretreatment to remove solids by microfiltration and

(b) concentration and purification of hemicelluloses by ultrafiltration and diafiltration. The process was performed batch-wise with a starting volume of approx 1 $m^3$. All liquid streams were analyzed regarding oligo- and polysaccharide and acetyl concentration, to estimate the concentration of hemicelluloses. Monosaccharide content, total solids, and ash were determined to evaluate the purification efficiency.

### Pretreatment

The process water was microfiltrated in a Vibratory Shear-Enhanced Processing (VSEP) unit (series L/P, New Logic, Emeryville, CA, USA) to remove the solids. The membrane stack consisted of 19 double-sided polytetrafluoroethylene membrane discs. The membrane pore diameter was 10 μm and the total membrane area was 1.57 $m^2$. The pump was a displacement pump (G-03, Wanner Engineering Inc., Minneapolis, MN). Microfiltration was carried out at a transmembrane pressure between 250 and 300 kPa and a temperature of 25°C. The vibration frequency was 50 Hz, which corresponds to the amplitude of 19 mm.

### Concentration and Purification

Ultrafiltration and diafiltration were performed in a DDS 20 LAB module unit (Alfa Laval Corp., Lund, Sweden). In earlier work *(12)*, it was found that the ETNA01PP membrane (Alfa Laval) had good performance for ultrafiltration of the process stream. In the same study it was shown that a membrane with higher cutoff had better separation capability. The ETNA membranes are made of surface-modified polyvinylidene fluoride, which has been found to be very resistant to fouling *(13)*. Thus, two ETNA membranes with different cutoffs were compared: ETNA01PP (1 kDa) and ETNA10PP (10 kDa) (Alfa Laval). Two different membrane stacks were used, one with six double-sided ETNA01PP membrane discs with a total membrane area of 0.21 $m^2$ and one with eight double-sided ETNA10PP membrane discs with a total membrane area of 0.28 $m^2$. The pump was a displacement pump (D-25, Wanner Engineering Inc.) and the circulation flow rate was measured with a rotameter. The permeate flow was measured gravimetrically with a balance (FX-3000, A&D Company Ltd., Tokyo, Japan).

The average transmembrane pressure was 1.0 MPa and the temperature 50°C. The circulation flow rate was 5.2 L/min, which corresponds to a cross-flow velocity of 0.5 m/s. Two temperature-equilibrated diavolumes of deionized water were added at the same flow rate as the permeate flow during diafiltration. The number of diavolumes corresponds to the ratio between the volume of water added during diafiltration and the constant volume of feed solution in the system *(14,15)*. The membranes were cleaned with 0.5 wt% Ultrasil 10 (Henkel, Düsseldorf, Germany) at 50°C for 45 min and thoroughly rinsed with deionized water before the experiments.

## Analysis

The ash content and total solids were determined according to the standardized methods of the National Renewable Energy Laboratory (NREL, US Department of Energy) *(16,17)*. The monomeric sugar composition and the concentration of oligo- and polysaccharides were analyzed by acid hydrolysis according to the standardized method of NREL *(18)*. Monomeric sugars were analyzed before and after acid hydrolysis and the oligo- and polysaccharide content was calculated from the difference in monosaccharide concentration before and after hydrolysis. Anhydro corrections of 0.9 and 0.88 were used for the hexoses and pentoses, respectively.

High-performance anion-exchange chromatography coupled with pulsed amperometric detection using an ED40 electrochemical detector (Dionex, Sunnyvale, CA) was used to analyze the monomeric sugars. The chromatograph was equipped with a gradient pump, (GP40, Dionex) an autosampler (AS50, Dionex), and a Carbo Pac PA10 guard and analytical column (Dionex). Millipore water with 2 m*M* NaOH was used as eluent at a flow rate of 1 mL/min, and the injection volume was 10 µL. D-mannose, D-glucose, D-galactose, D -xylose, and L-arabinose (Fluka Chemie AG, Buchs, Switzerland) were used as standards.

The acetic acid content was analyzed before and after acid hydrolysis and the concentration of acetyl groups in the hemicelluloses was calculated from the difference in acetic acid concentration before and after hydrolysis. The acetyl group concentration was multiplied by a factor of 0.98 to correct for the protonation. The acetic acid was analyzed using high-performance liquid chromatography equipped with a refractive index detector (Shimadzu, Kyoto, Japan) and an Aminex HPX-87H column (Bio-Rad, CA). Millipore water with 5 m*M* $H_2SO_4$ was used as eluent at a flow rate of 0.5 mL/min at 65°C. The injection volume was 20 µL. Acetic acid (Merck, Darmstadt, Germany) was used as standard. The hemicellulose concentration was defined as the sum of the concentrations of oligo- and polysaccharides and the acetyl groups.

## Economic Evaluation

The investment and the operating costs for the isolation method were calculated to evaluate the profitability of the process. The annual repayment of the investment costs was calculated with the annuity method:

$$C_{\text{repayment}} = C_{\text{investment}} \times \frac{i \times (1+i)^n}{[(1+i)^n - 1]} \quad (1)$$

where $C_{\text{investment}}$ is the investment cost of the equipment, $i$ is the interest rate, and $n$ is the depreciation time in years. An interest rate of 8% and 10 yr of depreciation time were used. The calculations were based on 8500

operating h/yr and an electricity cost of 3¢/kWh, in accordance with the Swedish pulp and paper industry.

A feed concentration of 0.5 g/L of hemicelluloses was used in the calculations and the process was designed to handle a feed of 400 $m^3$/h, which corresponds to a production rate of approx 4 metric tonnes (t) of hemicelluloses/d. This is the estimated demand of hemicelluloses for the production of barrier films in fiber-based packaging materials at Tetra Pak (Lund, Sweden). The concentration of hemicelluloses required for barrier film production in industrial scale is today unknown. In this calculation, the concentration of hemicelluloses in the product was chosen to be 30 g/L.

### Pretreatment

In the pulp and paper industry, drum filters are the standard method for removing fibers and solids from various process streams. One of the leading manufacturers of drum filters (Algas, Moss, Norway) suggested a drum filter with a 30-μm polyester cloth filter, based on their experience from similar applications. The drum filter had a net active filter area of 36 $m^2$, which would be sufficient to handle the design flow of 400 $m^3$/h according to the manufacturer. The energy demand of the filter is approx 21 kW. The recovery of hemicelluloses in the pretreatment step is expected to be very high because the content of suspended matter is very low. Therefore, a recovery of 100% was assumed in the calculations. In the laboratory experiments, removal of water insoluble matter was performed in a VSEP unit as a small-scale drum filter was not available. However, the quality of the water is expected to be equal irrespective of whether a VSEP unit or a drum filter is used for pretreatment.

### Concentration and Purification

Owing to the results obtained from the experimental study the ETNA10PP was chosen for the economic evaluation. Spiral wound elements (8 × 38 in.) with 30 mil spacers with three elements per pressure vessel were chosen to be used in the full-scale ultrafiltration plant. The estimated lifetime of these membranes are 24 mo (according to the manufacturer). The temperature of the process water in the pulping process is 80°C. However, the upper temperature limit for the ETNA spiral wound elements is 60°C. The process water must thus be cooled, e.g., in a heat exchanger. The investment cost of a shell-and-tube heat exchanger with 200 $m^2$ surface area was calculated with Icarus Process Evaluator (Aspen Tech, Cambridge, MA). The price of the cooling water used in the heat exchanger was taken from the literature *(19)*.

The ultrafiltration plant was assumed to have multistage recirculation design with the same membrane area in all stages. This is the most common design for ultrafiltration plants regardless of application. The investment and operating costs of the membrane plant, was calculated for different number of stages. The cost for one extra stage was included in the

Table 1
Economic Data Used to Calculate the Investment and Operating Costs of the Ultrafiltration Plant

| Costs | |
|---|---|
| Basic installation (€)[a] | 50,000 |
| Instrumentation, piping, and so on per stage (€)[a] | 80,000 |
| Membranes and housing (€/m$^2$)[a] | 150 |
| Cleaning equipment (€)[b] | 50,000 |
| Membrane replacement (€/m$^2$)[a] | 50 |
| Cleaning (€/yr)[c] | 300,000 |
| Maintenance[b] | 2% of investment cost |
| Number of operators[c] | 1 |
| Labor cost (€/h)[c] | 20 |

[a]Alfa Laval
[b]From ref. 15.
[c]Experience from the ultrafiltration plant at Stora Enso Nymölla mill.

calculations. This extra stage is necessary in the plant in order to be able to take one stage out of the operation for membrane cleaning and replacement, and still operate the ultrafiltration plant continuously. The calculations were based on membrane area and energy consumption of the ultrafiltration plant calculated by solving the mass balances in the process, i.e., the amount of hemicelluloses and process water entering and exiting each stage and the entire membrane plant. This was performed with the computer software Matlab (The Math Works Inc., Natick, MA). The flux in the different stages, i.e., as function of concentration, was obtained from experimental results. The energy requirement of the initial feed pump and the booster pumps was calculated for a plant operating at 1.0 MPa. The efficiency of the pumps was chosen to be 80% and the pressure drop in each spiral wound element was approximated to 0.08 MPa. Economic data were received from Alfa Laval, Stora Enso Nymölla mill (Sweden) and from estimates found in the literature *(15)*. These data are shown in Table 1.

## Results and Discussion

### *Flux During Concentration of the Hemicelluloses*

The concentration of total solids differed in different batches from the pulp mill. It was between 2 and 6 g/L, probably depending on how, and when, samples were withdrawn from the storage tank for process water. Although there was a variation in concentration of total solids in the raw process water, the pretreated process water had uniform properties with a concentration of total solids of 1.8 g/L, of which approx 30% was hemicelluloses. The pretreated process water was ultrafiltrated to increase both the purity and concentration of the hemicelluloses. The hemicelluloses

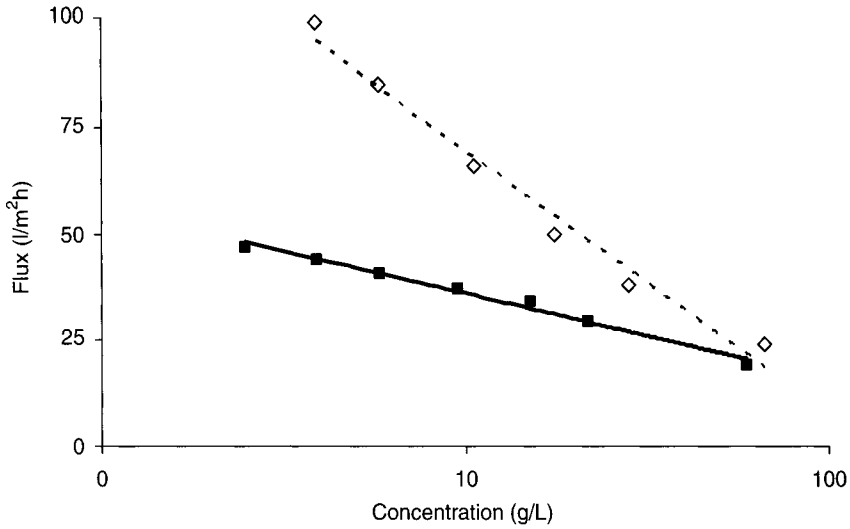


**Fig. 1.** Correlation between the flux and the concentration of hemicelluloses in the feed solution for the ETNA01PP (solid line) and ETNA10PP (dashed line) membranes.

were concentrated to 59 g/L with the ETNA01PP membrane and to 66 g/L with the ETNA10PP membrane. The retention of hemicelluloses was 98% for both membranes. The flux was significantly higher for the ETNA10PP membrane than for the ETNA01PP membrane, as shown in Fig. 1. The flux decreased as the hemicelluloses were concentrated in the feed. The relation between the flux and the concentration of hemicelluloses was determined by plotting the flux against the concentration on a logarithmic scale. The relation is linear, which is in accordance with the theory that states that this relation should be linear under limiting flux conditions *(20)*. This relation was used in the economic evaluation to calculate the flux in the different stages.

### *Purity During Concentration of The Hemicelluloses*

Purity increases during concentration using ultrafiltration if the retention of the product is higher than the retention of other compounds *(15)*. In earlier work *(12)*, it was found that a hydrophilic membrane with a cut off of 5 kDa had better separation capability with respect to hemicelluloses and contaminants (salts and monosaccharides) than a hydrophilic membrane with a cut off of 1 kDa. Based on these results, it was expected that the purity (defined as the ratio between the hemicelluloses and the total solids) would increase faster during the concentration of hemicelluloses with ETNA10PP. This is verified by Fig. 2, which shows the purity as function of hemicellulose concentration.

The composition of the total solids in the process water changed drastically during concentration of the hemicelluloses. Table 2 shows the composition after pretreatment by microfiltration and after concentration to 66 g/L with ultrafiltration using the ETNA10PP membrane. The ash is partially

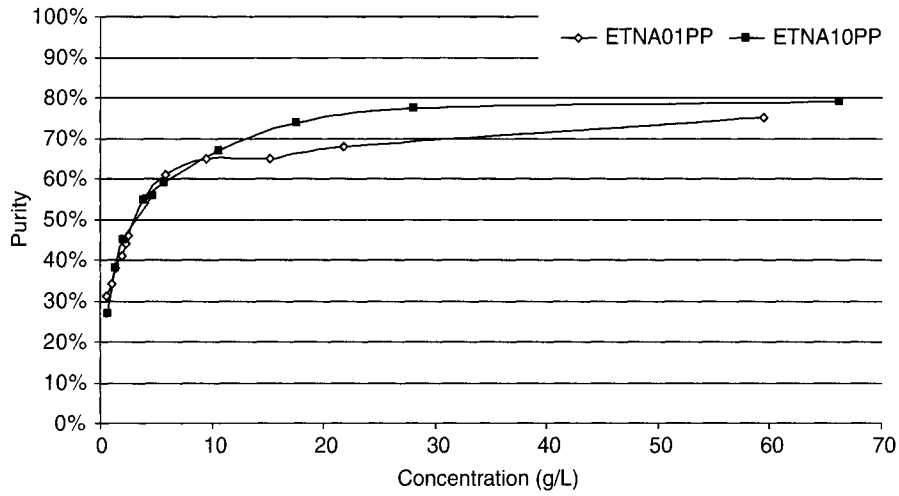


**Fig. 2.** The relation between the purity and the concentration of the hemicelluloses in the feed during ultrafiltration with the ETNA01PP and ETNA10PP membranes.

Table 2
Composition of the Process Water After Pretreatment by Microfiltration

| | Hemicelluloses (g/L) | Monosaccharides (g/L) | Ash (g/L) | Other organic matter (g/L) |
|---|---|---|---|---|
| After microfiltration | 0.7 (27%) | 0.2 (6%) | 0.8 (32%) | 0.9 (35%) |
| After ultrafiltration | 66.2 (79%) | 0.3 (0%) | 11.5 (14%) | 5.8 (7%) |

Composition expressed in grams per liter and percentage of total dry solids.

retained by the ultrafiltration membrane, which is somewhat unexpected. This is probably owing to ionic interactions with the hemicelluloses.

Diafiltration was investigated as a method to further increase the purity of the hemicelluloses after ultrafiltration. However, for the parameters used in the economic evaluation (the ETNA10PP membrane and a final hemicellulose concentration of 30 g/L), the purity was not increased significantly by diafiltration. Thus, diafiltration was not included in the economic evaluation.

## *Economic Evaluation*

### Pretreatment

The economic evaluation of the pretreatment step was performed based on the economic data received from the filter manufacturer Algas (*see* Table 3). The cost of pretreating a volume of process water corresponding to 1 t of product was calculated to be approx € 40.

Table 3
Economic Evaluation of the Pretreatment Step with a Capacity of 400 $m^3/h$

| Cost | € |
|---|---|
| *Investment* | |
| Equipment cost | 280,000 |
| *Annual* | |
| Capital cost | 40,000 |
| Energy cost | 5000 |
| Maintenance | 20,000 |
| Labor | 0 |
| Total annual costs | 65,000 |
| Cost of filtering a volume of process water corresponding to 1 t of product | 40 |

A drum filter with a 30-μm polyester cloth filter manufactured by Algas was used.

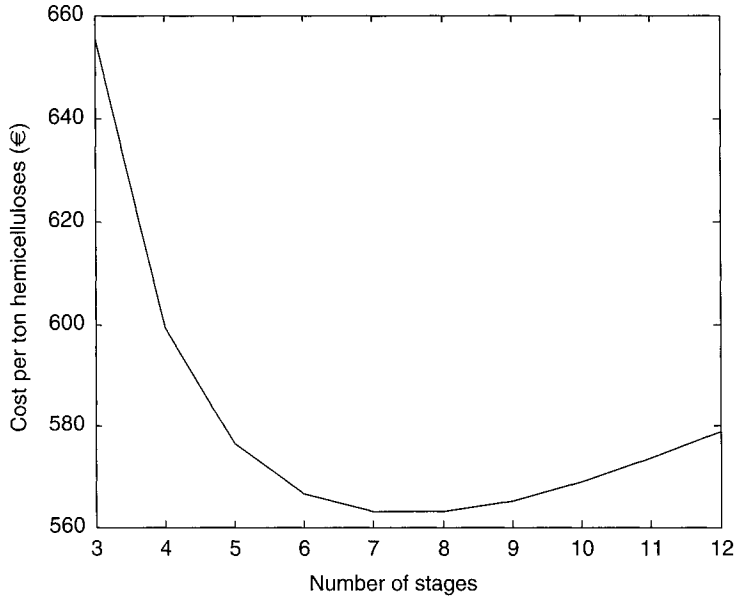


**Fig. 3.** The cost to concentrate 1 t of hemicelluloses to 30 g/L. The cost was calculated for a multistage ultrafiltration plant with varying number of stages.

## Concentration and Purification

The cost for concentration by ultrafiltration varies with the number of stages in the ultrafiltration plant, as shown in Fig. 3. The optimal number of stages for minimizing the cost was found to be eight stages. The total membrane area of the plant was 4000 $m^2$ and the recovery of hemicelluloses was 89%. The total cost to heat exchange a feed corresponding to 1 t of product and to increase the hemicellulose concentration to 30 g/L in an ultrafiltration plant with eight stages is € 630, as shown in Table 4.

Table 4
Costs Associated With Cooling 400 $m^3/h$ Process Water From 80 to 60°C and Ultrafiltrating to Increase the Hemicellulose Concentration to 30 g/L in an Ultrafiltration Plant With Eight Stages

| Cost | € |
|---|---|
| *Investment* | |
| Heat exchanger including installation | 210,000 |
| Ultrafiltration plant | 1,350,000 |
| Total | 1,560,000 |
| *Annual* | |
| Capital cost | 230,000 |
| Cooling water (1.5 ¢/$m^3$) | 85,000 |
| Energy cost | 40,000 |
| Maintenance | 30,000 |
| Labor | 170,000 |
| Membrane replacement | 100,000 |
| Membrane cleaning | 300,000 |
| Total annual costs | 955,000 |
| Cost to heat exchange and concentrate 1 t of hemicelluloses | € 630 |

There is a possibility that the future cost for ultrafiltration in a full-scale plant could be lower than calculated owing to the difference in operational conditions in the laboratory and the full-scale plant. First, in the laboratory study, the ultrafiltration was carried out at 50°C whereas the temperature in the full-scale ultrafiltration plant was set to 60°C. A higher temperature results in a higher flux through the decreased viscosity. Second, it is also probable that the flux would be higher in the spiral wound element than in the plate-and-frame module used in the laboratory, because the turbulence is greater in the flow channel of the spiral wound elements.

### Total Cost of the Isolated Hemicelluloses

The total cost of producing a solution containing 1 t of hemicelluloses was calculated to be approx € 670. The market price of barriers with similar properties made of ethylene vinyl alcohol is around € 5800/t. These numbers are of course not directly comparable, but even if costs for additional treatment and handling, such as further concentration, transportation, and addition of chemicals to improve the properties of the barrier are added, it is most likely that the price for the hemicelluloses will still be very competitive. If the concentration of hemicelluloses required for barrier film production in industrial scale is higher than the value used in this study (30 g/L), further concentration is needed. This can be accomplished either by further treatment with ultrafiltration or by evaporation. Of these two alternatives, ultrafiltration is probably the more cost efficient alternative because the energy

requirement of evaporation is significantly higher. However, to be able to perform the ultrafiltration to higher concentrations, further development of the method is necessary. An additional economic benefit when isolating hemicelluloses in the process water of thermomechanical pulp mills is that, the biological load on the sewage treatment plant will decrease when fibers and hemicelluloses are removed from the process water.

## Conclusions

This study has shown the potential to isolate hemicelluloses from process streams from thermomechanical pulping at a competitive cost, even though the initial concentration of hemicelluloses is very low. Further research and development is of course required to implement this process, but the calculated cost is sufficiently low to leave a great margin to the price of barriers made of petrochemicals with similar properties, i.e., ethylene vinyl alcohol barriers. This process was designed for a thermomechanical pulp mill that produces 0.6 million t pulp/yr. The total Swedish production of mechanical pulp is more than 3 million t/yr and the worldwide production is above 30 million t/yr. This gives some idea of the amount of hemicelluloses available for isolation from thermomechanical pulp mills.

## Acknowledgments

The Swedish Agency for Innovation Systems (VINNOVA) and the Swedish Energy Agency (STEM) are gratefully acknowledged for financial support, Alfa Laval for donating the ultrafiltration membranes, Tetra Pak and Algas for sharing important information, and Stora Enso Kvarnsveden mill AB for delivering the process water. The authors also wish to acknowledge Per Sassner for assistance with the economic evaluation in Icarus Process Evaluator.

## References

1. Hartman, J., Albertsson, A. -C., Soderqvist Lindblad, M., and Sjoberg, J. (2006), *J. Appl. Polym. Chem.* **100,** 2985–2991.
2. Grondahl, M., Eriksson, L., and Gatenholm, P. (2004), *Biomacromolecules* **5,** 1528–1535.
3. Soderqvist Lindblad, M., Ranucci, E., and Albertsson, A. -C. (2001), *Macromol. Rapid Comm.* **22,** 962–967.
4. Boussaid, A., Cai, Y., Robinson, J., Gregg, D. J., Nguyen, Q., and Saddler, J. N. (2001), *Biotechnol. Progr.* **17,** 887–892.
5. Parajo, J. C., Dominguez, H., and Dominguez J.M. (1998), *Bioresour. Technol.* **65,** 191–201.
6. O'Dwyer, M. H. (1923), *Biochem. J.* **17,** 501–509.
7. Hagglund, E., Lindberg, B., and McPherson, J. (1956), *Acta Chem. Scand.* **10,** 1160–1164.
8. Lundqvist, J., Teleman, A., Junel, L., et al. (2002), *Carbohyd. Polym.* **48,** 29–39.
9. Willfor, S., Rehn, P., Sundberg, A., Sundberg, K., and Holmbom, B. (2003), *Tappi J.* **2,** 27–32.
10. Palm, M. and Zacchi, G. (2003), *Biomacromolecules* **4,** 617–623.
11. Teleman, A., Nordstrom, M. and Tenkanen, M. (2003), *Carbohyd. Res.* **338,** 525–535.

12. Persson, T., Jönsson, A. -S. and Zacchi, G. (2005), Fractionation of hemicelluloses by membrane filtration, 14th European biomass conference and exhibition, Paris, France, October 17–21.
13. Wei, J., Helm, G. S., Corner-Walker, N., and Hou, X. (2006), *Desalination* **192,** 252–261.
14. Shao, J. and Zydney, A. L. (2004), *Biotechnol. Bioeng.* **87,** 286–292.
15. Cheryan, M. (1998), In: *Ultrafiltration and Microfiltration Handbook.* Technomic Publishing. Co., Lancaster, PA: pp. 298–304, 330–342.
16. Ehrman, T. (1994), Standard Method for Ash in Biomass, Laboratory Analytical Procedure-005, National Renewable Energy Laboratory, Midwest Research Institute for the Department of Energy, USA.
17. Ehrman T. (1994), Standard Method for Determination of Total Solids in Biomass, Laboratory Analytical Procedure-001, National Renewable Energy Laboratory, Midwest Research Institute for the Department of Energy, USA.
18. Ruiz R. and Ehrman T. (1996), Determination of Carbohydrates in Biomass by High Performance Liquid Chromatography, Laboratory Analytical Procedure-002, National Renewable Energy Laboratory, Midwest Research Institute for the Department of Energy, USA.
19. Wingren, A., Galbe, M., and Zacchi, G. (2003), *Biotechnol. Prog.* **19,** 1109–1117.
20. Blatt, W. F., Dravid, A., Michaels, A. S., and Nelsen, L. (1970), *Memb. Sci. Technol.* Plenum Press, New York, NY: pp. 47–97.

0273-2289/1559-0291 (Online)/07/136–140/753–764/$30.00

# Estimation of Temperature Dependent Parameters of a Batch Alcoholic Fermentation Process

**Rafael Ramos de Andrade,*[,1] Elmer Ccopa Rivera,*[,1] Aline C. Costa,[1] Daniel I. P. Atala,[2] Francisco Maugeri Filho,[2] and Rubens Maciel Filho[1]**

*[1]Laboratory of Optimization, Design and Advanced Control, School of Chemical Engineering, State University of Campinas, P.O. Box 6066, 13081-970, Campinas, SP, Brazil, E-mail: rafaelra@feq.unicamp.br, elmer@feq.unicamp.br; and [2]Department of Food Engineering, School of Food Engineering, State University of Campinas, P.O. Box 6121, 13081-970, Campinas, SP, Brazil*

## Abstract

In this work, a procedure was established to develop a mathematical model considering the effect of temperature on reaction kinetics. Experiments were performed in batch mode in temperatures from 30 to 38°C. The microorganism used was *Saccharomyces cerevisiae* and the culture media, sugarcane molasses. The objective is to assess the difficulty in updating the kinetic parameters when there are changes in fermentation conditions. We conclude that, although the re-estimation is a time-consuming task, it is possible to accurately describe the process when there are changes in raw material composition if a re-estimation of parameters is performed.

**Index Entries:** Alcoholic fermentation; kinetic parameters estimation; mathematical modeling; Quasi-Newton algorithm; *Saccharomyces cerevisiae*; ethanol production.

## Introduction

The interest in renewable energy sources tends to augment with the concern about exhaustion of fossil fuels and the increase in their price. The world meetings make clear that policies for renewable energy are essential to achieve sustainable development in a broad sense. Environmental protection, job creation, alleviation of external debts in developing countries, and security of supply are some of the key issues to mention *(1)*. Bioethanol (ethanol from biomass) is an attractive, sustainable energy source. Modeling potentially reduces the cost of the alcoholic fermentation process development by eliminating unnecessary experimental work. It allows the study of

*Author to whom all correspondence and reprint requests should be addressed.

the various process parameters interactions through simulation. Besides, it provides understanding of the process, which is helpful for operational policy definitions and can be applied for posterior optimization and control.

There are many minor problems associated with the alcoholic fermentation process to be solved nowadays. Among them is the lack of robustness of the fermentation in the presence of fluctuations in operational conditions, which leads to changes in the kinetic behavior, with impact on yield, productivity, and conversion. These changes are very common in plants of alcoholic fermentation; they occur not only because of the variations in the quality of the raw material but also because of variations of dominant yeast in the process. Also, the alcoholic fermentation process is exothermic and small deviations in temperature can dislocate the process from optimal operational conditions.

Temperature has an important influence on the alcoholic fermentation process, because it is usually difficult to support a constant temperature during large-scale alcoholic fermentation and it affects productivity as well as microorganism viability. Besides, terms of temperature influence on ethanol fermentation kinetics can be useful in strategies for process optimization (2). Still, there are few works in the literature on the mathematical modeling of the fuel ethanol fermentation considering the effect of temperature on the kinetic parameters. (2–4).

In this work we perform kinetic parameters optimization in an alcoholic fermentation process. The kinetics was determined as function of temperature from batch fermentations at temperatures from 30 to 38°C. Based on experimental data, a differential model consisting of rate expressions for cell growth, substrate consumption, and product formation was proposed. The resulting model has eleven parameters, five of which are known to be temperature dependent. In order to describe this dependence, one set of parameters was estimated for each considered temperature and in a subsequent step an equation describing the temperature dependence of each parameter was fitted to the resulting data. The performance of the proposed model in the presence of changes in raw material composition is assessed before and after parameters re-estimation.

## Materials and Methods

The microorganism used was *Saccharomyces cerevisiae*, cultivated in the Bioprocess Engineering Laboratory in the Faculty of Food Engineering/State University of Campinas, Campinas, SP, Brazil and obtained from an industrial fermentation plant. The growth medium for the inoculum contained 50.0 kg/m$^3$ of glucose, 5.0 kg/m$^3$ of $KH_2PO_4$, 1.5 kg/m$^3$ of $NH_4Cl$, 0.7 kg/m$^3$ of $MgSO_4 \cdot 7H_2O$, 1.2 kg/m$^3$ of KCl, and 5.0 kg/m$^3$ of yeast extract. The growth of microorganisms was performed in 500-mL flasks placed in a shaker at 30°C and 150 rpm for 24 h. The production medium was diluted using sugarcane molasses from an industrial ethanol fermentation plant. Sterilization was performed at 121°C for 20 min in autoclave.

Table 1
Initial Substrate Concentrations and Temperature for Experiments

| Experiments | $T$(°C) | $S_0$ (kg/m$^3$) |
|---|---|---|
| 1 | 30 | 127.6 |
| 2 | 31.2 | 86.8 |
| 3 | 34 | 119.1 |
| 4 | 36.8 | 84.6 |
| 5 | 38 | 118.8 |
| 6 | 34 | 168.1 |

A bioreactor (Bioflow III System; New Brunswick Scientific Co., Inc., Edison, NJ) with temperature and agitation control systems through proportional and integral differential (PID) controllers was used. The total working volume was 5 L. Agitation was controlled at 300 rpm and performed with two flat blade turbine disk impellers, with six blades each. Temperature was controlled at the fixed value for each fermentation. Dry cell mass was determined gravimetrically after centrifuging for 15 min at 3300 rpm (1219.68$g$), washing, and drying the cells at 70°C. Biomass concentration is given by the weight difference divided by total sample volume.

Viable cells were counted with the methylene blue staining technique (5). In this work the cell viability during batch fermentation was always close to 100%. Total reducing sugar and ethanol concentrations were determined by high-performance liquid chromatography (Varian 9010 model, Varian, Inc. Scientific Instruments, Palo Alto, CA). A SHODEX KS 801 column (Showa Denko, Tokyo, Japan) at 30°C was used. Ultrapure water obtained from Milli-Q Purification System (Millipore Corporation, Billerica, MA) containing Millipak membrane of 0.22 μm (diameter of pore) was mixed with $H_2SO_4$ (pH 1.4) and used as the eluent at a flow rate of 0.7 mL/min. The standards were mixed solutions of sucrose, glucose, fructose, and ethanol at concentrations from 0.1 to 40.0 kg/m$^3$. The experiments were performed following the initial substrate concentrations and temperatures depicted in Table 1.

## Parameter Estimation Problem

### *Batch Model*

For batch fermentation process, the mass balance equations that describe the concentrations of biomass, substrate, and ethanol are:

$$\frac{dX}{dt} = r_x \tag{1}$$

$$\frac{dS}{dt} = -r_s \tag{2}$$

$$\frac{dP}{dt} = r_p \tag{3}$$

where $X$ is the concentration of cell mass (kg/m$^3$), $S$ is the concentration of substrate (kg/m$^3$), and $P$ is the concentration of ethanol (kg/m$^3$). In this study the rates of cell growth, $r_x$ (kg/[m$^3$·h]), substrate consumption, $r_s$ (kg/[m$^3$·h]), and product formation, $r_p$ (kg/[m$^3$·h]), were expressed as functions of temperature, as described below. For fermentation with *S. cerevisiae*, experimental data has shown that cellular, substrate and product inhibitions are of importance *(2)*. In this study, the cell growth rate, $r_x$, includes terms for such types of inhibitions:

$$r_X = \mu_{max} \frac{S}{K_S + S} \exp(-K_i S) \left(1 - \frac{X}{X_{max}}\right)^m \left(1 - \frac{P}{P_{max}}\right)^n X \quad (4)$$

where $\mu_{max}$ is the maximum specific growth rate (h$^{-1}$), $K_s$ the substrate saturation parameter (kg/m$^3$), $K_i$ is the substrate inhibition parameter (m$^3$/kg), $X_{max}$ the biomass concentration when cell growth ceases (kg/m$^3$), $P_{max}$ the product concentration when cell growth ceases (kg/m$^3$), and $m$ and $n$ are parameters of cellular and product inhibitions, respectively. Luedeking–Piret expression *(6)* was used to account for the ethanol formation rate, $r_p$.

$$r_P = Y_{px} r_X + m_p X \quad (5)$$

where $Y_{px}$ is Luedeking–Piret growth associated constant (kg/kg) and $m_p$ is the Luedeking–Piret nongrowth associated constant (kg/[kg·h]). The substrate consumption rate, $r_s$, is given by:

$$r_S = (r_X / Y_X) + m_X X \quad (6)$$

This equation describes the sugar consumption during fermentation, which leads to cell mass and ethanol formation. $Y_x$ and $m_x$ are the limit cellular yield (kg/kg) and maintenance parameter (kg/[kg·h]), respectively. The first term of Eq. 6 considers that part of substrate is used for cell growth and the second one, for cellular maintenance that is the energy used for basic cell functions. According to the above description, there are 11 parameters to be estimated from experimental observations and some of them are temperature-dependent parameters ($\mu_{max}$, $X_{max}$, $P_{max}$, $Y_x$, and $Y_{px}$). This temperature dependence can be described by the following expression *(7)*:

$$\text{Temperature-dependent parameter} = A \cdot \exp(B/T) + C \cdot \exp(D/T) \quad (7)$$

## Optimization Using the Quasi-Newton Algorithm

Let $\theta$ specify the parameters vector, which contains all the temperature-dependent parameters. The objective of the optimization problem is to find out $\theta$ by minimizing the objective function *(8,9)*, min $E(\theta)$:

$$E(\theta)=\sum_{n=1}^{np}\left[\frac{(X_n-Xe_n)^2}{Xe_{max}^2}+\frac{(S_n-Se_n)^2}{Se_{max}^2}+\frac{(P_n-Pe_n)^2}{Pe_{max}^2}\right]=\sum_{n=1}^{np}\varepsilon_n^2(\theta) \quad (8)$$

The optimization is performed using the experimental data from fermentations in the temperature range of 30–38°C. $Xe_n$, $Se_n$, and $Pe_n$ are the measured concentrations of cell mass, substrate, and ethanol at the $n$th sampling time. $X_n$, $S_n$, and $P_n$ are the concentrations computed by the model at the $n$th sampling time. $Xe_{max}$, $Se_{max}$, and $Pe_{max}$ are the maximum measured concentrations and the term $np$ is number of sampling points. $\varepsilon_n(\theta)$ is the error in the output owing to the $n$th sample. Equations 1–6 were solved using a FORTRAN program with integration by an algorithm based on the fourth-order Runge–Kutta method. In order to model the fermentation experiments, the temperature dependent parameters ($\mu_{max}$, $X_{max}$, $P_{max}$, $Y_x$, and $Y_{px}$) in Eqs. 4–6 were determined by minimizing Eq. 8 using a Quasi-Newton (QN) algorithm. The FORTRAN IMSL routine DBCONF was used for this purpose. The optimization problem was implemented as a nonlinear programming problem written as:

Minimize Eq. 8

Subject to $l_p \le x_p \le u_p$, $p = 1, \ldots, 5$

where, $x_p$ is the temperature-dependent parameters. The $l_p$ and $u_p$ are specified lower and upper bounds on the variables, with $l_p \le u_p$. The parameters that are not temperature dependent had their values fixed according to the work of Atala et al. *(2)* as follows: $K_s$ = 4.1 kg/m$^3$, $K_i$ = 0.004 m$^3$/kg, $m_p$ = 0.1 kg/(kg·h), $m_x$ = 0.2 kg/(kg·h), $m$ = 1.0, and $n$ = 1.5. The optimization procedure was repeated for each temperature value (30, 31.2, 34, 36.8, and 38°C), resulting in five sets of the temperature dependent parameters ($\mu_{max}$, $X_{max}$, $P_{max}$, $Y_x$, and $Y_{px}$).

## *Influence of Temperature on the Kinetics*

After the temperature dependent parameters were optimized by using the QN algorithm, they were described by Eq. 7 as functions of temperature. The Levenberg–Marquardt algorithm was used for fitting all constants (*A*, *B*, *C*, and *D*), whose values are presented in Table 2. This table also shows the coefficient of determination ($r^2$) of the parameters fitting. Figure 1 shows the resulting dependence of $\mu_{max}$, $X_{max}$, $P_{max}$, $Y_x$, and $Y_{px}$ with temperature. The symbols (■) are the optimized values determined for each temperature using the QN algorithm and the lines represent the temperature dependence description of Eq. 7. It can be observed that the maximum specific growth rate occurs at a temperature of 34°C, considered the optimum condition for growth. Ethanol tolerance, limit cellular yield and $X_{max}$ decreases with temperature as expected.

Table 2
Constant Values in the Eq. 7 and Coefficient of Determination ($r^2$) of Parameters Fitting as Functions of Temperature for Batch Model Optimized by QN

| Parameter | ($r^2$) | $A$ | $B$ | $C$ | $D$ |
|---|---|---|---|---|---|
| $\mu_{max}$ | 0.999 | $-2.98 \times 10^{5}$ | -304.44 | $2.82 \times 10^{5}$ | -302.18 |
| $X_{max}$ | 0.999 | $7.20 \times 10^{-18}$ | 1284.40 | 10.24 | 48.58 |
| $P_{max}$ | 0.999 | $6.01 \times 10^{-22}$ | 1588.05 | 106.33 | -12.02 |
| $Y_x$ | 0.999 | $-2.98 \times 10^{-17}$ | 1194.15 | 11.73 | -5.60 |
| $Y_{px}$ | 0.997 | $-4.10 \times 10^{-78}$ | 5111.34 | 0.01 | 33.72 |

## Results

The mathematical model to be computed consists of Eqs. 1–6. The temperature dependent parameters $\mu_{max}$, $X_{max}$, $P_{max}$, $Y_x$, and $Y_{px}$ are given by Eq. 7 with the constants (A, B, C, and D) shown in Table 2, the parameters, which are not temperature dependent are fixed according to Atala et al. *(2)*. The profiles for ethanol, substrate, and biomass are shown in Fig. 2. It can be observed that the estimated model was able to fit batch experimental observations very satisfactorily and, therefore, the model can be applied for posterior optimization and controller process design. However, it should be stressed that when there are changes in operational conditions, the model kinetic parameters have to be re-estimated. It is worthwhile mentioning that, although the re-estimation is a time-consuming task, it is necessary to accurately describe the process when there are changes in raw material composition. Figure 3 shows the results for experiment 6 described in Table 1. The experimental data of this experiment were not used in the estimation procedure, but only to validate the model.

The residual standard deviation (RSD), Eq. 9, written as a percentage of the average of the experimental values, was the measurement used for characterizing the quality of the prediction of the model.

$$\mathrm{RSD}(\%) = \left( \frac{\sqrt{\mathrm{RSD}}}{\bar{d}_p} \right) 100 \tag{9}$$

where $\mathrm{RSD} = \frac{1}{np} \sum_{p=1}^{np} (d_p - x_p)^2$ in which $x_p$ and $d_p$ are, respectively, the value predicted by the mathematical model and experimental value, $\bar{d}_p$ is the average of the experimental values, and $np$ is the number of experimental points. The RSDs (%) for the batch model optimized by QN are shown in Table 3. The concentrations of biomass, substrate, and ethanol concentrations calculated using the resulting mathematical presented deviations of 4.9–23.3% from the experimental data.

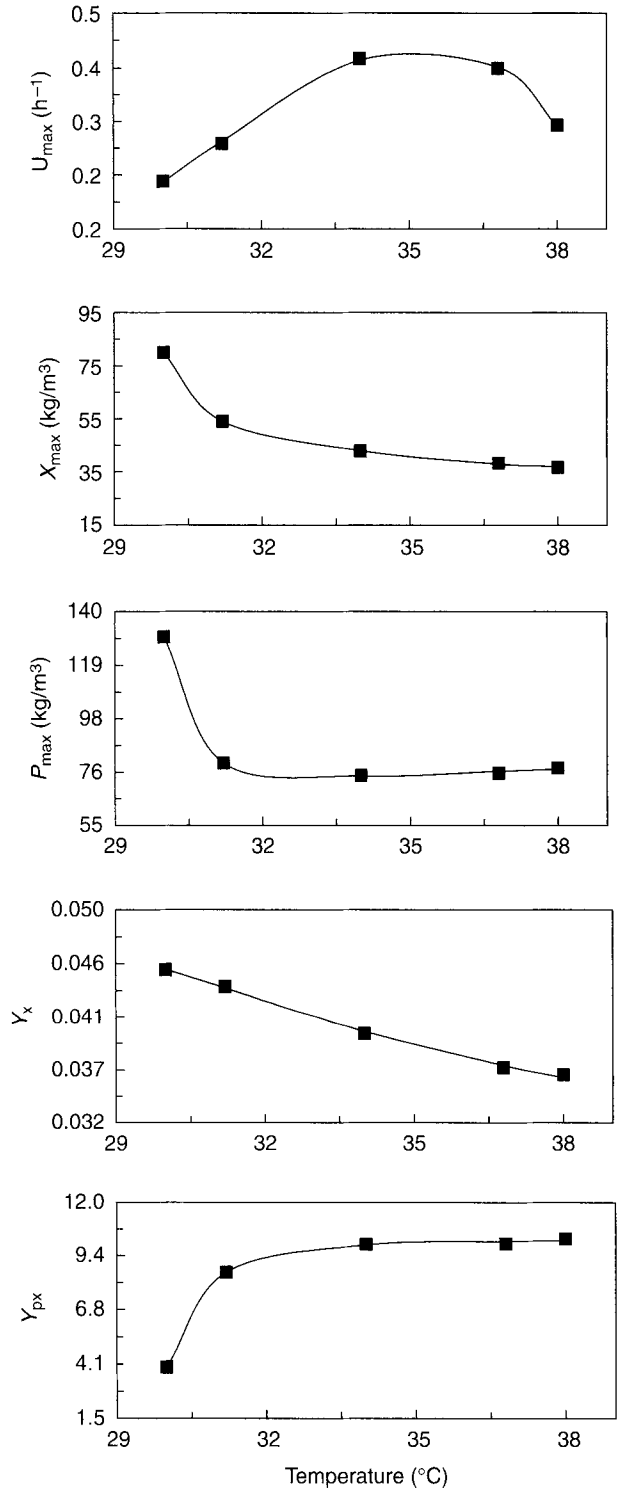


**Fig. 1.** Kinetic parameters optimized by QN algorithm at 30, 31.2, 34, 36.8, and 38°C, respectively.

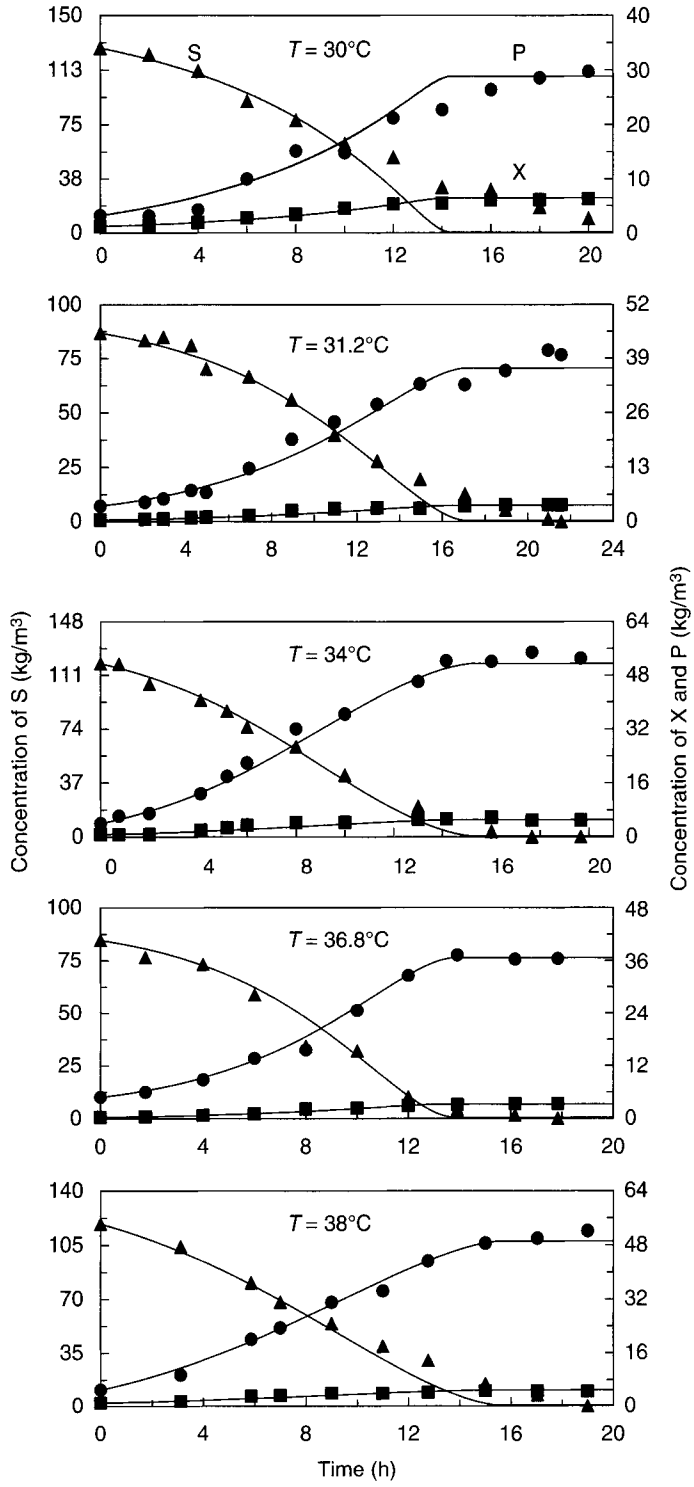


**Fig. 2.** Experimental and simulated data (QN—) from 30 to 38°C. Experimental data are for concentration of substrate, *S* (▲); cell mass, *X* (■); and ethanol, *P* (●).

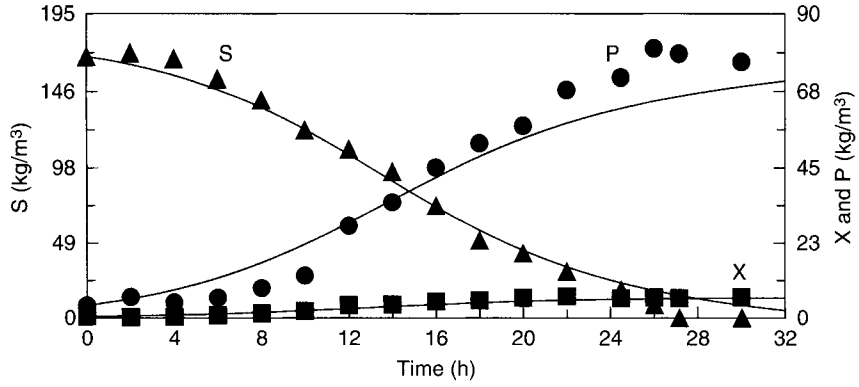


**Fig. 3.** Validation of the model. Experimental and simulated data for experiment 6 in Table 1. Experimental data are for concentration of substrate, *S* (▲); cell mass, *X* (■); and ethanol, *P* (●).

Table 3
RSDs (%) for the Batch Model

| | RSD (%) | | | | | |
|---|---|---|---|---|---|---|
| Output variable | $T$ = 30°C | $T$ = 31.2°C | $T$ = 34°C | $T$ = 36.8°C | $T$ = 38°C | $T$ = 34°C (validation) |
| *X* | 9.5 | 15.6 | 18.6 | 9.6 | 12.1 | 16.6 |
| *S* | 23.3 | 10.4 | 8.2 | 12.9 | 14.1 | 8.0 |
| *P* | 14.6 | 11.0 | 6.3 | 4.9 | 4.9 | 8.4 |

In order to test the model performance in the presence of fluctuations in raw material and culture medium compositions, an experiment performed at 34°C was considered. The only difference between this experiment and the experiments at 34°C shown in Figs. 2 and 3 are the molasses origin (molasses from a different harvesting) and the production medium, which, in this case, was diluted sugarcane molasses with addition of 1.0 kg/m$^3$ of yeast extract and 2.4 kg/m$^3$ of $(NH_4)_2SO_4$. The results are shown in Fig. 4A. The results after re-estimation of kinetic parameters are shown in Fig. 4B. The RSD (%) values for the model with and without parameters re-estimation are shown in Table 4.

## Discussion

The main objective of this work is to evaluate mathematical models to describe the alcoholic fermentation process in the presence of changes in operational conditions and fluctuations in the quality of raw material. These models are important to enable dynamic behavior studies, determination of control structures, optimization, and design of process controllers. It is

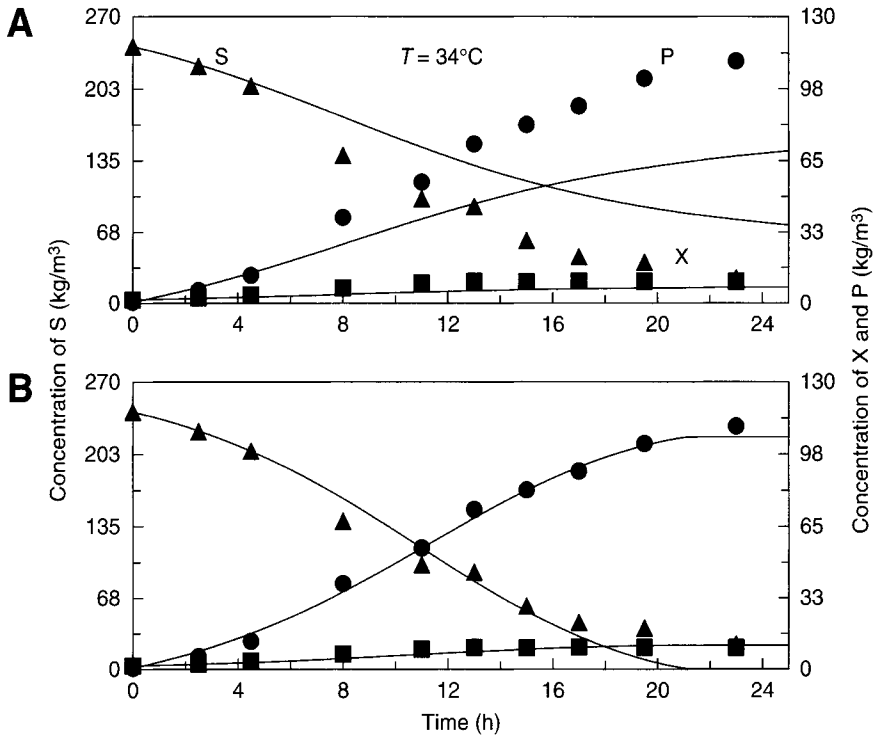


**Fig. 4.** Model performance in the presence of fluctuation in raw material composition. **(A)** Model without parameters re-estimation. **(B)** Model with parameters re-estimation. Experimental data are for concentration of substrate, *S* (▲); cell mass, *X* (■); and ethanol, *P* (●).

Table 4
RSD (%) for the Batch Model in the Presence of Fluctuations in Raw Material and Production Medium Compositions With and Without Parameters Re-estimation

| Output variable ($T$ = 34°C) | RSD (%) | |
|---|---|---|
| | Without re-estimation | With re-estimation |
| $X$ | 39.7 | 17.4 |
| $S$ | 36.1 | 13.2 |
| $P$ | 45.3 | 4.8 |

well-known from past studies that models, which do not have their parameters re-estimated when changes in operational conditions occur, do not describe the process accurately. Also, the description of the temperature dependence by the model is very important, although it transforms the parameter re-estimation problem into a much more complicated optimization problem.

In this work a procedure is presented for parameters re-estimation to follow more accurately the process behavior when changes in operational

conditions take place. The general methodology consists on keeping the parameters that are not temperature dependent and estimating those ones that are affected by temperature. The fitting procedure makes use of a double exponential function to find out the best relationship between parameters and temperature. The profiles of biomass, substrate, and ethanol concentrations calculated using the resulting mathematical presented deviations from 4.9 to 23.3% of the experimental data.

## Acknowledgments

The authors acknowledge Fundação de Amparo à Pesquisa do Estado de São Paulo (FAPESP) and Conselho Nacional de Desenvolvimento Científico e Tecnológico (CNPq) for financial support.

## Nomenclature

| | |
|---|---|
| $K_i$ | substrate inhibition coefficient ($m^3/kg$) |
| $K_s$ | substrate saturation parameter ($kg/m^3$) |
| $m$ | parameter used to describe cellular inhibition |
| $m_p$ | ethanol production associated with growth (kg/[kg·h]) |
| $m_x$ | maintenance parameter (kg/[kg·h]) |
| $n$ | parameters used to describe product inhibitions |
| $P$ | product concentration ($kg/m^3$) |
| $P_{max}$ | product concentration when cell growth ceases ($kg/m^3$) |
| $r_p$ | kinetic rate of product formation (kg/[m3·h]) |
| $r_s$ | kinetic rate of substrate consumption ($kg/[m^3 \cdot h]$) |
| $r_x$ | kinetic rate of growth ($kg/[m^3 \cdot h]$) |
| $S$ | substrate concentration ($kg/m^3$) |
| $T$ | temperature into the fermentor (°C) |
| $X$ | biomass concentration ($kg/m^3$) |
| $X_{max}$ | biomass concentration when cell growth ceases ($kg/m^3$) |
| $Y_{px}$ | yield of product based on cell growth (kg/kg) |
| $Y_x$ | limit cellular yield (kg/kg) |
| $\mu_{max}$ | maximum specific growth rate ($h^{-1}$) |

## References

1. Goldemberg, J., Coelho, S. T., Nastari, P. M., and Lucon, O. (2004), *Biomass Bioenergy* **26,** 301–304.
2. Atala, D. I. P., Costa, A. C., Maciel, R., and Maugeri, F. (2001), *Appl. Biochem. Biotechnol.* **91–93(1–9),** 353–366.
3. Aldiguier, A. S., Alfenor, S., Cameleyre, X., et al. (2004), *Bioproc. Biosyst. Eng.* **26,** 217–222.
4. Kalil, S. J., Maugeri, F., and Rodrigues, M. I. (2000), *Proc. Biochem.* **35(6),** 539–550.
5. Lee, S. S., Robinson, F. M., and Wang, H. Y. (1981), *Biotechnol. Bioeng.* **11,** 641–649.
6. Luedeking, R. and Piret, E. L. (1959), *J. Biochem. Microbiol. Technol. Eng.* **1,** 431–450.
7. Akerberg, K., Hofvendahl, K., Zacchi, G., and Hahn-Hägerdal, B. (1998), *Appl. Microbiol. Biotechnol.* **49,** 682–690.
8. Wang, F. S. and Sheu, J. W. (2000), *Chem. Eng. Sci.* **55,** 3685–3695.
9. Wang, F. S., Su, T. L., and Jang, H. J. (2001), *Ind. Eng. Chem. Res.* **40,** 2876–2885.

0273-2289/1559-0291 (Online)/07/136–140/765–776/$30.00

# Thermophilic Anaerobic Digester Performance Under Different Feed-Loading Frequency

JOHN BOMBARDIERE,[1,3] TEODORO ESPINOSA-SOLARES,*[,1,2] MAX DOMASCHKO,[1] AND MARK CHATFIELD[1]

*[1]Division of Agricultural, Consumer, Environmental, and Outreach Programs. West Virginia State University, Institute WV 25112-1000; [2]Agroindustrial Engineering Department, Autonomous University of Chapingo, Chapingo, 56230, Edo. de Mexico, Mexico, E-mail: espinosa@correo.chapingo.mx; and [3]Current position: Enviro Control Ltd., Singleton Court Business Park, Wonastow Road, Monmouth, UK.*

## Abstract

The effect of feed-loading frequency on digester performance was studied on a thermophilic anaerobic digester with a working volume of 27.43 $m^3$. The digester was fed 0.93 $m^3$ of chicken-litter slurry/d, containing 50.9 g/L chemical oxygen demand. The treatments were loading frequencies of 1, 2, 6, and 12 times/d. The hourly pH, biogas production, and methane percent of the biogas were less stable at lower feed frequencies. There was no statistical difference among treatments in methanogenic activity. The feed-loading frequency of six times per day treatment provided the greatest biogas production.

**Index Entries:** Biogas; chicken litter; digester stability; methane; methanogenic activity; thermophilic.

## Introduction

Feed input may be the most important factor in optimizing process control of an anaerobic digester. Feed-input volume, and concentration must be monitored and controlled carefully to ensure stable and efficient operating conditions. Although daily total carbon and total volume inputs into a digester have the greatest effect on digester efficiency, the frequency of feed input events within 1 d also affect performance. Kim et al. *(1)* studied process stability at different temperatures, mixing regimes, and feed frequencies. Biogas production from a single phase, mixed thermophilic laboratory digester continuously fed dog food slurry, yielded 16% more gas compared with the same type of digester fed only once per day.

Feeding events change several physical and biochemical parameters in the digester. Oxygen, carbon, volatile fatty acids, and other materials that affect

*Author to whom all correspondence and reprint requests should be addressed.

anaerobic microbes are introduced. Buhr and Andrews (2) reviewing the work of Golueke (3) reported the cyclic nature of a digester fed once per day. At 50°C, biogas release peaked sharply at the time of feed entry, then sharply decreased followed by a gradual increase over the following 24 h $CO_2$ release, partially caused by temperature reduction, and pH drop, because violative fatty acids (VFA) in the feed, were observed. An increase in biogas production throughout the day corresponded with a decrease in digester volatile acids concentration and an increase in digester pH compared with the time of feed input.

If the feed is not heated to or above digester-media temperature before input, a temperature reduction will occur. In a system using an external heat exchanger with a pump, the microbial consortia can be affected. For example, it has been documented that enzyme deactivation depends on mixing conditions (4). Excess shear force resulting from digestate being passed through a pump for long periods of time or by overmixing can disrupt the microbial communities dependant on each other for fermentation. Shigematsu et al. (5) worked with mesophilic acetate-degrading methanogenic consortia under continuous cultivation. They reported fluorescence *in situ* hybridization revealed dilution rate that modifies the consortia structure. Additionally, Sheng et al. (6), studying the role of extracellular polymeric substances (EPS) on the stability of sludge flocs under shear conditions, have shown that external layers are easily dispersible by shear forces, whereas the inner component is more stable.

For digester process control, feed input is the most important and simplest parameter to manage. More frequent feed events could allow more flexibility to change input to maintain steady-state conditions. Investigations at the West Virginia State University (WVSU, WV), Bioplex pilot-plant reactor have shown repeatable pH, biogas production, and biogas composition responses to changes in feed concentration and input volume (7). The goal of the current research is development of supervisory software that uses online real time feedback from a pH meter, biogas flowmeter, and gas chromatograph to adjust and control feed input based on feedback parameters. Considering that studies regarding feed-frequency influence on anaerobic digestion performance in available literature are limited, the purpose of this article is to test the effect of different feed frequencies on performance and stability in a thermophilic digester fed poultry-litter. The results will be used by our research team to define the feed frequency for the supervisory software trials.

## Materials and Methods

Experiments were carried out at the facilities of the Bioplex Project at WVSU. Diluted chicken-litter slurry was fed automatically into a 40-$m^3$ tank. The digester was operated in a semicontinuous process, being fed with fresh slurry every 24, 12, 4, or 2 h. The hydraulic retention time (HRT) was $29.5 \pm 1.7$ d. During the experiments, the slurry volume inside the tank was kept at $27.43 \pm 0.06$ $m^3$. The fermentation media in the digester was mixed through pumping the medium, for temperature control, and bubbling biogas. The digester liquid was pumped through an external heat exchanger

and recirculated back into the digester when internal digester temperature fell 0.1°C less than target. A gas blower extracted biogas from the top of the digester and recirculated the gas through a bubbling ring located at the bottom of the digester. According to the previous work, pumping could recycle close to six times the volume of the tank in 24 h as the bubbling rate was 0.01 gas volume/liquid volume/min, operating for 5 min every 60 min. In such conditions, pumping and bubbling, respectively, played the main roles in mixing and gas release from the liquid phase *(7)*. The digester operated under thermophilic conditions (56.7°C). The fermentation media was automatically heated when digester internal temperature fell below target. A pump recycled the work fluid (water and ethylene glycol mixture) for the heat exchanger. The digester effluent was discharged into a 5700-L sedimentation tank. The biogas flowed out by pressure differential through a Coriolis flowmeter, and then flared. Liquid effluent overflowed onto a 100-mesh separator screen and then into a holding tank.

Litter was obtained from a commercial poultry farm located in Moorefield, WV. The litter was taken from a broiler house using wood chips for bedding. Litter was maintained in the rearing house for six consecutive approx 42-d cycles (flocks) of production. Thus, litter resided in the house about 1 yr before disposal. Litter was received at 30–40% moisture, and then diluted with fresh water in a mix tank to 5–7% solids slurry. In the case of volatile acids (VA) and chemical oxygen demand (COD), methods 8196 and 8000 reported in the *Hach Water Analysis Handbook* were used *(8)*. Feed slurry samples were obtained from the feed inlet pipe, once per day, during feeding events. Effluent samples were taken at the time of discharge from the digester tank, before sedimentation or separation. A pipe extending into the top 1/3 of the working digester volume removed effluent by pressure-differential; therefore, the effluent was discharged from the tank during bubble mixing and feeding events when biogas pressure increased more than 2 kPa, because of rapid release of biogas during bubble mixing or input of liquid volume during feeding. Samples were taken once per day during bubble mixing, which occurred each hour, to ensure a representative sample of the substrate, as liquid and solid layers stratify between bubble mixing events. For days when feed input was one time in 24 h, samples were taken 1 h before feed input. For days when feed input was two times in 24 h, the samples were taken 1 h before the midday feed input. For days when feed input was 6 or 12 times/d, samples were taken at the hour before midday feed input. Biogas composition was measured with an online HP Gas Chromatograph (Hewlett-Packard Agilent Model: 5890 Series II GC, Santa Clara, CA) once per hour. Online pH, temperature, and biogas flow were recorded into a computer database every 5 min.

Feed frequencies tested included 1 feeding/d (T1), 2 feedings/d at 12 h intervals (T2), 6 feedings/d at 4 h intervals (T6), and 12 feedings/d at 2 h intervals (T12). Daily feed volume and concentration were, respectively, 0.93 ± 0.06 $m^3$ and 50.9 ± 5.8 g/L COD. Each treatment was run for at least seven

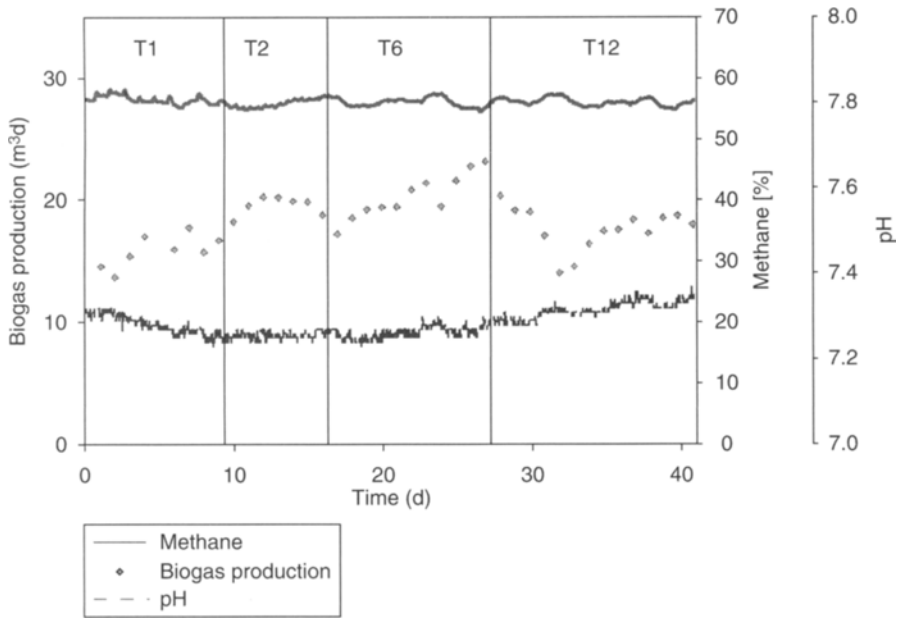


**Fig. 1.** Biodigester performance during the experiments.

consecutive days with data collection for three consecutive days once the digester had stabilized at the new feed frequency. The digester biochemical parameters along with biogas and methane percent measurements were used to determine steady state. Having similar hydraulic and carbon-loading rates, over a 4-d period, when the biogas production fluctuated less than 10% and methane percent fluctuated less than 2%, along with pH fluctuations within the digester of less than 0.2 and VA fluctuations inside the digester smaller than 10%, the digester was judged to be at steady state. Figure 1 shows the changes in biogas production, methane percentage, and pH during the experiments. Certainly, the steady state used in this article could be considered as a pseudo-steady-state, as it may be necessary to maintain a stable reactor for a period of three times the working HRT to assume steady state. Therefore, the steady state in this article was defined as stated in previous work *(7,9)*. This consideration has resulted in repeatable data from the WVSU pilot plant over a 4-yr period of operation and data collection.

For statistical analysis, an experimental unit was considered to be one 24-h period of continuous operation. Each treatment was sampled three times. Analysis of variance was performed using version 9.1 of the Statistica Analysis System (SAS) (SAS Institute Inc., Cary, NC). When the analysis of variance showed differences among treatments a Tukey test ($\alpha = 0.05$) was performed to compare means.

## Results and Discussion

Figures 2–5 show the performance of the reactor under different feed frequencies. For all cases the pH remained almost constant along the

Table 1
Digester Average Temperature Characteristics

| Treatment | Temperature[a] (°C) | Maximum deviation from target temperature (°C) | Time to reach target temperature after feeding (h) | Average daily recycled liquid ($m_{pumped}^3$ $m_{media}^{-3}$/d) |
|---|---|---|---|---|
| T1 | 56.50[b] | 2.0 | 6 | 4.174[c] |
| T2 | 56.60[d] | 1.0 | 3 | 3.843[c] |
| T6 | 56.62[c,d] | 0.7 | 2 | 3.858[c] |
| T12 | 56.64[c] | 0.5 | 1 | 3.737[c] |

[a]Data expressed as means from three replicates.
[b–d]Means with different letters in the same column showed statistical differences ($\alpha = 0.05$).

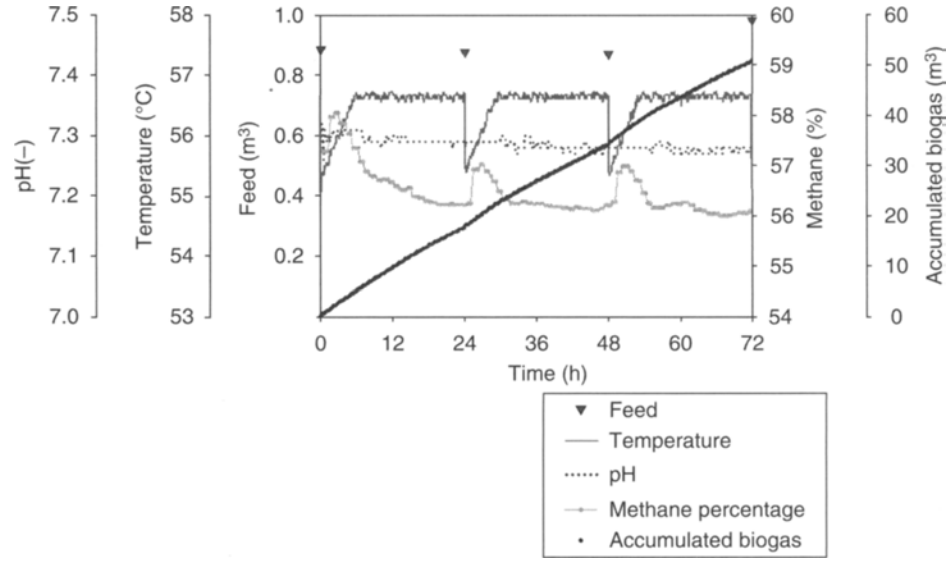


**Fig. 2.** Biodigester performance during feed intervals of 24 h.

experiments. Temperature of the media had a temporary reduction, dropping the temperature as the feed frequency increased. This was a result of feedslurry entering the thermophilic digester at ambient temperature, thus reducing digester temperature immediately after input. When average daily temperature of the digester was analyzed, significant differences between treatments were observed (Table 1). The temperature reduction and the corresponding recovery time of the process temperature for the treatments, incrementing in frequency (T1, T2, T6, and T12), were as follows: 2°C and 6 h, 1°C and 3 h, 0.7°C and 2 h, and 0.5°C and 1 h. These changes in temperature activated the heating system; as a result, the amount of recycled

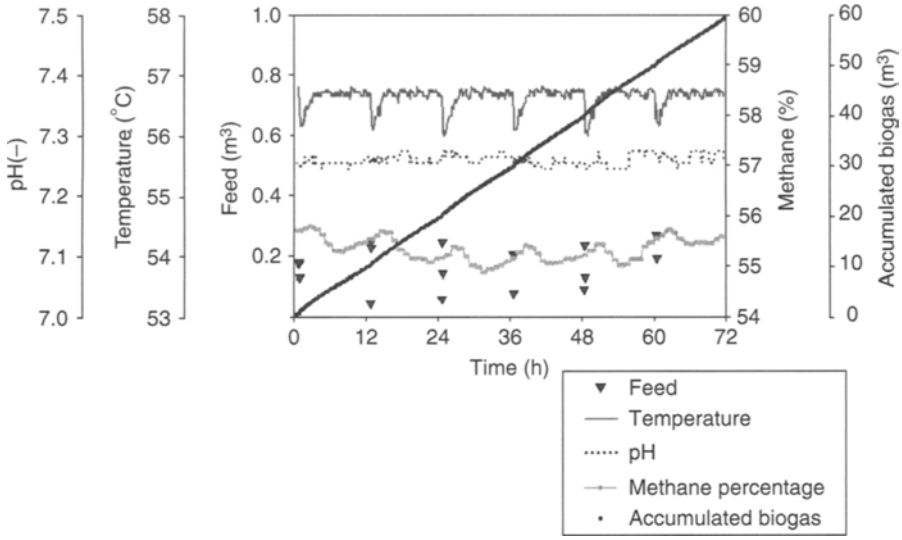


**Fig. 3.** Biodigester performance during feed intervals of 12 h.

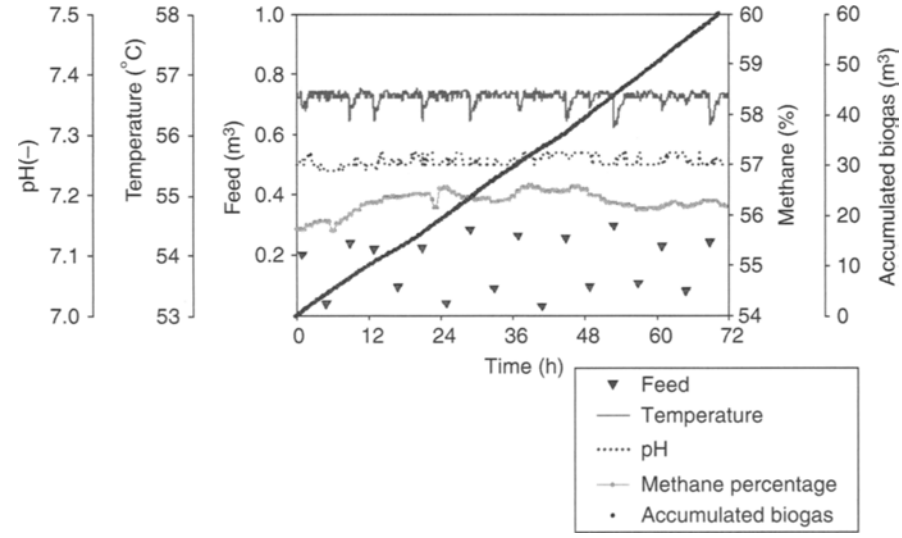


**Fig. 4.** Biodigester performance during feed intervals of 4 h.

liquid during the treatments was different, ranging from 3.7 to 4.2 $m_{pumped}^{3}$ $m_{media}^{-3}$ $d^{-1}$ (Table 1).

Pumping of the media contributed to release of the methane gas from the digestate. This phenomenon was registered mainly in the treatments T1 and T2 as an increment of methane in the gas phase followed by the pattern imposed by the temperature variations. For T6 and T12, considering the methane percentage variation in the gas phase, no trend was

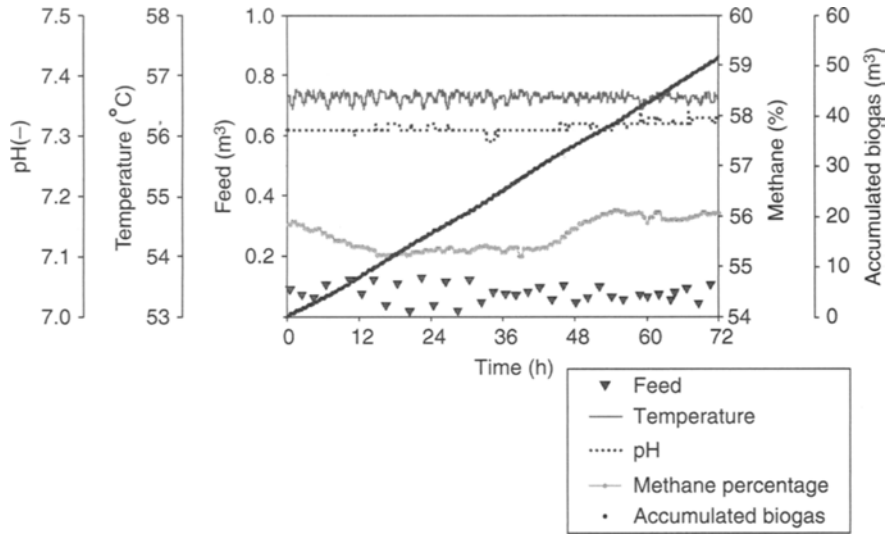


**Fig. 5.** Biodigester performance during feed intervals of 2 h.

observed. The biogas production was considered in steady-state conditions. In fact, the biogas produced per day along each one of the treatments was practically constant, this is easily observed in Figs. 2–5, wherein the slopes of the corresponding accumulated biogas are almost constant. Thus, the values of the slopes for the four incrementing frequency treatments (T1, T2, T6, and T12) were 0.729, 0.821, 0.834, and 0.708 $m^3/h$. As a result, the daily biogas production was statistically different, with treatments T6 and T2 in the group with the highest biogas production and T12 and T1 in the group with the lowest biogas production. The difference between the lowest gas production and the highest was close to 20% (Table 2). Regarding the COD loading, there was no statistical difference among treatments. However, a lower amount of carbon was supplied to T12; it had 88% of the amount supplied to T6. Nevertheless, a similar trend to total biogas production was observed when methanogenic activity was analyzed. Even though no statistical difference was observed in the methanogenic activity among treatments, the highest methanogenic activity was achieved by T6 and T2, with the maximum difference between the highest and lowest performing treatment, respectively T6 and T12, close to 7% (Table 2). It is important to note that besides the influence of feed frequency, temperature and mixing could have affected the digester performance.

Temperature reduction in the digester may have impacted the performance during feed-frequency one (T1). When temperature dropped from 56.7°C to 54.4°C, in a thermophilic anaerobic system fed poultry litter, a 35.8% reduction in biogas production occurred *(9)*. After the feed loading event at frequency one (T1), temperature dropped to 55.4°C, and did not reach the normal operating temperature of 56.7°C for 6 h. In fact, T1 was

Table 2
Feed Input and Biogas Average Daily Values

| Treatment | Feed ($m^3$/d) | COD loaded (kg/d) | Biogas production ($m^3$/d) | Methanogenic activity ($m^3/kg_{COD}$·d) |
|---|---|---|---|---|
| T1 | 0.879[a] | 50.4[a] | 17.1[b] | 0.203[a] |
| T2 | 0.905[a] | 52.0[a] | 19.6[a] | 0.209[a] |
| T6 | 1.017[a] | 53.8[a] | 20.5[a] | 0.215[a] |
| T12 | 0.932[a] | 47.5[a] | 17.2[b] | 0.201[a] |

Data expressed as means from three replicates.
[a,b]Means with different letters in the same column showed statistical differences ($\alpha = 0.05$).

the only treatment that was statically different from the other treatments when comparing average daily temperature (Table 1). This extended drop in temperature could have resulted in depressed biogas production during feed frequency one.

Recirculation of the digestate through the heat exchanger may have also impacted performance, because bubble mixing was kept constant throughout the experiment. When comparing the influence on methanogenic activity by the recycled liquid in each treatment, treatments T1 and T12 differed from T2 and T6 (Tables 1 and 2). The maximum performance was around 3.8 $m_{pumped}^3\ m_{media}^{-3}\ d^{-1}$, which is in the same order of magnitude as the one (4.55 $m_{pumped}^3\ m_{media}^{-3}\ d^{-1}$) reported by Lomas et al. *(10)* for the best performance in the treatment of piggery-slurry in a pilot plant. In addition, the pump run time after feed input varied between treatments (Table 1). In this system, recirculation for temperature control contributes to mixing; however, excessive mixing can damage the microbial consortia *(7)*.

Hydrolyzing bacteria appear to be more sensitive to mechanical stress than acetogenic and methanogenic bacteria. This may be owing to their position on the outer layer of the granule. Microbes in a digester form flocs or granules, held together by biofilms, with methanogens forming clusters in the middle of the biofilms *(11)*. Studying cellulose hydrolysis and methanogenesis, Song et al. *(11)* characterized the hydrolyzing bacteria on the biofilm on the outer surface of particles. The bacteria were found to be attached to the surface by EPS. Sheng et al. *(6)* found that the EPS on the outer layer of anaerobic flocs was completely dispersible at infinite shear intensity, whereas inner EPS layers were tightly bound and only dispersible under extremely unfavorable conditions, such as pH 11.0. In this experiment, it stands to reason that the increased pumping at feed frequency one damaged the hydrolyzing bacteria, disrupting the fermentation process resulting in depressed conversion of COD to biogas, whereas acetogenic and methanogenic bacteria remained relatively undisrupted, resulting in practically stable pH, VFA concentrations, and methane percent (Tables 2 and 3).

Table 3
Digester Parameter Average Daily Values

| Treatment | Digester pH (–) | Digester VFA (mg/L) | Biogas methane (%) |
|---|---|---|---|
| T1 | 7.29[b] | 1.714[a] | 56.5[a] |
| T2 | 7.26[c] | 1.770[a] | 55.3[c] |
| T6 | 7.26[c] | 1.876[a] | 56.3[a,b] |
| T12 | 7.31[a] | 2.053[a] | 55.6[b,c] |

Data expressed as means from three replicates.
[a–c]Means with different letters in the same column showed statistical differences ($\alpha = 0.05$).

Conversely, the feed frequency of T12 may have yielded less total biogas per kilogram of COD fed owing to decreased pump run time, resulting in less total mixing than the other treatments. Interestingly, pH and VFA concentration in the digester, and methane percentage in the biogas were stable for all treatments and there was little variation between treatments. However, the total biogas yield was different between treatments; with T1 and T12 significantly different from T2 and T6 (Table 2). This indicates parameters such as pH, VFA concentration, and biogas methane percentage may not be the best indicators of performance for optimizing and controlling the digestion process. Mechichi and Sayadi *(12)*, evaluating these and other parameters for process control of up-flow anaerobic filters for olive waste, concluded pH changes are too slow for early detection of process imbalance. VFA concentration and composition did show rapid response to perturbations, such as increased organic loading rate, change in HRT, and temperature fluctuations. The authors suggest accumulation of longer chain fatty acids than acetate and propionate are good indicators of process imbalance. In this experiment, VFA profiles were not measured.

From an operator's standpoint, more frequent feed input events present both benefits and challenges. For ease of operation and mechanical reliability, less frequent feedings are advantageous. Slurries containing bedding material, such as wood chips in poultry litter, can present materials handling problems, especially at 6–10% total solids. Pump, line, and valve clogging can occur, even when particle size is reduced. A single feeding would allow close monitoring and repair of the equipment used to move slurry into the digester at the time of operation. Continuous or intermittent feeding throughout the day and night would provide more opportunities for the feed system to clog or pump to malfunction, resulting in variable feed input and increased maintenance. For closer process monitoring and control, more frequent feedings would be desirable, especially with inconsistent or uncharacterized feedstocks. Digester pH, biogas production, and biogas composition change in response to changes in feed quality and quantity *(13)*. The more frequent the feed input, the more opportunity the operator has to modify the volume or concentration of the feed to maintain

steady-state conditions. This may be more important for plants using mixed feedstock, or regional plants receiving materials from different sources. The presence of inhibitors or toxic compounds may not be discovered until the material is fed and digester performance is impaired. Frequent feed events could limit or discontinue the loading of slurry containing inhibitory levels of compounds such as ammonia or antibiotics until the digester recovers. In contrast, 1 feeding/d would load large quantities of the slurry into the reactor, especially in systems operated at short retention times, reducing performance or causing cessation of methanogenesis.

## Conclusions

There were no statistical differences in the daily feed volume and concentration among treatments. Biogas production was greatest at feed frequencies two and six. Regarding methanogenic activity, a similar trend to biogas production was observed with T6 and T2 having the highest performance; however, there was no statistical difference among treatments. Biochemical and online parameters other than biogas volume showed little difference. The average daily temperature of the digester decreased as feed input frequencies decreased. This may have impacted the performance of once per day, and twice per day feedings. Preheating of feed slurry to temperatures at, or above digester operating temperature, before loading, would lessen the impact of the feed frequency on temperature, and as a result could lead to better overall performance. Digester pH, methane percent, and hourly biogas output were most stable at higher feeding frequencies. VFA concentrations of the digester changed very little between treatments, and remained stable throughout the experiment. This suggests parameters such as VFA concentration, pH, and biogas methane percentage may not be the best indicators of digester performance. Further work is needed in order to clarify the roles of temperature, and mixing on digester performance, which is left for future communications.

## Acknowledgments

The authors gratefully acknowledge the financial support from West Virginia State University, Division of Agricultural, Consumer, Environmental, and Outreach Programs and Autonomous University of Chapingo, Agroindustrial Engineering Department. The study was funded by USDA Administrative Grant 2004-06200. We would also like to acknowledge the following individuals for their contributions; Dr. David Stafford, Mike Easter, Scot Shapero, and Ami Smith.

## References

1. Kim, M., Younh-Ho, A., and Speece, R. E. (2002), *Water Res.* **36,** 4369–4385.
2. Buhr, H. O. and Andrews, J. F. (1977), *Water Res.* **11,** 129–143.

3. Golueke, C. G. (1958), *Sewage Ind. Wastes* **30,** 1225.
4. Ghadge, R. S., Patwardhan, A. W., Sawant, S. B., and Joshi, J. B. (2005), *Chem. Eng. Sci.* **60,** 1067–1083.
5. Shigematsu, T., Tang, Y. Q., Kawaguchi, H., et al. (2003), *J. Biosci. Bioeng.* **96,** 547–558.
6. Sheng, G. P., Yu, H. Q., and Li, X. Y. (2006), *Biotech. Bioeng.* **93,** 1095–1102.
7. Espinosa-Solares, T., Bombardiere, J., Domaschko, M., et al. (2006), *App. Biochem. Biotech.* **129–132,** 959–968.
8. Hach Water Analysis Handbook, Procedures 819b and 80a (online at http://www.hach.com). Hach Company, Loveland, CO.
9. Bombardiere, J., Espinosa-Solares, T., Domaschko, M., and Chatfield, M. (2006), in *Proceedings Seventh IWA Conference on Small Water and Wastewater Systems,* Mexico City, Mexico.
10. Lomas, J. M., Urbano, C., and Camarero, L. M. (2000), *Biomass Bioenergy* **18,** 421–430.
11. Song, H., Clarke, W., and Blackall, L. L. (2005), *Biotech. Bioeng.* **91,** 369–377.
12. Mechichi, T. and Sayadi, S. (2005), *Process Biochem.* **40,** 139–145.
13. Liu, K., Olsson, G., and Mattiasson, B. (2004), *Biotech. Bioeng.* **87,** 43–53.

0273-2289/1559-0291 (Online)/07/136–140/777–792/$30.00

# A Proposed Mechanism for Detergent-Assisted Foam Fractionation of Lysozyme and Cellulase Restored With β-Cyclodextrin

VORAKAN BURAPATANA, ELIZABETH A. BOOTH, IAN M. SNYDER, ALES PROKOP, AND ROBERT D. TANNER*

*Chemical Engineering Department, Vanderbilt University, Nashville, TN 37235, E-mail: robert.d.tanner@vanderbilt.edu*

## Abstract

Foam fractionation by itself cannot effectively concentrate hydrophilic proteins such as lysozyme and cellulase. However, the addition of a detergent to a protein solution can increase the foam volume, and thus, the performance of the foam fractionation process. In this article, we propose a possible protein concentration mechanism of this detergent-assisted foam fractionation: A detergent binds to an oppositely charged protein, followed by the detergent–protein complex being adsorbed onto a bubble during aeration. The formation of this complex is inferred by a decrease in surface tension of the detergent–protein solution. The surface tension of a solution with the complex is lower than the surface tension of a protein or a detergent solution alone. The detergent can then be stripped from the adsorbed protein, such as cellulase, by an artificial chaperone such as β-cyclodextrin. Stripping the detergent from the protein allows the protein to return to its original conformation and to potentially retain all of its original activity following the foam fractionation process. Low-cost alternatives to β-cyclodextrin such as corn dextrin were tested experimentally to restore the protein activity through detergent stripping, but without success.

**Index Entries:** Artificial chaperones; detergent stripping; protein refolding; protein renaturation; surface tension.

## Introduction

Foam fractionation has the potential to be an effective low-cost protein separation and concentration process *(1–5)*. Foam fractionation has a much lower cost than traditional protein separation techniques such as chromatography, ion exchange, electrophoresis, and ultrafiltration *(4,5)*. Selectivity can be imparted to the foam fractionation technique by varying the pH of the foamed solution *(6)*, the airflow rate used in the foaming, or the initial liquid volume. The low cost of foam fractionation suggests that the process could be used in the pharmaceutical industry wherein therapeutic protein drugs

*Author to whom all correspondence and reprint requests should be addressed.

need cost-effective purification and separation techniques, as downstream processing is one of the major costs in biopharmaceuticals production *(7)*. Foam fractionation is a versatile process that can be applied to other potentially industrial scale processes, such as, concentrating laccase C, a lignin-degrading enzyme that is used in chlorine-free bleaching processes *(8,9)*. Nonetheless, foam fractionation does not work well with hydrophilic proteins such as lysozyme, because such proteins often do not foam when aerated at low concentration *(10)*. One way to modify foam fractionation to concentrate hydrophilic proteins is to add a detergent to increase the foam volume. This has been demonstrated in previous studies wherein it has been observed that the addition of a detergent can enhance the concentration of hydrophilic proteins (like lysozyme and cellulase) in foam fractionation processes *(11–13)*. Unfortunately, the protein may be denatured during the process, but it is possible to restore some of the lost activity by adding cyclodextrin. The mechanism of this detergent-assisted foam fractionation has apparently not been explored; therefore, a molecular mechanism to model this process is proposed in this article for possible use in future process improvement studies.

Although cyclodextrins have been used successfully to restore activity to enzymes they are relatively expensive, particularly when used with industrial enzymes like cellulase, which can currently sell for just a few dollars per kilogram. It is the cyclodextrin's hydrophobic cavity and the inclusion complexes it forms that allow it to strip away the charged surfactant and restore the activity *(7)*. Other starches and dextrins may have the potential to remove the detergent from the cellulase if they are able to form a structure similar to the hydrophobic cavity of the cyclodextrin. Long linear dextrins may be able to form such hydrophobic chambers in transient states, capable of removing the detergent from the enzyme. However, little seems to be known about substituting other dextrins for cyclodextrins in order to reduce the cost of enzyme restoration *(7)*.

In order to concentrate a protein solution using a foam fractionation process, the protein must first adsorb onto a foamed air (or other gas) bubble surface. A hydrophilic protein like lysozyme is not likely to adsorb because it prefers to stay in aqueous solution. Without that adsorption step, the concentration of the resulting product "foamate" will be the same as the initial concentration. However, by adding a detergent, which forms a complex with the hydrophilic protein, the hydrophilic part of the detergent likely binds with the hydrophilic part of that protein. The hydrophobic part of the detergent is then free to be adsorbed on the bubble surface and is then free to be carried along with the attached protein out into the foam phase. At the same time, the water will drain as the foam rises to the top of the column making the protein even more concentrated in the foamate.

## Materials and Methods

Cellulase from *Trichoderma reesei*, lysozyme from chicken egg white, lyophilized cells of *Micrococcus lysodeikticus*, sodium dodecylsulfate (SDS), Pluronic F-68, and 3,5- dinitrosalicylic acid (DNS) were purchased from Sigma (St. Louis, MO). Cetyltrimethylammonium bromide (CTAB) was purchased from Fluka (Switzerland). Starch soluble, potato starch, corn starch, Whatman filter paper No. 1,3-cyclodextrin, bicinchoninic acid (BCA) assay kit, and 96-well microplate were purchased from Fisher Scientific (Pittsburgh, PA). The artificial sweetener stevioside (Stevia) was provided by Flavio F. DeMoraes from Maringa, Brazil. 10 m*M* pH 5.0 phosphate buffer prepared at time of use or deionized water was used as a solvent in the cellulase experiments *(14)*, and 10 m*M*, pH 8.5 Tris-HCl buffer was used in the lysozyme experiment *(15)*. The components used in preparing these buffer solutions were purchased from Sigma. All data except for the surface tension data and refolding with linear dextrins data are taken from earlier work *(11)*.

### Foam Fractionation

Semibatch foam fractionation experiments are carried out in a small custom made (with stopcock at the bottom) glass column ($2 \times 10$ cm$^2$). The schematic drawing of the apparatus is shown in Fig. 1, from a previous publication *(16)*. Twelve milliliters of protein solution is added to the column and medical grade air from a compressed gas cylinder is introduced (at a selected rate) through a fritted disc sparger (pore size 40–60 μm) imbedded at the bottom of the column. Water loss in the effluent air stream is minimized by humidifying the air before it enters the column. Air is allowed to continue to flow into the column at rates of 4, 8, and 12 mL/min until no more foam is generated. The produced foam is allowed to continuously collapse into a liquid product (the foamate in the overhead foam collector). The foamate volume is measured in a graduated cylinder. Each experimental condition is repeated in triplicate.

### Renaturation of Cellulase After Foam Fractionation

After foam fractionation of a cellulase and CTAB mixture, 350 μL of collected foamate is diluted with 150 μL of 13 m*M* β-cyclodextrin solution or varying concentrations of corn dextrin solution, potato starch solution, Stevia (a Brazilian sugar substitute) solution, or starch soluble solution. The resulting mixture is stored overnight before checking for its activity, both before and after addition of β-cyclodextrin and the other potential refolding solutions. The filter paper activity test *(17)* is used to determine the cellulase activity. The DNS assay *(18)* is used to measure the amount of sugar produced in that test.

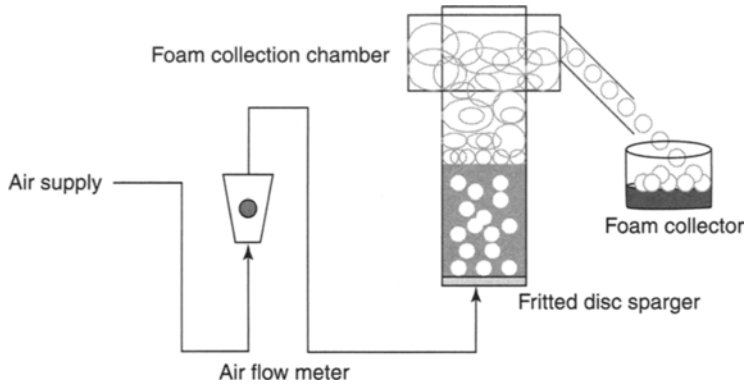


**Fig. 1.** Schematic drawing of the foam fractionation apparatus.

### *BCA Assay for Protein Concentration*

Twenty mililiters of collected cellulase samples are put into a 96-well microplate and the analysis is repeated in triplicate. Then, 180 µL of BCA reagent is added to each well-plate. The microplate is scanned after 30 min for the determination of absorbance at 562 nm *(19)*. For lysozyme, 20 µL of the sample is added to a well in a 96-well microplate. 180 mL of BCA reagent is then also added to each well and again carried out in triplicate. The microplate is incubated at 37°C for 2 h before being read by a Bio-Tek µQuant plate reader at 562 nm. Longer incubation times and higher temperatures are used to increase the light absorbance signal from the BCA assay, when necessary.

### *Lysozyme Activity Assay*

The protocol for this assay is taken from the Worthington Enzyme Manual *(20)*. Lyophilized *M. lysodeikticus* cells of 9.0 mg are first diluted in 25 mL of 0.1 *M* potassium phosphate buffer at pH 7.0. Then, after dissolving the *M. lysodeikticus* cells, the buffer solution is added to bring the final volume to 30 mL. Ten microliters of the samples are added to a 96-well microplate. BCA reagent of 290 µL are then added to each well. The assay is carried out in triplicate. The change in absorbance at 450 nm is scanned every minute for 5 min using the Bio-Tek µQuant plate reader. The activity of the substance is measured in units/mL and activity enrichment (AE) is defined as the activity per unit volume of the foamate divided by the initial activity per unit volume of the solution before foaming.

### *Surface Tension Measurement*

The surface tension of solutions is determined by the Wilhelmy Plate method using a Sigma 70 tensiometer from KSV Instrument Ltd. (Helsinki, Finland). The automated tensiometer apparatus determines surface tension

by slowly dipping a platinum-iridium plate into the surface of the liquid solution. Then, the microbalance inside the tensiometer measures the maximum force needed to pull the plate away from the liquid surface. The accompanying computer calculates the liquid surface tension based on the force measured. Twenty milliliters of liquid sample is placed into a glass cylinder, which in turn, is placed within the KSV Sigma 70 tensiometer. After pressing the start button on the computer interface, the surface tension of the liquid solution is measured five times and the results are then averaged.

The surface tension of six separate systems is measured to determine the critical micelle concentration (CMC) of various surfactants in different solvents. The CMC is the surfactant concentration wherein any additional amount of surfactant does not change the surface tension of the solution. First a 10.0 mg/mL SDS solution is added incrementally to deionized water, and the resulting surface tension is measured at various concentrations to determine the CMC of SDS in water. Then, a 10.0 mg/mL SDS solution is added incrementally to a 75.0 mg/L lysozyme solution to determine the CMC of SDS in 75.0 mg/L lysozyme solution. In addition, lysozyme is also incrementally added to deionized water to determine the CMC of lysozyme in water. Next, 1.0 mg/mL CTAB solution is added incrementally to deionized water to determine the CMC of CTAB in water. A 1.0 mg/mL CTAB solution is added incrementally to 200.0 mg/L cellulase solution to determine the CMC of CTAB in 200.0 mg/L cellulase solution. Finally, cellulase is also added to deionized water to determine the CMC of cellulase in water.

## Results and Discussion

### *Summary of Detergent-Assisted Foam Fractionation of Lysozyme*

Varley and Ball *(10)* tried to use foam fractionation to concentrate a lysozyme solution and reported that in order to foam lysozyme, a high-protein concentration of 2200.0 mg/L needed to be used. With this high lysozyme concentration, they obtained an enrichment ratio (ER) as high as 1.2 with a 0.02 protein mass recovery (MR). They also retained about 87% of the initial activity. The use of an SDS-assisted foam fractionation makes it possible to foam lysozyme at a lower concentration, which in the presented data, can result in a much larger ER (3.3). Results from the literature indicates that anionic surfactants such as SDS bind strongly with proteins and form protein–surfactant complexes; cationic surfactants (e.g., CTAB) on the other hand, have less tendency to interact with proteins, and non-ionic surfactants (e.g., Pluronic F-68) weakly bind to proteins *(21–23)*. For example, lysozyme at pH 8.5, the condition used for foaming, is cationically charged (on average) suggesting its strong desire to bind with anionic surfactants such as SDS *(21–23)*. It has been determined that a complex of lysozyme–SDS is more surface active than lysozyme or SDS alone *(24)*. Our direct surface tension measurements indicate that this enhanced

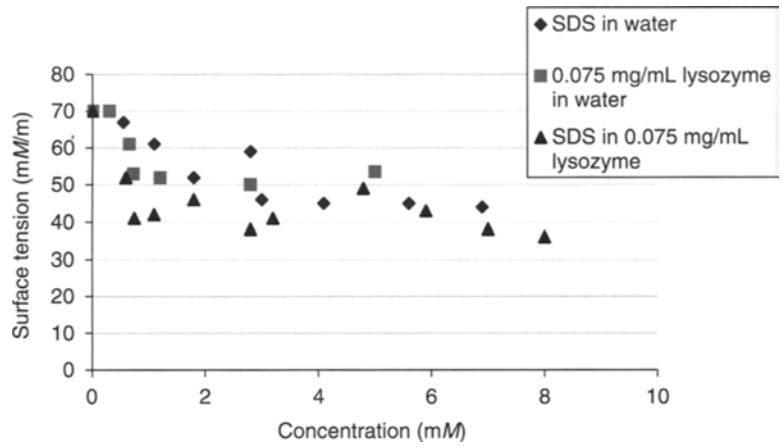


**Fig. 2.** Surface Tension measurements of SDS, lysozyme, and SDS–lysozyme complex. The surface tension is measured by the Sigma 70 (tensiometer) using the Wilhelmy Plate Method.

surface activity (Fig. 2). Thus, it is possible that the complex may foam better than its individual parts, which in fact is the case, resulting in better enrichment and recovery. From Fig. 2, the CMC of SDS in water is seen to be around 4 m*M*, the CMC of SDS in 75.0 mg/L lysozyme solution is around 1.5 m*M*, and the CMC for lysozyme in water is around 3 m*M*. Thus, the SDS-assisted foam fractionation of lysozyme (200.0 mg/L SDS = 0.7 m*M*) is operated below the CMC. Operating below the CMC is important to avoid the formation of miscelles. SDS normally binds with a protein by electrostatic interaction with the positively charged groups of amino acids of that protein *(25)*, so that the complex is likely to have strong electrostatic binding. Lysozyme does not show any loss of activity during foam fractionation probably because of the fact that lysozyme contains four disulfide bonds, which may make the lysozyme more resistant to structural change. Moreover, a minor change in structure as noted from CD measurements, is probably not enough to change lysozyme activity *(26,27)*. It is reported in the literature that without reducing the four disulfide bonds into lysozyme, a rapid dilution can effectively refold the denatured lysozyme into its native state *(28)*. In this foaming process, no reducing agent was used; therefore, the four disulfide bonds are likely to remain intact, making it more difficult for lysozyme to lose its enzymatic activity. A schematic for the SDS- and lysozyme-binding process is pictured in Fig. 3.

Of all three detergents tested (CTAB, Pluronic F-68, and SDS), addition of SDS yields the highest enrichment and recovery *(29)*. Addition of SDS to the foam fractionation of lysozyme improves both the enrichment and recovery when compared with foam fractionation of lysozyme without any additional detergent *(10)*. Although there is a slight change in

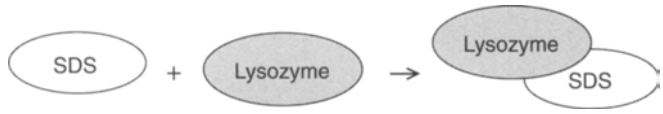


**Fig. 3.** SDS binds with Lysozyme. Owing to the four disulfide bonds lysozyme is resistant to structural changes caused by this binding. This means that the lysozyme activity remains intact in the binding process.

lysozyme secondary structure, there is no loss of lysozyme activity as a result of SDS-assisted foam fractionation. The SDS–lysozyme complex is more surface active than SDS or lysozyme alone because of the greater depression of surface tension with the complex than with either of the components. Operating SDS-assisted lysozyme foam fractionation at an airflow rate of 4 mL/min gives the best result because it yields the highest ER and leads to the recovery of about 86% of the initial enzyme, whereas operating the foam column at the other two airflow rates (8 or 12 mL/min) leads to 9% higher recovery and an enrichment loss of less than half.

### *Summary of Detergent-Assisted Foam Fractionation of Cellulase*

Without the addition of β-cyclodextrin solution, operating with additional 100.0 mg/L SDS at 12 mL/min is probably the best condition among the three detergents tested. This condition provides the lowest loss of activity. Although Pluronic F-68 does not lead to any loss of activity, it does not increase the protein concentration in the foamate, so it is not beneficial to this process. With the addition of β-cyclodextrin, CTAB is probably the best detergent among the three detergents tested. Operating the foam column with 100.0 mg/L CTAB at 12 mL/min airflow rate is wherein the cellulase in the foamate is enriched more than 1 in both mass and activity, and it also yields higher mass and activity recovery (AR) than SDS at the same flow rates *(11)*.

As Pluronic F-68 does not provide an increase in cellulase enrichment, it means that the cellulase complex does not adsorb at the air-liquid interface, and only Pluronic F-68 adsorbs and forms a foam layer. The foam then carries out the Pluronic F-68 with the original liquid solution intact. It is unlikely that Pluronic F-68 forms a complex with cellulase because nonionic surfactants such as Pluronic F-68 usually do not interact with proteins *(22,23)*. Pluronic F-68 can be used to recover roughly 55% of the initial protein without the loss of enzymatic activity but with no protein enrichment in the foamate. As an SDS-assisted foam fractionation can concentrate cellulase *(11)*, it is likely that SDS forms a complex with cellulase because anionic surfactants such as SDS usually bond strongly with proteins *(22,23)*. Some cellulose components at pH 5.0, the pH used in foaming are on average cationically charged and will interact strongly with the anionic SDS *(22,23)*. When foam is not present (not aerated), SDS alone does not decrease the cellulase activity compared with the control

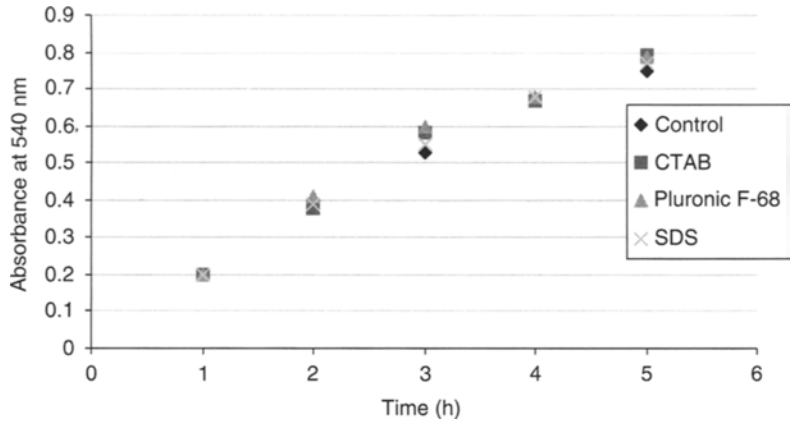


**Fig. 4.** Effect of adding different surfactants to a 200.0 mg/L cellulase solution without aeration. Absorbance response to the filter paper assay is shown in this figure.

run (of no added detergent) when tested in the filter-paper assay for 5 h. (as shown in Fig. 4). In that assay, a 200.0 mg/L cellulase solution is added to an equal value of a detergent (Pluronic F-68, SDS, or CTAB) to make 100.0 mg/L of detergent solution. Then the filter paper assay is performed, which results in an increased glucose concentration when there is an increased cellulose concentration. The increased glucose concentration reacts with the DNS solution causing a darkening of the solution. The darkened solution changes the absorbance readings determined by the plate reader and related back to the cellulose concentration. The activity is checked every hour for 5 h. The ER can be determined from the absorbance readings and is defined as the activity per unit volume of the foamate divided by the initial activity per unit volume of the solution before foaming *(11)*. The AE is defined as the activity per unit volume of the foamate divided by the initial activity per unit volume of the solution before foaming *(11)*. The MR is defined as the amount of protein in the foamate divided by the initial amount of protein *(11)*. The AR is defined as the total activity in the foamate divided by the total initial activity *(11)*.

$$\mathrm{ER} = \frac{C_{\mathrm{foam}}}{C_{\mathrm{initial}}} \tag{1}$$

$$\mathrm{AE} = \frac{A_{\mathrm{foam}}}{A_{\mathrm{initial}}} \tag{2}$$

$$\mathrm{MR} = \frac{C_{\mathrm{foam}} \times V_{\mathrm{foam}}}{C_{\mathrm{initial}} \times V_{\mathrm{initial}}} \tag{3}$$

$$\mathrm{AR} = \frac{A_{\mathrm{foam}} \times V_{\mathrm{foam}}}{A_{\mathrm{initial}} \times V_{\mathrm{initial}}} = \eta \times \mathrm{MR} \tag{4}$$

Thus, the damage occurring in the foam fractionation process of cellulase is probably caused by the foaming process, not from the surfactant added. The reorientation of a protein at a gas-liquid interface can cause surface denaturation, and is the main cause of protein denaturation in the foaming process *(30,31)*. Thus, this change in cellulase structure can result in a loss of enzymatic activity. SDS helps enrich the cellulase concentration as much as three and half times, but the activity only increases by 1.3-times at its maximum *(11)*. However, the addition of SDS only leads to a recovery of around 0.23 of the initial mass and only 0.1 of the initial activity. The addition of β-cyclodextrin with SDS creates a more dilute solution but does not provide any gain in the AE. The SDS and β-cyclodextrin pairing does not renature the enzyme well, in contrast to what has previously been reported in the literature *(32)*. CTAB tests are then carried out because it appears that CTAB and β-cyclodextrin work well with many of the proteins studied in the literature *(33–35)*. CTAB concentrates cellulase as well as SDS, but CTAB yields higher MR results. After foaming, cellulase specific activity decreases below that of the initial solution, which results in a difference between mass ER and AE ratio. Adding β-cyclodextrin (the stripping agent) solution increases the activity of the foamate as it dilutes the solution. The addition of artificial chaperones, which are substances to help proteins regain their desired folding (consisted of a detergent plus stripping agent) to the foam process, allows the cellulase to refold to its native state; thus, leading to an enzymatic activity increase. In this two step process, the detergent is likely to form a complex with the cellulase protein in the first step, preventing both aggregation and renaturation. In the second step, the stripping agent (cyclodextrin) takes away the detergent from the protein–detergent complex allowing much of the now concentrated protein to fold back to its native state.

This postulated mechanism is analogous to the well-studied natural chaperone system of GroEL/GroES *(33,34)*. In that system, GroEL first captures a denatured protein by binding to the exposed hydrophobic surfaces of that protein. Then, GroES interacts with GroEL to release the now natured protein. In the modified (for renaturation) foam fractionation process for cellulase, pictured here, the additional detergent (e.g., CTAB) binds with cellulase. CTAB does not necessarily unfold the native enzyme at room temperature, but it does dissolve any aggregated proteins *(33)*. Cationic detergents such as CTAB generally have a strong potential to bind with proteins. The surface tension curves (Fig. 5), shown here for cellulase, indicate that mixing CTAB with cellulase solution to form CTAB–cellulase complex makes the solution more surface active at least at a CTAB concentration of 0.5 m*M* (by lowering the surface tension) than CTAB or cellulase alone.

The resulting lower surface tension of the CTAB in a 0.2 mg/mL (200.0 mg/L) cellulase solution at a CTAB concentration before the CMC (1 m*M*) of CTAB likely indicates that there is a small interaction between cellulase and CTAB, particularly of the 0.5 m*M* concentration wherein the response

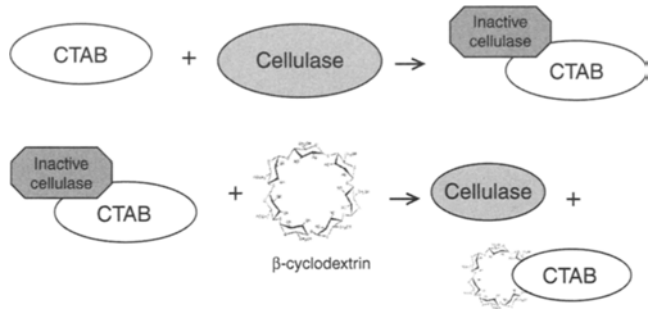


**Fig. 5.** Surface tension responses to an increase in CTAB or cellulase concentration in water and an increase in CTAB concentration in a 200.0 mg/L cellulase solution.

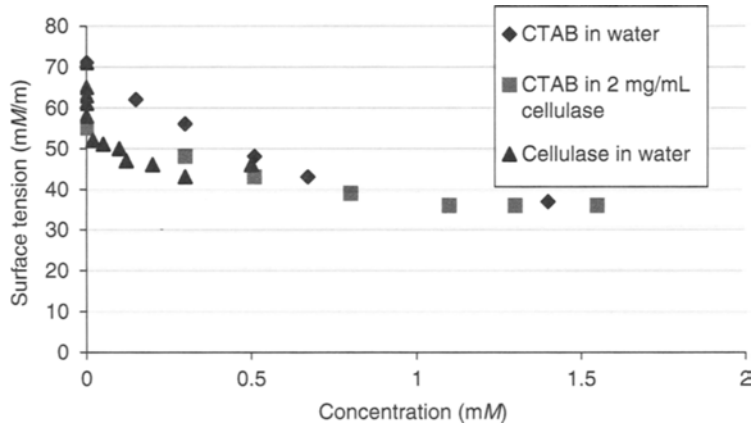


**Fig. 6.** Postulated mechanism for cellulase concentration in two steps. In step 1 cellulase and CTAB form a complex in order to concentrate the cellulase by foaming. In step 2 the CTAB is stripped away by the β-cyclodextrin.

is more than CTAB and cellulase alone. In order for the foam fractionation process to be able to concentrate a protein (such as cellulase) solution in the foamate, it is crucial that protein adsorption occurs on the foamed bubbles.

There are three possible mechanisms for adsorption of proteins in the presence of an interface and surfactants, as have been suggested *(36,37)*:

1. The protein and the surfactant do not form a complex but compete for adsorption sites on the bubble surface.
2. The protein and the surfactant form a complex, following the adsorption of only one complex at the interface.
3. Both protein and surfactant adsorb at the interface and form a solution complex.

After adsorption, foaming, and subsequent foam collapse, the now modified activity drops as suggested in the "inactive cellulase" state in the mechanism modeled in Fig. 6. The decrease in cellulase activity may be because of changes in both the secondary and tertiary structures *(30,37,38)*.

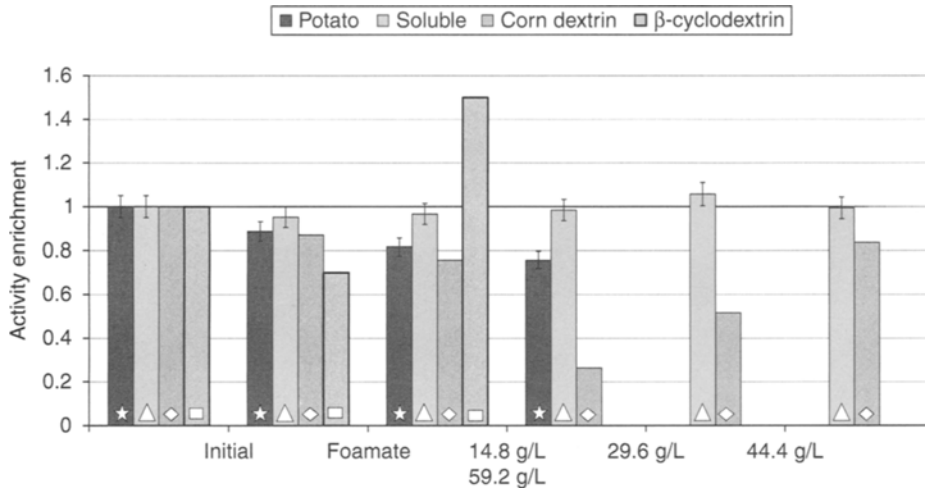


**Fig. 7.** Differences in the AE of cellulase before and after foam fractionation (foamate state) refolded with β-cyclodextrin, potato starch, starch soluble, and corn dextrin at different concentration levels. The chart shows that β-cyclodextrin is the only effective detergent stripping agent at the 14.8 g/L level. The normalized AE of 1 corresponds to the initial activity of 0.1 unit/mL.

The presence of detergent in the foamate can perhaps also prevent the protein from refolding back into its desired native state, and thus, retain its proper secondary and tertiary structure. As the initial detergent concentration (100.0 mg/L CTAB = 0.27 m*M*) is below the CMC of 1 m*M*, the detergent–protein complex is likely not to be in a micelle form *(39)*.

Restoration of the cellulase activity is performed by adding β-cyclodextrin solution to complete the artificial chaperone process. Because cyclodextrin binds more strongly to the nonpolar segment of the detergent than it does to a protein, it has the ability to separate a detergent from a protein *(33)*. From thermodynamic measurements, it has been demonstarted that cyclodextrin binds strongly to the hydrophobic segment of a detergent *(40–43)*. Because cyclodextrin can strip away the detergent from a protein–detergent complex the protein is now free to refold to its desired native state. As previously mentioned straight chain dextrins and starches are unable to remove the detergents from cellulase even at significantly higher concentrations than the β-cyclodextrin levels typically used for refolding. Results for the refolding of the foamate cellulase are shown in Fig. 7 for potato starch, starch soluble, corn dextrin, and are compared with β-cyclodextrin up to the 14.8 g/L level. It is noted that the 26.6 g/L, 44.4 g/L, and 59.2 g/L tests were carried out with corn dextrin, thinking at first that high levels kept improving the activity of cellulase. It turned out that glucose impurities present in the corn dextrin give a false-positive when using the filter paper assay. Athough there is some refolding with corn dextrin (as described by the filter paper assay, with a correction for the contaminating glucose), it is still small compared with β-cyclodextrin refolding.

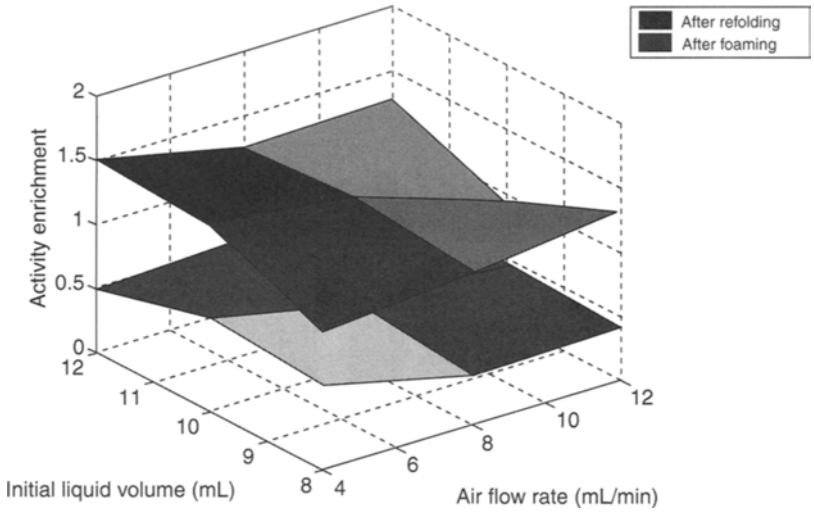


**Fig. 8.** Cellulase AE ratio for the foam fractionation of 200.0 mg/L Cellulase with 100.0 mg/L CTAB solution. The top graph illustrates the results from refolding with β-cyclodextrin solution.

However, the use of both CTAB and β-cyclodextrin together does not always refold an entire denatured protein *(32)*. This can be realized when the specific activity is calculated. The specific activity of cellulase occurs at its highest possible value before it is subjected to foam fractionation. After foam fractionation and refolding, the specific activity does not reach its initial value of 0.1 unit/mg indicating that all of the activity is not recovered and the entire denature molecule is not refolded *(11)*.

CTAB-assisted foam fractionation may concentrate different components of the cellulase complex than SDS-assisted foam fractionation. The operating pH is 5.0, but not all of pI's of the cellulase components are at 5.0. The most abundant component of cellulase produced from *Trichoderma reesei* is cellobiohydrolase I, which has a pI of 3.9 *(44,45)*. Cellobiohydrolase I likely has a net negative charge at pH 5.0 and interacts strongly with the cationic CTAB, but it may not interact as well with SDS because both are negatively charged. The cellulase component, β-glucosidase, has a pI around 6.5 *(29)*. It likely has a net positive charge at the operating pH of 5.0, so SDS probably binds stronger with this component than CTAB. However, the foam fractionation process does not have a high selectivity for distinguishing proteins with similar pI's *(7)*, so it is likely that other cellulase components are in the foamate as well. More experiments using two-dimensional gel electrophoresis or high-performance liquid chromatography are needed to determine if CTAB and SDS separate components of cellulase during the foam fractionation process. The results of applying the artificial chaperone system to the cellulase foam fractionation process are shown in previous study *(12)*. Typical results for the AE and the AR are shown in Figs. 8 and 9, respectively.

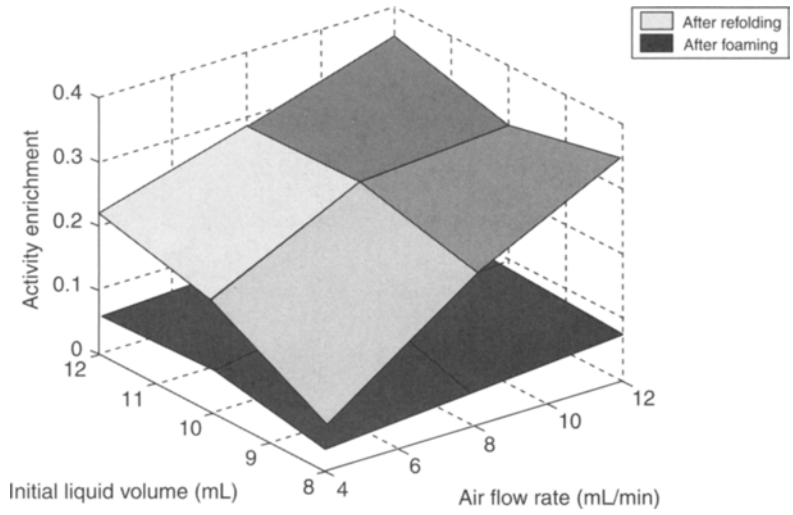


**Fig. 9.** Cellulase AR for the foam fractionation of 200.0 mg/L cellulase with 100.0 mg/L CTAB solution. The top graph illustrates the results from refolding with β-cyclodextrin solution.

The example underlying Figs. 8 and 9 uses a mixture of 200.0 mg/L cellulase and 100.0 mg/L CTAB as the initial solution, and the foamate is later diluted with β-cyclodextrin. There is a trade off between enrichment and recovery in this foam fractionation process. At the condition where the MR is the lowest, the mass ER is the highest. Therefore, it is difficult to determine the best operating conditions at one of these four points. Operating the column with a 12 mL/min airflow rate and a 12 mL initial volume and a 100.0 mg/L CTAB solution, it is chosen as the best point to operate (in the range of values tested) because it has the highest AR (*see* Fig. 9) compared with other points *(46–49)*. Just concentrating a denatured enzyme solution does not necessarily increase the value of the enzyme. What is needed is to increase the AE as well. It is noted that the discussed modified foam fractionation process may not be suitable for concentrating cellulase because of the loss in enzymatic activity.

## Conclusions

The decrease in surface tension of a mixture of a detergent and a protien, compared with the detergent and protein alone, indicates the possibility of a detergent–protein complex. The complex formation is consistent with the hypothesis that the detergent–protein complex adsorbs on the bubble surface and rises out of the liquid phase into the foam phase. Electrostatic interactions play an importat role in SDS–lysozyme foam fractionation process because the SDS is anionic and lysozyme is positively charged at the tested pH. Moreover, neither CTAB (cationic) nor Pluronic F-68 (nonionic) by themselves can concentrate lysozyme (a positively charged enzyme) in the

foam fractionation process. It is recommended that future research into this should include modeling the early time data during the refolding of cellulase with β-cyclodextrin to elucidate the early time dynamics in much the same manner as previously observed for the similar biomolecular mechanism of a substrate and enzyme in an enzyme kinetic reaction scheme.

## Acknowledgments

This work was supported in part by the USDA Grant No. 2001-52104-11476. We thank Professor Robert Balcarcel for allowing us to use Bio-Tek μQuant plate reader in his laboratory. We also thank Ph.D. candidate Tiffany Rau for her assistance in using the Bio-Tek μQuant plate reader.

## References

1. London, M., Cohen, M., and Hudson, P. B. (1954), *Biochim. Biophys. Acta* **13,** 111–120.
2. Schnepf, R. W. and Gaden, E. L. (1959), *J. Biochem. Microbiol. Technol. Eng.* **1(1),** 1–8.
3. Lemlich, R. (1968), *Ind. Eng. Chem.* **60(10),** 16–19.
4. Uraizee, F. and Narsimhan, G. (1990), *Enzyme Microb. Technol.* **12(4),** 315–316.
5. Uraizee, F. and Narsimhan, G. (1990), *Enzyme Microb. Technol.* **12(3),** 232–233.
6. Bacjleh, M., Ekici, P., Leupold, G., Coelhan, M., and Parlar, H. (2004), *J. Sep. Sci.* **27(12),** 1042–1044.
7. Kurganov, B. I. and Topchieva, I. N. (1998), *Biochemistry (Moscow, Russ Fed)* **63(4),** 413–419.
8. Gerken, N. M., Nicolai, A., Linke, D., Zorn, H., Berger, R. G., and Parlar, H. (2006), *Sep. Pur. Technol.* **49(3),** 291–294.
9. Gerken, B. M., Wattenbach, C., Linke, D., Zorn, H., Berger, R. G., and Parlar, H. (2005), *Anal. Chem.* **77(19),** 6113–6117.
10. Varley, J. and Ball, S. K. (1994), *Sep. Biotechnol.* **3,** 525–531.
11. Burapatana, V., Booth, E. A., Prokop, A., and Tanner, R. D. (2005), *Ind. Eng. Chem. Res.* **44(14),** 4968–4972.
12. Burapatana, V., Prokop, A., and Tanner, R. D. (2005), *Appl. Biochem. Biotechnol.* **121,** 541–552.
13. Luminita, A. B. (2005), *PhD Thesis*, Rechnical University of Munich, Munich, Germany.
14. Brown, A. K., Kaul, A., and Varley, J. (1999), *Biotechnol. Bioeng.* **62(3),** 291–300.
15. Noble, M., Brown, A., Jauregi, P., Kaul, A., and Varley, J. (1999), *J. Chromatogr. B* **711(1–2),** 31–43.
16. Burapatana, V., Prokop, A., and Tanner, R. D. (2004), *Appl. Biochem. Biotechnol.* **113–116,** 619–625.
17. Mandels, M., Anderotti, R., and Roche, C. (1976), *Biotechnol. Bioeng. Symp.* 21–33.
18. Loha, V., Prokop, A., Du, L. P., and Tanner, R. D. (1999), *Appl. Biochem. Biotechnol.* **77–79,** 701–712.
19. Smith, P. K., Krohn, R. I., Hermanson, G. T., et al. (1985), *Anal. Biochem.* **150(1),** 76–85.
20. (1993), *Worthington Enzyme Manual*, 5th ed. Worthington Biochemical Corporation: Lakewood, NJ.
21. Lu, R. C., Cao, A. N., Lai, L. H., Zhu, B. Y., Zhao, G. X., and Xiao J. X. (2005), *Colloids Surf. B* **41(2–3),** 139–143.
22. Lindman, B. (1993), In: *Interactions of Surfactants with Polymers and Proteins*, Ananthapadmamabhan, K. P. (ed.), CRC Press, Boca Raton, 203p.
23. Ananthapadmanabhan, K. P. (1993), In: *Interaction of Surfactants with Polymer and Proteins*, Ananthapadmamabhan, K. P. (ed.), CRC Press, Boca Raton, 319p.
24. Green, R. J., Su, T. J., Joy, H., and Lu, J. R. (2000), *Langmuir* **16(13),** 5797–5805.
25. Green, R. J., Su, T. J., Lu, J. R., and Penfold, J. (2001), *J. Phys. Chem. B* **105(8),** 1594–1602.

26. Postel, C., Abillon, O., and Desbat, B. (2003), *J. Colloid Interface Sci.* **266(1),** 74–81.
27. Lu, J. R., Su, T. J., Thomas, R. K., Penfold, J., and Webster, J. (1998), *J. Chem. Soc. Faraday Trans.* **94(21),** 3279–3287.
28. Goldberg, M. E., Rudolph, R., and Jaenicke, R. (1991), *Biochemistry* **30(11),** 2790–2797.
29. Vinzant, T. B., Adney, W. S., Decker, S. R., et al. (2001), *Appl. Biochem. Biotechnol.* **91–93,** 99–107.
30. Clarkson, J. R., Cui, Z. F., and Darton, R. C. (1999), *J. Colloid Interface Sci.* **215(2),** 323–332.
31. Clarkson, J. R., Cui, Z. F., and Darton, R. C. (1999), *J. Colloid Interface Sci.* **215(2),** 333–338.
32. Machida, S., Ogawa, S., Shi, X. H., Takaha, T., Fujii, K., and Hayashi, K. (2000), *FEBS Lett.* **486(2),** 131–135.
33. Rozema, D. and Gellman, S. H. (1996), *Biochemistry* **35(49),** 15,760–15,771.
34. Rozema, D. and Gellman, S. H. (1995), *J. Am. Chem. Soc.* **117(8),** 2373–2374.
35. Philip, J., Prakash, G. G., Jaykumar, T., Kalyanasundaram, P., and Raj, B. (2002), *Phys. Rev. Lett.* **89(26)**.
36. Wesley, R. D., Cosgrove, T., and Thompson, L. (1999), *Langmuir* **15(24),** 8376–8382.
37. Phillips, L. G., Hawks, S. E., and German, J. B. (1995), *J. Agric. Food Chem.* **43(3),** 613–619.
38. Phillips, M. C. (1981), *Food Technol.* **35(1),** 50.
39. Chatterjee, A., Moulik, S. P., Majhi, R., and Sanyal, S. K. (2002), *Biophys. Chem.* **98(3),** 313–327.
40. Liveri, V. T., Cavallaro, G., Giammona, G., Pitarresi, G., Puglisi, G., and Ventura, C. (1992), *Thermochim. Acta* **199,** 125–132.
41. Takahashi, S., Suzuki, E., and Nagashima, N. (1986), *Bull. Chem. Soc. Jpn.* **59(4),** 1129–1132.
42. Palepu, R. and Reinsborough, V. C. (1988), *Can. J. Chem.* **66(2),** 325–328.
43. Inoue, Y., Yamamoto, Y., and Chujo, R. (1983), *Carbohydr. Res.* **118,** 37–45.
44. Henriksson, H., Stahlberg, J., Isaksson, R., and Pettersson, G. (1996), *FEBS Lett.* **390(3),** 339–344.
45. Schulein, M. (1988), *Methods Enzymol.* **160,** 234–242.
46. Burapatana, V., Prokop, A., and Tanner, R. D. (2005), *Sep. Sci. Technol.* **40(12),** 2445–2461.
47. Linke, D., Zorn, H., Gerken, B., Parlar, H., and Berger, R. G. (2005), *Lipids* **40(3),** 323–327.
48. Linke, D., Zorn, H., Gerken, B., Parlar, H., and Berger, R. G. (2005), *Lebensmittelchemie* **59(129)**.
49. Linke, D., Zorn, H., Gerken, B., Parlar, H., and Berger, R. G. (2005), *Lebensmittelchemie* **59(16)**.

0273-2289/1559–0291 (Online)/07/136–140/793–804/$30.00

# Study on the Production of Biodiesel by Magnetic Cell Biocatalyst Based on Lipase-Producing *Bacillus subtilis*

MING YING[1–3] AND GUANYI CHEN*[,1,3]

[1]*Section of Bioenergy and Environment, Faculty of Environmental Science and Engineering Tianjin University, Weijin Road 92, 300072, Tianjin, China;* [2]*School of Chemical Engineering and Technology, Tianjin University; and* [3]*State Kay Lab of Internal Combustion Engine, Tianjin University, E-mail: chen@tju.edu.cn*

## Abstract

Production of biodiesel from waste cooking oils by a magnetic cell biocatalyst (MCB) immobilized in hydrophobic magnetic polymicrosphere is studied here. The cells of lipase-producing *Bacillus subtilis* were encapsulated within the net of hydrophobic carrier with magnetic particles ($Fe_3O_4$), and the secreted lipase can be conjugated with carboxyl at the magnetic polymicrosphere surface. Environmental scanning electron microscope, transmission electron microscope, and vibrating magnetometer, and so on were used to characterize the MCB. The MCB was proved to be superparamagnetic; and could be recovered by magnetic separation; moreover it could be regenerated under 48 h of cultivation. When methanolysis is carried out using MCB with waste cooking oils under stepwise additions of methanol, the methyl esters in the reaction mixture reaches about 90% after 72 h reaction in a solvent-free system. The process presented here is environmentally friendly and simple without purification and immobilized process required by the current lipase-catalyzed process. Therefore, the process is very promising for development of biodiesel fuel industry.

**Index Entries:** *Bacillus subtilis*; biodiesel; magnetic cell biocatalyst; magnetic polymicrosphere; waste cooking oils.

## Introduction

Up to now, biodiesel is usually produced through chemical-catalyzed process. Alkali or acid process always lead to large quantities of waste stream, which has to be treated before disposal. So lipase-catalyzed production of biodiesel has recently generated increasing interest because of its waste-free process *(1–3)*. However, the use of extracellar lipase as catalyst requires complicated recovery, purification, and immobilization process *(4)*. As part of a research program aimed at simplifying the process of

*Author to whom all correspondence and reprint requests should be addressed.

lipase-catalyzed biodiesel production from waste cooking oils, a magnetic cell biocatalyst (MCB) prepared with cells of *Bacillus subtilis* 1.198 were investigated. In this study, the *B. subtilis* cells were encapsulated in divinyl benzene magnetic polymicrosphere, which have superparamagnetic property. This kind of MCB can be better dispersed when it catalyzes the methanolysis reaction. It can also be more easily separated from reaction system, and stabilized in a magnetofluidized bed reactor by applying an external magnetic field. The use of magnetic particles can also reduce the capital and operational costs *(5)*. For these reasons, the process using MCB to produce biodiesel appears more promising for development of biodiesel industry.

In our previous work, we have reported the use of *Rhizopus oryzae* lipases efficiently for catalyzing the transesterification of waste cooking oils in a solvent-free medium. The cells of *R. oryzae* immobilized in polyurethane foam particles were used as whole cell biocatalyst in Kobe University (Japan). When methanolysis was carried out with stepwise additions of methanol, the level of methyl ester (ME) conversion was same as that using the extracellular lipase *(6–8)*. This forms the starting point of our research using cell-catalyzed biodiesel product. The lipase from *B. subtilis* used in this study is different from that of *R. oryzae* or *Candida antarctica* in term of the biochemical properties and three-dimensional structures *(9)*. First, lipolytic enzymes produced and secreted by *B. subtilis* include a lipase LipA (EC 3.1.1.3) and an esterase LipB (EC 3.1.1.1) *(10)*. *B. subtilis* 1.198 used in this study is a LipA-lipase overexpression strain. Second, LipA is a small protein with a molecular mass of 19.3 kDa *(11)*. The structures of LipA-lipase is clearly different from *R. oryzae* lipase studied early, which suggested no lid domain and interfacial activation *(12,13)*. This point will result in easy interaction with substrates in transesterification reaction system. Finally, LipA-lipase exhibits higher specific activities toward substrates with longer chain triacylglycerol, such as tricaprylin (C10 : 0), trilaurin (C12 : 0), and triolein (C18 : 1) Eggert et al. *(14)*.

As such, LipA-lipase of *B. subtilis* might be more suitable for biodiesel production. For the purpose of easily separating the catalyst from transesterification reaction system, and keeping stability in the fluidized-bed reactor by applying an external magnetic field, we encapsulated *B. subtilis* cells into the net of hydrophobic carrier with magnetic particles ($Fe_3O_4$) and prepared a MCB. Scanning electron microscope (SEM), transmission electron microscope (TEM), and vibrating magnetometer were used to characterize the MCB. The methanolysis activity was assayed at the same time.

## Materials and Methods

### Materials and Chemicals

The waste cooking oils were obtained from Yizhong restaurant. Olive oil (saponification value 175–195), vinyl acetate 2,2-azo-*bis*-isobutyronitrile (CR grade), and poly(vinyl alcohol) (Mr 72,000) were obtained from Tianjin

Kewei Reagent Company (Tianjin, China). Divinyl benzene (total isomers >80%) were obtained from Tianjin NanKai Chemical Factory (Tianjin, China), sodium dodecyl sulfonate, yeast extract, and tryptone were provided by Shanghai Sangon Biotechnology Co. Ltd (Shanghai, China). A neodymium permanent magnet (diameter 8 cm; magnetic field strength $2.4 \times 10^5$ A/m) from Institute of Metal Research Chinese Academy of science (Shenyang, China) was used for separation. All other chemicals were analytical grade and bought at local market.

### *Microorganism and Medium*

All experiments were carried out using *B. subtilis* 1.198. The basal medium was LB containing: tryptone 10.0 g, yeast extract 5.0 g, and NaCl 10.0 g in 1 L tap water. For solid slant medium, 20.0 g/L agar was added into above liquid medium. The immobilized medium used ATCC573 *Bacillus* medium, which contains $(NH_4)_2SO_4$ 1.3 g, $KH_2PO_4$ 0.37 g, $MgSO_4 \cdot 7H_2O$ 0.25 g, $CaCl_2 \cdot 2H_2O$ 0.07 g, $FeCl_3$ 0.02 g, glucose 1.0 g, and yeast extract 1.0 g in 1.0 L distilled water and pH is adjusted to 4.0 with 10 *N* $H_2SO_4$. The multiplication medium of magnetic cells is GYE including 20.0 g tryptone, 10.0 g sucrose, 5.0 g olive oil, 1.0 g $(NH4)_2SO_4$, 1.0 g $MgSO_4 \cdot 7H_2O$, 1.0 g $KH_2PO_4$, and 1.0 g Tween-80 in 1 L distilled water.

### *Preparation of MCB*

#### Synthesis of Lipophilic $Fe_3O_4$ Nanocolloids

According to the method described previously *(15)*, $FeCl_3 \cdot 6H_2O$ 41.9 g and $FeCl_2 \cdot 4H_2O$ 20.9 g were added to a three-necked flask containing 350 mL of distilled water, which was heated by thermostat water bath and stirred by a mechanical agitator. When temperature of thermostat water bath increased to 60°C, 50 mL of 0.5 mol $NaHCO_3$ was poured into the flask under vigorous agitation. Five milliliters stearic acid was dropped into the mixture gradually, and incubated for 20 min at 60°C before the mixture was cooled to room temperature naturally.

#### Cultivation of *B. subtilis* cells for immobilization

Mycelia collected from LB agar slants were inoculated into 5 mL of LB liquid medium. The cultures were incubated for 20 h at 37°C on a rotary shaker at 225 rpm. And then the seed suspension (grown for 20 h on LB medium) was used to inoculate with $4.0 \times 10^8$ cells/mL to 250 mL ATCC573 *Bacillus* medium in a 500-mL shake-flask, which was incubated at 37°C and 225 rpm. The *B. subtilis* cells were collected into 10 mL oleic acid in the late logarithmic growth phase, and cultivated for 1 h at room temperature and 225 rpm.

#### Synthesis of MCB

The MCB particles were synthesized by encapsulating the cells into the net of hydrophobic carrier with magnetic particles ($Fe_3O_4$) through divinyl

benzene radical suspension polymerization. In a basic preparation, 15 mL of the ferrofluid prepared as Synthesis of Lipophilic $Fe_3O_4$ Nanocolloids section, 10 mL of oleic acid *B. subtilis* cell suspension, and 1.8% 2,2-azo-*bis*-isobutyronitrile were dispersed in a mixture of 3.7 mL divinyl benzene and 16.8 mL vinyl acetate and sonicated for 10 min. The mixture was transferred into a 50-mL injector with a 60–70 μm of diameter pinhead. The mixture was injected drop by drop into a three-necked flask containing 300 mL aqueous solution of 10% poly(vinyl alcohol) plus 2.0 g/L sodium dodecyl sulfonate, which was put into a 30°C thermostat water bath and agitated at 300–500 rpm. Thereafter, the reaction mixture was maintained at 30°C stilly for 2 h. The magnetic cell microspheres were harvested by permanent magnet separation and washed three times with distilled water. Finally, the MCB was stored in 80% glycerol solution at 4°C before use.

### Multiplication Culture of Magnetic Cells

Magnetic *B. subtilis* cells were separated from the glycerol solution by magnetic separation. After washed with routinely physiological saline solution, the magnetic cells were immerged in GYE multiplication medium and cultivated for 1–3 d at 225 rpm. And then the magnetic cells biocatalyst were separated from culture medium and dried under a vacuum for about 24 h after washed three times with sterile water. Magnetic cells biocatalyst with a water content of approx 5% were obtained and can be used as a methanolysis biocatalyst.

## *Methanolysis Reaction*

The methanolysis were carried out at 40°C, 220 rpm and pH 6.5 in a 100-mL shake-flask incubating on a rotary shaker. The compositions of the reaction mixtures were as follows: waste cooking oils 68.85 g, 0.1 *M* phosphoric acid buffer (pH 6.5) 3.0 mL, and methanol 2.5 g with 3.0% MCB to the shake-flask. One molar equivalent of methanol was 2.5 g against 68.85 g waste cooking oil. To fully convert the oil to its corresponding MEs, when the ME content in the reaction mixture reached approx 30 and 60%, 2.5 g of methanol was added twice. In this case, the reaction mixture was incubated for 72 h. The composition of methanolysis products were analyzed by mass chromatography (MS) and the content of MEs were analyzed by capillary gas chromatography as described below.

## *Analysis*

One unit enzyme activity of MCB was defined as the amount of lipase, which liberates 1 μmol fatty acids from olive oils/min under the assay condition. The released fatty acids were determined by titration with 5 m*M* NaOH solution. The initial enzyme activity of MCB is about 4800 U/g assayed by this method. The ME content of the reaction mixture was quantified using an Agilent 6890N Series GC–MS system (Agilent

Technologied Corp.), and HP6890 Chemstation software was used for data analysis. The GC was equipped with a HP9091s-413 capillary column (300 μm × 30 m). For GC analysis, 500 μL of sample supernatant and 500 μL hexane as diluent were mixed in a 1.5-mL bottle. One microliter aliquot of the dilute sample was injected into the gas chromatograph. A split injector was used with a split ratio of 20 : 1 and the temperatures of injector and detector were set at 300 and 260°C, respectively. The carrier gas was nitrogen with a flow rate of 20 mL/min. An FID detector was used and the oven was initially held at 50°C, then elevated to 130°C at 20°C/min holding for 5 min, and finally to 260°C at 2.5°C/min. The oven was held at this temperature for 10 min before returning to 50°C. Total run time for this method was about 70 min. Calibration of the GC method was carried out by analyzing standard solutions of methyl palmitate, linoleic acid methylester, methyl oleate, and stearic acid ME. The standards were diluted in hexane-like reaction samples. ME yield was expressed as the percentage of MEs produced relative to the theoretical maximum based on the amount of original oils. In this article, ME yield is sometimes expressed as ME content or conversion.

### *Charaterization Analysis of MCB*

The cross-section morphology of MCB particles was observed with a JEM-100CX II TEM system (JEOL, Japan). The paramagnetic property of the dried MCB particles was analyzed with an LDJ 9600-1 vibrating sample magnetometer ([VSM], LDJ Electronics, MI). The particle size distribution and density of the magnetic microspheres was measured with a Mastersizer 2000 particle size analyzer (Malvern Instruments, UK). Scanning electron micrographs were taken by an JSM-6700F field emission SEM (JEOL, Japan). The crystal construction of MCB was determined by X-ray detector X'pert Pro (Panalytical, Dutch).

## Results and Discussion

### *Micromorphology of MCB*

The magnetic cells polymicrospheres were prepared according to the method described in Preparation of MCB section, and the morphology of the particle observed by SEM was shown in Fig. 1A. Some micropores on rough microglobules surface can be found; which is a typical copolymer beads. The cross-section of magnetic cells biocatalyst particles was observed by TEM after 48 h cultivation in GYE multiplication medium, and the photographs was shown in Fig. 1B. It can be seen that the cells of *B. subtilis* (on the cycles) were encapsulated into the internal gaps of copolymer beads. Some cells have already became dormant, but the movement of other cells can be observed under the lane of TEM.

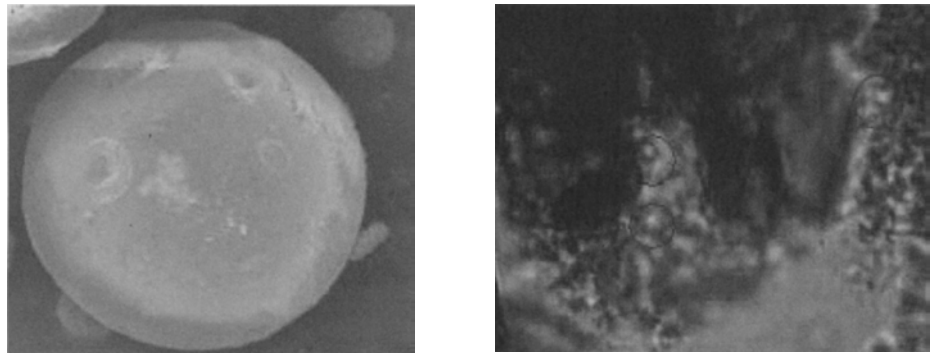


**Fig. 1. (A)** Surface features of the MCB particle observed with SEM. **(B)** Cross-section of the MCB particle observed with TEM.

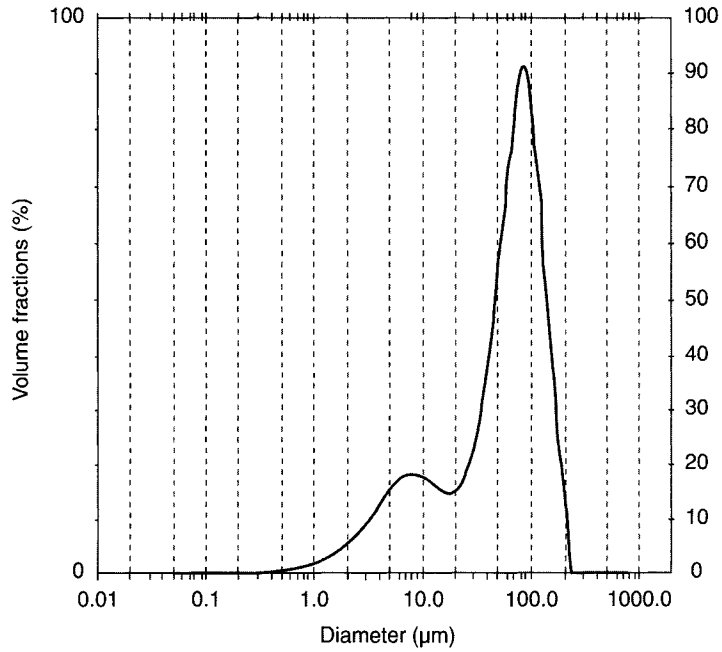


**Fig. 2.** Particle size distributions of MCB.

## *Crystal Construction of MCB*

The size distributions of MCB particles were analyzed by a Mastersizer 2000 particle size analyzer. The results are described in Fig. 2, which indicates the mean diameter is 64.7 μm, the density is 1.00 g/cm$^3$, and specific surface area is 0.5092 m$^2$/g. The magnetic particles for the preparation of the polymicrospheres were analyzed by X-ray diffraction, Fig. 3 shows the result. The spectrum of magnetic particles consisting with $Fe_3O_4$ spectrum of database indicates the core of polymicrospheres is $Fe_3O_4$ indeed. According to Scherrer

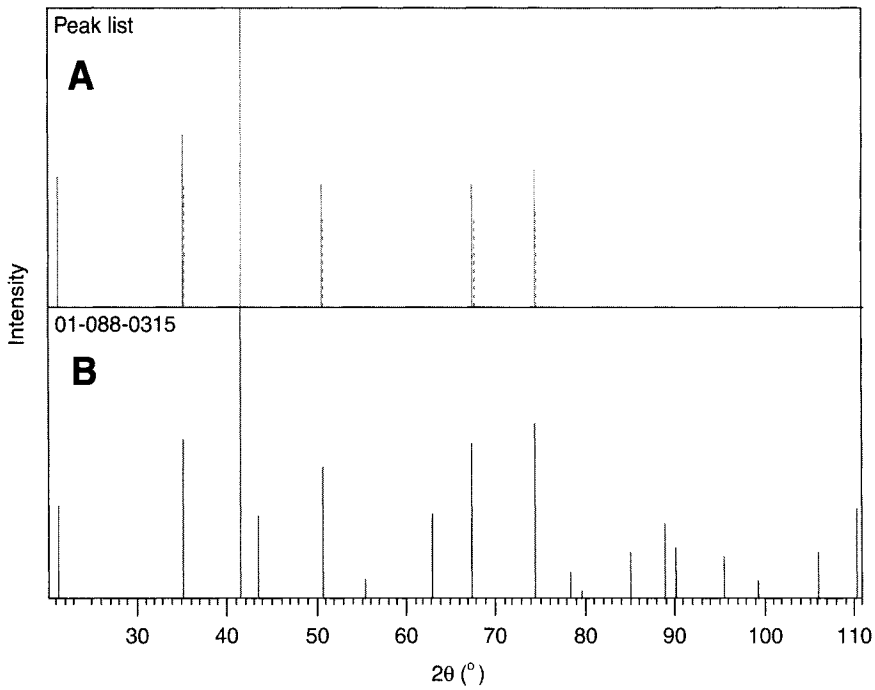


**Fig. 3.** XRD pattern of MCB comparing with standard pattern of $Fe_3O_4$, **(A)** XRD pattern of MBC. **(B)** Standard pattern of $Fe_3O_4$ in database.

equation $D_{XRD} = k\lambda/\beta\cos\theta$, the size of $Fe_3O_4$ is about 5.5–17.8 nm with a mean diameter of about 11.5 nm. For ultrafine magnetic particles, there exists a critical size, 25 nm, below which the microspheres can obtain single magnetic domains even in zero magnetic fields *(13)*. According to this magnetic theory, the MCBs prepared in this study are superparamagnetic.

### *Superparamagnetic Property of MCB*

Drawing the magnetization curve of MCB with a VSM is used to further analyze the magnetic property of the MCB particles at room temperature (300 K). The magnetization curve shown in Fig. 4 can be fitted as Langevin Eq. 1, which describes the superparamagnetic behavior well *(16)*. This provides a strong support to the superparamagnetic property of MCB

$$B = \varepsilon_m B_s \int_0^{\infty} \left[ \coth\left(\frac{kT}{\mu_0 B_s VH}\right) - \frac{kT}{\mu_0 B_s VH} \right] f(V)\mathrm{d}V \qquad (1)$$

where $B$ is the magnetization (emu/g), $B_s$ is the saturation magnetization of magnetite colloids (emu/g), $H$ is the applied magnetic field strength (Oe), $V$ is the volume of magnetite colloids ($cm^3$), $\mu_0$ is the permeability in vacuum, $T$ is the absolute temperature (K), and $k$ is the Boltzmann's constant. The values of saturation magnetization $B_s$, the remanence $B_r$, coercivity $H_c$, and maximum field strength $H_{max}$ measured by VSM are listed in Table 1 *(17)*.

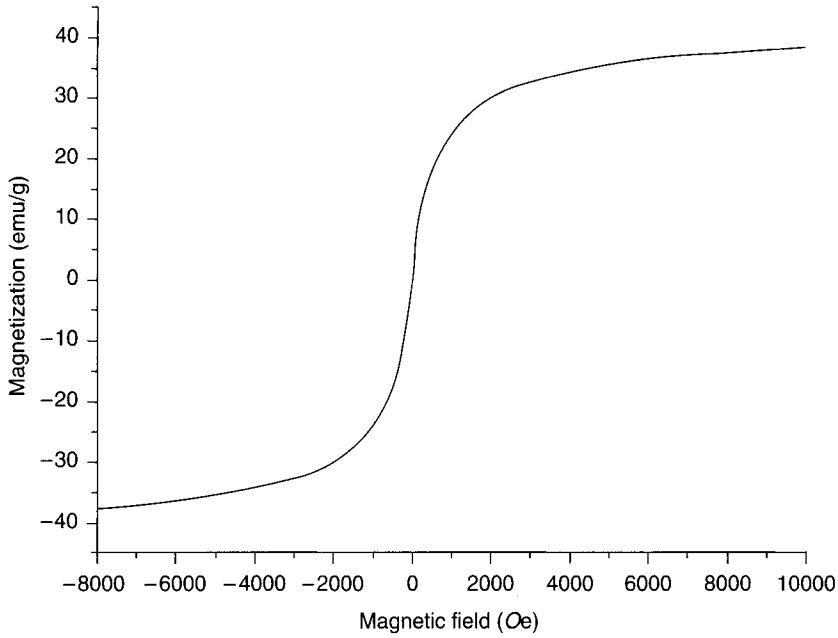


**Fig. 4.** Magnetization curves of MCB particle microspheres at 300 K. The solid line is calculated from the data measured by VSM.

Table 1
Some Magnetic Parameters of MCB Measured by VSM

| | |
|---|---|
| Maximum field strength ($H_{max}$ [Oe]) | 9960 |
| Coercivity ($H_c$ [Oe]) | −0.1094 |
| Remanence ($B_r$ [emu/g]) | 0.01004 |
| Saturation magnetization ($B_s$ [emu/g]) | 3.867 |

From the results of VSM, it can be seen that remanence (0.01004 emu/g) and coercivity (–0.1094 emu/g) were so small that hysteresis could hardly be observed *(18)*. This feature is also typical of superparamagnetism *(19)*. So the MCB particles could be easily settled within 22 s under the permanent magnet field. When the external magnet was removed, the MCB particles can be well dispersed by gentle shaking. The above conclusion indicates the advantage of the MCB, i.e., easy for recovery and recycling *(20)*.

## *Methanolysis Activity of MCB*

Figure 6 shows the composition of ME, which is converted by MCB from waste cooking oil. The reaction is under the conditions: temperature 40°C, pH 6.5, loading of MCB 3.0%, adding methanol in two stepwise and reacting for 72 h. The analytic result of Fig. 5 is listed in Table 2. It can be seen that all the components are ME and basically belong to longer carbon

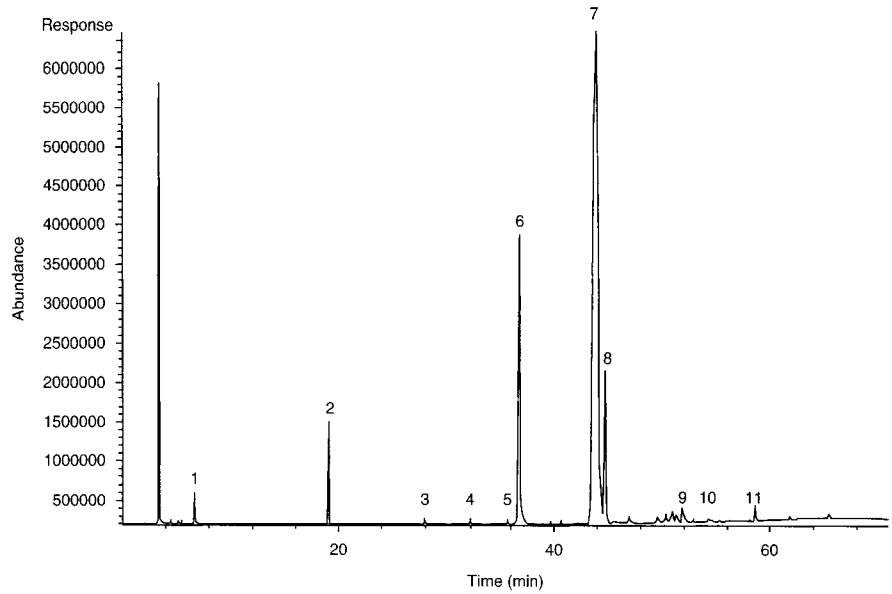


**Fig. 5.** The GC–MS spectrum of ME converted by MCB from waste cooking oil.

Table 2
Result of GC–MS Analysis on Chemical Composition of Methanolysis Production

| No. | Compositions name | Retention time (min) |
|---|---|---|
| 1 | Decanis acid and ME | 8.206 |
| 2 | Methyl tetradecanoate | 19.094 |
| 3 | 9-Hexadecenoic acid and ME | 28.495 |
| 4 | Hexadecanoic acid and ME | 33.758 |
| 5 | Pentadecanoic acid and 14-methyl ME | 37.725 |
| 6 | 8,11-Octadecadienoic acid and ME | 38.538 |
| 7 | 9-Octadecenoic acid and ME | 44.034 |
| 8 | Eicosanoic acid and ME | 46.396 |
| 9 | Docosanoic acid and ME | 53.046 |
| 10 | Tricosanoic acid and ME | 56.126 |
| 11 | Etracosanoic acid and ME | 59.217 |

chain ($>C_{12}$). The main components are octadecadienoic acid ME (C18 : 1; C18 : 2), which is involved in the range of biodiesel fuel *(21)*. The ME content analyzed by capillary gas chromatography is about 90%. All of the peaks are methyl ester except for the first one which is the diluent.

## *Regeneration Property of MCB*

The MCB particles can be repeated for use many times; however, the methanolysis activity will decrease gradually like immobilized lipase. The method of MCB regeneration was investigated in this study. When

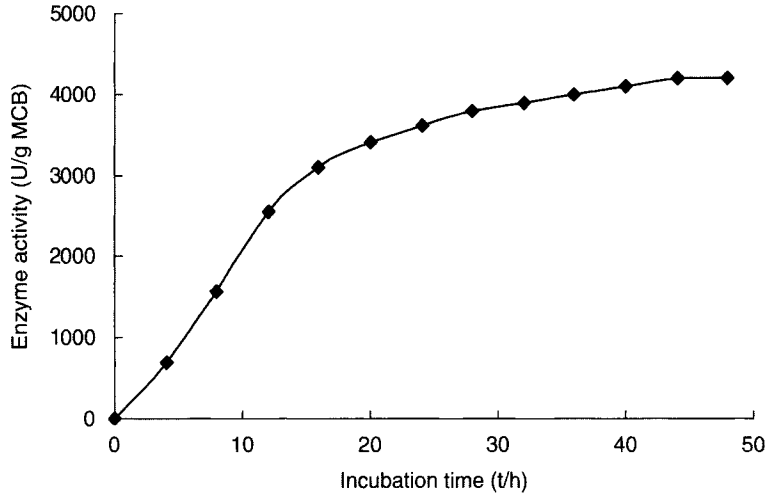


**Fig. 6.** Curve of enzyme activity change of MBC incubated in GYE medium.

enzyme activity of MCB decreases, the MCB particles separated from reactive mixture with a permanent magnet were washed with acetone and physiological saline solution before added into the GYE medium. The enzyme activity of MCB was assayed as described in Preparation of MCB section at interval of 4 h during 48 h cultivation. Figure 6 shows the curve of enzyme activity change when MCB particles regenerate. The results indicate *B. subtilis* cells encapsulated within polymicrosphere can propagate in the rich GYE medium, at the same time the enzyme activity of MCB increase gradually. All the results demonstrate the advantage of MCB in terms of easy regeneration, like cultivation of microorganisms.

## Conclusions

A novel method of immobilizing cells within magnetic material has been developed for production of biodiesel from waste cooking oils. This new type of biocatalyst was characterized by various techniques, and the results demonstrate the MCB particles have superparamagnetic property and have the advantages of easy recovery, recycling, and regeneration. The conclusions of our work indicate MCB can avoid the disadvantage of extracellular lipase-catalyzed reaction, such as complicated recovery, purification, and immobilization process required. Moreover, the methanolysis of waste cooking oils with MCB shows high conversion up to 90%. Further work should be concentrated on optimizing the various reaction parameters in order to shorten the reaction time and also on investigating kinetic behavior of methanolysis reactions, which may be included in the nonaqueous media.

## Acknowledgments

This work was financially supported by Ministry of Science and Technology (China) through National Key Fundamental Research Programme (Contract No. 200556617).

## References

1. Du, W., Xu, Y. Y., Liu, D. H., and Zeng, J. (2004), *J. Mol. Catalysis B: Enzymatic* **30,** 125–129.
2. Köse, Ö., Tüter, M., and Aksoy, A. H. (2002), *Bioresour. Technol.* **83,** 125–129.
3. Iso, M., Chen, B. X., Eguchi, M., Kudo, T., and Shrestha, S. (2001), *J. Mol. Catalysis B: Enzymatic* **16,** 53–58.
4. Oda, M., Kaieda, M., Hama, S., et al. (2005), *Biochem. Eng. J.* **23,** 45–51.
5. Bahar, T. and Celebi, S. (2000), *Enzyme Microb. Technol.* **26,** 28–37.
6. Kondo, A., Liu, Y., Furuta, M., Fujita, Y., Matsumoto, T., and Fukuda, H., (2000), *Enzyme Microbial. Technol.* **27,** 806–811.
7. Ban, K., Hama, S., Nishizuka, K., et al. (2002), *J. Mol. Catalysis B: Enzymatic* **17,** 157–165.
8. Ban, K., Kaieda, M., Matsumotoc, T., Kondo, A., and Fukuda, H. (2001), *Biochem. Eng. J.* **8,** 39–43.
9. Ruiz, C., Blanco, A., Pastor, F. I. J., and Diaz, P. (2002), *FEMS Microbiol. Lett.* **217,** 263–267.
10. Eggert, T., Brockmeier, U., Dröge, M. J., Quax, W. J., and Jaeger, K. E. (2003), *FEMS Microbiol. Lett.* **225,** 319–324.
11. Ruiz, C., Pastor, F. I. J., and Diaz, P. (2003), *Lett. Appl. Microbiol.* **37,** 354–359.
12. Eggert, T., Pouderoyen, G. V., Pencreac'h, G., et al. (2002), *Colloids Surf. B: Biointerfaces.* **26,** 37–46.
13. Pouderoyen, G. V., Eggert, T., Jaeger, K. E., and Dijkstral, B. W. (2001), *J. Mol. Biol.* **309,** 215–226.
14. Eggert, T., Pouderoyen, G. V., Dijkstrab, B. W., and Jaeger, K. E. (2001), *FEBS Lett.* **502,** 89–92.
15. M. Z. Y., Guan, Y. P., Liu, X. Q., and Liu, H. Z. (2005), *Chin. J. Chem. Eng.* **13,** 239–243.
16. Bean, C. P. and Livingston, J. D. (1959), *J. Appl. Phys.* **30,** 120–129.
17. Xue, B. and Sun, Y. (2002), *J. Chromatogr. A.* **947,** 185–193.
18. Chantrell, R. W. and Popplewell, J. (1978), *IEEE Trans. Mag.* **14,** 975–980.
19. Zhang, M. L. and Sun, Y. (2001), *J. Chromatogr. A.* **912,** 31–38.
20. Kobayashi, H. and Matsunaga, T. (1991), *J. Colloid Interface Sci.* **141,** 505–511.
21. Kröbitz, W. (1999), *Renewasble Energy* **16,** 1078–1083.

0273-2289/1559-0291 (Online)/07/136-140/805-816/$30.00

# Production of ω-3 Polyunsaturated Fatty Acids From Cull Potato Using an Algae Culture Process

ZHANYOU CHI,[1] BO HU,[1] YAN LIU,[1] CRAIG FREAR,[1] ZHIYOU WEN,[2] AND SHULIN CHEN*,[1]

*[1]Department of Biological Systems Engineering, Washington State University, WA 99163, E-mail: chens@wsu.edu; and [2]Department of Biological Systems Engineering, Virginia Polytechnic Institute and State University, VA 24061*

## Abstract

Algal cultivation for converting cull potato to docosahexaenoic acid (DHA) was studied. *Schizochytrium limacinum* SR21 was selected as the better producing strain, compared with *Thraustochytrium aureum* because of higher cell density and DHA content. Used as both carbon and nitrogen source, an optimal ratio of hydrolyzed potato broth in the culture medium was determined as 50%, with which the highest production of 21.7 g/L dry algae biomass and 5.35 g/L DHA was obtained, with extra glucose supplemented. Repeat culture further improved the cell density but not fed batch culture, suggesting limited growth was most likely caused by metabolites inhibition.

**Index Entries:** Docosahexaenoic acid; microalgae; omega-3 fatty acid; *Schizochytrium*; cull potato; fish oil.

## Introduction

ω-3 Polyunsaturated fatty acids (ω-3 PUFAs) are a group of fatty acids containing two or more double bonds, of which the last double bond is located at the third carbon atom from the methyl terminal. Docosahexaenoic acid (DHA, 22:6) is a particularly important ω-3 PUFA, with a 22-carbon chain and six double bonds. It has been reported that DHA is an essential nutrient during early human development *(1,2)*; it is supplied to the infant through the placenta during pregnancy and through human milk after birth. Being an important component of the photoreceptor cells of infants' retinas, DHA is also involved in the development of infants' brain tissues through incorporation in synaptic vesicles, myelin, and mitochondria. As a result of its important role in infant development,

*Author to whom all correspondence and reprint requests should be addressed.

inclusion of supplementary DHA in infant formulas is recommended by the World Health Organization *(3)*.

The conventional source of ω-3 PUFAs is mostly from fish oil. Cod, salmon, sardine, mackerel, menhaden, anchovy, tuna, and seal are generally used for fish oil production. The quality of fish oil is variable, being dependent on fish species, season, and geographical location of the catch site. As marine fish oil is a complex mixture of fatty acids with varying chain lengths and degrees of saturation, DHA needs to be refined from fish oil for use in nutraceutical/pharmaceutical applications. The purification of DHA from low-grade fish oil can be difficult and costly *(4)*, and in addition, marine fish stocks are subject to seasonal and climatic variations, and might not be able to provide a steady supply for the increasing demands of DHA. In fact, fish are not capable of synthesizing PUFA *de novo* and much of their PUFA is derived from the primary producer in the oceanic environment: the microalgae or algae-like microorganisms *(5)*.

DHA produced from heterotrophic algal culture is taking on a more and more important role and could, with increased economic viability, gradually substitute fish oil, as it offers better taste, odor, and stability *(5)*. Although a large number of microalgae contain DHA, only a few species have demonstrated production potentials on an industrial scale *(6)*, in that they can accumulate high oil contents in their biomass, produce a high percentage of total lipids as DHA, and reach high biomass densities in a short time. Strains from the *Traustochytrid* marine protists and dinoflagellate *Crypthecodinium cohnii* have traditionally been considered to have the most potential in a commercial setting, especially the former *(5)*, which belongs to the genus *Thraustochytrium* and *Schizochytrim.* Initial research on *Thraustochytrium* produced relatively low cell densities around 5.0–20.0 g/L as well as low DHA content in the biomass. Lately, although, new *Schizochytrium* strains have been isolated *(7)*. In initial research with these strains, the highest DHA productivities were 2.0 g/L·d using optimized media *(8)*. The lipid extracted from the cell was about 50% of the dry cell weight and the DHA content of the lipid was 34% of total fatty acids. Optimal culture conditions for the specific strain *Schizochytrium limacinum* SR21 have also been investigated. A high total fatty acids content, up to more than 50%, was obtained with corn steep liquor as the nitrogen source and an increase in carbon source concentration led to a high-DHA yield *(9)*. In this work, a DHA yield of > 4.0 g/L was obtained in both glucose and glycerol media at 9% and 12% concentrations, respectively, which indicated that *S. limacinum* SR21 is a promising algae strain for DHA production.

High-yield production culture of *Schizochytrium* strains has also been investigated *(10)*. With increased carbon (glucose) and nitrogen (corn steep liquor and ammonium sulfate) sources in the medium, 48.1 g /L dry cell weight and 13.3 g/L DHA were produced in a 4-d culture with 12% glucose. The lipid content was 77.5% of dry cells, and the DHA content was 35.6% of total fatty acids. With this excellent performance, this algae

strain was eventually applied to the commercial sector. The new high cell density fed batch fermentation process developed by the commercial sector splits the overall fermentation process into a biomass density increasing stage and a DHA production stage; resulting in biomass densities of at least 100.0 g dry cell/L in the fermentation broth and at least 20% of their dry cell weight as lipids *(11)*.

Even with such yield and productivity improvements, fish oil is still a substantial competitive threat to the new commercialized DHA productions from algae fermentation *(12)*. Urea crystallization, supercritical fluid extraction, and high-performance liquid chromatography are used for extraction and purification of DHA from fish oil, which are difficult and costly. However, several companies have developed microencapsulated fish oil products that claim to have resolved much of the odor, stability, and taste issues associated with fish oil whereas simultaneously removing the need for costly purification. Thus, it is still indispensable for research to continue to decrease the cost of production from heterotrophic algal cell cultivation. Using under-utilized cull potato to replace glucose as a carbon source and to provide the nitrogen source might be a good choice. There are more than 10–15% of harvested potatoes that are classified as culls, and therefore unfit for market or processors. Development of new markets for the culls is essential to the profit margins of the potato producers because the cost to grow the culls is $70–120/t, whereas presently they can be sold as an animal feed for only about $10–20/t. Converting the culls to a value-added bioproduct is an excellent way to develop new markets and overcome the cost to produce the culls, as they can provide starch, protein, vitamins, and salt nutrients for the fermentation process. In fact, microbial production of lactic acid from potato starch has been widely reported *(13)*. Various bacteria such as *Lactobacillus, Lactococcus* and *Streptococcus*, and the fungi *Rhizopus* were used as the producers, with hydrolyzed potato starch as the carbon source *(14–16)*. Among them, some strains of *Rhizopus oryzae* can use potatoes as the sole nutrient supply in the culture medium. With one of these strains, Liu et al *(17)* optimized the culture condition to produce 33.3 g/L lactate. This indicates that cull potato can be an effective feedstock for the production of lactic acid and potentially other valued nutraceuticals.

Compared with lactate, DHA is more valuable. If these potatoes can be converted to DHA, it will not only benefit the DHA manufacturers, in that this will significantly reduce the medium cost of the production process, but also the farmers because the high value-added product will better offset the production costs. Preliminary research for the development of such a process was investigated in this article. The specific objectives of this study were:

1. Selecting a high yield DHA producer algae strain.
2. Determining the optimum ratio of HPB to the whole medium.
3. Developing a higher cell density culture process.

## Methods

### Algal Strains

The alga strain *Thraustochytrium aureum* (American Type Culture Collection [ATCC] 34304) and *S. limacinum* SR21, (ATCC MYA-1381) were used in the experiments. The seed cells were cultured in artificial seawater medium, as described by the University of Texas at Austin, Culture Collection of Algae (UTEX) (http://www.bio.utexas.edu/research/utex/), with 5.0 g/L glucose, as well as 1.0 g/L yeast extract, and 1.0 g/L peptone.

### Culture Conditions

The culture medium for DHA production consisted of artificial sea water, 5.0 g/L corn steep solids (Sigma, St. Louis, MO), and 1.0 g/L ammonium acetate as nitrogen sources plus either pure glucose, or as described in the later experiments, a certain percentage of hydrolyzed potato broth (HPB). The initial medium pH was adjusted to 6.0 by addition of hydrochloric acid. The cells were cultured in 250-mL Erlenmeyer flasks at 20°C, with inoculums of 5 mL seed cells to 50 mL culture medium. After 6 d culture, the algae cells were harvested to conduct dry cell weight and fatty acid analysis.

To prepare HPB, cull potato was boiled and minced, mixed with certain volume of water and placed in a 5-L tank with agitation. Two enzymes, α-amylase and glucoamylase were used to hydrolyze the potato starch into glucose. The temperature used in the hydrolysis process was 55°C. After 4 d, the hydrolyzed broth was harvested and centrifuged to remove the solids. The glucose concentration in the liquid phase was determined and then diluted to 100.0 g/L with water.

### Cell Growth and Fatty Acid Analysis

The algae biomass in the broth was harvested and centrifuged, removed from the medium, and washed twice with distilled water. The biomass was then dried at 105°C for 3 h and weighed.

One milliliter of the same biomass was distributed to screw top glass tubes; then placed in a freeze dryer overnight. The preparation of fatty acid methyl ester (FAME) directly from algae biomass was used, putting to use a method as described in Indarti *(18)*. After freeze-drying, a 4 mL mixture of methanol, concentrated sulfuric acid and chloroform (1.7 : 0.3 : 2.0 [v/v/v]) were added into the tube. Four milligrams arachidonic acid (C20 : 4) or heptadecanoic acid (C17 : 0) was added as the internal standard. Tubes were placed inside a heated water bath at 90°C for 40 min. On completion of the reaction, the tubes were cooled down to room temperature and weighed again to dismiss leaking samples. Then, 1 mL of distilled water was added into the mixture and thoroughly vortexed for 1 min. After the formation of two phases, the lower phase containing the FAME was transferred to a clean, 10-mL bottle and dried with anhydrous $Na_2SO_4$. Half milliliter-dried

Table 1
Comparing Cultures of the *S. limacinum* SR21 with *T. aureum*

| Strain | Carbon source | Concentration (g/L) | Dry cell weight (g/L) | DHA yield (g/L) | DHA/ biomass (%) |
|---|---|---|---|---|---|
| *T. aureum* | Soluble starch | 30 | 7.7 | 0.65 | 8.4 |
| | Potato starch | 30 | ND[a] | 0.40 | ND[a] |
| *S. limacinum* | Pure glucose | 30 | 12.6 | 2.30 | 18.2 |
| SR21 | Potato glucose | 30 | 10.8 | 1.75 | 16.2 |
| | Pure glucose | 90 | 20.1 | 3.51 | 17.5 |
| | Potato glucose | 90 | 9.2 | 0.52 | 5.7 |

[a]Not determined, because residual potato starch was mixed with the algae biomass.

solutions were transferred into a vial and stored in a freezer (–20°C) for gas chromatography (GC) analysis. The method of FAME analysis using a GC was the same as reported by Wen and Chen *(19)*. Briefly, a GC machine from HP Inc. and a GC column from Restek (cat no: 12498) were used in this analysis. The parameters of this GC column are: 30 m × 0.32 mm ID × 0.25 μm.

## Results

### *Alga Strain Selection*

*T. aureum* can take starch directly as a carbon source to support its growth *(20)*, whereas *S. limacinum* SR21 grows poorly in starch *(9)*. The carbon in the cull potato mainly exists as starch. The cost of hydrolyzing the starch could be avoided if the starch could be utilized directly. In the preliminary work (data not shown) with *T. aureum*, the highest dry cell weight was obtained when the starch concentration was 30.0 g/L, thus, this concentration was used in this experiment. The performance of these two algal strains was compared, as shown in Table 1. *T. aureum* was cultured with both soluble starch (Sigma) and potato starch, whereas *S. limacinum* SR21 was cultured with two levels (30.0 g/L and 90.0 g/L) of pure glucose or a certain amount of HPB. Results of the study showed that *T. aureum* reached a maximum dry cell weight of 7.7 g/L, but with the same amount of carbon source, *S. limacinum* reached a maximum of 12.6 g/L dry biomass. Additionally, the DHA yield and DHA content in the biomass was much higher in *S. limacinum*. The fatty acids profile of *S. limacinum* SR 21 in the GC analysis was shown in Fig. 1.

Even higher dry cell weights and DHA yield were obtained with *S. limacinum* SR 21 when 90.0 g/L of glucose were used instead of 30.0 g/L. This indicated that *S. limacinum* SR 21 can grow well on a high carbon source concentration. Unfortunately, the culture result with HPB containing 90.0 g/L glucose was lower than its 30.0 g/L counterpart, which implies that inhibition occurred when a high percentage of HPB was used. These

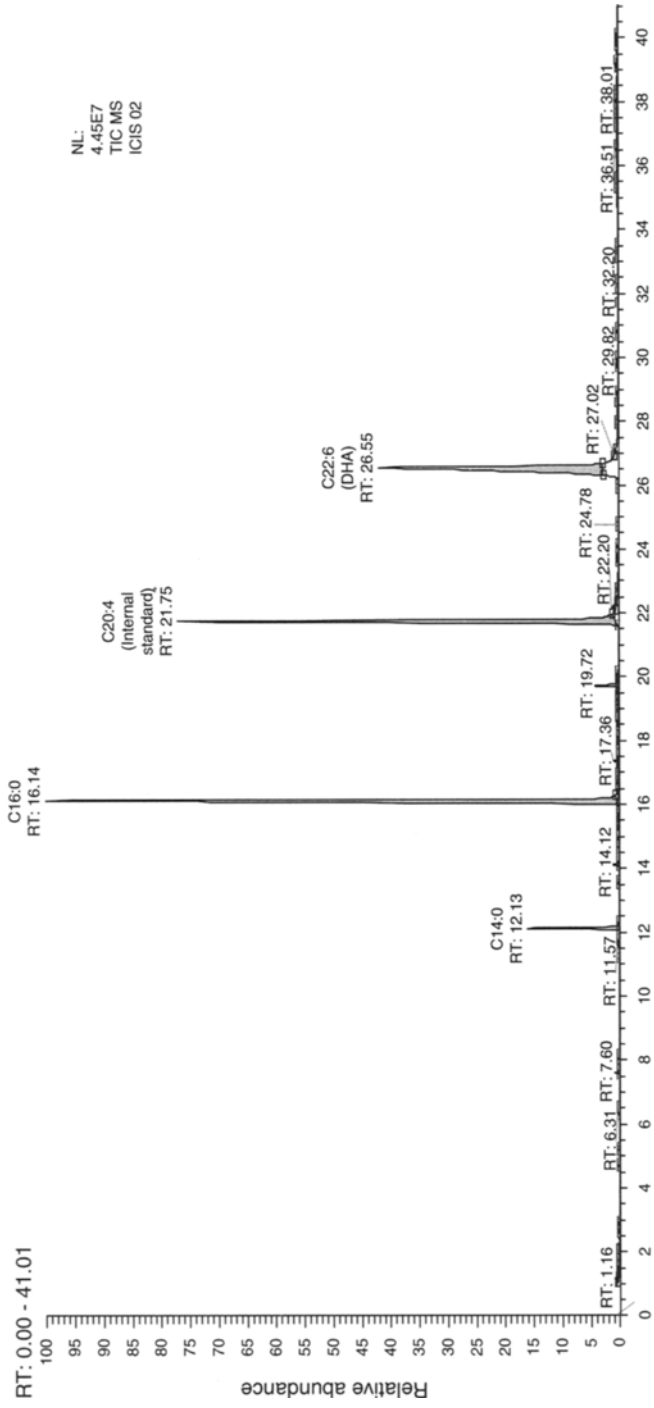


**Fig 1.** GC analysis of the FAME from *S. limacinum* SR 21.

Table 2
Culture Results With Various Concentration of HPB

| Carbon source | Nitrogen source added | HPB/ medium (% [v/v]) | Glucose concentration (g/L) | Nitrogen concentration (g/L) | Dry cell weight (g/L) | DHA yield (g/L) | DHA in biomass (%) |
|---|---|---|---|---|---|---|---|
| Group 1: HPB | 5.0 g/L Corn steep solids | 70 | 70 | 1.74 | 18.1 | 2.70 | 14.9 |
| | | 50 | 50 | 1.40 | 18.6 | 2.70 | 14.5 |
| | | 30 | 30 | 1.06 | 11.7 | 1.60 | 13.7 |
| | | 70 | 70 | 1.19 | 17.3 | 2.79 | 16.2 |
| Group 2: HPB | Without | 50 | 50 | 0.85 | 17.0 | 2.81 | 16.5 |
| | | 30 | 30 | 0.51 | 10.8 | 1.75 | 16.2 |
| Group 3: Pure glucose | 5.0 g/L Corn steep solids | – | 70 | 0.55 | 21.2 | 3.76 | 17.7 |
| | | – | 50 | 0.55 | 19.0 | 3.35 | 17.6 |
| | | – | 30 | 0.55 | 12.6 | 2.30 | 18.2 |

results show that the performance of *S. limacinum* was much better than *T. aureum* and although the latter can directly utilize starch, the production efficiency was too low. Thus, *S. limacinum* was used as the DHA producing strain in the ensuing experiments.

### *HPB Percentage Optimization*

As shown in Table 1, the growth of *S. limacinum* SR21 was inhibited with the use of a high HPB concentration, which has been inferred to be caused by the presence of a certain inhibitor in the HPB. One hypothesis was that a potential inhibitory source might be the high nitrogen source, in that the nitrogen content in the HPB was 1.7 g/L (total kjeldahl nitrogen [TKN]), which is equivalent to the nitrogen in 15.0 g/L of corn steep solids. It is well known that the C/N ratio strongly affects the lipids accumulation in the DHA producers, so determining the optimal HPB concentration and corresponding nitrogen concentration in the culture was necessary. In this experiment, the HPB culture was diluted to various concentrations, as shown in Table 2. The cultures with and without added nitrogen source (5.0 g/L corn steep solids) were also compared. The cultures with pure glucose were taken as the control.

Compared with the culture with 90.0 g/L pure glucose in which 20.1 g/L dry algae biomass was obtained, the biomass production in the culture with 90% HPB was only 9.2 g/L, as shown in Table 1. This indicates that there was severe inhibition in the culture with a high percentage of HPB. But in the range of 30–70%, the differences were not significant ($p > 0.05$, as shown in Table 3). This indicates that the inhibition were relatively moderate in the lower percentage of HPB, owing to the corresponding lower inhibitor

Table 3
The $p$-Value of Paired $t$-Test of Various Groups in Table 2

| | Dry cell weight | DHA yield | DHA content in biomass |
|---|---|---|---|
| Group 2 vs Group 3 | 0.062 | 0.040 | 0.026 |
| Group 1 vs Group 3 | 0.219 | 0.025 | 0.022 |
| Group 1 vs Group 2 | 0.049 | 0.018 | 0.036 |

Table 4
Culture Results of HPB Medium With Glucose Added ($n = 3$)

| Glucose added (g/L) | Dry cell weight (g/L) | DHA yield (g/L) | DHA content in biomass (%) |
|---|---|---|---|
| 0 | 16.3 ± 0.1 | 2.69 ± 0.04 | 16.5 ± 0.3 |
| 20 | 21.7 ± 1.0 | 5.35 ± 0.04 | 24.7 ± 1.2 |
| 40 | 20.7 ± 0.4 | 4.83 ± 0.02 | 23.3 ± 0.5 |

concentration in the culture. Therefore, the results of this study showed that the original hypothesis of the high nitrogen concentration in the culture being the cause of the growth inhibition was incorrect, because a higher biomass production was obtained in the HPB culture with extra nitrogen as compared with the culture without any nitrogen addition.

The earlier data showed that it was not necessary to add an extra nitrogen source to the HPB culture, because the culture without any extra nitrogen supported good growth of the algae. Also, the extra nitrogen significantly decreased the DHA content in the biomass, compared with the culture without nitrogen added (Tables 2 and 3). In fact, 0.55 g/L nitrogen was enough to support 20.0 g/L algae biomass growth using pure glucose (Table 2). An equivalent nitrogen concentration (0.51 g/L) existed in the 30% HPB, suggesting that this would be the optimal HPB concentration, but taking into consideration that a higher biomass concentration may be reached in future work, which will need more nitrogen, the percentage of 50% HPB was taken as the basic medium in the ensuing work.

## *Culture With Glucose Added to HPB*

Although the nitrogen concentration in the culture with 50% HPB is enough to support higher biomass density, the 50.0 g/L glucose in it may be a limiting factor, in that with the same concentration of pure glucose reported earlier, only 19.0 g/L dry biomass was obtained (Table 2). If this hypothesis is right, supplement of extra glucose in the culture should enhance the production. In this verification experiment, 20.0 g/L and 40.0 g/L pure glucose were added to the culture with 50% HPB with the results shown in Table 4.

Table 5
Repeat Culture Results ($n = 3$)

| Culture day | Dry cell weight (g/L) | DHA yield (g/L) | DHA content in biomass (%) |
|---|---|---|---|
| 6 | 20.1 ± 0.9 | 4.75 ± 0.05 | 23.7 ± 1.0 |
| 12 | 41.0 ± 1.0 | 9.14 ± 0.08 | 22.2 ± 0.7 |

Compared with the control, the added glucose significantly enhanced the cell density, to as much as 21.7 g/L dry cell biomass with 5.35 g/L DHA obtained in 6-d culture. However, there was no significant difference between the 20.0 and 40.0 g/L glucose added groups, which indicate that the glucose was no longer a limiting factor.

### *Feeding and Repeat Culture*

To develop a higher cell density culture, a fed batch culture was conducted with a defined medium. In practice, each component of the medium, at half the amount of the initial culture, was added to the end of the previous batch culture. Unfortunately, there was no further increase in yield with respect to addition of all the supplements (data not shown). This indicated that the reduced growth in batch culture was not caused by depletion of certain nutrients and must therefore be a result of inhibition owing to accumulation of some metabolites. To verify this hypothesis, a repeat culture was conducted. In practice, at the 6th d of this culture, the fermentation broth was centrifuged and the spent medium was removed and replaced with fresh medium at which point the culturing process was allowed to proceed for another 6 d. The results of this repeat culture are shown in Table 5. The cell density climbed to 41.0 g/L in the repeat culture, and the DHA yield in these cultures reached 9.14 g/L. This verified that some metabolites in the culture inhibited the cells' growth. The analysis to determine what the inhibitory factors are and the method of how to avoid the inhibition are to be conducted in future work.

## Discussion

Compared with *S. limacinum* SR 21, which has been proven to be a good DHA producer *(9)*, *T. aureum* obtained a much lower final cell density and DHA content, which led to very low production efficiency, even though *T. aureum* can take direct advantage of starch as a carbon source. Later experiments that used *S. limacinum* as the production strain within a HPB as both the carbon source and nitrogen source, attained similar results as that from the culture of pure glucose with added nitrogen source. This result along with the knowledge that the starch hydrolyzing process is widely used in the fermentation industry makes DHA production from cull potatoes a feasible and perhaps cost effective process. Also, this production efficiency may

be further increased if a simultaneous saccharification and fermentation process were to be used.

A higher ratio of carbon-to-nitrogen is preferred for this alga to accumulate fatty acids *(9)*, but the ratio of carbon-to-nitrogen in potato is not optimal for this process. To offset this, in this experiment, a HPB containing 100.0 g/L glucose was prepared, which correspondingly, contained 1.7 g/L nitrogen. The algae grew well in the culture without any extra nitrogen source having been added, which indicated that this amount of nitrogen was enough to support the algae's growth. This will significantly decrease the feedstock cost for DHA production, in that the cull potato provided both the carbon and nitrogen source. The low ratio of C/N in the original HPB caused a low DHA content in the biomass, but this was improved by reducing the percentage of HPB (reduction of the nitrogen source concentration) and adding extra glucose to the culture.

21.7 g/L dry cell biomass and 5.35 g/L DHA was obtained in the optimized culture. Compared with the results of the same algae strain by Yokochi et al *(9)* in which 4.0 g/L DHA and more than 30.0 g/L biomass was obtained with 90.0 g/L glucose in 50% concentration of seawater, we obtained less biomass production, but higher DHA yield. Although the productivity in these preliminary studies are still rather low, compared with the processes currently used commercially, they indicate cull-potato utilization is a feasible and promising way to produce DHA and in a more economically efficient manner because of the reduction in fermentation feedstock cost.

## Conclusions

1. Although it cannot directly utilize potato starch, *S. limacinum* SR21 is a better DHA producer with cull potato as raw material, in that it accumulated a high content of DHA in the biomass, and reached a high culture cell density.
2. The ratio of carbon-to-nitrogen in the potato is not optimal for the DHA production process, but it can be improved by reducing the percentage of HPB in the medium and adding extra glucose in the culture.
3. The process of converting underutilized cull potato to DHA is promising and worth further study to reach a high cell density culture.

## Acknowledgments

We thank Washington state potato commission (WSPC) and Washington State University IMPACT center for their funding support.

## References

1. Innis, S. M. (1994), *Can. J. Physiol. Pharmacol.* **72,** 1483–1492.
2. Makrides, M. and Gibson, R. A. (1995), *Br. J. Clin. Practice* **(Suppl. 80),** 37–44.

3. FAO/WHO Expert Committee (1998), Fats and oils in human nutrition. (http://www.fao.org/docrep/v4700E/v4700E0c:htm#infant%20nutrition). Accessed February 21, 2007.
4. Belarbi, E. H., Molina, E., and Chisti, Y. (2000), *Process Biochem.* **35,** 951–969.
5. Ward, O. P. and Singh, A. (2005), *Process Biochem.* **40,** 3627–3652.
6. Ratledge, C. (2004), *Biochimie* **11,** 807–815.
7. Honda, D., Yokochi, T., Nakahara, T., et al. (1998), *Mycol. Res.* **102,** 439–448.
8. Nakahara, T., Yokochi, T., Higashihara, T., et al. (1996), *J. Am. Oil Chem. Soc.* **73,** 1421–1426.
9. Yokochi, T., Honda, D., Higashihara, T., et al. (1998), *Appl. Microbiol. Biotechnol.* **49,** 72–76.
10. Yaguchi, T., Tanaka, S., Yokochi, T., et al. (1997), *J. Am. Oil Chem. Soc.* **74,** 1431–1434.
11. Bailey, R. B., DiMasi, D., Hansen, J. M., et al. (2003), US Patent, 6,607,900.
12. Martek Annual Report. (2005), (http://www.corporate-ir.net/library/11/116/116214/items/184075/2005_Annual.pdf). Accessed February 21, 2007.
13. Anuradha, R., Suresh, A. K., and Venkatesh, K.V. (1999), *Process Biochem.* **35,** 367–375.
14. Litchfield, J. H. (1996), *Adv. Appl. Microbiol.* **42,** 45–95.
15. Tsao, G. T., Cao, N. J., Du, J., and Gong, C. S. (1999), *Adv. Biochem. Eng.* **65,** 243–280.
16. Hofvendahl, K. and Hahn-Hägerdal, B. (2000), *Enzyme Microb. Technol.* **26,** 87–107.
17. Liu, Y., Wen, Z., Liao, W., et al. (2005), *Eng. Life Sci.* **5,** 343–349.
18. Indarti, E., Majid, M. I. A., and Hashim, R., et al. (2005), *J. Food Compos. Anal.* **8,** 161–170.
19. Wen, Z. Y. and Chen, F. (2000), *Biotechnol. Lett.* **22,** 727–733.
20. Bajpai, P. K., Bajpai, P., and Ward, O. P. (1991), *J. Am. Oil Chem. Soc.* **68,** 509–514.

0273-2289/1559-0291 (Online)/07/136-140/817-834/$30.00

# Hybrid Neural Network Model of an Industrial Ethanol Fermentation Process Considering the Effect of Temperature

IVANA C. C. MANTOVANELLI,[1] ELMER CCOPA RIVERA,[2] ALINE C. DA COSTA,*[,2] AND RUBENS MACIEL FILHO[2]

[1]*Department of Biotechnological Processes; and* [2]*Department of Chemical Processes, School of Chemical Engineering—UNICAMP, Cidade Universitária "Zeferino Vaz"—Caixa Postal 6066—CEP 13083-970–Campinas–SP—Brasil, E-mail: accosta@feq.unicamp.br*

## Abstract

In this work a procedure for the development of a robust mathematical model for an industrial alcoholic fermentation process was evaluated. The proposed model is a hybrid neural model, which combines mass and energy balance equations with functional link networks to describe the kinetics. These networks have been shown to have a good nonlinear approximation capability, although the estimation of its weights is linear. The proposed model considers the effect of temperature on the kinetics and has the neural network weights reestimated always so that a change in operational conditions occurs. This allow to follow the system behavior when changes in operating conditions occur.

**Index Entries:** Alcoholic fermentation; functional link networks; kinetic parameters estimation; mathematical modeling; process simulation; bioreactors.

## Introduction

A potential substitute for petroleum in Brazil is biomass, particularly sugar cane. The sugar cane industry is the largest alternative commercial energy production program in the world with ethanol and the almost complete use of sugar cane bagasse as fuel. Although the bioethanol production is running for several years it is clear that improvements are required to increase the process performance. The influence of temperature in the kinetics is a very important factor in the alcoholic fermentation process. It is difficult to support a constant temperature during large-scale alcoholic fermentation and variations in temperature affects productivity through changes in kinetics as well as in microorganism lifetime. The temperature in a typical industrial fermentor varies from 33.5°C (during the night) to

*Author to whom all correspondence and reprint requests should be addressed.

35°C (at the end of the day) owing to fluctuations in the cooling water temperature. In plants with poor temperature control the temperature in the fermentor goes up to 40°C. Thus, an accurate mathematical model must take the influence of temperature into account. Also, changes in operational conditions and fluctuations in raw material composition, both very common in alcoholic fermentation plants, results in kinetic changes and affects yield and productivity.

Owing to the difficulties described above, the main difficulty in model-based techniques for definition of operational strategies, control, and optimization for the ethanol production process is the problem of obtaining an accurate model. Thus, in this work a procedure for the development of robust mathematical models for the alcoholic fermentation process is evaluated. The objective is to obtain a model to be used as a simulator, making simpler not only the development and implementation of new control and optimization techniques, but also retuning of existing controllers as well as finding out new optimal operational conditions when operational changes occur.

In the last years, many studies of the mathematical modeling of alcoholic fermentation process have been performed *(1,2)*. However, although temperature has an important influence on this process, there are very few works in the literature considering the effect of temperature on the kinetic parameters. Among them are the works of Atala et al. *(3)* and Aldiguier et al. *(4)*. However, Aldiguier et al. *(4)* determined different values for kinetic parameters in different temperatures, but did not determine a temperature function to describe the kinetic parameters. Although phenomenological mathematical models provide understanding about the process, practical experience shows that they are only valid for the specific conditions in which they were determined. When there are changes in operational conditions, the model kinetic parameters have to be reestimated. The frequent reestimation, mainly when the parameters are described as functions of temperature, is difficult and time-consuming because of nonlinearities, great number of parameters, and interactions among them.

One way to deal with this problem is to use hybrid neural models *(5,6)*. As was demonstrated by Psichogious and Ungar *(7)*, it is simple to propose a bioreactor mathematical model through application of mass balances for the process variables. The really difficult part is the mathematical representation of the kinetics. A cell is a complex organism wherein thousands of enzyme-catalyzed reactions take place. The kinetic rates are most often poorly understood nonlinear functions; whereas the corresponding parameters are in general time-varying *(8)*. Literature presents a great number of approximate kinetic models, which take different factors into account, and the proper choice of the mathematical description of these expressions is object of discussion in many works *(2,3,9,10)*. Thus, hybrid neural models are suitable to model biotechnological processes, as they combine mass and energy balance equations with neural networks, which represent the unknown kinetics *(11)*. In this work a hybrid neural model is proposed to

model an industrial alcoholic fermentation process. The specific growth rate is described by a functional link network (FLN) *(12)*. These networks have been shown to have a good nonlinear approximation capability, although the estimation of its weights is linear. Because of this linear estimation, the FLNs training is rapid, requires low computational effort, and convergence is guaranteed, so that it has a large potential for online control and optimization implementations *(6)*.

## Industrial Alcoholic Fermentation Process—Phenomenological Model

The alcoholic fermentation process to be modeled is illustrated in Fig. 1. This is an existing plant, designed using the procedure of Andrietta and Maugeri *(13)* to a maximum production of 320 $m^3$ of anhydrous ethanol/d. The system is a typical large-scale industrial process made up of five continuous-stirred tank reactors attached in series and operating with cell recycle. Each reactor has an external heat exchanger to keep the temperature constant at an ideal level for the fermentation process. The feedstock, a mixture made up of sugar cane molasses and syrup and sources of nitrogen and mineral salts, is converted into ethanol by a fermentation process carried out using the yeast *Saccharomyces cerevisiae*. A set of centrifuges splits the outlet-fermented product into two phases. The light phase ($F_V$) is sent to a distillation tower in which the alcohol is finally obtained. The heavy phase is mixed with acid and diluted with water (flow rate $F_a$) before being recycled (flow rate $F_R$) to the first reactor. $F_S$ ($m^3/h$) is the flow rate of the cell purge stream, used to permit cell renovation and the withdrawal of secondary products accumulated into the fermentor. These process-operating conditions are real conditions of typical industrial distilleries in Brazil.

The mass and energy balances for the five fermentors are:
Global mass balance in *i*th fermentor:

$$\frac{dV_i}{dt} = \frac{F_{i-1} \times \rho_{i-1}}{\rho_i} - F_i \tag{1}$$

Substrate balance in *i*th fermentor:

$$\frac{d(S_i V_i)}{dt} = F_{i-1} S_{i-1} - F_i S_i - V_i X_i \frac{1}{Y_{X/S}} \mu_i \tag{2}$$

Product balance in *i*th fermentor:

$$\frac{d(P_i V_i)}{dt} = F_{i-1} P_{i-1} - F_i P_i + V_i X_i \frac{Y_{P/S}}{Y_{X/S}} \mu_i \tag{3}$$

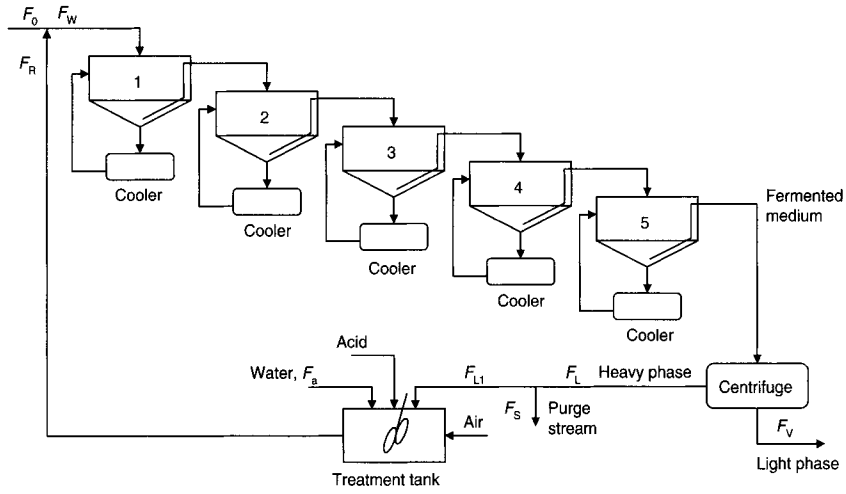


**Fig. 1.** Schematic illustration of an industrial plant for ethanol production.

Biomass balance in *i*th fermentor:

$$\frac{d(X_i V_i)}{dt} = F_{i-1}X_{i-1} - F_i X_i + V_i X_i \mu_i \tag{4}$$

Energy balance in *i*th fermentor:

$$\frac{d(V_i T_i)}{dt} = F_{i-1}T_{i-1} - F_i T_i + F_i(T_{Ci} - T_i) + \frac{V\Delta HX_i}{\rho_i Cp_i Y_{X/S}}\mu_i \tag{5}$$

Energy balances for the reagent fluid in *i*th heat exchanger:

$$\frac{d(T_{Ci})}{dt} = F_{Ci}(T_i - T_{Ci})\rho_i Cp_i - \left(\frac{UA_i}{V_{Ci}\rho_i Cp_i}\right)\mathrm{LMTD}_i \tag{6}$$

Energy balances for the cooling fluid in *i*th heat exchanger:

$$\frac{d(T_{J_i})}{dt} = \frac{F_{J_i}}{V_{J_i}}(T_{J_e} - T_{J_i}) + \left(\frac{UA_i}{V_{J_i}\rho_J Cp_J}\right)\mathrm{LMTD}_i \tag{7}$$

Logarithmic mean temperature difference (LMTD) for *i*th heat exchanger:

$$\mathrm{LMTD}_i = \frac{(T_i - T_{J_i}) - (T_{Ci} - T_{J_e})}{\ln(T_i - T_{J_i})/(T_{Ci} - T_{J_e})} \tag{8}$$

where the subscripts i refer to each stage (fermentor); $J_i$ and $J_e$ are indexes referring to water inlet and outlet of the cooler; C is an index referring to

process fluid at the cooler; $V$ ($m^3$) is the reactor volume; $T$ (°C) is the temperature; $F$ ($m^3/h$) is the flow rate; $S$ ($kg/m^3$), $X$ (g/L), and $P$ ($kg/m^3$) are the substrate, cell, and ethanol concentrations, respectively; ρ ($kg/m^3$), Cp (J/kg·°C), and $\Delta H$ (J/kg) are density, specific heat, and reaction heat, respectively; and $Y_{X/S}$ and $Y_{P/S}$ are the kinetic parameters of yield. A kinetic model was validated with typical industrial conditions for this process *(14)*. The specific growth rate used was proposed by Lee et al. *(2)*:

$$\mu = \mu_{MAX} \frac{S}{K_S + S}\left(1 - \frac{P}{P_{MAX}}\right)^n \left(1 - \frac{X}{X_{MAX}}\right)^m \tag{9}$$

where $\mu_{MAX}$ ($h^{-1}$), $P_{MAX}$ ($kg/m^3$), and $X_{MAX}$ ($kg/m^3$) are the maximum specific growth rate, the product concentration when cell growth ceases and the biomass concentration when cell growth ceases, respectively, and n and m are inhibitor terms coefficients. The maximum specific growth rate, $\mu_{max}$, is influenced by temperature and is calculated by the Arrhenius equation *(15)*:

$$\mu_{MAX} = Ae^{\frac{-E}{RT}} \tag{10}$$

According to Andrietta *(14)*, $P_{MAX}$ has a constant value below a critical temperature (32°C) and above this temperature its value is described by:

$$P_{MAX} = K_0 e^{aT} \tag{11}$$

The kinetic parameters and constants used with Eqs. 1–11 are given by $E$ = 6417 J/mol, $A = 4.5 \times 10^{10}$, $R = 8.314$ J/mol·K, $K_0 = 895.6$ kg/m$^3$, $a = -0.0676$ °C$^{-1}$, $X_{max} = 100$ kg/m$^3$, $n = 3.0$, $m = 0.9$, $K_s = 1.6$ kg/m$^3$, $Y_{P/S} = 0.445$, $Y_{X/S} = 0.033$ *(14)*. Table 1 shows the design parameters for the five fermentors.

The operations involved in the recycle (centrifuge, purge, dilution, and mixing) presents fast dynamics when compared with the fermentation process and can be considered in pseudo-steady-state. The concentrations of ethanol and substrate can be considered to remain constant in the value of the fermentor outlet at the centrifuge exit. Also, variations in density are considered negligible through the process. The equations are as follows:

$$F_W = \frac{F_0}{1 - RR} \tag{12}$$

$$F_R = F_W - F_0 \tag{13}$$

Cell concentration is kept constant in the recycle by manipulation of water flow rate, $F_a$. Mass balance on the dilution tank leads to:

$$F_{L1} = \frac{F_R X_R}{X_L} \tag{14}$$

Table 1
Design Parameters for the Five Fermentors

| Reactor | $A_i$ ($m^2$) | $V$ ($m^3$) | $F_c$ ($m^3/h$) | $F_J$ ($m^3/h$) | $V_c$ ($m^3$) | $V_J$ ($m^3$) |
|---|---|---|---|---|---|---|
| 1 | 76.361 | 433 | 400 | 400 | 20 | 20 |
| 2 | 63.242 | 370 | 350 | 350 | 20 | 20 |
| 3 | 31.061 | 366 | 180 | 180 | 20 | 20 |
| 4 | 6.809 | 359 | 60 | 60 | 20 | 20 |
| 5 | 2.869 | 333 | 28 | 30 | 20 | 20 |

$$F_a = F_R - F_{L1} \tag{15}$$

$$S_R = \frac{F_{L1} S_5}{F_R} \tag{16}$$

$$P_R = \frac{F_{L1} P_5}{F_R} \tag{17}$$

Mass balance on the centrifuge leads to:

$$F_V = F_W \frac{X_L - X_5}{X_L - X_V} \tag{18}$$

$$F_L = F_W - F_V \tag{19}$$

In the purge point we have:

$$F_S = F_L - F_{L1} \tag{20}$$

The concentrations of the first fermentor feeding are:

$$S_S = \frac{F_R S_R + F_0 S_0}{F_W} \tag{21}$$

$$P_W = \frac{F_R P_R}{F_W} \tag{22}$$

$$X_W = \frac{F_R X_R}{F_W} \tag{23}$$

The mathematical model is made by Eqs. 1–23 and solved using the fourth order Runge–Kutta method. The must feed flow rate used was $F_0 = 100\ m^3/h$. Other parameters used in the equations are: $\Delta H = -6.509 \times 10^5\ J/kg$, $\rho = 950\ kg/m^3$, $Cp = 4184.1\ J/kg{\cdot}°C$, $U = 1.464 \times 10^7\ J/h{\cdot}°C{\cdot}m^2$, $\rho_J = 1000\ kg/m^3$, $Cp_J = 4184.1\ J/kg{\cdot}°C$ *(14)*. The model does not consider cellular death because purge and recycle maintain the average age of cells in the process

from 7 to 10 d (young cells). Death rate is equal to the rate of cellular replacement and there is no accumulation of live cells or dead cells.

## Hybrid Neural Model

The phenomenological model described by Eqs. 1–23 was determined by Andrietta *(14)* considering a real industrial process operating in continuous mode. It was validated with industrial data and shown to describe the process dynamic behavior accurately. However, this model is not able to describe the process in the presence of changes in operational conditions. In 2005, Andrietta evaluated this same model and concluded that, for the current operational conditions in the factory evaluated, the model of Ghose and Thyagi *(1)* with some modifications led to a better description of the process dynamic behavior. He also determined the existence of four groups of kinetic parameters in different harvesting periods in the year, which indicates that, in order to describe the dynamic behavior of the plant for long periods of time, the mathematical model should have its kinetic parameters updated periodically. However, the reestimation of kinetic parameters, mainly if they are considered functions of temperature, is a difficult and time-consuming task.

In order to solve this problem we used a hybrid neural model in which the kinetics is described by FLNs. The great advantage of these neural networks is that the estimation of its weights is a linear problem, and so the reestimation is rapid and convergence is guaranteed. The hybrid model consists of the mass and energy balance equations (Eqs. 1–8 and 12–23) and a FLN, which describes the specific biomass growth rate. The choice of this kinetic rate to be described by the neural network was made based on the results of a sensitivity analysis of the process.

## Functional Link Networks

A neural network typically consists on many simple computational elements or nodes arranged in layers and operating in parallel. The weights, which define the strength of connection between the nodes, are estimated to yield good performance. Usually, in the training of neural networks, the inputs to a node are linearly weighted before the sum is passed through some nonlinear activation function that ultimately gives the network its nonlinear approximation ability. However, the same nonlinearity creates problems in learning the network weights, as nonlinear learning rules must be used, the learning rate is often unacceptably slow, and local minima may cause problems *(12)*. One way of avoiding nonlinear learning is the use of FLNs. In these networks, a nonlinear functional transformation or expansion of the network inputs is initially performed and the resulting terms are combined linearly. The obtained structure has a good nonlinear approximation capability and the estimation of the network weights is linear.

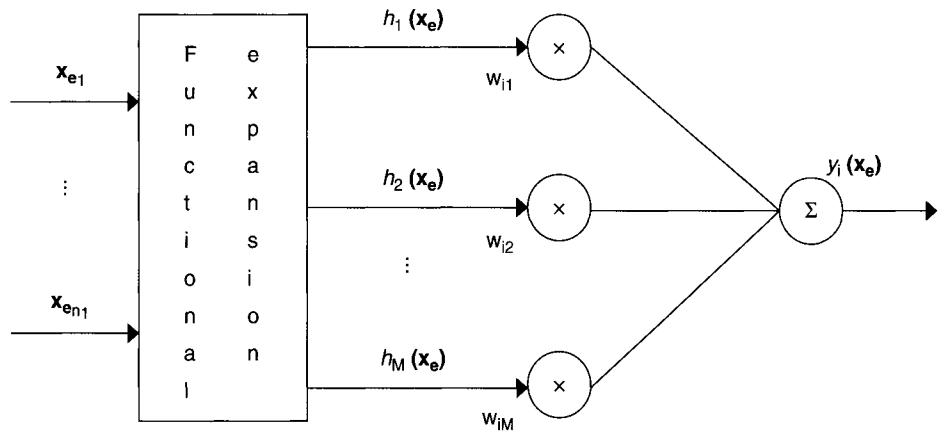


**Fig. 2.** General structure of a FLN.

The general structure of an FLN is shown in Fig. 2, where $\mathbf{x}_e$ is the input vector and $y_i(\mathbf{x}_e)$ is an output. The hidden layer performs a functional expansion on the inputs, which maps the input space of dimension $n_1$, onto a new space of increased dimension, $M$ ($M > n_1$). The output layer consists on m nodes, each one, in fact, a linear combiner. The input–output relationship of the FLN is

$$y_i(\mathbf{x}_e) = \sum_{J=1}^{M} w_{ij} h_J(\mathbf{x}_e), 1 < i \leq m \tag{24}$$

We use a modification in the structure of the FLNs, where the output given by Eq. 24 is transformed by an invertible nonlinear activation function. The new output is

$$y_i(\mathbf{x}_e) = f_i\left(\sum_{J=1}^{M} w_{ij} h_J(\mathbf{x}_e)\right), 1 < i \leq m \tag{25}$$

where $f_i$ is an invertible nonlinear function such as, for example, the sigmoidal function. Another modification in the FLNs used in this work is that the real inputs ($\mathbf{x}_e$) are transformed into a greater number ($n_z$) of auxiliary inputs ($\mathbf{z}$) before the functional expansion is performed. These modifications increase the nonlinear approximation ability of the network and yet, the estimation of the parameters remains a linear problem. A polynomial expansion of degree six is then performed on the new inputs. The generated monomials ($h_J[\mathbf{z}]$) are shown in Table 2.

Once the monomials are generated, the orthogonal least-squares estimator proposed by Billings et al. *(16)* is used to calculate the network weights ($w_{ij}$) and to eliminate the monomials, which are not significant in explaining the output variance. This reduces the size and complexity of the neural network and avoids overfitting of the data.

Table 2
Polynomial Expansion of Degree Six

| Degree | Monomials |
|---|---|
| 0 | 1 |
| 1 | $z_i$ $(i = 1, n_z)$ |
| 2 | $z_i z_j$ $(i = 1, n_z, j = i, n_z)$ |
| 3 | $z_i z_j z_k$ $(i = 1, n_z, j = i, n_z,$ and $k = j, n_z)$ |
| 4 | $z_i z_j z_k z_l$ $(i = 1, n_z, j = i, n_z, k = j, n_z,$ and $l = k, n_z)$ |
| 5 | $z_i z_j z_k z_l z_m$ $(i = 1, n_z, j = i, n_z, k = j, n_z, l = k, n_z,$ and $m = l, n_z)$ |
| 6 | $z_i z_j z_k z_l z_m z_n$ $(i = 1, n_z, j = i, n_z, k = j, n_z,$ $l = k, n_z, m = l, n_z,$ and $n = m, n_z)$ |

Table 3
Full Factorial Design With Axial Points and One Center Point

| Time (h) | $S_0$ (g/L) | $T_0$ (°C) |
|---|---|---|
| 10 | 158.8 | 29 |
| 20 | 158.8 | 34 |
| 30 | 201.2 | 29 |
| 40 | 201.2 | 34 |
| 50 | 150 | 31.5 |
| 60 | 210 | 31.5 |
| 70 | 180 | 28 |
| 80 | 180 | 35 |
| 90 | 180 | 31.5 |

## *Training of the Neural Network*

The network inputs ($\mathbf{x_e}$) are the process state variables: biomass, substrate and product concentrations, and temperature. The output is the specific growth rate. In this work, the state variables are considered accessible by direct measurement, but the output is not measurable. It can be estimated from measured experimental data by the discretization of the biomass balance equation. When dealing with noisy data, some kind of smoothing algorithm has to be applied to produce reliable rate values from biomass concentration data. Training was performed using a full factorial design, considering axial points and one center point, involving the variables $S_0$ and $T_0$. Both variables had their values changed every 10 h within the ranges 150–210 g/L ($S_0$) and 28–35°C ($T_0$). Ten hours is enough time for the process to reach a new steady state. Table 3 shows the factorial design.

During training and validation the performance of the FLN was measured by Eq. 26, given by Milton and Arnold *(17)*:

$$\text{cor} = \left( 1 - \frac{\sum_{k=1}^{N} [y_e(k) - y(k)]^2}{\sum_{k=1}^{N} [y_e(k) - \bar{y}_e]^2} \right) 100\% \tag{26}$$

where $y_e(k)$ is the real output, $y(k)$ is the network output, $\bar{y}_e$ is the mean value of the real outputs and $N$ is the number of training points. For validation, the disturbances encompassed a sequence of steps with random changes every 10 h within the ranges 162–198 g/L ($S_0$) and 28°C to 32°C ($T_0$). During training and validation the activation function that led to the best performance is given by Eq. 27:

$$f\left( \sum_{j=1}^{M} w_{ij} h_j(\mathbf{z}) \right) = \frac{1}{\sum_{j=1}^{M} w_{ij} h_j(\mathbf{z})} \tag{27}$$

The auxiliary input vectors were chosen for each reactor after many tests and are given in Table 4.

## Results

For the five process fermentors, the best performance of the FLNs was obtained using fifth degree monomials. Using four auxiliary inputs (as shown in Table 4) we generated 126 monomials for each of the five FLNs (each one describing the specific growth rate of one fermentor). After using the orthogonal least-squares estimator proposed by Billings et al. *(16)* to eliminate nonsignificant monomials, the number of monomials for each network was drastically reduced, as can be seen in Table 5, which shows the number of monomials and the performance of the five FLNs during validation (measured by Eq. 26).

The number of monomials in the FLNs can be considered equivalent to the number of connections (or weights) in a multilayer perceptron neural network.

The five FLNs are described by Eqs. 28–32:

$$\mu_{FLN}(\text{Fermentor 1}) = \frac{1}{-1.4295T^{1.18} + 1.1165 \times 10^{-23} X^{6.04} \frac{1}{S} P^{9.84} + 6.8689 \times 10^{-7} X^{6.04} P^{4.92} T^{1.18}}$$

$$\frac{1}{-5.0705 \times 10^{-13} X^{3.02} P^{4.92} T^{1.77} + 7.5585 \times 10^{-7} X^{3.02} T^{2.36} - 5.104 \times 10^{-24} \frac{1}{S} P^{14.76} T^{0.59}} \tag{28}$$

$$\frac{1}{+9.7211 \times 10^{-10} P^{4.92} T^{2.36}}$$

Table 4
Input Vectors of the Network

| Reactor | Vector (z) |
|---|---|
| 1 | $z = \left[ X^{3.02} \frac{1}{S} P^{4.92} T^{0.59} \right.$ |
| 2 | $z = \left[ X^{2.7} \frac{1}{S} \frac{1}{P^{4.0}} T^{0.6} \right]$ |
| 3 | $z = \left[ X^{3.0} \frac{1}{S} P^{4.90} T \right]$ |
| 4 | $z = \left[ X \frac{1}{S} P T^{0.4} \right]$ |
| 5 | $z = \left[ X^{1.25} \frac{1}{S} P T^{0.59} \right]$ |

Table 5
Performance and Number of Monomials for the FLN

| Reactor | Number of monomials | Performance (%) |
|---|---|---|
| 1 | 7 | 99.6870 |
| 2 | 6 | 99.6868 |
| 3 | 11 | 99.9895 |
| 4 | 18 | 99.7873 |
| 5 | 18 | 96.6931 |

$$\mu_{FLN}(\text{Fermentor 2}) = \frac{1}{-334.11 + 0.0060987X^{8.1}\frac{1}{P^{4.0}} + 1.1656 \times 10^{-14}X^{10.8}\frac{1}{S} - 7.2676 \times 10^{-7}X^{10.8}\frac{1}{P^{4.0}} \frac{1}{-4.5488 \times 10^{-11}X^{8.1}\frac{1}{S^{2.0}} + 8.6769 \times 10^{-9}X^{5.4}T^{1.8}}} \quad (29)$$

$$\mu_{FLN}(\text{Fermentor 3}) = \frac{1}{9039.3 - 323.37T - 0.00033194\frac{1}{S}P^{4.9} + 3.0911 \times 10^{-5}\frac{1}{S}P^{4.9}T - 9.6048 \times 10^{-7}\frac{1}{S}P^{4.9}T^2 \frac{1}{-8.9072 \times 10^{-11}P^{4.9}T^{3.0} - 5.2582 \times 10^{-11}X^{6.0}T^{3.0} + 9.2656 \times 10^{-8}X^{3.0}T^{4.0} \frac{1}{+2.7862 \times 10^{-5}\frac{1}{S^{3.0}}T^{2.0} + 9.9624 \times 10^{-9}\frac{1}{S}P^{4.9}T^{3.0} + 2.8483 \times 10^{-12}P^{4.9}T^{4.0}}}} \quad (30)$$

$$\mu_{FLN}(\text{Fermentor 4}) = \cfrac{1}{-2899.6 - 0.53749X\frac{1}{S^{2.0}}P + 0.27431\frac{1}{S^{2.0}}P^{2.0} - 0.017078\frac{1}{S}P^{3.0} + 2.0252PT^{1.2} \cfrac{1}{-2.3187\times10^{-6}X\frac{1}{S^{4.0}} - 0.0053256X\frac{1}{S^{2.0}}P^{2.0} + 0.21679X\frac{1}{S^{2.0}}PT^{0.4} \cfrac{1}{-0.043293XPT^{1.2} + 1.6239\times10^{-9}\frac{1}{S^{5.0}} + 1.8985\times10^{-7}\frac{1}{S^{4.0}}P + 1.5343\times10^{-5}\frac{1}{S^{4.0}}T^{0.4} \cfrac{1}{-3.8448\times10^{-7}\frac{1}{S^{3.0}}P^{2.0} + 0.0010677\frac{1}{S^{2.0}}P^{3.0} - 0.072847\frac{1}{S^{2.0}}P^{2.0}T^{0.4} \cfrac{1}{-2.9298\frac{1}{S^{2.0}}T^{1.2} + 2.3907\times10^{-5}\frac{1}{S}P^{4.0} + 0.0039741\frac{1}{S}P^{3.0}T^{0.4}}}}} \quad (31)$$

$$\mu_{FLN}(\text{Fermentor 5}) = \cfrac{1}{-7511.3\frac{1}{S} - 0.0046055\frac{1}{S^{2.0}}P + 10.992\frac{1}{S}P^{2.0} + 13.016T^{1.77} - 9.8779\times10^{-9}\frac{1}{S^{4.0}} \cfrac{1}{-0.23645\frac{1}{S}P^{3.0} - 0.00058067X^{3.75}\frac{1}{S^{2.0}} + 0.01669X^{2.5}\frac{1}{S^{2.0}}T^{0.59} \cfrac{1}{-0.15954X^{1.25}\frac{1}{S^{2.0}}T^{1.18} - 0.019771X^{1.25}T^{2.36} - 1.1657\times10^{-14}\frac{1}{S^{5.0}} \cfrac{1}{+1.3446\times10^{-9}\frac{1}{S^{4.0}}T^{0.59} + 5.2132\times10^{-9}\frac{1}{S^{3.0}}P^{2.0} - 7.4404\times10^{-8}\frac{1}{S^{3.0}}PT^{0.59} \cfrac{1}{+1.8348\times10^{-7}\frac{1}{S^{3.0}}T^{1.18} + 0.50787\frac{1}{S^{2.0}}T^{1.77} + 0.0013531\frac{1}{S}P^{4.0} \cfrac{1}{+0.00091873\frac{1}{S}P^{3.0}T^{0.59}}}}} \quad (32)$$

The quality of prediction of the proposed hybrid neural model was measured by the residual standard deviation (RSD) described as a percentage of average of the 'real' values, as described by Atala et al. *(3)*:

$$\text{RSD}(\%) = \frac{\text{RSD}}{\bar{Y}_i} \times 100 \quad (33)$$

$$\text{RSD} = \frac{\sqrt{\sum_{i=1}^{n}\left(y_i - y_{Pi}\right)^2}}{n} \quad (34)$$

In this equation $y_i$ is the "real" value (calculated by the deterministic model), $y_{Pi}$ is the value predicted by the hybrid model and $n$ is the number

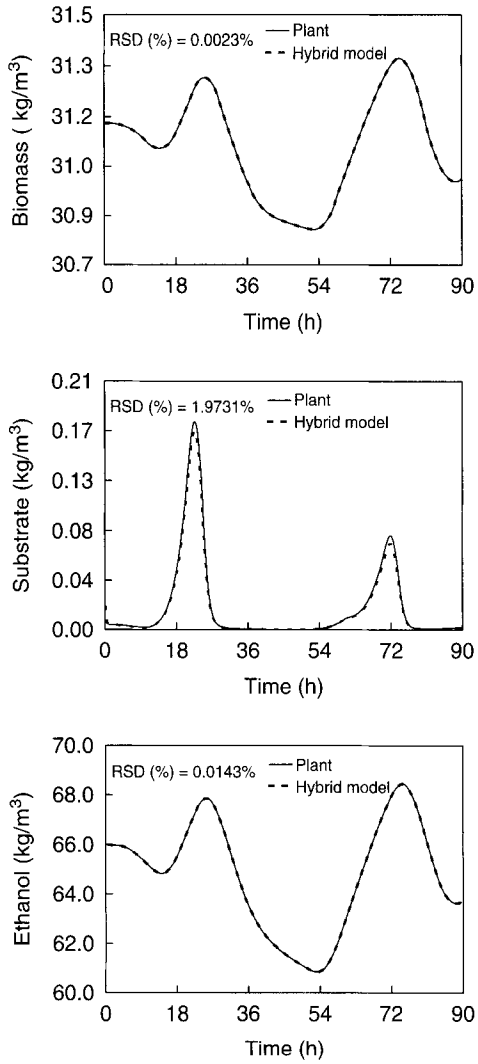


**Fig. 3.** Concentrations of biomass, substrate, and product in the fifth fermentor (deterministic model —, hybrid model ).

of points. Figure 3 shows the performance of the hybrid model to describe the dynamic behavior of the fifth fermentor when the process is subjected to the disturbances shown in Fig. 4. In this figure the disturbances performed for training of the neural networks are shown for comparison. Table 6 shows the values of RSD% obtained when we use the mathematical model to calculate concentrations of biomass, substrate, and product in the five fermentors. If a model without update of its parameters is used it is not possible to obtain good predictions, and errors over 50% might be found depending on the type and level of changes.

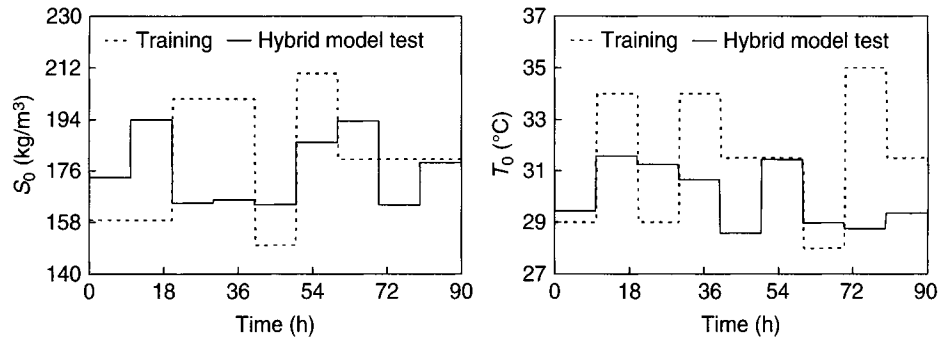


**Fig. 4.** Disturbances for the test of the hybrid model.

Table 6
Model Quality of Prediction Described by the RSD (%)

| Reactor | Biomass $X$ (kg/m$^3$) | Substrate $S$ (kg/m$^3$) | Product $P$ (kg/m$^3$) |
|---|---|---|---|
| 1 | 0.0037 | 0.1506 | 0.0323 |
| 2 | 0.0021 | 0.3097 | 0.0147 |
| 3 | 0.0020 | 0.7540 | 0.0126 |
| 4 | 0.0024 | 1.4294 | 0.0149 |
| 5 | 0.0023 | 1.9731 | 0.0143 |

## Discussion

Bioreactors are quite difficult to model because their operation involves microbial growth under constantly changing conditions. Past experience has shown the difficulties of using phenomenological models without kinetic parameters reestimation to describe the dynamic behavior of the process for long periods of operation, when there are changes in substrate and yeast conditions (a common situation in industrial plants). However, the reestimation of kinetic parameters in a phenomenological model is difficult and time-consuming, mainly when the kinetics dependence on temperature is taken into account. As the main nonlinearities and uncertainties are in the description of the process kinetic, the use of a hybrid approach whereby the kinetics is described by a FLN can simplify the reestimation step.

In this work, we have shown that a hybrid neural model combining mass balance equations with FLNs is able to describe the process dynamic behavior with a performance similar to that of a phenomenological model. However, the reestimation of the weights of a FLN is much simpler than the reestimation of kinetic parameters in a phenomenological model. The estimation of the FLN weights is a linear optimization problem, so it is very fast and convergence is guaranteed. The use of this approach enables the development of an online reestimation procedure.

## Conclusions

The proposed hybrid model seems to be a quite suitable approach to follow changes in the process that impact the system behavior. The reestimation of the hybrid model is easily done especially because the model is built-up using FLNs. These networks showed to have a good nonlinear approximation capability, although the estimation of its weights is linear. The proposed approach for hybrid modeling is able to deal with disturbances in transient phases of the process and different yeasts, because the identification procedures is carried out adequately with an appropriate set of data representative of the biotechnological process.

## Acknowledgments

The authors acknowledge Fundação de Amparo à Pesquisa do Estado de São Paulo (FAPESP) and Conselho Nacional de Desenvolvimento Científico e Tecnológico (CNPq) for financial support.

## Nomenclature

| | |
|---|---|
| $a$ | constant in Eq. 11 |
| $A$ | constant in Eq. 10 |
| $A_i$ | area of the $i$th heat exchanger ($m^2$) |
| Cp | reagent fluid heat capacity (J/kg·°C) |
| $Cp_J$ | cooling fluid heat capacity (J/kg·°C) |
| $E$ | activation energy (J/mol) |
| $f$ | activation function of the FLN |
| $F_a$ | water flow rate ($m^3$/h) |
| $F_{Ci}$ | reagent fluid flow rate to the $i$th heat exchanger ($m^3$/h) |
| $F_i$ | feed stream flow rate to $i$th reactor ($m^3$/h) |
| $F_{Ji}$ | cooling fluid flow rate in the $i$th heat exchanger ($m^3$/h) |
| $F_L$ | cell suspension flow from centrifuge ($m^3$/h) |
| $F_{L1}$ | cell suspension flow to treatment tank ($m^3$/h) |
| $F_0$ | fresh medium flow rate ($m^3$/h) |
| $F_R$ | cell recycling flow rate ($m^3$/h) |
| $F_S$ | purge flow rate ($m^3$/h) |
| $F_V$ | liquid-phase flow to rectification column ($m^3$/h) |
| $F_W$ | feed stream flow rate ($m^3$/h) |
| $h$ | monomials generated by the functional expansion |
| $K_0$ | constant in Eq. 11 |
| $K_s$ | substrate saturation constant (kg/$m^3$) |
| $LMTD_i$ | logarithmic mean temperature difference for the $i$th heat exchanger |
| m | constant in Eq. 9 |
| $m$ | number of outputs of the FLN |

| | |
|---|---|
| $M$ | number of monomials |
| n | constant in Eq. 9 |
| $n_z$ | number of auxiliary inputs |
| $P_i$ | product concentration in the *i*th reactor (kg/m$^3$) |
| $P_{MAX}$ | product concentration when cell growth ceases (kg/m$^3$) |
| $P_R$ | product concentration in the cells recycle (kg/m$^3$) |
| $P_W$ | feed product concentration (kg/m$^3$) |
| $R$ | universal gas constant (J/mol·K) |
| $RR$ | cell recycle rate |
| $S_i$ | substrate concentration in the *i*th reactor (kg/m$^3$) |
| $S_0$ | inlet substrate concentration (kg/m$^3$) |
| $S_R$ | substrate concentration in the cells recycle (kg/m$^3$) |
| $S_W$ | feed substrate concentration (kg/m$^3$) |
| $t$ | time (h) |
| $T_{Ci}$ | temperature of the reagent fluid in the *i*th heat exchanger (°C) |
| $T_i$ | temperature in the *i*th reactor (°C) |
| $T_{Ji}$ | cooling fluid temperature at the *i*th heat exchanger exit (°C) |
| $T_{Je}$ | inlet cooling fluid temperature in the *i*th heat exchanger (°C) |
| $U$ | global exchange coefficient (J/h·°C·m$^2$) |
| $V_i$ | volume of the *i*th reactor (m$^3$) |
| $V_{Ji}$ | cooling fluid volume in the *i*th heat exchanger (m$^3$) |
| w | FLN weights |
| $\mathbf{x_e}$ | input vector of the FLN |
| $X_i$ | biomass concentration in the *i*th reactor (kg/m$^3$) |
| $X_L$ | biomass concentration in the heavy phase from centrifuge (kg/m$^3$) |
| $X_{MAX}$ | biomass concentration when cell growth ceases (kg/m$^3$) |
| $X_R$ | cell recycling concentration (kg/m$^3$) |
| $X_V$ | biomass concentration in the light phase to rectification column (kg/m$^3$) |
| $X_W$ | feed biomass concentration (kg/m$^3$) |
| $Y_{P/S}$ | yield of product based on cell growth (kg/kg) |
| $Y_{X/S}$ | limit cellular yield (kg/kg) |
| **z** | auxiliary input vector |

*Greek letters*

| | |
|---|---|
| $\Delta H$ | reaction heat (J/kg) |
| $\rho_i$ | reagent fluid density in the *i*th reactor (kg/m$^3$) |
| $\rho_j$ | cooling fluid density (kg/m$^3$) |
| $\mu_i$ | specific growth rate in the *i*th reactor (h$^{-1}$) |
| $\mu_{MAX}$ | maximum specific growth rate (h$^{-1}$) |

## References

1. Ghose, T. K. and Tyagi, R. D. (1979), *Biotechnol. Bioeng.* **21,** 1387–1400.
2. Lee, J. M., Pollard, J. F., and Coulman, G. A. (1983), *Biotechnol. Bioeng.* **25,** 497–511.

3. Atala, D. I. P., Costa, A. C., Maciel Filho, R., and Maugeri Filho, F. (2001), *Appl. Biochem. Biotech.* **91(3),** 353–365.
4. Aldiguier, A. S., Alfenor, S., Cameleyre, X., et al. (2004), *Bioproc. Biosyst. Eng.* **26,** 217–222.
5. Costa, A. C., Alves, T. L. M., Henriques, A. W. S., Maciel Filho, R., and Lima, E. L. (1998), *Comput. Chem. Eng.* **22,** 859–862.
6. Harada, L. H. P., Costa, A. C., and Maciel Filho, R. (2002), *Appl. Biochem. Biotech.* **98(1–9),** 1009–1024.
7. Psichogios, D. C. and Ungar, L. H. (1992), *AIChE J.* **38,** 1499–1511.
8. Smets, I. Y., Claes, J. E., November, E. J., Bastin, G. P., and Van Impe, J. F. (2004), *J. Proc. Control* **14,** 795–805.
9. Nishiwaki, A. and Dunn, I. J. (1999), *Biochem. Eng. J.* **4,** 37–44.
10. Ricci, M., Martini, S., Bonechi, C., Trabalzini, L., Santucci, A., and Rossi, C. (2004), *Chem. Phys. Lett.* **387,** 377–382.
11. Patnaik, P. R. (2003), *Biochem. Eng. J.* **15,** 165–175.
12. Chen, S. and Billings, S. A. (1992), *Int. J. Control* **56,** 319–346.
13. Andrietta, S. R. and Maugeri, F. (1994), *Adv. Bioprocess Eng.* **1,** 47–52.
14. Andrietta, S. R. (1994), *PhD Thesis*, State University of Campinas, SP, Brazil.
15. Fogler, H. S. (1999), *Elements of Chemical Reaction Engineering*, 3rd ed. Prentice Hall, New York.
16. Billings, S. A., Chen, S., and Korenberg, M. J. (1989), *Int. J. Control* **49,** 2157–2189.
17. Milton, J. S. and Arnold, J. C. (1990), *Introduction to Probability and Statistics*, McGraw Hill, New York.

0273-2289/1559-0291 (Online)/07/136–140/835–846/$30.00

# Characterization of Thermostructural Damages Observed in a Seaweed Used for Biosorption of Cadmium

*Effects on the Kinetics and Uptake*

ANTONIO CARLOS AUGUSTO DA COSTA,* ADERVAL S. LUNA, AND ROBSON PAFUMÉ

*Universidade do Estado do Rio de Janeiro, Programa de Pós-Graduação em Engenharia Química, R. S. Francisco Xavier 524, Sala 427, Maracanã, Rio de Janeiro, RJ, Brasil, 20550-013, E-mail: acosta@uerj.br*

## Abstract

The effect of drying *Sargassum filipendula* on the kinetics and uptake of cadmium was studied. The maximum uptake was not reduced when oven-dried biomass was used for cadmium concentrations from 10.0 to 500.0 mg/L. Kinetics indicated better performance of the *in natura* biomass. Drying at 333 K affected the uptake capacity. Results fit the Langmuir model better than the Freundlich. This process followed pseudo-second-order kinetics. Thermogravimetric and infrared analysis confirmed that no structural damage occurred after drying, and no differences between the biomasses were observed. Temperatures from 303 to 328 K affected cadmium uptake capacity.

**Index Entries:** Cadmium; kinetics; *Sargassum filipendula*; thermal effects; uptake capacity; biosorption.

## Introduction

In the last few years, there has been an increasing concern about using biomasses for the recovery of metals from industrial solutions. This information has been confirmed in a recent review from Ahluwalia and Goyal *(1)* wherein *Aspergillus niger, Penicillium chrysogenum, Rhizopus nigricans, Ascophyllum nodosum, Sargassum natans, Chlorella fusca, Oscillatoria anguistissima, Bacillus firmus*, and *Streptomyces* sp. are presented as potential biosorbents under investigation. Authors say that lead, zinc, cadmium, chromium, copper, and nickel are potential targets for these studies. They also say that uptake capacities may range from 5.0 to 641.0 mg/g, indicating a wide

*Author to whom all correspondence and reprint requests should be addressed.

variability of biomasses and structural polysaccharides. The critical conclusion of the review paper is that information about different biosorbents is still inadequate for process scale-up and design, and also that the appropriate biomass choice and proper operational conditions need to be identified.

In order to fill part of this technological gap in the literature, a few authors are trying to establish the operational parameters for possible scale-up of processes or to confirm the feasibility of using certain types of biomasses for the accumulation of metals. Martins et al. (2) studied the adsorption of cadmium and zinc ions by the aquatic moss *Fontinalis antypiretica*, focusing on temperature, pH, and water hardness. Some process parameters, such as equilibrium data and pH were studied by Pavasant et al. (3) who investigated the green macroalga *Caulerpa lentillifera* as a biosorbent material. Padilha et al. (4) studied the effect of the counter ions on the uptake capacity of copper by a brown seaweed. Karthikeyan et al. (5), Villar et al. (6), and Martins et al. (2) also investigated some physico-chemical properties that may affect the biosorption process, and drew specific conclusions for individual metal-biosorbent combinations. The objective of the present work was to investigate the impact of drying *S. filipendula* at 303 and 333 K on cadmium uptake capacity and rate.

## Materials and Methods

### Seaweed Biomass

The brown seaweed *S. filipendula* (*Phaeophyceae*, *Ectocarpales*, *Fucales*, and *Sargassaceae*) used in this work was harvested from the sea and sampled. Seaweed was collected in the city of Recife, Pernambuco State, Brazil, at the Atlantic Ocean (W34°53′55″) in January 2006. Only one batch of seaweeds was collected (5.0 kg) for use in experiments. Other studies from the group indicated that the polysaccharide content of the seaweeds was practically the same during the whole year, with changes observed in the mannuronic and guluronic acids content. However, the total alginate content (mannuronic plus guluronic acid blocks) remains constant.

Part of the harvested biomass was extensively washed with distilled water to remove particulate material from its surface, and was oven-dried at 343 K for 24 h. Part of the harvested biomass was only sun-dried at an average temperature of 303 K (*in natura* biomass) for 24 h. One kilogram of biomass was subsampled for use in these experiments. In order to ensure that homogeneous samples were used, standard sampling techniques were applied. Dried biomass was cut, ground in a mortar with a pestle, and then sieved. The fraction with a diameter of 0.3–0.7 mm was selected for use in the biosorption tests. After drying, the biomass was stored in a dessicator.

### Cadmium Solutions

A stock cadmium solution (1000.0 mg/L) was prepared by dissolving cadmium chloride (Merck, Darmstadt, Germany) in 100 mL of deionized

distilled water (DDW) and quantitatively diluted to 1000 mL using DDW. Cadmium solutions of different concentrations were prepared by appropriate dilution of the stock solution with DDW.

### *Determination of Cadmium Concentration by Atomic Absorption Spectrometry*

The concentration of cadmium in the solutions before and after the equilibrium was determined by atomic absorption spectrometry, using a Perkin-Elmer (Frankfurt, Germany) Analyst 300 atomic absorption spectrometer equipped with a deuterium arc background corrector and an air-acetylene burner, and was controlled by an IBM personal computer. The hollow cathode lamp was operated at 4 mA, and the analytical wavelength was set to 228.8 nm. Glassware and polypropylene flasks used were immersed overnight in 10% (v/v) $HNO_3$ and rinsed several times with DDW.

### *Infrared Spectrometry*

The scope and versatility of infrared spectrometry as a qualitative analysis tool have been substantially increased by the internal reflectance technique, also known as attenuated total reflectance. When a material is placed in contact with the reflecting surface, the beam loses energy at those wavelengths whereby the material absorbs because of an interaction with the penetrating beam. This attenuated radiation, when measured and plotted as a function of wavelength, is an absorption spectrum that is characteristic of the material and is similar to an infrared spectrum obtained in the normal transmission mode. Using this technique, qualitative infrared absorption spectra are easily obtained from most solid materials without the need for grinding or dissolving or making a mull *(7)*. A Perkin-Elmer Spectrum One fourier transform infrared was used in the infrared spectrometry analysis of *S. filipendula* biomass.

### *Thermogravimetric Analysis of the Biomass*

Thermogravimetry (TG) or thermogravimetric analysis (TGA) provides a quantitative measurement of weight changes associated with thermally induced transitions. For example, TG can directly record the loss in weight as a function of temperature for transitions that involve dehydration or decomposition. Thermogravimetric curves are characteristic of a given compound or material owing to the unique sequence of physical transitions and chemical reactions that occur over definite temperature ranges. The rates of these thermally induced processes are often a function of the molecular structure. Changes in weight result from physical and chemical bonds forming and breaking at elevated temperatures. TG data are useful in characterizing materials as well as in investigating the thermodynamics and kinetics of the reactions and transitions that result from the application of heat to these materials.

TG, a valuable tool in its own right, is perhaps most useful when it complements differential thermal analysis (DTA). Virtually, all weight-change processes absorb or release energy and are thus measurable by DTA, but not all energy-change processes are accompanied by changes in weight. This difference in the two techniques enables a clear distinction to be made between physical and chemical changes when samples are subjected to both DTA and TG tests. In TG, the weight of the sample is continuously recorded as the temperature is increased. In this case, the biomass was placed in a crucible that was positioned in a furnace on a quartz beam attached to an automatic recording balance (Rigaku, model TAS 100, Japan) with a rate of 10°C/min and 30 mL/min of nitrogen.

### *Batch Biosorption Studies*

Batch biosorption experiments were performed using 50.0 mg of dried biomass (dried at 343 K or *in natura*), which was added to 25 mL of cadmium solution in 100-mL polypropylene flasks. The flasks were placed on a rotating shaker (Tecnal, Brazil) with constant shaking at 150 rpm (1.5*g*). For the kinetic study, two cadmium concentrations were tested: 10 mg/L and 100 mg/L. Three temperatures were selected: 303, 313, and 328 K; and the working pH was that of the solution (pH = 4.5). The biosorption time ranged from 3 to 300 min. At predetermined times, the flasks were removed from the shaker and the solutions were separated from the biomass by filtration through filter paper (Whatman no. 40, ashless). The equilibrium isotherms were determined using similar experimental conditions, by varying the initial cadmium concentration from 10 to 500 mg/L and using an equilibrium time equal to 2 h.

### *Metal Uptake*

The cadmium uptake was calculated by the simple concentration difference method. The initial concentration ($C_0$ [mg/L]) and metal concentration at any time ($C_t$ [mg/L]), respectively, were determined and the metal uptake ($q$ [mg metal adsorbed/g adsorbent]) was calculated from the mass balance as follows (Eq. 1):

$$q = \frac{(C_0 - C_t)V}{1000w} \tag{1}$$

where $V$ is the volume of the solution in milliliter before addition of seaweed, and $w$, mass of the sorbent in gram. Preliminary experiments had shown that cadmium adsorption losses to the flask walls and to the filter paper were negligible.

### *Equilibrium Modeling*

Modeling the equilibrium data is fundamental for industrial applications of biosorption. It gives information for comparison of different

biomaterials under different operational conditions for designing and optimizing operating procedures. In order to examine the relationship between sorbed ($q_e$) and aqueous concentrations ($C_e$) at equilibrium, the biosorption isotherm models of the Langmuir (Eq. 2) and Freundlich (Eq. 3) isotherms were tested for fitting our data.

$$\text{Langmuir isotherm } q_e = \frac{Q_0 K_L C_e}{1 + K_L C_e} \tag{2}$$

$$\text{Freundlich isotherm } q_e = K_F C_e^{\frac{1}{n}} \tag{3}$$

where $C_e$ is the liquid-phase concentration of metal at equilibrium (mg/L), $K_L$ the Langmuir constant (L/mg), $q_e$ the metal uptake at equilibrium (mg/g), $Q_0$ the maximum metal uptake capacity at equilibrium (mg/g), and $K_F$ and $n$ the Freundlich parameters.

### *Kinetic Modeling*

Two different kinetic models were used to fit the experimental data of cadmium biosorption on *S. filipendula*. The pseudo-first-order Lagergren model (Eq. 4):

$$\log(q_e - q) = \log q_e - \frac{k_{1,\,ads}}{2.303} t \tag{4}$$

where $q_e$ (mg/g) and $q$ (mg/g) are the amounts of adsorbed metal ions on the biosorbent at the equilibrium and at any time ($t$), respectively. And $k_{1,\,ads}$ is the Lagergren rate constant, and the pseudo-second order model is represented in Eq. 5 *(2,8)*:

$$\frac{t}{q} = \frac{1}{k_{2,\,ads} q_e^2} + \frac{1}{q_e} t \tag{5}$$

where $k_{2,\,ads}$ is the rate constant for second-order biosorption (g/mg/min).

## Results and Discussion

### *Infrared Spectrometry*

Results about the infrared spectra of both *in natura S. filipendula* and oven-dried *S. filipendula* biomasses are presented in Fig. 1. A comparison between the two infrared spectra indicates that no marked differences were observed.

Pavasant et al. *(3)* studied the biosorption of cadmium by the green macroalgae *C. lentilifera* suggesting the possibility of coupling between metal species and types of functional groups such as carboxylic (O–H bending),

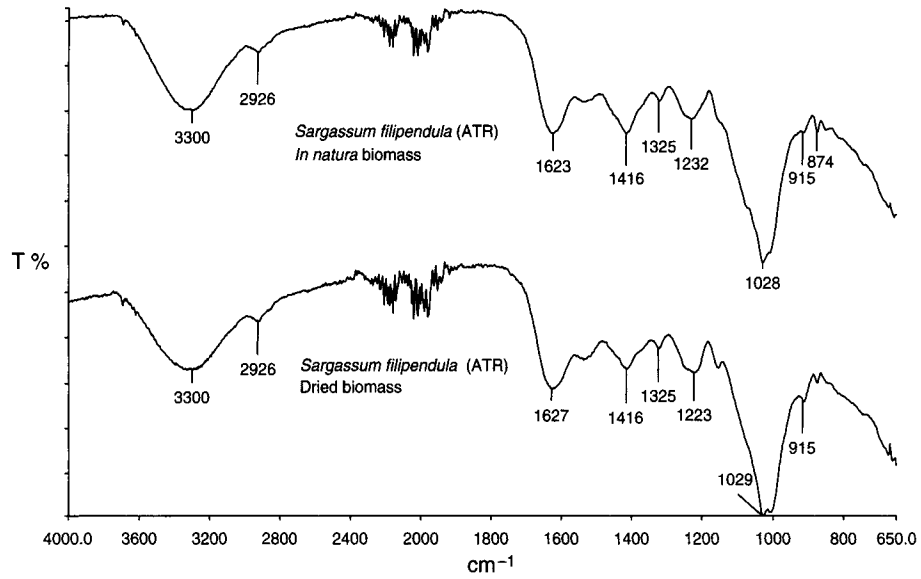


**Fig. 1.** Infrared spectra of *in natura S. filipendula* and oven-dried *S. filipendula* biomasses.

amine (N–H and C–N stretching), amide (N–H), amino (C–O), sulfonyl (S=O stretching), and sulfonate (S=O stretching).

## *TGA of the Biomass*

The results of the TGA of the biomass are presented in Fig. 2.

Results clearly indicate that there is a continuous loss of mass as a function of increasing temperature. From these results, it is possible to obtain an estimation of weight of biomass lost at the two temperatures used. For *in natura* biomass (sun dried at 303 K), the approximate weight loss is negligible, around 2.5%. On the other hand, for the oven-dried biomass (333 K) the weight loss is considerable, reaching 10%. Heating the biomass in an inert environment results in a loss of mass, which was probably associated with water. The DTA curve shows a significant thermal effect at 333 K.

## *Effect of the Initial Cadmium Concentration on Biosorption Equilibrium*

Figure 3 presents the results obtained when the Langmuir model was used to fit the experimental data; and Fig. 4 shows the experimental data fit for the Freundlich model (Table 1). The corresponding constants and the correlation coefficients ($R$) associated with each linearized form of both equilibrium models, for both types of biomasses and for temperatures tested, are presented in Table 1. The results indicate that the Langmuir isotherm best fits the experimental data over the experimental range studied because it has higher correlation coefficients. Statistically distinct results

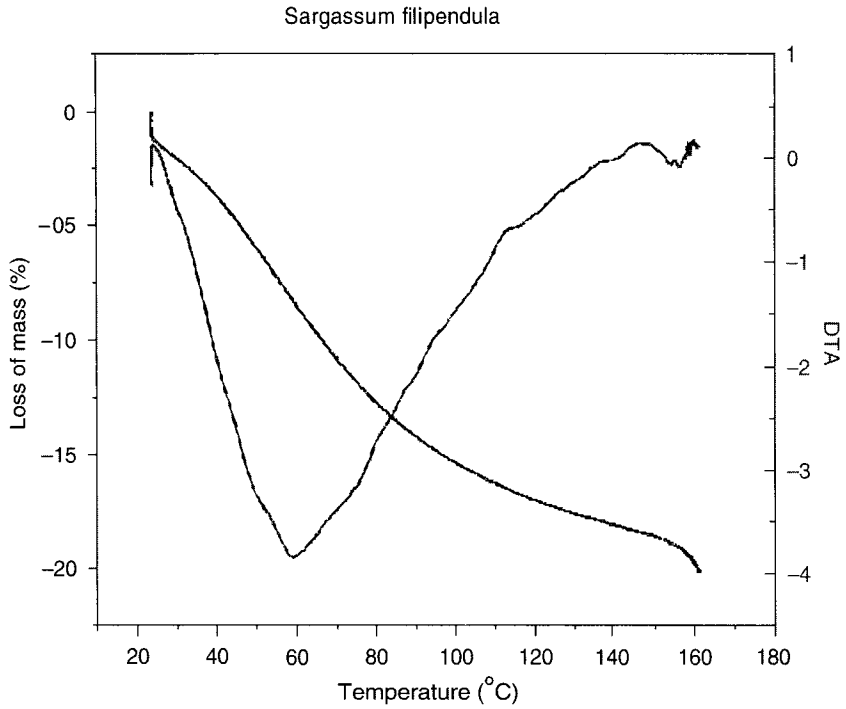


**Fig. 2.** Plot of loss of mass of *S. filipendula* biomass as a function of increasing temperature and DTA analysis.

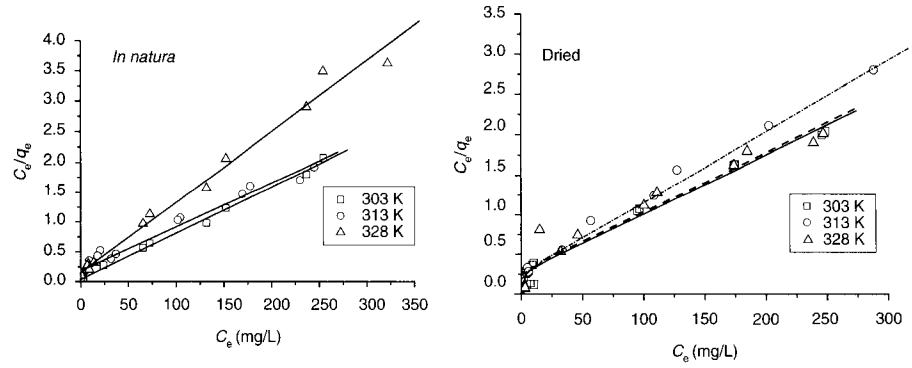


**Fig. 3.** Linear plots of experimental cadmium biosorption by *S. filipendula* biomass based on the Langmuir model.

were observed at an incubation temperature of 328 K ($Q_0$ = 85 ± 3 mg/g) and 313 K ($Q_0$ = 107 ± 2 mg/g) when *in natura* and oven-dried biomasses were used, respectively.

The constant $K_F$ from the Freundlich model ranged from 9.4 ± 1.2 to 22.8 ± 1.9 when *in natura S. filipendula* biomass was used, and ranged from 13.0 ± 1.4 to 19.9 ± 2.0 when dried *S. filipendula* biomass was used. Statistically distinct results were observed for all incubation temperatures

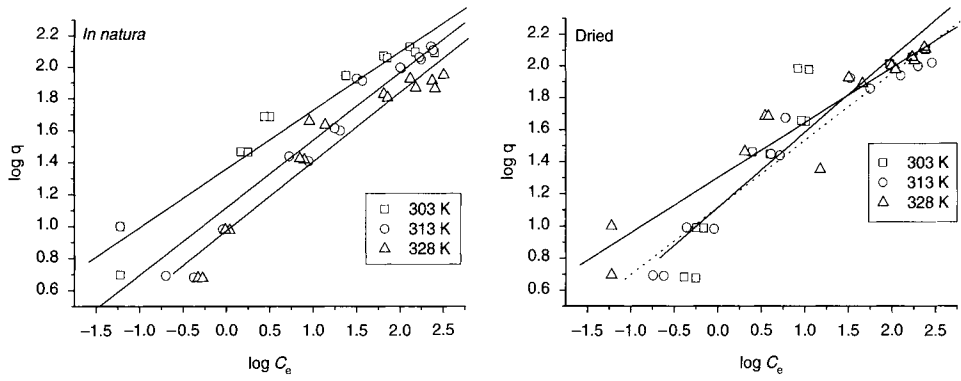


**Fig. 4.** Linear plots of experimental cadmium biosorption by *S. filipendula* biomass based on the Freundlich model.

Table 1
Freundlich and Langmuir Adsorption Constants Associated with Adsorption Isotherms of Cadmium(II) Ions by *S. filipendula* at Different Temperatures

| | Freundlich constants | | | Langmuir constants | | |
|---|---|---|---|---|---|---|
| $T$ (K) | $K_F$ | $N$ | $R$ | $Q_0$ (mg/g) | $K_L$ (L/mg) | $R$ |
| *In natura biomass* | | | | | | |
| 303 | 22.8 (1.9)[a] | 2.7 (0.2) | 0.9736 | 129 (2) | 0.20 (0.07) | 0.9981 |
| 313 | 13.1 (1.7) | 2.4 (0.2) | 0.9564 | 136 (7) | 0.04 (0.01) | 0.9843 |
| 328 | 9.4 (1.2) | 2.3 (0.2) | 0.9625 | 85 (3) | 0.08 (0.02) | 0.9936 |
| *Dried biomass* | | | | | | |
| 303 | 13.0 (2.3) | 2.1 (0.2) | 0.9235 | 128 (3) | 0.08 (0.02) | 0.9962 |
| 313 | 13.0 (1.4) | 2.4 (0.2) | 0.9662 | 107 (2) | 0.09 (0.03) | 0.9962 |
| 328 | 19.9 (2.0) | 2.9 (0.2) | 0.9588 | 127 (7) | 0.06 (0.03) | 0.9766 |

[a]Figures in parenthesis indicate standard deviations ($n$ = 3).

when *in natura* biomass was used, and a marked difference was observed when oven-dried biomass was used, with an incubation temperature of 328 K. The incubation temperature affected the uptake of cadmium.

## Biosorption Kinetics of Cadmium Ions

Figure 5 presents the results from the kinetic modeling of cadmium biosorption by *S. filipendula* biomass. These are based on the second-order model because it best fit the experimental data. Complete results from the modeling can be found in Table 2. Figure 5 is representative of the goodness of the fit to the second-order model in each experiment. Table 2 shows that using *in natura* and dried *S. filipendula* biomasses, did not affect the uptake capacity for initial cadmium concentrations of 10.0 and 100.0 mg/L. However, the incubation temperature proved to be a parameter that affected

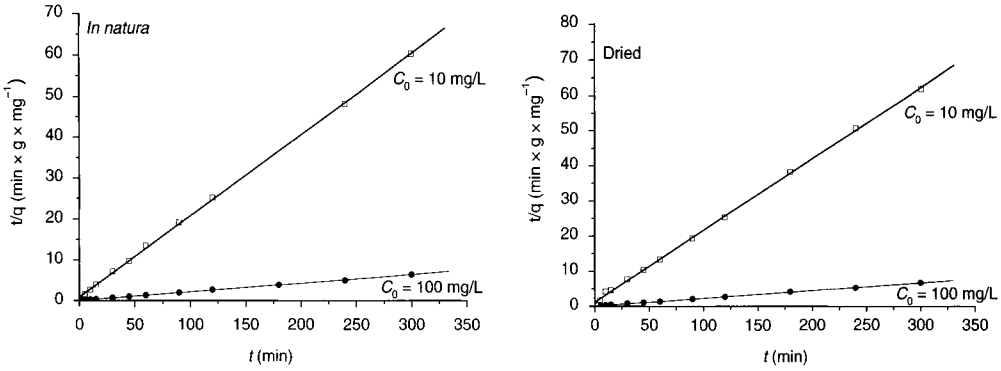


**Fig. 5.** Linear plots of the kinetic modeling of cadmium biosorption by *S. filipendula* biomass according to the second-order model at 303 K.

the uptake of cadmium, under certain experimental conditions. The results obtained for the parameter $q_e$ when *in natura* biomass was tested, showed that the incubation temperature affected the uptake of cadmium. For initial cadmium concentrations of 10.0 and 100.0 mg/L, the obtained $q_e$ values indicated that the higher the temperature, the smaller the $q_e$ value. On the other hand, the results obtained for $q_e$ when oven-dried *S. filipendula* biomass was used, showed that this biomass seemed to be less dependent than the *in natura* biomass with respect to the incubation temperature. For initial cadmium concentrations of 10.0 and 100.0 mg/L, the $q_e$ value remained constant with increasing temperature, according to the second-order equation.

A comparison of the results obtained from the kinetic modeling of the experimental $q_e$ values indicate a good fit to the pseudo-second-order model. Additionally, the correlation coefficients were close to 1.0, for all incubation temperatures tested. Hawari and Mulligan *(9)* worked with nonliving anaerobic granular biomass for the biosorption of cadmium found a $q_e$ value of 64.0 mg/g, as predicted by the Langmuir model, in comparison with a $q_e$ experimental value of 60.0 mg/g, which was considerably less than the results obtained in this work. Karthikeyan et al. *(5)* investigated the behavior of the green algae *Ulva fasciata* and the brown seaweed *Sargassum* sp. during the biosorption of copper. Authors found that *U. fasciata* could acquire copper up to 73.5 mg/gand *Sargassum* sp. up to 72.5 mg/g, with a rapid equilibrium and second-order kinetics. Martins et al. *(2)* observed that the aquatic moss *F. antipyretica* accumulated a maximum amount of cadmium of 28.0 mg/g biomass, independent of the temperature, with the results best fitting a Langmuir type model.

Villar et al. *(6)* compared the use of the red seaweed *Gelidium* sp. with an algal waste obtained from agar extraction for the biosorption of cadmium ions. They concluded that the results fitted well to the Langmuir and Redlich–Peterson models, with a maximum recovery of cadmium of

Table 2
Comparison Between Adsorption Rate Constants

| | First-order kinetic model | | | Second-order kinetic model | | | |
|---|---|---|---|---|---|---|---|
| T (K) | $K_{1,\ ads}$ ($min^{-1}$) | $q_e$ (mg/g) | $R$ | $K_{2,\ ads}$ (g/mg/min) | $q_e$ (mg/g) | $R$ | $q_{e,\ exp}$ (mg/g) |
| *In natura biomass ($C_0$ = 10.0 mg/L)* | | | | | | | |
| 303 | 0.021 (0.002) | 1.7 (0.2) | 0.9755 | 0.045 (0.009) | 5.04 (0.04) | 0.9998 | 4.86 (0.14) |
| 313 | 0.074 (0.008) | 2.7 (0.7) | 0.9686 | 0.106 (0.024) | 4.80 (0.02) | 0.9999 | 4.75 (0.02) |
| 328 | 0.104 (0.017) | 5.8 (1.8) | 0.9733 | 0.054 (0.012) | 4.71 (0.03) | 0.9998 | 4.64 (0.02) |
| *In natura biomass ($C_0$ = 100.0 mg/L)* | | | | | | | |
| 303 | 0.023 (0.005) | 10.8 (2.2) | 0.9077 | 0.007 (0.003) | 47.8 (0.4) | 0.9996 | 47.5 (0.9) |
| 313 | 0.035 (0.004) | 16.6 (3.6) | 0.9611 | 0.022 (0.032) | 42.8 (0.5) | 0.9993 | 43.0 (1.2) |
| 328 | 0.029 (0.016) | 6.1 (1.7) | 0.7862 | 0.061 (0.237) | 41.6 (0.5) | 0.9993 | 41.8 (1.3) |
| *Dried biomass ($C_0$ = 10.0 mg/L)* | | | | | | | |
| 303 | 0.040 (0.003) | 2.9 (0.3) | 0.9884 | 0.034 (0.006) | 4.91 (0.04) | 0.9997 | 4.76 (0.06) |
| 313 | 0.025 (0.011) | 3.0 (1.0) | 0.7288 | 0.234 (0.067) | 4.92 (0.01) | 0.9999 | 4.90 (0.02) |
| 328 | 0.017 (0.014) | 1.9 (1.1) | 0.4344 | 0.040 (0.017) | 5.07 (0.08) | 0.9991 | 4.97 (0.02) |
| *Dried biomass ($C_0$ = 100 mg/L)* | | | | | | | |
| 303 | 0.049 (0.005) | 23.1 (3.5) | 0.9773 | 0.006 (0.001) | 45.2 (0.3) | 0.9997 | 44.0 (0.9) |
| 313 | 0.024 (0.003) | 5.5 (0.5) | 0.9605 | 0.021 (0.009) | 46.4 (0.2) | 0.9999 | 46.4 (0.2) |
| 328 | 0.008 (0.016) | 15.0 (11.7) | 0.2537 | 0.001 (0.001) | 48.3 (4.8) | 0.9627 | 46.8 (0.3) |

$q_e$ estimated and coefficients of correlation, $R$ associated with the pseudo-first-order Lagergren, and the pseudo-second-order kinetic models ($w$ = 0.050 g, $V$ = 25 mL, agitation rate 150 rpm, pH = 4.5).

[a]Figures in parenthesis indicate standard deviations ($n$ = 3) of the numbers immediately above.

18.0 mg/g for pure *Gelidium* sp. biomass and 9.7 mg/g for the algal waste. Martins et al. *(10)* working with *Sargassum* sp. biomass for the biosorption of lead, found second-order kinetics during the uptake, which was not affected by the temperature in the range from 298 to 328 K. Their results fitted well to a Langmuir type equation, with a maximum biosorption of 1.26 mmol/g.

## Conclusions

- Fourier transform infrared spectra indicated no differences between the spectra for *in natura* and oven-dried *S. filipendula* biomasses.
- TG/DTA analysis indicated a loss of mass, which was probably associated to the presence of water and a thermal effect was observed at 333 K.
- Kinetic modeling followed a pseudo-second-order model based on the similarities between the experimental and theoretical $q_e$ values.
- Equilibrium modeling followed the Langmuir equation based on the correlation coefficients, which were close to 1.0. According to the Langmuir model, the $q_e$ value was equal to 129.0 ± 2.0 mg/g when *in natura* biomass was used and 128.0 ± 3.0 mg/g when dry biomass was used.

## Acknowledgments

Antonio Carlos Augusto da Costa and Aderval S. Luna would like to thank UERJ, through the Prociência Program. This work is part of the M.Sc. Thesis of Robson Pafumé.

## References

1. Ahluwalia, S. S. and Goyal, D. (2006), *Biores. Technol.* (in press).
2. Martins, R. J. E., Pardo, R., and Boaventura, R. A. R. (2004), *Water Res.* **38,** 693–699.
3. Pavasant, P., Apiratikul, R., Sungkhum, V., Suthiparinyanont, P., Wattanachira, S., and Marhaba, T. F. (2006), *Biores. Technol.* **97,** 2321–2329.
4. Padilha, F. P., de França, F. P., and da Costa, A. C. A. (2005), *Biores. Technol.* **96,** 1511–1517.
5. Karthikeyan, S., Balasubramanian, R., and Iyer, C. S. P. (2007), *Biores. Technol.* **98,** 452–455.
6. Villar, V. J. P., Botelho, C. M. S., and Boaventura, R. A. R. (2006), *Water Res.* **40,** 291–302.
7. Willard, H. H., Merritt, L. L., Dean, J. A., and Settle, F. A. (1988), *Instrumental Methods of Analysis,* 7th ed. Wadsworth Publishing Company, Belmont, California.
8. Ho, Y. S., Wase, D. A. J., and Forster, C. F. (1996), *Environ. Technol.* **17,** 71–80.
9. Hawari, A. H. and Mulligan, C. N. (2006), *Biores. Technol.* **97,** 692–700.
10. Martins, B. L., Cruz, C. C. V., Luna, A. S., and Henriques, C. A. (2006), *Biochem. Eng. J.* **27,** 310–314.

0273-2289/1559-0291 (Online)/07/136–140/847–858/$30.00

# Ethanol Fermentation of Various Pretreated and Hydrolyzed Substrates at Low Initial pH

ZSÓFIA KÁDÁR,*[,1] SAN FENG MALTHA,[2] ZSOLT SZENGYEL,[1] KATI RÉCZEY,[1] AND WIM DE LAAT[2]

*[1]Budapest University of Technology and Economics, Department of Agricultural Chemical Technology, Szent Gellért tér 4., H-1521 Budapest, Hungary, E-mail: zsofia_kadar@mkt.bme.hu; and [2]Royal Nedalco B.V. P.O. Box 6, 4600 AA, Bergen op Zoom, The Netherlands*

## Abstract

Lignocellulosic materials represent an abundant feedstock for bioethanol production. Because of their complex structure pretreatment is necessary to make it accessible for enzymatic attack. Steam pretreatment with or without acid catalysts seems to be one of the most promising techniques, which has already been applied for large variety of lignocellulosics in order to improve enzymatic digestibility. During this process a range of toxic compounds (lignin and sugar degradation products) are formed which inhibit ethanol fermentation. In this study, the toxicity of hemicellulose hydrolysates obtained in the steam pretreatment of spruce, willow, and corn stover were investigated in ethanol fermentation tests using a yeast strain, which has been previously reported to have a resistance to inhibitory compounds generated during steam pretreatment. To overcome bacterial contamination, fermentations were carried out at low initial pH. The fermentability of hemicellulose hydrolysates of pretreated lignocellulosic substrates at low pH gave promising results with the economically profitable final 5 vol% ethanol concentration corresponding to 85% of theoretical. Adaptation experiments have shown that inhibitor tolerance of yeast strain can be improved by subsequent transfer of the yeast to inhibitory medium.

**Index Entries:** Inhibitors; lignocellulose; *Saccharomyces cerevisiae*; toxicity; yeast adaptation; bioethanol.

## Introduction

Emission of greenhouse gases, especially carbon dioxide, has been steadily increasing since the industrial revolution. Apparently, the net carbon dioxide emission has been increasing exponentially during the last century mainly because of extensively growing energy demand. The transport sector, a key factor in economy as it facilitates movement of produced goods, accounts for more than 30% of the energy consumption in the European

*Author to whom all correspondence and reprint requests should be addressed.

Community (EC). Carbon dioxide emission from transportation is expected to rise by 50% from 1990 for year 2010 to about 1113 million t for which road transportation can be held responsible with its 84% share to the total carbon dioxide generated *(1)*. At the present time transport sector is 98% oil dependent. Increasing the use of biofuels in road transportation is one of the key tools by which EC can reduce carbon dioxide emission to a great extent and at the same time also decrease the dependency on imported energy. Directive 2003/30/EC clearly sets the target shares of biofuels in transport sector for EC member states. The short-term target was set at 2% in 2005; however, at the end of the year it was clear that the European Union would not reach it. The long-term target is to increase the use of biofuels in energy consumption to 5.75% by 2010, but probably it could also fail to reach this goal.

Bioethanol (produced from biomass) has been long recognized as a possible alternative fuel. It can be mixed into both gasoline and diesel. As an alternative, ethyl tertiary butyl ether (ETBE) produced from bioethanol is also accepted in the EC; however, only 47% is of biological origin. For the production of bioethanol, large varieties of materials are available. However, as the share of raw material cost is calculated to be about 50% of total expenditures, the choice of feedstock and ethanol yields are two of the most important factors affecting the economy of fuel alcohol production. Lignocellulosics, the most abundant renewable resources on Earth, represent an enormous potential for large-scale bioethanol production. In spite of this, hydrolysis of polysaccharides in these materials is not an easy task to accomplish for which the complex and highly compact structure of lignocellulosics is responsible *(2,3)*. To be an attractive substrate for ethanol fermentation, pretreatment of lignocellulosic raw material is necessary to open up the structure and make it accessible for enzymatic attack. Despite the extensive research undertaken in the last decades on pretreatments (physical, chemical, enzymatic, or combinations of these methods), nowadays none of the available processes could be used as a general process, owing to the differences in composition of lignocellulosics; however, steam explosion is known as a highly efficient and economically feasible method *(4,5)*.

During pretreatment a range of toxic compounds are formed. Olsson et al. *(6)* divided inhibitors into different groups depending on the origin: acetic acid is released when the hemicellulose structure is degraded-furfural, 5-hydroxymethyl furfural (HMF) are produced because of sugar (pentose and hexose) degradation, whereas aromatic compounds originated from lignin degradation. Formic acid is formed when furfural and HMF are broken down and levulinic acid is formed by HMF degradation. Quantitative and qualitative composition of the inhibitors arising during pretreatment depends on the type of applied pretreatment and also on the origin of lignocellulosic material *(6)*. A detailed review on the generation of inhibitors, on the mechanisms of inhibition and on detoxification methods (biological, physical, and chemical) was reported by Palmqvist and Hahn-Hägerdal *(7,8)*.

Biomass growth and ethanol production rate is hampered in the presence of weak acids (acetic and lactic acid) *(9–11)*. The inhibitory effect of these acids depend heavily on pH *(8,9)*, which can be reduced by maintaining higher fermentation pH. The tendency is to increase pH to values higher than 5.0 or even 5.5 *(12–17)* to demonstrate fermentability of pretreated raw materials; however, the optimum fermentation pH is in the range of 4.0–5.0 *(18)*. Above pH 5.0 bacteria can grow much faster than yeasts and on industrial scale uncontrollable fermentations will be observed in a non-sterile continuous process lay out. The principal bacterial contaminants in a distillery are those that form lactic acid. Some effects of contamination on flavor are known, but normally do not cause serious problems *(19)*. Although the production of fuel alcohol is not concerned with the taste of the product, any lactic acid formed subtracts from the yield of alcohol, furthermore, inhibit yeast growth and metabolism *(20)*. The production of lactic acid and other contaminants should therefore be avoided as much as possible. The development of these microorganisms is severely repressed at pH values under 5.0. This article presents a study on inhibitory effects of hemicellulose hydrolysates (HH) obtained after steam pretreatment of spruce, willow, and corn stover on ethanol fermentations at low pH (pH < 5.0) using an inhibitor resistant *Saccharomyces cerevisiae* strain, and a strategy to adopt the microorganism to inhibitors present in the hydrolysates.

## Materials and Methods

### Microorganisms and Culture Media

*S. cerevisiae* ATTC 26602, obtained from the American Type Culture Collection (ATCC), was used throughout this study. The yeast strain was maintained at –85°C in the mixture of 50 vol% glycerol and yeast, peptone, glucose (YPD) solution, which contained per liter demineralized water: 20.0 g of bacto peptone, 10.0 g of yeast extract, and 10.0 g of glucose. The pH was adjusted with 0.1 *M* KOH to 6.5 and sterilized for 15 min at 125°C. To control the procedure of freezing, yeast strain was plated on YPD agar contained per liter demineralized water: 20.0 g of bacto peptone, 10.0 g of yeast extract, 10.0 g of glucose, and 15.0 g of bacto agar. The pH was adjusted with 0.1 *M* KOH to 6.5 and sterilized for 15 min at 125°C.

### Yeast Cultivation

Starter culture of *S. cerevisiae* ATCC 26602 was grown in 1000-mL cap flasks containing 500 mL of culture medium. The medium for growth of yeasts contained per 0.5 L demineralized water: 114.0 g of Nedalco standard beet molasses (45–50% sugar content) and 1.2 g of $(NH_4)_2PO_4$. The pH was adjusted to 4.8 with 25% $H_2SO_4$, the medium was sterilized by autoclaving at 110°C for 30 min at 0.5 bar and was inoculated with freezed stock solution (1.5 mL) of yeast. After 1 d of incubation at 32°C cultures

were centrifuged at 1750*g* for 10 min (Rotanta 46, Hettich Zentrifugen, Germany), washed with demi water and harvested in demi water.

### Substrates

Spruce, willow, and corn stover containing about 45% cellulose based on dry matter were obtained from Sweden. Pretreatment of raw materials were carried out at Lund University (Sweden). Pretreatment of spruce, willow, and corn stover were carried out at 215°C for 5 min, 205°C for 4 min, and at 190°C for 5 min, respectively, with $SO_2$ impregnation. Pretreatment of willow was also carried out without $SO_2$ impregnation at 210°C for 14 min. Complete analysis of pretreated materials was carried out at the Budapest University of Technology and Economics (Hungary) (Table 1) according to the National Renewable Energy Laboratory Analytical Procedures. The liquid part of pretreated material (HH) was separated by centrifugation at 2625*g* for 10 min. Other batches of pretreated corn stover, originating from Italian National Agency for New Technologies, Energy and Environment, Italy (ENEA), pretreated at 190°C for 5 min and 210°C for 5 min, were also tested for ethanol fermentation.

### Fermentation Assays

Batch fermentations were carried out in stirred flasks with online measuring $CO_2$ production. Experiments were performed in 0.5- or 0.25-L capped flasks containing 100 or 50 mL of fermentation broth agitated at 300 rpm by magnetic stir bars and incubated in water bath at 32°C until the end of the fermentation (1 d). The fermentation medium contained per liter: liquid phase of pretreated material (HH) at different vol%, 16 mL of mineral solution, 1 mL of trace element solution, 1 mL of vitamin solution, and 1 mL of 30% (w/w) $FeSO_4 \cdot 7H_2O$ *(21)*. The mineral solution contained per liter *(12)*: 250.0 g of $(NH_4)_2SO_4$, 125.0 g of $KH_2PO_4$, 31.25 g of $MgSO_4$; the trace element solution contained per liter: 4.5 g $ZnSO_4 \cdot 7H_2O$, 1.0 g $MnCl_4 \cdot 4H_2O$, 0.3 g $CuSO_4 \cdot 5H_2O$, 0.3 g $CoCl_2 \cdot 6H_2O$, 4.5 g $CaCl_2 \cdot 2H_2O$, 0.4 g $Na_2MoO_4 \cdot 2H_2O$, 1.0 g $H_3BO_3$, and 0.1 g KI; the vitamin solution contained per liter: 0.05 g of biotin, 1.0 g calcium-pantothenate, 1.0 g nicotinic, 25.0 g inositol, 1.0 g thiamin-HCl, 1.0 g pyridoxin-HCl, and 0.2 g *p*-aminobenzoic acid. Glucose was added to the medium according to the cellulose content of the pretreated material (Table 1). The additional glucose was calculated as:

$$\text{Glucose(g)} = \frac{\begin{array}{r}[(\text{cellulose content}(\%) \cdot (\text{amount of HH(L)} \cdot \text{density of HH(kg / L)} / 0.9)] + \\ [(\text{cellobiose content}(\%) \cdot (\text{amount of HH(L)} \cdot \text{density of HH(kg / L)} / 0.95)]\end{array}}{100 \cdot \text{working volume(mL)}}$$

Harvested yeast was added to correspond to 1.5 g dry weight per liter. Dry matter content of harvested yeast was determined as described in Analytical Procedures section. The pH of the broth was adjusted initially to

Table 1
Composition of Pretreated Materials by Steam Explosion

| | Spruce | Willow ($-SO_2$)[a] | Willow ($+SO_2$)[a] | Corn stover | Corn stover[b] |
|---|---|---|---|---|---|
| *Pretreated material (%)* | | | | | |
| Dry matter | 23.76 | 18.61 | 24.70 | 10.03 | 35.01 |
| Cellulose[c] | 8.95 | 9.05 | 10.01 | 4.12 | ~9.62 |
| Lignin[c] | 7.40 | 5.08 | 5.38 | 1.50 | ~8.4 |
| Ash[c] | 0.01 | 0.10 | 0.09 | 0.29 | ~3.4 |
| *Liquid part: HH[d] (%)* | | | | | |
| Cellulose | 0.23 | 0.03 | 0.11 | 0.01 | nd |
| Glucose | 3.07 | 0.14 | 0.79 | 0.23 | nd |
| Mannose | 2.73 | – | – | – | nd |
| Xylose | – | 0.30 | 2.12 | 1.16 | nd |
| Arabinose | 0.07 | 0.01 | 0.05 | 0.12 | nd |
| Formic acid | 0.18 | 0.11 | 0.12 | 0.06 | nd |
| Acetic acid | 0.52 | 0.67 | 0.70 | 0.14 | nd |
| Levulinic acid | 0.13 | – | – | – | nd |
| HMF[e] | 0.38 | 0.10 | 0.10 | – | nd |
| Furfural | 0.25 | 0.22 | 0.15 | 0.01 | nd |

nd, not determined.
[a]Willow impregnated with (+) or without (–) $SO_2$.
[b]Pretreated at ENEA (Italy).
[c]Based on dry matter content.
[d]Based on pretreated material (mass/volume).

4.0 with 10% NaOH. Flasks were sampled at the end of fermentation, and analyzed for concentrations of biomass, sugars, metabolites, and ethanol by high-performance liquid chromatography (HPLC) at the following described conditions. Calculations were based on data obtained at the point from which no additional $CO_2$ production was achieved.

## *Analytical Procedures*

- Changes in biomass concentration throughout the fermentation process were measured by optical density measurement at 700 nm using a Perkin-Elmer Spectrophotometer. Dry matter content was determined according to a calibration line at 700 nm (Nedalco standard procedure): (dry weight [DW] (g/L) = $281[OD_{700}]^2 + 187.29[OD_{700}] + 9.822$).
- Sugars, ethanol, lactic acid, acetic acid, and glycerol were analyzed by Shimadzu HPLC on a Bio Rad column (HPX-87H), and detected by a refractive index (RI) detector. The working temperature was 65°C. $H_2SO_4$ (0.25 *M*) was used as eluent at a flow rate of 0.55 mL/min. Before HPLC samples were passed through a 0.2 µm pore size filter.
- Production of carbon dioxide was monitored online using a BAM-6 module (HaloteC, The Netherlands).

## Results and Discussion

The analytical characteristics of the pretreated materials and the HHs are summarized in Table 1. The HH consisted of soluble hemicellulose quantified as monomers (glucose, xylose, arabinose, and mannose) in different concentrations. Differences between softwood (spruce) and hardwood (willow) is noticeable in chemical composition. Hemicellulose of hardwood is rich in xylan polymers and contain small amounts of mannan, whereas mannose is a predominant sugar originating mainly from softwood (*5*). As xylose and mannose could not be separated on the applied HPLC column, therefore carbohydrate of pretreated spruce was assumed to be mannose, whereas at pretreated corn stover and willow, the sugar peak was interpreted as xylose (Table 1). The concentration of glucose in spruce HH is higher compared with the other pretreated substrates, demonstrating an easily degradable glucose containing biopolymer in spruce. Pretreatment of willow was carried out with and without $SO_2$ (which is used to improve hemicellulose recovery) in order to test the effect of $SO_2$ present in the HH on ethanol fermentation.

During steam explosion carbohydrate degradation products (furfural and HMF) and carboxylic acids (acetic, formic, and levulinic acids) were formed. Because hemicellulose of hardwood (willow) is more acetylated, pretreated willow resulted in the highest acetic acid concentration (Table 1). Overall the highest concentration of inhibitors were observed in pretreated spruce and it was the only pretreated material wherein levulinic acid formation was noticed as well. Presence of $SO_2$ did not dramatically affect the concentration of inhibitors in pretreated willow. Compared with pretreated woody substrates significantly lower inhibitor concentration was measured in hemicellulose hydrolysate of pretreated corn stover (originating from Lund) as shown in Table 1, wherein inhibitors are presented as w/w (%) of pretreated material (because of the structure of corn stover pretreated at ENEA, complete and accurate analysis could not be carried out). Lignin degradation products were not determined from HHs.

The effect of inhibitors present in steam pretreated lignocellulosic substrates was investigated using an inhibitor resistant yeast strain, which was previously selected by screening to have a resistance to inhibitory compounds generated during steam pretreatment. Of all tested strains *S. cerevisiae* ATCC 26602 seemed to grow best on toxic materials (data not shown). For fermentation studies pretreated materials were separated by means of centrifugation and the liquid part (HH) was used for fermentation. To test the fermentability of these pretreated lignocellulosic materials glucose was added to the HH (as described in Materials and Methods section) assuming that all cellulose (Table 1) could be hydrolyzed.

Fermentation of lignocellulosic substrates is usually carried out at pH 5.0–5.5. Running a fermentation under sterile conditions on large scale is not economical, and therefore it is important to keep the pH low (<4.5) to

prevent bacterial contamination and more organic acid formation with more inhibited process. Preliminary fermentation studies were carried out earlier (unpublished data) to test the effect of pH in the range of 4.8–3.8. Based on these preliminary investigations and on industrial considerations, fermentation of different steam exploded hydrolysate samples were tested at pH 4.0.

The fermentability of steam pretreated samples was tested under the same circumstances, only the ratio of hydrolysate was varied in a range of 30–94 vol% in the medium, containing minerals, vitamins, and trace elements (*see* Materials and Methods section). The results of ethanol fermentation on HHs are presented in Fig. 1A–D, wherein gas production rates (mL/min) are plotted vs fermentation time as a measure of actual volumetric ethanol production rate during the course of the process. In general, the $CO_2$ production profile showed the same curve with differences in lag phase. By increasing the ratio of HH in the medium the lag phase became longer indicating that the yeast requires an adaptation period because of inhibitors present in the fermentation broth.

Comparison of fermentation results represented by different steam-exploded lignocellulosic raw materials is in good agreement with inhibitor concentration of samples. The most inhibitory sample (Fig. 1A) has resulted at the highest dilution ratio, which was necessary to avoid the effect of inhibitors. Obtained ethanol concentrations on different HHs at the highest concentration wherein fermentation was not blocked by inhibitors, are summarized in Table 2. The ethanol yield was calculated from the ethanol concentration determined by HPLC at the end of the fermentation based on the potential fermentable sugars (glucose and mannose) concentration. Xylose concentration in the liquid fraction was also high (Table 1), but according to our knowledge this strain is not able to ferment xylose.

Even though rather high final ethanol concentration was achieved on pretreated spruce and willow, the concentration of HH could not be further increased because of inhibitors. Although corn stover could be fermented almost pure, the final ethanol concentration with 2.7 vol% is too low to be commercially interesting. However, with further increase (35%) in the dry matter content of pretreated corn stover (ENEA) the economically profitable final ethanol concentration was achieved (Table 2). Ethanol yields were comparable with data obtained in the literature on different pretreated and hydrolyzed lignocellulosic substrates: on spruce approx 0.40 g/g *(22)*, on wheat straw 0.43–0.46 g/g *(16)*, on willow 0.41–0.46 g/g *(10,23)* ethanol yield based on fermentable sugars have been reported.

By increasing the concentration of pretreated materials in the medium the molar ratio of ethanol/glycerol has been increased (data not shown). This tendency was observed on all substrates; however, the degree of change has differed. Glycerol is nontoxic to the yeast even at very high concentration. It plays a role under anaerobic condition in the maintenance of intracellular redox balance and acts as an osmotic regulator of the

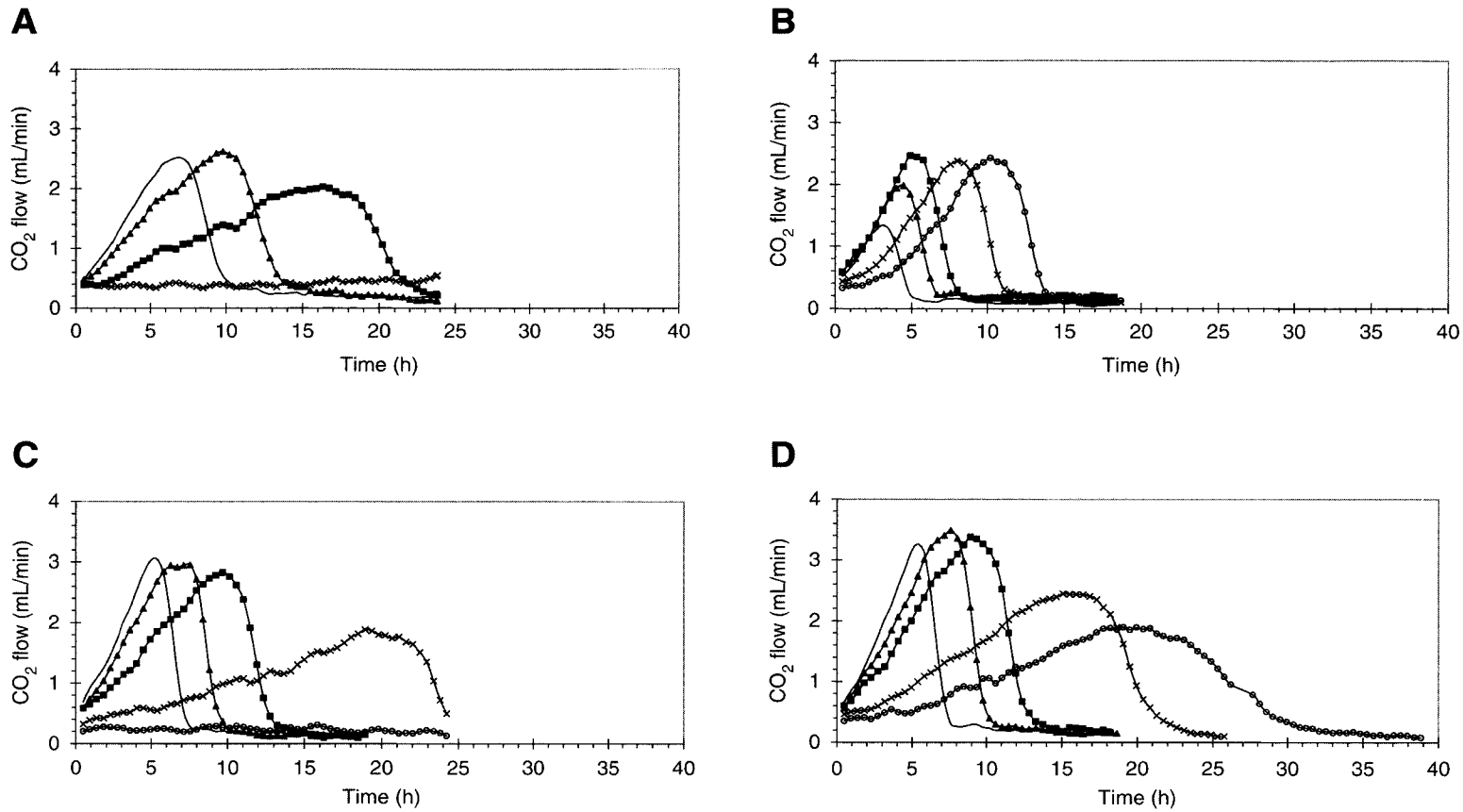


**Fig. 1. (A)** Fermentation of spruce HH at different vol% by *S. cerevisiae* ATCC 26602. 30% (–), 40% (-▲-); 50% (-■-), 55% (-×-). **(B)** Fermentation of corn stover HH at different vol% by *S. cerevisiae* ATCC 26602. 30% (–), 50% (-▲-); 70% (-■-), 85% (-×-), 94% (-○-). **(C)** Fermentation of willow HH (pretreated without $SO_2$ impregnation) at different vol% by *S. cerevisiae* ATCC 26602. 35% (–), 45% (-▲-); 55% (-■-), 64% (-×-), 67% (-○-). **(D)** Fermentation of willow HH (pretreated with $SO_2$ impregnation) at different vol% by *S. cerevisiae* ATCC 26602. 30% (–), 40% (-▲-); 50% (-■-), 59% (-×-), 67% (-○-).

Table 2
Ethanol Fermentation Results on Steam Pretreated Spruce, Corn Stover, and Willow With *S. cerevisiae* ATCC 26602

| Name | Substrate: Maximum volume (%) of HH | Substrate: Dry matter (%)[a] | Final ethanol (vol [%]) | Gross yield (%) |
|---|---|---|---|---|
| Spruce | 50 | 11.9 | 4.53 | 0.42 |
| Corn stover | 94 | 9.4 | 2.73 | 0.44 |
| Corn stover[b] | 75 | 15.8 | 5.03 | 0.49 |
| Willow ($-SO_2$)[c] | 64 | 11.9 | 4.09 | 0.48 |
| Willow ($+SO_2$)[c] | 65 | 16.6 | 5.74 | 0.50 |

[a]Corresponding to the concentration of HH.
[b]Pretreated at ENEA.
[c]Pretreated with (+) or without (–) $SO_2$.

cell *(24,25)*. Some of the inhibitors like acetic acid, furfural, and HMF were found to be a stimulator in the conversion of glucose to ethanol by *S. cerevisiae* in a certain extent rendering both a higher ethanol yield and lower byproduct (glycerol) yield *(26)*. Acetic acid has shown effect on growth energetic, leading to an increased ethanol yield *(15)*. Palmqvist et al. *(13)* have shown competition between furfural reduction and glycerol production in favor for furfural reduction, thus causing more sugar availability for ethanol production. Furfural and HMF are known to be reduced by yeast mainly to furfuryl alcohol *(13)*, 5-hydroxymethylfurfuryl alcohol, and slightly to 5-hydroxymethyl furan carboxylic *(12,13)*. During our fermentations, concentrations of HMF and furfural decreased and probably have been reduced by yeast to furfuryl alcohol and 5-hydroxymethylfurfuryl alcohol.

The fermentability of *S. cerevisiae* ATCC 26602 yeast strain was improved by adaptation to toxic components present in the pretreated lignocellulosic materials. Adaptation procedures were also performed on HH with added glucose in BAM6 module, followed by online measuring of $CO_2$ production (*see* Materials and Methods section). The simplified procedure for a rapid and reliable adaptation assay on spruce is shown in Fig. 2. During the procedure concentration (vol%) the HH was increased continuously (from 60% to 65%) in the fermentation broth. When the adaptation was succeeded at higher concentration, cells were separated at growing phase and reused in the next adaptation step.

To control the procedure of adaptation the fermentation ability of adapted and nonadapted yeast was tested on increased concentration of spruce HH. As can be seen from Fig. 3, *S. cerevisiae* ATCC 26602 could be adapted to higher concentration of inhibitors on spruce matrix with 5.2 vol% final ethanol concentration; however, this topic needs to be addressed in more detail in future studies.

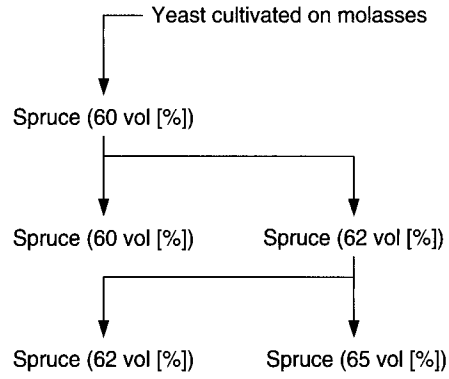


**Fig. 2.** Scheme of the adaptation procedure.

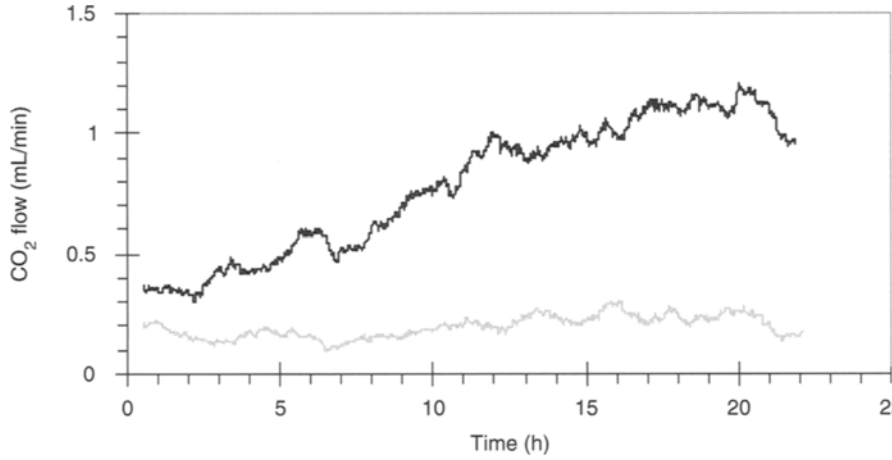


**Fig. 3.** Result of adaptation of *S. cerevisiae* ATCC 26602 on spruce HH at 65 vol%. Not adapted yeast (–), adapted yeast (–).

## Conclusions

This study aimed to test the fermentability of different steam pretreated lignocellulosic raw materials at low pH by the inhibitor resistant *S. cerevisiae* ATCC 26602 yeast. *S. cerevisiae* ATCC 26602 was found to be capable of ethanol fermentation at low initial pH (pH 4.0), which is necessary to avoid bacterial contamination. After steam pretreatment all tested lignocellulosic materials (pretreated willow, spruce, and corn stover) seem to be a possible substrate for economically profitable industrial ethanol production with final ethanol concentration of 5 vol%. Impregnation with $SO_2$ did not affect the applied microorganism, but was found to be necessary to improve the recovery of hemicellulose. Steam pretreated corn stover seems to be a promising substrate for bioethanol production. The main advantage of this agricultural waste (produced in huge amounts in Hungary) is that

the concentration of toxic compounds formed during pretreatment does not reach the critical level, at which fermentation of yeast would be blocked. The inhibitor tolerance of the selected *S. cerevisiae* ATCC 26602 was improved with continuous adaptation on steam pretreated spruce matrix. Under the same circumstances and inhibitor concentrations, the adapted yeast was able to ferment 5 vol% ethanol, the original, nonadapted yeast strain was incapable of ethanol fermentation.

Ethanol yields were rather high (in all cases above 0.42 g ethanol/g fermentable sugars) considering that none of these experiments were made on real fibrous substrate, only on filtrate, using added glucose as sugar component (according to cellulose content). In order to test the real process, the glucose should be derived from enzymatic treatment of the pretreated fiber material as performed in simultaneous saccharification and fermentation on the whole slurry. To obtain the least 5% (v/v) ethanol concentration rather high (approx 20%) dry matter concentration is needed, whereas further increasing the substrate concentration more than 15% of dry matter would result in reduced ethanol yield owing to insufficient mass transfer *(27)*.

## Acknowledgments

The study was financially supported by the Commission of the European Communities, Energy, Environment, and Sustainable Development Programme (project number ENK6-CT-2002-00604), by the Rubik Foundation and by the Leonardo Program. The authors would like to gratefully acknowledge also Lund University, Department of Chemical Engineering, and ENEA for performing pretreatments.

## References

1. Commission of the European Communities (2000), COM (2000) Final Report 769.
2. Claassen, P. A. M., van Lier, J. B., Lopez Contreras, A. M., et al. (1999), *Appl. Microbiol. Biotechnol.* **52,** 741–755.
3. Zaldivar, J., Nielsen, J., and Olsson, L. (2001), *Appl. Microbiol. Biotechnol.* **56,** 17–34.
4. Vallander, L. and Eriksson, K. E. L. (1990), *Adv. Biochem. Eng.* **42,** 63–95.
5. Szengyel, Zs. (2000), *PhD Thesis*, Lund University, Sweden.
6. Olsson, L. and Hahn-Hägerdal, B. (1996), *Enzyme Microb. Technol.* **18,** 312–331.
7. Palmqvist, E. and Hahn-Hägerdal, B. (2000), *Bioresour. Technol.* **74,** 17–24.
8. Palmqvist, E. and Hahn-Hägerdal, B. (2000), *Bioresour. Technol.* **74,** 25–33.
9. Narendranath, N. V., Kolothumannil, C. T., and Ingledew, W. M. (2001), *J. Am. Soc. Brew. Chem.* **59,** 187–194.
10. Olsson, L. and Hahn-Hägerdal, B. (1993), *Process Biochem.* **28,** 249–257.
11. Delgenes, J. P., Moletta, R., and Navarro J. M. (1996), *Enzyme Microb. Tech.* **19,** 220–225.
12. Taherzadeh, M. J., Gustafsson, L., Niklasson, C., and Lidén, G. (2000), *Appl. Microbiol. Biotechnol.* **53,** 701–708.
13. Palmqvist, E., Almeida, J. S., and Hahn-Hägerdal, B. (1999), *Biotech. Bioeng.* **62,** 447–454.
14. Palmqvist, E., Grage, H., Meinander, N. Q., and Hahn-Hägerdal, B. (1999), *Biotech. Bioeng.* **63,** 46–55.
15. Taherzadeh, M. J., Niklasson, C., and Lidén, G. (1997), *Chem. Eng. Sci.* **52,** 2653–2659.

16. Klinke H. B., Olsson, L., Thomsen, A. B., and Ahring, B. K. (2003), *Biotech. Bioeng.* **81,** 738–747.
17. Larsson, S., Palmqvist, E., Hahn-Hägerdal, B., et al. (1999), *Enzyme Microb. Tech.* **24,** 151–159.
18. Lin, Y. and Tanaka, S. (2006), *Appl. Microbiol. Biotechnol.* **69,** 627–642.
19. Makanjoula, D. B., Tymon, A., and Springham, D. G. (1992), *Enzyme Microb. Technol.* **14,** 350–357.
20. Narendranath, N. V., Hynes, S. H., Thomas, K. C., and Ingledew, W. M. (1997), *Appl. Environ. Microbiol.* **63,** 4158–4163.
21. Verduyn, C., Postma, E., Scheffers, W., and van Dijken, J. P. (1992), *Yeast* **8,** 501–517.
22. Persson, P., Andersson, J., Gorton, L., Larsson, S., Nilvebrant, N. O., and Jönsson, J. (2002), *J. Agric. Food Chem.* **50,** 5318–5325.
23. Palmqvist, E., Hahn-Hägerdal, B., Galbe, M., and Zacchi, G. (1996), *Enzyme Microb. Technol.* **19,** 470–476.
24. Maiorella, B. L., Blanch, H. W., and Wilke, C. R. (1984), *Biotechnol. Bioeng.* **26,** 1155–1166.
25. Albers, E., Larsson, C., Lidén, G., Niklasson, C., and Gustafsson, L. (1996), *Appl. Environ. Microbiol.* **62,** 3187–3195.
26. Sárvári, I. H. (2001), *PhD Thesis,* Chalmers University of Technology, Sweden.
27. Varga, E., Klinke, H. B., Réczey, K., and Thomsen, A. B. (2004), *Biotecnol. Bioeng.* **88,** 567–574.

0273-2289/1559-0291 (Online)/07/136–140/859–874/$30.00

# The Effects of Engineering Design on Heterogeneous Biocatalysis in Microchannels

FRANK JONES,*[,1] ROBERT BAILEY,[2] STEPHANIE WILSON,[1] AND JAMES HIESTAND[1]

[1]*University of Tennessee at Chattanooga, Chattanooga, TN 37403, E-mail: frank-jones@utc.edu; and* [2]*Loyola College in Maryland, Baltimore, MD 21210*

## Abstract

The results of a numerical study of the fundamental interactions of engineering design and micromixing on conversion in packed microchannels are presented. Previously, channel-based microreactors made of molded silicon plastic were designed, fabricated, and experimentally tested. These reactors have enzymes immobilized on the channel walls by various methods including layer-by-layer nano self-assembly techniques. They also contain molded packing features to add reactive surface area and to redistribute the fluid. An arbitrary but intuitively sensible packing arrangement was initially chosen and used in experimental studies. The current computer simulation study was undertaken to understand how static laminar mixing affects the conversion efficiency. The reactors previously used experimentally have been simulated using CFD-ACE+ multiphysics software (ESI CFD Inc., Huntsville, AL). It is found that packing significantly increases conversion when compared with empty channels over the entire flow rate range of the study ($0.25 < Re < 62.5$). The boost in conversion has an optimal point near $Re = 20$ for the particular geometry examined.

**Index Entries:** Catalase; enzyme; micromixing; microreactor; numerical simulation; heterogeneous catalysis.

## Introduction

The field of miniaturizing chemical process devices has exploded in the last decade. This has led to extensive studies of the behavior in microscale fluidic channels. Most of these studies lie in the general categories of heat transfer *(1)*, mixing *(2)*, and chemical reaction *(3)*. Investigators are striving to acquire the ability to fully use the inherent advantages of the small scale. This work investigates heterogeneous catalysis in microchannels by numerical analysis. It follows up on previous experimental studies by the authors whereby enzymes were immobilized on polydimethylsiloxane (PDMS) microchannel walls by various techniques including layer-by-layer nano self-assembly *(4,5)*. The channels were created using molds fabricated by micro electro mechanical systems (MEMS) techniques. Reaction behavior in

*Author to whom all correspondence and reprint requests should be addressed.

these channels was physically studied and later simulated using CFD-ACE+ computational software *(6)*.

Static mixing is critical for homogeneous and heterogeneous chemical reaction in microchannels. Numerous physical and computational studies pursuing applications in DNA sequencing, chemical analysis, separation, and environmental monitoring have investigated micromixing in the last several years. Static mixing is accomplished on the microscale by excavating grooves or fabricating structures in the channels *(7–9)*. An attempt has even been made to optimize the number and pattern of the packing to achieve best mixing *(7)*. Mixing can also be accomplished by complex twisting, splitting, and rejoining pores in three dimensions *(3)*. Current microreactor research is to be applied to a broad array of applications including biofuels. Microreactors are being used to produce biodiesel fuel. Both mixing of the reactants and the transesterification reaction take place in microchannels reducing processing time from hours or days to minutes. Although each channel produces a very small quantity, banks of channels packaged in suitcase-sized devices can be used to produce enough fuel for individuals or small communities *(10)*.

It is the objective of this article to examine the effects of packing on mixing and heterogeneous conversion in microchannels. Also, the reactors are examined over a range of flow rates in order to find optimum operating conditions for a given design. The ultimate goal, beyond the present study, is to vary the packing feature size, shape, locations, and density in order to optimize the microchannel's ability to promote the reaction. As MEMS techniques and enzymes are very expensive, acquiring the ability to optimize the packing design will allow microreactors to become even smaller and perhaps more efficient. In the fabrication process, micromolds are made using 10-cm silicon wafers. Smaller reactors will allow more to fit on the same mold, making them significantly cheaper. Essentially, the microfluidics industry is following the path of the microelectronics industry in making smaller and smaller devices.

## Theory

### *Descriptive Equations*

The flow, mixing, and heterogeneous liquid–solid reaction in microchannels are described by a complex set of coupled nonlinear partial differential equations. For this study, several assumptions are introduced that simplify these equations significantly:

- The density and viscosity of the bulk mixture are determined by the primary constituent, water. The very small concentration of the substrate (hydrogen peroxide) has no appreciable effect on these parameters. This also leads to minimal heating from reaction owing to the high heat capacity of the water and the low level of

reaction per unit enzyme per unit flow, so the flow is considered to be isothermal.
- The flow is steady state, incompressible, and because of low fluid velocity and the smallness of the channels, laminar.
- Chemical reactions are heterogeneous, taking place only at solid–liquid interfaces wherein enzyme is present.

With these assumptions the flow field (velocity and pressure) within a reactor microchannel is determined by solving the following forms of the conservation of mass (continuity) and Navier–Stokes (momentum) equations:

$$\nabla \cdot \mathbf{V} = 0 \tag{1}$$

$$\rho \mathbf{V} \cdot \nabla \mathbf{V} = -\nabla p + \mu(\nabla^2 \mathbf{V}) + \rho \mathbf{g} \tag{2}$$

where **V** is Cartesian velocity vector (m/s), ρ is bulk mixture density (kg/m$^3$), p is pressure (Pa), μ is bulk mixture absolute viscosity (N·s/m$^2$), and **g** is gravitational acceleration vector (m/s$^2$). The steady-state concentration field is governed by:

$$\mathbf{V} \cdot \nabla C_i - D_i \cdot \nabla^2 C_i = 0 \tag{3}$$

where, i is species indicator (one equation for each species), $C_i$ is concentration of species i (M), and $D_i$ is diffusivity of species i in solvent (m$^2$/s). The kinetics of the heterogeneous chemical reaction that takes place at the solid–liquid interfaces is described using the Michaelis–Menten model:

$$v = \frac{V_{max}[S]}{k_m + [S]} \tag{4}$$

where $v$ is reaction rate (mol/[s·m$^2$]), [$S$] is substrate concentration at the solid surface (M), $V_{max}$ is the maximum reaction rate (mol/[s·m$^2$]) $V_{max} = k_{cat}$ [$E$], $k_m$ is Michaelis constant (concentration that gives $v = V_{max}/2$) (M), $k_{cat}$ is turnover number (s$^{-1}$), and [$E$] is enzyme concentration at the solid surface (mol/m$^2$).

## *Boundary Conditions*

The boundary conditions associated with flow and reaction within microchannels are as follows. At the channel inlet, a uniform velocity distribution and substrate concentration were specified whereas at the channel exit, a fixed pressure boundary condition was assigned. A no-slip boundary condition (**V** = 0) was applied at all solid surfaces. If no enzyme is present on a solid surface, the concentration boundary condition is given by:

$$D_s \times \frac{d[S]}{dn} = 0 \tag{5}$$

where $D_s$ is the diffusivity of substrate in the solvent ($m^2/s$) and $n$ is distance in direction normal to the solid surface (m). If enzyme is present at the surface, the following boundary condition, which includes Michaelis–Menten kinetics, was applied to implement the steady, heterogeneous catalysis reaction:

$$-D_s \times \frac{d[S]}{dn} = \frac{V_{max} \times [S]}{k_m + [S]} \tag{6}$$

### Dimensionless Parameters

Two dimensionless parameters are of particular interest in this study. The first is the mass transfer Peclet number (*Pe*), which represents the ratio of advection to diffusion mass transfer rates. This parameter is defined as:

$$Pe = \frac{Ud}{D_s} \tag{7}$$

where $U$ is velocity magnitude (m/s) and $d$ is the smallest channel cross dimension (m). The second dimensionless parameter is the Reynolds number (*Re*), given by:

$$Re = \frac{\rho U d}{\mu} \tag{8}$$

The Reynolds number represents the ratio of inertial forces to viscous forces within the moving fluid, and it is a determining factor in transition from laminar to turbulent flow. As already mentioned, all flows in this study were laminar.

### Numerical Solution Method

The differential equations were solved numerically using the CFD-ACE+ computational package developed by ESI CFD Inc., located in Huntsville, Alabama *(11)*. CFD-ACE+ is a finite volume-based code that uses a variation of the semiimplicit method for pressure-linked equations consistent (SIMPLEC) algorithm *(12)*. As with all finite volume methods, two major approximations are used:

- The physical domain is broken down into a series of small control volumes (cells). The resultant collection of cells is referred to as the computational grid.
- The governing differential equations are replaced by a set of algebraic finite difference equations that approximate the requirements of the differential equations on each cell.

In general, the velocity, pressure, and concentration fields are linked, but owing to the small substrate concentrations considered in this study, the concentration field could be decoupled to enhance computational efficiency. The solution algorithm proceeds in two major steps. First, the velocities and pressures at the cell centers are calculated using an iterative pressure-correction approach (SIMPLEC). Once these flow field variables are determined, they are introduced into the approximated species conservation equation, and the concentrations at the cell centers are calculated iteratively *(11)*. CFD-ACE+ has been applied previously by the authors to simulate flow and reaction within microchannels, and validation through comparison with experimental data is described in ref. *6*.

## Modeling and Simulation Procedures

Two separate three-dimensional representations (models) of a single microreactor channel were created using CFD-ACE+. In each case, the channel was 500 μm wide ($x$-direction) by 125 μm deep ($y$-direction) by 50,000 μm long ($z$-direction). The first model, which considered a channel without internal features, used a structured grid with approx 720,000 cells. Grid points were clustered near the channel walls to more accurately resolve concentration gradients there. A portion of the grid is shown in Fig. 1A. A second model was developed for a channel with internal features that were shaped like triangular prisms. Because of the more complex geometry, an unstructured grid consisting of just over 1,000,000 cells was used. A portion of this grid is presented in Fig. 1B. Sensitivity studies performed with other grids indicated that the two earlier models provided sufficient resolution to capture important trends in the solutions. The chemical reaction considered in all of the simulations was the breakdown of hydrogen peroxide ($H_2O_2$) into oxygen and water in the presence of catalase (the enzyme catalyst):

$$H_2O_2 \xrightarrow{\text{Catalase}} H_2O + \frac{1}{2}O_2 \tag{9}$$

An active catalase surface concentration of $1.0 \times 10^{11}$ molecules/cm$^2$ was assigned at all solid surfaces wherein enzyme was present, and the $H_2O_2$ concentration at the channel inlet was set to 0.0147 $M$ (500 ppm). The fluid flow, mass transfer, and reaction kinetics parameters were taken from the open literature and are shown in Table 1. All computations were performed on personal computers equipped with a 3.0 or 3.6 GHz Intel Pentium 4 processors and 2 GB of random access memory (RAM). The computational times ranged between 7 and 11 h depending on Reynolds number and the presence or absence of internal features.

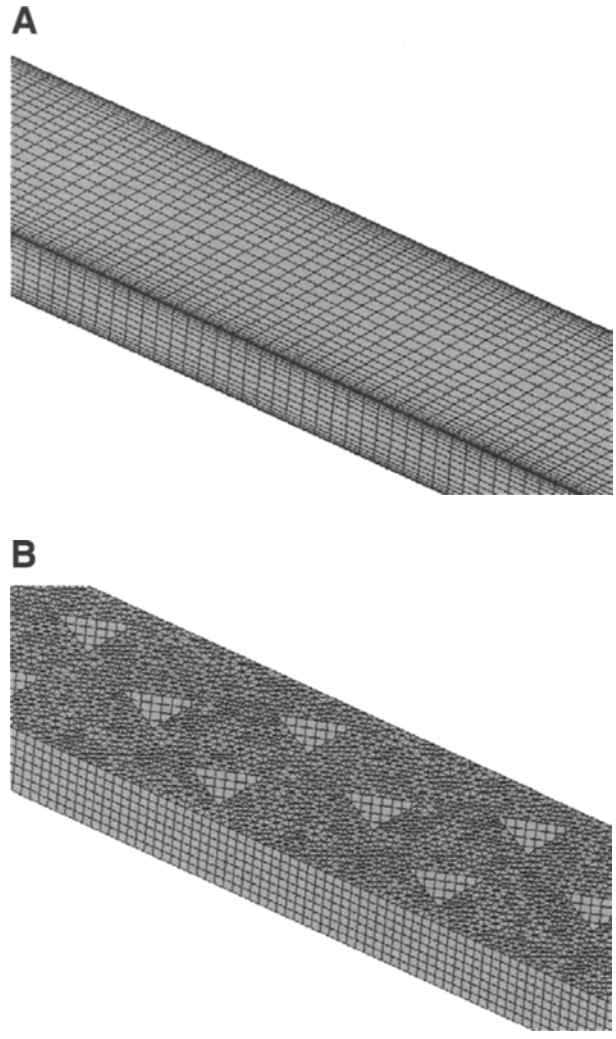


**Fig. 1. (A)** A portion of the structured grid used for a microreactor channel with no internal features. **(B)** A portion of the unstructured grid used for a microreactor channel with internal features.

Table 1
Flow, Mass Transfer, and Kinetics Parameters

| Property | Symbol | Value |
|---|---|---|
| Bulk mixture density *(13)* | $\rho$ | 998 kg/m$^3$ |
| Bulk mixture kinematic viscosity *(13)* | $\upsilon$ | $1.31 \times 10^{-6}$ m$^2$/s |
| Diffusivity of $H_2O_2$ in water (25°C) | $D_s$ | $1.0 \times 10^{-9}$ m$^2$/s |
| Michaelis constant for breakdown of $H_2O_2$ catalyzed by catalase *(14)* | $k_m$ | 0.025 *M* |
| Turnover number for breakdown of $H_2O_2$ catalyzed by catalase *(14)* | $k_{cat}$ | $1.0 \times 10^7$ s$^{-1}$ |

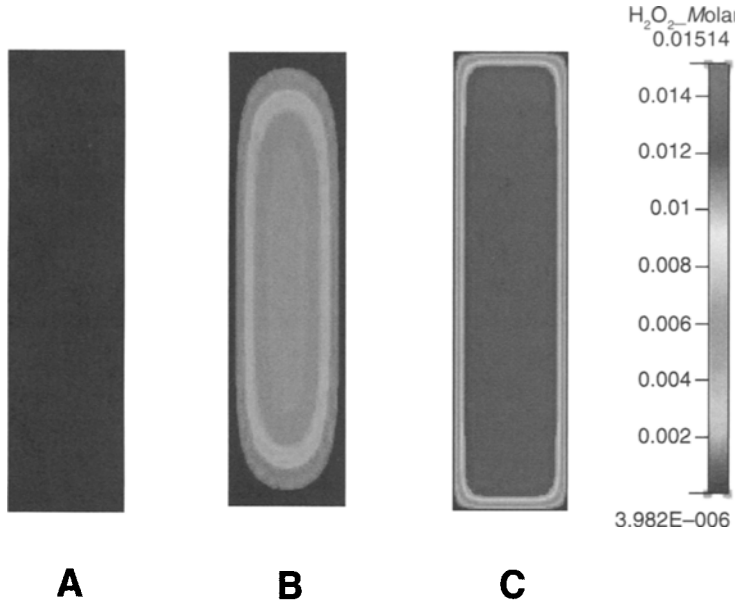


**Fig. 2.** Concentration profiles of the exit planes of various reactor channels. **(A)** Cross-section 50 × 12.5 μm², **(B)** 500 × 125 μm², and **(C)** 5000 × 1250 μm².

Table 2
Reactor Performances for Various Channel Sizes

| Scale (μm) (length × width) | Flow rate ($mm^3/s$) | *Re* | *Pe* | *X* (%) | Δ*P* (Pa) |
|---|---|---|---|---|---|
| 5000 × 1250 | 166.7 | 25 | 33,375 | 3.5 | 25 |
| 500 × 125 | 16.67 | 2.5 | 3338 | 62.5 | 1500 |
| 50 × 12.5 | 0.167 | 0.25 | 334 | 100 | 156,000 |

## Results and Discussion

### *The Effect of Scale on Conversion in Microchannels*

The effect of decreasing reactor cross-section on conversion should be dramatic for heterogeneous catalysis in channels simply because of increased proximity of reactant molecules to enzyme-coated walls as the scale becomes smaller. Previous experimental studies *(4,15)* used 50 mm long channels with 500 μm by 125 μm cross-sections with 1% (by mass) surface coverage of immobilized enzyme. The level of conversion in channels an order of magnitude larger (5000 × 1250 μm²) and an order of magnitude smaller (50 × 12.5 μm²) are compared with the experimental (nominal) scale. Each scale has a flow rate and surface area 100 times smaller than the next for proper comparison. The feed to all channels is 500 ppm hydrogen peroxide in water.

The calculated conversions at the exits for the three sizes are shown as concentration profiles in Fig. 2 and numerically in Table 2. The largest

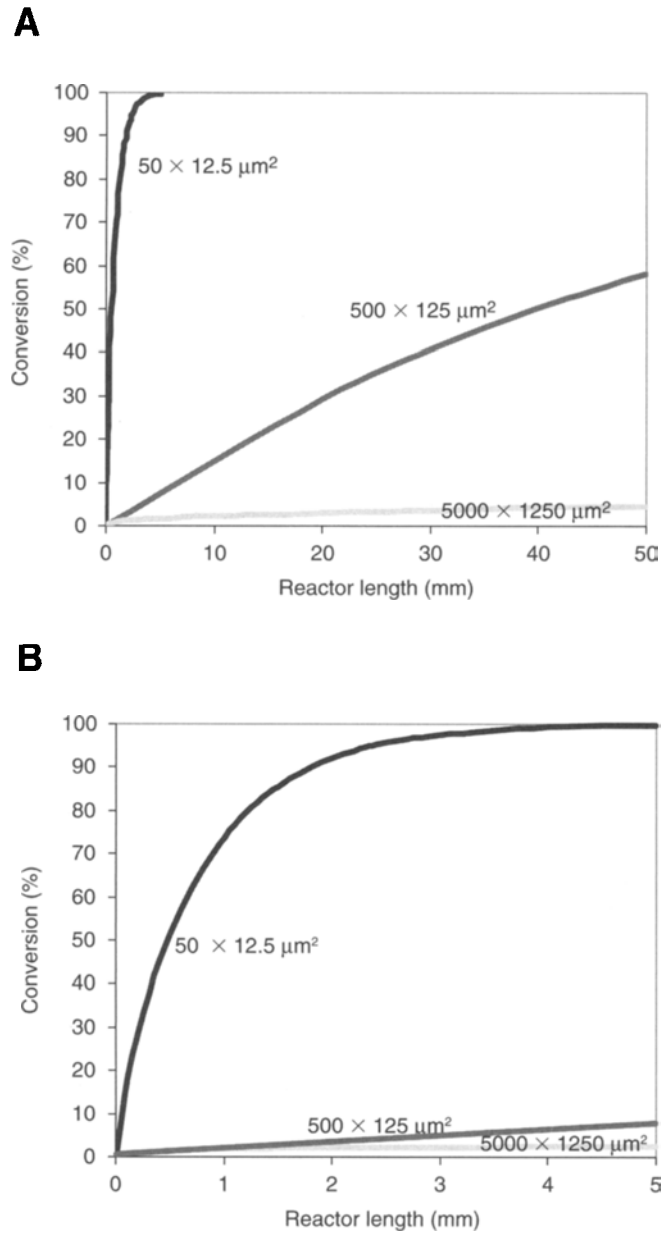


**Fig. 3. (A)** Conversions along the lengths of the reactor channels of Fig. 1. **(B)** Detail of the conversion profiles of the first 5 mm of the channels in Fig. 3 **(A)**.

channel has a conversion of 3.5%; the experimental scale, 62.5%; and the smallest channel, virtually 100% at their exits (50 mm length). In fact, the smallest channel reached complete conversion far before the exit. Fig. 3A shows the conversion vs length behavior in the channels. The channel with the smallest cross-section reaches 99% conversion in less than 5 mm. Part B of Fig. 3 is a blowup of the first 5 mm of the reactor channels. At the 3 mm point, the smallest scale has about 98% conversion compared

with 4% for the nominal scale, which is an increase of 2350% in the number of reactions per unit enzyme per unit flow.

The pressure drops grow dramatically as cross-section decreases (from 25 to 156,000 Pa). Although a pressure drop of 156,000 Pa is not experimentally prohibitive *(4)*, Fig. 3A reveals that a proper design for the smallest scale would be a reactor only 5 mm in length. The resulting pressure drop of about 1560 Pa would be almost identical to the full length nominal reactor. Clearly, smaller reactors would be cheaper to fabricate by standard MEMS techniques because more reactors would fit on a standard 10 cm wafer. Also, the smaller molded reactor would be cheaper to coat with (very expensive) enzyme *(5)*. Reynolds numbers are also shown in Table 2. They vary owing to the characteristic length (the smallest cross dimension) changing by a factor of 10 for each scale, but all flows are laminar.

Only lateral diffusion to flow can carry a reactant molecule to a wall for reaction in an empty channel. Parts (B) and (C) of Fig. 2 clearly show that centrally located process fluid remains largely unreacted at the channel exits. The Peclet number is a measure of the ratio of advection (transport owing to bulk fluid motion) to diffusion mass transfer. Lower Peclet numbers allow for adequate lateral diffusion in the 50 mm channel length and lead to higher conversions. As shown in Table 2, for Peclet number significantly higher than 334, advection dominates diffusion and fluid redistribution is required to improve conversion.

### *The Effect of Static Mixing on Conversion: Packed Channels*

Packing features are added to the empty channels to improve conversion by providing fluid redistribution and adding reactive surface area with coated packing. Fluid redistribution refers to the break-up of flow patterns to enhance fluid-solid contact. Because the flow is laminar, this is not mixing in the traditional sense. The term chaotic advection is sometimes used to describe this laminar phenomenon. Figure 4 shows a detail of the velocity field in a channel with the packing feature pattern used in all packed simulations and a flow rate of 25 cc/min ($Re = 62.5$). Triangular packing features with a perimeter of $125 \times 125 \times 140$ $\mu m^3$ and the full channel depth of 125 μm are located in a repeating pattern of three per 500 μm length (referred to as a unit cell) for a total of 300 features in the 50 mm channel. The packing adds 17.2% surface area and subtracts 10.5% channel volume. Therefore, packing reduces process fluid residence time by 10.5% when compared with equal flow rate simulations in empty channels.

Conversions for a Reynolds number range of 0.25 to 62.5 are shown in Fig. 5 for channels with and without packing features. Also shown are conversions for channels with uncoated packing, which will be discussed later. There are large improvements in conversion at all flow rates owing to packing except at $Re = 0.25$ wherein all channels achieve virtually 100% conversion. This is in spite of the fact that there is 10.5% less residence time for reaction in packed channels.

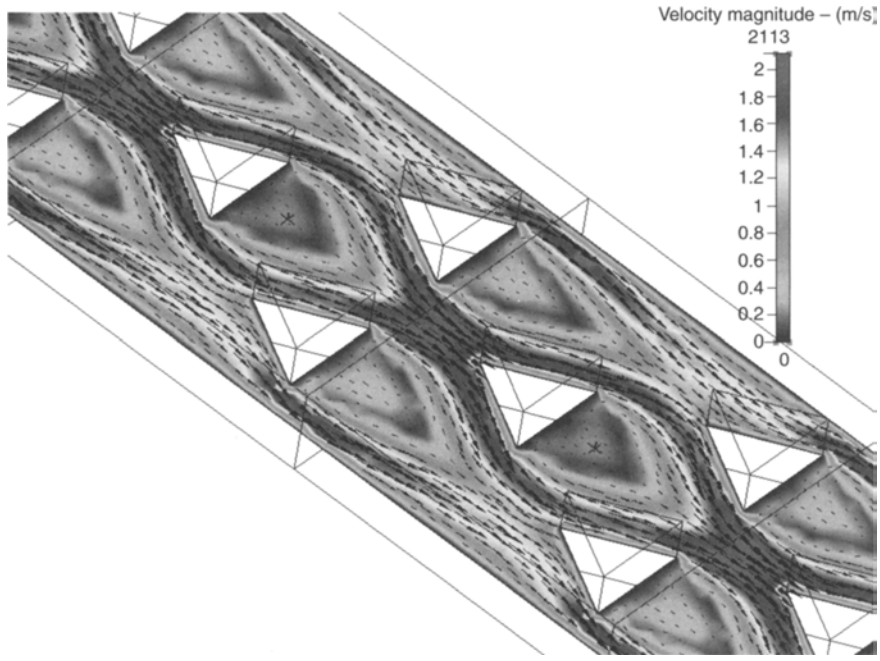


**Fig. 4.** Detail of the velocity field for $Re$ = 62.5 in packed channel with a 500 × 125 μm$^2$ cross-section. Packing is in a repeating pattern for the entire 50 mm long channel.

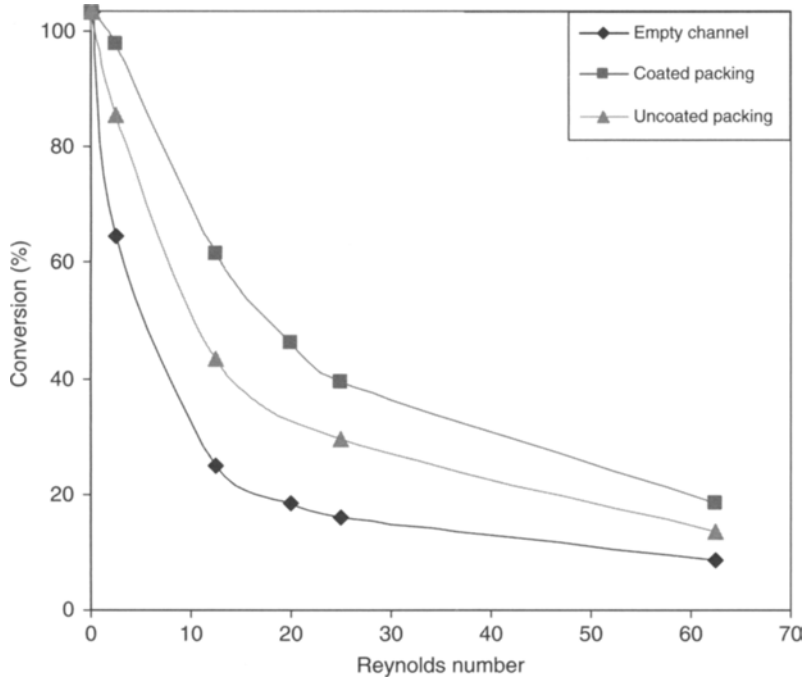


**Fig. 5.** Conversions for channels with and without packing and with uncoated packing at various Reynolds numbers.

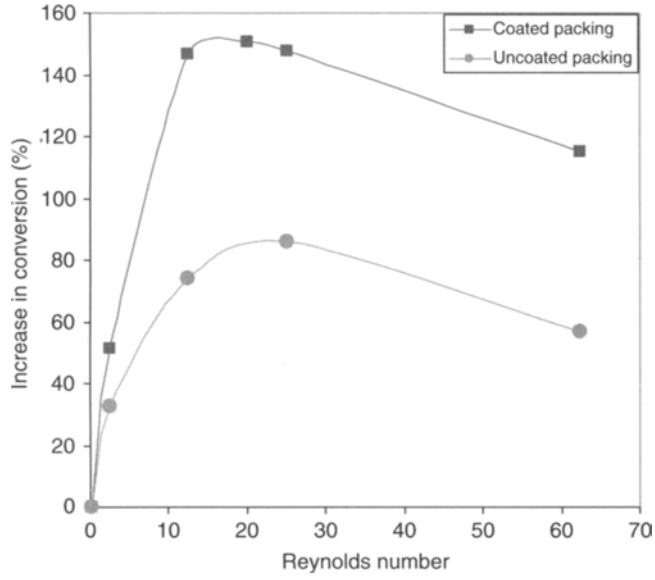


**Fig. 6.** Percentage increase in conversion owing to packing.

The level of conversion improvement varies greatly over the range of flow rates. For example, at a flow rate of 1 cc/min ($Re$ = 2.5), conversion increases from 62.5% for an empty channel to 94.5% for a packed channel. The conversion improvements over the entire range of flow rates for coated and uncoated packing are shown in Fig. 6. A peak in increase in conversion for coated packing over empty channels occurs near $Re$ = 20. Here, the packed channel has 151% more conversion than an empty one.

This discovery suggests an optimal use of this design. Previous experimental work was performed using packed channels and a nominal flow rate of 1 cc/min ($Re$ = 2.5). Simulations show that the maximum beneficial effect of packing on conversion is at 8 cc/min, which is eight times the nominal flow rate but still has almost half the conversion (44.7% vs 94.5%). This yields a 278% increase in reactions per enzyme. This increase in enzyme effectiveness can be explained by increased chaotic advection as flow speeds up. In fact, the number of reactions performed by each enzyme in packed channels increases over the entire flow rate range, because conversion never decreases as much as residence time. This behavior is consistent with experimental results in similar reactors wherein urea was reduced using immobilized urease (*5*). Table 3 contains conversions, Peclet numbers, and pressure drops for empty and packed channels at various flow rates. Packing increases pressure drop significantly. At a flow rate of 1 cc/min, an empty channel has a pressure drop of 1500 Pa, whereas packing causes an increase to 4100 Pa, a factor of about 2.73. This factor increases with flow rate, such that at a flow rate of 25 cc/min, the factor is 5.76. Pressure drops for packed channels also increase significantly more than linearly as flow rate increases.

Table 3
Conversions and Pressure Drops for Empty and Packed Channels

| *Re* | Flow rate (cc/min) | *Pe* | $\Delta P$ (Pa) (empty) | *X* (%) (empty) | $\Delta P$ (Pa) (packed) | *X* (%) (packed) |
|---|---|---|---|---|---|---|
| 0.25 | 0.1 | 334 | 200 | 100 | 400 | 100 |
| 2.5 | 1.0 | 3338 | 1500 | 62.5 | 4100 | 94.5 |
| 12.5 | 5.0 | 16,688 | 7900 | 24.2 | 24,600 | 59.6 |
| 20 | 8.0 | 26,700 | 12,700 | 17.8 | 44,900 | 44.7 |
| 25 | 10 | 33,375 | 15,800 | 15.4 | 60,500 | 38.2 |
| 62.5 | 25 | 83,438 | 39,800 | 8.4 | 229,300 | 18.0 |

Figure 7 shows the velocity fields taken at the vertical midplane in the channel entry regions for each of four flow rates. Four repeating unit cells (a total length of 2 mm of the 50 mm channel) are shown for each case. Entry lengths for hydrodynamically fully developed flows have been estimated from these figures in multiples of 0.5 mm. Entry lengths are 1, 1.5, 2, and 2.5 mm for Reynolds numbers of 0.25, 2.5, 25, and 62.5, respectively.

Three distinct flow fields appear in packed channels over the entire Reynolds number range of this study. The two slower flow rates ($Re = 0.25$, 2.5) appear to have creeping flow around packing features and slow flow near the outside walls that mostly returns to and mixes with more centrally located fluid (Fig. 7, top 2 images). Faster flow at $Re = 25$, has fast flow along the two upstream walls of each triangle and significant dead spots behind each triangle. There is also significant channeling around the central triangles. At the fastest flow rate ($Re = 62.5$), separate channels develop between the outside walls and their neighboring triangles (Fig. 7, bottom image). These channels remain largely separate from the central flow creating a significant opportunity for a large amount of fluid to flow near a reactive surface that is not seen in slower flow rates.

## *The Effect of Static Mixing in Packed Channels: Uncoated Packing*

Packing adds reactive surface area and static mixing to increase conversion. In order to separate these two effects, simulations were performed with the same packing configuration but with the surfaces of the triangles that are exposed to the flow not coated with enzyme. Uncoated packing reduces both reactor volume and residence time by 10.5% and reduces the active reaction area by 8.4% when compared with empty channels. In spite of these handicaps, reactors with uncoated packing perform significantly better than empty channels at all but the slowest flow rate ($Re = 0.25$ is virtual creeping flow) as shown in Fig. 5. For example, at $Re = 25$, fluid redistribution using uncoated triangles increases conversion from 15.4% to 28.6%. Coating the packing

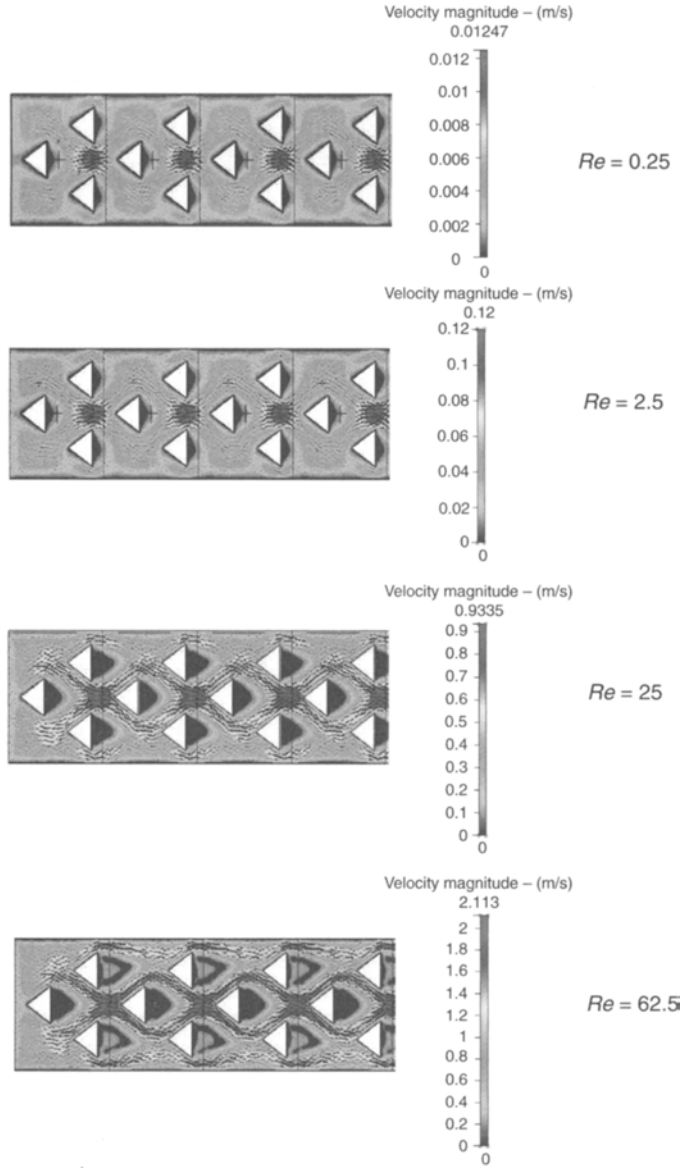


**Fig. 7.** Top view of the velocity fields in the vertical midplane near the channel inlet for various Reynolds number. Velocity scales at right.

increases the reactive surface area by 27% (vs uncoated) and further increases conversion to 38.2%. Figure 6 shows that the effect of static mixing on conversion over empty channels varies with Reynolds number and peaks around $Re = 20$, as it did for coated features.

## *The Effect of Flow Direction Using Triangular Packing*

When the flow direction in a packed channel is reversed, a significantly different flow field results. Figure 8 shows flow into the flat base of

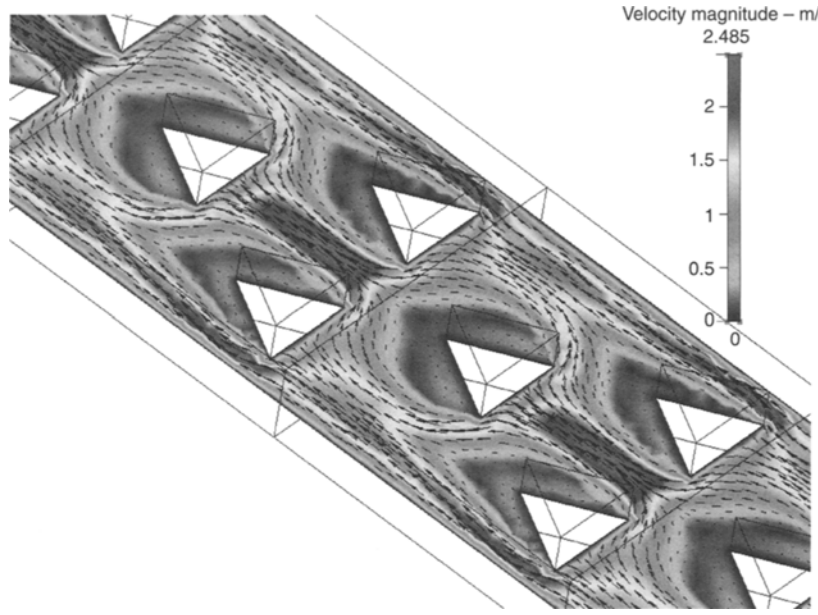


**Fig. 8.** Velocity field for reverse process flow at $Re = 62.5$.

the triangles for a Reynolds number of 62.5. As the packing now directs some flow in a direction lateral to the bulk flow, static mixing should be increased when compared with flow into the triangle points (*2*). It follows that increased mixing should increase conversion. However, inspection of the flow shows slow flow on both downstream faces of the triangles, reducing presentation of reactive surface area to the faster flows, which are essentially the majority of the process fluid, and hence, dictate the level of conversion. Ultimately, conversions for the reversed flow are found to be about the same as for flow into the points of the triangles. Flow into the flats increased conversion in all cases, but always by less than 1%. Simulations using uncoated packing with flow into the flats also resulted in conversions virtually the same as those with flow into the points.

## Conclusions

Heterogeneous catalysis in microchannels has been successfully simulated over a broad range of flow rates. It is found that static mixing (laminar flow redistribution) using triangular packing features significantly increases conversion over the entire range of flow rates ($0.25 < Re < 62.5$) when compared with the conversions in empty channels. There is a peak improvement to conversion at a Reynolds number near 20 for both coated and uncoated packing. Changing the mixing patterns significantly by reversing the flow into the bases of the triangles does not improve conversions.

## Acknowledgments

The authors gratefully acknowledge the support of the State of Tennessee through a Center of Excellence in Applied Computational Science and Engineering Grant (R04-1302-007).

## References

1. Ameel, T. A. (1997), *Int. Comm. Heat Mass Transfer* **24,** 1113–1120.
2. Nguyen, N. T. and Wu, Z. (2005), *J. Micromech. Microeng.* **15,** 1–16.
3. Zheng, A. I., Jones, F., Fang, J., and Cui, T. (2000), in *Proceedings of the Fourth International Conference on Microreaction Technology* (IMRET IV), pp. 284–292.
4. Jones, F., Forrest, S., Palmer, J., Lu, Z., Elmore, J., and Elmore, B. (2004), *Appl. Biochem. Biotechnol.* **113–116,** 261–272.
5. Wen, J., Elmore, B., and Jones, F. (2007), submitted to *Biotechnol Bioeng.*
6. Bailey, R., Jones, F., Fisher, B., and Elmore, B. (2005), *Appl. Biochem. Biotechnol.* **121–124,** 639–652.
7. Wang, H., Iovenitti, P., Harvey, E., and Masood, S. (2002), *Smart Mater. Struct.* **11,** 662–667.
8. Lin, Y., Gerfen, G. J., Rousseau, D. L., and Yeh, S. R. (2003), *Anal. Chem.* **75,** 5381–5386.
9. Wang, H., Iovenitti, P., Harvey, E., and Masood, S. (2003), *J. Micromech. Microeng.* **13,** 801–808.
10. Jovanovich, G. (2006), *Ind. Bioprocessing* **28(4),** 6.
11. ESI CDF Inc (2006), *CFD-ACE+ V2006 User Manual,* Huntsville, AL.
12. Van Doormaal, J. and Raithby, G. (1984), *Numer. Heat Transfer* **7,** 147–163.
13. Crowe, C., Roberson, J., and Elger, D. (2001), *Engineering Fluid Mechanics,* 7th ed. John Wiley & Sons Inc., New York.
14. DeTurck, D., Gladney, L., and Pietrovito, A. (1996), *The Interactive Textbook of PFP 96,* http://dept.physics.upenn.edu/courses/gladney/mathphys/subsection4_1_7.html, University of Pennsylvania, Philadelphia, PA.
15. Jones, F., Lu, Z., and Elmore, B. (2002), *Appl. Biochem. Biotechnol.* **98–100,** 627–640.

0273-2289/1559-0291 (Online)/07/136–140/875–884/$30.00

# Utilization of Condensed Distillers Solubles as Nutrient Supplement for Production of Nisin and Lactic Acid from Whey

CHUANBIN LIU,*,[1] BO HU,[2] SHULIN CHEN,[2] AND RICHARD W. GLASS[3]

*[1]Energy & Environmental Research Center, University of North Dakota, Gand Forks, ND, 58203, E-mail: cliu@undeerc.org; [2]Washington State University, Pullman, WA, 99164-6120; and [3]National Corn Growers Association, Chesterfield, MO, 63005*

## Abstract

The major challenge associated with the rapid growth of the ethanol industry is the usage of the coproducts, i.e., condensed distillers solubles (CDS) and distillers dried grains, which are currently sold as animal feed supplements. As the growth of the livestock industries remains flat, alternative usage of these coproducts is urgently needed. CDS is obtained after the removal of ethanol by distillation from the yeast fermentation of a grain or a grain mixture by condensing the thin stillage fraction to semisolid. In this work, CDS was first characterized and yeast biomass was proven to be the major component of CDS. CDS contained 7.50% crude protein but with only 42% of that protein being water soluble. Then, CDS was applied as a nutrient supplement for simultaneous production of nisin and lactic acid by *Lactococcus lactis* subsp. *lactis* (ATCC 11454). Although CDS was able to support bacteria growth and nisin production, a strong inhibition was observed when CDS was overdosed. This may be caused by the existence of the major ethanol fermentation byproducts, especially lactate and acetate, in CDS. In the final step, the CDS based medium composition for nisin and lactic acid production was optimized using response surface methodology.

**Index Entries:** Condensed distillers solubles; nutrient supplement; fermentation; lactic acid; *Lactococcus lactis*; nisin.

## Introduction

Total ethanol production in United States has grown significantly in recent years. In year 2005, 95 ethanol plants in 19 states produced a record 3.904 billion gal of ethanol, an increase of 17% from 2004 and 126% from 2001. Dry mill ethanol refineries accounted for 79% of production capacity, and wet mills 21% *(1)*.The accelerated growth of ethanol industry is believed to be capable of reenergizing rural and farm development through increased

*Author to whom all correspondence and reprint requests should be addressed.

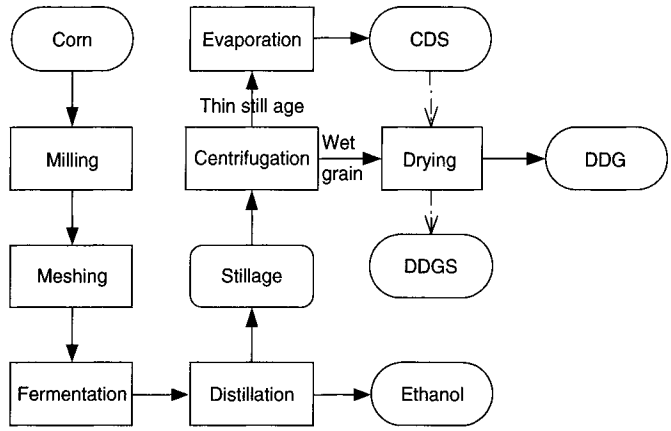


**Fig. 1.** Diagram of corn dry-milling process for ethanol and related coproducts production.

employment, enhancing local industry, and aiding our national security through increased reliance on domestic renewable energy and decreasing greenhouse gas emissions *(2)*.

The major challenge associated with the rapid development of ethanol industry is the usage of the coproducts, i.e., distillers dried grains (DDG) and condensed distillers solubles (CDS) *(3,4)*. In the dry mill ethanol process, as shown in Fig. 1 *(3,4)*, the corn kernels are first ground into a flour, or "meal," and mixed with water to form a slurry, called "mash." Enzymes are added to break down the starch to fermentable sugars. The mash is then pumped to the fermentors wherein yeast converts the sugars in the mash into ethanol. The fermented mash is pumped to the distillation tower wherein the ethanol is separated from the nonfermentable solids (the stillage). The stillage from the distillation system is sent through a centrifuge that separates the coarse grains from the solubles. The coarse grains are dried to produce DDG. Another coproduct, CDS, is also obtained in significant amount after the removal of ethanol by condensing the thin stillage fraction to a semisolid. In some dry-mill plants, CDS is mixed with the coarse grains from the centrifuge and then dried to produce dried distillers grains with solubles.

DDG and CDS are currently used as animal feed supplements *(3,4)*. As the growth of the livestock industries remain flat, dry mills will soon be faced with the need to identify new, potential customers to ensure that there are markets that will utilize these coproducts from the increasing number of dry mills coming online to meet the increasing ethanol demand. Therefore, alternative usage of CDS and DDG are urgently needed. The objective of this work is to study the feasibility of using CDS as a nutrient supplement for nisin and lactic acid coproduction from cheese whey. Nisin is an antimicrobial peptide produced by certain *Lactococcus* bacteria *(5)*, which has been accepted as a safe and natural preservative in more than 50 countries and is widely used as an antimicrobial agent in the food industry *(5–9)*. Biosynthesis of nisin is coupled with the growth of lactic acid bacteria and

lactic acid production *(8)*. Lactic acid is an important chemical for food processing. It can also be used as a raw material in the production of the biodegradable polymer poly(lactic) acid *(10)*. Our former study *(11)* has proved that simultaneous production of nisin and lactic acid is feasible, because the optimal conditions for nisin biosynthesis and lactic acid formation by *L. lactis* using whey as feedstock are almost the same. In this research, CDS was characterized and applied as nutrient supplement for simultaneous production of nisin and lactic acid from whey. Effects of CDS on nisin biosynthesis, lactic acid production, and bacteria growth were studied.

## Materials and Methods

### Characterization of CDS

The CDS used in this research was kindly provided by National Corn Growers Association, Chesterfield, Missouri. Analysis of total solids, total phosphorus, ammonia, total nitrogen, and crude protein in CDS were carried using Association of Official Analytical Chemists standard methods *(12)*. Water soluble peptides and amino acids were analyzed following the Ohnishi and Barr modified Lowry procedure *(13)* using the kit TP 0200 purchased from Sigma-Aldrich (St. Louis, MO). Acetate and lactate content in CDS were quantified by high-performance anion exchange chromatography using a Dionex DX-550 system. The detailed IC analysis conditions can be found at Liu et al. *(14)*.

### Determination of the Major Component of CDS

A size distribution study was conducted according to the flowchart shown in Fig. 2. Hundred grams of CDS was thoroughly mixed with 900 mL water at which point the mixture was sieved using two standard sieves (produced by CSC Scientific Co., Inc., Fairfax, VA): no. 45 with an opening diameter of 0.355 mm and no. 120 with an opening diameter of 0.125 mm. The solid particles retained by each sieve were thoroughly washed using deionized water at room temperature, then dried at 105°C for 6 h and weighed.

### Microorganisms and Media

*Lactococcus lactis* subsp. *lactis* (American Type Culture Collection [ATCC] 11454) was the nisin-producing microorganism used in this work. *Micrococcus luteus* (ATCC 9341) was used as an indicating microorganism in the bioassay used to measure nisin concentrations. The compositions of media used for the growth of these microorganisms are summarized as follows. Medium I, used for seed culture of *L. lactis* (pH 7.0), contained 5.0 g/L of glucose, 5.0 g/L of polypeptone, and 5.0 g/L of yeast extract (YE). Medium II, used for bioassay of nisin (pH 7.0), contained 10.0 g/L of glucose, 5.0 g/L of polypeptone, 5.9 g/L of YE, and 5.0 g/L of NaCl. Medium III, used for the main fermentation, contained 20.0 g/L of sweet whey powder (provided by WesternFarm Food Inc., Seattle, WA), 0.6 g/L for

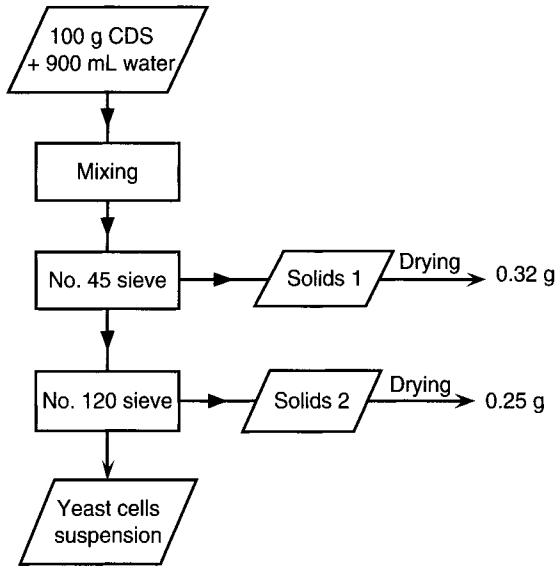


**Fig. 2.** Flowchart of CDS sieving experiment.

$KH_2PO_4$, 0.6 g/L for $MgSO_4$, and other nutrients, the amount of which are indicated in the experimental designs.

### *Cultivation Method*

Before main cultivation was performed, culture size was scaled-up by two steps in order to increase the amount of cells with high growth activity. Seed culture of *L. lactis* was conducted in 125-mL Erlenmeyer flasks placed on an orbital shaker at 160 rpm and 30°C for 8 h. Main fermentations were performed in a 5-L Bioflo 110 fermentor (New Brunswick Scientific, Edison, NJ) equipped with temperature, pH, dissolved oxygen concentration, and gas flow control systems. The working volume was 2 L. Air was supplied to the fermentor for aerobic cultivation conditions.

### *Analysis of Fermentation Products*

The viable cell concentration of *L. lactis* was determined as colony-forming units on agar plates. Concentrations of L-lactic acid and acetic acid in the medium and fermentation broth were analyzed using the high-performance anion-exchange chromatography method mentioned under "CDS Characterization" *(14)*. Nisin concentration was measured by a bioassay method based on the method of Shimizu et al. *(15)*.

## Results and Discussion

### *Characterization of CDS*

Because the detailed information of CDS composition was not available, the corn dry-mill byproduct needed to be characterized before using

Table 1
Characterization of the Corn CDS Applied in This Research

| Parameter | Content (g/100.0 g of CDS) |
|---|---|
| Total solids | 28.70 |
| Water | 71.30 |
| Total nitrogen | 1.20 |
| Total phosphorous | 0.31 |
| Crude protein | 7.50 |
| Water soluble peptides and amino acids | 3.16 |
| Ammonia | 0.11 |
| Lactate | 2.40 |
| Acetate | 0.15 |

it as nutrient supplement for nisin fermentation. Total solids, total phosphorus, ammonia, total nitrogen, crude protein, and water soluble peptides and amino acid profiles of CDS were analyzed, respectively, using standard methods. The content of the major ethanol fermentation byproducts, including lactate and acetate, which may have negative effects on bacteria metabolism, were also measured. The results are shown in Table 1.

### *Yeast Biomass is the Major Component of CDS*

CDS is the condensed thin stillage fraction of yeast fermentation broth left after the removal of ethanol by distillation. Therefore, CDS is a mixture of yeast cells and small grain particles. In order to know the major component in CDS, a sieve separation study was conducted. As shown in Fig. 2, a mixture of 100.0 g CDS and 900 mL water was sieved using two standard sieves, no. 45 with the opening diameter of 0.355 mm and no. 120 with the opening diameter of 0.125 mm. The solid particles retained by each sieve were thoroughly washed and dried up. Only 0.32 g of solids were retained by no. 45 sieve and 0.25 g of solids by no. 120 sieve. Compared with the total amount of CDS loaded in this experiment, 100.0 g wet base, which corresponds to 27.5 g dry weight, the percentage of the grain particles with the size larger than 0.125 mm in CDS was only 2.1%. Therefore, we can safely draw the conclusion that yeast biomass is the major component of CDS.

### *Water Soluble Nitrogen in CDS*

As yeast biomass is the major component of CDS, a certain amount of organic nitrogen in yeast cells should have been leached out during the long-duration heat treatment of distillation. The results in Table 1 indicate that, CDS has 7.50% crude protein but with only 42% of that protein being water soluble. The content of ammonia in CDS is very low at 0.11% and only contributes to 8.6% of the total nitrogen.

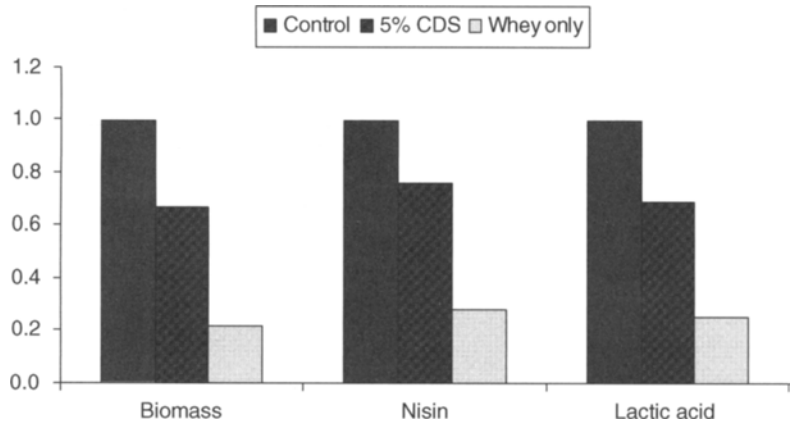


**Fig. 3.** Relative production of nisin, lactic acid, and biomass when 5% CDS alone was used as nutrient supplement.

## *CDS Alone as the Nutrient Supplement*

In order to quantify the performance of CDS, the optimal medium for nisin and lactic acid coproduction obtained in an earlier study *(11)* was used as a positive control, and the whey without any nutrient added was used as a negative control. $CaCO_3$ was provided to buffer the fermentation pH around 5.5. The biomass, nisin biosynthesis, and lactic acid formation after 24 h of fermentation were compared. As shown in Fig. 3, the production of nisin was very poor when bacteria grew on whey without addition of any nutrient. A significant increase (twofold) of nisin formation was seen when 5% of CDS (wet base) was added, although it was only 70% of that at the earlier optimized conditions *(11)*. Therefore, it can be concluded that CDS does provide essential nutrients for nisin production from whey.

## *Inhibition of Nisin Biosynthesis Owing to CDS Overdose*

As shown in Fig. 3, the stimulation of CDS on nisin production was observed when 5% of CDS (wet base) was added into fermentation medium. In the following experiment, more CDS was added into media in order to provide essential nutrients for nisin production from whey. Similarly, the optimal medium for nisin and lactic acid coproduction obtained in an earlier study *(11)* was used as a positive control, and the whey without any nutrient added was used as a negative control for the quantification of the performance of CDS. $CaCO_3$ was provided to maintain the fermentation pH around 5.5. The biomass, nisin biosynthesis, and lactic acid formation after 24 h of fermentation were compared. As shown in Fig. 4, the production of nisin decreased with the addition of more CDS in the media. The only explanation to this phenomenon is that CDS contains some inhibitory byproducts that have negative effects on the growth of lactic acid bacteria and the production of nisin. The byproducts of ethanol fermentation, i.e., acetate, lactate, and many others might be responsible for the inhibition observed.

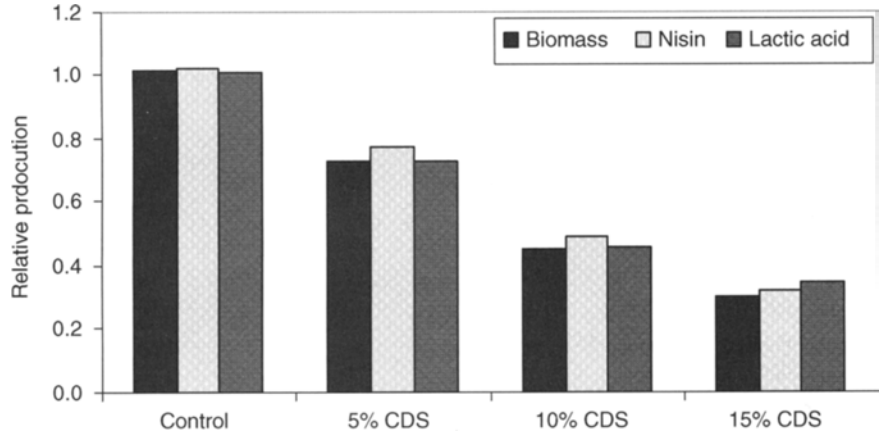


**Fig. 4.** Inhibition of biomass, nisin, and lactic acid production when CDS is overdosed.

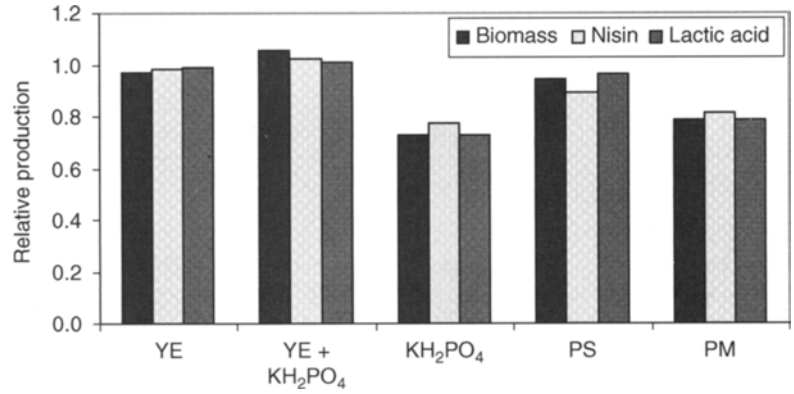


**Fig. 5.** Stimulation effects of different nutrient supplements on nisin, lactic acid, and biomass production (5% CDS + other nutrients). YE, yeast extract; PS, peptone from soy; and PM, peptone from meat.

## *Effects of Nutrient Supplements on Nisin and Lactic Acid Production*

Considering that the nisin producing strain *L. lactis* is a well-known, nutritionally fastidious microorganism requiring an abundance of nutrients for cell growth and metabolism *(5)*, nutrients in addition to CDS may be required for the simultaneous production of nisin and lactic acid. YE, peptone from meat (PM), and peptone from soy (PS), the most widely used organic nutrient supplements in such fermentation studies, as well as $KH_2PO_4$, were selected as the candidates for nutrient supplementation. The stimulation effects of these nutrient supplements on cell growth, nisin formation, and lactic acid production were studied. In addition to 5% of CDS; YE, PS, PM, and $KH_2PO_4$ were added to the media. The fermentation results are compared in Fig. 5. Similarly in Fig. 3, the optimal medium for nisin and lactic acid coproduction obtained in an earlier study *(11)* was used as a positive control, and the whey without any nutrient added was

Table 2
Central Composite Design of Factors in Coded Levels With Nisin, Biomass, and Lactic Acid Concentration as Response

| Run | Type | CDS | YE | Nisin (mg/L) | Biomass ($10^8$ colony forming units/mL) | Lactic acid (g/L) |
|---|---|---|---|---|---|---|
| 1 | Center | 0 | 0 | 82 | 12.2 | 18.7 |
| 2 | Center | 0 | 0 | 81 | 12.6 | 18.7 |
| 3 | Center | 0 | 0 | 81 | 12.2 | 18.8 |
| 4 | Center | 0 | 0 | 80 | 12.6 | 18.9 |
| 5 | Center | 0 | 0 | 80 | 12.4 | 18.8 |
| 6 | Axial | −1.41 | 0 | 67 | 8.4 | 11.8 |
| 7 | Axial | +1.41 | 0 | 30 | 5.4 | 8.5 |
| 8 | Axial | 0 | −1.41 | 56 | 8.4 | 13.6 |
| 9 | Axial | 0 | +1.41 | 80 | 12.6 | 17.6 |
| 10 | Fact | −1 | −1 | 30 | 5 | 8.8 |
| 11 | Fact | +1 | −1 | 37 | 5.8 | 8.9 |
| 12 | Fact | −1 | +1 | 67 | 11.2 | 18.7 |
| 13 | Fact | +1 | +1 | 39 | 8 | 9.0 |

used as a negative control. YE and peptone, as seen by the comparative yields with the controls shown in Fig. 3, are ideal sources of nutrient for nisin and lactic acid coproduction. $KH_2PO_4$ is essential, as the yield of nisin and lactic acid was around 2.7 times of the negative control. The combination of $KH_2PO_4$ and YE gave the highest yield of nisin and lactic acid.

### *Medium Optimization Using Response Surface Methodology*

The results shown in Figs. 3–5 indicate that, CDS is a good source of nutrients essential for nisin and lactic acid cofermentation; however, only a limited amount of CDS can be added for this purpose. Considering that CDS alone cannot provide sufficient nutrients for the well-known, nutritionally fastidious microorganism *L. lactis*, YE was selected as the auxiliary nutrient supplement in order to satisfy the requirement of nisin and lactic acid fermentation. The contents of them in the fermentation media were optimized through a statistically based design of experimentation in central composite design (Table 2) *(11)*. The coded and actual values of each variable are listed in Table 3. The fermentation media were made up of 50.0 g/L of whey, 1.0 g/L of $KH_2PO_4$, 30.0 g/L of $CaCO_3$, and the predetermined amount of the three variables were assigned by the central composite design. The content of nisin and lactic acid after 24 h of fermentation at 30°C were measured and presented as responses in Table 2.

After the responses were obtained, they were subjected to multiple nonlinear regression and optimization using the software Design-Expert (V6.0, 2001, Stat-Ease Inc., MN). The optimal conditions for nisin

Table 3
The Coded and Actual Values of the Factors in Central Composite Design

| Factor | Name | Axial (−1.41) | Low (−1) | Central (0) | High (+1) | Axial (+1.41) |
|---|---|---|---|---|---|---|
| A | CDS (g/L) | 0.50 | 15.00 | 50.00 | 85.00 | 99.50 |
| B | YE (g/L) | 0.05 | 1.50 | 5.00 | 8.50 | 9.95 |

biosynthesis and lactic acid formation were obtained by further numerical analysis of the three-dimensional response surface plots using the software. The solution to the maximal nisin biosynthesis was 37.31 g/L for CDS and 7.12 g/L for YE. The solution to the maximal lactic acid production was 36.74 g/L for CDS and 7.58 g/L for YE. Last, the solution to the simultaneous maximal production of nisin and lactic acid was 37.08 g/L for CDS and 7.34 g/L for YE. The results also reveal that the predicated values of nisin and lactic acid under these three conditions have no significant difference.

In order to confirm the optimal conditions obtained from the statistically based experimental designs, a verification experiment under the conditions of 37.0 g/L CDS and 7.5 g/L YE was conducted. After 24 h of fermentation 85.0 mg/L of nisin and 19.3 g/L of lactic acid were obtained. The result was very close to the predicted value. In addition, the nisin result also agreed well with the "ceiling concentration" of nisin previously reported by other researchers *(16,17)*. Therefore, the optimal conditions predicted from the statistically based experimental designs were valid. In brief, we aimed at verifying the feasibility of using CDS as a nutrient supplement for nisin and lactic acid coproduction by *L. lactis* from cheese whey. The results indicated that CDS is a good source of nutrients essential for nisin and lactic acid cofermentation; however, only a limited amount of CDS can be added for this purpose. The optimal concentration of CDS in fermentation medium was 37.0 g/L, when 7.5 g/L of YE was applied as auxiliary nutrient.

## References

1. Renewable Fuels Association (2006), http://www.ethanolrfa.org/industry/statistics/#A. Accessed February 13, 2007.
2. Wyman, C. E. (2001), *Appl. Biochem. Biotechnol.* **91–93,** 5–21.
3. Iowa Beef Center (2002), http://www.extension.iastate.edu/Publications/IBC18.pdf.
4. Hoffman, M. P. and Tsengeg, P. (2004), http://www.ag.iastate.edu/farms/04reports/w_/IncorporatingCondensed.pdf. Accessed February 13, 2007.
5. Parente, E. and Ricciardi, A. (1999), *Appl. Microbiol. Biotechnol.* **52,** 628–638.
6. Food and Drug Administration (2001), GRAS Notice No. GRN 000065, Rockville, MD.
7. Cleveland, J., Thomas, J., Montville, J. T., Nes, F. I., and Chikindas, L. M. (2001), *Int. J. Food Microbiol.* **71,** 1–20.
8. Sablon, E., Contreras, B., and Vandamme, E. (2000), *Adv. Biochem. Eng. Biotechnol.* **68,** 21–59.
9. Jack, R. W., Tagg, J. R., and Ray, B. (1995), *Microbiol. Rev.* **59,** 171–200.

10. Datta, R. and Tsai, S. P. (1997), In: *Fuels and Chemicals from Biomass*, ACS Symposium Series 666, Saha, W., Saha, B., and Woodward, J., eds. Oxford University Press, Oxford UK: pp. 224–236.
11. Liu, C., Liu, Y., Liao, W., Wen, Z., and Chen, S. (2004), *Appl. Biochem. Biotechnol.* **114,** 627–638.
12. Association of Official Analytical Chemists (1990), *Official Methods of Analysis*, 15th ed. AOAC International, Gaithersburg, MD.
13. Ohnishi, S. T. and Barr, J. K. (1978), *Anal. Biochem.* **86,** 193–200.
14. Liu, Y., Wei, L., Liu, C., and Chen, S. (2005), *Eng. Life Sci.* **5,** 343–349.
15. Shimizu, H., Mizuguchi, T., Tanaka, E., and Shioya, S. (1999), *Appl. Environ. Microbiol.* **65,** 3134–3141.
16. Kim, W. S., Hall, R. J., and Dunn, N. W. (1997), *Appl. Microbiol. Biotechnol.* **48,** 449–453.
17. Kim, W. S., Hall, R. J., and Dunn, N.W. (1998), *Appl. Microbiol. Biotechnol.* **50,** 429–433.

0273-2289/1559-0291 (Online)/07/136–140/885–896/$30.00

# Optimization of Tocopherol Concentration Process From Soybean Oil Deodorized Distillate Using Response Surface Methodology

**Vanessa Mayumi Ito,* César Benedito Batistella, Maria Regina Wolf Maciel, and Rubens Maciel Filho**

*Laboratory of Separation Process Development (LDPS), School of Chemical Engineering, State University of Campinas (UNICAMP), CP 6066, CEP13081-970; Campinas, SP—Brazil, E-mail: vanessa@lopca.feq.unicamp.br*

## Abstract

Soybean oil deodorized distillate is a product derived from the refining process and it is rich in high value-added products. The recovery of these unsaponifiable fractions is of great commercial interest, because of the fact that in many cases, the "valuable products" have vitamin activities such as tocopherols (vitamin E), as well as anticarcinogenic properties such as sterols. Molecular distillation has large potential to be used in order to concentrate tocopherols, as it uses very low temperatures owing to the high vacuum and short operating time for separation, and also, it does not use solvents. Then, it can be used to separate and to purify thermosensitive material such as vitamins.

In this work, the molecular distillation process was applied for tocopherol concentration, and the response surface methodology was used to optimize free fatty acids (FFA) elimination and tocopherol concentration in the residue and in the distillate streams, both of which are the products of the molecular distiller. The independent variables studied were feed flow rate ($F$) and evaporator temperature ($T$) because they are the very important process variables according to previous experience. The experimental range was 4–12 mL/min for $F$ and 130–200°C for $T$. It can be noted that feed flow rate and evaporator temperature are important operating variables in the FFA elimination. For decreasing the loss of FFA, in the residue stream, the operating range should be changed, increasing the evaporator temperature and decreasing the feed flow rate; $D/F$ ratio increases, increasing evaporator temperature and decreasing feed flow rate. High concentration of tocopherols was obtained in the residue stream at low values of feed flow rate and high evaporator temperature. These results were obtained through experimental results based on experimental design.

**Index Entries:** Deodorized distillate; free fatty acids; molecular distillation; response surface methodology; soya sludge; tocopherol.

*Author to whom all correspondence and reprint requests should be addressed.

## Introduction

Soybean oil deodorized distillate (SODD) is a complex mixture made up of fatty acids, sterols, tocopherols, sterol esters, hydrocarbons, breakdown products of fatty acids, aldehydes, ketones, and acylglycerol species *(1)*. It is an important source of natural tocopherols and phytosterols corresponding approx 10 and 20%, respectively. The SODD corresponds to approx 0.1 and 0.4% of crude soybean oil *(2)*. The economical value of SODD depends on tocopherols and phytosterols contents. Free fatty acids (FFA) represent 25–75% and acylglycerols about 3–56% of the SODD, depending on the raw material being refined and on the type and conditions of the refining process *(3)*.

Natural tocopherols are important antioxidants present in cereals and vegetable oils. Each one of these sources has different quantity of vitamin E. Vitamin E is the most efficient soluble, natural lipidic antioxidant and the main antioxidant membrane in mammal cells *(4)*. They avoid oxidation of vitamin A, β-carotene, and essential fatty acids *(5)*. Tocopherols prevent diseases like cancer, cardiovascular, and cataracts *(6)*. They are used in food, cosmetics, and pharmaceutical industries *(7)*. A mixture of α-, β-, γ-, and δ-isomers containing 60 wt% tocopherols is widely used as additive in many kinds of foods *(8)*. They are also used as an additive in paints based on natural oils *(9)*. Tocopherols are sensible to light, heat, alkali, and contaminant metals *(10)*.

Molecular distillation or short path distillation is characterized by a short exposure of the distilled liquid to the operating temperature and high vacuum *(11)*. This process has been applied to lipid-containing products, including monoglycerides production *(12)*, recovery of carotenoids from palm oil *(13)*, and purification of structured lipids *(14)*. Also, it can be applied to fuel product, like production of biodiesel from castor oil *(15)* and heavy petroleum characterization *(16)*. Ito et al. *(17)* studied the recovery of tocopherols and FFAs from SODD in function of the ratio (distillate flow rate [*D*]/residue flow rate [*R*]) of 0.96, and the tocopherol and FFA recovery curves had an optimum point at 73%. Martins et al *(18)* determined the best operating conditions of wiped film molecular distillator to concentrate tocopherols from SODD. Moraes et al. *(19)* studied this process experimentally and by simulation with good agreement.

To obtain maximum recovery of vitamin E, the molecular distillation process must be optimized and the response surface methodology (RSM) is an effective tool for this purpose. The main advantage of this methodology is the reduced number of experimental runs needed to provide sufficient information for statically acceptable results. According to preliminary experience, the process variables (condenser temperature and feed temperature) were not significant *(20,12)*. Then, in the feed flow rate ($X_1$) and evaporator temperature ($X_2$), process variables were selected for optimization of the unsaponifiable material from SODD through a molecular distillation process.

Nowadays, in several areas of process development, RSM are being applied. Chemical processes have many variables, which need to be optimized in relation to cost, yield, and purity taking into consideration the interactions among them. Maciel Filho et al. *(21)* evaluated atmospheric and vaccum petroleum residues using a two-level factorial design. The error repetition was estimated by three runs on the central point of the experimental design. Fregolente et al. *(22)* studied the optimization of distilled monoglycerides production through molecular distillation. The $2^3$ factorial design was used to evaluate the effects of reaction parameters and the central composite design to optimize the molecular distillation process. The objective of this work is to understand the relationships between the independent ($X_1$ and $X_2$) and dependent variables (Distillate flow rate/Feed flow rate [$D/F$]) ratio, $Y_1$; FFAs content in the distillate stream (FFAD), $Y_2$; and total tocopherols content in the residue stream (TocoR), $Y_3$.

## Materials and Methods

### *Materials*

SODD was provided by Bunge Ltda, (São Paulo, Brazil). All samples were stored in the refrigerator at 4°C until analysis. All solvents and reactants for the analysis were of analytical grade. A tocopherol kit consisting of α-, β-, γ-, and δ-tocopherol (purity ≥95%) was purchased from Calbiochem (San Diego, CA) and used as reference standards for tocopherols analysis.

### *Molecular Distillator*

Molecular distillation or short path distillation is a separation process characterized by short exposure of the feed inside the equipment, and so to the operating temperature, by high vacuum and by a small distance between evaporator and condenser (in the order of mean free path of the molecular involved) *(13)*. In this study, the centrifugal molecular distillator from Myers Vacuum Inc. (Kittaning, PA), with an evaporator area of 0.0046 $m^2$ was used. Figure 1 shows a scheme of this equipment. Two product streams are generated: distillate (rich in the volatile compounds that escape from the evaporator and reach the condenser, in this case FFA) and residue (rich in the heaviest compounds that remain in the evaporator surface, in this case tocopherols). The process conditions were maintained at 13.3 Pa, the feed temperature at 50°C, condenser temperature at 50°C, at $g$-force value equal to 5.5$g$. The molecular distillation experiments were conducted according to the following procedure: a sample of SODD was homogenized before feeding the equipment. For each molecular distillation run, samples of both streams (distillate [D] and residue [R]) were collected and submitted to FFAs and tocopherols analysis.

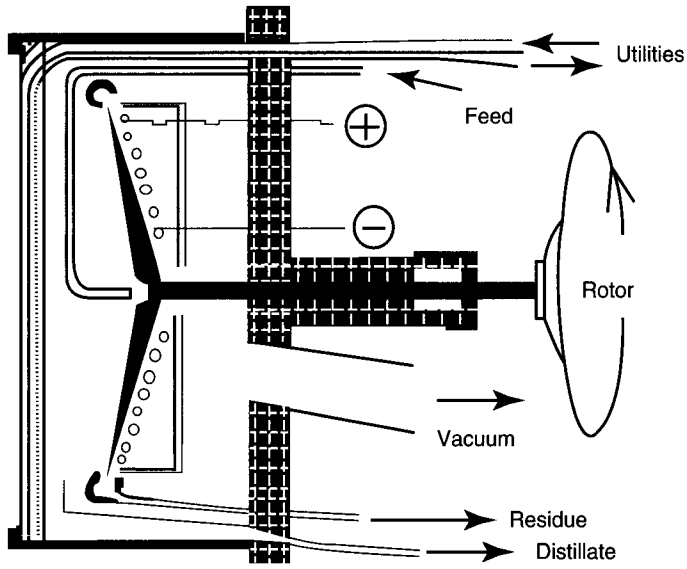


**Fig. 1.** Centrifugal molecular distillator scheme.

## *Response Surface Methodology*

A central composite design was used to study the dependent variables which are called responses, which are $D/F$ (split ratio), $Y_1$; FFAD, $Y_2$; and TocoR, $Y_3$. The independent variables were $X_1$ and $X_2$ representing feed flow rate and evaporator temperature, respectively. The experiments were carried out according to a $2^2$ complete factorial design plus three central points and four axial points, called star points. The distance of the star points from the center point is given by $\alpha = (2^n)^{1/4}$, where $n$ is the number of independent variables, for two factors $\alpha = 1.41$ *(23)*. Experimental values were chosen according to previous experience. Values of feed flow rate lower than 4 mL/min might be high enough to form a uniform thin film on the evaporator surface. An efficient mass and energy transfers were promoted by a uniform, thin film. For feed flow rate greater than 15 mL/min, the system operated with low effectiveness, because of the low residence time. The first significant FFA drops on the condenser wall sets the lower evaporator temperature level *(12)*. The settings for the independent variables were as follows (low/high values): evaporator temperature (°C), 140/190, and the feed flow rate (mL/min), 5.1/10.9.

Each variable to be optimized was coded at five levels, –1.41, –1.0, +1, and +1.41. This gives a range of 130–200°C and 4–12mL/min, to these variables, respectively, including the star points. Three replicate runs at the center (0, 0) of the design were performed to allow the estimation of the pure error. All experiments were carried out in a randomized order to minimize the effect of unexplained variability in the observed responses owing to

Table 1
Independent Variables and Their Levels for Central Composite Design in Optimization of Molecular Distillation Process of SODD

| | | Coded variable levels | | | | |
|---|---|---|---|---|---|---|
| Independent variables | Symbol | −1.41 (−α) | −1 | 0 | +1 | +1.41 (+α) |
| Feed flow rate (mL/min) | $X_1$ | 4.0 | 5.1 | 8.0 | 10.9 | 12.0 |
| Evaporator temperature (°C) | $X_2$ | 130 | 140 | 165 | 190 | 200 |

extraneous factors. The RSM was chosen to study the optimization of two selected factors, feed flow rate (*F*) and evaporator temperature (*T*). Table 1 shows the independent variables and the coded levels.

## *FFA Analysis*

FFA content was determined according to the method AOCS Ca 5a-40 *(24)*. This method uses titration with a standard alkali, NaOH. The FFA content is expressed as percentage of oleic acid ($C_{18:1}$). The expression is:

$$\text{FFA as oleic acid (\%)} = \frac{\text{Alkali volume (mL)} \cdot \text{Alkali normality} \cdot 28.2}{\text{Sample weight (g)}} \quad (1)$$

## *Tocopherol Analysis*

The method AOCS Ce 8–89 *(25)* was used to determine the α-, β-, γ-, and δ-tocopherol contents. A known amount of the sample was dissolved in hexane (approx 1 mg/mL) and 20 μL of the solution was injected into a high-performance liquid chromatography modular equipment made up of Waters delta 600 high-performance liquid chromatography pump (Mildford, MA), equipped with a fluorescence detector (Waters model 2475 multifluorescence). The flow rate of the mobile phase (hexane : isopropanol, 99 : 01 [v/v]) was set at 1.0 mL/min. The separation was conducted in a microporasil column 125 Å, with particle size of 10 μm and 3.9 × 300 $mm^2$ of dimension (Waters, Ireland). Figure 2 shows the tocopherols chromatogram. The tocopherols detected in the chromatograms were identified comparing the retention time of the compounds with the retention time of the standard solutions. Quantification of each type of tocopherols was done using calibration curves. The data processing was carried out through the Millennium software (Waters, Mildford, MA).

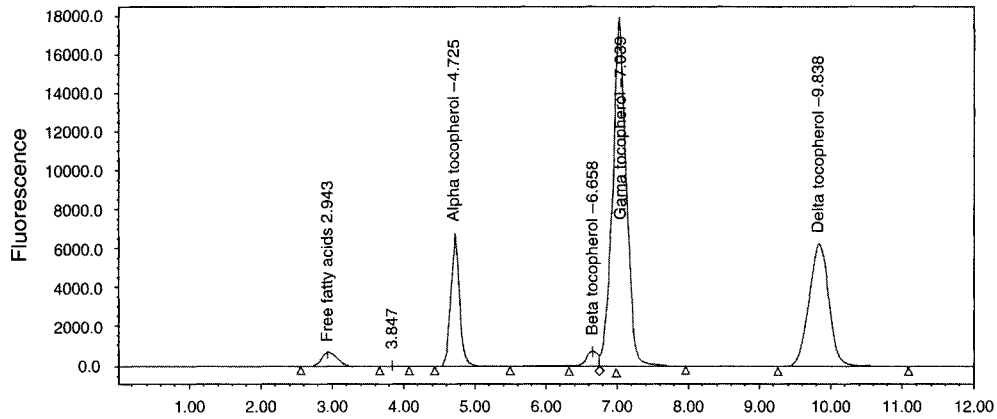


**Fig. 2.** Chromatogram of SODD for tocopherols analysis.

Table 2
Raw Material Characteristics

| Analysis | SODD |
|---|---|
| FFA (wt% as oleic acid) | 53.04 ± 1.10 |
| α-Tocopherol | 1.41 ± 0.25 |
| β-Tocopherol | 0.12 ± 0.05 |
| γ-Tocopherol | 1.95 ± 0.15 |
| δ-Tocopherol | 0.58 ± 0.09 |
| Tocopherol total | 4.06 ± 0.54 |

## Results and Discussion

The raw SODD was analyzed in relation to the FFA and tocopherols contents. Table 2 shows the characteristics of the SODD. The SODD used is brownish and semisolid at room temperature.

### *Experimental Design*

The response were analyzed using Statistica 7.0 software (StatSoft. Inc.). A quadratic polynomial regression model was assumed for predicting $Y_1$, $Y_2$, and $Y_3$. The model proposed for each response of $Y$ was:

$$Y = A + B_1X_1 + B_2X_2 + C_{11}X_{1^2} + C_{22}X_{2^2} + C_{12}X_1X_2 \quad (2)$$

where $A$ is a constant, $B_i$ is a first order model coefficient, $C_{ij}$ is a second order model coefficient, $X_1$ and $X_2$ are independent variables. The model fitting was evaluated by the coefficient of determination ($R^2$), and by the analysis of variance (ANOVA). Table 3 shows the coded levels and the responses obtained through the molecular distillation process (central composite design). The fitted coded models for the $D/F$ ratio, FFA content

Table 3
Coded Levels and the Results Obtained in the Molecular Distillation Process (central composite design)

| Run | $X_1$ | $X_2$ | $Y_1$ | $Y_2$ | $Y_3$ |
|---|---|---|---|---|---|
| 1 | −1 | −1 | 12.70 | 93.61 | 4.07 |
| 2 | +1 | −1 | 2.60 | 93.13 | 4.27 |
| 3 | −1 | +1 | 63.30 | 101.49 | 9.91 |
| 4 | +1 | +1 | 9.20 | 94.71 | 5.74 |
| 5 | −1.41 | 0 | 48.50 | 97.60 | 7.14 |
| 6 | +1.41 | 0 | 10.50 | 95.57 | 3.99 |
| 7 | 0 | −1.41 | 3.50 | 93.14 | 4.22 |
| 8 | 0 | +1.41 | 32.50 | 104.00 | 10.19 |
| 9 | 0 | 0 | 26.70 | 98.13 | 4.63 |
| 10 | 0 | 0 | 25.50 | 98.89 | 5.23 |
| 11 | 0 | 0 | 24.70 | 99.33 | 5.10 |

$X_1$, feed flow rate; $X_2$, evaporator temperature; $Y_1$, $D/F$ split ratio; $Y_2$, FFAs content in the distillate stream (FFAD); and $Y_3$, tocopherols content in the residue stream (TocoR).

in the distillate stream, and tocopherol content in the residue stream were shown in Eqs. 3–5. All the coefficients of Eq. 2 were considered:

$$Y_1 = 0.256 + 0.123X_1 - 0.142X_1^2 - 0.147X_2 + 0.015X_2^2 - 0.01122X_1X_2 \quad (3)$$

$$Y_2 = 98.78 + 3.10X_1 - 0.57X_1^2 - 1.27X_2 - 1.76X_2^2 - 1.58X_1X_2 \quad (4)$$

$$Y_3 = 4.99 + 1.97X_1 + 1.01X_1^2 - 1.05X_2 + 0.19X_2^2 - 1.09X_1X_2 \quad (5)$$

The model validation was determined by the ANOVA in relation to the responses $Y_1$, $Y_2$, and $Y_3$. Table 4 shows the ANOVA data. It can be concluded that there is no evidence of lack of Fit for the fitted models, because the calculated $F$ values $\left(\frac{\text{Mean square lack of fit}}{\text{Mean square pure error}}\right)$ are lower than the critical $F$ value ($F_{0.95,8,2} = 19.37$) at 95% confidence, for the three models. The results show the model for tocopherols content in the residue ($Y_3$). Equation 5 is predictive in the experimental conditions studied, because the percent of explained variable is high (98.7%) and the calculated $F$ value $\left(\frac{\text{Mean square regression}}{\text{Mean square residual}}\right)$ is more than 65 times higher than the critical $F$ value at 95% of confidence ($F_{0.95,2,8} = 4.46$). As a practical rule, regression can be considered useful to predict values, when the $F$ value $\left(\frac{\text{Mean square regression}}{\text{Mean square residual}}\right)$ is more than ten times higher than the critical $F$ value *(26)*. An excellent repeatability of results was obtained, the pure error is low in comparison

Table 4
ANOVA for the Fitted Models

| Source of variation | Model | Sum of square | Degree of freedom | Mean square | *F*-ratio |
|---|---|---|---|---|---|
| Regression | Eq. 3 | 0.35 | 2 | 0.18 | 57.97[a] |
| | Eq. 4 | 113.56 | 2 | 56.78 | 7.13[a] |
| | Eq. 5 | 50.52 | 2 | 25.26 | 65.70[a] |
| Residual | Eq. 3 | 0.006 | 8 | 0.0007 | – |
| | Eq. 4 | 14.28 | 8 | 1.78 | – |
| | Eq. 5 | 0.69 | 8 | 0.09 | – |
| Lack of fit | Eq. 3 | 0.0053 | 8 | 0.0007 | – |
| | Eq. 4 | 13.55 | 8 | 1.69 | – |
| | Eq. 5 | 0.49 | 8 | 0.06 | – |
| Pure error | Eq. 3 | 0.0002 | 2 | 0.0001 | 0.28[b] |
| | Eq. 4 | 0.74 | 2 | 0.37 | 0.24[b] |
| | Eq. 5 | 0.20 | 2 | 0.10 | 0.03[b] |
| Total | Eq. 3 | 0.363 | 10 | 0.036 | – |
| | Eq. 4 | 127.84 | 10 | 12.78 | – |
| | Eq. 5 | 51.21 | 10 | 5.12 | – |

Equation 3, explained variance (98.5%), explicable variance (96.95%); Eq. 4, explained variance (88.8%), explicable variance (99.42%); and Eq. 5, explained variance (98.7%), explicable variance (99.61%).

[a]*F*-ratio (regression/residual).

[b]*F*-ratio (lack of fit/pure error).

with the experimental values. As can be seen in Fig. 3, obtained from Eq. 2, the $D/F$ ratio increases, increasing the evaporator temperature and decreasing the feed flow rate. In the maximum conditions, almost all the feed was distilled. The maximum is got at higher temperature and lower feed flow rate levels.

Figure 4 shows the response surface for FFA in the distillate stream. To increase the deacidification of the SODD, the operating range needs to follow evaporator temperature increasing and feed flow rate decreasing. For SODD deacidification, it is not interesting to carry out the experiments at low evaporator temperature. The high evaporator temperature promotes the evaporation of lighter molecules from SODD, and consequently, increases the FFA content. Figure 5 shows the response surface for total tocopherol in the residue stream. In order to concentrate tocopherols, it is necessary to increase the evaporator temperature and to decrease feed flow rate. At high evaporator temperature, all the FFA were distilled and collected as distillate. But in this case, some loss of tocopherol can be observed.

For all the responses, the maximum value can be obtained at high evaporator temperature and low feed flow rate. To FFA at distillate stream, a large range can be used to get a maximum deacidification of SODD. The

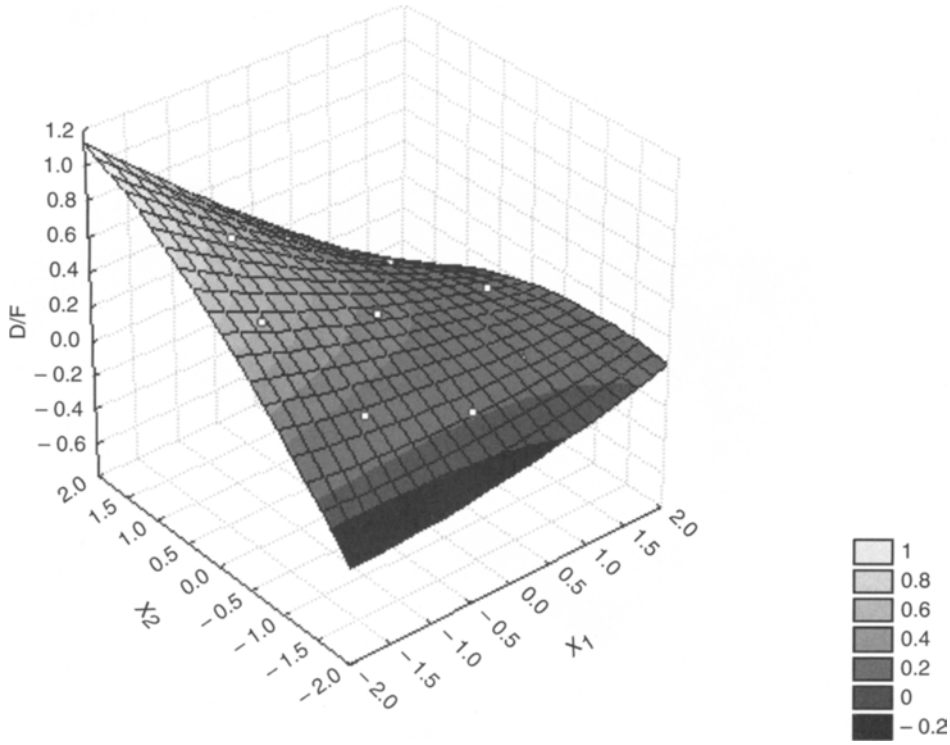


**Fig. 3.** Response surface for the $D/F$ split ratio.

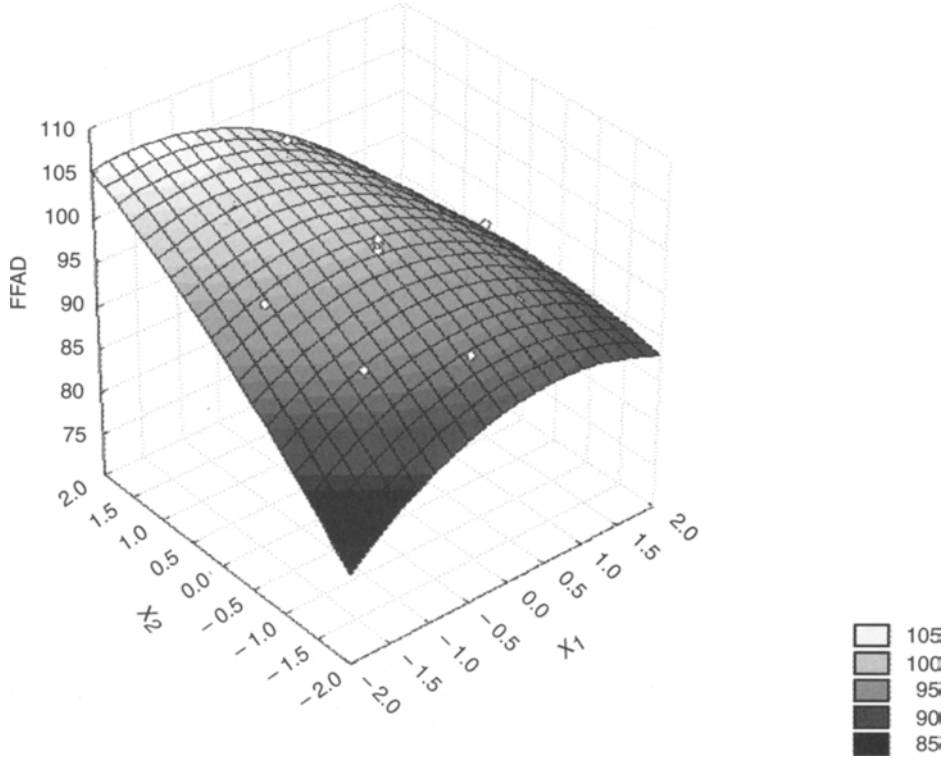


**Fig. 4.** Response surface for FFA content in the distillate stream.

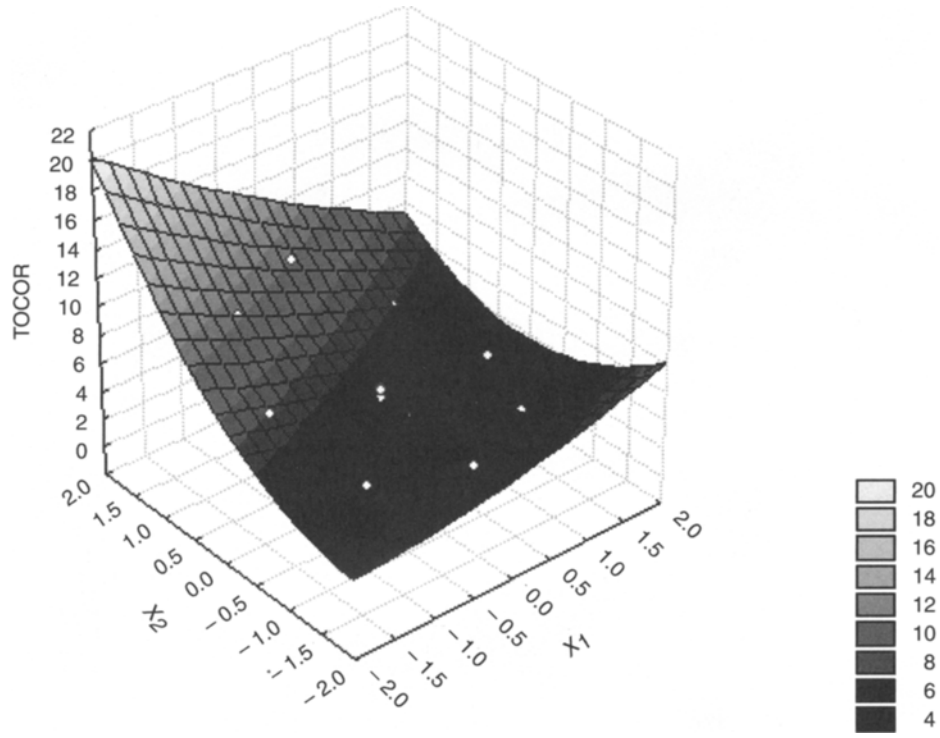


**Fig. 5.** Response surface for tocopherol content in the residue stream.

Table 5
Predicted and Experimental Responses for Molecular Distillation Process

| Real value | | Coded value | | Response | | |
|---|---|---|---|---|---|---|
| | | | | Experimental | Predicted | SD |
| $X_1$ | $X_2$ | $X_1$ | $X_2$ | | $Y_1$ | |
| 7.5 | 160 | −0.17 | 0.2 | 22.6 | 30.9 | 5.87 |
| 10.0 | 160 | 0.69 | 0.2 | 10.4 | 17.0 | 4.67 |
| | | | | | $Y_2$ | |
| 7.5 | 160 | −0.17 | 0.2 | 96.4 | 99.6 | 2.26 |
| 10.0 | 160 | 0.69 | 0.2 | 93.3 | 97.6 | 3.04 |
| | | | | | $Y_3$ | |
| 7.5 | 160 | −0.17 | 0.2 | 4.5 | 5.1 | 0.42 |
| 10.0 | 160 | 0.69 | 0.2 | 5.1 | 5.3 | 0.14 |

Units for $X_1$ and $X_2$ are mL/min and °C, $Y_1$ is a dimensional, $Y_2$ and $Y_3$ are %(w/w).

results are validated through the independent experiments for the molecular distillation process. The predicted $D/F$ ratio, FFA, and Tocopherols levels were close to the experimental data as shown in Table 5. The difference between the experimental and predicted responses is small. The data in Table 5 shows the validation of the fitted models through RSM.

## Concluding Remarks

In this study, RSM successfully optimized the conditions used in the deacidification of SODD and concentration of tocopherols. The generated regression models could be used to predict the SODD deacidification and tocopherols concentration. Results of this study might serve as a guideline for a scale-up of the molecular distillation process, such as a pilot plant, for concentration of vitamin E from SODD.

## Acknowledgments

The authors are grateful to FAPESP (Fundação de Amparo a pesquisa do Estado de São Paulo, no. 02/07844–5), CAPES (Coordenação de Aperfeiçoamento de Pessoal de Nível Superior), and CNPq (Conselho Nacional de Desenvolvimento Científico e Tecnológico) for the financial support.

## References

1. Ramamurthi, S. and McCurdy, A. R. (1993), *J. Am. Oil Chem. Soc.* **70(3),** 287–295.
2. Almeida, M. E. M. (2000), *PhD Thesis,* Food Engineering School, State University of Campinas (UNICAMP), Campinas, Brazil.
3. Ramamurthi, S., Bhirud, P. R., and McCurdy, A. R. (1991), *J. Am. Oil Chem. Soc.* **68(12),** 970–975.
4. Ruperez, F. J., Martín, D., Herrera, E., and Barbas, C. (2001), *J. Chrom. A.* **935,** 45–69.
5. Ferrari, R. A., Schulte, E., Esteves, W., Brühl, L., and Mukherjee, K. D. (1996), *J. Am. Oil Chem. Soc.* **73(5),** 587–592.
6. Stampfer, M. J., Hennekens, C. H., Manson, J. E., Colditz, G. A., Rosner, B., and Willett, W. C. (1993), *J. Med.* **56(12),** 1444–1449.
7. Chu, B. S., Baharin, B. S., and Quek, S. Y. (2002), *Food Chem.* **79(1),** 55–59.
8. Shimada, Y., Nakai, S., Suenaga, M., Sugihara, A., Kitano, M., and Tominaga, Y. (2000), *J. Am. Oil Chem. Soc.* **77(10),** 1009–1013.
9. Jeromin, L., Johannisbauer, W., Gutsche, B., Jordan, V., and Wogatzki, H. (1997), USP 5627289.
10. Tütem, E., Apak, R., Günaydi, E., and Sözgen, K. (1997), *Talanta* **44,** 249–255.
11. Batistella, C. B., Wolf Maciel, M. R., and Maciel Filho, R. (2000), *Comp. Chem. Eng.* **24,** 1309–1315.
12. Fregolente, L. V., Batistella, C. B., Maciel Filho, R., and Wolf Maciel, M. R. (2005), *J. Am. Oil Chem. Soc.* **82(9),** 673–678.
13. Moraes, E. B., Batistella, C. B., Alvarez, M. E. T., Maciel Filho, R., and Maciel, M. R. W. (2004), *Appl. Biochem. Biotechnol.* **113,** 689–711.
14. Xu, X., Jacobsen, C., Nielsen, N. S., Heinrich, M. T., and Zhou. D. (2002), *Eur. J. Lipid Sci. Technol.* **104,** 745–755.
15. Lima Silva, N., Wolf Maciel, M. R., Batistella, C. B., and Maciel Filho, R. (2006), *Appl. Biochem. Biotechnol.* 129–132.
16. Sbaite, P., Batistella, C. B., Winter, A., et al. (2006), *Petrol. Sci. Technol.* **24(3–4),** 265–274.
17. Ito, V. M., Martins, P. F., Batistella, C. B., Maciel Filho, R., and Wolf Maciel, M. R. (2006), *Appl. Biochem. Biotechnol.* 129–132.
18. Martins, P. F., Ito, V. M., Batistella, C. B., and Maciel, M. R. W. (2006), *Sep. Pur. Technol.* **48,** 78–84.
19. Moraes, E. B., Martins, P. F., Batistella, C. B., Alvarez, M. E. T., Maciel Filho. R., and Wolf Maciel, M. R. (2006), *Appl. Biochem. Biotechnol.* **129–132,** 1041–1050.

20. Ito, V. M., FAPESP (Fundação de Amparo a pesquisa do Estado de São Paulo) Report. 2004.
21. Maciel Filho, R., Batistella, C. B., Sbaite. P., et al. (2006), *Petrol. Sci. Technol.* **24(3–4),** 275–283.
22. Fregolente, L. V., Batistella, C. B., Maciel Filho, R., and Wolf Maciel, M. R. (2006), *Appl. Biochem. Biotechnol.* **129–132,** 680–693.
23. Burkert, J. F. M., Maldonado, R. R., Maugeri Filho, F., and Rodrigues, M. I. (2005), *J. Chem. Technol. Biotechnol.* **80,** 61–67.
24. AOCS (1998), Official Methods and Recommended Practices of the AOCS, 5th ed. Champaign, Method Ca 5a-40.
25. AOCS, (1998), Official Methods and Recommended Practices of the AOCS, 5th ed. Champaign, Method Ce 8–89.
26. Barros Neto, B., Scarminio, I. S., and Bruns, R. E. (2003), In: *Como Fazer Experimentos: Pesquisa e Desenvolvimento na Ciência e na Indústria,* 2nd ed. Unicamp, Campinas, 228p.

0273-2289/1559-0291 (Online)/07/136–140/897–908/$30.00

# Semicontinuous Production of Lactic Acid From Cheese Whey Using Integrated Membrane Reactor

YEBO LI,* ABOLGHASEM SHAHBAZI, SEKOU COULIBALY, AND MICHELE M. MIMS

*Bioenvironmental Engineering Program, Department of Natural Resources and Environmental Design, North Carolina A&T State University, 1601 East Market Street, Greensboro, NC 27411, E-mail: yli@ncat.edu*

## Abstract

Semicontinuous production of lactic acid from cheese whey using free cells of *Bifidobacterium longum* with and without nanofiltration was studied. For the semicontinuous fermentation without membrane separation, the lactic acid productivity of the second and third runs is much lower than the first run. The semicontinuous fermentation with nanoseparation was run semicontinuously for 72 h with lactic acid to be harvested every 24 h using a nanofiltration membrane unit. The cells and unutilized lactose were kept in the reactor and mixed with newly added cheese whey in the subsequent runs. Slight increase in the lactic acid productivity was observed in the second and third runs during the semicontinuous fermentation with nanofiltration. It can be concluded that nanoseparation could improve the lactic acid productivity of the semicontinuous fermentation process.

**Index Entries:** Cheese whey; fermentation; lactic acid; lactose; membrane; nanofiltration; semicontinuous.

## Introduction

Lactic acid is a natural organic acid and has many applications in the pharmaceutical, food, and chemical industries. It is used as acidulant and preservative, and recently its potential as substrate for the production of biodegradable plastic has been actively pursued *(1,2)*. Approximately half of the world's supply of lactate is produced by fermentation process. Although batch fermentation processes are currently used, a number of more advanced techniques have been investigated in order to improve the process efficiency *(3)*. Semicontinuous and continuous lactic acid production systems have been recently studied to improve the fermentation performance *(4–6)*. Cheese whey is an important byproduct from the cheese manufacturing industry. Typically, 100.0 g of milk yield, 10.0 g of cheese, and 90.0 g of

*Author to whom all correspondence and reprint requests should be addressed.

liquid whey (7). Cheese whey contains about 4.5–5% lactose, 0.6–0.8% soluble proteins, 0.4–0.5% (w/v) lipids, and varying concentrations of mineral salts (8). Therefore, there is an interest to utilize lactose from cheese whey in the production of value-added products such as lactic acid.

Lactic acid has been produced by fermenta tion of sugar-containing substrates such as cheese whey using *Lactobacillus helveticus* (2,9) and *L. casei* (4,5) in most of the previous studies. *Bifidobacterium longum* is a bacterium that can convert lactose into lactic acid and also produce an antibacterial compound, which can boost the immune system in its host. In recent years, there has been an increasing interest in the incorporation of the intestinal bacterial species, *B. longum*, into fermented milk products. Studies have demonstrated that *B. longum* in fermented milks have a variety of beneficial health effects in human and animal intestinal tract (10,11). Most previous studies on the fermentation process using *B. longum* have focused on the production of *B. longum* cell (12,13) for application in the food and pharmaceutical industry. The research on lactic acid production using *B. longum* is scarce.

Nanofiltration is a pressure-driven membrane process with a MWCO situated between reverse osmosis and ultrafiltration. The nanofiltration membrane has already been used in the demineralization of salted, acid, and sweet cheese whey (14). The process could separate monovalent salts and organics in the molecular weight range 200–1000 Da (15). Nanofiltration membrane with MWCO around 400 Da was demonstrated to retain about 97% of lactose and 12–35% of lactate at pH 3.3 in a nanofiltration membrane-reactor (1). Nanofiltration of cheese whey has been evaluated based on the permeate flux to improve the demineralization rate by Alkhatim et al. (16). The objectives of this study were: (a) to evaluate the performance of nanofiltration filtration membrane on the lactic acid purification, and (b) to evaluate the performance of semicontinuous production of lactic acid from cheese whey with and without nanofiltration.

## Materials and Methods

### Cheese Whey Media

Cheese whey media was prepared by dissolving 50.0 g of deproteinized cheese whey powder (Davisco Foods International Inc., Eden Prairie, MN) into a liter of deionized water and stirring for 5 min at ambient temperature to obtain 5% cheese whey concentration. The composition of the deproteinized cheese whey powder was as follows: crude protein (total nitrogen × 6.38) 6.8%, crude fat 0.8%, lactose 78.6%, ash 9.4%, and moisture 4.4%. The solutions were autoclaved at 103°C for 10 min before being used at the fermentation experiments.

### Microorganism and Culture Media

*B. longum* was obtained from the National Collection of Food Bacteria (NCFB 2259). Stock culture of this strain was maintained in 50% glycerol

and Man Rogosa Sharpe (MRS) broth media at –80°C. Active cultures were propagated in 10 mL MRS broth at a temperature of 37°C for 24 h under anaerobic conditions. This was used as a preculture to initiate cell production of higher volume with a 1% inoculation into 100 mL fresh MRS broth, and incubated at 37°C for 24 h.

### *Nanofiltration*

The nanofiltration system consisted of a recirculation pump, nanofiltration unit (SEPA CF II, Osmonics, Minneapolis, MN), and an online permeate weighting unit. The cheese whey broth was circulated from the fermentor to the nanofiltration membrane unit at a constant velocity through a positive pump (M03-S, Hydra-cell, Minneapolis, MN). The permeate was collected in a container placed on an electronic balance. The reading of the balance was continually recorded at 30 s intervals by a computer. The cross-flow velocity used in the experiments was 0.5 m/s. The transmembrane pressure levels used were 1.4, 2.1, and 2.8 MPa. Two nanofiltration membranes (DS-5DK and DS-5HL, Osmonics) were used in the experiments. Both the membranes could retain 98% of MgSO4 but had different levels of permeate flux. No MWCO information was provided by the manufacturer. The surface area of the membrane is 140 $cm^2$. The hold up volume of the membrane unit is 70 mL. The nanofiltration process lasted for 1 h.

An alkali–acid treatment method was applied to the membrane system in the following steps: (a) fully open the recirculation and permeate valves, (b) flush with tap water for 5 min, (c) circulate 2 L of 4% phosphoric acid for 10 min, (d) rinse with tap water for 5 min, (e) circulate 2 L of 0.1 N NaOH solution for 10 min, and (f) rinse with 10 L of deionized water for 5 min.

### *Semicontinuous Fermentation*

The fermentation was conducted in a stirred 1.5-L benchtop fermentor. The pH of the broth was maintained at the designated value by neutralizing the acid with 10 *N* ammonium hydroxide during fermentation. The agitation speed of the fermentor was maintained at 200 rpm, whereas the temperature was maintained at 37°C. Samples were withdrawn every 2 h during the first 6 h and every 12 h during the remaining fermentation process.

The preliminary semicontinuous fermentation experiments without membrane separation were conducted at pH 5.0–6.5 for 48 h. After 48 h, half of the broth (0.75 L) was pumped out and same amount (0.75 L) of fresh cheese whey (5%) was added. The fermentation lasted for another 48 h at the same condition. In the semicontinuous fermentation experiments with membrane separation, 0.75 L of broth was harvested from the fermentor using the nanofiltration unit described above. The 5DK membrane was used in the tests. The transmembrane pressure of the tests was maintained at 2.1 MPa. After membrane separation, 0.75 L of fresh cheese whey (5%) was added to replace the removed permeate. The membrane unit was flushed with boiling water for sterilization before each run of separation. In

order to compare the performance of semicontinuous fermentation without and with membrane separation, 0.75 L of broth was also harvested and replaced with 0.75 L of fresh cheese whey every 24 h in the semicontinuous fermentation without membrane separation. The fermentation experiments were replicated three times.

### *Analysis*

Lactose, lactic acid, and acetic acid were measured by high-performance liquid chromatography (Waters, Milford, MA) with a KC-811 ion exclusion column and a Waters 410 differential refractometer detector. The mobile phase was 0.1% $H_3PO_4$ solution at a flow rate of 1 mL/min. The temperatures of the detector and of the column were maintained at 35°C and 60°C, respectively. The performance of fermentation was evaluated with lactic acid productivity:

$$\text{Lactic acid productivity} = \frac{\text{Lactic acid produced (g / L)}}{\text{Total fermentation time (h)}} \quad (1)$$

The performance of membrane separation was evaluated by using three criteria: (a) permeate flux, (b) lactose retention, and (c) lactic acid recovery. The permeate flux was calculated by measuring the quantity of permeate collected during a certain time and dividing it by the effective membrane area for filtration.

$$\text{Permeate flux } (\text{Lm}^{-2}/\text{h}) \frac{\text{Permeate volume}}{\text{Membrane area} \times \text{time}} \quad (2)$$

The lactose retention (%) was defined as:

$$\text{Lactose retention} = \left(1 - \frac{\text{Concentration of lactose in the permeate}}{\text{Concentration of lactose in the feed stream}}\right) \times 100 \quad (3)$$

The lactic acid recovery (%) was defined as:

$$\text{Lactose recovery} = \frac{\text{Concentration of lactic acid in the permeate}}{\text{Concentration of lactic acid in the feed stream}} \times 100 \quad (4)$$

## Results and Discussion

### *Semicontinuous Fermentation Without Membrane Separation*

The preliminary semicontinuous fermentation without membrane separation was conducted at different pH to obtain the optimum fermentation condition. The averaged lactose, lactic acid, and acetic acid concentrations obtained during the fermentation with free cells of *B. longum* at different pH are shown in Figs 1–4. The results show that lactose conversion ratio was significantly affected by the pH ($p < 0.0001$). The lactose

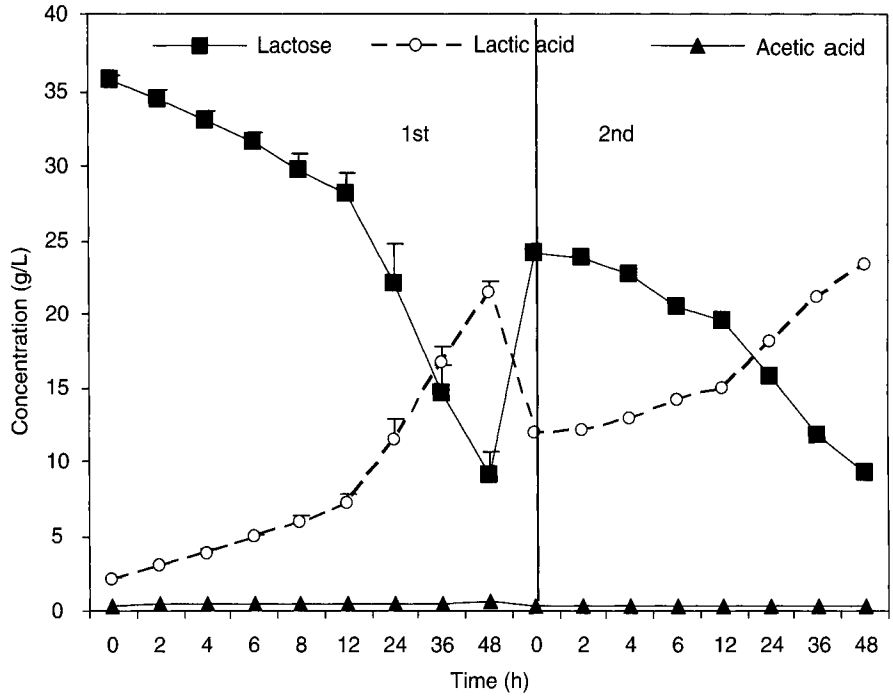


**Fig. 1.** Semicontinuous production of lactic acid from cheese whey (pH 5.0).

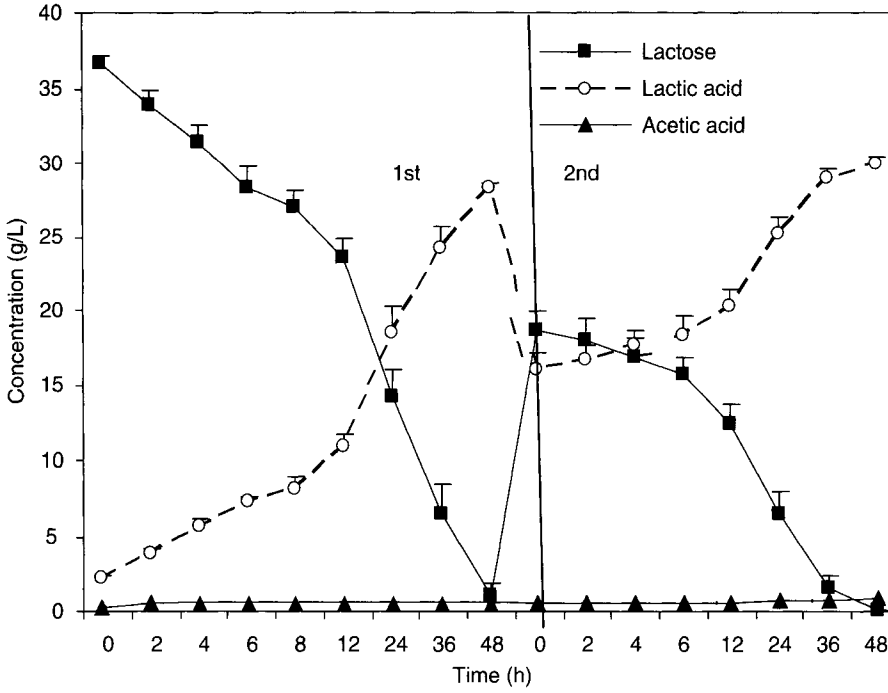


**Fig. 2.** Semicontinuous production of lactic acid from cheese whey (pH 5.5).

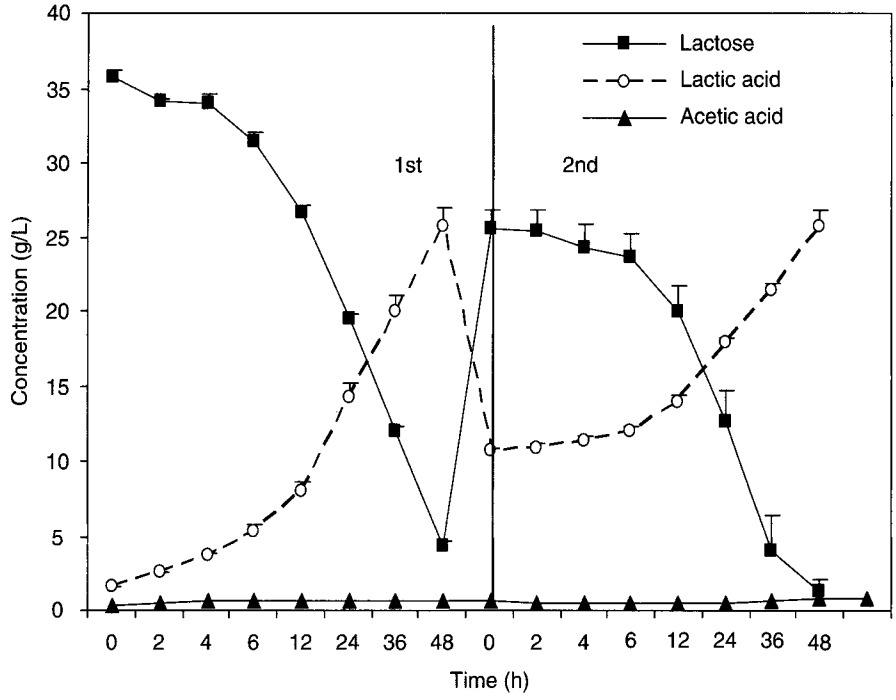


**Fig. 3.** Semicontinuous production of lactic acid from cheese whey (pH 6.0).

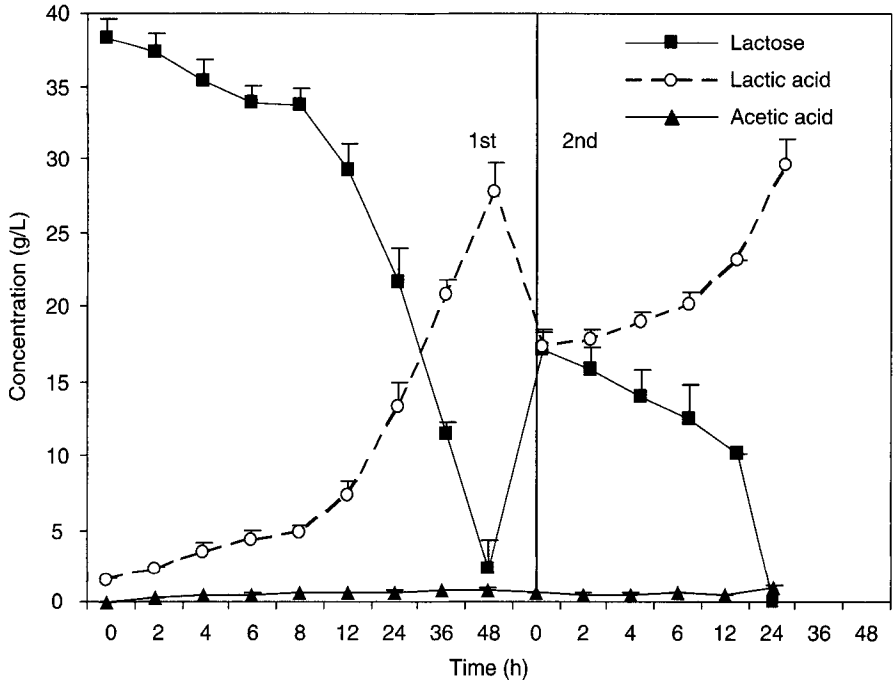


**Fig. 4.** Semicontinuous production of lactic acid from cheese whey (pH 6.5).

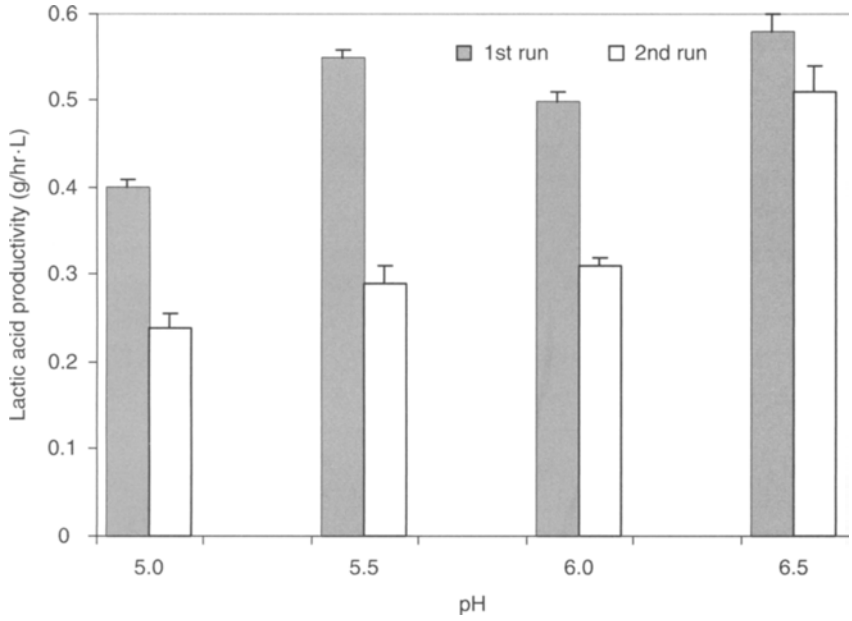


**Fig. 5.** Lactic acid productivity of the semicontinuous fermentation of cheese whey without membrane separation.

conversion ratio of 75, 97, 88, and 94% was obtained at pH 5.0, 5.5, 6.0, and 6.5 for the first run, respectively. The lactose conversion ratio of 62, 100, 89.5, and 100 was obtained at pH 5.0, 5.5, 6.0, and 6.5 for the second run, respectively. The lactic acid yield was between 0.72 and 0.76 g/g at pH values from 5.0 to 6.5. The pH has no significant effect on the lactic acid yield within the pH range of 5.0–6.5 ($p > 0.2$). The production of acetic acid was negligible in comparison with that of lactic acid production. As the initial lactose concentration of the second run was lower than that of the first run, most of the lactose could be converted during the second run. It can be seen from Fig. 5 that lactic acid productivity of the second run is much lower than that of the first run.

## *Nanofiltration of Fermentation Broth*

The nanofiltration testing results of permeate flux, lactose retention, and lactic acid recovery are shown in Table 1. The values in Table 1 are the average of two replicates. After 48 h of fermentation, nearly all the lactose in the fermentation was converted. In order to evaluate the performance of the membrane on the lactose retention, the lactose concentration in the broth was also adjusted to 10.0 g/L in some tests. It can be seen from Table 1 that when the membrane of 5DK was used, 100% of the lactose was retained at pressure of 2.1 and 2.8 MPa. Under the studied conditions, the membrane of 5HL could only retain about 70% of the lactose. In order to obtain pure lactic acid, membrane of 5DK was selected for the semicontinuous fermentation

Table 1
Permeate Flux, Lactose Retention, and Lactic Acid Recovery During Nanofiltration

| Membrane type | Initial concentration (g/L) Lactose | Lactic acid | Pressure (MPa) | Flux ($Lm^{-2}/h$) | Lactose retention (%) | Lactic acid recovery (%) |
|---|---|---|---|---|---|---|
| | 0 | 25.0 | 1.4 | 36.9 | – | 44.5 |
| | 0 | 25.0 | 2.1 | 45.4 | – | 34.2 |
| | 0 | 25.0 | 2.8 | 50.5 | – | 31.7 |
| 5DK | 10.0 | 30.0 | 1.4 | 21.9 | 98.0 | 44.2 |
| | 10.0 | 30.0 | 2.1 | 53.5 | 100 | 37.7 |
| | 10.0 | 30.0 | 2.8 | 59.3 | 100 | 30.0 |
| | 0 | 25.0 | 1.4 | 56.9 | – | 67.8 |
| | 0 | 25.0 | 2.1 | 58.1 | – | 56.0 |
| 5HL | 0 | 25.0 | 2.8 | 62.6 | – | 44.2 |
| | 10.0 | 30.0 | 2.1 | 50.4 | 69.0 | 70.8 |
| | 10.0 | 30.0 | 2.8 | 62.0 | 73.1 | 62.4 |

tests. It can be seen from Table 1, that permeate flux and lactose retention increased with the increase of transmembrane pressure. The lactic acid recovery in the permeate decreased with the increase of transmembrane pressure.

### *Comparison of Semicontinuous Fermentation With and Without Nanofiltration*

Figures 6–8 show the comparison of semicontinuous fermentation with and without nanofiltration. As the nanofiltration membrane could retain all the lactose, it can be seen from Fig. 7 that the initial lactose concentrations of the second and third runs of the tests were very close to that of the first run, whereas the lactose concentrations of the second and third runs were lower than that of the first runs in the tests without nanofiltration (Fig. 6). In the tests without nanofiltration, the lactic acid productivity of the second and third run was much lower than that of the first run (Figs. 6 and 8), whereas no decrease in lactic acid productivity was observed in the second and third runs when the nanofiltration membrane was used (Figs. 7 and 8). As the nanofiltration membrane could retain all the cells in the reactor, the initial cell density of the second and third runs with nanofiltration is much higher than that of tests without nanofiltration. It can be seen from Fig. 7 that the lactic acid concentration was increasing with runs, which was caused by the lower lactic acid recovery of the membrane. The selected membrane (5DK) could retain all the lactose, but it also had high lactic acid retention. The membrane need to be modified to increase the lactic acid recovery (reduce the lactic acid retention), whereas retain all the lactose in the future studies.

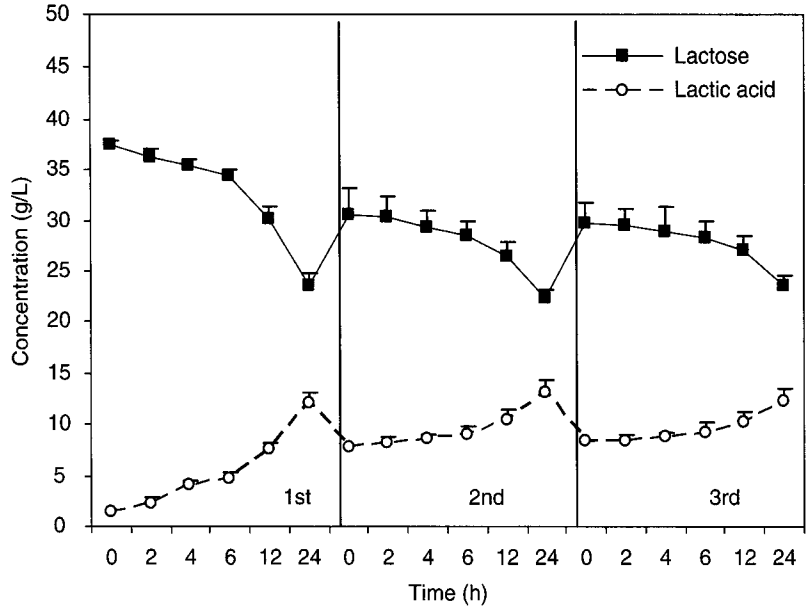


**Fig. 6.** Semicontinuous lactic acid production without nanofiltration (pH 5.5).

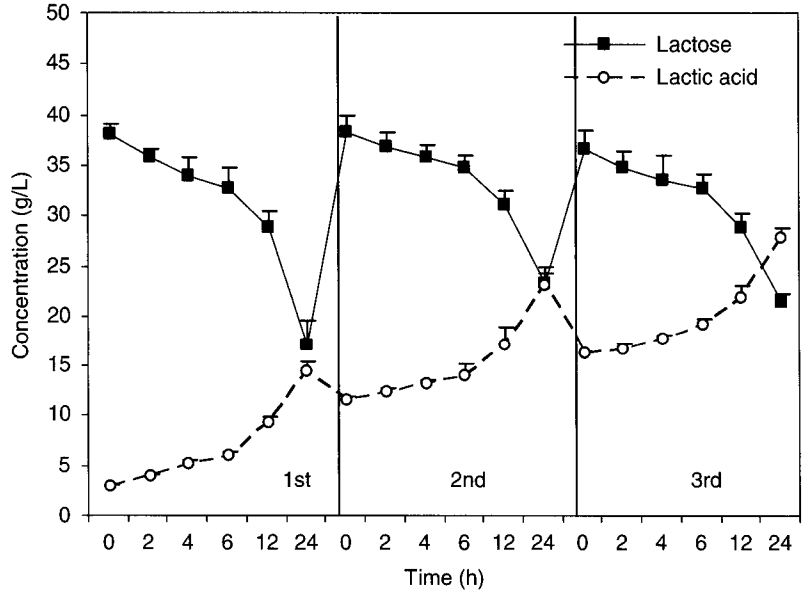


**Fig. 7.** Semicontinuous production of lactic acid from cheese whey with nanofiltration (pH 5.5).

## Conclusion

The semicontinuous fermentation without nanofiltration was tested at pH 5.0–6.5 and high lactose conversion and lactic acid yield were obtained at pH 5.5–6.5 in the first runs. The lactic acid productivity of the second runs was much lower than that of the first runs when the semicontinuous

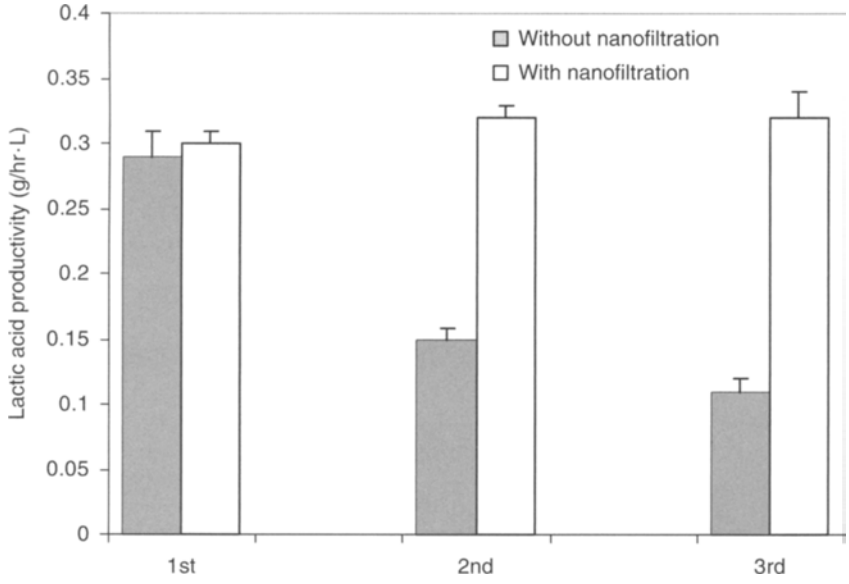


**Fig. 8.** Comparison of lactic acid productivity of semicontinuous fermentation with and without nanofiltration (pH 5.5).

fermentation was conducted without nanofiltration. Lactose retention ratio of 100% and lactic acid recovery of 38% was obtained with nanofiltration membrane of 5DK at pressure of 2.1 MPa. Membrane of 5HL could only retain about 73% of lactose, but could recover 62% of the lactic acid. When the nanofiltration membrane unit (5DK membrane) was integrated with the fermentor to harvest lactic acid every 24 h, higher lactic acid productivity was obtained for the second and third runs than the first run during the semicontinuous fermentation. Compared with the semicontinuous fermentation without nanofiltration, the lactic acid productivity of the subsequent runs increased.

## References

1. Jeantet, R., Maubois, J. L., and Boyaval (1996), *Enzyme Microbial. Technol.* **19,** 614–619.
2. Shahbazi, A., Mims, M. R., Li, Y., Shirley, V., Ibrahim, S. A., and Morris, A. (2005), *Appl. Biochem. Biotechnol.* **121–124,** 529–540.
3. Diosady, L. L. and Puzanov, T. (2005), *Int. J. Appl. Sci. Eng.* **3(1),** 19–25.
4. Bruno-Barcena, J. M., Ragout, A. L., Cordoba, P. R., and Sineriz, F.(1999), *Appl. Microbiol. Biotechnol.* **51,** 316–324.
5. Senthuran, A., Senthuran, V., and Hatti-Kaul, R. (1999), *J. Biotechnol.*, **73,** 61–70.
6. Mostafa, N. A. (1995), *Energy Convers. MGMT.* **37(3),** 253–260.
7. Kosikowski, F. V. (1979), *J. Dairy Sci.* **61,** 1149–1160.
8. Siso, M. I. G. (1996), *Bioresour. Technol.* **57,** 1–11.
9. Tango, M. S. A. and Ghaly, A. E. (2002), *Appl. Microbiol. Biotechnol.* **58,** 712–720.
10. Amrouche, T., Boutin, Y., and Moroni, O., (2006), *J. Microbiol. Methods.* **65 (1),** 159–170.
11. Baricault, L., Denariaz, G., Houri, J. J., Bouley, C., Sapin, C., and Trugnan, G. (1995), *Carcinogenisis* **2,** 245–252.

12. Doleyres, Y., Paquin, C., LeRoy, M., and Lacroix, C. (2002), *Appl. Microbiol. Biotechnol.* **60,** 168–173.
13. Song, S. H., Kim, T. B., Oh, H. I., and Oh, D. K. (2003), *World J. Microbiol. Biotechnol.* **19,** 721–731.
14. Van der Horst, H. C. (1995), *Int. Dairy Fed. Spec. Issue* **9504,** 36–52.
15. Eriksson, P. (1988), *Environ. Prog.* **7,** 58–62.
16. Alkhatim, H. S., Alcaina, M. I., Soriana, E. Iborra, M. I., Lora, J., and Arnal, J. (1998), *Desalination* **199,** 177–184.

0273-2289/1559-0291 (Online)/07/136-140/909-926/$30.00

# Functional Stability of a Mixed Microbial Consortium Producing PHA From Waste Carbon Sources

ERIK R. COATS,[1] FRANK J. LOGE,*[,2] WILLIAM A. SMITH,[3] DAVID N. THOMPSON,[3] AND MICHAEL P. WOLCOTT[4]

*[1]Department of Civil Engineering, University of Idaho, PO Box 441022, Moscow, Idaho 83844-1022; [2]Department of Civil and Environmental Engineering, University of California Davis, 1 Shields Avenue, Davis, CA 95616, E-mail: fjloge@ucdavis.edu; [3]Biotechnology Department, Idaho National Laboratory, P.O. Box 1625, Idaho Falls, ID 83415-2203; and [4]Department of Civil and Environmental Engineering, Washington State University, Pullman, WA 99164-2910*

## Abstract

Polyhydroxyalkanoates (PHAs) represent an environmentally effective alternative to synthetic thermoplastics; however, current production practices are not sustainable. In this study, PHA production was accomplished in sequencing batch bioreactors utilizing real wastewaters and mixed microbial consortia from municipal activated sludge as inoculum. Polymer production reached 85, 53, and 10% of the cell dry weight from methanol-enriched pulp and paper mill foul condensate, fermented municipal primary solids, and biodiesel wastewater, respectively. Using denaturing gradient gel electrophoresis of 16S-rDNA from polymerase chain reaction-amplified DNA extracts, distinctly different communities were observed between and within wastewaters following enrichment. Most importantly, functional stability was maintained despite differing and contrasting microbial populations.

**Index Entries:** Activated sludge; denaturing gradient gel electrophoresis; polyhydroxyalkanoates; wastewater; primary solids fermentate; foul condensate; environmental biotechnology.

## Introduction

Engineered biological systems have historically been utilized principally for the remediation and/or treatment of anthropogenic-derived pollution. Only in recent years has this environmental management discipline, appropriately referred to as environmental biotechnology *(1)*, been recognized for its potential to synthesize commodities and provide services beyond waste treatment *(1)*. However, this proposition is not

*Author to whom all correspondence and reprint requests should be addressed.

without challenges. Foremost, any proposed commodity-producing, biologically based process must be relatively easy to operate, stable, and largely self-correcting *(1)*, which demands functional stability within the anticipated diverse microbial community. Although this fundamental requirement is not necessarily congruent with all current biological treatment processes (e.g., biological nitrogen removal and biological phosphorus removal *[2,3]*), recent research applying advanced molecular techniques provides evidence of stable ecological functions within diverse and seemingly different mixed microbial populations *(4,5)*. In fact, ecological resilience and maintenance of function is proposed to be predicated on species diversity *(6)*.

Within the context of environmental biotechnology and commodity production are biologically derived polyesters known as polyhydroxyalkanoates (PHAs), which represent a potentially sustainable replacement to fossil-fuel based thermoplastics. Synthesis of PHAs, which serve as bacterial carbon and energy storage reserves, is currently estimated to be accomplished by over 300 different bacterial species in the form of cytoplasmic granules *(7)*. Biosynthesis is stimulated by either excess soluble carbon with a concurrent macronutrient limitation (typically limited on either nitrogen or phosphorus), a limitation in a terminal electron acceptor (with oxygen as the most common), or a so-called feast/famine environment wherein microorganisms realize a transient excess of soluble carbon without any other nutrient limitations *(8)*. Poly-3-hydroxybutyrate (PHB or P3HB) was the first PHA discovered (>75 yr ago), and hence is the most extensively characterized type *(9,10)*, although many more forms of hydroxyalkanoic monomer units have since been identified *(9)*. Common precursors to PHA synthesis include simple sugars such as glucose and fructose, and organic acids such as acetic and propionic acid. The type of carbon substrate dictates the polymeric structure of the PHA *(9)*, with some of the most commonly studied forms including PHB, poly-hydroxyvalerate (PHV), and poly-4-hydroxybutyrate. In turn, each form of PHA yields different polymer properties. PHB exhibits similar properties to polypropylene, including melting temperature and crystallinity, but the polymer is brittle on crystallization and exhibits little stress resistance *(9)*. Polymer improvements have been accomplished through copolymerization with PHV to increase ductility and impact resistance and lower processing temperatures *(9)*.

Current commercial PHA production practices utilize pure microbial cultures grown on renewable, but refined feedstocks (e.g., glucose) under sterile conditions *(11)*, and hence are not necessarily sustainable *(12,13)*. However, recognizing the apparent propensity for wild microbial consortia to synthesize the polymer *(14–16)*, commercial production of PHA would theoretically appear to be a natural extension of wastewater treatment. In fact PHA synthesis is empirically associated with certain municipal wastewater treatment processes *(17–19)*, although biological synthesis of PHA in full-scale wastewater treatment facilities, estimated at upwards

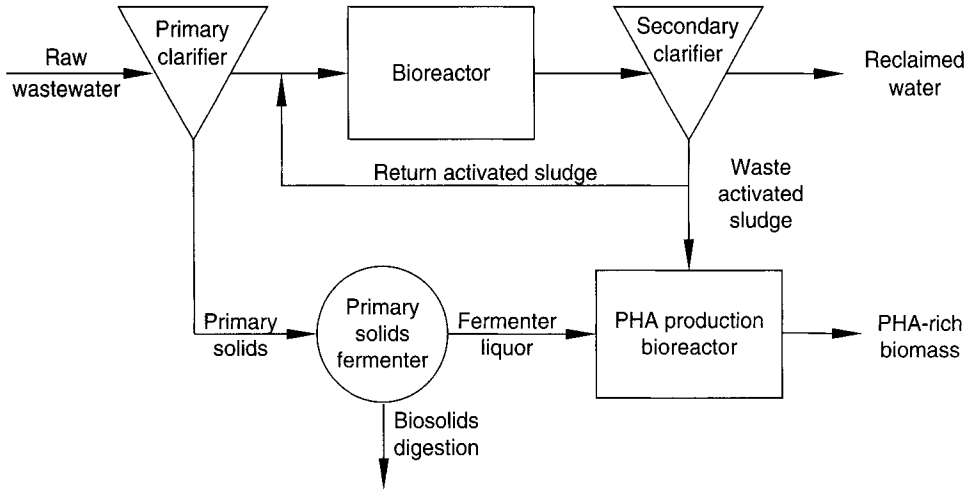


**Fig. 1.** Schematic diagram of proposed PHA production process integrated within a municipal wastewater treatment scheme.

of 4% (w/w) (data not shown), falls short of quantities necessary for commercial exploitation. Nevertheless, recognizing that many waste streams are rich in PHA precursors, the potential exists for PHA-production concurrent with wastewater treatment.

As proof of this concept, we have previously proposed and implemented an integrated PHA production and wastewater treatment process for municipal wastewaters (Coats et al., in review). In this scheme, wastewater treatment would occur in a biological treatment train designed to create selective environmental pressures necessary to achieve treatment objectives and concurrently enrich for microorganisms capable of producing PHA (Fig. 1). Mass production of PHA would occur in a separate biological reactor (termed a sidestream reactor) receiving biomass routinely wasted from the treatment reactor. Primary solids fermentate, derived from a primary solids fermentation reactor, would be supplied to both the wastewater treatment and PHA production reactors. Implementation of this integrated PHA production–wastewater treatment scheme resulted in a PHA yield of approx 10–22% (w/w) while concurrently realizing soluble carbon removal (Fig. 2); in the sidestream reactor, PHA production peaked at approx 53% (w/w) within 3.5 h (Fig. 3). Similar results were achieved in a sidestream reactor utilizing solids obtained from a wastewater treatment reactor operated under strictly aerobic conditions (data not shown). In all cases PHA production followed a feast-famine pattern, and maximum PHA production consistently occurred at a defined time-point after feeding concurrent with maximum reduction in readily metabolized soluble carbon. Importantly, copolymerization of both PHB and PHV was achieved (Fig. 3). The occurrence of this feast–famine condition is consistent with previous investigations *(8,14,15)* that focused on environmental matrices other than wild microbial consortia and wastewater.

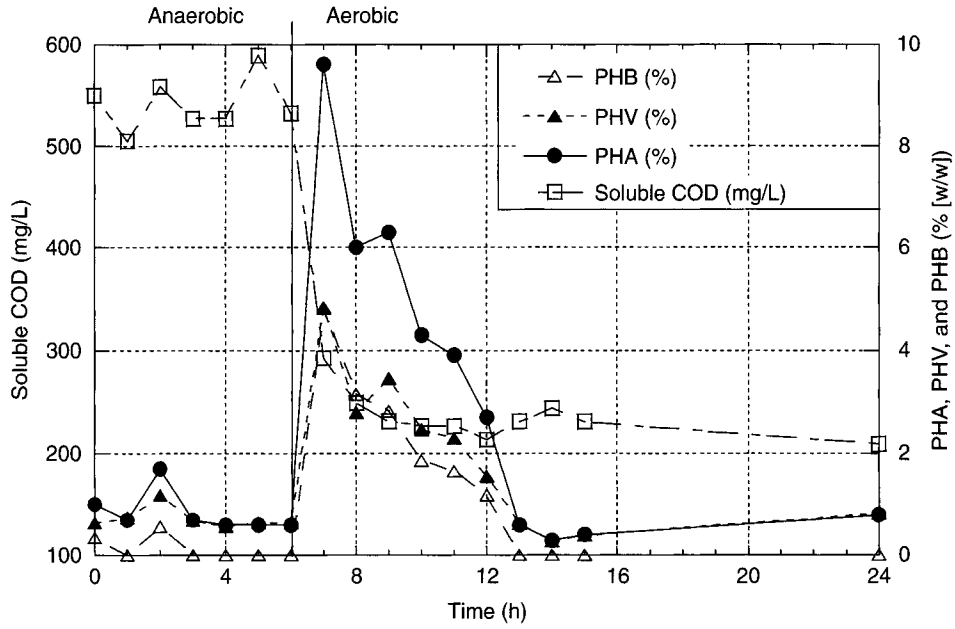


**Fig. 2.** Transient concentrations of soluble orthophosphate, COD, PHAs, PHB, and PHV in an anaerobic/aerobic SBR seeded with a mixed microbial consortium and fed fermentate (at $t = 0$) derived from municipal primary solids.

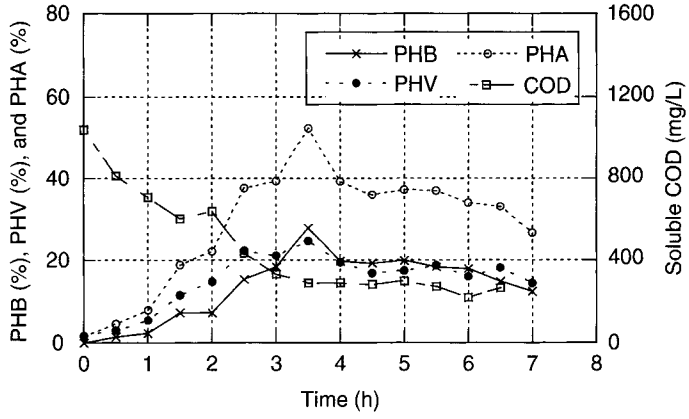


**Fig. 3.** Transient concentrations of soluble COD, PHAs, PHB, and PHV in a sidestream aerobic batch reactor seeded with cells obtained from the SBR in Figure 2 at $t = 24$ h and fed fermentate (at $t = 0$) derived from municipal primary solids.

The goal of the research presented herein was to extend the proposed PHA-wastewater treatment process to industrial wastewater, and to investigate the functional stability and general diversity of mixed microbial consortia within different PHA-producing wastewater environments. The specific objectives were to:

1. Demonstrate that PHA synthesis can be achieved by a mixed microbial consortium on industrial wastewaters.

2. Demonstrate process and functional stability in a municipal wastewater environment following process upset.
3. Preliminarily characterize the extent of microbial diversity of the PHA-producing consortium within a particular wastewater and among different wastewaters.

## Materials and Methods

### *Source of Microorganisms*

The mixed microbial seed was obtained from the Moscow, Idaho, wastewater treatment facility, which had been determined, through a series of preliminary facility screening studies, to be capable of synthesizing PHA. The microbial seed for the primary solids fermenter was obtained from the anaerobic digester at the Pullman, Washington wastewater treatment plant.

### *Source of Wastewater*

Foul condensate wastewater was obtained from the Lewiston, Idaho, Potlatch Corporation pulp and paper mill. Biodiesel-derived wastewater was provided by the University of Idaho, Department of Biological and Agricultural Engineering (Moscow, Idaho). Two batches of biodiesel wastewater were obtained, one with residual ethanol and one without, and each batch was fed into two reactors, one at 1% (v/v) and the second at 5% (v/v). Thickened primary solids, for operation of the fermentor were obtained from the Pullman, Washington wastewater treatment facility. Raw municipal wastewater was obtained from the Moscow, Idaho wastewater treatment facility.

### *Culture Conditions and Harvesting Procedures*

PHA production on pulp and paper mill foul condensate wastewater was accomplished in three 4-L completely mixed reactors. All reactors were operated as sequencing batch reactors (SBRs) on a 24-h cycle, with a solids retention time (SRT) of 4 d (reactor PO-A and PO-A1) or 6 d (reactor PO-C). Withdrawal and fill cycles of the SBR occurred almost immediately. Given that the mixture under reaction in the SBR was not permitted to settle before withdrawal, the hydraulic retention time (HRT) was equivalent to the SRT. Reactors PO-A and PO-C were continually aerated to maintain fully aerobic conditions; reactor PO-A1 was cycled every 12-h between anaerobic (first 12 h) and aerobic environments. Anaerobic conditions were established by bubbling nitrogen gas continuously into the reactor. Nitrogen gas and air were supplied through a 9-in. diameter Sanitaire® Silver Series II membrane fine bubble disc diffuser (Brown Deer, Wisconsin). PHB production on biodiesel wastewater was accomplished in 500-mL flasks incubated by shaking at 250 rpm for 4 d at 30°C.

Wastewater biosolids fermentate was produced in a 10-L completely mixed primary solids fermenter operated as a SBR, with a 24-h reaction time, and a SRT and HRT of 4 d. The daily decant was centrifuged at approx 10,000*g*, and the supernatant (e.g., fermentate) recovered. The fermentate-fed anaerobic/aerobic reactor (batch fed daily with fermentate) and the raw wastewater methanol fed reactor (batch fed daily raw wastewater and 5 mL of methanol to yield an initial concentration of approx 0.125% [v/v]), consisted of 4-L vessels continuously operated on a 24-h cycle (anaerobically for 6 h following feeding, then aerobically for 18 h) with a SRT and HRT of 5 d. Withdrawal and fill cycles of the SBR occurred almost immediately. Anaerobic conditions were accomplished through the continuous supply of nitrogen gas, and were verified utilizing a dissolved oxygen probe. Nitrogen gas and air were supplied through a 9-in. diameter Sanitaire Silver Series II membrane fine bubble disc diffuser.

### *Analytical Techniques*

Soluble chemical oxygen demand (sCOD or COD) tests were performed in accordance with Standard methods 5220-D *(20)*, with samples filtered through sterilized 0.22 μm filters before analysis (Millipore Corp, Billerica, MA). Hach high-range ampules (Hach Company, Loveland, Colorado) were utilized, with a Hach COD reactor and a Spectronic® 20 Genesys™ spectrophotometer. Biomass PHA content was determined by gas chromatography/mass spectrometry (GC/MS) as previously described *(21)*. Briefly, dried PHA-rich biomass samples were digested at 100°C in 2 mL each of acidified methanol (3% [v/v] sulfuric acid) and chloroform. Benzoic acid was added to the chloroform as an internal standard. Following vigorous vortexing of the mixture with 1-mL deionized water, PHA-rich chloroform was recovered for analysis. The chloroform phase was dehydrated by filtering the PHA-rich solution through sodium sulfate before analysis. GC/MS was performed on a Thermofinnigan PolarisQ iontrap GC/MS instrument (Thermo Electron Corporation, Waltham, MA) in positive electron impact mode. The sample was introduced using split injection. Separation was achieved on a ZB1 (15m, 0.25 mm ID) capillary column (Phenomenex, Torrance, CA) with helium as the carrier gas (1.2 mL/min) using a temperature program of 40°C (2 min) ramped to 200°C at 5°C/min. The Xcalibur software program (Thermo Electron Corporation) was used to analyze the data. The identity of the compounds was confirmed by retention time and mass spectral matching with known standards (Lancaster Synthesis, Ward Hill, MA) as methyl ester derivatives, and quantified based on the internal standard. Total cellular PHA content was determined on a weight basis (e.g., mass PHA : mass of dry biomass, [w/w]).

### *Molecular Methods*

Genomic DNA was extracted from 250 μL liquid samples using MoBio UltraClean Soil DNA isolation kit (MoBio Laboratories, Carlsbad, CA).

Polymerase chain reaction (PCR) was used to amplify bacterial 16S rDNA using the 341f-GC and 907r primers described by Ishii et al. *(22)*. Amplification was performed in 25 µL reaction mixtures that contained 0.4 pmol of each primer, 0.2 µ*M* of each dNTP, 10.0 µg/mL bovine serum albumin, 1X PCR buffer, 1.5 m*M* $Mg^{2+}$, 20 units/mL of *Taq* polymerase (buffer, dNTPs, bovine serum albumin, and RED*Taq*, [Sigma-Aldrich, St. Louis, MO]), and approx 100.0 ng target DNA. Reactions began with a 94°C denaturation for 5 min, followed by 30 cycles of 94°C for 1 min, 54°C annealing step for 1 min with a 72°C extension step for 1 min. Final extension was carried out at 72°C for 7 min. Presence of PCR products was confirmed by electrophoresis of 2 µL of the reaction mix on 1.5% agarose gels stained with 0.5 µg/mL ethidium bromide (Bio-Rad Laboratories, Hercules, CA). Four reactions from each sample were pooled to create a single 100 µL composite for denaturing gradient gel electrophoresis (DGGE) analysis.

DGGE *(23)* was performed with the D-Code system (Bio-Rad) at 60°C and 65 V for 900 min. Samples (25 µL) were loaded on a 6% (w/v) polyacrylamide gel (acrylamide : *N,N'*-methylene-bisacrylamide ratio, 37.5 : 1 [Bio-Rad]) in 1X TAE buffer. The denaturing gradient was formed by mixing two stock solutions of 6% acrylamide containing 40% and 80% denaturant (7 *M* urea [Bio-Rad] plus 40% [v/v] formamide [Sigma Chemical Co.]). The DNA was stained with 0.5 µg/mL ethidium bromide and imaged at 302 nm using an AlphaImager (Alpha Innotech Corp., San Leandro, CA).

## Results and Discussion

### *Production of PHA on Industrial Wastewater Treatment*

#### PHA Production in Foul Condensate Wastewater

Pulp and paper mill foul condensate wastewater is typically enriched with methanol, yielding a COD in excess of 10,000.0 mg/L. Methanol can be readily removed from the wastewater through biological processes; however, this wastewater is also nutrient limited, and the addition of nitrogen, phosphorous, and micronutrients is often necessary to achieve adequate removal of COD to meet permitted effluent discharge requirements *(24)*. Although these nutrient limitations are often viewed as troublesome from a conventional wastewater treatment perspective, the coupled high-carbon low-macro (micro) nutrient environment is potentially ideal for stimulating PHA synthesis. In addition, methanol is a quality carbon source for PHA synthesis *(25,26)*.

Utilizing a PHA-producing mixed microbial seed obtained from the Moscow, Idaho wastewater treatment facility, a foul condensate-fed SBR operated under fully aerobic conditions (reactor PO-A; SRT = 4 d) maintained a microbial consortium capable of producing PHA at 17.2% (w/w). Polymer production was moderately variable, with a 95% confidence interval of 10.4–24.0% (w/w), (Table 1); peak PHA synthesis was 85% (w/w).

Table 1
Summary of PHB Yield on Methanol-Enriched Foul Condensate Wastewater Obtained From a Pulp and Paper Mill, for Samples Collected and Analyzed Over a 4 mo Operational Period

| | PHB (% [w/w]) | | |
|---|---|---|---|
| Reactor | Average | 95% Confidence interval | Maximum |
| PO-A | 17.2 | 6.8 | 84.6 |
| PO-C | 5.0 | 1.3 | 7.5 |
| PO-A1 | 6.6 | 1.6 | 16.8 |

All reactors were operated as SBRs. Reactors PO-A and PO-C were operated under fully aerobic conditions, with a HRT and SRT of 4 and 6 d, respectively. Reactor PO-A1 was operated under alternating anaerobic/aerobic conditions (12 h AN, 12 h AE), with a HRT and SRT of 4 d. PHB yields represent dry weight concentrations (mass PHB : mass dry cell weight).

Reactor PO-C, which was also operated under fully aerobic conditions but with an SRT of 6 d, yielded PHA at 5.0 ± 1.3% (w/w), (95% confidence interval; Table 1); peak PHA synthesis was 7.5% (w/w). The reactors were operated for a period of 4 mo. Analysis of the biomass samples applying GC/MS techniques repeatedly verified both the presence and quantity of PHB (Fig. 4 presents a typical chromatogram). Biomass samples assayed for PHB were collected during routine reactor decant. COD levels in both reactors were consistently reduced by approx 10–20% (data not shown).

The variability in average and peak PHB yield in the fully aerated reactors can be attributed primarily to three factors. First, the sampling time-point may not have corresponded to peak cellular PHA concentration. As evidenced by the temporal distribution of PHA synthesis and degradation on fermentate (Figs. 2 and 3), the sampling time-point is critical, because the microbes will readily and rapidly metabolize the stored carbon. Temporal PHB synthesis within a given operational cycle was not assessed. Second, methanol content in the daily feed of foul condensate may have varied over time; recognizing that methanol is the primary substrate for PHB synthesis in foul condensate wastewater, such variation could significantly affect PHB yield. Conversely, excess methanol has been shown to have an inhibitory effect on overall biomass production and PHB synthesis (*27*). Third, monoterpenes represent the other primary organic carbon constituent in foul condensate (*28*); these carbon forms, which are much more structurally complex than methanol, are biodegraded through different metabolic pathways than methanol. These metabolic processes could have interfered with PHB synthesis.

In addition to the aforementioned factors, reactor operating conditions adversely influenced PHB synthesis. Increased HRT/SRT (e.g., reactor PO-C), which corresponded to an "older" microbial consortium, appeared to result in more carbon utilized for cell maintenance and growth and less for PHB

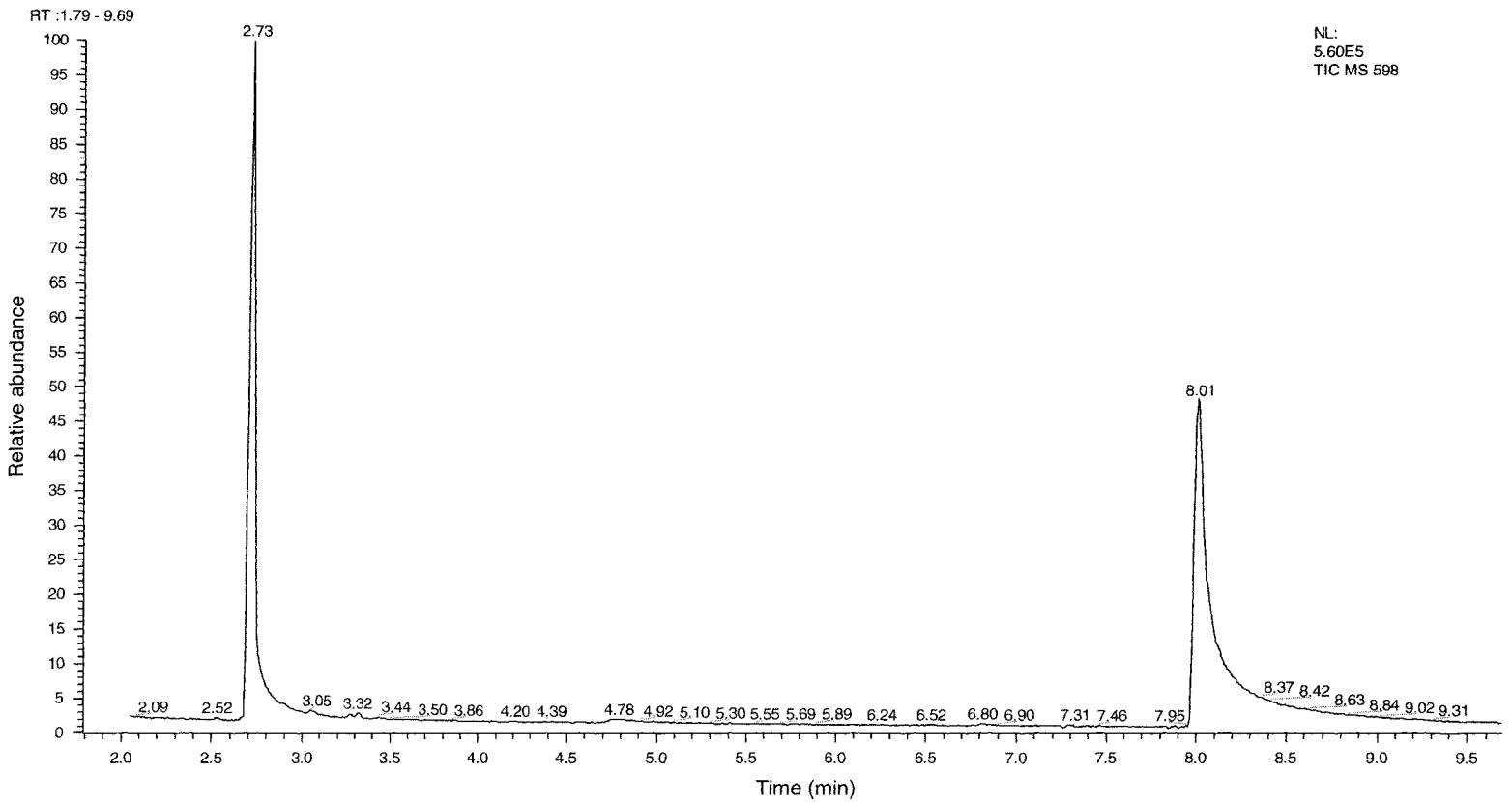


**Fig. 4.** Gas chromatograph plot of PHB-rich biomass produced on pulp and paper mill foul condensate. PHB methyl esters eluted at 2.73 min, whereas benzoic acid methyl esters (e.g., internal standard) eluted at 8.06 min. No other significant peaks occurred. PHB yield was estimated at approx 85% (w/w).

synthesis (Table 1). Further, as contrasted with reactor PO-A, PHB yield was significantly less under alternating anaerobic/aerobic reactor conditions (e.g., reactor PO-A1; average 6.9% [w/w], Table 1). The removal of oxygen appears to have created antagonistic conditions for PHB synthesis associated with nearly complete inhibition of microbial activity consistent with aerobic methanol oxidation by obligate methylotrophs *(29)*.

Methylotrophic bacteria are the principal microbial species associated with PHB synthesis on methanol *(30,31)*, and certain species are capable of producing upwards of 80% PHB *(30)*, which is consistent with our peak yield. The mechanism for stimulating polymer synthesis appears to be one of macronutrient limitation *(27,30)*, which is also consistent with our operations. However, previous research suggests carbon-to-macronutrient ratios may need to be optimized to maximize PHB synthesis *(27,30)*. In terms of process scale-up, site-specific investigations will be needed to optimize nutrient conditions. However, clearly there is potential to integrate polymer production into this industry as a value-added commodity generated during wastewater treatment.

## PHA Production in Biodiesel Wastewater

Biodiesel is a potential replacement or supplement to petroleum-based diesel fuels *(32)*. However, within the context of green engineering *(33)*, the "green" label is arguably a misnomer because the high strength coproduct wastewater stream *(32)* has simply shifted the environmental impacts within the overall life-cycle of the product. Biodiesel wastewater, which exhibits a COD in excess of 10,000,000 mg/L, principally consists of residual ethanol, glycerol, fatty acid ethyl (or methyl) esters, and residual fatty acids *(32)*. Glycerol, ethanol, and fatty acids are direct precursors to PHA synthesis *(25,26)*. Production of PHA on biodiesel wastewater is not presented here as the exclusive method of making this product "green", but rather as an example of how the production of commodities within the context of wastewater treatment (viewed here simply as raw materials) can be used to mitigate the shift in environmental impacts within the overall life-cycle of a product.

Utilizing biodiesel wastewater and a PHA-producing microbial seed derived from the Moscow, Idaho wastewater treatment facility, PHB yield ranged from approx 6% (w/w) on the ethanol-enriched biodiesel to approx 10% (w/w) on wastewater that contained no ethanol. Somewhat surprisingly, the yield on the ethanol-enriched biodiesel wastewater, which represents a diverse carbon substrate for PHA synthesis, was lower than the waste stream that contained no ethanol. Concurrent COD reduction was approx 67 and 60%, respectively. Considering the COD strength of biodiesel, this level of treatment is quite significant. Whereas PHB yield was low, reactor optimization would likely result in improved PHA yield concurrent with additional COD reduction. In fact, previous research with pure microbial cultures grown on biodiesel wastewater has yielded upwards of 42% PHA (w/w) *(32)*.

### *Process and Functional Stability following Process Upset*

A fermentate-fed SBR (identified as reactor FE-1) operated in an alternating anaerobic/aerobic scheme consistently maintained a microbial consortium capable of producing PHA (Fig. 2). The described conditions were replicated in three discrete reactors operated under steady-state conditions at different times over a 9 mo period. Comparable treatment efficiency and PHA production patterns were achieved each time. Each of these reactors was established with a new microbial seed obtained from the Moscow, Idaho wastewater treatment facility, with the primary solids fermenter operated with similarly new (e.g., fresh) material. Moreover, the reactor microbial seed and primary solids were obtained under different seasonal conditions (e.g., fall, winter, and spring) and under varying City wastewater conditions (e.g., with and without the contributions of the seasonally large university student populations in Pullman and Moscow). As further validation of this proposed process, the results presented herein were replicated at the University of California-Davis utilizing a mixed microbial seed derived from the Lincoln, CA wastewater treatment facility and primary solids derived from the Davis, CA wastewater treatment facility (data not shown).

As a contrast to the fermentate-fed wastewater treatment reactor, a mixed microbial seed derived from the Moscow, Idaho wastewater treatment facility was cultured on raw wastewater augmented with methanol (identified as reactor RW-1). The consortium generally utilized carbon at a constant rate throughout both the anaerobic and aerobic periods, and no appreciable PHA synthesis occurred (Fig. 5). A limited quantity of PHA was produced in the form of PHB. Clearly, this form of augmentation and reactor operation does not yield conditions suitable for concurrent PHA production and wastewater treatment. In fact, the results were comparable with those obtained on foul condensate wastewater when the reactor was operated under alternating anaerobic/aerobic conditions.

To evaluate how each established microbial consortium would function under dynamic nutrient feed conditions (e.g., process upset), recognizing that wastewater constituents can vary over time within a municipal wastewater treatment environment, the substrate to the respective reactors was switched. Specifically, the feedstock to reactor RW-1 was converted to fermentate (reactor identified as FE-2), and vice versa (FE-1 renamed as RW-2). As the reactors were batch fed daily, the conversion was effectively instantaneous. The induced "upset" conditions were associated with (a) a significant increase in COD (e.g., FE-1 to RW-2) and (b) a significant change in the carbon : nitrogen : phosphorus ratios in the substrate (e.g., RW-1 to FE-2 and FE-1 to RW-2). All other operating parameters remained the same. Two interesting mechanistic responses were observed. First, each microbial consortium ultimately switched metabolic responses. For example, the methanol-amended raw wastewater-fed reactor that was switched to fermentate, ultimately stabilized to cycle carbon consistent with the results

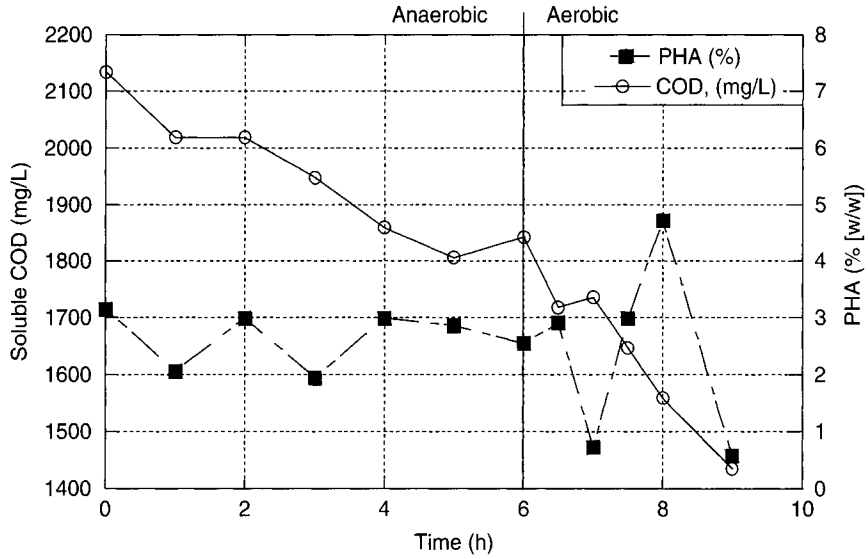


**Fig. 5.** Transient concentrations of soluble COD and PHAs in an anaerobic/aerobic SBR seeded with a mixed microbial consortium and fed raw wastewater and methanol (at $t = 0$).

shown in Fig. 2. Second, the microbial consortium in reactor FE-2 adapted to synthesize both PHB and PHV in copious amounts, whereas the consortium was previously producing only minimal amounts of PHB. Conversely, reactor RW-2 yielded negligible quantities of PHB, similar to RW-1.

### *Mixed Microbial Consortia for the Production of PHA in Wastewaters*

Whereas the fact that PHA could be produced by a mixed microbial consortium at a commercial level on various wastewaters certainly is significant, and that the consortia demonstrated robust functional capabilities, another observation carries similar weight. Quantitative PHA analysis on the original microbial seed indicated approx 0.2% (w/w) PHB and insignificant amounts of PHV, suggesting either limited numbers of PHA-producing organisms, or a limited production capacity. In either case, when exposed to more optimum PHA-producing conditions, this same PHA-producing consortium flourished.

### *Diversity of the PHA-Producing Microbial Population*

DGGE was performed to provide preliminary qualitative information regarding microbial community composition in the different reactors as a result of both the contrasting and altered feedstock conditions. The utilized primers amplified a bacterial 16S rDNA region corresponding to *Escherichia coli* positions 356–906. DGGE profiles indicate the number and relative abundance of the bacterial 16S rDNA amplicons in the reaction mixture. Each discrete band represents a single amplicon that corresponds

to a different bacterial strain present in the original sample. Despite biases of this method described in the literature *(34)*, this method nonetheless provides a "fingerprint" that can be used to describe similarities between and changes within microbial communities without the need for cultivation or cloning and sequencing.

DGGE analysis was performed on samples from: (a) reactors FE-1, FE-2, and RW-2, (b) two foul condensate reactors (PO-A and PO-C), (c) the original microbial seed from the Moscow, Idaho EBPR facility, and (d) the primary solids fermenter liquor (e.g., fermentate). The resulting fingerprints revealed starkly different microbial populations, with few common bands (Fig. 6). Patterns from FE-1 indicated the presence of at least eight different strains with two dominant strains relative to others within the lane. RW-2 contained only two distinct bands, which interestingly were not present in FE-1; this is of significance given that RW-2 was initially FE-1 before switching feedstock. The absence of common bands between these two samples indicates a complete change in the dominant communities present. FE-2 contained 5 faint bands; contrasting FE-1 and FE-2 revealed little apparent similarity between populations despite receiving the same substrate. The microbial seed from the Moscow, Idaho wastewater facility (lane D) exhibited eight bands of approximately equivalent intensity; additional faint bands were observed in replicate electrophoresis gels (data not shown), suggesting a rich, diverse community of bacteria present in the seed material. Fermenter liquor (lane E) contained five bands, two of which were dominant. Throughout all lanes, smears are interpreted as a large number of incompletely resolved bands likely resulting in an underestimate of diversity.

Potential explanations for the appearance and disappearance of bands between related reactors (e.g., FE-1 vs RW-2; FE-1 vs FE-2; all reactors contrasted with the microbial seed) include enrichment of strains that were originally beyond detection, addition of microorganisms in the feedstock, or microbial contamination. Feedstock effects are possible, because the clarified fermenter liquor feedstock contained low quantities of microorganisms. However, the DGGE profiles of FE-1 and FE-2 (Fig. 6) showed minimal-to-no influence of the dominant communities from the feedstock, as indicated by the predominant absence of common bands. The environmental pressure in these reactors appears to have selected a microbial consortium exclusive of not only the fermenter liquor feedstock but also the dominant microorganisms in the original seed. Raw wastewater from the City of Moscow (no DGGE sample collected) contained less than 200.0 mg/L total suspended solids (of which only a small portion would represent microbes). Thus, whereas this feedstock is potentially a source of inoculum, the cell density is low relative to the cell density established within the operating reactor. However, in the absence of DGGE profiles for the raw wastewater there is no way to characterize its influence on the resulting communities in the raw wastewater fed reactors.

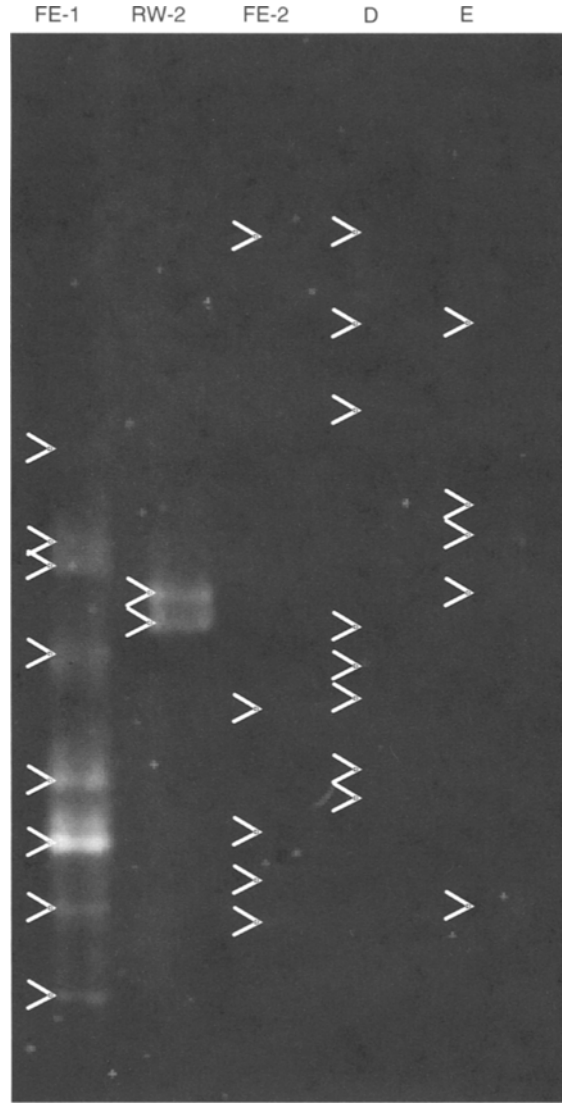


**Fig. 6.** DGGE gel of bacterial 16S rDNA PCR products amplified from mixed microbial consortium PHA-producing reactors, seed material from the Moscow, Idaho wastewater treatment facility (lane D), and the primary solids fermenter liquor (lane E). Lane FE-1 was inoculated with a microbial seed obtained from the Moscow, Idaho wastewater treatment facility and fed fermentate-rich wastewater. Lane RW-2 was previously run as FE-1 but was switched to a feedstock of raw wastewater and methanol. Lane FE-2 was previously run as RW-1 but was switched to a feedstock of fermentate-rich wastewater.

In contrast to the appearance and disappearance of multiple bands noted above, results from DGGE analysis on samples from reactors PO-A and PO-C (Fig. 7) indicated a loss of only one band and a subsequent change in the intensities of the other bands. The lower dilution rate of PO-C resulted in an increased sludge age (e.g., older microbial population) that appears to

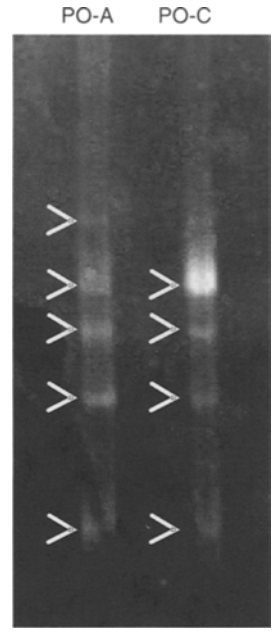


**Fig. 7.** DGGE gel of bacterial 16S rDNA PCR products amplified from mixed microbial consortium PHA-producing reactors. Lane PO-A represents a reactor operated at a HRT/SRT of 4 d, and lane PO-C represents a reactor operated at a HRT/SRT of 6 d. Both reactors were inoculated with a microbial seed obtained from the Moscow, Idaho wastewater treatment facility, fed pulp and paper mill foul condensate wastewater, and aerated continuously.

have enriched for one member of the community at the expense of at least one other, as well as decreased net PHA accumulation. Further, recognizing that PO-C did not receive as much substrate as PO-A, the reduced "feast" environment may have also facilitated the enhanced selection of non-PHA producing microbes.

A common approach to understanding the interplay between microbial community structure and function in biological wastewater treatment has relied on the identification of the microorganism present in either a single sample or a few samples over time *(35)*. Although there arguably is value in identifying which microorganisms are performing the critical functions associated with PHA synthesis, the task is certainly daunting, even with the many molecular tools available today. Conversely, an argument can also be made that phylogenetic specificity is not necessary to accomplish phenotypic stability; in fact, Rittman et al. *(1)* suggest that the field of environmental biotechnology within the context of full-scale engineered biological systems should focus on managing microbial communities rather than focusing on a "solves-all problems superbug."

The results presented herein demonstrate that a diverse microbial consortium can achieve a stable function under dynamic conditions, thereby

validating an application of this "function over structure" approach. Recognizing the diversity of municipal and industrial wastewater streams, and the associated diversity of bioreactor operating conditions necessary to treat these wastewaters, this apparently transcendent functional stability for PHA synthesis is viewed as a prerequisite condition for ultimate commercial development of the proposed PHA process. Taken together, these results suggest that nutrient conditions more significantly affect microbial function, rather than dominance of certain genotypes, and furthermore, that "functional redundancy" *(36)* results in retention of major or dominant community functions despite changes in community structure. These results further imply that if given a suitable carbon and energy source, reactor operational conditions such as induction of a feast/famine regime, the HRT, and/or the SRT, rather than starting inoculum composition, drive the microbial functions of PHA accumulation in a mixed microbial consortium.

## Conclusions

Based on the results presented herein, the following conclusions can be drawn:

1. The genetic capability to synthesize PHA appears to be common in mixed microbial consortiums present in conventional wastewater treatment bioreactors, as demonstrated through process success in two geographically distinct regions and on different waste carbon substrates.
2. The proposed process can recover from a process upset associated with instantaneous changes in either substrate carbon concentration or carbon : nitrogen : phosphorus ratios.
3. The genetic capability to synthesize PHA (e.g., function) is a critical factor for process success, rather than the presence of a specific microbial structure.
4. Successful integration of PHA production with wastewater treatment will demand optimizing bioreactor operations (e.g., SRT, HRT, and operating environment) with the substrate.
5. Additional investigations are necessary to develop appropriate design and operational criteria such that the proposed process can be successfully scaled up. Within this context, investigations should be conducted to identify the specific microbes-producing PHA, which could generate mechanisms to monitor and maintain process success.

## Acknowledgments

This material is based on work supported by the National Science Foundation under Grant Number DMI-0400337 and by the U.S. Department of Energy, Industrial Technologies Program, Forest Products Industries of the Future, under DOE-NE Idaho Operations Office Contract

DE-AC07-05ID14517. Any opinions, findings, and conclusions or recommendations expressed in this material are those of the authors and do not necessarily reflect the views of the funding agency.

## References

1. Rittmann, B. E., Hausner, M., Löffler, F., et al. (2006), *Environ. Sci. Technol.* **40,** 1096–1103.
2. Fuhs, G. W. and Chen, M. (1975), *Microbial. Ecol.* **2,** 119–138.
3. Wagner, M. and Loy, A. (2002), *Curr. Opin. Biotechnol.* **13,** 218–227.
4. Kaewpipat, K. and Grady, C. P. L., Jr. (2002), *Water Sci. Technol.* **46,** 19–27.
5. Stamper, D. M., Walch, M., and Jacobs, R. N. (2003), *Appl. Environ. Microbiol.* **69,** 852–860.
6. Peterson, G., Allen, C. R., and Holling, C. S. (1998), *Ecosystems* **1,** 6–18.
7. Lee, S. Y. (1996), *Trends Biotechnol.* **14,** 431–438.
8. Dionisi, D., Majone, M., Papa, V., and Beccari, M. (2004), *Biotechnol. Bioeng.* **85,** 569–579.
9. Madison, L. L. and Huisman, G. W. (1999), *Microbiol. Mol. Biol. Rev.* **63,** 21–53.
10. Lemoigne, M. (1926), *Bull. Soc. Chem. Biol.* (Paris). **8,** 770–782.
11. Braunegg, G., Lefebvre, G., and Genser, K. (2003), *J. Biotechnol.* **65,** 127–161.
12. Gerngross, T. U. (1999), *Nat. Biotechnol.* **17,** 541–544.
13. Scott, G. (2000), *Polym. Degrad. Stabil.* **68,** 1–7.
14. Carucci, A., Dionisi, D., Majone, M., Rolle, E., and Smurra, P. (2001), *Water Res.* **35,** 3833–3844.
15. Beun, J. J., Dircks, K., Van Loosdrecht, M. C. M., and Heijnen, J. J. (2002), *Water Res.* **36,** 1167–1180.
16. Dionisi, D., Renzi, V., Majone, M., Beccari, M., and Ramadori, R. (2004), *Water Res.* **38,** 2196–2206.
17. Comeau, Y., Hall, K. J., Hancock, R. E. W., and Oldham, W. K. (1986), *Water Res.* **20,** 1511–1521.
18. Mino, T., Arun, V., Tsuzuki, Y., and Matsuo, T. (1987), In: *Biological Phosphate Removal From Wastewaters*. vol. 4, Ramador, R. (ed.), Pergamon: Oxford, pp. 27–38.
19. Randall, A. A. and Liu, Y. -H. (2002), *Water Res.* **36,** 3473–3478.
20. Eaton, A. D., Clesceri, L. S., Greenberg, A. E. (1995), *Standard Methods for the Examination of Water and Wastewater*; 19th ed., APHA: Washington, DC.
21. Braunegg, G., Sonnleitner, B., and Lafferty, R. M. (1978), *Eur. J. Appl. Microbiol.* **6,** 29–37.
22. Ishii, K., Fukui, M., and Takii, S. (2000), *J. Appl. Microbiol.* **89,** 768–777.
23. Muyzer, G. and Smalla, K. (1998), *Antonie van Leeuwenhoek*. **73,** 127–141.
24. Slade, A. H., Nicol, C. M., and Grigsby, J. (1999), *Water Sci. Technol.* **40,** 77–84.
25. Yamane, T. (1993), *Biotechnol. Bioeng.* **41,** 165–170.
26. Ackermann, J. and Wolfgang, B. (1998), *Polym. Degrad. Stabil.* **59,** 183–186.
27. Kim, P., Kim, J. -H., and Oh, D. -K. (2003), *World J. Microbiol. Biotechnol.* **19,** 357–361.
28. Yoo, S. K. and Day, D. F. (2002), *Process Biochem.* **37,** 739–745.
29. White, D. (2000), *The Physiology and Biochemistry of Prokaryotes*, 4th ed. Oxford University Press, Inc., New York, NY.
30. Bourque, D., Pomerleau, Y., and Groleau, D. (1995), *Appl. Microbiol. Biotechnol.* **44,** 367–376.
31. Korotkova, N. and Lidstrom, M. E. (2001), *J. Bacteriol.* **183,** 1038–1046.
32. Ashby, R. D., Solaiman, D. K. Y., and Foglia, T. A. (2004), *J. Polym. Environ.* **12,** 105–112.
33. Anastas, P. T. and Zimmerman, J. B. (2003), *Environ. Sci. Technol.* **37,** 94A–101A.
34. Watanabe, K., Kodama, Y., and Harayama, S. (2001), *J. Microbiol. Methods* **44,** 253–262.
35. Seviour, R. J., Mino, T., and Onuki, M. (2003), *FEMS Microbiol. Rev.* **27,** 99–127.
36. Langenheder, S., Lindstrom, E. S., and Tranvik, L. J. (2006), *Appl. Environ. Microbiol.* **72,** 212–220.

0273-2289/1559-0291 (Online)/07/136–140/927–934/$30.00

# Separating a Mixture of Egg Yolk and Egg White Using Foam Fractionation

TIFFANY M. WARD,[1] ROSS A. EDWARDS,[2] AND ROBERT D. TANNER*,[1]

[1]*Department of Chemical Engineering, E-mail: robert.d.tanner@vanderbilt.edu; and* [2]*Department of Mechanical Engineering, Vanderbilt University, Nashville, TN 37235*

## Abstract

A mixture created by blending with a spatula, an egg yolk and an egg white from the same egg can serve as a binary system for testing to see how well foam fractionation can be used to separate two different groups of proteins naturally found together. This mixture of two phases is particularly attractive for such a study because the two phases can be visualized distinctly when in their separated states. It has been shown that air alone at a low flow rate and with little or no water added can effect visually clean separations of egg yolk from egg white, making this a "green" separation process. The white precedes the yolk in the process, which takes less than 10 min at a laboratory scale.

**Index Entries:** Egg albumin; egg protein; egg white; egg yolk; foam fractionation; protein separation; serum albumin.

## Introduction

Foam fractionation processes are promising methods for separating proteins found in water solutions. Other than the addition of air or another carrier gas, such as carbon dioxide, no other substances are needed to remove the foaming (hydrophobic) proteins from the other proteins found in a solution mixture. Therefore, contamination by exogenous chemical separation agents such as organic solvents is minimized. Natural fractionation phenomena occur in various processes such as the protein foam head formation in beer glasses, the breaking waves along ocean shorelines, in biological waste treatment plants *(1)*, and in commercial fermentation processes such as those used to create antibiotics and industrial enzymes like cellulase.

Foam fractionation is a simple and low-cost technique for separating and concentrating surface-active chemicals such as hydrophobic proteins. In foam fractionation, hydrophobic proteins are attached by adsorption to the gas bubbles, which then rise to the top of the bulk liquid at the surface *(2)*.

*Author to whom all correspondence and reprint requests should be addressed.

The proteins then become more concentrated as they rise because water is lost as they move upward through drainage.

Proteins are made up of long chains of amino acids. Chicken egg proteins are found in either the egg yolk or the egg white phases. The main constituent of an egg white is the protein, ovalbumin, which makes up 75% of the protein mass in the egg white (3). Other proteins that make up the egg white include conalbumin, ovomucoid, lysozyme, globulins (G2, G3), ovomucin, flavoprotein, ovoglycoprotein, ovomacroglobulin, avoinhibitor, and avidin (3). Egg yolk contains lecithin, a natural detergent and also apovitellenins I and VI and phosvitin (4).

Previous studies on foam fractionation show its feasibility for concentrating and separating proteins that foam. In general, foam fractionation is a very promising method for removing proteins from dilute solutions, for example, kudzu proteins from a retting solution and potato protein wastes in the potato industry (5). Many biopolymers including bovine serum albumin (blood), albumin, pepsin, and urease have been purified by foam fractionation. One of the key characteristics of this process is the speed with which the enrichment occurs because of the large gas-liquid interface generated in the bubbling process (6).

When an egg is cracked into a bowl and is beaten lightly with a spatula or whisk, it can be seen that even though the egg white and yolk incorporate into one another nicely, there still exists a boundary between the two phases. Separating the egg white from the egg yolk is a membrane called the vitelline membrane (4). When this mixture is placed into a foam fractionation column, a separation of the initial two phases, egg yolk and egg white, can be seen, suggesting a binary separation of the two phases. This two-phase system is a model system used here to explore how foam fractionation can be used to separate two optically different phases, each of which contain many proteins. To prove the binary separation of the egg white from egg yolk, the concentration of egg yolk and egg white of the foamate at various stages of foaming needed to be found. Optional spectroscopy used here to quantify the egg yolk and egg white separation, is a simple, noninvasive analytical technique with an infinitely broad range of applications in plant biotechnology and food processing.

Proteins are found in numerous other naturally occurring mixtures, which can be thought of as phases. In addition to water solutions of egg proteins, kudzu vine fermentation proteins, sweet potato proteins, and blood plasma proteins can be thought of as being consisting of visibly colored groupings or phases for analysis and for foam fractionation separation herein. Blood plasma contains groups of soluble proteins, the most abundant of which is serum albumin (7). It is interesting that the hydrophilic and hydrophobic carrier properties of albumins in a water solution render them suitable for separation from other proteins or protein groupings (phases) using foam fractionation. Perhaps even foam/bubble fractionation could also be used to separate plant-derived mixtures of hydrophilic tannin from

hydrophobic cellulose. The effect of physio-chemical parameters on the separation of proteins from human placenta extract using a continuous foam fractionation column has also been examined in previous studies *(8)*.

Because the egg yolk membranes appear to be fractionated and left behind in the bulk residue consisting mainly of egg yolk for the case of moderate hand premixing, perhaps the egg shell membrane can also be separated from other egg components by using foam fractionation. If so, then it might be possible to recover and concentrate those egg membranes, which are used as the substrate to grow viruses. This low-cost recovery could then perhaps be used as a first step in producing vaccines more quickly.

## Materials and Methods

### *Sample Preparation*

Grade A large white chicken eggs (Weiss Lake Pride, distributed by LA-127 Weiss Lake Egg Col, Centre, AL 35960) were purchased from a local grocery store and refrigerated at 5°C. Each egg was allowed to warm to approx 20°C because it was found that warm eggs foam better than cold eggs. The egg was then cracked, and the yolk and white (albumin) were separated by decantation into separate glass beakers. Owing to the high viscosity of fresh egg white, which made it hard to split and dilute with water, grade II crude, dried chicken egg white purchased from Sigma-Aldrich (St. Louis, MO) as Lot 88H1447, was used in its place. To create the calibration curve for the egg white, the dried egg white was diluted with water to the desired concentrations. For the yolk calibration curve, the whole yolk was weighed and then diluted down with water. More stirring was required to fully incorporate the yolk into the water than was required for the dried egg white. For the foam fractionation experiment, a whole egg was placed in a beaker and beaten lightly with a spatula for approx 5 min. For a separate experiment, another egg was placed into a blender (Blend Master 10, with a 350 W motor, made by Hamilton Beach/Proctor-Silex Inc., Washington, DC) and mixed on high speed for 5 min.

### *Experimental Procedure*

The experimental foam fractionation column used was made of glass with an inside diameter of 2 cm and a height of 10 cm. A porous ceramic (fritted) disk sparger with medium sized porosity was fitted inside the inner column wall near the bottom. Air from a compressed gas cylinder was introduced at a low rate (approx 35 mL/min) into the column after passing through a humidifying flask. The apparatus is shown in Fig. 1 and a typical spectrum of colors from a foaming experiment are described in Fig. 2. To test for the role of membranes in restricting the foaming process, the egg that was beaten by hand and an egg beaten vigorously in a blender to better break down the existing membranes were foamed in separate experiments. During the first experiment, the whole egg beaten by hand

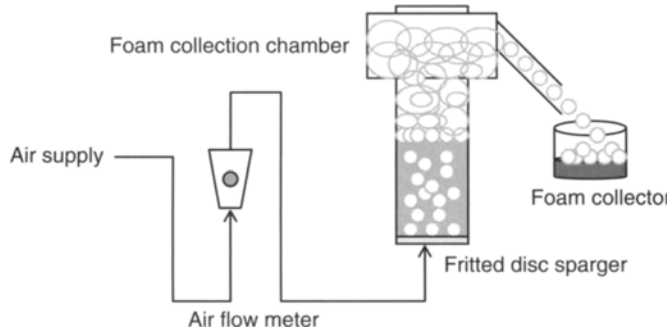


**Fig. 1.** Schematic drawing of the foam fractionation apparatus.

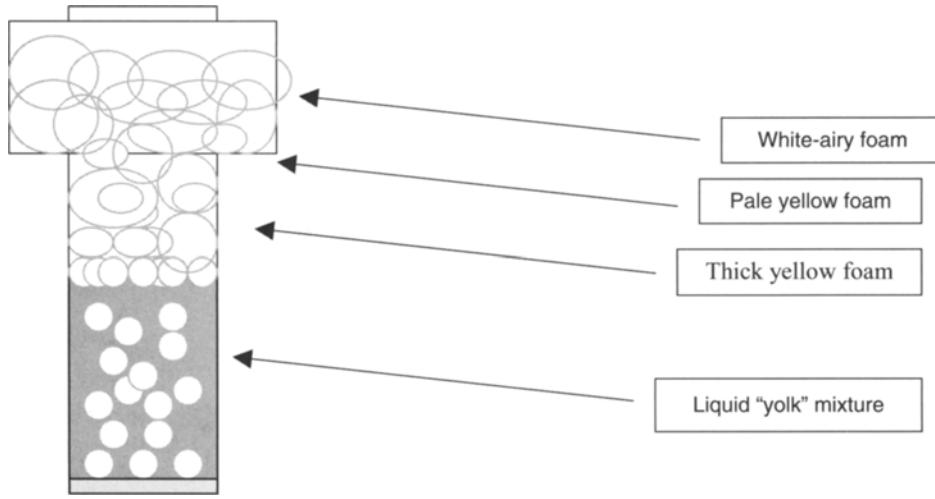


**Fig. 2.** Gradient of color in foaming within the column pictured in Fig. 1 of whole egg beaten by hand. This is observed before the collection of effluent foam to create the foamate in the foam collector.

was foamed. The second trial was done with the egg that was beaten by a blender. In each experiment foamate was collected at various time intervals and the absorbencies were read using a spectrophotometer.

## *Spectroscopy*

To initially determine how the egg phases absorb in the spectrophotometer, two samples, one of pure egg yolk and one of egg albumin (mostly ovalbumin, *[9]*) powder were diluted with water to reach the Beer's law concentration range (≤0.94 g/L for egg yolk and ≤4.44 g/L for egg white led to linear absorbance vs concentration curves). The spectrophotometer (Bausch and Lomb, Spec 20) was calibrated according to the instructions and then absorbencies were read for the given concentration at a wide range of wavelengths. Only wavelengths in the visible light range (<600 nm) were used.

Once the two desired wavelengths were selected the absorbance vs wavelength scans data of each of the two phases, white and yolk, were taken for different concentrations of pure egg yolk and pure egg albumin powder using the previously prepared samples. Calibration curves were created for both yolk and white and used to determine the concentrations of yolk and white for the samples of the foamate, which were collected at various time intervals. To test the linearity range of Beer's Law and establish the associated linear coefficients correlating absorbance with the underlying phase concentration, the absorbance of each sample was found. The smaller the concentration, the better Beer's Law is expected to hold and meet the assumption of linear superposition of the component absorbencies of the yolk and white, so that these phase components will equal the measured total absorbance.

## Results and Discussion

Visibly, when the egg was mixed by the blender on high speed for 5 min, the resulting mixture was "smoother" and more homogenous throughout as compared with the egg white and egg yolk that was blended by hand, mixing with a spatula. During the foam fractionation of a whole hand-beaten egg, the mixture was separated into two phases in the column. It took a few minutes for foamate to be produced, but once it started, the process went quickly. As seen in the schematic, shown in Fig. 2, the foamate at the top of the column was very white, and as foaming continued it increased in yellow color until the last of the foam left in the column was purely yellow. The yellow foam or yolk, could not make it out of the column at the flow rate we were using, but it remained in a foam-like state within the column, effectively creating a white foamate phase at the top of the column and a yellow residual liquid phase at the bottom of the column. The egg white foamed much more effectively than the yolk owing to the higher concentration of proteins; the lower concentration of fat in the white vs the yolk was especially because the fat in the yolk impedes foaming. It appeared that the egg mixture was reverting back into its original phases, egg white and egg yolk.

When the egg mixed by the blender was aerated, it began foaming immediately; however, there was no visible separation between the yolk and the white. Even when collected, the foam remained a pale yellow color as opposed to being separated out into white and yellow colors. The foamate was collected in a large container and after allowing it to sit for 5–10 min, the yellow yolk "dripped" to the bottom of the container and settled as a liquid. While doing so, the foamate on the top of the container became more and more white. Thus, a difference in the intensity of mixing before separation in the foam fractionation apparatus is a significant factor in the separation of the yolk and white phases. These experiments illustrate the ability of foam fractionation to separate visibly different

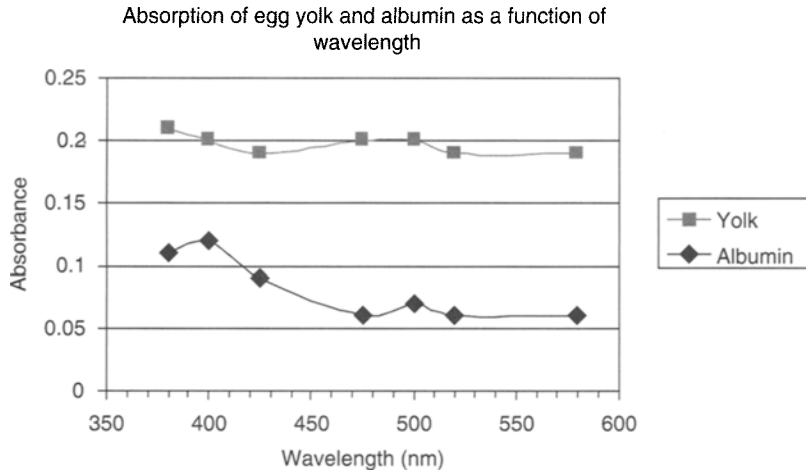


**Fig. 3.** The absorbance of a powdered egg albumin sample (concentration 4.44 g/L) and an egg yolk sample (concentration 0.94 g/L) scanned across the wavelength ranging from 380 to 580 nm.

phases from moderately mixed egg white and yolk solutions. The yellow color in the yolk mainly comes from the carotenoid, canthaxanthin *(10)*. This carotenoid most likely acts as a tracer, describing how the intensity of mixing allows spillover of the yellow color to the entire mixture of white and yolk when mixing is vigorous, and is retained in the yolk when mixing is gentle.

Figure 3 shows the results obtained by scanning a sample of egg yolk diluted with water and a sample of egg white powder diluted with water across a range of wavelengths. It can be seen that there are local peaks in the absorbance of egg white at 400 and 520 nm and a somewhat larger deviation in the absorbencies of egg white and egg yolk at 520 nm (than at 400 nm), wherein the white is close to its maximum absorbance. These two wavelengths were selected to create the calibration curves. In general, when both of the absorbing phases contribute to the total absorbance, the following set of equations can describe the system. For $\lambda_1$ = 520 nm, and $\lambda_2$ = 400 nm, the respective absorbencies are $A_1$ and $A_2$.

$$A_1 = k_1 C_w + k_3 C_y \tag{1}$$

$$A_2 = k_2 C_w + k_4 C_y \tag{2}$$

$$C_w = \frac{k_3 A_2 - k_4 A_1}{k_2 k_3 - k_1 k_4} \tag{3}$$

$$C_y = \frac{k_2 A_1 - k_1 A_2}{k_2 k_3 - k_1 k_4} \tag{4}$$

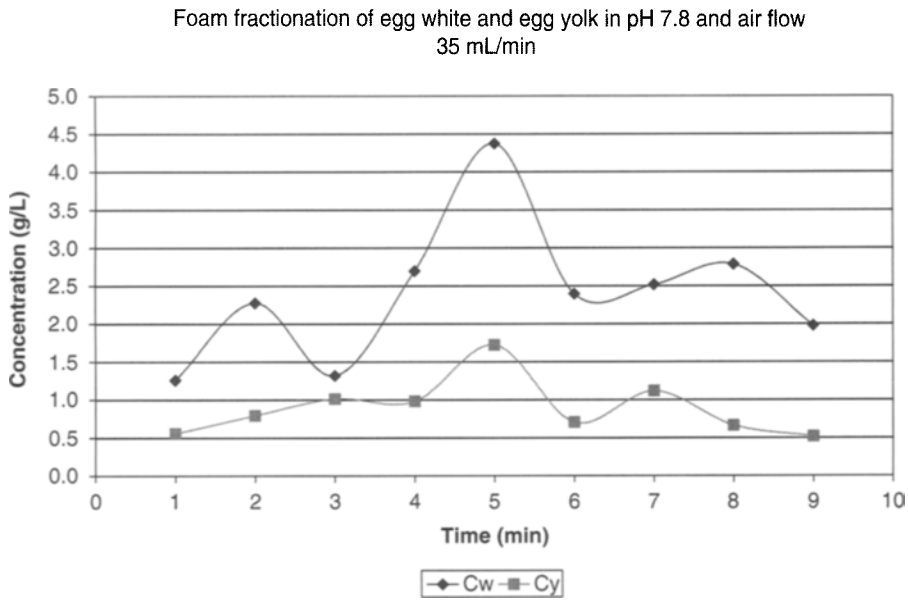


**Fig. 4.** The concentration of egg white and egg yolk foamate as a function of time at pH 7.8 and airflow rate of 35 mL/min.

The absorbance of an unknown sample found at either 520 nm or 400 nm, $A_1$ and $A_2$ respectively, can be found experimentally using a spectrophotometer for a sample with unknown concentration. It is imperative that $\lambda_1$ and $\lambda_2$ be selected to minimize the chance that the $(k_2k_3–k_1k_4)$ term (sometimes called the Wronskian in mathematics *[11]*) does not equal zero. Given $k_1$ and $k_3$ from the respective slopes from the developed calibration curves (consisting of three points each, in addition to the origin) for white and yolk at $\lambda_1 = 520$ nm, and $k_2$ and $k_4$ from the respective slopes of white and yolk (consisting of three points, respectively, at $\lambda_2 = 400$ nm [approx 420 nm], in keeping with earlier work with a different egg albumin absorbance-wavelength scan, absorbing at a local peak of 420 nm), Eqs. 1 and 2 can be combined to form Eqs. 3 and 4. Given $A_1$ and $A_2$ from experimentation, the concentration of egg white, $C_w$, and the concentration of egg yolk, $C_y$ can be calculated. Here, $k_1 = 0.013$ L/g, $k_2 = 0.028$ L/g, $k_3 = 0.24$ L/g, and $k_4 = 0.26$ L/g. Typical values of $C_w$ and $C_y$ as functions of time are given in Fig. 4. Because the egg white tended to be produced in higher concentration than the yolk, the egg white concentration is depicted above the yolk concentration. Thus, the visual observation noted in Fig. 2 is verified by the absorption results in Fig. 4. The actual measured effluent samples are diluted down (1000X) with deionized water to the concentration levels in order to read the respective calibration graphs in the Beer's law range. The actual reported concentrations take the dilution factor into consideration. It is suggested that future work focus on measurement of the effect of

the airflow rate and the pH on the foam fractionation process. If the airflow rate is reduced then the separation will take longer, but perhaps, the separation between yolk and white may be more extensive.

## Conclusions

The observed separation of a binary mixture from a whole egg using foam fractionation, demonstrates that it is possible to separate two phases of protein groups as a first step in more complete protein separations. This inexpensive method can possibly be used to separate other colored mixtures of proteins (such as seen in the separation of hydrophobic protein in beer foam from hydrophilic protein in the beer bulk phase, both within a glass of beer) found in natural substances. The similarity between egg albumin (ovalbumin) and blood albumin (serum albumin) might open up the possibility of less expensive separations before more complete chromatographic separations in the medical world. Blood albumin must be separated out of whole blood in order to use it in some medical applications such as the treatment of shock.

## Acknowledgments

We are pleased to acknowledge the initial assistance of the students of the Fall 2005 (ES 101, Section 8) Freshman Seminar in the Engineering School of Vanderbilt University: Grant M. Bouchillon, Paul A. Capelli, Sesha N. Pinnaduwage, and Grant T. England.

## References

1. Chai, J., Loha, V., Prokop, A., and Tanner, R. (1998), *J. Agric. Food Chem.* **46,** 2868–2872.
2. Burapatana, V., Booth, E., Prokop, A., and Tanner, R. (2005), *Ind. Eng. Chem. Res.* **44,** 4968–4972.
3. Wikipedia Contributors, "Egg White", *Wikipedia, The Free Encyclopedia,* http://en.wikipedia.org/wiki/Egg_white (accessed April 22, 2006).
4. Wikipedia Contributors, "Egg Yolk", *Wikipedia, The Free Encyclopedia,* http://en.wikipedia.org/wiki/Egg_yolk (accessed April 22, 2006).
5. Eiamwat, J., Loha, V., Prokop, A., and Tanner, R. (1998), *Appl. Biochem. Biotechnol.* **70–72,** 559–567.
6. Karger, B., Snyder, L., and Horvath, C. (1973), In: *An Introduction to Separation Science,* Wiley and Sons, New York, pp. 411–436.
7. Caprette, D. (2006), "Components of Mammalian Blood," *Experimental Biosciences,* http://www.ruf.rice.edu/bioslabs/studies/sds-page/blood_tissue.html (accessed April 25, 2006).
8. Bhattaharya, P., Ghosal, S. K., and Sen, K. (1999), *Sep. Sci. Technol.* **26,** 1279–1293.
9. *The Merck Index,* 10th ed., (1983), Windholz, M. and Rathway, N. J. (eds.), Merck & Co., Inc., no. 1880 990p.
10. Egg and Fowl Allergens, *LabSpec.* http://www.labspec.co.za/l_egg.htm (accessed April 27, 2006).
11. Rainville, E. D. (1958), Elementary Differential Equations, 2nd ed., The Macmillan Co., New York.

0273-2289/1559-0291 (Online)/07/136–140/935–946/$30.00

# Synthesis of Poly(Sorbitan Methacrylate) Hydrogel by Free-Radical Polymerization

GWI-TAEK JEONG,[1,6] KYOUNG-MIN LEE,[1] HEE-SEUNG YANG,[1] SEOK-HWAN PARK,[1] JAE-HEE PARK,[1] CHANGSHIN SUNWOO,[1,2] HWA-WON RYU,[1,2] DOMAN KIM,[1,2] WOO-TAE LEE,[2] HAE-SUNG KIM,[7] WOL-SEOG CHA,[8] AND DON-HEE PARK*,[1–5]

*[1]School of Biological Sciences and Technology, E-mail: dhpark@chonnam.ac.kr; [2]Faculty of Applied Chemical Engineering; [3]Research Institute for Catalysis; [4]Biotechnology Research Institute; [5]Institute of Bioindustrial Technology; [6]Engineering Research Institute, Chonnam National University, Gwangju 500-757, Korea; [7]Department of Chemical Engineering, Myongji University, Yongin 449-728, Korea; and [8]Department of Chemical Engineering, Chosun University, Gwangju 501-759, Korea*

## Abstract

Hydrogels are materials with the ability to swell in water through the retention of significant fractions of water within their structures. Owing to their relatively high degree of biocompatibility, hydrogels have been utilized in a host of biomedical applications. In an attempt to determine the optimum conditions for hydrogel synthesis by the free-radical polymerization of sorbitan methacrylate (SMA), the hydrogel used in this study was well polymerized under the following conditions: 50% (w/v) SMA as monomer, 1% (w/w) α, α′-azo-*bis*(isobutyro-nitrile) as thermal initiator, and 1% (w/w) ethylene glycol dimethacrylate as cross-liking agent. Under these conditions, the moisture content of the polymerized SMA hydrogel was higher than in the other conditions. Moreover, the moisture content of the poly(SMA) hydrogel was also found to be higher than that of the poly(methyl methacrylate [MMA]) hydrogel. When the Fourier transform–infrared spectrum of poly(SMA) hydrogel was compared with that of poly(MMA) hydrogel, we noted a band at 1735–1730/cm, which did not appear in the Fourier transform–infrared spectrum of poly(MMA). The surface of the poly(SMA) hydrogel was visualized through scanning electron microscopy, and was uniform and clear in appearance.

**Index Entries:** Free radical hydrogel; moisture content; polymerization; sorbitan methacrylate.

*Author to whom all correspondence and reprint requests should be addressed.

## Introduction

Biomaterials can be made up of metals, ceramics, biocompatible polymers, and their composites. Biocompatible polymers diverge regarding modulus from flexible elastomers to strong fibers, and can be readily processed into a variety of shapes. Hydrogels constitute one of the more promising classes of biomaterials. Hydrogels are hydrophilic polymeric networks, which have been shown to absorb significant quantities of water, in a range of 10% up to thousands of times their dry weight *(1–4)*. Recently, a host of studies have reported on the myriad possible applications of sugar-containing polymeric materials, which can be synthesized from sugar esters. Sugars are a relatively attractive group of multifunctional compounds, owing to the fact that they are both biologically relevant, and contain multiple hydroxyl groups. Sugar esters, which contain sugar molecules, have become the focus of increased interest of late, and have already been utilized in a variety of applications in the medical and industrial fields *(3–6)*. Sugars can also harbor functional glycosylation groups, which serve multifarious functions, evidencing different biological activity, surface activity, optical activity, optical separation activity, stereostructure, biodegradability, biocompatibility, and biostability, depending on the type of functional group harbored and the stereo-structural bonding methods utilized *(1,7)*.

The term "hydrogel" refers to a class of materials with the ability to swell in water, and to retain a significant fraction of that water within their structures. The classic hydrogel is a colloid gel consisting of water molecules held together by crosslinked molecular chains. The characteristic water absorption capabilities of hydrogels are dependent on the presence of hydrophilic groups within the substrate. Hydrogels have been used extensively in a host of biomedical applications, including wound dressings, artificial organs, and delivery carriers for bioactive agents, largely because of their considerable biocompatibility *(1,3,8,9)*. High moisture content and low interfacial tension with the surrounding biological environment are the two most salient factors regarding hydrogel biocompatibility *(10,11)*.

The moisture content of hydrophilic materials has important properties, and bears a great deal of importance in regard to other characteristics of the materials. In order to overcome the problems inherent to inadequate moisture content, acryl groups can be glycosylated using glycosyl materials, the molecules of which harbor a wealth of hydroxyl groups. Then, according to the regioselective synthesis method used and the degree of substitution, the glycosylated materials can be constructed for enhanced moisture contents *(12,13)*.

The development of acryl monomers such as poly(MMA), which have fairly simple structures with a small number of carbons, and exhibit polymerizational vinyl radical sharing among the hydroxyl and carboxyl groups, was followed rapidly by the development of a wide

variety of novel hydrogel polymers. This pursuit for new compounds was driven by competition for a favorable position within this new emerging market *(1,3)*.

The hydrogel synthesis of several glycosylated esters had reported *(2,14–16)*. The poly(MGAA) and poly(MGMAA) that seeded to applicable for wound dressing agent was well conformed by free-radical polymerization with α, α′-azo-*bis*(isobutyro-nitrile) (AIBN) *(2)*. Magnani et al. *(14)* reported polysaccharide hydrogels, which were made with polysaccharide components of hyaluronane, alginate, and carboxymethyl-cellulose. Sucrose-based hydrogels were found to be nontoxic, highly water absorbable, and eventually had applications for medical applications *(15)*. Draye et al. *(16)* reported the dextran dialdehyde crosslinked hydrogels for wound dressing agents. However, the hydrogel synthesis of poly(sorbitan methacrylate [SMA]) and its property have not previously reported.

Polymerization is the process by which monomer molecules are induced to react chemically, resulting in the formation of either linear chains or a three-dimensional network of polymer chains. There are many forms of polymerization, and different systems have been formulated for their categorization. The primary categories of polymerization are chain-growth reaction and step-growth reaction *(15)*.

The principal objective of this study was to determine the optimum conditions for the polymerization of SMA, which is glycosylated with sorbitan and vinyl methacrylate, and to compare the moisture content with poly(SMA) and poly(MMA). We conducted experiments in which the monomer, thermal initiator, and crosslinking agent were tested at a variety of concentrations for optimization of polymerization. The polymerized hydrogels were then assessed specifically regarding moisture content, which is one of the primary criteria relevant to the flexibility and biocompatibility of a constructed hydrogel.

## Materials and Methods

### *Chemicals*

Novozym 435 (Lipase B from *Candida antarctica*, EC 3.1.1.3, a nonspecific lipase immobilized on a macroporous acrylic resin, 1–2% moisture content, 10,000 Propyl Laurate Units/g) was purchased from Novo Nordisk A/S (Bagsvaerd, Denmark). The D-sorbitol and *t*-butanol used in this study was obtained from the Sigma-Aldrich Chemical Co. (St. Louis, MO). The *p*-toluenesulfonic acid (*p*-TSA) and MMA were purchased from Yakuri Pure Chemicals (Osaka, Japan). The vinyl methacrylate was purchased from Tokyo Kasei Kogyo Co. (Tokyo, Japan). AIBN, used as a thermal initiator in this study, was provided by Junsei Chemicals (Japan), and the ethylene glycol dimethacrylate (EGDMA) used in this study was from the Sigma-Aldrich Chemical Co. All other chemicals used were of analytical

grade, and the solvent was dried using molecular sieves (Yakuri Pure Chemicals Co.) for 1 d before use.

### 1,4-Sorbitan Preparation and Enzymatic Esterification

All dehydration reactions (sorbitol cyclization) for the synthesis of 1,4-sorbitan using *p*-TSA in a solvent-free process were conducted as was previously described *(4)*. The dehydration reactions were carried out for 2 h at 130 ± 1°C, under reduced pressure (200 mmHg). The reactor volume was 50 mL. The reaction temperature was controlled with an oil bath, equipped with a proportional and integral differential (PID) temperature controller. Agitation was conducted with a magnetic bar, spinning at approx 200 rpm.

We conducted esterification through alcoholysis. Esterification for the synthesis of 1,4-sorbitan esters with immobilized lipase was conducted as described in a previous report *(4)*. The reactions were initiated through the addition of 7.5% (w/v) of Novozym 435 and 0.05% (w/v) of hydroquinone, with an initial 1,4-sorbitan concentration of 50.0 g/L. The reaction of 1,4-sorbitan to vinyl methacrylate (at a molar ratio of 1 : 4) resulted in 170 min of synthesis at 45 ± 1°C. The reaction temperature was controlled using a water bath equipped with a PID temperature controller. Mixing was conducted using a magnetic stirrer, spinning at approx 200 rpm. The condenser prevented the evaporation of the reactant (*t*-butanol).

### Purification of SMA

After esterification, the mixture was filtered to remove enzymes, and dried under reduced pressure at 40°C. An equivalent volume of *n*-hexane was added to the reaction mixture. The mixture was then vigorously stirred for 2 h, and the upper phase was recovered and then vaporized at 40°C under reduced pressure. In order to separate the SMA and other compounds from the reaction mixtures, open column chromatography (PYREX®, 25 × 250 $mm^2$) was conducted, using silica gel (Merck 7734, 70–230 mesh, 300.0 g) and an autofraction collector, at 180-s time intervals. A chloroform : hexane (2.5 : 1 [v/v]) mixture was used as the mobile phase. The flow rate was 10 mL/min, and 20 mL volume of the sample was loaded into the chromatograph.

### Synthesis of Hydrogel by Free-Radical Polymerization

The synthesized and purified monomers, SMA and MMA, were then utilized in the free-radical polymerization process. The monomers were dissolved in chloroform. The initial volume of monomer solution was 5 mL. The thermal initiator (AIBN) and crosslinking agents (EGDMA) were added on the basis of the total monomer concentration. Free-radical polymerizations were conducted with five concentrations of monomer (10, 25, 50, 75, and 90% [w/v], respectively), 0.5–5% (w/w) of thermal initiator and 0.5–5% (w/w) of crosslinking agent, as was described in Table 1. Polymerization was allowed to proceed for 2 h at 70°C, without agitation.

Table 1
Experimental Conditions of Free-Radical Polymerization

| Experimental variables | Experimental conditions | | |
|---|---|---|---|
| | Monomer (% [w/v]) | Thermal initiator (% [w/v]) | Crosslinking agent (% [w/v]) |
| Monomer concentration | 10, 25, 50, 75, 90 | 1 | 1 |
| Thermal initiator concentration | 50 | 0.5–5 | 1 |
| Crosslinking agent concentration | 50 | 1 | 0.5–5 |

### *Purification of Poly(SMA) and Poly(MMA)*

In order to remove the initiator, unreacted monomer and impurities potentially present in the synthesized hydrogels, the poly(SMA) and poly(MMA) were purified as described below. At the end of the polymerization, the synthesized poly(SMA) and poly(MMA) hydrogels were immersed in 10 vol of ethanol (ethanol : reactant [v/v]) for 24 h, and subsequently treated with distilled water for an additional 24 h. Three treatments with ethanol and distilled water were applied. Then, the synthesized hydrogels were immersed in 10 vol of acetone for 24 h. Finally, after acetone removal, the hydrogels were washed with water, dried, and stored in a desiccator.

### *Structural Analysis of Poly (SMA) by FT–IR and SEM*

The poly(SMA) was structurally analyzed through Fourier transform–infrared (FT–IR) (Nicolet 520P, Nicolet). The FT–IR sample of polymerized SMA was used in powder form. The surface of the poly(SMA) synthesized under optimal conditions was then visualized through scanning electron microscopy (SEM; JSM-5400, JEOL).

### *Moisture Content Measurement of Poly(SMA) and Poly(MMA) Hydrogels*

Dried poly(SMA) and poly(MMA) hydrogels were cut to a diameter of 10 mm and a thickness of 5 mm, then immersed for 48 h in distilled water at room temperature. After removing the water from the surface of the hydrogels using filter paper, the hydrogels were then weighed. After weighing, the hydrated hydrogels were dried for 48 h at 40°C, and then measured. The moisture contents of the hydrogels were calculated through the following formula:

$$\text{Moisture content (\%)} = \frac{Ws - W_0}{Ws} \times 100$$

where $W_s$ is the weight of the swollen hydrogel (g) and $W_0$ is the weight of the dried hydrogel (g).

## Results and Discussion

In the free-radical polymerization process used in the synthesis of poly(SMA) from SMA, several factors have been shown to affect both the polymerization and moisture content, including the reaction solvent, reaction temperature, monomer, thermal initiator, crosslinking agent, and so on *(1,14)*. The initial step of this study involved the identification of factors likely to affect polymerization. In order to achieve this objective, we assessed the screening of several factors for the free-radical polymerization experiments, testing the monomer, thermal initiator, and crosslinking agent at different concentrations.

### *Effect of Different Monomer Concentrations*

Free-radical polymerizations were conducted with three different monomer concentrations (10, 25, 50, 75, and 90% [w/v], respectively of reaction solution), in order to characterize the effects inherent to monomer concentration. Figures 1 and 2 show the results regarding polymerization degree and moisture content. In Fig. 1, sample A, which had a lower monomer concentration (10% [w/v]) than the other samples, exhibited a lower degree of polymerization when compared with the others. Sample E, which contained an abundant quantity of SMA as a monomer, evidenced a higher degree of polymerization than did the other samples. Sample C exhibited a suitable degree of polymerization, with no decrease in total volume. The experiments in which MMA was used as a monomer exhibited similar tendencies to those in which SMA was used as a monomer. Sample F, with a lower concentration of MMA than the other samples, exhibited a lower degree of polymerization when compared with the others; and sample J, with an abundant amount of monomer, scored higher than the other samples. The moisture contents of the polymerized hydrogels are compared in Fig. 2. The moisture content of the polymerized hydrogels was altered by the residual water contained in the hydrogels. The moisture content of the hydrogels polymerized with SMA was found to be higher than in those polymerized with MMA. Also, the moisture contents of hydrogels containing 75% or higher concentrations of monomer were lower than in the other samples. The samples polymerized with 25 and 50% of monomer evidenced similar moisture contents, of approx 37%.

### *Effect of Different Thermal Initiator Concentrations*

In order to evaluate the effects of different concentrations of thermal initiator on polymerization, 0.5, 1, 2, 3, and 5% (w/w) of thermal initiator (AIBN), relative to total monomer concentration (50% [w/v]) was added to the monomer solution, and subsequently polymerized for 2 h at 70°C,

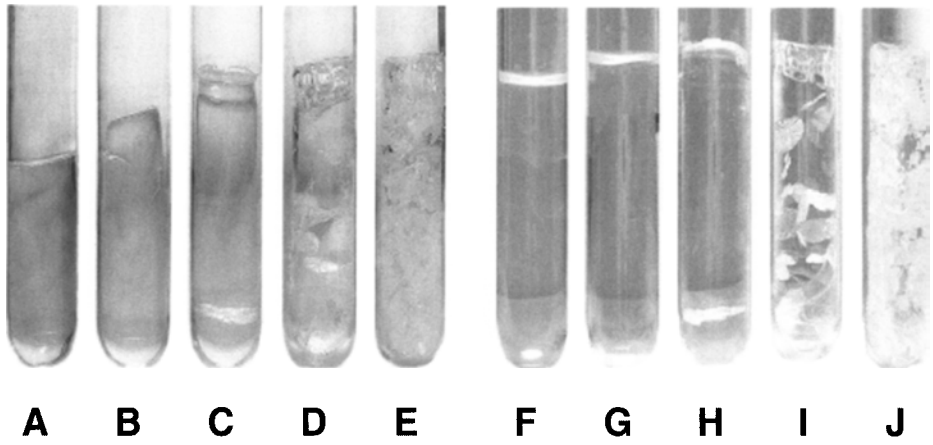


**Fig. 1.** Photographs of polymerization with different monomer concentrations. Monomers: SMA and MMA; **(A)** SMA 10% (w/v), **(B)** SMA 25% (w/v), **(C)** SMA 50% (w/v), **(D)** SMA 75% (w/v), **(E)** SM A 90% (w/v), **(F)** MMA 10% (w/v), **(G)** MMA 25% (w/v), **(H)** MMA 50% (w/v), **(I)** MMA 75% (w/v), and **(J)** MMA 90% (w/v).

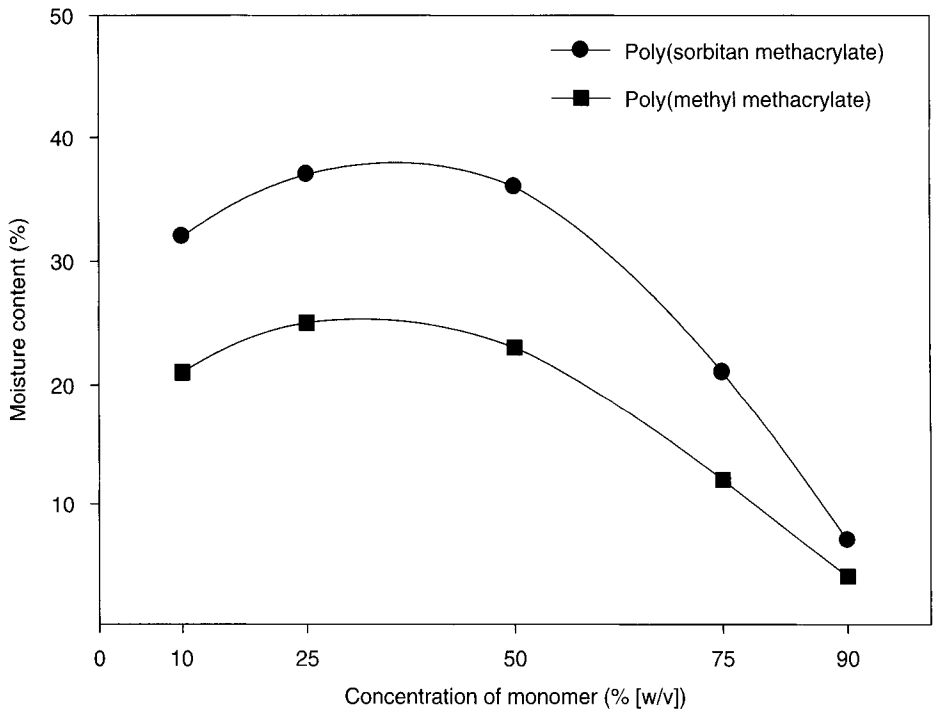


**Fig. 2.** Moisture contents of hydrogel polymerized with concentration changes of monomer.

without agitation. The results of polymerization are shown in Figs. 3 and 4. In Fig. 3, sample A, with lower thermal initiator concentration (0.5% [w/w]) than was seen in the other samples, exhibited a lower degree of polymerization when compared with the others. A greater degree of polymerization

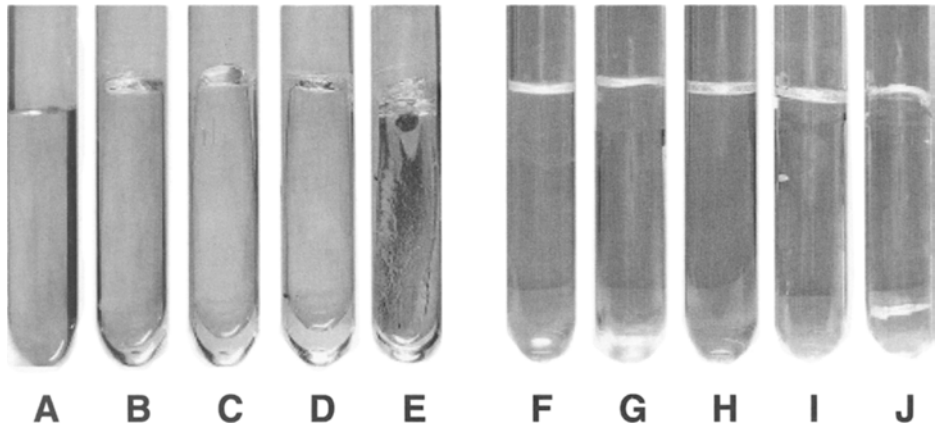


**Fig. 3.** Photographs of polymerization with different thermal initiator concentrations. Monomers: SMA **(A–E)** and MMA **(F–J)**; thermal initiator (AIBN) concentration, **(A)** 0.5% (w/w), **(B)** 1% (w/w), **(C)** 2% (w/w), **(D)** 3% (w/w), **(E)** 5% (w/w), **(F)** 0.5% (w/w), **(G)** 1% (w/w), **(H)** 2% (w/w), **(I)** 3% (w/w), and **(J)** 5% (w/w).

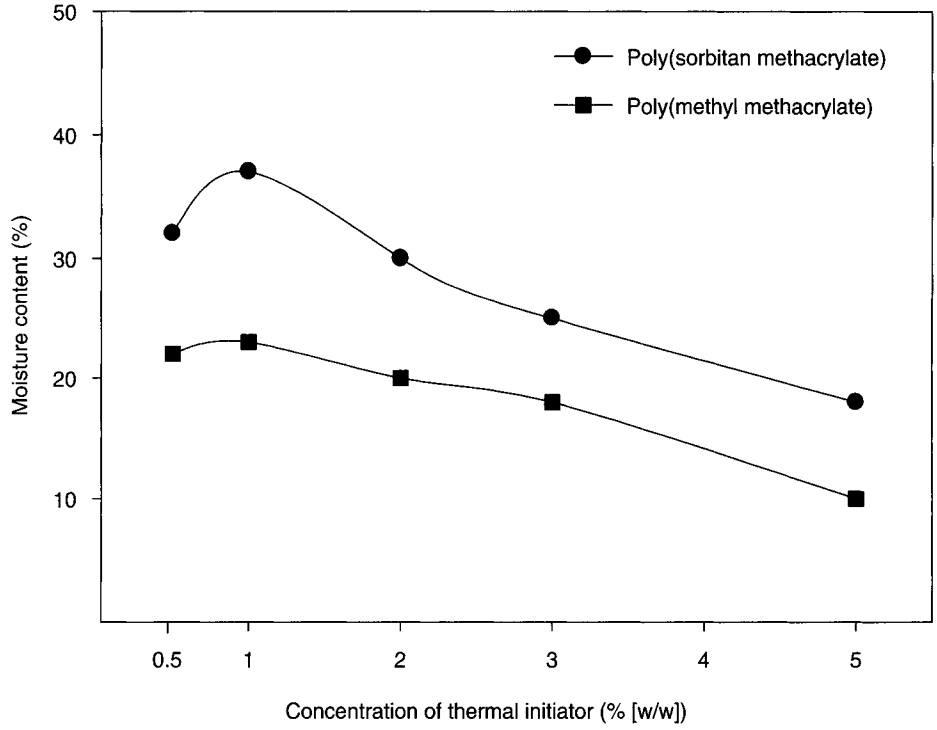


**Fig. 4.** Moisture contents of hydrogel polymerized with different thermal initiator concentrations.

was detected in sample E than in the other samples. Sample F, which contained less AIBN than the other samples, evidenced a degree of polymerization similar to the other samples. Polymerization degree, then, was not particularly influenced by the concentration of added AIBN, but when the

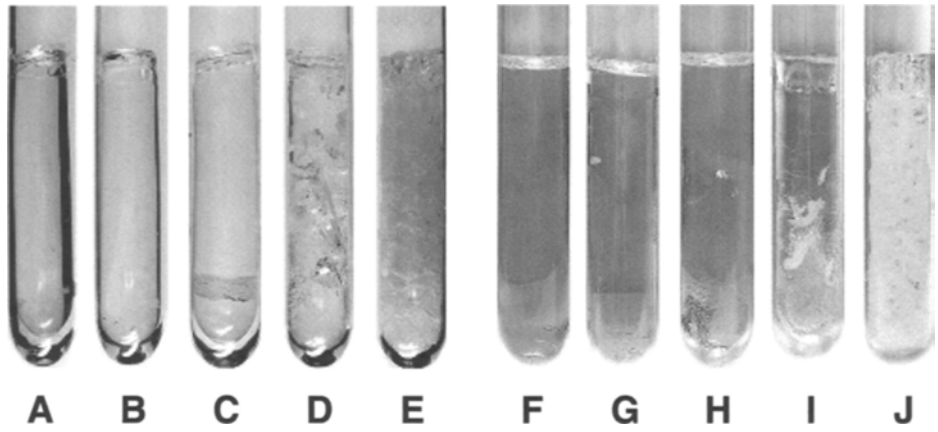


**Fig. 5.** Photographs of polymerization with different crosslinking agent concentrations. Monomers: SMA **(A–E)** and MMA **(F–J)**; crosslinking agent (EGDMA) concentration, **(A)** 0.5% (w/w), **(B)** 1% (w/w), **(C)** 2% (w/w), **(D)** 3% (w/w), **(E)** 5% (w/w), **(F)** 0.5% (w/w), **(G)** 1% (w/w), **(H)** 2% (w/w), **(I)** 3% (w/w), and **(J)** 5% (w/w).

AIBN concentration was in excess of 5% (w/w), node formation was detected. We noted no obvious differences in the types of monomers. Changes in moisture content according to the amount of added AIBN are presented in Fig. 4. The moisture contents of the hydrogels polymerized with SMA were generally higher than the hydrogels polymerized with MMA. The moisture contents of the hydrogel to which more than 3% (w/w) AIBN was added were lower than in the others. In the samples to which 1% (w/w) AIBN was added, the moisture content was higher than that of others.

### *Effect of Different Crosslinking Agent Concentrations*

The effects exerted by different concentrations of crosslinking agent (EGDMA; 0.5, 1, 2, 3, and 5% [w/w], respectively) on the degree of polymerization degree and moisture contents in the hydrogels were determined through free-radical polymerization, as is shown in Figs. 5 and 6. In Fig. 5, sample A, to which less EGDMA (0.5% [w/w]) was added than to the other samples, exhibited a lower degree of polymerization than was seen in the other samples. A higher degree of polymerization was detected in sample E (5% [w/w]) than in the other samples. Sample A evidenced a degree of polymerization comparable with those of the others. Node formation was detected in the samples to which more than 1% (w/w) EGDMA was added, the polymerized hydrogel evidenced nodes. The effects of EGDMA on hydrogel moisture contents are shown in Fig. 6. The moisture contents of hydrogels polymerized with SMA were found to be higher than those polymerized with MMA. The moisture contents of hydrogels containing 1% or more EGDMA were lower than those of the other samples. 0.5 and 1% (w/w) of EGDMA did not appear to influence the moisture contents of hydrogels of polymerized SMA to a significant

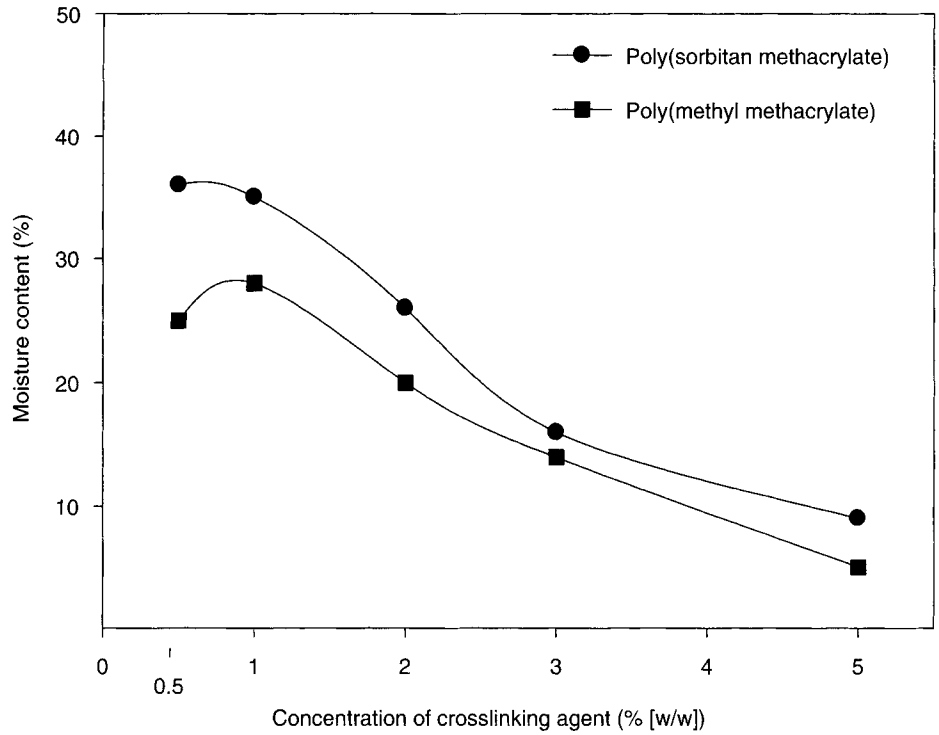


**Fig. 6.** Moisture contents of polymerized hydrogel with different crosslinking agent concentrations.

degree. Whereas, the moisture content of hydrogel of polymerized MMA is high at the concentration of 1% (w/w) of EGDMA.

### *Structure Analysis and Surface Observation of Poly(SMA)*

To confirm the polymerization of SMA, the structural analysis results of poly(SMA) were compared with the results of poly(MMA), through FT–IR spectroscopy. The FT–IR results are shown in Fig. 7. The band of polymerized SMA was confirmed at 1735–1730/cm (C=C), but the band of poly(MMA) was not confirmed. The band for the C–O span of the secondary alcohols appeared at 1200–1300/cm, and the O–H span evidenced a strong band at 2900–3000/cm, as well as a broad band at 3400–3500/cm, thereby indicating the presence of SMA. The surface of the poly(SMA), synthesized under optimal conditions and treated, was then observed through SEM, as was shown in Fig. 8. The surface was observed to have a uniform, clear appearance.

In this study, in order to maintain proper moisture contents in such hydrogel materials, we utilized SMA as a new monomer, which was glycosylated with a methacryl group and included many hydroxyl molecules for hydrogel polymerization, in order to overcome the aforementioned problem. Then, according to the selective synthesis method

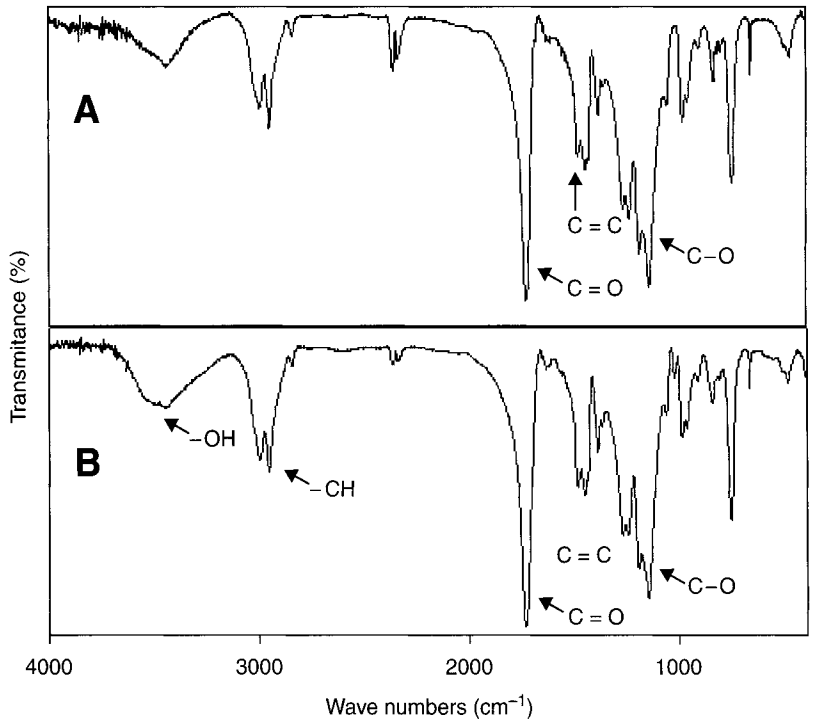


**Fig. 7.** Comparison of FT–IR spectra of poly(MMA) and poly(SMA). **(A)** Poly(MMA), **(B)** Poly(SMA).

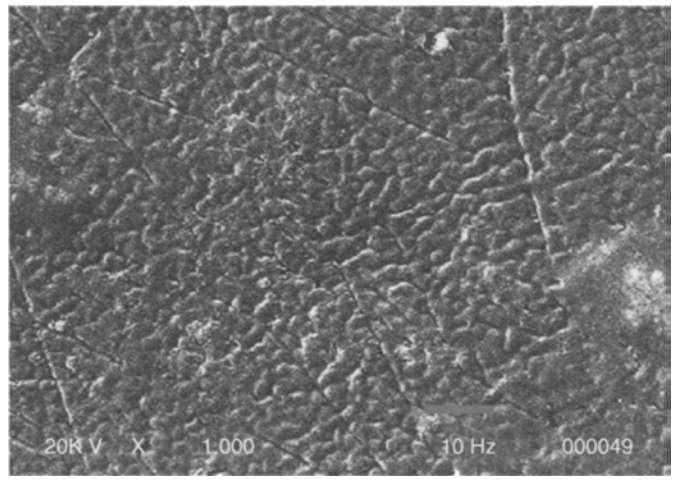


**Fig. 8.** SEM photograph of poly(SMA) under optimal conditions.

and degree of substitution, glycosylated materials such as SMA can enhance the moisture contents of polymerized hydrogels. Therefore, SMA is expected to prove an efficient monomer for sugar polymers with high hydrophilicity and biocompatibility, which might be used in the construction of medical materials.

## Acknowledgments

This work was supported by Korea Research Foundation Grant funded by the Korean Government (MOEHRD) (R05-2004-000-11185-0), and also supported partly by the Korean Ministry of Education & Human Resources Development through the second stage of BK21 program.

## References

1. Hanks, C. T., John, C. W., and Sun, Z. (1996), *Dent. Mater.* **12,** 186–193.
2. Park, D. W. (2003), *PhD Dissertation*, Yonsei University, Seoul, Korea.
3. Jeong, G. T., Byun, K. Y., Lee, W. T., et al. (2006), *Biochem. Eng. J.* **29,** 69–74.
4. Jeong, G. T., Lee, H. J., Kim, H. S., and Park, D. H. (2006), *Appl. Biochem. Biotechnol.* **129–132,** 265–277.
5. Park, D. W. and Kim, H. S. (2004), *J. Korean Oil Chem. Soc.* **21,** 37–44.
6. Berger, J., Reist, M., Mayer, J. M., Felt, O., Peppas, N. A., and Gurny, R. (2004), *Eur. J. Pharm. Biopharm.* **57,** 19–34.
7. Jeong, G. T. and Park, D. H. (2006), *Enzyme Microbiol. Technol.* (in press).
8. Taguchi, T., Kishida, A., Sakamoto, N., and Akashi, M. (1998), *J. Biomed. Mater. Res.* **41,** 386–391.
9. Coviello, T., Grassi, M., Rambone, G., et al. (1999), *J. Controlled Release* **60,** 367–378.
10. Kim, S. K., Shin, J. S., Moon, Y. U., and Lee, K. Y. (1996), *J. Korean Ind. Eng. Chem.* **7,** 136–144.
11. Cunningham, M. F. (2002), *Prog. Polym. Sci.* **27,** 1039–1067.
12. Jalbert, I. and Stapleton, F. (2005), *Contact Lens Anterior Eye* **28,** 3–12.
13. Liu, Z. and Pflugfelder, S. C. (2000), *Ophthalmology* **107,** 105–111.
14. Magnani, A., Rappuoli, R., Lamponi, S., and Barbucci, R. (2000), *Adv. Technol.* **11,** 488–495.
15. Chen, X., Martin, B. D., Neubauer, T. K., Linharbt, R. J., Dordick, J. S., and Rethwisch, D. G. (1995), *Carbohydr. Polym.* **28,** 15–21.
16. Draye, J. P., Delaey, B., de Voorde, A. V., Bulcke, A. V. D., Reu, B. D., and Schacht, E. (1998), *Biomaterials* **19,** 1677–1687.

0273-2289/1559–0291 (Online)/07/136–140/947–956/$30.00

# Hybrid Thermochemical/Biological Processing

*Putting the Cart Before the Horse?*

**ROBERT C. BROWN***

*Iowa State University, Center for Sustainable Environmental Technologies, 286 Metals Development Building, Ames, IA 50011, E-mail: rcbrown@iastate.edu*

## Abstract

The conventional view of biorefineries is that lignocellulosic plant material will be fractionated into cellulose, hemicellulose, lignin, and terpenes before these components are biochemically converted into market products. Occasionally, these plants include a thermochemical step at the end of the process to convert recalcitrant plant components or mixed waste streams into heat to meet thermal energy demands elsewhere in the facility. However, another possibility for converting high-fiber plant materials is to start by thermochemically processing it into a uniform intermediate product that can be biologically converted into a bio-based product. This alternative route to bio-based products is known as hybrid thermochemical/biological processing. There are two distinct approaches to hybrid processing: (a) gasification followed by fermentation of the resulting gaseous mixture of carbon monoxide (CO), hydrogen ($H_2$), and carbon dioxide ($CO_2$) and (b) fast pyrolysis followed by hydrolysis and/or fermentation of the anhydrosugars found in the resulting bio-oil. This article explores this "cart before the horse" approach to biorefineries.

**Index Entries:** Biochemical processing; biorefinery; gasification; lignocellulose; pyrolysis; thermochemical processing.

## Introduction

The Biomass Research and Development Technical Advisory Committee (2002) of the US Departments of Energy and Agriculture defines a biorefinery as: "A processing and conversion facility that (a) efficiently separates its biomass raw material into individual components and (b) converts these components into marketplace products, including biofuels, biopower, and conventional and new bioproducts" *(1)*. In the conventional view of a biorefinery, the separated components are monosaccharides and lignin. This separation involves physical and chemical pretreatments and enzymatic hydrolysis. The carbohydrate fractions are then biologically

*Author to whom all correspondence and reprint requests should be addressed.

converted into ethanol and other bio-based products. Lignin may be burned for process heat, gasified to syngas, or processed into bio-based products. Thus, biological treatments are followed by high-temperature thermochemical treatments. An alternative approach is to subject biomass to thermochemical treatments that yield a uniform intermediate product, which can then be biologically converted into a bio-based product. There are two distinct approaches to hybrid processing:

1. Fast pyrolysis followed by hydrolysis and/or fermentation of the anhydrosugars found in the resulting bio-oil.
2. Gasification followed by fermentation of the resulting gaseous mixture of carbon monoxide (CO), hydrogen ($H_2$), and carbon dioxide ($CO_2$).

## Bio-Oil Fermentation

Fast pyrolysis is the rapid thermal decomposition of organic compounds in the absence of oxygen to produce liquids, gases, and char *(2)*. Bio-oil from fast pyrolysis is a low-viscosity, dark-brown fluid with up to 15–20% water, which contrasts with the black, tarry liquid resulting from slow pyrolysis or gasification *(3)*. The bio-oil is a mixture of many compounds, although most can be classified as acids, aldehydes, sugars, anhydrosugars, and furans, derived from the carbohydrate fraction and phenolic compounds, aromatic acids, and aldehydes, derived from the lignin fraction. The higher heating values of pyrolysis liquids range between 17 MJ/kg and 20 MJ/kg with liquid densities of about 1280.0 kg/m$^3$. Assuming conversion of 72% of the biomass feedstock to liquid on a weight basis, yield of pyrolysis oil is about 560 L/t (dry) biomass.

Bio-oil fermentation is based on the observation that under rapid pyrolytic conditions, pure cellulose yields levoglucosan, an anhydrosugar with the same empirical formula as the monomeric building block of cellulose: $C_6H_{10}O_5$ *(4)*. Anhydrosugar is a sugar from which one or more molecules of water have been removed, resulting in the formation of an internal acetal structure (*see* Fig. 1). On the other hand, addition of a small amount of alkali inhibits the formation of levoglucosan and promotes the formation of hydroxyacetaldehyde and for slower heating rates and lower temperatures char rather than liquids is preferentially formed. These multiple reaction pathways for pyrolysis of cellulose are illustrated in Fig. 2 *(2)*.

Scott and coworkers *(5)* at the University of Waterloo in Ontario, Canada recognized that alkali in biomass catalyzed the char-forming pathway. If these cations are removed by soaking the feedstock in dilute acid before pyrolysis, the lignocellulose is depolymerized to anhydrosugars, primarily levoglucosan, at very high yields. Levoglucosan is readily hydrolyzed to glucose. Brown and his collaborators *(6)* evaluated the effect of alkali removal on the pyrolytic products of cornstover. Three pretreatments were evaluated: acid hydrolysis, washing in dilute nitric acid, and

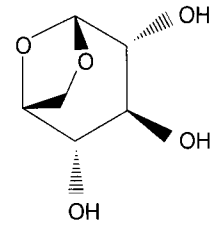


**Fig. 1.** Chemical structure for levoglucosan (1,6-anhydro-β-D-glucose).

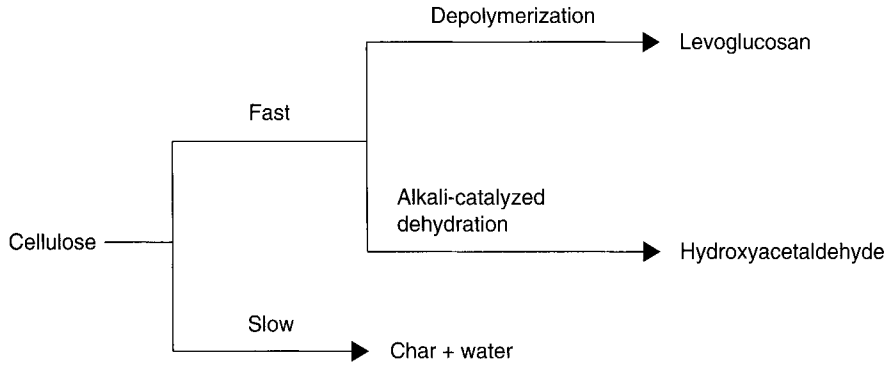


**Fig. 2.** Reaction pathways in fast pyrolysis.

washing in dilute nitric acid with the addition of $(NH_4)_2SO_4$ as a pyrolytic catalyst. All three acid treatments were able to substantially increase the yield of anhydrosugars, as shown in Table 1. Acid hydrolysis of this anhydrosugar yielded 5% solutions of glucose and other simple sugars.

The resulting glucose solutions can be fermented, as demonstrated by Prosen et al. *(7)*. However, the resulting substrate derived from the bio-oil contains fermentation inhibitors that must be removed or neutralized by chemical or biological methods. Chemical methods that have been evaluated on bio-oil derived substrate include solvent extraction, hydrophilic extraction, and adsorption extraction *(8)*. Khiyami *(9)* explored the use of biofilms of *Pseudomonas putida* and *Streptomyces setonii* to remove toxins from bio-oil.

One manifestation of a biorefinery based on fermentation of bio-oil is illustrated in Fig. 3. Fibrous biomass is pretreated with dilute acid to simultaneously remove alkali and hydrolyzes the hemicellulose fraction to pentose. The remaining fraction, containing cellulose and lignin, is pyrolyzed at 500°C to yield char, gas, and bio-oil. The bio-oil is separated into pyrolytic lignin and levoglucosan-rich aqueous phase. The char, gas, and lignin are burned to generate steam for distillation and other process heat requirements of the plant while the levoglucosan is hydrolyzed to hexose. The pentose and hexose are fermented to ethanol.

Table 1
Products (maf wt%) of Pyrolysis for Different Pretreatments of Cornstover

| | No pretreatment | Acid hydrolysis | Demineralization | Demineralization with catalyst |
|---|---|---|---|---|
| *Pyrolysis products (wt%)* | | | | |
| Char | 15.8 | 13.2 | 13.2 | 15.9 |
| Water | 2.57 | 10.6 | 10.4 | 7.96 |
| Organics | 59.1 | 67.2 | 68.5 | 67.7 |
| Gases | 22.6 | 9.02 | 7.88 | 8.44 |
| *Organics (wt%)* | | | | |
| Anhydrosugars | 2.75 | 22.3 | 23.4 | 28.1 |
| Aldehydes | 14.4 | 7.6 | 3.7 | 4.6 |
| Carboxylic acids | 6.0 | 1.5 | 1.3 | 1.1 |
| Acetol | 4.53 | Trace | Trace | Trace |
| Pyrolytic lignin | 33.40 | 16.89 | 17.74 | 20.08 |

maf: moisture, ash-free basis. From ref. *6*.

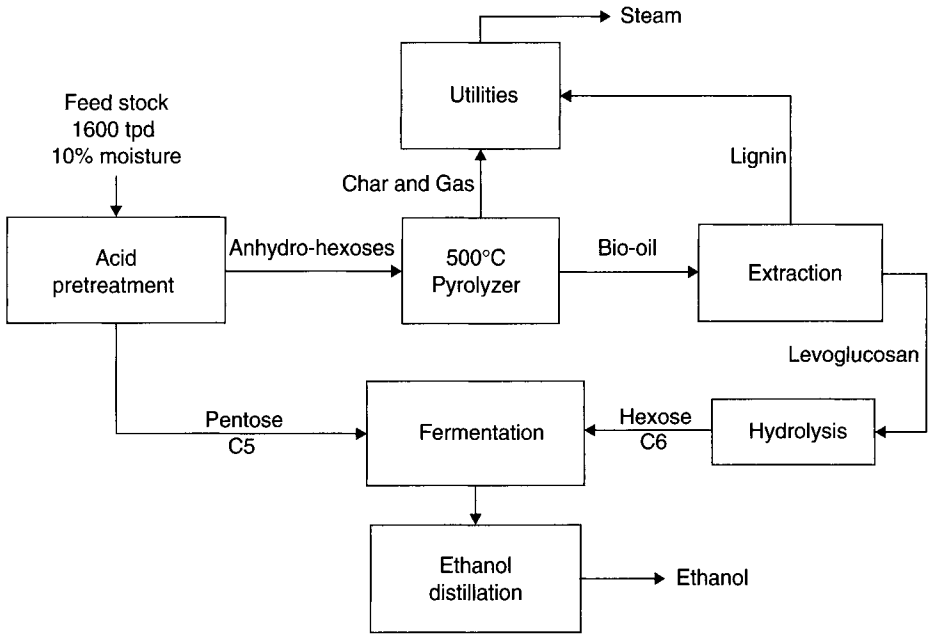


**Fig. 3.** Schematic of cellulosic biomass-to-ethanol based on fast pyrolysis *(10)*.

So and Brown *(10)* compared the cost of producing 95 million L/yr ethanol bio-oil fermentation, acid hydrolysis, and enzymatic hydrolysis. As summarized in Table 2, total capital investment for a plant based on fermentation of bio-oil was estimated to be $69 million, whereas the annual operating cost was about $39.2 million, resulting in an ethanol production cost of $0.42/L. This is about 23% higher than ethanol from plants based on acid hydrolysis and enzymatic hydrolysis of biomass, but well within

Table 2
Comparing Production Cost of Ethanol From Cellulosic Biomass for Three Conversion Technologies[a]

| | Fast pyrolysis | SSF[b] | Acid hydrolysis |
|---|---|---|---|
| Annual ethanol output | 95 million L | 95 million L | 95 million L |
| Annual biomass input | $240 \times 10^6$ kg | $244 \times 10^6$ kg | $238 \times 10^6$ kg |
| Total capital | $69 million | $64 million | $67 million |
| Raw materials ($46/t) | $11.1 million | $11.3 million | $11.0 million |
| Labor, utilities,[c] and maintenance | $6.18 million | $0.9 million | $2.13 million |
| Indirect costs | $8.07 million | $7.13 million | $7.21 million |
| Annual capital charges | $13.8 million | $12.8 million | $13.3 million |
| Annual operating costs | $39.2 million | $32.1 million | $33.7 million |
| Production cost of ethanol | $0.42/L | $0.34/L | $0.35/L |

From ref. *10*.
[a]1997 US$.
[b]Simultaneous saccharification and fermentation (enzymatic hydrolysis).
[c]Includes credit for steam generation for SSF and acid hydrolysis processes.

the uncertainty of the analysis (33%). The presence of lignin, hemicellulose, and various inorganic compounds in fibrous biomass results in more than a hundred chemical products, many of them not only unsuitable as a carbon and energy source for fermentations, but that are actually toxic to the microorganisms to be cultivated. Improved selectivity of pyrolytic reactions will be important in achieving high yields of fermentable carbohydrate. Understanding reaction pathways will be the key to success in this endeavor.

## Syngas Fermentation

Gasification is the high temperature (750–850°C) conversion of solid, carbonaceous fuels into flammable gas mixtures, sometimes known as synthesis gas or syngas, consisting of CO, $H_2$, $CO_2$, methane ($CH_4$), nitrogen ($N_2$), and smaller quantities of higher hydrocarbons. A number of microorganisms are able to utilize these gaseous compounds as substrates for growth and production. These include autotrophs, which use $C_1$ compounds as their sole source of carbon and hydrogen as their energy source and unicarbonotrophs, which use $C_1$ compounds as their sole source of both carbon and energy. Among the fermentation products are carboxylic acids, alcohols, esters, and hydrogen. In a comprehensive review on the prospects for ethanol from cellulosic biomass, Lynd *(11)* noted that syngas fermentation represents an "end run" with respect to acid or enzymatic hydrolysis of biomass because it avoids the costly and complicated steps of extracting monosaccharide from lignocellulose. It also has the potential for being more energy efficient because it effectively utilizes all the

constituents of the feedstock, whether cellulose, hemicellulose, lignin, starch, oil, or protein.

Syngas fermentation also has advantages compared with the use of inorganic catalyst in the production of synthetic fuels *(12)*. Most catalysts used in the petrochemical industry are readily poisoned by sulfur-bearing gases whereas syngas-consuming anaerobes are sulfur tolerant. In conventional catalytic processing, the $CO/H_2$ ratio of the syngas is critical to commercial operations whereas biological catalysts are not sensitive to this ratio; indeed, the water-gas shift reaction is implicit in the metabolism of autotrophic and unicarbonotrophic anaerobes. Gas-phase catalysts typically use temperatures of several hundreds of degree Centigrade and at least 10 atm whereas syngas fermentation proceeds at near ambient conditions. Finally, biological catalysts tend to be more product specific than inorganic catalysts.

Nevertheless, as described by Grethlein and Jain *(12)*, syngas fermentation has several barriers to overcome before it can be commercialized. Among these are relatively low rates of growth and production by anaerobes, difficulties in maintaining anaerobic fermentations, product inhibition by acids and alcohols, and difficulties in transferring relatively insoluble CO and $H_2$ from the gas phase to the liquid phase, whereby the anaerobes can utilize the gas. Of these, mass-transfer limitations probably represent the main bottleneck to commercializing this technology. However, studies by Worden and coworkers *(13)* give encouragement that the use of nontoxic surfactants and novel dispersion devices can enhance mass transfer through the generation of microbubbles to carry syngas into bioreactors.

Our syngas studies have focused on the coproduction of hydrogen and polyhydroxyalkonoates (PHA) from CO using the purple nonsulfur bacteria *Rhodospirillum rubrum* under dark reaction conditions *(14)*. PHAs are a class of polymers that are both bio-based and biodegradable with many applications in the production of plastic utensils and disposable medical supplies *(15)*.

Figure 4 illustrates the laboratory-scale system assembled to study syngas fermentation at Iowa State University. It consists of a 5.0 kg/h fluidized bed gasifier, a hot gas filter to remove particulate, a tar removal system based on activated carbon, and stirred tank reactor that serves as a syngas bioreactor. The system allows fermentation to be studied using realistic syngas mixtures derived from switchgrass, waste seed corn, and distiller's dried grains or artificial syngas when the gasifier is not operating. Typical gas composition from air-blown gasification with this system is 10 vol (%) $H_2$, 18 vol (%) CO, 5.6 vol (%) $CH_4$, 17 vol (%) $CO_2$, and 46 vol (%) $N_2$, with the balance being light hydrocarbons.

Figure 5 summarizes our studies to date. The stirred tank reactor used in our studies is only able to convert about 40% of the CO bubbled through it. This reflects a limitation in gas-to-liquid exchange rather than a theoretical limit. Indeed, *R. rubrum* consumes CO so quickly that it cannot be

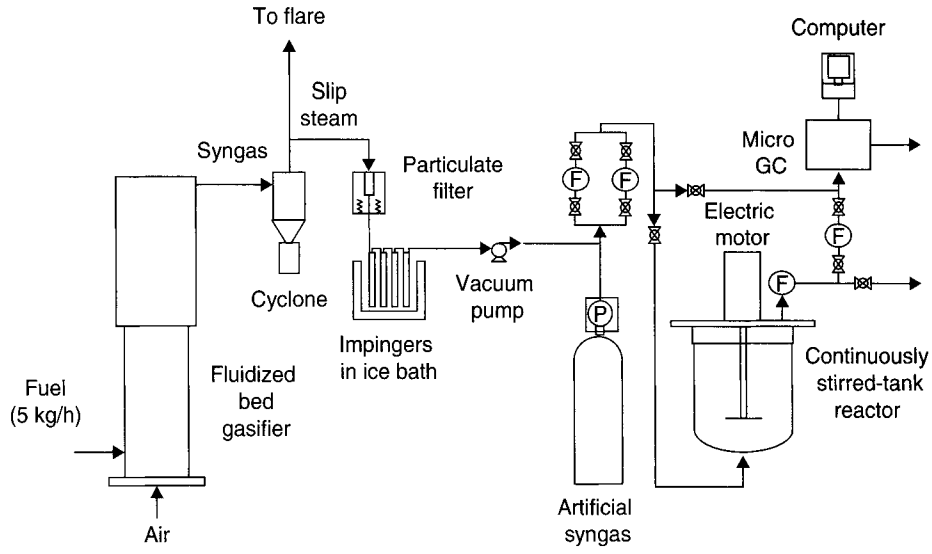


**Fig. 4.** Laboratory system for studying syngas fermentation.

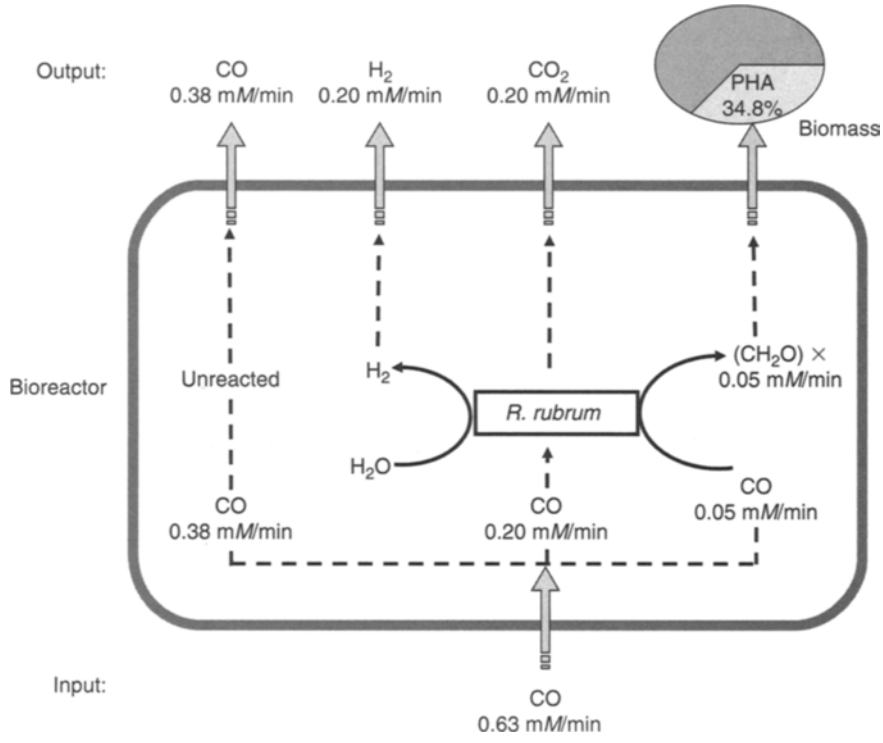


**Fig. 5.** Summary of results obtained from fermentation of syngas by *R. rubrum*.

detected in the liquid phase. Of the CO fermented, 20% is converted into cell mass and 80% is used in biologically mediated water-gas shift reaction to produce (extracellular) hydrogen. Of the cell mass, 35% is PHA. A biorefinery based on syngas fermentation to hydrogen and PHA is illustrated

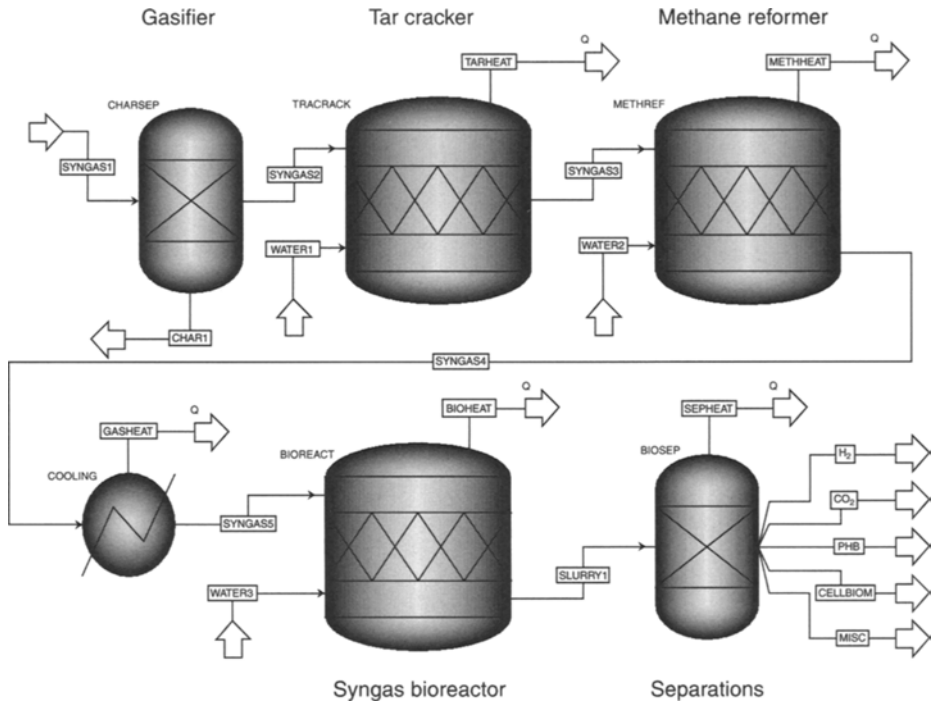


**Fig. 6.** Conceptual schematic of biorefinery to produce hydrogen and PHA coproducts from fibrous biomass.

in Fig. 6. Biomass is gasified in oxygen followed by additional steps to remove tar and methane from the syngas. No inorganic contaminant removal is thought necessary because the organisms are tolerant to sulfur and chlorine. The gas is cooled and passed through a bioreactor wherein CO is dissolved in the fermentation media and taken up by *R. rubrum*.

We have performed a preliminary economic assessment on this biorefinery concept, assuming 20 tons per day (tpd) of PHA and 55 tpd of hydrogen. The capital costs, detailed in Table 3, are estimated to be $103 million. The operating costs for this plant, shown in Table 4, yields a production cost of $2.80/kg of PHA assuming a credit for coproduct hydrogen equal to $1.90/kg, which is based on the US Department of Energy's long-term target price for this fuel. This PHA production cost compares favorably with the production cost of PHA from glucose, which may be as much as $5–7/kg.

## Conclusions

Thermochemical processing of biomass to produce substrates suitable for fermentation is a relatively new approach to bio-based products. The syngas route, by transforming all plant constituents into CO and $H_2$, is attractive for its efficient use of biomass. The fast pyrolysis route, by yielding a storable carbohydrate-rich liquid, allows the processing of solid

Table 3
Estimated Capital Costs for Biorefinery to Produce Hydrogen and PHA Coproducts From Fibrous Biomass

| | | |
|---|---|---|
| Gasifier | $18.6 million | Estimated from: Larson and Svenningsson *(16)* |
| Fermenter | $59.1 million | Estimated as 25% of total cost of an ethanol plant |
| Separation equipment | $25.3 million | Estimated as 30% of total costs of a fermentation plant |
| Grassroots capital | $103 million | – |

Table 4
Estimated Operating Costs for Biorefinery to Produce Hydrogen and PHA Coproducts From Fibrous Biomass

| | | |
|---|---|---|
| Annual $H_2$ output | $18.1 \times 10^6$ kg | Based on 20% CO to cell mass; 35% cell mass to PHA |
| Annual PHA output | $6.5 \times 10^6$ kg | |
| Annual input | $210.0 \times 10^6$ kg | 90% capacity factor |
| Total Capital | $119 million | – |
| Raw materials | $12.6 million | Purchased at $0.06/kg |
| Credit for $H_2$ | $34.3 million | Assumed to sell for $1.90/kg |
| Labor, utilities, and maintenance | $15.6 million | – |
| Indirect costs | $10.4 million | – |
| Annual capital charges | $13.9 million | 10% interest, 20 yr |
| Annual operating costs | $18.2 million | – |
| PHA production costs | $2.80/kg | – |

biomass to be decoupled from fermentation and offers prospects for distributed processing of widely dispersed biomass resources. Both have an advantage over cellulose hydrolysis in that they are able to process a wider variety of feedstocks, although this is especially true for the gasification route. Based on the current state-of-the-art, the syngas fermentation route has an advantage over the bio-oil fermentation approach owing to the larger amount of nonfermentable compounds in the bio-oil.

Compared with acid and enzymatic hydrolysis, relatively few resources have been devoted to developing hybrid thermochemical/biological routes to bio-based products. The reason for this circumstance is easy to understand: the original feedstocks of the fermentation industry were naturally occurring sugars and starches that were easily hydrolyzed to sugar. The fact that starch and cellulose are both polymers of glucose encouraged similar approaches to depolymerizing these two carbohydrates. In fact, cellulose is not only more recalcitrant than starch but it is imbedded in a matrix of lignin, which makes the process of releasing sugar

from lignocellulose much more difficult than for starch. Considering these difficulties, hybrid thermochemical/biological approaches to bio-based products deserves increased attention.

## Acknowledgments

I would like to acknowledge my collaborators in the field of hybrid thermochemical/biological processing, including Profs. Tony Pometto, Alan Dispirito, Ted Heindel, Basil Nikolau, and Tom Bobik; Drs. Young Do and Desmond Radlein; former and present graduate students Kim So, Scott Bents, Kevin Timmer; and undergraduate student Abbie Hancock. Support for this work has come from the Iowa Energy Center, the US Department of Agriculture, and the US Department of Energy.

## References

1. Roadmap for Biomass Technologies in the United States, Biomass Research and Development Technical Advisory Committee, United States Department of Energy and United States Department of Agriculture (2002). Available at www.biomass.gov-tools.us/pdfs.
2. Bridgwater, A. V. and Peacocke, G. V. C. (2000), *Renewable Sustain. Energy Rev.* **4,** 1–73.
3. Piskorz, J., Scott, D. S., and Radlein, D. (1988), *ACS Symposium Series No. 376.* Soltes, E. J. and Milne, T. A. (eds.), American Chemical Society, Washington, DC, pp. 167–178.
4. Evans, R. J. and Milne, T. A. (1987), *Energy Fuels* **1,** 123–137.
5. Scott, D. S., Czernik, S., Piskorz, J., and Radlein, D. (1989), *Energy from Biomass and Wastes XIII,* New Orleans, LA, USA, Publ by Inst of Gas Technology, Chicago, IL: pp. 1349–1362.
6. Brown, R. C., Radlein, D., and Piskorz, J. (2001), *Chemicals and Materials from Renewable Resources: ACS Symposium Series No. 784.* American Chemical Society, Washington, DC, pp. 123–132.
7. Prosen, E. M., Radlein, D., Piskorz, J., Scott, D. S., and Legge, R. L. (1993), *Biotechnol. Bioeng.* **42,** 538–541.
8. Brown, R. C., Pometto, A. L., Peeples, T. L., et al. (2000), *Proceedings of the Ninth Biennial Bioenergy Conference,* Buffalo, New York.
9. Khiyami, M. A. (2003), *PhD Thesis,* Iowa State University, Ames Iowa.
10. So, K. and Brown, R. C. (1999), *Appl. Biochem. Biotechnol.* **77–79,** 633–640.
11. Lynd, L. R. (1996), *Annu. Rev. Energy Environ.* **21,** 403–465.
12. Grethlein, A. J. and Jain, M. K. (1993), *Trends Biotechnol.* **10,** 418–423.
13. Worden, R. M., Bredwell, M. D., and Grethlein, A. J. (1997), *Fuels and Chemicals from Biomass,* ACS Symposium Series No. 666, Washington, DC: pp. 320–336.
14. Young, D., Smeenk, J., Broer, K. M., et al. Growth of *Rhodospirillum rubrum* on synthesis gas: conversion of CO to $H_2$ and poly-b-hydroxyalkonoate. *Biotechnol. Bioeng.*, in press.
15. Kessler, B., Weusthuis, R., Witholt, B., and Eggink, G. (2001), *Adv. Biochem. Eng./Biotechnol. Bioeng.* **71,** 159–182.
16. Larson, E. D. and Svenningsson, P. (1990) *Energy from Biomass and Wastes XIV.* Institute of Gas Technology, Lake Buena Vista, FL.

0273-2289/1559-0291 (Online)/07/136–140/957–970/$30.00

# Physical and Chemical Properties of Bio-Oils From Microwave Pyrolysis of Corn Stover

FEI YU,[1] SHAOBO DENG,[1] PAUL CHEN,[1] YUHUAN LIU,[2] YIQIN WAN,[2] ANDREW OLSON,[3] DAVID KITTELSON,[3] AND ROGER RUAN*,[1,2]

*[1]Center for Biorefining and Department of Bioproducts and Biosystems Engineering, University of Minnesota, 1390 Eckles Ave., St. Paul, MN 55108, E-mail: ruanx001@umn.edu; [2]Jiangxi Biomass Engineering Center, Nanchang University, Nanchang, China 330047; and [3]Center for Diesel Research, University of Minnesota, 111 Church St. S. E., Minneapolis, MN 55455*

## Abstract

This study was aimed to understand the physical and chemical properties of pyrolytic bio-oils produced from microwave pyrolysis of corn stover regarding their potential use as gas turbine and home heating fuels. The ash content, solids content, pH, heating value, minerals, elemental ratio, moisture content, and viscosity of the bio-oils were determined. The water content was approx 15.2 wt%, solids content 0.22 wt%, alkali metal content 12 parts per million, dynamic viscosity 185 mPa·s at 40°C, and gross high heating value 17.5 MJ/kg for a typical bio-oil produced. Our aging tests showed that the viscosity and water content increased and phase separation occurred during the storage at different temperatures. Adding methanol and/or ethanol to the bio-oils reduced the viscosity and slowed down the increase in viscosity and water content during the storage. Blending of methanol or ethanol with the bio-oils may be a simple and cost-effective approach to making the pyrolytic bio-oils into a stable gas turbine or home heating fuels.

**Index Entries:** Aging; chemical behavior; microwave pyrolysis; physical behavior; stability; bio-oils.

## Introduction

It is imperative to find/develop alternative renewable fuels to address issues arising from rapid consumption of petroleum oils and rising interest in environment protection *(1)*. Generally, the energy generated by direct combustion has a maximum efficiency of more than 30%. It is believed that burning bio-oils produced from the thermochemical conversion of biomass is more efficient *(2)*. Bio-oils with little upgrading treatments are already suitable for turbine fuel and home heating oil uses, and therefore receiving much attention. Solantausta et al. *(3)* tested bio-oils produced

*Author to whom all correspondence and reprint requests should be addressed.

from wood in a gas turbine, and concluded that the technical limitations to the use of the bio-oils in turbines could be minimized by optimizing their physical and chemical properties such as ash content, alkali content, heating value, and viscosity and modifying the gas turbine engine system. The ash present in the bio-oils reduces the protective oxide surface film of the engine (4). Alkali metal sulfates and chlorides can accelerate the oxidation process (5). The heating value of bio-oil is lower than for fossil fuel, and a significant portion of the bio-oil consists of water. The spray pattern and droplet size are influenced by fuel viscosity, which may be connected to the pressure drop in the fuel system lines because of high viscosity. Higher viscosities result in higher line pressure drops, requiring the fuel pump to work harder to maintain a constant fuel flow rate. Fuel viscosity also influences the performance of the fuel system control unit. Therefore, the bio-oils must be properly produced and/or improved in order to meet the gas turbine fuel specifications (6).

This study was aimed at characterizing the physical and chemical properties of the bio-oils produced from a novel microwave pyrolysis process. The understanding of their physical and chemical behaviors is important to the design and control of processing parameters, product specifications, and product storage and transportation. Blending bio-oils with combustible solvents such as methanol and ethanol is a practical approach to the improvement of the bio-oil shelf stability and performance. It has been reported that the presence of methanol or ethanol in the bio-oil provides a simple method for controlling the viscosity of the bio-oil (7), facilitating combustion, improving homogeneity, and enhancing stability (8). Therefore, the effect of methanol and ethanol blending on the viscosity and stability of the bio-oils were also studied.

## Materials and Methods

### Materials

Corn stover (provided by Agricultural Utilization Research Institute, Waseca, Minnesota) used in this experiment was dried in air and pulverized mechanically and sifted through a 2 mm sieve before pyrolysis. The properties of corn stover are given in Table 1 and minerals in Table 2.

### Apparatus and Process

Pyrolysis of corn stover was carried out in a microwave cavity oven by placing 150.0 g samples in a 1-L quartz flask, which in turn was placed inside the microwave cavity. The oven was purged with nitrogen gas at a flow rate of 200 mL/min for 2 min before microwave treatment to create an oxygen-free gas background. A constant power input of 600 W at 2450 MHz was supplied to the microwave oven. Heating of the corn stover last about 40 min, which is thought to be sufficient to allow complete pyrolysis according to preliminary experiments. The volatile pyrolyzates were condensed after passing through a water-cooling column and collected in a

Table 1
Properties of Corn Stover

| Properties | Corn stover |
|---|---|
| Bulk density, at 20°C (kg/m$^3$) | 557.0 |
| Volatile matter | 79.44 |
| Fixed carbon | 8.34 |
| Moisture | 7.66 |
| Ash | 5.75 |
| *Elemental composition (wt%)* | |
| Carbon | 40.35 |
| Hydrogen | 5.31 |
| Nitrogen | 1.12 |
| Sulfur | 0.09 |
| Oxygen (by difference) | 53.13 |
| Gross heating value (MJ/kg) | 24.5 |

bottle. This pyrolytic liquid is called bio-oil. The condensates adhering to the interior wall of the quartz flask were washed with ethanol into the pyrolytic liquid collection bottle. All liquid collected was concentrated at 40°C using a rotovap (Buchi R-141, Flawil, Switzerland) to a constant weight, and the weight recorded. All experiments and analyses were performed in triplicate with an experimental error ≤ ±1.0%.

## *Determination of Physical and Chemical Properties of Bio-Oils*

The ash content of the bio-oils was determined following the procedure outlined in ASTM D 482-80 for petroleum products. The solids content was determined as ethanol insoluble material by Millipore (No. 4, Whatman) Filtration method. The pH of the bio-oils was observed using a digital pH meter (Accumet model 8250, Fisher Scientific, Fair Lawn, NJ). The minerals in the bio-oils were analyzed using the Inductive Coupled Plasma-Atomic Emission Spectrometer (ARL 3560, Waltham, MA). The heating value was measured as calorimetric value (higher heating value) by a Parr 1341 Oxygen Bomb Calorimeter (Parr Instrument Co., Moline, IL). The elemental ratio (C/H/N/O/S) of the samples was analyzed using an elemental analyzer (Leco 600, St. Joseph, MI). Water in the bio-oils was determined using a Karl Fischer titrator (Schott, Mainz, Germany; ASTM D 1744). The dynamic viscosity of oils was determined with a rotational viscometer (Brookfield DV-E, Middleboro, MA; ASTM D 445). The Brookfield rotational viscometer is equipped with a cover for preventing the evaporation of volatiles. The kinematic viscosity of the bio-oils was calculated by the dynamic viscosity divided by the density. Measurements for samples were taken at 22°C.

The homogeneity of the samples was determined using following procedure: 500 mL sample was pumped using a peristaltic pump (MASTERFLEX 07518-10, Vernon Hills, IL) at room temperature from bottom to

Table 2
Minerals of Corn Stover and Bio-Oils by ICP Analysis

| Mineral (ppm) | Al | B | Ca | Cd | Cr | Cu | Fe | K | Mg | Mn | Na | Ni | P | Pb | Zn |
|---|---|---|---|---|---|---|---|---|---|---|---|---|---|---|---|
| Corn stover | 112.740 | 4.442 | 2389.500 | 0.120 | 0.506 | 3.530 | 149.880 | 10643 | 1642.800 | 23.082 | 15.049 | 4.440 | 429.820 | 1.680 | 40.417 |
| Bio-oils | 4.9215 | 2.848 | 6.833 | 0.0585 | 0.307 | 0.3965 | 7.589 | 3.127 | 1.8575 | 0.034 | 1.8155 | 0.953 | 1.5175 | 0.8215 | 0.7915 |

Table 3
Physico-Chemical Properties of Bio-Oils

| Properties | Units | Bio-oil | Conventional bio-oils |
|---|---|---|---|
| pH | | 2.87 | 2.0–3.8 |
| Moisture | wt% | 15.2 | 15–30 |
| Density at 20°C | g/mL | 1.25 | 1.1–1.4 |
| Dynamic viscosity at | mPa·s | | |
| 20°C | | 1270 | – |
| 40°C | | 185 | – |
| 50°C | | 60 | – |
| 80°C | | 34 | – |
| Gross heating value | MJ/kg | 17.51 | 15–19 |
| Elemental composition | wt% | | |
| C | | 60.66 | 55.3–63.5 |
| H | | 7.70 | 5.2–7.0 |
| N | | 2.02 | 0.07–0.39 |
| S | | 0.15 | 0.00–0.05 |
| Ash content | wt% | 0.04 | 0.03–0.30 |
| Solids content | wt% | 0.22 | <1 |

top for about 1 h per test. Samples were taken from the homogenized sample by pouring from the hose at the outlet of the pump. Microscope (×300 magnification) was used to capture the digitalized microscopic images of sample. The stability was determined using following procedure: 100 mL pyrolytic oils were placed in 150-mL amber bottles and stored at room temperature (22°C) or at elevated temperatures (40 or 60°C) in ovens over various time periods (30–60 d). After the designated time the samples were cooled rapidly and viscosity and water content were tested according to the methods described above.

## Results and Discussion

The bio-oils from our process are dark brown viscous liquid. Some key physical and chemical properties of the oils are described in Table 3. As can be seen, these properties were in the range of bio-oils from other pyrolysis processes but significantly different from those of petroleum derived diesels.

### *Ash Content*

The presence of ash in the bio-oil can cause erosion, corrosion, and gumming problems in the engine valves. The ash content of the bio-oils from microwave pyrolysis is 0.04 wt%. Problems associated with ash content become more serious when the ash content of the fuel is greater than 0.1 wt% *(9)*.

### Solids Content

The solids content of bio-fuel from our microwave pyrolysis is 0.22 wt%. It lies in the lower range of the solids content of other bio-fuels reported in the literature (Table 3). Depending on their size, solid particles can wear the fuel system, block the filter, and clog the fuel nozzle *(6)*. Thereby the solids content is important with respect to the particulate emissions during the combustion process. The larger and the more the particles, the more serious the solids content problem is.

### pH

The pH value of bio-oils from our microwave pyrolysis is 2.87. Most bio-oils have a pH in the range of 2.0–3.8 because of the presence of organic acids, mostly acetic and formic acid *(5)*. The acids in the bio-oils are corrosive to common construction materials such as carbon steel and aluminum, especially with elevated temperature and with the increase in water content. However, bio-oils are noncorrosive to stainless steels.

### Mineral Contents

The presence of superscale magnesium, calcium, and alkali metals in a fuel used for gas turbine is rather troublesome. The melting of metals and the condensation of metal oxides can cause accelerated corrosion and erosion of turbine blades *(10)*. Furthermore, sodium and potassium are responsible for high-temperature corrosion whereas magnesium and calcium are accountable for hard deposition. The metal limits for a gas turbine fuel are 1 ppm for sodium and potassium, 0.5 ppm for calcium, and 0.5 ppm for vanadium. The main source of minerals in the pyrolytic oils is the char residues carried by the pyrolytic vapors. The metal contents of the bio-oils were found to be: 3 ppm K, 2 ppm Na, and 7 ppm Ca (Table 2). They are lower than those of the bio-oils generated by other processes. The alkali metal and calcium concentration in bio-oils can be reduced by the organic solvent dilution, which is a simple and cost-effective method to improve the fuel quality.

### Heating Value

Bio-oils have a lower gross heating value than petroleum fuels and will therefore require an increased fuel flow to compensate the combustion in a firebox *(9)*. The gross heating value of our raw bio-oil sample is 17.51 MJ/kg (Table 3). It is similar as the gross heating values of bio-oils produced by other processes (15–19 MJ/kg) but lower than that of petroleum fuels (42 MJ/kg). The heating value of the bio-oils from microwave pyrolysis is approx 41.7% of a petroleum fuel oil. In other words, 2.4 kg of our bio-oil is required to provide the same energy as 1.0 kg of petroleum oil.

Table 4
High Heating Value of Bio-Oils and Bio-Oils With Solvent Addition

| Samples | High heating value (MJ/kg) |
|---|---|
| Bio-oils | 17.51 |
| Aqueous phase | 1.2 |
| Bio-oils with 10 wt% methanol | 16.21 |
| Bio-oils with 20 wt% methanol | 15.96 |
| Bio-oils with 30 wt% methanol | 13.47 |
| Bio-oils with 10 wt% ethanol | 14.15 |
| Bio-oils with 20 wt% ethanol | 12.07 |
| Bio-oils with 30 wt% ethanol | 11.98 |

The aqueous phase of pyrolytic liquid, methanol, and ethanol can be used as solvent to keep the bio-oils homogenous and low in viscosity. If the aqueous phase of pyrolytic liquid, methanol, and ethanol are to be blended into the bio-oils, it is important to determine the variations in the heating values of the blends. The gross heating value of the aqueous phase is 1.2 MJ/kg (Table 4), lower than that of the bio-oils. Methanol and ethanol also have lower energy density than the bio-oils. Therefore, the heating values of the blends are expected to be lower than that of the bio-oils.

### *Water Content*

The water content in the bio-oils from our microwave pyrolysis of corn stove is 15.2% (Table 3). The water likely came from two sources: the moisture in the raw corn stover and the water produced as a result of the dehydration reactions occurring during the pyrolysis. Therefore, water content can vary in a wide range (15–30%) depending on the feedstock and process conditions *(11)*. At this concentration water is usually miscible with the oligo-cellulosic derived components because of the solubilizing effect of other polar hydrophilic compounds (low-molecular-weight acids, alcohols, hydroxyaldehydes, and ketones) mostly originating from the decomposition of carbohydrates. The presence of water has both negative and positive effects on the oil properties. Obviously, it lowers its heating value, contributes to the increase in ignition delay, and the decrease in combustion rate compared with engine fuels. On the other hand, it improves bio-oil flow characteristics (reduces the oil viscosity), which is beneficial to combustion.

### *Viscosity*

In order to be considered as a gas turbine fuel, the bio-oils must meet certain viscosity standard. The viscosity of gas turbine oils is usually around 2.5–30 $mm^2/s$ at 40°C *(7)*. The kinematic viscosity of the bio-oils was difficult to determine because the level of the bio-oils in the viscometer

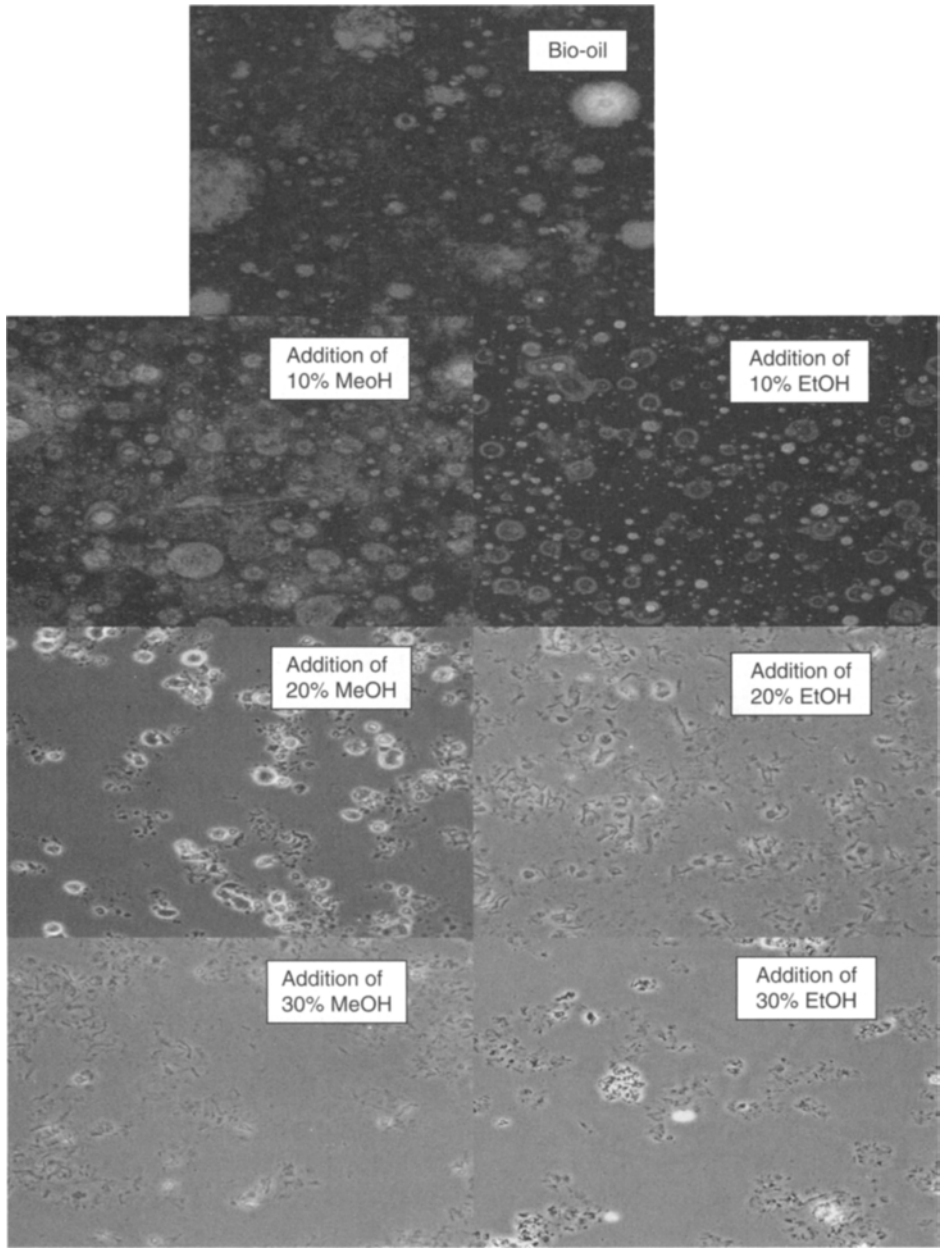


**Fig. 1.** Microscopic images of bio-oils and bio-oils with solvent addition (×300 magnification).

could not be read easily. Therefore, the dynamic viscosity was measured. Viscosity of our bio-oils was 185 mPa·s at 40°C (or 148 $mm^2/s$ at 40°C, calculated by the dynamic viscosity of bio-oils divided by the density), which is too high for gas turbine. As mentioned earlier, blending with organic solvent such as methanol and ethanol can reduce viscosity.

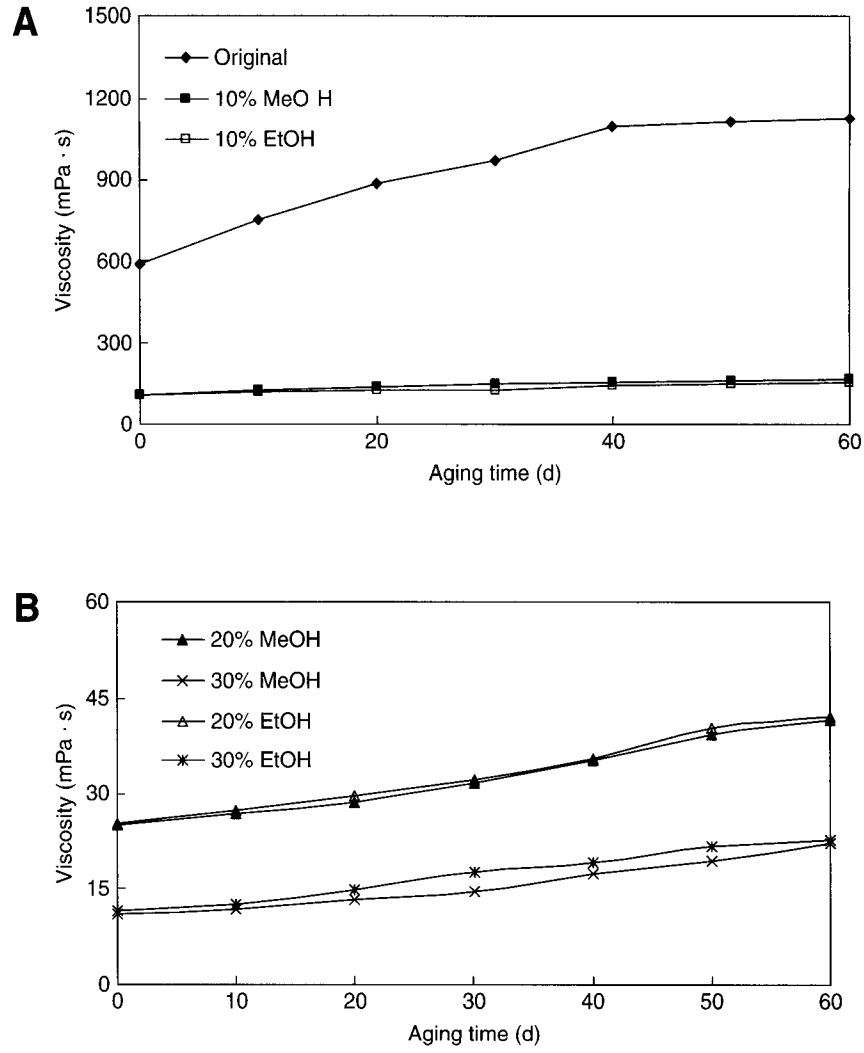


**Fig. 2.** Viscosity of bio-oils and bio-oils with solvent addition vs ageing period at room temperature.

It was found that the viscosity of the 10% methanol–bio-oil mixture was 3.7 $mm^2/s$ at 40°C, which should satisfy the atomization requirements.

### *Homogeneity*

Bio-oils from microwave pyrolysis appear to be a homogeneous liquid with black solid particles suspended in the liquid as revealed by the microscopy study (Fig. 1). These particles are char residues, or ashes and minerals entrained in the pyrolytic vapors emitted from the pyrolytic reactions. Some solid particles may form through crystallization and precipitation during storage. The solids content can be controlled with filtration before or after oil recovery process. Microscopic analysis of the 10–30% methanol or ethanol–bio-oil blends shows that methanol or ethanol improved the quality of the dispersion and the homogeneity. Moreover, the methanol

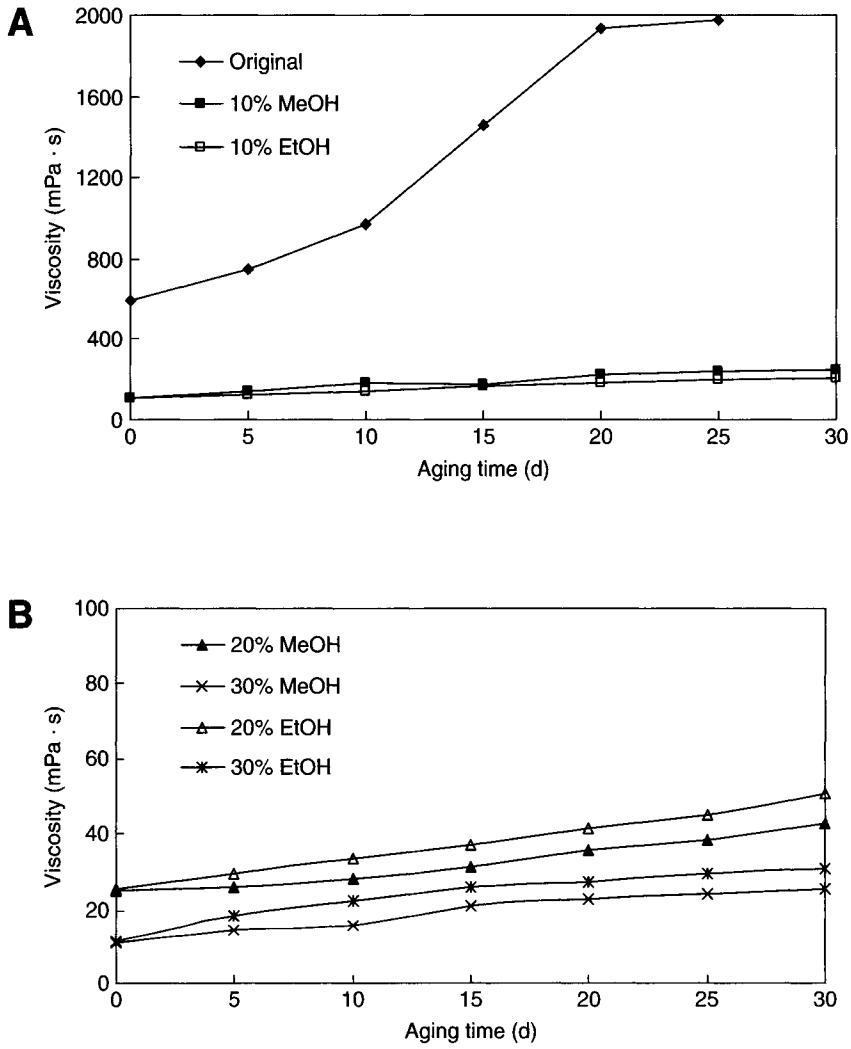


**Fig. 3.** Viscosity of bio-oils and bio-oils with solvent addition at 40°C.

or ethanol reduces the size of the aqueous phase droplets *(9)*. The water droplets in the bio-oil sample will agglomerate gradually and form larger size droplets, ultimately leading to sedimentation during storage. Methanol or ethanol is miscible with both components of the oil system and aqueous phase system, helping to form small particle size droplets, and hence, decrease considerably the sedimentation velocity and increase the stability of the emulsion. The comparison between the pure bio-oils and the blends indicates an increase in the number of droplets, which is translated to an increased homogeneity of the sample.

## *Aging*

Organic compounds in bio-oils samples can continue to react to form larger molecules during storage over time, which can contribute to

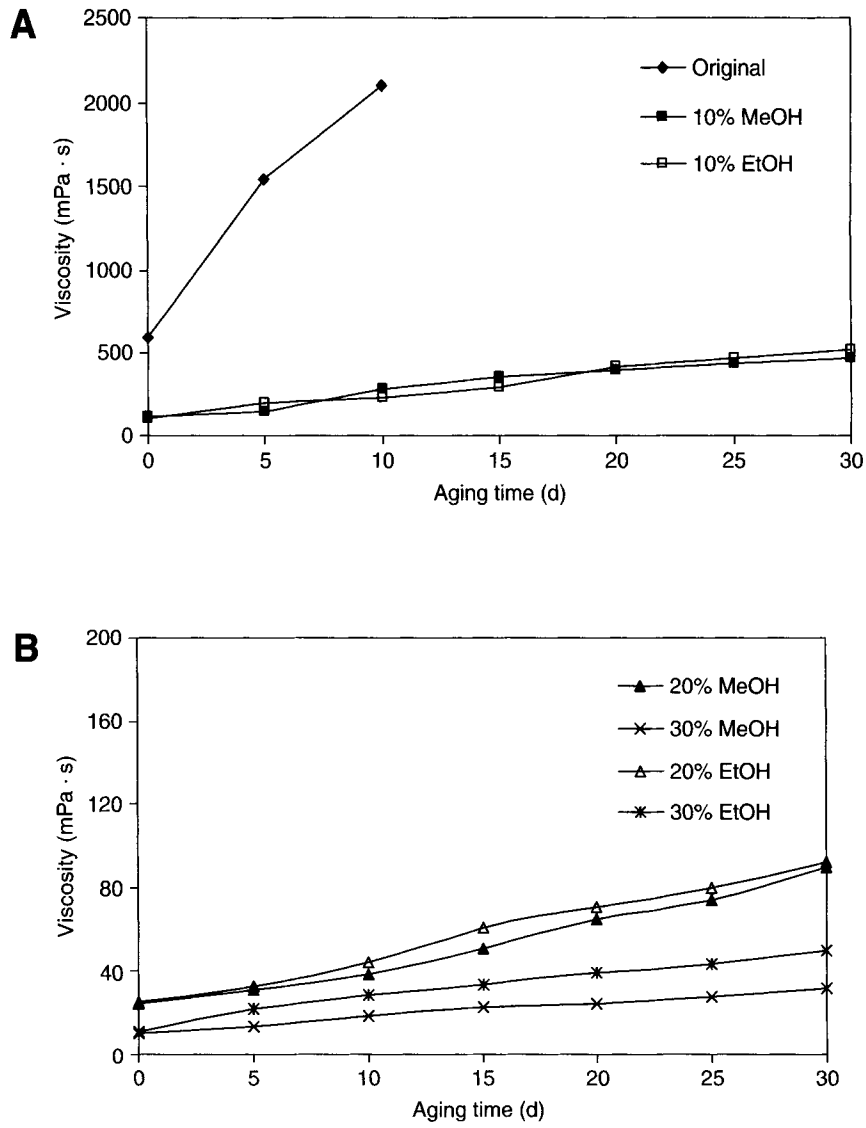


**Fig. 4.** Viscosity of bio-oils and bio-oils with solvent addition at 60°C.

increase in viscosity and water. The main chemical reactions are etherification and esterification occurring between hydroxyl, carbonyl, and carboxyl group components, in which water is a byproduct (*7*). Polymerization of double-bonded components also happened because of the instability of those chemicals.

The dynamic viscosity of the pure bio-oils and the solvent/oil blends was measured as a function of the aging time at different temperatures (Figs. 2–4). The results indicated that the viscosity of the pure bio-oils increased dramatically during the first 40, 20, and 10 d at storage temperatures of 22, 40, and 60°C, respectively, followed by a slow increase or a plateau. Addition of methanol or ethanol decreased the viscosity substantially.

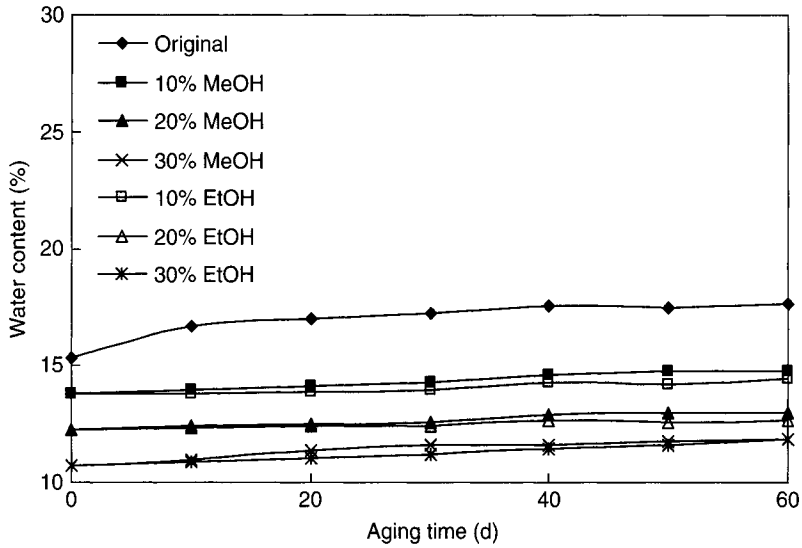


**Fig. 5.** Water content of bio-oils and bio-oils with solvent addition vs ageing period at room temperature.

The viscosity of bio-oils was reduced by the addition of solvent (regardless of methanol or ethanol), not only because solvent has a low viscosity, but also because they are good solvents for bio-oils. For example, a concentration of 10% methanol in bio-oils produced a mixture with a viscosity five times lower than that of original bio-oils, whereas 20% methanol in bio-oils decreased the viscosity of bio-oils by a factor of 24. The addition of methanol or ethanol also slowed down the increase in viscosity during storage.

Figures 5–7 show the water content of the pure bio-oils and the blends during the storage at different temperatures. The water content of bio-oils was reduced by the addition of solvent *(12)*. The observed water content increase from 15.27 to 17.60% during the 2 mo storage, was considered small. The increase was higher at higher storage temperatures. Similar results were obtained by Czernik et al. *(13)*. The aging rate (increasing rate for viscosity and water content) depends on bio-oils composition, which in turn affects the feedstock, pyrolysis types and conditions, the efficiency of solid removal and product collection, and storage conditions especially the storage temperature, which can affect exponentially the rates of chemical reactions during storage.

## *Phase Stability*

Phase separation may occur during a long-term storage of bio-oils, especially at high temperatures *(8)*. Our observation indicates that a low-viscosity water-rich layer appeared on the top whereas a high-viscosity tar-rich layer appeared at the bottom of the pure bio-oils. Such phase separation phenomenon occurred after 30 d at 40°C and 15 d at 60°C. The high-molecular weight tar may further become a gum and ultimately a

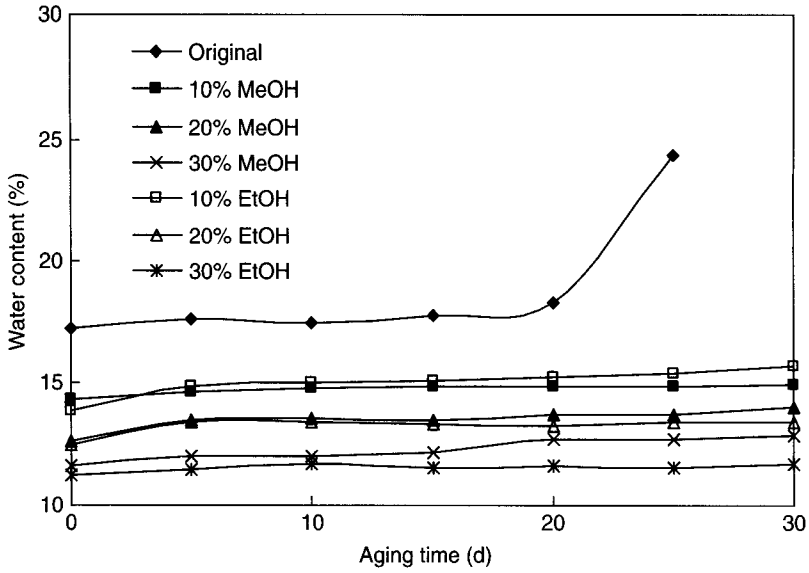


**Fig. 6.** Water content of bio-oils and bio-oils with solvent addition at 40°C.

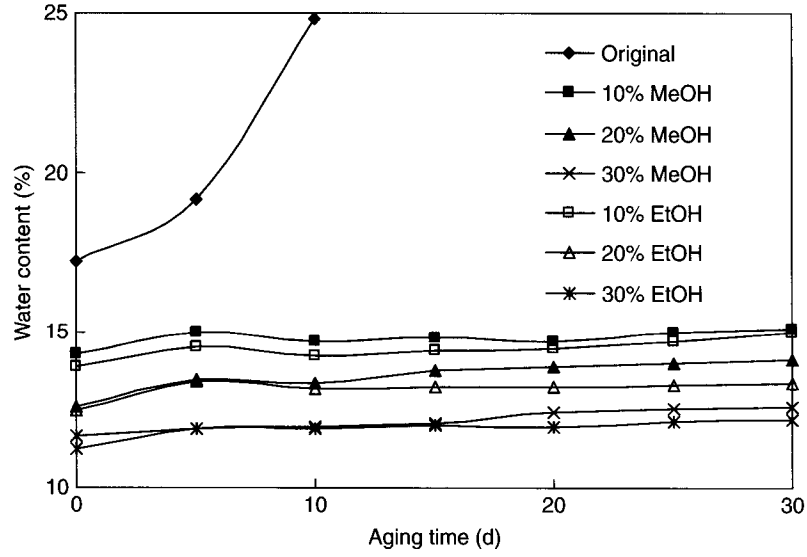


**Fig. 7.** Water content of bio-oils and bio-oils with solvent addition at 60°C.

carbonaceous clot. For the solvent–bio-oil blends, no phase separation was observed after 30 d of storage at 40°C and 60°C, suggesting that addition of methanol and ethanol to the pure bio-oils inhibited phase separation. The results suggested that a 10% methanol or ethanol addition to the bio-oils would be sufficient to prevent phase separation. This is particularly important to bio-oil storage at high temperatures.

## Conclusions

In this study, the physical and chemical properties of the bio-oils produced from a microwave-assisted pyrolysis of corn stover were investigated. The ash content and solids content in the bio-oils were relatively low. The gross heating value was about 41% of the petroleum oil. The bio-oils had undesirable pH, water content, and viscosity values if the bio-oils are to be used as gas turbine fuel. The bio-oils experienced an increase in viscosity accompanied by phase separation over a 30–60 d storage. Blending methanol or ethanol into the bio-oils was proved to improve the properties and stability of the bio-oils. Our study showed that addition of 0methanol or ethanol enhanced the homogeneity and greatly reduced the viscosity of the bio-oils, and slowed down the aging process. The solids content and large particles can be reduced through filtration before and/or after bio-oil recovery process. We believe that with further research and development, bio-oils from microwave-assisted pyrolysis of biomass are a promising candidate for gas turbine fuel and home heating oil.

## Acknowledgment

This work was supported by University of Minnesota IREE and Center for Biorefining and China Ministry of Education PCIRT Program (IRT0540).

## References

1. Scott, D. S., Piskorz, J., and Radlein, D. (1985), *Ind. Eng. Chem. Proc. Des. Dev.* **24,** 581–586.
2. Wornat, M. J., Porter, B. J., and Yang, N. Y. (1994), *Energy Fuels* **8,** 1131–1142.
3. Solantausta, Y., Nylund, N. O., and Gust, S. (1994), *Biomass Bioenergy* **7,** 297–306.
4. Aubin, H. and Roy, C. (1980), *Fuel Sci. Technol. Int.* **8,** 77–86.
5. Elliott, D. C. (1994), *Biomass Bioenergy* **7,** 179–186.
6. Diebold, J. P. and Czernik, S. (1997), *Energy Fuels* **11,** 1081–1091.
7. Boucher, M. E., Chaala, A., and Roy, C. (2000), *Biomass Bioenergy* **19,** 337–350.
8. Boucher, M. E., Chaala, A., Pakdel, H., and Roy, C. (2000), *Biomass Bioenergy* **19,** 351–361.
9. Peacocke, G. V., Russel, P. A., Jenkins, J. D., and Bridgwater, A. V. (1994), *Biomass Bioenergy* **7,** 169–178.
10. Olsson, J. G., Jaglid, U., Pettersson, J. C., and Hald, P. (1997), *Energy Fuels* **11,** 779–784.
11. Oasmaa, A. and Czernik, S. (1999), *Energy Fuels* **13,** 914–921.
12. Roy, C. and Caumia, B. (1986), *Fuel Sci. Technol. Int.* **14,** 531–539.
13. Czernik, S., Johnson, D. K., and Black, S. (1994), *Biomass Bioenergy* **7,** 187–192.

0273-2289/1559-0291 (Online)/07/136–140/971–984/$30.00

# Comparison of Diafiltration and Size-Exclusion Chromatography to Recover Hemicelluloses From Process Water From Thermomechanical Pulping of Spruce

ALEXANDRA ANDERSSON,*,[1] TOBIAS PERSSON,*,[2] GUIDO ZACCHI,[2] HENRIK STÅLBRAND,[1] AND ANN-SOFI JÖNSSON†,[2]

[1]*Department of Biochemistry; and* [2]*Department of Chemical Engineering, Lund University, P.O. Box 124, SE-221 00 Lund, Sweden, E-mail: ann-sofi.jonsson@chemeng.lth.se*

## Abstract

Hemicelluloses constitute one of the most abundant renewable resources on earth. To increase their utilization, the isolation of hemicelluloses from industrial biomass side-streams would be beneficial. A method was investigated to isolate hemicelluloses from process water from a thermomechanical pulp mill. The method consists of three steps: removal of solids by microfiltration, preconcentration of the hemicelluloses by ultrafiltration, and purification by either size-exclusion chromatography (SEC) or diafiltration. The purpose of the final purification step is to separate hemicelluloses from small oligosaccharides, monosaccharides, and salts. The ratio between galactose, glucose, and mannose in oligo- and polysaccharides after preconcentration was 0.8: 1: 2.8, which is similar to that found in galactoglucomannan. Continuous diafiltration was performed using a composite fluoro polymer membrane with cutoff of 1000 Da. After diafiltration with four diavolumes the purity of the hemicelluloses was 77% (gram oligo- and polysaccharides/gram total dissolved solids) and the recovery was 87%. Purification by SEC was performed with 5, 20, and 40% sample loadings, respectively and a flow rate of 12 or 25 mL/min (9 or 19 cm/h). The purity of hemicelluloses after SEC was approx 82%, and the recovery was above 99%. The optimal sample load and flow rate were 20% and 25 mL/min, respectively. The process water from thermomechanical pulping of spruce is inexpensive. Thus, the recovery of hemicelluloses is not of main importance. If the purity of 77%, obtained with diafiltration, is sufficient for the utilization of the hemicelluloses, diafiltration probably offers a less expensive alternative in this application.

**Index Entries:** Galactoglucomannan; diafiltration; microfiltration; polysaccharides; ultrafiltration; SEC; gelfiltration.

*Contributed equally to this work.

†Author to whom all correspondence and reprint requests should be addressed.

## Introduction

Hemicelluloses and cellulose are among the most abundant renewable polymeric materials on earth. Cellulose has become one of the most widely used resources, but hemicelluloses, as such, have not the same utility in our society. However, several potential applications have been described, e.g., the production of hydrogels *(1)* and barrier films *(2,3)*, hydrolysis and fermentation to ethanol *(4)*, and as a feedstock for xylitol production *(5)*. Thus, there is significant potential for the future utilization of hemicelluloses. A prerequisite for the increased use of hemicelluloses is that cost-effective methods of extracting hemicelluloses from different raw materials will be developed.

Extraction of hemicelluloses from different raw materials has been studied since the 1950s *(6–11)*. The method used here to isolate hemicelluloses from process water from thermomechanical pulping of spruce *(Picea abis)* is membrane filtration followed by a final purification step of diafiltration or size-exclusion chromatography (SEC). Earlier studies have been performed with similar methods, e.g., membrane filtration *(10,12)* and SEC *(13,14)*.

Spruce wood is an important raw material for the Swedish pulp and paper industry. The dominating hemicellulose in spruce is *O*-acetyl galactoglucomannan (GGM). GGM is a complex, substituted heteropolysaccharide containing an *O*-acetylated β-(1→4)-linked glucomannan backbone with α-(1→6)-D-galactosyl side groups attached to some of the mannosyl units *(15,16)*. GGM is partly dissolved in the process water during thermomechanical pulping and has been isolated and shown to have good properties for production of barrier materials intended for food packaging *(3)*. The aim of this study was to compare two purification techniques, diafiltration and SEC. The purpose was to isolate the hemicelluloses from smaller-molecular-weight compounds such as small oligosaccharides, monosaccharides, and salts. The purity, recovery, and size distribution of hemicelluloses after diafiltration and SEC were studied.

## Materials and Methods

### *Raw Material*

The raw material used in this study was process water from thermomechanical pulping of spruce, from Stora Enso Kvarnsveden Mill AB, Sweden. The process water originates from the final dewatering step of the pulp, using a disc filter. The total dissolved solids (TDS) of the process water were 3.8 g/L and the pH was 4.7. The amount of hemicelluloses, defined as oligo- and polysaccharides including acetyl groups, was 1.5 g/L. The process water was stored at 4°C and 0.2 mL/L of the biocide Nalco 7647 (Nalco, Leiden, The Netherlands) was added to prevent biological activity.

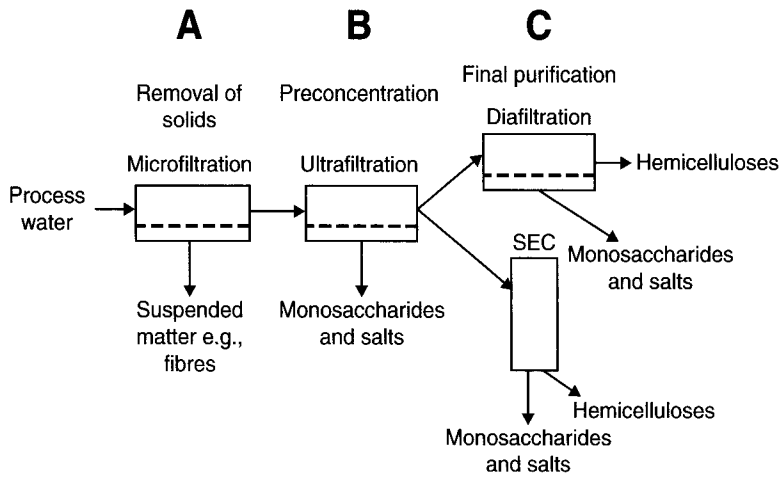


**Fig. 1.** Schematic illustration of the method used to isolate hemicelluloses from process water from thermomechanical pulping of spruce.

## *Procedure*

The method used to isolate hemicelluloses from the process water involves three steps: removal of solids by microfiltration (Fig. 1A), preconcentration of hemicelluloses by ultrafiltration (Fig. 1B), and purification by diafiltration or SEC (Fig. 1C). All liquid streams were analyzed regarding oligo- and polysaccharide content and acetyl-group concentration, to determine the concentration of hemicelluloses. Monosaccharide content, ultraviolet (UV)-absorbance, TDS, ash, and conductivity were determined to evaluate the purification efficiency.

### Removal of Solids

Microfiltration was performed in a vibratory shear-enhanced processing unit (series L/P, New Logic, Emeryville, CA), which is used in a wide variety of industrial separation and volume reduction (VR) processes *(17–19)*. The membrane stack consisted of 19 double-sided polytetrafluoroethylene membrane discs. The membrane pore diameter was 1 μm and the total membrane area was 1.57 $m^2$. The pressure was measured before and after the membrane stack. The pump was a displacement pump (G-03, Wanner Engineering Inc., Minneapolis, MN) and the permeate flow was measured with a flow meter (Promag 53, Endress+Hauser, Reinach, Switzerland).

Microfiltration was carried out at a transmembrane pressure of 200 kPa and a temperature of 22 ± 0.5°C. The vibration frequency was 49.9 Hz, which corresponds to an amplitude of 19 mm. The vibrations cause high shear forces to arise on the membrane surface and thereby prevents the formation of a filter cake, which otherwise would decrease the flux. The membranes were cleaned with 0.3 wt% Ultrasil 10 (Henkel Chemicals Ltd., Düsseldorf, Germany) at 35°C for 45 min, and thoroughly rinsed with deionized water before and after the study.

### Preconcentration by Ultrafiltration and Purification by Diafiltration

Ultrafiltration and diafiltration were performed in a DDS 20 LAB module unit (Alfa Laval Corp., Lund, Sweden). The membrane stack consisted of six double-sided ETNA01PP membrane discs (Alfa Laval Corp.) made of a composite fluoro polymer with cutoff of 1000 Da. The total membrane area was 0.21 $m^2$ and the pressure was measured with diaphragm pressure transmitters (dTrans p02, JUMO, Fulda, Germany), before and after the membrane stack. The pump was a displacement pump (D-25, Wanner Engineering Inc.) and the circulation flow rate was measured with a rotameter. The permeate flow was measured gravimetrically with a balance (FX-3000, A&D Company Ltd., Tokyo, Japan).

The microfiltration permeate was preconcentrated by ultrafiltration to 80% VR. Four temperature-equilibrated diavolumes of deionized water were added at the same flow rate as the permeate flow during diafiltration. The number of diavolumes corresponds to the ratio between the volume of water added during diafiltration and the constant volume of feed solution in the system *(20,21)*. The average transmembrane pressure was 1.0 MPa and the temperature was 60°C during both preconcentration and diafiltration. The circulation flow rate was 5.2 L/min, which corresponds to a cross-flow velocity of 0.5 m/s. The membranes were cleaned with 0.3 wt% Ultrasil 10 at 60°C for 45 min and thoroughly rinsed with deionized water before and after the study. The pure water flux was measured at 50°C and 1.0 MPa before and after the study, and after cleaning.

### Purification by SEC

SEC was performed on an INdEX 100/500 column (GE Healthcare, Uppsala, Sweden) with a diameter of 10 cm, packed with Superdex 30 chromatography media (GE Healthcare) to a height of 28 cm. Blue Dextran (GE Healthcare) was used to determine the void volume (684 mL), and acetone (Sigma-Aldrich Co, St. Louis, MO) was used to determine the total mobile volume of the column (1870 mL). Dextran T10 (GE Healthcare), maltose (Sigma-Aldrich Co.), and D-mannose (Fluka Chemie AG, Buchs, Switzerland) were used to calibrate the column. To determine the elution volumes for the standards, 6 mL of a 5 wt% solution was injected at a flow rate of 12 mL/min. The column was connected to a WellChrom high-performance liquid chromatography pump (K-1001, Knauer, Berlin, Germany), refractive index (RI) detector (K-2401, Knauer), and Filter-Photometer (K-2001, Knauer). The system was controlled with ChromGate computer software (Knauer).

SEC was performed on ultrafiltration retentate withdrawn at a VR of 80%. Six different SEC runs were performed in which the flow rates were 12 or 25 mL/min (9 or 19 cm/h) and sample volumes of 5, 20, or 40% of the total column volume were applied, respectively. The productivity of SEC is improved by increasing the sample volume or the flow rate of the

mobile phase. However, these actions result in band broadening, and hence, decreased separation *(22)*. A larger sample volume contributes greatly to a larger average retention volume, because of longer time required to apply the sample. The influence of flow rate on band broadening is well described by the van Deemter equation *(23)*. The study was performed at load-limiting conditions *(22)*. Degassed Millipore water was used as eluent and the column was washed with 4000 mL 2 wt% NaOH before the first SEC run. Two fractions were collected from each SEC run and the change of fraction occurred in the valley between the first and the second peak. With non-Gaussian elution profiles it can be difficult to determine the elution volume. Therefore, the center of each peak was used to calculate the elution volume.

### *Analysis*

The ash content and TDS were determined according to the standardized methods of the National Renewable Energy Laboratory (NREL, US Department of Energy) *(24,25)*. The absorbance at 205 nm in untreated samples was measured with a spectrophotometer (UV-160, Shimadzu, Kyoto, Japan) to indicate presence of lignin *(26)*. The conductivity was measured with a digital conductivity meter (PW9527, Philips, Amsterdam, The Netherlands) and calibrated with 0.01 *M* KCl (Merck, Darmstadt, Germany).

The monomer sugar composition and the concentration of oligo- and polysaccharides were analyzed by acid hydrolysis according to the standardized method of NREL *(27)*. Monomeric sugars were analyzed before and after acid hydrolysis and the oligo- and polysaccharide content was calculated from the difference in monosaccharide concentration before and after hydrolysis. Anhydro corrections of 0.9 and 0.88 were used for the hexoses and pentoses, respectively.

High-performance anion-exchange chromatography coupled with pulsed amperometric detection using an ED40 electrochemical detector (Dionex, Sunnyvale, CA), was used to analyze the monomeric sugars. It was equipped with a gradient pump (GP40, Dionex), an autosampler (AS50, Dionex), and a Carbo Pac PA10 guard and analytical column (Dionex). Degassed Millipore water was used as eluent at a flow rate of 1 mL/min, and the injection volume was 10 µL. D-Mannose, D-glucose, D-galactose, D-xylose, and L-arabinose (Fluka Chemie AG) were used as standards.

The acetyl content of the samples was measured by freeze-drying the filtrates and then redissolving them in 1% NaOH solution, to remove the *O*-acetyl moieties. The samples were then treated at room temperature overnight. The amount of acetic acid released was determined with high-performance liquid chromatography (GE Healthcare) using an Aminex HPX-87H column (BIO-RAD, Hercules, CA) at 65°C. Degassed 0.005 *M* $H_2SO_4$ was used as eluent, at a flow rate of 0.6 mL/min. Detection was performed with a RI detector (Erc - 7512, Erma Inc., Tokyo, Japan) and acetic acid (Merck) was used as standard.

## Results and Discussion

### *Pretreatment by Microfiltration*

Particles and suspended matter in the process water were removed by microfiltration. The average flux was 78 L/m$^2$h during concentration to 87% VR. The TDS were 3.8 g/L in the original process water and 3.2 g/L in the permeate. Turbidity decreased from 960 nephelometric turbidity units (NTU) in the process water to 4 NTU in the permeate. The oligo- and polysaccharide concentration including acetyl groups was 1.5 g/L in the process water and 1.3 g/L in the permeate. Hence, the recovery of oligo- and polysaccharides was 73%. A lower concentration in the permeate was expected, because oligo- and polysaccharides in or adsorbed onto the suspended matter were included in the analysis of the oligo- and polysaccharide concentration.

### *Preconcentration by Ultrafiltration*

The average flux was 69 L/m$^2$h during preconcentration by ultrafiltration to 80% VR. The concentration of oligo- and polysaccharides including acetyl groups increased from 1.3 to 5.7 g/L and the TDS from 3.2 to 10.0 g/L in the retentate. The flux decreased from 90 to 60 L/m$^2$h. The initial flux decrease is probably because of fouling and reduction of the Zeta potential of the membrane *(28)*. Galactan, glucan, and mannan were detected in a ratio of 0.8 : 1 : 2.8 in the ultrafiltration retentate, which is similar to that found in GGM *(15,29)*. No xylan or arabinan were detected.

### *Purification by Diafiltration*

In diafiltration the product is purified by removing permeable solutes by dilution with water. Diafiltration can be carried out in two ways: discontinuous or continuous, i.e., water is added in one batch or at the same rate as permeate is withdrawn. Continuous diafiltration was used as one of the methods to purify the hemicelluloses in the ultrafiltration retentate. If the retention is constant during diafiltration, the concentration of a solute *(i)* in the retentate can be expressed as *(21)*:

$$C_i = C_{0,i}\, e^{-V_d(1-R_i)} \tag{1}$$

where $C_{0,i}$ is the initial concentration of the solute, $V_d$ is the number of diavolumes, and $R_i$ is the retention of the solute. The conductivity decreased in accordance with Eq. 1 with a retention of 60%. Conductivity was used to measure the content of ions in the retentate during diafiltration, *see* Fig. 2. A small flux increase from 55 to 63 lx/m$^2$h during diafiltration implies that the retention of the oligo- and polysaccharides was high. Flux, purity, and recovery are important factors for the economy of the separation process. The purity is defined as the ratio between the

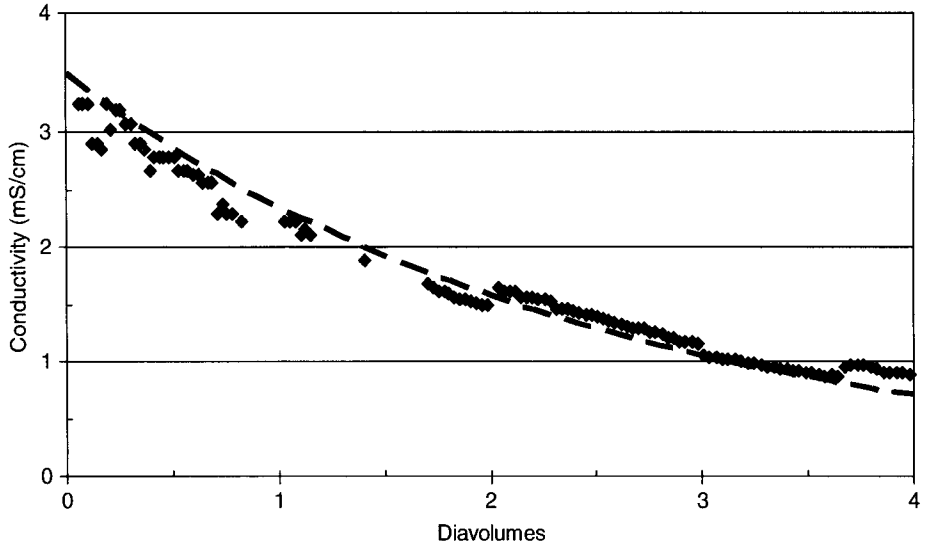


**Fig. 2.** Conductivity in the retentate during diafiltration of process water preconcentrated by ultrafiltration to 80% VR. The ash content in the ultrafiltration retentate was 0.2 g/g TDS. The dashed line was calculated from Eq. 1 with R = 60%.

mass of oligo- and polysaccharides and the TDS. The recovery during diafiltration can be calculated from *(17)*:

$$\text{Recovery} = \frac{m_r}{m_o} = e^{-V_d \cdot (1-R_i)} \tag{2}$$

where $m_r$ is the mass of oligo- and polysaccharides in the retentate, $m_{tds}$ is the total mass of dissolved solids, and $m_o$ is the original mass of oligo- and polysaccharides. Purity increased from 57 to 77% during diafiltration, but at the same time the recovery of oligo- and polysaccharides decreased by 16% compared with the ultrafiltration retentate. Figure 3 shows that the purity continued to increase with the number of diavolumes and a purer product was achieved as diafiltration progressed. However, as diafiltration proceeds, the recovery decreases. Optimal conditions are defined by 100% retention of the compound to be purified and 0% retention of contaminants. Equation 1 was used to calculate the average retention during diafiltration, presented in Table 1. The retention of oligo- and polysaccharides was high, which agrees with the small flux increase during diafiltration, whereas the retention of contaminants was smaller, but still much greater than zero.

The ash retention was constant during diafiltration and similar to the calculated retention of the conductivity (60%). The retention of lignin, on the other hand, increased during diafiltration from 42 to 85%. This was owing to the size distribution of the molecules. Both small carbohydrate degradation products and large lignin molecules and lignin bound to hemicelluloses in lignin-carbohydrate complexes *(30,31)* absorb UV-light at 205 nm. The small molecules pass through the membrane during diafiltration whereas

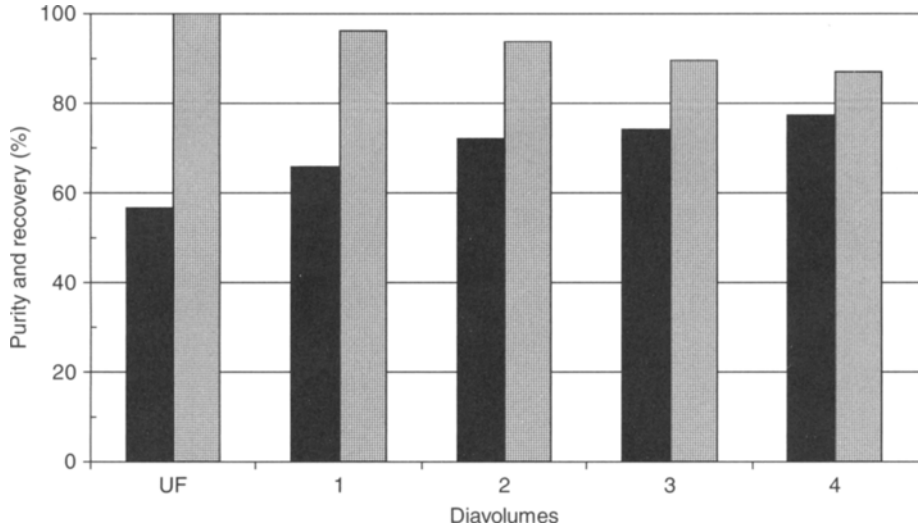


**Fig. 3.** Purity with respect to TDS (solid bars) and recovery of oligo- and polysaccharides (hatched bars) during diafiltration.

Table 1
Average Retention of Different Compounds During Diafiltration, Calculated With Eq. 1

| | Oligo- and polysaccharides | Monosaccharides | TDS | Lignin | Ash |
|---|---|---|---|---|---|
| Retention (%) | 97 | 38 | 89 | 63 | 63 |

the large molecules are retained, which increases the average molecular mass of the hydrophobic molecules and thus increases the retention. The pure water flux was 197 L/m$^2$h before ultrafiltration and 124 L/m$^2$h after preconcentration and diafiltration. After cleaning, the pure water flux was 204 L/m$^2$h. This flux decrease implies that the membranes are fouled during operation, but after cleaning, the original flux was restored.

## *Purification by SEC*

SEC was used as an alternative method to purify the hemicelluloses in the ultrafiltration retentate. The influence of different flow rates and sample volumes was studied. The resolution between two solutes depends on two effects, (a) increasing separation of band centers and (b) increasing bandwidth as bands migrate along the column. The resolution of two peaks is described by:

$$R_s = \frac{\Delta V_r}{W_{av}} \tag{3}$$

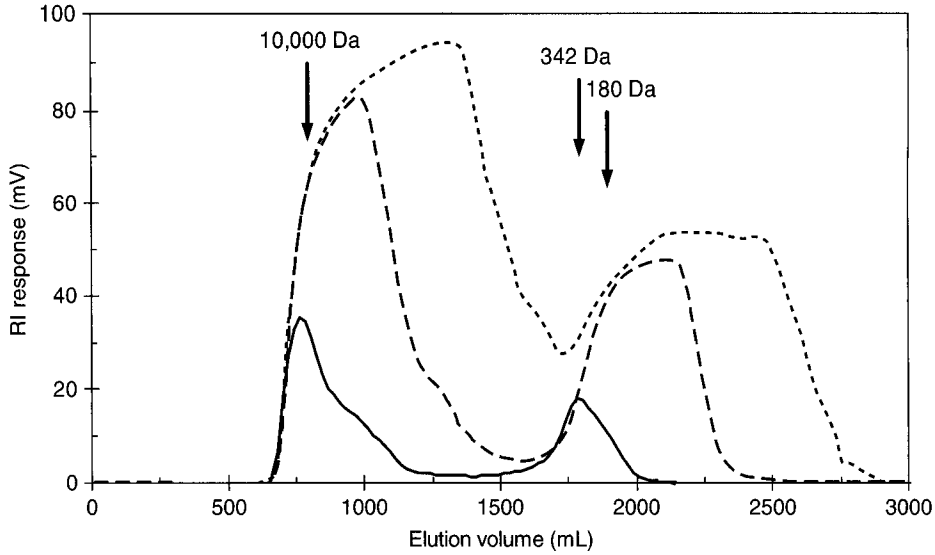


**Fig. 4.** RI elution profile from SEC of ultrafiltration retentate at a flow rate of 25 mL/min and sample volumes of 5% (solid line), 20% (dashed line), and 40% (dotted line) of the total column volume, which correspond to 94, 374, and 747 mL, respectively.

Table 2
Resolution and Recovery in SEC

| Flow rate (mL/min) | 12 | 12 | 12 | 25 | 25 | 25 |
|---|---|---|---|---|---|---|
| Sample volume (%) | 5 | 20 | 40 | 5 | 20 | 40 |
| Resolution | 1.8 | 1.4 | 0.7 | 1.9 | 1.7 | 0.7 |
| Recovery (%) | >99 | >99 | >99 | >99 | >99 | >99 |

The resolution was calculated from Eq. 3 and the recovery of GGM from Eq. 2, based on mannose residues.

where $\Delta V_r$ is the difference in elution volume between two solutes and $W_{av}$ is the average width of the two peaks *(22,32,33)*. Therefore, the flow rate of an eluent should affect the resolution of the peaks, but no significant difference was detected at the two flow rates investigated. At flow rates higher than 25 mL/min the maximum pressure drop for the column (300 kPa) was exceeded. Thus, higher flow rates could not be studied. Larger sample volume demands a longer loading time, which leads to increased peak width. Thus, the resolution of the peaks in the chromatogram decreases with increasing sample volume, *see* Fig. 4 and. Table 2. The recovery of GGM, based on mannose residues, was above 99% and independent of sample volume. The sample volume should not be more than 20% of the total column volume, as a resolution better than 1.5 is desirable for efficient product purification *(32)*.

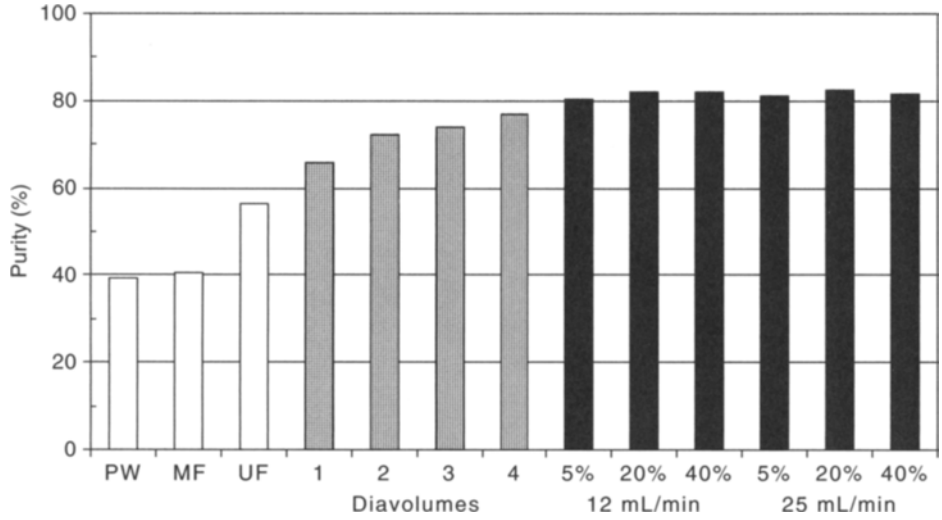


**Fig. 5.** Purity of oligo- and polysaccharides after primary filtration (white bars), after diafiltration (hatched bars), and after SEC (black bars). PW is the original process water, MF is after microfiltration, and UF is after preconcentration. The number of diavolumes during diafiltration and the eluent flow rate and sample volume, expressed as percent of total column volume during SEC are shown in the diagram.

## *Comparison Between Diafiltration and SEC*

The purification efficiency during diafiltration and SEC can be compared by calculating the purity of the oligo- and polysaccharides after the removal of low-molecular-weight compounds. Figure 5 indicates that the purity is somewhat higher after SEC than after diafiltration. However, the purity could probably be further increased during diafiltration by increasing the number of diavolumes. When diafiltration is used as the final purification step, the purity of the hemicelluloses is dependent on the purity of the feed. If the feed is highly contaminated with low-molecular-weight compounds, additional diavolumes are needed to obtain a pure product. If instead, SEC is used as the purification step, the purity of the feed is not important for the purity of the product, as long as the column is not overloaded. Separation is based completely on size and is independent of the concentrations of oligo- and polysaccharides over the range studied. Measurements of the UV absorbance also indicate a slightly higher purity of samples after SEC (*see* Fig. 6: small, UV-absorbing, hydrophobic molecules are easily separated from the hemicelluloses by SEC, but because they are retained by the ultrafiltration membrane, more diavolumes are needed to achieve the same purity).

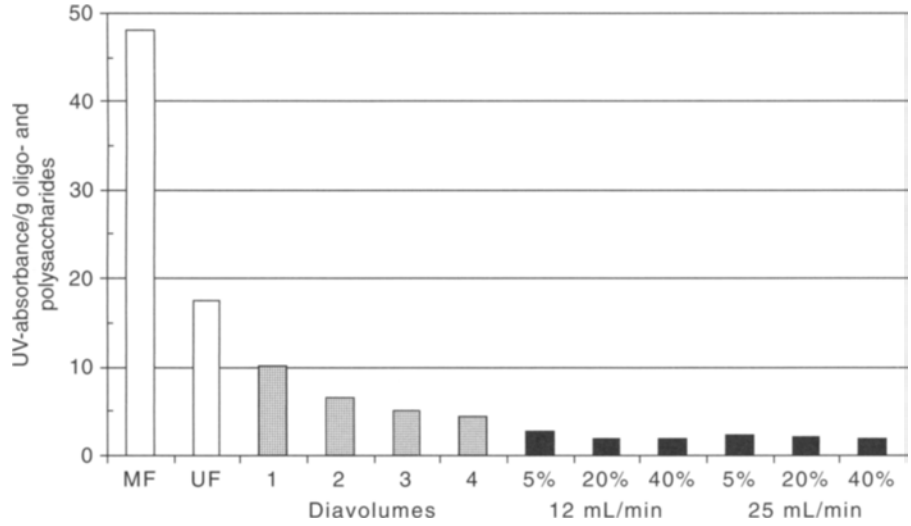


**Fig. 6.** The ratio between UV absorbance (205 nm) and grams of oligo- and polysaccharides before diafiltration (white bars), after diafiltration (hatched bars), and after SEC (black bars). MF is after microfiltration and UF is after preconcentration. The number of diavolumes during diafiltration and the eluent flow rate and sample volume, expressed as percent of total column volume during SEC are shown in the diagram.

## Conclusions

Both purification methods have been shown to efficiently remove low-molecular-weight compounds from the process water and to have high recovery of oligo- and polysaccharides. The two separation techniques used have advantages and disadvantages. SEC gives both higher purity and recovery than diafiltration. The purity of diafiltrated material could probably be increased by adding more diavolumes or by using a membrane providing better separation between contaminants and hemicelluloses. However, increasing the number of diavolumes decreases the recovery. SEC is preferably used when the raw material is expensive and there are high demands on recovery, for example, in the purification of valuable products such as pharmaceuticals. Process water from thermomechanical pulping is an inexpensive raw material, and consequently, diafiltration is probably the most cost-efficient purification method for the extraction of hemicelluloses from this process water. Both techniques should be economically evaluated and further optimized by using different operating conditions and materials to find the most suitable procedure.

## Acknowledgments

This study is part of a joint project called NovHemi. The aim of the project is to develop a process for the extraction of hemicelluloses from process and waste streams and to demonstrate the usefulness and advantages

of these hemicelluloses as renewable raw materials to make barrier films for food packaging. The Swedish Agency for Innovation Systems (VINNOVA) is gratefully acknowledged for financial support, and Alfa Laval for donating the ultrafiltration membranes. The Sven and Lilly Lawski Foundation is acknowledged for partial financial support.

## References

1. Soderqvist Lindblad, M., Ranucci, E., and Albertsson, A. -C. (2001), *Macromol. Rapid Commun.* **22,** 962–967.
2. Grondahl, M., Eriksson, L., and Gatenholm, P. (2004), *Biomacromolecules* **5,** 1528–1535.
3. Hartman, J., Albertsson, A. -C., Lindblad, M. S., and Sjoberg, J. (2006), *J. Appl. Polym. Sci.* **100,** 2985–2991.
4. Boussaid, A., Cai, Y., Robinson, J., Gregg, D. J., Nguyen, Q., and Saddler, J. N. (2001), *Biotechnol. Prog.* **17,** 887–892.
5. Parajo, J. C., Dominguez, H., and Dominguez, J. M. (1998), *Bioresour. Technol.* **65,** 191–201.
6. Teleman, A., Nordstrom, M., and Tenkanen, M. (2003), *Carbohydr. Res.* **338,** 525–535.
7. Hagglund, E., Lindberg, B., and McPherson, J. (1956), *Acta Chem. Scand.* **10,** 1160–1164.
8. Lundqvist, J., Teleman, A., Junel, L., et al. (2002), *Carbohydr. Polym.* **48,** 29–39.
9. Meier, H. (1958), *Acta Chem. Scand.* **12,** 144–146.
10. Willfor, S., Rehn, P., Sundberg, A., Sundberg, K., and Holmbom, B. (2003), *Tappi J.* **2,** 27–32.
11. Palm, M. and Zacchi, G. (2003), *Biomacromolecules* **4,** 617–623.
12. Gabrielii, I., Gatenholm, P., Glasser, W. G., Jain, R. K., and Kenne, L. (2000), *Carbohydr. Polym.* **43,** 367–374.
13. Palm, M. and Zacchi, G. (2004), *Sep. Purif. Technol.* **36,** 191–201.
14. Kringstad, K. (1965), *Acta Chem. Scand.* **19,** 1493–1494.
15. Timell, T. E. (1967), *Wood Sci. Technol.* **1,** 45–70.
16. Lundqvist, J., Jacobs, A., Palm, M., Zacchi, G., Dahlman, O., and Stalbrand, H. (2003), *Carbohydr. Polym.* **51,** 203–211.
17. Akoum, O., Jaffrin, M. Y., and Ding, L. -H. (2005), *J. Membr. Sci.* **247,** 211–221.
18. Akoum, O. A., Jaffrin, M. Y., and Ding, L. (2002), *J. Membr. Sci.* **197,** 37–53.
19. Takata, K., Yamamoto, K., Bian, R., and Watanabe, Y. (1998), *Desalination* **117,** 273–282.
20. Shao, J. and Zydney, A. L. (2004), *Biotechnol. Bioeng.* **87,** 286–292.
21. Cheryan, M. (1986), *Ultrafiltration handbook,* Technomic Publishing. Co., Lancaster, PA, USA: pp. 205–209.
22. Snyder, L. R. and Kirkland, J. J. (1979), *Introduction to Modern Liquid Chromatography,* Wiley Cop., New York: pp. 27–37, 617–623.
23. van Deemter, J. J., Zuiderweg, F. J., and Klinkenberg, A. (1995), *Chem. Eng. Sci.* **50,** 3869–3882.
24. Ehrman, T. (1994), *Standard Method for Ash in Biomass, Laboratory Analytical Procedure-005,* National Renewable Energy Laboratory, Midwest Research Institute for the Department of Energy, USA.
25. Ehrman, T. (1994), *Standard Method for Determination of Total Solids in Biomass, Laboratory Analytical Procedure-001,* National Renewable Energy Laboratory, Midwest Research Institute for the Department of Energy, USA.
26. Ehrman, T. (1996), *Determination of Acid-Soluble Lignin in Biomass, Laboratory Analytical Procedure-004,* National Renewable Energy Laboratory, Midwest Research Institute for the Department of Energy, USA.
27. Ruiz, R. and Ehrman, T. (1996), *Determination of Carbohydrates in Biomass by High Performance Liquid Chromatography, Laboratory Analytical Procedure-002,* National Renewable Energy Laboratory, Midwest Research Institute for the Department of Energy, USA.

28. Zhu, H. and Nystrom, M. (1998), *Colloids Surf. A: Physicochem. Eng. Aspects.* **138,** 309–321.
29. Sjöström, E. (1993), *Wood Chemistry Fundamentals and Applications,* Academic Press Inc., London: pp. 63–65.
30. Wallace, G., Russell, W. R., Lomax, J. A., and Jarvis, M. C. (1995), *Carbohydr. Res.* **272,** 41–41.
31. Karlsson, O., Ikeda, T., Kishimoto, T., Magara, K., Matsumoto, Y., and Hosoya, S. (2004), *J. Wood Sci.* **50,** 141–150.
32. Poole, C. F. (2003), *The Essence of Chromatography,* Elsevier, Amsterdam: pp. 51–59.
33. Harris, D. C. (1999), *Quantitative Chemical Analysis,* W.H. Freeman, New York: pp. 654–660.

# Author Index


**A**
Agobo, F. K., 653
Akin, D. E., 3
Alamouti, S. M., 267
Alhadeff, E. M., 17
Alizadeh, H., 395
Alriksson, B., 327, 339
Alvarez, M. E. T., 451
Alves-Prado, H. F., 27, 41
de Amorim, M. T. P., 573
Andersson, A., 253, 97
de Andrade, M. S., 515
de Andrade, R. R., 753
de Arauz, L. J., 515
Atala, D. I. P., 753

**B**
Baeza, J., 267
Baida, L. C., 27
Bailey, R., 859
Bakalinsky, A., 131
Balan, V., 207, 395
Ballesteros, I., 239, 353
Ballesteros, M., 239, 353
Batistella, C. B., 885
Benkö, Z., 195, 253
Benedicto, S. C. L., 185
Berlin, A., 267
Bernardes, O. L., 105
Berson, R. E., 289
Bevilaqua, J. V., 105
Bezerra, M. S., 185
Biswas, G., 207
Bocchini, D. A., 27, 281
Bombardiere, J., 765
Booth, E. A., 777
Borole, A. P., 437
Bradshaw, T. C., 395
Brígida, A. I. S., 67
Brown, S. D., 653
Brown, R. C., 947
Burapatana, V., 777

**C**
Cara, C., 379
Cardoso, V. L., 463, 471
Castro, E., 379
Cavalcanti, E. D. C., 57
Cha, W-S., 935
Chambliss, K., 301
Chatfield, M., 765
Chen, G., 793
Chen, P., 957
Chen, S., 689, 805, 875
Chen, S-F., 301
Chi, Z., 805
Cholewa, O., 555
Chung, P., 267
Coats, E. R., 909
Contiero, J., 27
Converse, A. O., 611
Converti, A., 539
Cos, O., 17
da Costa, A. C., 753, 817
da Costa, A. C. A., 835
Cotta, M. A., 93, 171
Coulibaly, S., 897
Coward-Kelly, G., 653
Crockett, E., 207

**D**
Dadi, A. P., 407
Dale, B. E., 207, 395
Dantas, M. A. A., 675
Dasari, R. K., 289
Davison, B. H., 437
Deng, S., 957
Dien, B. S., 171
Domaschko, M., 765
Drahos, E., 195
Duarte, E. R., 487
Duarte, M. C. T., 501
Dunlap, C. A., 93

**E**
Edwards, R. A., 927
Elander, R. T., 721
Espinosa-Solares, T., 765

**F**
Ferreira, A. L. O., 67
Filho, F. M., 753
Filho, R. M., 451, 487, 753, 817, 885
Flynn, P. C., 625, 639
Fonseca, R. R., 471
França, F. P., 463, 471
Frear, C., 805
Freer, J., 267
Freire, D. M. G., 57, 105

**G**
García-Aparicio, M. P., 353
Garcia-Gil, M., 301
Gáspar, M., 253
Ghafoori, E., 625, 639
Gilkes, N., 267
Glass, R. W., 875

Gomes, E., 27, 41, 281
Gonçalves, A. R., 501, 573
Gonçalves, L. R. B., 67, 185, 675
González, A., 353

H
Hanchar, R. J., 313
Hiestand, J., 859
Himmel, M. E., 1
Hotta, T., 155
Hu, B., 805, 875

I
Ishii, M., 555
Ito, V. M., 885

J
Jeffries, T. W., 653, 703
Jeng, H. T., 555
Jenkins, B. M., 423
Jeong, G-T., 583, 595, 935
Jones, F., 859
Jönsson, A-S., 741, 971
Jönsson, L. J., 327, 339
Jordan, D. B., 93
Jozala, A. F., 515

K
Kádár, Z., 847
Kale, S. P., 663
Kang, K-Y., 267, 367
Kim, D., 935
Kim, D-H., 583
Kim, H-S., 935
Kim, J-N., 529
Kim, T. H., 81
Kim, Y-J., 529
Kittelson, D., 957
Kobayashi, M. J., 539
Kumar, A., 639
Kunimura, J. S., 555

L
de Laat, W., 847
Labavitch, J. M., 423
Ladish, M. R., 171
Lago, R. C. A., 57
Langone, M. A. P., 105
Leal, M. C. M. R., 105
Lee, K-M., 935
Lee, W-T., 935
Lee, Y. Y., 81, 721
Leite, R. S. R., 281
Li, X-L., 93, 171
Li, Y., 897
Liao, W., 689
Lim, L. H., 115
de Lima, C. J. B., 463
Liu, C., 875
Liu, Y., 95, 805, 689
Loge, F. J., 909
Lu, C., 703
Luna, A. S., 835
Lunelli, B. H., 487

M
Macedo, G. R., 185
Machado, A. B., 451
Machado, O. L. T., 57
Maciel, F. M., 57
Maltha, S. F., 847
Mansoorabadi, K., 703
Mantovanelli, I. C. C., 817
Manzanares, P., 239, 353
Marins, E. D., 281
Martin, C., 339
Maximenko, V., 267
McCalla, D., 313
McKeown, C. K., 663
Mendonça, R., 267
Mielenz, J. R., 663
Mims, M. M., 897
Moore, K. J., 221
Moraes, E. B., 451
Moriya, R. Y., 501
Mosier, N., 171
Muñoz, C., 267

N
Negro, M. J., 239, 353
das Neves, L. C. M., 161, 539, 711
Nielson, C. D., 313
Nilvebrant, N-O., 327, 339
Nordin, A-K., 741
Nordmark, T. S., 131

O
Oliva, J. M., 239, 379
de Oliveira, K. S., 539
Olson, A., 957

P
Pafumé, R., 835
Pan, X., 367
Pan, Z., 423
Park, D-H., 529, 583, 595, 935
Park, J-H., 935
Park, S-H., 935
Penna, T. C. V., 515, 539, 555
Penner, M. H., 131
Pereira, N., Jr., 17, 141
Persson, T., 741, 971

Pessoa, A., Jr., 515, 711
Pinheiro, A. D. T., 67
Pinto, G. A. S., 67, 185, 675
Prokop, A., 777
Puranen, T., 195

**R**
Raman, B., 663
Ransom, C., 207
Réczey, K., 195, 253, 847
Ren, H., 221
Resende, M. M., 463
Richard, T. L., 221
Rivera, E. C., 753, 817
Roberto, I. C., 27
Rocha, M. V. P., 185
Rodrigues, T. H. S., 675
Romero, I., 379
Ruan, R., 957
Ruzene, D. S., 573
Ryu, H-W., 529, 935

**S**
Saddler, J. N., 267, 367
Sáez, F., 239, 379
Salgado, A. M., 17
Saville, B. A., 115
Schall, C. A., 407
Searcy, E., 639
Sérvulo, E. F. C., 463, 471
Shahbazi, A., 897
Silva, A. J. R., 471
Silva, D., 281
Da Silva, J. N. C., 141
Da Silva, R., 27, 41, 281
Sjöde, A., 327, 339
Smith, W. A., 909
Snyder, I. M., 777
Snyder, S. W., 739
de Souza, M. B., Jr., 141
Souza, M. C. M., 185
Stålbrand, H., 253, 971
Sticklen, M. B., 205, 207
Stowers, M. D., 313
Sunwoo, C., 935
Szengyel, Z., 195, 253, 847

**T**
Tanner, R. D., 777, 927
Teixeira, J. A., 573
Teter, S. A., 423
Teymouri, F., 313, 395
Thompson, D. N., 909
de Toledo, E. C. V., 487
Torry-Smith, M., 653
Toyama, H., 155
Toyama, N., 155

**V**
Valdman, B., 17
Valero, F., 17
Van Walsum, G. P., 30
Varanasi, S., 407
Vásquez, M. P., 141
Vehmaanperä, J., 195
Villeneuve, P., 57
Vitolo, M., 161, 711

**W**
Wan, Y., 957
Wang, D., 423
Ward, T. M., 927
Wee, Y-J., 529
Wen, Z., 805
Wenger, K., 653
Whitehead, T. R., 93
Wilson, S., 859
Wolcott, M. P., 909
Wolf-Maciel, M. R., 451, 487, 885

**X**
Xie, D., 367
Ximenes, E. A., 171

**Y**
Yang, H-S., 935
Yano, M., 155
Ying, M., 793
Yoon, S-L., 367
Yu, F., 957

**Z**
Zacchi, G., 741, 971
Zhang, R., 423
Zheng, Y., 423
Zhu, Y., 721
Zullo, L., 739

# Subject Index


2S albumin, 57

**A**

Acetone powder, 57
Acid and alkaline catalyzed ethanol pulping, 573
Acid hydrolysis, 339
Acid prehydrolyzate, 239
Acrylic acid, 487
Acrylic acid recovery, 451
Activated sludge, 909
Aging, 957
Agricultural residues, 339, 353
Agriculture, 611
Alcohol oxidase, 17
Alcoholic fermentation, 753, 817
Alkaline extraction, 253
Alkalophillus *Bacillus clausii*, 27
Ammonia fiber explosion, 207, 313, 395
Ammonium sulfate, 675
Anaerobic digestion, 625
Analysis, 301
Aqueous ammonia petreatment, 721
Arabinofuranosidase, 93
Arabinose, 313
Artificial chaperones, 777
Artificial compounds, 515
Aspen wood, 301
*Aspergillus niger*, 171
*Aspergillus oryzae*, 675
Assay, 131

**B**

β-glucosidase, 281
*Bacillus atrophaeus*, 539
*Baciullus pumilus*, 501
*Bacillus subtilis*, 471, 793
Bacterial cellulose, 529
Bagasse, 339
Barrier film, 741
Batch cultivation, 539
Bidimensional model, 487
Biobleaching, 501
Biochemical processing, 947
Bioconversion, 595
Biodiesel, 583, 793
Bioethanol, 81, 327, 847
Biofuel, 81
Biogas, 765
Biogas plant, 625
Bioindicator, 555
Biomass, 171, 221, 289, 379, 395, 663, 721
Biomass conversion, 81, 207
Biomass transportation, 639
Bio-oils, 957
Bioprocess, 437
Bioreactors, 529, 817
Biorefinery, 327, 947
Biosensors, 17
Biosorption, 835
Biosurfactant, 185, 463
Biosurfactant production, 471, 539
Biotechnological processes, 487

**C**

Cadmium, 835
Calcium carbonate, 689
Carbohydrate analysis, 253
Carbonic acid, 301
Carboxy-methylcelluose, 573
Casein, 539
Cashew apple bagasse, 675
Cashew apple juice, 185
Castor seeds, 57
Catalase, 161, 859
Catalysis, 93
Cell concentration, 653
Cellulase, 131, 141, 155, 171, 221, 267, 281
Cellulignin, 141
Cellulose, 155, 195, 207, 407, 663
Cellulose conversion, 353
Cellulosic ethanol, 395
Central composite rotatable design, 595
CGTase characterization, 41
CGTase production, 27
CGTase purification, 41
Cheese whey, 897
Chemical behavior, 957
Chemical bleaching, 573
Chicken litter, 765
Chloroperoxidase, 437
Cloning, 703
Coconut fiber, 67
Cofermentation, 721
Condensed distillers solubles, 875
Conidia, 155
Continuous process, 161
Corn stover, 301
Covalent attachment, 67
Crystal sugar, 471
Crystallinity, 367
Cull potato, 805
Cyclodextrin glucanotransferase, 27
Cyclomaltodextrin glucanotransferase, 4

**D**

*D*-value, 555
DDGS, 171
Deactivation, 115
Degree of polymerization, 367

Denaturing gradient gel electrophoresis, 909
Deodorized distillate, 885
Detergent stripping, 777
Diafiltration, 971
Digestate processing, 625
Digester stability, 765
Dilute acid pretreatment, 423
Docosahexaenoic acid, 805
Dynamic reduced model, 487

E
Economic evaluation, 741
Economics, 437
EDTA, 515
Egg albumin, 927
Egg protein, 927
Egg white, 927
Egg yolk, 927
Esterification, 595
Ethanol, 17, 105, 207, 267, 339, 379, 663
Ethanol potential, 423
Ethanol production, 141, 753
Ethanol transport, 639
Ethanol/water pulp, 501
Experimental design, 27
Endoglucanase, 207, 281
Environmental biotechnology, 909
Enzymatic, 437
Enzymatic hydrolysis, 141, 289, 339, 379, 395, 407, 423
Enzyme, 105, 267, 859
Enzyme immobilization, 67
Epoxides, 437
Esterification, 67
Experimental design, 463

F
Fed-batch, 711
Fermentable sugar, 423
Fermentation, 185, 267, 529, 653, 663, 711, 875, 897
Fermentation processes, 515
Fermentor, 195
Fiber size, 367
Fiber sludge, 327
Filter paper, 131, 155
Fish oil, 805
Foam frractionation, 927
Forest, 611
Foul condensate, 909
Free fatty acids, 583, 885
Free radical hydrogel, 935
Fuel ethanol, 93
Fumaric acid, 689
Functional link networks, 817
Fungal pellet, 689
Furfural, 239

G
Galactoglucomannan, 741, 971
Gasification, 947
Gelfiltration, 971
Gene expression, 703
*Gluconacetobacter*, 529
Gluconic acid, 161
Glucose, 161, 313, 379, 539, 711
Glucose 6-phosphate dehydrogenase, 711
Glucose isomerase, 115
Glucose oxidase, 161
Glycohydrolase, 93
Gram-negative, 515
Gram-positive, 515
Green fluorescent protein, 555

H
Hemicellulases, 171, 221, 281
Hemicellulose, 81, 93, 741
Herbaceous crop, 239
Heterogeneous catalysis, 859
Horseradish peroxidase, 17
Hybrid poplar, 367
Hydrolysis, 67, 267

I
Immobilized enzymes, 17, 115
Immobilized lipase, 105
Infrared spectra, 573
Inhibitors, 93, 847
Initial rates, 407
Inoculum size, 689
Ionic-liquid, 407

K
Kinetic parameters estimation, 753, 817
Kinetics, 115, 539, 835

L
Lactic acid, 721, 875, 897
*Lactococcus lactis*, 515, 875
Lactose, 195, 689, 897
Land requirements, 611
Ligation, 703
Lignin, 3, 81
Lignocellulose, 267, 313, 327, 353, 847, 947
Lipase, 57, 67, 437, 595
Lipopeptide, 471
Liquid hot water pretreatment, 379
Liquid–liquid extraction, 451

M
Magnetic cell biocatalyst, 793
Magnetic polymicrosphere, 793

Maize, 253
Manure, 625
Manure pipeline, 625
Mathematical modeling, 753, 817
Membrane, 897
Membrane reactor, 161
Metal ions, 689
Methane, 765
Methanogenic activity, 765
Methanol, 105
Microalgae, 805
Microfiltration, 971
Micromixing, 859
Microreactor, 859
Microspectrophotometry, 3
Microwave-assisted fractionation, 253
Microwave pyrolysis, 957
Model, 653
Modeling, 487
Moisture content, 935
Molecular distillation, 885
Municipal solid waste, 423

**N**
Nanofiltration, 897
Nisin, 515, 875
Non-Newtonian, 289
Nuclei, 155
Numerical simulation, 859
Nutriet supplement, 875

**O**
Olive tree residues, 379
Omega-3 fatty acid, 805
Optimization, 595, 529, 583, 703
Optimum size, 625
Organic acids, 301
Organosolv ethanol pretreatment, 367
Organosolv pulping, 501, 573

**P**
Particle suspension, 289
pH-stability, 555
Phenolic acid esters, 3
Physical behavior, 957
*Pichia stipitis*, 653
Pipeline transport, 639
Plant breeding, 3Plant breeding, 3
Polyhydroxyalkanoates, 909
Polymerization, 935
Polysaccharides, 971
Postfossil, 611
Potato dextrose broth, 689
Power transmission, 639
Pretreatment, 221, 301, 353, 339, 395
Pretreatment crystallinity index, 407
Pretreatment optimization, 239
Primary solids fermentate, 909
Process stimulation, 817
Protein refolding, 777
Protein renaturation, 777
Protein separation, 927
Protein stability, 93
*Pseudomonas aeruginosa*, 185, 463
Pyrolysis, 947

**Q,R**
Quasi-Newton algorithm, 753
Rail transport, 639
Raw materials, 185
Recombinant strain, 711
Red oak wood, 289
Reducing sugars, 407
Reed canary grass, 395
Renewable energy, 611
Renewable sugars, 451
Response surface methodology, 27, 885, 583, 595, 721
Rhamnolipid, 185, 463
*Rhizopus oryzae*, 689
Ricin, 57
*Ricinus communis*, 57
Rotary biofilm contactor, 529

**S**
Saccharification, 93
*Saccharomyces cerevisiae*, 141, 327, 487, 711, 753, 847
Saline crops, 423
*Sargassum filipendula*, 835
Sawdust slurry, 289
Scenario, 611
Schizochytrium, 805
SEC, 971
Semicontinuous, 897
Separation, 451
Sequential injection analysis, 17
Serum albumin, 927
Shake flask, 195
Ship transport, 639
Silage, 221
Silica gel, 115
Simulation, 451
Simultaneous saccharification, 141, 721
Simultaneous saccharificaton and cofermentation, 81
Size-exclusion chromatography, 253
Sodium chloride, 555
Solid state fermentation, 281, 675
Solka Floc 200, 195
Solvent, 105
Sorbitan ester, 595
Sorbitan methacrylate, 935
Soya sludge, 885

Soybean oil, 105, 463
Stability, 957
Steam pretreated corn stover, 195
Submerged fermentation, 27
Sugar-cane bagasse, 141
Sugar separation, 313
Surface-response methodology, 239
Surfactin, 471
Surface tension, 463, 777
Steam explosion, 353
Substrate characteristics, 367
Surface-active substances, 471
Sugarcane bagasse, 573
Sugarcane straw, 501

**T**
Tannase, 675
Tannic acid, 675
Thermal effects, 835
Thermal stability, 555
Thermochemical processing, 947
Thermodynamic characterization, 451
Thermomechanical pulp, 741
Thermophilic, 765
Thermostability, 115
Thermostable CGTase, 41
Tocopherol, 885
Toxicity, 847
Transgenic maize, 207
Transcriptomics, 663
Transportation cost, 639
*Trichoderma*, 155
*Trichoderma reesei*, 17
Truck transport, 625, 639
Tubular bioreactor, 487

**U**
Ultrafiltration, 741, 971
Uptake capacity, 835

**V,W**
Viscosity, 289
Waste cooking oils, 793
Wastewater, 909
Weight-average molecular weight, 253
Wet storage, 221
White-rot fungi, 3

**X**
Xylan, 327
Xylanase, 501
Xylanase supplementation, 353
Xylose, 313, 653, 703
Xylose recovery, 239

**Y**
Yeast, 703
Yeast adaptation, 847